

POST-MINING 2005
APRÈS-MINE

Symposium Proceedings

To the memory of
Francis Wojtkowiak

RESIDUAL SUBSIDENCE ANALYSIS AFTER THE END OF COALMINE WORK
M. AL HEIB, M. NICOLAS, J.F. NOIREL, F. WOJTKOWIAK

THE CHARACTERISTICS OF SOFT ROCKS AND THEIR EFFECT ON THE LONG TERM STABILITY OF ABANDONED ROOM AND PILLAR LIGNITE MINES
O. AYDAN, A. SAKAMOTO, N. YAMADA, K. SUGIURA, T. KAWAMOTO

A REAL-TIME MONITORING SYSTEM FOR THE ASSESSMENT OF STABILITY AND PERFORMANCE OF IN ABANDONED ROOM & PILLAR LIGNITE MINES
O. AYDAN, H. TANO, A. SAKAMOTO, N. YAMADA, K. SUGIURA

FLOODING OF THE SAAR-LORRAINE COAL MINES: COUPLING OF THE REGIONAL MODEL OF THE LOWER TRIASSIC SANDSTONES AQUIFER WITH A "BOX" MODEL OF THE MINING RESERVOIR
Y. BABOT, A. DUZAN, M. ECKART, H. KORIES, M. METZ, R. RENGERS

THE NATURE OF RISK IN GEOTECHNICAL ENGINEERING
G. B. BAECHER

GEOTECHNICAL INVESTIGATION AND REINFORCEMENT DESIGN OF SUBSIDENCE PRONE AREA
K-M BANG, W-K SONG

ASSESSMENT AND MAPPING OF THE ENVIRONMENTAL HASARD IN THE PMRP APPROACH: FROM THE APPLICATION TO DEVELOPMENT NEEDS
PH. BARANGER, M. KIMMEL, B. MAZENC, R. HADADOU, O. LEFEBVRE, C. FRANCK

INFLUENCE OF COAL MINE TIPS ON THE CHALK AQUIFER. SAMPLING METHODS FOR THREE DIMENSIONAL SULPHATE INFILTRATION STUDY
F. BARREZ, J. MANIA, J.L. MANSY, B. PIWAKOWSKI

DEEP SALT CAVERNS ABANDONMENT
P. BEREST, B. BROUARD, M. KARIMI-JAFARI

SALT AND BRINE PRODUCTION METHODS IN FRANCE: MAIN CONCLUSIONS OF THE INTERNATIONAL GROUP OF EXPERTS (IEG) COMMISSIONED BY THE FRENCH REGULATORY AUTHORITIES
P. BEREST, B. DIAMOND, A. DUQUESNOY, G. DURUP, B. FEUGA, L. LOHFF

GASES EMISSION MONITORING IN A POST-MINING CONTEXT
K. BESNARD, Z. POKRYSZKA

FAILURE MECHANISMS, STABILITY ASPECTS, AND ANALYSIS TECHNIQUES FOR ABANDONED CANADIAN METAL MINES
M.C. BÉTOURNAY

RISK EVALUATION AND RELATED STABILITY CONSIDERATIONS FOR ABANDONED CANADIAN METAL MINES
M.C. BÉTOURNAY

PETROFABRIC OF THE KEUPERIAN MARLS IN LORRAINE (FRANCE): CHARACTERIZATION AND EVOLUTION IN BRINE
E. BOIDIN, F. HOMAND, F. THOMAS, J. YVON

MODELLING UNCERTAINTIES IN PILLAR STABILITY ANALYSIS
M. CAUVIN, T. VERDEL, R. SALMON

THE POST-MINING CONTEXT AT DECAZEVILLE-FIRMI CONCESSION (AVEYRON, FRANCE): ANALYSIS OF IMPACTS RESULTING FROM THE CESSATION OF PUMPING AT THE CENTRAL SHAFT. SURVEY OF VARIOUS SCENARIOS RELATED TO THE WATER LEVEL OF THE PIT LAKE IN THE GRANDE DECOUVERTE
R. COJEAN, N. FRANCO, J.-C. LAZAREWICZ, A. BLACHÈRE, D. LEFORT, C. SORGI

A SEMI-DISTRIBUTED MODELLING OF THE EVOLUTION OF GROUNDWATER QUALITY IN FLOODED MINES IN THE LORRAINE IRON BASIN
P. COLLON-DROUAILLET, R. FABRIOL, M. BUES

PPRM : ENVIRONMENT RISK ASSESSMENT METHODOLOGY – MAIN STEPS
B. COSTE, Y. ITARD, D. ARTIGNAN

TYPOLOGY OF CONDITIONS FOR UNDERGROUND QUARRY PILLARS BASED ON GEOPHYSICAL INVESTIGATIONS
PH. COTE, X. DÉROBERT, O. ABRAHAM

CHARACTERISATION AND TYPOLOGY OF MINING EFFLUENTS : PROSPECTIVE APPROACH BASED ON FRENCH LEAD-ZINC DEPOSITS
S. COTEL, J. M. SCHMITT, B. COSTE, Y. ITARD

COMBINING CAVITIY SURVEY AND PRECISION DRILLING TO OPTIMIZE GALLERY EXPLORATION
J-P CRABEIL

LARGE SCALE APPLICATIONS OF COVERS WITH CAPILLARY BARRIER EFFECTS TO CONTROL THE PRODUCTION OF ACID MINE DRAINAGE
A-M. DAGENAIS, M. AUBERTIN, B. BUSSIERE, V. MARTIN

TYPOLOGY OF STRATA MOVEMENT RELATED TO OLD SOLUTION MINING OF SALT AT SARRALBE (LORRAINE, FRANCE)
X. DAUPLEY, H. CUCHE, M. GHOREYCHI

VULNERABILITY ASSESSMENT FOR MINING SUBSIDENCE HAZARD
O. DECK, T. VERDEL, R. SALMON

AIR-WATER INTERACTION AND TIME DEPENDENT COMPRESSIBILITY OF A SUBTERRANEAN QUARRY CHALK
V. DE GENNARO, C. SORGI, P. DELAGE

UNDERGROUND WORKINGS OF SLATE VEIN AND COTICULE IN THE COMMUNE OF VIELSALM (BELGIUM): THE GEOLOGICAL RISK MANAGEMENT THROUGH DATABASE AND GIS
X. DEVLEESCHOUWER, C. MULLARD, E. GOEMAERE

THE MRPP : A POWERFUL OPERATIONAL REGULATORY TOOL TO PREVENT AND MANAGE POST-MINING RISKS
C. DIDIER, J. LELOUP

MANAGING THE MINING SUBSIDENCE HAZARD IN LORRAINE
Y. DISSART, T. VERDEL

PSYCHOSOCIAL AND MEDICAL CONSEQUENCES OF MINING SUBSIDENCE IN LORRAINE
V. DODELER, C. TARQUINIO

COPPER RECOVERY FROM THE SLUDGES OF THE LARONDE MINE, CANADA
K. ELAMARI, M. BENZAAZOUA, B. BUSSIÈRE, M. ARCHAMBAULT

HYDRODYNAMIC STUDY OF THE LONG TERM EVOLUTION OF A SALT CAVITY AFTER COLLAPSING
J.B. FEBVAY, V. HAMM, C. OLTEAN, F. GOLFIER, R. FABRIOL, M.A. BUÈS

COLLAPSE/SUBSIDENCE: ROLE AND INFLUENCE OF OVERBURDEN IN LORRAINE IRON MINES CASE
J. FOUGERON, M. SOULEY, F. HOMAND

UNDERGROUND CAVITIES DETECTION AND CHARACTERIZATION USING 2D ELASTIC FULL WAVEFORM INVERSION IN THE SPACE-FREQUENCY DOMAIN
C. GÉLIS, J. VIRIEUX, G.GRANDJEAN, S. OPERTO, D. LEPAROUX

LONG TERM STABILITY ANALYSIS OF CAST IRON SHAFT LININGS AFTER COAL MINE CLOSURE AND FLOODING
F. HADJ-HASSEN, Y. BIENVENU, J.F. NOIREL, M. METZ

ENVIRONMENTAL CHARACTERIZATION OF THE ABANDONED KETTARA MINE WASTES (MOROCCO)
R. HAKKOU, M. BENZAAZOUA, B. BUSSIÈRE

MODELLING THE IMPACT OF BACK- FILLING MATERIAL ON THE WATER QUALITY OF FLOODED IRON MINES (LORRAINE, FRANCE)
V. HAMM, R. FABRIOL, L. VAUTE, G. FOURNIGUET, J-C BAUBRON

A STUDY OF THE EFFECT OF STRAIN RATE ON STIFFNESS AND STRENGTH IN SILTY MUDSTONE USING MULTISTAGE TRIAXIAL TESTING
O. HAMZA, R. STACE, D. REDDISH

POST MINING HAZARD ASSESSMENT IN NORTH RHINE-WESTPHALIA (GERMANY) AT THE EXAMPLE OF THE AACHEN HARD COAL MINING DISTRICT
M. HEITFELD, M. MAINZ, K. SCHETELIG

THE SPATIAL INFORMATION SYSTEM ERAMSIS IN THE SERVICE OF GEOTECHNICAL MONITORING
M. HELLER, R. MAUKE, M. MOHLFELD, J. SKRZYPPEK, J. CROISÉ

NATURAL PROCESSES AND SYSTEM EVOLUTION DURING MINE CLOSURE: NUMERICAL SIMULATION AND VISUALIZATION
M. HELLER, J. POPPEI, L. SCHLICKENRIEDER, B. FÖRSTER

LONG-TERM GEOMECHANICAL STABILITY AND INTEGRITY OF THE SALT BARRIER IN THE CENTRAL PART OF THE BARTENSLEBEN SALT MINE
S. HEUSERMANN, S. FAHLAND

A STUDY OF SINKHOLE HAZARD AT AREA OF LOCKED COLLIERY
A. KOTYRBA

CONTRIBUTION TO IMPROVE PILLAR ANALYSIS IN ABANDONED ROOM AND PILLAR SATL MINES
F. LAOUAFA & M. GHOREYCHI

BROOKS UNDER COLLIERY HEAPS IN THE WALLOON REGION
J.P. LARDINOIS, B. FLAMION, Y. ZECH

MANAGEMENT OF MINING-RELATED DAMAGES IN ABANDONED UNDERGROUND COAL MINE AREAS USING GIS
U. J. LEE, J. A. KIM, S. S. KIM, W. K. KIM, S. H. YOON, J. K. CHOI

TECHNICAL AND LEGAL ASSESSMENT OF A DISUSED UNDERGROUND QUARRY IN THE NEIGHBOURHOOD OF SAUMUR (FRANCE)
D. MATHON

EVALUATION OF POST MINING AREAS IN AUSTRIA WITH METHODS OF MINE SURVEYING AND MINING SUBSIDENCE ENGINEERING
G. MAYER, R. PILGRAM, B. RANDJBAR

INDUCED SEISMICITY IN A SALT MINE ENVIRONMENT EVALUATED BY A COUPLED CONTINUUM-DISCRETE MODELLING
D. MERCERAT, M. SOULEY, L. DRIAD, P. BERNARD

FROM DISCOVERY TO BACK FILLING OF POTENTIALLY UNSTABLE MINING VOIDS : THE CASE OF THIL (FRANCE)
D. MIDOT, A. MARNET, J-P GIONTA

MONITORING THE FLOODING OF A MINE GALLERY IN LORRAINE THROUGH ELECTRICAL-RESISTIVITY AND SASW SURVEYS – TRESSANGE PILOT SITE
J.M. MIEHE, A. BITRI, H. FABRIOL, G. GRANDJEAN, F. LEBERT, F. MATHIEU, G. RICHALET

ELECTRICAL METHODS FOR DETECTING AND CHARACTERIZING DISTURBANCES CAUSED BY SALT MINING: EXAMPLE OF THE LA MADELEINE SALT CONCESSION (LORRAINE, FRANCE)
J-M. MIEHE, F. MATHIEU, B. FEUGA, H. FABRIOL

RE-STABILISATION OF THE CARNALLITIC WORKING AREAS IN THE MERKERS POTASH MINE
W. MINKLEY, J. MÜHLBAUER

PLACE OF A SOCIO-ECONOMIC APPROACH IN THE WATERSHED-SCALE POST-MINING MANAGEMENT: EXAMPLE OF THE GOLD MINING DISTRICT OF ST-YRIEIX, FRANCE
J.F. ORRU, G. RECOCHE, Y. ITARD

HIGH RESOLUTION IMAGING OF GROUND SUBSURFACE: APPLICATION TO MINING SITES
B. PIWAKOWSKI, F. BARREZ, F. MEILLIEZ, J. MANIA

CAVITIES AS THE SOURCES OF ACID MINE PROCESS IN THE NIWKA-MODRZEJÓW COAL MINE (POLAND)
I. PLUTA, M. MAZURKIEWICZ

GAS MIGRATION FROM CLOSED COAL MINES TO THE SURFACE. RISK EVALUATION METHODOLOGY AND PREVENTION MEANS
Z. POKRYSZKA,C. TAUZIÈDE, C. LAGNY, Y. GUISE, R. GOBILLOT, J-M. PLANCHENAULT, R. LAGARDE

MODELING AND ASSESSMENT FOR SUBSIDENCE HAZARD IN INCLINED IRON MINING
V. RENAUD, J.-J. TRITSCH, C. FRANCK

LONG-TERM BEHAVIOUR PREANALYSIS OF THE BODOVALLE MINE (GALLARTA-VIZCAYA, SPAIN)
R. RODRIGUEZ, F. MARTIN DE LA ESCALERA, J. ELORZA, C. DEL OLMO, A. SAMPER

AN INTEGRATED CAVITY FILLING TECHNIQUE FOR ABANDONED UNDERGROUND ROOM AND PILLAR LIGNITE MINES AND UNDERGROUND QUARRIES
A. SAKAMOTO, N. YAMADA, K. SUGIURA, M. HAMADA

SOME EXAMPLES OF THE CAVITY FILLING ALONG TRANSPORTATION ROUTES ABOVE ABANDONED ROOM AND PILLAR LIGNITE MINES IN TOKAI REGION
A. SAKAMOTO, N. YAMADA, K. SUGIURA, T. KAWAMOTO

SAFETY ASSESSMENT FOR THE LAND SURFACE IN THE VICINITY OF THE POTASH SHAFT NEUSTAßFURT VI
K. SALZER, W. MINKLEY

ASSESSMENT OF THE WATER INFLOW TO THE MINE WORKINGS BY NUMERICAL MODELLING
Y. SHENG, D. REDDISH

INTERFEROMETRY OF SPATIAL RADAR IMAGES FOR POST-MINING SURVEILLANCE: EXPERIMENT FEEDBACK
E. SIMONETTO, D. RAUCOULES, C. CARNEC

HIGH RESOLUTION MICROGRAVITY INVESTIGATIONS FOR THE DETECTION AND CHARACTERISATION OF SUBSIDENCE ASSOCIATED WITH ABANDONED, COAL, CHALK AND SALT MINES
P. STYLES, S. TOON, M. BRANSTON, R. ENGLAND, E. THOMAS, R. MCGRATH

SOLUTION OF UNDERGROUND MINE GAS EMISSIONS ON SURFACE OF ABANDONED MINING SITES WHERE STEEP DEPOSITED COAL SEAMS HAVE BEEN EXPLOITED
G. TAKLA, K. FROML

MICROSEISMIC MONITORING OF ABANDONED SALT MINES BENEATH NORTHWICH, CHESCHIRE, UK.
S.M. TOON, P. STYLES

DEVELOPMENT AND VALIDATION OF A METHOD TO PREDICT COAL PILLAR LIFE IN SOUTH AFRICA
N. VAN DER MERWE

DEVELOPMENT OF TOOLS FOR MANAGING THE IMPACTS ON SURFACE DUE TO CHANGING HYDROLOGICAL REGIMES SURROUNDING CLOSED UNDERGROUND COAL MINES
M. VESCHKENS, W. UNLAND, H. KORIES

EFFECT OF WATER ON THE MECHANICAL BEHAVIOUR OF SHALES
J. WAKIM, F. HADJ-HASSEN, M. TIJANI, J.F. NOIREL

MINE WATER MANAGEMENT AND THE WATER FRAMEWORK DIRECTIVE
C. WOLKERSDORFER

To the memory of Francis…



Three years ago, Francis Wojtkowiak opened in Nancy the first « post-mining symposium », as the President of GISOS.

After having studied geology in Nancy, he post-graduated a PhD on the topic of “cracks generation in rocks under mechanical stresses”. He then joined BRGM and later on ANTEA for about 25 years, period during which he has been deeply involved in geotechnics and especially rock mechanics related to mining activity. He became an expert recognised internationally in this domain. In 1995, he joined INERIS where he was in charge of high responsibilities within the ground and underground division. He notably contributed to develop the “post-mining” activities, especially within the Lorraine iron ore basin where he was born while his father was a miner.

In 2002, he became president of GISOS. His great involvement contributed to the development of this scientific group and facilitated the organisation and achievement of some of the major GISOS successes like the “Tressange flooding experiment” and the “GISOS post mining symposium”.

He has always been deeply involved in national and international geotechnical scientific networks. He has been General Secretary of the French Society of Rock Mechanics as well as many other scientific or technical associations (CFGI, SIM, AFTES, AFPS…).

Last February, Francis left us. He was 52 years old. He faced his disease with a courage and a love for life that caused the admiration of all of those who had the privilege to accompany him during his last weeks.

He has always been aware of the transfer of the expertise and knowledge he has accumulated during all those years. He left us many scientific and technical publications denoting the various abilities of Francis by their relevance, their clearness, their practical character and the quality of their drafting. He also spent lot of time, kindness and energy to transmit his knowledge to young engineers at the first stage of their career. I was one of them and my gratitude to him is even larger.

We have not only lost the last GISOS president, we also lost a joyful and brilliant colleague. For lot of us we also lost a friend and, for some of us, a very close one.

Today, as the second GISOS post-mining symposium opens, we miss him so much. The absence of his voice and of his laugh during these days will be a cruel miss. But we know that he was very attached to this symposium. He took part, until his last days, to the organisation committee. We know that this symposium will also be that of Francis.

RESIDUAL SUBSIDENCE ANALYSIS AFTER THE END OF COALMINE WORKEXAMPLE FROM LORRAINE COLLIERY, FRANCE

Al Heib M.[(1)], Nicolas M.[(2)]. and Noirel[(2)] J.F., Wojtkowiak F.

[1] INERIS LAEGO - Ecole Nationale Supérieure des Mines de Nancy, Parc de Saurupt – F 54042 Nancy Cedex, France. vincent.renaud@ineris.fr

[2] Charbonnage de France, 2, rue de Metz, 57802 Freyming-Merlebach,

ABSTRACT : This paper describes the residual movements associated with the deep coalmines. The studied case relates to works located into Lorraine coal basin. The paper is divided into two sections. The first one describes subsidence phenomena, especially the residual phase in terms of amplitude, duration and localization. The second one focus on Morsbach case: the total and residual subsidence measurements will be analyzed and compared to the state of the art as well as the currant knowledge. The results of the analysis show that the duration of residual movements does not exceed 24 months and their amplitude is about 5% of total subsidence. We analyze also the declarations of the mining damage during and after the mining period. Damages occur, after this period are probably due to late observations.

KEY WORDS: *coalmines, residual subsidence, mining damage, subsidence measurements.*

Résumé : Cet article décrit les mouvements résiduels associés à l'exploitation des mines de charbon à grande profondeur. Le cas traité concerne le secteur de Morsbach, influencé par une exploitation de charbon en Lorraine. L'article se décompose en deux parties : la première partie décrit le phénomène d'affaissement, et particulièrement la phase résiduelle de l'affaissement (amplitude, durée, localisation), la deuxième partie est consacrée au cas de Morsbach, pour lequel nous analyserons les mesures d'affaissement (totales et résiduelles) par rapport à l'état de la connaissance. Les résultats de l'analyse montrent que la durée de l'affaissement résiduel ne dépasse pas 24 mois et que son amplitude est de l'ordre de 5% de l'affaissement total. Nous avons également analysé les déclarations des dommages et des dégâts miniers pendant et après l'exploitation. Les dommages observés après l'arrêt des travaux sont probablement dus à des observations tardives.

MOTS CLES : mines de charbon, mesures d'affaissement résiduel, dégâts miniers.

1. Introduction and objectives

The last panel of Lorraine French coalmines has been mined in 2004. The subsidence prediction during the mining period was completely controlled. Today, we focus on the residual subsidence phase. The problem is the existence of other movements whose amplitudes are comparables to residual subsidence. In this paper, we will discuss various processes can led to ground movements comparable to residual mining subsidence. The analysis of a case studies make it possible to improve knowledge and city management of zones where risks of residual subsidence can occur. One of them is the Morsbach city (57), well documented, from Lorraine colliery. It enables us to check the classical rules describing the evolution of mining subsidence during and after the mining period. This case also offers an interesting opportunity because the data related to subsidence measurements and mining

works are complete. We will examine the final subsidence under the city of Morsbach (1996) and consequences on the existing and future buildings of the sector.

2. Mining Subsidence: Theoretical aspects and definitions

The underground excavations induce the bending and the deconsolidation of the overlying strata. The induced displacements are transmitted on the surface and form a subsidence trough (figure 1). This subsidence trough extends on a surface above the exploited area; its volume remains less than the extracted one due to the bulking effect. Figure 1 indicates schematically the geometry of the subsidence profile. The characteristics of the subsidence trough are: influence angles (or limit angle) and maximum subsidence amplitude Am.

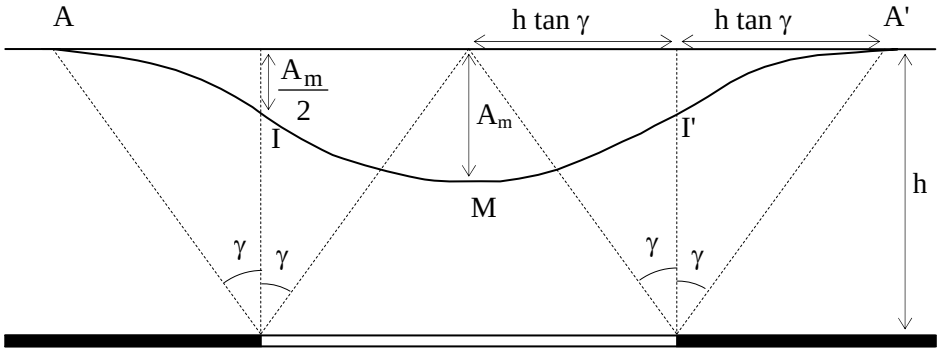


Figure 1: Theoretical subsidence trough above a single panel at critical width in horizontal seam (after Proust, 1964)

The movement at the surface has a vertical component, the subsidence itself, and a horizontal component. The displacement is systematically oriented towards the centre of the trough. Horizontal displacements generate differential displacements and those induce horizontal strain in compression and extension (figure 2). The damages occurring on infrastructures are mainly induced by the horizontal strain, the zones in tension being, in general, more unfavourable than those in compression.

When the ratio “width of the zone/depth” is greater than 1.4, for an influence angle of 35° (typical value of Lorraine coalmines), the configuration is said supercritical and the subsidence amplitude is maximum. A sub-critical surface requires a correction of the subsidence value, and maximum of tilt and strain values. The correction depends on the geometry of the zone. The maximum tilt (P_{max}) is calculated using the following empirical relation: $P_{max} = \beta\ Am/H$ (Am: maximum subsidence, b: depends on the nature of strata). The maximum horizontal strain ε_{max} is calculated using the following empirical relation: $\varepsilon_{max} = \alpha\ Am/H$. In the context of the Lorraine coal basin, the experience feedback highlights that β is considered equal to 3 and α is generally taken equal to 0.75.

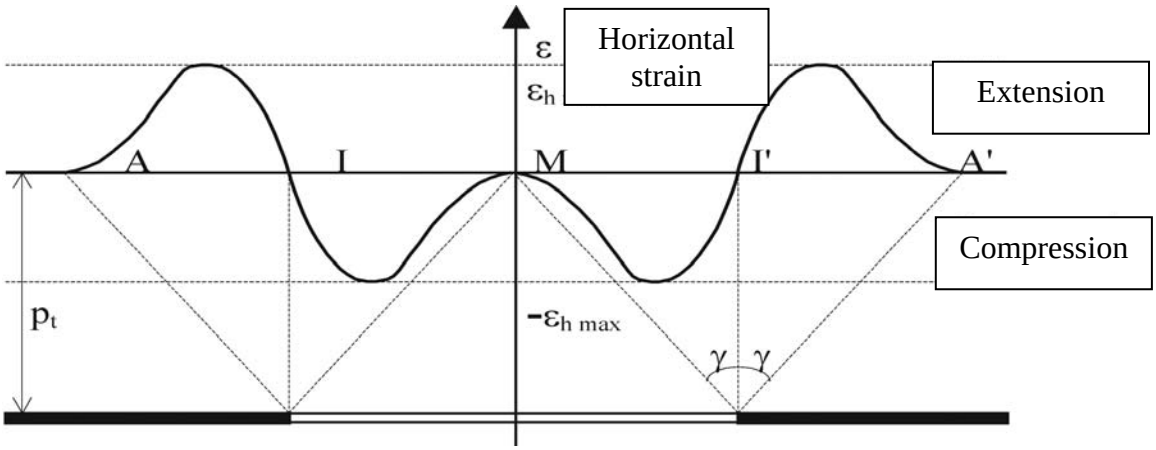


Figure 2: Theoretical horizontal strain variations above a supercritical single panel (Proust, 1964)

3. Phases of mining subsidence

The final subsidence can be divided into three phases as illustrated in figure 3, (Wojtkowiak, 1997). Phase I known as initial subsidence, corresponds to the period when the face of extraction penetrates the cone of influence. This cone is defined by the influence angle and the depth of the considered point, until passing to the vertical of this one. This phase is generally associated to 10 to 15 % of final subsidence. Phase II known as principal or accelerated subsidence corresponds to the period when the face of extraction moves away from the vertical of the point, until it leaves the cone of influence of this point. In the United-Kingdom coalmine, 97 % of final subsidence is reached at this stage. From the bibliography, the corresponding value of subsidence varies between 80 to 90 % of Am.

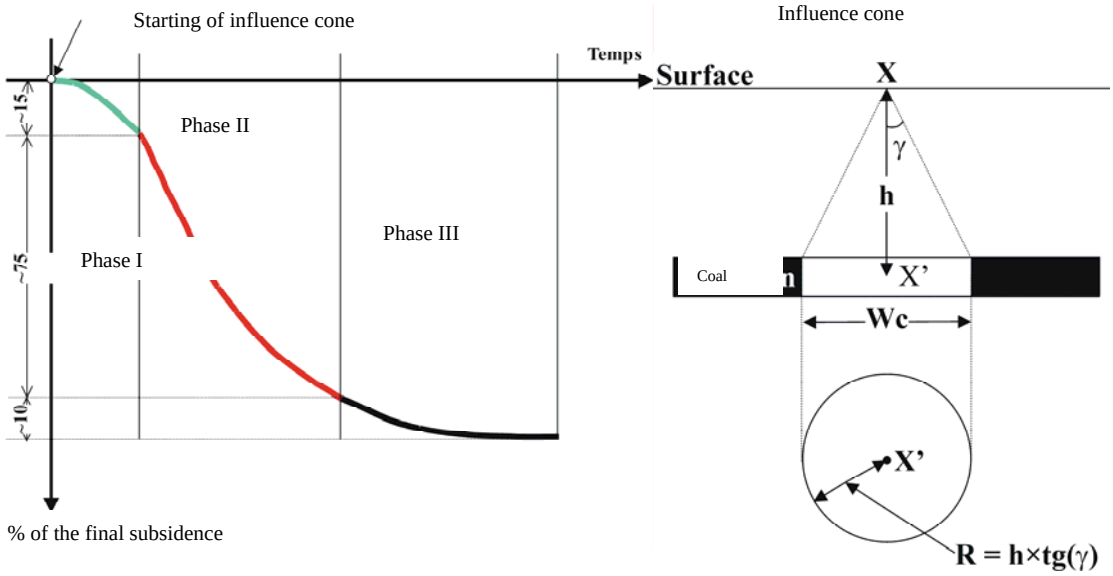


Figure 3: (a) Typical evolution of a subsidence profile with time; (b) cone of influence of a point located on the surface

Phase III, known as residual subsidence (also named differed or delayed subsidence) is constitutes the final phase of subsidence. It continues after the extraction phase or when the front of the face is out of the area that influences completely the considered point. Residual subsidence represents only some fraction of the total subsidence. After this last phase, subsidence is supposed finished and surface is stabilized.

4. Mining Damage Classification

Subsidence can induce damages on buildings and infrastructures. The damage severity depends both on the characteristics of the subsidence trough and the nature of the structures. The values presented in table 1-a classify the damage on structures in five categories. These values are determined from many back-analysis of many cases for ordinary buildings. Deck et *al*. (2003) after analysing various classifications available in the international bibliography propose three levels of damage scale. Table 1-b specifies the definition of each of these three classes of damages or degradations. Deck, (2002) has checked that this table is well correlated with the values of deformation thresholds given in table 1-a.

Damage classes	Horizontal strain (mm/m)	Tilt (‰)	Radius of curvature (km)
Very slight	$\varepsilon<0,5$	<2,5	>50
Slight	$0,5< \varepsilon <1$	<5	>20
Appreciable	$1< \varepsilon <2$	<10	>11
Severe	$2< \varepsilon <3$	<15	>8
Very severe	$\varepsilon>3$	>15	<6

Table 1-a: Scale of damage

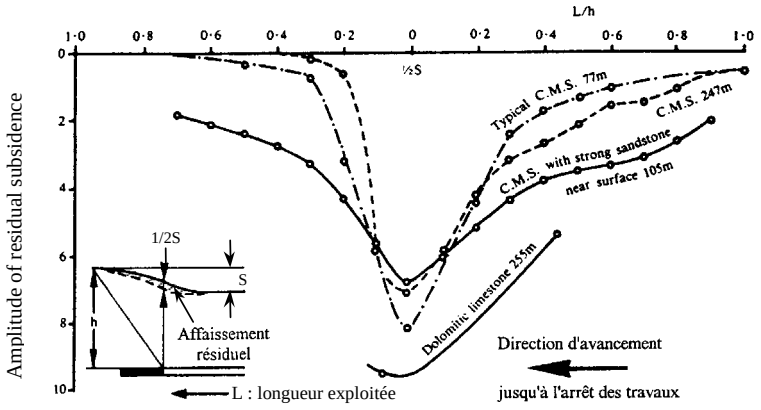
Classification of degradations	Description
Architectural	Low-size cracks in the plasters, wedging of the doors and the windows.
Functional	Instability of structural elements, blocking of doors and windows.
Structural	Sever degradation or collapse of the principal structural elements. Possibility of rupture of certain parts. Partial or total rebuilding is necessary. Major risks for the residing.

Table 1-b: Classification of scale of damages on the surface structures proposed by Deck et *al*., 2003

5. Residual subsidence

5.1. Amplitude and shape of residual subsidence

The amplitude of residual subsidence is generally about 1 to 10% of final subsidence (figure 3). This value is largely allowed by the whole French and foreign authors. The amplitude depends on many factors: thickness of the mined seam, depth, backfilling and goaf methods as shown in figure 5, the amplitude of residual subsidence is maximum in the vicinity of the inflection point of the subsidence trough. On both sides of this point, the amplitude of residual subsidence decreases significantly. Generally, residual subsidence decreases with the mine depth. One can highlight that, during the last two or three years of residual subsidence phase, that the amplitude of subsidence is negligible. The settling speed is decreasing over this duration. A great part of residual subsidence is given at the end of the first year (40 to 90 %), sometime before, (80 % after one month in a USA mine). In the Nord and Pas-de-Calais collieries, in France, residual subsidence does not exceed 5 mm per year after 18 months and 2 mm per year after 26 months in most cases.



S : subsidence ; L : length of long-wall ; h : depth of underground excavation

Figure 5: Residual subsidence for various coverings according ratio length exploited/depth (after NCB, 1975).

5.2. Duration of residual subsidence

Table 2 presents bibliographical data related to the duration and amplitude of the residual subsidence phase. We specified for each case the treatment method (goaf, backfilling) and the nature of strata. The duration of the residual subsidence phase is about 12 to 18 months, but this duration is often less long, i.e. about 3 to 4 months when the exploitation is carried out in an already disturbed zone (several seams, goaf...). There are some isolated cases resulting from geological contexts and/or particular exploitation, for these cases, the duration of residual subsidence can appreciably be raised and spread out over one period of 4 to 6 years.

Cases	Mining conditions	Residual subsidence
U.K. (Many basins)	Long-wall method and plastic layers	Less than 12 months ; 5-6 % of the total subsidence
UK (Durham Coalfield)	Tow mines with high resistance strata	1) 8 % of total subsidence after 4 years, and 9 % after 6 years. 2) 6.8 % of total subsidence after 4 years
West Germany	Many mines using long-wall method	5 years, with 75 % from the first year
Australia	Long-wall with caving method	3 to 7 months
India	Long-wall in virgin ground	10 months to 15 month for 10 to 30 % of total subsidence
	Long-wall method - in already extracted zones.	2 to 4 months; 5 to 10 % of total subsidence
USA	Long-walls method	10 % of total subsidence 1 month and 12 % after 17 months
France : Nord-Pas-de-Calais Albi - Carmaux	Plastic strata ; in already extracted zones.	99 % of total subsidence after 3 to 4 years
France : Provence, Lorraine And Blanzy	Resistant strata ; in already extracted zones	2 to 3 years

Table 2: Duration and amplitude of residual subsidence phase (after Aissaoui, 1999)

5.3. Consequences of residual subsidence on structures and infrastructures

Residual subsidence does not affect the surface constructions because the residual horizontal strains, which are more prejudicial, are practically small. One does not have specific study undertaken on the damage that mining works can induce during residual phase. One can however roughly estimate the horizontal strain and the tilt starting from relations established

for the active phase. Maximum residual subsidence reaches only a small proportion of maximum subsidence (10%) in active phase. The residual maximum strain and tilt result from those in active phase in the same proportion. Since the horizontal strains reach in active phase, 0.1 to 3 mm/m (more rarely higher values), the order of magnitude of the additional horizontal strain, will be 10^{-2} to 10^{-1} mm/m in residual phase.

6. Other causes of ground movements

Other types of phenomena can induce movements of the same order of magnitude as residual mining subsidence (the pumping of ground water, compaction of soil, seasonal climatic variations or exceptional weather conditions of long duration, etc). These phenomena exist in mining zones like everywhere else. It appear to be very difficult to distinguish between what result from mining residual subsidence and what is ascribable to other natural causes.

As an example the natural variations of soil water content induces vertical displacements of the surface (Holzer and Pampeyan, 1981). The amplitude is equal to residual subsidence, and often in proportions much more important when man causes a major reduction in the piezometric level. The cases of Mexico City (Morales et *al*., 1991), and Fremont Valley in California are well-known examples.

Ground movements may also result of the hydrocarbon exploitation. They are very similar to those related to mining (Bau et *al*., 1999). The main difference comes from the great extension of the subsidence (10^2 to 10^4 km^2). In fact, due to depth and extension of the extracted hydrocarbons area, the hydrocarbons subsidence is comparable to a whole coalfield. Subsidence above the fields of hydrocarbon extraction develops a residual phase, during which the fluids move in-depth until finding a state of equilibrium.

The compaction of the soil depends on the water content variation that can be related on pumping, the climatic change, the increase in the stresses, etc. The order of magnitude of compressing can be similar with that of residual subsidence of mining origin.

7. Subsidence analysis of the eastern sector under Morsbach district

7.1. Presentation of study sector

The exploitation of the Marienau sector - commune of Morsbach started in 1970, used initially the method of the backfilling long-wall, when, later used the long caving faces method. The last panel was exploited at 1000 m depth. All seams belong to the upper bright burning coal (beam of Laudrefang). The field of Marienau is limited by the anticline Simon, the synclinal of Marienau and the fault of Fockloch. The thickness of the sandstone bed, above the carboniferous beam, is about 250 m. The least deep and oldest panels are in the east of the sector. The exploitation developed towards the west while deepening. The depth of the exploited panels lies between 470 m and 1070 m. The dip of the seams varies from 10° in the east of the sector, to 30° in the west of the sector. The total of 49 panels have been extracted from 13 seams with a variable thickness ranging from 1 to 3 m. The average thickness is 2.1 m. At the surface, above the exploitation, there are a forest and few structures. On the other hand, west of the highway, one can note the presence of several cities and principal roads.

7.2. Analysis of subsidence measurements

Charbonnages de France performed regular subsidence measurements before, during and after the exploitation. The levelling loop contains significant number of points. The levelling started in 1961, has been carried out by the services of Charbonnages de France. The final subsidence of studied sector has a dissymmetrical form, resulting from the geometry and number of exploited seams, which are more numerous in the east. The maximum amplitude of subsidence is 11.74 m, in the east of the sector. The curves of iso-subsidence are tight side, in the area corresponding to the forests (figure 6). The maximum tilt Pmax of the ground calculated from the curves of iso-subsidence is equal to 10% (this tilt is different from the one measured on existing buildings). The tilt does not exceed 2% in the urban zone of the Morsbach city. Figure 6 presents the location of a section going from the centre of the subsidence trough to outside the zone of influence.

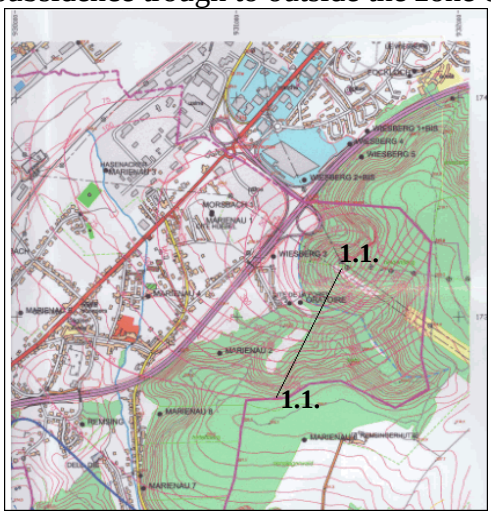


Figure 6: Final subsidence and location of cut A-B

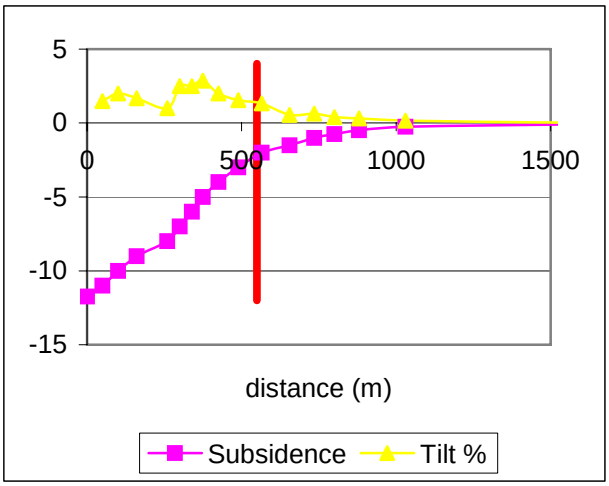


Figure 7: Subsidence (m) and tilt of Profile A-B

The figure 7 shows subsidence and tilt profiles. The angles of influence are difficult to determine due to the complex geometry of underground excavations and the surface topography. The angle of influence in flat seam equals 35° (without dip). In the case of an inclined seam, there are two angles: an upstream angle equal to 35° less the dip of the seam and a downstream angle equal to 35° plus the dip of the seam. For studied example, we calculated, using subsidence measurements, downstream angle (south-eastern) equal to 49°.

7.3. Measurements and prevision comparison

The cumulated average thickness of the 7 exploited seams at the centre of the subsidence trough is equal to 15 m. The surface exploited in each seam is supercritical. The maximum subsidence (Am) predicted by the following expression: Amax = w * f1 * f2 * g
- W: height of opening, - f1 and f2 empirical factors where f1 depends on the mode of treatment of the extraction area. It equals, for the Lorraine exploitations: 0.1 for a hydraulic stowing; 0.5 for a pneumatic stowing and 0.9 for caving. The depth factor f2 is equal to 1 for depths ranging up to 500 to 600 m and 0.8 for depths greater than 800 m (for the French coalmines). g: factor depends on the geometry of excavation of sub-critical panels. Maximum calculated subsidence, for a coefficient f1 ranging between 0.8 and 0.9, to take into account of the presence of certain backfilled panels, is between 12.7 m and 13.5 m. The forecast of subsidence by the method described above is close to the subsidence measured at the centre of the trough (11.75 m). The maximum tilt calculated according to the empirical relation (cf § 2) is equal to 4.5 %. The measured maximum tilt differs from the theoretical calculation of the maximum tilt. This difference is probably due to the

dissymmetrical shape of the subsidence trough. The urban zone of the Morsbach city is in the zone where the tilt is less than 2%.

7.4. Characteristics of residual subsidence

The closure of the exploitation of the Marienau sector under the Morsbach city took place in 1996. The depth of the last panel is 1000 m. It is considered that the phase of residual subsidence started from this date. Subsidence measured in 1996 was 35 cm. On this date the subsidence was mainly affected by the exploitation of the last active panel. The subsidence measured in 1997 was only 20 cm, in 1998 the residual subsidence is null because no measurable movement has been detected. The cumulated value of residual subsidence thus lies between 20 and 55 cm. The period of stabilization of subsidence is less than two years. The results of these observations, in Lorraine coal basin, are conforming to the data resulting from the bibliography. Consequently, this period is also lower than 5 years, maximum period of stabilization noted in other basins. The location of maximum residual subsidence is north of the exploitation zone, at the edge of mining work. The distance between the location of the maximum subsidence and that of the maximum residual subsidence is 700 m. If one adopts the maximum value of residual subsidence of 55 cm, residual subsidence is equal to 5% of maximum subsidence. The residual tilt can be calculated using the empirical relation (§ 2). In this case this residual tilt is equal to 0.2 %, the maximum tilt increased from 1.8% (before residual subsidence phase) to 2% (after residual subsidence phase).

7.5. Subsidence effects on structures of Morsbach city

We determined the number of structures damaged induced by the exploitation. All concerned structures are located at the west of the exploited zone, under Morsbach city. Before 1991, the exploitation carried on non-urbanised area. The data thus relating to the three following periods are summarized in table 3.

Damage type	Recent panels 1991-1995	Residual phase 1996-1998	Stabilized phase 1999-2003
Architectural	41	44	13
Functional	29	5	10
Structural	4	2	1
Total	74	50	24

Table 3: Number of damaged structures due to exploitation at Morsbach city

Let us specify that certain structures were considered in several classes of damage of which we held account in our analysis. The total number of cases was 74 for the period 1991-1995; it is of 24 cases for the period of 1999-2003. The total number of damaged structures thus clearly decreased between 1996 and 2003. It is noted that the number of cases of structural damage is significantly decrease. The total number of cases corresponding to the structural damage is 7 compared to 148 retained. Only one case of structural damage was retained for stabilized phase. According to the observations, this case has been appeared during the active phase of subsidence and only declared during residual phase.

8. Conclusion

In this study, we present an analysis of the residual subsidence measured after the closure of the exploitation. The studied sector was Marienau – Morsbach city. The exploitation ended at the end of 1996. The maximum subsidence measured at the centre of the trough corresponds to the forecast given by empirical calculation. The basin has a dissymmetrical form. The maximum tilt in the East (non-urbanized zone) is 10% but reaches only 2% in the west (urban zone of Morsbach city). Residual subsidence is obtained after less than 2 years. This duration is in conformity with the forecast. The amplitude of residual subsidence is less than 5 % of total maximum subsidence at the centre of the trough. The supplement of maximum tilt due to residual subsidence is estimated at 0.2%. The damage of the structures is especially associated to the active phase of subsidence. After the period of stabilization, the number of complaints falls appreciably. The complaints are primarily due to late declarations of the existing damage.

9. References

Aissaoui K., 1999 : *Amélioration de la prévision des affaissements dans les mines à l'aide des approches empiriques, numériques et analytiques*. Thèse INPL – LAEGO.

Bau, D., Gambolati, G., Teatini, P. 1999: *Residual land subsidence over depleted gas fields in the northern adriatic basin*. Environmental And Engineering Geoscience. Win 1999, Vol 5 (4), pp. 389 - 405

Deck O., Al Heib M., Homand F. 2003: *Etude de la vulnérabilité du bâti soumis aux conséquences des affaissements miniers*. Après-mines 2003, Nancy, p 1 - 11 (CD-ROM).

Morales, R., Murillo-Fernandez, R., Hernandez-Rubio, A. 1991: *Subsidence of the former Texcoco Lake*. Land Subsidence, Proc. 4th Int. Symp., Houston, Texas, USA, IAHS Publ. n° 200, pp. 35 - 43

Holzer, T. L., Pampeyan, E. H. 1981 *Earth fissures and localized differential subsidence*. Water-Resources-Research, Vol.17, n°1, Feb. 1981, pp. 223 - 227

NCB, 1975 : *Subsidence Engineer's Handbook*. National Coal Board, London.

Proust A. 1964. : *Étude sur les affaissements miniers dans le Bassin du Nord et du Pas-de-Calais*. Revue de l'Industrie Minérale, juin - juillet 1964, 46, n° 6 et 7, 68.

Wojtkowiak, F. 1997 : *Evolution du phénomène d'affaissements pendant et après l'exploitation totale de couches de charbon*. Exposé à la Conférence mondiale sur le développement durable des anciens pays charbonniers. Lille, mars 1997

A REAL-TIME MONITORING SYSTEM FOR THE ASSESSMENT OF STABILITY AND PERFORMANCE OF IN ABANDONED ROOM & PILLAR LIGNITE MINES

AYDAN, Ömer[1], TANO, Hisataka[2], SAKAMOTO, Akio[3], YAMADA, Noritoshi[3], SUGIURA, Kenrou[3]

[1]TOKAI UNIVERSITY, Department of Marine Civil Engineering, Shizuoka, Japan. ; aydan@scc.u-tokai.ac.jp

[2]NIHON UNIVERSITY, Department of Civil Engineering, Koriyama, Japan. ; tano@civil.ce.nihon-u.ac.jp

[3] TOBISHIMA CONSTRUCTION COMPANY, Nagoya Branch, Japan.; Akio_Sakamoto@tobishima.co.jp; Noritoshi_Yamada@tobishima.co.jp; ,kenrou_sugiura@tobishima.co.jp

ABSTRACT: The authors have been involved with the stability of abandoned mines beneath urbanized residential areas in Tokai region. These abandoned lignite mines were in operation until 1960s. There is a great concern about the stability of these abandoned mines during large earthquakes. The 2003 Miyagi Hokubu earthquake caused great damage to abandoned mines and resulted in collapses. The authors describe an integrated real-time monitoring system and they report some measured data up to now. The responses of monitoring system during a large roof collapse under gravitational condition as well as during and after two earthquakes are presented and their implications are discussed.

KEYWORDS: Abandoned mine, Earthquake, Multi-parameter monitoring.

RESUME : Les auteurs ont été impliqués par la stabilité de mines de lignite abandonnées se trouvant à l'aplomb de secteurs résidentiels de la région de Tokai. Ces mines étaient en exploitation jusque dans les années 60. La stabilité de ces mines abandonnées pendant de grands tremblements de terre est une préoccupation majeur. Le tremblement de terre de Miyagi Hokubu en 2003 a induit de nombreux dommages dans d'anciennes mines qui se sont soldés par des effondrements. Les auteurs décrivent un système de surveillance en temps réel et ils présentent quelques-unes des données mesurées. L'article présente et analyse les réponses du système de surveillance pendant un effondrement majeur du toit des exploitations sous l'effet de la gravité, aussi bien que pendant et après deux tremblements de terre. Les implications de cette analyse sont également discutées.

MOTS-CLEFS : Mine abandonnée, Tremblement de terre, Surveillance multi-paramètre.

1. Introduction

Lignite was extensively extracted using room and pillar mining technique in Tokai region of Central Japan until 1960s. These mines are abandoned since then and many of these areas have become urbanized. There is a growing concern on the response and stability of areas situated above the abandoned-lignite mines in Japan due to urbanization in recent years during earthquakes as well as in long-term.

One of such areas is Mitake town in Gifu prefecture of Japan, which was well known for mining activities until 1960s. Since the abandonment of the mines, some caving and collapses occurred in the town and the town authorities are also concerned with the stability and performance of the

abandoned mines during earthquakes. Expected Tokai earthquake or Tonankai earthquake may particularly cause extensive damage in the town.

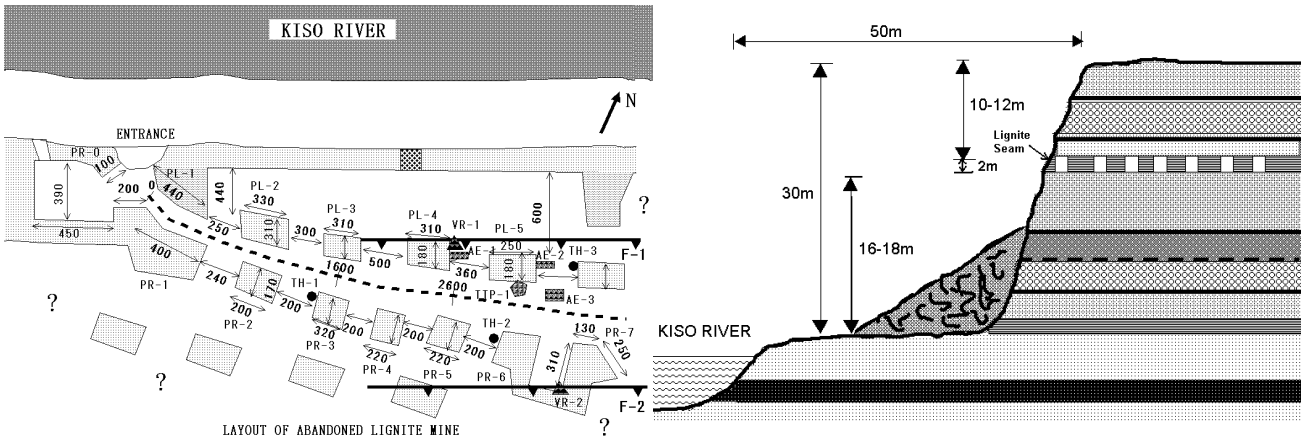
The authors have initiated a research program for investigating the stability and performance of an abandoned room and pillar lignite mine in Mitake town. A continuous measurement and monitoring program of acoustic emissions, electrical potential variations, temperature and humidity has been initiated since March 2004 besides intermittent measurements of deformation of the mine, pH values of underground water, seismic wave velocity and some index tests such as Schmidt hammer rebound value and needle penetration tests. Furthermore, certain areas within the mine are photographed in order to see the degradation process of the mine with time.

In this article, the authors describe the integrated real-time monitoring system and measured data up to now. The responses of monitoring system during a large roof collapse under gravitational condition as well as during and after two earthquakes are presented and their implications are discussed.

2. Mine Layout and Geology

The mine is situated nearby Kiso River, which was used for transporting the extracted lignite through boats. It seems that two lignite seams were exploited during mining operations, which were terminated about 40 years ago. Mining was mainly carried out using room-pillar method. Dimensions of a typical pillar were 2x2m and the seam height was about 1.8-2m. The extraction ratio varies from place to place. The section, which is monitored by the authors, can be sometimes 6-7m wide. However, a typical width of rooms is about 3-4m (Figure 1(a)).

The overburden ranges between 10-12m and it consists of relatively thick beds of sandstone, siltstone and mudstone. Although their strength is lower than lignite seam, they have few joints. The mined seam is about 16-18m above the river level and Figure 1(b) shows a typical vertical cross-section. The lignite extraction extends to a distance of about 40-50m from the entrance. Debris from mining operations or cliff collapses is found below the entrance level as shown in Figure 1(b). The slope of debris is about 35-40^{o} and it consists of relatively large pieces of rock blocks.



(a) Plan view of the instrumented area (b) Cross-section

Figure 1: Plane view of the instrumented area of the abandoned mine and a typical cross-section

3. Rock Mass Conditions

Rock layers generally dip towards SE with a gentle inclination and it has been folded. The folding axis is aligned in the direction of NE-SW. There are three lignite seams and their thickness ranges between 1-6m. The thickness of lignite seam at the mine is about 2m and it consists of intercalated mudstone and sandstone layers whose thickness ranges between 5 to 15cm. Joints are generally perpendicular or sub-perpendicular to layering and their spacing ranges between 10 to 60cm. The joint interval becomes smaller within lignite seam while it is widely spaced in mudstone and sandstone layers. Normal faults having a slight sinistral or dextral lateral sense are observed in the mine. The strike of major normal faults is aligned with the flow direction of Kiso River, which pass nearby the mine.

Rock mass classifications are done according to RMR and Q-system rock mass classification systems. RMR values correspond to BASIC RMR values, implying that no corrections are implemented. Rock masses are broadly classified as typical rock mass and fractured zone. Results are summarized in Table 1.

Table 1: Classification rates according to RMR and Q-systems

Rock mass	RMR	Q-value
Typical	37 - 53	2.08 - 2.50
Fractured	26 - 29	0.83 - 1.00

4. Instrumentations and Items of Measurements

It is also known that when rock starts to fail, the stored mechanical energy in rock tends to transform itself into different forms of energy. Experimental studies by the authors showed that rock indicates distinct variations of multi-parameters during deformation and fracturing processes. These may be used for the real-time assessment of the stability of rock structures (Aydan et al. 2001, 2003, 2005). The multi-parameter measurement system involve electric potential (EP) variations, acoustic emissions (AE), rock temperature (RT), temperature and humidity of the abandoned lignite mine. Measurements are initiated in March 2004 and the measurements of deformation of the mine, pH values of underground water, seismic wave velocity and some index tests such as Schmidt hammer rebound value and needle penetration tests are also carried intermittently. Furthermore, certain areas within the mine are photographed in order to see the degradation process of the mine.

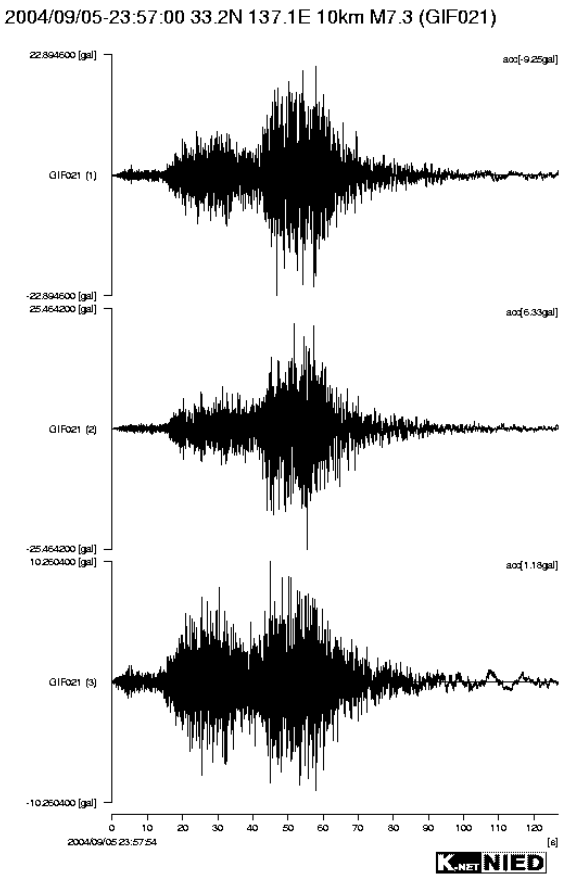
The temperature and humidity sensors are installed at certain spacing from the mine entrance as shown in Figure 1(a). Presently 4 temperature and humidity devices operate in the abandoned mine. Pillar denoted as LP5 has two temperature sensors, one of which was embedded at a depth of 10cm from the pillar surface while the other one is fixed on the pillar surface.

Initially two geo-electric potential monitoring devices are set-up as shown in Figure 1(a). These two devices are just located on normal faults. An additional geo-electric potential monitoring device was installed in Pillar denoted LP5. The electrical resistance of ground is in the order of $K\Omega$ while the impedance of the devices is in the order of $M\Omega$. Therefore, the measured electric potential variations by the devices are directly related to those of surrounding rock mass.

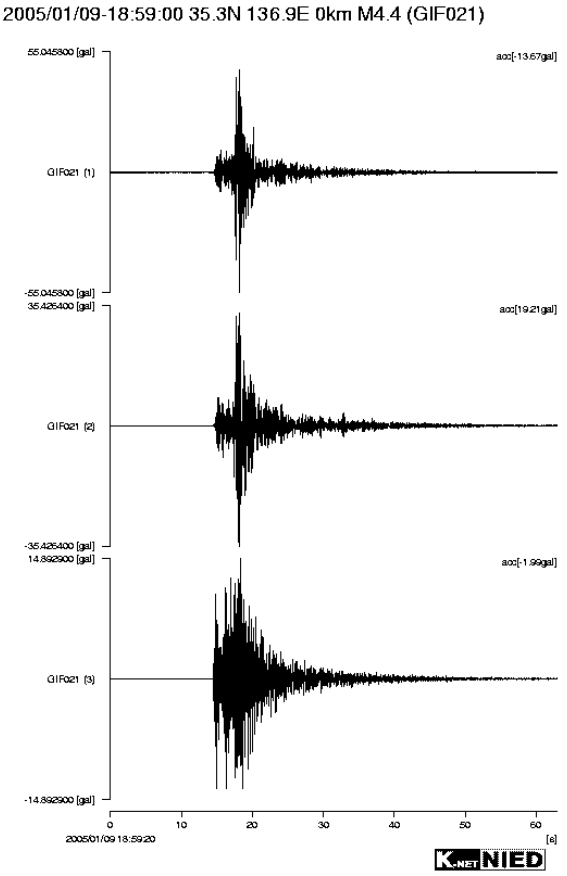
The AE system was developed by the second author and it is limited only to counting AE events (Tano et al. 2005). Pulse signals, which correspond to AE waves exceeding a threshold are discriminated through a pulsar and recorded onto a pulse counter (logger) as AE rate counts. Such limited specification of the rate counting reduces the system cost so that it is capable of using two AE systems as one set. One of the AE systems is called an active unit while the other one is called a dummy unit. The active unit is directly attached onto the rockmass while the dummy AE sensor is not in contact with the rockmass. If signals are counted on both systems simultaneously, the count of active unit is neglected from the measured data. This active-dummy counting system can improve the reliability of the AE monitoring and check the noise condition in field.

5. Earthquakes During Monitoring Period

One of the purposes of this study is to monitor the behaviour of the abandoned during earthquakes. Two earthquakes relevant to the site took place during the monitoring period. The first earthquake, which is officially named as Tokaido-oki earthquake with a magnitude of 7.3, occurred on September 5, 2004. Although the epicentre of the earthquake was 236km away from the mine, the maximum ground acceleration caused by this earthquake was more than 20gal and the shaking period was greater than 20s (Figure 2(a)). In January 9, 2005, an earthquake, named as Komaki earthquake with a magnitude of 4.7, took place 25km away the mine and the maximum ground acceleration was more than 50gal at a nearby strong-motion station (Figure 2(b)) (K-Net, NIED) These two earthquakes also provided some unique data on the response of the abandoned mine during earthquakes.



(a) Tokaido-oki earthquake



(b) Komaki earthquake

Figure 2: Acceleration records at Mino-kamo city induced by Tokaido-oki and Komaki earthquakes

6. Instability Problems During Monitoring

Besides instrumental monitoring, the visual inspection and photographing of the abandoned mine were carried out periodically. Since the data download is carried out at intervals of two-months period, the visual inspections and photographing of certain locations were done at each time of data download. The first remarkable collapse was observed when the authors visited the mine on May 14, 2004 after the visit on March 23, 2004. Since the collapse was not observed during the visit to the mine on March 23, 2004, it should have take place during the period between these two visits. The collapsed area (3m x 2m) was bounded by pillars denoted PL3, PL4, PR3 and PR4, and 25cm thick sandstone roof layer was fallen down as seen in Figure 3(a).

There was no remarkable collapse within the area of instrumentation until the earthquake on September 5, 2004. The authors visited the mine on September 17 and there were some notable roof collapses as seen in Figure 3(b). However, there was no remarkable collapse induced by the Komaki earthquake on January 9, 2005. Besides these major collapses in the mine, rock mass in the roof and pillars continues to degradate. The degradation of rock mass occurs in the form of flaking of rock pieces from the roof and pillars fall due to cyclic saturation and drying. Furthermore, some cracks in pillars continue to open up.



(a) Roof collapse between March 23 and May 17 (b) Roof Collapse due to Tokaido-oki earthquake

Figure 3: Some views of instability in the abandoned lignite mine

7. Results and Discussions

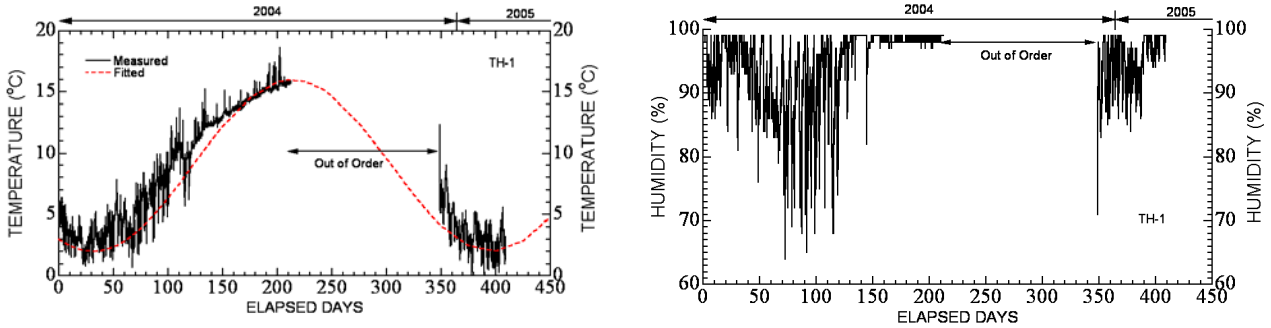
The measurements involve the environmental and stability conditions within the mine. First environmental conditions are described and then the measurements of acoustic emissions and geo-electrical potential measurements are presented in relation to some specific instability events during the period of measurements.



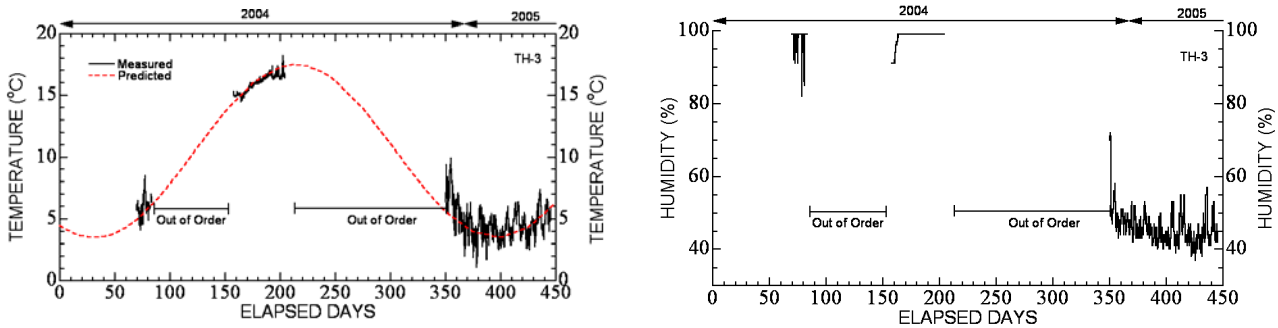
Figure 4: Some fracturing, crack opening in pillars and flaking of roof layers

7.1. Environmental Measurements

The environmental measurement items are the temperature and humidity of the mine, pH of ground water. Temperature and humidity variations in the abandoned mine during the period between March 10, 2004 and May 14, 2005 are shown in Figure 5. The overall temperature fluctuation for one year is about 12^{o} and the daily temperature variation ranges between 2-4^{o}. The humidity variation ranges between 60-100%. These results indicate that the soft sedimentary rocks would be subjected to cycles of wetting and drying. This observation clearly indicates that rocks would degradate, if they were prone to variations of water content.



(a) Temperature and humidity variations nearby the entrance of the mine



(b) Temperature and humidity variations inside the mine (40m away from the entrance)

Figure 5: Temperature and humidity variations in the mine

Figure 6 shows the temperature variations on the surface and inside of the pillar denoted LP5. The general trend of the temperatures at the pillar surface and 10cm inside the pillar surface are quite similar. However, the fluctuations of temperature at the surface are much larger than those inside the pillar. This simply implies that thermal loading in rock would be very high near the pillar surface. As a result the rock would be prone to degradation due to the daily and yearly cyclic thermal loading. Furthermore, the yearly variation of temperature is somewhat asymmetric.

The pH measurements were carried out at 4 different locations in the mine. The pH values are almost the same at measurement locations. They generally vary between 6.4 and 8.2. The pH values decreases during rainy summer season and increases during dry winter seasons.

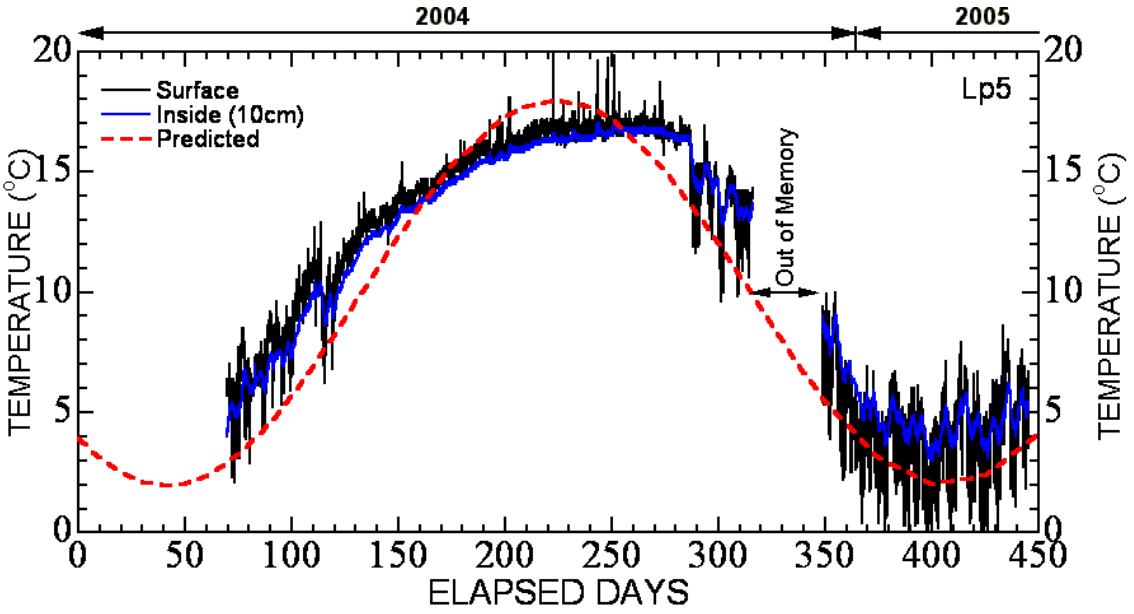


Figure 6: Variations of temperature on the surface and inside pillar denoted LP5

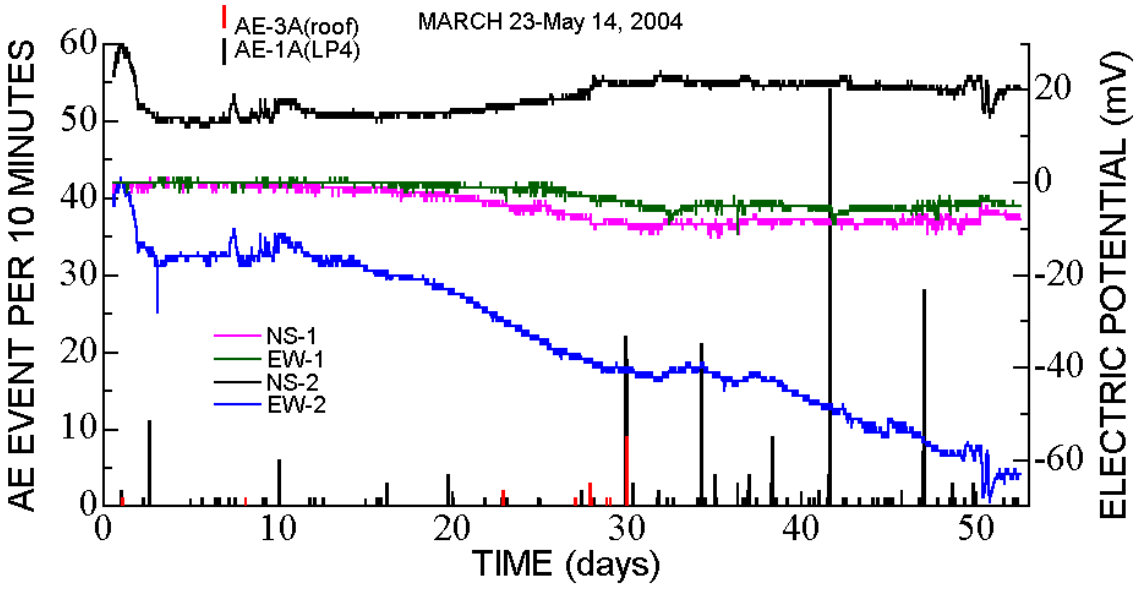


Figure 7: Variations of geo-electric potential and acoustic emission (AE) counts

7.2. Measurements Associated with Stability

Since three major events associated with mine stability took place during the period of monitoring, the monitoring results are discussed separately in the following subsections.

7.1 Period between March 23, 2004 and May 17, 2004

Geo-electric potential variations and acoustic emission (AE) counts per 10 minutes are shown in Figure 7 during March 23 and May 17. As seen from the figure there is almost one to one correspondences between geo-electric variations and acoustic emission counts. However, the fluctuations of the geo-electric potential starts much earlier than AE events as also observed in laboratory tests (Aydan et al. 2002, 2003, 2005) on samples from this mine and other sites. The collapse area is very close to the AE device set on pillar denoted PL4. More than 50 AE counts measured on May 2, 2004. However, high acoustic emission activity started to occur after April 20, 2004. Geo-electric potential variations started to occur about 10 days before the high acoustic emission activity. The geo-electric potential variation vectors indicated that the instability was located to the west of the devices. The actual event was observed about 5-10m west of the geo-electric devices.

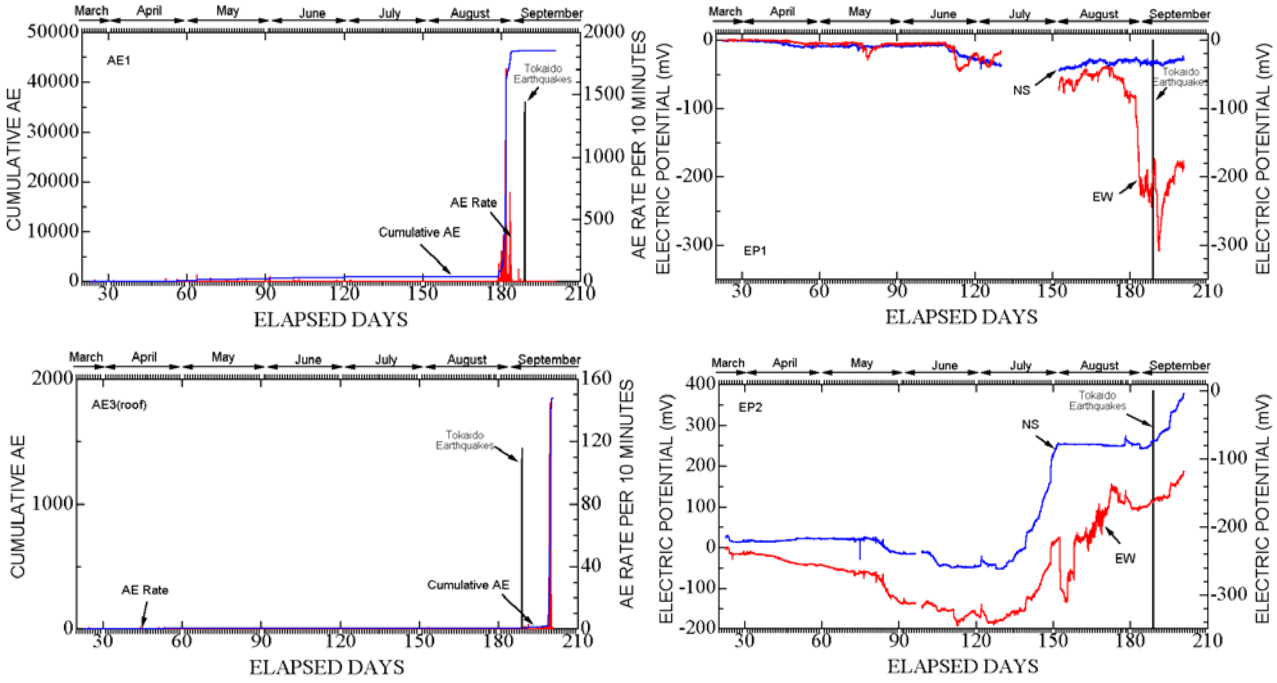


Figure 8: Variations of geo-electric potential and acoustic emission (AE) counts

7.2 Period Before and After Tokaido-oki Earthquake of September 5, 2004

Both geo-electric potential variations and AE counts per 10 minutes are shown in Figure 8. The acoustic emissions observed at the device numbered AE1 (PL4) before the earthquake. This pillar has a secondary normal fault to the principal one and a crack on the opposite side of the pillar continues to open-up, these acoustic emissions should be directly related to the fracturing of this pillar. EP1 device is also next to this pillar and very large geo-electrical variations occur during the acoustic emission activity. AE3 device is between pillars LP5 and PR5 indicated high acoustic emission activity just after the earthquake and the AE count was more than 400 on September 12. EP2 geo-electric device is about 5m to the south of AE3 and the geo-electric potential started to

increase after the earthquake. The major collapses were observed near pillar LP5 and PL7, which are about 10m to the east of the AE device. The geo-electric potential vector of EP2 indicated that the instability locations were directed to NE. As for EP2 device the location was to the east. Particularly it is of great interest that the geo-electric potential vectors can be used to locate the spot of instability. Furthermore, it seems that geo-electric potential variations are also influenced by the crustal geo-electric potential variations associated with earthquakes. Since the Tokaido-oki earthquake was to SW of the site, the variations of geo-electric potentials point out the location of the source of geo-electric potential signals. It should be also noted that AE counts are generally associated with events whose sources are within the vicinity of 10m. Therefore, a dense network of the AE devices could be useful to locate the exact location of the instability spots. The combinations of these measurements together with geo-electric potential measurements can distinguish near-field and far-field events.

7.3 Period Before and After Komaki Earthquake of January 9, 2005

Geo-electric potential variations and AE counts per 10 minutes are shown in Figure 9 in association with the 2005 Komaki earthquake. Some acoustic emissions observed at the device numbered AE1 (PL4) before and after the earthquake. As said previously, this pillar has a secondary normal fault to the principal one and a crack on the opposite side of the pillar (its picture is shown in Figure 4) continues to open-up, these acoustic emissions should be directly related to the fracturing of this pillar. EP1 device is also next to this pillar and very large geo-electrical variations occur during the acoustic emission activity. Furthermore the geo-electrical potential vector indicates that the events have been occurring to the SW of the device. A new acoustic emission numbered AE5 was installed in December 2004 between pillars PL4 and LP5. The acoustic emission events measured by AE1 and AE5 occur almost simultaneously. During these events, the geo-electric potential measuring device EP1, which is close to AE1 and AE5 have fluctuations in the measured responses indicated. Both EP1 and EP2 geo-electric potential measuring devices indicate that some instability problems to the South or SW of the their location may be taking place. Since the observations are limited to a certain area due to concern of roof collapses and pillar failures, we could not confirm the implications of these geo-electric potential measurements by visual inspections. However, the effects of the 2005 Komaki earthquake could not be observed in view of the measurements shown in Figure 9.

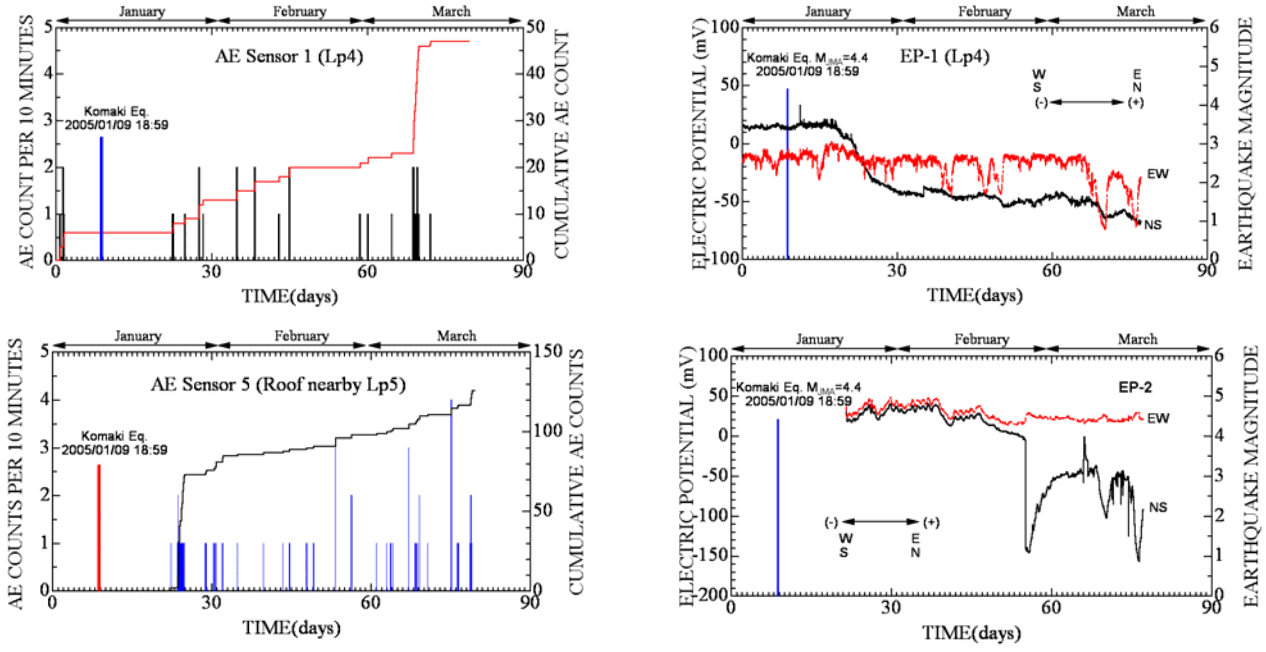


Figure 9: Variations of geo-electric potential and acoustic emission (AE) counts

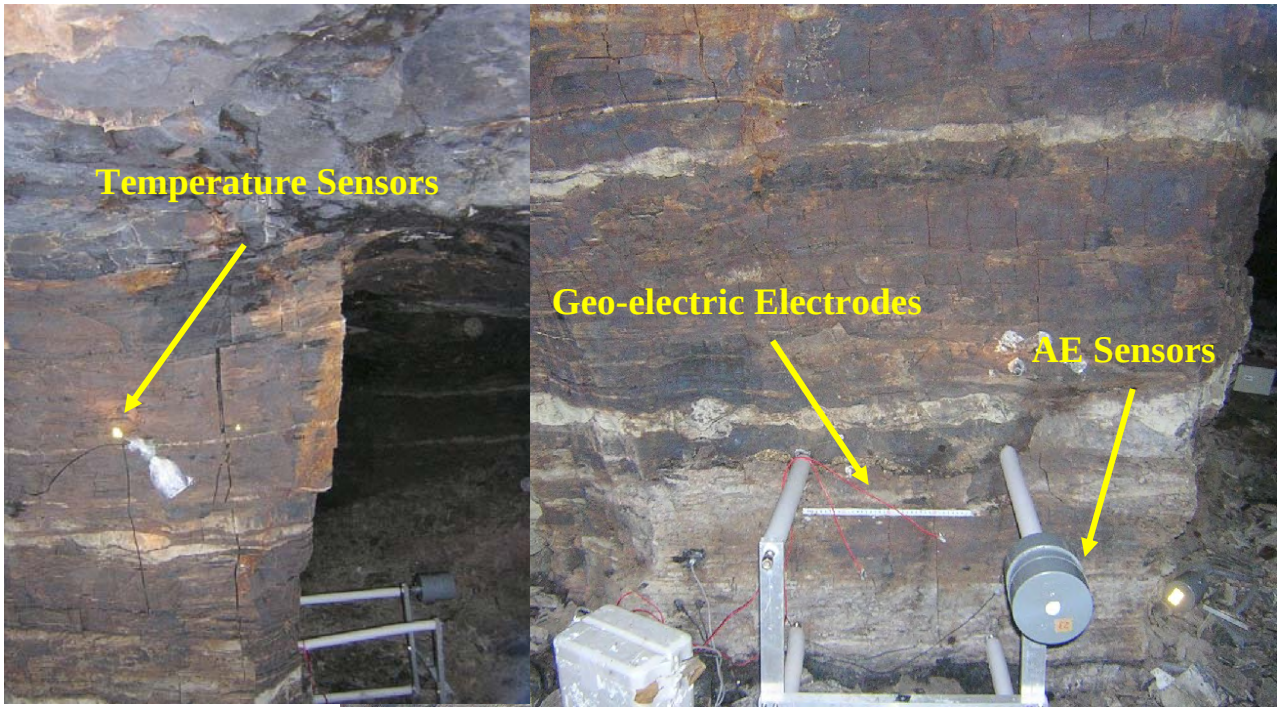


Figure 10: Instrumented pillar LP5.

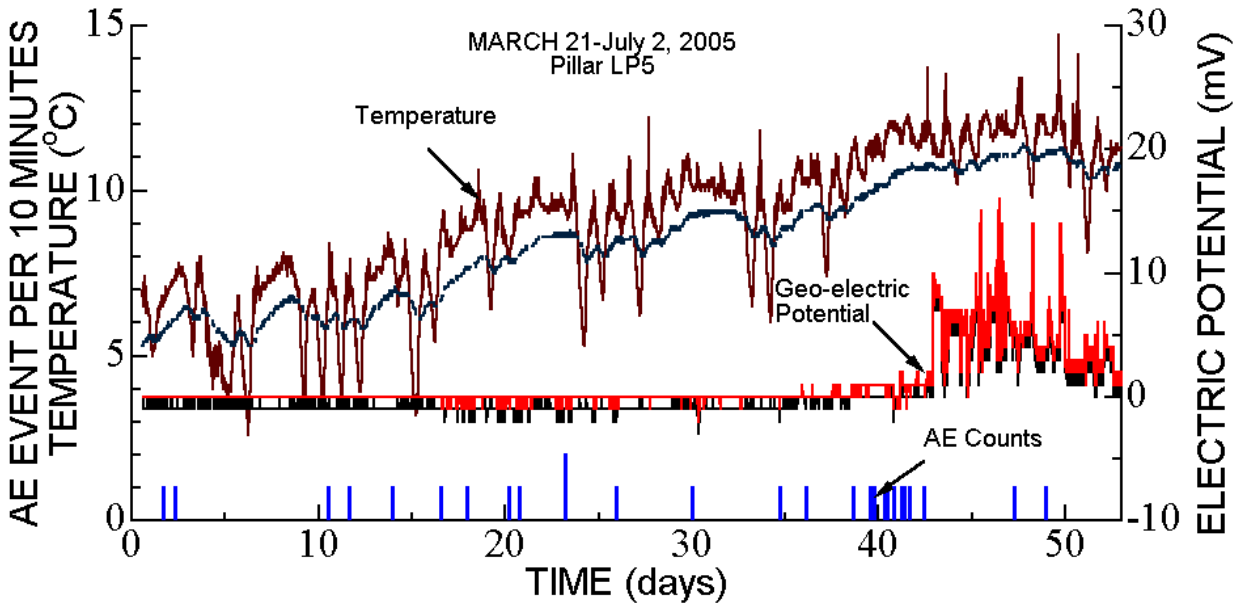


Figure 11: Multi-parameter response of Pillar LP5 during March 21 and July 02, 2005

7.4 Multi-parameter Observations on Pillar LP5 During March 21, July 02, 2005

Pillars resemble to the samples under uniaxial compression tests in laboratory. A geo-electric potential measuring device was recently installed in the pillar denoted LP5 in addition to temperature and acoustic emission measurements. Compared with the initial state of this pillar, vertical cracks in this pillar were open up further. The geo-electrical potentials were measured in vertical (UD) and horizontal (NS) directions. Figure 10 shows the instrumented pillar LP5. Figure

11 shows the variations of geo-electric potential, temperature and AE events during March 21 and July 02, 2005. As it is noted from the figure, some acoustic emission events have been taking place. This implies that the crack opening and propagation has been occurring. Particularly the AE events have been increasing since the beginning of June, which roughly corresponds to rainy Munson season in Japan. Simultaneously, geo-electric potential variations become larger. This may indicate that overall electric resistivity of the pillar decreasing so that the geo-electrical potentials associated with crack development become more amplified. The temperature variations seem not to be associated with the AE and geo-electric potential variations.

8. Conclusions

The authors described a real-time monitoring system and its application to the investigation of the stability and performance of an abandoned room and pillar lignite mine in Mitake town. During the monitoring period, two earthquakes relevant to the site occurred and their effects on the abandoned mine were observed both instrumentally and visually. Both geo-electrical potential and acoustic emission (AE) measurements are indicators of forecoming instability problems related to seismic loading as well as degradation and creep of surrounding rocks and variation of surcharge loadings. The main conclusions from this study may be summarized as follows:

- Temperature and humidity measurements indicate that surrounding rock is subjected to daily and yearly cycles of wetting and drying and thermal loading. These undoubtedly cause further degradation of surrounding rock and it can be counted as one of the causes of instability in long term.
- AE counts are generally associated with events whose sources are within the vicinity of 10m. Therefore, a dense network of the AE devices could be useful to locate the exact location of the instability spots.
- The geo-electric potential measurements indicate that it is possible to infer the for-coming instability problems and their locations and timing. However, it seems that geo-electric potential variations are also influenced by the crustal geo-electric potential variations associated with earthquakes. The combinations of geo-electric potential measurements together with Acoustic Emission (AE) measurements together can distinguish near-field and far-field events.

Acknowledgements

The authors sincerely thank the graduate students of Aydan Laboratory of Department of Marine Civil Engineering of Tokai University for their help during the installation and gathering data. We also thank Emeritus Prof. Dr. Toshikazu KAWAMOTO of Nagoya University for his invaluable suggestions and encouragement for the development and application of this multi-parameter system for real-time stability and environmental monitoring of the abandoned mine as well as pointing out the importance of instability problems associated with abandoned lignite mines.

9. References

Aydan, Ö., Minato, T. and Fukue, M. (2001). *An experimental study on the electrical potential of geomaterials during deformation and its implications in Geomechanics*. 38th US Rock Mech. Symp., Washington, Vol.2, 1199-1206, 2001.

Aydan, Ö., Ito, T., Akagi, T., Watanabe, H., Tano, H. (2002). *An experimental study on the electrical potential of geomaterials during fracturing and sliding*. Korea-Japan Joint Symposium on Rock Engineering, Seoul, Korea, July, 211-218.

Aydan, Ö., Tokashiki, N., Ito, T., Akagi, T., Ulusay, R., Bilgin, H.A. (2003). *An experimental study on the electrical potential of non-piezoelectric geomaterials during fracturing and sliding*. 9th ISRM Congress, South Africa, 73-78.

Aydan, Ö., Daido, M., Tano, H., Tokashiki, N., Ohkubo, K. (2005). *A real-time multi-parameter monitoring system for assessing the stability of tunnels during excavation*. ITA Conference, Istanbul,, 1253-1259.

Aydan, Ö., Sakamoto, A., Yamada, N., Sugiura, K., Kawamoto, T. (2005). *The characteristics of soft rocks and their effect on the long term stability of an abandoned room and pillar lignite mine*. Internation Symposium on Post Mining , PostMining 2005, Nancy.

K-Net NIED (2004,2005) : Strong motion records of 2004 Tokaido-oki abd 2005 Komaki earthquakes. http://www.bosai.ac.jp/

Tano, H., Abe, T., and Aydan, Ö. (2005). *The development of an in-situ AE monitoring system and its application to rock engineering with particular emphasis on tunneling*. ITA Conference, Istanbul, 1245-1252.

THE CHARACTERISTICS OF SOFT ROCKS AND THEIR EFFECT ON THE LONG TERM STABILITY OF ABANDONED ROOM AND PILLAR LIGNITE MINES

AYDAN, Ömer[1], SAKAMOTO, Akio[2], YAMADA, Noritoshi[2], SUGIURA, Kenrou[2], KAWAMOTO, Toshikazu[3]

[1]TOKAI UNIVERSITY, Department of Marine Civil Engineering, Shizuoka, Japan. ; aydan@scc.u-tokai.ac.jp

[2] TOBISHIMA CONSTRUCTION COMPANY, Nagoya Branch, Japan.; Akio_Sakamoto@tobishima.co.jp; Noritoshi_Yamada@tobishima.co.jp; ,kenrou_sugiura@tobishima.co.jp

[3]NAGOYA UNIVERSITY, Emeritus Professor, Nagoya, Japan.; choman@poem.ocn.ne.jp

ABSTRACT: It is well known that some caving, collapses and subsidence take place from time to time in the areas where abandoned room & pillar type mines exist. The authors have been involved with the stability of abandoned mines beneath urbanized residential areas in Tokai region and there is a great concern about the stability of these abandoned mines during large earthquakes as well as in long term. The 2003 Miyagi Hokubu earthquake caused great damage to abandoned mines and resulted in many collapses. The authors present the experimental results on the characteristics of soft rocks from abandoned lignite mines in Tokai Region as well as the results of some analyses of their effects on the long-term stability of abandoned lignite mines.

KEYWORDS: Abandoned mine, Earthquake, Soft rocks, Degradation, Creep

RESUME : Il est bien connu que l'effondrement et l'affaissement surviennent de temps en temps à l'aplomb d'anciennes mines abandonnées. Les auteurs ont été impliqués par la stabilité de mines abandonnées se trouvant dans des secteurs résidentiels de la région de Tokaï. L'évaluation de la stabilité de ces mines abandonnées durant de grands tremblements de terre, aussi bien que dans le long terme, est une préoccupation majeur. Les mines abandonnées se sont endommagées suite au En 2003, le tremblement de terre en Miyagi Hokubu a endommagé de nombreuses mines abandonnées et induit de nombreux effondrements. Les auteurs présentent les résultats expérimentaux sur les caractéristiques des roches déformables en provenance des mines abandonnées de lignite de la région de Tokaï, aussi bien que les résultats de quelques analyses de leurs effets sur la stabilité à long terme de ces mines.

MOTS-CLEFS : Mine abandonnée, Tremblement de terre, Roche déformable, Dégradation, Fluage

1. Introduction

Some caving, collapses and subsidence take place from time to time in the areas where abandoned room & pillar type mines exist (Figure 1). If the area is urbanized, it presents a great concern to the municipalities as well as people living in those areas. Furthermore, if the seismicity of areas is high, the risk of collapses due to earthquakes may amplify those concerns. The 2003 Miyagi Hokubu earthquakes clearly indicated that such areas may experience roof collapses, subsidence as well as the ejection of underground waters from the mines (Aydan and Kawamoto, 2004) (Figure 2). The authors have been involved with the stability problems of some abandoned mines in Tokai Region of Japan and they have been investigating their performance and responses in long term as well as during earthquakes. Samples were obtained from some abandoned mines in Tokai region and various tests such as Brazilian tests, uniaxial compression tests, creep tests as well as degradation tests as a function of water content variation were carried out. During some compression tests,

multi-parameter measurements such as AE, electrical potential, resistivity, magnetic field in addition to conventional load and deformation measurements, which may be of great value for the assessments of in-situ monitoring results of such mines, were also performed. On the bases of these experiments, some stability analyses for the assessment of the long-term stability of abandoned room and pillar mines as well as during earthquakes have been carried out and their implications are discussed. The authors present the experimental results on the characteristics of soft rocks from abandoned lignite mines in Tokai Region as well as the results of analytical and numerical analyses of their effects on the long-term stability of abandoned lignite mines and underground quarries.



(a) Collapse of Oya Underground Quarry



(b) Collapse of abandoned lignite mine in Mitake

Figure 1: The collapse of underground quarry and an abandoned lignite mine



(a) Caving



(b) Caving and sandy water discharge

Figure 2: Caving and sandy water discharges in Yamoto town caused by 2003 Miyagi earthquake

2. Soft Rocks of Abandoned Lignite Mines in Tokai Region

The geological age of soft rocks associated with lignite deposits differ from location to location. Figure 3 shows the distribution of lignite deposits in Tokai region. While the age of lignite field within Nakamura unit of Mizunami formation at Mitake belongs to the Miocene era, the lignite field belonging to Yadagawa unit of Seto formation at Nagakute does to Pliocene. Therefore, rocks of Mitake are older than those at Nagakute. As a result, their physical and mechanical

characteristics are expected to be different from each other. There are four lignite seams in Mitake and the second and the third seams were extracted. The thickness of the third seam is 1-3m thick. Although the number of lignite seams at Nagakute is four, the seams are much thinner (less than 1m). Sedimentary rocks at Mitake are broadly classified as lignite, sandstone, siltstone and mudstone with conglomerate layers at the base of the formation above the pre-Tertiary rocks. Although sedimentary rocks of Nagakute can be geologically classified in the same manner, the cementation is poor and sometimes non-cemented sand layers are found below lignite seams. Rock samples were obtained through boring at Mitake town. On the other hand, samples from Nagakute site were prepared from blocks extracted from a recent excavation in association with a cavity-filling site.

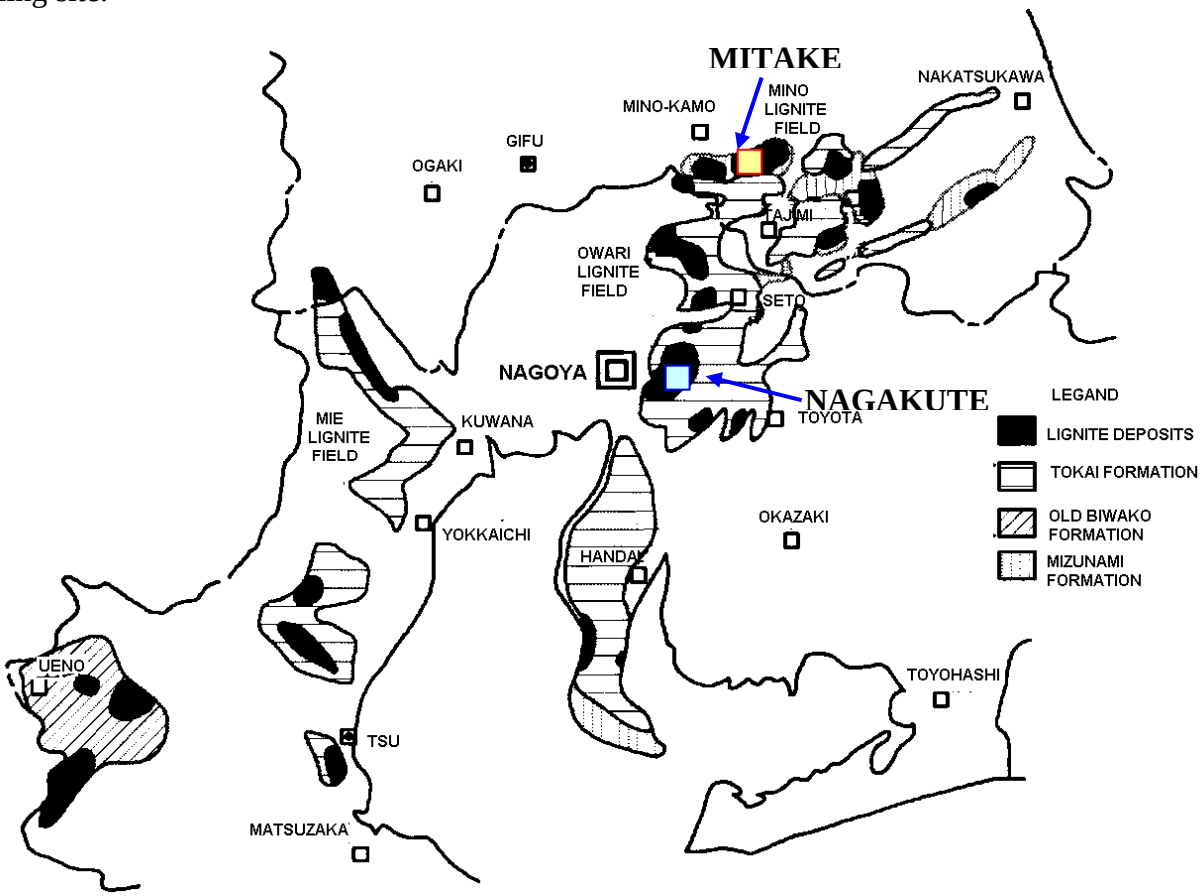


Figure 3: Lignite deposits in Tokai region and locations of sites

3. Physical and Mechanical Tests

Physical tests involve unit weight, water content, porosity, needle penetration index, elastic wave velocity while mechanical tests are uniaxial compression and Brazilian tests. In addition some creep and relaxation tests are also performed. Table 1 and Table 2 give physical and mechanical properties of rock samples at Nagakute and Mitake, respectively. Table 3 gives the parameters of yield functions for Mitake rocks obtained from uniaxial compression and Brazilian tests. Needle penetration index tests are quite useful for inferring the mechanical properties of soft rocks. Figure 4 and Figure 5 show the results for Mitake and Nagakute soft rocks together with those other soft rocks.

Table 1: Physical and mechanical properties of soft rocks from Nagakute site

Rock Type	Unit Weight (kN/m^3)	Water Content (%)	Compressive Strength (MPa)	Elastic Modulus (MPa)	NPI (N/mm)
Lignite	7.1-18.2	30.2-35.3	2.3-3.2	86.8-167.9	16-28
Mudstone	15.6-16.5	7.3-17.1	0.3-2.2	15.2-77.8	2-22

Table 2: Physical and mechanical properties of soft rocks from Mitake site

Rock Type	Unit Weight (kN/m^3)	Water Content (%)	Compressive Strength (MPa)	Elastic Modulus (MPa)	Vp (km/s)	NPI (N/mm)
Lignite	10.6-14.1	12.6-27.2	4.0-6.0	1800-1860	1.6-2.3	22-33
Sandstone	16.8-19.2	15.4-19.8	2.3-7.0	328-	1.6-2.7	20-71(dry)
Mudstone	15.6-16.5	9.5-13.3	1.0-1.5	38-150	1.3-1.5	2-22

Table 2: Parameters of yield functions for soft rocks from Mitake site

Rock Type	Mohr-Coulomb				Aydan					
	Lower		Upper		Lower			Upper		
	c MPa	φ (°)	c MPa	φ (°)	A (MPa)	b	σ_t (MPa)	A (MPa)	b	σ_t (MPa)
Lignite	0.67	52.4	1.05	52.4	3.0	0.66	0.430	4.0	0.50	0.670
Sandstone	0.40	52.4	0.70	63.4	2.5	0.66	0.250	5.0	0.50	0.351
Mudstone	0.35	16.7	0.40	28.8	1.1	0.58	0.518	1.7	0.58	0.518

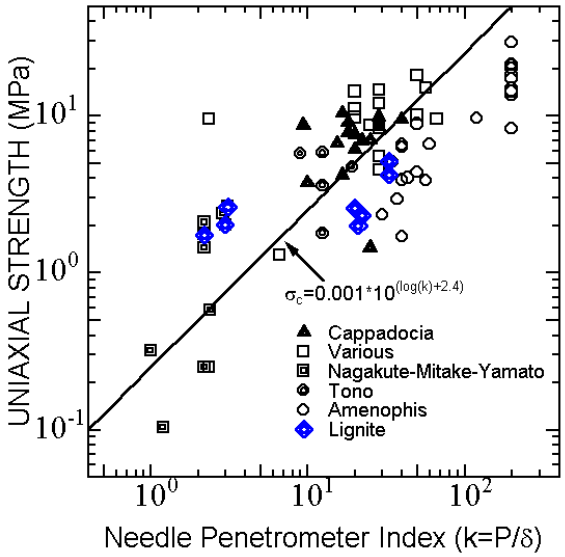


Figure 4. NPI versus compressive strength

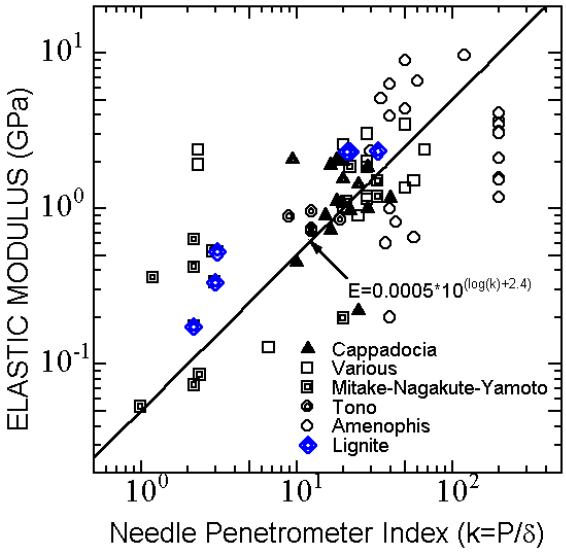


Figure 5. NPI versus elastic modulus

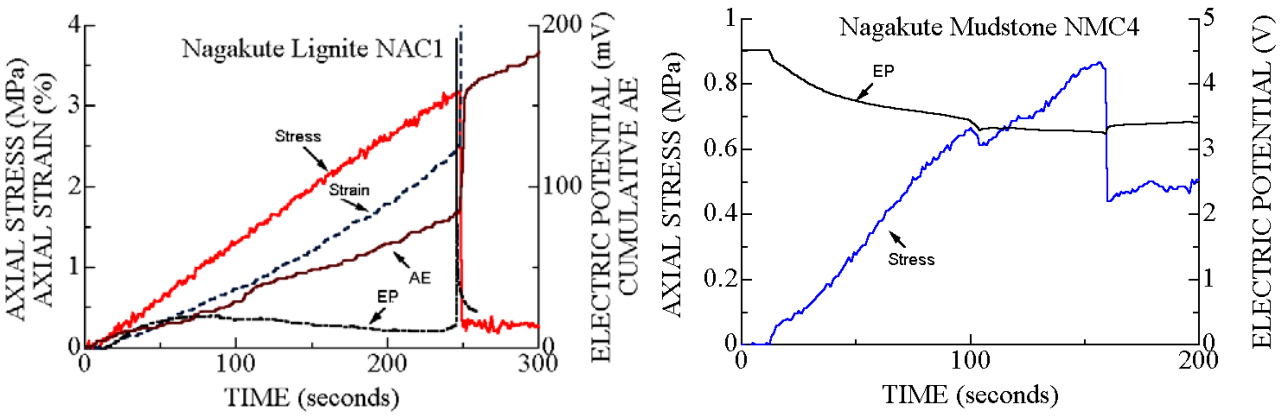


Figure 6: Multi-parameter response of Nagakute rocks during uniaxial compression tests

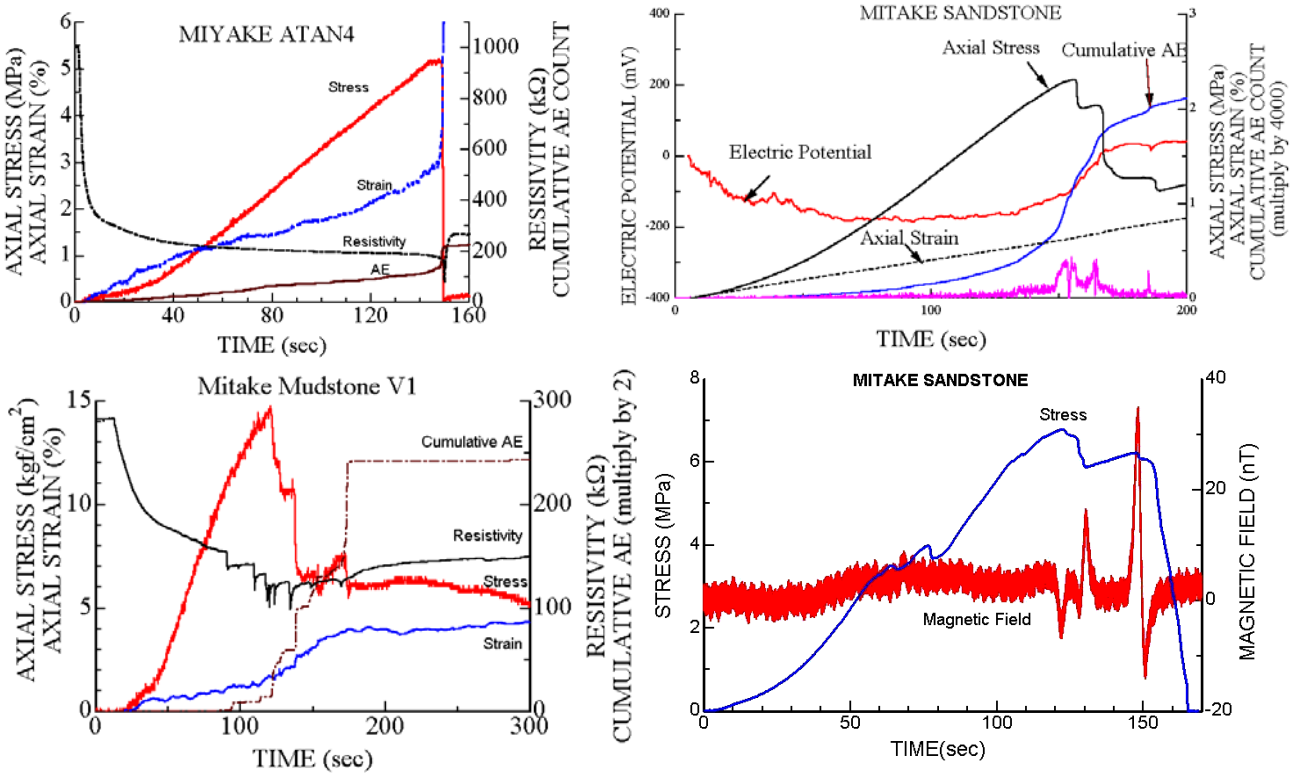


Figure 7: Multi-parameter response of Mitake rocks during uniaxial compression tests

The mechanical properties of soft sedimentary rocks are influenced by the water content. The compressive strength and elastic modulus of soft rocks generally decrease with the increase of water content. During some experiments, electric potential, electrical resistivity, magnetic force, acoustic emission (AE) were measured besides conventional load and displacement. The main purpose of such measurements was to establish some experimental bases for the real-time monitoring of multi-parameters for the stability assessment of an abandoned mine in Mitake (Aydan et al. 2005). Figure 6 and Figure 7 show some experimental multi-parameter responses measured during experiments on Nagakute and Mitake samples.

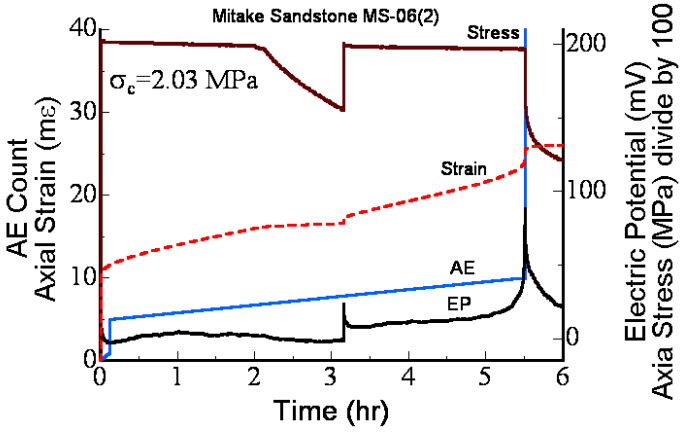


Figure 8: Creep test result on sample MS-06

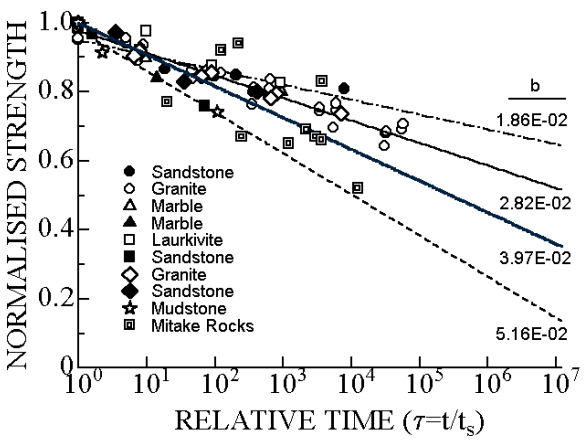


Figure 9: Comparison of normalized long-term strength of Mitake soft rocks with other rocks

4. Long-term Properties of Mitake Soft Rocks

One of the main parameters influencing the long-term stability of abandoned mines is the creep strength characteristic of rocks. A series of creep tests on sandstone samples were carried out. In these tests, variations of electric potential and acoustic emissions were also measured in addition to applied axial stress and induced axial strain. Figure 8 shows the responses measured in one of the creep tests. Aydan and Nawrocki (1996) proposed the following function for the long-term strength of rocks normalized by their short-term strength.

$$\frac{\sigma_{cl}}{\sigma_{cs}} = 1 - b \ln\left(\frac{t}{t_s}\right)$$

The coefficient *b* in the above functions is determined to be 0.0397 from the creep experiments shown in Figure 9.

5. Degradation of Soft Rocks by Cycles of Wetting & Drying

Some of sedimentary rocks are prone to degradation due to cycles of wetting and drying. This mainly occurs due to the suction of water by some minerals such as clay minerals. As a result, rock disintegrates after each cycle of wetting and drying. Soft rocks in Mitake and Nagakute exhibit such behavior as seen in Figure 10. The same phenomenon observed in abandoned mines. The degree of degradation differs depending upon the environmental conditions within the mines. However, the degree of degradation rocks close to the entrance of the mines is much higher than those far away from the entrance. Figure 11 shows some examples of degradation as a result of cycles of wetting and drying.



Figure 10: Some examples of disintegration of soft rocks of Mitake.

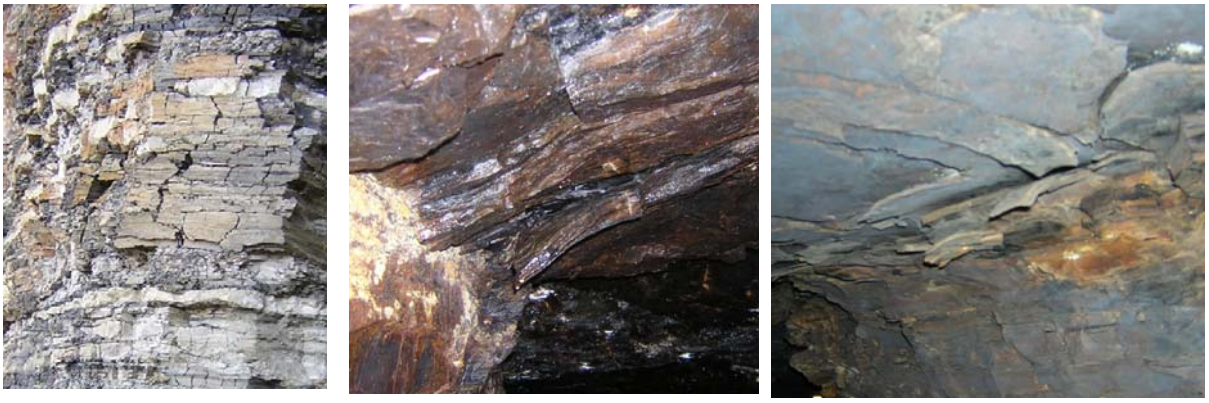


Figure 11: Some examples of disintegration in the abandoned mine.

A series of tests were carried out to understand the mechanism of degradation during wetting and drying cycles. The tests involve the measurement of the weight, shrinkage, electric potential or electric resistivity and acoustic emissions of the sample. The weight is measured to obtain the water content with time, and acoustic emissions and electrical potential are measured to observe if cracking is taking place during the drying process. The electrical resistivity is measured to correlate the water content to the electrical resistivity, which could be utilized to infer the water content in-situ as a non-destructive testing method. Furthermore, the temperature and humidity of the sample environment are measured simultaneously. Figure 12 shows a view of a typical experimental set-up. We report the experimental results for a sandstone sample only as shown in Figure 13. On the same sample, electrical potential and electrical resistivity tests were carried out. As noted from the figure, some cracking starts to occur after about 3 hours and the cracking activity reaches its maximum value after about 10-12 hours. This roughly corresponds the peak of drying rate. The samples shrinks and it simply implies that when the minerals losses the water, they are volumetrically shrinking. As a result of this phenomenon, cracking would be induced in samples if their tensile strength were insufficient. It is also interesting to note that some samples were fractured or lost their cohesion during the saturation process (Figure 14(a)).

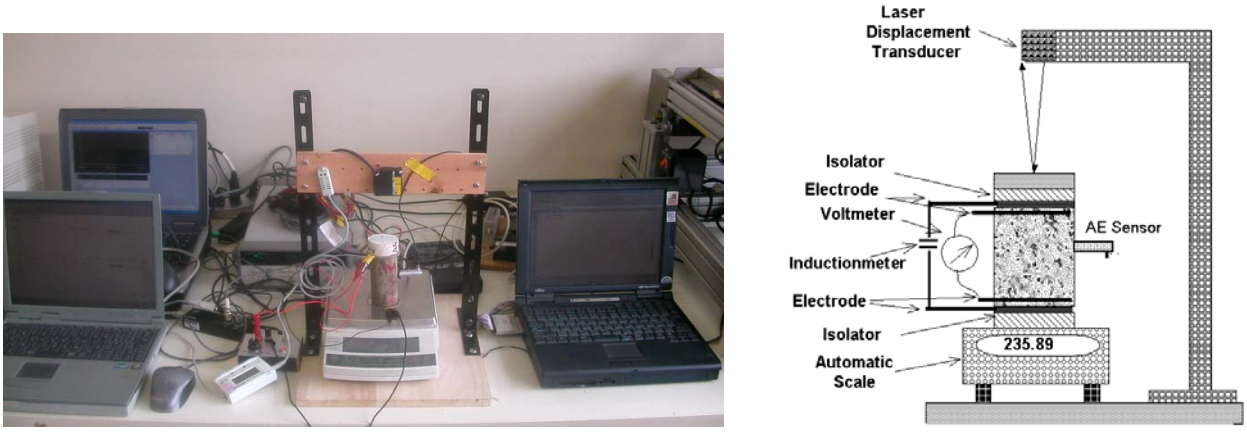


Figure 12: A view of the degradation test and its illustration

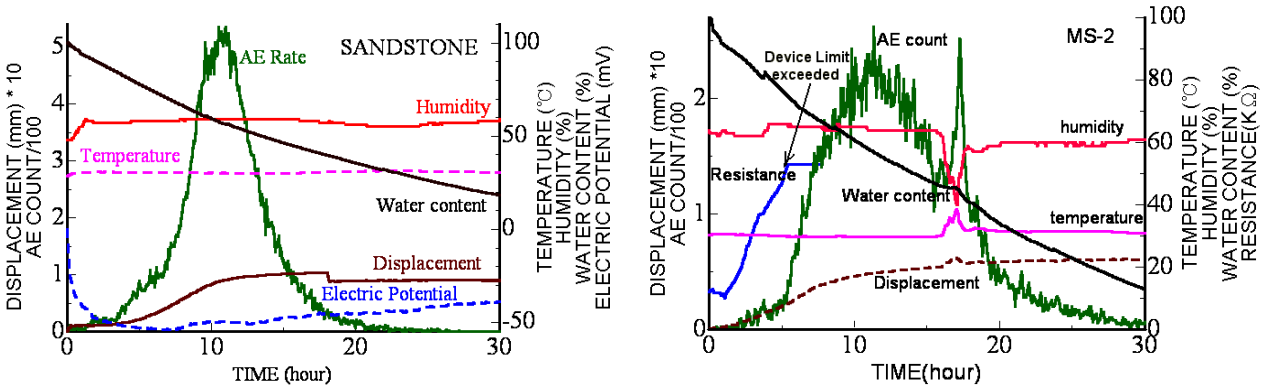


Figure 13: Degradation tests on Mitake sandstone sample numbered MS-02



(a) Cracking upon submerging in water (b) Drying induced cracking

Figure 14: Cracking of sandstone samples induced by submerging in water or drying

6. Stability Assessment

In this section, we first consider the long-term stability of the abandoned mine using the rock classification methods. Then the long-term stability of the abandoned mines is assessed by considering the effects of degradation and creep loading on the stability of abandoned mines where the excavation is carried out by room and pillar technique. For the simplicity, we will use the tributary area approach for pillar stability and arching approach for roof layers in developing our theoretical equations.

6.1. Assessment by Rock Classification Methods

Although there are many rock classifications, RMR and Q-System were chosen for the assessment of the stability of the abandoned mine. The ratings of rock mass of the abandoned mine have been already presented in the other paper by the authors (Aydan et al. 2005) and they are also given in Table 3. The span of the opening ranges between 2 and 6m. For the rates given in Table 3 and the range of opening span, the results are plotted in the stability charts proposed by Bieniawski (1985) and Barton (1995) as shown in Figure 15. As noted from the figure, RMR system predicts that the openings should had been already collapsed totally many decades ago. Although roof collapses were observed within the abandoned mine, the abandoned mine is still stable in broad terms. It seems that the RMR system is somewhat over-conservative for the stand-up time of the underground cavities. On the other hand, the estimations by the Q-System seem to be more reasonable as the support requirement would be necessary. However, the required support system would be light.

Table 3: Classification rates according to RMR and Q-systems

Rock mass	RMR	Q-value
Typical	37 - 53	2.08 - 2.50
Fractured	26 - 29	0.83 - 1.00

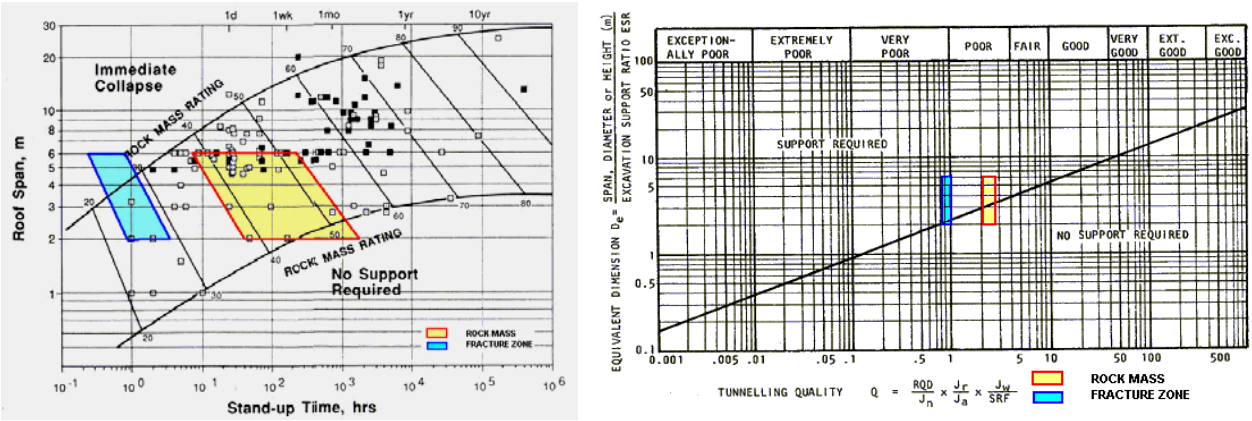


Figure 15: Comparison of observed and suggested stand-up time or stable opening span.

6.2. Stability Assessment of Pillars

The tributary area is simple yet effective method to assess the overall stability of the pillars. Let us assume that the geometry of a representative pillar and its overburden load can be modeled as shown in Figure 16. From the assumed geometry, it is easy to show that the average pillar stress is

$$\sigma_p = \rho g H \frac{A_t}{A_p} \text{ or } \sigma_p = \sigma_V \frac{A_t}{A_p} \qquad (1)$$

Where ρ : is unit weight of rock

g : is gravitational acceleration

H: Overburden

A_t: Area supported by pillar

A_p: Area of pillar

$\sigma_V = \rho g H$

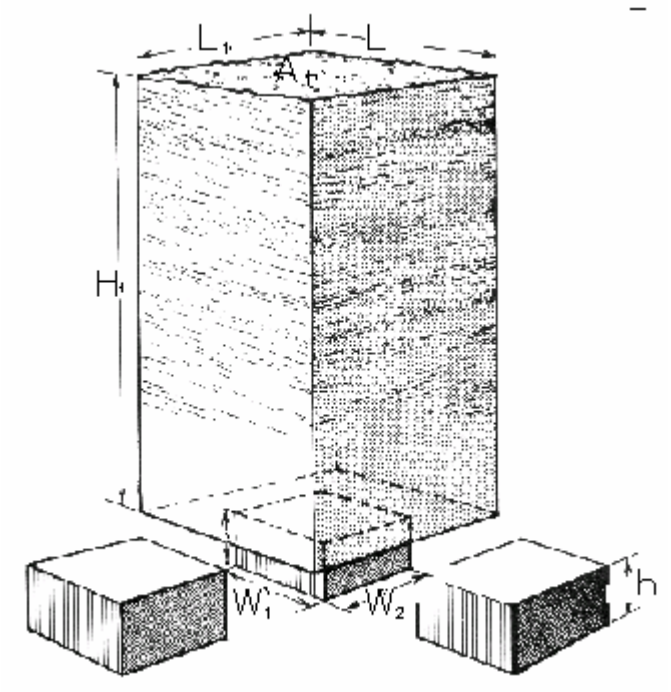


Figure 16: Model for pillar stability analyses

(a) Effect of Degradation

The effect of degradation of rock by the cycles of wetting and drying cause the flaking of rock near the surface and it falls under the effect of gravity. This process repeats itself endlessly, which subsequently cause the reduction of the area of the pillar. As a result, the normalized stress on the pillar may be given as

$$\frac{\sigma_p}{\sigma_{p0}} = \frac{1}{1 - \dfrac{\Delta L \times (L_{10} + L_{20})}{A_{p0}} + \dfrac{\Delta L^{\,2}}{A_{p0}}} \qquad (2)$$

The degradation process may be approximated using some functional forms. For the simplicity, we assume that the degradation is a linear function of time and it is given in the following form:

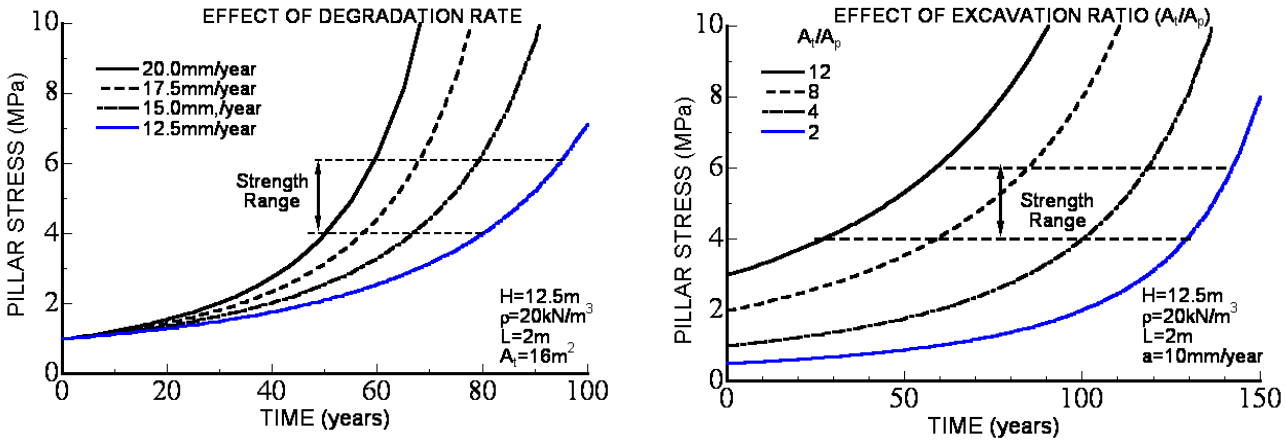
$$\Delta L = a \cdot t \qquad (3)$$

Where constant *a* is called as degradation rate. Since the uniaxial strength of the lignite seam ranges between 4 to 6 MPa, the computed results for long-term stability of the abandoned mine for varying the degradation rate and tributary area ratio are shown in Figure 17. As expected, the computed results imply that if the degradation rate is higher or tributary area ratio is larger, the failure time of the pillar would become shorter.

(b) Effect of Creep Loading

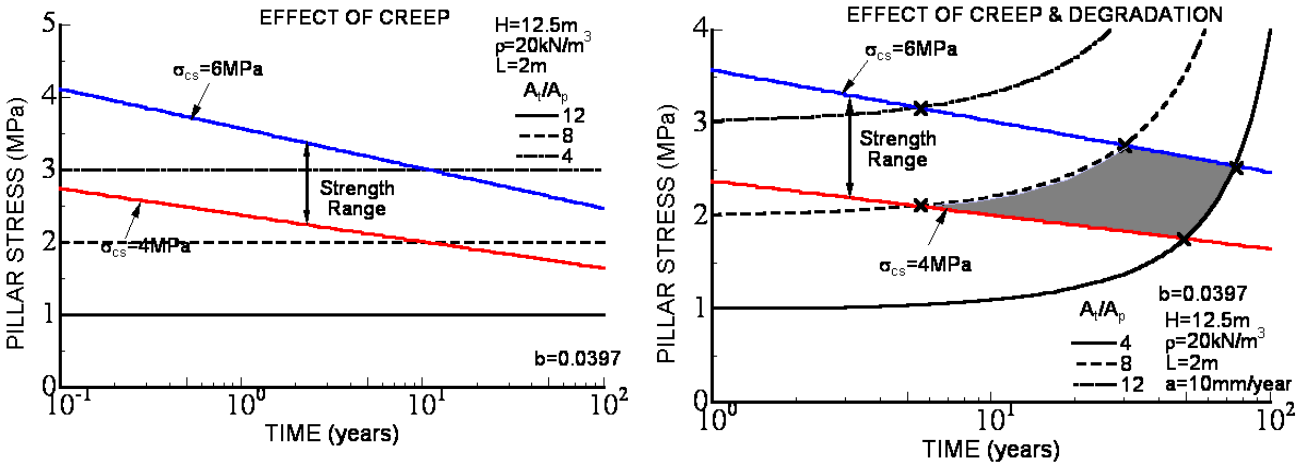
As explained in Section 4, the long-term strength of rock under creep loading would be mobilized. The long-term strength of rock depends upon the level of the sustained loading with respect to its strength in short-term tests. Figure 18(a) shows the computed results for the failure time of pillars with the consideration of long-term strength of pillars. From the results it is inferred that the failure time would be shorter if the tributary area (excavation ratio) increases. This type of situations may be observed when the abandoned mines are fully submerged. However, it should be noted that the long-term strength properties for saturated conditions should be used under such situations. Figure 18(b) shows both effects of long-term strength and degradation rate. Compared with the failure time

of pillar under the condition of creep loading only, the failure time of pillars become shorter. The shaded range probably corresponds to the actual situation of the abandoned mine that the authors have been investigating (Aydan et al. 2005). For the lower bound strength range, the stability problems of pillars would occur after 5.6 to 50 years while it would be after 30 to 75 years for the upper bound strength range.



(a) Effect of degradation rate (b) Effect of excavation ratio (tributary area)

Figure 17: Effects of degradation and tributary area on failure time of pillars



(a) Effect of creep loading only (b) Effect of creep loading and degradation

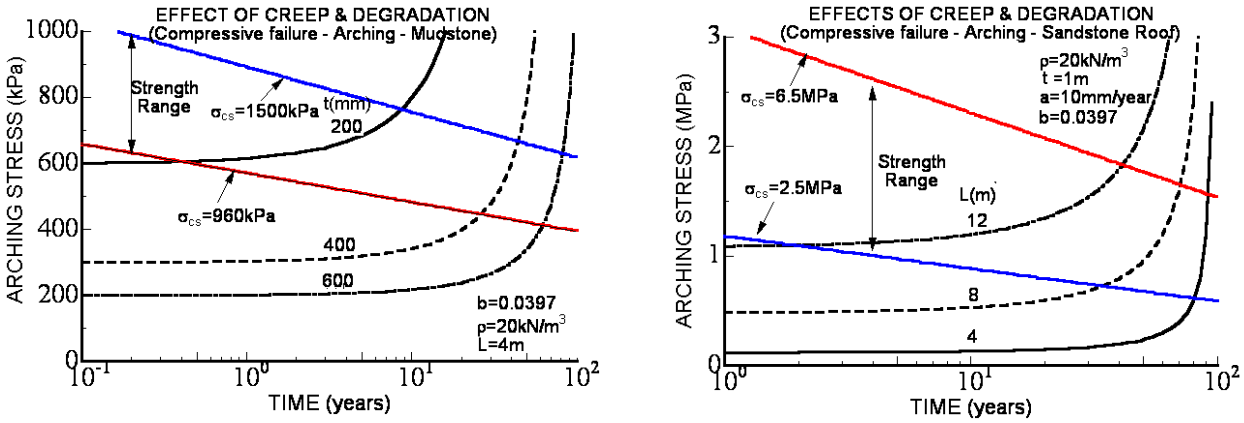
Figure 18: Effects of degradation and creep loading on failure time of pillars

6.3. Stability Assessment of Roof

The stability of roof layers can be checked against various forms of failure. Although roof layers may crack due to bending stresses, their ultimate failure would be governed by arching phenomenon (although shear failure may be conceived, it is not generally likely to occur) within the roof layers. If the fiber stress exceeds the compressive strength at the crest of arch within roof layer, the roof layer will collapse. Under such a condition, the following relation can be derived (i.e. Aydan, 1989):

$$\sigma_c = \frac{3}{8}\rho g L\left(\frac{L}{t}\right) \tag{4}$$

Where L and t are the span and thickness of roof layer, respectively. The effect of degradation can be imposed on the thickness of roof layer while the effect of long-term strength can be imposed on the compressive strength of roof layers. Figure 19 shows some computational results for the effect of creep loading and degradation for mudstone roof and sandstone roof.



(a) Mudstone roof (b) Sandstone roof

Figure 19: Effects of degradation and creep loading on failure time of roof

7. Stability Assessment During Earthquakes

Many collapses observed in the abandoned mine area of Yamoto town due to the 2003 Miyagi-Hokubu earthquake (Aydan and Kawamoto, 2004). However, there is no available approach to consider the effect of earthquakes on the stability of abandoned room and pillar mines. The appropriate consideration would require the solution of the equation of motion. However, we will propose a simple approach based on the seismic coefficient approach used in the seismic design of structures in earthquake engineering. When the pillar is in full contact with overburden layers, the stress on a pillar may be given as follows

$$\sigma_p = \rho g H \frac{A_t}{A_p}\left[1 + 6\alpha \frac{H}{w}\cdot\frac{y}{w}\right] \tag{5}$$

The maximum compressive and tensile stress would occur at the both sides of the pillar. If the tensile strength between the roof layer and pillar is assumed to nil and the yielding takes to a certain depth from the side of pillar, the maximum compressive stress on the pillar side can be obtained as follows

$$\sigma_p = \sigma_{po}\frac{1}{(1-\xi)^2}\left[1 + \frac{6}{(1-\xi)}\left(\alpha\frac{H}{2w} - \xi\right)\right] \tag{6}$$

Where $\xi = \dfrac{e}{w}$, $e = w - w^*$, $A_p^* = w^* \cdot w^*$, $\sigma_{po} = \rho g H \dfrac{A_t}{A_p}$. The relation between the normalised yield distance and seismic coefficient α for no-tension condition between roof layer and pillar is obtained after some manipulations as follows,

$$\alpha = \frac{w}{3H}\left[5\xi + 1\right] \tag{7}$$

The seismic coefficient at the collapse of the pillar may be obtained for the condition that the maximum compressive stress obtained from equations (6) and (7) is same. Figure 20 shows an example of computation. Model tests on room and pillar mines on shaking table indicated that the roof layers also fail by bending. Therefore the load condition under horizontal shaking is assumed to be consisted of gravitational load inducing the bending stresses and linearly varying axial stress along the rood axis from tension to compression due to horizontal shaking. On the basis of this assumption, the seismic coefficient at the time of roof layer failure by bending is obtained as follows:

$$\alpha = \frac{\sigma_t}{\rho g w (A_t / A_p - 1)} - \frac{w}{2H}(A_t / A_p - 1) \qquad (8)$$

Figure 21 shows a computed diagram for the relation between overburden ratio and seismic coefficient for various failure modes for the chosen parameters shown in the same figure. These results indicate that the shallow mines are prone to roof failure while the deeper mines are prone to pillar failure for actual strong ground motions during earthquakes.

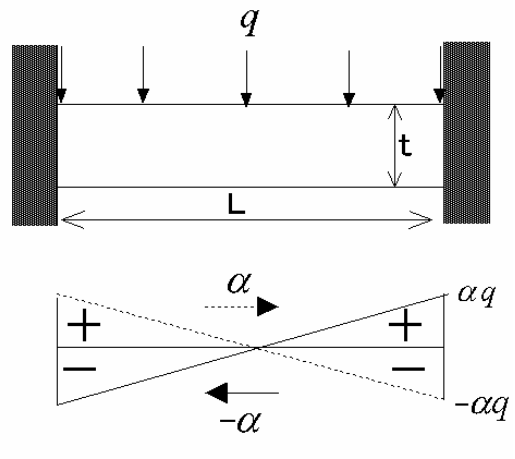


Figure 20. Seismic loading model for roof

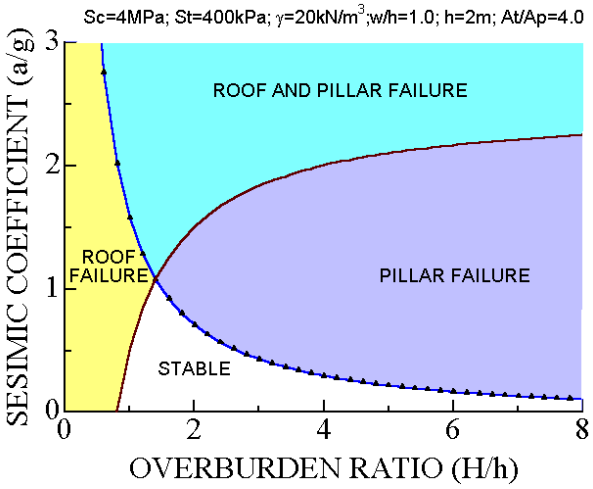


Figure 21. Seismic stability chart for abandoned mines

8. Conclusions

The authors presented some experimental results on the physical, mechanical and degradation characteristics soft rocks in Tokai region. The experimental results indicated that these soft rocks are prone to degradation in long term. A series of stability analyses was carried out to investigate the effects of degradation and creep failure and earthquake loading. These stability analyses results indicated that many abandoned room and pillar lignite mines are prone to collapse in long term as well as during earthquake shaking. Therefore, some measures against the collapse or subsidence of these abandoned mines are urgently needed.

9. References

Aydan, Ö. & Kawamoto, T. (2004). The damage to abandoned lignite mines caused by the 2003 Miyagi-Hokubu earthquake and some considerations on its causes. 3rd Asian Rock Mechanics Symposium, Kyoto, 525-530.

Aydan, Ö., Daido, M., Tano, H., Tokashiki, N., Ohkubo, K. (2005). *A real-time multi-parameter monitoring system for assessing the stability of tunnels during excavation*. ITA Conference, Istanbul,, 1253-1259.

Aydan, Ö., Sakamoto, A., Yamada, N., Sugiura, K., Kawamoto, T. (2005). *The characteristics of soft rocks and their effect on the long term stability of an abandoned room and pillar lignite mine*. International Symposium on Post Mining, PostMining 2005, Nancy.

FLOODING OF THE SAAR-LORRAINE COAL MINES: COUPLING OF THE REGIONAL MODEL OF THE LOWER TRIASSIC SANDSTONES AQUIFER WITH A "BOX" MODEL OF THE MINING RESERVOIR

BABOT Yves[1], DUZAN Alexandre[1], ECKART Michael[2], KORIES H.[2], METZ Michel[3], RENGERS Rudolf.[4]

[1] ANTEA, Parc Club des Tanneries, 15 rue du tanin – BP 312 Lingolsheim – 67834 Tanneries Cedex – France ; a.duzan@antea-ingenierie.fr ; y.babot@antea-ingenierie.fr

[2] DEUTSCHE MONTAN TECHNOLOGIE GmbH, Am Technologiepark 1 – 45307 Essen – Deutschland. Michael.Eckart@dmt.de

[3] CHARBONNAGES DE FRANCE GSA, 2 av. Emile Huchet - 57802 Freyming-Merlebach – France. Michel.metz@charbonnagesdefrance.fr

[4] DEUTSCHE STEINKOHLE AG, Shamrockring – 44623 Herne – Deutschland

ABSTRACT: Charbonnages de France (CdF) and Deutsche Steinkohle AG (DSK) has mandated the ANTEA/DMT working group to draw up a transborder groundwater / mining reservoir coupling model for the Center-East sector. This coupling makes it possible to calculate pumping flows, according to pressure losses between mines, in order to prevent brackish water intrusion from mines to the Lower Triassic Sandstones aquifer.

KEYWORDS: FLOODING, COUPLING MODEL, MINING RESERVOIR, LOWER TRIASSIC SANDSTONES AQUIFER.

RESUME: Les sociétés Charbonnages de France (CdF) et Deutsche Steinkohle AG (DSK) ont mandaté le groupe de travail ANTEA/DMT pour élaborer un modèle couplé nappe / réservoir minier transfrontalier sur le secteur Centre Est. Ce couplage permet de calculer en fonction des pertes de charge entre les mines, les débits à pomper de façon à empêcher les eaux minéralisées de la mine de remonter dans la nappe des grès du Trias inférieur.

MOTS-CLEFS: ENNOYAGE, MODELE COUPLE, RESERVOIR MINIER, NAPPE DES GRES DU TRIAS INFERIEUR.

1. Introduction

In agreement with the French company Charbonnages de France (CdF), Deutsche Steinkohle AG (DSK) has mandated the ANTEA/DMT working group to draw up a transborder model for dealing with groundwater in the main mining areas in Lorraine and Germany (cf. fig. 1) The aim of this modelling exercise is to couple the model of the Lower Triassic Sandstones (LTS) aquifer with the BOX model of the mining reservoir (Centre-East sector) so as to provide answers to the important hydrogeological issues arising as a result of the planned mine closures and the flooding that results from them.

The technical reason for this initiative is the fact that no uniform water level will be established in the mining reservoir. This implies that the behaviour of the flooding volume flows between the mining concessions is highly complex and can no longer be estimated by means of simple analytical evaluations.

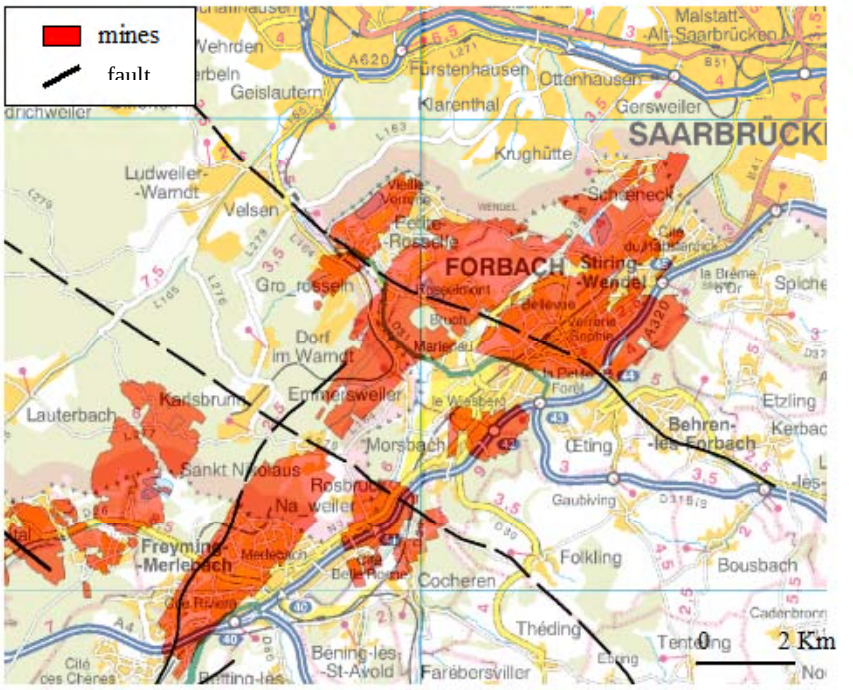


Figure 1: Saar-Lorraine coal mines (Centre East sector)

2. Coupling of the hydrogeological model of the LTS aquifer with the BOX model

ANTEA's VAL hydrogeological model and DMT's BOX model operate according to the so-called "volume evaluation" method. They use square meshing, which facilitates the production of a common grid. The advantage is that complicated couplings such as the transmission of volume flows between the models can be eliminated. It also allows calculations to be carried out in a transient state on the rise of the water level with interaction between the mines and the LTS aquifer.

The overall model consists of 26 layers, the first section of which represents the LTS aquifer. The other sections in the model consist of 17 evaluation units corresponding to individualised mining reservoirs (BOXES). The coupling of the two models is shown in Figure 2.

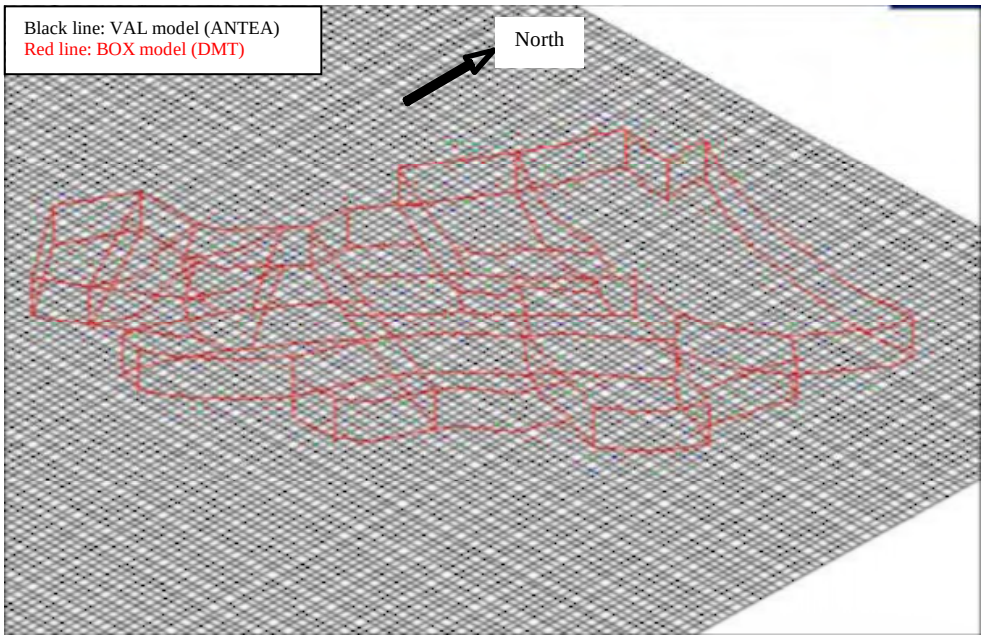


Figure 2: Coupling of the hydrogeological model of the LTS aquifer with the BOX model

3. Long-term future status forecasts of the overflow rate at the Gustave shaft

For reasons of security, simulations have been carried out with different hydraulic conductivities for the galleries. The variation in this parameter plays an important role in the water levels in the different mining areas (BOXES).

- "Optimistic" variant (hydraulic short-circuit between the galleries)

The differences in level which appear in relation to the discharge level at the Gustave shaft are negligible in all the BOXES due to the fact that the galleries are in a hydraulic short-circuit. The overflow rate at +192 m NGF (French datum level) at the Gustave shaft is very high: 12 m^3/min.

- "Realistic" variant (average hydraulic conductivity of the galleries)

In the case of this variant, differences of a few decimetres appear in the Forbach box to the East and in the Merlebach box to the South as well as differences of approximately 4 to 5 m between the Gustave shaft and the Forbach area, and 7 to 8 m between the Gustave shaft and the Merlebach area (cf. fig. 3). The overflow rate at +192 m NGF at the Gustave shaft is 8.4 m^3/min.

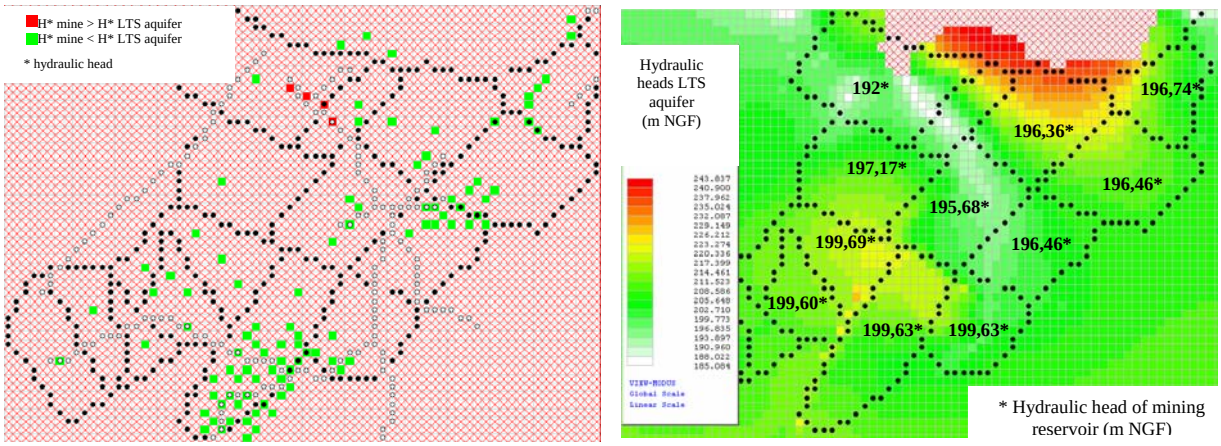


Figure 3: realistic variant

➢ "Pessimistic" variant (very limited hydraulic conductivity of the galleries)

The pressure losses induced by the low hydraulic conductivity of the galleries lead to increases in pressure in the mining reservoir in relation to the LTS aquifer in the Freyming-Merlebach and Forbach sectors (cf. fig. 4). This situation causes a risk of contamination of the LTS aquifer by the waters from the mining reservoir. On the other hand, the overflow rate at +192 m NGF at the Gustave shaft is now only 3.2 m^3/min.

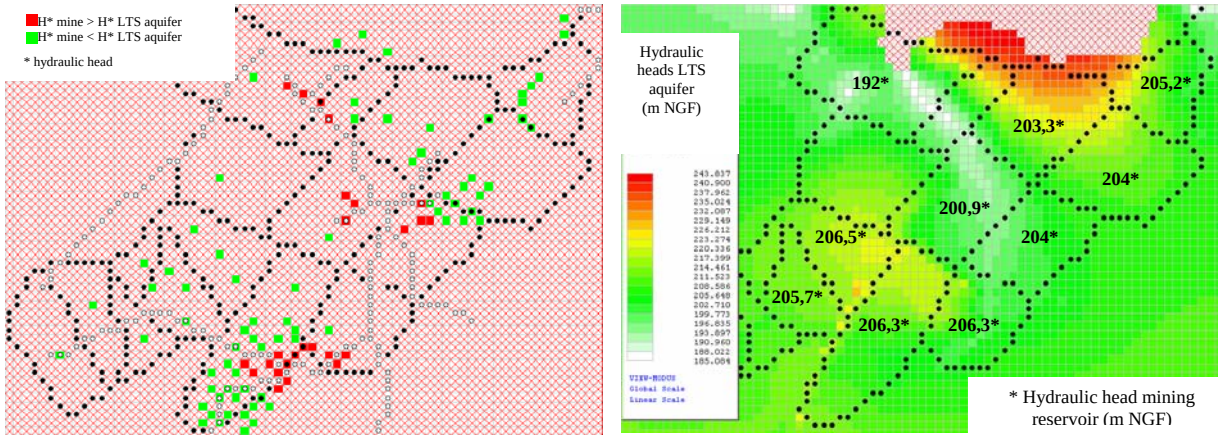


Figure 4: pessimistic variant

4. Behaviour over time of the final flooding phase

Due to the importance of the flows entering from the French side, the workings will be filled up in just a few years. The rate of rise of the water level, however, slows considerably when the level of the mine water in the workings comes close to that of the great piezometric depressions in the Lower Triassic Sandstones (cf. fig. 5). This rate of rise of the water level in the final phase depends to a great extent on the porosity of the Sandstones, in other words on its absorption capacity.
The BRGM estimates the absorption capacity of the Sandstones due to its porosity to be 10 %. This value was worked out on the basis of the interregional hydrogeological model. On the other hand, locally, the measures taken by the HBL on the boring samples of LTS give a porosity of approximately 5 % only. We must accept here that that laboratory studies do allow the fracture systems to be taken into account. The total absorption capacity due to porosity can only be judged

by means of observations in the evaluations of larger areas. As a result of these uncertainties, we will look at not only the 10% hypothesis, but also that of an absorption capacity of 5%.
The work of HEITELE argues in favour of the hypothesis of relatively high porosities. In this document, effective porosities varying between 5 and 15% have been determined on samples of Lower Triassic Sandstones. The document indicates on this subject that: "As Lower Triassic Sandstones contains a low proportion of binders coming from ferrous and clayey minerals with a homogenous granulation, which could be qualified as averagely to roughly clastic, this may explain the relatively high level of its porosity".

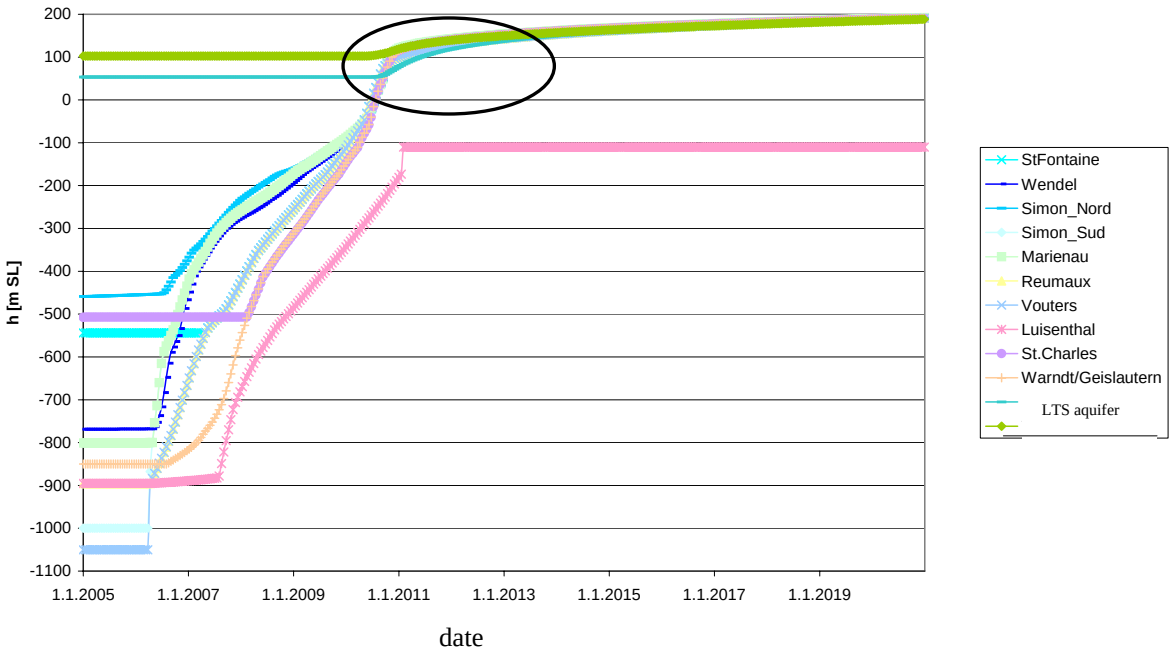


Figure 5: Flooding phase and final phase of the rise of groundwater (porosity 5%)

The next figure shows an extract from the first phase of the rise of water level in the Lower Triassic Sandstones:

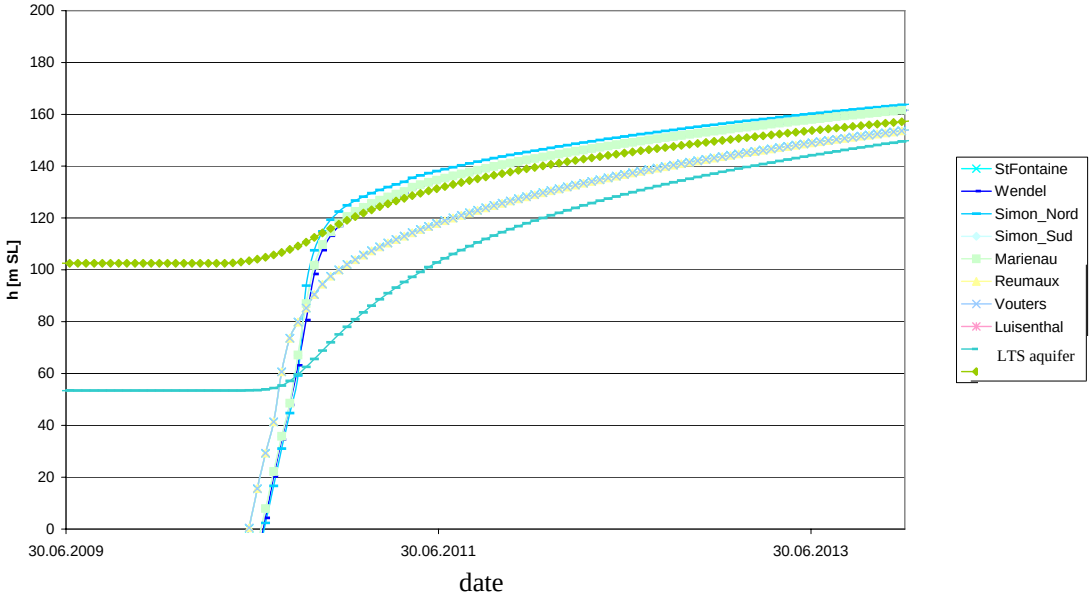


Figure 6: Extract from the flooding phase and the final rise of the groundwater (porosity 5%)

The following figure shows the rise in the final phase in the event of 10% LTS porosity. Furthermore, a small residual void has been integrated into the calculation which is likely to fill up, which leads to a slightly more rapid rise of the water level in the mining reservoir. As a result, the workings will also be flooded approximately six months earlier. This half-year is, however, negligible compared to the much longer total flooding period that we find with a 10 % porosity.

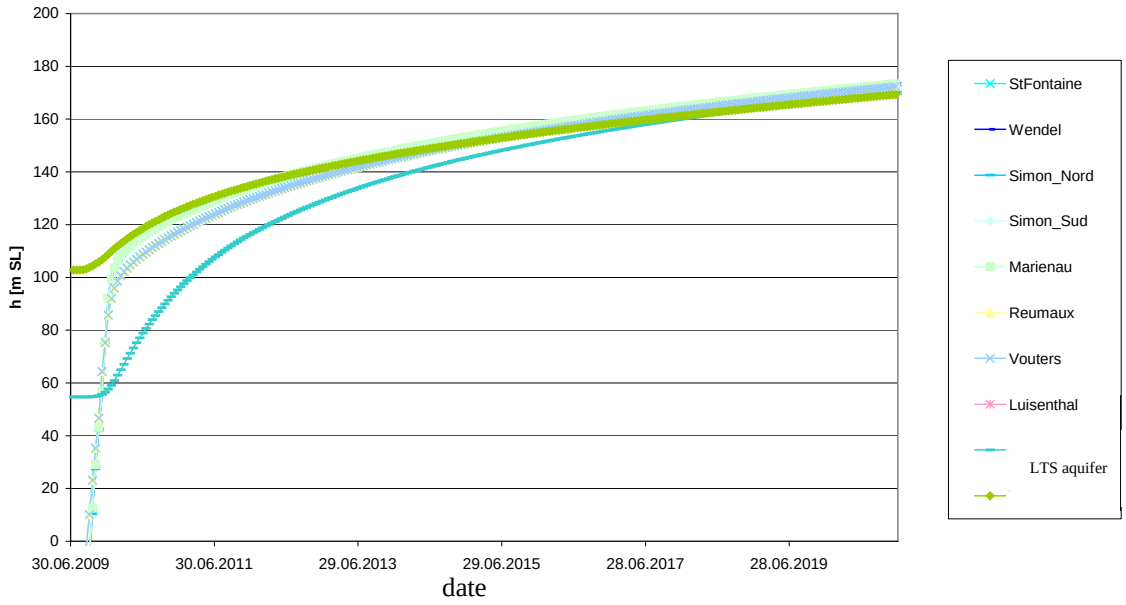


Figure 7: Flooding phase and final phase of the rise of the groundwater (porosity 10%)

An analysis of the rise curves clearly shows that over a period of time of 3 to 5 years, once the mining reservoir is almost full, there will temporarily be sectors where the water levels in the mining reservoir will be higher than in the LTS aquifer, which will create an upward flow. These are in particular the sectors where the piezometric funnels of Vouters and Marienau/Wendel are situated. This phenomenon can be explained by the fact that at other infiltration points away from the cone of depression, the flow of the water from the LTS aquifer continues downwards; this water, however, spreads inside the mine so as to form a relatively uniform water level, which may be higher locally than the water level in the LTS aquifer.

Due to the fact that the boundary conditions of the model for the status "drawdown – current situation" and "final phase" are specified separately depending on the problems that arise, a problem remains in calculating the total flooding until the final status. As far as the curves above are concerned, the model has been started from "the current status". In this way, we keep these boundary conditions for all the calculation, which leads to a lack of precision in the final phase of the calculation. Given the problems to be dealt with, the exact way in which the last stage of the final phase rolls out over time becomes of secondary importance, which makes it possible to tolerate these deviations at this stage.

5. Conclusions

The maximum overflow rate in the final flooding phase of the Gustave shaft is 12 m^3/min. This flow rate is calculated for an optimistic option in which the galleries retain all their hydraulic conductivity. In a rather more "realistic" option, the overflow rate is reduced to approximately 8.5 m^3/min, due to differences in level of approximately 4 to 5 m between the Gustave shaft and Forbach and approximately 7 to 8 m between the Gustave shaft and Merlebach, due to the deterioration in the conductivity in the galleries.
In the event of very poor hydraulic properties of the galleries (pessimistic variant), the water levels on the French side exceed the +200 m NGF mark in the mining reservoir. Consequently, the volume flow towards the Gustave shaft is reduced to approximately 3-4 m^3/min. This hypothesis leads us to fear a rise in the mine water level in the Lower Triassic Sandstones, in particular in the Rosselle valley area.
Before arriving at the long term future status, a very slow final phase of filling up the LTS aquifer should be expected after the very rapid filling up of the mining reservoir. The time needed to fill the LTS aquifer from a level of 100 m NGF up to the level of the Gustave shaft (+192 m NGF) will be at least 15 years (LTS porosity of 5%), but will probably be considerably longer (porosity of the Sandstones of 10%).
An analysis of the rise curves clearly shows that over a period of time of 3 to 5 years, once the mining reservoir has filled up first, there will temporarily be local sectors where the water levels in the mining reservoir will be higher than in the LTS aquifer, which will lead to an upward flow. These are in particular the cones of depression (Vouters and Marienau/Wendel).
To avoid the contamination of the Lower Triassic Sandstones aquifer by the intrusion of brackish mine water it will be necessary to dewater in different sectors of the mining reservoir in order to keep the hydraulic head of this reservoir lower than that of the Sandstones aquifer.
To avoid the risks (even in the pessimistic hypothesis), the method of management chosen by CdF is pumping at the Vouters and Simon 5 shafts (in France), maintaining a water level at about + 193 m NGF in the mining reservoir; the residual flow rate at the Gustave shaft will then be very low.

6. References

Vaute L., (2004). *Scénarios d'exploitation de la nappe des grès du Trias inférieur dans le département de la Moselle, Rapport final*. BRGM/RP – 52822-FR.

Heitele H., (1968). *Opérations d'infiltration dans la zone des GTi du sud de la Sarre*, thèse A, Université de Tübingen.

THE NATURE OF RISK IN GEOTECHNICAL ENGINEERING
LA NATURE DU RISQUE EN INGÉNIERIE GÉOTECHNIQUE

BAECHER Gregory[1]

[1] UNIVERSITY OF MARYLAND, College Park, MD 02174 USA; gbaecher@umd.edu

ABSTRACT: People built tunnels, dams, mines, and other geotechnical structures long before there was a formal discipline of geotechnical engineering. Although many impressive projects were built, the ability of engineers to deal with geotechnical problems in analytically rigorous ways that allowed them to learn from experience and to catalogue the behavior of soils and rocks was limited. A similar transformation has taken place over the past few decades in dealing rationally with risk. These methods are now being widely applied to geotechnical and underground engineering, with sometimes misleading—or at least, confused—results. This paper discuss the application of modern concepts of risk to geotechnical and underground engineering, focusing on what the results of such applications mean.

KEYWORDS: Risk, Uncertainty, Probabilistic analysis.

RESUME: Des tunnels, des barrages, des mines et d'autres ouvrages ont été construits bien avant que ne se constitue la géotechnique en tant que discipline scientifique. Bien que des ouvrages impressionnants aient été réalisés, l'aptitude des ingénieurs à traiter les problèmes géotechniques de manière analytiquement rigoureuse, qui leur a permis d'apprendre par l'expérience et de classifier le comportement des roches et des sols, fut néanmoins limitée. Une transformation analogue s'est produite durant les dernières décennies en ce qui concerne le traitement rationnel du risque. Ces méthodes ont maintenant été largement appliquées à l'ingénierie géotechnique ou à celle des travaux souterrains conduisant parfois à des résultats erronés ou confus. Aussi, le présent papier traite de l'application des concepts modernes de risque dans ces domaines et met l'accent sur la signification des résultats auxquels ils aboutissent.

MOTS-CLEFS : Risque, Incertitude, Analyse probabiliste.

1. Introduction

Probabilistic methods, long established in other engineering disciplines, are finding increasing acceptance in geotechnical engineering practice, for example, in the Netherlands (e.g. TAW, 1998) (Jorisson and Vrijling, 1998), Hong Kong (Morgenstern, 2002), Canada (Hartford and Stewart 2002), and even the US (Von Thun 1996). Risk assessment is becoming common among dam owners (ANCOLD, 2003), and ICOLD has recently published a Bulletin on Risk Assessment in Dam Safety Management (ICOLD 2005). Other development work has been ongoing in Europe and around the world for several years (e.g. EuroCode7). More recently, the California Bay-Delta Authority levee seismic risk assessment study, ongoing at the time of writing, represents a major advance in application of risk analysis in the management of important earth structures.

This paper−an extension of issues touched on by Christian (2004)−addresses questions about the meaning of uncertainty and probability and how the meanings given to those terms affect the meanings of the results obtained from risk analysis. The focus is on understanding uncertainty and risk rather than on controlling their influences in practice (e.g., Peck, 1969). In this regard, the discussion is relevant to those aspects of geotechnical engineering where standard solutions as embodied in codes are not applicable.

Uncertainty is a basic part of geotechnical engineering. Indeed, a major attraction for many students entering geotechnical engineering is that the problems presented are not cut and dried. As the geologic environment varies from site to site, so does each project present a new challenge. Properties of soils and rocks, loads, environmental constraints, and geotechnical configurations must be calculated anew. Furthermore, some of these can never be known exactly, even after extensive investigation. The geotechnical engineer must learn to face uncertainty and provide for it.

Geotechnical engineers have developed strategies to deal with uncertainty. It is usually unrealistic and almost always uneconomical to provide enough margin to encompass extreme eventualities. The best known and most widely cited strategy is the observational method, in which the engineer acknowledges the possibility of unfavourable circumstances and determines how to tackle them if they arise, but employs remedial methods only if observations made during construction reveal that the unfavorable circumstances do in fact exist. A similar philosophy lies at the heart of the New Austrian Tunneling Method (Einstein *et al.* 1996).

2. Uncertainty

What does it mean for something to be uncertain? Questions about the meaning of uncertainty, and about the conflict between necessity and chance, have a history dating at least to classical antiquity.

The word *uncertainty* is used to mean many things, but most people take *uncertainty* to be a primitive term, that is, a term whose meaning is accepted but undefined. Indeed, people have written entire books on the subject of uncertainty without defining the word.

The definition for *uncertainty* in the U.S. Water Resource Council's *Principles and Guidelines* for project evaluation (USWRC 1983), the guidance for federal water resource projects in the U.S., is that "uncertainty describes situations wherein lack of certainty is not describable by [numerical] probabilities." This is a limited−and limiting−definition, but aligns with Knight (1921), who introduced this well-known distinction into the business literature between the notions of "risk" and "uncertainty." In his view, *risk* refers to situations wherein one can assign probabilities, and *uncertainty* refers to situations wherein one cannot.

Keynes (1937) expresses the distinction as follows,

> By uncertain […] I do not mean merely to distinguish what is known for certain from what is only probable. The game of roulette is not subject, in this sense, to uncertainty […]. The sense in which I am using the term is that in which the prospect of a European war is uncertain, or the price of copper and the rate of interest twenty years hence […]. About these matters there is no scientific basis on which to form any calculable probability whatever. We simply do not know.

Knight's narrow definition is not widely used in engineering today, although it is still common in the popular literature on investing (Bernstein 1996). Nonetheless, many economists and decision theorists reject Knight's distinction. Current thinking is that, while a decision-maker may choose not to assign probabilities to vague uncertainties, in making practical decisions he or she always does so, at least implicitly. Keynes continues,

> [Under uncertainty] there is no scientific basis on which to form any calculable probability whatever. We simply do not know. Nevertheless, the necessity for action and for decision compels us as practical men to do our best to overlook this awkward fact and to behave exactly as we should if we had behind us a good Benthamite calculation of a series of prospective advantages and disadvantages, each multiplied by its appropriate probability waiting to be summed.

In a practical decision the quantification of probability always occurs, if only implicitly. This suggests that probabilities are "beliefs," not states of nature, and therefore that there is no such thing as a "true" probability. We return to this topic, below.

Despite the decision theoretic view of uncertainty as inevitably quantitative, there are indeed issues for which we almost completely lack confidence and about which it is nearly impossible to assess credible numerical probabilities. Among such issues are, for example, the economic impact of climate change decades in the future and long-run geological processes in the evaluation of nuclear waste repositories. Such considerations are recognized but cannot be measured, quantified, or expressed statistically. Thankfully, they are only infrequently the subject of engineering risk analysis.

3. Is the world random?

What does it mean for something to happen by chance? As Keynes notes, the risks in roulette have to do with randomness. *Random* means lacking an inherent plan or purpose, without definite aim, direction, rule, or method. Does randomness have a place in geotechnical engineering, and does it need to be accommodated in risk analysis?

In the century following Newton, philosophers and scientists thought of the world as determined by physical laws. These physical laws and a set of initial conditions fully determined the future state of the world. Laplace (1814) began his *Philosophical Essay on Probabilities* with the often quoted passage, "[A]ll events, even those which on account of their insignificance do not seem to follow the great laws of nature, are a result of it just as necessarily as the revolutions of the sun" (translation by Bell 1902). This *doctrine of necessity* had profound implications. Laplace wrote,

> Given for one instant an intelligence which could comprehend all the forces by which nature is animated and the respective situation of the beings who compose it–an intelligence sufficiently vast to submit these data to analysis – it would embrace in the same formula the movements of the greatest bodies of the universe and those of the lightest atom; for it, nothing would be uncertain and the future, as the past, would be present to its eyes.

By the beginning of the 19th century, the scientific community came to see the world as completely determined by natural laws, both in the past and into the future. This had implications that gripped intellectual debate: if the world was determined by natural laws, what room was left for human volition and the random unpredictability of nature (Hacking 1990)?

Laplace reasoned that, although the world may follow a *doctrine of necessity*, human intelligence is limited and thus perceives randomness because it knows no better. Probability theory was needed not to describe randomness, but to describe man's ignorance: probabilities described the mind, not the world. Today, this philosophy is sometimes referred to as "probabilism" (Jaynes 2003).

At the turn of the 20th century, Peirce (1998) refuted Laplace's position, "[G]iven the state of the universe in the original nebula, and given the laws of mechanics, a sufficiently powerful mind could deduce from these data the precise form of every curlicue of every letter I am now writing." Rejecting the doctrine of necessity, he suggested, "[T]he apparently universal laws that are the glory of the natural sciences are a by-product of the workings of chance." This view that the workings of physical world are random at the most basic level is a central belief of modern physics, and randomness is central to modern evolutionary biology.[1]

---

[1] In recent years a new consideration has arisen on the nature of chance: *chaos*. The origins of chaos theory lie in the observation that, for complicated non-linear systems, small changes in initial conditions can lead to

Thus, in contemporary thought, two views of necessity and chance exist. One follows Laplace and the doctrine of necessity. The other follows Peirce and the doctrine of a stochastic physics. Portions of the high-energy physics community subscribe to the second view, but most geotechnical engineers, we suspect, subscribe to the Laplacian view. Stated simply: the world is deterministic; things occur necessarily according to natural law; the only source of uncertainty is man's limited knowledge. This seems to be the philosophy on which most engineering risk analysis is based.

4. Natural variation

Sometimes, we treat uncertainties due to limited knowledge *as if they were due to chance* because we have too little understanding of their mechanisms or too few data to model them in a way that provides more predictive power, or because it is just easier. Randomness at the macro scale in a risk analysis is an assumption; it is not an inherent quality of the world. In principle, one ought to be able to predict whether a tossed coin will land heads-up or heads-down, but it is more convenient to assume that coin tossing is a random process with a consistent frequency of "heads". This random model may predict the outcomes of the tosses of a coin at least as well as a model of the mechanics and aerodynamics of coin flipping.

Rainfall and runoff are processes that are usually modeled as random processes. Does this mean that rainfall and runoff are unpredictable attributes of nature? Not necessarily. Given advances in atmospheric science and hydrology, it is becoming common for weather models to be used in predicting rainfall, and thus runoff and flood heights. Such models are being considered for use in predicting extreme floods for dam safety studies. When flood discharges are predicted by mechanistic modeling, they are no longer assumed to be random processes. Their uncertainties become those of model and parameter errors.

Human factors in risk analysis present particularly interesting examples of how deterministic processes are treated as if they were random. For example, a wanderer comes to a parting of the ways along the road to Rome and does not know which path to take. Not all roads lead to Rome (at least not in this example), so what is the probability that the wanderer gets to Rome instead of, say, Genoa? This might be modeled as a random event–the wanderer chooses one road, and it may or may not be the one that leads to Rome–although clearly there is nothing random about which road does lead to Rome. The uncertainty is not of the world but in the mind of the wanderer, yet in risk analyses we might treat this as a random variable (Rescher 1995).

The evolution of the idea of *randomness* since classical antiquity (David 1962) has concerned natural processes about which we have too little understanding to allow predictions about individual realizations, like the roll of dice, patterns of the weather, when and where earthquakes occur. All we know is the relative frequency with which they occur. Such unpredictable occurrences have been called *aleatory* by Hacking (1975) and others, after the Latin *aleator*, meaning "gambler" or "die caster." This term is now widely used in risk analysis, especially in applications dealing with seismic hazards, nuclear safety, and severe storms.

In applying probability measures to such uncertainties, the meaning of term *probability* is taken to be the frequency of occurrence in a long or infinite series of similar trials. In this sense, probability is interpreted for operational matters to be a property of the system (*i.e.*, a property of nature) inde-

---

large changes in final conditions. Since the initial changes are too small to be modeled feasibly, final conditions become unpredictable and, for practical purposes, due only to chance.

pendent of anyone's knowledge of it or evidence for it. We may or may not know what the value of this probability is, but the probability in question is a property for us to learn. It is innate; there is a "true" value of this probability. Two observers, given the same evidence, should converge to the same numerical estimate.

5. Limited knowledge

The second aspect of uncertainty concerns what we know. The truth of a proposition, guilt of an accused, or the presence of a liquefiable layer of soil are unknown. Such things have been called *epistemic*, from the Greek (Hacking 1975). This term, too, is now widely used in risk analysis to distinguish imperfect knowledge from randomness.

The term *probability*, when applied to imperfect knowledge, is taken to mean the degree of belief in the occurrence of an event or truth of a proposition. We may or may not know what the value of the probability is, but the probability in question can be learned by interrogation. There is, by definition, no "true" value of this probability. Probability is a mental state and therefore unique to the individual. Two observers, given the same evidence, may arrive at different probabilities and both be right.

How do epistemic uncertainties manifest in risk analyses? It is convenient to consider two types of risk analyses that are common in engineering. The first uses a direct calculation of the derived distribution of some uncertain variable based on uncertainties in a set of input variables, and boundary and initial conditions. The first-order second-moment (FOSM) method and first-order risk method (FORM) are examples of this type of analysis. FOSM was used to evaluate the risk of the James Bay dikes (Christian *et al.* 1994). The U.S. Army Corps of Engineers (1996) also uses it to assess levee safety (USACE 1999). In a direct-calculation approach, epistemic uncertainties enter the analysis as model and parameter uncertainties.

Model uncertainties reflect the inability of a model or design technique to represent a system's true physical behavior precisely, or the analyst's inability to identify the best model, or a model that may be changing in time in poorly known ways (*e.g.*, seismic zonation changing as more geological data become available). The models used to approximate naturally varying phenomena need to be fit to natural process by observing how those processes work, by measuring important features, and by statistically estimating parameters of the models.

Parameter uncertainties result from an inability to assess exactly the parametric values from test or calibration data due to limited numbers of observations and the statistical imprecision attendant thereto. These include data uncertainties deriving from (i) measurement errors, (ii) inconsistency of data, (iii) data handling and transcription errors, and (iv) poor representativeness of sampling schemes due to time and space limitations (Kulhawy and Trautmann 1996).

The second type of risk analysis model uses an event-driven logic in which initiating events are presumed and all possible chains of subsequent events (either logical or chronological) are laid out in a tree-like pattern. This is the sort of model used in most dam safety evaluations (Bowles *et al.* 1999). It is also central to probabilistic seismic hazard analysis (Budnitz *et al.* 1997). In this event-driven approach, epistemic uncertainties enter the analysis both as unique events, and as parameter or model uncertainty. Note that, in addition to the conventional meaning of the word, an *event* may be a condition such as the existence of liquefiable soil.

Probabilities associated with unique phenomena reflect uncertainty about the truth of a scientific theory, a popularly held doctrine, or the occurrence of a specific historical event when inadequate or conflicting accounts are involved. These probabilities are of a special nature since, by definition,

they cannot be defined with respect to repeatable experiments. The probabilities involved are subjective and typically vary from one person to another. Using probability as a measure of uncertainty about unique phenomena enlarges its domain of application to propositions that do not meet the requirement of repeatability. For example, the arrangement of playing cards in a single deal is unique and can be determined exactly by simply looking through the deck. However, at the time of the deal, bridge or poker players do not know the distribution and are forced to treat it probabilistically, modifying their evaluations as more information becomes available during the play of the hand. The same intellectual processes apply to the description of the geometry and properties of a geologic profile–or the cross-section of an existing dam or mine profile that is being evaluated.

6. A taxonomy of uncertainty

A series of (U.S.) National Research Council reports (1995, 1996, 2000) develops a terminology for describing uncertainties in risk analysis (Figure 1). Aleatory uncertainty has also been called natural variability, random variability, stochastic variability, objective uncertainty, or external uncertainty (Table 1). The term, *natural variability*, seems the most intuitive of these and was preferred. Epistemic uncertainty has also been called knowledge uncertainty, subjective uncertainty, or internal uncertainty. The term *knowledge uncertainty* similarly was preferred. Knowledge uncertainties were further divided into three sub-categories: model uncertainty, parameter uncertainty, and uncertainty about unique events.

In addition to natural variation and knowledge uncertainty, *decision-model uncertainty* describes our inability to understand decision objectives or, at least, how alternative projects or designs should be evaluated. This is a third type of uncertainty, somewhat different in character from the first two. This uncertainty includes, for example, uncertainty in discount rates and the appropriate length of planning horizons. In many current applications of geotechnical risk and risk analysis the influence of decision-model uncertainty is for the most part ignored.

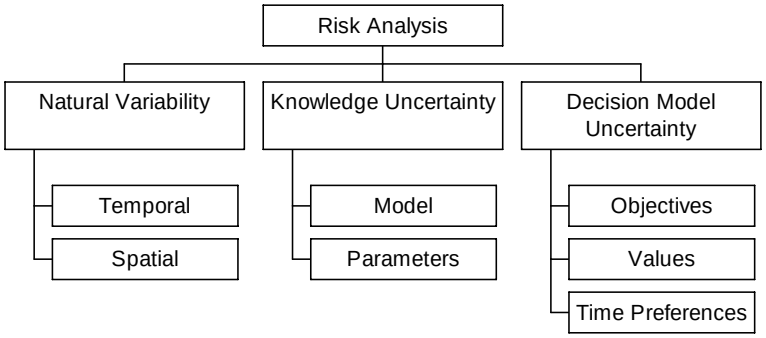


Figure 1. Taxonomy of uncertainties in engineering risk analysis.

The familiar case of flood frequency analysis demonstrates how the two principal types of uncertainty manifest in risk analysis. The annual peak flow frequency curve summarizes historically observed exceedances, reflecting what is presumed to be the natural variability (aleatory uncertainty) of flood flows. The error bands about this curve reflect knowledge (epistemic) uncertainty about the natural process. The frequency curve reflects the irresolvable variation of nature, assigned to chance. The error bands on the curve reflect our lack of perfect knowledge about the statistically estimated parameters of the curve, assigned to ignorance. Collecting more data improves our estimates of the parameters and thus reduces the error bands about the frequency curve, but no amount of data changes the underlying frequency distribution represented by the exceedance curve.

It is crucial that the framework for risk analysis distinguish clearly between natural variability and knowledge uncertainty. The effects of these different sources of uncertainty on risk calculations can

be large. For example, spatial variations in rock fill properties within an embankment, treated as natural variations, average out from one section of embankment to the next in most engineering calculations. High values at one place balance against low values at another. In contrast, parameter uncertainty in the average value, treated as knowledge uncertainty, introduces a systematic effect into the calculation. If mean strength is overestimated at one location, it is overestimated in every location.

7. Probability

We take for granted today that uncertainties should be denominated in the language of probability. It comes as no surprise that, just as there is a duality in *uncertainty* between natural variability and limited knowledge, so, too, there is a duality in *probability* divided between relative-frequency and degree-of-belief (Hacking 1975). Historically, these have been seen as opposing one another, but in practice they are simply applications of a common mathematical theory to different things. For example, we apply the same differential calculus to both groundwater flow and magnetic fields without thinking that these are in opposition. Mathematical probability theory is a logical framework over-arching the notions of frequency and belief and encompassing both.

From the duality in probabilistic philosophy, modern statistical practice, too, has evolved in two principal schools of thought. These might be called the traditional or frequentist school and the Bayesian or degree-of-belief school. Much of engineering risk analysis has been dominated by frequentist approaches, although Bayesian approaches are becoming ever more common.

Table 1. Categories of uncertainty and associated schools of probabilistic and statistical thought.

Uncertainty	Probability	inference
Aleatory	Relative frequency	Fisher, Neyman-Pearson
Epistemic	Degree of belief	Bayesian

The principal difference between traditional and Bayesian approaches is that the former take probability to be a property of the world which has some specific although imprecisely known value, whereas the latter take probability to be a degree of belief, which may be applied to a property of the world. Probability in the traditional sense is a natural frequency over time or space; it has some fixed value, and it makes no sense to speak of a probability distribution over this frequency. In contrast, probability in the Bayesian sense is a belief about the world; thus, it does make sense to quantify degrees of belief about the value of any parameter, even a measure of natural variation.

8. Risk analysis

In this paper the Laplacian view is adopted, that the world is deterministic and knowable, but information about the world is limited (or to paraphrase Matheron (1989), Mprobability is in the model, not in the world). Uncertainty in risk analysis, therefore, comes uniquely from limited knowledge. Despite this, many or even most risk analyses focus on random uncertainties: floods, earthquakes, geologic properties, and other things are treated as stochastic. How do we reconcile a view that the world is deterministic with the risk analysis presumption that the world is random?

The answer is that modelers find it mathematically convenient to treat the world as if some uncertainties are not due to limited knowledge but are actually random. It is important to remember,

however, that the distinction is artificial; it is not inherent in the physical system. Dividing uncertainty between natural variability and limited knowledge is an active choice by the modeler. Consider the trending variation of soil strength properties along the length of a levee (Figure 3). The strengths increase toward the right, but erratically. In making a stability calculation, one assesses an average strength and then modifies (reduces) that value by some increment to account for the variation about the average.

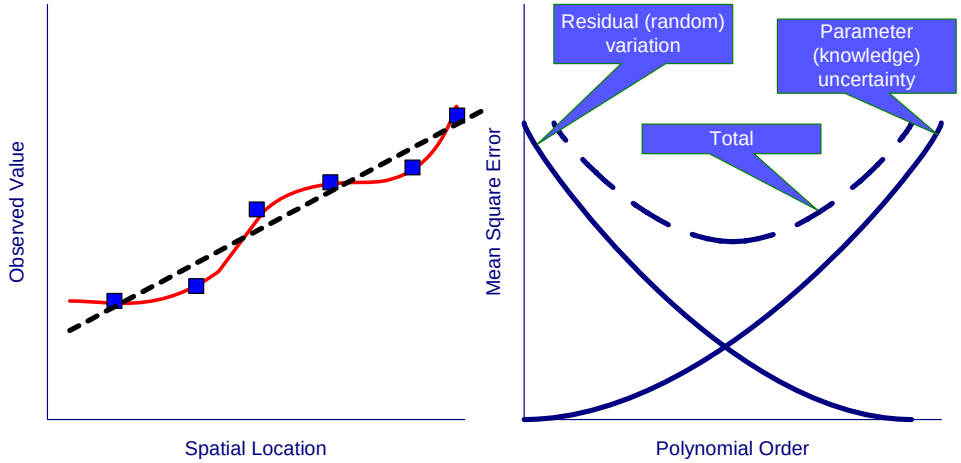


Figure 2. Alternate models for the spatial variation of soil properties

In the simplest case, one could use a fixed spatial average of soil strength and subtract from it a large increment reflecting the relatively large standard deviation about the full-length average. Alternately, one could fit a linear spatial trend to the soil strength data and subtract from it a smaller increment reflecting the relatively smaller standard deviation about the linearly-trending average. Indeed, as the order of the trend approached the number of data points, the standard deviation about the trend would approach zero. On the other hand, the statistical confidence with which one could estimate the parameters of the trend would become ever smaller – that is, the statistical uncertainty in the trend parameters would become ever larger – as the order of the trend curve increased. As the order of the curve approaches the number of data points, the number of remaining degrees of freedom approaches zero, and the parameter uncertainty increases without limit., there may be some optimum between these extremes.

9. The meaning of risk analysis results

An implication of making the trade-off between natural variability and limited knowledge is that what is meant by a predictive probability may change. Consider the “probability of excessive settlement” of a long levee. As stated above, this could mean the portion of the levee that can be expected to experience the excessive settlement, or the probability of overall settlement of the entire levee. Confusion over this issue is frequent in the literature, where the temporal or spatial fraction of adverse performance of a single large structure is sometimes used to verify a probabilistic prediction.

The meaning of a risk calculation depends on how the modeling assumptions are made; specifically, on how the total uncertainty is divided between natural variability and limited knowledge. To the extent that all the uncertainty is assumed to be natural variation, the probability of adverse performance refers to a temporal or spatial fraction. To the extent that all the uncertainty is assumed to be due to limited knowledge, the probability refers to a chance of complete failure. Almost always,

the uncertainty is apportioned between natural variability and limited knowledge, so the probability itself is a mixture.

A second implication of the trade-off between natural variability and limited knowledge is that the variability of performance is a function of scale, as can be seen in the prediction of performance on the James Bay dykes of HydroQuébec™ (Christian et al. 1994). To the extent that uncertainty is presumed to be natural variability, uncertainty averages over space and time. The variability of soil properties among large specimens will be less than among small specimens. The variability among *in situ* tests that mobilize large soil volumes will be less than the variability among *in situ* tests that mobilize small soil volumes. The converse is true of behaviors that rest on extreme properties. Seepage conditions and piping that depend on the most transmissive element of a formation become both more variable and more extreme with scale. Rock slope failures that depend on the least favorably inclined joint become more variable and also more probable as the volume of rock mass becomes larger.

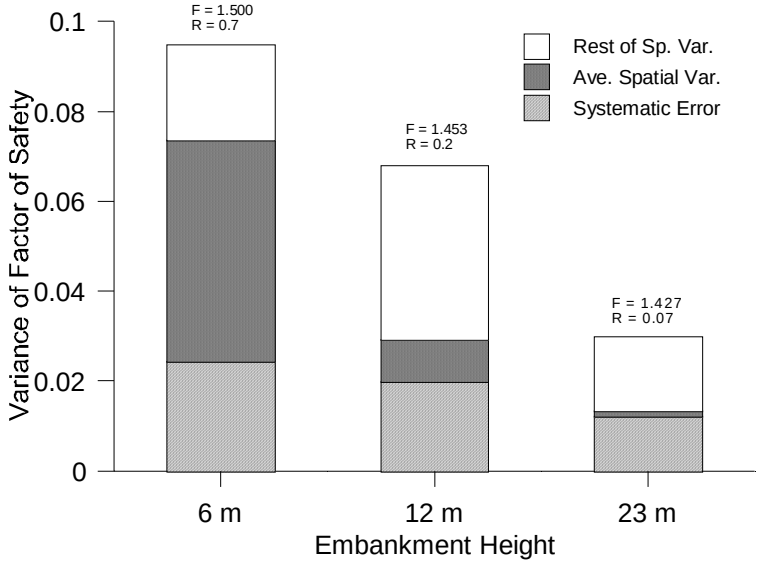


Figure 3. Variance of the factor of safety against slope failure for three elevations of dykes at James Bay (Christian et al 1994). Cross-hatched bar corresponds to epistemic uncertainty arising from parameter and model uncertainty. Remaining bar corresponds to aleatory uncertainty arising from spatial variation of soil properties. This spatial variation overages over soil volumes (stippled bar) generating a scale effect.

A third implication of the trade off between aleatory and epistemic uncertainty is expressed by the expected value of sample information (EVSI). EVSI is a concept from decision theory alluding to how much one should be willing to pay for the results of gathering (sampling) more information. To the extent that uncertainties are moved to the natural variation column, a floor is created beneath which uncertainty cannot be reduced. For example, fitting a linear regression line to data means that even with large numbers of observations there will always be a residual error about the line. Increasing amounts of information can be gathered, but this only makes the estimate of population parameters (e.g., the regression line) more precise. In contrast, gathering more information about knowledge uncertainties reduces those uncertainties.

Ladd and Da Re (2001) examined the consequences of different ways to develop the statistical parameters for the risk analysis of an underwater slope failure. They computed a 0.24 probability of failure on the basis of the mean values and standard deviations of the shear strength measured in field vane tests. As an alternative, they used the SHANSEP method (Ladd and Foott 1974) to estimate strength. This places the uncertainty in the values of the parameters entering the SHANSEP formulas rather than in the measured strengths themselves. It is analogous to moving from treating floods as purely random processes to incorporating model and parameter uncertainty in predicting

flood patterns. Ladd and Da Re found that the probability of total failure of the embankment was again 0.24 when uncertainties in the parameters alone were considered. When they added the additional effects of uncertainty in the analytical model, the probability rose to 0.26. Finally, when they also incorporated the natural variability effects of local soil properties, they computed a 0.32 probability of failure, which now included approximately a 0.06 probability of a local failure.

10. Should natural variation and knowledge uncertainty be combined?

What does it mean to have a degree of belief about a frequency, or, said in a different way, what does it mean for there to be a probability of a probability? When a model is chosen, certain uncertainties are taken to be due to natural variability. The parameters for the models of these uncertainties have to do with frequencies. But one does not know the values of these parameters with precision, for they themselves are estimated from data. Such estimates can be made using traditional statistical techniques, and they result in estimators and confidence limits. These are not probabilistic descriptions of the uncertainties in the parameters but conditional statements of how such estimators function in repeated sampling from the same population. This is illustrated by the example of the liquefaction regression models described above. On the other hand, estimates can be made with Bayesian techniques, in which case the resulting probability distributions apply directly over the space of parameters. The latter approach is obviously necessary if parameter (and model) uncertainties are to be integrated out mathematically to yield an aggregate risk or risk.

The issue of probabilities of probabilities, that is, of specifying probability distributions over model parameters which are themselves probabilities (frequencies) has been the subject of extensive debate (Von Mises *et al.* 1939; De Finetti 1990; Mosleh and Bier 1996). Mosley and Bier, extending Kaplan and Garrick's (1981) argument for a "probability of frequencies" framework, propose a hierarchy of conditional probabilities based on underlying conditions (i.e., hypotheses or propositions). There is an extension of this approach to include probability assessments directly over alternate models (Hoeting *et al.* 1999), but a number of subtle issues arise in the model uncertainty arena which complicate this practice.

An approach now gathering momentum in closely related fields of risk analysis–seismic safety, nuclear power plant risk, and high-level waste disposal–is to use conditional statements of risk, in which a family of probability distributions is generated over aleatory uncertainties. Each member of the family of distributions is conditioned on a non-exceedance probability for the epistemic components of uncertainty (Pate-Cornell 1999). In this way, the assessment of risk avoids the difficulties of convolving different types of uncertainty. While this approach provides an interesting way of portraying complex risk analysis results, its usefulness is limited to cases in which a small number of epistemic uncertainties dominates the analysis.

11. Final comments

Risk analysis for geotechnical projects, and mining and environmental engineering more generally, involves uncertainties about processes in the natural world and about the performance of man-made structures in response to natural processes. Presuming a Laplacian view–the world obeys natural laws and acts in deterministic ways–leads inevitably to a conclusion that all the uncertainties dealt with in risk analysis are caused by limited knowledge: there is no such thing as randomness (Veneziano 1994). Nonetheless, one assumes hypothetically that some of these uncertainties are actually due to natural variation of an inherently random character over time or space. This presump-

tion, without which the enterprise of risk analysis would be made much more difficult, has strong implications of which practitioners need to be aware.

12. Acknowledgements

The author wishes to thank Drs. John T. Christian and Desmond N.D. Hartford, the co-authors, respectively, of *Risk and Statistics in Geotechnical Engineering* (Wiley 2003) and *Risk and Uncertainty in Dam Safety* Telford 2004) for their many contributions to the concepts in this paper.

13. References

ANCOLD (Australian National Committee on Large Dams Inc.) (2003). Guidelines on Risk Assessment

Baecher, G.B. and Christian, J.C. (2003). *Reliability and statistics in geotechnical engineering*, John Wiley and Sons, London and NY.

Bernstein, P. L. (1996). *Against the gods : the remarkable story of risk*. New York, John Wiley & Sons.

Bowles, D. S., Anderson, L. R., Evelyn, J. B., Glover, T. F. and Van Dorpe, D. M. (1999). *Alamo dam demonstration risk assessment.* Proceedings of the Australian Committee on Large Dams (ANCOLD) Annual Meeting, Jindabyne, New South Wales:

Budnitz, R. H., Apostolakis, G., Boore, D. M., Cluff, L. S., Coppersmith, K. J., Cornell, C. A. and Morris, P. A. (1997). *Recommendations for Probabilistic Seismic Hazard Analysis: Guidance on Uncertainty and Use of Experts, NUREG/CR-6372*. Washington, DC, U. S. Nuclear Regulatory Commission.

Christian, J. T. (2004). *Geotechnical Engineering Risk: 'How well do we know what we are doing?' - The 39th Terzaghi Lecture.* Journal of Geotechnical and Geoenvironmental Engineering, ASCE **130**, to be published.

Christian, J. T., Ladd, C. C. and Baecher, G. B. (1994). *Risk Applied to Slope Stability Analysis.* Journal of Geotechnical Engineering, ASCE **120**(12): 2180-2207.

David, F. N. (1962). *Games, gods and gambling; the origins and history of probability and statistical ideas from the earliest times to the Newtonian era*. New York,, Hafner Pub. Co.

De Finetti, B. (1990). *Theory of probability : a critical introductory treatment*. Chichester ; New York, Interscience Publishers.

Einstein, H. H., Halabe, V. B., Dudt, J.-P. and Descoeudres, F. (1996a). *Geologic Uncertainties in Tunneling.* Uncertainty in the Geologic Environment, ASCE Conference, Madison, WI.

Eurocode 7 Geotechnical design. (1997). *Comité Européen de Normalisation.* The European Commission

Hacking, I. (1975). *The Emergence of Probability*. Cambridge, Cambridge University Press.

Hacking, I. (1990). *The taming of chance*. Cambridge England ; New York, Cambridge University Press.

Hartford, D.N.D and Baecher, G.B. (2004). *Risk and Uncertainty in Dam Safety*, Thos. Telford, London.

Hartford, D.N.D. and Stewart, R.A. (2002) *Risk Assessment and The Safety Case in Dam Safety Decisions.* Proceedings of the 12th Biennial Conference of the British Dams Society, Thomas Telford..

Hoeting, J. A., Madigan, D., Raftery, A.E., and Volinsky, C.T. (1999). *Bayesian Model Averaging: A Tutorial (with discussion).* Statistical Science , 14 :4, 382--417. Corrected version available at http://www.stat.washington.edu/www/research/online/hoeting1999.pdf..

ICOLD (2005). *Risk Assessment in Dam Safety Management. A reconnaissance of Benefits. Methods and Current Applications*. Report 130, Paris.

Jaynes, E.T. (2003). *Probability theory: The logic of science*, Cambridge University Press.

Jorisson, R. and Vrijling, J.K (1998) *The transition to a Risk-Based Concept of Dike Design for the Netherlands*. Paper No. 310. ICCE98.

Kaplan, S. and Garrick, B. J. (1981). *On the quantitative definition of risk.* Risk Analysis, 1(1): 11-27.

Keynes, J. m. (1937). *The General Theory*. Quarterly Journal of Economics: 209-233.

Knight, F. H. (1921). *Risk, uncertainty and profit*. Boston, New York,, Houghton Mifflin Company.

Kulhawy, F. H. and Trautmann, C. H. (1996). *Estimation of In-Situ Test Uncertainty.* Uncertainty in the Geologic Environment, Madison, WI, ASCE: 269-286

Ladd, C. C. and Da Re, G. (2001). *Discussion of Factor of Safety and Risk in Geotechnical Engineering by J. M. Duncan.* Journal of Geotechnical and Geoenvironmental Engineering, ASCE **127**(8): 710-714.

Ladd, C., C. and Foott, R. (1974). *New design procedure for stability of soft clays.* Journal of the Geotechnical Engineering Division, ASCE **100**(7): 763-786.

Laplace, P. S. (1814). *Philosophical Essay on Probabilities*. New York, Dover Publicatons, Inc., A. I. Dale translator and editor.

Matheron, G. (1989). *Estimating and Choosing: An Essay on Probability in Practice*, Berlin, NY, Springer-Verlag.

Morgenstern, N.R. (2002). *Performance in Geotechnical Practice.* The Inaugural Lumb Lecture, Hong Kong Institution of Engineers, May.

Mosleh, A. and Bier, V. M. (1996). *Uncertainty about probability: A reconciliation with the subjectivist viewpoint.* IEEE Transactions on Systems, Man, and Cybernetics--Part A: Systems and Humans **26**(3): 1083-1090.

National Research Council (1995). *Flood risk management and the American River basin: An evaluation*. Washington, DC, National Academies Press.

National Research Council (1996). *Understanding risk: Informing decision in a democratic society*. Washington, DC, National Academies Press.

National Research Council (2000). *Risk analysis and uncertainty in flood damage reduction studies*. Washington, DC, National Academies Press.

Orr, T.L.L and Farrell, E.R. (1999) *Geotechnical Design to Eurocode 7* Springer Verlag

Pate-Cornell, E. M. (1999). *Conditional uncertainty analysis and implications for decision making: The case of WIPP*. *Risk Analysis* **19**(5): 995-1002.

Peck, P. B. (1969). *Ninth Rankine Lecture: Advantages and Limitations of the Observational Method in Applied Soil Mechanics.* Geotechnique **19**(2): 171-187.

Peirce, C. S., Cohen, M. R. and Dewey, J. (1998). *Chance, love, and logic : philosophical essays*. Lincoln, University of Nebraska Press.

Rescher, N. (1995). *Luck : the brilliant randomness of everyday life*. New York, Farrar Straus and Giroux.

TAW (Technical Advisory Committee for Water Retaining Structures), 1998. *Guidelines on the Basis for Water Defence*, The Netherlands.

U.S. Army Corps of Engineers (1996). *Risk-based analysis for flood damage reduction studies.* Washington, DC, US Army Corps of Engineers.

Veneziano, D. (1994). *Uncertainty and Expert Opinion in Geologic Hazards.* The Earth, Engineers, and Education: A symposium in Honor of Robert V. Whitman, Cambridge, Department of Civil and Environmental Engineering, MIT: 102-124

Von Mises, R., Neyman, J., Sholl, D. and Rabinowitch, E. I. (1939). *Probability, statistics and truth*. New York, The Macmillan Company.

Von Thun, L. (1996). *Risk Assessment of Nambe Falls Dam.* Uncertainty in the Geologic Environment, Madison, WN, 604-635.

Water Resources Council (1983). E*conomic and environmental principles and guidelines for water and related land resources implementation studies.* Washington, DC, Executive Office of the President.

GEOTECHNICAL INVESTIGATION AND REINFORCEMENT DESIGN OF SUBSIDENCE PRONE AREA

BANG Ki-Mun[1], SONG Won-Kyong[2]

[1] DAEWOO ENGINEERING COMPANY, 9-3 Sunedong Bundanggu Suwon - 463-825 Kyonggido, - Korea. ; bkm21@dweng.co.kr

[2] KOREA INSTITUTION OF GEOSCIENCE AND MINERAL RESOURCES, 30 Gajeongdong Yuseonggu - 305-350 Daejeon, - Korea. ; songwk@kigam.re.kr

ABSTRACT: This report presents a case study on site investigations and an assessment of ground stability for an area classified into potentially unstable because of surface subsidence. The subsidence results from excavated cavities of an old coal mine in underground and exerts a threat on the national road No. 35 that passes through this area. For the complete understanding of geological structure and mined cavities, geophysical survey, boring and in-situ and laboratory tests were carried out. Based on the geotechnical informations ground stability assessment has been made using theoretical and numerical techniques. Then reinforcement design for improving the stability of the road has been performed for the area where mined cavities are located within the depth of 30m from the surface.

KEYWORDS: Subsidence, Mined cavities, Reinforcement, Site investigation, Ground stability

RESUME : Ce rapport présente un cas d'étude décrivant les investigations de site et l'estimation de la stabilité d'une zone classée potentiellement instable à cause du risque d'affaissement. L'affaissement résulte de l'exploitation d'une mine de charbon en souterrain et exerce une menace sur la route nationale No. 35 qui traverse la zone considérée. Afin de comprendre la structure géologique et de reconnaître les cavités exploitées, une investigation géophysique, une campagne de sondages et des caractérisations de laboratoire ont été réalisés. Sur la base de cette information, une estimation de la stabilité des terrain a éte faite à l'aide de méthodes théoriques et numériques. Ensuite un renforcement a été dimensionné pour améliorer la stabilité de la route se trouvant à la verticale de cavités situées à moins de 30m de la surface.

MOTS-CLEFS : Affaissement, Cavités de mine, Renforcement, Investigation de site, Stabilité des terrain

1. Introduction

Ground subsidence occured in an area where there was an undergorund coal mine. This subsidence gives a threat to safty of the ntional road No. 35. A proper measure to improve the stability of the ground around the road was required but it was very difficult to obtain the solution because of lack of documents concernig the underground cavities excavated during mining work.

This study wsa carried out to assess the ground stability around the national road and to take an appropreate measure. First of all, site investigation was done, which is divided into preliminary and detailed investigation. During the preliminary stage, site investigation was done in a regional scale to select potentially unstable zones. Detailed investigations including borings, geophysical surveys and in-situ and laboratory tests were conducted on these unstable zones. Then reinforcement design was done based on geotechnical information obtained from these investigations.

2. Ground condition

Several mining tunnels are distributed under the national road No. 35 (Fig. 1). Most of them except the 1st level are considered to give no significant effect on the stability of the road because they are located at the depth of over 100m below the surface. The depth of the 1st level is approximately 60m below the surface.

In fact, ground deformations due to underground cavities on this level are found in many places around the road as shown in the figure 1. The figure 2 shows some examples of ground movement occured in this zone.

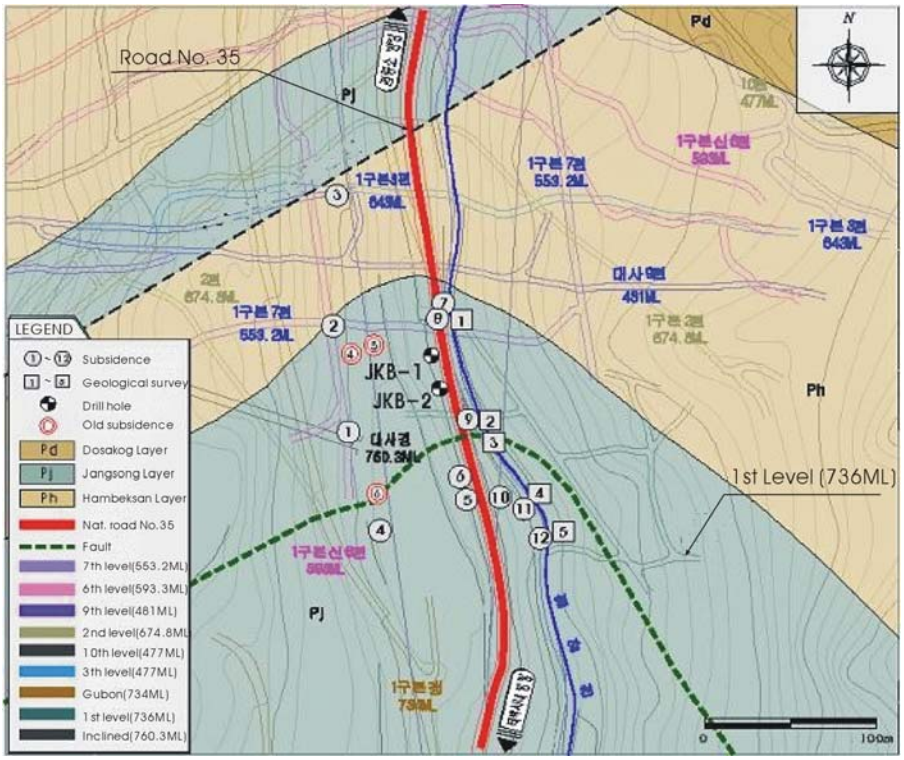


Figure 1. Distribution of gangways and subsidence places around the national road No. 35



Figure 2. Evidence of subsidences; sinkhole with a diameter of 5m (left) and deformation of the national road No. 35 (right)

3. Geotechnical investigation

In order to understand the geological condition under the ground surface, electrical resistivity surveys were carried out along the both sides of the road (Figure 3). The survey shows that a low resistivity region is present at the depth of around 20m below the surface. This depth is similar to that of the 1st level gangway. Appearance of low resitivity region in the geophysical survey images is considered as an extension of disturbed zone above mined cavities.

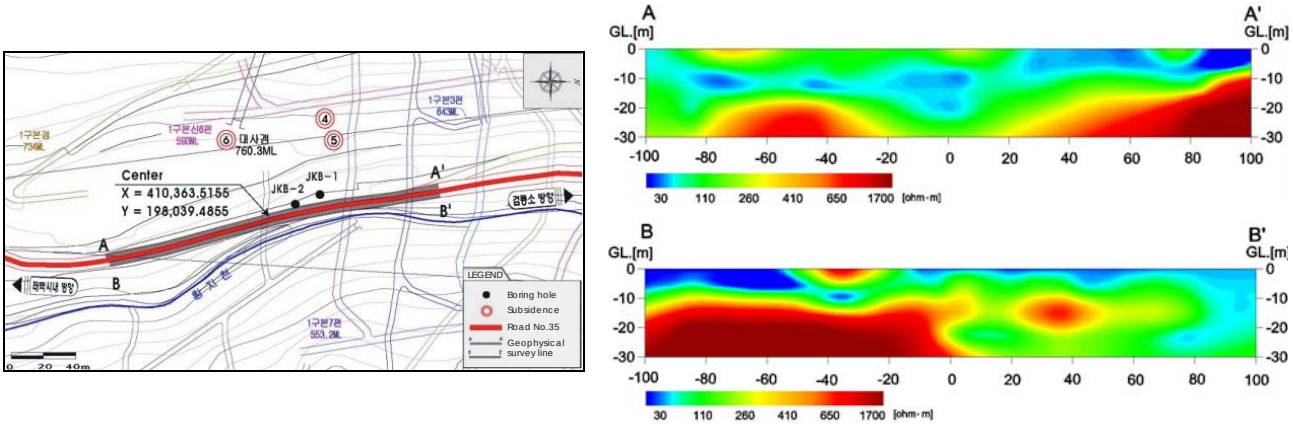


Figure 3. Electrical resistivity survey

Two boreholes were drilled at the places where low resistivity values are exhibited (refer to the figure 3). Thick coal seams were found from the cores and especially some fragments of support timbers were recovered in the borehole JKB-2 (Figure 4). Furthermore, even the presence of a mined cavity was detected from these cores. It was confirmed from this borehole survey that mining work had been actively done in this zone and caused ground movement.

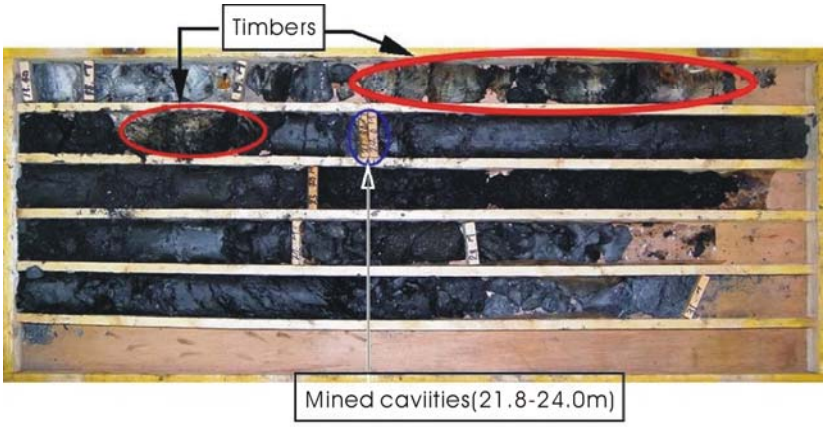


Figure 4. Support timbers and mined cavity found in drill cores

4. Numerical analysis

Numerical analysis was conducted to estimate the necessity of the ground reinforcement on the studied area. A section acrossing the national road was taken for the model and the physical

properties used in the model are described in the table 1. It was assumed that 70% of coal seam was mined out and the rest was preserved as pillars.

Table 1. Input properties

Layer	E, MPa	ν	c, MPa	ϕ, deg	γ, kg/m^3
Weak rock	300	0.25	2.0	30	2,200
Moderate rock	3,000	0.20	2.5	35	2,300
Coal seam	29	0.30	0.2	20	2,000

Figure 5 represents a contour of vertical displacement. Vertical displacement of over 30cm occured at the place where the road passes. This value exceeds the allowable displacement for roads, 10cm. Therefore a proper measure is required to improve the stability of the ground.

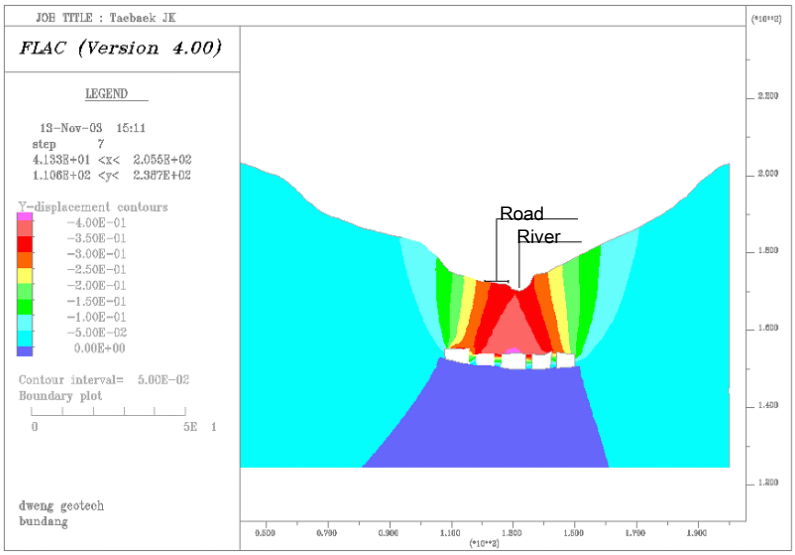


Figure 5. Contour of vertical displacement around the road

5. Reinforcement design

5.1. Limit angle

The extent of ground subsidence can be defined by limit angles (Figure 6). Limit angle in dip and raise side are not equal in inclined coal seams. Three angles of limit, τ_1, τ_2 and τ_3, can be determined using empirical formulae suggested by SHE(National Coal Board, 1975), Rom(1964) and Ren et al. (1987). Considering the curves depicted in the figure 6, the maximum limit angle in dip side, τ_3, varies between 46 and 64 degrees.

5.2. Influence depth

Vertical displacement of ground surface according to the depth of mined cavities was estimated using numerical analysis. Geometry of the models was simplified and three models having 30m, 50m and 70m depth of cavities were simulated (Figure 7). Maximum vertical displacements for these models were 26.3cm, 9.6cm and 8.2cm, respectively. It was known that, when the depth of

mined cavities exceeds 50m, vertical displacement of the ground becomes smaller than the allowable limit value, 10cm.

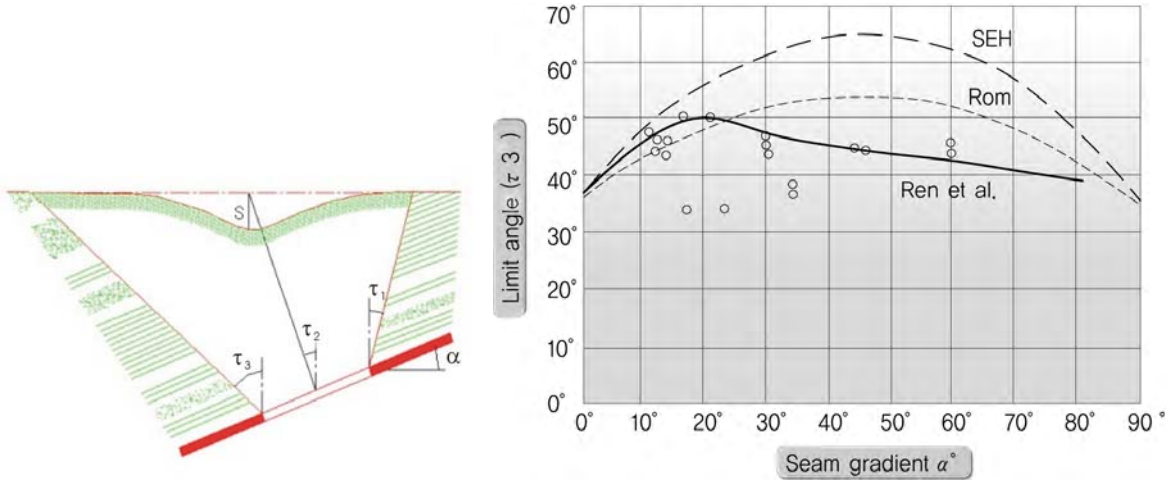


Figure 6. Comparison of the maximum limit angles derived from different empirical formulae

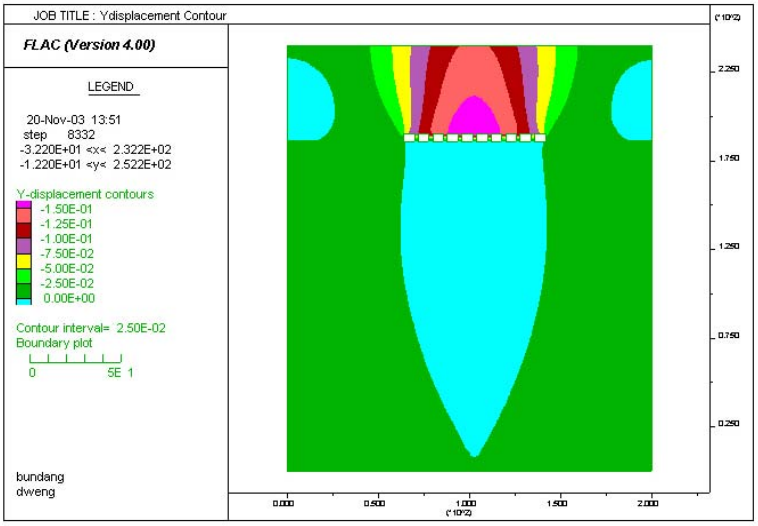


Figure 7. Contour of vertical displacement of the ground for the model with mined cavities 50m deep

5.3. Reinforcement design

Based on the results of theoretical and numerical analyses mentioned above it was decided that the reinforcement was required to the areas where mined cavities existed within the depth of 30m from the surface and appropriate method for reinforcement was the grouting of the ground under the road with cement.

The grouting holes were planned to reach up to the depth of the bottom of the cavities and to be drilled in both sides of the road (Figure 8). The whole length of the reinforcement on the ground surface is 95m.

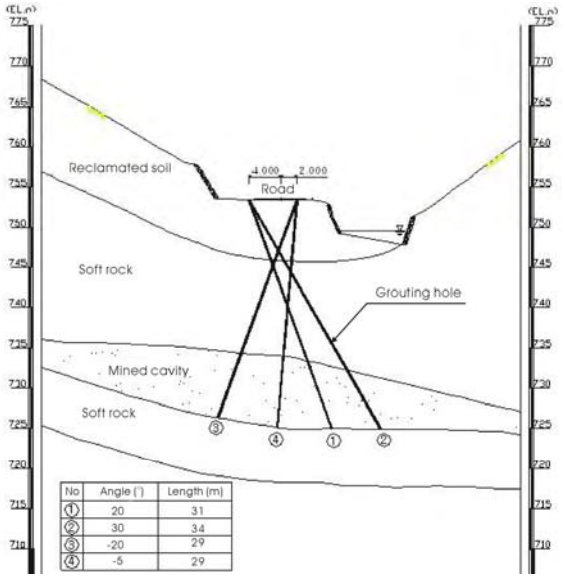


Figure 8. Reinforcement design with cement grout

6. Conclusion

It was known from detailed geotechnical survey that the national road No. 35 exposed a risk of ground deformation due to undergorund mined cavities. The studied area is considered as unstable because ground subsidence is being still developed.

The extent of reinforcement was determined from the analysis of limit angles and influence depth. The most proper method for reinforcement is borehole grouting with cement. The reinforcement is required to the areas where mined cavities existed within the depth of 30m from the surface.

7. References

National Coal Board, 1975, *Subsidence engineer' handbook*, London, 1-111.

Ren, G., Reddish, D. J. and Whittaker, B. N. (1987), *Mining subsidence and displacement predicting using influence function methods*, Mining Science and Technology, Vol. 5, 89-104.

Rom, H., (1964*), A limit angle system*, Mitt. Markscheidew., 71, 197-199.

ASSESSMENT AND MAPPING OF THE ENVIRONMENTAL HASARD IN THE PMRP APPROACH: FROM THE APPLICATION TO DEVELOPMENT NEEDS.

BARANGER Philippe[1], KIMMEL Marion[1], MAZENC Bernard[1], HADADOU Rafik[1], O. LEFEBVRE[1], C. FRANCK[1]

[1] GEODERIS, 1 rue Claude Chappe-Europlaza Bat C2, 57070 Metz Cedex 3.;

philippe.baranger@industrie.gouv.fr;marion.kimmel@industrie.gouv.fr;bernard.mazenc@industrie.gouv.fr; rafik.hadadou@industrie.gouv.fr;olivier.lefebvre@industrie.gouv.fr;christian.franck@industrie.gouv.fr

ABSTRACT: The integration of the environmental aspect within the framework of the Plan of Mining Risk Prevention (PMRP) led to develop a specific methodology for the evaluation and mapping of the hazard related to the water and soil pollution. A first approach was proposed and tested on three old heavy metal mining sites. These works raised some technical difficulties for the evaluation of the environmental mining hazard, requiring a large research and development support. These R&D requirements must be especially focused on the way of evaluating the various hazard levels while considering both intensity and probability of occurrence of the pollution. The space-time evolution of the pollution will have particularly to be considered in the hazard assessment.

KEYWORDS: PMRP, mining hazard, environmental impact, mining environment.

RESUME : La prise en compte du volet environnemental dans le cadre du Plan de Prévention des Risques Miniers (PPRM) a conduit à développer une méthodologie spécifique pour évaluer et cartographier l'aléa minier relatif à la pollution des eaux et des sols. Une première approche a pu être proposée et testée sur trois anciennes mines de type polymétallique. Le retour d'expérience issu de ces travaux a permis de soulever un certain nombre de difficultés techniques liées à l'estimation de l'impact minier environnemental et nécessitant d'importants besoins en recherche et développement. Ces besoins doivent notamment porter sur la façon d'évaluer les différents niveaux d'aléa tout en croisant les facteurs intensité et probabilité d'occurrence de la pollution. L'évolution spatio-temporelle de la pollution devra tout particulièrement être considérée dans l'évaluation de l'aléa.

KEY WORDS: PPRM, alea minier, impact environnemental, environnement minier

1. Introduction

The closure of a mining site is responsible for various impacts associated with the pollution of sediments, soils, and water. The resulting environmental hazard is now taken into account within the framework of the PMRP from the decree of 16 June 2000.

While the estimation of the hazard related to field instability is based on an already proven methodology, this is not the case for the environmental hazard calling for a specific methodological approach.

A methodological work has thus been carried out to incorporate the environmental aspect within the framework of the PMRP. A first approach has already been proposed to estimate and map the environmental risk (Ineris, 2004). It is based both on the drawing up of a global conceptual model of the system and on a qualitative and quantitative analysis of the various compartments involved in the transfer of pollution (surface water; groundwater soils and sediments).

2. A review of the current methodology

The proposed approach has been applied and tested on three concrete cases of old heavy metal mining sites, one located in Brittany region and the other two in Rhone Alps region.

Three main types of mining hazards were evaluated and mapped: the “surface water pollution” hazard , the “groundwater pollution” hazard and the “soil pollution” hazard.

The hazard was assessed with data collected during a prior informative phase, essentially based on the legal obligation reports established for the closure of the mining site. An example of an informative map is shown in figure 1.

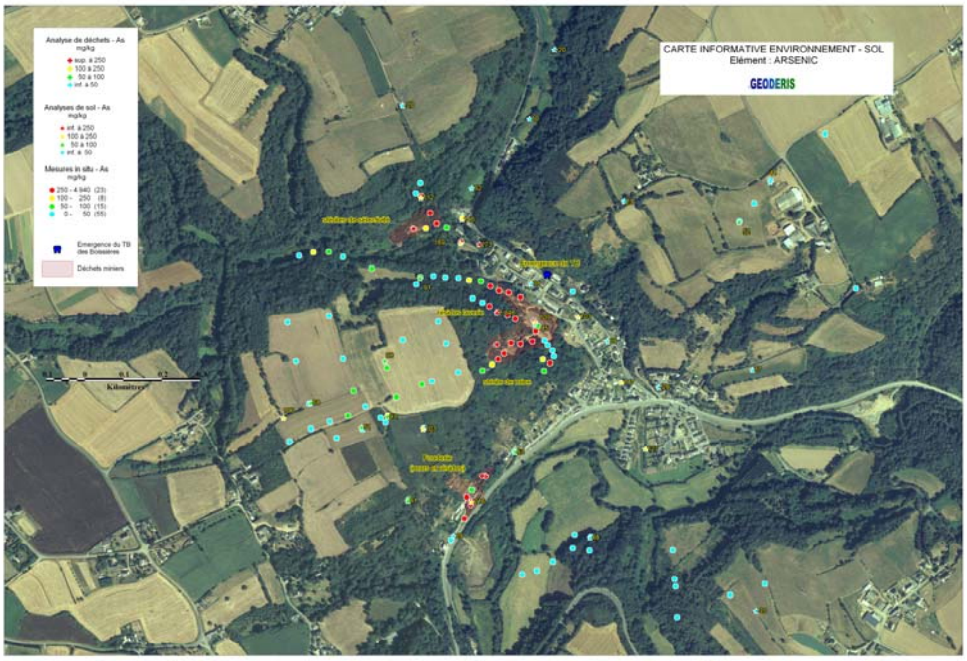


Figure 1: Example of a soil informative map; arsenic content on an old mining site located in Brittany region.

2.1. The “surface and groundwater” hazard

For the three sites, the hazard was assessed considering that the water pollution was stabilized in space and over time. In this case the hazard level can be then assimilated directly to the intensity of the pollution.

The hazard levels were defined on the basis of the French system for the water quality evaluation (SEQ : Agences de l’eau , 1999, 2002). The advantage of this system is that it is common to all water partners and consistent with the European framework directive proposal for community action in the water field. It should be remembered that the general principle of this tool is to assess the physical/chemical quality of the water and its suitability for performing the natural functions of aquatic environments and anthropic uses.

The measured contents of chemical elements are compared with threshold values defining water quality classes and indices as well as the suitability classes of this water for the various entropic uses and the “biological potentialities” function. The suitability classes and associated colour codes are shown in table 1. The global suitability class of the water is determined, for each use, by the most penalising parameter for this use. A use is disadvised if the water suitability for this use is either poor (Orange), or unsuitable (Red).

Table 1.Suitability classes of water defined by the SEQ referential (Agences de l'eau, 1999)

	Very good suitability
	Good suitability
	Fair suitability
	Poor suitability
	Unsuitability

For the specific methodology associated with the environmental part of the PMRP approach, only the most representative parameters of the mining impact (sulphates, pH, metals and metalloids) are taken into account for the determination of the suitability class of the water. This class does not therefore represent the global quality of the water which could be also affected by pollution not directly related to the mining activity (pollution of agricultural origin, industrial origin, etc.).

The suitability classes are then used to determine the intensity classes. Each class of intensity is defined according to the uses and functions examined individually (table 2). For example, the intensity class is considered to be "very low" if no use or function is disadvised. It is considered to be "medium" if the suitability for the "biological potentialities" function and for the use "drinking water supply" are disadvised.

Table 2. Intensity classes determination according to uses and the "biological potentialities" function.

Intensity	**Very low**	**Low**	**Medium**	**High**	**Very high**
Disadvised uses and functions	None	Drinking water supply	Drinking water supply Biological potentialities	Watering Drinking water supply Biological potentialities	Irrigation Watering Drinking water supply Biological potentialities

The intensity classes and thus the hazard levels (pollution supposed to be stabilized in space and over time) is mapped on the basis of the color code reported in table 2.

However, it should be noted that the use of the SEQ referential is not always suitable for the mining context. Indeed, the assessment of the mining water impact on the surface water network may be sometimes distorted in particular because the iron and manganese concentrations are not taken into account in the SEQ referential. Some of the threshold values defined in the SEQ referential also raised the question of the quality of the analytical data available for the hazard assessment. Indeed, it sometimes appears that the analytical detection limits used to acquire these data are higher than the threshold values defined in the SEQ referential, especially for the "biological potentialities" function.

2.2. The" soil pollution" hazard

As for water, the "soil pollution" hazard was determined assuming that the pollution was stabilized in space and over time.

Considering the lack of a French system of threshold values applicable for soils and sediments, a referential was established on the basis of sanitary risk calculations for reference scenarios considered to be relevant (table 3).

However, such approach led to very low threshold values, well below the regional geochemical background. It was thus initially decided to exclude this parameter from the hazard assessment.

For some chemical elements (i.e, Ag) the calculated threshold values were completely unsuited to french soils. These values were thus replaced by an "average national geochemical background" (table 3).

Table 3. Threshold values considered for soil referential (mg/kg). The values corresponding to the "average national geochemical background" are underlined.

Scenarios	**Pb**	**Cu**	**Cd**	**Zn**	**Ag**	**Hg**	**Ni**	**As**
Agricultural / Residential with a vegetable garden / Commercial	40	47	1	140	10	0,3	35	29
Residential without a vegetable garden / Parcs	330	8 800	15	28 000	500	24	390	29
Industrial with soil covered or not	3 200	48 000	100	270 000	11 000	150	1 100	29

Each measured concentration is first compared with the threshold values. This comparison makes it possible to check whether the concentration is compatible with the considered scenarios. The global suitability of the soil for the scenario is determined by the most penalising parameter. An example is given for a mining waste sample collected on one of the sites considered (table 4).

Table 4. Example of suitability evaluation for the considered scenarios : mining waste sample collected on an old mining site located in Rhone Alps region. Red color : not suitable (lower than the threshold value); blue color : suitable (higher than the threshold value)

Chemical elements	Concentrations	Agricultural / Residential with a vegetable garden / Commercial	Residential without a vegetable garden / Parcs	Industrial with soil covered or not
Cu (ppm)	**19200**			
Pb (ppm)	**129**			
Zn (ppm)	**97000**			
Cd (ppm)	**158**			
As (ppm)	**111**			
Ag (ppm)	**1.8**			
Ba (ppm)	**871**	**X**	**X**	**X**
Sr (ppm)	**118**	**X**	**X**	**X**
Al (%)	**12.9**	**X**	**X**	**X**
Fe (%)	**20.2**	**X**	**X**	**X**
TOTAL				

The intensity class is then determined on the basis of the scenarios for which the sample may present risks for human health (table 5).

Table 5. Intensity classes determination according to scenarios.

Intensity	Very low	Low	Medium	High
Disadvised scenarios	None	Agricultural Residential with a vegetable garden Commercial	Agricultural Residential with and without a vegetable garden Commercial	Agricultural Residential with and without a vegetable garden Commercial Industrial with soil covered or not

The intensity classes and thus the risk levels (pollution supposed to be stabilized in space and over time) is mapped on the basis of the color code reported in table 5 (figure 2).

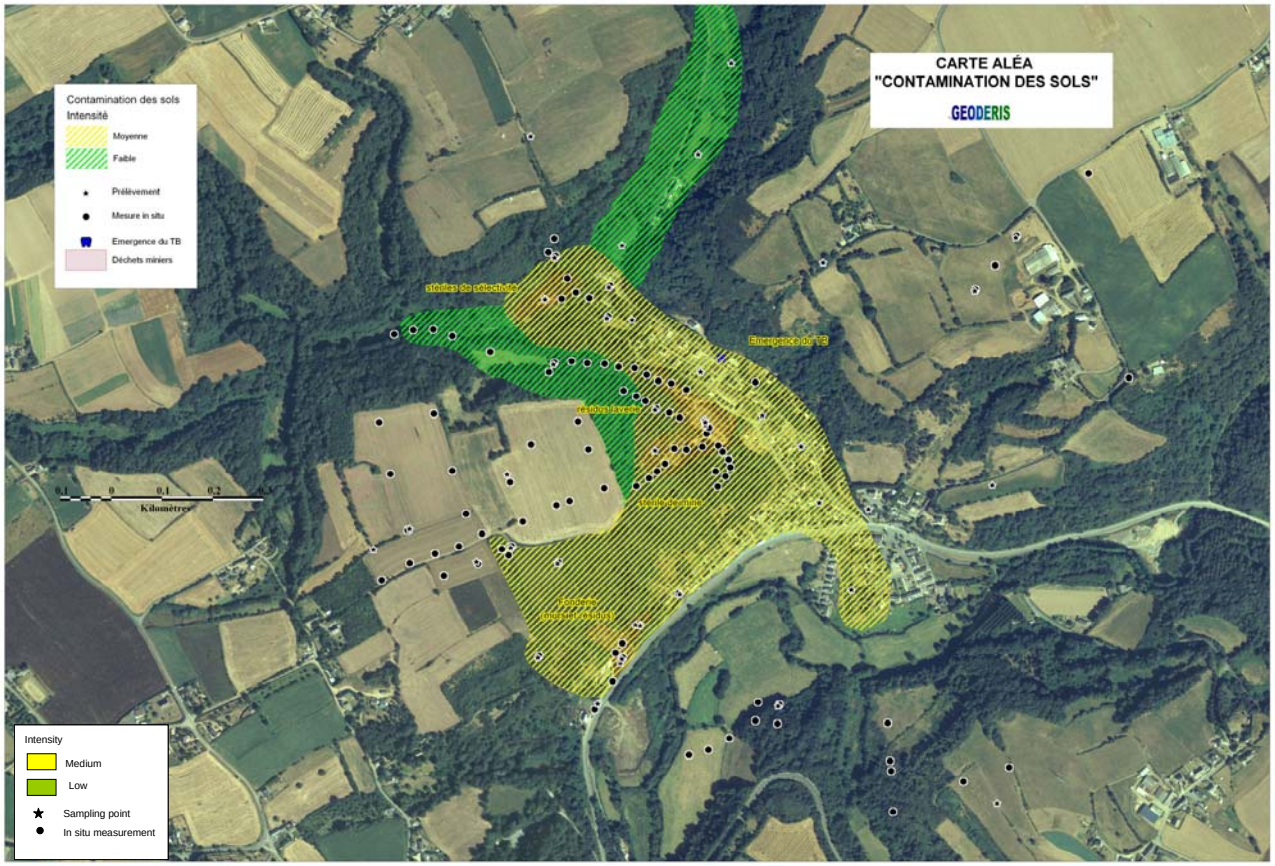


Figure 2: Example of a hazard level mapping established for soils and sediments; case of an old mining site located in Brittany region

3. Research and development needs

The experience feedback resulting from the previous works raised some difficulties and needs in research and development. Several points need to be examined :

- The method used for the determination of intensity classes for waters
- The need for additional data
- The typology of solids considered in the hazard assessment for soil pollution
- The choice of threshold values for soils. The regional geochemical background
- The way of considering the probability term in the hazard assessment for soil and water pollutions: assessment of the site predisposition to the appearance of environmental disorders.
- The way of considering the space/time variation of the pollution in the hazard assessment

3.1. The method used for the determination of intensity classes for waters

The approach used to assess intensity classes for waters is based on the definition of possible uses (SEQ referential). That means that stake concept is indirectly considered. It thus produces a real ambiguity between the risk, depending on the hazard and the stakes, and the hazard, depending on the intensity and the probability of occurrence of pollution. In this context, the mapping of a hazard level implies an estimation of the suitability for a given use and does not represent an overall assessment of the level of an environmental damage. The lesson learned from the previous works also shows that a reliable assessment of the hazard through the SEQ referential can only be possible with a large number of data which are not always available.

This point need to be examined to improve the existing methodology by developing some approaches where hazard levels can be assessed independently of possible uses. For water, results of the SEQ evaluation could simply be reported on the environmental informative map without being directly related to the hazard level assessment.

3.2. The need for additional data

The lesson learned from the previous works clearly shows that the data set contained in the legal obligation reports established for the closure of a mining site must be generally supplemented by additional data for achieving a reliable hazard assessment. This is especially true for soils and sediments for which little or sometimes no qualitative information are available in these reports.

For water, the use of the SEQ referential will also often require a lot of additional data collected on the whole studied area and at various periods of the year, covering all the hydrogeological conditions (low- and high-water periods).

In the PMRP context, it is essential to consider that these additional investigations need to be well oriented to optimize the number of data to be acquired. As far as possible, the expert in charge of the hazard assessment will try to promote the extrapolation of existing data towards the area where data are not available.

3.3. The typology of solids considered in the hazard assessment for soil pollution.

The works already carried out showed that the type of solids used for the hazard assessment (mining waste, soils, sediments, dust) must be better considered and examined. The information available is generally limited to the analysis of mining waste and rarely to soils or sediments. These data alone will only lead to a simple mapping of the sources of pollution and consequently to a partial hazard assessment. The acquisition of additional data then becomes essential, notably in the case of soils located in the vicinity of the mining site which are likely to be impacted by flying dust from slag located in the site. These investigations may be greatly facilitated by portable field analyzers combining both advantages of rapidity and cost (example of portable XRF analyzers).

Sediments should be also better investigated because of there accumulation capacity for a large number of pollutants. They then become very good indicators to follow the environmental impact of the mining activity.

A particular attention must also be paid to the analysis of suspended matter. Such material can be responsible for high environmental disorders but is almost never taken into account in the hazard assessment due to lack of data.

3.4. The choice of threshold values for soils. The regional geochemical background

We have seen that the determination of hazard classes was based for soils and sediments on a system of threshold values essentially determined by sanitary risk calculations (table 3). However, these values proved to be extremely low for all pollutants, which, in a context of a geochemical anomaly, raised the question of the regional geochemical background in the soil hazard assessment. Moreover, the choice of an "average national geochemical background" as threshold value must be excluded from the current methodology because it has no real meaning in a mining environment context (geochemical anomaly context). The selection of suitable threshold values taking into account the regional geochemical background for soil hazard assessment still requires considerations. These considerations must be conducted in close cooperation with the participants involved in the field of contaminated land and waste management. Some considerations could also be brought to sanitary risk calculations to make them less penalizing, specially by considering the speciation of pollutants.

3.5. The way of considering the probability term in the hazard assessment for soil and water pollutions: assessment of the site predisposition to the appearance of environmental disorders.

In the current methodology, the environmental hazard is assessed only on the basis of pollution intensity. The probability that a point or an area could be affected by this pollution is not taken into account. The way of considering this probability term is not easy and the concept of a site's predisposition to the appearance of environmental disorders has been proposed as an alternative to the concept of probability (Ineris 2004). However, this approach remains to be better defined in the current methodology. The concept of geo-environmental model and of site typology may, in this case, represent an interesting way of research. The potential environmental impacts of each family of mining sites could be predicted by simple intrinsic parameters (parameters relating to topography, geology, hydrogeology, mineralogy, geochemistry, etc.). Such an approach should involve, on the one hand, the elaboration of the conceptual model of the site and on the other, the definition of scenarios taking into account the pollution directly related to the mining activity.

3.6. The way of considering the space/time variation of the pollution in the hazard assessment.

As it is reported above, the environmental mining hazard assessment is currently based on the assumption that the pollution is stable in space and over time. However, such an assumption is often difficult to verify within the framework the PMRP, especially because hydrogeochemical models are generally not available due to the lack of data and because it remains difficult to obtain a statistical approach of the mining phenomena. In some cases, such assumption is even wrong because the pollution intensity is characterized by significant variations in space and over time. This can be illustrated by examples of mining sites that shown significant variations in the chemistry of their outflow over periods of several tens of years.

A reliable estimation of hazard should thus involve taking the space/time variation of pollution into account. One possible way could be to use a coupled modeling approach describing both chemical processes and transport of chemical elements. It calls, however, for a large amount of quantitative data on waters, soils and sediments and it is not easily applicable to complex systems, especially to fractured systems. The use of these approaches within the framework of the PMRP thus remains inappropriate except acquiring a great number of data.

If we refer to the conceptual models developed by Schmitt et al. (1996) for a polymetallic mine, by Younger (1999) for coal mines, or by Collon et al. (2004) for iron mines, another way of considering the space/time variation of the pollution would consist in developing some simplified and pragmatic modeling approaches. There too, the geo-environmental model and site typology approach could be an interesting support for this research.

4. Conclusions

The methodology drawn up within the framework of the environmental part of the PMRP was applied to the case of three old mining sites. Hazard maps were thus elaborated for soils and sediments. The lessons learned from these initial works show that the current methodology still needs to be improved. The research effort associated with these considerations should of course be based on the experience already acquired at the international level and in the field of contaminated land and waste management.

This effort should notably be focused on the way of assessing the various levels of hazard while combining the intensity of the pollution and its probability of occurrence. The way of considering the space/time variation of the pollution in the hazard assessment should be also examined. An approach based on the concept of site typology could be promising and would need to be tested on several reference sites.

Another point which should be examined is the choice of suitable threshold values taking into account the regional geochemical background for the hazard assessment for soil and sediment pollution. This point absolutely needs to be discussed in close concertation with participants involved in the field of contaminated land and waste management.

In addition to these methodological requirements, it appears that a reliable hazard assessment will often need some additional data acquisition for water, soils and sediments. Indeed, available quantitative data remain generally not sufficient in the legal obligation reports established for the closure of the mining site. In the framework of the PRMP, it will be essential to focus this data acquisition on the real means of the environmental mining hazard assessment and to optimize the number of data to be acquired. For waters, attempts will notably be made to obtain data over the various hydrogeological conditions that can be found on the studied area. These data mainly consist in flow rate measurements and in analysis of the representative parameters of the mining impact and of the main pollutants (measurements of pH, conductivity, sulphates, metals and metalloids contents….).

For soils and sediments, these additional data acquisitions will be greatly facilitated by portable field analyzers combining both advantages of rapidity and cost (example of portable XRF analyzers).

5. References

Agences de l’eau (1999). *Système d’évaluation de la qualité des cours d’eau*. Etudes des Agences de l’eau n°64, rapport de présentation SEQ-eau, version 1.

Agences de l’eau (2002). *Système d’évaluation de la qualité des eaux souterraines*. Etudes des Agences de l’eau n°80, rapport de présentation, version 0.

Collon P., Fabriol R., Bues M. (2004). *Ennoyage des mines de fer de lorraines : impact sur la qualité de l’eau.* C.R. Geoscience, Vol. 136, Issue 10, p.889-899.

Ineris (2004). *L'élaboration des plans de prevention des risques miniers, Guide méthodologique, Volet technique relatif à l'évaluation de l'aléa*. Ouvrage collectif INERIS, BRGM, GEODERIS, ENSMP, IRSN, CSTB.

Schmitt J.M., Combes P (1996). *Impact hydrogéologique et hydrochimique de l'abandon d'une mine métallique. Cas de l'Argentière*. Les techniques, décembre 1996, p. 38-47.

Younger P.L. (1999). *Predicting temporal changes in total iron concentrations in groundwaters flowing from abandoned deep mines: a first approximation*. Journal of Contaminant Hydrology, 44, pp 47 – 69.

INFLUENCE OF COAL MINE TIPS ON THE CHALK AQUIFER. SAMPLING METHODS FOR THREE DIMENSIONAL SULPHATE INFILTRATION STUDY.

BARREZ Frédéric[1], MANIA Jacky[1], MANSY Jean-Louis[2], PIWAKOWSKI Bogdan[3]

[1] POLYTECH'LILLE, Département Génie Civil, UMR CNRS 8107 (LML), Avenue Paul Langevin, Cité Scientifique, 59655 Villeneuve d'Ascq, France. Frederic.barrez@eleves.polytech-lille.fr ; Jacky.mania@Polytech-lille.fr.

[2] UNIVERSITE de LILLE 1, Laboratoire de sédimentologie et de géodynamique, Bât. SN5 , UMR CNRS 8110 (PBDS), Cité Scientifique, 59655 Villeneuve d'Ascq, France. Jean-louis.Mansy @univ-lille1.fr.

[3] ECOLE CENTRALE de LILLE, Groupe électronique acoustique IEMN-DOAE, UMR CNRS 8520, Cité Scientifique, 59655 Villeneuve d'Ascq, France. Bogdan.Piwakowski@EC-lille.fr.

ABSTRACT: The coal basin of the Nord-Pas-de-Calais region (France) shows a very strong deterioration of the Chalk aquifer quality. In order to better model the hydrodynamism and to improve knowledge on the chemical interactions, sampling according to depth of the groundwater is undertaken. The low-flow sampling and the profiles of the in-situ physicochemical parameters allow the observation of various vertical heterogeneities of the aquifer. The areas where the coal mine tips are localised appear very interesting to study. The sulphates released by the pyrite oxidation allow a "artificial tracing" and give a visualization of the flow as well as information on the implied chemical processes between the oxidizing and reducing zones.

KEYWORDS: chalk, low-flow sampling, sulphate, chemical profiles, coal mine tips.

RESUME : Le bassin minier du Nord-Pas-de-Calais (France) montre une très forte dégradation de la qualité des eaux de l'aquifère de la Craie. Afin de mieux modéliser l'hydrodynamisme et d'améliorer les connaissances sur les interactions chimiques, un échantillonnage des eaux souterraines en fonction de la profondeur est entrepris. L'utilisation de la méthode low-flow associée à la réalisation de diagraphies de quelques paramètres in-situ, permet de visualiser les différentes hétérogénéités verticales de l'aquifère. Les zones où sont localisés les terrils miniers, apparaissent très intéressantes à étudier. Les sulfates rejetés par l'oxydation de la pyrite permettent un "traçage artificiel" et donnent une visualisation des écoulements ainsi que des renseignements sur les processus chimiques impliqués entre les zones oxydantes et réductrices.

MOTS-CLEFS : craie, échantillonnage low-flow, sulfate, diagraphies chimiques, terrils.

1. Introduction

The chalky aquifer contains the major water resources of Nord-Pas-de-Calais region (France) for the production of drinking water. Many anthropic stressors, pasts and presents, have lead to deterioration of groundwater quality of this aquifer in particular in the Carvin/Hénin-Beaumont/Douai triangle. This area constitutes a part of the coal mining basin of Nord-Pas-de-Calais. The coal extraction has lead to industrial (metallurgy and siderurgy) and urban boom which cause serious environmental problems today (heavy metals, sulphates, hydrocarbons…). Sometimes to that may be added agricultural pollutions (in particular, nitrate pollution at the West of the study area). This addition of pollutants and their sources (obsolete industrial zones, present industries,

Deûle Canal, urban zones…) require a constant monitoring of the groundwater and an increased knowledge of the chemical processes in the three dimensions of space.

In this area, Sterckeman et al. (2000) have carried out a study on the vertical distribution of heavy metals in the unsatured zone. But in the satured zone, few studies have been carried out into its vertical distribution. Chalk aquifer is often considered as a homogeneous hydrologic unit, where elements are mixed together quickly at depth. Therefore, the samples are widely acquired on the middle screen after purging 3-5 casing volume of the borehole. The complex chemical processes and the groundwater flow system lead to a study yet the hydrochemical regime in the three-dimensional. Recently, at the southern England in an equivalent aquifer, Schürch et al. (2004) showed that evolution of oxygen concentration determines geochemical groundwater zones which can explain chemical evolution profiles as residence time of water which is an important factor.

In this study, the goal is to bring new methods to characterize chemical water evolutions of the aquifer according to the depth. Assessing to the depth dimension constitutes a way to improve the understanding of the pollutant transfer across the aquifer. This also may, eventually, determine the penetration depth of some pollutants, relative residence time of water, maximal flow zone… In this paper we are interested by the sulphate anion which was the subject of a recent study by Denimal et al. (2002). These authors showed by using the isotopic ratios of sulphur the salting out of sulphates in great quantity in the Chalk aquifer by coal mine tips. It is also an interesting anion because it is in important concentration in many zones of the aquifer and it is easy to measure (but the techniques adopted, in particular low-flow sampling, can be applied to other elements). This study represents a start point to define the stratification of the hydrochemistry of the aquifer and to characterize the parameters which contribute to modify it.

2. Study area

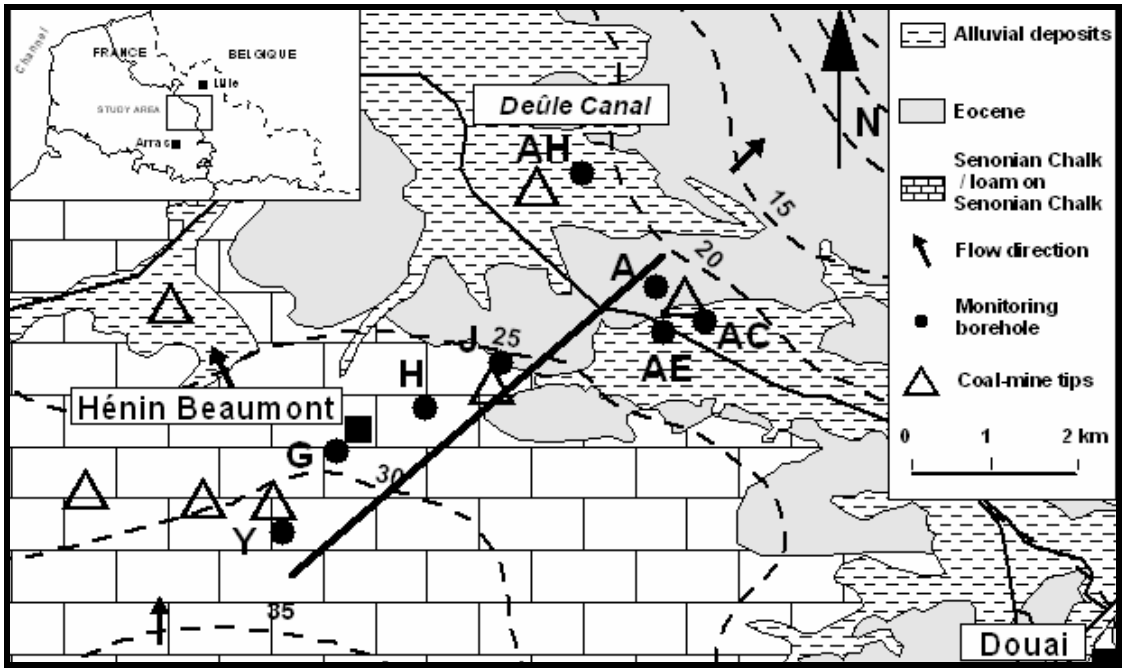


Figure 1. Geological map showing the locations of the boreholes sampled. Generalised piezometric levels are contoured at intervals of 5m above mean sea level.

Global study site is located at the unconfined-confined boundary of the Chalk aquifer (figure 1). At the North-East, Louvil Clay (Tertiary Formation) protects it from pollutant vertical transfers, while

at the South, chalk outcrops (santonian chalk here). Chalk aquifer consists of Santonian-Coniacian formations and the upper part of Turonian (~ 50 meters thickness). The flow direction is S-N for the west part of the study area and SW-NE for the east part. A cone of depression is located at the North-East of the sector.

The water of this area can sometimes be characterized by a strong sulphate mineralization. Previous work has pointed out several possible sources of sulphate in the coal basin (Bernard, 1979; Droz, 1985; Denimal et al., 2002):

- The dissolution of evaporate minerals present in the Carboniferous limestone formation, which can locally contaminate, per ascensum, the chalk aquifer.
- The dissolution of gypsum contained in the Tertiary formations (Argile de Louvil, Sables d'Ostricourt).
- Sulphates of anthropogenic origin linked to wastewater discharge and/or agricultural practices.
- The weathering of mine tips.

In the coal basin, there are many coal mine tips coming from the old mining extraction. The oxidation of the pyrite contained by Carboniferous siltstones causes the release of sulphate that may be transferred to the aquifer:

$$FeS_{2(S)} + 3{,}5\ O_2 + H_2O \leftrightarrow Fe^{2+} + 2\ SO_4^{2-} + 2\ H^+$$

Sometimes, the pyrite can also lead to a denitrification in acid conditions (Pauwels and Talbo, 2004):

$$5\ FeS_2 + 14\ NO_3^- + 4H^+ \rightarrow 7\ N_2 + 10\ SO_4^{2-} + 5\ Fe^{2+} + 2\ H_2O$$

This last phenomenon could be implied in the reduction of the nitrate concentration downstream of some coal mine tips (localised at the unconfined zone of aquifer) like that of Noyelles-sous-Lens, located at the West of the study area (Barrez et al., 2004). In this area, such chemical reactions are perceptible on both sides of this coal mine tip on drinking water borehole. At the upstream, flow is polluted out of nitrate (on average 100 mg/l) but not very charged in sulphate (approximately 50 mg/l). At the downstream, water appears very charged in sulphate ion (730 mg/l) but less nitrated (approximately 50 mg/l). This type of denitrification, although very localised, would take part in the global denitrification at the passage in captivity at the NE of the area. Mariotti et al. (1988) have shown a denitrification in this sector by absence of correlation between $\delta^{15}N$ with the inverse of nitrate concentrations.

This denitrification forms part of a whole of redox reactions which take place at the time of the passage unconfined to confined aquifer. In this direction, the order in which the reactions are expected to occur from a thermodynamic point of view (but not necessarily realized) is aerobic respiration, denitrification, Mn reduction, Fe reduction, SO_4 reduction and $C0_2$ reduction/methane fermentation (Stumm and Morgan, 1981; Mariotti, 1994; Groffman and Crossey, 1999; Christensen et al., 2000). At the passage in captivity, sulphate concentration decreases also at the same time of the decrease of redox potential.

Here the passage in captivity occurs about the level of the Deûle Canal which delimits an unconfined zone at the South-West and a confined zone at the North-East. In the Western part of the sector, the aquifer meets many unconfined/semi-confined zone successions in particular under the alluvial deposits. Consequently, although coal mine tips can release a great quantity of sulphate (sometimes, the concentrations can easily exceed 2 g/l for Chalk aquifer in unconfined zone downstream some coal mine tips) this physical property of the aquifer leads to a strong reduction of sulphate concentration by the process of sulphato-reduction.

3. Methods

To carry out samplings according to depth, several methods are possible. Here are some examples for a sampling with a direct mobilization of the aquifer (dynamic sampling):

- The sampling starting from the drilling of a whole of boreholes to variable depths.
- The sampling to various depths at the same time of the drilling (Caritat et al., 1998).
- The sampling using a bailer after the purge of 3-5 casing volume of borehole.
- The sampling using Dual Pumping Technique: two pumps are used simultaneously with a separate variation of the flows, one placed under the water table and the other near the bottom. Concentration profiles are obtained by applying algorithms compared to speeds of the pumps (Thullner et al., 2000).
- The sampling using Low-Flow technique: pumping is made with low-flow in order to mobilize only one small part of the aquifer.

There are many other methods as well as combined methods. The low-flow technique has many advantages: low-flow purging tends to minimize the turbidity caused by pumping (Puls and Barcelona, 1995; Puls and Paul, 1997), it is the cheapest (except for the use of bailer) and most practical setup. Therefore we chose this method for sampling according to the depth.

Low-flow sampling procedures are gently different from U.S. Environmental Protection Agency recommendations (Puls and Barcelona, 1995). The authors recommend to sample with a flow rate (often <1 l/min) to minimize drawdown (<0.1 m) until field parameters stabilization (Puls and Barcelona, 1995, Creasey and Flegal, 1999). We notice that for Wilson (1995, in Thierrin et al., 2001), water sample is representative of the ambient groundwater when variations of temperature, conductivity, dissolved oxygen, pH do not respectively exceed ± 0.5°C, ± 10 µS/cm, ± 0.2 mg/L O_2 and ± 0.1 pH unity. But flow rate depends largely on the hydraulic conductivity and the depth spacing between two samples. Here, conductivity of the chalk aquifer is high and on the study site, the filtered zone borehole observation is often about or superior to 10 m. Furthermore, for depth borehole, we need long tube which allows temperature's equilibration of the sampling water when the tube is out of borehole. With a very low-flow rate, the temperature parameter is severely affected by the extern temperature and the stability of parameters is very slow. Consequently, we chose to conserve a minimize drawdown (<0.1 m) but with a flow rate adjust from 1.5-3 l/min.

Procedure sampling consisted on 2 stages here in the following order:

- First the profiles of temperature, conductivity, dissolved oxygen, pH and redox potential were established by a multiparameter probe KLL-Q SEBA before pumping. The parameters were measured every meter (except in the case of very deep boreholes) while descending the probe. The measurements taken from the bottom to the top can lead to mistakes: at the bottom of the borehole, chalky mud is sometimes present and is stucked on the electrodes.
- Next we use a low-flow purging technique; the pump was put down and the samples were acquired all the every meters once stability of field parameters was obtained.

For the analysis of the cations, 20 ml of sample were collected and 0.45 µm filtered and acidified by 50 µl addition of pure HNO_3. The cations were determined by ICP-OES. Analysis for Cl, NO_3-N, NO_2 and SO_4 were performed by colorimetric method on 500 ml unacidified samples. HCO_3 is measured by potentiometric method using 0.02N HCl acid (Norm NF T90-036, 1977).

In this communication, the results are only presented for sulphates. The sampling campaign was conducted during the winter 2005 (February-March) but on some boreholes, a sampling campaign could already have been carried out during the summer 2004 (June-July).

4. Results

4.1. General evolution

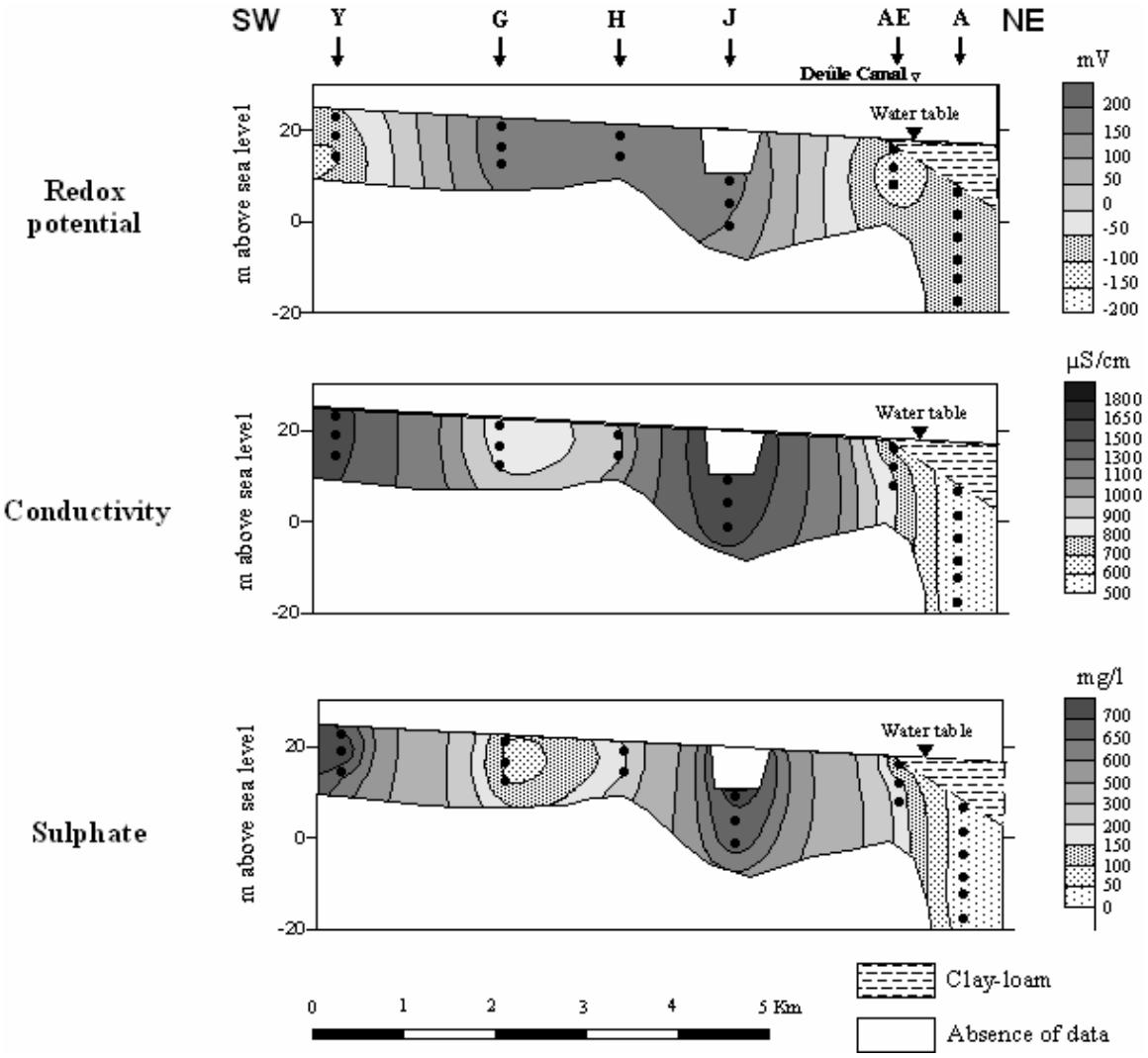


Figure 2. Evolution profiles of redox potential, conductivity and sulphate concentration. The points represent the samples.

Evolution profiles for the Winter 2005 of redox potential, electrical conductivity, sulphate concentration is showed figure 2. The boreholes used (technical featured are presented in the table 1) were projected on line about perpendicularly to the global flow direction. In this area, the aquiferous part has a thickness of more than 50 meters from the surface. Here, the variations of the parameters are dual: in space and depth. It appears much less important according to depth because the scales horizontal and vertical are different.

The aquifer becomes gradually captive to the North after the Deûle Canal. It can explain that the redox potential decreases at the North (values of redox potential are > 150mV for the boreholes G and H while the values are < -50mV for AE and A). For the low redox potential measured to the borehole Y (about between -60 mV and -100 mV), this is explained by this location in a hydrocarbons polluted zone.

For the limit between unconfined/confined zones, it is essential to determine redox potential. Sulphate concentration in the groundwater is not only function of the sulphates brought by a source

of pollution, it depends also on the redox process which can lead to the sulphato-reduction for low redox potential. It is the same chemical process which allows a fast reduction of sulphate concentration when the aquifer becomes confined (notice that the decrease of sulphate can be induced by dilution also).

The electrical conductivity is function of global mineralization degree of water (global mineral species content, generally ionized species) and varies according to temperature. The leaching of the soils lead to the dissolution of salts such carbonates, sulphates, chlorides… Moreover, industrial and agricultural practices discharge salts too and induce an increase in electrical conductivity. In this area, the electrical conductivity is function of sulphate concentration mainly (figure 3) which is often the major anion of the groundwater. The electrical conductivity profiles provide excellent way to detect source of sulphate provisions.

The electrical conductivity profile (figure 2) shows two principal sources of sulphate around the boreholes Y (located in industrial area and around a coal mine tip) and J (located at the downstream of a coal mine tip) with conductivity > 1500µS/cm. The minimum level measured is for the borehole A, located in the captive zone. The boreholes G and H are located in a town (moreover G is located at the upstream of coal mine tip), with an electrical conductivity strong enough for the Chalk aquifer (~ between 800 and 1000 µS/cm). The borehole AE is located at the downstream of an industrial zone but at the limit of confined/unconfined zone. There is maybe a process of sulphato-reduction because in this area, a strong smell of H_2S is detected in the water sampled. This process fits into the scheme of decrease of redox potential (<< 0mV for the borehole AE) with the transition to the captivity of the aquifer.

The sulphate concentration profiles show obvious sources of sulphate pollutions: the boreholes Y and J have the maximum level of sulphate concentration with a maximum of 772 mg/l for Y and 712 mg/l for J. For the borehole J, Denimal et al. (2002) showed that sulphate concentration was produced by the leaching of the coal mine tip.

The concentrations of the other boreholes on this profile are lower. The maximum for G is 96 mg/l and for A, 22 mg/l (at the level of the borehole A, the aquifer is captive; there is no direct source of pollution and the sulphato-reduction is possible).The maximum concentration for the boreholes H and AE are slightly higher (respectively 196 mg/l and 177 mg/l), this can be explain by their locations. We notice that for these boreholes, in the first meters the soil was made of Carboniferous siltstones which contain pyrite. These materials were used quite often for embankment work.

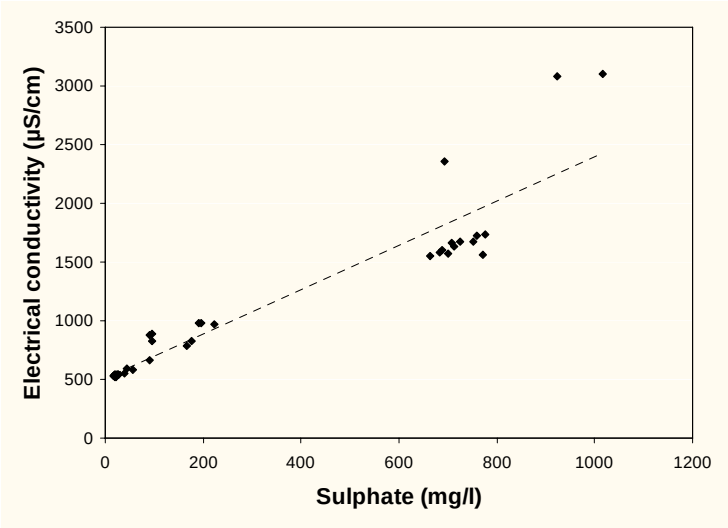


Figure 3. Electrical conductivity vs sulphate concentration. Other elements can modify the electrical conductivity like the calcium. The relation is thus not completely linear.

Remark :

The monitoring boreholes used belong to private companies. They were not drilled for the purpose of this study (except the borehole A). We retained only those which had a filtered zone higher than 8m. For the borehole J, the filtered zone is between 20 and 30m of depth. The first 10m below the water table are not screened.

Table 1. Technical features of used boreholes.

Boreholes	*Location*	*Depth (m)*	*Filtered zone (m above sea level)*	*Elevation number above sea level (Thickness of covering before chalk)*	*Water table (m above sea level)*	*Global state of the Chalk aquifer*
A	Lateral / downstream of a coal mine tip and Deûle Canal	128m	17 to – 100.5m	27.5m (21m)	Summer 2004: 19m Winter 2005: 18.5m	Confined
G	Town	20m	22.5 to 12.5m	31.5m (3.3m)	22m	Unconfined
H	Town	20m	21 to 13m	33m (4m)	19.6m	Unconfined
J	Downstream of a coal mine tip	29.5m	13 to 3m	33m (4.5m)	Summer 2004: 23.4m Winter 2005:23m	Unconfined
Y	Industrial zone	25.5m	26 to 15m	41m (few meters)	20.5m	Unconfined
AC	Lateral / downstream of a coal mine tip and Deûle Canal	24m	18 to 7m	31m (13m)	20.5m	Confined
AE	Industrial zone	21m	17 to 7m	28m (10m)	17m	Semi-confined
AH	Downstream of a coal mine tip	24m	14 to 4m	29m (14.5m)	15.8m	Confined

4.2. Local observations. Examples of sulphate concentration evolution and the first interpretations.

Values of the following graphs represent the state of the aquifer for the first meters, except for the monitoring borehole J (tubed on the first ten meters). For the technical features, to refer to table 1.

The majority of values were taken during winter 2005. However for some boreholes, an analysis campaign could already have been carried out during the summer 2004. A complete study would require the analysis of the evolution of the parameters according to depth for each borehole, but also the analysis of the evolution of the parameters according to time as well as the evolution of boreholes located within the study perimeter. We will take only some examples to show the interest to integrate the "depth" dimension and the "time" dimension.

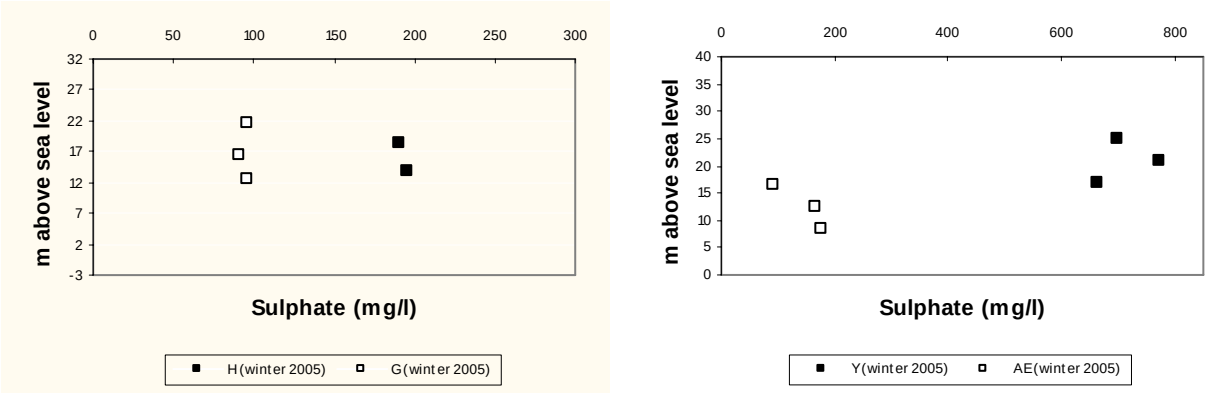


Figure 4. Evolution profiles of sulphate concentration for the boreholes H-G (urban zone) and Y-AE (industrial zone).

The figure 4 shows the evolution of sulphate concentration for 4 boreholes (H, G, Y and AE). Here, the values for the boreholes in the urban zone are pretty constant according to depth (for H about 195 mg/l and for G, 95 mg/l). The differences observed are partially produced by the precision of measurements (sampling, colorimetric analyses…). Moreover, there is no major source of sulphate around them, this could explain this homogeneous state of the aquifer according to the depth.

For the monitoring boreholes Y and AE, there are important differences according to the depth. The sulphate concentration of the samples is much lower for the first sample located one meter under the level of water table (for AE; 91 mg/l and Y; 700 mg/l), than that located approximately 5 meters below (respectively 166 mg/l and 772 mg/l). We even notice that the maximum concentration is reached at the middle screen for the borehole Y (at the bottom, the sulphate concentration measured is 664 mg/l). A phenomenon of dilution could explain the fact that for these two boreholes the higher part of the groundwater has a weaker concentration in sulphate. Two assumptions can be planned to explain this observation:

- The aquifer is in period of refill (which corresponds to this sampling period), the water which feeds it in the higher part is much less mineralized (because of the important rains, there is a dilution effect).
- These boreholes are not located directly under the sulphate contamination source; the higher part of the aquifer would correspond to a contribution side of a less mineralized water (the higher part of the chalk is generally most hydraulically active it is the most fractured and weathered).

These two phenomena can be complementary, but if it is the first which prevails, for the period of lowest water level, dilution should strongly decrease. We should thus observe an homogenization of the sulphate profile, contrary to the second phenomenon where the concentration profile should

always show a weaker concentration to the top. It may be nevertheless that here the water dilution due to the period of groundwater refill is lower during the summer.

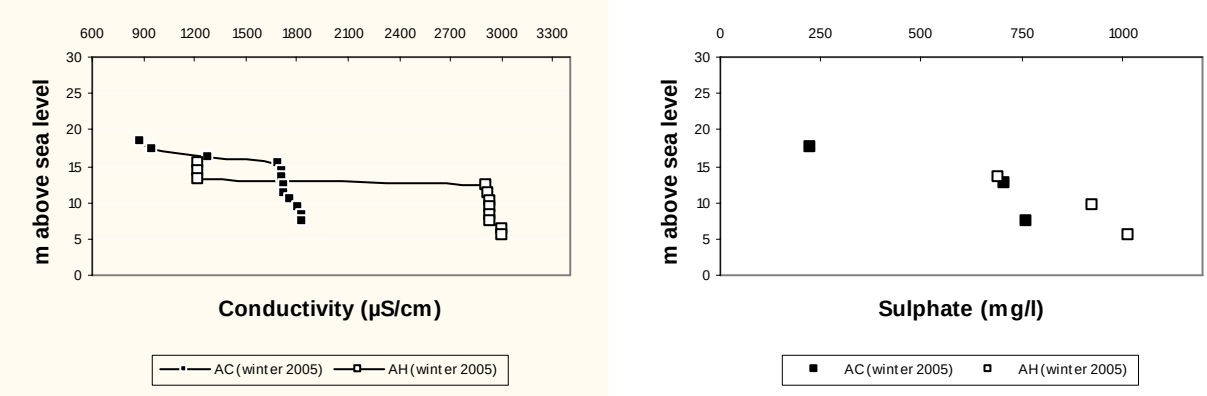


Figure 5. Evolution profiles of conductivity and sulphate concentration for the boreholes AC-AH (downstream of a coal mine tip).

The figure 5 shows the evolution profiles of sulphate concentration and conductivity for the boreholes AC and AH which are localised at the downstream of a coal mine tip. The alluvial deposits can also provide sulphate ions for AC, also located downstream of the Deûle Canal. The beginning of the screened zone corresponds to the level of the water table for the borehole AH and 3 meters below for the borehole AC (these two boreholes are in confined zone).

Increase of electrical conductivity profile (about 900 µS/cm at the upper part of the aquifer to 1800 µS/cm ten meters below for the borehole AC and about 1200 µS/cm to 3000 µS/cm for the borehole AH) strongly reflects the variations of the sulphate concentration which increase according to depth (223 mg/l to 760mg/l for AC and 692 mg/l to 1016 mg/l for AH). In the first meters of the aquifer, sulphate concentration is much less important than at ten meters depth. We can note the same evolutions as Y and AE, here the phenomenon is amplified (AH and AC are at the downstream of an important source of sulphate).

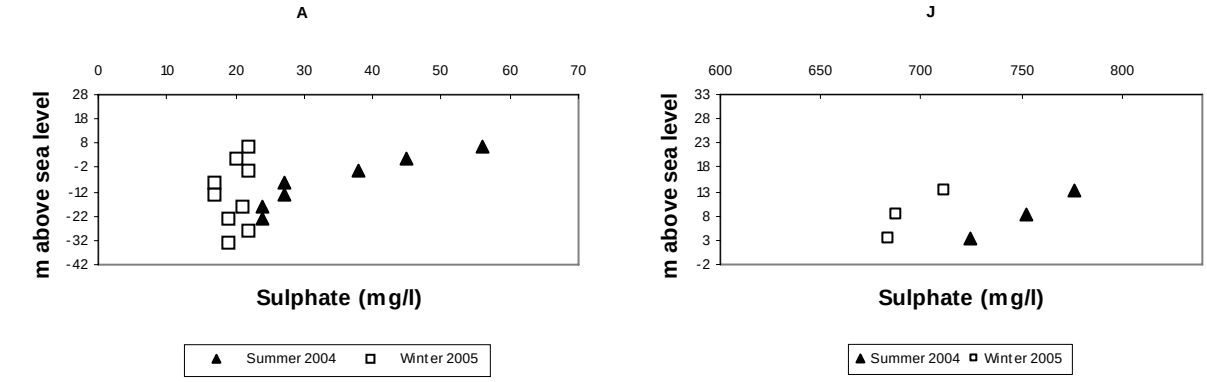


Figure 6. Evolution profiles of sulphate concentration for the boreholes A (confined zone) and J (downstream of a coal mine tip) and comparison between the summer 2004 and the winter 2005.

The evolution according to the time are also well worth studying. The figure 6 shows the evolution of sulphate concentration according to the depth and for two periods of sampling: Summer 2004 and Winter 2005. The borehole A, located in a confined zone, near a coal mine tip and downstream of the Deûle Canal shows that during the winter, the sulphate concentration is homogeneous according to depth (about 20 mg/l). During the summer (here sampling was taken at the end of June), the upper part of the aquifer has a higher concentration (up to 56 mg/l) than that located in

the lower part, the sulphate concentration was stabilized around 25 mg/l. This could be explained by a flushing effect. During this period, in the most hydraulically active part of the aquifer, there is a fast renewal of the water of the aquifer (here, the water from the upstream is more mineralized). It is pretty certain that a delay time is also observed; the time of transit between the moment when the unconfined zone of the aquifer is in refill and the moment when the water arrives in the confined zone. When the flow is less important, the homogenization of the water column would occur due to the fractures of chalk but also to the physico-chemical processes (like the sulphato-reduction).

For the borehole J (figure 6), we will point out that the first ten meters are tubed, we do not have measurements on the upper part of the aquifer. It's possible that the first sample under the water table was less concentrated than that located 5 meters below. But for the moment, the lack of drillings in this zone and experiences feedback do not make it possible to advance this assumption. On the graph, sulphate concentration is high (about 675 to 775 mg/l, depending on the depth and the period of sampling) because J is located at the downstream of a coal mine tip. However, the sulphate concentration decreases according to depth between 13m and 3m above sea level for the two periods of sampling (respectively from 776 mg/l to 724 mg/l for the sampling of summer 2004). Moreover, the graph (figure 6) shows that the concentrations measured at the time of sampling in summer 2004 are higher than those measured for the sampling carried out at the time of the winter 2005 (for example, the concentration decrease from 776 mg/l to 712 mg/l between the sampling of summer 2004 and winter 2005). The dilution operated by the refill of the groundwater can explain at least partially this reduction of concentration.

5. Conclusion

The sampling of chalk aquifer according to depth has been proved a very useful tool to the understanding of the hydrodynamism of the aquifer and the chemical interactions. That could also make it possible to improve positioning of monitoring boreholes and sampling protocols. The few examples shown in this paper indicate that the Chalk aquifer is not homogeneous according to the depth. Several factors can induce these vertical heterogeneities: seasonal variations, differences between the top and the bottom of the aquifer, periods of refill, zones of contamination, the thickness of the cover, the passage in captivity, the oxygen concentration reduction, the lithological variations…

The sampling by low-flow method as well as the physicochemical profiling seems a very good way to reach the characteristics of the Chalk aquifer on a few meters scale. The samplings in other areas at various periods of time will make possible the constitution of a data base necessary to the development of a hydrodynamic model for this aquifer.

6. Acknowledgements

The authors are grateful to Charbonnages de France (particularly Mr Blanchart) for their assistance and to Nord-Pas-de-Calais Region and the European Union for their financial support (contract n° 105/2638).

7. References

Barrez F., Mania J., Mansy J.L., Piwakowski B., Van Vliet-Lanoë B., Meilliez F. (2004) *Evolution piézométrique et hydrochimique de la nappe de la craie dans l'Ouest Douaisien.* Journées Nationales de Géotechnique et de Géologie de l'ingénieur, Lille, 8p.

Bernard D. (1979). *Contribution à l'étude hydrogéochimique de la nappe de la craie dans le Nord de la France. Etat et acquisition du chimisme de l'eau*. PhD Thesis, University of lille.

Caritat P. de, Danilova S., Jæger Ø., Reimann C., Storrø G. (1998). *Groundwater composition near the nickel-copper smelting industry on the Kola Peninsula, central Barents Region (NW Russia and NE Norway).* J. Hydrol., 208, 92-107.

Christensen T.H., Bjerg P.L., Banwart S.A., Jakobsen R., Heron G., Albrechtsen H.-J. (2000). *Characterization of redox conditions in groundwater contaminant plumes*. J. Contam. Hydrol., 45, 165-241.

Creasey C. L., Flegal A.R. (1999). *Elemental analyses of groundwater: demonstrated advantage of low-flow sampling and trace-metal clean techniques over standard techniques.* Hydrogeology Journal, 7, 164-167.

Denimal S., Tribovillard N., Barbecot F., Dever L. (2002). *Leaching of coal-mine tips (Nord-Pas-de-Calais) and sulphate transfer to the chalk aquifer: example of acid mine drainage in a buffered environment*. Environ. Geol. 42, 966-981.

Droz B. (1985). *Influence de la structure et de la nature des terrains du Valenciennois sur la qualité de la nappe de la craie (Nord de la France). Apport du krigeage à l'hydrochimie réginale et gestion qualitative des eaux souterraines.* Thesis, University of Lille.

Groffman A.R., Crossey L.J. (1999). *Transcient redox regimes in a shallow alluvial aquifer.* Chem. Geol., 161, 415-442.

Mariotti A., Landreau A., Simon B. (1988). *^{15}N isotope biogeochemistry and natural denitrification process in groundwater: application to the Chalk aquifer of northern France*. Geochim. Cosmochim. Acta, 52, 1869-1878.

Mariotti A. (1994). *Dénitrification in situ dans les eaux souterraines, processus naturels ou provoqués: une revue*. Hydrogéologie, 3, 43-68.

Pauwels H., Talbo H. (2004). *Nitrate concentration in wetlands: assessing the contribution of deeper groundwater from anions*. Water Research, 38, 1019-1025.

Puls R.W., Barcelona M.J. (1995). *Low-flow (minimal drawdown) ground-water sampling procedures.* U.S. Environmental Protection Agency Report EPA/540/S-95/504, 7p.

Puls R.W., Paul C.J. (1997). *Multi-layer sampling in conventional monitoring wells for improved estimation of vertical contaminant distributions and mass.* J. Contam. Hydrol., 25, 85-111.

Schürch M., Edmunds W.M., Buckley D. (2004). *Three-dimensional flow and trace metal mobility in shallow Chalk groundwater, Dorset, United Kingdom*. J. Hydrol., 292, 229-248.

Sterckeman T., Douay F., Proix N., Fourrier H. (2000). *Vertical distribution of Cd, Pb and Zn in soils near smelters in the North of France*. Environmental. Pollution, 107, 377-389.

Stumm W., Morgan J.J. (1981). *Aquatic Chemistry. An introduction emphasizing chemical equilibria in natural waters (2^{nd} Ed.).* Wiley-Interscience, 780p.

Thierrin J., Steffen P., Cornaz S., Vuataz F.D., Balderer W., Looser M. (2001). *Guide pratique de l'échantillonnage des eaux souterraines (rapport provisoire).* Office fédéral de l'environnement,

des forêts et du paysage, section protection des eaux et pêche (OFEFP)/Société suisse d'hydrogéologie (SSH), 56p.

Thullner M., Höhener P., Kinzelbach W., Zeyer J. (2000). *Validation of the dual pumping technique for level-determined groundwater sampling in a contaminated aquifer*. J. Hydrol., 235, 104-116.

Wilson N. (1995). *Soil and ground water sampling.* CRC Lewis Publishers, Boca Raton / London / Tokyo, 188 p.

SALT AND BRINE PRODUCTION METHODS IN FRANCE: MAIN CONCLUSIONS OF THE INTERNATIONAL GROUP OF EXPERTS (IEG) COMMISSIONED BY THE FRENCH REGULATORY AUTHORITIES

BÉREST Pierre[1], †DIAMOND Bill[2], DUQUESNOY Antoine[3], DURUP Gérard[4], FEUGA Bernard[5], LHOFF Lothar[6]

[1]LABORATOIRE DE MÉCANIQUE DES SOLIDES, École polytechnique - Route de Saclay - 91128 Palaiseau Cedex – France. berest@lms.polytechnique.fr

[2] SOLUTION MINING RESEARCH INSTITUTE – Past Executive Director

[3]GEO-ENGINEERING STATE SUPERVISION OF MINES - P.O. Box 8 2270 - AA Voorburg - The Netherlands. a.j.h.m.duquesnoy@minez.nl

[4]GAZ DE FRANCE - Direction Transport - Centre d'Expertise et de Services (DES-ST) - 91-98 Bd Victor Hugo - 92115 Clichy – France. gerard.durup@gazdefrance.com

[5]GEODERIS – BP 25198 – 57075 Metz Cedex 3 – France. bernard.feuga@industrie.gouv.fr

[6]LANDESBERGAMT CLAUSTHAL-ZELLERFELD - Hindenburgplatz 9 – Germany. lothar.lhoff@LBA.niedersachsen.de

ABSTRACT: The French authorities commissioned a group of experts to discuss trends in salt mining techniques (solution mining and dry mine) and abandonment methods. Safety margins in the stable caverns methods, methods in which caverns may become instable, methods including deliberate collapse were discussed; recommendations were provided on such topics as post-abandonment monitoring, risks related to a well crossing through the salt formation and the specific problems related to dry mines abandonment.

KEYWORDS: Brine production; Cavern abandonment; Salt mine abandonment; Salt caverns stability.

RESUME : Les autorités françaises ont demandé à un groupe d'experts de discuter les tendances actuelles dans les techniques de production du sel par dissolution ou par mine sèche, ainsi que les méthodes d'abandon correspondantes. Les marges de sécurité nécessaires à la création de cavernes stables, les méthodes dans lesquelles les cavernes peuvent devenir instables et celles dans lesquelles l'effondrement est délibérément recherché ont été examinées. Des recommandations ont été formulées quant à la surveillance postérieure à l'exploitation, aux risques associés à un sondage traversant la formation salifère, et aux problèmes particuliers soulevés par l'abandon des mines sèches.

MOTS-CLEFS : Production de saumure; abandon des cavernes souterraines; abandon des mines de sel; stabilité des cavernes dans le sel.

Preface

In Spring 2002, the French regulatory authorities commissioned an international group of experts (IEG) to prepare a report including descriptions of the major trends in salt mining techniques and abandonment methods, and giving recommendations with respect to France, with special emphasis on the long-term safety and environmental aspects of the Lorraine salt mining.

The six members of the IEG were Pierre Bérest, Bill Diamond, Gérard Durup, Antoine Duquesnoy, Bernard Feuga and Lothar Lhoff. The experts acted as individuals. Alain Buffet, a former engineer-geologist in a French salt mining company, and Ignace Salpeteur, acting as a scientific liaison with the contractor (BRGM) also took part in the IEG meetings.

The IEG had three plenary meetings in October 2002 at Bad Ischl (Austria), in December 2002 and February 2003 in Paris. Hearings of the solution mining companies operating in France were organized. The IEG invited several scientific experts to express their views. Comments from Yves Babot (Antea, France), Professor Emmanuel Ledoux (École des Mines de Paris, France), David Challinor (Great Britain), Andrzej Kunstman (Kemchop, Poland), Professor Pedro Ramirez (Madrid School of Mines, Spain) were especially helpful. Various working documents were prepared; one of these documents was presented during the Chester and Wichita SMRI Meetings (Bérest et al., 2003 and 2004). The French regulatory authorities (Paul Cattaert, Head of the Underground Mining Department, Ministry of Industry) gave permission to publish the Main Conclusions of the IEG Report. The present paper includes the Main Report of the IEG. A reference list, a paragraph on Lorraine dry salt mines and several figures were added.

Bill Diamond passed away a few days before the last IEG meeting. The IEG benefited from his spirit, his ethical sense and his remarkable knowledge of the salt industry. His loss was irretrievable for the IEG members, as it was for the salt community worldwide.

French salt deposits

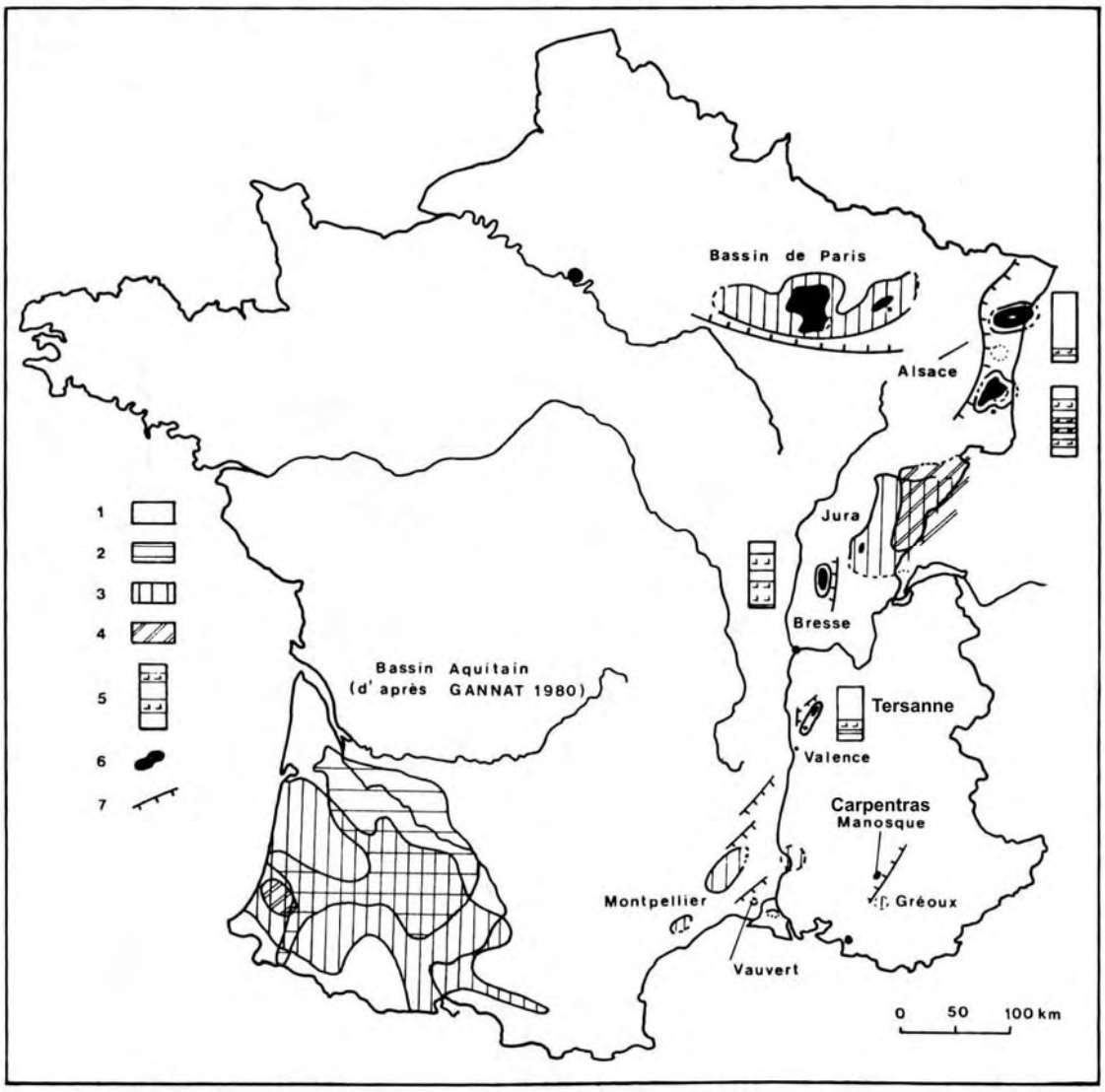


Figure 1. Main French salt deposits, after Friès et al. (1983). 1. Oligocene 2. Lias 3.Upper Trias 4. Middle Trias (Muschelkalk) 5.Existence of several distinct salt layers 6. Zones where storage can be considered (depth larger than 100m, smaller than 1600m, salt content larger than 80%)

The French salt deposits are represented on Figure 1. Solution Mining took place in several different districts. However brine production was most active by far in the shallow eastern fringe of the Lorraine salt deposit, 300 km east of Paris.

1. Introduction

The French regulatory authorities have commissioned an international group of experts (IEG) to prepare a report that includes descriptions of the major trends in salt-mining techniques and abandonment methods worldwide, and to provide recommendations, with respect to France, on the long-term safety and environmental aspects with a special emphasis on the Lorraine salt mining.

1.1. Introductory remarks

Salt production is a very old human activity. In China, solution mining has been performed for more than 20 centuries. Dry mines were opened during the Middle Ages in Austria and Poland, but salt was extracted during the Iron Age in Hallstatt, Austria. It was only during the XIX century that salt production became a truly industrial activity.

Dry mines in salt-bedded formations more often used the room-and-pillar method. Extraction ratios were quite high and often more than 80% at a 200-m depth. This ratio was too high, when compared to pillar, roof or floor strengths and frequently led to overburden collapse, or to partial roof failure often followed by mine flooding.

Brine production first began in natural salt-water springs; brine outlets were enlarged or deepened. Then brine was pumped out to increase the production rate; for this purpose, wells were equipped with a unique tube which, in most cases, was not cemented to the ground. Pumping led to groundwater flow to the roof of the salt formation. Soft water flowed down through the un-cemented annulus between the rock and the production well or entered the dissolution zone at the salt roof (brine aquifer) through discontinuities, either natural or induced by salt extraction. The origin of the soft water and the exact place where dissolution took place generally were unknown. The resulting dissolution was spread over a large horizontal area. Only a thin layer of salt was dissolved, and the process resulted in a trough of large horizontal extension at the surface, although trough depth and slopes were small. In fact, the consequences were often insignificant - except in some cases, when hydrogeological or topographical conditions allowed active dissolution even after deliberate pumping had stopped.

A higher salt-extraction ratio, by means of solution mining, was reached later, when deeper wells, penetrating inside the salt formation, allowed higher caverns to be created. The well was equipped with a tube whose shoe was significantly deeper than the salt roof depth. Brine was pumped out through this tube. Pumping drew soft water to the cavern; soft water flowed into the cavern from overlying water-bearing strata through the well external annulus, or was provided by the preexisting brine aquifer at the salt roof. Caverns enlarged as they moved upward through the salt mass and eventually reached the roof of the salt formation. In many cases, the upward migration of caverns resulted in overburden collapse when the roof span became large enough.

The extraction ratio was made still larger when neighboring individual caverns merged, as (often alternately) some wells could be used as injection wells, and other wells could be specialized as brine withdrawal wells. Hydrofraccing was sometimes used, allowing neighboring caverns to merge at an early stage of their development. Keeping the ground level stable was not given a high priority: caverns collapsed unexpectedly from time to time; the main concern was to extract as much salt as possible before ground movements became so large that the injection/withdrawal equipment was unusable. This method was accepted as long as the mining company was the landowner. When the company did not own the land, salt extraction tended to stop before being

completed, to keep the ground stable (according to the empirical rules progressively drawn from earlier local experience).

1.2. Recent evolution of brining techniques and environmental concerns

Large changes in production circumstances have been experienced in the past few decades, especially since the 70s.

The long-term consequences of underground activities raise greater public concern. Better environmental protection has become an objective widely shared by the public. This is especially true in densely inhabited areas of Europe, where mining has been active in the past. Mining companies are sensitive to these changes. Better long-term planning of land use is made more difficult when old mining works threaten the stability of large ground-surface areas.

Advances in basic knowledge and measurement techniques allow better control of cavern growth.

On the one hand, a large amount of empirical data is available: the conditions leading to undesirable situations are better understood and, more positively, the conditions allowing avoidance of undesirable situations are identified more clearly. On the other hand, geophysical investigation techniques have experienced very significant progress: they allow a better understanding of the hydrogeological and geological context. Cavern development can be controlled during the complete life cycle of a cavern. Routine use of sonar measurement is probably one of the most significant advances. Leveling techniques have become more accurate, and new progress may be expected from airborne measurements. The balance between injected and withdrawn fluid volumes, by recording the salt content in withdrawn brine, can be performed automatically at a low cost. The same is true for hydraulic head and salinity measurements performed in control wells. Numerical simulations and laboratory tests have reached a high standard of quality. The leaching process is simulated routinely when involving the most safety-demanding uses of solution-mined caverns (hydrocarbon storage). Stimulated by the research dedicated to nuclear waste disposal, rock mechanics use numerical simulation and benefit from advances in understanding the rheological behavior of rock salt and other evaporitic rocks.

These developments are available worldwide. The solution-mining industry is gathered globally in such organizations as the Solution Mining Research Institute (SMRI), whose membership includes most of the major companies in North America and Europe. Technical meetings are organized frequently and provide descriptions of successes and failures, information on recent innovations, scientific research, regulations and recommendations. The "state-of-the-art" is no longer a vague notion but, rather, the result of extended exchanges inside the international community.

1.3. Specific questions asked of the IEG

It is in the context of the changes presented above that the consequences of the long-term behavior of dry mines and brine fields must be addressed. The topics of interest in this report must be more precisely defined. Taking into account the history of salt production in France and the geological environment in Lorraine, we will focus on shallow caverns and mines (say, 200 m deep) dug out or leached out in bedded-salt formations. In sharp contrast with domal salt formations, these bedded-salt formations whose thickness is relatively small (approximately 100 m in Lorraine) are characterized by horizontal or sub-horizontal layers, including interbedded layers of rocks such as marls and anhydrite. The interbedded layers, whose periodicity is somewhat erratic, are from 1-mm to 10-m thick. Domal salt, which does not exhibit a marked horizontal stratification, raises very different problems: zones in which the salt is homogeneous can often be found in a salt dome.

The long-term behavior after abandonment is a problem common to any type of mine. However, salt mines (as well as potash or other evaporitic minerals) exhibit some specific features in this respect. Salt is an extremely soluble material; besides the underground geometric changes induced by the mined voids, one must also consider possible later changes induced by underground water flow taking place after mine abandonment. These changes include new groundwater flow, or a drastic increase of natural groundwater flow made possible by the existence of the mining openings or by the disorders the openings create in the natural state of the underground layers. These groundwater flows are able to generate active salt dissolution, even after salt production has been completed, leading to delayed but sometimes significant consequences for ground-level stability. Moreover, for dry mines, water flooding (which, in the long term, is unavoidable) may have more severe consequences than in the case of any other mineral substance: the depths of troughs or craters at surface is often much larger than the height of (underground) galleries; and they may appear in unexpected areas — even away from the horizontal contour of the mine, a feature rarely found in other mines.

1.4. Each site is specific

The IEG experts emphasize the fact that each site is specific. Automatically applying rules resulting from empirical experience drawn from one site to a new site is the exact opposite of good engineering practice. Site-specific geological and hydrogeological conditions, together with brining or mining methods, must be taken into account. However, the IEG experts are convinced that certain general lessons may be drawn from experience; these lessons are part of what is known as the "state of the art".

2. Brine production methods in Lorraine

At this step a brief description of the effects at the surface caused by the basic brine production methods is helpful (more precise explanation will be provided later):

- The “stable cavern” method leads to no significant ground movement during brine production or after the claim was classified. Long-term stability is certain.
- The “deliberate collapse” method leads to complete collapse of all the caverns (small or no voids are left). Collapse is completed during the brine production period.
- The “unstable cavern” method neither leads to complete cavern collapse nor to long-term stability.
- In the “wild brining” method, water inlet is not controlled, often resulting in an “unstable cavern”.

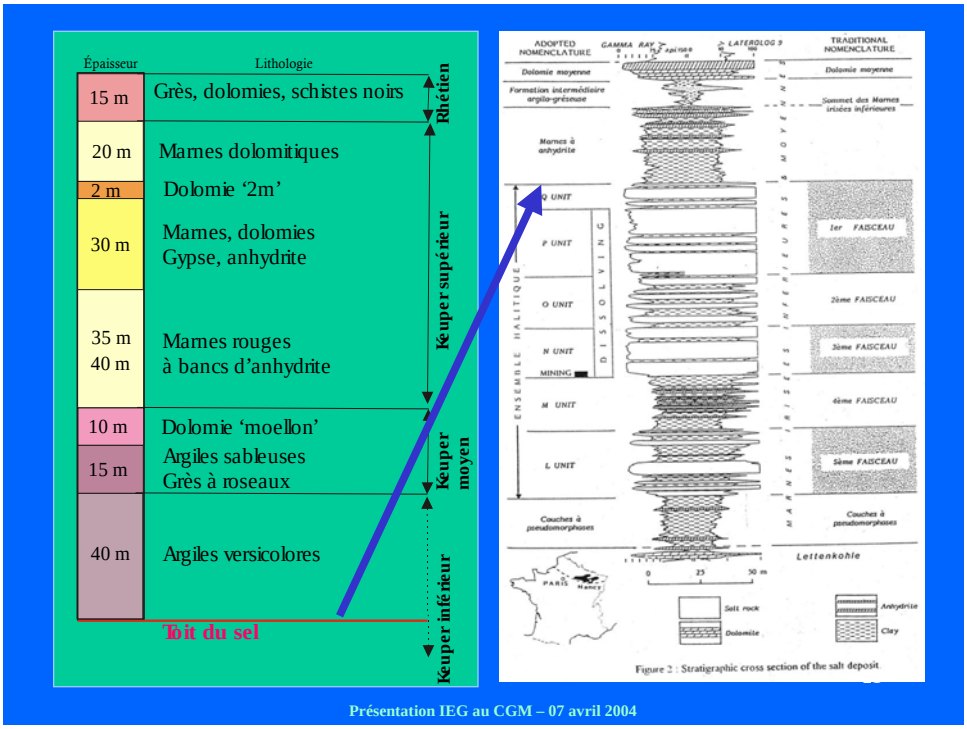


Figure 2. Lithologic description and layers denomination (after Marchal, 1982, modified). The seven dry mines opened in Lorraine are located in the lower part of the "3ème faisceau" (3rd unit, or N unit, or 11th layer), where the bottom of recent solution-mined cavern is also located. Cavern top may reach the top of the salt or Q unit. In such a case, stoping takes place up to the "Dolomie moyenne", often also called "Dolomie de Beaumont" (Beaumont Dolomite). Cratering takes place when this stiff layer is not able to withstand the overburden weight.

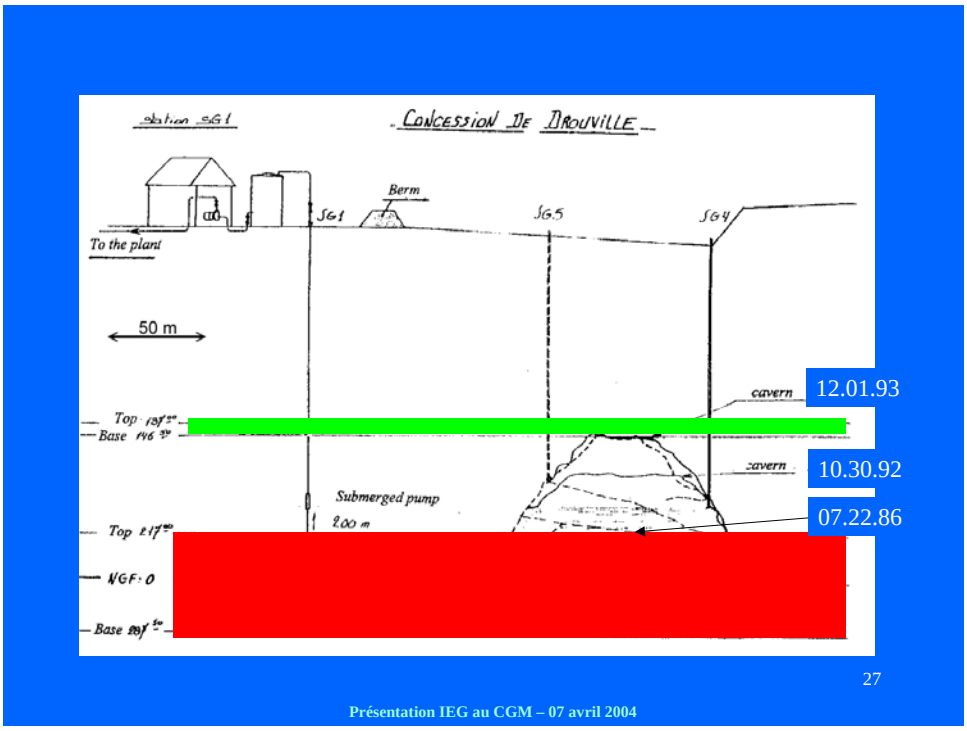


Figure 3 – In the case of the SG4-SG5 cavern, the cavern roof reached the Beaumont Dolomite layer by 1993 – Long-term stability could not be taken for granted, and it was decided to enlarge the cavern, which eventually collapsed (after Buffet, 1998).

2.1. "Stable Cavern" method

The "Stable Cavern" method, which is defined more precisely below, is the most widespread brining method. It is considered worldwide as an admissible brining option, provided that state-of-the-art practice, in a salt formation which allows operating according such a method, are applied during the design, operation and abandonment of the caverns. This method is the only considered brining option in such countries as the Netherlands or Germany. However, it must be noted that, even were these two countries considered to be comparable to France from the perspective of mining hazards and environmental protection, differences do exist: for instance, in Germany, salt (or potash) can be found in salt domes in which deeper cavern can be created; in the Netherlands, ground-level conservation is, in general, a more stringent constraint than it is in France. A precise definition of a “stable” cavern is needed at this step. The use of the term “stable cavern” implies underground openings whose existence has no practical adverse impact for the cavern environment from chemical, hydrological or mechanical perspectives. In other words, this method leads to negligible risks of:

- crater or sinkhole creation,
- significant subsidence, and
- contamination of drinkable water resources by underground salty waters.

The term "no practical adverse impact” is worth a comment here. In a closed and abandoned cavern, after thermal equilibrium is reached, pressure will slowly build up as cavern shrinks, due to salt creep. If the cavern remains perfectly tight, pressure ultimately will reach overburden pressure and the cavern will remain stable for an extremely long period. However caverns are likely not to be perfectly tight. In fact, it is likely that a closed cavern will release brine slowly and that the brine will seep to the surrounding salt mass or flow upward to an above lying aquifer, along the cemented access wells, even after the well has been plugged properly. In such a case, the cavern slowly shrinks, due to salt creep triggered by the gap between the overburden pressure at cavern depth and the brine pressure in the cavern. However, when the considered cavern is located at a shallow depth (say, less than 200 m below ground level), when it is properly designed, and when the extraction ratio is not too high, this closure process is so slow that its ultimate consequence (i.e., the complete closure of the cavern) will be reached only after a period of thousands or tens of thousands years. During this process, the cavern brine pressure will remain intermediate between the overburden pressure and the pressure resulting from a brine-filled column; as a result, brine will be expelled slowly from the cavern. Brine flow rates will remain small enough to ensure a large dilution of the brine. It is important, of course, to verify that no significant drinkable groundwater resource is available within a short distance from the cavern.

Even though this expert group emphasizes that each particular case must be thoroughly scrutinized, the IEG thinks that the consequences of the just-mentioned very long-term closure process, which are delayed and slow, need not to be taken into consideration. More generally, the IEG considers that the stable cavern method, when operated according to state-of-the-art practice in a salt formation which allows operating according to such a method, exhibits fewer drawbacks than production methods that lead to a deliberate collapse of the caverns.

2.2. Methods in which caverns may become unstable

The IEG is convinced that, according to today's standards, the worst method, by far, is any method leading to the creation of unstable caverns - i.e., caverns which did not collapse but whose geometrical shape, or location inside the salt mass, is such that collapse or severe subsidence may occur some day. Apart from the public safety, hydrogeological and environmental aspects, such a situation generates an unacceptable constraint for any further use of the ground surface. In fact, when a cavern appears unstable, two options may be considered: deliberate cavern collapse (However, the conditions leading to such a collapse are difficult to predict.); or monitoring the unstable cavern for an indefinite time (including the development of an emergency plan, in case rapid evolution occurs).

In the past, methods have been used that, though not deliberate, led to unstable caverns. Their associated risks should be eliminated before classifying the corresponding claim. These methods must not be accepted when considering present or future brine field operations. In principle, in such new fields, the stability prediction, made when production stops, must be certified and validated by the available scientific knowledge. Scenarios, prepared before cavern abandonment, should describe the evolution of such quantities as pressure build up, brine flow expelled from the cavern, surface subsidence, cavern shape or cavern roof location. These scenarios must be validated, within a small margin of uncertainty, through in-situ measurements performed for a sufficiently long period. In any case, there should be no chance of significant impacts on water resources.

2.3. Safety margins in the stable cavern method

When designing and operating a stable cavern, wide margins of safety must be included, and the transition from a "stable" to an "unstable" situation must be prevented. Such transitions have been observed before in Lorraine. A large margin of safety must be selected to avoid potential adverse consequences of incorrect assessment of the geological uncertainties, poor cavern operations or post-abandonment human activities. Prevention of such change requires the following.

2.3.1 Better understanding of the precise geometrical, mechanical, physical or chemical conditions leading to cavern collapse

This understanding, with regard to caverns in Lorraine, is insufficient at this time. It could be made significantly better if empirical data resulting from more than one century of brining operations, along with the lessons drawn from laboratory tests and numerical computations were used appropriately. It is desirable, from this perspective, that companies share the information they have gathered concerning actual collapses, their mechanisms, and the conditions that made them possible. Experts from universities or industry should be asked to analyse these empirical data. This information quite clearly does not belong to the expertise that must legitimately be protected. Clearly, gathering this information would be beneficial to the entire salt-mining industry. The paper by A. Buffet (1998), dedicated to the SG4-SG5 caverns collapse in the Gellenoncourt brine field, provides a good example of what can be achieved in this domain. It is also desirable that the hydrous, mechanical, chemical and geometrical conditions leading to collapse be clarified. The IEG feels that, in this respect, old beliefs transmitted through oral tradition prevail over explanations that are more scientific. The IEG heard several foreign experts who stated that understanding of cavern collapse conditions was a concern in many brine fields; current advances in several Earth-Science domains indicate that conclusive results can be achieved. Significant results are still available. Such scientific efforts will solidify a solid base for such issues as operating parameters, maximum horizontal cavern size, thickness of the salt slab left at cavern roof, cavern spacing, etc.

2.3.2 Conservative application of rules

Before standard designing rules resulting from scientific studies become available, and before empirical lessons can be drawn from the operation of caverns using the new brining methods proposed by the companies in Lorraine, the IEG strongly suggests that the rules proposed today be applied in a conservative manner. Results from recent studies conducted by École des Mines de Paris (Vouille, 1999; Humbert and Vouille, 2001) provide some insight in this regard.

The expert group emphasized that each site is specific. Rock properties are far from being identical when distinct sites are considered. Advances had been and will be experienced in the understanding of the mechanical behaviour of rocks. The IEG thought that it was not in charge of providing precise dimensioning rules but, rather, of assessing the methods used by the companies and their consistency with the state of the art.

Underground caverns and galleries generally are dimensioned through a comparison between the rock strength – as measured in the laboratory – and the (as computed) stress distribution that results from excavation. This method is not well suited to the case of a viscoplastic rock (as rock salt definitely is), as the above-mentioned rock strength is measured through "instantaneous" tests and does not account for the long-term behaviour of the rock. Experts prefer tracking the "onset of dilatancy" during triaxial lab tests; the onset of dilatancy (or irreversible increase of the sample volume) provides a value of the stress boundary below which it is generally considered that long term stability of the rock is certain. This stability domain is generally expressed in terms of the "deviatoric stress" (which is larger when the state of stress is far from isotropic) and the "mean stress".

In the above-mentioned studies, the deviatoric stress is used as a criterion to define the stability domain. The numerically-computed state of stress in the rock mass must belong to this stability domain - except maybe in small zones at the vicinity of the cavern wall. Furthermore, a large safety margin (say, from 1.6 to 2) - must be respected inside a pillar between two neighbouring caverns. In the mentioned studies, the safety margin is taken as the ratio between the measured dilatancy boundary stress and the computed deviatoric stress.

It is mentioned that the deviatoric stress must remain smaller than 9 MPa (the dilatancy boundary stress) and cavern dimensioning is such that the computed deviatoric stress in the pillar is kept significantly smaller than this 9 MPa limit. The experts think that the method used in the reports is compatible with the state-of-the-art and that the proposed dimensions and figures, that the IEG did not try to validate, are not unreasonable. A practical consequence of these figures is that 80 meters appear as a reasonable value for the maximal horizontal extension of the caverns and that 40 meters is an admissible minimal distance between two caverns.

The salt roof thickness left between the top of the cavern and the roof of the salt formation is an important parameter in the case of the Lorraine salt caverns: a direct contact between cavern brine and above-lying marly layers results in weathering of these layers. Computations prove than a relatively thin salt layer (2.5 metres) is enough to provide mechanical stability. However geological uncertainties (for instance, when salt roof location is concerned) remain, and a safety margin must be kept. A salt thickness of approximately 10 meters must be kept, as a direct contact between brine and marly layers must absolutely be avoided.

In one of the mentioned studies (Humbert and Vouille, 2001), the strength of the rock layer below the base of the third unit (eleventh layer) is considered to be very weak, and the authors suggested to leave a thick salt slab below cavern bottom. This suggestion would imply that solution-mining of the base of the third unit (eleventh layer) cannot be allowed anymore. The IEG is not completely

convinced that forbidding solution-mining of the base of the third unit (eleventh layer) is necessary from a stability point of view.

The experts believe that the dimensioning methods exposed in the above-mentioned reports are consistent with the state-of-the-art. The recommended criteria are in the same range as what is suggested elsewhere. These criteria should be reassessed when sufficient experience is available, and when a good fit has been observed between predictions and observations for such phenomena as ground-surface subsidence, cavern-shape evolution and evolution rate, etc.

2.3.3 Use of Adequate Measurement Techniques

Adequate measurement techniques, defined by the state-of-the art and the recommendations issued by the solution-mining industry, must be used. The objective is to check, as often as appropriate, that the observed evolutions match the predictions. The IEG emphasizes the importance of at least two logs, the sonar survey and the gamma ray log. These logs allow to monitor cavern shape and cavern roof location. A reasonable frequency for a sonar survey is one year (one month for a gamma ray survey), but the actual frequency must be based on such considerations as cavern size and shape. Had these types of frequent measurements been performed in the past, several problematic evolutions could have been avoided. For good monitoring results, the leaching process must be performed such that the cavern shape remains simple, so that a complete picture of the cavern can be achieved through a sonar survey. The injected water volume/withdrawn brine volume must be balanced and the volumes compared thoroughly to detect any anomalous evolution as early as possible. With regard to levelling measurements, it is better that a reference state (before brine-field operation begins) be available. Levelling must follow recommendations such as those issued by the SMRI. Measurement frequency must be adapted to the salt production rate, cavern size and cavern growth rate, and it must take into account the lessons drawn from experience. The frequencies suggested above are considered as a mean reasonable value; the IEG thinks that frequencies much lower than these would be unwise.

Generally speaking, the IEG is convinced that applying the above-mentioned rules and procedures will allow "stable" caverns to be created.

2.4. Deliberate collapse

“Intensive” or “par pistes intensives” methods - or, more precisely, “deliberate collapse” methods, which allow to focus salt extraction and some of its drawbacks in a small area, are being used in Lorraine. These methods are not widely used in other countries, where cavern collapse usually is seen as an undesirable exception to good mining practice. Intensive methods have several drawbacks, some of which are certain, while others are potential. These methods lead to irreversible changes in the ground surface. The consequences of such changes must be examined on a case-by-case basis (some of its drawbacks can be mitigated) and be assessed by taking into account not only the ground-surface uses no longer possible today, but also the uses that may be not be possible in the long term (say, for instance, in several decades). The IEG did not try to perform such assessments for the existing brine fields, as the group was told that the consequences were not considered to be inadmissible.

Rather, the IEG focused on the potential hazards possibly raised by the creation of opened vertical discontinuities resulting from cavern collapse. These may include uncontrolled dissolution because of either shallow water flow to a collapsed area (funnel effect) or soft groundwater flow from shallow water-bearing strata to the roof of the salt formation through the collapsed chimney. Some obstacles to such a large water flow do exist and, first of all, the density of the brine resulting from

salt leaching. It is likely that the changes will often be negligible; however, the IEG did question hydrogeologists, who stated that precise and certain predictions in this domain are still out of reach when long-term predictions are concerned. The existence of a salt roof dip, or the existence of (even small) hydraulic head gradients can promote change that can have a significant accumulated effect even after long periods. There exist several cases, some of them being well-documented, in which unexpected dissolution took place at a distance from the collapsed areas; they were generated by fluid flow at the salt roof that collapse had made possible. With regard to the Lorraine case, the IEG examined the existing brine fields operated according to the "intensive" method, as well as the conditions that would allow such brine fields to be opened in the future. When existing brine fields are considered, two local factors must be taken into account:

- the company that plans to use the intensive method seems to be able to support its prediction by a large amount of empirical data accumulated over several decades (This experience provides some credibility for its prediction — for example, when conditions leading to cavern collapse are considered.); and
- no significant amount of drinkable water exists above the salt formation. (However, such a method requires that attention be paid to the creation of uncontrolled water flow. Hydrogeological studies have already been performed, and the IEG strongly suggests that these efforts be continued and that, in particular, the hydrogeological role of the crater in its environment be clarified. These efforts must be integrated in a study of the relations between aquifer layers at the scale of the whole hydrogeological system There should be no doubt concerning the long-term evolution of the voids.)



Figure 4 - Haraucourt Brine Field (courtesy Solvay Company)

Generally, when considering the licensing of future brine fields that will use the intensive method, the following criteria must be met.

1. The conditions leading to cavern collapse must be identified clearly. Only a small amount of uncertainty is acceptable.

2. It must be proven that the geological and hydrogeological context will not allow the development of later dissolution near, or at a distance from, the collapsed caverns.
3. It must be determined that, after the collapse of the caverns, appropriate remediation of the ground surface is possible and that the cavern collapse does not impair foreseeable ground uses.
4. No drinkable-water resource must be threatened by the consequences of the brining operation.
5. Public safety near the collapsed cavern must be guaranteed.
6. Public safety and water-resource conservation cannot rely on the maintenance of permanent works or the injection or withdrawal of fluids for an indefinite time.

2.5. Wild brining, hydrofraccing

Brining methods based on direct inflow of groundwater in the salt formation is called "wild brining". These methods lead to risks of later collapse or significant cumulated subsidence, whose occurrence or exact localization cannot be predicted. The IEG advises against all variations of wild brining methods. In Lorraine, one production operation can be considered a wild brining operation. This operation should be converted, as soon as possible, into a more controlled brining activity - one in which the company has better insight as to where the brine comes from. Another technique leading to uncontrolled production conditions is hydrofraccing, which also should be prohibited.[In Lorraine, hydrofraccing was prohibited several years ago].

3. Post-abandonment monitoring (all methods)

After brining has been completed, the brine production fields must be monitored for a long-enough period to verify that unfavourable mechanical or hydrogeological change has not occurred and that the predictions performed before abandonment fit the observed changes. In the Netherlands, the monitoring period is 30 years. The IEG recommends that the monitoring period be at least 20 years. One important objective will be to verify that there is a good fit between predicted and observed changes. In many countries (the Netherlands, Spain and the USA's New York State, Tully brine field – see Briggs and Sanford, 2000), an abandonment plan is submitted to the mining authorities before brining is completed. This plan includes a prediction of the expected changes over 2 or 3 decades. An objective of the measurement program is to check that observed data fit these predictions. The plan may make a provision for re-evaluation of the measurement frequency, in one direction or the other, whenever the observed results suggest that it is needed. Parameters to be measured include surface levelling, which is an important parameter and relatively easy to measure. Very slow ground-surface changes are expected when the brining methods proposed by the Lorraine companies are considered. The IEG strongly recommends that such abandonment plans be made mandatory

For stable caverns, it is generally accepted that, in a group of hydraulically connected caverns, at least one well must remained open (unplugged). This is necessary at least for two reasons. On one hand, cavern-brine warming must be expected, as the temperature of the injected water is in many cases significantly colder than the rock mass at cavern depth; this heating process will continue over a long period — especially when the cavern is large. Such warming, which is recorded through thermometers set inside the cavern, generates brine thermal expansion and pressure build-up in a closed cavern. From time to time, the cavern must be vented through the unplugged well to prevent too high a pressure build-up. The effects of this warming must disappear before the remaining open wells can be unplugged.

On the other hand, pressure and temperature changes, ground displacements, will be predicted through computations before abandonment. Measurements performed after abandonment will allow to validate these predictions. Changes in pressure build-up will result both from brine warming and cavern creep, and the respective parts taken by these two mechanisms must be assessed correctly. It is suggested that these measurements, which are extremely useful but indirect or global, be complemented by further measurements that will verify that no unexpected cavern change takes place. In the wells to be kept open will be performed sonar measurement and logs (such as the gamma-ray log) to provide local information. Companies also must keep informed of any technical advances that could help to confirm the long-term prediction and provide solid information should claim classification be required. The abandonment plan must also define the monitoring of water-bearing strata near the caverns. Wells will be used to make piezometric recordings, and the water salt content as a function of depth will be measured periodically. Here, again, a prediction of the expected changes must be provided before brining is completed. For intensive brine fields, special attention must be paid to the hydrogeological parameters, as risk to groundwater flow is of utmost importance. The abandonment plan will describe site reclamation.

The experts ask themselves whether or not they should suggest how long a period of time predictions must consider. This question is related to the responsibility our societies accept toward future generations and, as such, is far beyond the scope of this report. The IEG tried to assess the credibility of long-term predictions. The IEG thinks that, based on a 20-30 year long monitoring period, quantitative predictions can be made for a one century-long period of time; and that qualitative predictions (the sense of the evolution of the main phenomena) can be made for a several-centuries long period of time.

4. Risks related to a well crossing through the salt formation

In many cases, a bedded-salt formation is protected from above- and under-lying groundwater by impervious layers. Even though the hydraulic heads of various aquifers are not uniform, no water flow can take place through the salt formation. The same can be said when a properly cased and cemented well crosses through the salt formation. However, improper cementing, steel corrosion, etc., may lead to downward or upward water flow along the well. In such cases, salt dissolution , cavern creation, and contamination of water-bearing layers, are made possible. Such a risk is not directly related to salt mining or cavern brining but it is of importance in Lorraine, and the IEG felt it was helpful to draw attention to it. Subsidence provoked by such a mechanism occurred once in Lorraine. Provisions should be made to prevent such accidents.

This paragraph, that illustrates the possible effect of a poorly abandoned well crossing through a salt formation, is not part of the IEG report. In the case of the famous Haoud Berkaoui collapse, the Albian aquifer hydraulic head is larger than the surface aquifer head by 2.5 MPa (Figure 5). A well was drilled to a depth of 2500 m. The well was abandoned inadequately and water began to flow from the Albian aquifer to the surface aquifer, leaching the salt formation and progressively creating a large cavern (Morisseau, 2000). A similar phenomenon was experienced at Dieuze in Lorraine (Bérest et al., 2004); however consequences were much less severe.

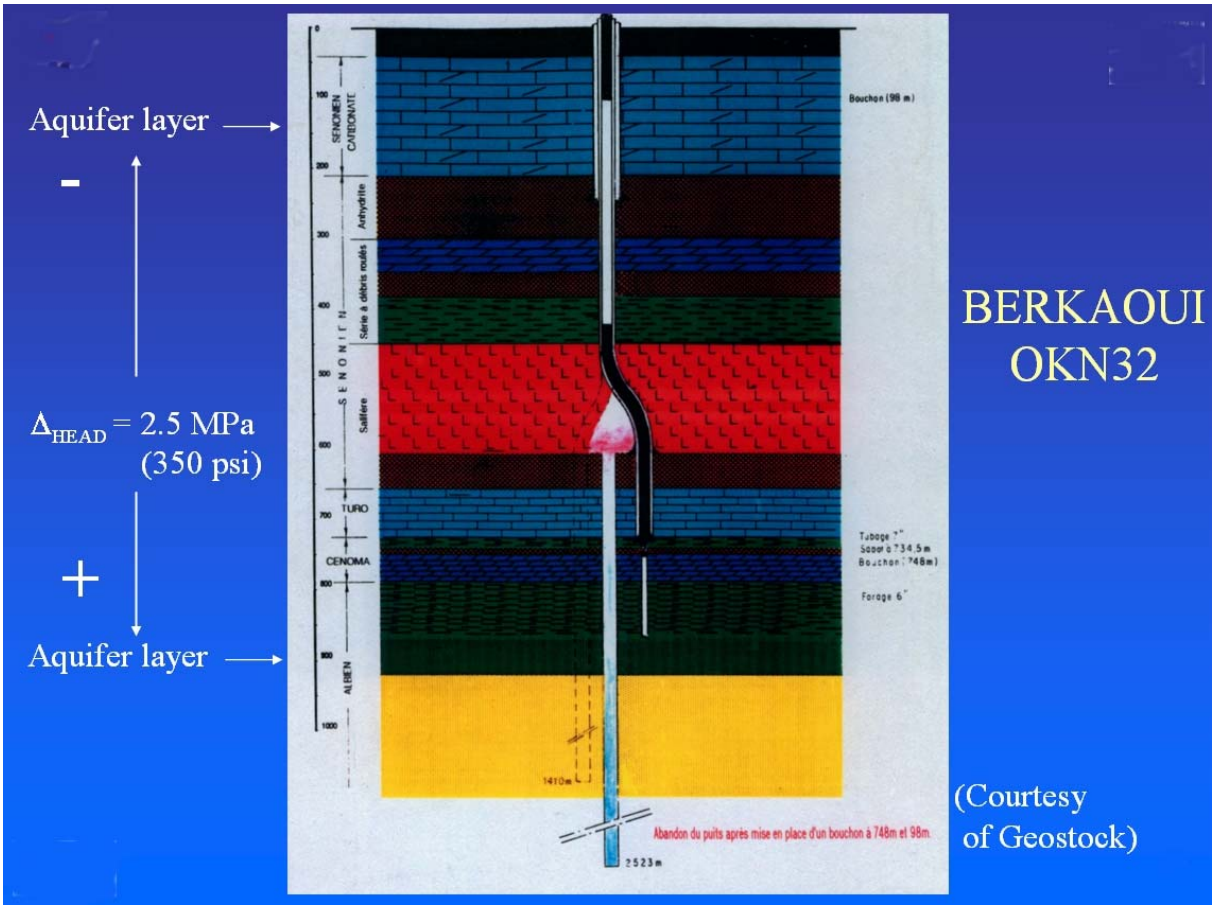


Figure 5 – Haoud Berkaoui collapse

5. Dry mines abandonment

The IEG was asked to provide an opinion regarding dry-mine abandonment. Two dry mines still exist in Lorraine: the Varangéville Mine and the Einville Mine. The Varangéville Mine is still active. Mining works are separated from above-lying groundwater by 60 m of salt and poorly permeable layers. The extraction ratio, particularly below densely inhabited areas, is small, except in old panels below less densely inhabited areas. It is recommended that, within a couple of years, studies be performed to define an abandonment method. The smaller Einville Mine causes more immediate concerns. It has been inactive for more than 50 years. The extraction ratio was large, and, in some places, only a thin layer of salt was left between the mining voids and the overlying water-bearing strata; wild brining takes place within a small distance. An abandonment method must be defined and implemented as soon as possible. The IEG collected information related to mine-flooding accidents and dry-mine abandonment methods in other countries. This information can be found in Annex 2.1. Main conclusions are briefly summarized below.

Mine flooding is a very common — but often unexpected — accident. Water or brine inflow, which, in many cases, remains low for long periods, may increase suddenly and so rapidly that no control is possible. Flooding results in intense and localized salt dissolution, as well as in the creation of sinkholes that can be significantly deeper than the mine height. It has been observed, at least in domal salt (but also in the Dieuze Mine, in the Moselle *département*), that the major part of the mine is more stable after flooding than it had been before flooding. Four abandonment methods can be considered:

- deliberate collapse of the mine;

- filling the mine with solid debris (and brine);
- shaft plugging and/or monitoring of the site; and
- flooding of the mine with water or brine.

Deliberate collapse is often difficult to plan and perform, as an exact assessment of mine stability is difficult. Filling the mine with debris is extremely costly in most cases. Shaft plugging is a difficult task when long-term tightness is desired; no definite end of the monitoring period can be predicted. Monitoring does not address the main concern of what must be done when water inflow appears. Deliberate flooding before abandonment has several significant advantages. The risk of later groundwater movement to the mine is lowered considerably, and the mine is more stable when the mine and the shafts are filled with brine. The IEG observed that mine flooding before abandonment is mandatory in salt domes in northern Germany. The existence of marly layers in the Lorraine mine environment raises some concerns, as these layers may become significantly weathered when in contact with water or brine, making deliberate flooding less favorable. Field data, however, are not completely conclusive: for instance, the old Dieuze Mine remained intact more than a century after being flooded. The IEG strongly recommends that further studies be performed to assess the deliberate-flooding option. With regard to Einville, the IEG suggests that these actions be given a high priority.

6. Conclusions and recommendations

1. The primary conclusion of the IEG is that the stable cavern method is considered to the most desirable brining method worldwide. When properly applied, it has negligible safety and environmental risks in the long term provided that the local conditions and operating methods be taken into consideration.

2. The wild brining method is an uncontrollable mining method that does not comply with recent evolutions in brining techniques. Existing wild brining activity must be converted to controlled activity.

3. The development of a deliberately collapsed cavern as a standard method (intensive method which allows high extraction ratios) creates a barrier to any future economical use of the ground surface, apart from safety, hydrogeological and environmental aspects. When the intensive brining method which allows using high extraction ratio, is permitted, several requirements must be taken into account, such as accurate prediction of the cavern collapse, absence of future harm to regional drinkable-water resources or future uncontrolled dissolution favored by the existence of the crater, and lack of needed permanent remedial measures.

4. The worst case is that of a cavern designed to remain stable but which degenerates into an unstable cavern. This case - which did exist in Lorraine- must be avoided absolutely in the future, which implies the following :

    a. Cavern development must be controlled during its complete life cycle (via routine control techniques like sonar and gamma ray logging, which currently are available).

    b. Conditions leading to cavern collapse in Lorraine should be understood sufficiently; lessons should be learned from the operations of the salt companies that were or are active in Lorraine, leading to better scientific knowledge.

c. In order to create inherently stable caverns, specific dimensioning rules should be implemented. Such rules have been suggested in the report.

d. Long-term predictions must be founded on a sound scientific basis.

e. Long-term predictions formulated when cavern brining is completed must be supported by later observations performed during a 20-30 year monitoring period.

f. Quantitative predictions can cover a period of at least one century when (e) has been properly performed

g. Qualitative considerations can be made for a period of several centuries after cavern abandonment.

5. An abandonment plan, including description of leveling, pressure and temperature measurements, backfilling, remediation, etc., must be submitted to the authorities before brine field abandonment. The plan must specify expected changes of the measured parameters to allow for comparison with observed changes.

6. In countries other than France, deliberate-flooding of dry mines is considered the best option for domal salt. For the case of bedded salt, studies must be performed to assess the adverse impact of mine flooding on mine stability.

7. References

Archives CSMSE - *Note sur l'accident de 1873 à la mine de Varangéville*. Archives of Compagnie des Salins du Midi et des Salines de l'Est ("A note on the 1873 Varangéville Mine accident", unpublished.)

Bauer S.J., Ehgartner B.L., Neal J.T. (2000) - *Geotechnical Studies Associated with Decommissioning the Strategic Petroleum Reserve Facility at Weeks Island, Louisiana : A Case History*. Proc. Technical Class and Technical Session SMRI Fall Meeting, San Antonio, p. 146-156.

Bekendam R., Oldenziel C., Paar W. (2000) –*Subsidence Potential of the Hengelo Brine Field (Part I). Physico-Chemical Deterioration and Mechanical Failure of Salt Cavern Roof Layers.* Proc. Technical Class and Technical Session SMRI Fall Meeting, San Antonio, p. 103-118.

Briggs P., Sanford K. (2000). *The Ups and Downs of Post-Closure Subsidence Monitoring at the Tully Valley Brine Field, New York.* Proc. Technical Class and Technical Session SMRI Fall Meeting, San Antonio, p.57-74.

Buffet A. (1998) - *The collapse of Compagnie des Salins SG4 and SG5 drillings.* Proc. SMRI Fall Meeting, Roma, p. 79-105.

Buffet A., Hilly J., Marchal C. (1993) – *Relationship between the Composition of Raw Brines Originating from the Mining of Lorraine Salt Rock (NE France) and the Lithology of the Deposit*. Proc. 7th Symp. on Salt, Kyoto, H. Kakihana, H.R. Hardy Jr, T. Hoshi, K. Toyokura eds., Elsevier, Vol. I, p.195-204.

Carosella M.E. (1978) - *The Use of Salt Domes for the Strategic Petroleum Reserve*. Proc. 5th Symp. on Salt , A.H. Coogan and L. Hauber ed., Northern Ohio Geological Society Inc. Pub., Vol. II, p. 69-75.

Cochran, M.H. (2004). *Conceptual changes to Kansas Department of Health and Environment salt dissolution mining regulations article 43*. Proc. SMRI Spring Meeting, Wichita, p.133-136.

Cosenza P. (1996) - *Sur les couplages entre comportement mécanique et processus de transfert de masse dans le sel gemme*. Thesis, Paris VI University ("Coupling between Mechanical Behaviour and Mass Transfer in Rock Salt")

DARPMI (2001) Direction de l'Action Régionale et de la Petite et Moyenne Industrie, Ministère de l'Economie et des Finances – *L'après-mine de sel en France* - ("Post Salt-Mining in France", Internal Report, February 2001, unpublished.)

Duffaut P., Bonvallet J. (1979) - *Mine de sel de Varangéville. Poursuite de l'exploitation dans la concession Rhône-Poulenc*. BRGM Report, n° 79 SGN 708 GEG, prepared for the French Ministry of the Industry, unpublished.

Feuga B. (2003) - *Old salt mine at Dieuze (France) revisited 150 years after being abandoned*. Proc. SMRI Fall Meeting, Chester.

Fokker P., Steeneken P., Kruse G.A.M. (2000) - *Predictable and Manageable Subsidence above Deep Salt Caverns*. Proc. Technical Class and Technical Session, SMRI Fall Meeting, San Antonio, p.209-216.

Friès G., Bérest P., Beaudoin B. (1983) - *Eléments d'un inventaire des gisements de sel français* - Annales des Mines (Paris), May-June 1983, p. 39 – 46 (Elements of an inventory of the French Salt Deposits)

Gendzwill D.J., Prugger F.F. (1990) - *Seismic activity in a flooded Saskatchewan potash mine*. In C. Fairhurst, editor, Proc. 2nd Int. Symp. on Rockbursts and Seismicity in Mines, Minneapolis, 8-10 June 1988, Balkema, Rotterdam, p. 115-120.

Gowan S.W., Trader S.M., Van Sambeek L.L. (1999) - *The discovery of an apparent brine pool associated with anomalous closure patterns and the eventual failure of the Retsof salt mine*. Proc. S.M.R.I. Fall Meeting, Washington DC, p. 241-272.

Gowan S.W., Trader S. (2000) - *The mechanism of sinkhole formation above the collapse of a small yield-pillar panel in the Retsof salt mine*. Proc. Technical Class and Technical Session, SMRI Fall Meeting, San Antonio, p. 313-332.

Griffith A.E. (1991) - *Tennant's ills*. Ground Engineering, November 1991, p.18-21

Hoffman E.L., Ehgartner B.L. (1997) - *Using Three Dimensional Structural Simulations to Study the Interactions of Multiple Excavations in Salt*. SAND 97-1017C Report, Sandia National Laboratories, Albuquerque, N.M.

Jeremic M.L. (1994) - *Rock Mechanics in Salt Mining*. A.A. Balkema, Rotterdam, 532 pages.

Johnson K.S., Gonzales S. (1978) – *Salt deposits in the United States and Regional Geological Characteristics Important for Storage of Radioactive Waste*. Y/OWI/SUB-7414/1 Report, Office of Waste Isolation (OWI), US-DOE, Earth Resource Associates, Inc., Athens, GA, p. 60.

Johnston K.S. (2001) - *Sinkholes associated with Petroleum Boreholes Drilled Through Salt Deposits in the USA*. Proc. SMRI Fall Meeting, Albuquerque, p.8-17.

Kunstman A.S., Urbanczyk K.M. (2003) - *Catastrophic flooding of Wapno salt Mine (1977) and controlled flooding of Solno Mine (1986-1991) – reasons, circumstances, consequences*. Proc. SMRI Fall Meeting, Chester.

Kupfer D.H. (1980) - *Problems associated with Anomalous Zones in Louisiana Salt Stocks, USA*. Proc. 5th Symp. on Salt, Hamburg, May-June 1979, The Northern Ohio Geological Society, Inc., Vol. II, p. 119-134.

Lolan W.E., Valadie R.J., Ballou P.J. (1998) - *Remote Operated Vehicle (ROV) Design, Cavern Survey and Gel Plugging Agent Application to Repair Louisiana Offshore Oil Port (LOOP) Cavern 14*. Proc. SMRI Fall Meeting, Roma, p. 327-345.

Maas K. (2001) - *Analysis, Modelling and Simulation of recent Subrosion in a flooded Potash Shaft*. Proc. SMRI Fall Meeting, Albuquerque, p. 272-281

.

McCauley T.V., Ratigan J.L., Sydansk R.D., Wilson S.D. (1998) - *Characterization of the Brine Loss Zone and Development of a Polymer Gel Plugging Agent to Repair Louisiana Offshore Oil Port (LOOP) Cavern 14*. Proc. SMRI Fall Meeting, Roma, p. 391-406.

Marchal C. (1982) – *Le gîte salifère keupérien de Lorraine-Champagne et les formations associées - Étude géométrique - Implications génétiques*. Thesis, Nancy I University (The Keuper salt deposit of Lorraine-Champagne and associated formations – Geometrical study – Genetic implications)

Minoux G. (1956) - *Programme technique pour l'exécution d'un forage AEP de l'Usine Kuhlman.* BRGM (Regional Service of Lorraine) report n° A 938 (Technical program for a water well drilling in the Kuhlman factory, in French, unpublished).

Morisseau J.M. (2000) - *Uncontrolled leaching of salt layer in an oil field in Algeria*. Proc. Technical Class and Technical Session, SMRI Fall Meeting, San Antonio, p. 330-333

Nichols N.W, Wu K.K., Kravitz J.H., O'Gorman F.E., Risbeck J.S., Durfee J.W., Wilcox W.R., Feehan R.D., Lilly D.P. (1981) - *The Jefferson Island Mine Inundation, November 20, 1980*. Mine Safety and Health Administration, U.S. Department of Labour, Report n° 202 031 (131 p.)

O'Gorman F., Stafford S. (1980) - *Jefferson Island: when courage, training, saved 52 in mine flood*. Mine Safety and Health Administration, U.S. Department of Labour, Report n° 205 957 (6 p.)

Payment K.A. (2000) - *Loss of the Retsof salt mine: legal analysis of liability issues*. In R.M. Geertma, editor, Proc. 8th World Salt Symp., Salt 2000, The Hague, The Netherlands, Elsevier Science publishers B.V., Amsterdam, Vol. I, p. 399-404.

Poyer C., Cochran M. (2003) - *Kansas Underground Storage Regulations*. Proc. SMRI Fall Meeting, Houston, p.199-204.

Prugger F.F. (1980) - *The flooding of the Cominco potash mine and its rehabilitation*. Proc. 5th Symp. on Salt, Hamburg, May-June 1979, The Northern Ohio Geological Society, Inc., Vol. I, p. 333-340.

Rölleke F.J. (2000) - *Subsidence and Sinkholes over Flooded Potash Mines in Northern Germany*. Proc. Technical Class and Technical Session, SMRI Fall Meeting, San Antonio, p. 87-101.

Spiers C.J., Urai J.L, Lister G.S., Boland J.N., Zwart H.J. (1986) - *Long-term rheological and transport properties of dry and wet salt rocks*. Final Report, Commission of the European Communities, EUR 11848.

Thoma H., Seifert G., Kuehn F. (2000) - *Examples of the Development of Sinkholes above Flooding or Flooded Salt Mines in Central Germany and Ways of Remote Detection of Areas with a Potential Risk of Fall.* Proc. Technical Class and Technical Session, SMRI Fall Meeting, San Antonio, p. 163-184.

Thoms R.L., Gehle R.M. (1994) - *The Jefferson Island mine flooding revisited*. SMRI Spring Meeting, Houston.

Thoms R.L., Gehle R.M (2000) - *Winnfield mine flooding and collapse event of 1965*. Proc. Technical Class and Technical Session, SMRI Fall Meeting, San Antonio, p. 262-274.

Van Sambeek L.L. (1996) - *Dissolution-induced mine subsidence at the Retsof salt mine*. Proc. SMRI Fall Meeting, Cleveland, p. 289-309.

Van Sambeek L., Thoms R. (2000) - *Pre- and Post-Flooding Surface Subsidence Rates at the Retsof, Belle Isle, Jefferson Island Salt Mines*. Proc. Technical Class and Technical Session, SMRI Fall Meeting, San Antonio, p. 75-85.

Van Sambeek L.L. (1993) - *The IMC K2 Mine Flooding*. SMRI Fall Meeting, La Fayette.

Van Sambeek L. *An introduction to Subsidence Over Salt and Potash Mining Facilities*. Proc. Technical Class and Technical Session SMRI Fall Meeting, San Antonio , p.1-10.

Van Sambeek L. (2000) - *Subsidence Modelling and the use of the SMRI SALT_SUB SID Software*. Proc. Technical Class and Technical Session, SMRI Fall Meeting, San Antonio, p. 11-22.

Van Sambeek L.L., Gowan S.W., Payment K.A. (2000) - *Loss of the Retsof salt mine: Engineering analysis*. Proc. 8th World Salt Symposium, Salt 2000, The Hague, Netherlands, Elsevier Science Pub. B.V., Amsterdam, Vol. I, p. 411-416.

Vouille G. (2001) - Communication to the GEODERIS Salt Expert Group, Metz, France. Unpublished

Walters R.F. (1978) - Land subsidence in Central Kansas Related to Salt Dissolution. Kansas Geological Survey Bull. 214, p.1-81.

Wilhelm St., Poppei J., Mayer G., Schwarz R., Klubertanz G., Siegel P., Förster B. (2002) - Influence of chemical reactions on the flow system and contaminant transport in a former salt mine. Proc. Int. Conf. Uranium Mining and Hydrogeology III. Freiberg, Sept. 2002.

8. Addendum : Lorraine dry mines

This paragraph is not part of the IEG report. It was added for the reader's information.

Seven dry mines were opened in Lorraine, all of them located in the lower part of the 11th layer (see figure 2). In fact two shafts were dug out at Tonnoy and Crevic, but no mine was worked from these two shafts. The Vic-sur-Seille Mine, opened in 1821, was abandoned a few years later, because water or unsaturated brine inflow could not be controlled. The Dieuze Mine, whose roof was 115 m deep, was flooded by saturated brine in 1864. In 2002 a sonar survey from a borehole drilled to the mine (figure 6) showed that it was in very good condition (Feuga, 2003). Only three mines are still open. The smaller is the Einville Mine, which has been inactive since 1949. Saint-Nicolas and Rosières Mines were linked to form the Varangéville Mine, which is still active (figure 7). The red circle on the Varangéville mine map shows the location of mine collapse that occurred in 1873 (Bérest et al., 2003).

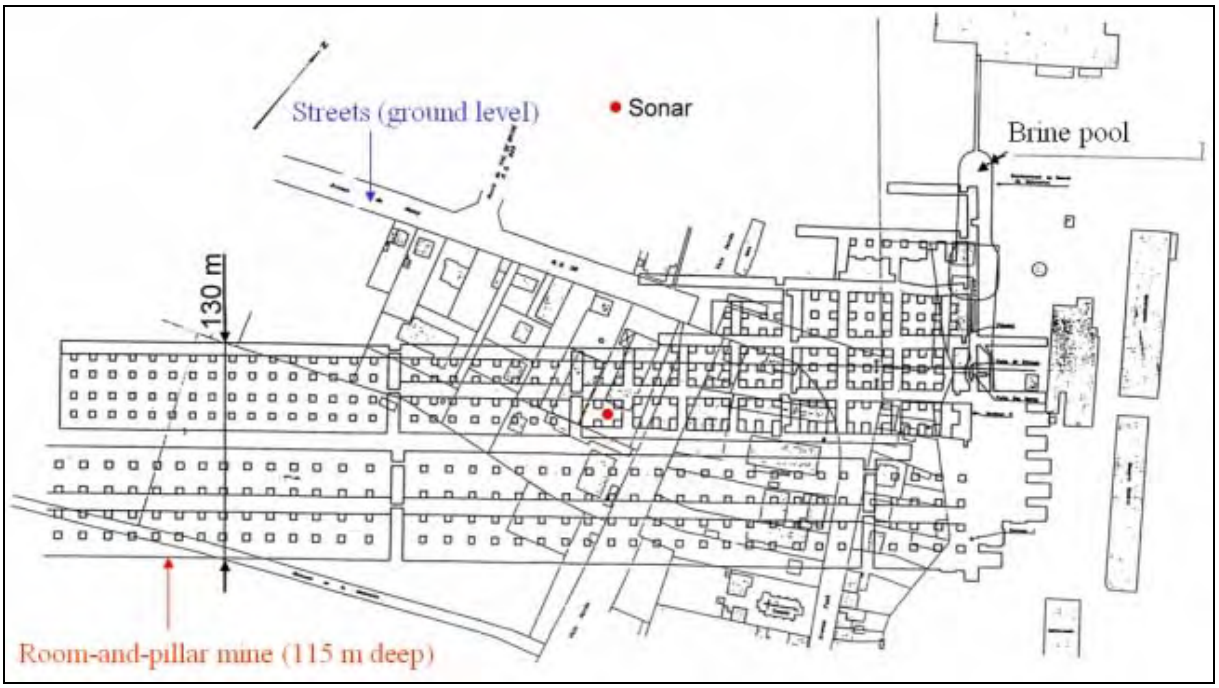


Figure 6. Plan of Dieuze salt mine (after Feuga, 2003)



Figure 7. Plan of Varangéville salt mine

DEEP SALT CAVERNS ABANDONMENT

BEREST Pierre[1], BROUARD Benoit[2], KARIMI-JAFARI Mehdi[1]

[1] LABORATOIRE DE MECANIQUE DES SOLIDES, Ecole Polytechnique, 91128 Palaiseau Cedex – France ; berest@lms.polytechnique.fr; karimi@lms.polytechnique.fr

[2] BROUARD CONSULTING, 101 rue du Temple 75003 Paris – France ; Contact@Brouard-Consulting.com

ABSTRACT: The behaviour of sealed and abandoned deep salt caverns is discussed. In such a cavern brine pressure builds up due to brine thermal expansion and cavern convergence, possibly leading to hydro-fracturing of the rock mass. However brine (micro) permeation through the cavern walls may release brine pressure, leading to a final equilibrium such that brine outflow balances cavern convergence rate. These phenomena are described and the ability to predict long-term evolutions is assessed. To validate these notions, an in situ test was performed.

KEYWORDS: Cavern abandonment, Salt permeability, Salt creep, In situ test.

RESUME : On discute du comportement à long terme de cavernes profondes réalisées dans un massif de sel après que ces cavernes ont été fermées et abandonnées. Dans une telle caverne, la pression de la saumure augmente en raison du réchauffement de la saumure et de la convergence de la caverne. Toutefois la (micro) perméabilité du sel permet une détente partielle de la saumure contenue dans la cavité, et l'apparition d'un équilibre dans lequel la perte de volume par convergence est égale au débit de saumure sortant de la caverne. Ces phénomènes sont décrits et on discute la qualité des prévisions d'évolution. Un essai in situ permet de valider les notions proposées.

MOTS-CLEFS : Abandon des cavernes souterraines, Perméabilité du sel, Fluage du sel, Essai in situ.

1. Introduction

In the past several years there has been concern about the long-term behaviour of deep underground salt caverns after they have been sealed and abandoned. By "deep" we mean caverns whose depths range between 400 and 2000 m and whose horizontal dimensions are significantly smaller than their depth (in such caverns there is no risk of a collapse leading to the creation of a sinkhole). Such deep caverns are leached out from a salt formation. A (typically) 1000-m deep well is cased and cemented to the salt formation. Soft water is injected into a central string and brine is withdrawn from the annular space between the string and the casing. After a year or so a 10,000 to 1,000,000 m^3 cavern is created. In many cases the cavern is later used for hydrocarbon storage (crude oil, LPG or natural gas); however there are several new projects in which caverns are used for disposal of nonhazardous, low level nuclear or industrial wastes, or carbon dioxide. These caverns will be abandoned some day; their long-term behaviour must be predicted (Ghoreychi and Cosenza, 1993; Brassow and Thoms, 2000; Dusseault *et al.*, 2001). The Solution Mining Research Institute which represents companies, consultants and research centers involved in the solution mining industry has set this problem at the center of its research program (Ratigan, 2000).

In most cases, prior to abandonment, the cavern will be filled with brine. Then a special steel plug will be set at casing seat or at a milled "window" above the casing seat, and cement will be poured in the well, isolating a large "bubble" of brine, the evolution of which is the concern of this paper.

The brine initial pressure results from the weight of the brine column which filled the well before it was plugged; this pressure is called *halmostatic* and is equal to P_h (MPa) = 0.012 H (m), where H is the average cavern depth. After the cavern is sealed, the brine pressure will build up, as proven by many "shut-in pressure tests" (see for instance, Fokker, 1995; Bérest *et al.*, 2000). Typical build up rates are 3 to 10 MPa/year, but much faster rates can be observed in very deep (say deeper than 2000 m) caverns. The final value of cavern brine pressure is of utmost importance. In a salt formation the natural state of stress in general is isotropic and the geostatic pressure at cavern depth, or H, is P_∞ (MPa) = 0.022 H (m). Several authors (Bérest and Brouard, 1995; Wallner and Paar, 1997) fear that brine pressure eventually reach a figure larger than the geostatic pressure, leading to hydrofracturing, upward brine flow through fractures and pollution of drinkable water. To which point such a scenario can be alleviated by taking into account salt (micro) permeability will be discussed later.

2. Factors contributing to pressure evolution

Behaviour of a sealed cavern is governed by four main phenomena (1) *brine thermal expansion* (2) *salt mass creep* (3) *brine permeation through the cavern walls* (4) *leaks through the casing or casing shoe*. These phenomena result in brine pressure change through *cavern compressibility*. These notions will be developed in the following paragraphs.

2.1. Cavern compressibility

When a certain amount of liquid is injected in a closed cavern or when cavern brine is heated, or when cavern shrinks due to rock mass creep, cavern pressure increases. The relation between the cavern pressure increase rate, or $\dot{P}_i$, and the volume change rate, or Q, is linear during a rapid evolution and the proportionality constant is the cavern compressibility or βV_c:

$$Q = \beta V_c \dot{P}_i \tag{1}$$

Cavern compressibility can be simply measured when injecting brine and measuring the resulting brine pressure build-up. Cavern compressibility is the slope of the curve (injected brine versus brine pressure). An example is provided on Figure 1.

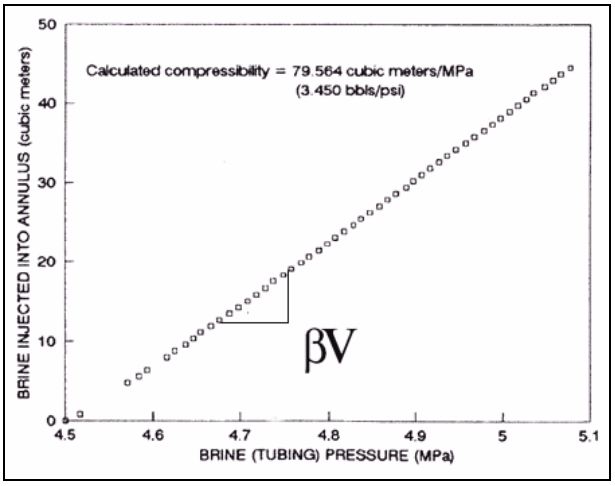


Figure 1 - Measurement of cavern compressibility [After Thiel, 1993].

Cavern compressibility, or βV_c, is proportional to cavern volume, or V_c. The compressibility factor, or β, is the sum of the cavern brine compressibility factor ($2.57 \cdot 10^{-4}$ MPa^{-1} is typical) and the cavern compressibility factor, which depends upon both rock-salt elastic properties and cavern shape. A typical value of the cavern compressibility factor is $1.4 \cdot 10^{-4}$ MPa^{-1}, making $\beta = 4 \cdot 10^{-4}$ MPa^{-1}; however larger values are sometimes met, for instance when the cavern is somewhat flat (Bérest *et al.*, 1999). In fact "instantaneous" compressibility and "long-term" compressibility must be distinguished. The above mentioned figures stand for a rapid test; when long term behaviour is considered, such phenomena as additional dissolution make the "long-term" compressibility larger (brine concentration at saturation, or the amount of brine that can be dissolved in a given mass of water, is a function of pressure and temperature; any pressure increase results in a (delayed) additional dissolution; as brine volume is smaller than the sum of the volumes of the water and the salt, the brine pressure increase is followed by a slight delayed pressure decrease of the initial pressure increase by 4 to 5 %, Van Sambeek *et al.*, 2005; this phenomenon cannot be observed during a short test).

2.2. Brine thermal expansion

In many cases, brine thermal expansion is by far the prominent factor explaining brine pressure build-up in a closed cavern. Its effects slowly reduce with time, but, in a big cavern, they can be effective during several decades.

The temperature of rock increases with depth, a typical value being T_R = 45°C at a depth of H = 1000 m, but caverns are leached out using soft water pumped from a river, lake or shallow aquifer whose temperature is cooler. Brine temperature at the end of leaching, or T_i^o, is close to the soft water temperature and significantly smaller than rock temperature. When the cavern remains idle, after leaching is completed, the initial temperature difference, or $T_R - T_i^o$, slowly resorbs with time, due to heat conduction in the rock mass and heat convection in the cavern brine. Appropriate heat-transfer equations can be written as follows:

$$\begin{cases} \dfrac{\partial T}{\partial t} = k_{salt}^{th} \Delta T \\ \int_\Omega \rho_b C_b \dot{T}_i d\Omega = \int_{\partial\Omega} K_{salt}^{th} \left(\partial T / \partial n \right) da \\ T_i(t) = T_{wall} \\ T(t=0) = T_R \text{ and } T_i(t=0) = T_i^o \end{cases} \tag{2}$$

The temperature in the rock mass is T; brine temperature is T_i. The first equation holds inside the rock-salt mass (k_{salt}^{th} is the thermal diffusivity of salt, $k_{salt}^{th} \approx 3 \cdot 10^{-6}\ m^2/s$) ; the second equation is the boundary condition at cavern wall ($K_{salt}^{th} = k_{salt}^{th} \rho_{salt} C_{salt}$ is the thermal conductivity of rock-salt, K_{salt}^{th} = 6 W/m/°C is typical, and $\rho_b C_b$ = $4.8 \cdot 10^{-6}$ J/m^3/°C is the volumetric heat capacity of brine). The third equation stipulates that rock temperature at cavern wall is equal to the average brine temperature in the cavern, or T_i, which is roughly uniform, a reasonable assumption as thermal convection stirs brine cavern effectively. The last equation describes the initial temperature distribution in the rock formation.

The exact temperature evolution in an actual cavern can easily be predicted through numerical computations. Back-of-the envelope estimations can be reached simply: dimensional analysis proves that heat transfer in the rock mass is governed by one characteristic time, $t_c = R^2/\pi k_{salt}^{th}$, where R is defined by $V_c = 4\pi R^3/3$, or $t_c(\text{years}) \approx V_c^{2/3}(\text{m}^2)/800$. The second equation of (2) provides a second characteristic time, or $t'_c = t_c/\chi$, $\chi = \rho_b C_b/\rho_{salt} C_{salt}$, which is of the same order of magnitude as t_c. In the case of a roughly spherical cavern, $2t_c$ is the time after which approximately 75% of the initial temperature difference has been resorbed. When V_c = 8,000 m^3, $2t_c \approx 1$ year; when V_c = 512,000 m^3, $2t_c \approx$ 16 years. The average temperature change rate (from leaching completion time to twice the characteristic time) is $\dot{T}_i =$ 0.75 (T_R - T_i^o)$/2t_c$ - i.e., when $T_R - T_i^o = 25°\text{C}$, $\dot{T}_i$ = 18°C/year in a 8,000 m^3 cavern and $\dot{T}_i$ = 1.2°C/year in a 500,000 m^3 cavern.
In a opened cavern, a temperature increase leads to thermal expansion and brine outflow at ground level, $Q_{th} = \alpha_b V_c \dot{T}_i$, where α_b is the brine thermal expansion coefficient, $\alpha_b \approx 4.4 \cdot 10^{-4}$/°C. In a closed cavern temperature increase leads to pressure build up:

$$\dot{P}_i = (\alpha_b/\beta)\dot{T}_i \tag{3}$$

The ratio α_b/β is close to 1 MPa/°C: when an initial temperature difference of 25°C is resorbed, after a time equal to several times t_c, the related pressure build up should be 25 MPa, far exceeding the initial difference between geostatic and halmostatic pressure which is P_∞ - P_h (MPa) = 0.01 H (m), or 10 MPa at a 1,000-m depth, and possibly leading to salt fracture. How fast this difference is resorbed depends on cavern size; the initial rate is 18 MPa/year (but rapidly decreasing) in a 8,000 m^3 cavern and 1.2 MPa/year in a 500,000 m^3 cavern. An example is provided in Figure 2. The three caverns (A, B, C) were leached out at the same time in the same salt formation and are at comparable depth. For technical reasons, leaching was stopped for a couple of weeks and advantage was taken of this stop to perform shut-in pressure tests. As-observed, pressure build-up rates were 4 MPa/year, 5.9 MPa/year and 10 MPa/year on the 346,000 m^3, 147,000 m^3 and 48,600 m^3 caverns, respectively, clearly highlighting the influence of cavern size on pressure build-up rate.

2.3. Salt mass creep

All solution-mined caverns converge as they gradually, and quite slowly, shrink. The driving force is the difference between the geostatic pressure (P_∞) and the cavity internal pressure (P_i). At this step a few comments on the mechanical behavior of salt are helpful. Most experts agree on the main features of steady-state rock-salt behaviour:

a) In the long term, rock-salt flows even under very small deviatoric stresses.
b) Creep rate is a highly non-linear function of applied deviatoric stress and temperature.
c) Steady-state creep is reached after several weeks or months when a constant load is applied to a sample; it is characterized by a constant creep rate.
d) Transient creep is triggered by any change in the state of stress; it is characterized by high initial rates (following a deviatoric stress increase) that slowly reduces to reach steady-state creep.
e) When deviatoric stress is large, salt experiences damage and dilatancy: its permeability drastically increases. The same occurs when salt is in contact with brine whose pressure is higher than the minimum principal stress (Fokker, 1995).

Main features of steady-state creep are captured by the following simple model (Norton-Hoff power law):

$$\dot{\varepsilon}_{ss}^{ij} = A\exp\left(-\frac{Q}{RT}\right)\frac{1}{n+1}\frac{\partial}{\partial\sigma_{ij}}\left[(\sqrt{3J_2})^{n+1}\right] \tag{4}$$

Where J_2 is the second invariant of the deviatoric stress tensor; A, n, Q/R are model parameters.

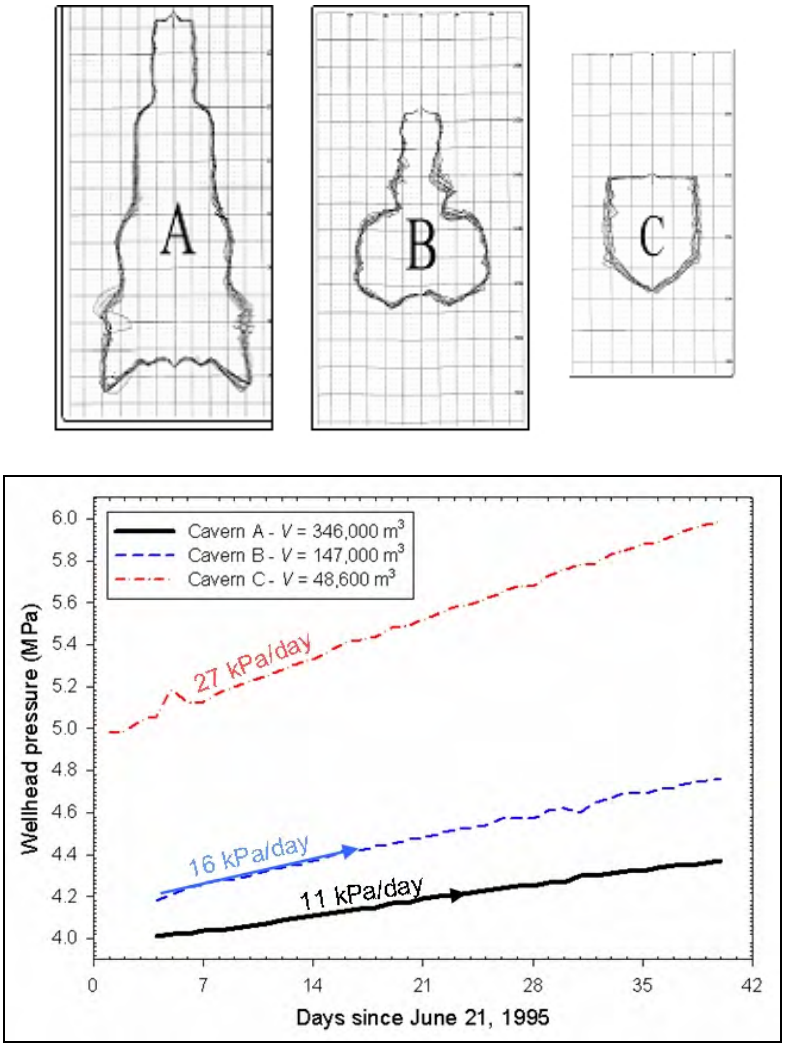


Figure 2 – Pressure Build-Up Due to Brine Thermal Expansion in a Small, Big, and Medium Size Cavern.

Values of these parameters were collected by Bérest and Brouard, 1998: for 12 different salts, the constant n is in the range n = 3-6, illustrating the highly non-linear effect of the applied stress on the strain rate, and Q/R ranges from 4,000 to 10,000 K. Several authors suggest constitutive laws which take into account transient creep. Here again, numerical computations allow to assess cavern convergence (i.e., loss of volume) as a function of time and cavern pressure history. The steady-state formulation (4) allows to obtain a closed-form solution for the idealized case of a perfectly spherical cavern that, over a long period of time, is submitted to an internal pressure (P_i) smaller than the natural geostatic pressure (P_∞) at cavern depth (H). In this solution the long-term deviatoric stress is much smaller (when n > 1) than in the corresponding elastic solution and the volume change rate is:

$$\dot{V}_c/V_c = -\frac{3}{2}\left[\frac{3}{2n}(P_\infty - P_i)\right]^n A\exp\left(-\frac{Q}{RT_R}\right) = A^*(P_\infty - P_i)^n \tag{5}$$

An immediate consequence of this solution is that, as long as the cavern brine pressure is smaller than the geostatic pressure, the cavern shrinks, leading to cavern pressure build-up ($\dot{P}_i > 0$) in a closed cavern.

$$\dot{P}_i = \left(1 \big/ \beta \right) \dot{V}_c / V_c \tag{6}$$

A typical value of the initial shrinkage rate (when cavern depth is H = 1000 m and pressure is still close to halmostatic) is $\dot{V}_c / V_c$ = -3·10^{-4} year^{-1}, although there are large variations according to site-specific salt properties and cavern shape. Such a shrinkage rate in a closed cavern will lead to a pressure build-up rate of $\dot{P}_i = (1/\beta)\dot{V}_c / V_c$ = 0.75 MPa/year when β = 4·10^{-4} MPa^{-1}. Two comments must be made:

1. Pressure build-up progressively leads to smaller creep rates, because the difference $P_\infty - P_i$ between geostatic pressure and brine pressure reduces with time (it reduces even faster when brine thermal expansion is taken into account).
2. In most cases, and at least in a freshly leached out cavern, the contribution of cavern shrinkage to pressure build-up is much smaller than brine's (see Paragraph 2.2). It is only in a very deep cavern (H = 2000 m) that cavern shrinkage due to salt creep governs cavern pressure evolution. The reason is two-fold: the initial difference between geostatic pressure and brine pressure is proportional to cavern depth, $P_\infty - P_i = 0.01\,H$, making the cavern convergence rate proportional to H^n; rock temperature, or T_R, is increasing with depth and the cavern convergence rate is proportional to $\exp(-Q/RT_R)$.

2.4. Leaks

As will be seen later, rock salt permeability in most cases is exceedingly small. The real problem is usually the "piping", that is, the cemented well that connects the cavern to the ground surface. While correct and robust well designs prevent most leakages, full scale testing is necessary to ensure that acceptable tightness exists. Tightness tests are performed before commissioning a cavern (and from time to time during cavern operation). It is often considered that the maximum allowable leak rate during such a test is Q_{leak} = 1000 bbls/year (Thiel, 1993) or 160 m^3/year, a relatively high figure (in a 100,000 m^3 cavern, when cavern compressibility is β = 4·10^{-4} /MPa, the pressure drop rate generated by such a leak is $\dot{P}_i = -Q_{leak} / \beta V_c = -4$ MPa/year, a figure larger than cavern convergence rate due to salt creep.) However it can be assumed that such a leak, which is effective when the cavern is in operation, will be made much smaller or even nil when the casing would have been plugged and filled with cement before cavern abandonment.

2.5. Salt permeability

For every standard engineering purpose, rock salt can be considered as an impermeable rock. Its matrix hydraulic conductivity is small and no fractures exist in a massive salt formation. The generally small permeability numbers resulting from laboratory tests are scattered ($K_{salt}^{hyd} = 10^{-21}$ m^2 to 10^{-18} m^2). Few in situ tests have been performed. A 1-year-long test, performed in a well and supported by the SMRI (Durup, 1994) gave $K_{salt}^{hyd} = 6 \cdot 10^{-20}$ m^2. Such figures are extremely small (hydrogeology textbooks generally define an impermeable rock as a one whose permeability is smaller than $K_{salt}^{hyd} = 10^{-17}$ m^2.) When short-term use of salt caverns is considered, salt cavern are

extremely safe from the perspective of product confinement. However when very long-term behaviour is considered, the general picture changes. When brine warming becomes negligible, even tiny losses of fluids, due to high cavern stiffness, can significantly lessen the effect of cavern creep and prevent cavern pressure from reaching high levels. To be more specific, consider the case of a spherical cavern with radius *R*, excavated in a salt mass with permeability K_{salt}^{hyd}, cavern brine pressure P_i and natural pore brine pressure P_o (The existence of a pore brine pressure uniform throughout the rock salt mass is arguable, as salt porosity is small – often smaller than 1% - and pore connectivity is likely to be poor. However the (few) in situ tests performed in salt mines or salt caverns prove that the notion of a pore pressure is consistent with test results. It is often assumed that pore pressure is equal to halmostatic pressure. However tests performed at the WIPP site proved that pore pressure was higher than expected (Dale and Hurtado, 1997) and more recently several observations made at a storage site (de Laguerie *et al*., 2004) strongly suggest that pore pressure in this specific site was smaller than halmostatic. However for simplicity we assume in the following that $P_o = P_h$.) If μ_b is the brine dynamic viscosity ($\mu_b = 1.4 \cdot 10^{-3}$ Pa.s) then, assuming Darcy law, steady-state brine seepage rate from a closed cavern is:

$$Q_{perm} / V_c = 3K_{salt}^{hyd} \left(P_i - P_o \right) / \left(\mu_b R^2 \right) \tag{7}$$

This rate is quite small (for instance, $P_i - P_o = 7$ MPa, *R* = 12.5 m and $K_{salt}^{hyd} = 10^{-20}$ m^2 leads to $Q_{perm} =$ 0.25 m^3/year) but it can balance creep rate, especially when cavern brine pressure is high.

2.6. Pressure evolution in a closed cavern

Pressure evolution in a closed cavern result from the effects of brine thermal expansion, cavern convergence due to salt creep, brine permeation through the cavern wall and (possible) leaks. The following equation captures these four effects:

$$\begin{cases} \beta \dot{P}_i = \alpha_b \dot{T}_i \left[t / t_c \right] + A^* \left(P_\infty - P_i \right)^n - 3K_{salt}^{hyd} \left(P_i - P_o \right) / \left(\mu_b R^2 \right) - Q_{leak} / V_c \\ P_i \left(t = 0 \right) = P_o = P_h \end{cases} \tag{8}$$

We assumed that pore pressure is halmostatic ($P_o = P_h$). For simplicity, leaks through the casing in a sealed cavern will be supposed to be negligible ($Q_{leak} = 0$). Note that (8) only holds when a slow evolution is considered, as *steady-state* formulations of cavern convergence rate and brine outflow rate are taken into account. $\dot{T}_i$ becomes negligible after a period of time larger than several times t_c (keep in mind that t_c can be several decades long in a large cavern). In other words, equation (7) proves that after a long period of time, brine pressure rate ($\dot{P}_i$) vanishes and cavern pressure reaches an equilibrium value, or $P_{eq,}$ such that:

$$A^* \left(P_\infty - P_{eq} \right)^n = 3K_{salt}^{hyd} \left(P_{eq} - P_o \right) \tag{9}$$

And $P_o < P_{eq} < P_\infty$: the equilibrium pressure is smaller than geostatic and larger than halmostatic. This equilibrium pressure is reached when cavern volume loss rate exactly balances brine outflow from the cavern.

3. Assessing the value of long-term predictions

Our goal is to predict the long-term evolution of a sealed and abandoned cavern. The cavern may be filled with pure brine or with some chemical or radioactive wastes, and the meaning of “long-term” is not the same in these three examples. We assume in the following that we want to be able to

make accurate quantitative predictions about a period of, say, 3 centuries and to make qualitative predictions when longer periods of time are considered. The quality of the assumptions made above – all contributing to pressure history in a closed cavern – must be assessed.

Cavern compressibility was measured in dozens of caverns (it is a fundamental pre-requisite to any interpretation of a cavern tightness test, a mandatory test for most caverns) and values of β = 4 to 5 10^{-4} MPa^{-1} are generally reported. No smaller figures have been found (brine compressibility is a lower bound for cavern compressibility). It was said that "long-term" cavern compressibility is slightly higher than "short-term" cavern compressibility, but the difference is small. Larger figures are met in flat caverns, or when the cavern contains an even small amount of gas, which is much more compressible than brine. However larger compressibility values make pressure build-up rate slower, a significant advantage in the context of cavern abandonment.

Brine thermal expansion is a well described phenomenon; the various constants such as $\alpha_b, K_{salt}^{th}, k_{salt}^{th}$ are well known and their range of variation from one site to another is small. The system of equations (2) is robust (it leads to excellent temperature evolution predictions because conduction is the only heat transfer process in an impermeable rock, and because thermal convection in the cavern, which stirs brine and makes its temperature uniform through the cavern, is generated by the natural geothermal gradient, a perennial source of energy). Furthermore, brine expansion rate vanishes to zero when very long term evolutions are considered.

Salt creep has been extensively studied. No other rock has given rise to such a comprehensive set of laboratory experiments, motivated, to large extent, by the specific needs of nuclear waste storage¸ see for instance the proceedings of the five Conferences on the Mechanical Behaviour of Salt (Hardy and Langer, 1984 and 1988, Hardy *et al*., 1996, Aubertin and Hardy, 1998, Cristescu *et al*., 2002). Dedicated numerical models, able to accommodate sophisticated constitutive laws, have been written. However, actual cavern convergence data are rough, scarce, and somewhat inaccurate (Bérest, 2005a); they make validation of sophisticated models uncertain. It was said that the constants in mechanical constitutive laws vary to large extent from one site to another, in sharp contrast, for instance, with the constants in the thermal model. Laboratory experiments generally have been performed on rock samples submitted to relatively large deviatoric stresses; it has been argued (Bérest *et al*., 2005b) that the constitutive laws inferred from these tests do not apply to the much smaller deviatoric stresses that will be encountered in the vicinity of an abandoned cavern experiencing high cavern brine pressure (creep rates should be much faster than is expected from standard laboratory results).

Salt permeability is by far the most uncertain factor in long-term cavern behaviour. The concept of a homogeneous isotropic permeability (i.e., a uniform value of K_{salt}^{hyd} through the whole salt mass) is probably incorrect. Bedded salt contains a fair amount of impurities and it can be suspected that their permeability is much larger than the permeability of pure salt. Salt permeability is strongly influenced by the state of stress, and several authors believe that most of the (small) permeability observed during in situ tests in salt caverns is induced by cavern creation and operation (more precisely, either by tensile or high deviatoric stresses developed at the cavern wall, when the cavern fluid pressure is very high or very small, respectively.)

Uncertainties remain, and the present state of knowledge does not allow to perform blind predictions (i.e., predictions based on laboratory measurements). In situ tests must be performed before decommissioning a cavern. Such a test is described in Paragraph 4. Note that, as far as possible, in situ tests must not be used to back-calculate model parameters but rather to check that model parameters, which are to be independently determined, were accurately assessed before the test.

4. In situ test in the EZ53 cavern

4.1. Objective of the test

The objective of the test was to verify that pressure build-up in a sealed cavern does not reach geostatic values but, rather, due to the combined effects of salt creep and salt (small) permeability, will vanish when a certain steady-state value of the cavern pressure (larger than halmostatic, but significantly smaller than geostatic) is reached. The cavern selected for the test was the EZ53 cavern of the Gaz de France storage site in Etrez, France. Its volume is small (7500 m^3) and its depth is 950 m. It was leached out in Spring 1982, i.e., 15 years before the test. The test was supported by the SMRI.

4.2. Brine thermal expansion

From Spring 1982 to Winter 1983, the thermal behaviour of the EZ53 cavern was monitored via cavern brine temperature measurements; they confirmed that 65% of the initial temperature difference between the rock mass and the cavern brine has been already resorbed after 250 days, which is consistent with the value of the characteristic time, t_c (years) $\approx V_c^{2/3}(\mathrm{m}^2)/800$ = 6 months (see Paragraph 2.2.). Temperature profiles were performed 14 years later, in February and March 1996, a few weeks before the test: they strongly suggested that thermal equilibrium was reached at that time, and that brine thermal expansion could be disregarded.

4.3. Salt creep

The rock salt belonging to the so-called upper layer of the Etrez salt formation, in which the EZ53 cavern had been leached, was studied by Pouya (1991) who fit laboratory data to the Norton-Hoff constitutive law described in Paragraph 2.3 and suggests the following parametric values: A = 0.64 MPa^{-n}, Q/R = 4100 K, n = 3.1. With these figures a simple estimation of cavern convergence rate in a 950-m deep cavern can be reached, see Formula (4); it is $\dot{V}_c/V_c$ = - 3 10^{-4} $year^{-1}$. Several weeks before the test, the EZ53 well-head was left opened and Brouard (1998) measured the brine outflow from the cavern. As the cavern had been at rest for most of the time since the end of leaching, and brine thermal expansion was nil, this outflow was considered as representative of steady-state cavern creep. The outflow was 6 liters per day, or $\dot{V}_c/V_c$ = - $3\cdot10^{-4}$ $year^{-1}$; this perfect agreement between observed and computed figures must be considered as partly fortuitous, but it does provide some confidence in the estimation of the mechanical behaviour of the cavern.

4.4 Brine permeation

Etrez salt permeability has been studied by Le Guen (1991) who found for some samples an intrinsic permeability of $K_{salt}^{hyd} = 10^{-21}$ m^2. Durup (1994) has performed an in situ permeability test on the EZ58 well, which belongs to the same salt formation as EZ53 and has similar depth. Durup found that pore pressure, P_o, was very close to halmostatic pressure, or $P_o = P_h$, and suggested an average value of $K_{salt}^{hyd} = 6\cdot10^{-20}$ m^2 for the 150-m high EZ58 well. This larger figure is consistent with the generally accepted effects of scale on rock permeability; as explained below, still larger values were found when interpreting the EZ53 test, performed in a *cavern* instead of a *well*.

4.5. Leaks

An important difference between a shut-in test and an actual cavern abandonment lays in the fact that during a shut-in test the cavern is closed at the well-head – and not sealed at the bottom of the well. During the test, leaks can occur in the well through the casing, the casing shoe or through the well-head. Such leaks would lead to severe misinterpretation of a sealed cavern long-term behaviour. To assess these leaks, an oil column was lowered down to a depth of 864.5 m (i.e., below the casing shoe depth) in the annular space between the cased and cemented casing and a central string. A small amount of oil was also injected in the central string. Pressure evolutions were measured at the well-head both in the annular space and in the central string. Oil density is smaller than brine density. Any oil leak through the casing (or through the well-head) results in a rise of the oil/brine interface and a difference in the evolution of the two pressure measured at the well-head. This system proved to be quite effective. In fact a leak (on day 315 after the test began) was detected through curve observation before being observed – and repaired – in the field.

4.6. Test results

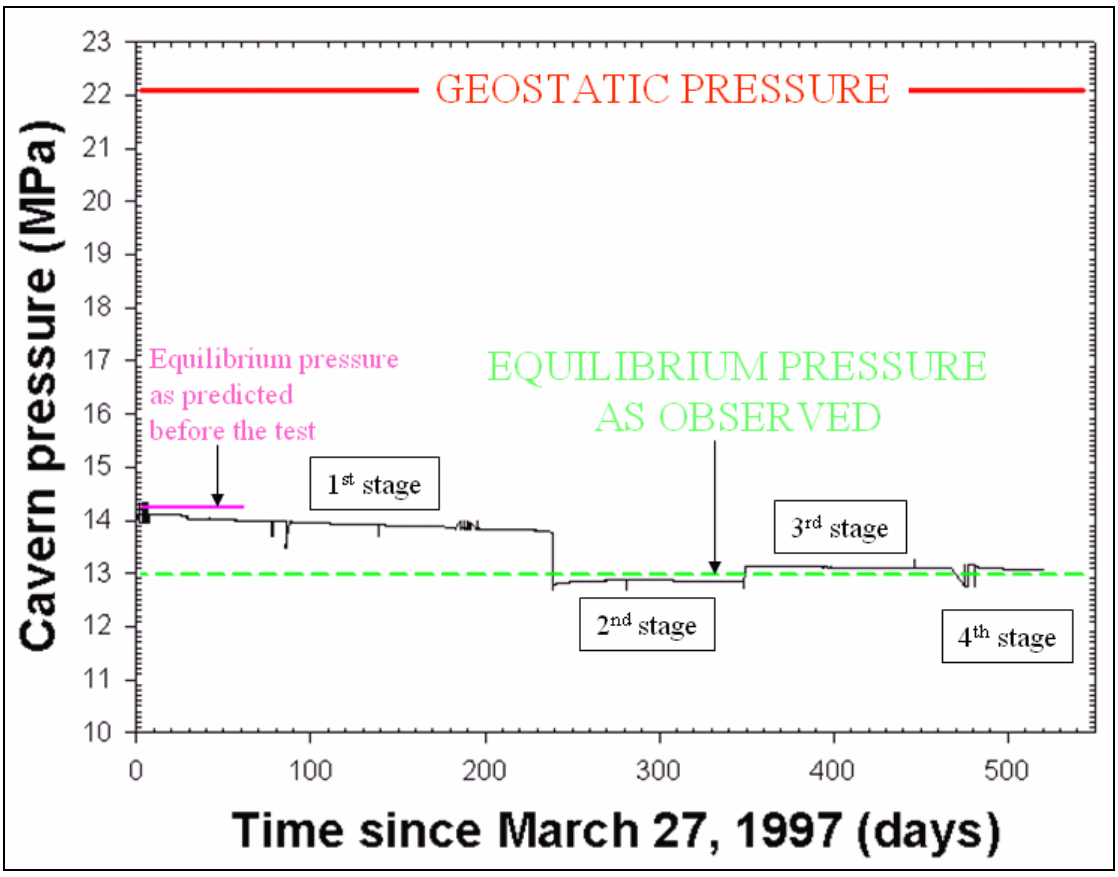


Figure 3 – Cavern evolution during the EZ53 test.

The test basically consists of a “trial and error” process (Figure 3) to approach the expected steady-state pressure. Different pressure levels are tested successively; each level is selected to trigger a change in pressure rate sign, providing upper and lower bounds for the steady-state equilibrium value. The test lasted 540 days and 4 steps were managed. From the test it can be inferred that the equilibrium is $P_{eq} = 13.0 \pm 0.1$ MPa. The equilibrium pressure is much smaller than the geostatic pressure, which is $P_{\infty} = 20.5$ MPa at a 950-m depth, and larger than halmostatic pressure which is

$P_h = 11.2$ MPa. A $P_{eq} = 14.3$ MPa figure had been predicted before the test. While EZ53 creep, which had been measured through in situ tests, can be considered to have been reasonably well estimated, it is logical to conclude that cavern permeability must be larger than estimated through earlier well tests; a $K_{salt}^{hyd} = 2 \cdot 10^{-19}$ m^2 value can be back-calculated; the variations in cavern volume and cavern brine volume are then of the order of $Q_{perm} \approx 1.4$ m^3/year. This test proved that in this site an equilibrium pressure did exist and that its value could be relatively well predicted. A similar test was performed in a 700-m deep cavern in another site (Brouard *et al*., 2004) and two additional tests are currently performed in shallow caverns in France and Germany; these two tests are supported by the SMRI.

5. Conclusions

It was proved that in a sealed cavern brine pressure evolution is governed by brine thermal expansion, cavern convergence due to salt creep and brine permeation through the cavern wall. In a (micro) permeable formation brine pressure will not exceed a figure smaller than a geostatic value – provided that thermal expansion can be disregarded. After a long period of time, a large volume of rock salt around the cavern will be impregnated by brine expelled from the cavern. The final equilibrium pressure can be accurately predicted provided that cavern thermal history, rock salt permeability and rock salt mechanical behaviour are known. An in situ test proved that most phenomena were relatively well described: cavern compressibility and brine thermal evolution can be very accurately measured and computed; cavern convergence can be fairly well predicted; large scale permeability of salt formations can be estimated through an in situ test but remains a partly opened question.

6. References

Aubertin M. and Hardy R.H., editors (1998). *Proc. 4th Conf. Mech. Beh. of Salt*, Montreal, June 1996. Trans Tech Pub., Clausthal-Zellerfeld, Germany, 658 pages.

Bérest P., Bergues J. and Brouard B. (1999). *Review of static and dynamic compressibility issues relating to deep underground caverns.* Int. J. Rock Mech. Min. Sci., 36(8), 1031–1049.

Bérest P., Brouard B. and Durup G. (2000). *Shut-In Pressure Tests – Case Studies*. Proc. SMRI Fall Meeting, San Antonio, 105-126. (Proceedings of the "SMRI Meetings" are available at: SMRI-3336, Lone Hill Lane, Encinitas, CA 9204-7262, USA. These Proceedings are edited as a separate volume since the Fall 1996 Meeting).

Bérest P., Blum P.A.,Charpentier J.P., Gharbi H., Valès F. (2005b). *Very slow creep tests on rock samples*. Int. J. Rock Mech. & Min. Sc. 42, 569-576.

Bérest P. (2005a). *In situ testing in salt caverns.* Proc. Technical Class, SMRI Spring Meeting, Syracuse.

Brouard B. (1998). *On the behavior of solution-mined caverns (in French).* Thesis Dissertation, Ecole polytechnique, France.

Brouard B. and Bérest P. (1998). *A classification of salt according to their creep properties.* Proc. SMRI Spring Meeting, New Orleans, 18–38.

Brouard B., Bérest P., Héas J.Y., Fourmaintraux D., de Laguérie P., You T. (2004). *An in situ test in advance of abandoning a salt cavern*, SMRI Fall Meeting, Berlin, 45-64.

Brassow C.L. and Thoms R.L. (2000). *Use of solution-mined caverns for the disposal of hazardous and industrial waste products*. Proc. 8th World Salt Symp., R.M. Geertman ed., Elsevier, 229-235.

Cristescu N., Hardy R.H. Jr. and Simionescu R.O., editors (2002). *Proc 5th Conf. Mech. Beh. of Salt,* Bucarest, August 1999, Balkema, 466 pages.

Dale T. and Hurtado L.D. (1997). *WIPP air-intake shaft disturbed-rock zone study*. Proc. 4th Conf. Mech. Beh. of Salt,. Montréal, June 1996. Trans Tech Pub., Germany, 525-535.

de Laguerie P., Héas J.Y., Fourmaintraux D., You Th., Brouard B., Bérest P. (2004). *Decommissioning and abandonment procedure of LPG caverns at Carresse (France)*. SMRI Fall Meeting, Berlin, 27-44.

Durup J.G. (1994). *Long term tests for tightness evaluations with brine and gas in salt*. Proc. SMRI Fall Meeting, Hannover

Dusseault M.B., Bachu S. and Davidson B.C. (2001). *Carbon dioxide sequestration potential in salt solution caverns in Alberta, Canada. Proc*. SMRI Fall Meeting, Albuquerque, 77-96.

Fokker P.A. (1995). *The Behavior of Salt and Salt caverns*. Thesis Dissertation, Delft University of Technology, The Netherlands.

Ghoreychi M. and Cosenza P. (1993). Quelques aspects de la sûreté à long terme des stockages dans le sel. Proc. *4ème Colloque Franco-Polonais*, Nancy, 209–217.

Hardy R.H. Jr and Langer M., editors. (1984). *Proc. 1st Conf. Mech. Beh. of Salt,* Pennsylvania , November 1981. Trans Tech Pub., Clausthal-Zellerfeld, Germany, 901 pages.

Hardy R.H. Jr and Langer M., editors. (1988). *Proc. 2nd Conf. Mech. Beh. of Salt,* Hannover, September 1984. Trans Tech Pub., Clausthal-Zellerfeld, Germany, 781 pages.

Hardy R.H. Jr, Langer M., Bérest P. and Ghoreychi M., editors. (1996). *Proc. 3rd Conf. Mech. Beh. of Salt,* Palaiseau, September 1993. Trans Tech Pub., Clausthal-Zellerfeld, Germany, 621 pages.

Le Guen C. (1991). *Mesure de la perméabilité de roches très peu perméables et étude de son evolution sous solicitation sthermomécaniques*. PhD Thesis, ENPC, France.

Pouya A. (1991) *Correlation between mechanical behaviour and petrological properties of rock salt*. Proc. 32nd US Symp. Rock Mech., Balkema Rotterdam, J.C.Roegiers ed., 385-392.

Ratigan J. (2000). *A Status Report on the SMRI Cavern Sealing and Abandonment Program*. Proc. SMRI Fall Meeting, San Antonio, 164-178.

Thiel, W.R. (1993). *Precision Methods for Testing the Integrity of Solution Mined Underground Storage Caverns.* Proc. 7th Symp. on Salt, Elsevier Science Publisher, Amsterdam, **1**, 377-383.

Van Sambeek L., Bérest P., Brouard B. (2005). *Improvements in Mechanical Integrity Tests for Solution-Mined Caverns used for mineral production or liquid-product storage.* Topical Report RSI-1799, prepared for the Solution Mining Research Institute.

Wallner M. and Paar W.A. (1997). *Risks of progressive pressure build up in a sealed cavern*. Proc. SMRI Fall Meeting, El Paso, 177-188.

GASES EMISSION MONITORING IN A POST-MINING CONTEXT

BESNARD Katia[1], POKRYSZKA Zbigniew[1]

[1] INERIS, Unité Eaux Souterraines et Emissions de Gaz - Parc Technologique Alata – BP 2 – 60550 Verneuil-en-Halatte - France. Katia.Besnard@ineris.fr; Zbigniew.Pokryszka@ineris.fr

ABSTRACT: Closed mines are often sources of dangerous gas emission. Flammable and/or toxic gases or deoxygenated air can be transmitted to the surface through existing aerodynamic links like abandoned shaft or galleries and fissures in rock. The gases issued from closed mines may generate public health and safety concerns and these problems are encountered for nearly all mine types. For the last 10 years, INERIS has developed in situ gas monitoring methods whose objectives are (i) to characterise gas emissions and to improve our knowledge of the processes governing their migration; (ii) to allow their risk evaluation and, eventually, to enable gas detection and alarm triggering. After briefly presenting each method, we will focus on some typical examples of monitoring by continuous automatic in-situ measurements that we have set up.

KEYWORDS: gas emission; abandoned mines; monitoring; in-situ measurements.

RESUME : Les mines abandonnées sont fréquemment le lieu de dangereuses émissions de gaz. Des gaz inflammables, toxiques et/ou de l'air désoxygéné peuvent migrer vers la surface à travers les anciennes infrastructures minières (puits, galeries…) ou des fissures dans le recouvrement. Les émanations de gaz à partir des mines abandonnées peuvent poser des problèmes de sécurité et de santé publique. Au cours de la dernière décennie, l'INERIS a développé des méthodes de monitoring in situ dont les objectifs sont (i) de caractériser les émissions de gaz et approfondir notre connaissance des processus gouvernant leur migration et (ii) d'aider à l'évaluation des risques et, le cas échéant, de permettre la détection des gaz et le déclenchement d'alarmes. Après avoir brièvement présenté chaque méthode, nous nous attarderons sur quelques exemples de surveillance par des mesures in situ en continu que nous avons mis en place.

MOTS-CLEFS : émission de gaz; mines abandonnées; surveillance; mesures in-situ.

1. Introduction

Problems of mine gas issuing at the surface have been encountered all over the world in all types of active or closed mines.

Mine gas develops in underground reservoirs formed by residual voids left by the mining activity. It can migrate to surface under the effect of several mechanisms and thereby presenting considerable hazards for individuals and property (explosions, intoxication, asphyxia, etc). Therefore it is crucial to have technical means to monitor gas emissions characteristics.

The intent of this paper is to briefly present the various methods that we have at our disposal. We then focus on three sites in a post-minig context in which we have set up gas monitoring systems.

2. Mine gas hazards on surface

2.1. Mine gas

In underground closed mines, they are often residual cavities resulting from the mining activity: abandoned rooms and pillars sectors, partial filling in, caving, galleries… or voids due to the increase in the porosity of surrounding strata resulting from their distressing and fracturing. This forms a true underground reservoir in which gases can build up. The composition of the gas mixtures in this volume considerably varies from one mine to another.

The gases most commonly found in mining contexts are oxygen, nitrogen, carbon dioxide and methane, and less often, hydrogen sulphide and carbon monoxide. In a simplified way, one can distinguish two origins for these gases: they can be geological gases, contained in rock before mining or the result of (bio)geochemical reactions in the deposit or in surrounding rocks, during or after mining. Thus the coal spontaneous combustion in abandoned mines causes frequently toxic gas emissions to the surface.

The major noxious gases are the very poisonous carbon monoxide and carbon dioxide. Hydrogen sulphide is extremely poisonous, but rarely occurs in dangerous quantity. Moreover mine gas is generally accompanied by a variable degree of oxygen depletion. Mine gas consequently presents several hazards including asphyxia, due to the oxygen concentration being too low, intoxication, due to the presence of carbon monoxide and hydrogen sulphide and, to a lesser extent, carbon dioxide, and finally ignition or explosion, due to the presence of hydrocarbons. These hazards are, of course, increased when the mine gas rising to the surface accumulates in locations accessible to the public.

2.2. Factors governing the migration of mine gas to the surface

Noxious gases or deoxygenated air can be transmitted on the surface through existing aerodynamic links like abandoned shaft or galleries and fissures in rock.

The gaseous mixtures build up in the reservoir formed by residuals voids can be transmitted to the surface when the pressure within the reservoir is higher than the atmospheric pressure. The different reasons for such a positive pressure differential between the reservoir and the surface are mostly:

- A dilatation of the atmosphere in the mine, due to a decrease of the atmospheric pressure at the surface;
- An increase of the pressure inside the reservoir due to :
    - The hydrostatic pressure imposed by rising water levels. The displacement of gas and reduction in storage volume add to the effect ;
    - The release of gas initially trapped;
- The production of gas by geological gas desorption and/or (bio)geochemical reactions that can lead to local overpressures within residual voids.

Any thermal gradient between the underground reservoir and the surface will also lead to gaseous migration. In this case, the air flow may reverse direction from one season to another.

These causes of surface gas emissions may occur simultaneously.

Therefore the gases issued from closed mines may generate public health and safety concerns and these problems are encountered for nearly all mine types.

2.3. Incidents caused by gas from closed mines

In France, few accidents or incidents associated with emissions or accumulations of coal mine gas after mine closures have fortunately been reported. Some cases have, however, been reported and looked into (Pokryszka and al, 2000). In the United Kingdom, on the other hand, ten or more incidents of this type have occurred over the last 50 years (Robinson, 2000). Other incidents or accidents have been reported in some countries with coal mining industries (Kral and al, 1998; Novotny and al, 2001).

Some residential areas of the iron basin of Lorraine (in the Northeast of France) are affected by noxious gas emissions (under-oxygenated and noxious gas loaded mixtures). The most spectacular phenomenon occurred in the built-up area of Moyeuvre-Grande in Moselle, especially in the district of the town located very close to the former underground mine workings in which some inhabitants observed faulty working gas cookers and boilers (Grabowski and Pokryszka, 2003).

The occurrence of gas in salt and potash mines and caverns has often been mentioned in the literature and in the historical reports of mine operations. Numerous mines in operation have experienced sudden, usually unexpected, expulsions of gas or continuous gas emissions. Incidents or accidents, sometimes very spectacular, occurred in mines due to gas emissions. At the beginning of the century, several potash mines of northern Europe were abandoned because of problems caused by gas outbursts (Gimm, 1968). In the early history of salt mining (prior to the current practice of evacuating the mine prior to blasting), many fatalities resulted from gas outbursts. A large portion were due to secondary factors, such as a methane explosion, suffocation, and poisoning (Dorfelt, 1966). Even with the practice of mine evacuation, outburst gases have in some cases filled the mine, blown out of the mine shafts, and caused fatalities at the surface. In one case, the heavier-than-air gas (CO2) gas blew out of the mine shafts for 25 minutes, flowed down a hill into a populated area, and killed 3 people. Several potash mines were abandoned due to a high number of casualties (Baar, 1977). These types of incidents can also occur after mine closures.

3. Gas monitoring methods

3.1. In-situ direct gas measurements or/and gas sampling and laboratory analysis

The gas composition can be determined by in situ direct measurements with portable gas sensors. The sensors have to be frequently calibrated with several gas standards covering the range of interest. Relative uncertainties in the readings are generally <5%. Portable gas detectors can either monitor :

• a single specific gas, e.g. methane, carbon dioxide, etc ;

• all volatile organic carbon (VOC) gases, or total hydrocarbons ;

• all flammable gases as a total ;

• oxygen ;

• a combination of flammable gas(es), oxygen, carbon dioxide and other gases such as hydrogen sulphide or nitrous oxide. Separate sensors being used for each gas/ group of gases and the values being reported separately.

Portable gas detectors are point source detectors. They measure the concentration of the gas at the sampling point of the instrument. The unit of measurement is % volume ratio, % lower explosive

limit (LEL) for flammable gas, ppm for low-level concentrations (and toxic gases) or mg/m^3. There are a number of techniques used for gas detection.

Those detectors give a first idea of gas composition in an area. They allow the measurement of numerous points and numerous gases but there are just periodic and limited measurements.

Gas samples may conjointly be collected in order to be analysed in laboratory. Such analyses are more precise concerning gas concentrations.

3.2. Continuous automated monitoring of old mining sites

Gas monitoring can be accomplished by an automatic continuously operating station located on site. Continuous gas emission monitoring systems refer to a package of gas sampling system, gas analysers and other sensors of aerodynamics or meteorological parameters that are integrated with a data acquisition and data logging system. Continuous automated gas measurements can be performed in former mine workings, in soil, in air and at particular gas emissions points on surface (old shafts, fumaroles, faults…).

In a continuous emission monitoring system, a sample of gas is continuously withdrawn from the chosen source point and presented to various gases or other parameters sensors. Gas concentrations and other parameters are measured, recorded and stored as data. The data is used to generate reports, alarms... This system offers the advantages of choosing the most appropriate analysis technique for the desired components and concentration ranges.

3.3. Gas flux measurements on surface.

The measurement of the gas flow out of soil is probably the best method to detect and estimate the importance of gas emissions at the surface. It can be measured by placing accumulation chambers at discrete locations on surface and monitoring the rate of gas that accumulates in the chamber. INERIS has been developing and validating such methods since 1992 (Pokryszka et al., 1995). These methods, which were originally intended for landfills and contaminated ground, quickly found an application in mines (Pokryszka et Tauziède., 1999).

The method uses a chamber that avoids perturbing too much the environment (cf. Figure 1). The gas escapes from the covered area then accumulates in the chamber. In this way it is possible to monitor how the atmosphere becomes enriched in a studied gas. A sample of the mixture is fed to an analyser and then returned to the chamber. By monitoring the rate at which the recirculated mixture is enriched in the gas, it is possible to deduce the local gas flow at the given point. The dimensions of the chamber and the operating parameters of the method were optimised at the design stage on a test rig using known gas flows. The measurement system used is relatively simple to operate. The total time necessary for an individual measurement is of the order of 5 to 10 minutes, so that a large number can be made daily (from 40 to over 60 points according to the difficulties of the site).

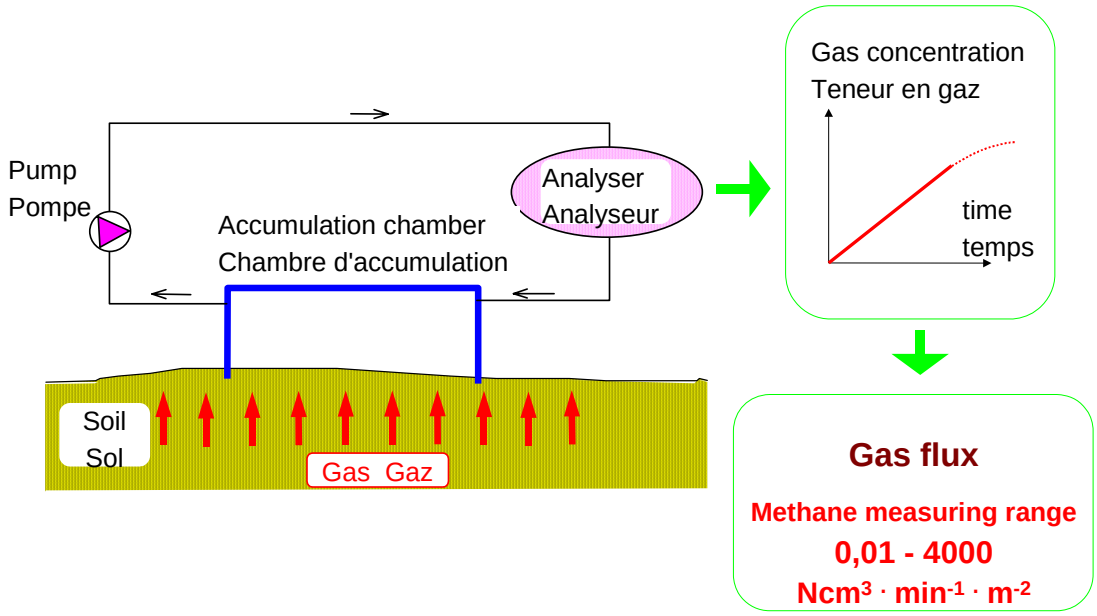


Figure 1. INERIS method of gas flow measurement on the soil surface

The method has already been applied in an operational manner for methane on the surface emissions diagnostics and appraisal on number of old mines sites in France, Czech Republic and Spain. The procedures involved in this method are protected by a European patent No. 96-05996.

The research work is now in progress at INERIS to adapt this method for CO_2 and radon emissions measurement on the surface of closed mines.

4. Examples of gas monitoring

4.1. Gases concentrations and aerodynamics parameters measurements in a closed iron mine

An automatic continuously operating station has been set up at the entrance of a former gallery connected to a closed iron mine in Lorraine, in Moyeuvre-Grande area. This area is affected by noxious gas emissions (under-oxygenated and noxious gas loaded mixtures).

In order to estimate the importance of these possible gas emissions, we have studied the influence of the aeraulic conditions within the underground voids on the gas flow from the old workings to the surface. We thus measured some aeraulic parameters in a former gallery, and interpret them in terms of process.

The monitoring device measures some aerodynamics parameters and gases concentrations. It is constituted by:

- A temperature sensor, that measures the air temperature old mining workings ;
- A barometric pressure sensor;
- A differential gas pressure sensor that measures the pressure difference between the old workings and external atmosphere;
- An O_2 and a radon gas sensors that measure the air composition in the gallery ;
- A data acquisition and data logging system.

Table 1 summarises the monitored parameters, their measure range and the sensors' characteristics. Figure 2. shows the monitoring station.

Table 1. Monitored parameters and the sensors' characteristics

Parameter	Sensor's measure range	Sensor	Sensor's accuracy	Acquisition frequency
O_2	0 to 25 (%vol.)	Polytron 2, Dräger	1% (± 0,1% O_2)	30 min
temperature in the gallery	-20 to +40 (°C)	PT 385, Prosensor	± 0,3°C	30 min
Atmospheric pressure	600 to 1060 (hPa)	Analogic barometer, PTB 101B, Vaisala	± 0,15 hPa	30 min
Differential pressure	-1 to 10 (Pa)	FCO 332, Furness Control	1%	30 min
radon	0 to 10 000 (Bq/m^3)	Barasol probe, Algade	65 Bq/m^3 h^{-1} (±0,8 imp.)	50 min

We also have at our disposal a measure of the outer atmospheric temperature.

The continuous monitoring of aeraulic parameters in the former gallery shows us that:

- The differential pressure between the outer atmosphere and the measured point in old workings, which is relatively close to the entrance (400 m), is low, in a range of -1 to 7 Pa. It is positive in summer and fluctuates around zero in winter;
- Theoretically the possible gas flow to the surface is low and goes preferentially through the fractures. This flow is higher in summer than in winter when it tends to zero and can even reverse.

These results give us data about the gas emissions from the former workings to the surface through the overburden. However, we need to perform other measurements in order to assess the importance of the flux through the fractured rocks.



Figure 2. Automatic continuously operating station at Moyeuvre-Grande

4.2. Monitoring of gas emission in deep boreholes in an operational salt mine

We have set-up an automatic continuously operating station in the context of an active salt mine in Lorraine. There, the salt is mined by the method of solution mining. Fresh water is injected through wells drilled into the salt bed, around 200m deep, to dissolve the salt and the resultant brine is then pumped to the surface. Dissolution of the salt forms a cavern in the salt deposit.

The objective of the experiment are (i) to identify the presence of gas within the salt deposit and (ii) to qualify and quantify the gas emission during the salt dissolution until the cavern collapses.

A continuous monitoring of the gaseous composition above the salt roof is allowed by the mean of an equipped drilling that emerges near the salt cavern. The gas mixture is measured by a withdrawal of the gas at the bottom of the drilling and its analysis by a specific device. The withdrawal and analysis of the gas are done continuously in a closed cycle (the gases are injected back in the drilling). This drilling is closed and allows the build up of the gases that can potentially be emitted at the salt roof.

The device is constituted by:

- Two flexible pipes: one channels the gas from the bottom of the drilling to the measure system and the other injects back the analysed gas at the bottom of the drilling;
- An automatic continuously operating station with :
  - Gas sensors;
  - A pump;
  - A data acquisition and data logging system.

The methods of analysis are non-destructive; therefore the gases can be injected back in the drilling in order to modify the composition of the gas and the pressure in the drilling.

Since the drilling has been equipped, in 2004, the system works under in-situ conditions. However, the salt exploitation is stopped and until now the composition of the air above the salt is the same as the atmosphere.

Moreover in situ direct measurements with portable gas sensors have been realised several times in the neighbour drillings above the future collapsed area. For that we insert a flexible pipe in the drilling. The CO_2, CH_4, H_2S, CO and O_2 concentrations are measured for each drilling. We noticed a spatial heterogeneity of the composition of the air in the drillings. The air is sometimes similar to the atmosphere and is sometimes enriched by methane or hydrogen sulphur.

4.3. Underground fire monitoring in an old mine of brown coal

On the site of the former lignite mine of Bois d'Asson, in Provence-Alpes-Côte d'Azur (SE of France), a spontaneous combustion has been noticed in 1999 through an old adit located close to the surface. Since the gas emissions on the site have been monitored by periodic in situ direct measurements with portable gas sensors.

We have set up a monitoring system in order to monitor the evolution of the combustion by measuring the underground temperature at various locations. This system also allows data logging and acquisition and transmission of these data by GSM.

The system consists of:

- Four temperature sensors placed in particular points of the site (Figures 3 to 5):
  - In the affected gallery;
  - In a fumarole at the surface above the gallery;
  - In the soil, 0,5m depth in a location where there is no influence of the coal heating;
  - In the atmosphere in a sun-protected location;

  The two least points are references in order to take the meteorological and climatic conditions into account.
- A station for data acquisition, data logging and data transmission by GSM (cf. Figure 6);
- An autonomous electric supply with two batteries, a loader and a solar panel (cf. Figure 7).

After one year, the experience has shown that the system works well. Thanks to the temperature measurements and the data teletransmission, it is possible to better follow the evolution of underground fire on this old mining site.



Figure 3. Temperature sensor at the entrance of the gallery



Figure 4. Outer temperature sensor



Figure 5. Sensor in a fumarole



Figure 6. Sensor in the soil



Figure 7. Box that protects electrical and electronic elements.



Figure 8. Whole view of the station

5. Conclusion

After mine closures gas emission risks may persist. Gases accumulated in post-mining voids can migrate to the surface through aerodynamic links. This may lead to risks of accidents on surface like explosions, asphyxia or intoxications.

Methods have been set up to monitor the sites where there are risks. Continuous automated systems associated with data teletransmission appear to be the best method to monitor old mine sites.

INERIS has developed efficient methods that have been validated in several post mining sites. These methods can now be used in the case of gas hazards in other closed mines sites.

6. References

Grabowski, D., Pokryszka, Z. (2003) *Noxious gas emissions from the closed iron mines to the built-up areas on the surface.* Proceedings of the 10th International Congress on Rock Mechanics ISRM 2003, 8-12 septembre 2003, Johanesbourg, Afrique du Sud, vol. 1.

Kral, V., Paletnik, M, Novotny, R. (1998) *Methane from closed-down mines in the soil*. Proc. of the international conference on coal-bed methane technologies of recovery and utilisation, GIG (eds), Katowice (Poland)

Novotny, R., Platenik, M., Takla, G., Kral, V. (2001) *Reduction of uncontrollable mine gas emission in the Czech part of Upper Silesian hard coal basin devastated by past mining activity.* Proc. of the 7th international mine ventilation congress, Research & Development Center EMAG (eds), Cracow (Poland).

Robinson, R. (2000) *Mine gas hazards at the surface environment.* Mining Technology, 109(3), 228-236.

Pokryszka, Z., Tauziède, C. (1999) *Method of measuring surface emission of methane*. International Conference on Latest Achievements in the Field of Mine Ventilation, Fire and Methane Hazard Fighting, , Szczyrk, Poland, 22-24 April 1999.

Pokryszka, Z., Tauziède, C. (2000) *Evaluation of gas emission from closed mines surface to atmosphere* – Proc. of the 6th international conference on environmental issues and management of waste in energy and mineral production, Calgary (Canada) – Balkema (eds)

Pokryszka, Z., Tauziède, C., Cassini, P. (1995) *Development and validation of a method for measuring biogas emissions using a dynamic chamber*. 5th International Landfills Conference - Sardinia'95, Proceedings vol III, CISA eds, Cagliari.

RISK EVALUATION AND RELATED STABILITY CONSIDERATIONS FOR ABANDONED CANADIAN METAL MINES

BÉTOURNAY, Marc C.
CANMET, Mining and Mineral Sciences Laboratories, Natural Resources Canada, Ottawa, Ontario, Canada, K1A 0G1
mbetourn@nrcan.gc.ca

ABSTRACT: A comprehensive engineering manual has been issued on the subject of site stability in response to a requirement for better risk assessment and risk mitigation for Canadian abandoned metal mines. This article establishes the basis for quantified risk assessment, and the calculation of the hazard probability and consequence aspects that comprise the risk value. This is outlined for factor of safety-based probabilistic, empirical probability, and numerical modeling applications. Clear geomechanics considerations such as hazard failure mechanisms and their development are also presented. The article provides outlines for land use and selection of remediation measures based on risk.

KEYWORDS: Abandoned metal mines, failure mechanisms, hazards, consequences, risk

RÉSUMÉ : Un manuel pratique a été publié à propos de la stabilité des sites pour répondre à un besoin d'améliorer l'évaluation et la réduction des risques associés aux mines métalliques abandonnées canadiennes. Cet article présente les bases d'une évaluation quantifiée du risque, ainsi que le calcul de la probabilité d'occurrence et des conséquences en particulier financières. Cette évaluation est faite sur la base de facteur de sécurité à base probabiliste, une probabilité empirique, et l'application de modélisation numérique. Des considérations géomécaniques précises telles que les mécanismes de ruptures sont également présentées. Cet article fournit également un choix de méthodes de traitement du risque.

MOTS-CLEFS : Mines de métaux abandonnées, mécanismes de ruptures, dangers, conséquences, risque

1. Introduction

Canada's mining history has left an important legacy of inactive mine sites with serious implications on the perpetuity of site hazards and risks that could be associated with them.
Mine closure in Canada requires planning to evaluate and mitigate long-term rock mass movements affecting surface integrity. To strengthen regulations, coupled with new approaches to liability and responsibility, regulatory agencies are requiring that better derived long-term risk assessment and risk mitigation be achieved during mine decommissioning or during reviews of abandoned ones. Also, pressures are exerted on municipal and provincial jurisdictions to use available land for alternate use.
The Canadian Shallow Stope Mine Decommissioning Manual, produced for the regulatory agencies (Bétournay, 2004a), has established a site management approach (Figure 1) that requires an in-depth understanding of site geomechanical aspects and the nature, timing and path development of potential failure mechanisms. Detailed representation of such rock mass behaviour is essential to quantify the risk associated with all potential hazards, upon which remediation decisions, site use and risk management must be based.

2. Geomechanical Aspects

Because Canadian metalliferous orebodies usually extend to the upper limit of bedrock, shallow underground stopes have been routinely created close to, or through to surface. Geological terrains are geomechanically poorer than at depth. Overburden and bodies of water can be close by, which

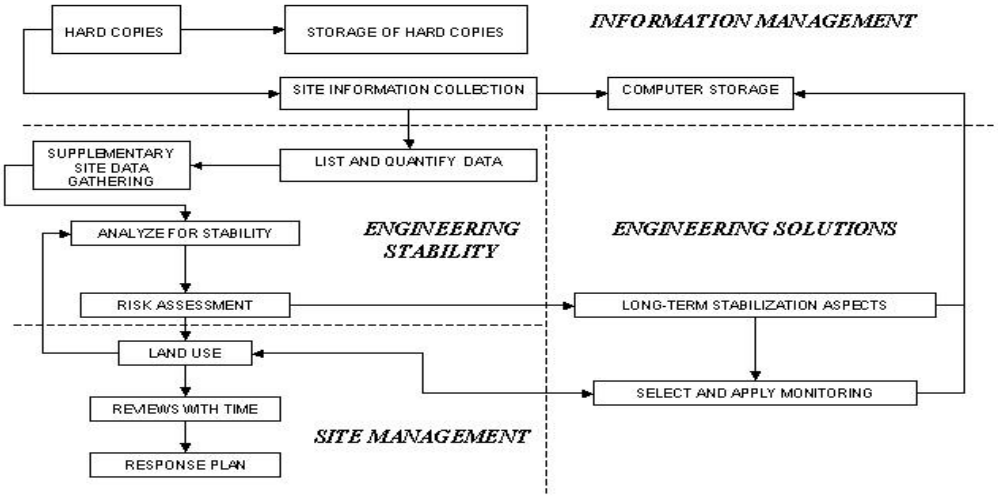


Figure 1. Canadian metal mine shallow stope decommissioning process (Bétournay, 2004a).

represent elements of care.

Rock mass instabilities predominantly originate with geological discontinuities (joints, faults) and rock fabric (foliation, bedding, etc.). Lateral ground stresses can be important in providing confinement, but laterally-extensive mining eliminates this advantage. When rock material has poor self-support capabilities, failure by exceeding rock mass strength is possible. When the rock mass is poorly jointed, of high quality, extensive lateral stope dimensions, or very thin pillars can be stable in the short term.

Obtaining a detailed understanding of rock mass conditions and defining the engineering characteristics of the rock masses are required to: obtain a representative sense of site conditions; carry out stability analyses with a maximum level of confidence; extract potential future dominant failure influences and types; and, form the basis for ground remediation and monitoring application. Sufficient rock mass coverage will provide a high degree of certainty of range of values and distribution of features.

The characterization result obtained can then be used to compare the site conditions to common rock mass environments. A review of shallow stope case studies (Bétournay, 1995) indicates that several common Canadian metal mine rock mass environments can be identified, in which a possible number of failure mechanisms can occur (Figure 2).

Rock mass movements at stope peripheries can be sudden and massive, piecewise and continuous, irregular in time, or one type followed by another. They may never reach surface because of re-equilibration, lack of space for failed material, or changes in geology or stope configuration.

Failure of shallow stopes is taken to denote rock mass movements that start from the shallow stope and develop to the top of bedrock. It has been shown that failures of shallow stopes will not always begin within the surface crown pillar above the shallow stope (Bétournay, 1995). It could start in the stope hangingwall or footwall. However, most of the time, the failure paths run close to or in the surface crown pillar. Design and evaluation of stability and risk should therefore address the

question “Which portion of the rock mass is mobilized in a failure to surface?” rather than “What should be the thickness of the surface crown pillar?”.

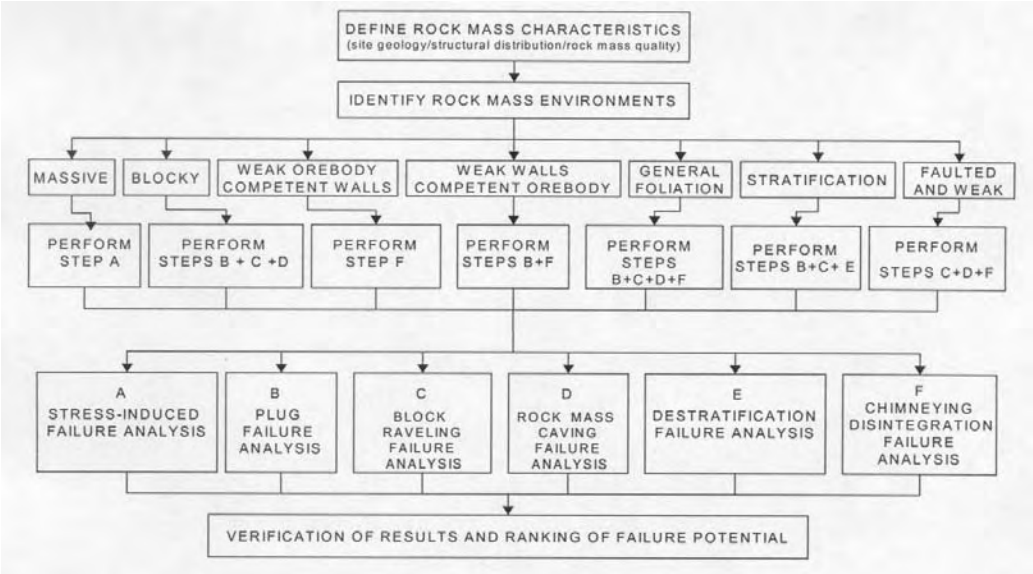
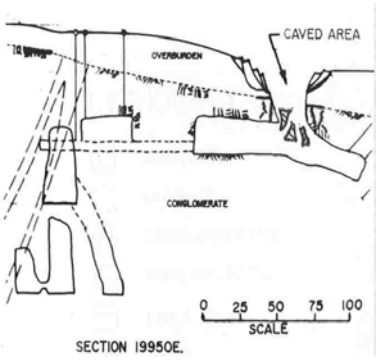


Figure 2. Shallow stope stability evaluation flow chart (Bétournay, 2004a).

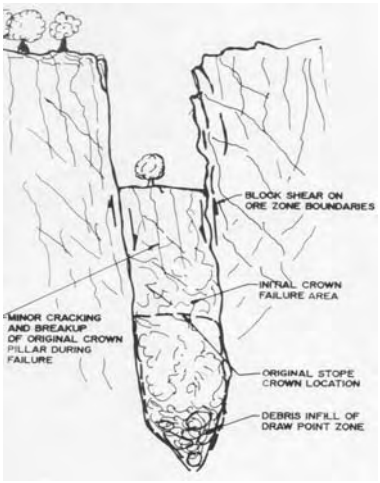
There are six common failures mechanisms associated with metal mines (Figure 3). Rock fracturing entails the rupture of a high quality surface crown pillar rock mass with collapse into the shallow stope. Large rock mass plugs fall suddenly into the underlying stope as an integral block, delineated by well-defined boundary plane discontinuities. Ravelling is a peripheral block-by-block failure without a stable cavity reached; a special case of ravelling is peeling of thin laminae, leading to the destabilization of the surface crown pillar. Tensile failures of stratified rock occur with dipping strata at stope walls and with shallow dipping strata at the base of surface crown pillars. Disintegration occurs as upward piecewise progression of a weak rock mass forming a limited cavity, or through progressive thinning of the surface crown pillar from rock material alteration and piecewise failure. Block caving is the rock mass break-up and gravity mobilization of blocks (flow) towards and into an opening leading to a progressive failure front moving towards surface.
There is normally little subsidence associated with the failures. The top of bedrock, and hence the overburden, is only affected when the failure front is near to it. This translates to localized ground movement which can be limited in its damage if proper surface access restrictions and infrastructure/activities are located elsewhere.

3. Risk Assessment

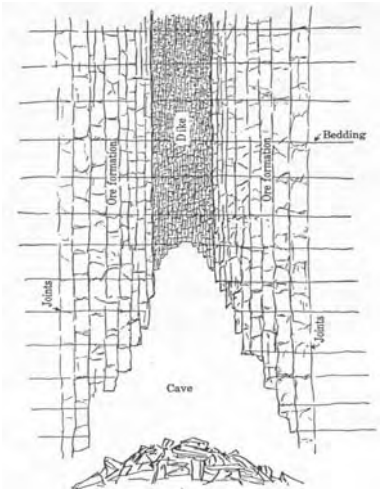
Increasing concern over the impact of mining activity on public safety and site use are focusing considerable attention on the identification of site hazards and risk associated with them. The notion of absolute safety is not realistic, however, especially when considering the variations of geomechanical elements within a rock mass and the difficulty to completely quantify them. This is important when considering the weaker, more variable shallow portion of bedrock.
The decision at which level analysis is carried out should primarily be based on the initial perception of the risk involved (Figure 4); although this may be modified once a preliminary evaluation has been completed. Where there is a potential for oss of life, detailed quantitative analysis should be the norm.



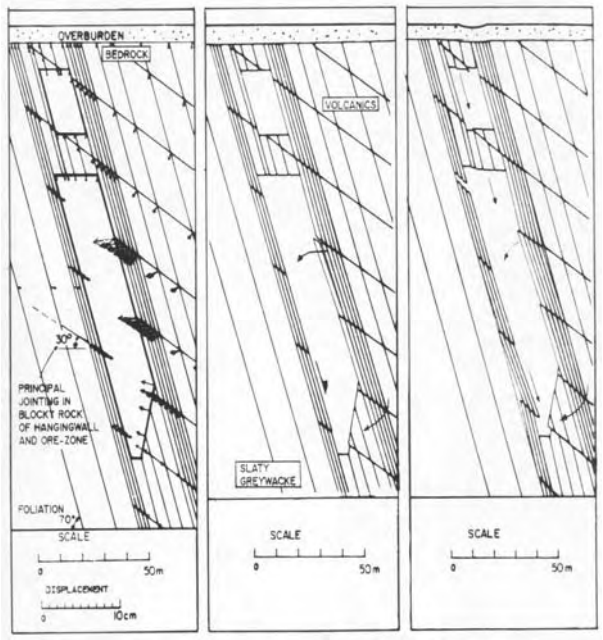
(a)



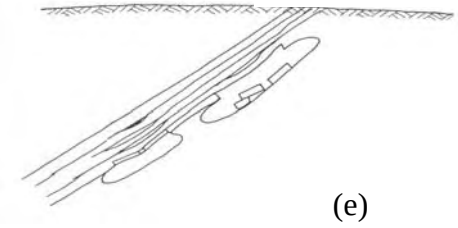
(b)



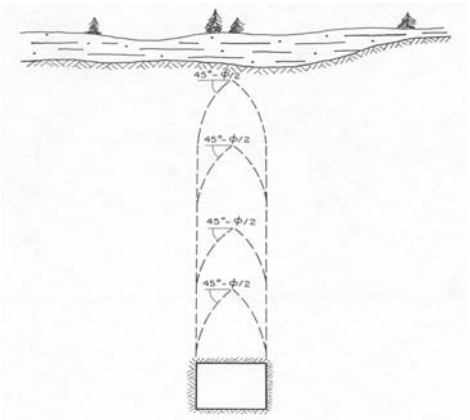
(c)



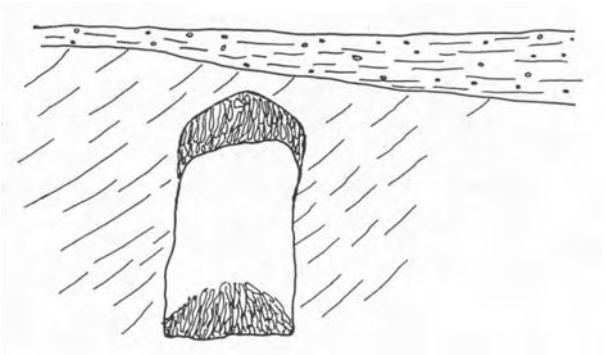
(d)



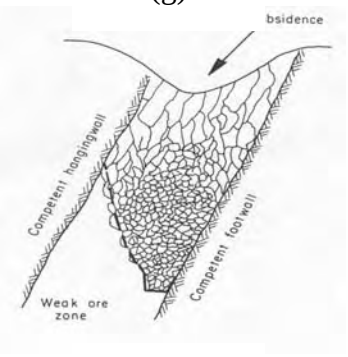
(e)



(g)



(f)



(h)

Figure 3. Common failure mechanisms of shallow stopes of hard rock mines: (a) rupture, (b) plug (Golder Associates, 1990), (c) ravelling (Crane, 1929), (d) delamination (Golder Associates, 1990), (e) strata failure, (f) alteration disintegration, (g) chimneying disintegration, (h) block caving (Bétournay, 2004a).

Frequency of occurrence	Severity			
	Catastrophic	Major	Minor	Negligible
Frequent	A	A	A	C
Probable	A	A	B	C
Occasional	A	B	B	D
Remote	A	B	C	D
Improbable	B	C	C	D

Action Guide

Risk level	Analysis
A	Detailed quantitative
B	Semiquantitative
C	Qualitative
D	Not required

Figure 4. Frequency-severity matrix and action guide (Canadian Standards Association, 1991).

Risk is defined as the combination of the probability of a hazard occurring (e.g. failure mechanism) and the consequence that it can lead to (measured impacts):

$$R = Px \times Cx \quad (1)$$

A detailed quantitative analysis of risk should ideally be performed at mine closure when the existing information can be gathered and decisions about site remediation and management must be taken. Too often is vital information lost after mine closure.

Sufficient data accurately reflecting existing conditions are required for proper consideration and minimize any significant degree of uncertainty in rock mass and parametric value coverage.
Figure 5 outlines the process and pathway to follow for shallow stope risk analysis, and includes hazard identification, probability of occurrence, consequence impact assessment, hazard-specific risk calculation and broader site risk evaluation.
A probabilistic hazard assessment can provide a level of safety for a particular condition, including the effect of the variability of input parameters, and, in limit equilibrium equations, presented in another article for this conference (Bétournay, 2005). The failure mechanisms presented earlier have been represented by factor of safety equations (except for block caving) (Bétournay, 2004a). A probabilistic assessment based on an empirical approach can also be carried out and will be described further in the article.
Ideally, the practitioner will understand the failure process for the numbers to have any meaning. For example, plug failures anticipating shearing of a blocky rock mass or block ravelling in inherently weak rock material is not realistic.
The results are presented as a probability that the factor of safety will be less than a certain value. Two methods are commonly used to obtain the distribution of factors of safety for a given hazard: the Monte Carlo method, which uses a random number generator to determine a value for each of the normally distributed equation variables and a factor of safety for each set of such values. The second, based on the fact that a quantity calculated from an equation containing normally distributed variables will itself be normally distributed (Rosenbleuth, 1972), uses values at each standard deviation on either side of the mean. This produces 2^n probability solutions (n=number of variables).

For example, in deciding the minimum level of safety for a given failure type, the factor of safety will be less than 1.0 which can be calculated from:

$$P(-\infty < Fs < b) = \Phi\left(\frac{b-\bar{V}}{S}\right) - \Phi(-\infty) \qquad (2)$$

where b = distribution variable value considered (e.g. Fs-1.0)
S = standard deviation of the variable's normal distribution
$\bar{V}$ = mean of the distribution

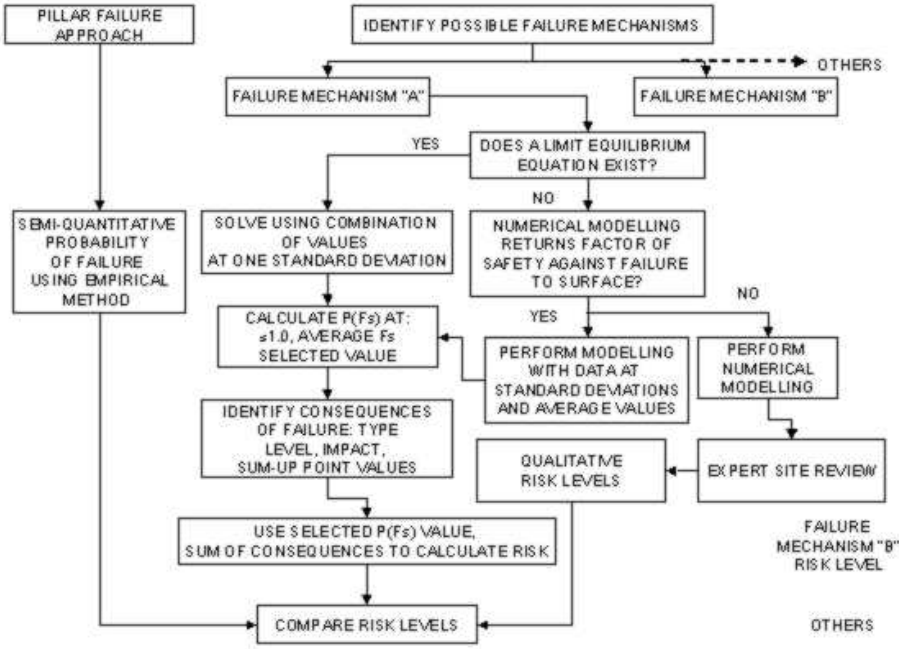


Figure 5. Shallow stope risk analysis (Bétournay, 2004a).

The empirical method uses a statistical critical surface crown pillar span line to separate essentially stable cases from essentially failed cases (Figure 6). In this semi-quantitative method, failure is expected to occur whenever rock mass quality is locally less than the critical quality for the crown zone and periphery. The procedure is to obtain the critical minimum rock mass quality using the critical span line equation and chart at the critical span value. The location of this point versus the mean rock mass quality value provides the critical offset from the mean and related probability of concern.

The application of several, properly failure mechanism-matched numerical modelling runs using representative failure criteria would have to be carried out using a sensitivity analysis, i.e. using a comprehensive variation in parameters to obtain a cross-section of realistic factors of safety from which probabilities could be derived. This would provide a qualitative level of hazard. In all approaches, a comprehensive comparative review of the results is required before the application of consequence measures to arrive at realistic risk identification.

What are the reference values against which the obtained probability can be compared to verify against an acceptable level of confidence against failure? In part, the small number of cases associated with each failure mechanism, has prevented the development of reference values. This compares with significantly more cases related to coal mining.

Consequences of failure (the impact of a hazard on potential receptors), form the other portion of risk calculation. Various categories of impact consequences can be considered (Table 1), depending on the location of the underground mine. If an all-encompassing evaluation is required,

a common factor system of measurement must be defined, such as a point scale, since the measure of impact includes various subjects.
The relative value assigned to such elements is difficult to determine and admittedly controversial and must be the subject of protracted debates and resolution between all stakeholders in the regulatory/mine owner/local residents strategy. Table 2 offers an arbitrary relative comparative scale and arrived at by pair-wise comparisons of Table 1. It distributes a constant number of points among the consequences reflecting relative importance. By adding up all of the anticipated impact consequences, the total rating value can be used against probability of hazard occurrence to arrive at a quantified risk value for a particular failure mechanism.

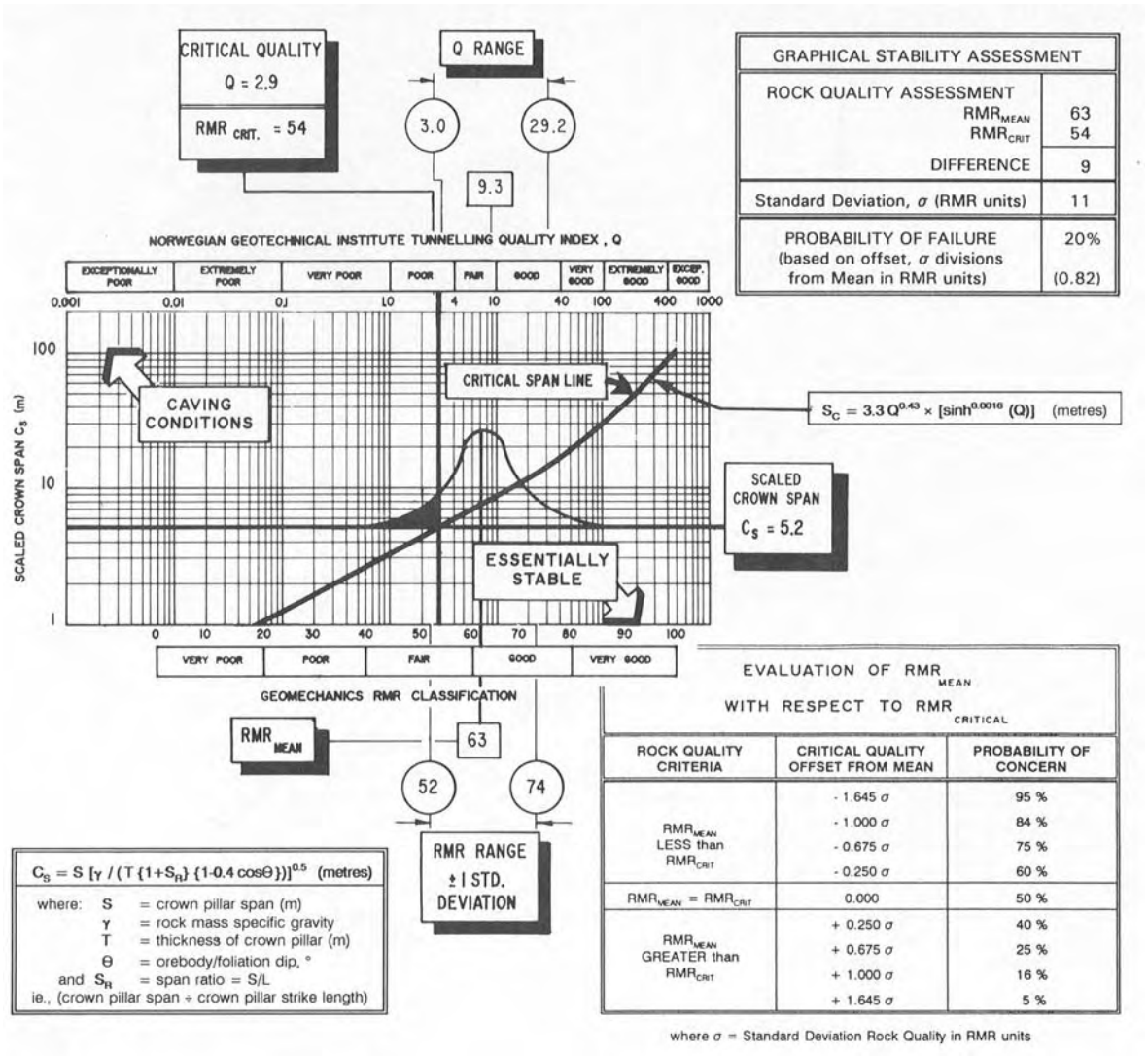


Figure 6. Example application of scaled crown-span concept to evaluate probability of failure for a surface crown pillar of known geometry (Carter and Miller, 1995). Q index from Barton et al. (1974), RMR index from Bieniawski (1973).

Specific risk identification, extent and overview of targeted issues to be addressed (Table 3) can also be performed using the "what if/checklist" technique (Center for Chemical Process Safety, 1992). For each risk, the impact and likelihood of occurrence are estimated using the agreed-to scales (the estimated probability classification ranges can be arranged to suit the needs (e.g. remote areas versus populated centres)). In this exercise, participation from the cross-section of stakeholders as well as an expert(s) on abandoned mines is required.

Table 1. Example of a cross-section of hazard impact consequences for shallow stopes (Bétournay, 2004a).

	PUBLIC						ECONOMIC			ENVIRONMENTAL	
Qualifying Level	Safety	Water Source	Social	Cultural	Trust	Services	Land-owner	Public	Industry	Species	Habitat
4	loss of life	unuseable	different residence, lifestyle	loss of object, structure	community disruption	complete, long-term	high (>20% of property value)	high (>$250K)	high (>$250K)	major (serious loss)	major (total)
3	serious injury	partial use with treatment	change in residence, lifestyle	significant damage to object, structure	community activism	partial, long-term	moderate (5-20%) of property value	moderate ($50-250K)	moderate ($50-250K)	moderate (partial loss)	moderate (replace-able)
2	minor injury	acceptable quality	disruption in residence, lifestyle	repairable damage to object, structure	disapproval	short-term	low (<5%) of property value	low (<$50K)	low (<$50K)	minor (localize d loss)	minor (replace-able)
1	negligeable or no impact										

Table 2. Example of priorization of consequence of impact and possible point values (Bétournay, 2004a).

Consequence	Value	Consequence	Value	Consequence	Value	Consequence	Value	Consequence	Value
Loss of life	500	High public expenditure	26	Lost community trust	13	Low private cost	9	Disruption in residence	4
Serious injury	50	Significant damage to object	22	Partial loss of services	12	Minor injury	8	Community disapproval	3
Loss of services	40	Moderate public expenditure	20	Moderate industry cost	12	Moderate species loss	7	Minor species loss	2
Loss of species	40	Moderate private cost	18	Partial water use	12	Community activism	7	Minor habitat loss	1
Loss of object	30	High industry cost	18	Change in residence	10	Repairable object	7	No effect	0
Loss of habitat	30	Different residence	16	Acceptable water	10	Moderate habitat loss	6		
Unuseable water	30	Low public expenditure	13	Low industry cost	10	Short-term service loss	5	MAXIMUM TOTAL	1,000

Table 3. Qualitative risk assessment scales, population consideration (Bétournay, 2004a).

Numerical Rank	**1**	**2**	**3**	**4**	**5**
Qualitative Description	Very low	Low	Possible	High	Very high
Probability/Likelihood					
Qualitative Description	Rare, very unlikely	Unlikely but not impossible	Moderate, just as likely	Likely	Almost certain, will probably arise
Probability	0.0-0.1	0.1-0.4	0.4-0.6	0.6-0.9	0.9-1.0
Health and Safety Consequences/Impact					
Qualitative Description	Negligible	Minor	Moderate	Major	Catastrophic
People	At most first aid	Local medical aid	Disabling injury	Life threatening	Fatality(ies)

4. Land Use

As a general rule, the location of current and new human activity, surface infrastructure and buried service components must be established on a "favourable terrain" basis, requiring a careful examination of the ultimate area of influence around and above the shallow stope, and related risk analysis. Table 4 presents an example of a qualitative risk matrix that indicates land use potential.

Table 4. Example of land use activity risk matrix (Bétournay, 2004a).

Hazard Probability	High	□			
	Medium	□	□		
	Low	□	□		
		1	2	3	4
	Degree of consequence				
□ land use potential					

No activity that would potentially compromise the safety of people should be undertaken in the area of hazard influence (permanent structures, infrastructure, recreational areas). Existing infrastructure over inactive mines requires re-examination and remediation measures undertaken where possible, in order to reduce hazard consequences to low levels. As a rule, two generic options are available for land use. It is based on manageable decisions that avoid degrees of human access guidelines, which are always difficult to match with a range of probability of failure, especially when the body of case studies is limited:

- Prohibited, no public access: rock mass and surface considerations are within area of influence of instability; minimum site remediation applied

  Examples:

  - Remote use

    - secondary use: land fill, nature preserve
    - geothermal energy

- Limited to routine use of the site depending on the nature of the risk activity considered for the site and monitoring applied:
  Examples:
  - Partial use:
    - with specific site remediation to reduce risk: surface storage
  - Routine use options:
    - with removal of hazard and stabilization of the rock mass: partial public access

5. Remediation Measures

Three options are available to the site operator to control the long-term behaviour of rock masses around shallow underground mine openings:

- Leaving the site as-is
- Carrying out long-term monitoring and/or mitigating possible hazards by removing, or engineering the stabilization of potential unstable rock mass elements
- Removing immediate risk by closing access or relocating the infrastructure

To date there are no specific regulatory obligations in Canada requiring remediation type versus given risk level or failure consequences. Table 5 outlines the broad remediation options to counter site risk.

Table 5. Shallow stope remediation options (Bétournay, 2004a)

METHODS	USE	RISK REDUCTION	EFFECTIVE LIFE	APPROXIMATE COST	ADVANTAGES	DISADVANTAGES
Signs monuments	Warn and alert	None	Temporary <25 years	<$200 each	Inexpensive; easy to install; site-wide coverage	No risk mitigation; subject to vandalism, degradation, vegetation overgrowth
Fence (chain link)	Limit access	Preventing consequence of hazard	Temporary <50 years	$80-$200 per linear meter	Inexpensive; simple to install; prevents entry	Ongoing inspection needed; corrosion, vandalism, theft
Concrete cap	Prevent access	Preventing consequence of hazard (surface crown pillar)	Long-term >50 years	$4,500/$m^2$ of area of coverage	Potential support; hazard prevented; alternative site use possible	Costly; deterioration over time
Structural bridge	Limit access	Preventing consequence of hazard	Long-term >50 years	>$1,000,000	Hazard prevented	Very costly; analysis of stability for footings; deterioration over time
Backfilling	Prevent access	Preventing hazard	Permanent (provided fill mass and retaining structure failures do not occur)	>$40/$m^3$ (e.g. hydraulic fill)	Permanent support (if contained); hazard prevented; alternative site use possible; ongoing failures stopped	Very costly; underground bulkheads required; fill settlement
Surface crown pillar removal by blasting	Prevent access	Preventing hazard	Permanent	$15/$m^3$	Removal of hazardous surface crown pillar, periphery; water filling for habitats	Partial hazard removal; periphery can still fail

Remediation should be selected on the basis of:

- The effectiveness of a measure to prevent access or reduce hazards
- The level of site risk (probability of occurrence; present/future consequences, anticipated site use, etc.)
- The serviceable life of the selected measure
- The future value of the mine opening
- The associated cost of the mitigating measure

6. Case Study

A major site definition and investigation of an abandoned gold mine in northern Ontario found the surface crown pillar of a shallow underground stope under an important highway to be under failing conditions (Bétournay, 2004b). It provides the only access to remote communities and mining operations. Alteration disintegration had developed over 25 years in metamorphic foliated iron rock, leaving only a 1 m thick surface crown pillar. Furthermore, there was evidence that the pillar was moving downward as a plug along the foliation and well-developed cross joints. The probability of plug failure was calculated to be 0.7 with planar plug boundaries, but upon further considerations, it was concluded that the "stepped" foliation surface was preventing sudden failure. Considerable consequences could occur from this hazard: loss of life, high public expenditure, high industry cost, community trust and disruption in services. The provincial government made a decision that the safety of the road could not be assured. Various options were discussed to mitigate or avoid the hazard such as diverting the highway to avoid other abandoned underground stopes, building a concrete plate under the highway to span the stope (with or without blasting the surface crown pillar), filling the stope, or placing a temporary bridge over the potential cave area while final options were evaluated. Given the high degree of consequences, and the fact that filling would be very costly and the fill not effectively contained underground, the option of a permanent bridge over the stope was selected at the cost of CDN$1.8M. The foundation of the new bridge was designed taking into consideration the failure development of the pillar and stope peripheries. Construction was completed eight years after the temporary bridge was put in place. To date, the complete failure of the surface crown pillar has not occurred.

7. References

Barton, N., Lien, R. Lunde, J. (1974). *Engineering Classification of Rock Masses for the Design of Tunnel Support*, Rock Mech. Volume 6 #4, 189-236.

Bétournay, M.C. (1995). *The Stability of Shallow Stopes of Hard Rock Mines,* McGill University Ph.D. Thesis, 611.

Bétournay, M.C. (2004a). *Canadian Manual for Metal Mine Shallow Stope Decommissioning*, CANMET Mining and Mineral Sciences Laboratories, Division Report 04-022(TR), Natural Resources Canada, 142 p.

Bétournay, M.C. (2004b). *Stability Evaluation and Remediation of a Critical Northern Canada Highway Over an Abandoned Gold Mine*, Proceedings 5th Biennial Workshop on Abandoned Mines, U.S. Interstate Group on Abandoned Mines, 71-80.

Bétournay, M.C. (2005). *Failure Mechanisms, Stability Aspects and Analysis Techniques for Abandoned Canadian Metal Mines*. Proceedings Post Mining 2005, Nancy.

Bieniawski, Z.T. (1973). *Engineering Classification of Rock Masses*, Trans. South Afri. Inst. Civil Eng., Volume 15, 335-344.

Canadian Standards Association (1991). *Risk Analysis Requirements and Guidelines*. CAN/CSA-Q634-M91, 42p.

Carter, T.G., Miller, R.I. (1995). *Crown Pillar Assessment – Planning aid for Cost-effective Remediation*, Trans. Instn. Min. Metal., Volume A104, 41-57.

Center for Chemical Process Safety (1992). *Guidelines for Hazard Evaluation Procedures, With Worked Examples*; 2nd Edition. American Institute of Chemical Engineers.

Crane, W.R. (1929). *Subsidence and Ground Movement in the Copper and Iron Mines of the Upper Peninsula, Michigan*. U.S. Bureau of Mines, Bulletin 295.

Golder Associates (1990). *Crown Pillars Stability Back Analysis*, CANMET, Energy, Mines and Resources Canada Contract 01sq23440-8-9074.

Rosenbleuth, E. (1972). *Point Estimates for Probability Moments*. Proc. Nat. Acad. of Sci., U.S.A., Vol. 10, 3812-3814.

FAILURE MECHANISMS, STABILITY ASPECTS, AND ANALYSIS TECHNIQUES FOR ABANDONED CANADIAN METAL MINES

BÉTOURNAY, Marc C.
CANMET, Mining and Mineral Sciences Laboratories, Natural Resources Canada, Ottawa, Ontario, Canada, K1A 0G1
mbetourn@nrcan.gc.ca

ABSTRACT: Canadian shallow stopes of hard rock mines, usually affected by inherently weak or complex rock mass conditions, can be subject to various types of failure mechanisms. This article reviews the associated common rock mass settings and specific geomechanical stability aspects that are associated with them. The effectiveness of conventional rock mechanics approaches is contrasted to the analysis requirements of the failure mechanisms. Dedicated numerical, analytical and empirical methods are presented as well as their limitations.

KEYWORDS: Abandoned metal mines, failure mechanisms, analysis

RÉSUMÉ: Les chantiers peu profonds des mines de métaux canadiennes, creusés la plupart du temps dans des massifs de faible résistance ou à structure complexe, peuvent être sujets à divers mécanismes de rupture. Cet article passe en revue les différents aspects liés à la stabilité géomécanique associés aux différents types de massifs rocheux. L'efficacité des méthodes conventionnelles de mécanique des roches est comparée au besoin d'analyse des mécanismes de rupture. Des méthodes numériques, analytiques et empirique dédiées sont présentées, ainsi que leurs restrictions.

MOTS-CLEFS : Mines de métaux abandonnées, mécanismes de ruptures, analyses

1. Introduction

Canada's mining legacy includes over 10,000 known inactives sites, most of which are related to the extraction of metal commodities. Stakeholders, especially the engineer of record, regulatory agencies and land owners, face difficult stability considerations related to the confidence of knowledge about a site. This most often pertains to shallow stopes (usually within 50 m of surface) and the variability in rock mass properties. Canadian metalliferous orebodies usually extend to the upper limit of bedrock, where geological terrains have variable rock mass quality, poorer than those at depth. Overburden and bodies of water can be close by and cover the mineralized bedrock. Ground stresses may not be sufficient to prevent gravity failures. When rock material has poor self-support capabilities, failure by exceeding rock mass strength is possible. When the rock mass is poorly jointed and of high quality, extensive lateral stope dimensions, and very thin pillars can be stable in the short term.
There is a wide variability in rock mass mobilization that can lead to failure even for a given rock mass setting (Figure 1).

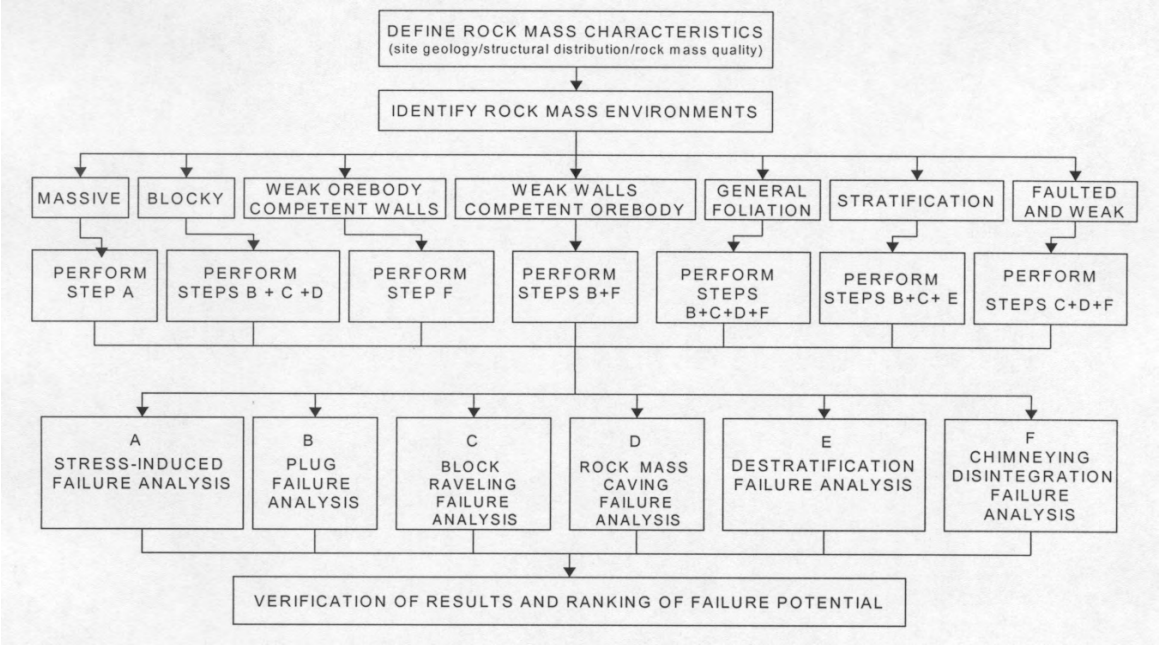


Figure 1. Shallow stope stability evaluation flow chart (Bétournay, 1995).

2. Failure Mechanisms

Case studies indicate that several common Canadian metal mine rock mass settings can be identified (Figure 2), in which a possible number of failure mechanisms can occur (Figure 3) (failure taken here to denote rock mass movements that start from the shallow stope and develop to the top of bedrock).

Rock mass movements at the periphery of shallow stopes can be sudden and massive, piecewise and continuous, irregular over long periods of time or one type followed by another and may not ever reach surface because of re-equilibration, lack of space for failed material and failure continuation, or changes in geology or stope configuration.

The six common failures mechanisms associated with metal mines are: rock fracturing, which entails the rupture of a high quality surface crown pillar rock mass (structure capping the stope) with collapse into the shallow stope; large rock mass plugs which fall suddenly into the underlying stope as an integral block; ravelling, a peripheral block-by-block rock mass failure without a stable cavity form reached; tensile failures of stratified rock occurring from dipping strata at stope walls and with shallow dipping strata at the base of surface crown pillars; disintegration, occurring as an upward, piecewise progression of a weak rock mass forming a limited cavity, or through progressive thinning of the surface crown pillar from rock material alteration and piecewise failure; and block caving, the rock mass break-up and gravity mobilization of blocks (flow) towards and into an opening leading to a progressive failure front moving towards surface.

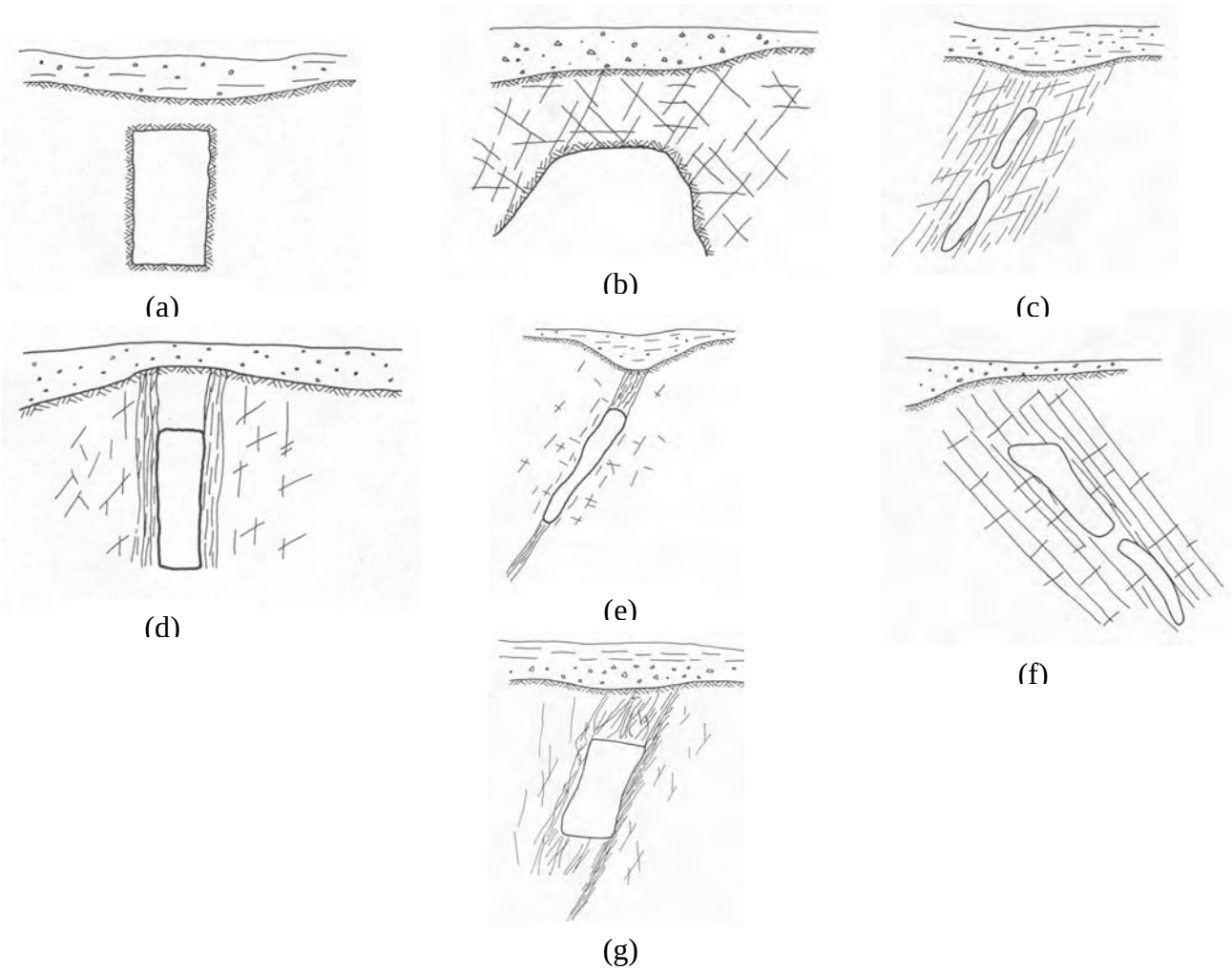
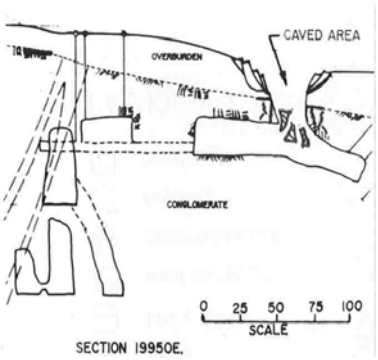
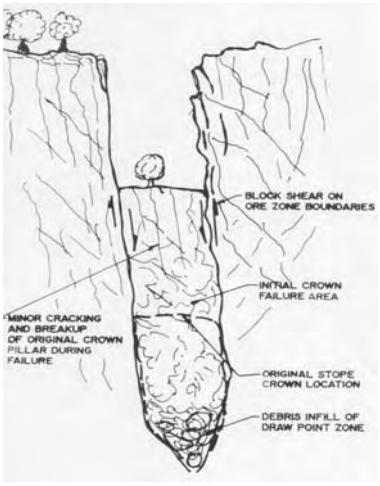


Figure 2. Common rock mass settings of shallow stopes of Canadian metal mines: (a) poorly jointed, (b) jointed and blocky, (c) weak, schistose orebody, (d) weak, schistose walls, (e) generally foliated, (f) stratified, (g) fault-weakened, altered (Bétournay, 1995).

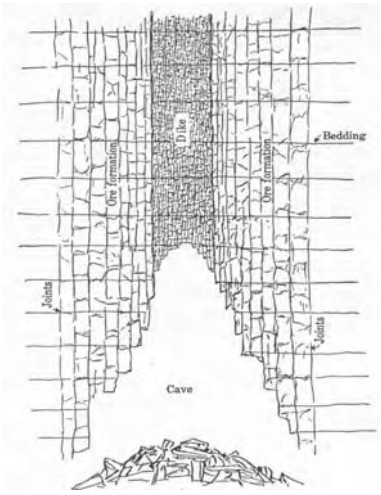
Plug failures have usually occurred on well-defined and uninterrupted discontinuities with low shear strength such as faults, foliation, or sheared contacts, bounding the periphery of the surface crown pillars of shallow stopes. Failure can occur when the surface crown pillar thickness/plug height, can be extensive, up to 660 m, where frictional properties of the bounding surfaces are very low (e.g. φ<8E). Plug failure potential depends considerably on the confinement available from redistributed tectonic stress around the stope to resist the plug's displacement. In areas of high extraction with numerous shallow stopes distributed locally or regionally, lateral confinement is effectively reduced or eliminated in those pillars centrally located (Bétournay, 2004a). The dip of the delimiting discontinuities is also important in reducing the potential for such occurrences (Bétournay, 1995). A further reduction in failure potential is obtained when the bounding planes are not continuous, i.e. contain intact rock segments. In failed cases, no precursor movements were noted. Failure occurred suddenly and completely.



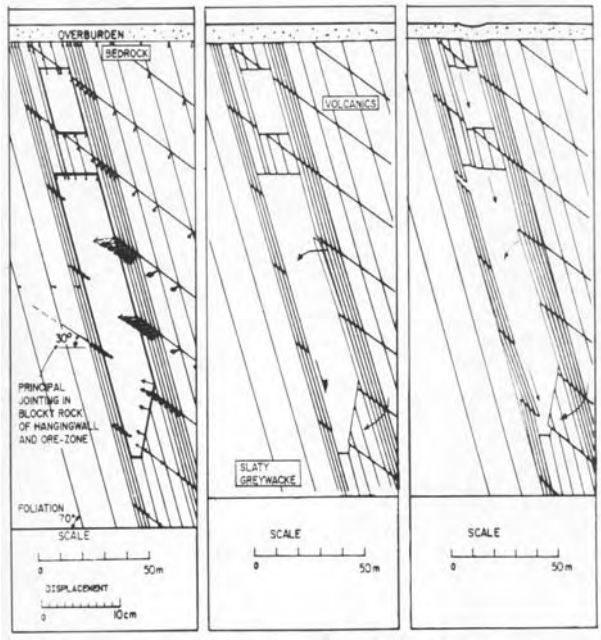
(a)



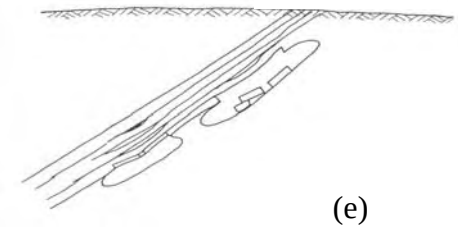
(b)



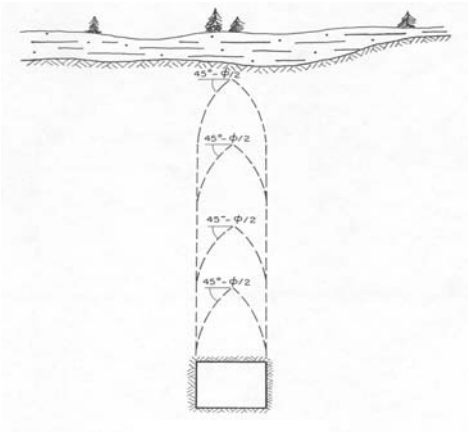
(c)



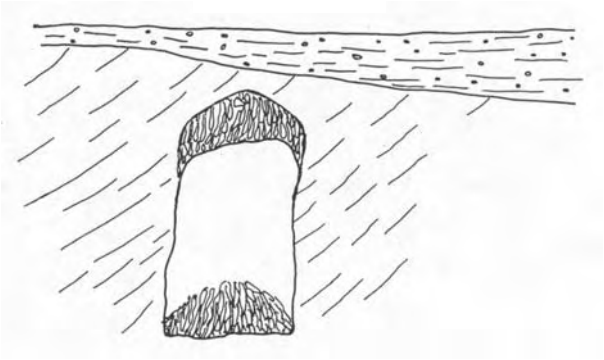
(d)



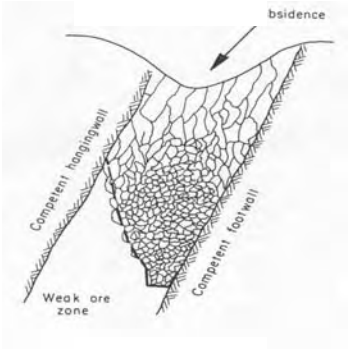
(e)



(g)



(f)



(h)

Figure 3. Common failure mechanisms of shallow stopes of hard rock mines: (a) rupture, (b) plug (Golder Associates (1990), (c) ravelling (Crane 1929), (d) delamination (Golder Associates, 1990), (e) strata failure, (f) alteration disintegration, (g) chimneying disintegration, (h) block caving (Bétournay, 2004a).

Ravelling from an unsupported periphery of unfavorably oriented rock blocks is commonplace when the tangential stress is insufficient to provide confinement for self-support. The blocks fail progressively (without the remainder of the rock mass mobilizing on a large scale) unless a stable-self supported arch cavity is formed. The examination of various case studies (Bétournay, 1995) has shown that, in the worst cases of block size/weight, the required tangential compressive stress to maintain stability is of the order of 0.5 to 1.0 MPa. A special case of ravelling, that of easily parting laminas ("delamination"), may occur despite the initial confining benefits of compressive tangential peripheral stress because of the thinness of the rock piece/small contact surface area.

Metal bearing ore occasionally occurs in sedimentary terrains where stratification (~ 8-50 cm thick) is well developed (e.g. lead-zinc Mississippian deposits, uranium deposits) or in a host rock capped by sedimentary beds. Stratification may also occur as a result of faulting or metamorphism. While there has been no reported failure to surface in these types of terrains, observations indicate that progressive failure of subsequent strata leave behind an arched failure surface, reflecting rapidly decreasing failed strata spans which stabilize the rock mass close to the original shallow stope periphery. Predicted failure heights using the strata failure analysis approach presented later, are very similar to actual failures, about 1/4 to 1/6 of the longest span, depending on rock material properties and strata thickness (Bétournay, 2004b).

Alteration disintegration progression is heavily dependent on oxidation of disseminated pyrite and kaolinization of certain feldspar minerals. Chimneying disintegration occurs in weak rock (e.g. severely altered rock; sericitic or chlorite schists; graphitic slate) with very low cohesion (<0.2 MPa), providing poor self-support capability. It is a continuous upward progressive failure by gravity that most often leads to the creation of vertically-sided cavities that cut across weak rock fabric and leaves openings that have spans less than 5 m. In the case of a weak, dipping homogeneous material bounded by competent hangingwall rock, the development of disintegration follows the contact, leaving behind a dipping chimney. The mechanism requires a shearing path of no resistance. The upper boundary for chimneying disintegration occurs when the rock mass can no longer be sheared effectively, e.g. with an increase in of sound rock portions. As a lower bound, if the underground opening is created large enough, caving of weak material will occur instead of chimneying disintegration (Rice, 1934).

Although rock mass caving initiation can begin with block ravelling, the mechanical action of breaking the integrity of the rock mass and mobilizing it is difficult to accurately quantify or predict. Very few cases of this type of failure as an unplanned event have been reported.

3. Stability Aspects

Failures of shallow stopes will not always begin within the surface crown pillar above the shallow stope (Bétournay, 1995). It could start in the hangingwall or footwall. The failure paths run close to or in the surface crown pillars. Rock mass behaviour should be considered as "Which portion is mobilized in a failure to surface?" rather than focus only on the pillar and what should be its thickness. This requires stability analysis based on failure mechanisms rather than conventional approaches which rely on the pillar thickness to width ratio, which can falsely lead to an assumption that a thicker rock mass is safer. In Canada, analyses were based on personal experience or on the elastic beam theory to avoid a thinner beam. There was little variation in the ratio used despite variations in terrain quality (Bétournay et al, 1988). Case studies of failures in very weak rock masses have shown that stopes are subject to failures initiated at deep (275 m) or at shallow levels.

Blocky rock masses can continuously ravel when joints are unfavourably dipping (Bétournay, 1995). Thin pillars (<3 m) can remain in place when high rock mass quality values are registered.

Table 1. Timing of shallow stope failures based on case studies.

Failure Type	Timing Once Failure Initiated
Pillar rupture	Instantaneous after fracturing and fall
Plug failure	Instantaneous once initiated
Ravelling	Several metres per day to several metres per month
Strata failures	One strata per day to one strata over several months
Alteration disintegration	One meter over twenty years
Chimneying disintegration	One to twenty metres per day
Block caving	Twenty to three hundred metres per year

Once failure is initiated, if no changes in conditions occur, most failure mechanisms will develop in relatively short time spans (Table 1) (should the ground support not be effective and stope space available to allow for its continuation). Carter and Miller (1995), considering the case studies used to derive a dedicated empirical stability evaluation method (described later in this article), made some broad observations on time dependent failure considerations. A bi-modal occurrence of failure has been observed. Initially, after mine closure (about 20 years), failed cases reach an ~3% failure rate, ascribed to failures based on rock mass "defects", while a second peak of ~2.5% failures is reached in the 60-year timeframe, reflecting "wearing out" effects. With pre-existing rock mass configurations that will not rapidly lead to failures, it is anticipated that, without major influences to such a rock mass, a shallow stope is not expected to fail until a much later time frame.

Conventional rock mechanics approaches (e.g. beams, plates, arches, etc.) will not represent actual shallow stope failure behavior: i.e. the nature, extent or relative potential for shallow stope failures in discontinuous or weak rock masses. Only in certain circumstances such as intact rock failure (e.g. from a good quality rock mass, from strata) can these be considered. Conventional empirical rock mass characterization methods are not specific to shallow mining rock mass cases and do not adequately encompass very weak rock mass cases. A more specific method particular to the failure mechanisms has been developed and is presented later.

4. Numerical Modelling Application

The most flexible stability analysis technique is numerical modeling. It provides the possibility of obtaining approximate solutions to the behaviour of surface and/or underground excavations while considering a large number of influencing factors such as tectonic stresses, rock and rock mass properties, geometry and proximity of openings, and ground support. Matching the problem to the selection of a particular numerical code depends on a proper understanding of the case and the anticipated failure mechanisms.

Block type failures (plug, ravelling, block caving) require distinct element or block codes. Plug type failures require a 3D application in order to respect the limited dimensions of the problem. Weak materials with large displacements should be modelled using non-linear codes. Elasto-plastic material response has been used successfully for indicating failure areas, failure progression to surface obtained with a finite-element 3D code with the allowance for the application of a death and

birth option for elements. In cases with weak schists, where codes with such an option were not used, the results identified failure areas around openings but did not indicate the ultimate extent of failure (Bétournay, 1995). For competent, poorly jointed rock masses, modeling using a linear, elastic approach is suitable. In many cases, thin surface crown pillars and those between open pits and underground can fail from high tensile stress concentrations. The use of a failure criterion to capture the ensuing rock mass response will provide the extent of the potential failure areas.

5. Analytical Equations Application

Plug Failure

The equation to calculate the factor of safety against downward falling of a plug, using the Coulomb criterion, defined by vertical or outward dipping discontinuities (Figure 4), is composed of upward shear resistance provided by the imposed normal forces induced by the in situ stresses and the cohesion along the surface, divided by the driving force of the block, its weight plus the downward force provided by the force in the case of a block with non-vertical dipping sides:

$$Fs = \frac{\sum_{i=1}^{n}\left(c_i A_i + \left(\left(\sum_{j=1}^{m}\sigma_{nj}A_j\right) - \frac{\gamma_w (H_i - d)^2 b_i}{3}\right)\tan\phi_{ri}\right)\sin\psi_i}{V\rho g + \left(\sum_{i=1}^{n}\left(\sum_{j=1}^{m}\sigma_{nj}A_j\right) - \frac{\gamma_w (H_i - d)^2 b_i}{3}\right)\cos\psi_i} \quad (1)$$

where ψ_i= dip of the i^{th} block side, n= total number of block sides, V= plug volume, ρ= mass density, g= constant of gravity, c_i, A_i, φ_{ri}= cohesion, area, angle of friction of ith side, m= total number of elements on the j^{th} side, σ_{nj}, A_j=normal stress, area on the jth element of one side, d=depth to the water table, b_i=width of i^{th} side, H_i=vertical distance from surface to ith side bottom, γ_w= unit weight of water

The possibility that a plug may slide on an inclined surface can also be considered. Sliding can be evaluated only if the block side opposite the sliding side is of equal or lesser dip and the dip of the other sides is either vertical, or away from the stope. In a simple consideration, the analysis includes consideration of the sliding and opposite side of same strike and equal or lesser dip, and two other sides parallel, vertical, with strike orthogonal to the other two sides (equation 2, Figure 4). The normal stress imposed to each block side must be the redistributed natural ground stresses imposed to the bounding discontinuities. The stress on the boundary planes will depend on the effect of the shallow stope on the natural stress field, and on the effects of neighboring mining activity such as an open pit, stopes on-strike or on-dip. It is normal for representative values to be significantly different (compressive or tensile) than natural stresses. Redistributed stresses returned from numerical modelling can be used in this case.

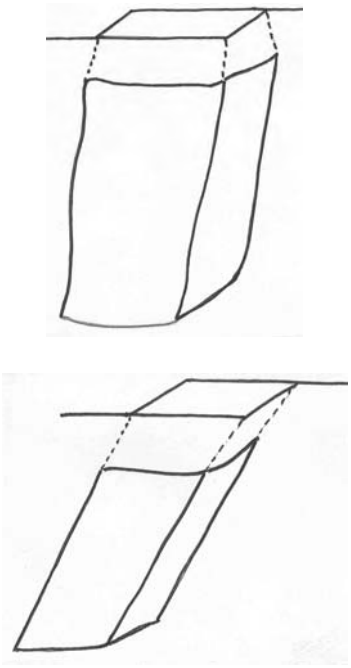


Figure 4. Representation of a falling and a sliding plug.

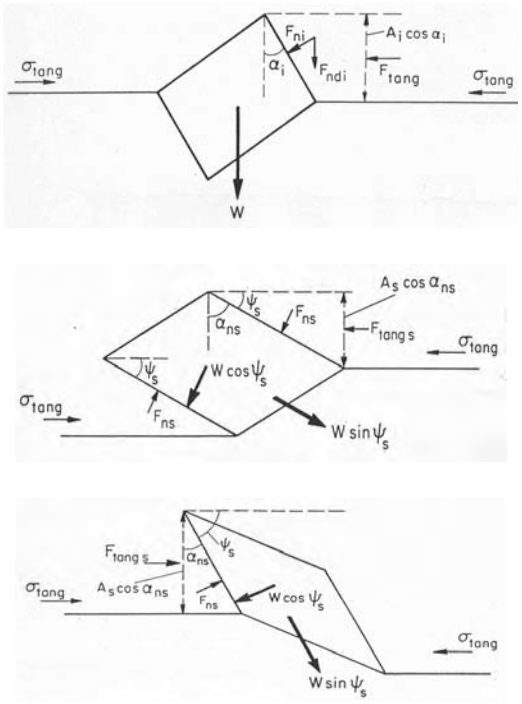


Figure 5. Force distribution on stope periphery falling and sliding blocks, 2D analysis.

$$Fs = \frac{c_s A_s + \left(\left(\sum_{j=1}^{m} \sigma_{nsj} A_{sj} \right) + V\rho g \cos\psi_s - \frac{\gamma_w (H_s - d)^2 b_s}{3} \right) \tan\phi_{rs}}{V\rho g \sin\psi_s + \left(\sum_{j=1}^{m} \sigma_{n2\,j} A_{2\,j} - \frac{\gamma_w (H_s - d)^2 b_s}{3} \right) \sin(\psi_s - \psi_2)}$$

$$+ \frac{c_2 A_2 + \left(\left(\left(\sum_{j=1}^{m} \sigma_{n2\,j} A_{2\,j} \right) - \frac{\gamma_w (H_s - d)^2 b_2}{3} \right) \cos(\psi_s - \psi_2) \right) \tan\phi_{r2}}{V\rho g \sin\psi_s + \left(\sum_{j=1}^{m} \sigma_{n2\,j} A_{2\,j} - \frac{\gamma_w (H_i - d)^2 b_i}{3} \right) \sin(\psi_s - \psi_2)} \qquad (2)$$

$$+ \frac{\sum_{i=3}^{4} \left(c_i A_i + \left(\left(\sum_{j=1}^{m} \sigma_{nij} A_{ij} \right) - \frac{\gamma_w (H_i - d)^2 b_i}{3} \right) \tan\phi_{ri} \right)}{V\rho g \sin\psi_i + \left(\sum_{j=1}^{m} \sigma_{n2\,j} A_{2\,j} - \frac{\gamma_w (H_i - d)^2 b_i}{3} \right) \sin(\psi_s - \psi_2)}$$

where s, 2 = subscripts to denote the sliding and its opposite side, ψ= dip of a plug side

Ravelling

In the case of ravelling, a simple limit equilibrium approach can be used to examine the initiation and possible continuation of falls or slides of parallelpiped blocks from the stope periphery until the state of ground stress is such to stabilize these movements. In it, the peripheral tangential stress is used as the clamping stress that may or may not be sufficient and allow a block to fall or slide from the periphery (Figure 5). The analysis is two-dimensional. Two joint families making up the block

are used, in a given plane, although more are possible. This approach is conservative but commonly used (Brady and Brown, 1985). The limit equilibrium equation is:

$$Fs = \frac{\sum_{i=1}^{2} \left(c_i + \sigma_{tang} \cos^2 \alpha_i \tan \phi_{ri} \right) A_i \cos \alpha_i}{W + \sum_{i=1}^{2} A_i \sigma_{tang} \cos^2 \alpha_i \sin \alpha_i} \quad (3)$$

where W= block weight, A_i= length of the block's i^{th} side (unit length in third direction), α_i= internal block angle between vertical and the i^{th} block face, σ_{tang}= tangential stress at that point of the periphery (from numerical modelling)

In reality, numerical modelling, or a re-appraisal of the peripheral stress, should be redone progressively to review the tangential stress value used in deriving the factor of safety.
The final shape of the block fall outline is compared to the bedrock boundary. The following equation (Bétournay, 1995) calculates the ultimate cavity height above a stope produced by block ravelling in a regularly-spaced two joint set 2D consideration:

$$H = \frac{L \sin(\psi_1 - \omega) \sin \psi_2}{\cos \omega \sin(180 - (\psi_1 + \psi_2))} \quad (4)$$

where ω= dip of the crown periphery, ψ_1= dip of the discontinuity in the direction of the crown periphery, ψ_2=dip of the discontinuity in the direction opposite the crown periphery, L = stope span

The analysis of a sliding block in the direction of the sliding motion can be performed by using:

$$Fs = \frac{2c_s A_s + (2\sigma_{tang} A_s \cos^2 \alpha_{ns} + W \cos \psi_s) \tan \phi_{rs}}{W \sin \psi_s} \quad (5)$$

where α_{ns}= angle between normal to periphery and block sliding surface, ψ_s= sliding side dip, c_s, φ_{rs}, A_s= cohesion, angle of friction, length of the sliding side (unit length in the third direction)

The block slide and block fall analyses should be performed for each rock mass sector that shows varying joint orientations and properties. Ground support forces can be input into these equations. This analysis is simplified compared to rock mass block movements that can be indicated by discontinuum modelling codes, but can be combined with finite element modelling if a such a code is not available. Furthermore, discontinuum codes do not return factors of safety.

Strata Failures

Elastic beam and plate approaches respectively overestimate and underestimate the imposed stress to a rock strata and the resulting height of the failure cavity (Bétournay, 2004b). Representative results are obtained when the material is considered with variable tension and compression moduli of elasticity, and strata stacking considered. Strata loading, common in field observations, indicates that the strata will fail at progressively shorter intervals, leaving behind cavity shapes. Using the analogy of the Fayol experiments (Sterling, 1977), with multiple beam stacking, the incremental deflection imposed on the lowest beam decreases until any additional beam do not affect the deflection of the lowest beam, and do not themselves deflect. The load on each stratum is the sum of all the fractions of loads given by the overlying strata, as well as that of its own weight.

$$p_{j+1} = \gamma_r t \cos \theta \sum_{i=1}^{n-j} \frac{1}{i} \quad (6)$$

where j= j^{th} stratum that has failed (j ∃0), γ_r= unit weight of rock, t= strata thickness, i= i^{th} stratum numbered from the lowest stratum, n= the total number of strata loading the lowest stratum, θ= strata dip, j+1= lowest unfailed stratum which would be at equilibrium

Failure will not occur if the imposed stress for a given stope span is equal to the stratum tensile resistance (equation 7).

This means that the highest possible stable stratum span can only occur under self-load (p_1). If

$$T_s = \frac{p_{j+1} L^2{}_{j+1} \left[1 + \left(E_c / E_t \right)^{1/2} \right]}{4t^2} - \sigma_a \qquad (7)$$

where E_c = the modulus of elasticity in compression stress, E_t = modulus in tension, , L_{j+1} = length of lowest unfailed stratum, σ_a= axial confinement

detached strata load this first stratum, the additional load will reduce the lowest stratum stable span. The general mechanical development of failure, for a stratum of "two materials", can be described as follows: when the tensile stress is imposed by self load, or that of several detached strata, the load surpasses the tensile strength at the beam end, a vertical crack grows from the top of the beam towards its neutral axis. This reduction in remaining thickness amplifies the imposed compressive stress at the bottom of the stratum, by a factor inversely proportional to the square of the remaining thickness, $1/t^2$. A shear failure grows upward from the lower stratum at the abutment, oriented at 45E+ φ /2 (φ=material internal angle of friction).

The failure reaches a distance of d from the end of the stratum, shortening it by:

$$d = t \tan(45^0 + \phi/2) \qquad (8)$$

which is used to calculate the total number of strata failed, j, for L_{j+1}

$$L_{j+1} = L - 2jd \qquad (9)$$

If the stope span is greater than the stable pan L_{j+1}, the failure height, orthogonal to stratification, is:

$$H_c = jt \qquad (10)$$

An iterative process is carried out to balance the remaining number of detached strata loading the lowest stable strata, and the total number of failed strata using equations (6)-(10).

If the number of failed strata, j, is higher than the number of strata loading, n, the span L_{j+1} is too long for the number of detached strata. This indicates that all detached strata will fail, followed by higher single stratum to arrive at the stable $L_{j+1.}$ Without knowing the number of anticipated detached strata loading a lowest stratum in equilibrium, a "worst case" situation can be adopted. For example, a 50^{th} detached strata only ads 0.02 of its weight to the lowest stratum. Equation (7) is redone to obtain an L_{j+1} with this higher p giving the smallest stable span for the "worst" loading. H_c then includes all the strata failed from original stope span to $L_{j+1.}$

If cavity height is already known, the process to obtain the number of loading strata on the lowest stratum in equilibrium is to start with the measured H_c and proceed sequentially in reverse to calculate n the number of loading strata.

Chimneying Disintegration

Chimneying disintegration commonly results in the formation of isolated holes in weak rock, developping in an upward fashion to surface. Since some degree of cohesion is needed in order for the cavity walls to remain integral, the rock can be considered as a c-φ geotechnical material.

The problem is set up in a similar fashion as mobilization of shear resistance along an active earth pressure in soil slopes. This is also representative of the shearing and cross-cutting of material fabric (e.g. schistocity), seen in case studies. Once an underground opening is created, its roof starts to deform. If these displacements are great enough, the shear strength of the material is mobilized, along active pressure rupture lines, Figure 3. A first rupture line, shaped as a dome, develops in the stope periphery and involves the fall of rock. This is seen in actual failed cases. Rupture lines continue to develop sequentially above the cavity. The most simple approximation of the rupture line is to use a 2D circular shear slip surface, as has been assumed in active pressure shear failures (circular) in slopes of cohesive soils, of weak rock material or even rubble.

By using a method of slices (Figure 6) commonly used to calculate the factor of safety related to active pressure slope circular arc failures, the factor of safety against chimneying disintegration is:

$$Fs = \frac{1}{\gamma_r\left(\frac{(45^0+\phi/2)\pi r^2}{360}-\frac{h_{1h}N}{2}\right)}\sum_{i=1}^{n}\frac{s}{\sin\left(\tan^{-1}\left(\frac{(h_{ih}+h_{(i+1)h})0.5}{N+(i-1/2)s}\right)\right)}\cdot c_m\cos\left(\tan^{-1}\left(\frac{h_{ih}+h_{(i+1)h}0.5}{N+(i-1/2)s}\right)\right) \quad (11)$$

where n= number of slices selected (even number), s= slice width, i= slice number, b= stope half-span, r= radius of the rupture arc= $\frac{b}{1-\cos(\alpha/2)}$, N= r-b, α/2= 45E+ φ/2, φ= rock mass angle of friction at σ_n = 0, c_m= rock mass cohesion, γ_r= rock unit weight, $h_{1h}=\sqrt{b(2r-b)}$, $h_{ih}=\sqrt{l_i(2r-l_i)}$, $l_i= b-(i-1)s$

A review of several chimneying disintegration failed and unfailed cases (Bétournay, 1995) provides a numerical correlation between the largest span L of the stope and rock mass cohesion c_m at Fs=1:

$$L_{critical} = 100c_m \quad (12)$$

where L= metres, c_m = MPa

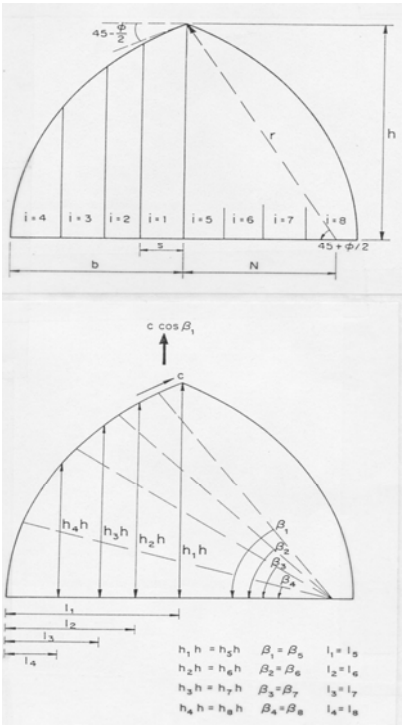


Figure 6. Method of slices application to calculate shear strength resisting chimneying disintegration initiation (example using eight slices) (Bétournay (1995).

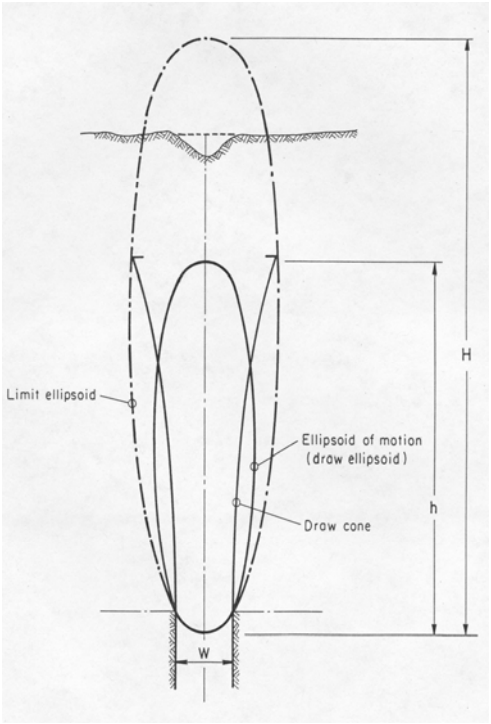


Figure 7. Ellipsoid drawing pattern for caved rock, Janelid and Kvapil (1966).

Block Caving

Block caving is common in blocky or crumbly rock mass conditions. Space must be available for material to mobilize into, from the crown zone. Janelid and Kvapil (1966) outlined model material flow patterns that approximate the geometry of the failure envelope above the stope (Figure 7). The volume that has caved into a stope is defined by the draw ellipsoid. The limit ellipsoid contains the zone of broken material that has then moved and expanded to fill this volume. If the rock mass in the limit ellipsoid moves, subsidence occurs if it intersects surface; if the draw ellipsoid intersects surface, failure of the surface crown pillar is registered. The maximum height of an opening failure will depend on the space available in the stope. If no failed material is extracted, the initial collapse of the rock mass leads to caved rock spilling into the space, stopped when it reaches the roof. The possibility of a complete surface crown pillar failure can be obtained by calculating the amount of caved material that will fill the void using a representative bulking factor (β=1.1-1.4, e.g. schist to blocky ground), with $V_{caved}= V_{in\text{-}stope}+V_{removed}$, and comparing it to the volume of the draw ellipsoid:

$$V_e = \frac{4}{3}\pi ab^2 \tag{13}$$

where a, b= respectively the semi-major and semi-minor axes of the draw ellipsoid

Its height, 2a, is then compared to the thickness of the pillar. For verifying a subsidence impact of the limit ellipsoid, its eccentricity is used:

$$\varepsilon = \sqrt{\frac{3W^2}{4h^2} - \frac{6V_{caved}}{h^3} + 1} \tag{14}$$

where W= stope width, h= limit ellipsoid height

The height h is compared to pillar thickness. Model studies have yielded eccentricities of 0.92-0.98 and the height of the limit ellipsoid is to be roughly 2.5 times the height of the draw ellipsoid.

6. Empirical Method Application

One dedicated empirical approach has been created (Golder Associates, 1990), based on 230 shallow stope case studies, including 32 failures. The cases plotted mostly in the 0.1 to 30 range of the NGI Q value (Figure 8). A best-fit line was derived to separate failed and unfailed cases. While approximate rock mass quality and stope geometry details were used in many of these cases (since original information was not available), the method can be used to provide a "sense" of this demarcation line. The expression of the limit ($F_s = 1$) surface crown pillar dimensions, considering the rock mass quality Q is outlined in equation (15).

$$Cs = L\left(\frac{\gamma r}{t(1+L/S)(1-0.4\cos\psi)}\right)^{0.5} \tag{15}$$

where L= stope span, S= stope strike length, t= surface crown pillar thickness, ψ= major discontinuity dip, γ_r= rock unit weight (tons/m^3)

The statistical average of critical span versus rock mass quality is:

$$Cs = 3.3Q^{0.43}(\sinh^{0.0016}(Q)) \tag{16}$$

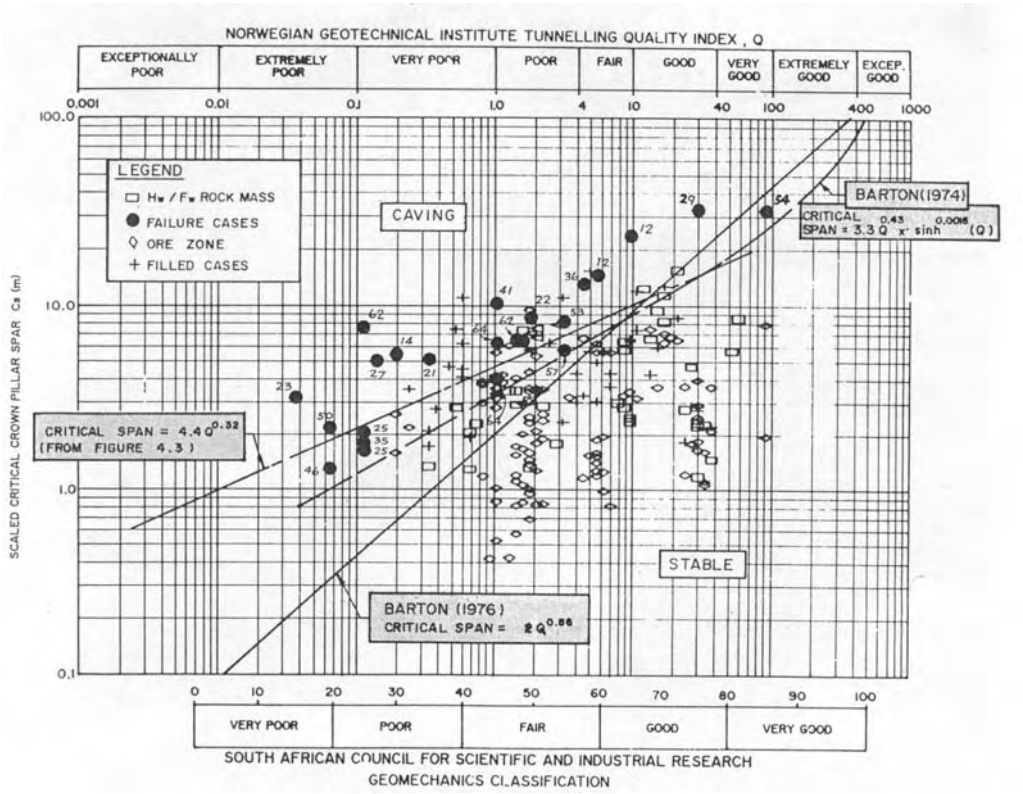


Figure 8. Critical empirical span for surface crown pillars (Golder Associates, 1990).

The process to evaluate the relative stability of a stable surface crown pillar ($F_s > 1$) uses the chart in Figure 8 or the above equation to obtain C_s which is then used to calculate the required mining span or thickness using equation (15). The approach has been shown to be reliable for application in blocky rock masses where ravelling and block caving will predominate. In very poor rock mass conditions (Q<0.1), minimum surface crown pillar thicknesses are predicted which are far less than the actual depth of the initiation of failures (Bétournay, 1995).

7. References

Bétournay, M.C., Nantel, S., Lessard, D. (1988). *Summary of 24 Surface Crown Pillar Case Studies*. Can. Inst. Min. and Metal. Bull., Volume 80 #917, 73-77.

Bétournay, M.C. (1995). *The Stability of Shallow Stopes of Hard Rock Mines*, McGill University Ph.D. Thesis, 611p..

Bétournay, M.C. (2004a). *Stability Effects and Failures from Extensive Hard Rock Mining*, Proceedings 6th North American Rock Mechanics Symposium, Houston, CD Proceedings.

Bétournay, M.C. (2004b). A *Failure Model for Stratified Rock Masses of Hard Rock Mines*, Proceedings 6th North American Rock Mechanics Symposium, Houston, CD Proceedings.

Brady, B.H., Brown, E.T. (1985). *Rock Mechanics for Underground Mining*. Allen and Unwin, 527p.

Carter, T.G., Miller, R.I. (1995). *Crown Pillar Assessment – Planning Aid for Cost-Effective Remediation*, Trans. Instn. Min. Metal., Volume A104, 41-57.

Crane, W.R. (1929). *Subsidence and Ground Movement in the Copper and Iron Mines of the Upper Peninsula, Michigan*. U.S. Bureau of Mines Bulletin 295.

Golder associates (1990). *Crown Pillars Stability Back Analysis*, CANMET, Energy, Mines and Resources Canada Contract 01sq23440-8-9074.

Janelid, I., Kvapil, R. (1966). *Sublevel Caving*. Int. J. Rock Mech. Sci., Volume 3, 129-153.

Rice, G.S. (1934). *Ground Movement from Mining in Brier Hill Mine*, Norway, Michigan. Proceedings Am. Inst. Min. & Met. Eng., Volume 109, 118-152.

Sterling, R.L. (1977). *Roof Design of Underground Openings in Near-Surface Bedded Formations*. University of Minnesota PhD. Thesis.

PETROFABRIC OF THE KEUPERIAN MARLS IN LORRAINE (FRANCE): CHARACTERIZATION AND EVOLUTION IN BRINE.

BOIDIN Elie[1] , HOMAND Françoise[1], THOMAS Fabien[2], YVON Jacques[2]

[1] LaEGO, Rue du Doyen Marcel Roubault - BP 40-54501 Vandoeuvre-lès-Nancy Cedex, France; Elie.Boidin@ensg.inpl-nancy.fr ; Francoise.Homand@ensg.inpl-nancy.fr

[2] Laboratoire Environnement et Minéralurgie, UMR 7569 CNRS/INPL-ENSG, BP 40-54501 Vandœuvre-lès-Nancy Cedex ; Fabien.Thomas@ensg.inpl-nancy.fr

ABSTRACT: In Lorraine, the keuperian salt working creates mines and solution cavities. In both, brine can be in contact with the rocks enclosing the salt strata and can contribute to these rocks degradation. The researches resumed here were carried out to characterize the petrofabric of the rocks surrounding the keuperian salt, and to understand its evolution when this rock-stratigraphic formation is immerged in brines. X-Ray diffraction, Hg porosimetry, visible and electronic microscopies were used to study the petrofabric; these analytical methods and brine titrating were also coupled with a batch test to study the evolution in brine environment. Whatever the brine and the duration of the test the anhydrite facies keeps its petrofabric. Concerning the argillite facies, the anhydrite hydration was clearly shown and seems to be the origin for these facies degradation.

KEYWORDS: underground salt working, argillite, anhydrite, brine, petrofabric.

RESUME: En Lorraine, l'exploitation du sel keupérien est à l'origine de mines et de cavités de dissolution. Dans ces deux contextes, une saumure peut rentrer au contact avec l'encaissant argilo-anhydritique du sel et de ce fait contribuer au délitage de celui-ci. Les recherches présentées ici ont été entreprises afin de caractériser la pétrofabrique de la série encaissante et de comprendre son évolution en présence de saumure. Pour ce faire, la diffraction-X, la porosimétrie au mercure, les microscopies visible et électronique ont été employées. Ces techniques, associées à des dosages en saumure, ont été couplées à des expériences de type « batch » mettant en jeu les lithologies majeures et une saumure de cavité. Quelque soient la durée d'immersion et la saumure employée, la pétrofabrique du faciès anhydrite n'évolue pas. Concernant le faciès argilite prélevé, l'hydratation du minéral anhydrite a été clairement mise en évidence et cette réaction semble être à l'origine du délitage.

MOTS-CLEFS : exploitation souterraine de sel, argilite, anhydrite, saumure, pétrofabrique.

1. Introduction

When underground water or brine come into connection with brines in salt formations, interactions with the salt strata or surrounding strata, can cause severe problems in salt mines. In such a case, pillars are quickly dissolved and some rock failure and subsidence appear, as for example in 1992 in Louisiana, in Saskatchewan and in the Urals (Daupley and al., 2004).In the salt workings of Lorraine (eastern France), and particularly in the Varangéville mine, pillar collapse is thought to result from brine weathering by decreasing of the wall spring rate, as shown by Vouille (1986) and Homand (2003). In the vicinity of this mine, and in a similar keuperian marl formation, sinkholes occurred above man-made cavities in salt deposits, especially the SG4 and SG5 cavities (Buffet, 1998). The origin of rock failure may be similar to that of the pillar collapse in the neighbouring salt working.

The question of the micro-mechanistic origin of rock failure at the contact with brine still remains opened, particularly at the petrographic scale. Therefore, the present work aims at understanding the origin of such phenomena by studying the physico-chemical interactions between the brine and the minerals of the keuperian marls of Lorraine, and their consequences on the petrofabric of the rock. The objective was to follow the evolution, transformation or migration of mineralogical species and of their interfaces in the rock during contact with the brine. Therefore batch weathering experiments were carried out, in which representative samples were contacted with various brines during more than 1 year. According to time, the chemical composition of the brines was analyzed, and the evolution of the petrofabric was studied by visible and electron microscopes observations.

2. Materials and methods

2.1. Geological background and lithology

The “Marnes Iriseés Inférieures” (lower iridescent marls) studied here belong to the middle part of the upper Triassic serie of Lorraine. It is composed of three formations which are, from the bottom to the top: the phantom crystal strata, the halite formation and the so-called "marls with anhydrite" (figure 1). The corresponding sediments and evaporites have been deposed and formed between 230 and 220 Ma in mudflats environments which were periodically connected to the German sea (Rashid, 1995; Hilly and Marchal, 1999).

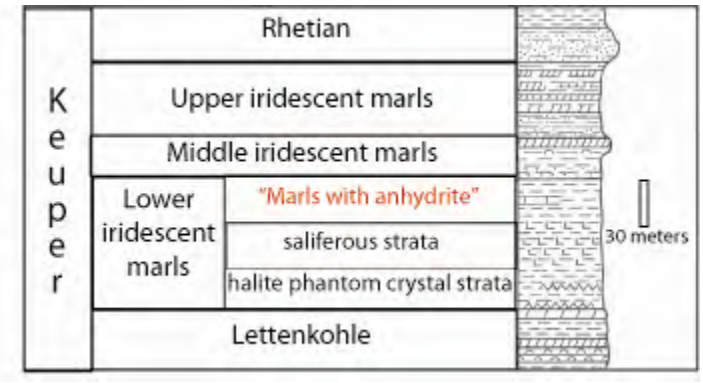


Figure 1: Stratigraphic cross section of the keuper in Lorraine (modified from BRGM, 1980)

Recent mineralogical characterisation of the keuperian marls of Lorraine revealed that the two major mineral components are clays and anhydrite (Rashid, 1995, Homand, 2003). Therefore, the argilite character is dominant, and it is recommended that this formation should be named "anhydrite-rich argilite".

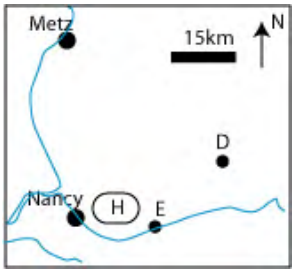


Figure 2: Location of studied drillings; H: Haraucourt Plateau; D: Dieuze; E: Einville.

The samples used for the study were collected from four drilled cores: SG 79 and CB3129 located in the Haraucourt plateau where the salt is still worked, one drilling above the Einville mine and one above and through the Dieuze Mine (figure 2). The batch experiments were carried out on the CB 3129 sample, which was the most homogeneous.

The stratigraphic logging of the four drilling cores revealed that keuper marls are composed of a decimetrical and metrical alternance of argilite and anhydrite. The anhydrous calcium sulphate is generally chicken-wire shaped, but can be sometimes laminar. Gypsum has not been observed in any sample. Most of the anhydrite laminae constitute some convolutes which might be the result of differential compaction or tectonic movement. In certain cases, the relative high density of argilite indicates the presence of diffuse microscopic anhydrite in the clay matrix. Cracks filled by anhydrite were observed, with either straight or sinuous shape, which indicates at least two steps of buckling.

2.2. Preparation and analytical methods

For the purpose of mineralogical analysis, samples were cut from cores, dried at 50°C until constant weight, and powdered with a mean granular radius smaller than 40 micrometers. The clay fraction was concentrated by selective leaching of sulphates. To this end, dialysis bags (14,000 Dalton) were filled with raw powders and immersed in distilled water. The distilled water was renewed when the conductivity outside the bags had increased to a maximum. The leaching was considered achieved when the conductivity was that of distilled water. X-Ray diffraction was carried out using a Bruker D8 device.

The porosity of the samples was quantified using an Autopore IV mercury porosimeter. The dimensions of the dried samples were 17*17*25 cm.

Microscope analysis of the petrofabric required the production of 30 µm thin-sections. In order to maintain the water-soluble minerals such as anhydrite or other minerals formed during the batch experiments, the samples were acetone-dehydrated. A low viscosity three components epoxy resin was used for embedding. In order to prevent the thermal dehydration of hydrated mineral such as gypsum, the resin was polymerized at low temperature (40°C). The final polishing of the thin-sections was achieved using isopar lubrication fluid. The final thickness was controlled by the third order birefringence of the anhydrite crystals with visible microscopes. Scanning electron microscopes (Hitachi 2500 and Philips XL30, carbon metallization with 20kV accelerating voltage) and visible microscope observations were performed on the thin-sections.

2.3. Batch experiments

Cylindrical samples with a 36 millimeters diameter were cored from the CB3129 core. In order to minimize the mineralogical and petrofabric heterogeneities between reactors, the two mains lithologies, a massive chicken-wired anhydrite facies and a greyish argilite containing centimetric chicken wires, were sampled on a unique continuous core for each lithology. Amounts of 200 g of solid were immersed in different fluids. The fluids were distilled water, a pure NaCl saturated brine, and a «cavity brine». The «cavity brine», provided by SOLVAY Company, was extracted from a cavity in contact with the halite formation but isolated from the keuper marl.

The batch experiment was run for 393 days at room temperature. Liquid and solid fractions were sampled after 46, 106, 200, 247, and 393 days. According to the mineral species present in the halite formation (Marchal, 1983; Marchal and al; 1991; Fontes and Matray, 1992; Buffet et al.,

1993; Rashid, 1995; Fanlo and Ayora; 1997), the fluids were analyzed for Mg, Fe and Ca by ICP-AE spectrometry (Dionex DX 120), and for SO_4^{2-} and Cl^- by ion chromatography (Dionex 500).

3. Results

3.1. In-situ petrofabric and mineralogy

depth (m)	lithology	Mineralogy of the fraction greater than 2µm				
		anhydrite	magnesite	quartz	celestite	halite
159,3	Red argilite with microscopic anhydrite	X	X			x
165 (batch sample)	Grey argillite with centimetric chicken-wired anhydrite	X	x	x	x	
166,8	red argillite with centimetric chicken-wired anhydrite	X	X			x
168	Red argilite with microscopic anhydrite	X	x			x
172,5	Purple argilite with centimetric cracks fille by anhydrite	X	x	x		x
174,4	grey argilite with centimetric cracks fille by anhydrite	X	x	X	x	
141,65 (batch sample)	Chicken-wired anhydritre	X		x		
141, 35	Laminated anhydrite	X				

Table 1: Semi-quantitative mineralogy of eight samples coming from the CB3129 cores

Table 1 shows the results from XRD on eight samples from the CB3129 drilling cores. The only mineral common to all samples is anhydrite. The very low peak intensities of magnesite, quartz and celestite indicate that the abundance of these minerals do not exceed few percents. With regard to the clay mineralogy, the analysis reveals in each sample the presence of chlorite, illite and disordered interlayered chlorite/smectite.

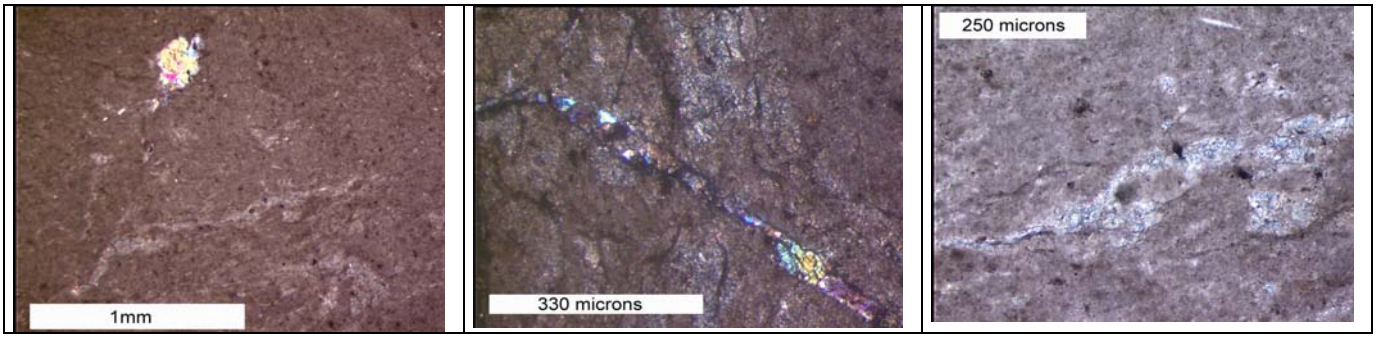


Figure 3: Some configurations of anhydrite crystals inside the clay matrix; left: aggregate; middle: filling of microcrack; right: diffuse crystals in clay matrix (polarized and analysed optical microscopy).

Concerning the petrofabric of argilites, scanning electron and optical microscope analyses of samples from the four drilling cores show that anhydrite is present either diffusely inside the matrix, or concentrated in microaggregates to which idiomorphic quartz is often associated (figure 3, 4). In regard to these configurations, the crystal habit of anhydrite is idiomorphic and prismatic. The great

axis of these crystals does not exceed 50 µm. Anhydrite has been also observed as filling material in variously sized cracks. In the case of microcracks, the crystal habit was similar to the above one. In the case of macrocracks, anhydrite displays a fibrous shape, the great axis of which was approximately 500 µm. Macro cracks were the only location where celestite was observed (figure 4).

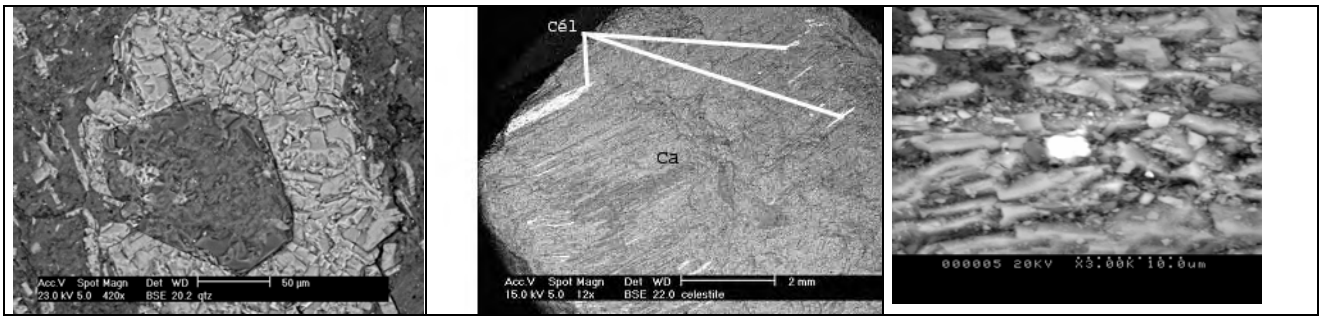


Figure 4: Accessory minerals in argilite faciès; left: quartz; middle: celestite; right: pyrite (BSE electron microscopy).

Pyrite was also locally observed in the clay matrix. The fact that it was not identified by XRD indicates that its amount in the bulk rock is less than one percent. Magnesite is present in a diffuse way inside the clay matrix. Halite is punctually present in the clay matrix and is also an accessory mineral.
In the anhydrite lithology, the only crystal habit of anhydrite was similar to that inside argilite microaggregates.

3.2. Porosity of the samples

Drilling	Depth (m)	lithology	free porosity	uncertainty (%)	mean acces radius Class (µm)	mean acces radius radius (µm)	Fn/Tn
Dieuze	29,45	Red argilite with chicken-wires	13,65	0,25	0,261-0,0018	0,00734	0,736246
	30,55	Greyish argilite with anhydrite laminae	11,6	0,37	0,627-0,0018	0,00819	0,7047388
	69,25	Greyish argilite with anhydrite laminae	6,52	0,16	0,109-0,0018	0,00344	
	88,5	Purple argilite	7,71	0,27	0,236-0,0018	0,00344	0,5357887
	96,15	Greyish argilite with anhydrite laminae	3,03	0,1	0,00734-0,00	0,00344	0,506689
	120,9	Greyish argilite with anhydrite laminae	8,56	0,75	0,0712-0,001	0,00344	0,7697842
	125,2	Red argilite with chicken-wires	12,03	0,9	0,0414-0,001	0,00344	0,752816
	128,7	Greyish argilite	10,64	3,71	0,137-0,0018	0,00308	0,7414634
	69,25<Z<88,5	Purple argilite	3,18	0,16	0,0886-0,001	0,00249	
Einville	1	Black argilite	9,23		0,0985-0,003	0,00383	0,6064389
	4	Black argilite	10,88	3,58	0,0794-0,001	0,00344	
CB 3129	165,2	Greyish argilite with chicken-wires	2,45	0,14	0,152-0,0018	0,00249	0,6862745
	165,5	Greyish argilite with chicken-wires	10,86	0,36	0,109-0,0018	0,00277	0,7685775
	166	Greyish argilite with chicken-wires	4,12	0,01	0,0986-0,002	0,002	0,6776316
	168	Chicken-wired anhydrite	0,38	0,12	6,71-3,50	3,51	0,1455939

Table 2: porous media properties of 15 samples from three drillings.

Mercury porosimetry reveals that the mean access radii decrease with increasing depth (Table 2). The observation of a clear sample depth dependent relation indicates that the preparation, and particularly the drying, has partially preserved the in-situ texture of the samples.

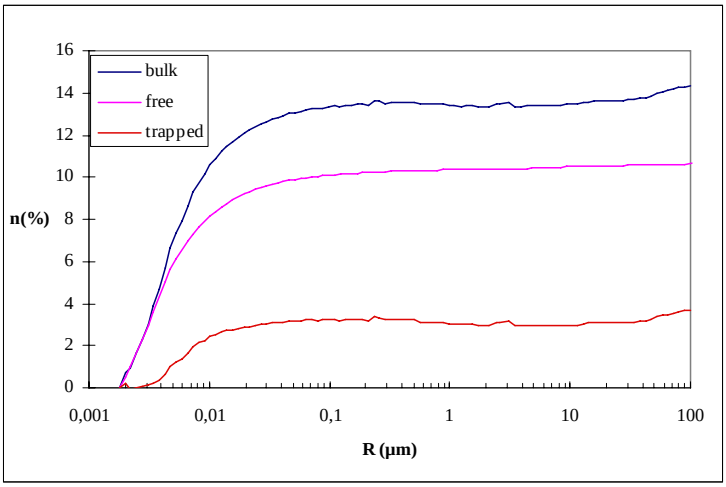


Figure 5: Significant pattern of the argilite porosity (sample Dieuze 128,70m).

Fifteen samples were analysed in order to study their connected porosity. Concerning the argilites, the main porosity is free in all studied cases. Another characteristic of this lithology is that the pattern of the access radius versus porosity is unimodal as those from the "Meuse-Haute Marne argillite" (Auvray, 2005). The predominance of the free porosity and its unimodal pattern suggest that the voids geometry is mainly crack shaped (Remy, 1993). Opposite, it was shown that the "Meuse-Haute Marne argillite" where trapped porosity is predominant has a porous medium dominated by a network of subspherical voids connected by "bottle necks" (Sammartino, 2001). The comparison between free porosity volume in argillites and in anhydrite reveals that the main accessible porosity is located in the clay matrix or at its boundaries.

3.3. Batch experiments

After 46 days of immersion, and whatever the fluid, all the argilite cylinders were more or less disrupted into centimetric fragments. In NaCl brine and «cavity brine», the main shape of the cylinder can still be recognized but centimetric fragments were detached and cracks appeared across the cylinders (figure 6). In distilled water, disruption was accompanied by the formation of macroscopic acicular crystals after 200 days of immersion. The anhydrite samples displayed no macroscopic changes whatever the fluid and experiment time.

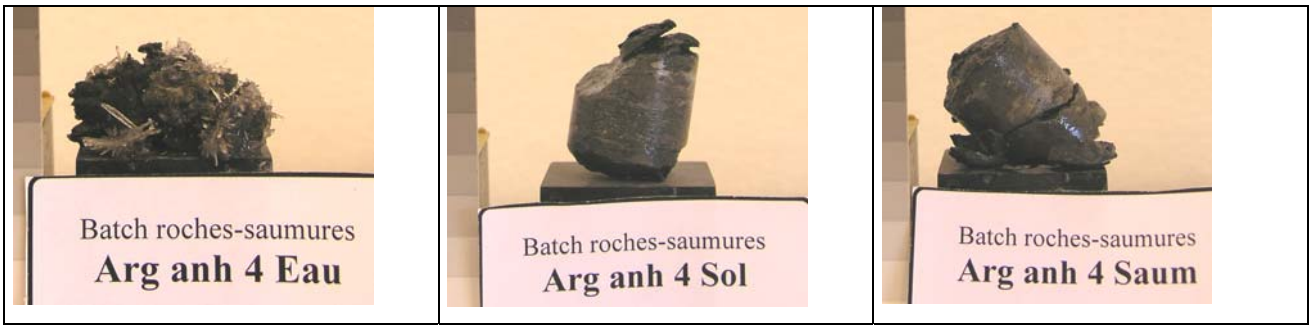


Figure 6: Significant views of argilite cylinders after 287 days of batch experiment.
Left : in distilled water; middle: in NaCl brine; right: in «cavity brine».

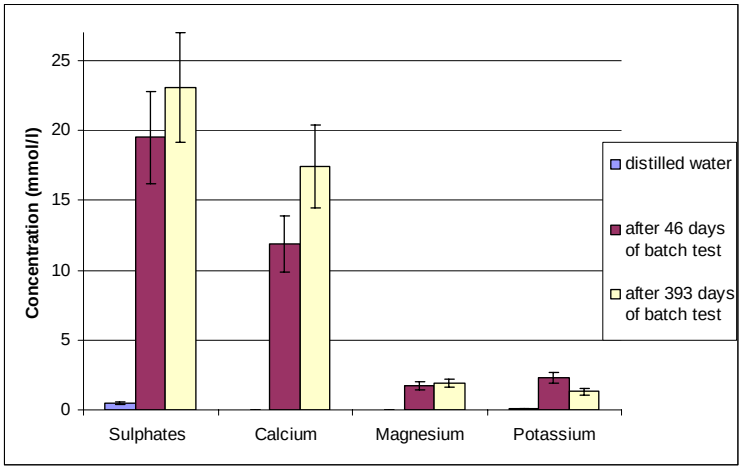


Figure 7: Evolution of the ion concentrations in the “distilled water / argilite batch”.

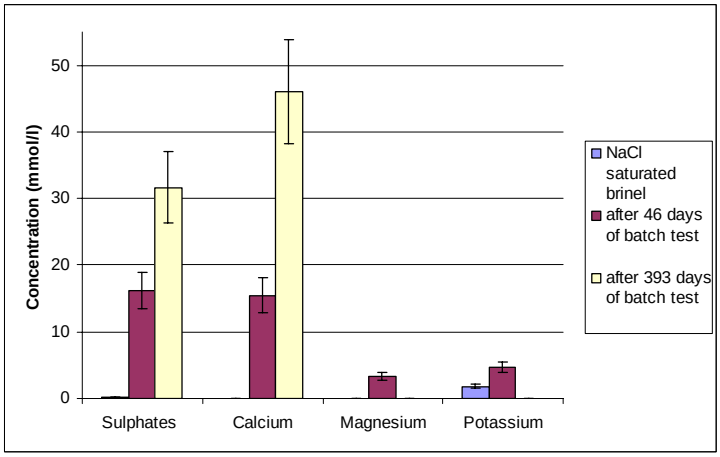


Figure 8: Evolution of the ion concentrations in the “NaCl saturated brine / argilite batch”.

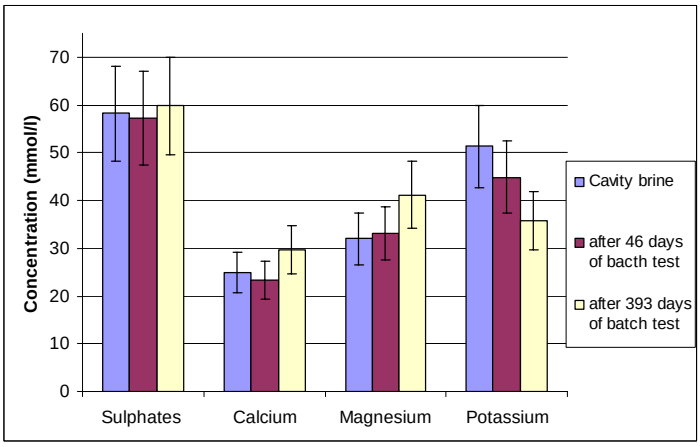


Figure 9: Evolution of the ion concentrations in the “«cavity brine» / argilite batch”.

Analyses of the fluids after 46 and 393 days show significant differences among the studied systems. In distilled water, sulphate and calcium appear in roughly similar amounts, and increased weakly with time. Small amounts of magnesium are also dissolved (Figure 7). According to the semi-quantitative XRD analysis, these relative amounts may correspond to dissolutions of anhydrite and magnesite. In NaCl Birne, the release of sulphate and calcium strongly increase with time,

whereas magnesium and potassium are detected only at 46 days (Figure 8). In «cavity brine», sulphates, calcium and magnesium were not significantly modified along the experiment (Figure 9). Only potassium seems to decrease. Similar results are observed on the anhydrite samples.

Iron was quantified in the reactors filled by «cavity brine» and by initially distilled water. On both lithologies, the corresponding concentration decreases during the experiment (figure 10).

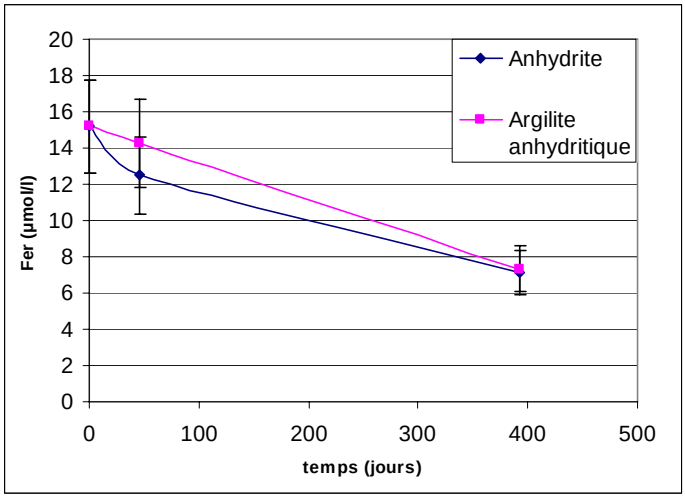


Figure 10: Evolution of dissolved iron in «cavity brine». Blue: anhydrite facies; pink: argilite faciès

Microscope analyses on thin-sections show significant evolutions on the argillite and anhydrite petrofabric, especially when rocks are immerged in distilled water. After 106 days of immersion in water, cracks were partly or totally filled with prismatic gypsum which migrating through the clay matrix (figure 11). Dissolution figures were also observed in this matrix. In anhydrite lithology, the differences with the initial petrofabric are located in a 150 µm border at the boundary of the anhydrite sample. The initial petrofabric is replaced by xenomorphic and prismatic anhydrite. The intergranular space is filled with gypsum. On the external part of this border, millimetric and prismatic gypsum include xenomorphic anhydrite crystals (figure 12). The argilite samples immerged in brine also show prismatic gypsum; as for the samples immerged in distilled water, this neoformed mineral is only located in open cracks (figure 13).

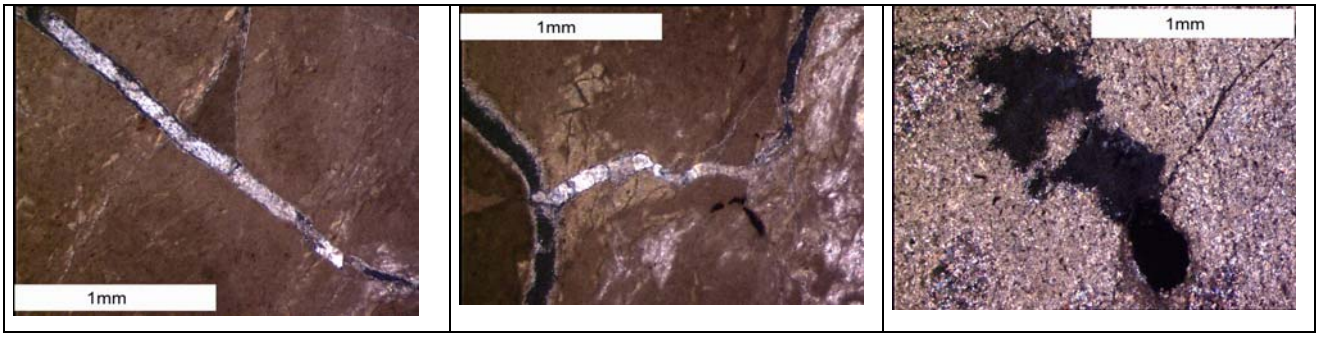


Figure 11: Cracks filled with gypsum and dissolution area in argilite after 106 days in distilled water (polarized and analysed light).

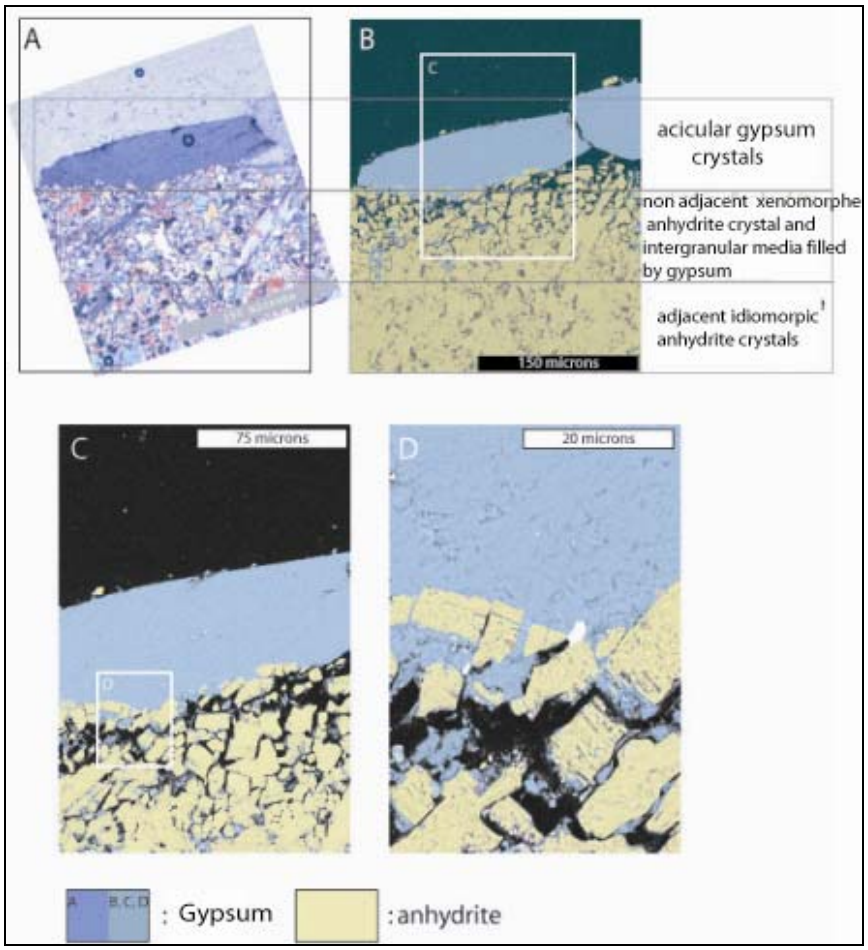


Figure 12: Reaction border on the sample boundary of anhydrite facies after a 287 days immersion in distilled water.

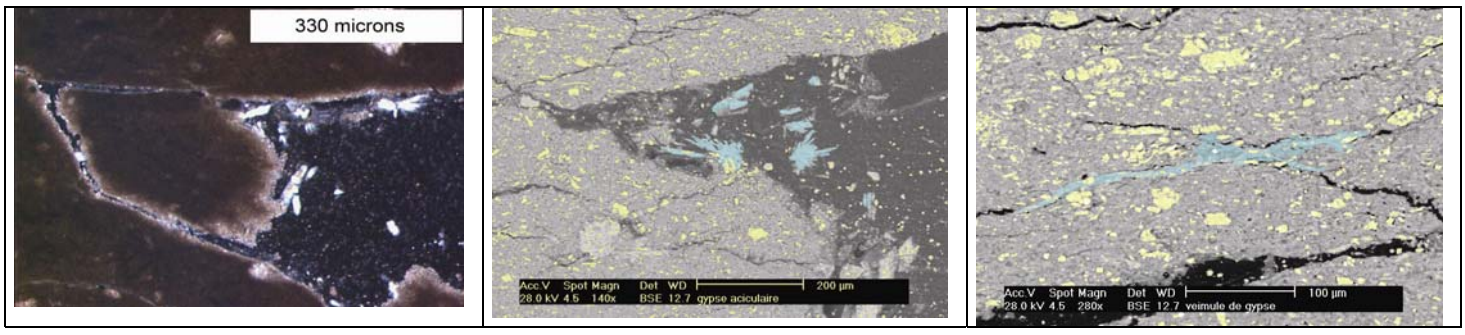


Figure 13: Gypsum filling in opened cracks observed after immersion of argilite in «cavity brine».

4. Discussion

4.1. Origin of the rock failure during brine immersion

Two hypotheses can be put forward to explain the mechanistic origin of mechanical weakening of the rocks, induced by the brine. On one hand, exportation of mineral species by dissolution in the fluid may decrease the mechanical resistance of the rock. On the other hand, in-situ mineralogical transformations and/or physico-chemical processes resulting in volume increase may provoke local disturbances.

The mineralogical characterization of the keuper marl reveals two species which are potentially able to swell in aqueous environment and thus to contribute to rock failure: swelling clays such as smectites and interlayered chlorite smectites, and anhydrous calcium sulphate (anhydrite).

As far as swelling clays are concerned, their hydration-dehydration is related to the activity of water (or to the relative pressure in vapour phase). Two swelling steps are classically described (Jin, 1994, Berend et al., 1995). Below 0.96 in relative pressure or activity coefficient, crystalline swelling is driven by the hydration of the interlayer compensating cations, and results in an increase of the basal distance. Nevertheless, this kind of swelling is known to be inactive at the macroscopic scale: the volume increase due to the interlayer swelling is compensated by the decrease of the pore volume (Bihannic, 1998). For higher activities, electrostatic repulsion and osmotic forces result in macroscopic swelling, called osmotic swelling, and finally in dispersion of the clay particles in diluted suspensions. In the present case, the high salt concentration in the brines (6 Mol/l for saturated NaCl) lead to an activity of water close to 0.8 that ranges in the field of microscopic swelling (Mulder *et al.*, 1992). Therefore, osmotic swelling of the clays, accompanied by volume increase is not a major mechanism of rock failure.

In regard to the argillite lithology, the microscopic analyses revealed the presence of gypsum in the cracks after immersion in «cavity brine», whereas the cracks in the initial petrofrabric were totally filled with anhydrite. Thus, this neo-formed mineral seems to result from the hydration of the anhydrite in the cracks during brine leaching. Moreover, the mercury porosity analyses have shown that the porous media is mainly located in the clay matrix or at is boundary. So water can flow along the “in-situ” anhydrite and cause its hydration and transformation into gypsum.

Though anhydrite can coexist with water at room temperature for a long time, the system anhydrite-water is known as a metastable one, where the real solid equilibrium phase is gypsum, therefore hydration of the anhydrite is highly possible. Anhydrite conversion into gypsum has been extensively studied for civil engineering purposes (Delporte, 1988; Evrard *et al.*, 1984, 1987; Nüesch et al, 1995; Einstein, 1996). The principle for metastability breaking up is to destabilise anhydrite by catching either calcium or sulphate from its surface; this can be achieved by trying to promote, at least temporarily, the formation of mineralogical species from the jarosite, ettringite or syngenite families, by adding to the solution alkaline metals alone or in combinations with ferric iron or aluminium. Thus the main decrease of dissolved Fe and K quantities in «cavity brine» during batch experiment seems to be the result of jarrosite/natrojarrosite and/or syngenite precipitations. By this way, the hypothesis of anhydrite hydration is strengthened.

In the hydration process of anhydrite, one mole (136 g) of anhydrite with a unit volume mass close to 3 $g.cm^{-3}$ is converted into one mole of gypsum (172 g) with a unit volume mass close to 2,32 $g.cm^{-3}$. An elementary calculation reveals then a volume expansion close to 163 % resulting from hydration. Swelling pressures of some anhydrite-rich argilites, which are between 1Mpa and 5Mpa (Einstein, 1996), are moreover in the range of the tensile strengths (Homand, 2002) of those from the lower iridescent marls. In terms of pressure, anhydrite hydration can creates opened cracks and thus be the origin of the Keuper “marls” degradation.

Thin-sections of anhydrite immerged in «cavity brine» do not show any gypsum. Since the iron and potassium quantities decrease in brine during the batch experiment, an anhydrite hydration promoted by temporary jarosite and or syngenite may be possible. In this case, the gypsum must has been detached from thin-sections during polishing. This hypothesis is consolidated by the fact that gypsum crystals from argillite thin sections have moved between optical and electronic microscope analysis. Nevertheless, this possible hydration may be relatively superficial as the one observed on sample immerged in distilled water. In order to explain the preservation of the anhydrite facies during batch experiment, we incriminate the low permeability, justified by the low porosity of anhydrite lithofacies: it may prevent the water access to internal anhydrite crystals.

4.2. Conclusion

The rocks surrounding the keuperian salt strata in Lorraine are dominantly composed of argilite and anhydrite instead of “marls” with anhydrite. The clay fraction contains some smectites and disordered interlayered chlorite/smectite.

The batch experiments by immersion of two types of keuper marls samples (the one dominantly argilite, the other dominantly anhydrite) in various fluids (distilled water, NaCl brine, «cavity brine») allowed to put forward and to support a hypothesis about the micro-mechanistic origin of rock failure. The hydration of anhydrite in the open porosity of the argilite rock results in its transformation into gypsum, promoted by the presence of iron and potassium in the brine. The volume increase associated to this mineralogical transformation causes internal pressure which results in disruption of the rock, mediated by the presence of clay veins with lower mechanical cohesion. The non-hydration of massive anhydrite is supposed due to its very low permeability that limits the access of water.

5. References

Auvray C. (2005). *Essais de perméabilité- ouvrages SUG 2005, SUG 2006*. LaEGO report for ANDRA, LG.CA.PSI.RPRE.05.0220.A1. 31p.

Berest P., Brouard B., Durup G. (1998). *Abandon des cavités salines.* Revue Française de Géotechnique, vol.82, 115-122.

BRGM (1980). *Synthèse géologique du basin de Paris. Geologic synthesis of the Paris basin*. Vol. 1, mémoires du BRGM n°101, variously paginated.

Buffet A., Hilly J., Marchal C. (1993) - *Relationship betwen the composition of raw brines originating from the mining of Lorraine salt rock (NE France) and the lithology of the deposit* - 7th Symposium on Salt, Vol. 1, 195-203.

Buffet A. (1998). *The collapse of Compagnie des Salins SG4 and SG5 Drillings*. Symposium of Rome, SMRI, 1998 .

Daupley X. (2004). *Typologie des mécanismes et des phénomènes de mouvement de terrain liés aux exploitations de sel.* INERIS report, DRS-04-56179/R01, 80 p + appendix.

Delporte C. (1988). *L’anhydrite de Faulquemont et sa valorisation sous forme de béton sulfate: mécanisme d’hydratation et mise au point d’accélérateur de prise hydraulique*. Phd Thesis, INPL, 232 p + appendix.

Einstein H. H. (1996). *Tunnelling in Difficult Ground- Swelling Behaviour and Identification of Swelling Rocks. Rock Mechanics and Rock Engineering*. Vol. 29, Iss. 3, 113-124.

Evrard O., Brice J.F. & Delporte C. (1984). *Brevet Français N° de publication 2 559 145, N° d'enregistrement 84017 12*. SMA.

Evrard O., Brice J.F. & Delporte C. (1987). *Brevet Européen N° d'enregistrement 84/ 400.533.0. SMA.*

Fanlo I., Ayora C. (1998). *The evolution of the Lorraine evaporate basin: implications for the chemical and isotope composition of the Triassic ocean.* Chemical Geology, Vol. 146, Issues 3-4, 135-154.

Fontes J.C., Matray J.M. (1993). *Geochemistry and origin of formation brines from the Paris Basin, France*. Chemical Geology, Vol. 109, Issues 1-4, 177-200.

Homand F. (2002). *Caractérisation physique et mécanique du sondage Cerville 3129*. LaEGO report for SOLVAY company, LG.FH.SOL.PSI.RPRE.02.0512.A, 31 p.

Hilly J., Marchal C. (1999). *Les gisements évaporitiques de Lorraine. Evaporite deposits of Lorraine.* Bulletin d'information des géologues du basin de Paris, Vol. 36, Issue 1, 20-24.

Marchal C. (1983). *Le gîte salifère keupérien de Lorraine-Champagne et les formations associées; Etude géométrique; Implications génétiques. The Keuper saliferous deposit in the Lorraine-Champagne region and associated formations; geometrical aproach, genetic implications* Sciences de la Terre, Memoires, Vol.44, 1-25.

Mulder T., Berend I., Yvon J., Tisot J.P. (1992). *Analyse du gonflement d'un interstratifié irrégulier kaolinite-beidellite. Aspects cinétiques et influences de la compaction initiale et de la salinité.* C.R. Ac. Sci. Paris t. 315, série II, 453-459.

Rashid H. (1995). *Contribution à l'étude d'un bassin évaporitique triasique. Les Marnes irisées inférieures.* Phd Thesis, UHP Nancy, 121 p + appendix.

Remy J.M. (1993). *Influence de la structure du milieu poreux carbonaté sur les transferts d'eau et les changements de phase eau-glace. Application à la durabilité au gel des roches calcaires de Lorraine*. Thesis, INPL, 253 p + appendix.

Sammartino S., (2001). *Construction d'un modèle conceptuel d'organisation de la porosité et de la minéralogie dans les argilites du site de Bure*. ANDRA report. D RP 0ERM 01-018\A, 68 p + appendix.

Vouille G. (1986). *Mine de Varangéville-comportement mécanique des marnes du mur en présence de saumure*. Ecole des Mines de Paris - Centre d'Etudes de Mécanique des Roches (CEMR), report n° R 86/3 for CSME company, 23 p + appendix.

MODELLING UNCERTAINTIES IN PILLAR STABILITY ANALYSIS

CAUVIN Maxime[1], VERDEL Thierry[1], SALMON Romuald[2]

[1] LAEGO – Ecole des Mines de Nancy, Parc de Saurupt – CS 14234 – 54042 Nancy Cedex – France. maxime.cauvin@mines.inpl-nancy.fr ; thierry.verdel@mines.inpl-nancy.fr

[2] INERIS, Parc Alata –BP 2 – 60550 Verneuil-en-Halatte – France. romuald.salmon@ineris.fr

ABSTRACT: Many countries are now facing problems related to their past mining activities. One of the greatest problems they have to deal with concerns the potential surface instability. In areas where a bord-and-pillar extraction method was used, deterministic methodologies are generally used to assess the risk of surface collapses. However those methodologies suffer from not being able to take into account all the uncertainties existing in any risk analysis. Through the practical example of the assessment of a single pillar stability in a very simple mining layout, this paper introduces a logical framework that can be used to incorporate the different kinds of uncertainties related to data, models as well as to specific expert's choices in the risk analysis process. Practical recommendations and efficient tools are also provided to help engineers and experts in their daily work.

KEYWORDS: Uncertainties, Risk analysis, Monte Carlo simulations, Pillar stability.

RESUME : De nombreux pays se trouvent aujourd'hui confrontés à des problèmes liés à leur histoire minière passée, et notamment à celui de l'instabilité des terrains de surface. Des méthodes déterministes sont généralement utilisées dans les zones anciennement exploitées par la méthode des chambres et piliers, pour évaluer le risque d'effondrement de surface. Cependant, ces méthodes ne permettent pas de prendre en compte les différentes incertitudes qui existent dans toute analyse de risque. Cette étude, à travers l'exemple du calcul de stabilité d'un pilier de mine extrait d'un environnement très simple, présente une démarche logique pouvant être utilisée pour incorporer les incertitudes, liées aux données aussi bien qu'aux modèles ou aux choix spécifiques des experts, dans les processus d'analyse de risque. Des recommandations pratiques et des outils efficaces pouvant permettre d'aider les ingénieurs et les experts dans leur travail de tous les jours sont également présentés.

MOTS-CLEFS : Incertitudes, Analyse de risque, Simulations de Monte Carlo, Stabilité de pilier.

1. Introduction

Many countries are facing problems related to abandoned underground mines. In France, iron ore has been industrially mined all around the Lorraine Region (North-Eastern France) from the middle of 19th to the end of the 20th century. The most common mining method was pillar extraction but a bord-and-pillar partial extraction method was sometimes used under sensitive zones to protect houses and surface infrastructures from subsidence during the exploitation. In those areas, some collapses already occurred, either during the mining operation or a long time after it. Even though numerous studies have already been carried out, researchers still go on developing and improving their works in order to understand the reasons of such collapses.

Today, one of the greatest issues of the work of state organisations having to manage the consequences of those past mining activities is to deal with the problem of potential surface instability. In the Lorraine region, INERIS and GEODERIS developed a multi-criteria analysis in

order to realise a risk map covering all the iron ore mining areas (Merad *et al.*, 2004). In The Netherlands, a deterministic method was applied successfully in the recent past to investigate the necessity of underground support measures to protect the surface from collapsing above shallow abandoned bord-and-pillar limestone workings (Bekendam, 2004). Even though those methods are perfectly efficient in their field of competence, they suffer from not being able to take into account all the uncertainties inherent to geotechnical problems.

In the past decades, literature about the use of probabilistic methods in geotechnical engineering became more and more comprehensive (Einstein, 1996; Baecher and Christian, 2003). For the purposes of any risk analysis, one may distinguish between four classes of uncertainty ranging from a very general to a very specific degree. Uncertainty can thus be attributed to (1) the scientific, economical and politic context of the study; (2) the expertise laying on deterministic human choices; (3) the use of models; and (4) the randomness and/or the lack of knowledge on data (figure 1). It can be shown from figure 1 that these four classes of uncertainty are not totally independent and that dealing with the uncertainty associated to a specific class may have impact on uncertainties of lower classes. However, the way of treating uncertainties is different between all the categories. In the higher classes, uncertainties are very difficult to deal within a quantitative way while tools exist to help considering lower classes uncertainties.

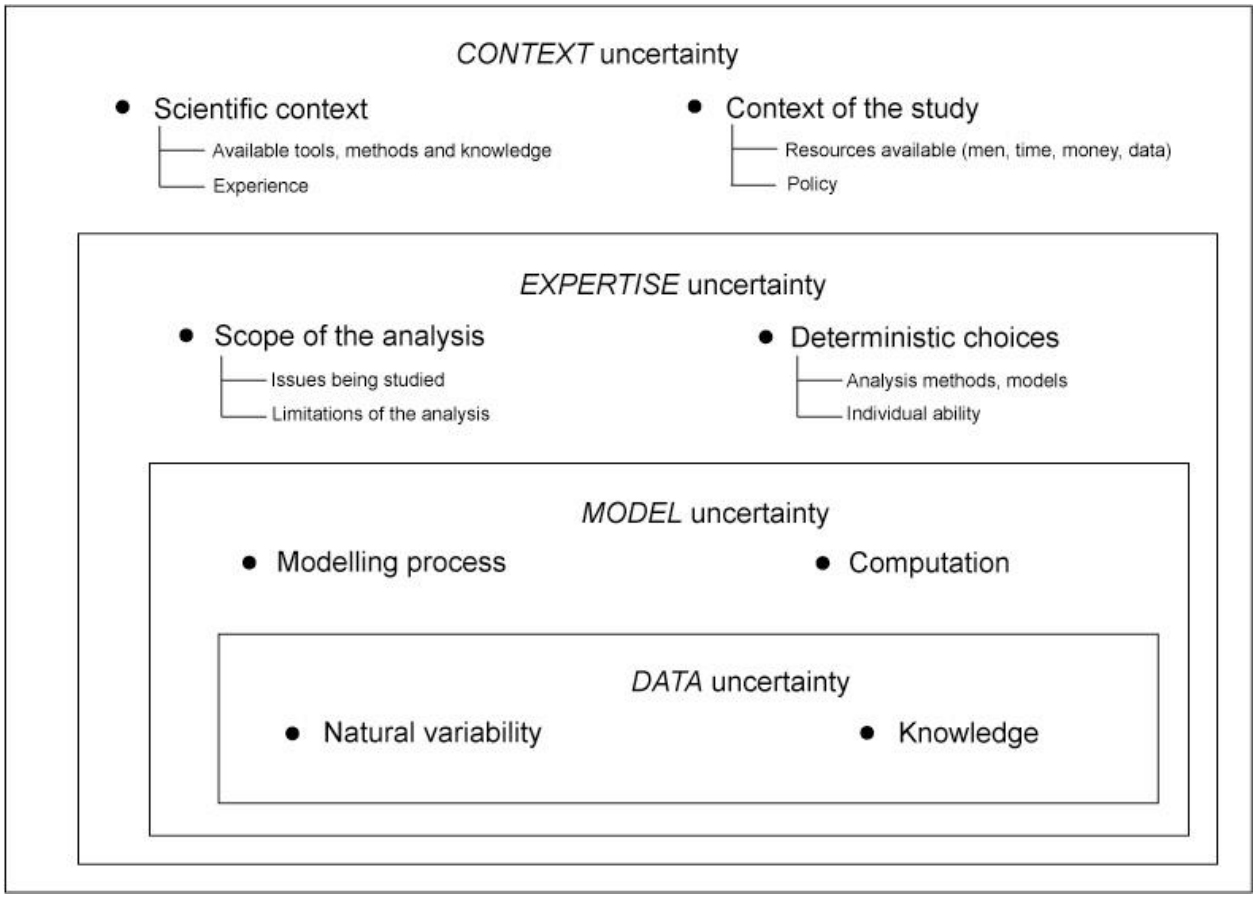


Figure 1. Possible scheme distinguishing between the different categories of uncertainty in engineering risk analysis.

In geotechnical engineering, most of the probabilistic studies that have been undertaken concern slope stability analysis. This geotechnical field indeed offers a really efficient framework for the incorporation of uncertainty into slope design (El-Ramly *et al.*, 2003) because physical phenomena are relatively well known and modelled. Nevertheless probabilistic studies are relatively rare in the mining field. Efforts have started to be made for the last couple of years in New-Zealand (Richards *et al.*, 2002) or in Great Britain (Swift and Reddish, 2002) after surface collapse events in order to

determine where further such collapses are likely to occur in the future. Even though those studies give really interesting results and make it possible to quantify the risk of future surface collapses, they do not take into account all the different kinds of uncertainties.

The study presented herein focus on the practical assessment of a single pillar stability in a very simple mining layout. It provides a methodology to incorporate different kind of uncertainties related to data, models or specific expert's choices. Different engineered recommendations will thus be given.

2. Classical deterministic approach

Bord-and-pillar method of mining is commonly used to extract ore from horizontally bedded sedimentary strata. Pillars are often left intact to provide permanent support to the undermined roof. In such a context of exploitation, economical considerations and safety assessment are the two most important issues at stake. Over the past few decades, several works about pillars have been carried out by a number of researchers and engineers either to determine optimal design pillar sizes (Salamon and Munro, 1967; Van der Merwe, 2003) or to assess long-term pillar stability (Bekendam, 2004).

The conventional methods used to assess the stability of mine pillars are based on deterministic (empiric or analytic) approaches. They usually adopt the safety factor (SF) as an indicator of the stability of the pillar. This safety factor is defined as the ratio of the pillar strength (R) over the mean vertical stress acting on pillar (S). Theoretically, a SF value greater than 1 thus means the system is stable while a SF value lower than 1 means it is unstable. In practice, a threshold value higher than 1 is generally used at the design level to incorporate uncertainties.

Several methods can be used to determine both of S and R. S is generally calculated using the Tributary Area Theory, which considers the total overburden load directly over the pillar and the portion of the galleries at its perimeter:

$$S = \gamma D \frac{(l + b_l)(L + b_L)}{lL}, \qquad (1)$$

where l and L are the pillar width and length, b_l and b_L the bord width and length, γ the average volumic weight of the overburden and D, the mining depth.

Pillar strength can be calculated by laboratory measurements on samples or by back analysis of past collapses. In the Lorraine region, several field investigations have been made after the historical surface collapses events and a back-analysis of the data lead experts to evaluate the long-term strength of the pillars to be 7.5 MPa.

In the present approach, the mining layout being studied is very simple. It consists in a grid of 3 by 3 rectangular pillars that allows to take into account the mining environment of the central pillar (figure 2). Dimensions of pillars and characteristics of the mining area have been extracted from a huge database containing information about all the Lorraine mines. The exploitation panel selected for the purpose of the study is between 130 and 150 m deep and 500 m wide. Pillars have a 12 by 8 m rectangular shape, roads are 4 m wide and the seam is 4 m high. The overburden is assumed to have a mean volumic weight of 25 $kN.m^{-3}$. Using the tributary area theory and a constant strength value of 7.5 MPa, the pillar is assessed to be stable with a safety factor equal to 1.09.

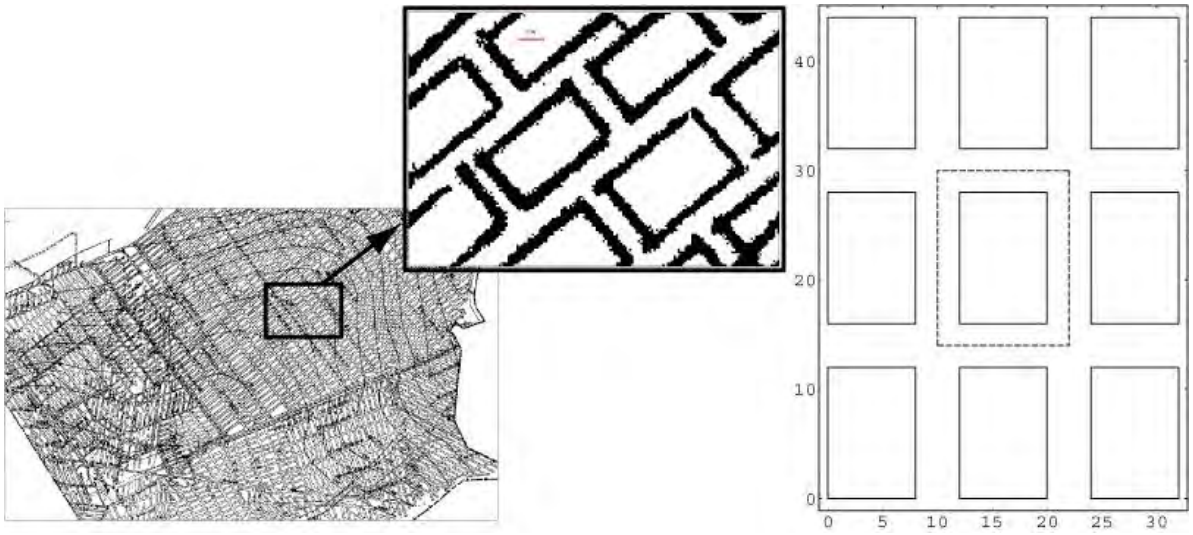


Figure 2. Extract of a mining map and selection of the nine pillar mining layout.

3. Taking into account the uncertainty on input parameters

Considering figure 1, uncertainty on input data can be linked to the spatial and temporal natural variability of mechanical and geological parameters as well as to the lack of knowledge making it difficult to assess exactly the parameter values used in models.

In our case of interest, both kinds of input data uncertainty can be found. '*Physical*' parameters, as γ, are affected by natural variability. They are indeed geological averaged values obtained from sample measurements. On the other side, epistemic uncertainty is predominant for parameters as the long-term strength of the pillar (R) that has been evaluated from a statistical back-analysis of several surface collapses occurred in the iron ore basin.

The determination of the nature of the uncertainty is far more difficult for the geometrical parameters such as pillar dimensions or mining depth. These are usually determined from mining paper maps archived by mining companies or regional authorities, and which are generally at a 1:5000 scale. At such a scale, a pencil line thickness on the map is equivalent to more than 1m in the mine. For classical Lorraine pillars, such a map inaccuracy may lead to a 10 % error on the values used for pillar dimensions and obviously to significant errors in the risk analysis process. It has been considered in this study that uncertainty due to the map inaccuracy belongs to '*model uncertainties*' as maps are models aiming to help engineers to represent the reality.

In geotechnical engineering, a very efficient way of taking into account uncertainty on input parameters is to define statistical distribution functions for each of the parameters (Kim and Gao, 1995). Unfortunately, available information is frequently poor and test data are often inefficient to characterize the statistical moments required in the distribution functions. When test data are unavailable, those parameters may be estimated from literature or judgement and experience of experts (USACE, 1999).

Once distribution functions are defined, Monte Carlo simulations may be used to propagate uncertainties in the deterministic model. The principle of such simulations is to take one random value from the distribution of each input parameter and to calculate the output value of the function. Each calculation gives one outcome. A great number of simulations allows to obtain a frequency distribution of the output values. Mean value, standard deviation or other statistical moments of the

studied parameter may thus be estimated. The greater the number of simulations, the more accurate the computed statistical moments.

For this study, a simulation method has been built allowing all the parameters to be defined by a mean value and a standard deviation. This method has been computed using Mathematica software. For the construction of the mining layout, each position of the corners of the nine pillars is randomly distributed around a mean value. In order to respect mine design reality, the assumption was made here that the roads are cut in a straight line. Map inaccuracy is supposed to lead to a 1 m error on pillar dimensions. Figure 3 presents different layouts that can be obtained from random simulations. For illustrating the difference between them, safety factors (SF) and extraction ratios (τ) were calculated for a 140 m thick overburden.

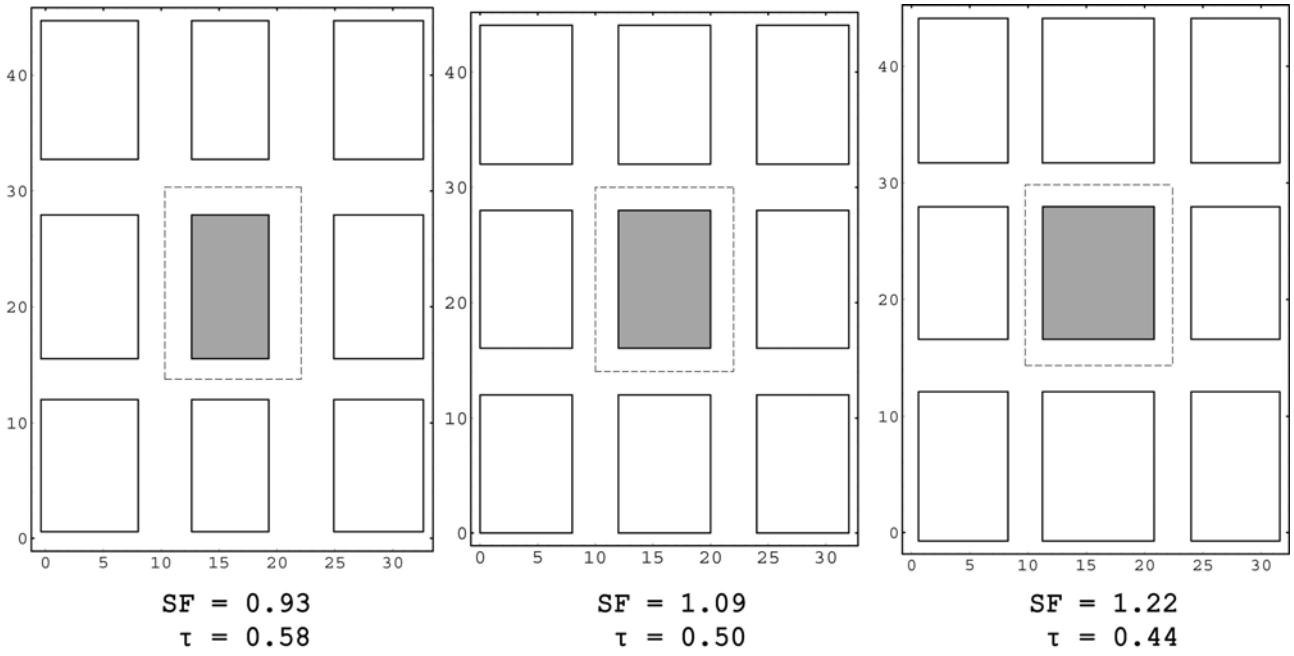


Figure 3. Three mining layouts computed from random simulations.

In order to describe statistically other input parameters, several assumptions had been made. All parameters had been characterized by a mean and a maximal error. Normal distributions were chosen to fit all the parameters. Such an assumption may be valid for parameters that have been determined from back-analysis of several past events (as R) or that are considered to be traditional mean values of sedimentary rock properties (as γ). It is more opened to criticism for parameters, as h or D, that are described in the available database by a minimal and maximal value. However, it will be shown later that the choice of a specific distribution function has only a weak influence on the result (see table 2). The maximal errors chosen for the parameters are considered to be the boundaries of the 95 % confidence interval of those normal distributions. When no information was available, maximal errors were roughly assumed to be 10 % of the mean value. Table 1 summarizes the statistical values chosen for each of the input parameters.

Table 1. Statistical values used for input parameters.

Parameter		Symbol	Mean value	Maximal error	Distribution law
Pillar length	(m)	L	12	1	Uniform
Pillar width	(m)	l	8	1	Uniform
Bord length = bord width	(m)	b	4	1	Uniform
Pillar height	(m)	h	4	0.5	Normal
Mining depth	(m)	D	140	10	Normal
Average volumic weight	($MN.m^{-3}$)	γ	0.025	$2.5e^{-3}$	Normal
Long-term strength	(MPa)	R	7.5	0.5	Normal
k-Strength constant	(MPa)	k	4.4	(–)	Constant
Mining span	(m)	A	500	(–)	Constant
Number of pillars	(–)	N	31	(–)	Constant
Coefficient of geostatic stress	(–)	K_0	0.5	(–)	Constant
Young modulus of pillar material	(GPa)	E_p	13	(–)	Constant
Young modulus of wall material	(GPa)	E_w	5	(–)	Constant
Poisson ratio of pillar material	(–)	ν_p	0.33	(–)	Constant
Poisson ratio of wall material	(–)	ν_w	0.33	(–)	Constant

Using the previously described method, the statistical analysis of a large number of computed simulations made it possible to evaluate the mean value and the standard deviation of the safety factor. Figure 4 presents the obtained distribution function. From a practical viewpoint, it would be of interest to estimate p_f, the probability of 'design failure', defined as the probability that the computed safety factor is less than the target value of stability, i.e. 1:

$$p_f = \Pr ob(SF < 1) . \quad (2)$$

p_f is in this case equal to 23.5 %.

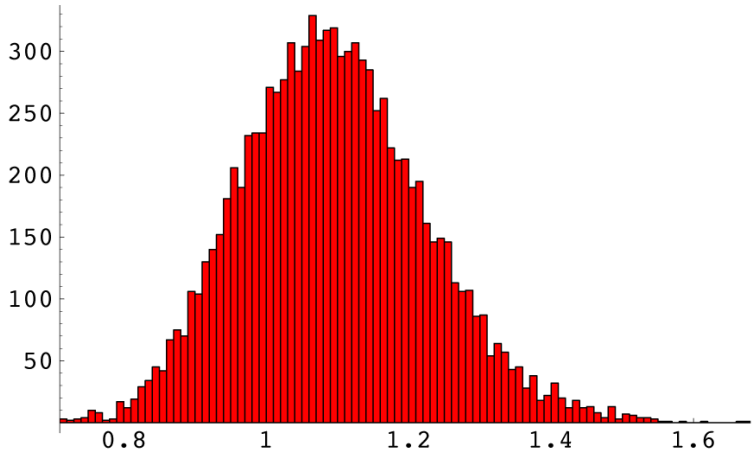


Figure 4. Distribution of the safety factor when uncertainties exist on input parameters.

While using of Monte Carlo method, an important parameter to take into account is the number of computed simulations. The greater the number of simulations, the more accurate the computed statistical moments but the longer the computation. In this study, a parametrical study has been carried out in order to investigate this parameter. Figure 5 presents for different numbers of simulations the ranges of variation of computed means of safety factors, as well as times to compute them. It can be shown that, for 10000 simulations, the computation time is still reasonable and the range of variation of the computed safety factor is less than 1 %.

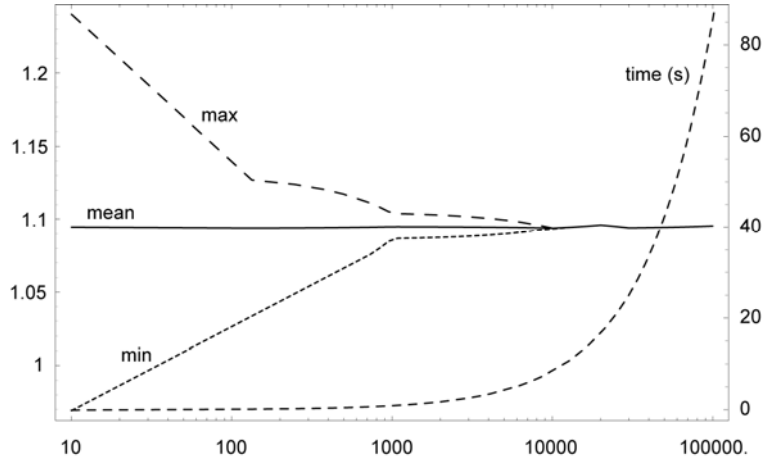


Figure 5. Range of variation of results and computation times for different numbers of simulation.

4. Taking into account the uncertainty related to the choice of a specific model

As presented earlier, uncertainty in risk analysis can also be attributed to some of the expert's choices. Assessing a risk generally requires using specific methodologies and mathematical models. For example, in our current example of pillar stability assessment, the choice has been made to compare the strength of the pillar to the stress acting on it. Two models have thus been used to estimate both of those parameters. Actually, models are no more than abstractions of the state of nature and no matter how sophisticated they are, they are unable to capture the nature entirely. The most effective approach to estimate the previously named '*model uncertainty*' would be to rely on field observations and use databases to do back-analyses. However, in geotechnical studies, it is usually very difficult to have historical observations to compare with results of model predictions and most of the times, only the uncertainty related to the choice of specific models (classified as '*expert uncertainty*') is taken into account.

In a study by Husein Malkawi *et al.* (2000), uncertainty associated with the use of different slope stability models was addressed by evaluating the relative performance of some simplified methods compared to the most rigorous and accurate one. In this study, it has been chosen to consider models as input parameters. Such a choice allows taking into account both the existence of several mathematical models and the inability of the analyst to identify the best one.

In our work previously described, two mathematical models have been used: the tributary area method has been chosen to calculate the stress acting on the central pillar of the mining layout and a constant value model has been used to evaluate the strength of a pillar. Nevertheless, even if both of the models are really convenient because simple, they also have disadvantages.

The two main drawbacks of the tributary area method are that (1) it makes the assumption that each pillar is carrying the load of a vertical rock column over it, this may only be valid for central pillars from large horizontally stratified mining environments, and (2) it does not take into account the nature of the overburden. Even though numerical simulations such as finite elements methods are today the most common methods used to compute stresses acting on pillars, they can only be used for specific sites where geology and mining geometry are known. Nevertheless, for the purpose of this study, whose aim is to be as general as possible, it has been chosen to use results from Coates' work about stresses acting on pillars (Coates, 1970). His approach makes it possible to take into account the extent of the mined area, the stress component parallel to the seam, the relative

deformation properties of pillar, roof and floor rocks, and the positions of the pillars in the mining zone. The general solution for the mean pillar stress becomes:

$$S_2 = \gamma D\left(1+\frac{2\tau - K_0\frac{h}{A}\frac{(1-2\nu_w)}{(1-\nu_w)} - \frac{\nu_p}{(1-\nu_p)}K_0\frac{h}{A}\frac{E_w}{E_p}}{\frac{h}{A}\frac{E_w}{E_p} + 2(1-\tau)\left(1+\frac{1}{N}\right) + 2\frac{l\tau}{A}\frac{(1-2\nu_w)}{(1-\nu_w)}}\right) \quad (3)$$

$$\text{with } \tau = 1-\frac{Ll}{(L+b)(l+b)}, \quad (4)$$

where τ is the extraction ratio, K_0 the coefficient of geostatic stress, A the extend of the mining area, N the number of pillars, E_p, E_w and ν_p, ν_w the Young modulus and Poisson ratios of pillar and wall (roof and floor) materials.

For the purpose of the study, the assumption had been made that only the parameters that are present both in equations (1) and (3) are aleatory. The impacts of those equations on the result may thus really be compared. Table 1 presents the values chosen for all the parameters. Some of these had been extracted from local databases and some are roughly estimated.

In our case of study, the use of the tributary area theory leads to a stress value of 6.87 MPa while Coates' formula gives a value of 6.66 MPa. It confirms the general belief that the tributary area theory is rather a conservative approach.

Concerning the strength of a pillar, it is now common cause that it depends on the strength of the material of which it is composed as well as its dimensions, and more specially its width-to-height ratio (Salamon and Munro, 1967; Van der Merwe, 2003). Using Van der Merwe's method on a very extensive database of failed and stable Lorraine iron ore pillars, it was found that the strength of those pillars can be expressed as follows (Cauvin, 2004):

$$R_2 = k\sqrt{\frac{w}{h}} \quad (5)$$

$$\text{with } w = 2\frac{Ll}{L+l}. \quad (6)$$

Here, w is the equivalent width that has to be used for rectangular pillars and k a constant value that can be related to the strength of the pillar material. The determination of k lays on the assumption that, on average, pillar failure occurs for a safety factor equal to 1.

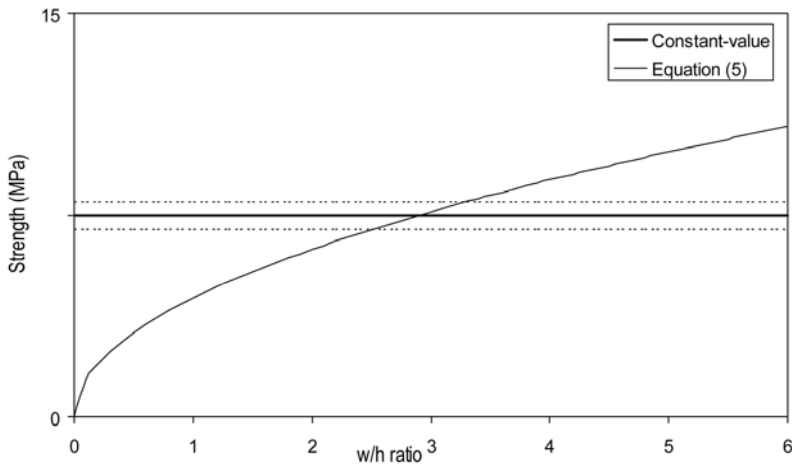


Figure 6. Comparison between the two different models estimating pillar strength.

Figure 6 shows the comparison between the two different models (constant-value versus equation (5)). For a w/h-ratio higher than 2.9, R_2 is bigger than 7.5 MPa.

Those different physical models have been implemented in the simulation method. Basically, like for input parameters, one random model is chosen among the two that exist to evaluate the strength of the pillar and the stress acting on it. The computation is then done following the same procedure as described in part 3. A degree of confidence can be chosen for models allowing taking into account decisions of experts as well as historical considerations. For example, if in a panel of 5 experts, 3 think that it is better to use a constant-strength value to express the strength of the pillar, the strength model used in the computation have a probability of 3/5 (0.6) to be this one. In one other way, in the Lorraine region the tributary area theory was originally used by miners to design the underground workings. It thus seems logical to preferably use this formula to assess the risk of pillar failure. Figure 7 shows the results obtained by the simulation method, assuming that the input parameters are perfectly known. It has been chosen here to assign a confidence degree of 75 % for the tributary area theory while the models for the pillar strength are equally "trusted".

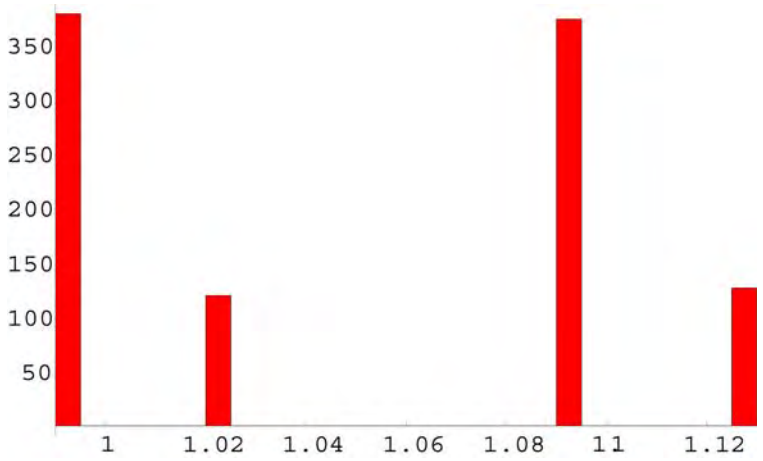


Figure 7. Computed safety factors, taking into account the existence of different models.

It can then be shown in this case that one on the four combinations gives a safety factor less than 1. This Safety Factor corresponds to the ratio between R_2 (equation 5) and S (equation 1).

Figure 8 presents the distribution function obtained for the safety factor when uncertainties on input parameters and on models are simultaneously taken into account. In comparison with the previous results, the probability of 'design failure' increases from 23.5 % to 34 %.

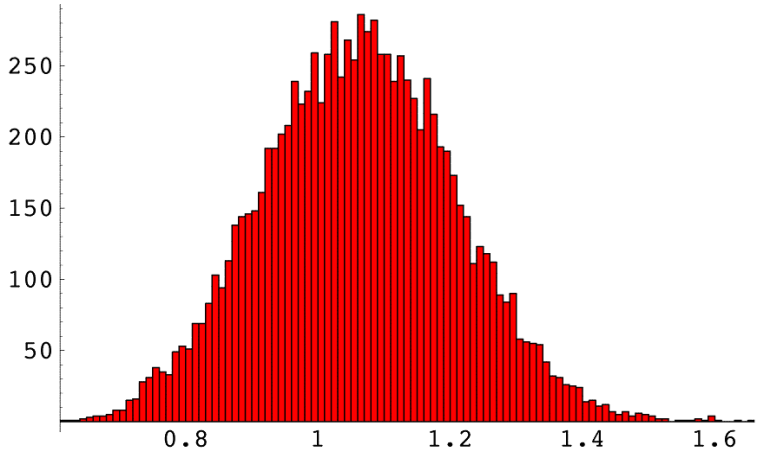


Figure 8. Distribution of the safety factor when uncertainties exist both on input parameters and models.

5. Taking into account the method used to "propagate" uncertainties

Monte Carlo simulations have been chosen as the method used to propagate uncertainty on input parameters into deterministic models. We are fortunately here in a case within which it is possible to do so. Problems with Monte Carlo simulations are that they may require huge time of computation.

However others methods exist to "transfer" the uncertainty concerning the input parameters on the output of a model. The Point Estimate Method (PEM) is one of them. It is known for its simplicity and is commonly used in geotechnical studies. One of the greatest advantages of such a method is that it is easily computable in numerical simulation processes. In PEM, each random variable is defined by two numbers: the mean value plus or minus the standard deviations of the variable. Using those points, it allows to obtain accurate approximations of the mean value and the variance of unknown output variables. For more details about the method, a detailed algorithm is presented in Isaksson (2002). The main drawback of PEM is that it does not provide any information about the shape of the distribution of the output parameter. Moreover, using complex functions or numerous correlated variables may lead to an inaccuracy of the results.

In our case of interest, Monte Carlo simulations allowed to obtain the distribution function of the pillar safety factor (figure 4). The mean value and the standard deviation of this parameter can thus be estimated to be respectively 1.095 and 0.126 after 10000 simulations. Using PEM, they have been found to be respectively 1.104 and 0.163.

6. Analysis of variance

Engineers and experts clearly ask today for efficient tools that can help them to solve the tough dilemma they face. They indeed have to give quick and accurate answers to problems full of uncertainties. One of their greatest needs is thus to reduce the uncertainty on the results they give (in this study, the standard deviation of the calculated safety factor is about 0.14) in a rapid and cheap way. For time and economic reasons, it is obvious that engineers cannot study all the sources of uncertainty but can only try to focus on some of them. The study presented herein provides a tool that makes it possible to identify the parameters whose uncertainty has the greatest impact on the result.

Table 2 presents the relative influences of five different sources of uncertainty on the total variance of the computed safety factor. The map inaccuracy and the use of human-made database, expert-made hypothesis or models (as back-analysis) to estimate parameter values may have impacts on the input parameters. But, as presented in part 4, the choice of specific models to deal with a problem may also have impacts on the result. In order to obtain Table 2, each source of uncertainty has been investigated separately. Normal and uniform distribution have been used in the Monte Carlo simulations to fit the input parameters. It can be shown that the choice of a specific distribution function has only a weak influence on the result. It can also be highlighted that in our case of interest, almost half of the total variance of the computed safety factor is due to the map inaccuracy. It has also to be specified here that the differences between the relative influences of D, γ and R on the total variance can be totally explained by the differences between the maximal error on mean ratios as the rule they play in the calculation of the safety factor is exactly the same (see equation 1).

Table 2. Relative influence of the different sources of uncertainty on the computed safety factor.

Source of uncertainty	Concerned parameters	Maximal error / Mean	Variance of the computed safety factor		Variance / Total variance (%)
			Normal distribution	*Uniform distribution*	
Map inaccuracy	L, l, b	~ 0.10	$7.78e^{-3}$	$9.89e^{-3}$	47
Use of database	D	0.07	$1.59e^{-3}$	$2.05e^{-3}$	9
Expert-made hypothesis	γ	0.10	$3.18e^{-3}$	$4.05e^{-3}$	19
Use of models	R	0.07	$1.37e^{-3}$	$1.77e^{-3}$	8
Choice of models	(–)	(–)	$2.82e^{-3}$		17

7. Conclusions and practical recommendations

Table 1 introduced a possible scheme to classify the different categories of uncertainty that can be encountered in a risk analysis study. This paper provides a logical framework that can be used to reduce several kinds of uncertainties. Defining statistical distribution functions for input parameters may help engineers to deal with the problem of '*data uncertainties*' inherent to the study of a natural system. It can also be pointed out here that the definition of the characteristics of those distribution functions requires the expert to make some choices (evaluation of mean values, maximal errors, …), so that the '*expertise uncertainty*' is also involved. Choices had also to be made regarding the nature of the distribution functions fitting the parameters. In our study, normal and uniform distributions have both been used and it can be shown that such a choice has only a weak influence on the results. Table 2 illustrates that the variance of the computed safety factor is only slightly bigger when uniform distributions have been chosen for all the input parameters (in this case, p_f equals 24.6 %) than when normal distributions have only been used (p_f = 21.4 %). More generally about '*expertise uncertainty*', this work may guide engineers through their analysis process in giving them a methodology to follow. It thus allows to break free from the individual ability or from the deterministic choices of the expert in charge of the analysis.

It has been said in introduction that the methods currently used to assess the risk of surface collapse do not generally integrate the taking into account of all the uncertainties inherent to the study of a natural system. In fact, it is not exactly true. Most of the times, uncertainties are introduced in the evaluation process in an indirect, if not unconscious, way. This integration is basically part of the expert's analysis process and is affected by '*expertise uncertainty*'. For instance, in the example we used, finding a safety factor greater than 1 means the system has to be stable. However the value of 1.092 is very close to 1, meaning that we are thus very close to the stability. Experts usually use deterministic threshold values for safety factor (1.2/1.3/1.5/3) in order to integrate uncertainties inherent to the evaluation and to be side of the safety. Generally, the more damaging the consequences of an event, the greater the chosen threshold value.

Nevertheless, using such threshold values does not allow the expert to assess '*how stable the situation is*'. Taking explicitly into account uncertainties on input parameters by the use of distribution functions makes it possible for the expert to represent himself an order of magnitude of what he is talking about, e.g. in our case of interest 23.5 % of the computed safety factors are less than 1. Expressing such a quantified result now sets the problem of its interpretation. In fact, we are now talking in terms of risk and acceptance. It is now up to the stakeholders, not either to the engineers, to decide whether the situation is acceptable or not, and whether uncertainty on the result has to be reduced or not.

8. References

Baecher G.B., Christian J.T. (2003). *Reliability and Statistics in Geotechnical Engineering*, John Wiley and Sons, London and New York, 2003.

Bekendam R.F. (2004). *Stability and subsidence assessment over shallow abandoned room and pillar limestone mines*. Engineering Geology for Infrastructure Planning in Europe. A European Perspective. Springer-Verlag, Berlin Heidelberg 2004, 657-670.

Cauvin M. (2004). *Elaboration d'une méthode permettant de distinguer risque d'effondrement brutal et risque d'effondrement progressif des terrains suite à une exploitation du sous-sol*. Rapport de stage de fin d'études, Ecole des Mines de Nancy.

Coates D.F. (1970). *Principes de la mécanique des roches*. Monographie 874, Direction des Mines. Ministère de l'Energie, des Mines et des Ressources.

Einstein H.H. (1996). *Risk and risk analysis in rock engineers*. Tunnelling and Underground Space Technology, Vol. 11, No. 2, 141-155.

El-Ramly H., Morgenstern N.R., Cruden D.M. (2003). *Probabilistic stability analysis of a tailings dyke on presheared clay-shale*. Canadian Geotechnical Journal, 40: 192-208 (2003).

Husein Malkawi A.I., Hassan W.F., Abdulla F.A. (2000). *Uncertainty and reliability analysis applied to slope stability*. Structural Safety 22 (2000) 161-187.

Isaksson T. (2002). *Model for Estimation of Time and Cost Based on Risk Evaluation Applied on Tunnel Projects*. PhD Thesis, Division of Soil and Rock Mechanics, Royal Institute of Technology, Stockholm, Sweden.

Kim K., Gao H. (1995). *Probabilistic Approaches to Estimating Variation in the Mechanical Properties of Rock Masses.* Int. J. Rock Mech. Min. Sci. & Geomech. Abstr. Vol. 32, No. 2, 111-120.

Merad M.M., Verdel T., Roy B., Kouniali S. (2004). *Use of a multi-criteria decision-aids for risk zoning and management of large area subjected to mining-induced hazards.* Tunnelling and Underground Space Technology, 19, (2004), 125-138.

Richards L., Mazengarb C., Beetham D., Brathewaite B., Smith W. (2002). *Waihi Underground Workings Stage II Investigations (Risk Assessment & Mitigation)*. New Zealand: Hauraki District Council (online) http://www.hauraki-dc.govt.nz/news/Mining-issues/MineworkingsReport/

Salamon M.D.G., Munro A.H. (1967). *A study of the strength of coal pillars*. Journal of South African Institute of Mining and Metallurgy, September 1967.

Swift G.M., Reddish D.J. (2002). *Stability problems associated with an abandoned ironstone mine*. Bull Eng Geol Env (2002) 61:227-239.

US Army Corps of Engineers (1999). *Risk-Based Analysis in Geotechnical Engineering for Support of Planning Studies*. Engineer Technical Letter, 1102-2-556, 28 May 1999.

Van der Merwe J.N. (2003). *Linear Coal Pillar Strength Formula for South African Coal*. Journal of South African Institute of Mining and Metallurgy, June 2003.

THE POST-MINING CONTEXT AT DECAZEVILLE-FIRMI CONCESSION (AVEYRON, FRANCE): ANALYSIS OF IMPACTS RESULTING FROM THE CESSATION OF PUMPING AT THE CENTRAL SHAFT. SURVEY OF VARIOUS SCENARIOS RELATED TO THE WATER LEVEL OF THE PIT LAKE IN THE GRANDE DECOUVERTE.

COJEAN Roger[1], FRANCO Nicolas[2], LAZAREWICZ Jean-Claude[3], BLACHERE Agnès[4], LEFORT Dorothée[4], SORGI Claudia[5]

[1] ECOLE des MINES de PARIS, Institut des Géosciences, Centre de Géologie de l'Ingénieur, UMLV, Bât. IFI, 5 Bd Descartes, Champs-sur-Marne, 77454 Marne-la-Vallée, cedex 2. roger.cojean@ensmp.fr

[2] CHARBONNAGES de FRANCE, Direction Technique Nationale, 4 square François Margand, BP 534, 42007 Saint-Etienne, Cedex 1. nicolas.franco@charbonnagesdefrance.fr

[3] CHARBONNAGES de FRANCE, Direction Technique Nationale, BP1, 13590 Meyreuil. jean-claude.lazarewicz@charbonnagesdefrance.fr

[4] Bureau d'Etudes CESAME, ZA du Parc, Secteur Gampille, 42490 Fraisses. cesame.environnement@wanadoo.fr

[5] INERIS, Parc Technologique ALATA, BP 2, 60550 Verneuil-en-Halatte. claudia.sorgi@ineris.fr

ABSTRACT: Within the frame of the Survey related to the cessation of mine workings in Decazeville-Firmi concession, various impacts resulting from the cessation of pumping at the Central Shaft were assessed. Mainly these impacts are related to groundwater behaviour in the abandoned underground coalmines, hydrochemistry of waters discharged to the environment, ground stability concerns and coal gas emanations. This analysis allowed the choice of the most appropriate elevation of the pit lake level in the Grande Découverte, with the necessity to continue the pumping. Two main objectives were reached. The elected elevation is high enough to result in a permanent chemical stratification, which allows the pumping of the superficial waters and its discharge to natural watercourses without any treatment. The elected elevation is low enough to avoid any problem of inflow of water or ground stability at some particular places which might have been threatened by the rising of the piezometric level of the mining aquifer. Lastly, the elected elevation of the pit lake allows a quality scenery design around the pit lake.

KEYWORDS: Coal mine. Impacts of cessation of pumping. Pit lake. Mine groundwaters. Ground stability

RESUME : Dans le cadre de la constitution du Dossier d'arrêt des travaux miniers dans la concession de Decazeville-Firmi, différents impacts résultant de l'arrêt du pompage au Puits Central ont été étudiés. Ces impacts sont principalement relatifs au comportement de l'aquifère minier, à la qualité des eaux restituées au milieu naturel, à la stabilité des terrains et aux gaz de mines. Cette étude a conduit à la définition de la meilleure cote du lac minier de Decazeville dans la Grande Découverte, en respectant deux principaux objectifs, avec la nécessité de poursuivre le pompage. La cote retenue est suffisamment élevée pour permettre l'établissement d'une stratification chimique permanente dans le lac minier, ce qui rend possible le pompage par soutirage de la tranche d'eau superficielle du lac et sa restitution au milieu naturel sans traitement particulier. La cote est suffisamment basse pour éviter tout problème de venue d'eau ou de stabilité des terrains en quelques zones particulières qui auraient pu être menacées par la remontée du niveau piézométrique de l'aquifère minier. Enfin, la cote retenue permet de réaliser un aménagement paysager de qualité autour du lac minier.

MOTS-CLEFS : Mine de charbon. Impact de l'arrêt de pompage. Lac minier. Aquifère minier. Stabilité des terrains.

1. Introduction

The paper is devoted to the analysis of the post-mining context at Decazeville-Firmi concession (Aveyron, France). Complex technical conditions resulting from the past coalmine workings, discussions related to the assessment of various potential impacts and the choice of the most appropriate level of the pit lake in the Grande Découverte are at the origin of a long procedure which took place during four years, from 2001 to 2004. During this time, dialogues occurred between Charbonnages de France, its engineering and technical consultants (mainly Ecole des Mines de Paris – Centre de Géologie de l'Ingénieur, CESAME, INERIS), the Midi-Pyrénées DRIRE (Regional Direction for Industry and Research), the local and regional authorities (Villefranche-de-Rouergue Sous-Préfecture and Rodez Préfecture) and the elected representatives of the concerned communes. After several investigations in the fields of hydrogeology, engineering geology and geomechanics, and presentation of the obtained results to the various concerned authorities, a general technical and consensual agreement was obtained. In a brief way, the paper describes the main steps of the corresponding scientific or technical investigations which allowed to address and solve the impact problems (Cesame, 2000, 2004; Charbonnages de France, 2001; Cojean, 2002, 2003, 2004; Ineris, 2000, 2003; Lefort, 2000).

2. Regional geological setting

According to geological investigations mainly due to Vetter P. (1968) and later research works resulting from the coal mining works, the litho-stratigraphic sequence of the coal basin, as well as the tectonic deformation phases are well known (Figures 1 and 2).

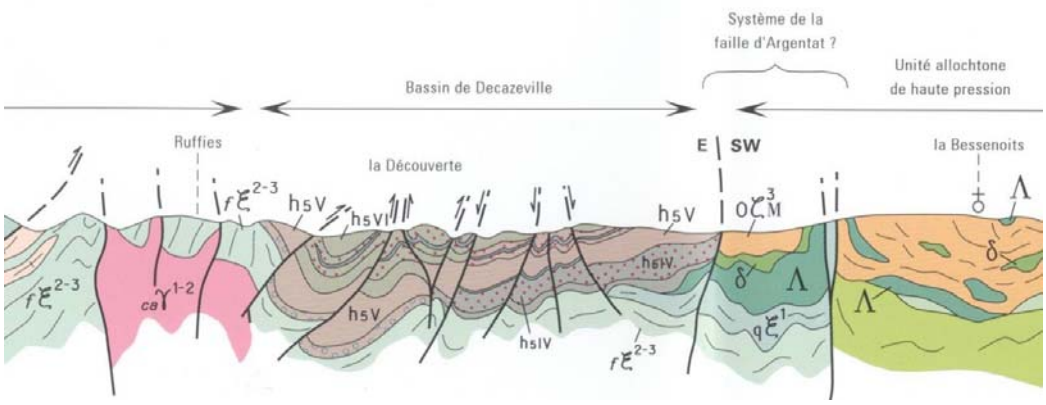


Figure 1. Geological cross section of Decazeville coal basin. The Stephanian series is represented in the central part of the cross section. La Découverte is concerned by the Bourran (h_{5VI}) cycle. Old underground coal works are mainly related to the Bourran (h_{5VI}) and Campagnac (h_{5V}) cycles. (after BRGM. 2001. Decazeville geological map, 1/50000).

The sedimentary sequence consists of several cycles or "assises" dated from Middle Stephanian series (Carboniferous period). In a stratigraphical order, the cycles are arranged as follows: Brayes cycle, Volcanic complex, Auzits cycle, Banel cycle, Campagnac cycle and Bourran cycle.



Figure 2. Elisabeth open pit, Firmi. Photo dated 1896. Saint-Eugène anticline, Campagnac cycle. (in Vetter P., 1968).

Each cycle is made up of conglomerates, sandstones, shales and coal layers. The major tectonic phase occurred at the end of the Paleozoic era and resulted in a general compression of the coal basin, with the folding and faulting of geological strata (Figures 2 and 3).

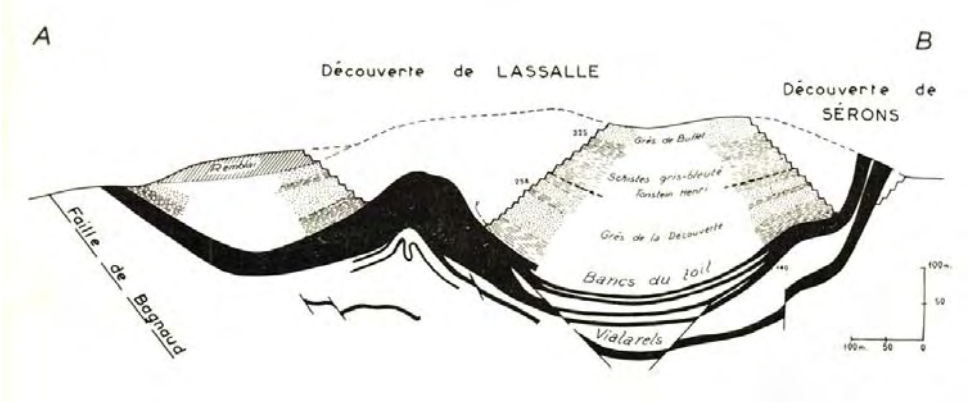
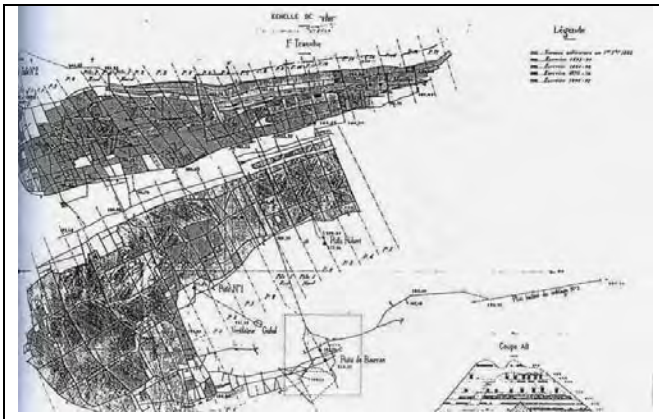


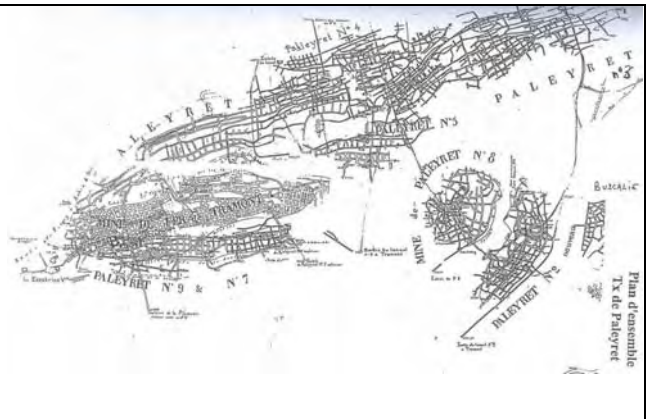
Figure 3. NE-SW geological cross section. Lassale (Grande Découverte) and Sérons open pits. Bourran cycle. (after Vetter P., 1968).

3. Past coalmine workings

Decazeville coal mining basin experimented three major mining periods. From 1360 to 1744, numerous private exploitations developed. Then, from 1744 to 1946, the period of large mining companies took place. In 1946, nationalization of mining companies and creation of Charbonnages de France occurred. It was a period of intense mining activities, with peak productions, then decline due to the international economic coal context and progressive lowering of the regional coal resources (Charbonnages de France, 2001).



a) Bourran underground coalmine workings



b) Paleyrets underground coalmine workings

Figure 4. Detailed old mining maps. a) The Bourran map is related to mine workings dated before 1893, with detailed drawings concerning backfilled horizontal slices during the period 1893-1897. b) The Paleyrets map is related to mine workings dated from 1830 to 1947, with detailed drawings concerning exploration galleries, abandoned coal chambers and pillars. In addition, the old Tramont abandoned iron chambers and pillars can be noted down. (after Charbonnages de France archives).

Underground mining works were performed according to a large variety of mining methods (Figure 4). Some of them were partial exploitations such as the method of *chambers and pillars* that left important residual voids at the end of the exploitations in case of abandonment. Other ones were total exploitations with an integral void treatment such as the stoping methods by successive horizontal slices: the *cut and fill method* that is working upwards or the *undercut and fill method* that is working downwards.

During the recent period of large opencast exploitations and especially the progressive deepening of the Grande Découverte, as well as other open pits in the surroundings, old mining works were partly intersected. Field analyses allowed to investigate the old backfilling operations as well as the mechanical behaviour of grounds after mining subsidence.



a) Old gallery backfilled by slime materials



b) Old timbered and backfilled mining works

Figure 5. Intersections of old mine workings during the deepening of the Grande Découverte.

4. Post-mining conditions

The post-mining context was analysed in a detailed way, considering the following causes for concern and corresponding impacts on the environment and constructions (Feuga, 2005; Fabriol, 2005):

- Type and behaviour of the mining aquifer;
- Ground stability concerns;
- Impacts of various scenarios related to the cessation of pumping and the water level in the pit lake;
- Risks resulting from mining gases, surface mining facilities, waste dumps and tips, specific equipments.

Only the first three items are presented in this paper.

4.1. The mining aquifer

The question of underground waters was investigated considering the different types of aquifers as well as their properties by reference to the problem of discharges and the question of water pressures and ground stability (Cesame, 2000; Cojean, 2002; Younger et al, 2002; Schmitt et al, 2003). The Carboniferous rock masses can be considered as made up of three different hydrogeological units that were more or less intensively modified by the mining works and associated mining subsidence. The Table 1 summarizes the characteristics of these units.

As a matter of fact, the water-bearing formation can be considered as mainly determined by the old coalmine workings, generally backfilled by permeable materials, while discharge questions and water inflows are concerned. However, for underground water pressures and stability problems, the hydraulic continuity has to be underlined as the major concern and may result from continuous water paths through low or very low permeability formations. So, in order to completely investigate these questions, very detailed consultations of old mine working drawings were performed in order to understand the connections between different mining works or to identify the presence of dams in particular cross-cut drifts.

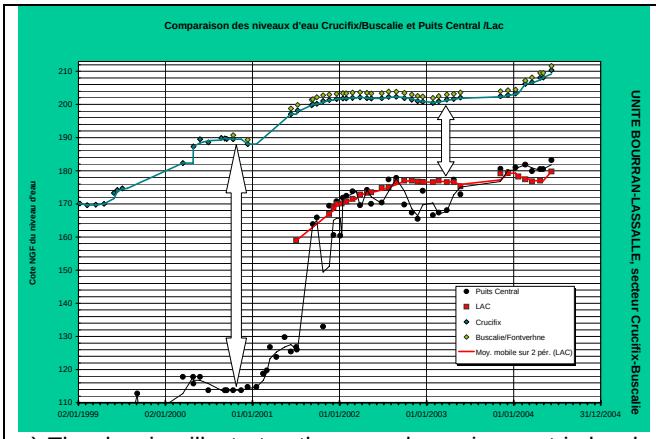
In addition, a piezometric network was installed to get a good understanding of the underground water behaviour and improve the knowledge of water pressure distributions in some specific places.

Table 1. Hydrogeological behaviour of the mining aquifer. Storativity and transmissivity are highlighted. In addition, the exchange function related to interactions between underground water and storage rocks has to be considered for physico-chemical, hydro-biological and thermal processes. It controls water quality.

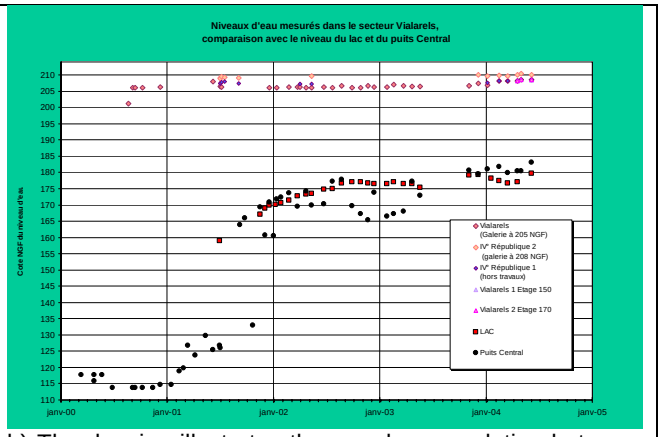
Mining aquifer	Storativity function	Transmissivity function
Carboniferous rock masses directly related to the old coalmine workings. *Very high permeability.* *Very high porosity.*	Very significant role	Very significant role
Carboniferous rock masses altered by the old coalmine workings and subsidence phenomena. *Medium to low fracture permeability.* *Medium to low porosity.*	Moderately significant role	Poor role
Carboniferous rock masses unaltered by the old coalmine workings. *Low (subsurface zones) or very low permeability.* *Low (subsurface zones) or very low porosity.*	Very poor role	Very poor role

As an illustration, conclusions resulting from the analysis of data related to two piezometers are presented in Figure 6. In the two cases mining connection was existing, but it can be seen that the

hydraulic connection does not have the same reaction while the hydraulic gradient is lowering due to the rising of the water level in the Central mineshaft (Puits Central) which is used as a pumping shaft.



a) The drawing illustrates the very close piezometric levels for two nearby piezometers (upper dots and curve: Buscalie and Crucifix), the correlation between these piezometric levels and the level of water in the Central mineshaft and the adjacent pit lake (lower dots and curves)



b) The drawing illustrates the very low correlation between the piezometric levels of different piezometers in the area of Vialarels (upper dots) on one hand and the level of water in the Central mineshaft and the adjacent pit lake (lower dots) on the other hand.

Figure 6. Hydrogeological connections between several coalmine workings and the Central mineshaft (Puits central).

Taking advantage of these different investigations a synthetic map was provided (Figure 7) which illustrates the different hydrogeological units and connections with the Central mineshaft.

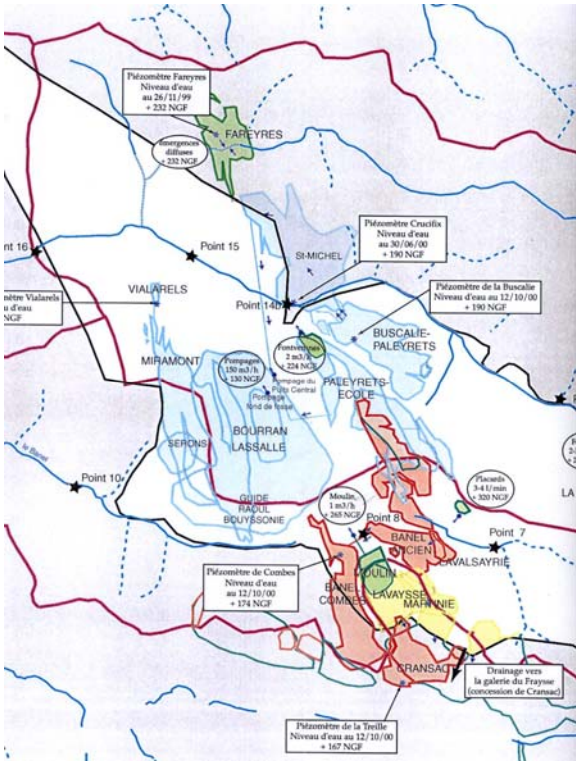


Figure 7. Synthetic map showing different mining aquifers connected to the Central mineshaft (Bourran-Lassalle, Paleyrets and Buscalie sectors) and other mining aquifers with no connection to the Central mineshaft (Banel, Placards, Martinie-Moulin and Firmi sectors). (after Cesame, 2000).

4.2. The ground stability concerns

Ground stability questions were investigated by reference to potential mining subsidence, collapse of abandoned rooms and pillars exploitations and sinkhole processes (Ineris, 2000; Piguet and Wojtkowiak, 2000; Cojean 2002; Wojtkowiak et al, 2002; Al Heib et al, 2003).
The areas which formerly were affected by mining subsidence were delimited. Presently, no residual subsidence can be expected in these places. However, reactivation of mining subsidence as a response to the rising of the general water level in the mining aquifer had to be considered. Different observations in the world show that some low uplift process can be expected. It has to be noted down that these processes occur at a regional scale. On the contrary, at a local scale, the rising of underground water level can result in local reactivation of settlement due to the washing out of infilling materials in sloping galleries for shallow exploitations.
The collapse of partial exploitations such as rooms and pillars is a concern for exploitations with a depth lower than 50 meters. The present stability conditions were investigated using the data provided by colliery archives. Long term stability conditions were analysed, taking into account the lowering of strength of pillars due to the rising of water levels in the exploitations. It was necessary to carry out additional boreholes in some places in order to clarify particular situations where safety problems were at stake.
The sinkhole hazard was also investigated considering possible scenarios of cavities at the crown of an underground mine working turning into successive bell holes reaching to the surface. For this purpose, additional boreholes have allowed to precise the risks associated to these processes and gave some essential data for stability calculations.
Lastly, ground stability questions were also analysed for underground iron mines, connected to the coalmine workings, which would be concerned by the rising of the regional piezometric level as a response to the cessation of pumping at the Central mineshaft.
As it can be noted down, any ground stability problem is closely connected to underground waters and corresponding water pressures. That is the reason why it is necessary to analyse the roles of mining aquifers in post-mining conditions by respect to discharge and water inflow questions, as well as by respect to piezometric levels and water pressures.

5. Election of the most appropriate water level in the pit lake

At the beginning of the Survey related to the cessation of mine workings in Decazeville-Firmi concession, comparative scenarios were analysed. At the beginning of the investigations, the scenario of a lake level at the 211 m elevation was considered. It was corresponding to a total cessation of pumping and made it possible to have a gravitational flow of water towards the surface watercourses, but consequences concerning ground stability concerns and water inflow in some places were not completely solved. Then a scenario of a lake level at the 170 m elevation was analysed. It allowed to cancel any ground stability problem, but long term pumping had to be taken into account as well as water treatment.

Finally an intermediate solution appeared to be appropriate. It was established according to the following thinking. The option had to make it possible to discharge water towards the surface watercourses without any treatment. But potential ground stability problems had to be limited and residual cases to be solved, especially for two cases related to Vialarels area in the town of Decazeville and Combes area in a nearby village. A consequence was that pumping had to continue.

Some world expertise concerning the behaviour of pit lakes is available as well as French expertise concerning coalmining works, especially at Blanzy (Saône et Loire). Pit lake evolution is complex and depends on geometrical parameters related to the watershed, hydro-chemical parameters

concerning the lake supply from surface and underground flows, characteristics of the connection between the lake and the mining aquifer and climatic parameters. The seasonal thermal stratification is well known for lakes in general. But for mine lakes, a chemical stratification can also take place. A permanent confined and mineralized body of water appears at the bottom of the lake and does not participate to the seasonal thermal convection processes. This zone appears below a narrow transitional zone called the chemocline, the corresponding lakes being described as meromictic lakes. According to the expertise coming from Blanzy (Paquette et al, 2000), three main factors seem to control this chemical stratification with threshold values:

- The maximum depth of the lake has to be larger than 25 m;
- The mean depth (ratio volume/surface: V/S) has to be larger than 15 m;
- The hollow index ($1000 \times V/S^{3/2}$) has to be larger than 50.

In addition, two additional factors may play a significant role: the ratio watershed surface/lake surface (BV/S) and the age of the lake.

As a consequence, in a first step, various scenarios concerning the water elevation in the pit lake were studied and led to the results presented in Table 3.

According to the accepted threshold values, it appears that the most appropriate water elevation is 195 m, taking into account a small safety margin (Figure 10). Then it will be possible to pump a superficial water slice within a specific structure designed to pump water with no disturbance of the chemical stratification of the lake.

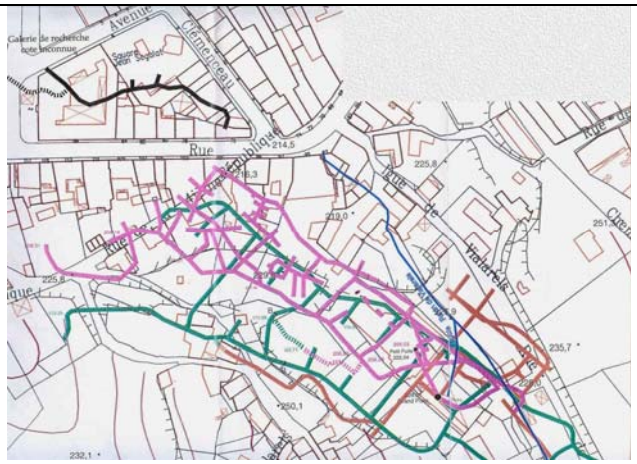
Table 3. Analysis of factors controlling the chemical stratification in the pit lake.

Water elevation in the pit lake	170 m	185 m	190 m	195 m	204 m	211 m
Maximum depth (m)	16	31	36	41	50	57
Volume V (m^3)	220 000	920 000	1 330 000	1 800 000	2 800 000	3 750 000
Surface S (m^2)	33 000	77 000	87 000	97 000	124 000	155 000
Mean depth V/S (m)	6,7	11,9	15,3	18,6	22,6	24,2
Hollow index $1000 \times V/S^{3/2}$	36,9	42,9	51,9	59,7	64,2	61,5
Ratio BV/S	47	20	18	16	12	10

In a second step, the consequences related to ground stability problems resulting from the 195 m elevation were considered.

The Vialarels area in Decazeville was closely analysed. This area consists in three different levels of galleries (Figure 8-a), the highest voids being locally at a 6 meters depth. These mining works were completed in 1916, and different small mining damage occurred during and after mining: small settlements, gas emanations, minefires. Infilling and reinforcement works were carried out. The hydraulic connection between Vialarels area and the mining aquifer connected to the Central mineshaft (where pumping was taking place) was specifically analysed using maps and additional piezometers which were progressively set up. The hydraulic connection appeared to be very poor (Figure 6-b), especially due to the presence of a permanent dam erected across the single cross-cut gallery connecting Vialarels area and the rest of the mine. In fact the water table in this area is mainly dependant on the recharge corresponding to direct meteoritic waters, but there is also a small

flow which leaks (probably through the dam) to the mining aquifer connected to the Central mineshaft. This leak can probably be influenced by the level in the pit lake if it is upper than 195 m. That is the reason why a pumping station will be designed to pump water out in case of heavy rainstorm on this area.



a) Mining works at Vialarels area. Three different levels of galleries can be observed.



b) Rooms and pillars iron mines at Combes area. These exploitations are connected to the Central mineshaft thanks to coal galleries.

Figure 8. Mining works at Vialarels area and Combes area.

Also the Combes area was analysed in a detailed way. In this place, old underground iron mines are connected to the coal mines and the Central mineshaft. The three dimensional characteristics and location of the chambers and pillars iron mines were studied thanks to the colliery archive documents (Figure 8-b) and knowledge related to the mining aquifer. It resulted that only a few houses were potentially concerned by modifications of stability conditions due to a variation of water level up to 195 m in the rooms and pillars of iron mines. Appropriate decisions will be taken for this particular case.

Finally additional analyses were performed about some other places, limited in extension, were similar impacts were identified.



Figure 10: Aerial view of the pit lake in the Grande Découverte. The Central mineshaft is on the right of the lake. In the top left corner, Decazeville town and Vialarels area. In the bottom right corner, Combes area.

As a consequence of these investigations in the field of mining groundwater and ground stability, the 195 m elevation was accepted as the best solution for the water level of the pit lake (Figure 10). In addition this level allows a quality scenery design around the pit lake.

6. Conclusion

As a conclusion, different major subjects that were investigated in the case of Decazeville-Firmi concession can be underlined.

The post-mining contexts are always complex and need integrated investigations mainly in the field of mining groundwaters, ground stability and gas emanations. The questions of underground waters have to be studied considering the discharge as well as the water pressure problems.

The monitoring of the mining aquifer by piezometric networks is necessary in order to improve the understanding of these complex groundwater systems.

The reference to colliery archives is essential to obtain a good knowledge of past mining works. Unfortunately the corresponding data are sometimes partial or difficult to be interpreted. So it is necessary to consider that boreholes investigations are sometimes necessary in order to accurately describe the subsoil conditions.

In the field of pit lakes, expertise begins to be accumulated but it is necessary to be careful and to implement monitoring devices in order to follow the chemical stratification process, as it is done in the case of Decazeville.

7. References

Al Heib M., Josien J.-P., El Shayeb Y. (2003). *Paramètres d'affaissement pour la hiérarchisation des zones à risque dans le bassin ferrifère lorrain.* Symposium Après-mines 2003, Nancy. 11p.

BRGM (2001). Carte géologique de la France à 1/50 000. N°859, Decazeville. Notice explicative 94p.

CESAME (2000). *Etudes hydrogéologique et hydrologique de la concession minière de Decazeville-Firmi (Aveyron).* 160p. et Annexes.

CESAME (2004). *Les travaux miniers sous le quartier de Vialarels à Decazeville. Bilan des connaissances.* 21p et Annexes.

Charbonnages de France – HBCM – Direction des Sites Arrêtés et de l'Environnement (2001). *Arrêt des travaux dans la concession de Decazeville-Firmi. Mémoire.* Tomes 1 et 2, 204p, Annexes techniques et plans.

Cojean R. (2002). *Compte-rendu d'expertise. Dossier d'arrêt des travaux miniers dans la concession de Decazeville-Firmi (Aveyron).* 36p. *Note complémentaire*. 9p. Rapports Armines-CGI.

Cojean R. (2003). *Note complémentaire au Compte-rendu d'expertise relatif au dossier d'arrêt des travaux miniers dans la concession de Decazeville-Firmi (Aveyron). Scénarios de cote du lac minier et impacts.* 11p. Rapport Armines-CGI.

Cojean R. (2004). *Note complémentaire au Compte-rendu d'expertise relatif au dossier d'arrêt des travaux miniers dans la concession de Decazeville-Firmi (Aveyron). Scénarios de cote du lac minier et impacts.* 4p. Rapport Armines-CGI.

Fabriol R. (2005). *La gestion de l'eau des mines en phase post-extractive.* Revue BRGM Géosciences, N°2, septembre 2005, 66-71.

Feuga B. (2005). *Quelques aspects de l'après-mine.* Revue BRGM Géosciences, N°1, janvier 2005, 24-29.

INERIS (2000). *Bassin houiller d'Aubin-Decazeville. Concession de Decazeville et Firmi. Analyse des effets en surface des travaux miniers souterrains.* 29p et Annexes.

INERIS (2001). *Guide méthodologique pour l'arrêt des exploitations minières souterraines.* 130p et Annexes.

INERIS (2003). *Bassin houiller d'Aubin-Decazeville. Concession de Decazeville et Firmi. Analyse des effets de l'ennoyage à la cote +170 m NGF des eaux de l'aquifère minier sur la stabilité des mines de fer.* 17p et Annexes.

INERIS (2003). *Bassin houiller d'Aubin-Decazeville. Concession de Decazeville et Firmi. Analyse des effets de l'ennoyage à la cote +210 m NGF des eaux de l'aquifère minier sur la stabilité des mines de fer.* 17p et Annexes.

Lefort D. (2000). *Etude hydrogéologique du bassin houiller de Decazeville (Aveyron).* Thèse professionnelle. Mastère Géologie de l'ingénieur et de l'environnement. Ecole des Mines de Paris - Centre de Géologie de l'Ingénieur et Bureau d'Etudes Cesame. 50p.

Paquette Y., Blachère A., Lefebvre O., Guise Y., Barrière J.-P. (2000). *Les lacs miniers des exploitations à ciel ouvert de charbon du massif central : qualité et évolution.* Chronique de la recherche minière, N°541, 85-101.

Piguet J.-P., Wojtkowiak F. (2000). *Affaissements et déformations au-dessus des exploitations minières : mécanismes et évolution dans le temps.* Mines et Carrières. Industrie Minérale. Juin 2000. 36-46.

Schmitt J.-M., Combes P., Ledoux E. (2003). *Qualité des eaux après fermeture des mines : remplissage initial, évolution transitoire, stabilisation à long terme et gestion environnementale.* Symposium Après-mines 2003, Nancy. 10p.

Vetter P. (1968). *Géologie et paléontologie des bassins houillers de Decazeville, de Figeac et du détroit de Rodez.* Tome1 : Description géologique, 442p. Thèse d'Etat. Houillères du Bassin d'Aquitaine, Albi.

Wojtkowiak F., Baubron J.-C., Cattaert P., Vassiliadis G. (2002). *Maîtrise de l'impact hydraulique, sur le bâti de surface, de l'ennoyage de mines souterraines arrêtées du bassin ferrifère lorrain (France).* 9ème Congrès International IAEG, Durban, Afrique du Sud, Décembre 2002. 10p.

Younger P. L., Banwart S. A., Hedin R. S. (2002). *Mine water. Hydrology, Pollution, Remediation.* Environmental Pollution, Volume 5. 442p. Klower Academic Publishers.

A SEMI-DISTRIBUTED MODELLING OF THE EVOLUTION OF GROUNDWATER QUALITY IN FLOODED MINES IN THE LORRAINE IRON BASIN

COLLON-DROUAILLET Pauline[1], FABRIOL Robert[2], BUÈS Michel[3]

[1] GEGENA, CREA, 2 esplanade Roland Garros - 51100 Reims – France ; pauline.collon@univ-reims.fr

[2] BRGM, 1 av. du parc de Brabois - 54500 Vandoeuvre-lès-Nancy Cedex - France; r.fabriol@brgm.fr

[3] LAEGO, Rue du Doyen Marcel Roubault - BP 40 - 54501 Vandoeuvre-lès-Nancy Cedex - France; Michel.Bues@ensg.inpl-nancy.fr

ABSTRACT: In Lorraine (France), closure and flooding of ancient mine workings led to a degradation of the groundwater quality, making it unsuitable for human consumption. The two models presented here were developped after the identification of the chemical mechanisms responsible for this phenomenon (Collon et al., 2004) in order to reproduce and predict the evolution of groundwater chemical composition in the Southern part of the lorraine Iron Basin. Based on a Network of Chemical Reactors (NCR) type global approach, two types of modelling are produced: one considers the basin in its totality and calculates the composition of the groundwater only at the overflow point, the other is semi-distributed in order to reproduce the concentrations observed in the four monitoring wells of the basin.

Keywords: Modelling, groundwater quality, mine flooding

RESUME : En Lorraine (France), l'abandon et l'ennoyage des anciens travaux miniers a entraîné une dégradation de la qualité de l'eau souterraine, la rendant impropre à la consommation humaine. Les deux modèles présentés ici ont été développés après la mise en évidence des mécanismes chimiques responsables de ce phénomène (Collon et al., 2004), pour reproduire et prédire l'évolution de la composition chimique de l'eau dans la partie Sud du bassin Ferrifère Lorrain. Basées sur une approche globale de type Réacteurs En Réseau (RER), deux types de modélisation sont réalisées : l'une considère le bassin dans sa globalité et ne calcule la composition de l'eau qu'au point de débordement, l'autre est semi distribuée, de manière à reproduire les concentrations observées dans les quatre puits de contrôle du bassin.

MOTS-CLEFS : Modélisation, qualité de l'eau, ennoyage des mines.

1. Introduction

Mine drainage is one of mining undesirable effects on the environment. In Lorraine, the flooding of the abandonned workings over the past 20 years has led to a degradation of groundwater quality, as indicated by high concentrations of SO_4, Ca, Na, Mg, K, Mn and B, making it unsuitable for human consumption. As this accumulated water in abandoned iron mines will, in the long run, represent a resource of around 300 million m^3 for the Lorraine, it is necessary to predict its future quantitative and qualitative evolution.

Most of the hydro-geochemical model that were applied to simulate the impact of mining on water ressources have been developed for mine tailings, considered similar to porous media (*e.g.*, Elberling *et al.*, 1994; Salomons, 1995; Lin *et al.*, 1997; Bain *et al.*, 2000; Neumann and Sami, 2002). The mine drainage is most often treated either hydrodynamically (*e.g.*, Therrien and Sudicky, 1996; Bochenska *et al.*, 2000; Adams and Younger, 2001; Hauns *et al.*, 2001) or chemically (*e.g.*, Appelo *et al.*, 1998; Brown *et al.*, 1998; Chen *et al.*, 1999; Mayo *et al.*, 2000;

Razowska, 2001; Eary *et al.*, 2003) and only few models couple mine reservoir hydrogeology and chemistry (*e.g.*, Bain *et al.*, 2001).

Based on these studies and on the available poor spatially distributed data, we adopted a Network of Chemical Reactors (NCR) global approach to predict the future evolution of water quality in the Lorraine Iron Basin (LIB).

2. Method

2.1. Principles of the model

The association of reactors in series and parallel was originally developed for process engineering (Villermaux, 1993). Thereafter, it has been used to model the reactive transfer of pollutants in soils (Jauzein *et al.*, 1989; Baranger et Kervévan, 1998), the tailing effluents (Altmann, 1995) and the composition of water discharge from flooded mines (Collon *et al.*, 2003).

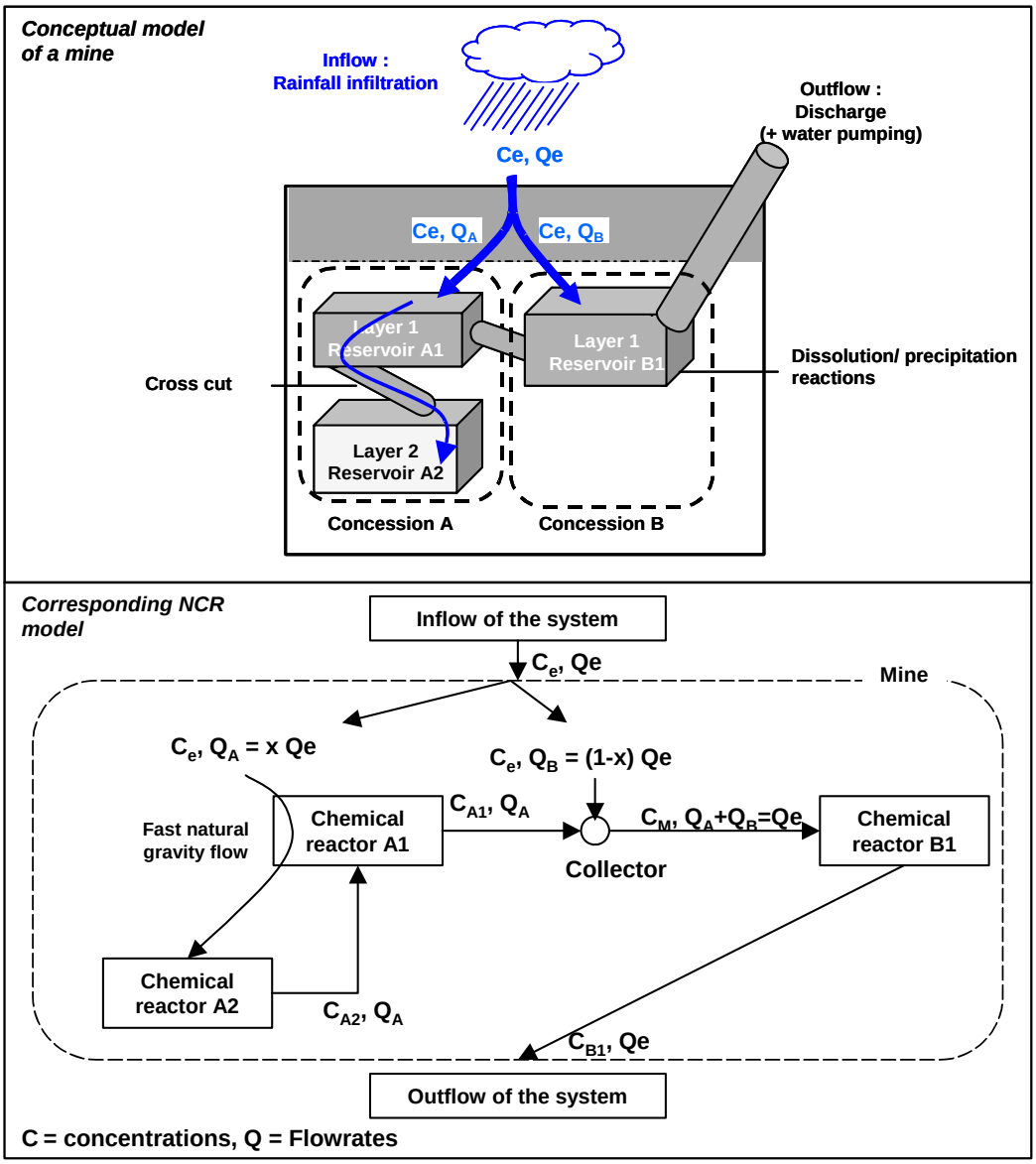


Figure 1. Principle of mine reservoir modelling with a network of chemical reactors – NCR model

Conceptually, the mining system is divided into hydraulically connected concessions or reservoirs (figure 1a). So, by representing each reservoir of this system with a reactor, the mine is represented as a NCR (figure 1b). Only advective mass transfer is taken into account between two reactors. At any time t, each reactor is characterised by an inflow Q_e, an outflow Q_s, a volume of water V that varies with water table fluctuations, and a mass of rock M. Groundwater circulating in a reservoir reacts with the minerals in the reservoir rock and its composition changes. Each reactor is described by the step by step summation of a mass-balance equation that enables to directly express the concentration of any chemical element or compound at time step t:

$$C(t_n)\,V(t_n) = V(t_0)\,C(t_0) + \sum_{i=1}^{n-1}\left[Q_eC_e + V(t_i)\,r(t_i) - QsC(t_i)\right]\Delta t_i \qquad \text{with } n \geq 2 \tag{1}$$

where:

Q_s = outflow rate (l/s)
Q_e = inflow rate (l/s)
C_s = outflow concentration (mol/l)
C_e = inflow concentration (mol/l)
C(t) = concentration in the reactor (mol/l)
V(t) = volume of water in the reactor (l) at time t (hence V_0 = volume of water at time t=0)
r(t) = production or consumption rate (= reaction rate) of a given chemical element or compound (mol/l/s)

The inflow rate Q_e was estimated using rainfall data, the outflow discharge rate and the numerical package TEMPO® based on signal-processing methods (Pinault *et al.*, 2001). This method does not require any hypothesis concerning the internal structure of the reservoir (type of flow, porosity, permeability,...), which is an advantage when no spatially distributed data is available.

A chemical kinetic model, based on the classical approach, is used to estimate the reaction rate r(t). It was built in order to reproduce the water-rock reactions observed in closed reactor tests and leaching column tests that were carried out on rocks of the LIB (Collon *et al.*, 2004). If we consider a dissolution-precipitation reaction of a mineral A_nB represented by the equation:

$$A_nB \leftrightarrow nA^+ + B^{n-} \tag{2}$$

then the rate of reaction is the difference between the dissolution rate (r_{diss}) and the precipitation rate (r_{pcp}):

$$r(t) = r_{diss} - r_{pcp} \tag{3}$$

$$r(t) = (Ctl)\; k_{pcp}\,[K\,(A_nB) - (A^+)^n\,(B^{n-})] \tag{4}$$

where:
K is the equilibrium constant related to the kinetic constants: $K = k_{diss}/k_{pcp}$,
(X) is the activity of X.
The factor (Ctl) enables to introduce the concept of specific surface area into the model:

$$Ctl = Fg\; b_{AnB}\,[m(t)]^{2/3} \tag{5}$$

Where:

$$F_g = \frac{9.756}{Gr}\,\frac{M_R}{\rho_R}$$

with M_R is the total mass of rock in (kg by litre of water) - 2.04 kg/kg of water in our laboratory experiments -
Gr is the mean grain size of the rock (m)
ρ_R is the mean density of the rock (kg/m^3) - 2.6 10^{-3} kg/m^3 -

The parameter Fg expresses the influence of initial rock granulometry: Fg = 10^6 for the granulometry of 2.5 mm used in the closed reactor tests, and Fg = 0.26 10^6 in the leaching experiments, where the average granulometry is 29 mm.

The coefficient b_{AnB} (dimensionless) represents the accessibility of the mineral AnB in the block of rock; it is a constant specific to each mineral and each sample. It was fitted on experimental results.

The mass of a mineral at time t, *i.e.* $[m(t)]^{2/3}$ (in mol), enables us to take into account the variation of the surface with the available mineral quantity. The initial value m(0) for each mineral in each studied rock sample was evaluated by a mineralogical study (Collon *et al.*, 2004).

The ion activity in water (A^+) and (B^{n-}) was calculated using the Debye-Hückel equation. The activity of the solid (A_nB) and that of water were considered to be 1. The fugacity of the gaseous compounds similar to perfect gases was considered to be equal to their partial pressure.

Equilibrium constant values, K, for mineral dissolution/precipitation reactions (25 °C, 1 bar), ion complexation reactions in water, and O2 and CO2 gas exchange reactions at the water-air interface, were taken from the PHREEQC database (Parkhurst and Appelo, 1999).

In our model, ion complexations are described by kinetic reactions, with the kinetic constants being set arbitrarily to account with their fast rates compared to those of mineral dissolution and precipitation. The kinetic constants were defined on the basis of experimental laboratory results: different scenarios were tested by modifying them. The best agreement with experimental data from the closed reactor tests was obtained with a model based on 12 chemical elements (Al, C, Ca, Fe, K, H, Mg, Na, O, S, Si and Sr), 19 mineral dissolution and precipitation reactions, 25 aqueous speciation reactions, O_2 and CO_2 dissolution and degassing, and 4 cationic exchange reactions (Collon *et al.*, 2004; Collon *et al.*, in press).

Table 1 gives an example of each type of reaction considered in the model (dissolution/precipitation, aqueous complexation, dissolution/degassing and cationic exchange).

Table 1. The kinetic model of five types of chemical reactions

Type of Reaction	Reaction	Rate
Dissolution/ precipitation	$CaSO_4,2H_2O \leftrightarrow Ca^{++} + SO_4^{--} + 2\ H_2O$	$r(t) = (Ctl)\ k_{pcp\text{-}gyps}[K - (Ca^{++})(SO_4^{--})]$
Dissolution/ precipitation	$FeS_2 + 3.75\ O_2 + 3.5\ H_2O \leftrightarrow 4\ H^+ + Fe(OH)_{3aq} + 2\ SO_4^{2-}$	$r(t) = (Ctl)\ k_{pcp\text{-}pyr}[K\ (O_2) - (H^+)(SO_4^{--})(Fe(OH)_{3aq})]$
Aqueous complexation	$H_2O \leftrightarrow H^+ + OH^-$	$r(t) = k_{pcp\text{-}H2O}[K - (H^+)\ (OH^-)]$
Dissolution/ degassing	$CO_{2(g)} \leftrightarrow CO_2$	$r(t) = k_{pcp\text{-}CO2}\ [K\ P_{CO2} - (CO_2)]$ *
Cationic exchange	$X_Na + 0.5\ Ca^{++} \leftrightarrow Na^+ + X_Ca_{0.5}$	$r(t) = (Ctl)\ k_{pcp\text{-}XNa}[K\ (X_Na)(Ca^{++})^{0.5} - (Na^+)(X_Ca_{0.5})]$

* P_{CO2} is the partial pressure of $CO_{2(g)}$

The NCR numerical simulators were built using Matlab® software and its graphic interface, Simulink® (Collon *et al.*, in press). The mining system is represented as an assemblage of reactors in series and parallel (figure 2) where the reactors determine the concentrations in each part of the reservoir and the masses extracted at a given time. To create the network, a distributor and a collector are required. These are characterised by:

$$\text{Distributor} \qquad Qe\ Ce = (\Sigma Qe)\ Ce$$

$$\text{Collector} \qquad \Sigma(Qe\ Cs) = (\Sigma Qe)\ Cs$$

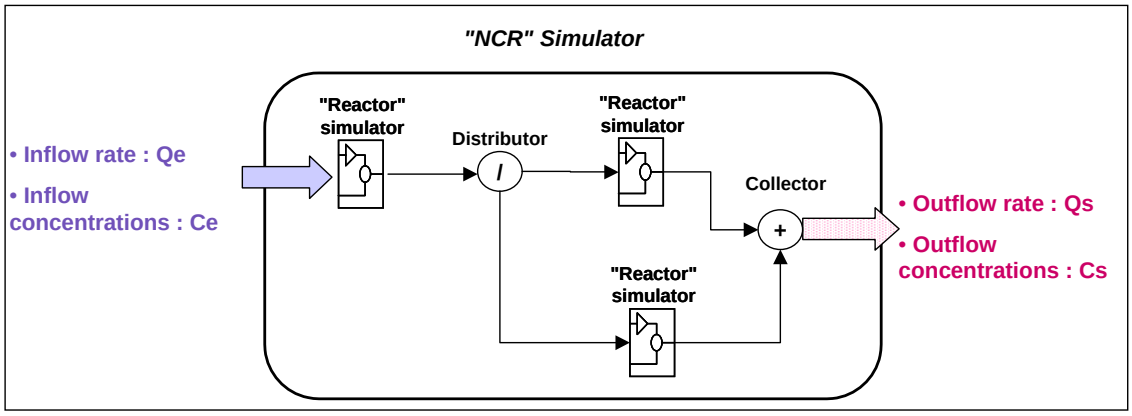


Figure 1. Flow chart of a network of chemical reactors (NRC)

2.2. *Site description*

Located along the eastern edge of the Paris Basin (France), the Lorraine iron-ore deposit extends from the Luxembourg border and the Moselle area to the Woëvre area in the West. The Pont-à-Mousson anticline causes a disruption in the mineralisation, thus creating two basins of unequal size: (i) the Briey-Longwy Basin to the North and (ii) the Nancy Basin to the South. Faults subdivide the Briey-Longwy Basin into three major structural units: the North, the Central, and the South Basins (figure 3). At the moment, the modelling is carried on the South Basin, whose mines were closed in 1995. The gradual flooding of the mine workings ends with the beginning of the overflow at the Tunnel of Moyeuvre in October 1998. Four mine shafts and the overflow point constitute a surveillance system set up for quantitative and qualitative groundwater monitoring. Thus, modelling results would be compared to *in situ* measurements.

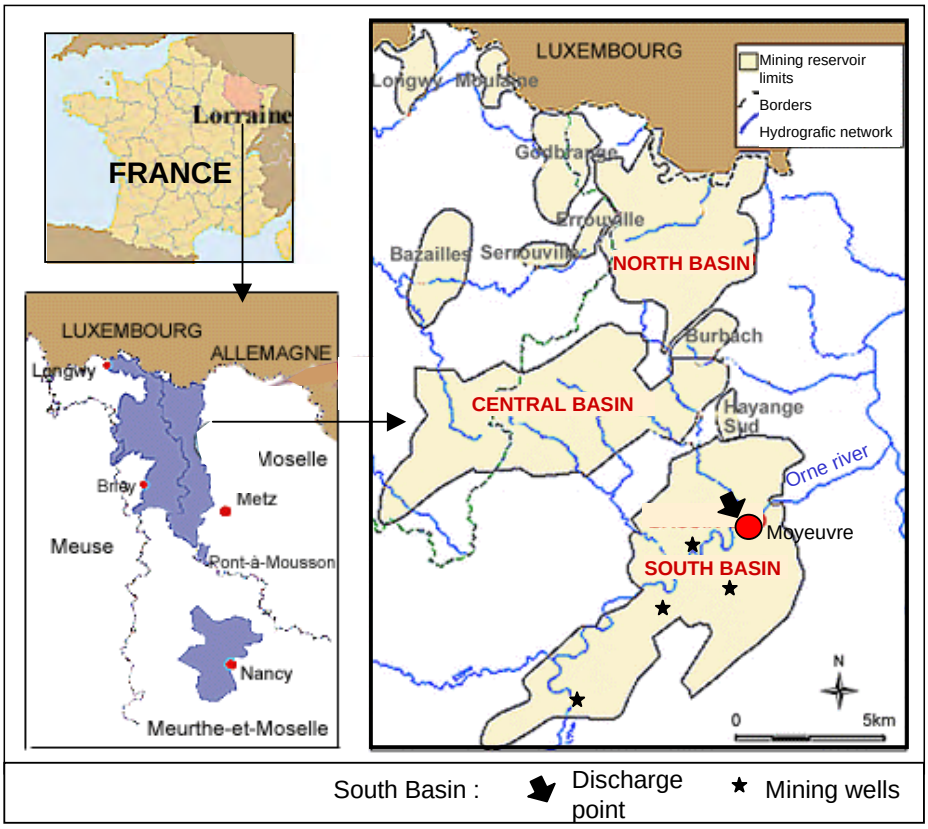


Figure 3. Geographic location of the Lorraine Iron Basin

Dated as Aalenian (Late Lias) the iron-bearing formation overlies Early and Middle Toarcian impermeable deposits. The Lorraine iron-bearing deposit is composed of alternating marly levels (intercalations) and ferruginous limestone (mineralised intervals) corresponding to a regressive sequence. Its thickness varies from 0 to 65 m with an average of 40 m. Nine mineralised intervals, distinguished by their colour, are recognised in the LIB, although generally no more than two were mined in a single concession. In the South basin, five mineralised layers have been mined, named from the bottom up as the green, brown-black, grey, yellow and red layers. The transition from a marly facies to an overlying mineralised facies is gradual via a metre-scale intermediate or "basal" layer. On top of the grey and yellow layers, *i.e.* in the hanging wall, transition into the next overlying marl intercalation occurs via a coarse-grained shelly limestone level known locally as '*crassin*'. The iron-bearing formation is overlain by about 5 m of micaceous marl, followed by a Dogger (Bajocian) limestone succession, some 50-60 m thick, which constitutes a major karstic aquifer. Mining has caused the fracturing and partial destruction of the impermeable level, enabling water from the Dogger limestone aquifer to infiltrate into the mine galleries.

Based on a mineralogical study and tests in closed reactors carried out on rock samples from the North Basin, which is still being mined, three groups of rocks have been differentiated according to their composition and their chemical reactivity in contact with water (Collon, 2003; Collon *et al.*, 2004):

(i) "shelly limestone" or "*crassin*",

(ii) "marly intercalations",

(iii) and "marly hanging wall".

The *crassin* group is composed of the rocks with the lower reactivity - producing less than 200 mg/l of sulphate when in contact with water -: the hanging-wall rocks of the grey and yellow layers and the iron ore. They are both made up of carbonates, quartz and goethite, but in different proportions.

The marly intercalations are characterised by their strong reactivity with water. In addition to the same minerals that make up the *crassin*, they contain pyrite, sulphate (mostly gypsum), phyllosilicates (ferriferous chlorite, illite, kaolinite, and mica), plagioclase and microcline. It is these minerals, and notably gypsum, that explain the degradation of the water quality observed on site (Collon *et al.*, 2004).

The marly hanging walls group is constituted by the hanging walls of the green, brown-black and red layers. Containing smaller quantities of the same minerals as the marly intercalations, they have a slightly lower chemical reactivity.

Two types of mined zones can be distinguished in the South Basin where the room and pillar method was used: the "gallery zones", where the pillars are still standing, and the "collapsed zones" where the pillars have been pulled. In the collapsed zones, the water is in contact with marly intercalations rocks, while it reacts only with *crassin*-type rocks in the galleries in grey and yellow layers. In the green, brown-black and red layers, the hanging-wall rocks react like the marly hanging walls, while the iron ore and basal layer react like the *crassin.* Based on the average dimensions of the galleries we estimate that, in these zones, water is in contact with a "mixed rock" composed by 34% marly hanging wall and 66% *crassin*.

Thus, three types of kinetic chemical reactor have been built. Each of them represents one of the three types of exploited areas encountered in the mine, in which the water reacts with a type of rock:

(i) "crassin" in the galleries zones (grey and yellow layers),

(ii) "marly intercalations" in the collapsed zones,

(iii) "mixed rock" in galleries within marly hanging wall zones.

There are distinguished by the parameters depending on the composition of the rocks which were estimated by laboratory experiments and mineralogical studies (Collon *et al.*, 2004; Collon et al., in press).

2.3. Non-distributed model

In a first step, the South Basin can be considered as a single unit of three parallel reactors, each corresponding to one of the mine zones; i.e. "collapsed" zone, "*crassin* gallery" zone and "gallery with marly hanging wall" zone (figure 4).

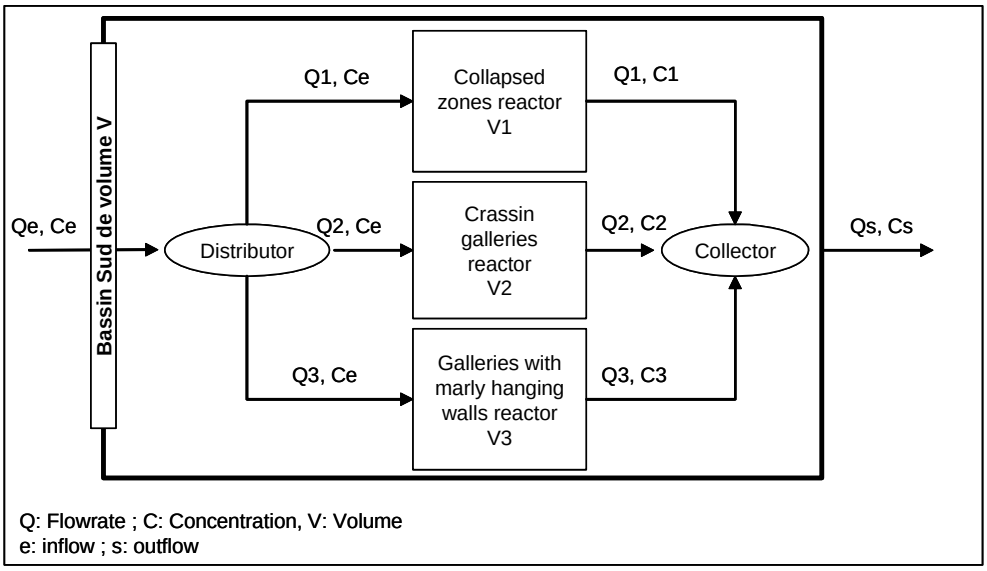


Figure 4. Flow chart of the reactor model of the South Basin

The hydrological model mentioned previously is used to estimate the total volume of water contained in the South Basin (V = 230 10^6 m^3) and the total recharge Qe, calculated from 1995 using a daily time step (figure 5a), when the water overflowed through the Moyeuvre tunnel (altitude = 172.5 m above NGF datum). Dewatering water having a composition similar to that of Dogger water, the total inflow Qe entering the system with a concentration Ce is defined as:

$$Qe = Q_{recharge} - Q_{dewatering} \quad (6)$$

where $Q_{recharge}$ is the estimated recharge and $Q_{dewatering}$ is the dewatering rate measured on site.

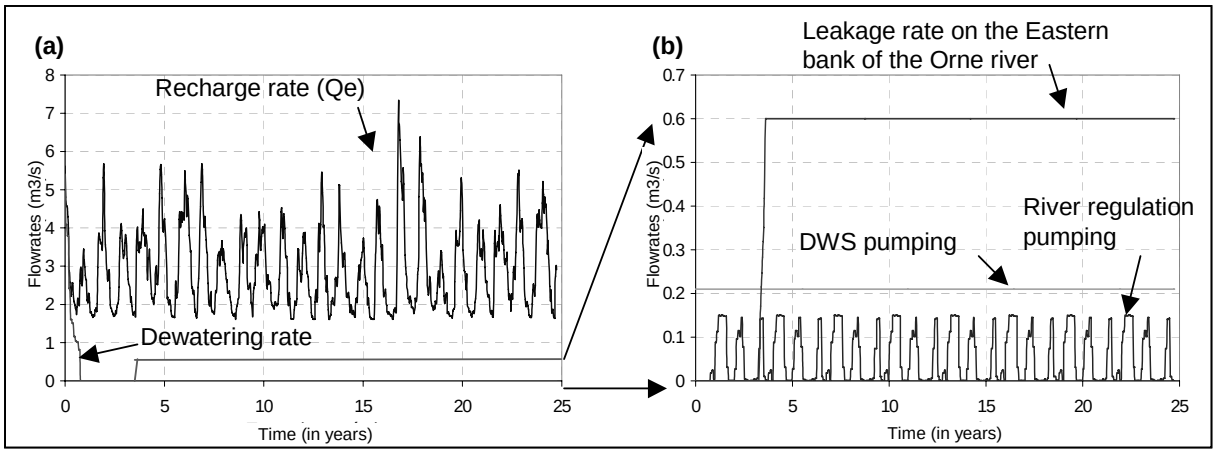


Figure 5. (a) Estimated recharge of and measured dewatering pumping rate in the mine reservoir
(b) Fixed outflow rates : river regulation, leakage, drinking water supply (from Vaute et al., 2004)

Since dewatering has stopped, water is pumped for drinking water supply and river regulation from the flooded parts of the mine. As opposite to the dewatering water, this water is highly mineralised. Thus, it is considered as "outflow" with fixed flow rates in the model. Leaks have also been observed in the alluvial plain below the level of the Moyeuvre tunnel overflow, and they have been estimated at 0.6 m^3/s (Vaute *et al.*, 2004). So, the total outflow rate of the system is defined as:

$$Q_{dis} = Qe - (Q_{DWS} + Q_{reg} + Q_{leak}) \quad (7)$$

Where Q_{dis} is the discharge rate, Q_{DWS} is the drinking water supply rate, Q_{reg} is the river regulation rate and Q_{leak} is the leakage rate (figure 5b).

For each ore-bearing layer, the zones mined in the galleries and the collapsed zones were digitized with MapInfo® from mine plans of each South Basin concession. Based on these maps, the total mined surface has been estimated to be equal to 138.6 km² comprising 53.6 km² of "*crassin* galleries" (38.7%), 26.5 km² of "galleries with marly hanging walls" (19.1%), and 58.5 km² of "collapsed zone" (42.2%). The volume V_n and the inflow Q_n of each reactor "n" are assumed to be directly proportional to its relative area, *e.g.*: V_1 = 42.2% V and Q_1 = 42.2% Q.

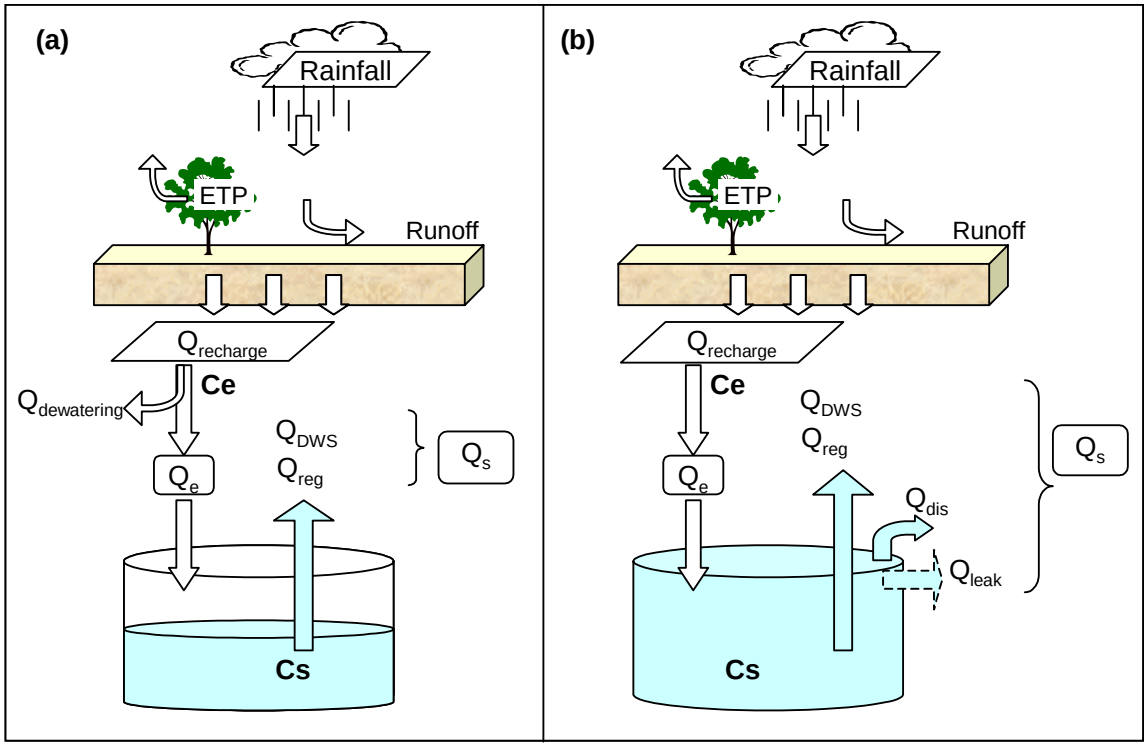


Figure 6. The two phases of hydrological functioning of the reservoir:
(a) filling and (b) overflow (Ci = inflow concentration, Co = outflow concentration)

The flooding of the South Basin mines began on 20/5/1995, date taken as time t = 0. Two phases can be distinguished in the model of the hydrological functioning of the reservoir (figure 6). Indeed, the flooding of the mine workings with no overflow constitutes a transient regime representing the first phase. It ends when the mine workings are full. Then starts the second phase where the mine system overflows.

2.4. Semi-distributed model

The non-distributed model makes it possible to predict the evolution of water quality observed at the overflow point, in the Tunnel of Moyeuvre. But, it gives no information on the spatial

distribution of the chemical concentrations in the Basin groundwater. As chemical monitoring of water quality is available at four wells of the South Basin, we developed a semi-distributed model to evaluate the accuracy of the NCR in accounting for the spatial variability of the concentrations.

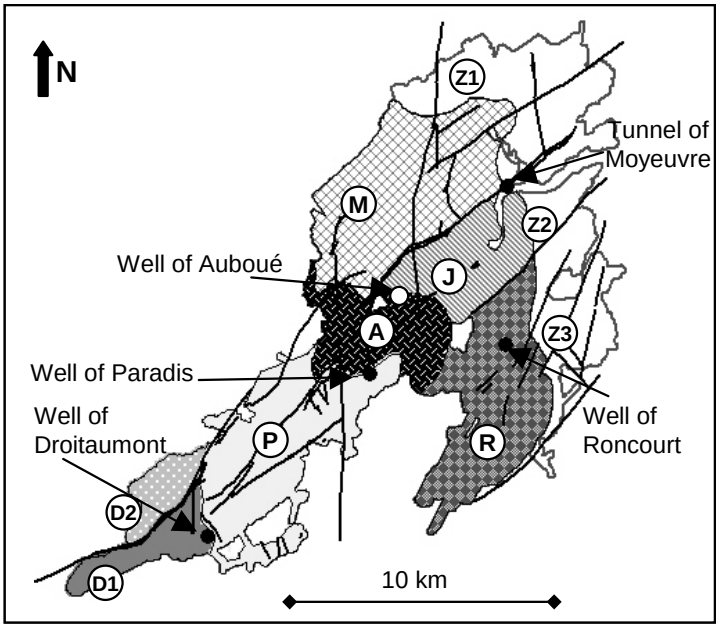


Figure 7. Breakdown of the South Basin into sectors: (D1) Droitaumont 1, (D2) Droitaumont 2, (P).Paradis, (A) Auboué, (R) Roncourt, (J) Joeuf, (M) Moyeuvre; Z1, Z2 and Z3: non-flooded areas.

Seven sectors have been delimited in the South Basin: Droitaumont 1 and 2, Paradis, Auboué, Roncourt, Joeuf and Moyeuvre (figure 7). For three sectors - Droitaumont 1, Paradis and Auboué – the geographical limits have been established in accordance with the mine topography. Major structural faults delimit the other zones, while the overflow level separate the Z1, Z2 and Z3 sectors, located above, from Roncourt, Joeuf and Moyeuvre, located below.

Table 2. Characteristics of the seven areas (S_{basin} = 159 km²)

Sectors	**Symbol**	**S_{rel}** (%)	**V_{sector} (m^3)**
Droitaumont 1	D1	4.2 %	$8.46\ 10^6$
Droitaumont 2	D2	3.0 %	$6.24\ 10^6$
Paradis	P	16.8 %	$4.16\ 10^7$
Auboué	A	8.3 %	$2.44\ 10^7$
Roncourt	R	14.6 %	$4.8\ 10^7$
Joeuf	J	8.5 %	$3.68\ 10^7$
Moyeuvre	M	19.2 %	$7.17\ 10^7$
Z1		14.2 %	non-flooded*
Z2		2.3 %	non-flooded*
Z3		8.9 %	non-flooded*

* Located above the overflow altitude (172 m NGF), these zones will never be flooded.

Considering that the inflow rate Qe is the result of the rain flow infiltration through the Dogger limestone, the total recharge in each sector is supposed to be proportional to its relative surface area S_{rel} (table 2): $Q_{sector} = S_{rel} \times Qe$. The volume in each sector is assumed to be proportional to the

distribution of total exploited surface area (E_{total} = 139 km²) in each sector (E_{sector}): $V_{sector} = E_{rel} \times V$ (table 2).

Each sector is represented as a unit of three parallel reactors (one reactor for each type of mining zone), similar to those used for the non-distributed model.

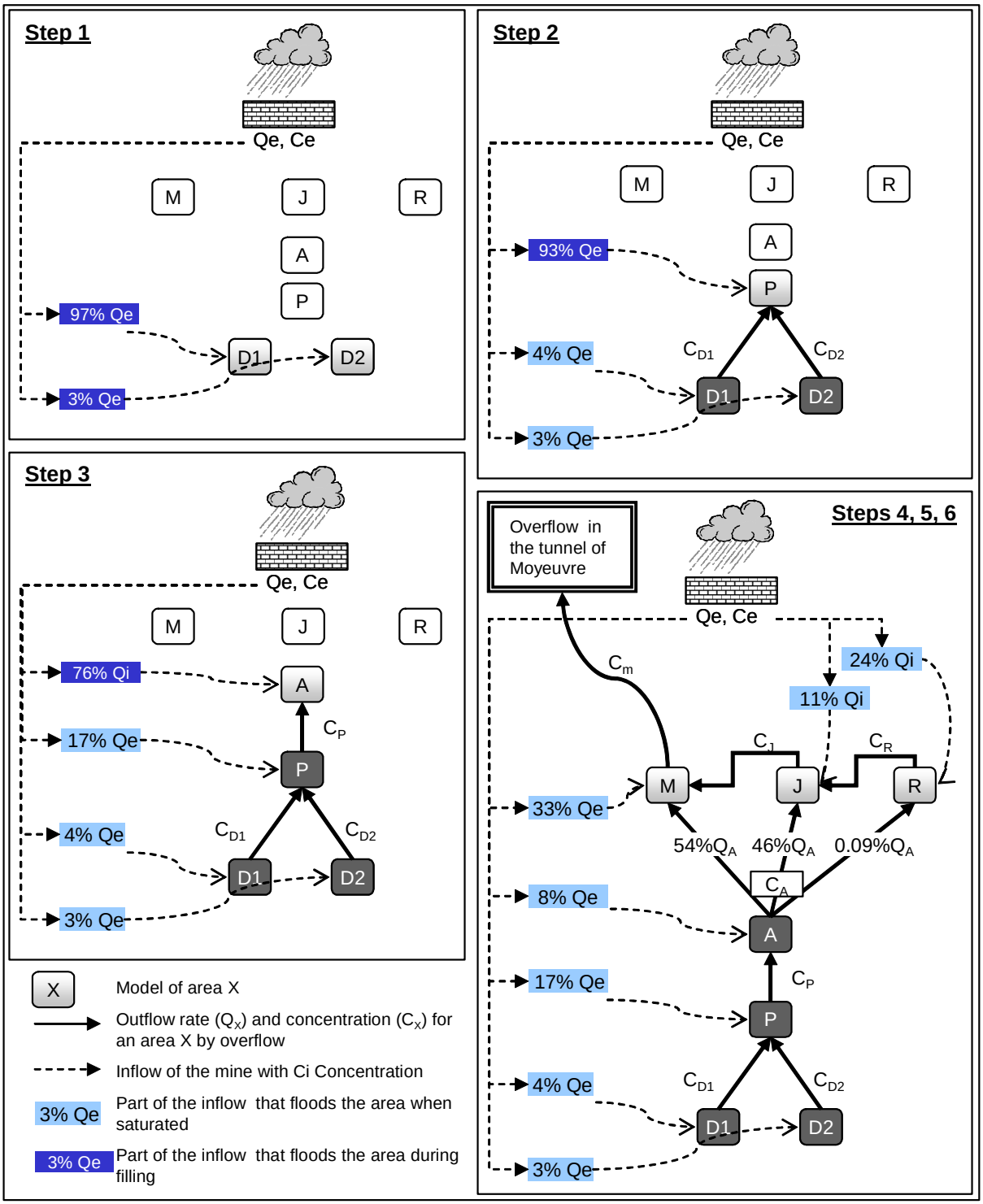


Figure 8. Schematic diagram of the hydraulic flow in the South Basin (Collon *et al.*, 2005)

The hydrological functioning of the mine is split into six phases detailed in the figure 8. Considering gravity, the rainfall water is assumed to be drained by the upper sectors towards the

lower sectors. Due to the short transfer times, the initial chemical composition is not modified and remind close to the Dogger water. Thus, in the first phase Droitaumont 1 receives 97% of the inflow rate, while Droitaumont 2, less hydraulically connected to the fellow sectors, is only recharged by the rainfall on its surface area (3%Qe). Once a sector N is flooded, it overflows in the upper sector with a new composition C_N. The flooded sectors only receive the rainfall water in proportion to their relative surface area, while the sector in "the flooding phase" drains the upper sectors. Located at the same depth, Moyeuvre, Joeuf and Roncourt start to fill up at the same time, when Auboué is saturated. They receive a part of Auboué overflow that is proportional to the surface contact they share with this sector. The water drained by the unflooded upper zones - Z1 for Moyeuvre, Z2 for Joeuf and Z3 for Roncourt – adds to the rainfall water that fall on their surface and recharges this sectors. The observed leakage rate is included as an imposed outflow rate for the Moyeuvre sector.

3. Results and discussion

At mine scale, the reference rock mass M_R (on the basis of 1 litre of associated water) and the average granulometry G_R of the rocks are unknown. Depending only on the mining method used, these two parameters are assumed to be identical for both the "crassing galleries" and the "galleries with marly hanging walls". They were determined by fitting the SO_4 concentration simulated with the non distributed model to the SO_4 concentration measured during the first three years at the overflow (table 3).

Table 3. Rock mass, M_R, and average granulometry, G_R, determined by fitting of simulated SO_4 concentrations and those measured at the overflow

	G_R (m)	M_R (kg)
Galleries	0.2	3.5
Collapsed zones	0.4	4

The concentrations simulated with the non-distributed model are in good agreement with the evolution observed at the Tunnel of Moyeuvre of the Na, Ca, Mg and HCO_3 concentrations, the pH, and the SO_4 concentration after the first three years used for fitting (figure 9). These results show that the non-distributed model can predict the evolution of water quality observed at the overflow of the South Basin for the major elements SO_4, Na, Ca, Mg and HCO_3 with a precision of ± 10% and it provides an order of magnitude for minor elements such as K. Thus, as observed in the older abandoned iron-ore mines of the LIB, it appears that the quality of the water at the overflow point will progressively improve with the leakage of the rocks, and will reach again, after several years, the authorized concentrations for human consumption.

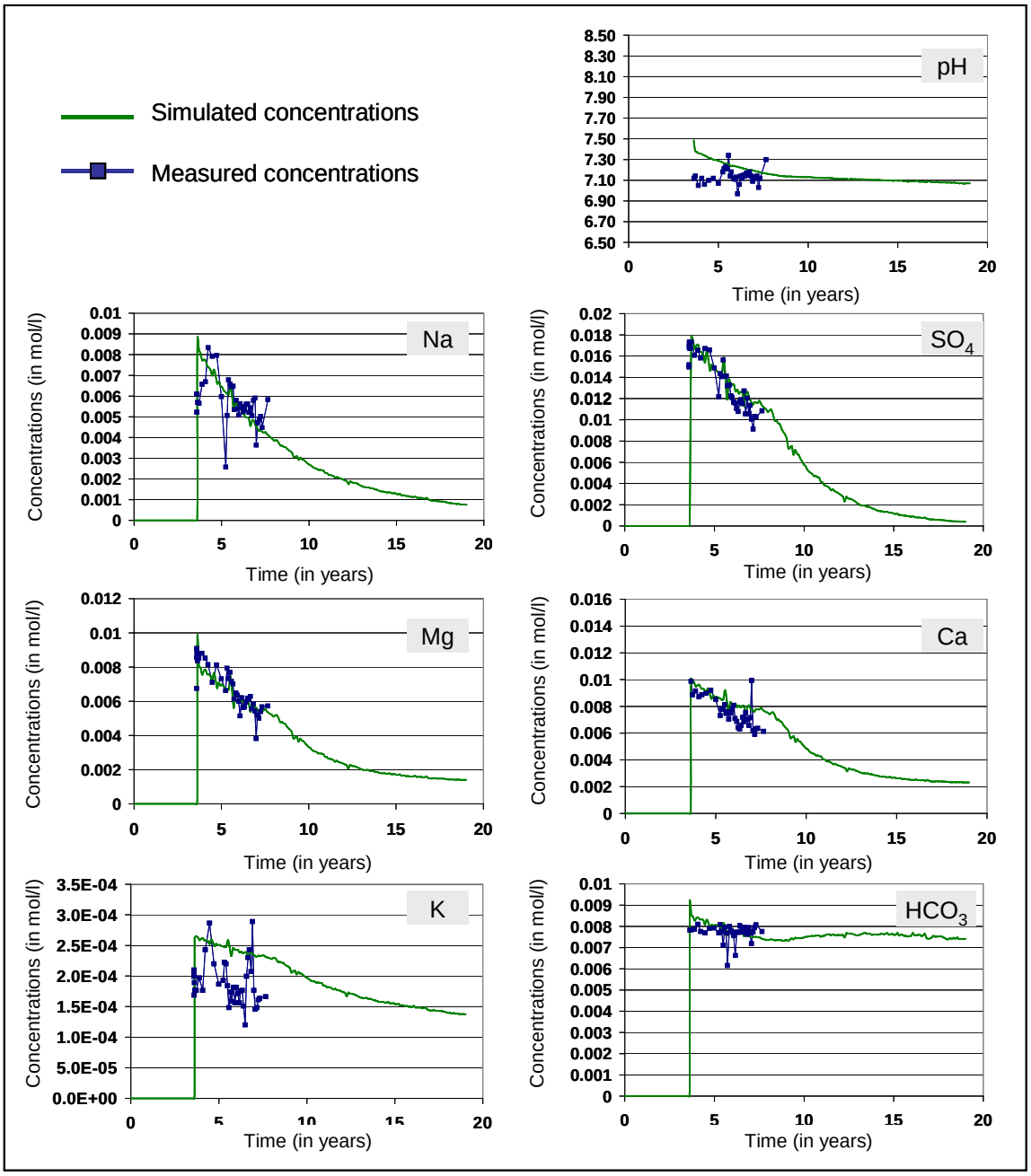


Figure 9. Simulated and measured concentrations at the overflow of the South Basin

The results of the semi-distributed model are more variable (figure 10). The evolution of pH and HCO_3 are always well reproduced, probably due to the buffer action of the CO_2 pressure and the presence of carbonates. Furthermore, the simulated concentration of minor elements such as K falls always within the range of possible maximum and minimum concentrations calculated by our model. Considering the major elements SO_4 (figure 10), Ca, Mg and Na, the concentrations are well reproduced in Roncourt, Auboué and at the overflow point in Moyeuvre. In Auboué, the high fluctuations of the observed concentrations correspond to important rainfall and could be explained by a poor impermeability of the well. The delay between the increase of calculated and observed concentrations in Roncourt is due to an artefact. Indeed, as the well is located in the middle-level, the sector starts to fill up and shows positive concentrations, even though the well is still above the water level. For the others sectors, the wells are located at the outflows of the sectors and the concentrations are represented when the sectors are flooded. In Droitaumont and in Paradis, the

observed concentrations are a lightly underestimated. Despite the orders of magnitude of the observed concentrations being correctly reproduced, this shows the limits of the approach: the positions of the wells and the effective hydraulic connections have not been taken into account. Indeed, the well of Paradis is located in a collapsed zone where three layers have been exploited, but only one (the grey layer) is connected with surrounding concessions. This can produce a hydraulic confinement of the well, not taken into account in the model.

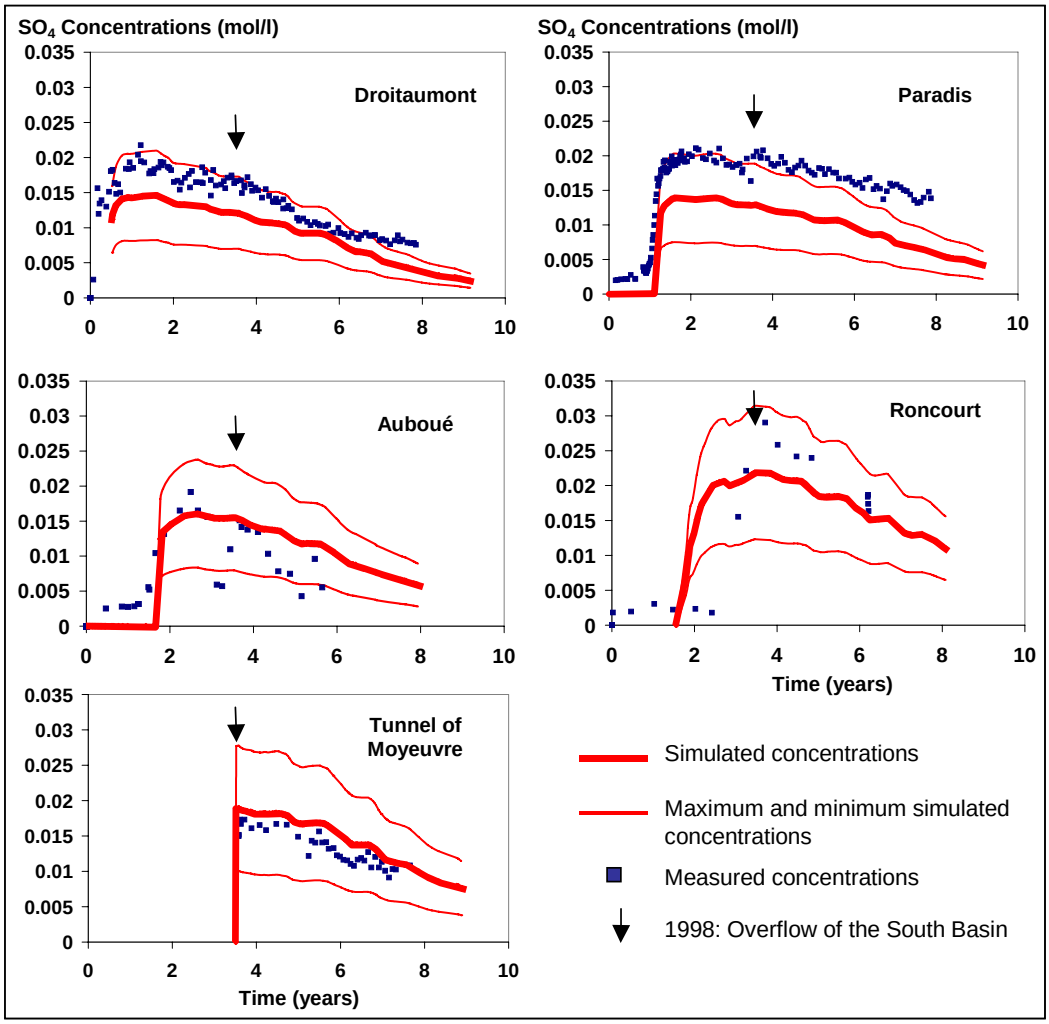


Figure 10. Measured and simulated SO_4 concentrations in the four wells and at the overflow point of the South Basin.

Thus, the global modelling based on a NCR approach (Network of Chemical Reactors) is an interesting approach to predict the evolution of water quality at the overflow. It accounts for the large-scale homogeneity of the South Basin, and characterises the convergence towards the overflow of the water coming from different areas of the mine workings and its mixing near this point. Although encouraging, the results of the semi-distributed model show the need to specify the spatial organisation of water flow in the reservoir in order to reproduce the evolution of chemical concentrations in the different monitored wells.

Acknowledgments

This work is part of the research programme carried out by GISOS (Research Group for the impact and safety of artificial underground cavities).

References

Adams R., Younger P.L., (2001). *A strategy for modelling ground water rebound in abandoned deep mine systems*, Groundwater, Vol. 39, No. 2, p. 249-261

Altmann S., (1995). *Measurement and modeling approaches for solving water pollution problems related to mining activities*. Mineral Deposits, Pasava, Kribek & Zak eds. Balkema, Rotterdam ISBN 90 5410550 X, p. 3-9

Appelo C.A.J., Verweij E., Schäfer H., (1998). *A hydrogeochemical transport model for an oxidation experiment with pyrite/calcite/exchangers/organic matter containing sand*. Applied geochemistry, Vol. 13, p. 257-268

Bain J.G., Blowes D.W., Robertson w.d., Frind E.O., (2000). *Modelling of sulfide oxidation with reactive transport at a mine drainage site*. Journal of Contaminant Hydrology, Vol. 41, p. 23-47

Bain J.G., Mayer K.U., Blowes D.W., Frind E.O., Molson J.W.H., Kahnt R., JenkBall U., (2001). *Modelling the closure-related geochemical evolution of groundwater at a former uranium mine*. Journal of Contaminant Hydrology, Vol. 52, p. 109-135

Baranger P., Kervèvan C., (1998). *SCS: Specific Chemical Simulators dedicated to chemistry-transport coupled modelling Part II - A simplified coupled modelling approach based on Networks of Chemical Reactors.* Goldschmidt Conference 1998, Toulouse, Mineralogical Magazine, Vol. 62 A, p. 114-115

Bochenska T., Fiszer J., Kalisz M., (2000). *Prediction of groundwater inflow into copper mines of the Lubin Glogow Copper District.* Environmental Geology, Vol. 39, No 6, p. 587-594

Brown J. G., Bassett R.L., Glynn P.D., (1998). *Analysis and simulation of reactive transport of metal contaminants in ground water in Pinal Creek Basin, Arizona.* Journal of Hydrology, Vol. 209, Issues 1-4, p. 225-250

Chen M., Soulsby C., Younger P.L., (1999). *Modelling the evolution of minewater pollution at Polkemmet Colliery, Almond catchment, Scotland.* Quarterly Journal of Engineering Geology, Vol. 32, p. 352-362

Collon P. (2003). *Evolution de la qualité de l'eau des mines abandonnées du bassin ferrifère lorrain. De l'expérimentation en laboratoire à la modélisation in situ.* Thesis INPL, October 2003, 247 p.

Collon P., Fabriol R., Buès M., (2003). *Variabilité minéralogique des intercalaires marneux du bassin ferrifère lorrain. Conséquences sur la qualité de l'eau dans la mine.* Colloque "Après-mine 2003", Nancy, 5-7 February 2003. CD ROM.14 p.

Collon P., Fabriol R., Buès M., (2004). *Ennoyage des mines de fer lorraines : impact sur la qualité de l'eau - Flooding of the iron mines of Lorraine: impact on the water quality.* Comptes Rendus Géoscience 336, p. 889-899

Collon P., Fabriol R., Buès M., (in press). *Modelling the evolution of water quality in abandoned mines in the Lorraine Iron Basin.* Journal of Hydrology.

Eary L.E., Runnells D.D., Esposito K.J., (2003). *Geochemical controls on ground water composition at the Cripple Creek Mining District, Cripple Creek, Colorado*. Applied Geochemistry, Vol. 18, p. 1-24

Elberling B., Nicholson R.V., Scharer J.M. (1994). *A combined kinetic and diffusion model for pyrite oxidation in tailings: a change in controls with time.* Journal of Hydrology, Vol. 157, Issues 1-4, p 47-60

Hauns M., Jeannin P.-Y., Atteia O., (2001). *Dispersion, retardation and scale effect in tracer breakthrough curves in karst conduits.* Journal of Hydrology, Vol. 241, p. 177-193

Jauzein M., André C., Margrita R., Sardin M., Schweich D., (1989). *A flexible computer code for modelling transport in porous media: Impact*. Geoderma, Vol. 44, p. 95-113

Kervèvan C., Thiéry D., Baranger P., (1998). *SCS: Specific Chemical Simulators dedicated to chemistry-transport coupled modelling Part lll - Coupling of SCS with the hydro-transport modelling software MARTHE*. Goldschmidt Conference 1998, Toulouse, Mineralogical Magazine, Vol. 62 A, p. 773-774

Lin C.-K., Trujillo E.M., White W.W., (1997). *A three-dimensional, three-phase geochemical kinetic model for acid rock drainage.* 4th International Conference on Acid Rock Drainage, Vancouver, British Columbia, Canada, May 30 – June 6, 15 p.

Mayo A.L., Petersen E.C., Kravits C., (2000). *Chemical evolution of coal mine drainage in a non-acid producing environment, Wasatch Plateau, Utah*. USA, Journal of Hydrology, Vol. 236, p. 1-16

Neumann I., Sami K., (2002). *Structural influence on plume migration from a tailings dam in the West Rand, Republic of South Africa*. In: YOUNGER P.L., robins N.S. (eds). *Mine Water Hydrogeology and Geochemistry*. Geological Society, London, Special Publications, Vol. 198, p. 337-347

Parkhurst D.L., Appelo C.A.J., (1999). *User Guide to PHREEQC (Version 2): A computer program for speciation, batch-reaction, one-dimensional transport, and inverse geochemical calculations*. U.S. Geological Survey Water-Resources Investigations, Report 99-4259, 312 p.

Pinault J-L., Plagnes V., Aquilina L., Bakalowicz M., (2001). *Inverse modeling of the hydrological and the hydrochemical behavior of hydrosystems: Characterisation of karst system functioning*. Water Resources Research, Vol. 37, No. 8, p. 2191-2204

Razowska L., (2001). *Changes of groundwater chemistry caused by the flooding of iron mine (Czestochowa Region, Southern Poland),* Journal of Hydrology, Vol. 244, p. 17-32

Salomons W., (1995). *Environmental impact of metals derived from mining activities: processes, prediction, prevention.* Journal of Geochemical Exploration, Vol. 52, p. 5-23

Therrien R., Sudicky E.A., (1996). *Three-dimensional analysis of variably-saturated flow and solute transport in discretely-fractured porous media*. Journal of Contaminant Hydrology, Vol. 23, p. 1-44

Vaute L., Nguyen The D., Fabriol R., Pinault J.-L., BAUBRON J.-C. (2004). *Une méthode de modélisation hydrogéologique inverse appliquée à un problème d'ingénierie : l'abaissement du niveau d'un réservoir minier ennoyé dans le bassin ferrifère lorrain.* Revue Française de Géotechnique, No. 106-107, p. 85-94

Villermaux J., (1993). *Génie de la réaction chimique, conception et fonctionnement des réacteurs*. TEC & DOC - Lavoisier, 448 p.

PPRM : ENVIRONMENT RISK ASSESSMENT METHODOLOGY – MAIN STEPS

COSTE Bernard[1], ITARD Yann[1], ARTIGNAN Dominique[1]

[1] BRGM Mineral Resources Division – Post Mining Unit, 3, Avenue C. Guillemin – BP 6009 – 45060 Orléans Cedex 2, - France. b.coste@brgm.fr – y.itard@brgm.fr d.artignan@brgm.fr

ABSTRACT: The main steps of an Environment Risk Assessment consist in 1. Determination of the contamination for assessing the soil and water quality; 2. Preparation of a soil model in horizontal and vertical directions; 3. Elaboration of a hydrodynamic and transport model ; 4. Detailed environmental risk assessment. This methodology has proven to be very useful, but remains a heavy tool for PPRM concern.

KEYWORDS: PPRM (Mining Risk Prevention Plan), Risk Assessment, groundwater modelling, pollution, metals.

RESUME : La réalisation d'une étude de risque environnementale comporte quatre étapes principales : 1. évaluation de l'impact sur la qualité des sols et des eaux ; 2. modélisation en 3D de la pollution des sols 3. modélisation hydrodynamique et hydrochimique ; 4. caractérisation détaillée des risques. Le canevas de cette méthodologie, relativement lourde à mettre en application, constitue un outil dont on doit s'inspirer pour la réalisation des PPRM.

MOTS-CLEFS : PPRM (Plan de Prévention des risques Miniers), Etudes de risques, Modélisation, Pollution, Métaux

1. Introduction

The scope of an environmental PPRM (Mining Risk Prevention Plan) is to evaluate and map the risks linked to pollution due to historical mining activities (Artignan.D., Cottard .F. 2003, a and b). It needs to provide a complete assessment of the extent of contamination of the soil and water (surface water and ground water) in the surroundings area of a mining site. The level of contamination is based on a risk assessment approach. The main steps of risk assessment methodology are introduced hereafter before to discuss its adaptation to PPRM.

2. Risk Assessment Methodology

The **risk assessment methodology** is based on:

· identification of sources of potential concern;
· characterisation of key substances;
· characterisation of pathways;
· exposure assessment;
· risk characterisation (human health risk and ecological risk).

In such a study, **four subsequent steps** are to be distinguished:

1. Determination of the contamination for assessing the soil and water quality;

2. Preparation of a soil model in horizontal and vertical directions;
3. Elaboration of a hydrodynamic and transport model;

2.1. Determination of the contamination

A pollution is defined when the soil composition deviates from the normal composition for a substance which is present in concentration greater than the natural one, or "background value" as a result of human activities (Darmendrail D. and al, 2000; Laperche V., Mossmann J.R., 2004). Pollution is regarded as having a net detrimental effect upon environment and its components. The **background** level is relative, and natural values may vary as a function of the locality from which the soil is sampled: standard metal concentration in soils from Belgium, for example, is lower than in soil from a zone with a large variety of rock types including plutonic rocks and metamorphic rocks.

Determination of the contamination requires the availability of a set of data on soils and water quality integrating analytical results of previous studies and complementary field investigations and analyses.

2.1.1 Data available

In terms of **environmental impacts on ground** linked to an old mine it is necessary to characterise different **release components** of the former activities and summarise the **effects of emissions to air and to water:**

- The components released to air are sulphur dioxide SO2 and metals (largely in the form of particulate matter) i.e. copper, zinc, nickel, lead, cadmium and arsenic,
- Constituents released to water include all metal contaminants reported to be present, as well as pH (hydrogen ion activity).

The effects of releases on ground contamination are linked to deposition of metals (dust fall) from air and direct or indirect effect of discharge of effluent. A set of data about soil or water quality may be available : previous studies, monitoring network.

2.1.2 Field and laboratory investigations

The set up of the program of field investigations and analyses is related to the objectives of the next steps (modelling and risk assessment) and takes into account the results and gaps of previous studies. Data reported in these documents and natural setting are used to define the areas to be investigated, the depth of the boreholes, and the location of the piezometers to be drilled.

2.1.2.1 Fieldwork

The fieldwork carried out includes the following activities:

- Detailed topographical survey of the studied areas and mapping,
- Drilling and installation of new piezometers
- Hydraulic tests for defining the water-permeability and pumping tests in piezometers
- Measurement of the piezometric groundwater levels in the piezometers located within the studied area
- Collection and analysis of soil and water samples (chemical analysis).

International standards (ISO standards) or national standards (NF, AFNOR) will be used as guidance on the collection, handling and storage of soil and water.

2.1.2.2 Laboratory analysis

Laboratory analysis include chemical analyses of water samples, and chemical analyses, leaching tests and mineral characterization of soil and waste.

All samples (water and soil) are investigated in a certified laboratory and 10 %, water and soil samples, are send for analytical control to an other laboratory (Quality Assurance, Quality control procedure).

Chemical analysis of soil samples and water samples

The determinations include specific parameters of mining pollutions (in the case of a polymetallic mine (sulphide): pH, Conductivity, SO_4, heavy metals (Cu, As, Cd, Cr, Pb, Se, V, Zn, Fe, Mn, Ni, Ag, Hg) and hydrocarbons). In case of soil and waste, mineralogical determination and leaching attack are useful to test the **mobility of metals** and predict the **impacted groundwater quality** (Table 1: low pH, conductivity, SO4 and metals).

Table 1 : Typical results from groundwater quality in a mining area.

Components	**Piezo**	**PL-18**	**PL-6**	**PL-20**	**E-2**	**PL-10**	**PL-9**	**PL-7**
pH		4.5	3.8	4.1	3.7	3.4	3.0	3.7
SO_4	**mg/l**	4,592	2,010	1,660	1,541	3,180	3,765	893
Conductivity	**µS/cm**	5,390	2,780	2,390	2,090	3,500	4,600	1,467
Pb	**mg/l**	**1.20**	**0.12**	**0.50**	**0.14**	**0.12**	**0.24**	**0.29**
Zn	**mg/l**	**157.0**	**3.30**	**30.70**	**19.38**	**29.10**	**13.70**	**9.10**
Cu	**mg/l**	**1,197**	**337**	**288**	**63.70**	**37.80**	**30.30**	**26.75**
Ni	**mg/l**	2.35	22.13	1.00	0.78	1.17	1.17	0.65
Cd	**mg/l**	**6.75**	**0.023**	**1.08**	**0.81**	**0.63**	**0.54**	**0.41**
Ag	**mg/l**	0.04	0.03	0.02	0.01	<0.01	0.02	0.02
As	**mg/l**	0.12	0.08	0.05	<0.05	0.17	0.17	<0.05
Cr	**mg/l**	0.06	0.14	<0.05	<0.05	0.22	0.08	<0.05
V	**mg/l**	<0.01	<0.01	<0.01	<0.01	<0.01	<0.01	<0.01
Fe	**mg/l**	<0.10	8.20	0.15	0.55	5.60	218.0	0.30
Mn	**mg/l**	50.10	36.90	16.00	16.56	55.10	115.0	15.42
Se	**mg/l**	<0.01	0.02	0.01	<0.01	<0.01	<0.01	<0.01
Hg	**mg/l**	<0.001	<0.001	<0.001	<0.001	<0.001	<0.001	<0.001

2.2. Soil model in horizontal and vertical direction

For a good representation of results in both a horizontal and vertical direction a 3D-software may be used:

- To manage field and drill hole data, regardless of the data source (boreholes, profiles, boundaries, topographic contours, spot samples) and the data format (sample descriptions, analysis tables, well logs, codes, coordinates), interpolate and model data on maps and sections,

· To produce high-quality graphics (maps and sections as multi-layer graphic documents).

As input : description, coordinates (X, Y, Z), analytical results for each well, borehole or superficial soil samples (table 2). The modeling of results includes results of previous reports and new results.

Table 2 : Results from leaching tests according to depth (Boreholes from 0 to 4 m)

Borehole N°	Sample	Depth, m	Cu, mg/kg	Pb, mg/kg	Zn, mg/kg	Ni, mg/kg	Cd, mg/kg	As, mg/kg
BHA-6	S-1	0.0-0.5	1.0	<1.0	<1.0	<1.0	<0.50	<1.0
	S-2	0.5-2.0	120.8	<1.0	70.1	5.0	1.0	2.5
	S-3	2.0-4.0	14.10	1.0	68.0	2.58	<0.50	<1.0
BHA-22	S-1	0.0-0.5	3.55	<1.0	4.80	1.11	<0.50	<1.0
	S-2	0.5-2.0	108.1	<1.0	23.92	1.49	1.05	<1.0
	S-3	2.0-4.0	<1.0	<1.0	<1.0	<1.0	<0.50	<1.0
BHA-24	S-1	0.0-0.5	2,673	3.1	258.0	9.34	19.70	<1.0
	S-2	0.5-2.0	14.50	2.04	21.57	1.40	2.0	<1.0
	S-3	2.0-4.0	<1.0	1.0	4.48	<1.0	<0.50	<1.0

2.3. Hydrodynamic and transport model

Hydrodynamic and transport model contribute to solving underground hydrodynamic problems in various contexts: groundwater management, civil works, environmental assessment, mining operations, etc. In particular, they have been extensively used to model industrial sites concerned by contaminated groundwater and complex drainage systems.

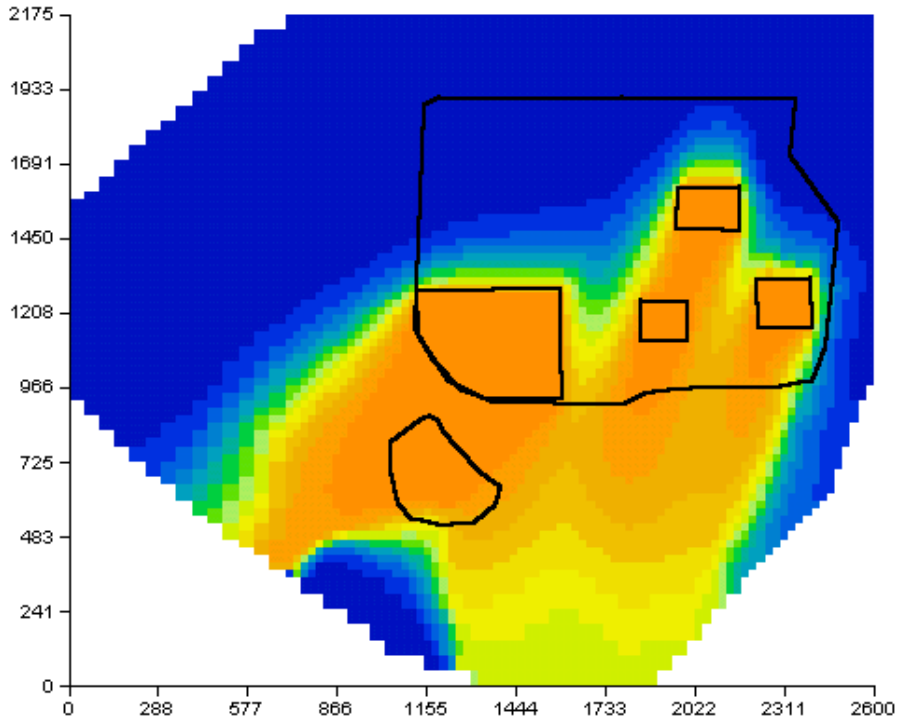


Figure 1: Simulation of pollutant spreading model (Plume 20 years later)

The objectives of the hydrodynamic and transport model are to:

· Assess the groundwater conditions under and around the mining site (groundwater levels, water flows).
· estimate the spreading of the pollutant from the site to defined targets (rivers, drinking water well)

The hydrodynamic and transport model comprises the following tasks :

· construction of the model,
· calibration of the hydrodynamic model,
· simulation of scenarios of pollutants spreading.

The contaminant transport model aims to determine how the contamination spreads through groundwater and to estimate how the concentration of contaminant could evolve near the targets. The needed transport parameters (diffusion coefficient, dispersion coefficient, retention coefficient) may be set to common value found in the literature. The migration calculations may be performed for sulfates and heavy metals.

2.4. Environmental risk assessment

In detailed risk assessment, the basic principles are as follows:

· Risk assessment should take into account current and future uses of a site and its surroundings.
· Receptors to be considerd are humans, water resources, ecosystems and buildings.
· For human health risk assessment the maximum tolerable excess lifetime cancer risk to be used for defining remedial objectives a theoretical risk of 10^{-5} could be set as a target value. A risk greater than 10^{-4} should be considered as unacceptable.
· Assessment of groundwater pollution must reflect both present and future use. In particular, local water management schemes define the areas that should be protected as future resources for drinking water supply.
· Risk assessment for ecosystems and buildings should proceed on a case-by-case basis, according to the current practical state-of-the-art.

The following methodology for detailed risk assessment is carried out using specific exposure scenarios that are as realistic as possible for the site and its environment.

2.4.1 Problem formulation

Problem formulation defines the framework for the risk assessment in term of characterization of the main sources of pollution, pathway assessment and target identification. Typical constituents considered in the risk assessment of mines include all metal contaminants reported to be present, as well as pH (hydrogen ion activity) with particular attention to seven metals Cu, Zn, Ni, Pb, Cd, Cr, Se, Hg and As.

2.4.1.1 Sources characterisation:

An initial site screening may eliminate site a part of the site from the assessment if (1) the site (or part of the site) has no source (no contamination identified), (2) contamination was removed by

prior clean up activities, (3) the site has no potential of physical instability in the environment (geotechnical aspects), and (4) no exposure route to the human and ecosystem exists (i.e. perched water).

During a contaminant data review, data are segregated by medium (soil and water). The sample concentrations for each contaminant in each medium are compared with the site background.

A number of contaminants are eliminated from consideration in each medium through comparison with risk based criteria, reference values (example: the allowable amount of contaminant in water for human health).

2.4.1.2 Pathway assessment

Describe the exposure possible from subsurface (0.15-3 m), and surface (0.0-0.15 m) soils, surface water, and sediments. Several routes are typically considered, including ingestion (soil and water), inhalation, and dermal contact. Indirect exposures are also incorporated (ingestion of contaminated food sources).

2.4.1.3 Target identification

One inventory of the main target exposed directly or indirectly to the pollution will be done in-site and out-site.

2.4.1.4 Toxicity assessment

Toxicity to humans is not usually measured directly by intentionally exposing people. Rather, it is determined indirectly, usually by extrapolation of animal studies to humans. Two types of toxic effects: 1) acute (happening rapidly after a single exposure such as breathing fumes from a chlorine spill), and 2) Chronic (happening after repeated long term exposure such as smoking, breathing polluting air). Chronic effects fall into 2 categories, carcinogenic and non-carcinogenic effects.

Toxicity assessments are based on a dose response concept: as you increase the dose (exposure), the response (toxicity) also increases. For all non-carcinogens, it is assumed that there is a dose below which no effect occurs (a threshold. See LOAEL = Lowest Observable Adverse Effect Level). For carcinogens, it is assumed that even the smallest dose can cause an effect (no threshold). Toxicity assessment are usually taken from the literature and specific databases (ASTR website, Berger, L.L. 2001; Bradley, R.W. and J.B. Sprague. 1985; Cusimano, R.F., and al. 1986). For heavy metals, toxicity is speciation-dependent (Campbell, P.G.C. 1995).

2.4.2 Analysis and characterization of exposure

Personal exposure studies: measure the amount of a substance in the body. It is usually appropriate after a short term exposure, when the full amount of the substance taken in may still be in the body (see Public Health Agencies or representatives)

Environmental exposure studies: measure the amount of a substance in the environment, determine the route of exposure, and estimate how much is in contact with the population and/or ecosystem. Variability over time in the concentration of the substance in the environment may lead to uncertainty.

A **Conceptual model** is produced as description and visual representation of predicted relationships between humans / ecological entities and the stressors to which they may be exposed.

2.5. Risk characterization

Risk characterization, the final phase of the risk assessment, combines the information on toxicity and the occurrence of exposure. Conclusions presented in the risk characterisation should provide clear information to risk managers in order to be useful for environmental decision making. When risk characterisation is completed, the risk assessor should be able to estimate ecological and human health risks, and indicate the overall degree of confidence in the risk estimate. If the risks are not sufficiently defined to support a management decision, risk managers may elect to proceed with another iteration of one or more phases of the risk assessment process.

3. PPRM and Risk Assessment

BRGM has applied a pragmatic approach in Detailed Risk Assessment in :

- France and abroad to many industrial sites with the objective to propose the best mitigation measures taking into account the future development plans of the site,
- India in the fields of mining and ore processing: 1) iron ore mines in the State of Goa, and 2) Sukinda Valley chromite mines in the State of Orissa.. The main objectives of the project in both areas were to undertake a Regional Environmental Assessment (REA) of existing and potential environmental impacts of mining operations, characterize the risks for human health and the environment based on a source-pathways-target approach, and develop an Environmental Management Plan (EMP) incorporating regional and mine-site-specific solutions in terms of both environmental management and technical improvement. The measures proposed in the context of sustainable development are commensurate with acceptable levels of environmental impact and improved economic operation under the technical, legislative and socio-economic conditions of India (Biswas. T. and al, 2000; Coste B. and al, 2001).

The scope of PPRM is risk based land management. The application of Risk Assessment Methodology to PPRM looks possible with adaptation to mine specificities. Specificities to take into account for environmental management of mining sites are in the field of regulation and policy, industrial and natural setting.

3.1. regulation and policy framework

In 1999 the “Post mining law” introduced the PPRM as an administrative tool to prevent and manage post mining hazards (law n° 99-245, 30 march 1999). Environment mining hazards mentioned in n°2000-547 decree (19 June 2000) concern : soil and water pollution, gas and radiations.

In addition to this main text, the PPRM depends on others national and European regulation in the field of waste, soils and water quality:

- national approach on contaminated sites developed by French Ministry for Environment for twelve years,
- EU legislative framework for site specific Risk Assessment (Ferguson C. and al 1998; Ferguson and Kasamas H. 1999)

In France and many European countries, pollution of groundwater is considered as the major risk arising from contaminated soils and sites. Protection of groundwater in the EU is tackled by different thematic regulations such as the Water Framework Directive (in the broadest sense), the Groundwater Directive (specifically) and the Landfill Directive.

A mine specific aspect is the management of dumps and tailings dams (Greffié C. and al 2004; BRGM 1997). The EU is now discussing a directive defining the status of mining residues, and the way they should be managed in the future. The future mining waste directive should be implemented in French legislation.

3.2. industrial and natural setting

In term of environmental risk management, a mining site may be considered as brownfield and megasite *(large industrial site*). For environmental risk assessment, geochemical background is the main specificity about its natural setting.

3.2.1 brownfield and megasite

- As brownfield: maintenance and renewal of industrial and other economic activities are an essential basis for a sustainable remediation and redevelopment of such areas, and require stakeholders participation in the scenario of development process.
- As megasite: megasites defined as regions with large-scale groundwater, soil and/or sediment contaminations require a special approach with respect to the risk assessment (proportionate risk reduction versus costs involved in the remediation and regional approach with a large place for modelling). At megasite scale, the contaminations are not completely removable.

3.2.2 geochemical background

The natural setting looks very different from one mine to an other: many coal mines as other megasites (metallurgical plants, coke plant) are located in urban areas, but uranium, lead-zinc or gold mines are situated in open country. In the first case the detailed risk assessment will be orientated for human health, and in the second one it will integrate human health and ecosystems.

The high level of regional geochemical background around the site is a specificity of mining sector (metals, radionucleides). For each parameter the natural geochemical background and anthropic pollutions are both components for characterisation of risk exposure. As far as geochemical background and anthropogenic inputs are not of the same nature (mineralogy, speciation, quantity), both have to be evaluated separately in term of risks.

4. Conclusion

The main steps of Environment Risk Assessment consist in 1. Determination of the contamination for assessing the soil and water quality; 2. Preparation of soil model in horizontal and vertical direction; 3. Elaboration of a hydrodynamic and transport model; 4. Detailed environmental risk assessment. Environmental risk assessment will be more or less detailed depending on data available on soils and water quality (first step), modelling being useful to interpolate results in space (soils - 3D Software) and expected evolution (groundwater - hydrodynamic and pollutants spreading).

Using such a methodology in France to undertake PPRM means:

- Adaptation to the French regulatory framework (Post mining law…),
- technical adaptation in the context of PPRM taking residual pollution (anthropic) plus geochemical background into account (high level of natural metal content),

· financial adaptation to objectives of the study and the size of the sphere of environmental influence of the mine.

5. References

Agency for Toxic Substances and Disease Registry – Public Health Statement. Available at http://www.atsdr.cdc.gov/ToxProfiles/phs9008.html.

Artignan.D., Cottard.F. (2003) - Méthodologie pour la réalisation de la phase informative du volet risque-pollution d'un PPRM - BRGM/RP-52048-FR

Artignan D., Cottard F. (2003) – Eléments à prendre en compte pour l'évaluation des impacts environnementaux dans l'élaboration d'un Plan de Prévention des Risques Miniers (PPRM). Rapport BRGM/RP-52049-FR

Darmendrail D., Baize D., Barbier J., Freyssinet P., Mouvet C., Salpéteur I. et Wavrer P. (2000) - Fond géochimique naturel. Etat des connaissances à l'échelle nationale. BRGM/RP –50518-FR,

GREFFIE.C., ARTIGNAN.D., DESCHAMPS.Y., ITARD.Y. (2004) - Caractérisation des pollutions potentielles relatives aux sites miniers du territoire français métropolitain - Rapport BRGM/RP-52816-FR -.

Berger, L.L.. 2001. Copper toxicity in Sheep. Available at http://www.saltinstitute.org/stm-2.html

Biswas.T., Babu.Rao.B., Sinha.B.P., COTTARD.F., COSTE.B., Jucker.C. (2000) Regional Environmental Assessment and Management of Mines in India., in SWEMP 2000 - International Symposium on Environmental Issues and Waste Management in Energy and Mineral Production - 6th - Calgary - Alberta - Canada - 30/05-02/06/2000, p. 11-16 [Paru]

Bradley, R.W. and J.B. Sprague. 1985. The influence of pH, water hardness, and alkalinity on the acute lethality of zinc to rainbow trout *(Salmo gairdner*i). Can. J. Fish. Aquat. Sci. 42: 731–736.

BRGM (1997) – Les résidus miniers français : typologie et principaux impacts environnementaux potentiels. Rapport BRGM R39503

Campbell, P.G.C. 1995. Interactions between trace metals and aquatic organisms: critique of the free-ion activity model. *I*n: A. Tessier and R. Turner (eds.), Metal speciation and bioavailability in aquatic systems. John Wiley & Sons Inc., New York, N.Y. pp. 45–102.

Coste B., Cottard.F., Itard.Y., Jucker.C. (2001) Environnement minier en Inde : Etudes d'impacts à l'échelle régionale., Chronique de la Recherche Minière, n° 541. p. 57-64 [Paru]

Coste B.and Itard Y. 2005 Projet méthodologie après-mine, module environnement : Définition des méthodes et outils d'intégration de la pollution des sols et des eaux dans les PPRM BRGM/RP-53969-FR

Cusimano, R.F., D.F. Brakke and G.A. Chapman. 1986. Effects of pH on the toxicities of cadmium, copper, and zinc to steelhead trout *(Salmo gairdner*i). Can. J. Fish. Aquat. Sci. 43: 1497–1503.

Ferguson, C., Darmendrail, D., Freier, K., Jensen, B.K., Jensen, J., Kasamas, H., Urzelai, A and Vegter, J. (editors) 1998 Risk Assessment for Contaminated Sites in Europe; Volume 1, Scientific Basis. LQM Press, Nottingham

Ferguson, C. and Kasamas, H. (editors) 1999. Risk Assessment for Contaminated Sites in Europe; Volume 2, Policy Frameworks. LQM Press, Nottingham.

Laperche V., Mossmann J.R. (2004) – Fond géochimique : Réflexions sur les applications possibles à la de gestion des sites et sols pollués en France. RP-53344-FR

TYPOLOGY OF CONDITIONS FOR UNDERGROUND QUARRY PILLARS BASED ON GEOPHYSICAL INVESTIGATIONS

Philippe COTE[1], Xavier DEROBERT[1], Odile ABRAHAM[1]
[1]Laboratoire Central des Ponts et Chaussées, Department of Soil Mechanics and Site Surveying, BP 4129, 44341 BOUGUENAIS, France

e-mail: philippe.cote@lcpc.fr

ABSTRACT: The planning of needed reinforcement works within an occupied underground quarry leads to a detailed comparative diagnostic of a large set of pillars. In order to complement the conventional observations of rock mining specialists, it has been decided to test a number of additional non-destructive tools stemming from geophysical techniques. GPR and seismic tomography investigations have been selected and specific simplified methodologies developed to minimize the time of experimentation. Various synthetic criteria can be extracted from geophysical interpretations; their joint analysis has yielded a pillar classification based on damaging condition.

KEYWORDS: Ground penetrating radar, seismic tomography, multi-criteria analysis, pillar, damage.

RESUME : La planification de travaux de renforcement dans une carrière souterraine occupée a nécessité la mise en place de diagnostics comparés sur un grand nombre de piliers. En complément des observations classiques des spécialistes de mécanique des roches, il a été décidé de tester des techniques non destructives issues de la géophysique. Les méthodes radar et tomographie sismique ont été sélectionnées et des méthodologies spécifiques ont été mises au point en vue de réduire les durées d'acquisition. Plusieurs critères peuvent être extraits des interprétations géophysiques, leurs analyses conjointes permettent de construire une typologie des piliers basée sur leur état de détérioration.

MOTS CLES : Radar géologique, tomographie sismique, analyse multicritères, pilier, détérioration.

1. Introduction

An underground gypsum quarry has revealed stability problems that necessitate local reinforcements. The extraction technique has involved pillars and chambers. The quarry is presently used for a number of activities requiring the participation of many employees. Ensuring stability of the occupied portion constitutes a major concern for the quarry owner. This occupied portion covers an area of about 2 ha. The typical pillars display a cubic shape with an edge length of around 7 m. The gallery width also lies on the order of 7 m. The main pathology observed was a large variation in pillar condition without any real spatial organization or any clear relationship with the load. The primary apparent symptoms were, for some pillars, a high degree of cracking, opened cracks and local collapses. In order to manage reinforcement of the set of pillars, it was decided to include an investigation tool with the classical mining observations and classifications. The aim herein has been to obtain comparative images of the inner conditions for an entire set of pillars. The first step towards reaching this goal consisted of conducting a test campaign involving seismic tomographies and GPR profiling. An investigation methodology was apparently conceivable, yet it proved necessary to build a specific system for the purpose of performing seismic tomographies within a reasonable time frame. After building such a system, an extensive investigation campaign concerning 45 pillars yielded a state classification for this pillar set.

Ground penetrating radar (GPR) proves to be a very useful technique for carrying out geological non-destructive testing (NDT), which serves to detect dielectric contrasts at boundary planes by the reflection of electromagnetic (EM) pulses. The degree of crack detection depends on various parameters, such as the equivalent target section and the filling of cracks with clay, water or air. In general, the dielectric attenuation of a rock remains very low, thereby providing several meters of radar investigation (Stevens et al., 1995; Toshioka et al., 1995). The literature mentions some results regarding the coefficient of reflection as a function of both dielectric contrast and incident angle of the target section, which may be modeled in order to predict the expected potential resolution (Dérobert, 2003; Olhoeft, 1998). Although this technique is quick and easy to use, its major limitation lies in an inability to yield information on the state of stresses in the structure.

For this reason, a complementary seismic tomography campaign has been aimed at producing, in a non-invasive fashion, a map of the internal mechanical properties within pillars. By means of measuring travel times of the compression wave between source and receiver points around the pillar, it is then possible to derive a compression wave velocity map. In the case of an a priori homogeneous material, the appearance of a lower-velocity zone indicates that the material has weathered locally. Seismic transmission tomography based on travel times is more sensitive to zones of micro-cracking than it is to isolated cracks, especially if the micro-cracks are not closed and if the material has been damaged. In the case of a homogeneous medium, the difference in travel times, both with and without an isolated crack, might very well be of the same order of magnitude as the level of accuracy in the measured times. Seismic amplitudes or rising times are more sensitive to cracking than travel times, but remain substantially more difficult to implement within real investigation processes (Spathis et al., 1983). Consequently, radar and seismic tomography are fully complementary, by virtue of their ability to provide different information in the geological diagnostic process (MacCann et al., 1988).

2. Testing campaign

2.1. GPR investigations

A GSSI GPR system was associated with a 500-MHz shielded antenna. The range was selected in order to ensure reaching the backs of the pillars, i.e. 170 ns for an average thickness of 7 m. The choice of frequency originated from a compromise between the maximum investigation depth and resolution. Since several pillars were targeted by this initial GPR investigation, including some with inaccessible sides, the highest frequency able to reach the other side of the pillars had to be adopted. A time-varying gain was applied to provide amplitude compensation for the medium attenuation as well as spreading loss of the traveling signals. The results yield a similar amplitude to the reflected pulses from both the surface and bottom of the pillar.

Measurements were performed at a height corresponding to the minimum section of the pillar, i.e. around 1.30-1.40 m, at which point the horizontal seismic tomography was conducted (Fig. 1). The advantage of using the minimum section is to ensure that each radar echo detected before the back of the pillar corresponds to an internal heterogeneity inside the pillar. Moreover, this section corresponds to that of the maximum stresses sought by mining specialists.

To obtain an indication of the inclination of fractures, a series of parallel profiles has been generated. The time lag recorded for a few successive profiles, from the same presumed crack, can yield an estimated indication of the angular direction of the crack (Fig. 1). 3D radar processing has already been studied (e.g.: Grandjean and Gourry, 1996; Grasmueck, 1996). The straightforward methodology developed herein, based on the comparison of a few successive profiles, is merely a

simplification in order to obtain confirmation of the occurrence of the crack and then a rough estimation of the level of crack inclination. As observed in Figure 1, the shape of the pillars does not justify processing a large number of radar profiles. Depending on the actual shape of the investigated pillars, two or three radar profiles have been developed at a spacing of 40 cm. Moreover, a thin carriage, including a survey wheel, has been built to allow recording accurate scans, at constant height, from the rough pillar surface.

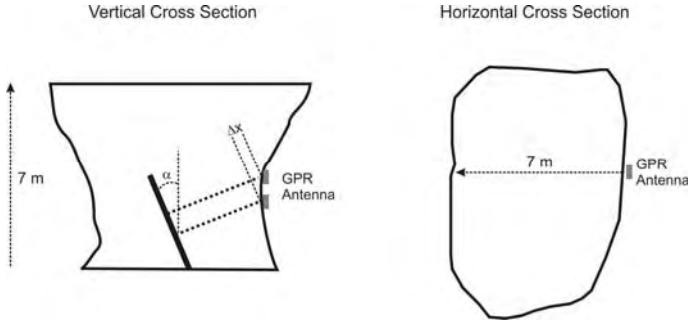


Figure 1 : Typical shape of a pillar and position of the antennas for the different investigations.

Successive processing steps have been carried out in order to localize cracks and damaged zones from the various sides (Fig. 2a). Following a vertical high-pass filter over 250 MHz on the profiles, the first step consisted of implementing a topographic correction, in assuming a known and constant velocity; this step entailed comparing the thickness of different pillars along with the corresponding double travel times. Results from the velocity measurements fluctuated from 11.6 to 11.9 cm/ns, these measurements take into account the possibility of errors due to the 3D shape of the pillar. A constant velocity for each pillar was then assumed. Topographic correction enables comparing the perpendicular, or opposite, radar profiles from the same pillar section and localizing the cracks detected from the various sides. In order to accomplish this step, geometrical data from a surveyor were utilized; this data also proved necessary for the seismic tomographies.

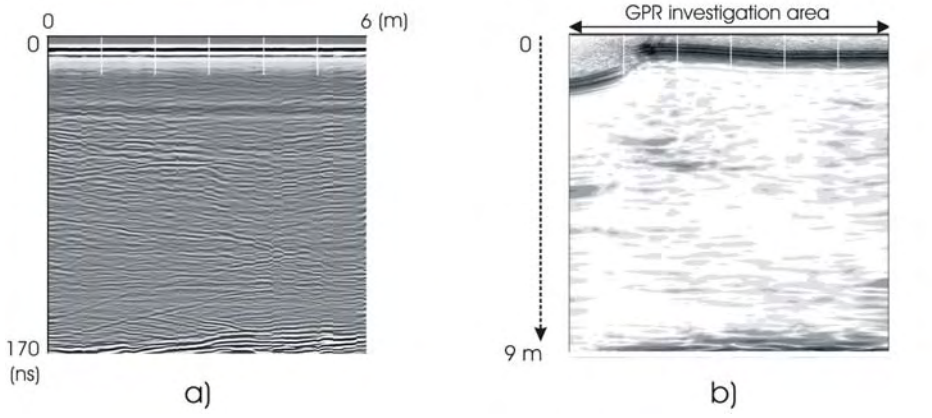


Figure 2: Processing applied to GPR data. a): example of rough data; b) final profile after topographic correction, migration and Hilbert transform.

Afterwards, frequency bandpass filters were applied in order to remove the noise; this step focused primarily on the major reflectors. The next step involved the use of time migration to establish a relationship between time and distance. A Kirchhoff method was employed, with a specific hyperbolic width of 2 m, in relation to the number of scans per meter. Since migration attenuates signal amplitude, a constant gain value of 3 was applied on the profiles. The chief limitation of this process pertains to the fact that migration on its own does not incorporate topography and may distort the surface shape. By compensating for this distortion with a new surface normalization, it

was possible to displace reflectors slightly from their correct positions. This problem is primarily concentrated at the edges of the pillars or when the topography features a sizable gradient. Lehmann and Green (2000) adapted a topographic migration to GPR data and substantiated its recommended use whenever the surface gradient exceeds 10%. For the particular application herein, some basic calculations can show that the positioning error remains below 0.5 m (even though some areas display surface gradients of over 10%), which may be considered as an acceptable approximation. This processing was ultimately achieved with a Hilbert transform in order to present the reflected energy (Fig. 2b). The result is a map showing dark plots that correspond to fracture zones. All of these steps can be considered as part of classical processing in the localization of fractures or damaged areas; furthermore, they provide the basis for radar imaging.

2.2. Seismic tomography investigations

Even though the geometry of a pillar is essentially 3D, measurements here were carried out in 2D. In the present case, the experimental and processing times for 3D seismic analyses are indeed prohibitive since a large number of pillars are being studied.

Given that the major zone of interest lies around the pillar's smallest section, it was decided to perform a horizontal tomography at this particular spot. In most cases, the four sides of the pillar were all accessible, thereby allowing for a good level of ray coverage. A vertical tomography was similarly performed with source and receiver points located on two opposite faces. The objective was twofold: to control the state of the pillar vertically, and to ascertain whether the horizontal tomography plane was located in the area of the pillar where velocities are highest. This approach served to prevent against any misinterpretation of artefacts that may arise from a 3D velocity distribution in which the horizontal tomography plane may be surrounded by higher horizontal velocity zones. Under such circumstances, the ray paths would not lie within the tomography plane, as presumed during the inversion process, and the calculations performed would be erroneous due to an incorrect ray geometry assumption.

During an initial series of experiments, an optimum spacing for the source and receiver points was determined such that the information contained on the tomography maps would be sufficient to perform the same diagnostic evaluation as with a denser map. It was shown that the total number of rays could be reduced from about 2,000 to 500 without noticing any major loss in information on the interpreted tomographic map. In the horizontal tomography, about 10 equidistant source-receiver points were located on each side. Sources and receivers never lie on the same face. In the vertical tomography, 18 equidistant source points were located on one side and 18 equidistant receiver points on the opposite side. Next, as for GPR interpretation, the surveyor data enabled determining coordinates for each of the source-receiver points.

A multi-channel acquisition system (10 bits, 1 MHz/channel) was used to collect and store the seismic signals. Since the shortest source-receiver travel times amount to approximately 0.1 ms, the sampling frequency was set at 1 MHz, in order to ensure acquiring a sufficient number of points for picking the arrival times. The source consisted of a hammer coupled with an accelerometer, while the receivers were accelerometers attached onto the pillar wall. Both the receiver and source signals were recorded for all possible source-receiver combinations. The time pickings were subsequently carried out in the laboratory. These arrival times and coordinates were then fed into the inversion process.

The tomography algorithm employed in this paper is that known as "RAI-2D" (Côte et al., 1992); it has already led to numerous applications in both soil surveying (Abraham et al., 1998) and structural NDT (Côte and Abraham, 1995; Abraham et al., 1996). RAI-2D has been inspired by the Simultaneous Iterative Reconstruction Technique (SIRT - Gilbert, 1972). The field of investigation is discretized into a mesh of points, on which the seismic velocity gets defined. One of the key

features of RAI-2D pertains to its influence zones, which as opposed to a fixed block-discretization grid are used when selecting rays to calculate slowness at a given grid point. The size of these influence zones constitutes one of the adjustment parameters that allows RAI-2D to adapt its convergence process to the type of actual data. This algorithm is also characterized by its use of circular analytical rays. The level of accuracy for civil engineering purposes inherent in this simple and rapid inversion technique, which has been widely tested using both synthetic and field data, is similar to that provided by other more complex methods based on matrix inversions and sophisticated ray path computations.

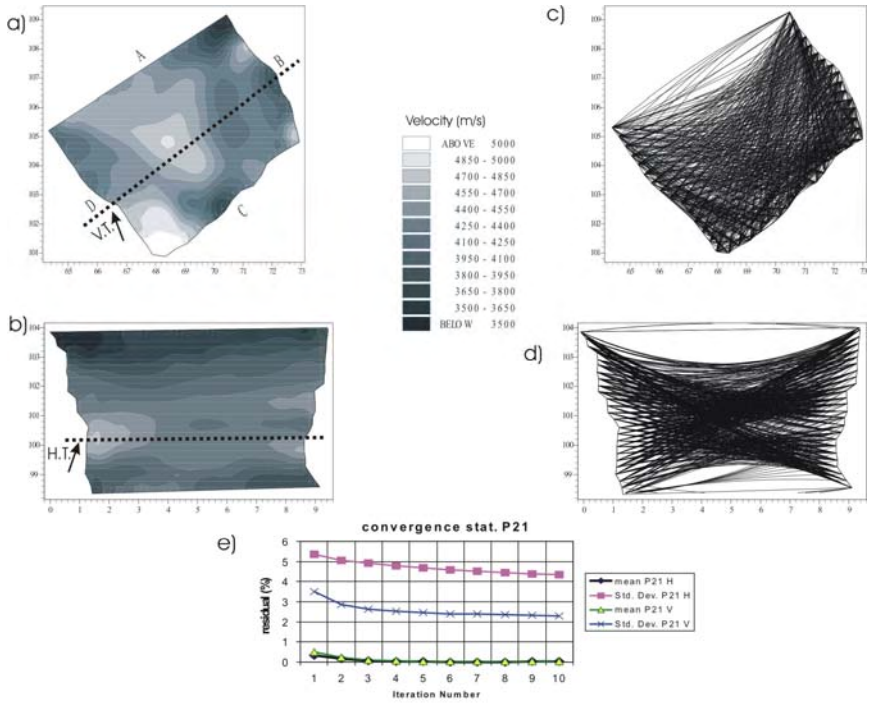


Figure 3: Horizontal (a) and Vertical (b) seismic tomographies of Pillar 21. The position of the vertical tomography plane (respectively horizontal) is indicated as dotted line on the horizontal tomography map (respectively vertical); (c) and (d): corresponding ray density; (e): convergence parameters expressed in terms of percentage of the mean travel time.

It is recommended to include certain complementary information with the final velocity map in order to guarantee the quality of the survey and facilitate its interpretation.

First of all, algorithm convergence should be tracked from a statistical point of view (mean residual, standard deviation). Furthermore, the residual statistics of each source and receiver should be checked so as to eliminate those sources and/or receivers displaying out-of-scale statistical values. Secondly, since both the precision and resolution of the velocity map are linked to the ray coverage, the plot of rays should at least be studied. For instance, in zones with few rays, the velocity value is less precise than in zones with well-distributed and large numbers of rays.

As an example, Figure 3 shows the horizontal and vertical seismic tomography results for Pillar 21. In both cases, the grid size is 0.4 m x 0.4 m and the results observed are those obtained after 10 iterations. Both inversions did converge correctly (Fig. 3e). The number of rays equals 625 for the vertical tomography and 675 for the horizontal tomography (Figs. 3c and 3d).

The vertical tomography (Fig. 3b) indicates that the highest velocities are located near the smallest horizontal pillar section, as would be expected. The information on the top and bottom of the tomography plane is less precise than in the middle due to ray bending (Fig. 3d). Moreover, lateral variations are less distinct than vertical variations due to the pseudo-parallelism of the entire set of

rays. The major benefit of this tomography is to confirm that localization of the horizontal one does not yield any artefacts as a result of high-velocity heterogeneities outside the horizontal plane.

For the horizontal tomography (Fig. 3a), face A was inaccessible. Information in the vicinity of this face is less accurate than in the other parts of the pillar. The degree of confidence in the velocity distribution may be illustrated by the ray-tracing map (Fig. 3c). As the rays cross one another in an increasingly dense pattern, the inversion becomes more accurate. The general organization of velocities in this tomography reveals, as a major fact, the presence of a high-velocity inner core embedded in slower materials. The highest velocities (corresponding to the soundest materials) observed in this core amount to approximately 4,800 m/s, while the lowest surrounding the core are around 4,000 m/s. The mean velocity of the whole pillar comes to 4,440 m/s. Otherwise, in the corners (e.g. between faces C and D), the majority of the rays are quite short and may at times be strongly affected by inaccuracies in either geometry or time picking. In these areas, the contrasts observed must be carefully compared with other information, such as local visual inspections.

2.3. Conclusions on the first testing campaign and methodology definition

Few pillars were tested during this first campaign. In order to compare information from both techniques, it was decided to plot, over the horizontal tomography, information on the fractures detected by the radar.

The horizontal tomographies were computed in accordance with the previously-described methodology:

- analysis of the residual statistics,
- verification of the absence of 3D artefacts from the vertical tomography analysis,
- analysis of the ray coverage in order to avoid interpreting unexplored areas, and
- plotting of maps with homogenized scales (for space and velocities) in order to generate comparisons.

The information derived from GPR can be summarized as follows:

- the radar profiles acquired for each face at two different heights (8 radar profiles for a standard pillar) are treated as previously described;
- the various echoes corresponding to inner fractures are localized on each of these profiles;
- each echo is then plotted over the seismic tomography using the following conventions (Fig. 4): color change to identify measurement face, different thickness depending on echo strength, dotted or continuous lines to separate the two measurement heights.

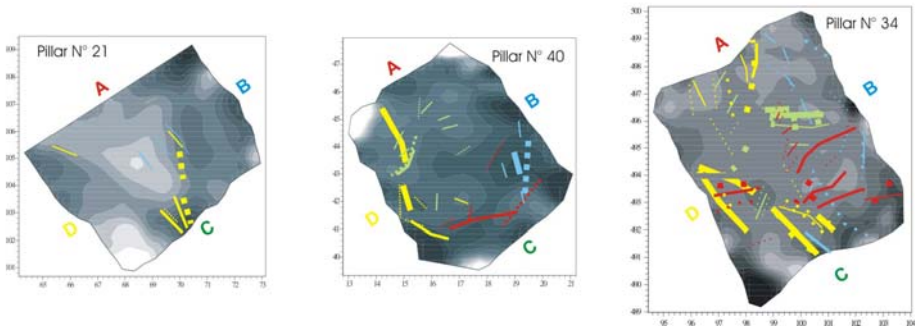


Figure 4: Horizontal tomographies and radar synthesis for 3 pillars.

Figure 4 illustrates such results for three pillars. The mean velocities observed are 4,440 m/s for P21, 4,300 m/sec for P34 and 3,990 m/sec for P40. These differences are not large enough to

actually attribute poor material quality to the slowest velocity, yet are significant enough to establish discrepancies in pillar behavior in the context of this very homogeneous geological formation. Moreover, one important feature that can be identified is the degree of inner homogeneity within the pillar. Large differences in this homogeneity may be observed; for example, Pillar P21 exhibits a high-velocity inner core whose shape can be correlated by small radar-detected fractures. Another important feature to be taken into account in a comparative study is the degree of fracturing in each pillar. From a synthesis comparison of P21 and P34, it is clear that P34 presents a greater degree of fracturing. In addition, it is possible to analyze the inner fractures with precision. As an illustration, P34 displays strong cracks observed from face D. The detection of these echoes is localized at the same place for both of the profiling heights. These fractures are thus located in a near sub-vertical plane.

Over the small number of pillars tested, a cross-interpretation of these two techniques has shown sizable variations in terms of mean velocity, inner homogeneity, and number and size of fractures. For this reason, the quarry owner decided to extend this test to a more extensive set of pillars in the quarry. In order to conduct such investigations at a large scale, it has been necessary to build a specific seismic acquisition system to obtain operating times that fulfill material and staff constraints. For GPR investigations, use of the current set of standard instruments is compatible with the prescribed methodology.

2.4. Definition of an adapted seismic acquisition system

The methodology for acquiring seismic data on pillar tomographies requires the following:

- a high analogous-digital conversion rate: typically 1 MHz per channel is necessary to yield acceptable picking time accuracy for the shortest rays (even though the received signal spectrum is quite weak over 10 kHz);
- a sufficiently high resolution to avoid any gain adjustment (16 bits presently seems to be quite common);
- a total number of channels high enough to simultaneously implement on 3 pillar faces (typically in the tens of receivers per face);
- a lightweight and packaged acquisition system, so as to authorize investigations in areas not always easily accessible; and
- a specific channel devoted to the triggering signal; this will allow for some relative shifting in the plots in order to increase picking time accuracy.

The new acquisition system has been built in accordance with these indications; the system derived is in fact similar to a modern seismograph (32 channels), yet with high-frequency sampling (1.2 MHz/channel). Consequently, the level of resolution cannot reach that of present seismometers (24 bits). This system has been built with a 16-bit sampling unit. The various tests conducted revealed an effective resolution of roughly 12 bits. The driving software includes all classical aspects (channel parameterization, time or frequency trace visualization, time picking, etc.); it is associated with a set of 32 accelerometers and their conditioning tools. Moreover, since this system is PC-based, it has been possible to implement the RAI-2D tomography algorithm and obtain a global tomographic system. A number of acceptance tests were held on site; they enabled finalizing the software processes and determining which rate could be envisaged for pillar tomographies. It has been observed that a rate of 2 pillars per day (4 tomographies) was indeed possible, in case of easy access to local site conditions.

3. Extensive measurement phase

An extensive measurement phase has been carried out in the quarry. A set of 45 pillars were selected in an area displaying some disorders. An extract of the synthetic results is presented in Figure 5. When local access conditions were simple, the forecasted rate proved realistic: 2 pillars per day for tomographies and 4 pillars per day for GPR. Unfortunately, for a significant number of pillars, access was rather difficult for the operating team; in these cases, the rate may be quite heavily affected and drop to 1 pillar a day for tomographies and 2 a day for GPR.

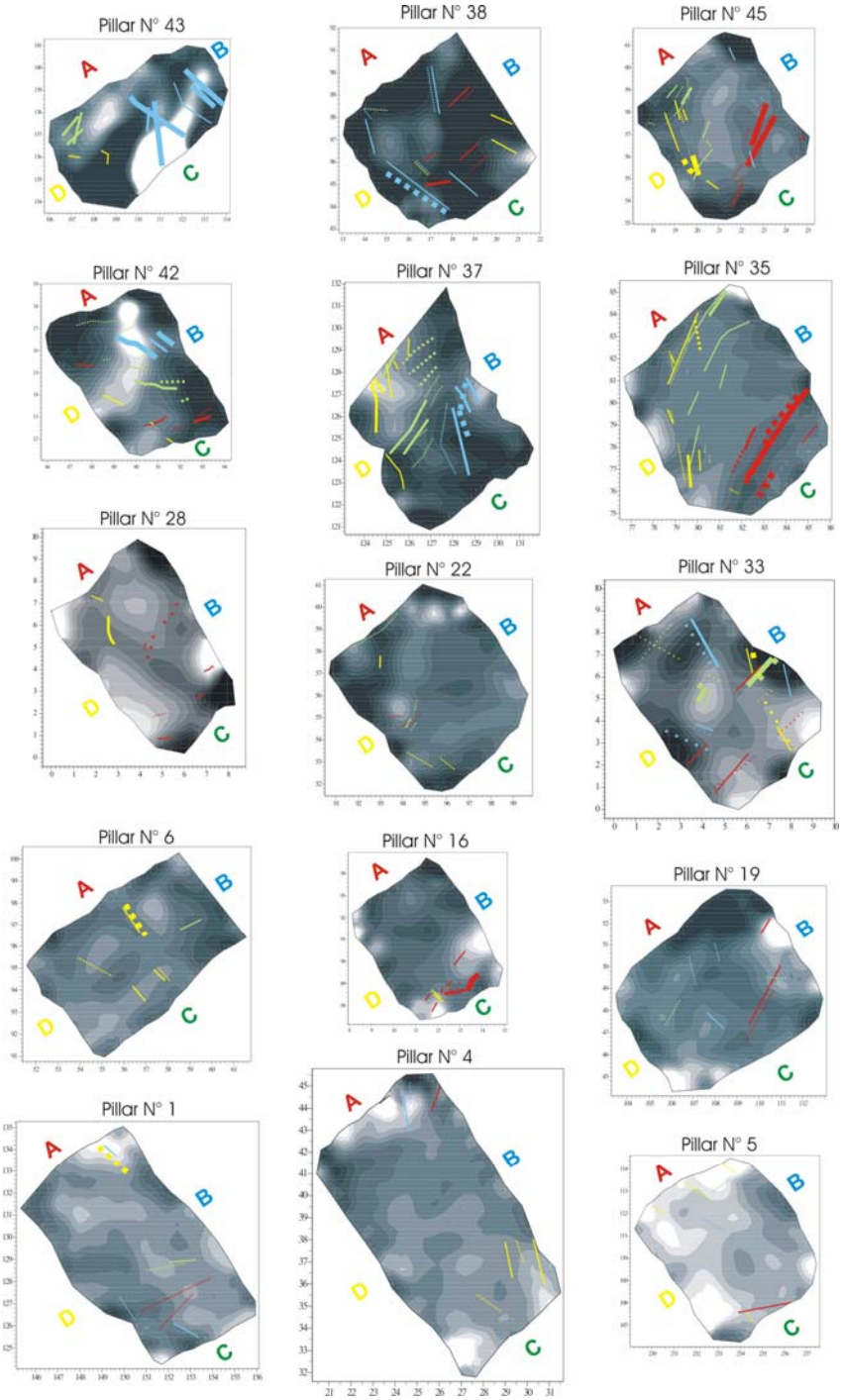


Figure 5: Horizontal tomographies and radar synthesis for a set of pillars extracted from the extensive investigations. The representation rules are identical as for Fig. 4.

As previously noted, a great variability in seismic velocities has been recorded (Fig. 5). This variability can be viewed not only as a discriminating factor between pillars but also as an inner observation inside pillars, in which certain areas may be distinguished. As a common practice in a defined material, it is possible to associate the weakest areas with the lowest seismic velocities; such an association can yield an initial typology based on the global mean velocity observed for each pillar. The corresponding histogram (Fig. 6a) illustrates the mean velocity distribution for the entire set of pillars. Many pillars are positioned in the vicinity of the median (4,150 m/sec). It would be possible to arbitrarily define 4 separate zones, which sort the pillars from "slowest" to "fastest".

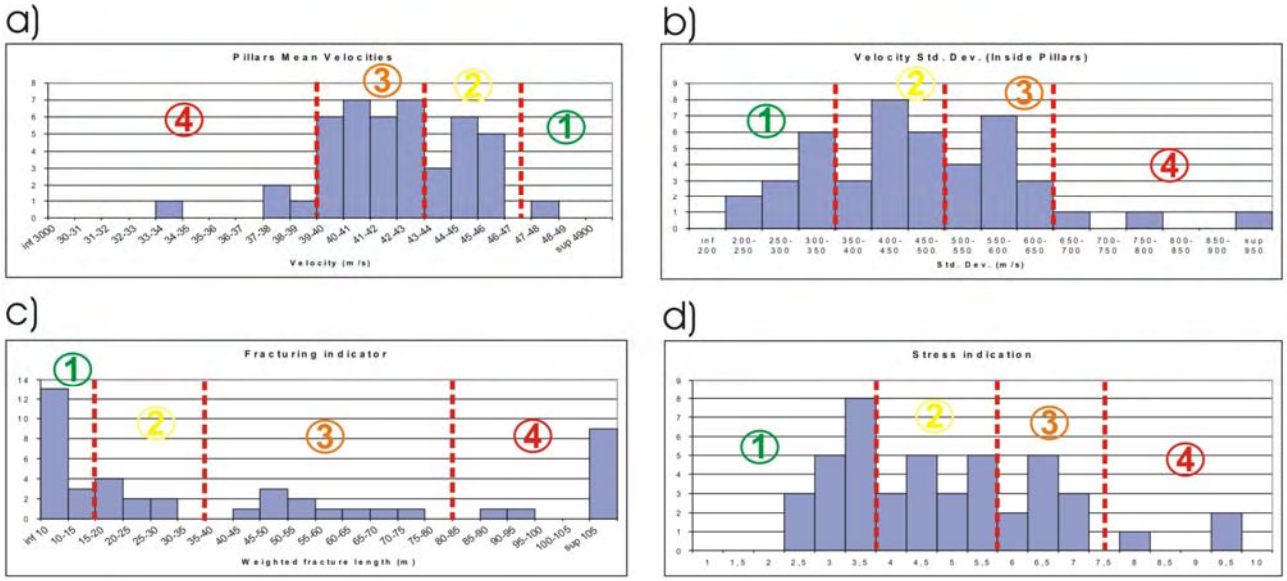


Figure 6: Pillars classification following four criteria. Mean velocities (a) and homogeneity (b) from sonic tomographies ; Fracturing estimation (c) from GPR and stress indicator (d) from global geometry.

Another typology can be analyzed by classifying pillars with respect to their homogeneity; this requires qualifying the velocity distribution at each pixel of the tomographic result. In the case of a homogeneous pillar, a simple Gaussian distribution would be observed. If the pillar has been subdivided into several mechanically-differentiated parts, the velocity histogram would then be more complex. One simple way to quantify the degree of pillar homogeneity consists of calculating the standard deviation of velocities in the tomography. Figure 6b depicts the distribution of these standard deviations for the entire set of pillars. Here once again, it is quite simple to discriminate among categories that qualify pillar homogeneity.

A third typology may now be introduced in order to discriminate pillars relative to their degree of fracturing (Fig. 6c). It is possible, for each pillar, to calculate a fracture rating that takes the following into account:

- total length of fractures detected,
- weighting factor of each of them (from radar reflectivity amplitudes),
- "GPR coherency" (reproducibility from different faces and heights), and
- “seismic coherency” (coherency of fracture localization relative to the borders of areas identified in the horizontal tomographies).

The fracture rating obtained has been plotted in Figure 6c. Here again, it may be observed that this index distinguishes quite well the pillar population into 4 areas: the first one corresponds to pillars without any major detected fractures (16 pillars belong to this category), while the last area corresponds to pillars displaying a very high degree of fracturing.

Moreover, it is possible to introduce an additional typology. The quarry owner has indicated the classification of pillars by their stress state, as deduced from their geometry and load. The corresponding histogram (Fig. 6d), shown here on a relative scale, provides a 4-class distribution of the pillars.

This set of parameters serves to build a multi-criteria analytical base for this pillar set. It must be pointed out that this process is not altogether free of subjectivity. The choice of each border in the various histograms is not exclusive. Moreover, different possibilities can be envisaged to implement the radar and tomographic results in this database. As an initial approach, the four selected parameters are considered to be of equal weight. It is always feasible to implement more complex discrimination rules for each parameter. Keep in mind however that a global classification does in fact show very little sensitivity when refining any of the individual assessment criteria.

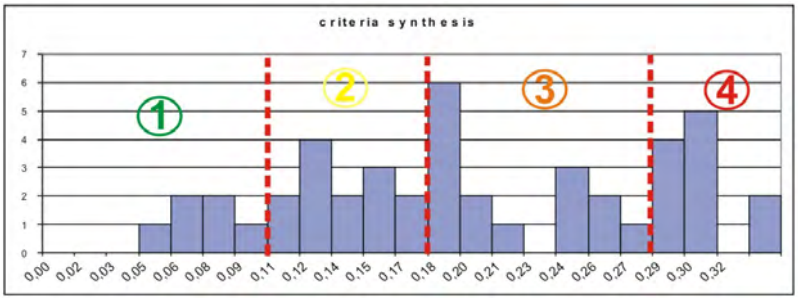


Fig. 7: Global synthesis of the four selected criteria.

The global typology may be summarized in a histogram deduced from the four selected criteria (Fig. 7). Two extreme types of behavior can be isolated. With a global assessment criterion of less than 0.1 (arbitrary unit), 6 pillars are qualified as being sound. With a criterion over 0.29, 11 pillars are qualified as being heavily-damaged. Between these two extreme categories, 28 pillars can be isolated and classified as exhibiting from least to heaviest damage. It would be possible to separate these 28 pillars into two categories, i.e.: a criterion between 0.1 and 0.18 corresponds to nearly-sound pillars, whereas a criterion of between 0.18 and 0.29 corresponds to quite heavily-damaged pillars.

In any attempt to validate this classification, it is important to check the stability of the global classification when deleting one of the parameters. Each line in following table (Tab. 1) corresponds to an identified pillar, numbered between 1 and 45. The first four colored left-hand columns correspond to the individually-selected parameters (mean velocity, homogeneity, stress and degree of fracture). The colors themselves represent the four qualification classes of each pillar for each parameter. The order of green, yellow, brown and red corresponds to the spectrum from sound to damaged qualifications. The column entitled "Synthesis" indicates the global classification described earlier. The four subsequent columns correspond to a classification (normalized, for comparison) of the global criterion less one parameter (alternatively radar, stress, homogeneity and mean velocity). It is interesting to note the rather good level of stability in the classification obtained. The majority of pillars classified as damaged or heavily-damaged retain their qualification in any event, while the individual parameters observed alternately do not lead to any stable classification. The selected parameters would thus appear to be complementary and the global classification may be used as a tool for reasonably managing the reinforcement works.

Pillars	Veloc.	Std Dev	Stress	GPR	synthesis	Synth - GPR	Synth - stress	Synth - std.dev.	Synth - veloc.
1	4460	307	5,79	9,91	0,04	0,049	0,05	0,03	0,04
2	4471	261	6,61	7,8	0,05	0,061	0,03	0,06	0,05
3	4533	251	6,77	8,585	0,05	0,060	0,02	0,06	0,05
4	4424	357	6,24	4,76	0,06	0,086	0,06	0,04	0,07
5	4748	340	7,06	4,85	0,07	0,092	0,04	0,06	0,09
6	4265	289	7,24	10,84	0,09	0,106	0,06	0,10	0,09
7	4158	438	6,07	4,98	0,09	0,125	0,11	0,05	0,09
8	4105	432	6,08	7,39	0,10	0,127	0,11	0,06	0,09
9	4420	336	7,56	17	0,11	0,126	0,08	0,11	0,13
10	4055	449	6,15	12,505	0,11	0,139	0,13	0,08	0,11
11	4117	350	5,55	48,32	0,12	0,077	0,16	0,11	0,12
12	4220	483	6,40	8,48	0,12	0,150	0,13	0,07	0,13
13	4557	425	7,21	23,63	0,13	0,138	0,11	0,10	0,16
14	4022	461	5,91	27,99	0,13	0,137	0,17	0,10	0,14
15	3928	466	6,77	13,265	0,14	0,177	0,15	0,11	0,14
16	4247	588	6,57	5,31	0,15	0,193	0,16	0,07	0,16
17	3936	568	6,22	5,5	0,15	0,194	0,17	0,08	0,15
18	4250	488	6,71	29,07	0,15	0,161	0,16	0,11	0,18
19	4083	574	6,48	18,4	0,16	0,195	0,19	0,10	0,18
20	4505	344	7,15	67,59	0,17	0,109	0,16	0,18	0,21
21	4444	357	7,38	58,5	0,17	0,126	0,16	0,18	0,20
22	3988	484	7,73	9,6	0,17	0,214	0,14	0,13	0,18
23	3734	638	6,05	6	0,17	0,229	0,21	0,09	0,17
24	4515	401	6,64	72,44	0,17	0,111	0,19	0,17	0,22
25	3861	682	5,93	6	0,17	0,230	0,22	0,07	0,18
26	4023	566	5,85	48,28	0,19	0,173	0,24	0,13	0,21
27	4301	441	7,53	51,63	0,19	0,170	0,18	0,18	0,23
28	4223	556	6,99	44,52	0,20	0,198	0,22	0,15	0,24
29	4528	525	7,75	63,18	0,23	0,196	0,22	0,20	0,29
30	3989	520	7,94	46,96	0,23	0,234	0,22	0,21	0,26
31	4318	620	9,19	18,665	0,24	0,294	0,19	0,18	0,29
32	4422	325	7,63	117,285	0,24	0,124	0,25	0,29	0,31
33	4109	536	6,62	89,54	0,25	0,184	0,30	0,23	0,30
34	4290	240	6,23	170	0,26	0,050	0,32	0,35	0,32
35	4222	354	5,60	169,6	0,28	0,074	0,37	0,33	0,34
36	4380	243	6,32	186,3	0,28	0,049	0,35	0,37	0,35
37	3761	456	5,72	132,3	0,28	0,148	0,37	0,30	0,31
38	3379	591	7,38	53,32	0,28	0,291	0,31	0,25	0,28
39	4152	440	7,99	108,15	0,29	0,196	0,29	0,31	0,35
40	3994	591	6,23	108,18	0,29	0,198	0,36	0,25	0,34
41	3962	546	5,78	131,56	0,30	0,168	0,39	0,28	0,35
42	4001	783	9,26	15,845	0,30	0,377	0,26	0,20	0,35
43	4082	912	7,97	20,1	0,30	0,372	0,31	0,15	0,36
44	4137	445	7,16	148,53	0,32	0,169	0,37	0,35	0,39
45	4065	605	8,36	91,26	0,32	0,275	0,33	0,30	0,39

Tab. 1: Global table classification of 45 pillars.

4. Conclusion

This work has been performed in order to define a non-destructive tool capable of guiding the quarry owner in planning reinforcement works inside the quarry. It has been demonstrated that a combination of seismic tomographies and GPR investigations may lead to a global classification of a set of pillars. These two geophysical methods have proven herein to be quite complementary. Seismic tomography is able to identify variations in material soundness while GPR serves to locate cracks. Their combined assessment allows establishing criteria for the purpose of qualifying the overall state of pillars. The methodology employed to determine the various criteria is, of course, not unique. A dose of subjectivity may be introduced into the process. One key to this process is to verify the complementarity of individual criteria as well as the stability of proposed classifications.
Moreover, when examining a particular pillar (classified as among the most heavily-damaged), the various maps interpreted from GPR and tomographies, in addition to visual inspections, enable considerably refining the diagnostic and the specification of necessary reinforcements.
One of the major drawbacks regarding sonic tomographies pertains to the time needed for conducting measurements. The design and development of a specific system has allowed minimizing this time. In considering some of the accessibility problems involved, these experiments would require at least one day per pillar for a team to complete both investigations (seismic tomography and GPR). This order of experimental cost, when added to the cost of the multiple interpretation processes, most likely relegates such a methodology to very specific underground quarries.

5. References

Abraham O., Derobert X., Alexandre J., (1996). *Seismic and electromagnetic tomography applied to historical buildings: a case history*. 2nd Meeting EEGS, Nantes. 232–235.

Abraham O., Ben Slimane K., Cote Ph., (1998). *Seismic tomography: factoring anisotropy into iterative geometric reconstruction algorithms*. Int. J. Rock Mech. Mining Sci. 35 1 , 31–41.

Cote Ph., Lagabrielle R., Gautier V., (1992). *2D and 3D Reconstructions Using Pseudo-rays.* EAEG, Paris, 242–243.

Cote Ph., Abraham O., (1995). *Seismic Tomography in Civil Engineering*. NDT-CE, Berlin, 459–466.

Dérobert X., (2003). *Techniques radar appliqués au genie civil.* Guide Technique ERLPC, LCPC, 110 p.

Gilbert P., (1972). *Iterative methods for the three dimensional reconstruction of an object from projections.* J. Theor. Biol.,105–117.

Grandjean G., Gourry C., (1996). *GPR data processing for 3D fracture mapping in a marble quarry Thassos, Greece* . J.Appl. Geophys. 36 1, 19–30.

Grasmueck M., (1996). *3-D ground-penetrating radar applied to fracture imaging in gneiss*. Geophysics 61 4, 1050–1064.

Lehmann F., Green A.G., (2000). *Topographic migration of georadar data*. Proc. 8th Int. Conf. on GPR, Gold Coast, Australia, 23–26 May. 163–167.

MacCann D.M., Jackson P.D., Fenning P.J., (1988). *Comparison of the seismic and ground probing radar methods in geological surveying*. IEE Proc. 4 , 380–391, part F.

Olhoeft G.R., (1998). *Electrical, magnetic, and geometric properties that determine ground penetrating radar performance*. Proc. 7th Int. Conf. on GPR, Lawrence, KS, USA, 27–30 May.

Spathis A.T., Blair D.P., Grant J.R., (1983). *Seismic pulse assessment of the changing rock mass condition induced by mining.* Int. J. Rock Mech. Mining Sci. 22 5 , 303–312.

Stevens K.M., Lodha G.S., Hollowaay A.L., Soonawala N.M., (1995). T*he application of ground penetrating radar for mapping fractures in plutonic rocks within the Whiteshell Research,Area, Pinawa, Manitoba, Canada*. J. Appl. Geophys. 33 1–3 , 125–141.

Toshioka T., Tsuchida T., Sasahara K., (1995). *Application of GPR to detecting and mapping cracks in rock slopes*. J. Appl. Geophys. 33 1–3 , 119–124.

CHARACTERISATION AND TYPOLOGY OF MINING EFFLUENTS: PROSPECTIVE APPROACH BASED ON FRENCH LEAD-ZINC DEPOSITS

CARACTERISATION ET TYPOLOGIE DES EFFLUENTS MINIERS : APPROCHE PROSPECTIVE REALISEE SUR LES GISEMENTS FRANÇAIS DE PLOMB-ZINC

COTEL Solenn[1], SCHMITT Jean-Michel[1], COSTE Bernard[2], ITARD Yann[2]

[1] : Ecole des mines de Paris, CIG, 35, Rue Saint-Honoré 77305 Fontainebleau cedex
[2] : BRGM, av. C. Guillemin, 45060 Orléans Cedex 2

ABSTRACT: The characterisation of the water running out the main lead-zinc French deposits has been undertaken for identifying the key parameters controlling the water quality. The objective is to set up a correlation between geological and gitological characteristics of the deposits and the chemistry of the perennial mining effluents running out after the mine closure. The optimisation of the long-term management of mining water requires to enhance this water characterisation and to open the approach to the other main types of deposits.

Keywords: lead-zinc deposits, mining water typology, long-term management.

RESUME : La caractérisation des eaux des principales mines de plomb-zinc françaises a été entreprise dans le but d'identifier les paramètres qui contrôlent la qualité de ces eaux. L'objectif est d'établir une corrélation entre les caractéristiques géologiques et gîtologiques des gisements et la chimie des rejets d'effluent miniers qui continuent durablement après la fermeture des mines. Afin d'optimiser la gestion sur le long terme des émergences minières, cette caractérisation des eaux devra être approfondie et élargie aux autres grands types de gisements français.

MOTS-CLEFS : Mines de plomb zinc, typologie des eaux de mine, gestion à long terme.

1. Introduction

In France, water from lead-zinc mines closed in the last twenty years is treated before being discharged into the natural environment. This is the case of the mines of Largentière (Schmitt & Combes 1996, Kimmel & Daupley 2003), Malines (Combes *et al.*1994), and Saint-Salvy (Combes & Schmitt 1994), which have their own treatment stations (neutralization with lime). These stations were imposed on the operator by prefectoral orders issued on the basis of hydrogeological surveys taking account of the quantitative and qualitative aspects of the flooding of the mines after the cessation of dewatering. The forecasts are based on hydrodynamic and hydrochemical models (Schmitt *et al.* 2003, Banks 1997, Cidu *et al.* 2001, Younger 1997, Salomon 1995).

Some twenty years later, a closer understanding of the mechanisms governing the minewater chemistry has emerged as crucial for the optimization of their long-term management. The first step presented here, the characterization of all the various types of water from French lead-zinc mines (treated or not), was carried out as part of a DEA (Diploma of Advanced Studies) course entitled Typology and hydrogeochemistry of closed lead-zinc mines (Cotel, 2005).

2. Typology of French lead-zinc deposits

This typology is the result of a bibliographic search on French lead-zinc deposits (GIS-France, etc), undertaken with the aim of characterizing the sites and identifying the parameters controlling their pollutant content so as to furnish the data necessary for selecting the sites to be sampled.

2.1. French lead-zinc deposits

The study concerns the various types of French lead-zinc deposits (figure 1), among which 120 are of medium to large scale, i.e. having a significant output (over 1000 t metal) (Demange 1972, 1973, Cassard & Itard 2003, Artignan & Messin 2004, Cottard *et al.* 2002, Coste & Delpont 2003, Combes *et al.* 1994). The classification factors adopted were selected in order to optimally reflect the various parameters controlling the water quality (host rock lithology, gangue, ore composition,…).



Figure 1**:** Map of France of Pb-Zn deposits sampled

2.2. Selection criteria of sampled deposits:

Of the 120 closed French Pb-Zn mines, some fifty mines in 13 main mining districts meet the following double criterion:

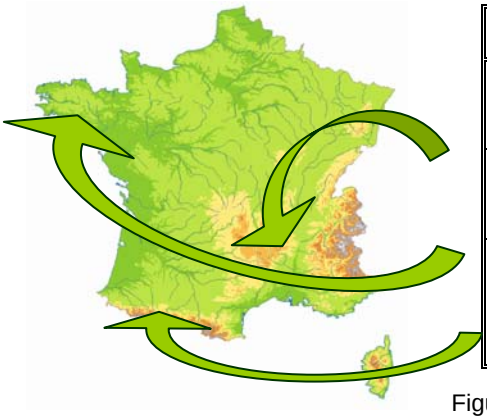
- more than 2000 t metal tonnage extracted,
- deposit appraised at over 10 000 t.

To determine a minewater typology representative of the various types of deposit, the sampling campaigns were planned on the following selection criteria:

- ✓ more than 2000 t metal tonnage extracted and a deposit appraised at over 10 000 t,
- ✓ the presence of drainage to varying degrees of certainty,
- ✓ the geological (characteristics of the ore, gangue and surrounding material) and economic (mining period, etc) features of each deposit,
- ✓ the presence of other potentially interesting deposits nearby.

3. Sampling programmes and analyses

In the time allotted to the study, the sampling programmes were prepared by meticulously selecting some twenty representative deposits. They were focused on three lead-zinc districts (figure 2): the Cevennes, Brittany and the Pyrenees (and 2 sites in the South Massif Central).



Mining District	Mines for sampling (Forecast)
Cevennes	St-Sébastien, La Croix-de-Pallière, Villemagne**,** Les Malines, Largentière
Brittany	Pontpéan, Trémuson, Huelgoat Poullaouen, La Touche
Pyrénées (+ Massif Central pp.)	Figeac, Villefranche, Pierrefitte, Sentein, Arrens, Chèze, St-Salvy, Peyrebrune, Pranal, Roure, Pontgibaud, La Brousse

Figure 2: Deposits prospected for minewater collection

3.1. Water sampling procedure

Samples are taken according to a precise procedure:

In the minutes after each sampling, a part of the raw sample is subjected, in situ, to a set of measurements. These measurements include:



- temperature,
- pH and redox potential,
- electrical conductivity,
- dissolved oxygen,
- alkalinity (TAC) by titration method.

Figure 3: Field measurement device

The remaining portion of the raw sample, intended for analysis, is filtered at 0.45 µm. Immediately after filtration, the sample is divided into two fractions, the first for analyzing anions, and the second previously acidified and sent for determination of cations and metals. The sampling points are photographed and accurately located by GPS. Upon returning from the field, these points are plotted on a topographic map.

3.2. Chemical analyses of water samples

The water sample was subjected to complete chemical analysis to determine the speciation and thermodynamic state. To do this, the major species were analyzed: anions (HCO3-, F-, Cl-, NO2-, Br-, NO3-, SO42-) and cations (Li+, Na+, NH4+, K+, Mg2+, Ca2+), silica, and the 9 metals (Fe, Cu, Pb, Cd, Zn, Co, Mn, Ni, Al, As) often present in minewater.



Figure 4: Central gallery, St Sébastien

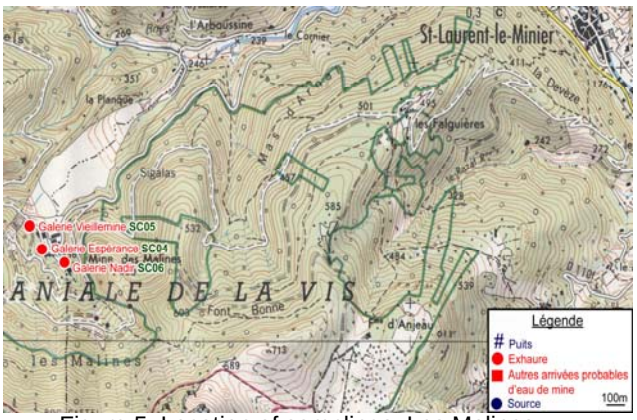


Figure 5: Location of samplings, Les Malines

3.3. Raw results

The results are given in Annex. A total of 31 minewaters were sampled and analyzed. On the whole, these waters display a wide range of hydrochemical types, although the Pyrenees and Brittany minewaters appear to be less varied than in the Cevennes. Very different waters were also observed in the same mine. These remarks will now have to be explained in light of the characteristics of the deposits.

4. Interpretation of results

The goal of this part is to identify the parameters controlling the pollutant content of the waters from the closed Pb-Zn mines. In concrete terms, this means correlating the characteristics of the deposits of the closed mines with the chemical data from the water issued from them. The first step is the determination of a minewater speciation and chemical typology. The second phase is the determination of a deposit typology, with the aim of identifying the parameters controlling the pollutant content. The conclusion will help reconsider which chemical typology can explain the cause of the various water types.

4.1. Minewater speciation and typology

The objective is not only to determine the typology of these waters, but also to present and use the results of the field surveys.

4.1.1 Speciation calculation

CHESS geochemical speciation code

The CHESS model developed at CIG by J. Van der Lee (1998) is used to calculate the speciation of a geochemical system, i.e. to determine the concentrations and activities of the various chemical species present in the various phases (solid, liquid, gas) and the state of saturation with respect to potential minerals. CHESS can also be used to simulate a reaction path, for example, to

model the changes in the chemical system as a function of the variation of certain variables (Eh, pH) or of an activity (pCO_2, etc).

The aim of this speciation calculation is to understand the origin of the waters sampled, to identify their state of equilibrium with respect to the various mineral phases, particularly the precipitation that they can induce. These factors serve to clarify the hydrological classification of the waters and also to assess their potential environmental impact.

Results and interpretation

The results are given in Annex (bottom part of Table). The main problem encountered in the speciation calculations is the significant virtually general ionic disequilibrium of the minewater. In nature, a water sample is normally electrically neutral. To obtain this neutrality, the concentration of the major anion or cation is generally adjusted, but this equilibration has its limits; the concentration of a species cannot be modified beyond the analytical error without jeopardizing the representativity of the data. Certain analyses unfortunately have to be discarded for this reason.

4.1.2 Minewater typology

Typology as a function of major anions and cations

This typology, which is not specific to minewater nor to potentially polluted water, only accounts for the major ions. The aim is to individualize the waters of the same geochemical type. Each sample was accordingly plotted on a PIPER diagram. This type of representation takes account of the anions SO_4^{2-}, HCO_3^- and Cl^- and the cations Na^+, Mg^{2+} and Ca^{2+}. These are generally the major ions in all the waters and this is also confirmed in our own case.

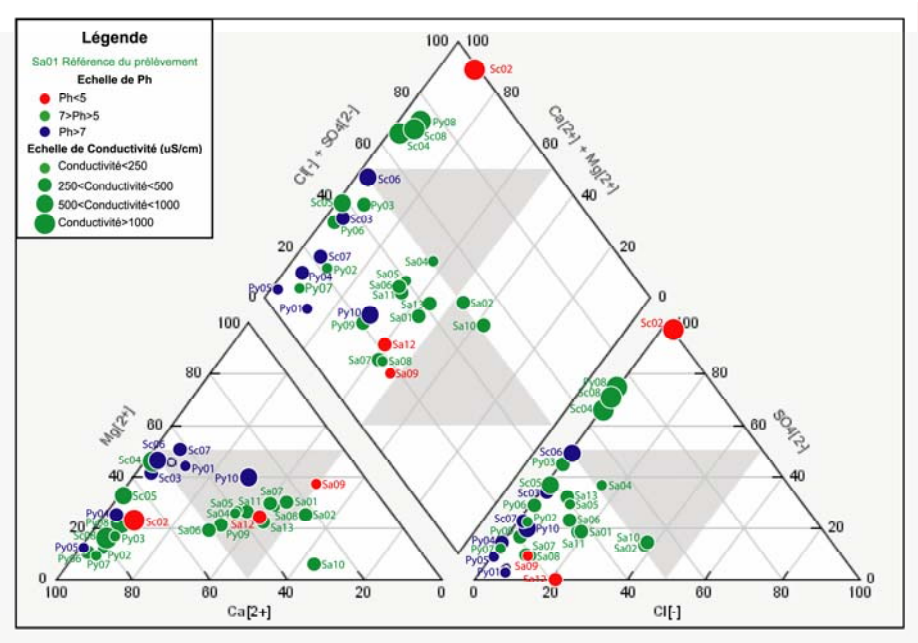


Figure 5: Positioning of water samples on a PIPER diagram with pH and conductivity scales

We find a wide hydrogeochemical variety in the minewaters: four types of water exist in terms of the cations (magnesium, calcium, sodium and combined type) and three in terms of anions (sulphate, hydrogenocarbonate and combined type).

Hydro-geochemical typology

This considers the waters as a whole, and therefore takes account of the field measurements, all the concentrations known by chemical analysis of the water, and the results of the speciation calculations (total dissolved load or TDS, CO_2 fugacity, equilibrium states). Observation of the overall data led to the definition of five hydro-geochemical groups. The waters grouped in a given unit are not identical but display close similarities. The parameters used to classify these minewaters effectively are: pH, redox potential, TDS, CO_2 fugacity, hydrochemical type, minerals at equilibrium and metals content.

4.1.3 Choice of representative chemical parameters

All the field measurements and all the concentrations known by chemical analysis of the waters are not equally important for determining the parameters controlling the pollutant content of the minewater. By considering the criteria used to determine the final minewater typology and the conclusions of the survey on minewater quality and impact, four important chemical parameters were selected for the vast majority of the effluents from the closed Pb-Zn mines:

- pH and TDS,
- zinc content and iron content.

Other chemical parameters, corresponding to aggregates of metals, were envisaged but considered to be less discriminating.

Table 1: Quantification of the mineralization, mine flooding and combined parameters.

	Place name	Mineralization (Min.) parameter				Mine flooding parameter	Min. and flooding parameter
		Pyrite	Pyrrhotite	Chalcopyrite	Note	Note	Note
Massif Armoricain	Trémuson	abund.	-	-	**6**	**1**	**9**
	La Touche	v abund.	-	-	**9**	**2**	**15**
	Huelgoat	abund.	-	rare	**6**	**2**	**12**
	Poullaouen	abund.	-	rare	**6**	**1**	**9**
Cévennes	Largentiére	freq.	-	rare	**3**	**1**	**6**
	St Sébastien	v abund.	-	-	**9**	**2**	**15**
	La Croix de P.	abund.	-	-	**6**	**2**	**12**
	Les Malines	abund.	-	-	**6**	**2**	**12**
	Villemagne	freq.	-	freq.	**4**	**2**	**10**
Montagne Noire	Peyrebrune	freq.	rare	rare	**3**	**2**	**9**
	St Salvy	abund.	-	-	**6**	**2**	**12**
Pyrénées	Arrens	freq.	freq.	freq.	**5**	**3**	**14**
	Pierrefitte	freq.	abund.	freq.	**6**	**3**	**15**
	Sentein	freq.	freq.	freq.	**5**	**3**	**14**
	Aulus	freq.	freq.	freq.	**5**	**3**	**14**

4.2. Typology and selection of the deposits' physical characteristics

By observing the criteria of the environmental database and the conclusions of the survey on minewater quality and impact, five independent physical parameters were selected:

- host material, mineralization,
- mine flooding, closure date,
- a secondary parameter: tonnage extracted.

The aim is to try to correlate the characteristics of the deposits or of the closed mines with the chemical data from the water issued from them. For each physical parameter, it was therefore necessary to find a grading system compatible with a graphic representation of the result. In practice, a grade was allocated to each data class corresponding to the parameters.

5. Conclusion

This study allowed the construction of an environmental database of all the French Pb-Zn mines, the taking of samples and a typology of the water from these mines, with the identification of the parameters controlling their pollutant content. These results are consistent with those declared in previous studies devoted to certain groups of deposits, and could also allow a preliminary qualitative estimate of the effluents from the closed lead-zinc mines, based on a limited number of simple parameters:

- mineralogical composition of the host material (presence or absence of carbonates),
- initial characteristics of the mineralization (abundance of iron sulphides),
- degree of mine flooding (presence of residual sulphide mineralization in unsaturated zone).

The parameters considered above are also inadequate to explain how very different qualities of drainage water can be observed in a given mine. It was therefore decided to clarify the heterogeneity of the water quality in a given deposit by constructing a phenomenological model of the change in water quality, focusing on two deposits (Les Malines and St-Salvy). Prior to the construction of the model, a new sampling campaign was already completed on the two deposits selected: sampling in a low water period (late summer 2005) broadened to a larger number of emergence points, and their impact on the natural environment (upstream and downstream sampling).

It is also obvious that the same type of systematic study can be applied:

- to other types of mineralization, such as fluorine, sulphide orebodies, gold, coal and uranium,
- media other than water, such as soil, wastes and sediments.

Acknowledgments

This work is part of the research programme carried out by GISOS (Research Group for the impact and safety of artificial underground cavities).

Gratitude is expressed to F. Aye (BRGM-SA) and P. Derouet (MetalEurop) for giving us access to their mining sites, and to M. Viard (Mica Environnement) and C. Sauzay (MINELIS) for technical assistance

References

D. ARTIGNAN, M. MESSIN, *Méthodologie d'élaboration d'un PPRM, Volet risque-pollution - Cas du site de Trémuson (22)* BRGM/RP 52831-FR document provisoire, rapport BRGM, mars 2004, 54 p.

D. BANKS, P.L. YOUNGER, R.T. ARNESEN, E.R. IVERSEN, *Mine-water chemistry : the good, the bad and the ugly*, Environmental Geology, Vol 32, 1997, P.157-174

D. CASSARD, Y. ITARD. (2003) *Metallogenic & environmental information systems: A modern Tool for the Sustainable Development of Mineral Resources.*, in NATO Workshop "Mineral Resource Base of the Southern Caucasus and Systems for its Management in the XXI Century - Tbilisi - Georgia - 04/2003, (actes du workshop), A.G. Tvalchrelidze and G. Morizot (eds.) - NATO Publisher, p. 167-180

R. CIDU, C. BIAGINI, L. FANFANI, G. LA RUFFA and I. MARRAS, *Mine closure at Monteponi (Italy) : effect of the cessation of dewatering on the quality of shallow groundwater*, Applied Geochemistry, Volume 16, Issue 5, April 2001, P. 489-502

P. COMBES, J.M. SCHMITT et E. LEDOUX, *Etude de la qualité des eaux – Région de St Laurent le Minier* . Rapport ENSMP/ARMINES, octobre 1994, 25 p.

P. COMBES, J.M. SCHMITT, *Qualité des eaux à l'exutoire de Combe Maurel*, LHM/RD/94/57, rapport ENSMP/ARMINES, 1994, 13 p.

B. COSTE, G. DELPONT, *Diagnostics environnementaux de trois mines de l'Aveyron, du Lot et des Hautes Pyrénées*, BRGM/RP 52740, rapport BRGM, décembre 2003, 34p.

S. COTEL. *Typologie et hydrogéochimie des effluents des anciennes mines métalliques : cas des mines de Pb-Zn française*. 2005, Rapport CIG/ARMINES-LHM/RD/05/11

F. COTTARD, I. BOUROULLEC, Ph. DUTARTRE, L. FLEURY, *Audits environnementaux de six mines fermées ou abandonnées de la région Midi-Pyrénées* BRGM/RP 51538, rapport BRGM, février 2002,.

M. DEMANGE, *Contribution à l'étude des gisements plombo-zincifères français*, Extrait du Bulletin du BRGM, Deuxième série - Section II – n°1, 1973, 30 p.

M. DEMANGE, *Typologie et dimensions des gisements plombo-zincifères français*, Thèse Université d'Orsay Paris XI, 1972, 165 p.

M. KIMMEL, X DAUPLEY, *Synthèse de la phase informative en vue de la réalisation d'un plan de Prévention des Risques Miniers – Largentière*, Dossier technique, décembre 2003, 61 p.

W. SALOMONS, *Environmental impact of metals derived from mining activities : processes, prediction, prevention*, Journal of geochemical Exploration, Vol.52, 1995, P. 5-23

J.M. SCHMITT, P. COMBES et E. LEDOUX, *Qualité des eaux après fermeture des mines : remplissage initial, évolution transitoire, stabilisation à long terme et gestion environnementale*, Colloque "Après-mine 2003", Nancy, 5-7 February 2003. CD ROM. 10 p.

J.M. SCHMITT, P. COMBES, *Impact hydrogéologique et géochimique de l'abandon d'une mine métallique. Cas de Largentière (Ardèche, France)*, Mines & Carrières, Les Techniques V. suppl. Déc. 1996, P. 38-47.

J.M. SCHMITT, E. LEDOUX et P. COMBES, *Etude hydrochimique relative a la fermeture de la mine de Noaihac – St Salvy* LHM/RD/94/24, rapport ENSMP/ARMINES, 1994, 60 p.

J.M. SCHMITT, J. VAN DER LEE, L DE WINDT, *Séminaire 'CHESS' de modélisation géochimique appliquée aux problèmes d'environnement*, Rapport Armines, LHM/RD/04/22, 2004, 132 p. + Annexes.

J. Van der LEE J., *Thermodynamic and mathematical concepts of CHESS.* Rapport Technique, École des Mines de Paris, CIG/ARMINES, LHM/RD/98/39, 1998, 99 p.

P. L. YOUNGER, *The longevity of minewater pollution: a basis for decision-making*, The Science of The Total Environment, Volumes 194-195, 24 February 1997, P. 457-466

Annex : Analytical results and speciation calculations (spring 2004)

1. Cevennes

Name		SCO2	SCO3	SCO4	SCO5	SCO6	SCO7	SCO8
Location of samples		St Sebast. Mine	La Croix de P. Mine	Malines Mines			Villemagne Mine	Largentière Mine
		Central Gallery	Gallery	Esperance Gallery	Old mine Gallery	Nadir Gallery	TB 843	Perruquette Spring
Date		01/04	01/04	01/04	01/04	01/04	01/04	01/04
. Field msmts.	Temp. in °C	10.6	12.4	13.3	13.1	11.6	9.3	15.3
	pH	2.98	7.02	6.36-6.42	6.96-7.04	7.62-7.64	7.5	6.79
	Eh /ENH in mV	748	314	223	295	299	477	196
	TDS. in mg/L	520	884	2774	488	807	322	1845
	O_2 diss. in mg/L	7.8	4.9	1.6	7.2	9.3	9.5	3.9
Anions in mg/L	HCO_3^-	0.0	311.1	205.0	158.6	224.5	158.6	219.6
	F^-	0.055	1.00	2.08	0.17	< 0.1	< 0.1	< 0.5
	Cl^-	5,41	7.73	10.21	3.67	4.28	4.77	7.15
	NO_3^-	1.75	< 0.4	< 1	0.97	< 0.1	1.34	< 0.5
	SO_4^{--}	498.9	254.8	1541	174.0	311.4	68.73	928.8
Cations in mg/L	Na^+	3.05	3.60	4.63	2.13	2.78	3.26	11.00
	NH_4^+	0.55	< 0.2	< 0.4	< 0.1	< 0.1	< 0.05	< 0.2
	K^+	1.40	< 0.2	6.93	0.64	1.60	1.15	7.61
	Mg^{++}	9.46	58.99	193.3	25.09	60.09	25.77	51.66
	Ca^{++}	38.33	135.3	381.8	96.65	122.6	47.99	403.2
Silica	SiO_2 (aq) en mg/L	14.9	< 1	< 1	< 1	< 1	< 1	8.6
Metals in µg/L	Fe	2 795	406.0	79 620	165	11.1	8.6	13 720
	Cu	151	< 0.4	8.7	< 0.4	< 0.4	< 0.4	< 0.4
	Pb	923	12.9	5.0	39.7	34.9	2.1	24.7
	Cd	32	1.0	18.4	34	11.4	18.8	2.8
	Zn	6 790	140	33 470	14 170	9 480	5 010	6 250
	Co	62	< 1	51	< 1	< 1	< 1	41
	Mn	1 982	16.1	1 629	23.5	10.1	30.4	590
	Ni	107.1	< 1	285	12.9	36.3	6.4	98.6
	Al four	34 880	50	6.1	6.0	8.6	14.8	11.8
	As four	907	56	< 10	< 10	< 10	< 10	117
Ionic balance %		-37.2	10.0	12.7	15.7	11.3	14.5	11.7
Elec bal.	Poss/Imposs	SO_4^{2-} $\triangle SO_4^{2-}$=26%	SO_4^{2-} $\triangle SO_4^{2-}$=18%	SO_4^{2-} $\triangle SO_4^{2-}$=9%	Ca^{2+} $\triangle Ca^{2+}$=26%	SO_4^{2-} $\triangle SO_4^{2-}$ =16%	Ca^{2+} $\triangle Ca^{2+}$=29%	SO_4^{2-} $\triangle SO_4^{2-}$=12%
	Diseq. value	-1.449e-6	4.4096e-6	1.6711e-5	9.0567e-6	4.2063e-6	6.4265e-6	8.4965e-6
Present state	minx at eq.	Coesite	Calcite	Corundum Ferrite-Mg	$Fe(OH)_3$ Smithsonite	Corundum Dolomite-D	Magnetite	Siderite Chalcedony
		CristobaliteA	-	$ZnCO_3{:}H_2O$ $Fe(OH)_3$	Ferrite-Ca	Aragonite	Smithsonite	Cerusite Calcite
		-	-	-	-	-	-	Mordenite Smectte
	f(CO2)	-	$10^{-1.59}$	$10^{-1.2}$	$10^{-1.88}$	$10^{-2.35}$	$10^{-2.38}$	$10^{-1.54}$
	IS (Anglesite)	-0.2676	-	-2.46	-2.52	-2.95	-	-2.12
	IS (Cerusite)	-	-0.21	-1.00	0.21	0.27	-0.94	-0.09
	IS (Smithsonite)	-	-2.01	-0.62	-0.20	0.25	-0.16	-0.82
	IS (Wurtzite)	-	-	-	-	-	-	-
	IS (Franklinite)	-	-	-	-	-	-	-
	IS (Ferrite-Zn)	-	7.96	8.48	9.31	8.00	7.10	8.82
	IS ($ZnCO_3.H_20$)	-	-1.46	-0.08	0.34	0.82	0.45	-0.32
	IS (Sphalerite)	-	-	-	-	-	-	-
Equilib. state	minx precipitates	Qz Hematite	Dolomite-O	Hematite Sphalerite	$ZnCO_3{:}H_2O$	Dolomite-O	Dolomite-O	Hematite Qz
		-	Hematite Diaspore	$CoFe_2O_4$ Diaspore	Hematite Diaspore	$ZnCO_3{:}H_2O$ Diaspore	Hydrozincite Diaspore	Sphalerite Nontronite-Ca
		-	-	CdS Chalcocite	Cerusite	Hematite Cerusite	Hematite	$CoFe_2O_4$ Galena CdS
.nit.s tat	Eh /ENH in mV	100	-140	-90	-100	-120	-170	-118
	CO2	Pas de CV	0.04	0.05	0.0075	0.025	0.0075	0.025

(Temp. = temperature, TDS. = totale dissolved, init. stat Pro. = Probable initial state, Bal. elec. = Electrical Balance, diss. = dissolved)

2. Brittany

Name		SA 01	SA 02	SA 04	SA 05	SA 06	SA 07	SA 08	SA 09	SA 10	SA 11	SA 12	SA 13
Location of samples		Tremuson Mine		Huelgoat Mine			Poullaouen Mine			La Touche Mine			
		Cavalier shaft	TB. Boissières	Terrils Gallery	Lavoir Gallery	Charrioteurs Gallery	Pape II shaft	St Georg shaft	Other shaft ?	Dewater 40 m D	Dewater 80 m D	Dewater 40 m G	Red waterGaly
Date		3/5	3/5	4/5	4/5	4/5	4/5	4/5	4/5	5/5	5/5	5/5	5/5
Field Msmts.	Temp. in °C	12.6	14.3	11.2	11.1	11.5	14.2	13.9	13.5	11.9	11.8	12.2	13.5
	pH	6.42	6.98	6.02	5.8	6.27	?	6.13	4.68	6.39	6.43	3.82	5.79
	Eh in mV	434	383	433	370	403	476	469	520	480	433	703	356
	TDS. in mg/L	436	275	322	272	251	361	281	349	231	332	410	662
	O_2 dis. in mg/L	4.65	7,36-7,2	6.7	4.8	6.3	217	5.1	8.05	7.61	5.6	7.14	1.61
Anions in mg/L	HCO_3^-	107.4	63.4	20.1	24.4	47.0	61.0	62.8	4.9	24.4	68.9	0.0	27.5
	Cl^-	37.18	37,32	14.75	14.93	14.9	14.63	15.84	16,07	26.32	24.71	22.37	25.48
	NO_3^-	5.39	32.39	1.66	0.68	2.60	13.33	1.36	33.87	41.80	7.31	3.00	< 0.05
	SO_4^{--}	70.60	37.99	67.90	72.26	62.34	41.09	31.74	40.66	27.89	70.99	202.5	215.3
Cations in mg/L	Na^+	30.1	32.61	12.49	12.53	12.69	16.11	13.20	11.64	27.56	22.15	24.31	28.98
	NH_4^+	0.52	< 0.04	< 0.04	< 0.04	< 0.04	< 0.04	< 0.04	0.3	< 0.04	< 0.04	< 0.04	< 0.04
	K^+	2.51	2.83	1.48	1.66	1.52	1.92	2.74	3.79	1.96	2.61	3.97	2.27
	Mg^{++}	22.8	14.89	8.48	9.12	8.47	13.13	9.9	2.08	3.49	15.57	14.75	15.74
	Ca^{++}	30.48	24.50	24.70	24.87	34.97	21.47	16.24	16.64	27.03	37.69	36.12	44.01
Silice	SiO_2 aq in mg/L	30.23	16.16	15.51	16.94	15.76	15.96	8.46	10.20	25.13	19.50	44.42	25.92
Metals in µg/L	Fe	8.2	67.6	243.6	88.7	77.1	10.7	23.5	26.8	172.2	71.4	2 392	38 305
	Cu	22.3	2.6	5.9	15.7	11.6	4.4	< 1	13.5	< 1	< 1	118	< 1
	Pb	4.4	2.6	242	443	538	37.1	53.8	5 135	14.8	9.8	86.8	119
	Cd	3.2	< 0.2	21.9	25.5	16.5	56.1	18	64	< 0.2	0.9	38.1	43.4
	Zn	595	74	2 885	2 846	1 461	1 597	5 405	10 840	56	234	6 639	5 461
	Co	3.3	3.6	14.5	26.1	22.8	5.0	4.5	7.2	1.4	2.4	72.3	22.4
	Mn	1 500	462	217	410	464	895	525	141	32.8	147	1 004	573
	Ni	12.0	< 1	42.1	50.0	45.5	20.7	20.1	32.0	< 1	9.7	104.5	28.5
	Al four	14.3	5.9	14.4	25.5	9.3	3.8	406	384	4.7	15.2	8 939	2 758
Ionic balance %		10.8	15.1	18.3	14.3	20.5	18.4	14.3	5.6	18.9	20.6	12.2	26.3
Elec Bal	Poss/Imposs	SO_4^{2-} $\triangle SO_4^{2-}$=30%	imp. $\triangle SO_4^{2-}$=68%	SO_4^{2-} $\triangle SO_4^{2-}$=30%	SO_4^{2-} $\triangle SO_4^{2-}$=23%	imp. $\triangle SO_4^{2-}$=43%	SO_4^{2-} $\triangle SO_4^{2-}$ =30%	SO_4^{2-} $\triangle SO_4^{2-}$=29%	SO_4^{2-} $\triangle SO_4^{2-}$ =15%	Imp. $\triangle SO_4^{2-}$=76%	imp. $\triangle SO_4^{2-}$=52%	SO_4^{2-} $\triangle SO_4^{2-}$=18%	SO_4^{2-} $\triangle SO_4^{2-}$=15%
	Diseq. value	0.0014193	0.0005384	1.0814e-7	1.0275e-7	0.0005687	2.0014e-7	1.3869e-7	1.4974e-7	0.0004387	0.000774	3.342e-6	3.013e-6
Present state	minx at eq.	CristobaliteB	CristobaliteA	Coesite	Coesite Cerusite	Coesite	CristobaliteA	Chalcedony	CristobaliteA	Cronstedtite-7A Coesite	Albite Coesite	Beidellite-H	Coesite Gismondine
		Coesite Co_2SiO_4	Coesite	CristobaliteA	CristobaliteA	CristobaliteA	Coesite	CristobaliteA	Anglesite	$Fe(OH)_3$ CristobaliteB	Cronstedtite-7A	CristobaliteB Trevorite	Sanidine-high
		-	-	-	-	-	-	-	Chalcedony	Corundum	Celadonite Corundum	Jarosite-Na	CristobaliteB Scolecite
	f(CO2)	$10^{-1.46}$	$10^{-2.26}$	$10^{-1.75}$	$10^{-1.45}$	$10^{-1.67}$	$10^{-1.18}$	$10^{-1.33}$	$10^{-1.04}$	$10^{-2.01}$	$10^{-1.56}$	-	$10^{-1.05}$
	IS (Anglesite)	-	-	-1.28	-1.01	-1.16	-2.40	-2.34	-0.20	-	-2.92	-1.42	-1.29
	IS (Cerusite)	-1.08	-1.12	-0.22	-0.09	0.68	-0.56	-0.32	-0.83	-0.97	-0.90	-	-1.08
	IS (Smithsonite)	-2.29	-2.76	-2.70	-	-2.37	-2.35	-1.73	-	-	-2.96	-	-2.96
	IS (Wurtzite)	-	-	-	-	-	-	-	-	-	-	-	-
	IS (Franklinite)	-	-	-	-	-	-	-	-	-	-	-	-
	IS (Ferrite-Zn)	3.86	6.70	6.05	2.77	5.62	3.53	5.1	-1.03	5.47	5.02	-0.39	4.88
	IS ($ZnCO_3$,H_20)	-1.75	-2.24	-2.13	-2.27	-1.8	-1.83	-1.21	-	-	-2.40	-	-2.43
	IS (Sphalerite)	-	-	-	-	-	-	-	-	-	-	-	-
Equilibr. state	minx precipitates	Qz $CoFe_2O_4$	Qz Hematite	Qz Hematite	Qz $CoFe_2O_4$	Qz Cerusite	Qz $CoFe_2O_4$	Qz Diaspore	Qz Diaspore	Qz Hematite	Qz Nontronite -Ca	Qz Nontronite -H	Qz Diapore
		Hematite	CoFe2O4	CoFe2O4	-	CoFe2O4 Hematite	Hematite	Nontronite -Mg $CoFe_2O_4$	$CoFe_2O_4$	Nontronite -Ca $CoFe_2O_4$	Diaspore $CoFe_2O_4$	CoFe2O4	Nontronite -Ca $CoFe_2O_4$
Init. stat	Eh in mV		-150	-80	-70	-95	-82	-95	-5	-120	-105	40	-38
	CO2	0.25⇒Imp.	0.4⇒Imp.	0.42	0.18	Imp.	Imp.	Imp.	0.04	0.33⇒Imp.	Imp.	Imp.	Imp.

Remark: samples Sa 03 Sa 14 and Sc 01 correspond to the sampling od a spring and water from tailings.

3. Pyrenees + South Massif Central

Name		Py 01	Py 02	Py 03	Py 04	Py 05	Py 06	Py 07	Py 08	Py 09	Py 10
Location of samples		Aulus	Sentein	Pierrefitte				Arrens	St Salvy		Peyrebrune
		Interior Gallery	Rouge Gallery	Estaing Gallery level 3	Estaing Gallery level 4	Vieillemine Gallery 1154E	Couledous Intermediate Gallery	Gallery 992	Main Mine	Rouquis Gallery	New shaft Gallery
Date		29/6	26/6	30/6	30/6	30/6	01/07	01/07	2/7	2/7	2/7
Field Msmts.	Temp in °C	15.8	12.2	11.2	11.2	13.2	7	9.2	17	15.5	17.9
	pH	7.64	7.00	7	7.95	7.96	6.99	6.75	6.62	6.77	7.42
	Eh in mV	545	353	422	421	427	457	468	224	198	358
	TDS. in mg/L	258	156	264	257	189	270	121	1555	260	502
	O_2 diss. in mg/L	10.4	8.7	4.9	6.8	7.3	6.56	7	3	0.6	3.35
Anions in mg/L	HCO_3^-	169.6	59.8	69.5	140.3	117.1	95.2	53.7	136.6	97.6	237.9
	F^-	< 0.05	< 0.05	< 0.05	< 0.05	< 0.05	< 0.05	< 0.04	< 0.2	< 0.05	1.49
	Cl^-	7.2	1,48	1.23	1.29	1.03	1.41	1.02	4.84	5.87	9.87
	NO_3^-	6.78	11.12	2.25	5.21	0.94	0.71	0.41	< 0.2	< 0.04	< 0.1
	SO_4^{--}	7.05	32.65	107.2	39.15	17.83	82.14	18.56	889.3	50.15	114.9
Cations i mg/L	Na^+	5.18	0.98	2.20	1.41	0.34	1.08	0.97	19.51	8.00	26.82
	NH_4^+	< 0.04	< 0.04	< 0.04	< 0.04	< 0.04	< 0.04	< 0.04	0.29	< 0.04	< 0.05
	K^+	0.51	0.60	1.10	1.47	0.59	2.07	0.90	25.77	3.67	4.59
	Mg^{++}	18.3	3.42	7.78	9.52	3.85	4.68	1.72	54.85	6.62	37.11
	Ca^{++}	31.05	37.51	69.49	65.44	49.96	69.52	22.65	299.9	38.74	76.08
Silice	SiO_2 aq in mg/L	2.8	2.9	3.6	4.1	2.3	3.9	3.5	12.5	11.4	3.3
Metals in µg/L	Fe	8.9	22 620	42.5	13.3	28.9	39.7	38.8	5 640	11 360	23.4
	Cu	8.2	2.2	1.8	13.8	< 1	1.5	1.5	< 1	< 1	< 1
	Pb	6.6	2.8	3.5	< 1	< 1	2.2	2.8	2.3	2.3	14.7
	Cd	1.5	0.5	9.5	1.0	< 0.5	4.4	< 0.5	13.1	17.9	0.7
	Zn	62	51	4 495	380	104	1 234	38	7 143	3 340	432
	Co	1.8	1.4	2.5	2.1	< 1	1.6	< 1	23.8	4.9	2.9
	Mn	2.4	8.1	279	69.6	4.0	24.5	10.8	6 256	1 795	217
	Ni	< 1	< 1	14.8	< 1	< 1	< 1	< 1	27.5	9.4	5.8
	Al four	5.7	8.2	1.1	3.3	2.7	8.1	4.3	12.2	5.3	6.0
Ionic balance %		1.7	58.3	23.4	24.2	19.2	18.4	3.0	4.0	27.3	20.4
Elec. Bal	Poss/Imposs	Ca^{2+} $\triangle Ca^{2+}$=1%	Ca^{2+} $\triangle Ca^{2+}$=25%	Ca^{2+} $\triangle Ca^{2+}$=36%	Ca^{2+} $\triangle Ca^{2+}$=35%	Ca^{2+} $\triangle Ca^{2+}$=23%	Ca^{2+} $\triangle Ca^{2+}$=23%	Ca^{2+} $\triangle Ca^{2+}$=3%	SO_4^{2-} $\triangle SO_4^{2-}$=3%	Ca^{2+} $\triangle Ca^{2+}$=40%	Imp $\triangle Ca^{2+}$=64%
	Diseq value	-2.2251e-7	1.4191e-6	4.0951e-6	-6.1966e-7	-2.7008e-7	4.068e-6	1.1427e-7	1.2468e-6	3.0269e-6	0.0039101
Present state	minx at 'eq.	Magnetite	Quartz	Paragonite Tridymite	Co_2SiO_4 Tridymite	Montmor-K Aragonite	Laumontite Chalcedony	Tridymite Quartz	Smectite Kyanite	Clinoptilolite Siderite	Celadonite Quartz
		Calcite	Microcline	Quartz Chalcedony	Aragonite Ferrite-Ca Qz	Calcite	Tridymite Corundum	Chalcedony	$Fe(OH)_3$ CristobaliteA	Zn_2SiO_4 CristobaliteA	Calcite Cerusite
		-	K-Feldspar	-	Laumontite Chalcedony	Beidellite-K Qz	-	K-Feldspar Microcline	Ferrite-Ca	Celadonite	Cronstedtite-7A
	f(CO2)	$10^{-2.5}$	$10^{-2.28}$	$10^{-2.23}$	$10^{-2.59}$	$10^{-2.99}$	$10^{-2.1}$	$10^{-2.1}$	$10^{-1.55}$	$10^{-1.86}$	$10^{-2.05}$
	IS (Anglesite)	-	-	-	-	-	-	-	-2.979	-	-
	IS (Cerusite)	-0.49	-1.06	-0.94	-	-	-1.04	-1.13	-1.31	-1.17	-0.17
	IS (Smithsonite)	-1.76	-2.95	-1.021	-0.81	-1.39	-1.51	-	-1.10	-1.09	-1.03
	IS (Wurtzite)	-	-	-	-	-	-	-	-	-	-
	IS (Franklinite)	-	-	-	-	-	-	-	-	-	-
	IS (Ferrite-Zn)	6.47	11.31	7.61	7.65	8.07	6.39	4.77	7.98	9.44	7.90
	IS (ZnCO3,H20)	-1.27	-2.39	-0.45	-0.24	-0.85	-0.86	-2.74	-0.63	-0.59	-0.58
	IS (Sphalerite)	-	-	-	-	-	-	-	-	-	-
Equilib. state	minx precipitates	Dolomite-O Diaspore	Hematite	Qz Zn2SiO4	Dolomite-O Qz	Dolomite-O Qz	Qz	Qz	Imp a calc	Qz Hematite	Dolomite-O Diaspore
		Nontronite -M	Nontronite -C	Hematite	Zn2SiO4 Diaspore	Nontronite-Ca	Nontronite-C	Nontronite -C	-	Sphalerite Nontronite-C	Nontronite-M
		CoFe2O4	CoFe2O4	Nontronite-C CoFe2O4	Nontronite-C CoFe2O4	Diaspore	Diaspore CoFe2O4	Diaspore	-	-	CoFe2O4
Init. stat	Eh in mV	-205	<Eh mini	-140	-210	-215	-135	-135	-100	-130	-175
	CO2	0.005	0.00032	0.02⇒Imp.	0.003	0.003	0.001	Pas de CV	0.01⇒Imp.	0.001	0.017⇒Imp.

Remark: ions whose contents are always lower than the detection threshold are not given in this Table.

COMBINING CAVITIY SURVEY AND PRECISION DRILLING TO OPTIMIZE GALLERY EXPLORATION

CRABEIL Jean Paul

FLODIM- Immeuble "Le Rond Point" – 79 avenue Lattre de Tassigny – 04100 MANOSQUE - FRANCE

Email : foldom@wanadoo.fr

ABSTRACT: Combining underground survey and precision drilling in order to determine as well as possible an underground space and to appreciate its extension is a practice that remains under-developed. Maintaining such a partnership throughout a campaign of investigation works can be extremely valuable for underground exploration. This collaboration can help the field supervisor in charge to reduce random drilling in order to obtain useful wells, from which a survey specialist will get most information. Today, improvements in vertical or precision drilling have been reached and survey interpretation techniques allow visualizing and reconstructing underground space in real time or so, three dimensional viewers showing junctions to the network of galleries already built. Advancement of the global field operations can then be followed step by step and the ratio efficiency over cost wil likely be better.

KEYWORDS: Survey, cavity, Sonar, Laser, Imaging

RESUME : Pour apprécier au mieux la présence de vides souterrains et en reconnaître correctement les extensions, il serait souhaitable dans bien des cas de revoir le couple forage – mesures de cavité qui n'est pas toujours utilisé de manière optimale. Une coopération pendant la durée d'une campagne d'investigation pourrait en effet être particulièrement enrichissante pour reconnaître au mieux des espaces souterrains. Une telle collaboration permettrait en effet au responsable du chantier de réduire de manière significative le forage aléatoire grâce à l'utilisation immédiate du résultat des mesures. Aujourd'hui, des améliorations dans la verticalité ou la précision des forages sont bien réelles, de nouvelles techniques d'interprétation allégée permettent de reconstituer les espaces mesurés en temps réel ou presque et des outils informatiques de visualisation 3D permettent de gérer les raccords avec le réseau de galeries déjà construit. L'avancement du chantier global pourrait alors être suivi étape par étape et le rapport efficacité de la reconnaissance sur coûts engagés serait probablement bien meilleur.

MOTS-CLEFS : Mesure, cavité, Sonar, Laser, Imagerie

1. INTRODUCTION

To recognize and dimension underground spaces only accessible by wells, Laser and Sonar technics are usually carried out. The survey is then run with a Sonar measuring instrument for the cavities filled with water, brine, hydrocarbon or pressurized gas and with a Laser measuring probe together with an imaging system for those filled with air.

In such a confined space it is often impossible for a man to run in-situ exploration for three main reasons : depth and related pressure (depth of brine or storage cavities can be over 1000m),

safety (divers and cavers lives cannot be endangered) and cost (large diameter wells are very expensive).

Even, data acquisition with automatic systems can be more efficient and much faster than with a mine surveyor inside the cavern. Correlation with surface data will also be better.

Throughout this presentation, we will go through the main following topics :

- review Sonar and Laser acquisition and interpretation existing technologies,
- comment some of the difficulties that can be encountered during cavity surveys,
- present new developments made in data processing for reconstruction and visualization of cavities (shape, dimension and texture),
- analyze the concept of useful well which breaks right in the middle of a galery.
- conclude on the combination of cavity survey and precision drilling.

2. ACQUISITION AND INTERPRETATION TECHNIQUES CARRIED OUT.

2.1. Sonar measuring instrument and its systems (rotation, tilt, stabilization, orientation)

A Sonar instrument usually incorporates the following modules:

- Rotation system with adjustable steps,
- Tilt system with adjustable steps,
- Acoustic system with 2 or more transducers,
- A velocimeter for the speed of sound,
- Orientation system with fluxgate and gyroscope positioning devices,
- Calculator and transmission systems,
- Power supply.

2.2. Sonar emission and reception

Sonar emission is the result of a wave propagation hitting a cavity wall, if possible with a 2° to 3° solid angle which is determined by the frequency and the size of the transducer used. An Echo Sonar results from the propagation wave returning to the probe.

The quality of the reception of an echo Sonar is determined by the distance, the medium, the angle on the cavity wall and also on the texture on which it is reflected.

2.3. Laser measuring instrument and its systems (rotation, tilt, stabilization, orientation and imaging)

A Laser instrument usually incorporates the following modules:

- Emission-reception laser systems,
- Rotation and tilt systems,
- Lighting systems,
- Orientation and stabilization systems,

- Digital video camera,
- Digital still camera,
- Data transmission telemetry system.

2.4. Laser pulse

The laser beam is extremely thin. The quality of the returning signal depends on 3 factors:

- The angle upon which the laser beam enters in contact with the cavity wall,
- The distance to measure,
- The texture and the colors of the wall.

2.5. Cavity imaging

A panoramic view over 360° is obtained through a large number of digital pictures, which are combined. New software can assemble a 360° view within a few minutes.

2.6. Acquisition of measuring points

Acquisition software allows to gather data points in manual mode by single shots or in automatic mode by horizontal or tilted sections, to replay the digital signals and to ensure full storage of raw and interpreted data.

2.7. Griding and validation

The data points recorded are presented according to their orientation, checked and validated. The specialist forbids himself to leave the field acquisition without being sure that the griding is completed and that there is no unexplored area left in the cavity.

2.8. Data treatment and interpretation

From the cloud of points recorded during the acquisition, the specialist can proceed to the various steps required for interpretation:

1) Construction of vertical sections, azimuth per azimuth, interpreting points issued from horizontal or tilted cross-sections,
2) Calculation, from the set of sections, the main characteristics of the cavity : radius, diameters, orientations, surfaces and volumes,
3) Reconstruction of horizontal cross-sections, which are reprocessed from the vertical sections, taking into account specific shapes,
4) Wire-framed models,
5) Computer generated images presented with modern viewers.

3. Main difficulties that can be encountered during cavity surveying

3.1. Total reflections upon smooth surface (Sonar & Laser)

Sonar reflections upon an interface brine/air or brine/hydrocarbons will give points which aren't representative and which have to be corrected. A laser beam in a river won't supply good information either and some data points will have to be cancelled.

3.2. Temperature and velocity gradients (Sonar)

Similar to marine acoustics, if temperature and liquid saturation is not constant throughout the medium, then the direction of the sonar beam will not be straight.

3.3. Multiple echoes from one single shot (Sonar)

It is important to record the full trace of the echo because for one single shot there can be several burst of interest in the signal which all have to be integrated in the interpretation.

3.4. Detected anomalies during cavity imaging (Laser)

When running cavity imaging, one can often see natural anomalies such as stalactite, stalagmite, unconsolidated materials, free blocks, large fissures ... or unexpected materials or equipment (for revisited old mines) such as piles, casing ...

These heterogeneities may alter especially the laser data because acquisition is run through very thin rays.

3.5. Angle of incidence upon cavity walls (Sonar & Laser)

More the angle of incidence between the emission signal and the cavity wall is small, more the data acquisition becomes difficult. In case of sonar, the limit to run a correct survey is somewhere between 5 and 10 degrees. In case of laser, it also depends on the shape, the texture and the color of the cavity wall.

3.6. Instability of the magnetic North (Sonar)

We experienced many cases where the compass is disturbed during acquisition. Of course, this occurs when measurements are recorded through steel casings or in iron mines. But, we have also noticed that it can take place in cavities at unexpected depths and times without the presence of metallic particles. Theories concerning electrical streams seem to be at the origin of this disorder but the real causes remain unexplained. For sure, this situation is materialistic independent of the measuring equipment. To avoid this problem, gyros have to be implemented to get rid of magnetism instability.

3.7. Stabilization of Sonar and Laser equipments (Laser, Sonar and Sonar Gas)

Handling of the winch (pulling out and running in the equipment inside the cavity) produces torsion effects to the cable which holds the downhole tools. Therefore, systems have to be added to the probe in order to reduce the rotation speed of its body. Systems with wings such as for torpedoes exist for the Sonar instrument. Systems with stabilization gyros have to be integrated

for Gas Sonar or for Laser instruments in high cavities. Once stabilization is ensured, the specialist can start to run horizontal or tilted sections acquisition.

3.8. Particles in suspension during cavity leaching (Sonar)

When leaching a salt cavity, there are always insolubles which can be of any size. Most are thin particles that may take a long time to settle down. The sonar response is perturbed by these particles. When the density of these particles is considerable, the echoes become difficult to read. This is very frequent for the bottom survey of high size cavities.

3.9. Problems due to running water or even water curtain for Laser acquisition (laser)

Even if the cavity is dry, the well may intercept water saturated formations. Then, there can be water drops, water filets or even water curtains running along the casing.

3.10. Difficulty of obtaining 360° panoramic view (Imaging)

When the well is tangential to the wall of the gallery or when there is too much running water alongside the casing, then the lighting of the pictures is difficult to set and panoramic views may become impossible to obtain.

3.11. Measurements through casings (Sonar)

- Measurements through casings in air or gas cavities are impossible with standard methods.

- For Sonar, plastic casing does not lower the quality of the echoes but tilting is impossible.

Now, as it concerns measurements through one or two steel casings, the alteration of the signal is important and any of the following parameters may deteriorate considerably the survey :

. quality of the casing itself (corrosion, deposits, thickness)

. quality of the cavity wall(salt, percentage of insolubles, angle of incidence)

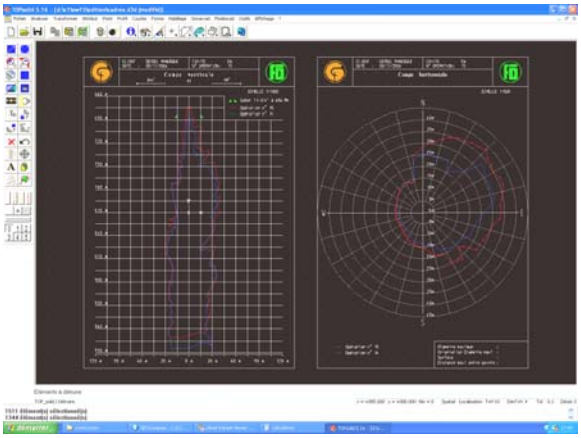
. centralizing of the probe within two casings

. presence of particles.

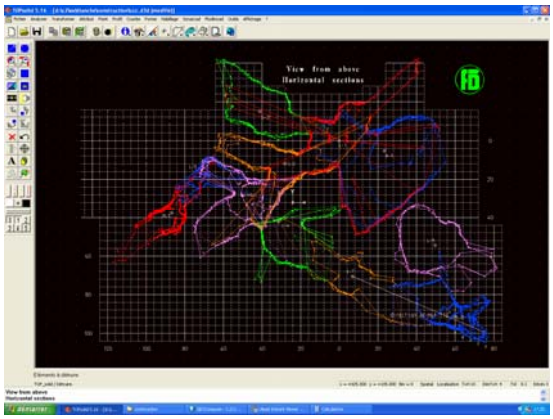
4. NEW DATA PROCESSING FEATURES

New developments made in data processing allow the specialist to reconstruct and obtain a three dimensional visualization of a cavity where he can study its shape, dimension and texture.

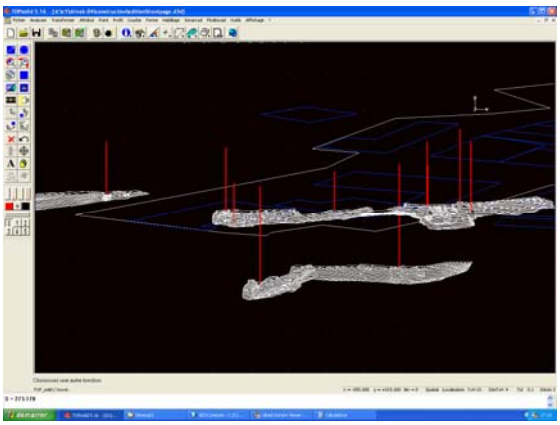
This is really useful to evaluate the results of each leaching phase. One can visualize the cavity before (in blue) and after (in red) the last leaching phase.



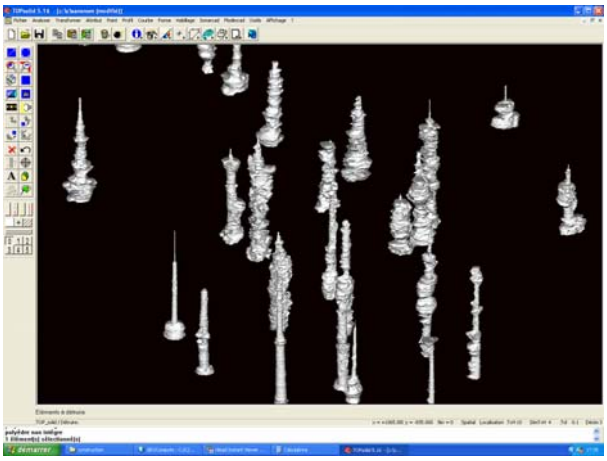
It also allows to follow step by step the advancement of underground spaces for real time mapping before filling up voids. The results of the previous single surveys are added every time in a different color in order to follow the construction of an underground space.



Associating drilling and measurements views can optimize global understanding of the investigation works and help to determine the best position of the next wells to be drilled.



Modern viewers offer the capability to manipulate three dimensional presentations of one or several cavities in space. User friendly, the viewer is helpful and interesting to realize quick and specific presentations or to pinpoint problems to be solved.



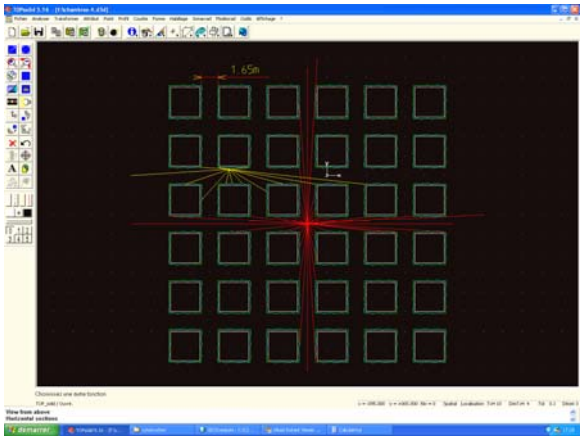
5. ANALYSING THE CONCEPT OF USEFUL WELL WHICH BREAKS RIGHT IN THE MIDDLE OF A GALLERY

The first Sonar or Laser single results should be a source of significant information at the beginning of investigation works. Indeed, if the deviation of a well can be minimized or controlled, then reaching the center of the gallery can bring not only more information concerning the gallery itself but also help to position the following wells which have to be drilled and which will become useful wells. Combining cavity survey with well positioning will improve the drilling efficiency and help to better recognize the network extensions.

Quite a few examples have showed that in spite of a signifiant percentage of voids, the percentage of drilled wells showing cleary a whole gallery remains low. A well reaching the edge of a cavity might not detect the true void even with weight recording equipments on the drilling rig and might conclude to a decompressed zone. Also, a well falling along side a gallery wall can be dangerous for the survey equipments and provide only partial information.

Let’s imagine a model of chambers and pillars. These pillars have a square base of 3 meters and galleries are 2 meters wide. The raw percentage of voids can be estimated at 64%, but the percentage of chances of finding a true void allowing the rotation and the tilt of the equipments is only of 57%. If the pillars do not have a perfect square base but have significant asperities or if the wall of the gallery is not vertical, then the percentage of reachable void may fall beneath 50%.

Now let’s take real cases of old coal mines where the upper galleries can be very narrow (from 1.2 to 1.5 meters wide). Even if the percentage of void is estimated at more than 50%, the percentage of chances to intercept a measurable void can drop down to a figure of less than 30%. Furthermore, the efficiency of an acquisition is greatly influenced by the position of a well inside a gallery. It is obvious that a well issuing in the intersection of two galleries will provide much more information than a well falling near a pillar (figure beneath).



6. CONCLUSION

From all the above topics, we come to the following points :

- Sonar and Laser in-situ data acquisition give reliable and precise results, even under difficult environment.

- New PC viewers (imaging and 3D) clearly show cavities or cavity networks and quickly give a real understanding of the underground conditions.

- Free voids have more chances to be detected and will give more information if drilling breaks in the middle of the cavity rather than alongside the wall (in this case, weight recording instruments are not always reliable or are difficult to interpret).

- Good vertical or directional drilling competences now exist in the market and geotechnical contracts should take into account the ability to run precision drilling and not only a price for a given amount of meters.

So, in order to determine as well as possible an underground space and to appreciate its extension and characteristics, we feel it is important to take under consideration a new working method where drilling and surveying competences are associated.

Such a collaboration in the field should will reduce random drilling in order to realize and obtain useful wells, from which a specialist can get most of its survey and transfer precise information to the project supervisor.

This should now be possible as new interpretation techniques allow to quickly reconstruct, visualize and run real time 3D maping, showing junctions to the existing network of galleries already built and because precision drilling should be able to obtain a high percentage of success if its surface position is well determined by the previous results.

Such an approach should help the supervisor in charge to follow up the field project step by step, to take the right decisions upon clear informations and to improve its ratio efficiency over cost.

LARGE SCALE APPLICATIONS OF COVERS WITH CAPILLARY BARRIER EFFECTS TO CONTROL THE PRODUCTION OF ACID MINE DRAINAGE

DAGENAIS Anne-Marie[1], AUBERTIN Michel[2], BUSSIÈRE Bruno[3], MARTIN Vincent[2]

[1] URSTM, 445 boul. de l'Université Rouyn-Noranda Québec - Canada, J9X 5E4; anne-marie.dagenais@uqat.ca

[2] INDUSTRIAL NSERC POLYTECHNIQUE-UQAT CHAIR, École Polytechnique, CP 6079, Succ. Centre-Ville, Montréal, Québec – Canada, H3C 3A7; michel.aubertin@polymtl.ca; vincent.martin@polymtl.ca

[3] INDUSTRIAL NSERC POLYTECHNIQUE-UQAT CHAIR, UQAT, 445 boul. de l'Université, Rouyn-Noranda, Québec - Canada, J9X 5E4; bruno.bussière@uqat.ca

ABSTRACT: Covers with capillary barrier effects (CCBE) have been used in recent years as part of the closure plan for mines having an acid mine drainage (AMD) problem. These covers can be used to limit oxygen and/or water migration. Different evaluation methods were used as part of a monitoring program to evaluate the efficiency of CCBE built at mining sites in Quebec, Canada and Nevada, USA. Results obtained from the monitoring program indicate these covers can, when properly designed and constructed, effectively reduce water infiltration in the case of a semi-arid climate, and limit oxygen migration in the case of more humid climatic conditions.

KEYWORDS: Covers, Acid mine drainage, Monitoring, Modelling, Behaviour and performance.

RÉSUMÉ : Des couvertures à effets de barrière capillaire (CEBC) ont récemment été utilisées pour la restauration de sites miniers ayant un problème de drainage minier acide (DMA). Ce type de recouvrement aide à contrôler la formation de DMA en limitant l'infiltration d'eau et/ou l'apport d'oxygène vers les résidus miniers réactifs. Différentes techniques d'auscultation ont été mises en place pour comprendre et évaluer le comportement de recouvrements construits sur différents sites miniers au Québec, Canada, et au Nevada, USA. Les résultats obtenus indiquent que des CEBC adéquatement conçues et construites peuvent effectivement réduire l'infiltration d'eau en climat semi-aride, alors qu'elles limitent efficacement la migration de l'oxygène en climat plus humide.

MOTS-CLEFS : Couverture, drainage minier acide, auscultation, modélisation, comportement et performance.

1. Introduction

Acid mine drainage (AMD) ensuing from the oxidation of sulphide minerals contained in mining wastes remains one of the critical environmental challenges for the mining industry. The oxidation reaction can cause acidification and heavy metal release in surface and ground water. To inhibit the acid formation, one must exert control on the constitutive elements (i.e. sulphide, water, or oxygen) of the oxidation reactions. Over the last decade or so, construction of cover with capillary barrier effects (CCBE), used to limit oxygen and/or water migration, has been a part of the closure plans for various mines with an AMD problem,

In a humid environment, studies have shown that preventing oxygen from reaching the sulphidic minerals is a practical approach for controlling AMD generation (*e.g.* SRK 1989; MEND 2001). A CCBE built for a humid environment can reduce oxygen ingress toward the underlying reactive waste rock or tailings, by maintaining one of its layers close to full saturation (e.g. Nicholson et al., 1989; Collin and Rasmuson, 1990). In arid and semi-arid climates, it is difficult to build a cover

system which maintains a layer close to saturation. Under these climatic conditions, the cover is subjected to extended dry periods, and the effect of evaporation (and evapotranspiration) would render it ineffective as an oxygen barrier (MEND, 2001). A CCBE built in a relatively dry climate should rather aim at controlling the influx of water to the reactive waste rock or tailings by diverting it or storing it for later evaporation. This type of cover is sometimes referred to as a "Store, divert and release" (SDR) cover (i.e. Zhan et al. 2001; Martin et al. 2005).

The optimization of the CCBE design (either for humid or arid climates) requires work involving simultaneous laboratory and field experiments combined with the application of numerical tools. This paper presents the advances made in this area through the authors' work using various experiments and tools, and referring also to recent cases where covers have been constructed on tailings impoundments and a spent leach pad (equivalent to a waste rock pile). First, a brief review of the fundamental principles governing the behaviour of CCBE is presented. It is followed by the description of laboratory and field work that lead to the construction of a full-scale CCBE. Applications of full-scale CCBE on actual mine sites are then presented. Finally, the conclusion sums up the challenges and the knowledge gained from the application of these covered systems.

2. Fundamentals of a CCBE

Capillary barrier effects appear when unsaturated flow occurs in layered soils of different hydraulic properties (Rasmuson and Erikson, 1986; Nicholson *et al*., 1989; 1991; Aubertin *et al.*, 1995, 1996, 1999). Under unsaturated conditions, the coarse-grained soil placed under a fine-grained material tends to drain easily, hence reaching a low volumetric water content θ. At low θ values, such coarse-grained soils (sand or gravel) have a low unsaturated hydraulic conductivity that limits downward movement of water which can be present in the fine-grained soil layer above. The fine textured soil then acts as a reservoir where water is stored by capillary forces. A more detailed description of capillary barrier effects can be found in Nicholson et al. (1989), Collin and Rasmuson (1990), Morel-Seytoux (1992), Aubertin et al. (1995, 1996), Khire et al. (1999), and Bussière et al. (2003a).

Figure 1 is a schematic illustration of a CCBE used in a humid climate. These covers usually contain three to five layers made of different materials. Each layer has to play one (or more) specific role(s). In Figure 1, the coarse-grained soil (support layer or capillary break layer) placed underneath the fine-grained soil (moisture-retaining layer) limits downward movement of water and prevents desaturation of the moisture-retaining layer. The top coarse-grained material placed over the fine-grained soil layer acts as a drainage layer and also limits loss of water by evaporation from the surface. The other two layers (protection and surface layer) are protective layers against erosion and biointrusion (Aubertin et al., 1995). In the system, the water retention layer is designed to maintain a high degree of saturation at all time. The diffusion of gas (oxygen) through this nearly saturated layer is low enough to prevent the significant production of AMD (Nicholson *et al*., 1989; Collin and Rasmuson, 1990; Yanful, 1993; Aubertin *et al*., 1995, 1999; Mbonimpa *et al*., 2003). Example of such CCBE applications can be found in Yanful et al. (1993, 1999), Aubertin et al. (1997a, 1999), Ricard et al. (1997, 1999), Khire et al. (1999), Lundgren (2001), Bussière et al. (2003a), and Dagenais et al. (2001, 2005). Some of these cases are described in the following.

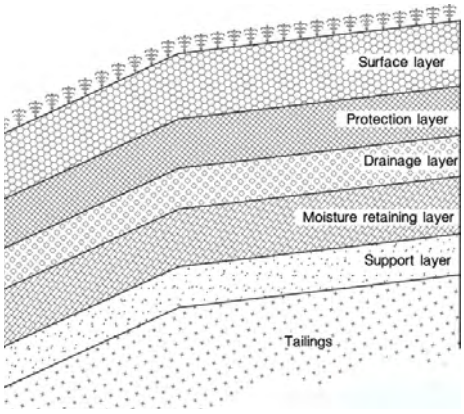


Figure 1. Typical configuration of a CCBE used to limit oxygen ingress to the reactive tailings (Aubertin et al., 1995).

Under arid or semi-arid climatic conditions, SDR covers use the capillary barrier effect created by the superposition of materials of different hydraulic properties to limit the downward flow of water at their interface. Again here, downward infiltration is limited by the placement of a fine-grained material layer over a coarser material. During a storm event on a flat area, the infiltrating water is stored in the fine grained layer for later evaporation release (e.g. Wilson et al. 1995; Williams et al. 1997). For an inclined cover, the water can also be diverted down the slope along the interface in the layered system (Ross, 1990; Stormont, 1995, 1996; Harries et al. 1997; Zhan et al., 2001; Bussière et al., 2003b; Martin et al., 2005; Aubertin et al. 2006).

Different techniques can be used to evaluate the efficiency of a CCBE. Monitoring the cover' hydrogeological behaviour is done with sensors measuring the volumetric water content θ and suction ψ, placed in the different layers of the cover (Yanful et al., 1993; Wilson et al., 1995; Aubertin et al., 1995, 1997a, 1999; Khire et al., 1999; Zhan et al., 2001). For a cover built in a humid climate, field measurements are expected to show low θ in the capillary break layer and a high θ in the moisture-retaining layer. The suction (negative pressure) ψ in the moisture-retaining layer should not exceed the material air entry value (i.e. suction at which the largest pores start to desaturate). For a SDR cover, the water content θ should remain low in the coarse grained material serving as a capillary break, while it can vary in the storage layer. Other monitoring techniques can involve the measurement of water infiltration and water quality. Also, for a CCBE used as an oxygen barrier, the measurement of the oxygen gradient or flux through the cover can provide valuable information on its actual efficiency (e.g. Elberling et al. 1994; Aubertin et al. 1995, 1999; Bews et al., 1997; Bussière et al., 2002, Mbonimpa et al., 2002, 2003).

3. Laboratory and field experiments

A study, spanning over more than ten years, was conducted by the authors on the hydrogeological behaviour of CCBE aiming at a reduction of AMD generation (Aubertin et al., 1995, 1997b, 1999; Bussière et al. 2003a, 2005). The initial phase of the project started with the hydro-geotechnical properties characterisation of various tailings. The favorable hydraulic properties (water-retention properties and hydraulic conductivity) of non acid generating tailings make them a very effective material to be used in a CCBE, as the moisture retaining layer, to limit oxygen migration (e.g. Aubertin et al. 1995, 1997a; Aachib et al. 1998).

3.1. Laboratory testing

Column tests combined with 1D numerical simulation were used to study the hydrogeological and geochemical behaviour of layered systems, in which the capillary layer was made of clean (non acid generating) tailings. The efficiency of these systems to limit AMD generation has been evaluated by comparing control columns where reactive tailings were covered by a layered system to a reference column containing only reactive tailings (Aubertin et al., 1995, 1997b; Aachib et al., 1998). Figure 2a presents the laboratory experimental set-up.

The column tests results show that the tailings layer, placed between two sand layers, stayed close to saturation, even during dry periods lasting up to 60 days. This high water content reduced the oxygen flux to the tailings underneath. The column tests also helped validating the numerical calculations on water distribution, as shown in Figure 2b. Leachate collected from the columns confirmed the efficiency of the CCBE as pH remained high and sulphates values remained low for the control column (with cover) compared to the reference column, as can be seen in Figure 3.

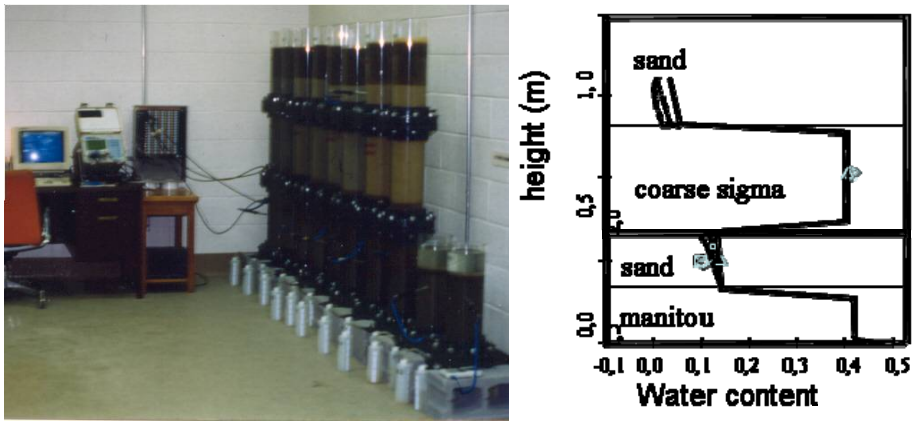


Figure 2. a) Experimental set-up for the column tests, and b) results from monitoring (symbols) and simulation (lines) (adapted from Aubertin et al., 1997b; Aachib et al. 1998).

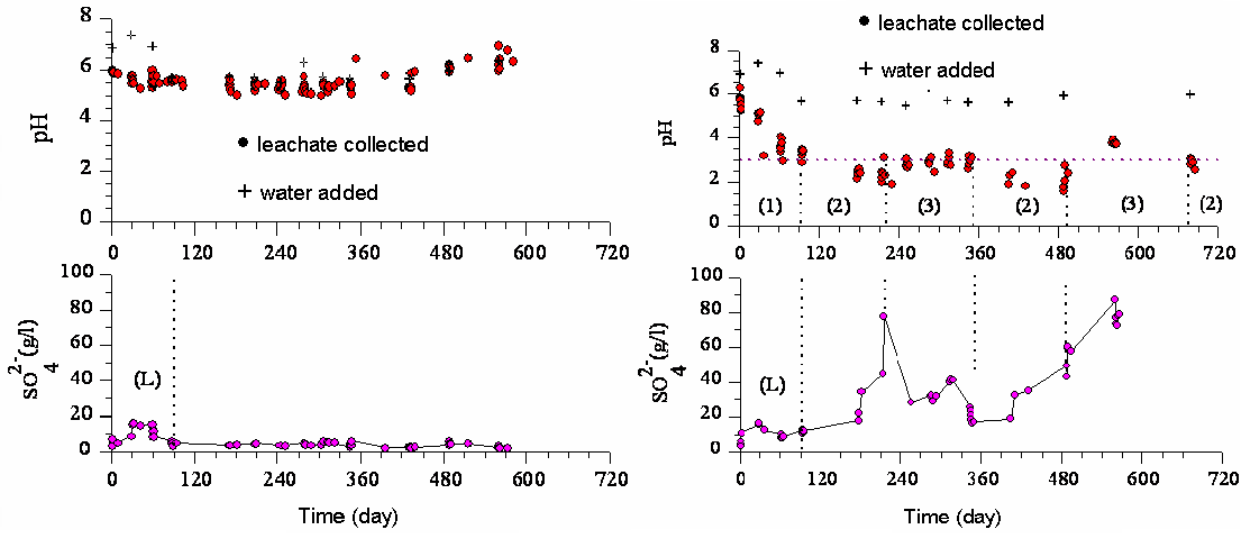


Figure 3. a) pH and sulphate from control column b) pH and sulphate from reference columns (Aubertin et al., 1997b).

3.2. Field testing

To complement the previous laboratory studies, experimental cells were constructed in 1995 to evaluate, on a larger scale and under more realistic conditions, the performance of CCBE using silty materials as the moisture-retaining layer (Aubertin et al., 1999; Bussière, 1999). Figure 4a presents a view of the cells at the end of the construction phase; the site is located on the Manitou mine site, near Val-d'Or, Québec.

The results showed the capillary barrier effects necessary to maintain a high degree of saturation in the moisture-retaining layer were present in all cells for the four years of monitoring. Figure 4b presents the low θ of the sand layer creating the capillary effects and the high θ in the moisture retaining layer for the year 1998. In figure 5, water quality of the leachate confirmed the efficiency of the CCBE to limit acid mine drainage production: the pH was between 6 and 7 for the covered cells compared to a pH lower than 3 for the control cell. Sulphates and metals loading were reduced by more than two orders of magnitude in the covered cells. The information gathered from these field plots over 4 years confirmed the efficiency of CCBE to control AMD production.

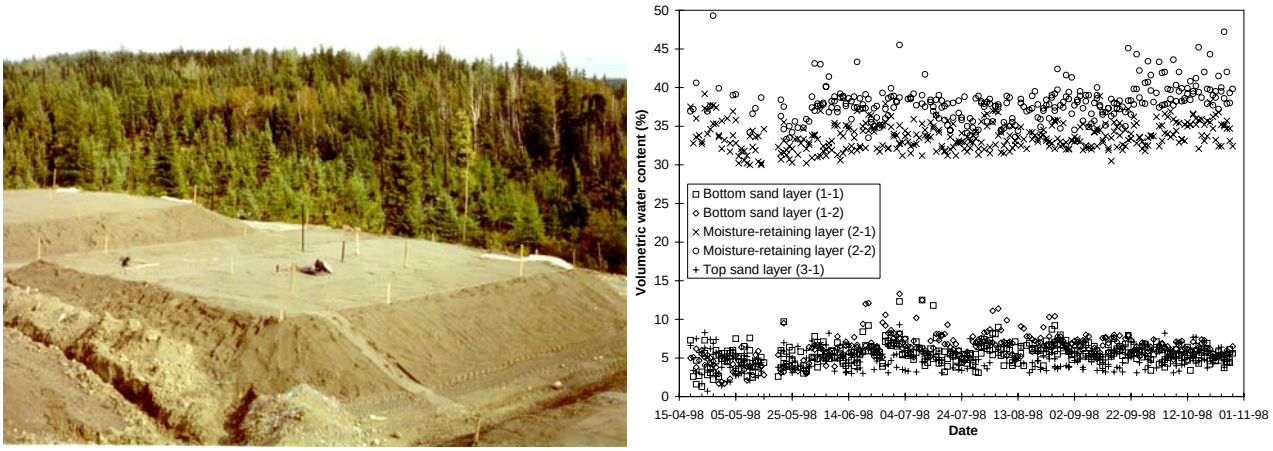


Figure 4. a) Experimental cells constructed at the Manitou mine site; b) value of θ measured in 1998 in the CCBE of one of the experimental cell (after Aubertin et al. 1999 and Bussière, 1999; see also Bussière et al., 2005).

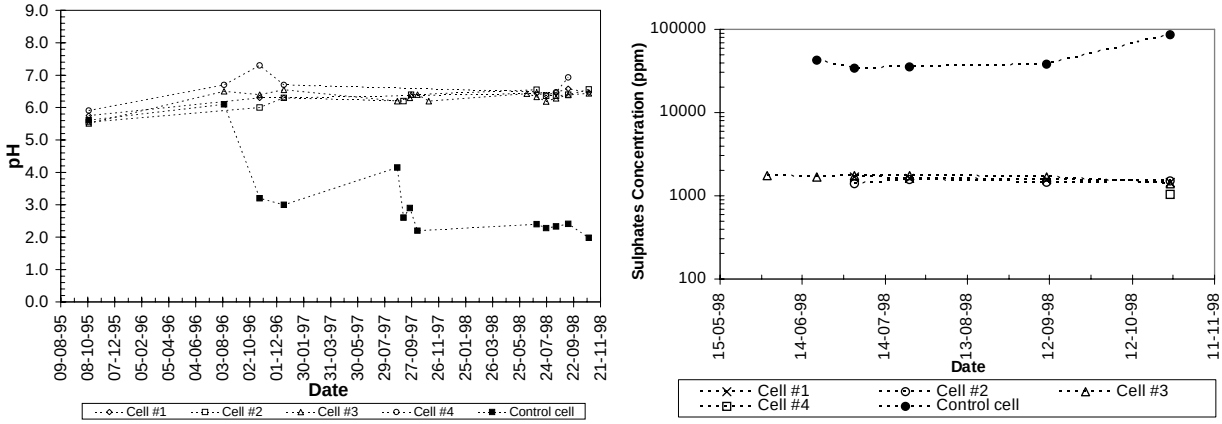


Figure 5. Water quality collected at the bottom of cells a) pH b) Sulphates concentration (Bussière et al., 2005).

4. Large scale applications of CCBE

As mentioned above, CCBE have been shown, through laboratory column tests and in situ test cells, to be a practical means of preventing AMD generation. These experimental evaluations have lead to the application of large scale covers at various locations over the past years. Three cases are described here.

4.1. LTA mine site

The cover constructed at the LTA site is one of the first large scale covers with capillary barrier effects constructed in a humid climate on an acid generating tailings impoundment. The LTA site is located near Malartic, in the Abitibi region (Québec). This 60-hectare cover is made of three layers: a capillary break layer 0.5 m thick, a moisture-retaining layer of 0.8 m thick made of non acid-generating tailings and a 0.3 m thick protection layer put on top. The design objective was to reduce oxygen migration through the CCBE. The design objective was to obtain a degree of saturation $S_r \geq 85\%$ (for a porosity n of 0.44, this corresponds to θ of about 37%) in the moisture-retaining layer (Ricard et al., 1997, 1999; Bussière et al, 2003c). After its construction in 1996-1997, instruments were installed in the CCBE to monitor its response over time.

Two different types of hydraulic behaviour have been observed on the nearly flat area of the LTA site: capillary barrier effects are active in the cover where the water table is deep, and the cover is nearly saturated by capillary rise when the phreatic surface is close to or in the CCBE. For instance, Figure 6 shows θ values obtained at the monitoring station CS96-1 where the water table is deep, and at station CS96-5 where the water table is high. One can see that θ of the sand layer for this last station is large compared to the one measured in the sand layer at station CS96-1. In both situations, the degree of saturation in the moisture-retaining layer remains above 85% (Bussière et al., 2003c).

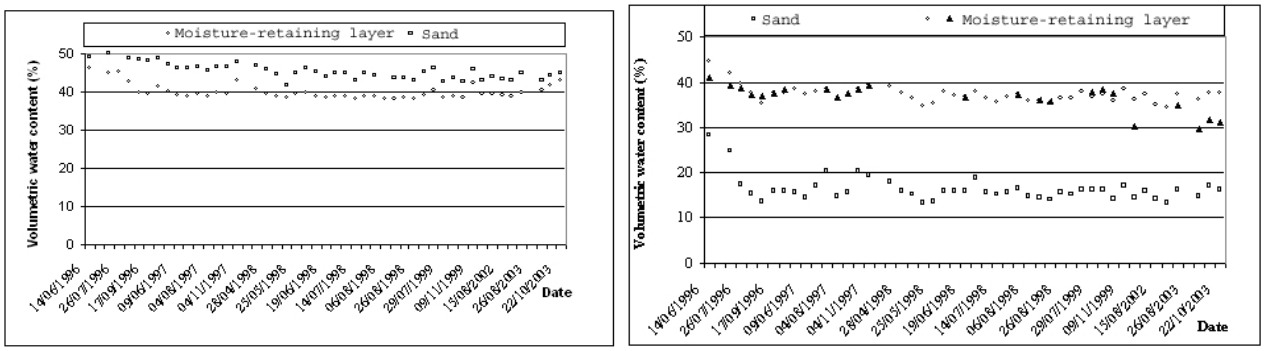


Figure 6. Volumetric water content measured in the sand layer and the moisture-retaining layer at the LTA site a) station CS96-5 b) station CS96-1 (adapted from Bussière et al., 2003c).

A small aerial portion of the cover constructed on the LTA site is located on the sloping side of the tailings dams. CCBE on an inclined slope are affected by both horizontal and vertical flow. It is more difficult to maintain the desired θ in the moisture-retaining layer along the upper parts of a slope, and this possible desaturation can influence the performance of the cover (Aubertin et al. 1997b). To study this subject further, a laboratory model was constructed and 2D simulations were conducted. Results showed a significant effect of the geometry on pressure and water distribution. This effect is illustrated in Figure 7, which shows θ values measured at the base and at the top of a sloping two layer system (obtained from measurements during inclined box tests ; Bussière, 1999; Bussière et al., 2000, 2003a). A numerical study based on the LTA site was also performed to quantify the effects of geometry on the performance of the CCBE. The results showed the possible

desaturation that may sometimes occur near the upper part of the cover along the slope. These results have led to the concept of suction breaks aimed at reducing the possible decrease in the degree of saturation in the cover (Aubertin et al. 1997b). This approach was tested following the construction of test areas on the sloping cover, where hydraulic breaks have been added. Part of this work is still ongoing. Results obtained to date on the LTA site, combined with numerical calculations, have confirmed the positive contribution of such suction breaks on the moisture distribution and on the ability of the cover to control the oxygen flux (Bussière et al. 2000; Maqsoud et al. 2005).

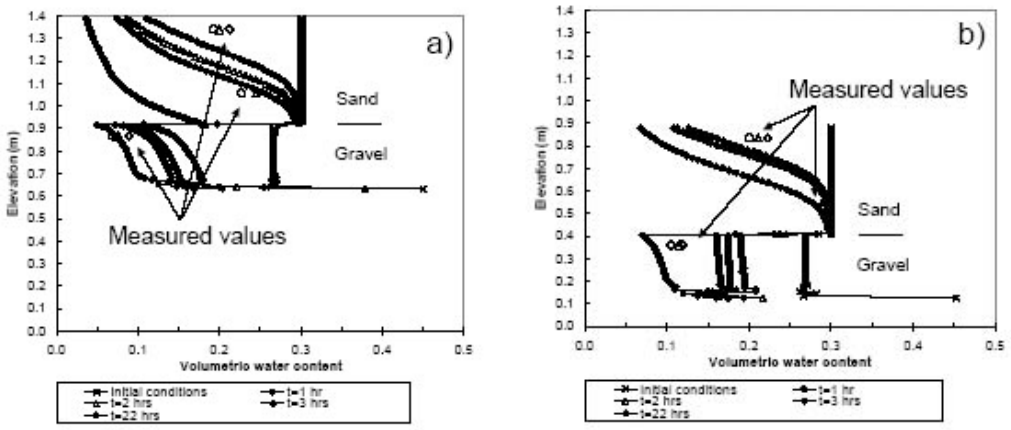


Figure 7. Measured (symbols) and calculated (lines) values of θ taken at a) top of the slope b) bottom of the slope in an inclined layered system tested in the laboratory (Bussière, 1999; Bussière et al., 2003a).

4.2. Lorraine mine site

A cover fairly similar to the one constructed on the LTA site was used at the Lorraine site, located in the Témiscamingue area, Québec. The 12-hectare CCBE built on this site is composed of three layers: a 0.3 m thick capillary break layer; a 0.5 m thick moisture-retaining layer; a protection layer 0.3 m thick. The targeted oxygen diffusion flux value was set at 20 to 40 g/m^2/year, which is comparable to that of a stagnant water cover. For steady state conditions using Fick's first law, this corresponds to an effective diffusion coefficient D_e of 1.1×10^{-9} to 2.2×10^{-9} m^2/s, which translates into a degree of saturation of about 88 % for the fine grained soil (porosity of 0.38) in the water retention layer serving as the oxygen barrier (Nastev and Aubertin, 2000; Dagenais et al., 2001, 2005).

The layered cover was also instrumented after its construction. The volumetric water content and suction measurements, made between 1999 and 2003, show that the capillary barrier effects are effective where needed on the site (i.e., where the water table is below the tailings surface). For instance, Figure 8 shows that for a representative monitoring station (B-5), measured suctions in the lower sand layer ranged from 2 to 12 kPa, draining this coarse material to a degree of saturation as low as 20 %. Suctions measured in the silt typically vary from 0 to 25 kPa, which is below its air entry value; the degree of saturation measured in situ is typically above 88%, although it can vary from 80 to 100 % at different locations (Dagenais et al., 2001, 2005; Dagenais, 2005).

The CCBE performance at the Lorraine site was also examined in term of reducing the oxygen flux diffusing to the reactive tailings. Oxygen fluxes were calculated, with Fick's laws, using the effective diffusion coefficient D_e determined from modified oxygen consumption tests done at 7 different locations on the cover in 2000 (Dagenais, 2005). Some of these results are presented in Table 1; these show that the oxygen flux through the CCBE varies from 0.2 to 39 g/m^2/year. The

flux calculated from the θ measured at the test stations are also presented in Table 1. Both estimation methods give results that are fairly close to each other, with fluxes that are almost always inferior (or very close) to the targeted flux adopted for the cover design (see details in Dagenais, 2005).

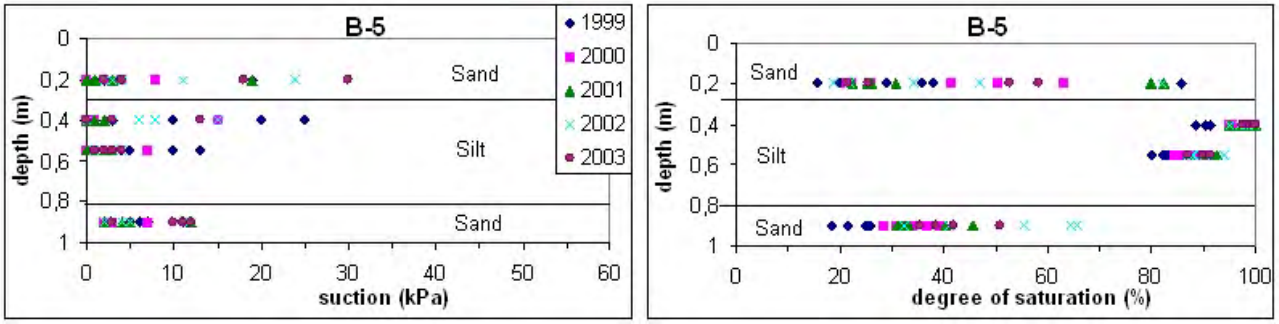


Figure 8. Measured values for suction and degree of saturation in the Lorraine mine site cover (station B-5).

Table 1. Oxygen flux (g/m^2/year) calculated from the modified oxygen consumption tests and from volumetric water content measurements (Dagenais, 2005).

Test	2	3	4	5	6	7	8
Modified oxygen consumption test	39	0.2	1.9	9.4	10.6	5.6	29
Volumetric water content	6.5	0.3	0.9	0.2	0.3	0.1	3.2
Design flux	20 - 40						

4.3. Goldstrike mine site

A simple cover was installed on the AA heap leach pad of the Barrick Goldstrike mine, located near Elko, Nevada. This SDR cover uses the capillary barrier effects to limit the downward flow of water into the leached ore (a material similar to waste rock). Following a series of laboratory tests and of numerical analyses, the cover was built on the leach pad. Instruments were added to examine the cover performance under natural and irrigated conditions. The SDR cover is made a 0.6 m thick monolayer of fine grained material (name Carlin silt). Figure 9 shows θ measurements in the cover (at 15 cm, 45 cm) and in the leach pad (at 75 cm, 120 cm) for one of the test cells; the amount of water added (large amount, in this case) during the irrigation test is also shown. The infiltration tests performed indicate that the cover can hold significant moisture during a wetting period; for most cases, there was little change in the moisture in the leach pad despite the increase water content in the cover (Zhan et al., 2001). However, for very larger water inflow, the diversion capacity can be exceeded, as illustrated in Figure 9 (i.e. after le large addition of water early in the test).

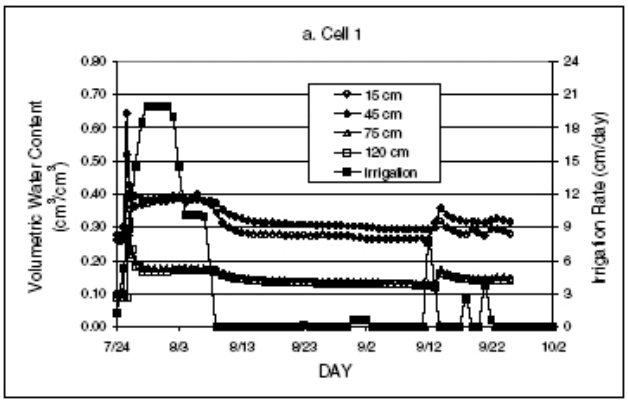


Figure 9. Measured water content at various depth and applied irrigation rate a) cell 1 b) cell2 (after Zhan et al., 2001)

Numerical simulations in 2D have shown that the SDR cover response is sensitive to many factors, such as variations in the material properties, dump slope angle and length, potential evaporation over the area, and precipitation duration and intensity (e.g. Bussière et al., 2003b; Martin et al., 2005; Aubertin et al. 2006). These analyses have also shown that the diversion capacity of the monolayer cover can be exceeded following very large precipitation events, in accordance with the data obtained in situ (as shown in Figure 9). To handle such extremely wet conditions, a multilayered SDR cover can be more suited as it can divert larger volumes of water on a longer diversion length. Examples of such alternate design for SDR covers are presented in Martin et al., (2005) and Aubertin et al. (2006).

5. Conclusion

The application of covers with capillary barrier effects (CCBE) to mine sites having an acid mine drainage problem was developed in recent years. It was shown that well designed CCBE can be effective in controlling the water and/or oxygen flux to the reactive tailings and waste rocks underneath. The process leading to an optimum design is an iterative one which includes laboratory material characterisation, physical modelling, validated numerical calculations for parametric study, and field test plots. Various materials and configurations can be used in covers. The key element is the difference in the hydraulic properties of the chosen materials, which is required to create the capillary barrier effects at the interface between materials with different texture.

Once constructed, monitoring programs are required for a CCBE to assess its hydrgeological response and to evaluate its effectiveness in limiting downward water flow and/or oxygen flux. Monitoring results form the LTA and Lorraine sites, located in Québec, indicate that capillary barrier effects are well developed in these covers, which can thus maintain the moisture-retaining layer close to saturation (S_r generally superior to 85 %). This is required to reduce the oxygen flux at acceptable levels through a cover built for a wet climate. The oxygen fluxes estimated from volumetric water content or from the modified oxygen consumption tests have been shown to be lower than 40 g/m^2/year, a flux comparable to that of a water cover. The field and modelling data obtained on the inclined portion of the LTA cover also illustrate the important role of the slope angle and length on the water distribution in such layered systems. On the other hand, the measurements made on the sloping cover at the semi-arid Barrick Goldstrike mine site showed that it is effective in diverting water along the sloping area. The results shown here, and in other referenced work, thus indicate that many factors, such as cover configuration, material properties, layer thickness, slope length and angle, and climatic conditions may influence the efficiency of the cover. These must be taken into account when assessing the reclamation option.

6. References

Aachib, M., Aubertin, M., Chapuis, R. P. (1998). *Essais en colonne sur des couvertures avec effets de barrière capillaire,* In Proc. 51st Canadian Geotechnical Conference, Edmonton, Vol. 2, 837-844.

Aubertin, M., Chapuis, R.P., Bouchentouf, A. and Bussière, B. (1997a). *Unsaturated flow modeling of inclined layers for the analysis of covers*. Proc. 4th ICARD, Vancouver, Vol. 2, 731-746.

Aubertin, M., Aachib, M., Monzon, M., Joanes, A.-M., Bussière, B., Chapuis, R. P. (1997b). *Étude de laboratoire sur l'efficacité des barrières de recouvrement construites à partir de résidus miniers*, Report NEDEM/MEND, Project 2.22.2b. Ottawa..

Aubertin, M., Bussière, B., Aachib, M., Chapuis, R. P. (1996). *Une modélisation numérique des écoulements non saturés dans des couvertures multicouches en sols*, Hydrogéologie, 1, 3-13.

Aubertin, M., Bussière, B., Monzon, M., Joanes, A.-M., Gagnon, D., Barbera, J.-M., Aachib, M., Bédard, C., Chapuis, R. P., Bernier, L. (1999). *Étude sur les barrières sèches construites à partir de résidus miniers. Phase II : Essais en place*, Report NEDEM/MEND Project 2.22.2c, Ottawa.

Aubertin, M., Chapuis, R. P., Aachib, M., Bussière, B., Ricard, J.-F., Tremblay, L. (1995). *Évaluation en laboratoire de barrières sèches construites à partir de résidus miniers*, Report NEDEM/MEND, Project 2.22.2a, Ottawa.

Aubertin, M. Cifuentes, E., Martin, V. Apithy, S. Bussière, B. Molson, J. Chapuis, R.P. Maqsoud A. (2006).*An investigation of factors that influence the water diversion capacity of inclined covers with capillary barrier effects.* Proc. Unsaturated Soils 2006, Arizona (to be published).

Bews, B. E., O'Kane, M. A., Wilson, G. W., Williams, D., Currey, N. (1997). *The design of a low flux cover system, including lysimeters, for acid generating waste rock in semi-arid environments*, Proc. 4th ICARD Vancouver, Vol. 2, 747-762.

Bussière, B. (1999). *Étude du comportement hydrique de couvertures avec effets de barrière capillaire inclinées à l'aide de modélisations physiques et numériques*, Ph.D. Thesis, Mineral Engineering. École Polytechnique de Montréal, Canada.

Bussière, B., Apithy, S., Aubertin, M., Chapuis, R. P. (2003b). *Diversion capacity of sloping covers with capillary barrier effect*, Proc. 56th Annual Conference and 4th Joint IAH-CNC and CGS Groundwater Specialty Conference, CD-Rom, Winnipeg.

Bussière, B., Aubertin, M., Chapuis, R. P. (2000). *The use of hydraulic breaks to limit desaturation of inclined capillary barriers*, Proc. 53th Canadian Geotechnical Conference, Montréal.

Bussière, B., Aubertin, M., Chapuis, R. P. (2003a). *The Behavior of Inclined Covers Used as Oxygen Barriers*, Canadian Geotechnical Journal, Vol. 40, 512-535.

Bussière, B., Aubertin, M., Mbonimpa, M., Benzaazoua, M. Molson, J. (2005). *In situ test cells for the evaluation of silty covers with capillary barrier effects*, submitted for publication.

Bussière, B., Dagenais, A.-M., Mbonimpa, M., Aubertin, M. (2002). *Modification of Oxygen-Consumption Testing for the Evaluation of Oxygen Barrier Performance*, Proc. 55th Canadian Geotechnical Conference and 3rd joint IAH-CNC and CGS Groundwater Specialty Conference, Niagara Falls, 139-146.

Bussière, B., Maqsoud, A., Aubertin, M., Martschuk, J., McMullen, J., Julien, M. (2003c). *Results from the monitoring program at the LTA site: hydraulic behavior of the cover*, Proc. CIM Conf. (CD-ROM), Montréal.

Collin M., Rasmuson, A. (1990). *Mathematical modeling of water and oxygen transport in layered soil covers for deposits of pyritic mine tailings,* Acid Mine Drainage : Designing for Closure. GAC-MAC Annual Meeting, 311-333.

Dagenais, A.-M. 2005. *Techniques de contrôle du drainage minier acide basées sur les effets capillaires*. Ph.D. Thesis. École Polytechnique de Montréal.

Dagenais, A.-M., Aubertin, M., Bussière, B., Bernier, L., Cyr, J. (2001). *Monitoring at the Lorraine Mine Site: a Follow-Up on the Remediation Plan*, Proc. National Association of Abandoned Mine Land Programs Annual Conf. : Land Reborn (CD-Rom), Athens, Ohio..

Dagenais, A.-M., Aubertin, M., Bussière, B., Cyr, J. (2005). *Performance of the Lorraine mine site cover to oxygen migration*, Proc. SME Annual Meeting, (CD-Rom), Salt Lake City.

Elberling, B., Nicholson, R. V., Reardon, E. J., Tibble, P. (1994). *Evaluation of Sulphide Oxidation Rates: a Laboratory Study Comparing Oxygen Fluxes and Rates of Oxidation Product Release*, Canadian Geotechnical Journal, 13, 375-383.

Harries, J. R., Levins, D., Ring, B., Zuk, W. (1997). *Management of Waste from Uranium Mining and Milling in Australia*, Nuclear Engineering and Design, 176 (1-2), 15-21.

Khire, M. V., Benson, C. H., Bosscher, P .J (1999). *Field Data from a Capillary Barrier and Model Predictions with UNSAT-H*, Journal of Geotechnical and Geoenvironmental Engineering, 125 (6), 518-527.

Lundgren, T. (2001). *The Dynamics of Oxygen Transport into Soil Covered Mining Waste Deposits in Sweden*, Journal of Geochemical Exploration, 74, 163-173.

Maqsoud, A. Bussière, B. Mbonimpa, M. Cissokho, F. Aubertin, M. (2005) *Suction break to control slope-induced moisture variation in layered covers.* Proc. Can. Geot. Conf. (CD-Rom), Saskatoon**.**

Martin, V., Aubertin, M., Zhan, G., Bussière, Chapuis, R. P. (2005). *An investigation into the hydrological behaviour of exposed and covered waste rock dumps*, Proc. SME Annual Meeting, (CD-Rom),Salt Lake City.

Mbonimpa, M., Aubertin, M., Aachib, M., Bussière, B. (2003). *Diffusion and Consumption of Oxygen in Unsaturated Cover Materials*, Canadian Geotechnical Journal, 40, 916-932.

Mbonimpa, M., Aubertin, M., Dagenais, A.-M., Bussière, B., Julien, M., Kissiova, M. (2002). *Interpretation of Field Tests to Determine the Oxygen Diffusion and Reaction Rate Coefficients of Tailings and Soil Covers*, Proc. 55th Canadian Geotechnical Conference and 3rd joint IAH-CNC and CGS Groundwater Specialty Conference, Niagara Falls, 147-154.

MEND (2001). *MEND Manual, Vol. 4- Prevention and Control*, Report 5.4.2, Ottawa.

MEND (2004) *Design, construction and performance monitoring of cover systems for waste rock and tailings*, Report 2.21.4, Ottawa.

Morel-Seytoux, H. J. (1992). *The capillary barrier effect at the interface of two soil layers with some contrast in properties*, Hydrowar Report 92.4, Hydrology Days Publ., Atherton, CA.

Nastev M., Aubertin M. (2000). *Hydrogeological modelling for the reclamation work at the Lorraine mine site Québec*, Proc. 1st Joint IAH-CNC-CGS Groundwater Specialty Conference, Montréal, 311-318.

Nicholson, R. V., Akindunni, F. F., Sydor, R. C., Gillham, R. W. (1991). *Saturated Tailings Covers above the Water Table: the Physics and Criteria for Design*, Proc. 2nd Int. Conf. on Abatement of Acidic Drainage, Montréal, Vol. 1, 444-460.

Nicholson, R. V., Gilham, R. W., Cherry, J. A., Reardon, E. J. (1989). *Reduction of acid generation in mine tailings through the use of moisture-retaining cover layers as oxygen barriers*, Canadian Geotechnical Journal, 26, 1-8.

Rasmuson A., Erikson J. C. (1986). *Capillary barriers in covers for mine tailings dumps*, Report 3307, The National Swedish Environmental Protection Board.

Ricard, J.-F., Aubertin, M., Firlotte, F. W., Knapp, R., McMullen, J., Julien, M. (1997). *Design and construction of a dry cover made of tailings for the closure of Les Terrains Aurifères Site, Québec, Canada*, Proc. 4th ICARD, Vancouver, Vol. 4, 1515-1530.

Ricard, J.-F., Aubertin, M., Pelletier, P., Poirier, P. (1999). *Performance of a dry cover made of tailings for the closure of Les Terrains Aurifères site, Malartic, Québec, Canada*, Proc. Sudbury'99 Conf., Mining and the Environment II, Vol.1, 155-164.

Ross, B. (1990). *The diversion capacity of capillary barriers*, Water Resources Research, 26 (10), 2625-2629.

SRK. (1989). *Draft Acid Rock Drainage Technical Guide*, BC AMD Task Force, Vol. I and II.

Stormont, J. C. (1995). *The effect of constant anisotropy on capillary barrier performance*, Water Resources Research, 31, 783-785.

Stormont, J. C. (1996). *The effectiveness of two capillary barrier on a 10 % slope*, Geotechnical and Geological Engineering, 14, 243-267.

Williams, D.J., Wilson, G.W. Currey, N.A. (1997). *A cover system for a potentially acid forming waste rock dump in a dry climate.* Proc. 4th Int. Conf. on Tailings and Mine Waste, Fort Collins, Colorado, Balkema, 231-235.

Wilson, G. W., Barbour, S. L., Swanson, D., O'Kane, M. (1995). *Instrumentation and modelling for saturated/unsaturated performance of soil covers for acid generating waste rock*, Hydrogéologie, 4, 99-108.

Yanful, E. K. (1993). *Oxygen Diffusion through Soil Covers on Sulphidic Mine Tailings*, Journal of Geotechnical Engineering, ASCE, 119 (8), 1207-1228.

Yanful, E. K., Riley, M. D., Woyshner, M. R., Duncan, J. 1993. *Construction and Monitoring of a Composite Soil Cover on an Experimental Waste Rock Pile near Newcastle, New Brunswick, Canada*, Canadian Geotechnical Journal, 30, 588-599.

Yanful, E. K., Simms, P. H., Payant, S. C. (1999). *Soil Cover for Controlling Acid Generation in Mine Tailings: a Laboratory Evaluation of the Physics and Geochemistry*, Water, Air and Soil Pollution, 114, 347-375.

Zhan, G., Aubertin, M., Mayer, A., Burke, K., McMullen, J. (2001). *Capillary cover design for leach pad closure*, Transaction: SME Annual Meeting, Denver, pp. 104-110.

TYPOLOGY OF STRATA MOVEMENT RELATED TO OLD SOLUTION MINING OF SALT AT SARRALBE (LORRAINE, FRANCE)

DAUPLEY Xavier[1], CUCHE Hervé[2], GHOREYCHI Mehdi[1]

[1] INERIS, Parc Technologique ALATA – BP 2 – 60550 Verneuil-en-Halatte Cedex, - France.;
Xavier.Daupley@ineris.fr ; Mehdi.Ghoreychi@ineris.fr

[2] SOLVAY, Rue de Ransbeek 310 - 1120 Bruxelles - Belgique. Herve.Cuche@solvay.com

RESUME : Dans l'objectif de la fermeture des cavités de dissolution de sel situées près de Nancy (Est de la France) appartenant à la Société Solvay, l'INERIS a entrepris d'importantes investigations sur le site ainsi que divers forages. Elles ont été complétées par des essais de laboratoire et des travaux de modélisation numérique et d'une analyse des mouvements de terrain. Ces travaux complémentaires ont permis d'étudier le comportement à long terme des cavités au regard du risque de rupture du recouvrement. Les résultats ont abouti à conclure que, du fait de la présence des terrains déformables au sein du gisement de Sarralbe, les grandes cavités sont déjà effondrées et, pour l'essentiel, totalement fermées, tandis que des petits chenaux de dissolution ont pu demeurer ouverts sans donner lieu à un fluage significatif du sel du fait de la faible profondeur (de l'ordre de 250 m). Au-delà de l'objectif de cette étude, les investigations réalisées et leurs conclusions présentent un intérêt méthodologique dans le contexte de l'abandon d'exploitations de sel, d'un point de vue de l'évaluation à long terme de leur impact sur la sécurité des personnes et des biens et sur la protection de l'Environnement.

MOTS-CLEFS : affaissements, dissolution, sel, stabilité, long terme, mesures topographiques.

ABSTRACT: In the view of closure of solution-mining cavities in salt near Nancy (East of France) belonging to Solvay Company, INERIS undertook different investigations on the site as well as several boreholes. They were completed by laboratory tests and modelling as well as the analysis of strata movement. These complementary works allowed to study long term behaviour of cavities regarding the risk of collapse of the overburden. The results came to the conclusion that because of presence of deformable strata in Sarralbe deposit, large cavities have already collapsed and now mostly closed. Meanwhile, small dissolution channels might have remained open without any significant salt creep due to their rather small depth (almost 250 m). Beyond the objective of the performed study, the investigations and their conclusions are of a methodological interest for the propose of salt mines closure with respect to the evaluation of their long term impact on the safety of people and properties as well as Environment protection.

KEY-WORDS : subsidence, dissolution, salt, stability, long term, topographic measurements

1 Introduction

After a long period of exploitation, France as some other industrial countries is dealing with mine closure. Long term impacts of cavities on public safety, properties and the Environment bring to undertake specific investigations. They are of major importance for the cavities created by salt mines and solution mining, due to the high solubility of salt in water and the continuous creep of this material.

As a matter of fact, hydrogeological context, overburden characteristics, geometry and dimensions of cavities, their depth and the exploitation method have to be analysed in detail. This requires to

collect all the data available and to complete them by field measurements, laboratory tests and modelling. Such investigations have been performed prior to the definitive closure of Sarralbe solution-mining cavities situated near Nancy (East of France).

2 Context and characteristics of Sarralbe deposit

Many investigations were undertaken during the period 1999-2001 in order to evaluate residual risks related to the solution-mining of salt by Solvay company in Sarralbe near Nancy and to establish the administrative abandonment procedure. At the request of SOLVAY, INERIS was in charge of this work. It was based on the data provided by Solvay (salt production, topography monitoring, etc.), prospection works on the boreholes, characterisation of mechanical behaviour of rocks (LAEGO), hydrogeological studies (ANTEA) and numerical modelling of long term behaviour of the site (The Ecole Polytechnique).

2.1 Location

In Sarralbe region, Solvay Company has got licence for 37 zones (concessions) located at the border of Lorraine and Alsace (Departments of Moselle and Bas-Rhin). Ten of them have been mined out by solution-mining. The location of the dissolution area is shown in figure 1.

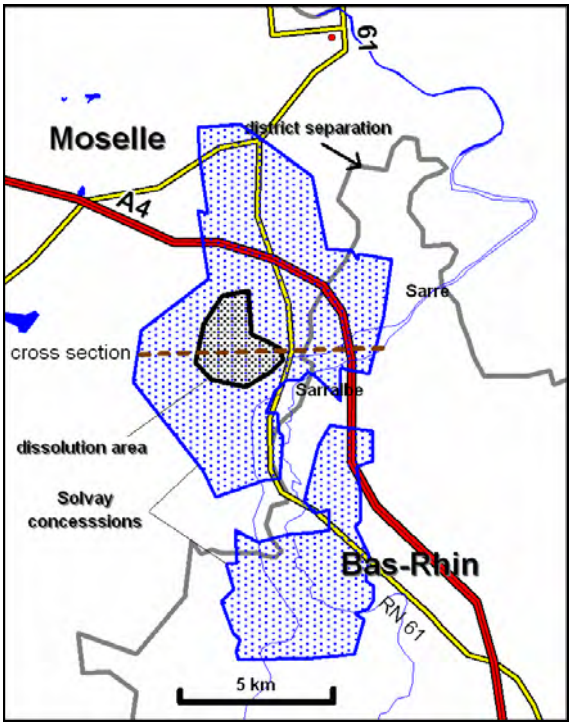


Figure 1. Location of concessions and solution mining in Sarralbe

2.2 Geology

Salt has been mined out in Lorraine from Sarralbe region (NE) to Nancy (SW). Halite is present at two levels :

- the most recent formation, in Keuper marls forming upper triassic. This is the case of the salt mines of Varangeville, Einville, Vic and Dieuze and solution mines of Haraucourt plateau (Nancy region).
- the oldest formation in the grey layers of middle Muschelkalk, at Sarralbe, situated at North-East extremity of Sarreguemines Synclinal, the area considered in this paper.

Figure 2 shows two lithological deposits present in Sarralbe and Nancy. The difference between these two regions basically depends on thickness of the salt deposit : 20 m at Sarralbe compared to 80 m at Nancy. The difference is also due to the presence or absence of the stiff dolomite layer of Beaumont which is found only in Nancy area but not in Sarralbe.

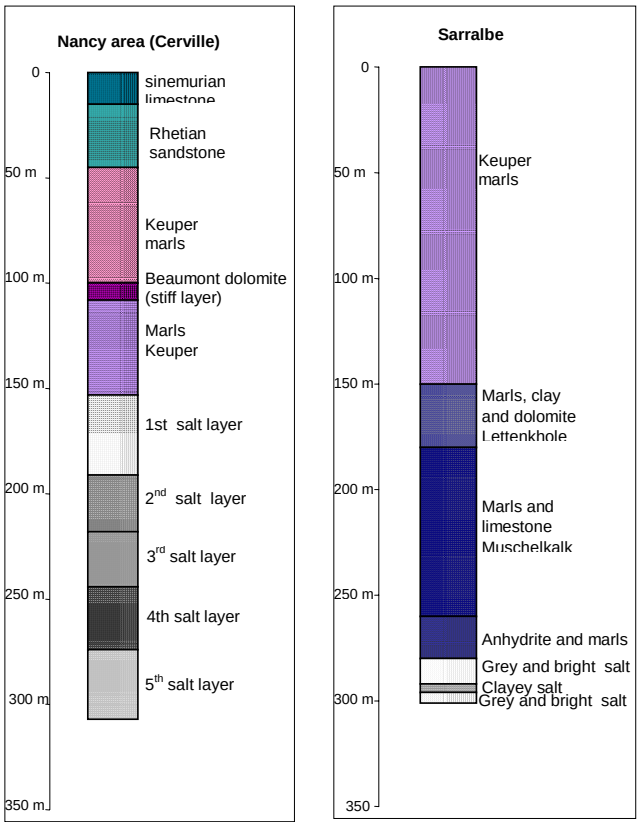


Figure 2 : Lithological series of triasic salt deposit and overburden in Lorraine (France).

The geological context of Sarralbe region is known thanks to many boreholes drilled for the purpose of exploration and exploitation of the deposit. The strata form a synclinal with the axis oriented in NNE-SSE (see cross-section in figure 3 and its location in figure 1).

In the mining area, salt deposit is found between 220 and 290 m of depth. Its thickness changes from 20 to 22 m in average, including irregular beds of marl and anhydrite with a cumulated thickness of 3 m.

The overlying strata are constituted by marl limestones and limestones of Muschelkalk and Lettenkohle besides a thick deposit of keuper marl (150 m in the mined out area).

The analysis of geological data, in particular those provided by the boreholes drilled during the year 2000 allowed a qualitative knowledge of the over-all mechanical behaviour of the strata forming the overburden : except for a few stiff layers of a few meters thick that are found in Muschelkalk limestone, the overburden strata are of poor mechanical properties that can be qualified as “globally

deformable". There is no stiff layer which the mechanical properties could have allowed large cavities to remain open in time.

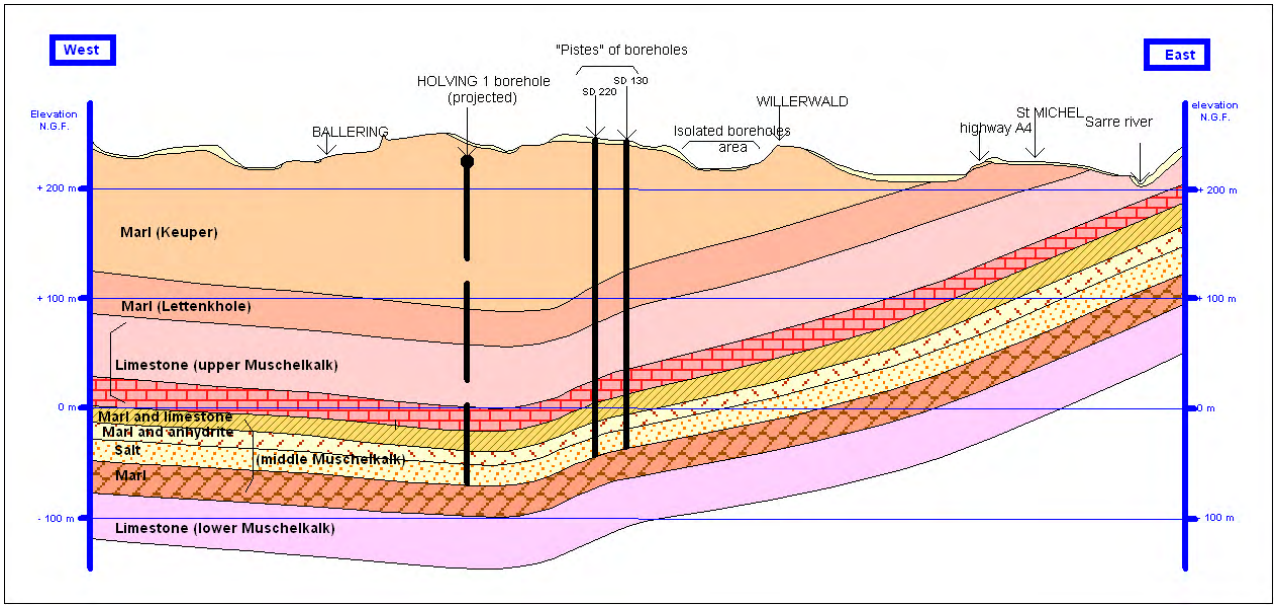


Figure 3. cross section of salt deposit and overburden in Sarralbe

3 Mining method

The main industrial solution-mining was done using different techniques : first through isolated boreholes drilled at deposit roof, then using the technique of group of boreholes (1884-1947) and finally by means of the so-called technique of "piste" of boreholes (1943-1983).

3.1 Isolated boreholes and group of boreholes

The first boreholes drilled at Sarralbe, called isolated boreholes have always been constituted by two holes with the maximum distance of 20 m. The cavities created at salt roof by introducing fresh water finished to be in communication (figure 4). One of the two boreholes was used to introduce fresh water, the other one for the brine extraction. This method was not optimised and did not allow an efficient dissolution of the deposit in all its thickness. It leaded too an out of control of lateral extension of dissolution.

By early XXth, groups of 10 to 20 boreholes were drilled (figure 4). After the communication between different boreholes was established, a part of them became fresh water in-flow boreholes where as the other part was used for the brine extraction. This corresponds to the initiation of whatever became later on the method of solution mining by "pistes" and boreholes.

The dissolution was always done to achieved a better control of the extension of the dissolved zones and a more efficient exploitation of the deposit thickeness. This became possible thank to the deeper boreholes and their optimal distribution in space. Figure 5 shows the groups of boreholes. Note that the different dissolution techniques performed at the salt roof allowed extracting of 5,4.10^6 tonnes of salt between 1884 and 1947.

3.2 Pistes of boreholes

In the following, the terme « piste » of boreholes is defined as a set of aligned boreholes. By the years 1930, the dissolution method of “piste” and boreholes was under operation at Sarralbe. This method is specific to Solvay Company. It is still under operation in other deposits, especially for the thick salt deposit of Cerville (Meurthe-et-Moselle). The method has been subjected to a favourable evolution leading to a rationalisation of mining that has begun with the group of boreholes in the first half of XXth century. The basic evolution feature of this method is related to the two following aspects :

- the dissolution is done from the floor to the roof of deposit ;
- it is oriented in the direction of boreholes line.

A piste is formed with boreholes drilled up to the basis of the salt deposit. The distance beetwen the boreholes is 50 m. They are placed in the direction of the highest slope line. First, all the boreholes are put in communication by creating dissolution channels using an air blanket. After achievement of channels formation, the piste can be mined out. Fresh water is introduced in the boreholes located in front of the piste and the brine is extracted through the backward boreholes.

The method allows salt mining with a maximum extraction ratio from floor to roof with an appropriate control of the dissolved zones.

At Sarralbe, two pistes roughly parallel with a distance of 200 m were mined out. The « piste 100 » compromises 52 boreholes and the « piste 200 », 40 boreholes. They resulted in the extraction of 8.64 millions of tonnes of salt. It has to be noticed that while mining was stopped at 1983, half of the « piste 200 » was not yet mined out. Only the dissolution channel, a few meters high, was already formed.

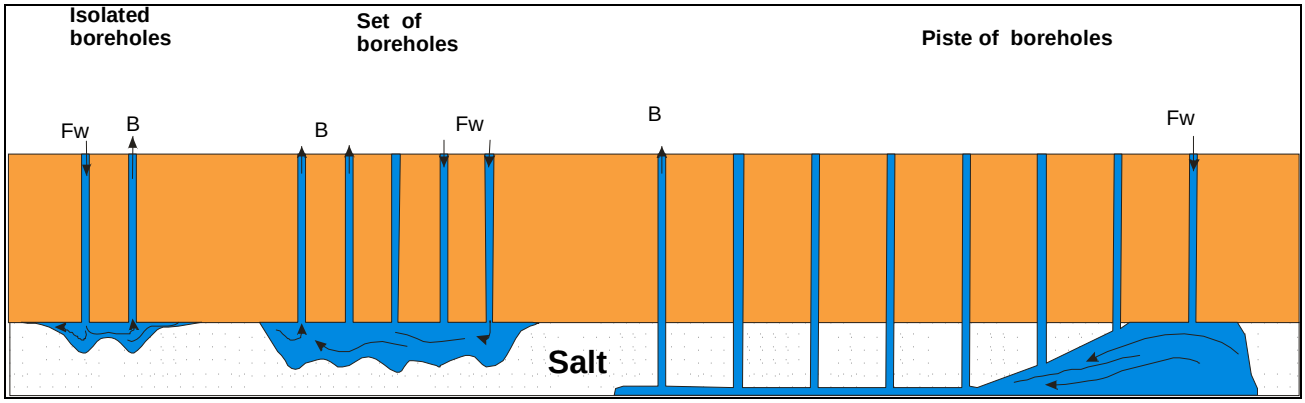


Figure 4 : cross section showing different solution mining techniques used at Sarralbe
(B : brine, Fw : fresh water)

The data available on the exploitation Sarrable pistes (extracted salt, Sonar, other investigations) allow to give some indications on the dimension and the extensions of the void spaces created by dissolution : dissolution channels were formed with a maximum height of 4 to 6 m and a lateral extension of 50 to 60 m. The solution-mining led to mine out the whole thickness of the salt layer, about 20 m in average. Moreover, the cavities were extended 40 to 50 m around the piste axis.

4 Strata movement induced by solution mining in Sarralbe

It has to be underlined that the different techniques of solution-mining used in Sarralbe have not resulted in any malor collapse. Only subsidence has occurred.

4.1 Features and rates of subsidence

Strata movement induced by dissolution could be analysed in detail thanks to the measurements provided by the topographic survey carried out from the beginning of mining period at the end of XIX th century.

Topographic measurements were taken systematically for the first boreholes (double boreholes or group of boreholes). Further more, an extended topographic network was set up for the exploitation. A few plots have been kept and followed by measurement until 2000. As a matter of fact, data are available almost 20 years after the mining was stopped.

4.1.1 Subsidence amplitude and extension

Mining at salt roof

For isolated boreholes formed by double ones, the measured subsidence is about 1 m (table 1). For the two groups of boreholes, that of “spond” and “brook”area, the maximum amplitude of basin subsidence reaches 3.9 and 5.6 m respectively. The number of mined out boreholes appears to be proportional to the maximum amplitude of subsidence. This denotes the fact that the group of boreholes were subject to communication. Therefore, the residual width/depth ratio was developped and resulted in the increase of soil subsidence amplitude.

Figure 5 shows the subsidence extension within the area of basic group of boreholes. The values of subsidence were extrapolated from the values of total subsidence for each borehole head measured in 1938.

Pistes of boreholes

In the area of mined pistes, the average value on subsidence is 3 m where and the maximum reaches 4.4 m. Above the area that has not been exploited, that is to say where there is only dissolution channel, no sensitive soil displacement has been registred neither during mining nor since the mining has been stopped in 1983.

By measuring the cavities dimensions using ultrasonic technique, the value of subsidence influence angle was estimated to be 37° where the limits of dissolution zone are known

Table 1. subsidence magnitude in Sarralbe

	Maximum subsidence in meters	Average subsidence in meters	Exploited boreholes
Isolated boreholes I, IV and V	1.09	0.96	2
Isolated boreholes II	2.4	2.4	4
Isolated boreholes III	3.7	3.7	6
Set of boreholes – “spond” area	3.9	3.2	10
Set of boreholes – “doerenbach brook” area	5.6	3.7	23
« Pistes » of Boreholes	4.4	3	50

4.1.2 Subsidence ratio

For each solution-mining technique, boreholes pistes and set of boreholes, the values of subsidence ratio (volume of subsidence over cavities volume) are relatively small. They change between 0.2 and 0.4 respectively for the exploitation by « boreholes pistes » and « set of boreholes ».

The results of numerical modelling (see paragraph 5), the mechanical properties of the strata and the subsidence amplitude agree on the fact that the small values of subsidence ratio are explained by the following factors :

- the small width of voids compared to the depth (sub-critical exploitation). This is the case specially for the pistes where the ratio cavity width over its depth is less that 0.5 ;
- the residual voids. Basically, the void spaces which have not been filled with the bulking of the collapsed strata are concerned ;
- the results of the different investigations indicate that most of the cavities has already collapsed. Only small cavities might be still open (not fully collapsed). This is particularly the case of the dissolution channels.

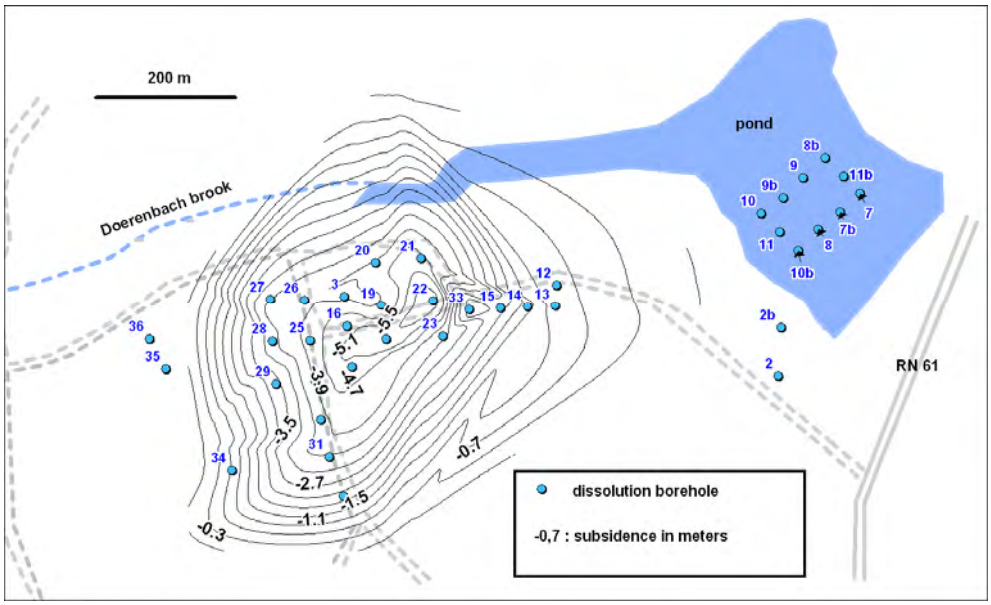


Figure 5 : subsidence extension at the aera of basic group of boreholes (cumulative values to 1938)

4.2 Subsidence evolution in time

Subsidence has been measured in time for the basic group of boreholes (Daerenbach brook area) and for the pistes. The main features of the time-dependent behavior of subsidence are as follows (see figures 7 and 8 for the basic group of boreholes).

The subsidence has basically occurred during the mining period. It is well correlated with brine extraction without any significant delay (figure 7). No jump has been observed for the subsidence plots. This clearly shows that the overburden has never failed since there is not any stiff layer in the overburden able to keep a large cavity open in time.

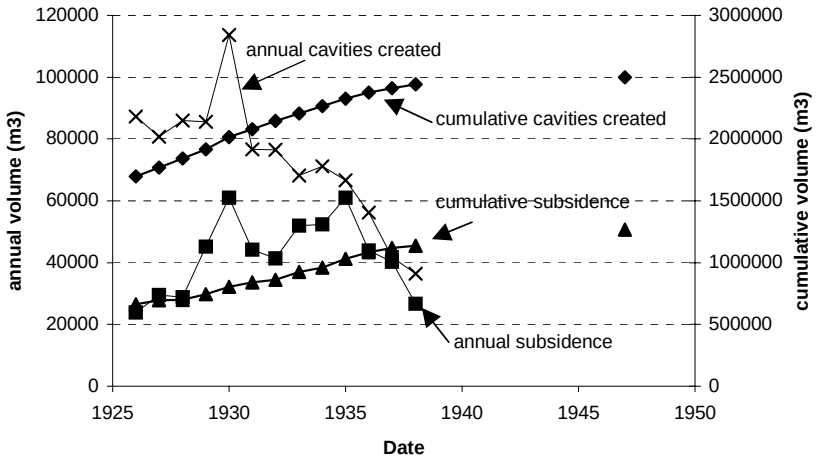


Figure 7 : Basic group of boreholes (Daerenbach brook area). Comparison between cavities and subsidence volumes (cavities assumed to be full of brine)

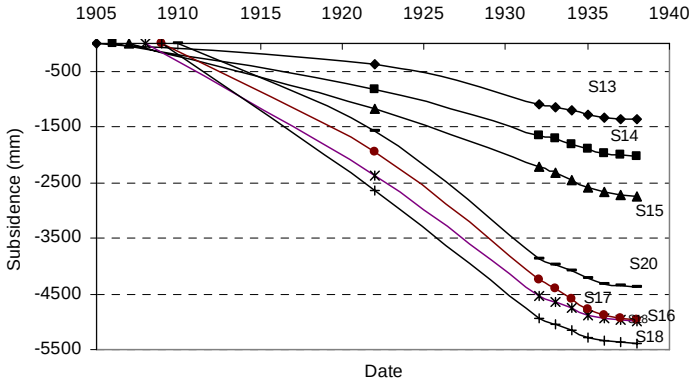


Figure 8 : subsidence evolution of basic group of boreholes (Daerenbach brook area).

The residual subsidence rate is negligible (less than mm/year) a few years after the end of mining (and so today). This result shows that salt (thin layer fully mined out) does not play any significant role on the overall behavior of the strata and upon the long term displacement of the surface. Figure 8 shows the subsidence evolution until 1938 for a part of boreholes belonging to the basic group. These boreholes have not been under operation for several years. For the exploitation by pistes, the topographic measurements taken at several occasions during the last 10 years and their comparison with the measurements made during the mining period show up that at present, there is no measurable displacement that can be measured on surface. The latest measurements (of the order of 1 cm) have been made locally in 1998. One can wander whether they are not related to the natural “breathing” of the soil rather than to a real subsidence.

5 Modelling

Evaluation of long term evolution of cavities and its impact on the soil surface and possible future structures and population required to model different kinds of cavities according to the solution mining methods.

In order to take into account, as far as needed, cavities, layers, their constitutive models and their properties, Finite Element computations were made. A special attention was paid to the modelling of the failure of various layers in the overburden. The results provided by the laboratory tests performed on the cores taken from a borehole (especially drilled for the purpose of this study) guided to select the appropriate constitutive models : brittle elastic for limestone, Cam Clay elasto-plastic model for clays and marls, elasto-viscoplastic model for salt (Norton law).

Using the values of mechanical properties obtained by laboratory tests, as reference values, a series of calculations was systematically made in the view of a sensitivity study. A wide range of the parameters values as well as the cavities dimensions were introduced in the model in order to evaluate in a satisfactory way, the effects of various data on the model results and conclusions. This priority required many modellings with iterative time-consuming computations (non linear and time-dependent behavior of rocks). In this condition, only 2D computations were feasible. They were done both in plane strain condition (for the pistes) and using axisymetric assumption (for the group of boreholes, on the basis of circular iso-subsidence curves, as shown in figure 5).

We emphasise on the fact that in spite of the fantastic progress of computers and modelling in the latest decades, accurate computation of the subsidence induced by a cavity collapse cannot be described precisely by any existing model (discrets elements, distinct elements, finite elements, etc). In fact, the bulking factor can easily reach a high value close to 0.3 (30 % of additional volume created by the void spaces among the blocs of rock) where as the models cannot take amount of this factor. Consequently, the calculated values of the subsidence amplitude and extension are usually exagerated in comparison with the reality. This is the reason why in this study, we preferred to calibrate the parameters of the model using the topographic measurements. This required systematically a very significant reduction of the mechanical properties of the overburden indicating that the overburden is globally very deformable.

The model being calibrated, long term stability of the caverns and the overburden was then investigated in different cases : group of boreholes, pistes, channels.

This evaluation was based on the concept of limit load theorem which is very common in soil mechanics (e.g. slope stability calculation). The idea is that for given values of mechanical properties, collapse takes place when a critical load value is reached.

In a numerical computation, this method requires a step by step decrease of the mechanical properties (e.g. strength, cohesion …). A sudden jump of displacements (for example, the cavity convergence) indicates that the limit load is reached and the cavity can no longer remain stable (overburden failure). In practice, for given values of overburden load and cavity width, different computations are made by decreasing continuously the mechanical strength of the overburden. The cavity closure and the soil subsidence (computation results) are then increased. This is shown in figure 9 for different values of cavity width. On can observe that the strength limit is increasing with the cavity width; that is to say under a given load, a small cavity is more stable than a large one (a large cavity needs a stronger overburden in order to remain stable, in comparison with a small one).

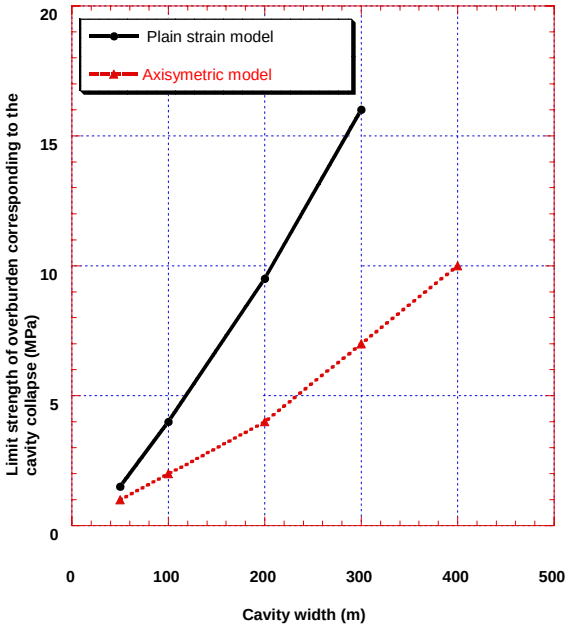


Figure 9 : Evolution of the limit load as a function of the cavity width

The following basic results came out of various computations :

1. there is clearly a mechanical (and hydraulic indeed) interaction between neighbouring cavities. Consequently the overall behaviour of the group of boreholes can be assimilated to that of a large cavity containing individual cavities. This is conform to the topographic data. Also, the computed values of subsidence are very close to the measured ones (figure 10) ;
2. the measured values of subsidence amplitude (a few meters) cannot be explained unless the roof fall and the cavities collapse are considered. This result denotes that most of the cavities has already collapsed ;
3. in spite of the fact explained above, the value of subsidence coefficient (subsidence volume over caverns volume) is almost small, between 0.2 to 0.5 depending on the exploitation context. This result fits well the measurements. Nevertheless, the calculated values of angle of influence (related to the lateral extension of subsidence) are higher than the measured values. This is due to the continuous feature of the model (in fact any significant subsidence does induce an overburden fracturing where as the model remains continuous anyhow) ;
4. the behaviour of dissolution channels is governed by salt properties : good strength and rather small creep at a depth of 200 –300 m.

The results of the calculations indicate that many channels remain probably still open. Their creep rate is very small and does not lead to any measurable effect on the soil surface (figure 11). On the whole, the results of modelling allow to conclude that the overburden has clearly a “soft” behaviour with poor mechanical properties. Cavities were already closing during the solution mining period and the most subsidence has already occurred at short term. Moreover the residual subsidence due to the open cavities and the channels is negligible and cannot result in any disorder of the overlying structures. Nevertheless, in case any heavy structure is planned in future, special investigations and operations have to undertaken prior to any construction of this type.

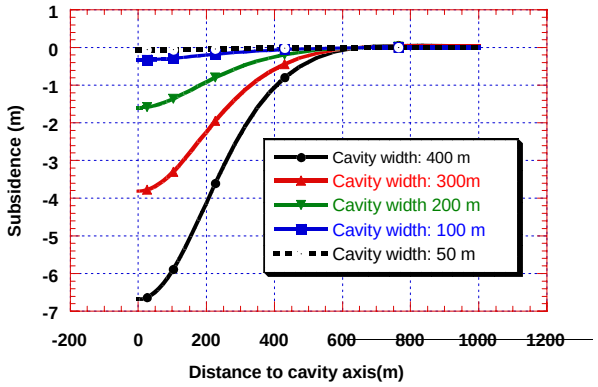


Figure 10 : Soil subsidence calculated for different widths of an axisymetric model of cavity

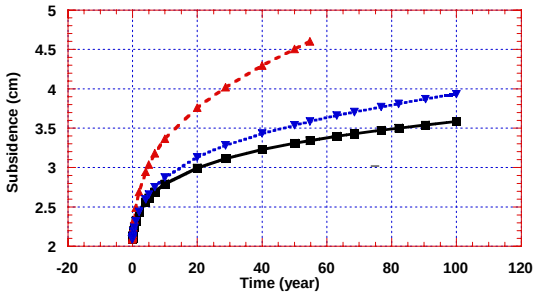


Figure 11 : Time dependent evolution of the soil subsidence above a channel modelled in axisymetric representation (calculation with 3 sets of model parameters)

6 General conclusions with respect to closing of salt mines.

The main interest of this study is due to the fact that mining has systematically been accompanied with a topographic monitoring from the beginning of the industrial solution-mining period. The investigations show up clearly that the geological context of Sarralbe site can be distinguished from that of the salt deposit in Nancy area (figure 12) :

- within the Nancy area, the Beaumont dolomite layer, very stiff and resistant, can potentially fail and generate large collapse. In fact, presence of a stiff layer in the overburden makes it possible to create large caverns. When the cavity becomes larger than a critical value (see the case of Gelloncourt cavity and the pistes reference) deflection of the dolomite layer leads to its failure resulting in the collapse of the overlying strata presenting poor mechanical properties. One has to notice that in Nancy region, the deposit thickness is nearly 80 m and the so-called “intensive” technique allows creation of few ten meters high cavities.
- Beaumont dolomite stiff layer does not exist in Sarralbe overburden which is globally “soft” with poor mechanical properties. In addition, the thickness of the salt layer (about 20 m) and, as a matter of fact, the cavities height are much smaller in Sarralbe in comparison with Nancy. Void spaces created by dissolution are easily filled because of the roof fall (bulking). The overlying strata are deformed smoothly leading to surface subsidence. The topographic measurements discussed in this paper showed up that the amplitude of the surface subsidence can reach a few meters. The subsidence is almost stabilised a few years after the brine extraction has been stopped.
- an intermediate case of the overburden behaviour and the induced effects at surface has been analysed by Wassemann (1980) and Bekendam (1997) in Twenth (Netherlands). It deals with a salt deposit, about 50 m thick, mined out by isolated boreholes and groups of boreholes. This mine induced a significant surface subsidence of a few meters, a few years after the exploitation was stopped. Like within Nancy area, the cavity formed by dissolution is characterised by an upward evolution in consolidated layers. But there is no stiff layer able to keep open the cavity for a long time. When the cavity reaches the basis of unconsolidated clays, these layers are subjected to a deflexion above the cavity leading to their failure and fall. The material fill the available volume and result in a significant surface subsidence. It has to be underlined that the subsidence rate was a few mm/year while the cavity was located at lower layers with rather good mechanical properties. Later on, as the cavity reaches the soft clay base, it is collapsing and generates subsidence of few m/year.

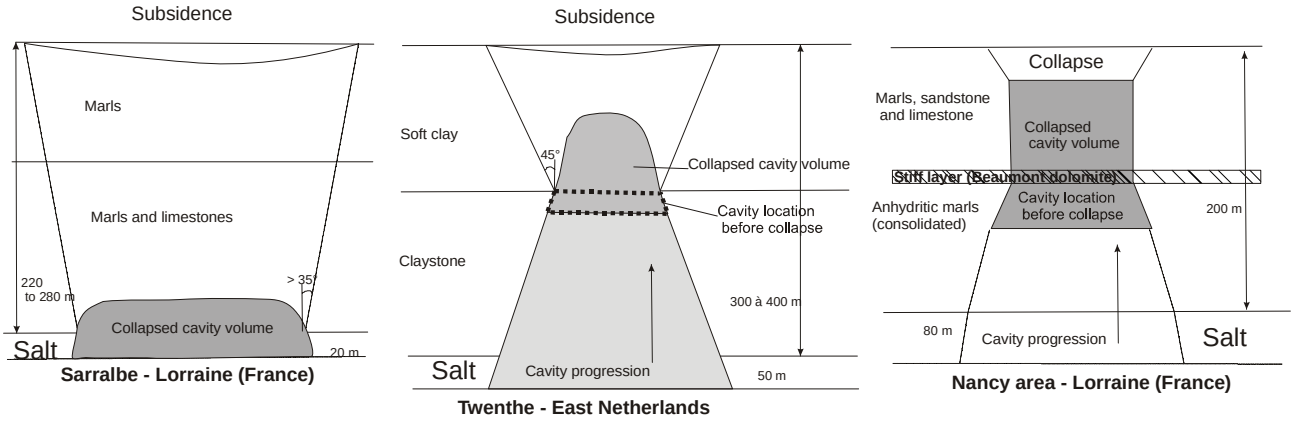


Figure 12 : schematic representation of the cavity evolution for different bedded salt contexts and induced soil movements.

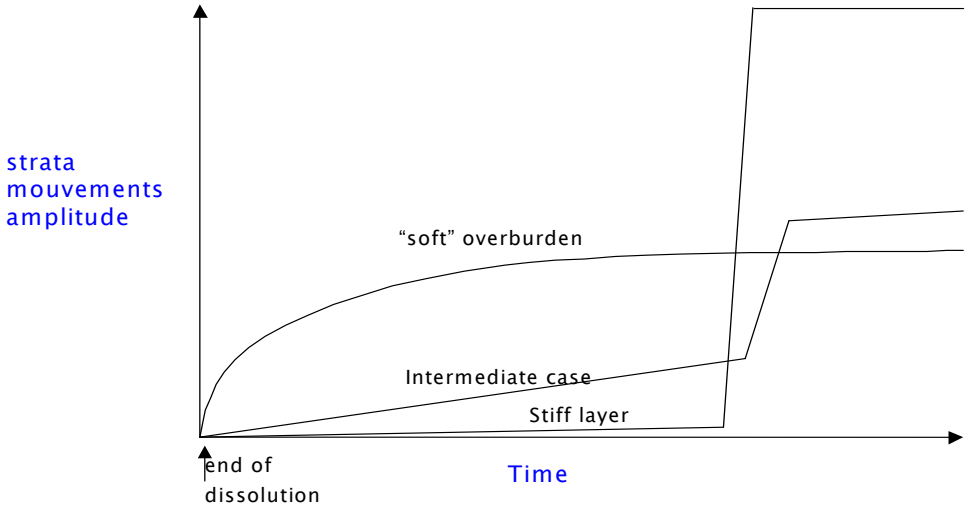


Figure 13 : schematic representation of the strata movement amplitude evolution for different bedded salt contexts

The analysis of the surface effects induced by mining in Sarralbe compared to the Nancy case and to that of Twenth highlights the important role of geological context especially the nature and the mechanical properties of the overburden. This role is decisional on the mechanisms of evolution of the cavities and on the surface effects. In particular, evolution in time of the effects are different as it is shown in figure 13. Theses differences are of a great importance for the long term management of salt mines regarding the impact on the future urbanism development and also with respect to an efficient monitoring system.

7 References

Bekendam R.F., (1997), *Stoping in weak rock over solution cavities in the Hengelo Field, the Netherlands, and its expression in terms of surface subsidence*, S.M.R.I. spring 1997 meeting, Cracow Poland.

Buffet A. (1998), *The collapse of compagnie des salins SG4 and SG5 drillings*. S.M.R.I., fall meeting, Rome.

Ghoreychi M., Daupley X., Baujart C., (2002), *Incidences du comportement mécanique et des processus de transport sur l'évolution à long terme des sites d'exploitation de sel*, JNGG 2002, 8-9 octobre 2002, Nancy.

Ghoreychi M., Daupley X. (2003), *Devenir à long terme d'exploitations abandonnées de sel*, Après mine 2003, Nancy / Revue Française de Géotechnique, N°106-107, 2004

Ghoreychi M., Daupley X., (2003), *Mechanical – transport processes in salt : consequences for abandonment of underground exploiations*, ISRM 2003-Technology roadmap for rock mechanics, South African Institute of Mining and Metallurgy.

Wassmann T.H., (1980), *Mining subsidence in Twente, East Netherlands*, Geologie en Mijnbouw, volume 59, pp 225-231

AIR-WATER INTERACTION AND TIME DEPENDENT COMPRESSIBILITY OF A SUBTERRANEAN QUARRY CHALK

DE GENNARO Vincenzo[1], SORGI Claudia[2], DELAGE Pierre[1]

[1] ENPC (CERMES, Inst. Navier), 6-8 Av. B. Pascal, F 77455 Marne-la-Vallée Cedex 2 - France; vincenzo.degennaro@enpc.fr; pierre.delage@enpc.fr

[2] INERIS, Direction des Risques du Sol et du Sous-Sol, Parc Technologique ALATA, BP n° 2, 60550 Verneuil-en-Halatte – France; claudia.sorgi@ineris.fr

ABSTRACT: In this paper the effect of suction and time on the mechanical response of a quarry chalk during eodometer tests is investigated. The water retention properties of the chalk, giving the changes in fluid content as a function of the suction applied, are studied and related to the changes in relative humidity in the quarry, chalk mineralogical composition and microstructure. Like in partially saturated geomaterials, it is recognised that chalk yielding is suction dependent, in that for decreasing suction (i.e. increasing water content) chalk softens. Preliminary results showing the effect of suction on the viscous behaviour of the chalk are also presented. The importance of the hydromechanical coupling associated to suction cycles and the induced cyclic changes in mechanical strength of chalk is emphasised, with regard to the long term behaviour of chalk pillars.

KEYWORDS: chalk, quarries, suction, viscosity, oedometer.

RESUME : On présente dans cet article les résultats d'une série d'essais de compressibilité réalisés à l'oedomètre pour étudier l'effet de la succion et du temps sur le comportement mécanique d'une craie de carrière. Les caractéristiques de rétention de la craie, donnant l'évolution de la saturation relative en eau en fonction du niveau de succion, ont été analysées et mises en relation avec les changements d'hygrométrie dans la carrière, la composition minéralogique de la craie et ses propriétés microstructurales. On montre que, comme dans les sols non saturés, l'écrouissage de la craie dépend du niveau de succion imposé, et qu'une réduction du niveau de succion (i.e. augmentation de la teneur en eau) augmente sa compressibilité. Des résultats préliminaires permettant de quantifier l'effet de la succion sur le comportement visqueux de la craie sont également présentés. On souligne l'importance du couplage hydromécanique existant dans cette craie, associé aux effets des cycles de succion sur sa résistance mécanique, en relation plus particulièrement avec le comportement mécanique à long terme des piliers des carrières.

MOTS-CLEFS : craie, carrières, succion, viscosité, oedomètre.

1. Introduction

Abandoned subterranean quarries constitute a potential risk in areas where their collapse may affect surface infrastructures and buildings. Quarries in chalk are quite numerous in France, for this reason a specific research is being conducted in the Estreux quarry (North of France) by INERIS, aimed at investigating the possible factors affecting the long term stability of the host chalk formation.

For mineworkings a number of collapse phenomena are documented in literature (among others: BLPC, 1973; Masson, 1973; Bonvallet, 1979; Bell et al., 1999; Talesnick et al., 2001; Lord et al. 2002; Grgic et al., 2003; Sorgi 2004). These collapses are mostly related to the destructuration (weathering) of the rock of the pillars due to external (i.e. physico-chemical processes,

environmental conditions) or internal (intrinsic) factors. The timing of these collapses is not easy to predict. They often occur without any manifest precursory symptom or external action, indicating that time effects (weathering, aging) may have serious consequences on the structural stability of the rock.

It seems now well accepted that the collapse of mine pillars is mainly due to the aging and the progressive degradation of the rock material, submitted to a constant state of stress. In the case of Estreux quarry chalk, moreover, the average relative humidity (RH) varies cyclically between 100 and 80%. Due to the well known sensitivity of chalk to water action, it is believed that these changes in RH may affect dramatically chalk mechanical behaviour, increasing degradation phenomena and the risk associated to the occurrence of instabilities. It was then decided to investigate the retention properties of the chalk to check more in detail its state of saturation and its influence on the mechanical behaviour.

In this paper, preliminary results of oedometric tests on samples at various degree of water saturation are presented. Partial water saturation was imposed controlling the suction during the tests. It is shown that increasing water content (i.e. decreasing suction) decreases the yield stress and increases the time dependent sensitivity. Viscous behaviour under constant load (creep) and constant degree of saturation is also analysed. The examination of the experiments is proposed and results are discussed within the general framework adopted to describe the behaviour of unsaturated soils.

2. General framework

Chalk is considered as a multiphase geomaterial, and it is known from the mechanics of unsaturated soils that multiphase geomaterials behave quite differently as compared to geomaterials that contain only one fluid (saturated soils or porous rocks). In particular, they experience collapse when wetted under a constant load, indicating that an increasing proportion of wetting fluid, mainly located at the inter-granular contacts, soon causes failure.

Because pressure discontinuity through the interface between two immiscible fluids (e.g. air and water) gives rise to capillary pressure, strength loss due to wetting can be viewed as the consequence of the loss of capillary bonding between soil particles. Nonetheless, in clays for example, the chemical activity of the soil particles adds chemical fluid-mineral interactions. Neglecting the gravitational potential, the action of capillary and chemical interactions can be derived from the matric potential and the osmotic potential of the pore water, respectively. Both are part of the chemical potential μ_w of the pore fluid, its definition is derived from the Gibbs free energy (e.g. Sparks, 1998):

$$\mu_w = \mu_w^o + RT \ln a_w \tag{1}$$

where μ_w is the chemical potential of the pore water solution, μ^o_w is the chemical potential of pure water, a_w is the activity of the pore water solution ($a_w = 1$ for pure water and $a_w \to 0$ increasing solutes concentration), T is the temperature (absolute Kelvin's scale) and R is the constant of the ideal gas (8.3143 $Jmol^{-1}K^{-1}$). When expressed in terms of pressure, the chemical potential is usually called total suction in unsaturated soil mechanics, and defined as

$$s = -\frac{\rho_w}{M_w} RT \ln a_w \tag{2}$$

where the sign minus is introduced in order to ensure that s is strictly positive, ρ_w is the water density and M_w is the molecular weight of water (18 $gmol^{-1}$). For partially saturated states,

equilibrium of pore water with its vapour phase allows to simplify in eq. (2) the expression of the activity coefficient a_w of pore water into the ratio between the partial vapour pressure p_w of the pore water and the partial vapour pressure p_{ow} of the pure water at a reference state ($a_w = p_w / p_{ow}$), this ratio defines the relative humidity RH (%) = $100a_w$. If we neglect the effect of dissolved solutes in pore water (accounted in the osmotic suction, s_o), the activity of pore water is only due to its pressure and the geometry of the pore space (i.e. matric suction s_m is equivalent to capillary bonding). Thus, total and matric air-water suctions are identical and are computed through

$$s = u_a - u_w = -\frac{\rho_w}{M_w} RT \ln(RH) \qquad (3)$$

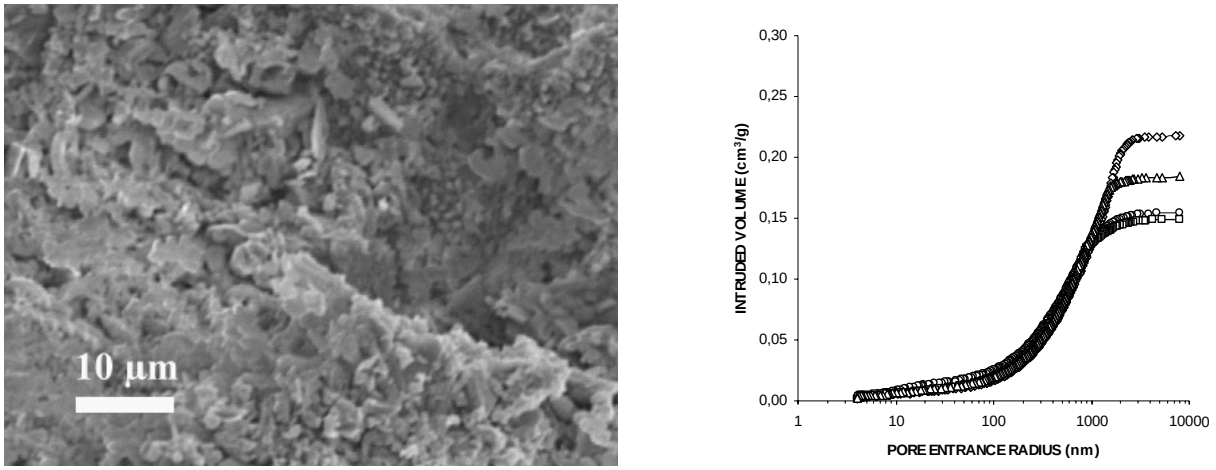
where u_a is the air pressure and u_w is the water pressure.

To describe the mechanical behaviour of unsaturated soils the usual mono-tensorial approach based on the effective stress concept (Terzaghi, 1936) is no longer valid (e.g. Wheeler & Karube, 1996; Gens, 1996). Indeed, matric suction is considered as an independent stress variable (Coleman, 1962; Fredlund & Morgenstern, 1977), and is usually admitted to act as a pure hydrostatic stress tensor. The other possible stress variable is the net stress $\boldsymbol{\sigma} - u_a\mathbf{I}$, being $\boldsymbol{\sigma}$ the total stress tensor and $\mathbf{I}$ the unit tensor (both here are second order tensors). This hypothesis enables to account for hydromechanical coupling in the behavioural features of multiphase geomaterials. Its validity has been verified on multiphase reservoir chalks, where the non-wetting fluid is oil rather than air (Delage et al., 1996; Pasachalk1, 2001; De Gennaro et al., 2003 and 2004; Pasachalk2, 2004). Within this theoretical framework, based on equation (3), hydro-mechanical coupling associated to hygrometry changes (i.e. suction changes) has been considered has one of the main factors affecting the stability of the underground quarries in chalk. In this paper we discuss some of the experimental evidences corroborating the proposed general framework for chalks.

3. Tested chalk: characterisation and sample preparation

The chalk used in this study comes from Estreux quarry (north of France). Blocks of Estreux chalk were retrieved at 25 meters depth. At the temperature and the hygrometry inside the quarry, 11° C and nearly 100% of relative humidity, respectively, the chalk was almost completely water saturated (natural water content w = 20.7%). The SEM image and the MIP curves of Estreux chalk are presented in Fig. 1. SEM picture displays evidence of a clayey matrix (flat platelets) and microfossils (Fig. 1a). The clay fraction was identified as glauconite, which is often present in chalks from the north of France, giving a typical greenish colour (BLPC, 1973; Bonvallet, 1979). Probably due to the presence of microfossils, porosity of Estreux chalk is quite high, in the range 35 to 37 % (average void ratio e_o = 0.566). MIP curves identify a narrow family of pores, with an average pore entrance radius value in the range 500 to 800 nm (Fig. 1b). We note a certain scatter in the values of the intruded volume at higher pore entrance radii (> 2000 nm) which seems likely to depend on the natural variation of the porosity, and is amplified by the reduced dimension of MIP samples.

Samples used for laboratory tests were cored from a unique block (same orientation) and then resized on a lathe. For water saturated samples this procedure was performed as much quick as possible, in order to avoid evaporation, adding water if necessary. Samples of about 38 mm diameter and 20 mm high were used for the oedometer tests (excepted one test on dry chalk, performed on a sample 50 mm in diameter). For the retention tests, samples had a diameter of about 20 mm and their height ranged between 20 and 25 mm. Dry samples were obtained after a heating period of 24 hours at 105° C.



(a) (b)

Figure 1. (a) SEM picture of Estreux chalk, (b) Mercury Intrusion Porosimetry curves.

4. Experimental techniques and apparatuses

Due to the key role played by suction on the behaviour of chalk, experimentation required a set of testing procedures allowing suction control. The two methods used were: (i) the osmotic technique, (ii) the vapour phase control.

4.1. The osmotic technique

The osmotic technique (Williams and Shaykewich, 1969; Kassiff & Benshalom, 1971; Delage et al., 1992; Dineen & Burland, 1995) allows to control suction by osmosis through a regenerated cellulose semi-permeable membrane behind which a solution at a given concentration of large molecules of polyethylene glycol (PEG) is circulated. The concentration of PEG solution define the corresponding value of suction applied, obtained by previous calibration. To apply the desired suction during experiments, apparatuses should allow the contact of the chalk sample with the semi-permeable membrane and the PEG solution.

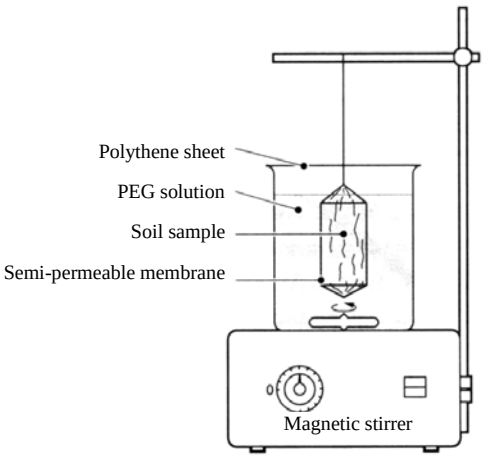


Figure 2. Experimental setup used to control suction by osmotic technique (Cui & Delage, 1995).

The layout of the experimental setup used to apply the desired suction level to chalk samples during water retention tests is shown in Fig. 2. The method (Cui & Delage 1995, De Gennaro et al. 2003) consists in inserting the chalk sample in tube-shaped semi-permeable membrane and in plunging it into a container full of PEG solution placed on a magnetic stirrer. For the determination of the imbibition curve, dry samples were inserted. Due to its wetting properties, water could infiltrate chalk under a controlled suction and expels a given volume of air. In the case of the drainage curve, the samples were saturated with water before being inserted. Due to the higher suction imposed by the concentred PEG solution, the pore water is expelled from the porous network of the chalk, crosses the membrane and is released into the PEG solution. In both cases the fluid transfer come to an end when the osmotic suction imposed by the solution and the matric suction of the sample are at equilibrium.

4.2. The vapour phase control

The vapour phase control allows total suction control by means of PEG solutions (Fig. 3a) or saturated salt solutions (Fig. 3b). Suction in this case is controlled by the ambience relative humidity imposed by the solution, taking care that isothermal condition is fulfilled. During all the retention tests presented in this paper a temperature of 20° C ± 0.5° C was ensured. The use of PEG or saline solutions depends on the level of desired suction. In this study PEG solutions were used for total suction levels lower than 2.5 MPa (RH = 98.2%), the minimum value of total suction attained by saturated saline solutions being 4.2 MPa (RH = 97% with K_2SO_4 salt).

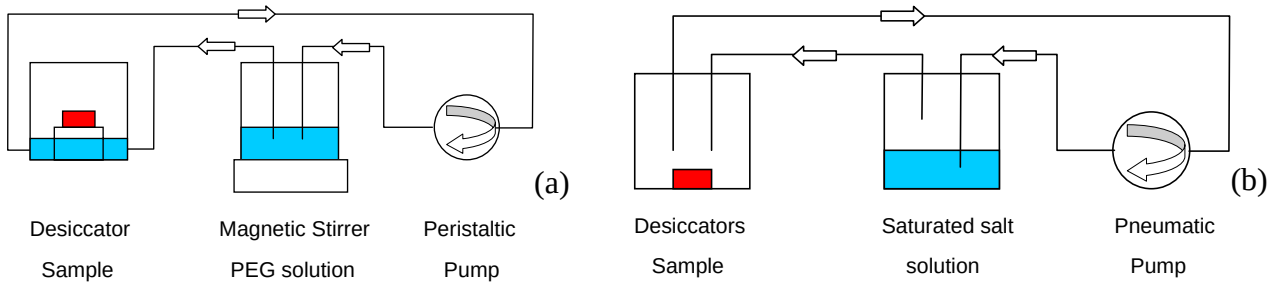


Figure 3. Vapour phase control: (a) using PEG solution, (b) using saturated salt solutions.

4.3. The suction controlled oedometer

One sample in this study was subjected to a mechanical test under suction controlled condition. This type of test was performed in the osmotic oedometer (Fig. 4). During oedometric tests chalk samples were subjected to incremental loading (applied instantaneously) and the evolution of the vertical strain during each loading stage was measured. This procedure is well established in soil mechanics. The value of the vertical strain is defined as the strain corresponding to the effective stress state (in saturated soil), i.e. the state of stress for which the excess pore fluid pressure is zero (end of primary consolidation). In a multiphase chalk, excess pore pressures of water during consolidation could modify the suction. Then, the actual vertical strain value should correspond to the condition of equilibrium of suction. In this device suction is controlled via the osmotic technique. The bottom of the sample is in contact with a semi-permeable membrane below which a solution of PEG is circulated (Kassiff & Benshalom, 1971; Delage et al., 1992). In order to control the suction level, water exchanges through the membrane were monitored through visual observation of the water level in a graduated tube placed in the bottle that contains the PEG solution.

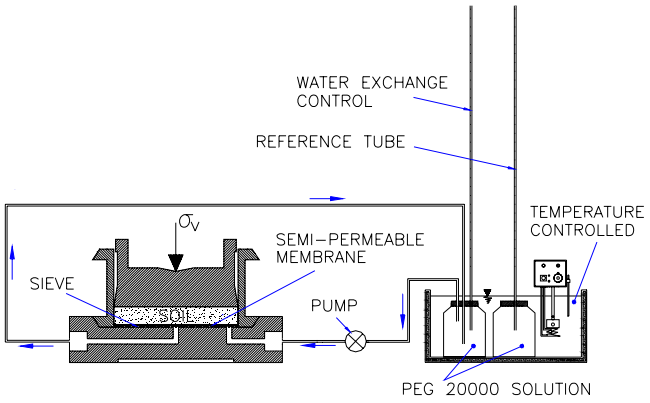


Figure 4. The osmotic oedometer.

In order to reach the desired net vertical stress, the sample was loaded using a high pressure oedometer frame with a double lever arm that allowed a maximum vertical stress of approximately 60 MPa on a sample 50 mm in diameter. At each loading stage, the stabilisation of the PEG level in the tube was checked.

5. Retention properties

The retention properties of Estreux chalk define the relationship between the degree of saturation S_{rw} and the suction s (the retention curve) in an air-water saturated chalk sample. Depending on the driving fluid used to modify the relative saturation of the sample, two curves can be established, following an imbibition path (water driving) or a drainage path (air driving). Retention curves have been obtained using one of the two techniques of suction control described previously.

MIP data were also used to obtain the retention curve following a drainage path. In fact, during mercury penetration the imposed pressure p_c is equal to the capillary pressure given by Laplace's equation : $p_c = (2\sigma\cos\theta)/r$, where σ is the surface tension, θ the contact angle between mercury and chalk (σ = 0.482 N/m and θ = 147°, respectively) and r is the pore entrance radius. The values of surface tension and contact angle in Laplace's equation for chalk in contact with water and air are σ_{aw} = 0.072 N/m and θ_{aw} = 0°. Using Laplace's equation, and imposing the equality of the pore entrance radius, air-water suction s can be derived knowing p_c values from MIP as follows

$$s = u_a - u_w = p_c \frac{\sigma_{aw}\cos\theta_{aw}}{\sigma\cos\theta} \qquad (4)$$

Obviously this relation is valid admitting only capillary interaction between chalk, air and water. Retention curves of Estreux chalk are presented in Fig. 5. It can be seen that a suction level of 1.5 MPa is necessary to expel water and reduce the chalk water saturation degree following a drainage path. This value of suction is also called "air entry value". It is straightforward to observe that retention curve following a drainage path obtained using osmotic or vapour phase technique, give by far higher values of suction than the same curve derived from MIP data using Laplace's equation (i.e. admitting only capillary effects). It follows that air-water interactions of different nature probably exist in this chalk. These interactions are likely to be the consequence of the activity of the clayey matrix of Estreux chalk and may involve other physico-chemical processes (i.e. adsorption, dissolution, etc.). It is believed that the knowledge of the extent of these interactions is of great importance in defining the macroscopic mechanical response of this rock.

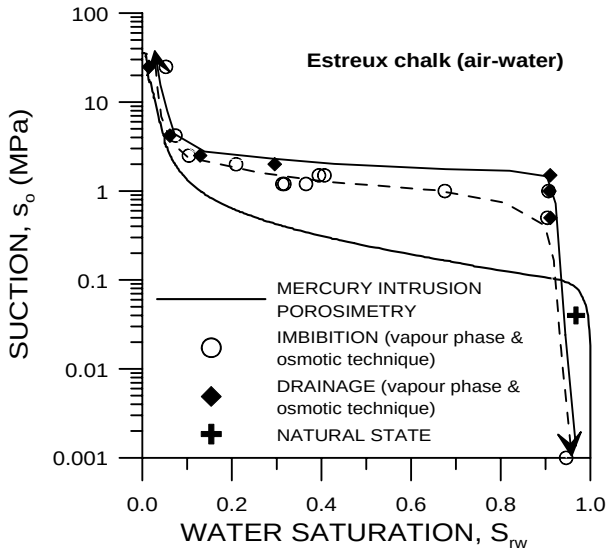


Figure 5. Retention curves of Estreux chalk.

Another indicator supporting the hypothesis of the existence of possible physico-chemical interactions is the small hysteresis observed in Fig. 5 between the imbibition path and the drainage path. In fact, significant hysteretic behaviour is often associated to capillary interaction and ink-bottle effect, leading to the entrapment of a given amount of water in the porous network, whereas physico-chemical interactions often produce reduced hysteresis. Note that, based on eq. (3), 1.5 MPa suction corresponds to a relative humidity of 99.8%.

Available measurements of the initial suction of Estreux chalk (at natural state) by filter paper (Fig. 5), gave values of about 40 kPa, in good agreement with the almost fully saturated state of the material. This corroborates also the in situ measurements of RH, indicating almost complete water vapour saturation at the time of the sampling. It is also interesting to observe that the residual water saturation is attained for suction values between 4.2 and 24.9 MPa. The former corresponds to RH = 97% (with K_2SO_4 salt), the latter to RH = 83,5% (with $(NH_4)_2SO_4$ salt). Thus, changes of few percentage points in RH may drastically reduce the relative saturation of the rock. Also, available measurements in the quarry gave minimum RH value of about 80%, which is sufficient, based on the retention curves plotted in Fig. 5, to attain almost complete de-saturation. Thus, the natural evolution of the relative humidity inside the quarry can lead to the two extreme saturation states (S_{rw} = 100% and S_{rw} = 5%), with changes in suction values between 0 and 24.9 MPa (i.e. the full range of attainable suction values). Consequently, due to the hydromechanical coupling, suction changes due to relative humidity could act as an additional load on the rock pillars and may affect, at long term, the stability of the underground quarry. The effects of these changes on material strength are quantified in the next section by means of suction controlled eodometric tests.

6. Results of oedometric tests

6.1. Compressibility curves

Figures 6 shows the results of three compression tests performed on chalk samples having various amounts of water: water saturated, dry and partially saturated under 1.5 MPa of controlled suction. The water saturation degrees (S_{rw}) of the samples and the corresponding level of suction can be

estimated from the retention curve of Fig. 5. Thus, the water saturated sample has s = 0 MPa, the dry sample has s > 24.9 MPa and at 1.5 MPa of suction the chalk has $S_{rw} \cong 90\%$ (i.e. is almost water saturated).

The analysis of the consolidation curves (Fig. 6a) for the water saturated sample, using the usual graphical methods employed in soil mechanics, did not permit to identify any significant point where changes in excess pore fluid pressure were apparent. Indeed, these methods seem not reliable for chalk, which is characterised by consolidation curves showing continuous vertical strain of the sample as soon as the loading is applied. Because of the order of magnitude of the permeability in this soft rock is quite high (about $1x10^{-8}$ m/s) and the compressibility of the soil skeleton quite low (due to inter-granular bonding), it is believed that after 24 hours of consolidation any excess pore fluid pressure is reasonably dissipated. This observation is in agreement with the analysis proposed by Lade and de Boer (1997), about the concept of effective stress in soil and rocks, and the general results of poroelasticity (Biot, 1941; Rice & Cleary, 1976; Coussy, 1995), showing that in a porous medium, the amount of the applied total load transferred instantaneously to pore water pressure increases when the drained bulk modulus decreases. Thus, it seems likely that the reduced compressibility and the rather high permeability are sufficient in chalk to prevent excess pore fluid pressure generation during instantaneous loading (i.e. stepwise oedometric loading). If this holds true, the delayed volumetric strain of chalk, as observed during oedometric tests (Fig. 6a), should be essentially due to creep and the solid skeleton settles continuously, although the excess pore pressure is zero. This result should be corroborated by pore pressure measurements during applied loading.

In order to reproduce the compressibility curves for Estreux chalk, the time of consolidation was 48 hours for stress levels lower than σ_o (conventional yield stress, as defined in Fig. 6b), and it was extended to seven days for loading steps in the plastic regime. The rational behind this choice was to have an insight into the creep behaviour of the rock. The compressibility curves of the chalk show clearly strength dependency on suction. It is interesting to observe that since the imposed suction level in Estreux chalk gives a water saturation degree that is close to the fully water saturated state (Fig. 5), compressibility curve under suction control at 1.5 MPa is also close to that obtained on a fully water saturated sample (Fig. 6b).

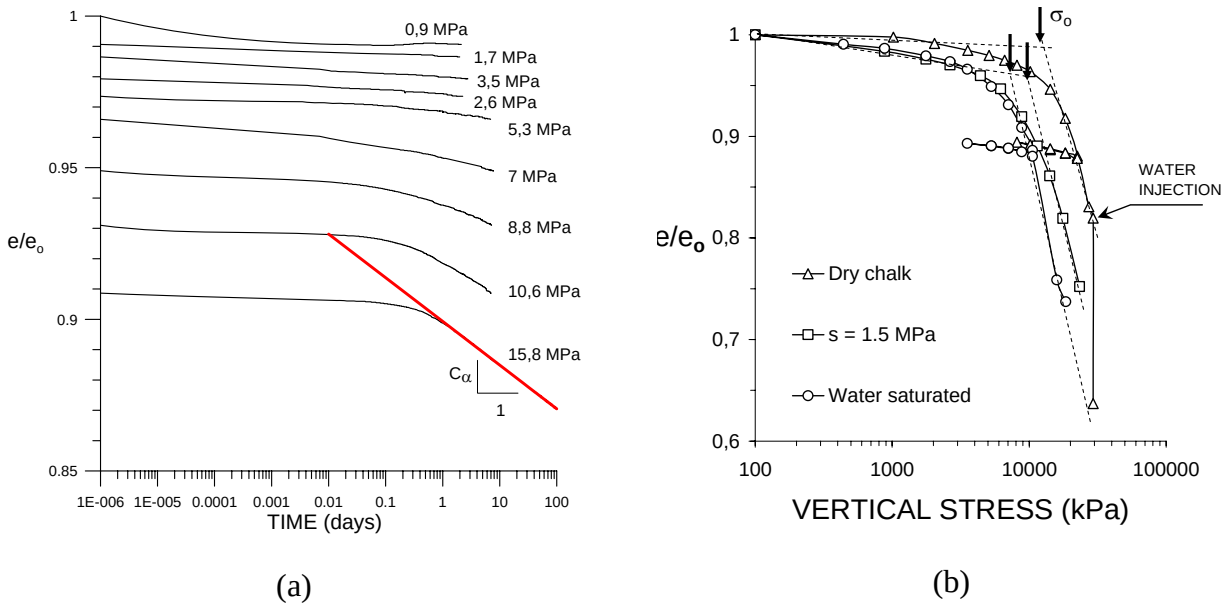


Figure 6. Results of oedometer tests : (a) Consolidation curves, (b) compressibility curves.

Nonetheless, the effect of suction is present, and it can be observed that the yield stress σ_o (the stress at which rock compressibility notably raises) increases with increasing suction, i.e. with lower degrees of water saturation.

Figure 6b also shows the collapse phenomenon of a dry chalk due to water imbibition. This was obtained by water injection under a vertical load of 29.3 MPa. In this test, the initial air-water suction (certainly higher than 24.9 MPa) was reduced to zero. Thus, based on the results shown in Fig. 5, the initial degree of water saturation of the dry sample, certainly less than 5%, was increased to the final value of 100% under zero suction. Water was infiltrated from the bottom to the top of the chalk sample, imposing few tens of centimetres of pressure head. The final point in Fig. 6b has been obtained after twelve days of continuous infiltration, and defines a total decrease of 0.183 in e/e_o ratio (vertical path). This variation of the void ratio corresponds to a compressive volumetric strain of about 6.6%. This collapse is significant, at the end of the process the final point is on the compression curve of the saturated chalk (Fig. 6b), in agreement with the double oedometer approach proposed by Jennings & Knight (1957) to assess the collapse susceptibility in unsaturated soils. The reduced amount of water menisci at the dry state doesn't seem to justify the magnitude of this breakdown as the consequence of the capillary loss solely. Consequently, it seems likely that the inter-granular links have a significant physico-chemical component, and are progressively weakened by the infiltration of water at the level of the inter-grain contacts. Pressure solution creep (Hellmann et al. 2002) is often mentioned to account for physico-chemical processes associated to rock weathering. This type of water-rock interaction bears a number of common features with the phenomena associated to suction. This point should certainly be the object of further researches, in order to better quantify the basic mechanisms at the origin of the chalk deformation.

The results presented so far are compatible with the water weakening effect in chalks, extending this effect to the partial saturation in both fluids under a controlled suction.

6.2. Viscous behaviour

Moving from the results presented in Fig. 6a, the analysis of the creep behaviour of Estreux chalk has been conducted quantifying the creep rate developing during each of the loading steps under oedometric conditions. The examination of the curves presented in Fig. 6a for the water saturated sample, plotting the evolution of the ratio e/e_o as a function of the logarithm of time, permits to define the classical creep coefficient C_α given by

$$\frac{de}{e_{oi}} = C_{\alpha i} d(\log t) \tag{5}$$

where e_{oi} is the void ratio at the beginning of loading stage i, $C_{\alpha i}$ is the slope of the consolidation curve vs time at long-term (Fig. 6a). Since equation (5) is valid for each of the hydraulic configuration, $C_{\alpha i}$ coefficients were assessed for all the loading stages of the three tests in Fig. 6b. Results are summarised in Fig. 7, plotting the evolution of C_α as a function of the applied vertical stress for all the tests. It is straightforward to note that both suction and vertical stress influence the creep rate. The creep rate varies linearly with the applied vertical stress, while it decreases when the level of suction increases, moving from a fully saturated to a completely dry environment. Similar results are in agreement with findings by Alonso et al. (2005) on the creep behaviour of partially saturated rockfill.

Note that, since suction influences the yield stress of the material, it is very likely that the influence of suction on creep could be reconducted to the similar effect on yield stress, assuming a normalizing factor for the effect of suction. This is the object of ongoing studies.

Parameter C_α describes adequately the viscous behaviour of Estreux chalk. Indeed, changes in creep rate due to suction (i.e. relative humidity) and load changes are easily accounted for when considering the results shown in Fig. 7. It is believed that these preliminary results can be useful for both practical applications, such as the assessment of the long-term stability of chalk pillars under various mechanical and environmental conditions, and theoretical developments (modelling approaches).

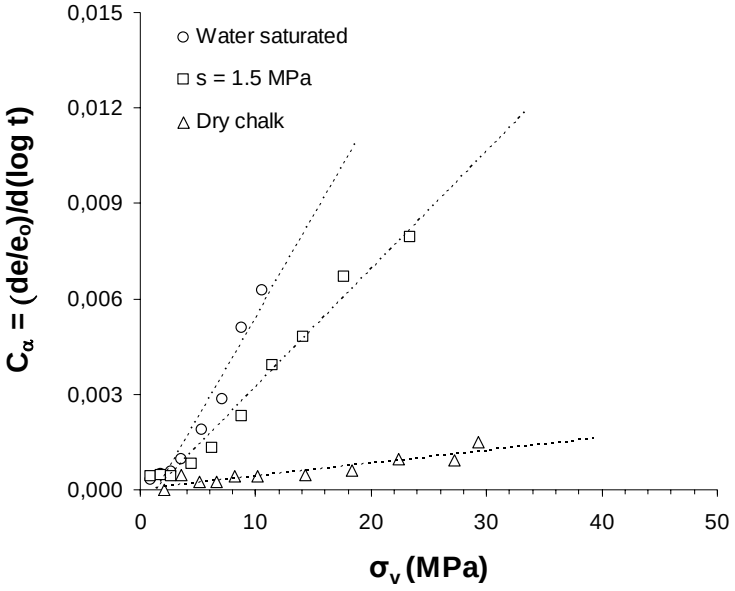


Figure 7. Evolution of creep parameter Cα vs vertical stress for various hydraulic configurations.

7. Conclusions

The experimental data presented in this paper are aimed at showing some effect of suction on the compressibility and the long term behaviour of a quarry chalk.

The role and the importance of the retention properties and their knowledge are emphasised, in order to better understand the coupled hydromechanical behaviour of partially saturated chalks. Compressibility and time-dependent behaviour have been studied in close relation with the influence of air-water suction. It has been shown that a number of common behavioural features exist between unsaturated soils and partially saturated chalks. Chalk is made stronger by increasing suction levels, which in turns means decreasing water contents. Its long-term deformation has consistently been related to the hygrometry changes by means of suction. The water weakening effect in chalk is considered here in a more comprehensive framework, introducing the air-water suction as an independent stress variable capable to account for the water-rock interactions.

8. Acknowledgements

The results on Estreux chalk have been obtained during the French National Project BCRD co-ordinated by INERIS. The collaboration of Mrs. M. Audiguier (Ecole des Mines, Paris - SEM images of Estreux chalk), Mr. J.V. Candel Hernandis and Mr. G. Priol is also acknowledged.

9. References

Alonso E.E., Olivella S., Pinyol N.M. (2005). *A review of Beliche dam*. Géotechnique, 55 (4): 267-285.

Bell F.G., Culshaw M.G., Cripps J.C. (1999). *A review of selected engineering geological characteristics of English chalk*. Engineering Geology, 54: 237-269.

BLPC (1973). *La craie*. Bulletin des Laboratories des Ponts et Chaussées, Special V190 pp.

Biot M. A. (1941). *General theory of three-dimensional consolidation*. Journal of Applied Physics, vol. 12 : 155-164.

Bonvallet J. (1979). *Une classification géotechnique des craies du nord utilisée pour l'étude de stabilité des carrières souterraines*. Revue Française de Géotechnique, 8 : 5-14.

Coleman, J.D. 1962. *Stress strain relations for partly saturated soils*. Correspondence Géotechnique, 12 (4): 348-350.

Coussy O. (1995). *Mechanics of Porous Continua*. Transl. by F. Ulm, John Wiley & Son Ltd.

Cui Y. J., Delage P. (1996). *Yielding and plastic behaviour of an unsaturated compacted silt*. Géotechnique, 46 (2): 291-311.

De Gennaro V., Delage P., Cui Y.J., Schroeder Ch., Collin F. 2003. *Time-dependent behaviour of oil reservoir chalk: a multiphase approach*. Soils and Foundations, 43 (4): 131-148.

De Gennaro V., Delage P., Priol G., Collin F., Cui Y.J. 2004. *On the collapse behaviour of oil reservoir chalk*. Géotechnique, 54 (6) : 415 - 420.

Delage P., Suraj De Silva G.P.R., Vicol T. 1992. *Suction controlled testing of non saturated soils with an osmotic consolidometer*. 7th Int. Conf. Expansive Soils, Dallas, 206-211.

Delage P., Schroeder C., Cui Y.J. 1996. *Subsidence and capillary effects in chalks*. EUROCK '96, Prediction and performance on rock mechanics and rock engineering 2, 1291-1298, Turin, Italy.

Dineen K., Burland J.B. 1995. *A new approach to osmotically controlled oedometer testing*. Proc. 1st Int. Conf on Unsaturated Soils UNSAT'95, Paris : 459-465.

Fredlund D.G., Rahardjo H. 1993. *Soil mechanics for unsaturated soils*. John Wiley, New York.

Gens A. (1996). *Constitutive modelling : application to compacted soils*. Proc. 1st Int. Conf on Unsaturated Soils UNSAT '95 : General Report, Paris : 1179-1200

Grgic D., Homand F., Hoxha D. (2003). *A short- and long-term rheological model to understand the collapses of iron mines in Lorraine, France*. Computers and Geotechnics 30 (2003):557–570

Jennings, J.E. & Knight, K. (1957). *The additional settlement of foundations due to collapse of sandy soils on wetting*. Proc. 4th Int. Conf. on Soil Mechanics and Foundations Eng., vol. 1 : 316-319.

Hellmann, R., Renders, P.J.N., Gratier, J-P. and Guiguet, R. (2002). *Experimental pressure solution compaction of chalk in aqueous solutions. Part1. Deformation behaviour and chemistry*. In: Water-Rock Interactions, Ore Deposits, and Environmental Geochemistry: A Tribute to David A. Crerar; The Geochemical Society (Hellmann & Wood Eds.), Special Publication no. 7: 129-152.

Kassiff G., Ben Shalom A. 1971. *Experimental relationship between swell pressure and suction*. Géotechnique, 21, 245-255.

Lade, P. V. & Boer, R. (1997). *The concept of effective stress for soil, concrete and rock.* Geotechnique 47, No. 1, 61-78.

Lord, J.A., Clayton, C.R.I., Mortimore, R.N. 2002. *Engineering in chalk.* CIRIA Eds., 334 pp.

Masson M. 1973. *Pétrophysique de la craie*. Bulletin des Laboratoires des Ponts et Chaussées, spécial V: 23-48.

Pasachalk1 (2001). *Mechanical Behaviour of PArtially and Multiphase SAturated CHALKs Fluid-skeleton Interaction : Main Factor of Chalk Oil Reservoirs Compaction and Related Subsidence*. Publishable Final report, European Joule III contract N° JOF3CT970033: 80 pp.

Pasachalk2 (2004). *Mechanical Behaviour of PArtially and Multiphase SAturated CHALKs Fluid-skeleton Interaction : Main Factor of Chalk Oil Reservoirs Compaction and Related Subsidence. Part 2*. Publishable Final report, Energy, Environment and Sustainable Development Programme, contract N° ENK6-2000-00089: in print.

Priol G. (2005). *Comportement mécanique différé et mouillabilité d'une craie pétrolifère*. ENPC, PhD thesis: 217 pp.

Rice, J. R., and M. P. Cleary (1976). *Some basic stress-diffusion solutions for fluid-saturated elastic porous media with compressible constituents*. Reviews of Geophysics and Space Physics, vol. 14, pp. 227-241, 1976.

Sorgi C. (2004). *Contribution méthodologique et expériementale à l'étude de la diminution de la résistance des massifs rocheux par veillissement*. BCRD Rapport Final (conv. 2001-01111), INERIS-DRS : 132 pp.

Sparks, D.L. (1998). *Soil physical chemistry*. CRC Press, 432 pp.

Talesnick, M.L., Hatzor, Y.H. & Tsesarsky, M. (2001). *The elastic deformability and strength of a high porosity, anisotropic chalk*. Int. J. of Rock Mech. & Min. Sci., 38 : 543-555.

Terzaghi K. (1936). *The shearing resistance of saturated soils and the angle between the plane of shear*. Proc. 1st Int. Conf. Soil Mech., Vol. 1 : 54-56.

Wheeler S.J., Karube D. (1996). *Constitutive modelling*. Proc. 1st Int. Conf on Unsaturated Soils UNSAT '95 : General Report, Paris : 1323-1356

Williams J., Shaykewich C.F. (1969). *An evaluation of polyethylene glycol PEG 6000 and PEG 20000 in the osmotic control of soil water matric potential*. Can. Geotech. J., 102 (6): 394-398.

VULNERABILITY ASSESSMENT FOR MINING SUBSIDENCE HAZARD

DECK Olivier[1], VERDEL Thierry[1], SALMON Romuald[2]

[1] LAEGO – LABORATOIRE ENVIRONNEMENT GEOMECANIQUE ET OUVRAGES. Ecole des Mines de Nancy – Parc de Saurupt – F 54042 – Nancy Cedex. Olivier.Deck@mines.inpl-nancy.fr; Thierry.Verdel@mines.inpl-nancy.fr

[2] INERIS – INSTITUT NATIONAL DE L'ENVIRONNEMENT INDUSTRIEL ET DES RISQUES. Parc Technologique ALATA - Rue Jacques Taffanel - BP 2 - 60550 Verneuil-en-Halatte. Romuald.Salmon@ineris.fr.

ABSTRACT: After the last mining subsidence events, which occurred in the iron-ore field in Lorraine (France) in 1996, 1997 and 1999, and because of the thousand hectares of undermined areas, the assessment of vulnerability of buildings and territories became necessary for risk management. The ten last years highlight evolutions of the vulnerability concept and its assessment method between the first risk management decisions and current risk assessment. These evolutions reveal a lot about the complexity of the vulnerability concept and about difficulties to develop simple and relevant methods for its assessment.

The objective of this paper is to present this evolution and to suggest different improvements compared to other concepts and methods developed in other countries (USA, Poland...) and for other hazards (flood, industrial...). These improvements take into account more various kinds of elements in the vulnerability meaning (buildings, people, roads, public facilities and public functions) as well as they deal with method of assessment in relation to the subsidence intensity and vulnerable elements.

KEYWORDS: Vulnerability, Subsidence, Stakes, Assessment Methods.

RESUME : Depuis les affaissements miniers survenus en Lorraine en 1996, 1997 et 1999, et en raison des milliers d'hectars souminés, l'évaluation de la vulnérabilité des habitations et des territoires est devenu une nécessité pour permettre une meilleure prévention des risques. Les dix années écoulées depuis les premières décisions prises en réaction au risque d'affaissement minier montrent une évolution importante des méthodes employées. Ces évolutions sont révélatrices de la complexité du concept de vulnérabilité et de la difficulté à trouver des méthodes pertinentes et opérationnelles pour l'évaluer.

Cet article a pour objectif de présenter cette évolution et de donner des perspectives d'amélioration au vu des méthodes employées dans d'autres pays (Etats-unis, Pologne) et vis-à-vis d'autres aléas (sismique, inondation, accidents industriels). Ces perspectives portent sur les différents enjeux qui contribuent à la vulnérabilité (personnes, bâtiments, infrastructures, équipements publics...) et sur les méthodes de caractérisation de la vulnérabilité en fonction des enjeux et de l'intensité de l'affaissement.

MOTS-CLEFS : Vulnérabilité, Affaissement, Enjeux, Méthodes d'Evaluation.

1. Introduction

"La Lorraine" is a French territory, which has important underground natural resources of iron, coal and salt. The industrial need for large quantities of raw materials at an acceptable cost has led to large underground mines, especially between 1900 and 1990. Because of the extraction methods,

such underground mining works create underground voids, which may cause mining subsidence phenomena, i.e. significant movements at surface. These may then result in serious damage to structures built in the area of influence of such movements. Subsidence is planned, during mining works, in the case of total extraction mining methods ("caving-in" method in coal mines, for example). Such methods are the most profitable and were used in the iron-ore field when no build elements exist on the ground surface. On the other hand, mining subsidence is of a highly accidental nature when it takes place over mines that use abandoned rooms and pillars method even though this method should have allowed an endless ground stability. Indeed, in the latter case, the operator has deliberately left in place natural or artificial pillars sized to withstand the weight of the overburden. Such a method is less profitable and is used under urbanized areas in order to avoid subsidence and damages to structures. Recent cases of mining subsidence (1996, 1997 and 1999) that have taken place in the Lorraine iron mining area denote the hazard of such mining works when left abandoned.

The cases of subsidence in Lorraine led public authorities to carry investigations over the entire Lorraine iron-mining field in order to assess hazard, vulnerability and risk of the whole territory. The first investigations highlighted the existence of about 20 km^2 of urbanised areas undermined by abandoned works consisting of rooms and pillars.

The first part of this paper is a presentation of the last subsidence phenomena and on the identification of damage.

The second part deals with different aspects of the vulnerability concept through a bibliography study. It is then proceeded to a description and a discussion, in a third part, of evolutions of methods used in the iron-ore field for the vulnerability assessment.

The last part deals with possible evolutions of the vulnerability and risk assessment methods for mining subsidence hazard. Some improvements can be carried out with an explicit split of the vulnerability components and some others with careful considerations about influence attached to the different vulnerability and risk components.

2. Mining subsidence in the iron-ore field

Mining subsidence often produces significant horizontal and vertical movements at the ground surface (Table 1). The maximum value “Sm” of the vertical subsidence is usually considered as a characteristic of the trough. This parameter is relatively easy to estimate for undermined areas. However, the horizontal strain of the ground “ε”, its curvature and its slope “T”, are the three main causes of structural damage. The maximum values observed for these parameters (“εm”, “Tm”) can be disastrous for a structure if the movements are imparted integrally. The measurement of these parameters entails significant difficulties either when a site of mining subsidence is instrumented, or in a case where cave-in has not yet taken place and prediction is regarded. The real measurements of movement often reveal that the vertical movement is in agreement with its theoretical value, but the slope and the horizontal strain deviate slightly from theory and the curvature even more.

Table 1: Description of the five last subsidences in the iron-ore field and the associate damage.

	Subsidence characteristics[2]	Physical damage	Cost	Others consequences
Auboué (Metz street) 1996	Sm = 1.7m $\varepsilon m \approx 15\ 10^{-3}$	130 buildings[2] roads, pavements,	13,9 millions € **Erreur ! Signet non**	150 families evacuated[1]

	Tm = 2.5%	sewerage system1	**défini.**	300 peoples left their village for good[1] Nursery school closed[1]
Auboué (Coinville city) 1996	Sm = 1m εm ≈ 8.5 10^{-3} Tm = 3.5%	100 buildings[2] roads, pavements[1]		
Moutiers (high quarter) 1997	Sm = 1.4m εm ≈ 18 10^{-3} Tm = 1.2%	70 buildings[2]		A pub is closed[1]
Moutiers (near the stadium) 1997	Sm > 0.5m εm > 6 10^{-3} Tm = ?	60 buildings[2]		
Roncourt 1999	Sm = 0.65m εm ≈ 6.5 10^{-3} Tm = 1%	18 buildings[2]		
[1] Zihri (2004) ; [2] Deck (2002)				

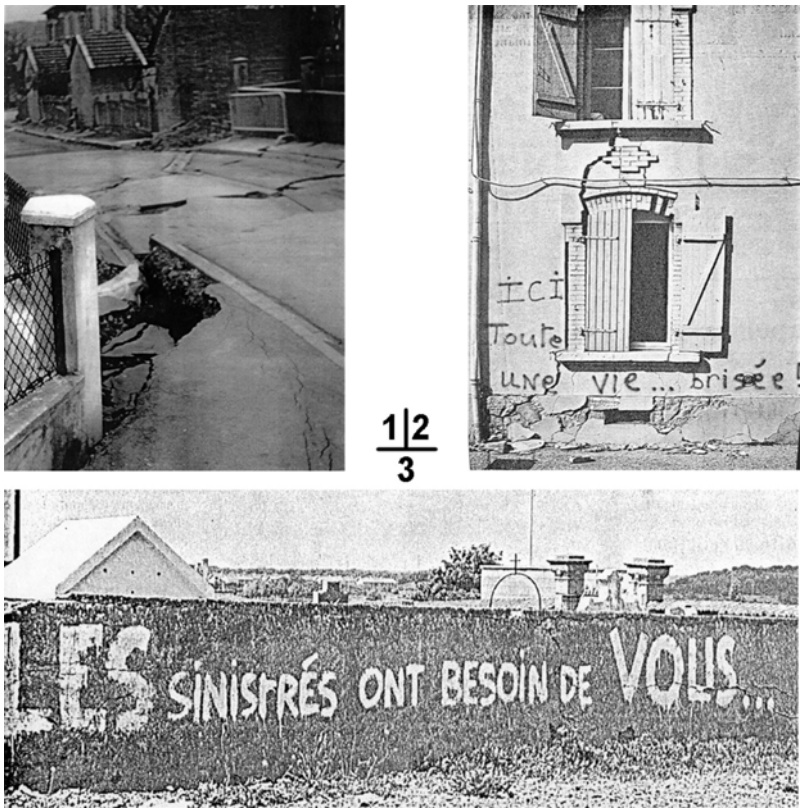


Figure 1: Example of mining damage in the iron-ore field (1: Road damage in Auboué, 1954; 2: Building and social damage in Auboué, 1996 "*Here, all a life is broken!*"; 3: Social damage in the iron-ore field « *Disaster victims need you...* »

Prediction of building damage may be performed on the basis of threshold values for ground movements (especially horizontal ground strain) and buildings characteristics (especially length and structural strength). But an accurate building damage prediction is difficult in the light of uncertainties about the real ground and structure behaviour.

Consequences induced by subsidence are various (Table 1, Figure 1):

- physical, with buildings, roads, pavements and networks damage;
- economical with the cost of physical reparations and compensations;

- social with important psychological impact on both disaster victims and other people of the area who suffer from an impression of a lack of public support and answer to their fears;
- political and media related because the whole territory became a key point for a political debate and media reports for many months.

3. The vulnerability concept in the scientific litterature

The concept of vulnerability is usually used in many definitions of risk. A comparison of these definitions is useful to grasp whole the notions included in this term.

The Vulnerability is a component of Risk. The United Nations, through the International Strategy for Disaster Reduction define Risk as "the probability of harmful consequences, or expected losses (deaths, injuries, property, livelihoods, economic activity disrupted or environment damaged) resulting from interactions between natural or human-induced hazards and vulnerable conditions » (UN/ISDR 2004). They adopt the classical convention expressed by the notation: Risk = Hazards x Vulnerability. Vulnerability is then defined by « the conditions determined by physical, social, economic, and environmental factors or processes, which increase the susceptibility of a community to the impact of hazards. »

In France, the Ministry of Environnement and Sustainable Development, defines the vulnerability by the « level of foreseeable consequences of one natural phenomenon upon stakes » in which stakes are « people, goods, activities, means, heritage... likely to be affected by a natural hazard » (MATE, 1997). In case of industrial risk, the same Ministry suggests a slightly different definition: « the vulnerability of an area or a place is the appreciation of target sensibility against particular effects. » (MEDD, 2003).

Griots and Ayral (2001) make an inventory of 17 definitions of vulnerability, which lead to split the vulnerability concept into two elementary notions: the notion of damage, consequences, losing level... and the notion of sensibility, susceptibility, weakness, predisposition... This last notion is also highlighted by Bogardi (2004, United Nations University), who underlines the "stochastic" nature of vulnerability.

In the seismic field, the European Macroseismic Scale used the vulnerability in the strict sense of the buildings strength: it "incorporates a compromise, in which a simple differentiation of the resistance of buildings to earthquake generated shaking (vulnerability) has been employed in order to give a robust way of differentiating the way in which buildings may respond to earthquake shaking. The Vulnerability Table is an attempt to categorise in a manageable way the strength of structures, taking both building type and other factors into account. This is a development from previous scales, which used only construction type as an analogue of vulnerability. » (EMS, 98). Nevertheless, the seismic field has a strong foothold in the evolution of the vulnerability term. Recent studies show an increase of assessment of both social and material vulnerability. Balandier (2004) lists different kinds of elements at risk (urbanized areas, roads, networks, power plants, community facilities), which are relevant for social vulnerability.

Still in the seismic field, Teramo et al. (2005) introduce a methodology of urban and territorial seismic vulnerability related both to engineering studies and social priority levels. They first highlight the impossibility for administrations to plan suitable prevention interventions due to the use of usual approaches based on the building weakness and the earthquake loss estimate (as in the EMS 98 case). They identify different vulnerability related to three kinds of elements:

- the vulnerability related to the "morpho-typological characters of buildings" (as the EMS 98 vulnerability);

- the vulnerability related to "the collective or public system" (distribution of services, productive stakes, public buildings...);
- the vulnerability related to "the critical spatial elements" (streets, safety routes, strategic structures...).

Each vulnerability is assessed with two functions, which model the seismic weakness/reliability and the social or strategic priority levels within the system.

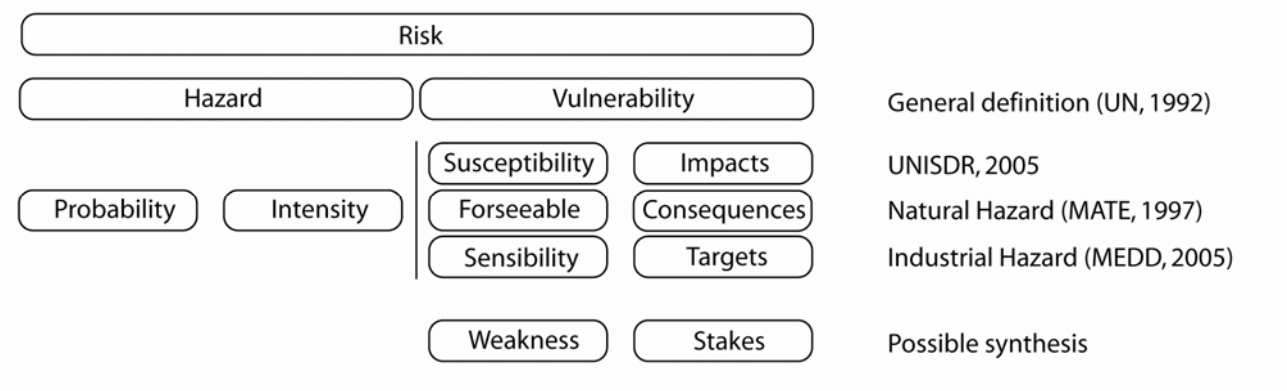


Figure 2: Synthesis of different definition for the Vulnerability term.

Studying vulnerability means to make the assessment of damage upon different kinds of stakes: human physical and psychological integrity, goods (buildings, roads, factories, properties...), economic (cost of reparations, decrease of activities, lost of stocks...), environmental (induced pollutions, ecosystems damage...)... The study of vulnerability requires identifying all the stakes, which may be damaged in case of natural phenomena or industrial accidents. But this step of the analysis is not sufficient to perform a real damage assessment since stakes may be damaged with varying level depending on accident intensity. For this reason, we choose a possible synthetic definition of vulnerability, which highlights the necessity to combine identification of stakes and the study of their weakness (Figure 2). This synthesis is in agreement with the vulnerability assessment methodology presented by Teramo et al. (2005).

On the basis of similar considerations, Bogardi (2004) still reveals uncertainties due to several points:

- the question of "how far should vulnerability be seen as the "susceptibility" alone or being rather the product of hazard exposure and that very susceptibility?"
- the question of the "proper scale (national, regional, community, household or individual) to capture and to quantify vulnerability";
- the question of "whether (social) vulnerability can adequately be characterized without considering simultaneously the response (coping) capacity of the same social entity"

The first question can be clarified with help of the Figure 2 where the "weakness" is assumed to be quite similar to susceptibility. From a theoretical point of view, weakness of stakes may be dependant from the intensity of Hazard. Considering that this intensity may be very different, regarding to its probability, the study of vulnerability might lead to as many elementary studies as the number of various hazard intensities. Because of the number of studies that this theoretical point of view would lead, engineers used to make a single assessment of vulnerability and thus make the hypothesis of the independence of weakness and hazard intensity.

The second question is also considered by Balandier (2004) and highlights that a same risk element has not the same importance depending on the kind of hazard and the surface area (country, city, district...) because of their relative importance.

The last question refers to the "resilience" concept, which is largely discussed by Klein et al. (2003). On the basis of several definitions they suggest to restrict this term to describe:

- "the amount of disturbance a system can absorb and still remain within the same state or domain of attraction;
- the degree to which the system is capable of self organisation;
- the degree to which the system can build and increase the capacity for learning and adaptation."

In conclusion, the vulnerability term has many different meanings. The most important is then to clearly define the held meaning before any study. It is important to notice that the vulnerability is always a subjective concept, due to the number of different stakeholders, administration or insurance companies who have to support the consequences of hazard occurrences. The results of the vulnerability studies are then dependant on the end user.

4. Evolution of the vulnerability concept and its method of assessment in the iron-ore field between 1996 and 2005

4.1. The first hierarchy

In reaction to recent subsidences, in 1996 (Auboué), 1997 (Moutiers) and 1999 (Roncourt) and sinkholes in 1998 (Moyeuvre), public authorities ordered investigations to become aware of the extent of the problem.

Because of the lack of knowledge regarding to the subsidence phenomena, a first hierarchy was based upon two main considerations:

- the subsidence probability, through the value of the extraction ratio;
- the subsidence intensity, through the value of the maximal subsidence.

This first hierarchy was in agreement with the regulations of the French urban code (article R111-2 and R111-3). It defines three kinds of areas, depending on the maximal possible subsidence, and associates recommendations for building projects (Table 2; Kouniali, 2001).

Table 2: First hierarchy of risk in the iron-ore field and its associate recommendations.

Maximal subsidence < 1m	Surface of building < 400 m2, Maximal length < 25m, Number of floors ≤ ground floor + 3
Maximal subsidence < 2.5 m	Surface of building < 150 m2, Maximal length < 15m, Number of floors ≤ ground floor + 1
Maximal subsidence > 2.5 m	Forbidden

This first hierarchy is called step 1 in the **Erreur ! Source du renvoi introuvable.**. It mainly deals with urban side of vulnerability and was unsuitable for other side of vulnerability, especially human, social and economical.

4.2. The multicriteria hierarchy

Supplementary investigations were necessary to both go deeper into the hazard assessment and the human vulnerability assessment. Merad and al. (2004) developed a method, based upon a multicriteria analysis. Because of mathematical functions included in the method, it allows to manage with a « complex decision-making problem where the available information is uncertain and imprecise and where knowledge is incomplete » (Merad and al., 2004). This method uses weight factors for all criteria, which allow to highlight their relative importance in the risk assesment.

One of the main goals was to identify areas requiring specific surveillance because of the importance of existing stakes. This leads to the second step of **Erreur ! Source du renvoi introuvable.**, which deals with identifying stakes.

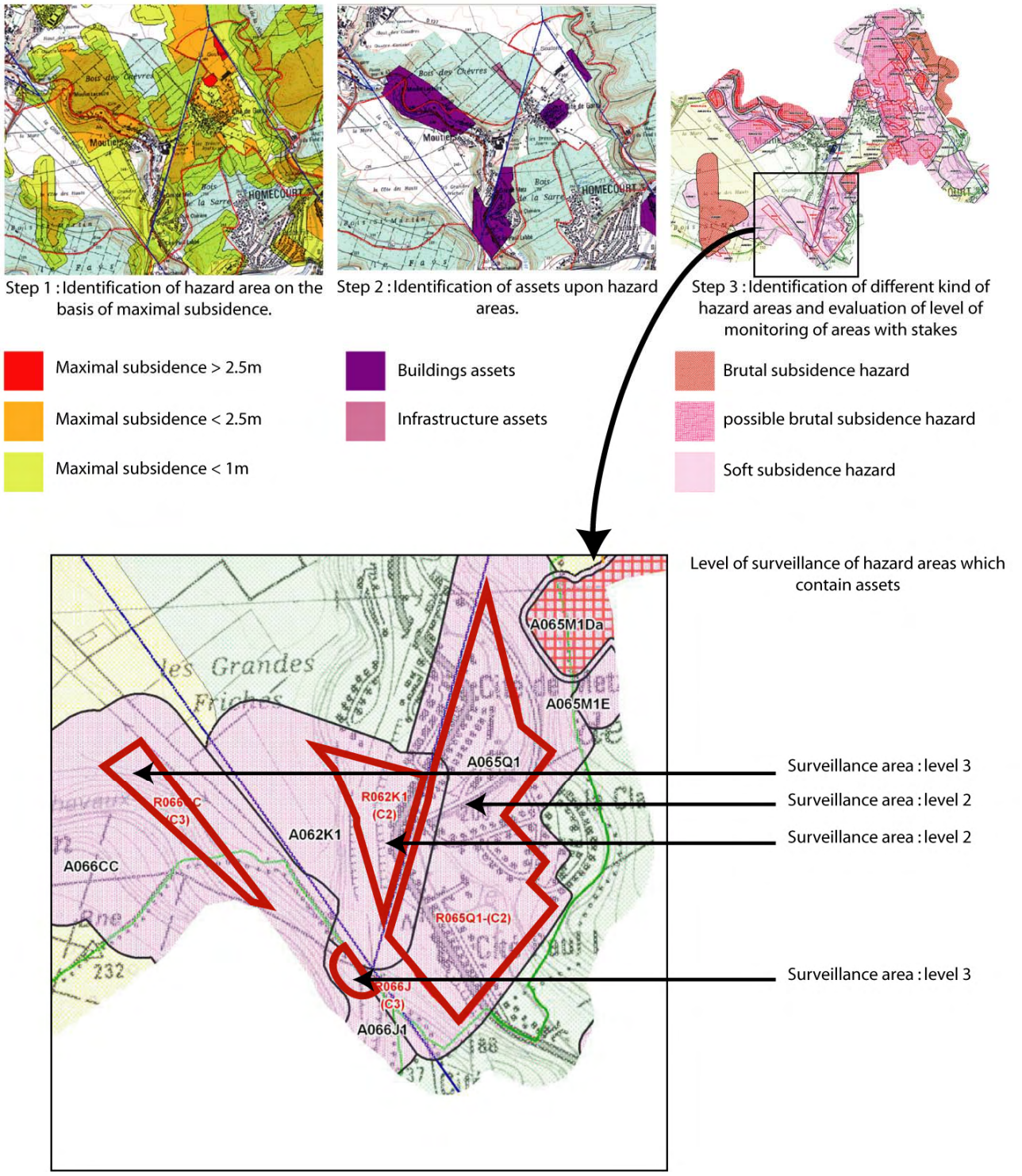


Figure 3 : Evolution of risk assessment in the iron-ore field.

Two kinds of stakes were identified: buildings stakes and infrastructure stakes. The Figure 4 shows the methodology used to determine the vulnerability of each kind of asset. In case of buildings stakes, no other stakes are taken into account. Buildings stakes are assessed through 5 levels from « business park » which induce a small vulnerability level because of its single daily activity to « city » which induce the strongest vulnerability level because of its both daily and nightly activities and because of the number of concerned people. This typology is mainly devoted to the population safety and to a lesser degree to the economic or structural vulnerability although those

kinds of vulnerabilities are indirectly taken into account since they increase with the population numbers. The associated recommendations are listed in the Table 3.

The choice to distinguish between two kinds of stakes (buildings stakes and infrastructure stakes) shows a will to favour human vulnerability upon others kinds without an explicit weighting.

The weights linked with the probability, intensity and vulnerability criteria raise an important question connected with the previous definition of risk. If the risk is the outcome of hazard and vulnerability, do weight for each component have to be equals? In this case, weight of hazard reach a sum of 46 while vulnerability weight factors reach « only » between 2 and 14, depending on the stakes. This difference leads to results, which are more dependent on hazard than on vulnerability, that is focuses on prevention rather than crisis management

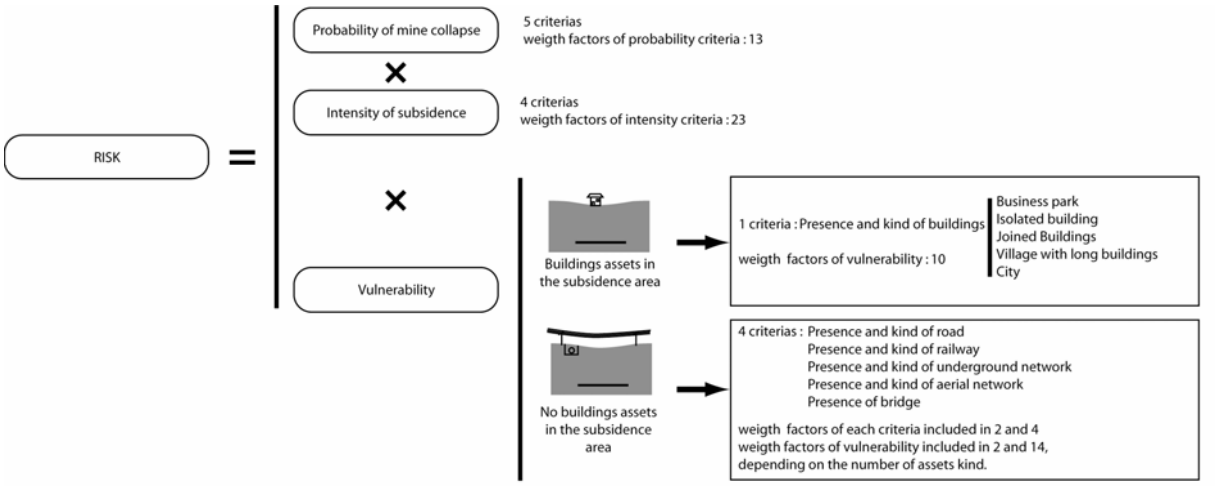


Figure 4: Description of criteria and weight factors used in the actual assessment of risk, hazard and vulnerability in the iron-ore field.

Table 3: Second hierarchy of risk in the iron-ore field and its associate recommendations.

Level 1 of surveillance area	Real-time monitoring.
Level 2 of surveillance area	Regular monitoring which will become a real-time one at the first forewarning.
Level 3 of surveillance area	Supplementary are required to assess the need of regular monitoring.
Level 4 of surveillance area	No monitoring is required. Levelling measurements are only made.

This methodology has been applied to constructed areas (civil security objective). An extension of the methodology has been applied to non urbanised areas in a perspective of land use planning

4.3. The Mining Risk Prevention Plan (MRPP)

The last step for the mining risk assessment and management is currently in completion stage. MRPP will provide a legal framework for all municipalities to both identify hazards and their current or foreseen stakes upon their territory. These plans aim to identify most sensitive areas with regards to risk development and establish rules for a proper management of territories according to post-mining constraints. MRPP are introduced by Didier (2005). They consist of four steps :

- Mining exploitation data collection and structuring ;
- Hazard assessment ;
- Stakes assessment ;

- Rules and regulations for existing and future constructions.

The "stakes assessment" step aims to identify all existing stakes within studied territories as well as possible future projects. It enables to identify threatened populations and most sensitive infrastructures. This step ends with a map of stakes. Several maps may be carried on to fit the goal of the study (civil security, land use planning…).

The MRPP framework is intended to be applied over potentially hazardous mining field. Its construction is based on the experience of already existing prevention plans for other hazards (flood, fire…). MRPP global methodology is the result of the experience of former REP (Risk Exposition Plan) that applied in 80's. Within REP, vulnerability had to be assessed through an exhaustive study of susceptibilities. At the scale of a town, this task appeared to be too complex and long. This led to define MRPP methodology with a requirement for simplicity and quick results.

In Lorraine, MRPP will lead to a third hierarchy with no significant difference in term of vulnerability assessment compared to the previous one. More generally, the application of the MRPP will not give methods to asses the vulnerability. Consequently, the next part presents a possible improvement of the current method for a better assessment of vulnerability

5. Improvements for a better vulnerability assessment

In a report for the Ministry of Environment and Sustainable Development and for the Ministry of Industry, Economy and Finance, Deck (2003) suggested some evolution to improve the current taking into account of the vulnerability in the French iron ore field. These proposals take into account the further remarks about the previous sections:

- Before any vulnerability study, it is obviously necessary to define the meaning of the term vulnerability. In the case of the iron-ore field, we saw that the objective was both the safety of citizens and the mitigation of risk with the prescription of rules for new buildings. The studied area is the whole iron-ore field, which is composed of more than one hundred small cities and villages. The scale of this study is far greater than the town one. Proposals for a better assessment of the vulnerability need to be related to this scale. They must allow a better hierarchy of every urbanized area (small villages or districts) in comparison with one another and especially guarantee the homogeneity of the evaluation of towns vulnerabilities ;
- Previously presented hierarchies underestimate the societal consequences and do not take into account the "resilience";
- Current hierarchy appears to give more importance to the hazard criteria than to the vulnerability ones (Figure 4). This situation is probably the reflection of the skills of experts who made this analysis. It is clear that the risk analysis is made by engineers, who are more keen on hazard concept than on the vulnerability one because of the number of its different dimensions: social, politic, economic... Giving exactly the same weight to vulnerability and hazard criteria comes from a theoretical point of view of the risk problematic. The increase of the vulnerability weight factors lead to direct safety measures towards vulnerable areas, although no certitude exist about the hazard occurrence. Conversely, a decrease of the vulnerability weight factors leads to limit safety measures to the highly probable hazard areas. The difference is equivalent to favour preventive cost or to favour compensation cost.

Proposals are synthesised on Figure 5 and discussed afterwards. They are mainly connected with the first two remarks.

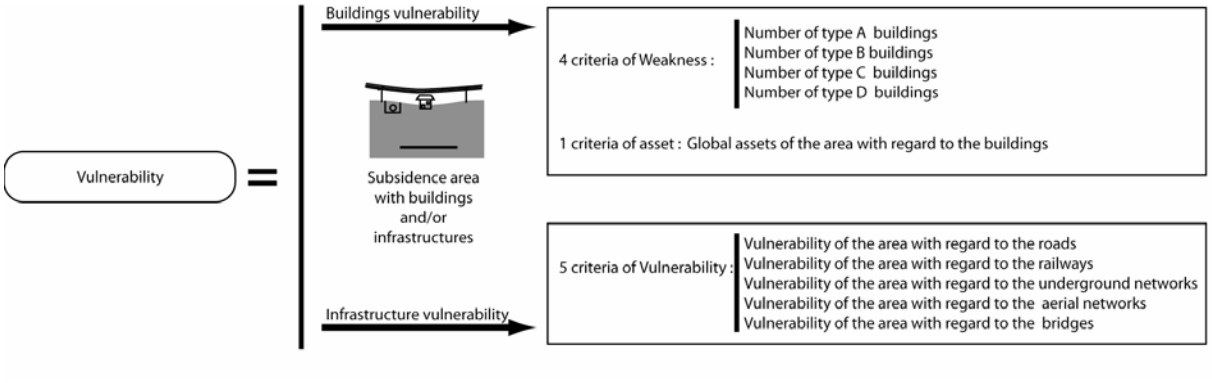


Figure 5: Propositions for a better assessment of the vulnerability in the iron-ore field.

For a more accurate vulnerability assessment, the every weak elements must simultaneously be considered into the analysis. In accordance with the section, which deals with literature, it may be useful to split vulnerability into different components.

For buildings, the current method assesses vulnerability through one criterion that identifies the nature of the building. We propose to split building vulnerability into two components: **weakness** and **stakes**. For networks, we choose to keep a single criterion but with a quite different definition than previously. These choices are in agreement with the problematic because most of urbanized areas are small one and previous subsidences show that buildings were the most critical constructions due to their weakness and stakes. Secondly, the use of explicit criteria for the weakness allows to consider results of the seismic field as a model for these criteria.

Figure 6 shows a classification of different kinds of buildings into four classes of **weakness**. This classification is modelled on the one used in the EMS 98. We based our proposal on statistical studies performed on the iron-ore damaged buildings (Deck, 2003) and on a architect study about the typology of buildings for one typical village in Lorraine.

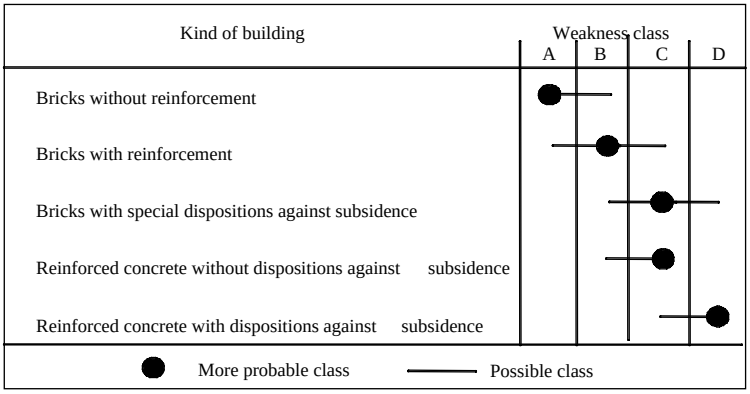


Figure 6 : Classification of buildings into 4 classes of weakness.

The Figure 6 can then be used to determine the number of buildings in each weakness class. This lead to consider 4 criteria to assess the weakness of buildings : number of class A, B, C and D buildings. These criteria are directly connected with the economic consequences of subsidence because the class A buildings will be more damaged than those of class B for similar subsidence phenomena. These four criteria are neither connected with social or environmental consequences dues to building damage, nor to the resilience.

For this reason, we define another criterion **(stakes),** which allows a qualitative assessment of stakes connected with building and to take into account the resilience, and mainly the degree to

which the village is capable of self organisation. The Table 4 describes three possible levels for this criterion.

Table 4: Indicators of stakes connected with buildings.

Slight	Medium	Strong
Individual consequences due to a slight importance of stakes or a slight quantity of possible damaged buildings.	Collectives consequences due to a strong importance of stakes or a big quantity of possible damaged buildings. Consequences over the society running are possible (social and economic equilibrium).	Collectives consequences with possibility of series of accidents: In addition to the collectives consequences previously described, a possibility of a series of accidents exist due to the very strong importance of stakes (hospital, emergency services...) or because some problems are identified in the hazard area (chemical factories, petrol station...).

For the infrastructure vulnerability assessment, we choose to keep the same number of criteria (five) than for the current method, but with a different meaning in order to take into account both the weakness and the stakes asset. Because of the lowest importance of the infrastructure vulnerability compared to the building's one, and because of the necessity to keep a relevant method for risk assessment, it is necessary to synthesize weakness and asset assessment into a single vulnerability criterion for each of the five kinds of infrastructure (roads, railways, underground networks, aerial networks, bridges). Table 5 describes five possible levels for each of these five criteria. The reference to the scale of consequences follows the thesis of Zihri (2004). This evaluation way allows to integrate both the weakness, the stakes assets and the resilience concept seeing that the social, economical and political response of the community is required and then assessed.

Table 5: Indicators of damage levels due to the infrastructure weakness and stakes.

Null	Slight	Medium	Strong	Very Strong
No infrastructure in the area	Combination of weakness, stake asset and resiliance of the infrastructure lead to think that damage will only affect...			
	...a few people (individual consequences)	...people, economy, running of whole a village.	...people, economy, running of whole an administrative region.	...people, economy, running of whole a state or of administrative region of different states

The Table 6 shows a comparison for a theoretical area between the current method of vulnerability assessment and the proposed one. On the basis of one area with 50 buildings, 1 main road, 2 shops, with no possibility to rehouse people for less than 10 Km and with a public debate and many information given to population about the risk of subsidence.

Table 6 : A exemple of comparaison between the currently method of vulnerability assessment and the proposal one

Current method		Proposal method	
1 criterion for building vulnerability	The whole area is classed as village one	4 criteria for building weakness	The four criteria of building weakness allow the assessment of possible economic damage : 5 buildings in class A 15 buildings in class B 22 buildings in class C 8 buildings in class D
		1 criterion for building stakes	Medium value of stakes connected with buildings due to the important number of concerned buildings and due to the difficulty to rehouse people.
5 criteria for infrastructure vulnerability	The 5 vulnerability criteria of infrastructures (bridge, road, railway, aerial netwok, underground	5 criteria for infrastructure vulnerability	Medium value for road infrastructure vulnerability. Null values for railway and bridge infrastructure

	network) are not taken into account because of the presence of buildings.		vulnerability because there is no such infrastructure. Sligth values for aerial and underground network because few of them might be damaged

6. Conclusion

The study of vulnerability with the prospect of risk assessment appears to be sensitive because of the gap between the social expectations and the difficulty to formalize a coherent and unbiased methodology.

A bibliographic approach allows to identify different concepts, which may be included in the vulnerability term. We choose to split this term into two elementary components: the weakness and the stakes. The weakness allows to characterize the possible structural damage to physical elements like buildings and infrastructures. The weakness is directly connected to the economic loss due to reparations. The stakes allow to characterize the importance of other damage due to the social, economical, civil... use of the damaged physical element.

Both of these two components are really subjective. Several preliminary considerations are necessary to precise the meaning of the vulnerability before using it in a risk assessment study.

- What is the scale of the study (national, regional, community...)?
- What is the balance between the weight factors for hazard criteria and for vulnerability criteria? An upper weight factor for vulnerability leads to favour civil protection, an upper weight factor for hazard leads to favour land use planning.
- Does the social vulnerability have to be taken into account? In this case, the concept of resilience need to be incorporated in the analysis. Improvements suggested for the vulnerability assessment in the iron-ore field show a pragmatic but subjective way to take into account the resilience concept. Nevertheless, It is necessary to be very cautious with this resilience assessment method because this term and its proper meaning is still uncertain.

These questions need to be answered before any vulnerability study. They all refer to the question of who is the end user and what does he want to do with the result? Much confusion may be raised because of an inappropriate use of vulnerability assessment study : some of its aspect may be relevant for one objective or one kind of end-user but not for other ones. In a single hazard area, the vulnerability will be very different for one citizen with an individual worry, for the municipality with collective worry or for the insurance companies with business worries.

The case of the Lorraine iron-ore field reveals the complexity of the vulnerability assessment, which may need several consecutive studies to go deeper in the analysis with the increase of stakes and knowledge about the present hazard. A consequence of these consecutive studies is the evolution of the hierarchy and the necessity to explain it both to citizens and end-users. This highlights the necessity to clarify the objectives of the study, so that results should not be interpreted in a different way than the expected one.

7. Bibliography

Balandier P. (2004). *Urbanisme et Aménagements – Objectifs et problématiques*. Collection Conception Parasismique, cahier n°3, Les grands Ateliers de l'Isle d'Abeau.

Bogardi J.J. (2004). *Hazards, risks and vulnerabilities in a changing environment: the unexpected onslaught on human security*. Global Environmental Change, 14, pp. 361-365.

Deck O. (2002). *Etude des conséquences des affaissements miniers sur le bâti - Propositions pour une méthodologie d'évaluation de la vulnérabilité du bâti*. Thèse de Doctorat de l'INPL (Nancy, France).

Deck O. (2003). *Réduction de la vulnérabilité par prise en compte du risque dans l'aménagement - Etude des interactions sol-structures - Application au cas des affaissements progressifs*. Rapport INERIS DRS-02-45828/RN.

Didier C., Leloup J. (2005). *PPRM : a powerful technical and administrative tool to prevent and manage post mining hazards*. Colloque Post-Mining - GISOS, 16-17 novembre 2005.

EMS (98). *European Macroseismic Scale 1998*. Cahiers du Centre Européen de Géodynamique et de Séismologie, Vol. 15, Editor. G. Grünthal.

Griot C. et Ayral P.A. (2001). *Terminologie en science du risque*, d'après le document de travail du colloque international "Dire le risque : le risque mis en examen", Mèze, 18-20 mai 2001.

Klein R.J.T., Nicholls R.J., Thomalla F. (2003). *Resilience to natural hazards: how useful is this concept?* Enviromental Hazards, 5, pp. 35-45.

Kouniali S. (2001). *Sécurité des personnes et urbanisme après la fermeture d'un grand bassin minier sédimentaire: le cas des mines de fer de Lorraine*. Les techniques de l'Industrie Minérale, n°10, juin 2001, pp. 91-95.

MATE (1997). *Plans de prévention des risques naturels prévisibles – Guide général*. La documentation Française

MEDD (2003). *Circulaire du 02/10/03 du MEDD sur les mesures d'application immédiate introduites par la loi 2003-699 en matière de prévention des risques technologiques dans les installations classées*.

Merad M., Verdel T., Kouniali S. (2004). *Use of multi-criteria decision-aids for risk zoning and management of large area subjected to mining-induced hazards*. Tunnelling and Underground Space Technology, 19, pp. 125–138.

Teramo A., Bottari D., Termini D. et Bottari C. (2005). *A methodological approach for the evaluation of urban and territorial vulnerability*. Pure and Applied Geophysics, , 162, pp. 659-670.

UN/ISDR (2004). *Living with Risk - A global review of disaster reduction initiatives* (2004 version).

Zihri G. (2004). *Risques liés aux ouvrages souterrains*. Constitution d'une échelle de dommages. . Thèse de Doctorat de l'INPL (Nancy, France).

UNDERGROUND WORKINGS OF SLATE VEIN AND COTICULE IN THE COMMUNE OF VIELSALM (BELGIUM): THE GEOLOGICAL RISK MANAGEMENT THROUGH DATABASE AND GIS

DEVLEESCHOUWER Xavier, MULLARD Cyril, GOEMAERE Eric

GEOLOGICAL SURVEY OF BELGIUM, Dpt VII of the Royal Belgian Institute of Natural Sciences, Rue Jenner, 13 - B-1000 Bruxelles - Belgique; Xavier.Devleeschouwer@naturalsciences.be; Cyril.Mullard@naturalsciences.be; Eric.Goemaere@naturalsciences.be

ABSTRACT: From the XVIIth century to the seventies, the commune of Vielsalm (Province of Luxembourg, Belgium) was the centre of an intensive exploitation of slate vein and coticule. Localized in suburban and forest areas, these old underground exploitations have developped into danger zones both on the surface and below. The Geological Survey of Belgium approached the problematic of the "mining" risk by a geomatics method. The GIS application allows to inventory, to cartography the old underground workings with a high precision and finally to delimitate previously unknown risk zones. A high density of shafts and gallery entrances is observed or confirmed during field campaigns. The GIS tool highlights the presence of galleries just below a recently populated district of Vielsalm (Cahai quarter). A collapse hazard must be taken into account but the GIS analysis could permit to manage the risk incurred by the population through monitoring and securing these potentially danger zones by the authorities.

KEYWORDS: slate vein, coticule, underground exploitations, GIS, geological risk.

RESUME : Du XVII^{e} à la fin des années 1970, la commune de Vielsalm (Province du Luxembourg, Belgique), fut le siège d'une exploitation intensive d'ardoise et de coticule. Ces anciennes carrières souterraines, localisées en milieu périurbain et forestier, laissent place aujourd'hui à de nombreuses zones de danger tant en surface qu'en profondeur. Le Service Géologique de Belgique a abordé la problématique du risque "minier" par une approche géomatique. L'application SIG créée permet d'inventorier, d'identifier précisément les anciens sites extractifs souterrains et in fine de délimiter des zones à risques auparavant inconnues. Outre la forte densité de puits, elle met en évidence des habitations du récent lotissement de Cahai situées à l'aplomb d'anciennes galeries. L'aléa d'un effondrement souterrain doit être pris en compte mais l'analyse SIG devrait permettre de gérer le risque encouru par la population grâce à une surveillance et une sécurisation accrue des zones potentiellement dangereuses par les autorités compétentes.

MOTS-CLEFS: ardoises, coticule, exploitations souterraines, SIG, risque géologique.

1. Introduction

1.1. Geographical context

The studied area is located in the Vielsalm commune in the southeastern part of Belgium (Province of Luxembourg). Vielsalm lies at an average altitude of 360 m and is surrounded by three hills culminating at 530-550 m. The Salm valley, from the name of the Salm river, flows between these hills where quarries and underground exploitations are known.

Slate vein have been exploited in several places near the villages of Ottré-Bihain, Vielsalm and Salmchâteau. In this paper, we will focus on the slate vein exploited in and around Vielsalm. Slate vein have been intensively mined in two main deposits located in the north and southern part of the hill named "Thier des Carrières" between the villages of Vielsalm and Salmchâteau on the eastern side of the Salm river. Other exploitations are also known on the opposite side of the Salm river. Coticule deposits are found, on the hills named "Thier de Regné", "Thier del Preu" and "Thier du Mont", near the villages of Salmchâteau, La Comté, Grand Sart, Bihain and Lierneux, in both sides of the road between Salmchâteau and Baraque de Fraiture (figure 1).

1.2. Geological setting

The Vielsalm area is located in the Caledonian Stavelot-Venn Massif that is the best-exposed Lower Paleozoic inlier in the allochthonous Variscan Ardennes Nappe in Belgium. The Ardennes in southern Belgium consists of an allochtonous domain thrusted onto an autochtonous unit during the Variscan orogeny. Rocks from the Early Cambrian up to the Middle Ordovician in age correspond to the oldest rocks present in this allochton. They have been deformed during the Caledonian orogenic phase. During the Devonian-Carboniferous times, an extensional basin was formed in the stable continental shelfal platform in the south of the Lower Old Red Sandstone with sedimentay deposits related to transgressive-regressive cycles. As a result, Lower Devonian to Upper Carboniferous sediments unconformably overlies this Caledonian Massif. All these strata were subsequently deformed during the Late carboniferous Variscan orogeny. The Hercynian metamorphism (360-420°C; 2-3 Kbar) characterizing the Stavelot-Venn Massif is probably due to burial and/or tectonic loading of sheets (Ferket *et al*., 1998). The Lower Paleozoic is a complex structure composed of Cambro-Ordovician sedimentary (slates, siltstones, sandstones, black shales) and rare magmatic rocks (rhyolites and dacites) according to Lamens and Geukens (1984, 1985), Lamens (1986). The deposits are Ordovician in age and correspond to the Salm Group subdivided into three stratigraphical formations (respectively, from base to top, Jalhay, Ottré and Bihain Formations). As shown on the geological map (figure 1), the slate vein (S) and coticule (C) deposits have been exploited in the Formation of Ottré. The Ottré Formation (230 m thick) is composed of red siltstones, slates, red slates alternating with 1-15 cm thick yellowish coticule beds and violet chloritoid-rich slates. These sedimentary rocks are enriched in iron and manganese (pastly mined in the Lienne valley). This formation is sliced by several thrust faults and bordered to the east by the Lower Devonian sedimentary series (Lochkovian and Pragian rocks) overlying an angular unconformity (figure 1).

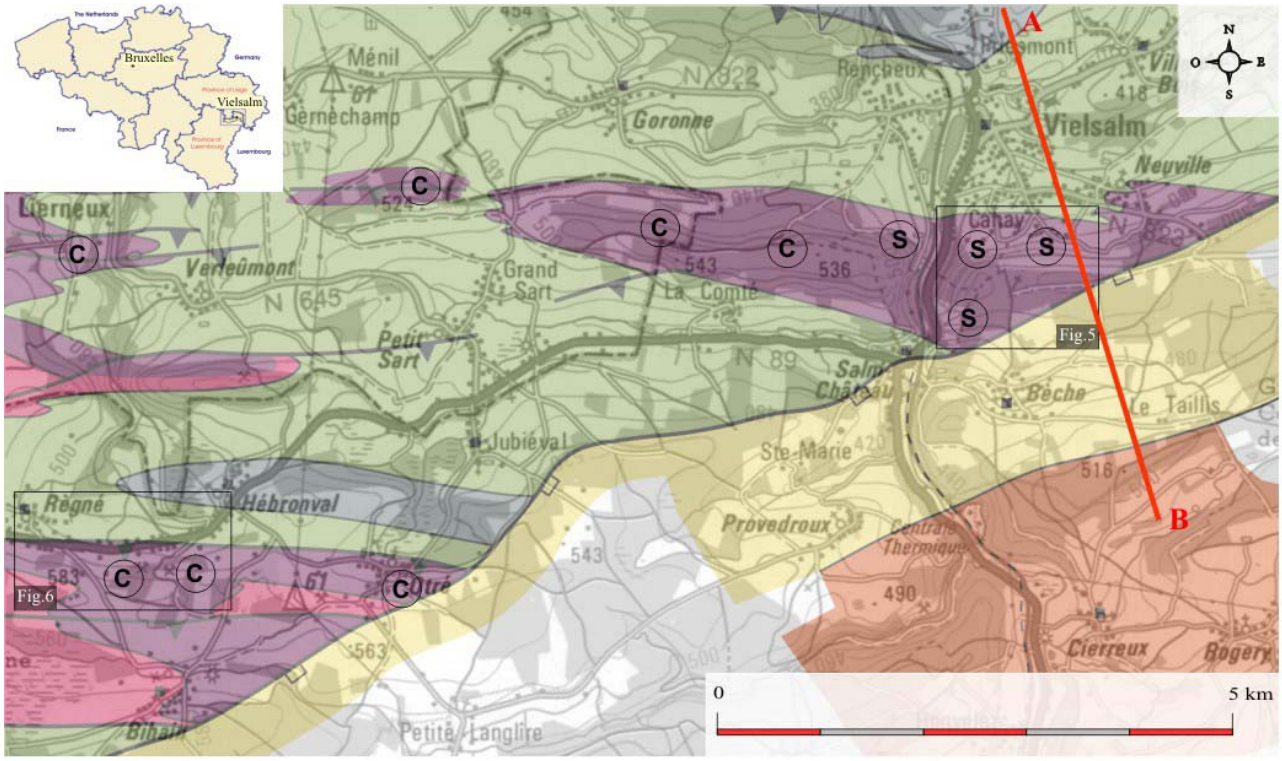
1.3. Definitions

By definition, slate is a dense, fine-grained fissile rock formed by low-grade regional metamorphism of pelitic sediments (shales and mudstone) or more rarely by fine-grained tuffs. Slates are characterized by a single, perfect cleavage (slaty cleavage), enabling it to split into parallel-sided sheets. The cleavage may be parallel to or at an angle to the bedding of the precursor sedimentary rock. Fossils may be preserved but are invariably distorted. Folds are often apparent on the field. True slate is hard and compact and does not undergo appreciable weathering. They are generally dark grey, green or black in color and individual grains cannot be distinguished with the naked eyes. Specific mineral components are responsible for the various colors: carbon and manganese (black), hematite (red and purple), chlorite and ferrous iron oxide (green) for examples.

Slate is the term common in use and means any 'flat rectangular' roofing product used in Europe for hundreds of years with surviving examples dating to the 8th century. This term is relatively ambiguous and in contradiction with the geological one's. Moreover, slate is found also in the literature and used by scientists to describe sandstones, limestones and similar non-metamorphic

roofing products. The most frequently encountered, traditional terms are stone slates or grey slates but they are also called flagstones or tile stones or sclaites (in Scotland). Each of these terms is used to distinguish them from metamorphic ‘blue’ slates. The objection to the stone slate term is that sandstones and limestones are not, petrographically, slates. They have not been metamorphosed and consequently they split along bedding rather than cleavage planes. This is certainly true and some geologists prefer the retronym tile stone to distinguish them from true slates. In the following text, we use the terms ‘slate’ and ‘slate vein’ to distinguish the surroundings rocks (called in the belgian literature “quartzophyllades”) from those found in veins, exploited in underground workings and used as roofing products. It’s important to notice that slates have been used also, in the Vielsalm commune, as stones for the houses (walls, door and window frames, etc.) and for some bridges, or as decorative elements in the houses (facing of the chimneys and the sinks, like benches and staircases) and even in the cemeteries and churches or as religious monuments like slate cross.

Coticule is a very fine-grained highly manganiferous metamorphic rock mainly composed of spessartine garnet (micrometric size), mica and quartz. These yellowish rocks are described petrographically for the first time in Belgium by Renard (1878). They are typically very rich in manganese (up to 24 wt% MnO), poor in iron (less than 1 wt% FeO or Fe2O3) and are generally very rich in garnet (> 40 wt%) and rather poor in quartz (< 30 wt%) (Lamens, 1986). Coticule is a natural abrasive stone used to sharpen and hone razor, surgery and knife blades for examples. Coticule have been commercialized and sold as whetstones everywhere in the world (Europe, Asia, United States, etc.). More quartz-rich varieties occur closely associated with these rocks but were not exploited due to their lower quality as abrasive rocks. These varieties consist of millimeter-scale alternation of greenish quartz-rich laminae and yellow garnet-rich laminae (Lamens et al., 1986). Similar rocks, also of Lower Ordovician age, occur in Wales, Ireland, Norway, New England, Massachusetts, Newfoundland and Nova Scotia according to Kennan and Kennedy (1983). They differ from the Belgian coticule by their mineralogical composition (quite nearly pure quartz-garnet rocks) and by a coarser grained facies. A deposition by possible density currents of fine carbonate mud in basinal setting, manganese replaced calcium in the carbonates probably after burial and the formation of spessartine during metamorphism explain the origin of the coticule veins in the Stavelot-Venn Massif (Lamens, 1986 and Lamens et al., 1986).



Geological map : layout from F. GEUKENS *(Aardkundige Mededelingen - vol. 3 - 1986)* & R. LEGRAND *(Geological Survey of Belgium - Archives)*, drawn up by G.VANDENVEN (1996, unpublished map) and modified by C.MULLARD.

Legend

Tectonic structures

- Angular unconformity
- Thrust faults
- Vielsalm thrust

Exploitation areas

- (C) "Coticule"
- (S) Roofing slate

Stratigraphy

Myrs				
± 245	HERCYNIAN OROGEN			
± 350				
± 360	**DEVONIAN**	Lower	Pragian	
			Lochkovian	
± 418	CALEDONIAN OROGEN			
± 450	**ORDOVICIAN**	Middle (Llanvirn)	Bihain Formation	SG
		Middle (Arenig)	Ottré Formation	SG
		Lower (Tremadoc)	Jalhay Formation	SG
± 488	**CAMBRIAN**	Upper	La Gleize Formation	RG

SG : Salm Group RG : Upper part of Revin Group

Geological profile

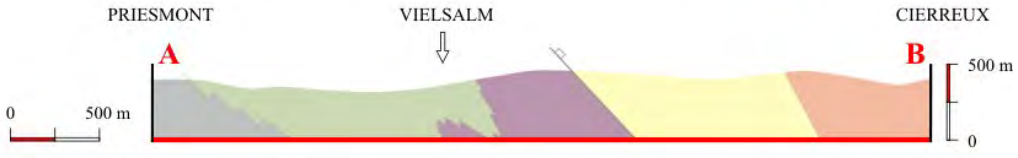


Figure 1: Simplified geological map superimposed to the Belgian topographic map (1/100.000 scale-map) of the area between Lierneux and Vielsalm. Legend, stratigraphic table and geological profile come to supplement and illustrate the geological map.

1.4. Purposes of the program DB-ARCO

Slate vein and coticule mining constitute an essential activity during the industrial revolution and a phase of the development of the country before the First World War. Today, the belgian mining activity is almost extinct in our country except for some local exploitation. The development of the mine at short to mid-term was established to guarantee an optimal output, profitability and the security during the exploitation. Up to recent times, the behavior of the mine after its abandonment and the future consequences on the environment were not posed. The questions related to the "post-mine" behavior of the underground exploitations concern almost all the natural resources which were, in a more or less close past, extracted from the subsurface deposits in Belgium. Some phenomena and disorders were observed and are known historically but there is an important gap in the awakening of the still active processes today in all of these abandoned and unknown underground workings.

The purposes of the DB-ARCO program (databank about slate vein or "ardoises" and coticule) in the Vielsalm commune are developed step by step and are the followings: 1- to gather all the 'mining' data (mining plans, mining profiles, etc.), 2 - to inventory the abandoned mined sites, 3 - to cartography the underground workings of the slate vein and coticule deposits using GIS methods, 4 - to confirm and validate the data with field works (GPS measures of the gallery entrances, shafts, surface infrastructures, etc.), 5 - to determine medium- and long-term behavior of these cavities, 6 - to assess their surface repercussions, 7- to draw up, if possible, risk-reduction procedures, and finally 8 - to suggest methods for monitoring high-risk areas.

2. The slate vein and coticule exploitation

The exploited slate vein (below 20 m thick, figure 2) in Vielsalm is subdivided into four terms detailed here successively from top to base. The best quality roofing products correspond to the vein called "Deliveine", 4 m thick in average. The term "Les Trois Grès", 2 m thick, is composed of unusable rocks. The 4 m thick term "Fleur de grosse veine" gives good quality and hardness products. The "Grosse pierre" term, 6 m thick in average, gives medium quality product. The slate vein is delimited on both sides (base and top) by a thin and unusable white sandstone layer called in Walloon patois "cresse". At the base, a slate layer named "Sous la blanche Peau" corresponds to slates enriched in ottrelite and used as building stones. The exploitation begins with the "crabotage" technique when the crosscut gallery has reached the whole slate vein. The technique consists to dig manually a space in the original cavity allowing to start the exploitation of the future chamber. This step starts at the top of the slate vein and continues towards the base (Voisin, 1987). The dashed brown lines indicate the dimensions of the abandonned chamber after exploitation.

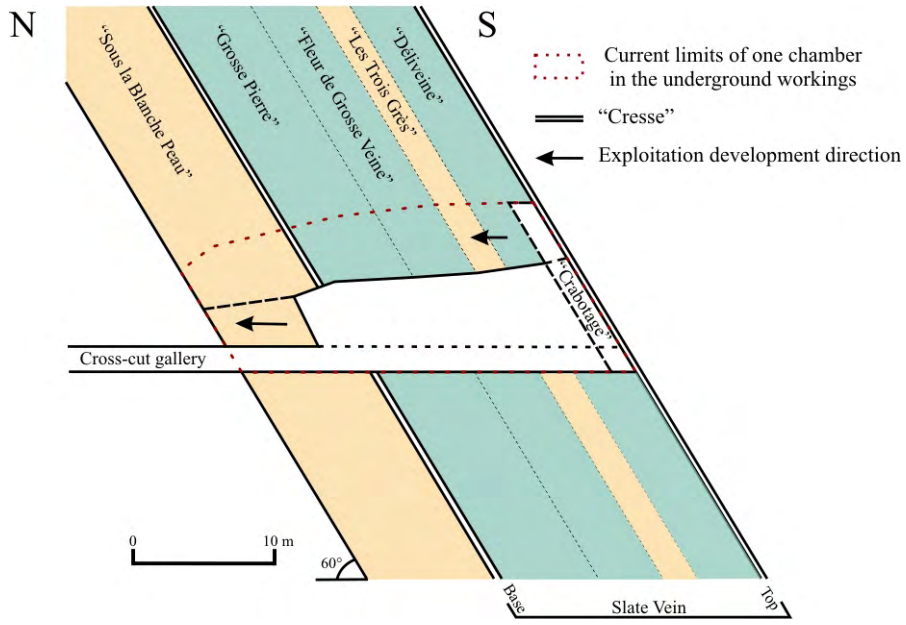


Figure 2: Simplified vertical projection of the underground workings inside one chamber. The slate vein is around 20 m thick in the Vielsalm area and almost 30 m thick. The layers are tilted with a dip of 60° towards the south (right side of the picture) after Ruche (1946) and modified by Mullard.

The high quality of these veins exploited in Vielsalm is attested in the literature. Some administrative journals of the Luxembourg Province describe, in 1903, that the church of Vielsalm have a slate roof dating from the beginning of the XVIIIth century. The use of natural resources in the Vielsalm area is known from the "Iron Age" as attested by archaeological traces on the top of the "Thier des Carrières" hill. Furthemore, the Romans used also the materials for their houses but the following works has destroyed all the exploitation traces. During around ten centuries, the exploitation of the slate vein was almost completely abandoned. The first texts indicating a commercial exploitation in Vielsalm date back to the year 1481. It seems to be located again on the "Thier des Carrières" hill. The materials were exported in the neighboring countries such as the Netherlands, Great Britain, Germany, France, Luxembourg, Italy, Spain, etc. Between 1835 and 1850, around 20-28 open pits are exploited by 150-250 working mans (Graulich, 1987). Slate vein were initially mined in quarries and later in underground workings, starting from 1865-1870 with the gallery named "les Houlands" in the "Thier des Carrières" (Graulich, 1987). At that time, the quarries will not undergo any more transformations. On the other hand, the only evolution at the surface concerns the extension and the development of the spoil heaps that will contribute to modify considerably the local topography.

The exploitation of the coticule in trenches evolved to underground workings through the diggings of many shallow shafts from which a superimposed system of small, narrow and sinuous galleries following the layers of coticule. The slate vein extraction differs from that of coticule. Initially, the quarrymen dug in open quarries, but later they crosscut 150 to 450 meters long galleries on the hillside until they reached the slate vein. The slate vein deposit was exploited in rooms (following the method of room and pillar) of a maximum height of 30 meters. In Vielsalm, the maximum depth of the underground workings could reach 60 to 70 meters due to several superimposed exploited levels and limited by the water table level. The lower levels, generally flooded, as well as the dewatered galleries and their exits are practically unknown and probably sealed. Shafts are used as emergency exits and ventilation of the galleries. The early end of the underground workings and the small size of the exploited slate vein deposits explain the scarcity and the weak precision of the mining plans, the lack of geographical reference marks and the small number of usable historical documents.

3. GIS and database development

In cooperation with the Walloon Region, the Geological Survey of Belgium approached the problematic of the "mining" risk by a geomatics methodology. The GIS tool allows to centralize various types and dispersed semantic and geographic data. Technically, this GIS application is based on the creation of two complementary modules (a relational data base management system under Microsoft Access 2000 (Copyright © 1992-1999 Microsoft Corporation) and a cartographic management system under ESRI® ArcView 8.3 (Copyright © 1999-2002 ESRI Inc.) connected by a geodatabase (Devleeschouwer et al., 2005, 2006). The “mining” plans of the underground workings of Vielsalm, constituting the background documents and starting point of the project, were georeferenced using geographical reference frameworks. First difficulties arise in the differences between the current field situation that represents the reality and the “mining” plans generally older than the closing of the underground workings. This procedure (figure 3) was established in two steps. First, similar anchor points are found on the limits of the cadastral parcels both on the “mining” plans and the digital vectorized georeferenced land register of the Vielsalm commune. Secondly, GPS measures during field campaigns are necessary to identify and inventory the surface elements represented on the “mining” plans such as the shafts and gallery entrances but also the buildings related to exploitation at the surface. These new coordinates points allow to use the shafts or gallery entrances present on the “mining” plans as new anchor points to increase the accuracy of the georeferencing procedure. The last step consists in vectorizing the “mining plan” inside the GIS. The original “mining” plan (figure 4), with the underground workings (chambers, galleries, etc.) and the associate profiles, shows that chambers have been exploited at different levels down to 60-70 meters below the surface. The main problem encountered during the vectorization step of these underground workings corresponds to the superposition of the whole exploited levels (blue, green and yellow surfaces) but drawn one in another. The only solution, when it’s impossible to decipher the drawing, consists to vectorize the wrapping surface of the whole exploited chambers for all the levels as indicated by the brown coloured surface on the figure 4. Several vectorized layers are thus created in the GIS; they correspond to the underground chambers, the main galleries and the junction galleries that link two underground exploitation areas at the same level, the shafts and the gallery entrances. Figure 7 presents all the vectorized data for the “Thier des Carrières” hill with a buffer of 10 m applied to all the vectorized objects due to several errors accumulated during the procedure (GPS measures, accuracy of the vectorized cadastral parcels, etc.).

The first results show a high density of shafts (from 0,3/ha on the “Thier des Carrières” to 1,6/ha on the “Thier de Regné”) in the old exploited zones. The GIS application highlights the structure of the underground workings (rooms and galleries) projected on current topographic maps and delimitates the risk zones still untreated. The two following pictures illustrate the differences in the exploitation methodology between slate vein (figure 5) and coticule (figure 6). Figure 5 presents the known and measured gallery entrances related to the underground workings of the slate vein exploitation levels. Almost all the gallery entrances are found on the north side of the “Thier des Carrières” hill. The old quarries are now delimitated on the northern wall by spoil heaps (grey surfaces) and to the south by 20 m height cliff of rocks, underlined on the picture by a black surface and trees alignments.

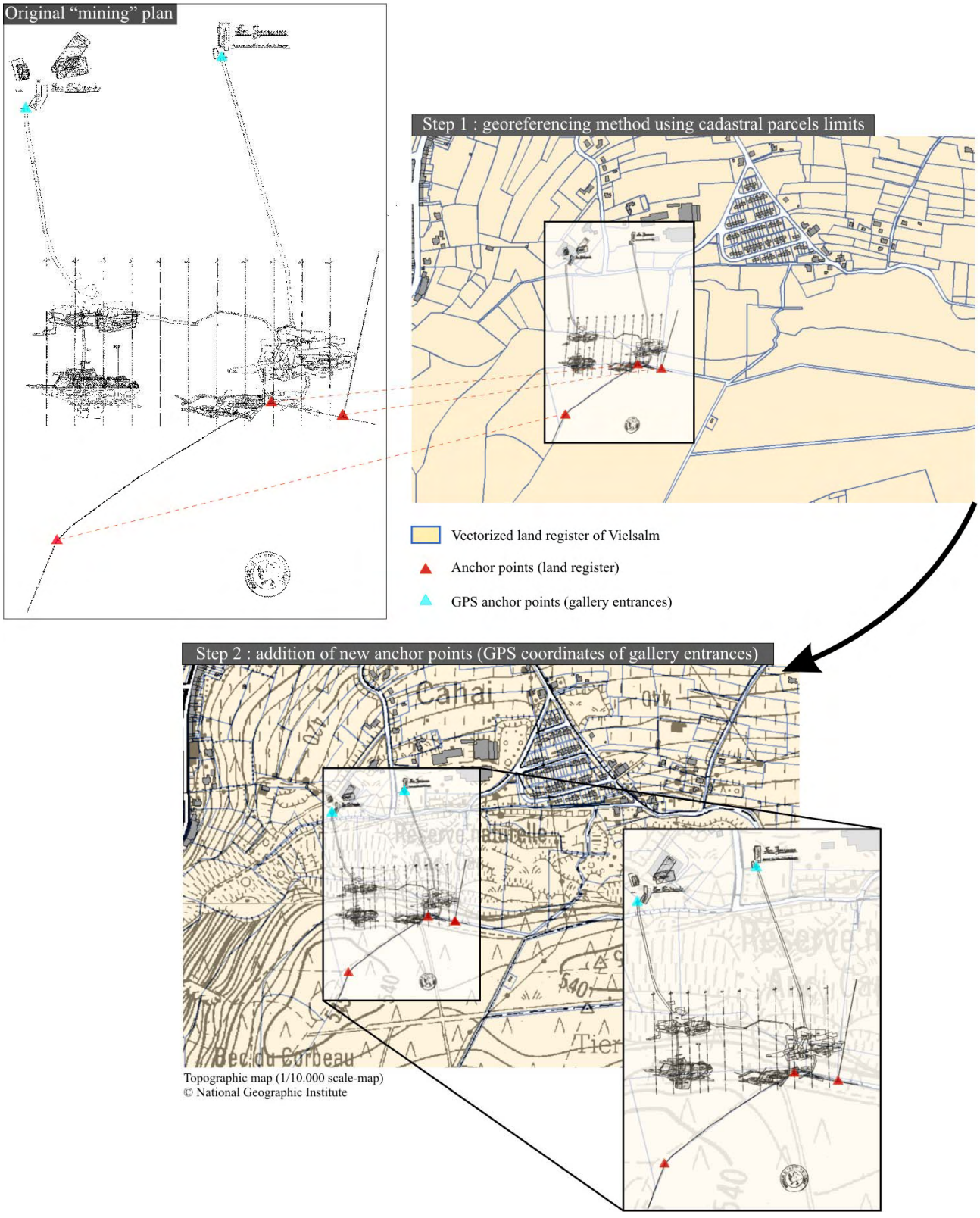
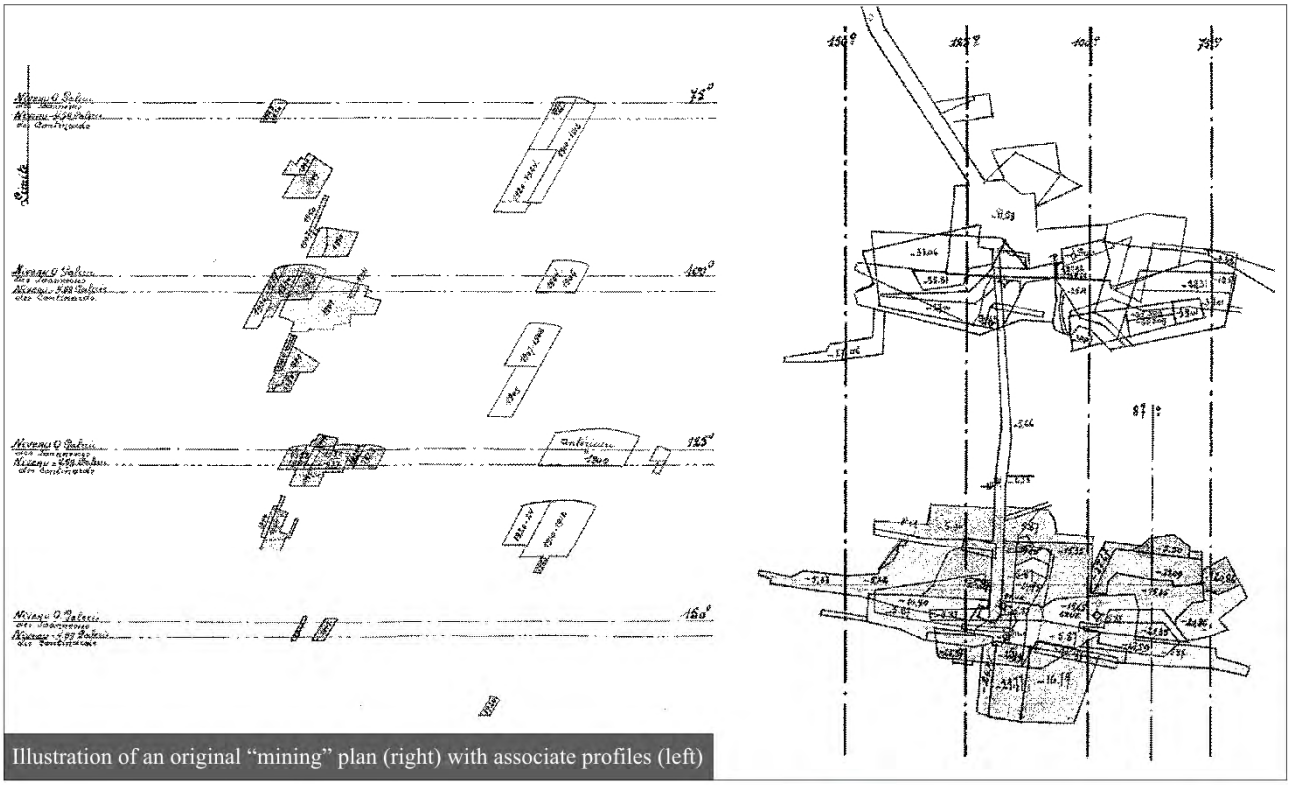


Figure 3: Illustration of the two-steps procedure used for georeferencing the old "mining plans". The step 1 shows the research of similar anchor points between the cadastral parcel limits drawed on the plan and those reported on the digital vectorized land register. The second step needs GPS measures during field campaigns to increase the number of anchor points and consequently the precision of the method.



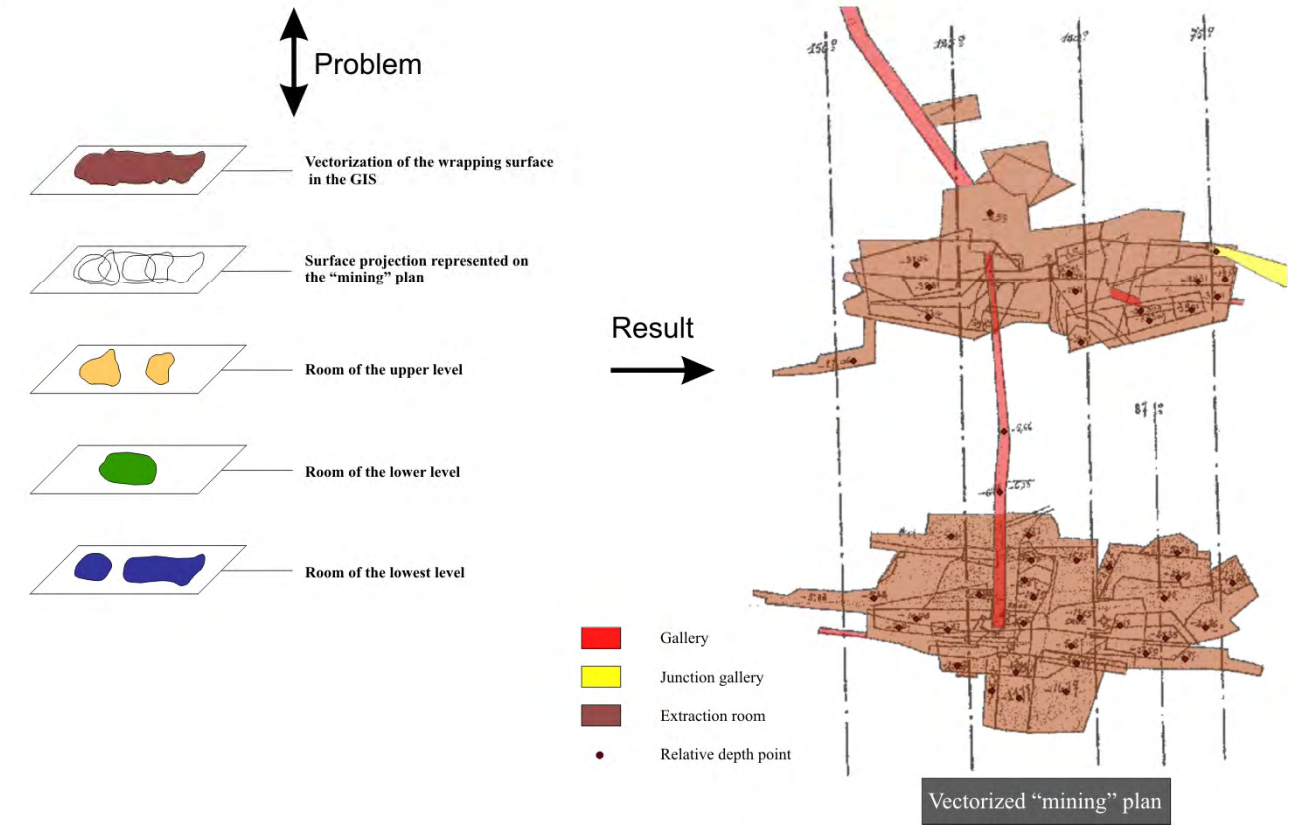


Figure 4: Illustration of a original “mining” plan with the underground workings (chambers, galleries, etc.) on the right and the associate profiles on the left. The main problem during the vectorization step corresponds to the superposition of several exploited chambers at different levels (blue, green and yellow surfaces) but drawn one in another. The solution consists to vectorize the wrapping surface of all the exploited chambers as indicated by the brown coloured surface.

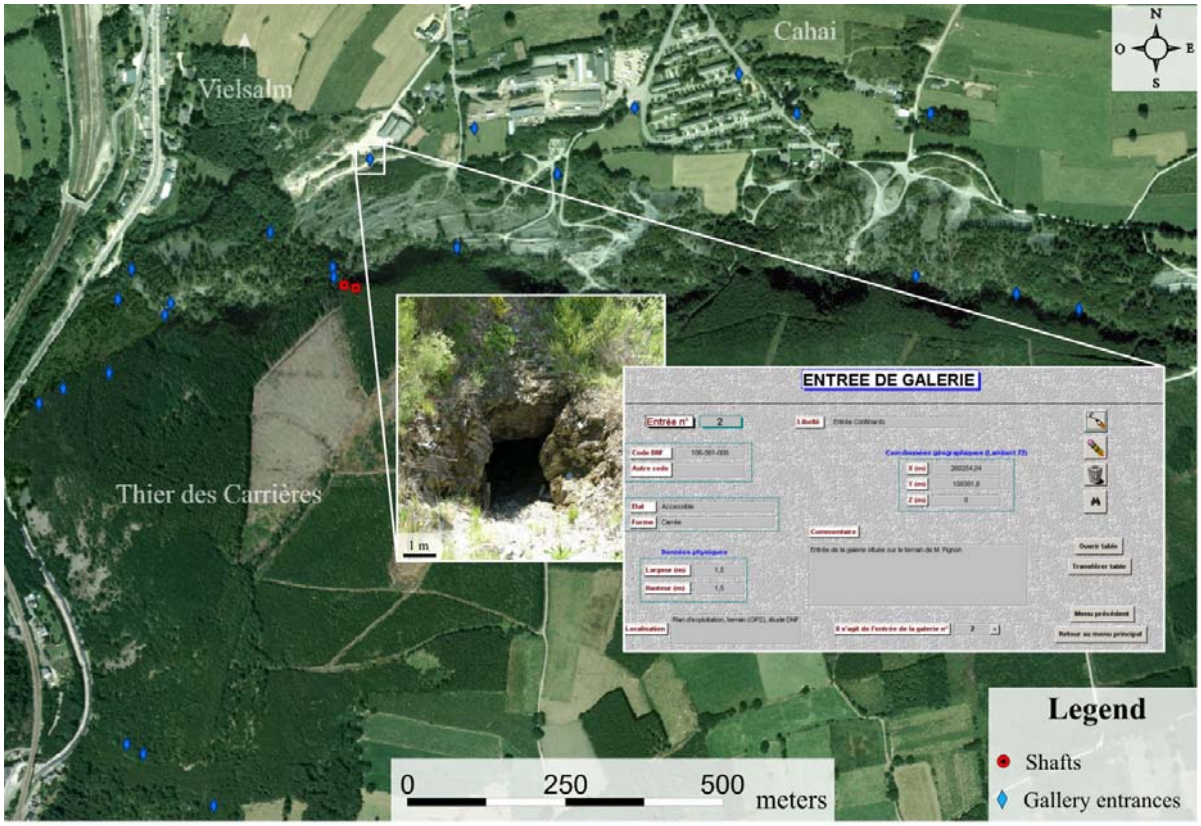


Figure 5: Gallery entrances and shafts observed and confirmed by field campaign. They are essentially located on the northern part of the “Thier des Carrières” hill.

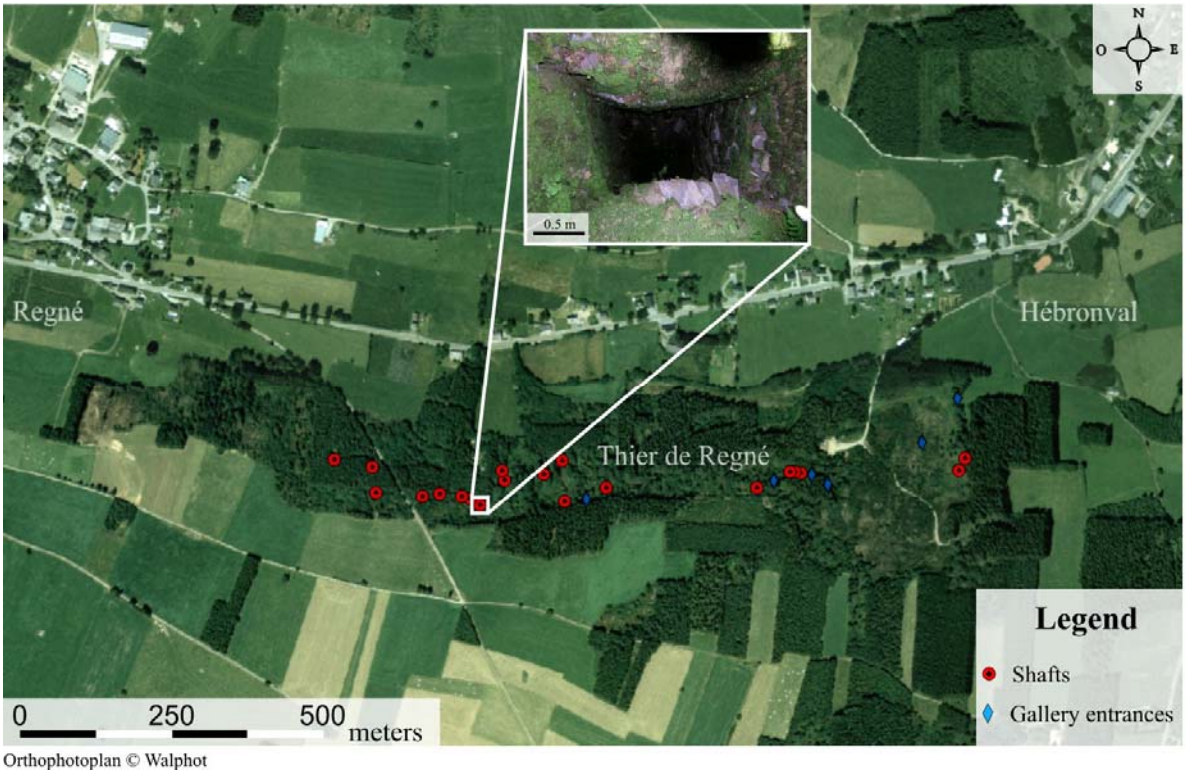


Figure 6: Shafts and gallery entrances observed during field campaigns on the “Thier de Regné” hill.

Some galleries have their entrances at a distance higher than 400 meters and crosscut the hill underneath the spoil heaps as illustrated by the photo of the gallery entrance “Les Continards”. In contrary, almost only shafts and few gallery entrances indicate the coticule exploitation on the “Thier de Regné” hill. The shafts are found in forest areas with a high vegetation cover and new campaigns could reveal some missed shafts. They are found along foot walk, only covered for some of them by old wooden decayed boards.

4. Potential hazards and risks generated by old underground slate quarries

The commune of Vielsalm is now affected by the presence of numerous holes and cavities due to the long period of intensive underground workings of slate vein and coticule as well as the juxtaposition of many concessions. The abandoned “mines” have developped into danger zones both on the surface and below. For example, the space analysis highlights the presence of galleries just below a district recently built in Vielsalm (Figure 7). An uncertainty margin of 10 meters is applied to each geographical object due to the inaccuracy of the georeferencing procedure. Some local disorders can be seen with a deformation of the road related to the presence of one gallery near the surface.
The open quarries are regularly faced with collapses of their vertical or sloped walls. These events at the surface generate cascading collapses in the lower levels. The ventilation and extraction shafts located close to footpaths and in wooded zone constitute a danger for the walkers. Dissimulated by the vegetation in the forest, these shafts represent many potential traps.

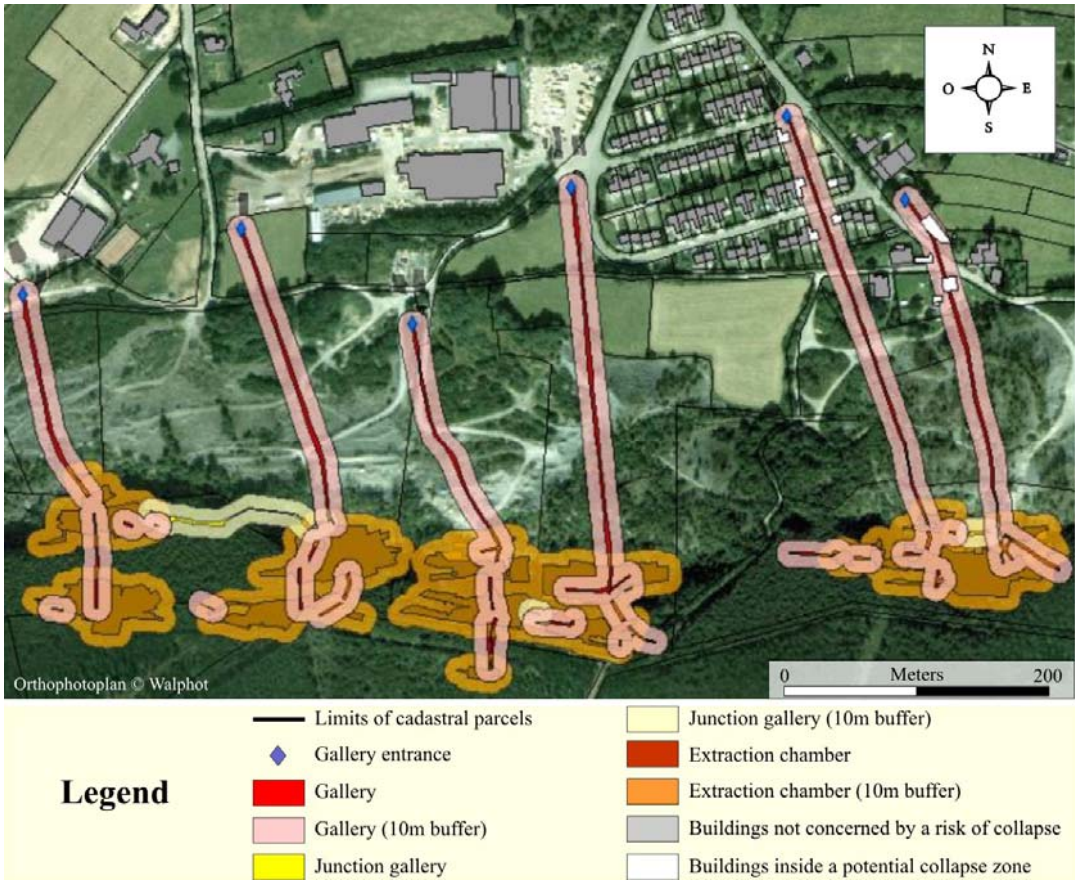


Figure 7: Spatial analysis to define the buildings of the Cahai quarter faced with the presence of underground galleries. Depending on the 10 m buffer used on the vectorized objects, 2 to 9 buildings must be considered in the case of collapse hazards of a gallery.

The numerous gallery entrances as well as the non protected inclined shafts enable minerals collectors and others to enter, without authorization, the network of galleries and rooms of extraction, where the danger is always present: collapse of galleries under spoil heaps ("verdou" or “verdô” in Walloon patois), decayed wooded posts and beams, the collapse of the fillings of the ventilation shafts, roof collapse of the exploited rooms, flooding of the lower levels, etc. The underground workings of Vielsalm present a high "mining" risk. Their exits are partially sealed to preserve unique bats population.

5. Conclusions

The development of such GIS application (geomatics approach) often requires the exhumation of old "paper" data (archives) that must be scanned, vectorized and formatted with a considerable cost. A highly performing GIS tool and thus the capacity to answer precisely to complex requests depends on the quality of the data stored in the databases. GIS application made by the GSB is utilizable for decision-making, but also correspond to a management tool of the territory for the official authorities (Ministry of the Walloon Region). The application permits to classify the zones as safe or unsave and to identify areas where further investigation on the field is necessary to analyze the risk and to secure the sites. The tool allows to reduce the risk incurred by the population by monitoring and increasing security of the potentially danger zones. It is the first step of a larger program of risk analysis that will integrate many physical, geophysical and mechanical parameters.

The program DB-ARCO, started in 2004 in the Vielsalm commune, has been pursued in the slate basin of the Bertrix-Herbeumont area (Aise valley) near the French border. The ultimate goals of the current program would be the study of all the sites where underground workings of slate vein have been observed. Fourteen Belgian communes must be considered for further investigations in the following years. A special attention will be given to the Warmifontaine underground exploitation where a large area including a part of the village collapsed in 1912.

6. References

Devleeschouwer X., Goemaere E. and Mullard C. (2005). *In Vielsalm, Belgium, Abandoned Underground Quarries Managed with GIS*. ESRI news, GIS in action, Summer 2005 - Online version: http://www.esri.com/news/arcnews/summer05articles/in-vielsalm.html.

Devleeschouwer X., Mullard C. and Goemaere E. (2006, accepted). *Management of abandoned slate and coticule underground quarries by means of GIS*. Vielsalm (Belgium), IAEG2006, 10th IAEG Congress, Nottingham, 6-10 September 2006, abstract.

Ferket H., Muchez P., Schroyen K. and Sintubin M. (1998). *Metamorphism in the Stavelot-Venn Massif: a study of quartz veins in the basal Devonian conglomerates (Lochkovian)*. Aarkundige Mededelingen, Vol. 9, 7-16.

Graulich O. (1987). *L’industrie ardoisière à Vielsalm*. Mémoire de Licence en Histoire de l’Université de Liège, 178 pages, unpublished.

Geukens F. (1986). *Commentaire à la carte géologique du Massif de Stavelot*. Aarkundige Mededelingen, Vol. 3, 15-30.

Kennan P.S. and Kennedy M.J. (1983). *Coticules - a key to correlation along the Appalachian-Caledonian orogen ?* In: Schenk P.E. (ed.), Regional trends in the geology of the Appalachian - Caledonian - Hercynian - Mauretanide Orogen, 355-361.

Lamens J. (1986). *Depositional history of Salmian (Lower Ordovician sediments in Belgium)*. Aarkundige Mededelingen, Vol. 3, 125-138.

Lamens J. and Geukens F. (1984). *Volcanic Activity in the Lower Ordovician of the Stavelot Massif, Belgium.* Mededelingen van de Koninklijke Academie voor Wetenschappen, Letteren and Schone Kunsten van België, Vol. 46/4, 3-13.

Lamens J. and Geukens F. (1985). *Volcanic Activity in the Lower Ordovician of the Stavelot Massif, Belgium*. Bulletin de la Société belge de Géologie, T. 94/1, 29-40.

Lamens J., Geukens F. and Viaene W. (1985). *Geological setting and genesis of coticules (spessartine metapelites) in the Lower Ordovician of the Stavelot Massif, Belgium*. Journal of the Geological Society, Vol. 143, 253-258.

Mullard C. (2004). *Mise en place d'un SIG appliqué à la gestion des carrières souterraines d'ardoise et de coticule de Vielsalm, Belgique*. Mémoire du DESS SIG, Cartographie et Développement territorial de l'Université de Haute Bretagne - Rennes, 117 pages, unpublished.

Renard A. (1878). *Sur la structure et la composition minéralogique du coticule et sur ses rapports avec le phyllade oligistifère.* Mém. Cour. Acad. Roy. Belgique, Vol. 41, 1-42.

Ruche J. (1946). *L'industrie ardoisière en Belgique.* Mémoire de Licence en Sciences Economiques de l'Université de Liège, 214 pages, unpublished.

Voisin L. (1987). *Les ardoisières de l'Ardenne*. Editions Terres Ardennaises, 257 pages.

THE MRPP : A POWERFUL OPERATIONAL REGULATORY TOOL TO PREVENT AND MANAGE POST-MINING RISKS

DIDIER Christophe[1], LELOUP Jacques[2]

[1] INERIS – Direction des Risques du Sol et du Sous-Sol - Parc Technologique Alata BP n°2 – 60550 Verneuil en Halatte – France. Christophe.Didier@ineris.fr

[2] Ministère de l'Economie, des Finances et de l'Industrie – 5 Place des Vins de France, Bâtiment ATRIUM – 75573 Paris Cedex 12 - France. Jacques.Leloup@industrie.gouv.fr

ABSTRACT: Even if most French mining sites are definitively closed, potential risks remain above the abandoned exploitations. In addition to surface instability, some mining sites may be affected by dangerous gas emissions or by flooding events or environmental degradations. Those kinds of disorders strongly influence the land use management of the concerned areas. In order to post and manage properly those risks, French State has developed a powerful operational regulatory tool : the MRPP (Mining Risk Prevention Plan). MRPP aims to identify the most sensitive areas subject to "post mining hazards" and to define technical and regulation rules able to manage the principles of the future urbanism development on surface. The present paper proposes a methodological description of MRPP in order to explain the nature and objectives of the procedure.

KEYWORDS: post-mining management, prevention, hazard, regulation, MRPP.

RESUME : Bien que la plupart des sites miniers français sont désormais fermés, les risques liés à ces anciennes exploitations n'ont pas pour autant disparu. Outre les risques de mouvements de terrain, certains sites peuvent être affectés par des émissions de gaz dangereux, des phénomènes de type inondations ou des impacts environnementaux parfois sensibles. Ce type de désordres influence fortement l'utilisation possible des terrains de surface concernés. Afin d'afficher et de gérer au mieux ces risques, l'état français a développé un outil opérationnel et réglementaire puissant : le PPRM (Plan de Prévention des Risques Miniers). Les objectifs du PPRM sont d'identifier les secteurs les plus sensibles aux risques liés à l'après-mine et de définir le cadre réglementaire permettant de gérer au mieux les principes du futur développement de l'occupation de surface. L'article propose une description méthodologique de la réalisation des PPRM afin d'en expliquer la nature et les objectifs.

MOTS-CLEFS : gestion de l'après-mine, prévention, aléas, principes réglementaires, PPRM.

1. Introduction

For several centuries, the French mining industry, considered to be one of the flagships of national industry, was a source of wealth for the country. In just a few decades, under the combined effect of diminishing resources and international competition, most mining operations were gradually forced to close.

Once a symbol of pride and solidarity, this industry is now often identified with the development of problems or a source of nuisance. As a matter of fact, closing down mining operations has not led to the complete and permanent elimination of risks and harmful effects likely to affect surface land within the geographical limits of old workings. During the period following operations therefore, traditionally known as the "post-mining" period, several kinds of disorders may develop, sometimes as soon as work has ceased but also much later.

Apart from surface instability (subsidence, collapse), some old mining sites may be affected by emissions of gases likely to be dangerous. The irreversible disturbance to underground water circulation caused by mining operations may also be the source of nuisance, both for the water circulation scheme (low point flooding, changes in water course flowrates) and its quality (water or soil pollution).

These phenomena may have major consequences for people, activities and property on the surface (support work or development, moving populations). They are also likely to have a major influence on regional development in mining areas.

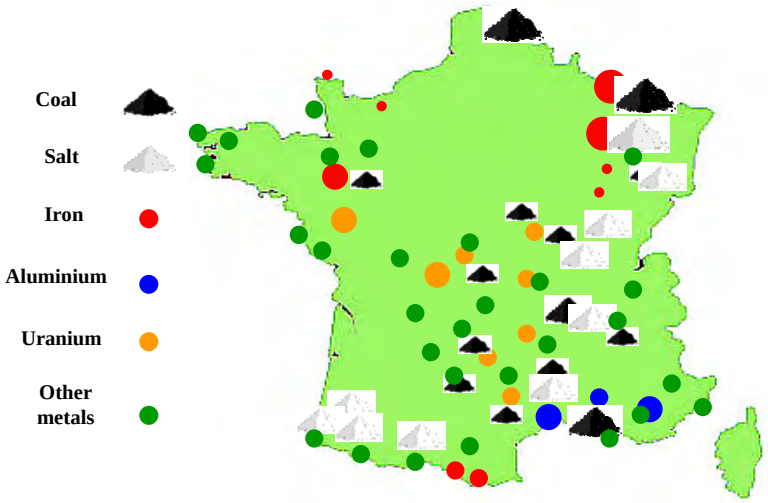


Figure 1. Major mining fields having been exploited in France.

To post and manage these various risks to an optimal degree, the French State has developed a high-performance and operational regulatory tool: Plans de Prévention des Risques Miniers (PPRM) (Mining Risk Prevention Plans - MRPP) are intended to identify the sectors most likely to develop risks or nuisances in the long term and draw up rules for managing land use according to the various constraints linked to the post-mining period.

The present paper gives a brief account of the principles subtending the drafting of MRPPs, with respect to both the administrative procedure and risk evaluation, as well as defining regulatory measures.

2. The MRPP, a tool for risk prevention management

2.1. The MRPP in French risk prevention policy

In France, the State is responsible for posting the risk and including it in regional development management. For this purpose, the State introduced "Plans de Prévention des Risques naturels prévisibles" (PPRN) (Predictable natural risk prevention plans - NRPP) in **law n° 95-101** of 2 February 1995.

Based on the successful application of these tools, their field of application was expanded to include mining risks through **law n° 99-245** of 30 March 1999. This law introduced the "Plans de Prévention des Risques Miniers" (PPRM) (Mining Risk Prevention Plans -MRPP). The rare differences which justify the introduction of a specific procedure for handling mining

risks particularly include the type of risks involved and the funds and procedure for compensating victims in the event of accident.

2.2. Administrative procedure for drafting an MRPP

The Prefect, as the regional State representative, initiates the procedure for drawing up an MRPP via a "prescription order". This order defines the limits of the study and the type of risks involved. The prevention procedure is applied, as far as possible, to global physical units, called "risk basins" defined by natural parameters and/or operations and not by administrative limits.

Apart from the administrative departments involved, all town councils in the communities concerned are systematically requested to give their opinion. The Prefect also submits the draft plan for public enquiry among the populations concerned.

At the end of these various consultations, the possibly modified MRPP is approved by Prefectural order. The regulatory constraints it defines take precedence over the Local Town Planning plans drawn up by the individual communities.

2.3. The main phases of drawing up an MRPP

2.3.1 The Information phase

The information phase of an MRPP is designed to collect all available information (including further investigations if these are found to be strictly necessary). It requires an on-site investigation and consultation of archives.

This phase gives rise to the production of an informative map which is used as a basis for diffusing essential information to the population, because it helps to justify the prevention procedure undertaken by summarising the disorder and harmful effect which has affected the site in the past.

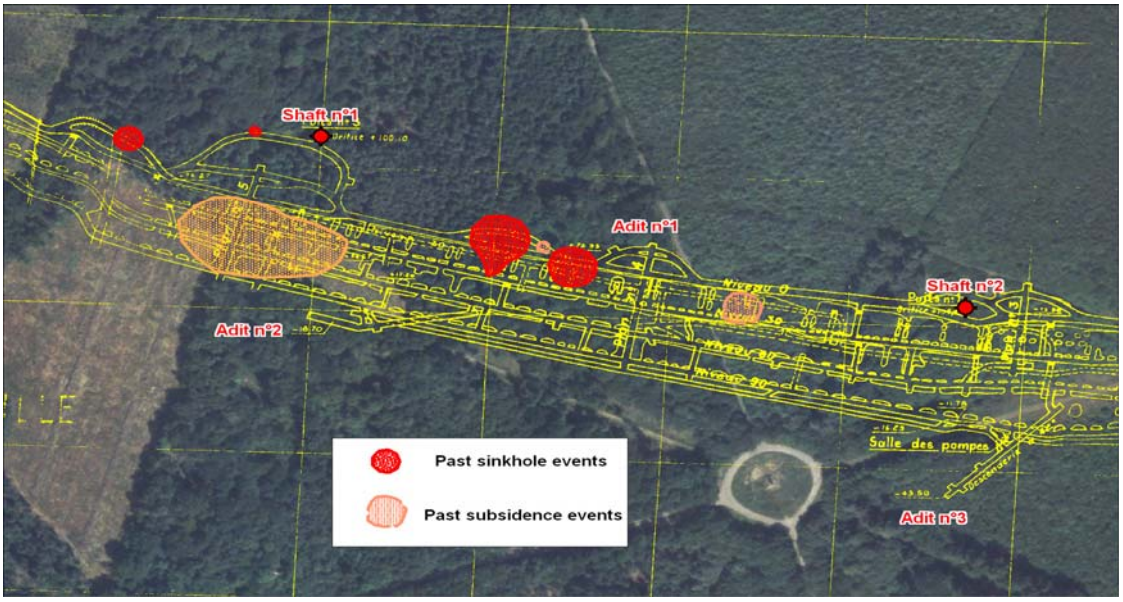


Figure 2. Example of an information map.

2.3.2 The Hazard evaluation phase

The hazard evaluation phase is intended to locate and list the zones exposed to potential phenomena, according to the intensity of the predictable events and the zone's predisposition to their development. This evaluation does not include the type of surface occupation.

It ends with the drafting of maps which locate the hazard zones identified by the evaluation procedure.

2.3.3 The Factor assessment phase

This phase includes drawing up an inventory of all existing factors in areas subject to one or more risks and identifying the potential future projects which could develop as a result. It is used to identify populations subjected to a non-zero risk level, particularly listing the most sensitive equipment or public establishments. It results in the production of a map including all the factors concerned.

2.3.4 The Regulatory zoning phase

The regulatory zoning phase defines homogeneous zones in terms of prohibitions, instructions or recommendations concerning land use, for both new and existing projects. The principles of this zoning are particularly based on confrontation between the levels of risks previously identified and the assessment of existing and future factors characterising the surface.

A set of rules is drawn up which is directly linked to this zoning. It is intended to define, clearly and operationally, the regulatory measures which apply to each regulatory zone.

3. Description of the main mining-related risks covered by the MRPP

Edict n° 95-101 of 5 October 1995 limits the risks covered by MRPPs to phenomena which are potentially dangerous to people and property. They will be grouped into four main themes detailed in the following paragraphs.

3.1. Modification of water flow scheme

Almost all underground mining took place below groundwater level, therefore requiring the use of dewatering pumps to allow ore extraction to take place. At the end of extraction operations, stopping the dewatering pumps allows the groundwater to rise to a level close to its premining level, which leads to the development of an underground reservoir which is discharged at one or more points, into the surface hydrographic network.

During operations, major modifications may have irreversibly altered the initial conditions in the supporting rock formation. Extraction work may also have led to surface subsidence, for instance, or created artificial groundwater vents. In addition to this, benefiting from dewatering pumping and lowering of the groundwater level, some sensitive zones may have taken advantage of this "dry period" to undertake development in terms of surface and/or underground occupation.

It is therefore easy to understand the need to pay particular attention to the possible consequences of rising groundwater levels on surface property and activities once dewatering is no longer taking place.

Several potential risks can be identified. They are described briefly below:

- *Modification of the discharge scheme* (change in flow, appearance of new discharge points or reactivation of old ones).
- *Appearance of wet zones or marshes* (inadequate drainage capacity for surface land).
- *Flooding of subsoil and low points* (groundwater level shallow beneath the surface, with possible impact on underground structures such as cellars, etc.).
- *Modification of water flow scheme* (may increase flood flow in certain water courses or reduce flow in others, particularly at low water).
- *Sudden flooding* (sudden discharge of a very strong water or mudflow, through an exit connected to a mining reservoir).



Figure 3. Discharge through an adit (left) and development of a wet zone close to an other adit (right).

3.2. Surface instability

Mining operations consist of extracting large quantities of material with the intention of marketing part of it in the form of usable ore. These excavations, whether underground or open-cast, have irreversibly altered the rock formations in which the ore is found.

Concerning **underground workings**, which represent most French mining operations, the method of exploitation used depends mainly on the geological configuration of the seam and the evolution of techniques. From the point of view of residual risks, there are two main methods: operations providing voids backfilling after extraction and those which lead to persistent residual voids once the workings are closed down.

For the first (working, stoping…), surface instabilities are generally limited to low amplitude movements. It is mainly the development of subsidence which is to be feared, as well as damage to buildings or infrastructure. For operations leading to large persistent residual voids (rooms and pillars, dissolution cavities…), the stability of old workings may be compromised by aging material or changes in the environment of underground mining works. Apart from the possibility of subsidence, this type of operation may also be the source of collapses.

In **open-cast mining**, extraction consisted of digging large pits from which the ore was extracted. The choice of operating method was based on the optimisation of economic profitability (limit the volume of waste to be cleared) and the stability of the mine structure (avoid slopes which are too steep). These rocky fronts often eventually suffer instabilities from simple rock falls to the massive slumping of an entire slope front. The combination of rock fracturing and the morphology of the slopes of the pit generally determine the volume of

rock mass which is potentially unstable. The nature of the surrounding rock formation also plays a major part in the development of any instability.

At the same time, mining operations, whether underground or open-cast, have often led to the constitution of bulky **mine waste deposits** close to the extraction sites. Although waste materials are generally stored in dry conditions and constitute piles of material commonly known as slag heaps or waste dumps, operating residues are mostly discharged into basins confined by retention dykes built round the edge of the storage zone. The rupture of deposit structures of any kind generally leads to the unfavourable evolution of one or more factors governing the mechanical behaviour of excavation or other waste.

The main potential risks characterising the potential for earth movement is described in the following.

- *Settling* (recompaction of a mound of loose rock affected by underground workings. The induced movement is usually only slight).
- *progressive subsidence* (gradual, flexible re-adjustment of surface layers. Phenomena which often cause damage but are rarely dangerous).
- *Sinkholes* (sudden appearance on the surface of a sink-hole. The sudden nature of the instability makes these potentially dangerous events).
- *General collapses* (collapse of all or part of an operation, often dynamic. Phenomena which are potentially very dangerous).
- *Slides or slope movements* (characteristics of deposits or slopes of stripping operations in loose rock: slides, gulley erosion).
- *Flows*: (potentially dangerous disorders likely to affect people and property in the neighbourhood of old deposit structures).
- *Rockfalls* (characteristic of pit slopes in open-cast mines excavated in hard rock formations, with steep slopes).

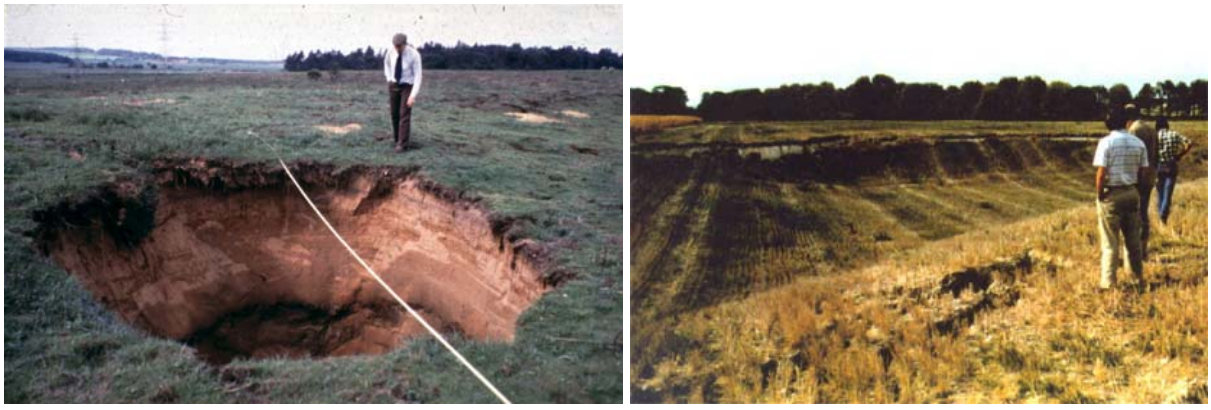


Figure 4. Example of a sinkhole (on the left) and of a general collapse (chalk mine on the right).

3.3. Mine gas emission on surface

After closing a mine, if not completely flooded, mining voids form an underground reservoir in which mine gasses accumulate. Depending on the ore extracted and the gases present in the deposit, the residual mine atmosphere may differ greatly in composition from one site to another.

Under the effect of various mechanisms, usually resulting from the pressure gradient between the underground workings and the outdoor atmosphere (rising groundwater, atmospheric pressure drop), mine gases may be forced to the surface through natural (fractures, cracks…) or artificial (shafts, drifts…) drains.

Depending on the type and composition of this mine gas, surface gas emissions may constitute several risks or nuisances to people and property. The safety of surface occupants may be affected if the gas is trapped in non-ventilated spaces (cellars, underground networks...). The main dangers for people are: ignition or explosion (methane), intoxication (CO, CO_2, H_2S…), asphyxia (oxygen deficit) or irradiation (radon).

- *Ignition (CH_4)*: methane, generally trapped in coal, is a non-toxic gas which is physiologically inoffensive. It is essentially its inflammability or explosivity which, when mixed with oxygen in certain proportions, makes methane such a dangerous gas.
- *Intoxication (CO, CO_2, H_2S)*: found in the ore being mined, resulting from the slow combustion or decomposition of organic or sulfuretted material, or resulting from the action of acid water on land, these gases are highly toxic and can be fatal at high concentrations. They attack the nervous system and the body's respiratory system.
- *Irradiation (radon)*: Radon is found in old underground uranium mines, but also in other underground spaces if the surrounding land contains even tiny quantities of uranium. Radon is a radioactive element which can be dangerous to humans when inhaled. Its effects increase the risk of lung and bronchial cancer.
- *Deoxygenated air*: Oxygen deficit situations (accumulations of mine gas or oxygen consumption) are likely to be encountered in all kinds of mining operations, particularly coal mines. Mine gas therefore represents a risk of asphyxia for people. An oxygen-poor atmosphere leads to a disturbance of the respiratory and blood systems of anyone exposed to it. A strong deficit can rapidly lead to death.

3.4. Water and soil pollution

Environmental modifications and disturbances induced by mining operations are likely to cause more or less important deterioration in the quality of environmental parameters in the area of the mine, reflected in the appearance of abnormal environmental contamination. This deterioration mainly affects underground or surface water and sediments and soils. It may also concern the atmosphere, particularly in the presence of ionizing radiation or toxic particle emissions.

The environmental impact results from complex and varied physico-chemical phenomena, closely linked to the type of substance mined and the mineralogy of the surrounding rock formations as well as the mining method used.



Figure 5. Effect on surface water of an abandoned coal mine discharge.

To assess the importance of environmental risks and nuisances, it is usual to reason in terms of "sources" (pollutant type and toxicity), "vectors" (water, soil, air) and "targets" in contact with this pollution (human activities, ecosystems…).

The main **sources** involved result from inorganic chemical contaminants (metals, sulfates…) or organic contaminants (hydrocarbons, phenol compounds...). They may particularly originate in old mine workings (soil leaching as the groundwater level rises), deposits of surface processing residues or structures storing industrial products used during mining operations.

Concerning contamination **transfer vectors**, underground and surface waters play a major role with air carrying toxic dust or ionizing radiation.

The main **targets** likely to be affected by these environmental nuisances are humans and, more generally, land and water ecosystems (biotopes and the organisms living in them). These targets may come into contact with various contaminants, either directly or indirectly via the food chain: water, plants, fruit and vegetables, fish, farm animals, etc.

4. Identifying, listing and mapping the hazards and factors involved

4.1. Principles for identifying and mapping hazards

4.1.1 Definition

A hazard corresponds to the probability that a given phenomenon will take place on a given site during a reference period, reaching a qualifiable or quantifiable intensity. Characterising a hazard is therefore usually based on the **predictable intensity of the phenomenon** with its **probability of occurrence.**

The **intensity of the phenomenon** corresponds to the amplitude of disorder, sequels or harmful effect likely to result from the feared phenomenon. This notion includes both quantification of the consequences of the feared events (size of a crater, height of water…) and the potential severity of their effect on humans, property and soil use, likely to potentially characterise the site after a certain time (possibility of victims or damage, existence and/or cost of prevention measures...).

The **probability of occurrence** reflects a site's sensitivity to being affected by any of the phenomena analysed. This is a concept which is particularly difficult to quantify considering the complexity of the mechanisms of evolution, the heterogeneous nature of the environment and the very partial nature of the information available. Therefore, within the context of hazard evaluation linked to the post-mine period, priority is given to the notion of a site's **predisposition** to suffer disorder or nuisance. Evaluation of this predisposition depends on the combination of different factors which are favourable or unfavourable to the initiation and development of the mechanisms in question.

4.1.2 Qualification of classes of intensity

The intensity of the phenomenon characterises the amplitude of the expected repercussion if the feared event takes place. Each type of phenomenon has one or more corresponding representative physical values which can be used to characterise the consequences of the

feared events. It is therefore the size of craters which defines the intensity of sinkholes and the estimated flowrate or depth of water which characterises the impact of flooding.

To evaluate the intensity of the feared phenomena, the expert attempts to evaluate the predictability, even approximate, of the physical values judged to be representative, for each selected phenomenon, using all the information collected. By referring to guide values which define the main classes of intensity, he can then define the class to which the feared phenomenon belongs within the context studied.

These reference values have been defined as part of the production of the methodological guide covering drafting of an MRPP. Some of the main national experts who are well-known in their field met in working groups, each dedicated to a particular theme. The guide values proposed are provided for information and can be adapted to the context by the expert in charge of evaluating risks. They also help to produce a homogeneous approach at national level, by limiting the subjectivity of the analysis inherent in the sensitivity of each expert.

As an example, the following table shows the classes of intensity of various phenomena which are representative of several classes of sequels.

Classes of intensity	Flooding	Surface instability
	Discharge modification (flowrate in dm^3/s).	Diameter of crater left by sinkholes
Limited	Seepage (< 1)	Ø < 3 m
Moderate	Small stream (< 10)	3 m < Ø < 10 m
High	Large stream	Ø > 10 m

4.1.3 Qualification of classes of predisposition

Determining predisposition is first based on a back analysis of the same type of disorder or nuisance on the site or a similar site. In addition, evaluation is also based on the analysis of scenarios and mechanisms of occurrence of phenomena likely to affect surface land, the combination of parameters promoting this occurrence and helping to raise the class of predisposition. For example, a very thick overburden, limited dimensions of residual voids and the presence of resistant layers in the overburden will make this site less predisposed to develop surface subsidence than a shallow site of operations located under an exclusively marly overburden.

Predisposition to triggering disorder can also be affected by the "incompleteness" of information available, which is often considerable in the case of very old operations. It is regularly necessary to manage the lack of available information by using the idea of "presumption".

While it would not be safe to limit yourself to only proven data, it would also be unreasonable to assign the same level of susceptibility to zones for which you only suspect that the feared phenomenon could develop as with those for which the hazard is confirmed. Therefore, a site's predisposition to the occurrence of disorders can be weighted by this idea of presumption, incorporating doubt resulting from gaps in the information.

4.1.4 Identification of classes of hazards

The principle of hazard qualification consists of combining criteria used to characterise the intensity of a feared phenomenon with criteria used to characterise its class of predisposition.

Several principles, explicit or implicit, can be used to combine qualitative values or cross-reference qualitative and quantitative criteria. For information, techniques can be noted by rating, upgrading, multi-criteria listing etc.

If the cross-referenced table principle is selected, a synthesis matrix is used, constituted as shown in the following table. To avoid complicating restitution maps, we shall limit ourselves to **three classes of hazard level** as far as possible: low, moderate and high hazard level.

Predisposition / **Intensity**	**Slightly sensitive**	**Sensitive**	**Very sensitive**
Limited	*LOW HAZARD*		
High			
Very high			*HIGH HAZARD*

4.1.5 Hazard mapping

The hazard has to be mapped for the entire sector concerned by the MRPP so as to reveal which sectors are most likely to develop risks or nuisances. Feedback tends to show that a scale of 1/10 000 is often used to reach a satisfactory compromise between MRPP principles (small scale) and communities' requirements (large scale). 1/5 000 can also be envisaged, mainly in small operations in an urban environment. Depending on the size of the study zone, diffusion could be envisaged in "paper" form but it is increasingly in "computer" form, using the powerful tools of Geographical Information Systems (GIS).

The hazard zoning contours are based on technical parameters (geology, operations…). They therefore have no reason to follow the contours of the plots of land. When, as if often the case, several potential phenomena coexist on the same plot, several risk maps can be drawn up, one per phenomenon, to avoid overloaded graphics and making them illegible.

Hazard mapping includes surface areas concerned by the possible effects of phenomena resulting from mining activities. It therefore takes into account the possible lateral extension of disorders or nuisances initiated in underground spaces and developing as far as the surface. It also includes the uncertainties inherent in the available information and results of estimates and models required to evaluate the area of influence of the risk.

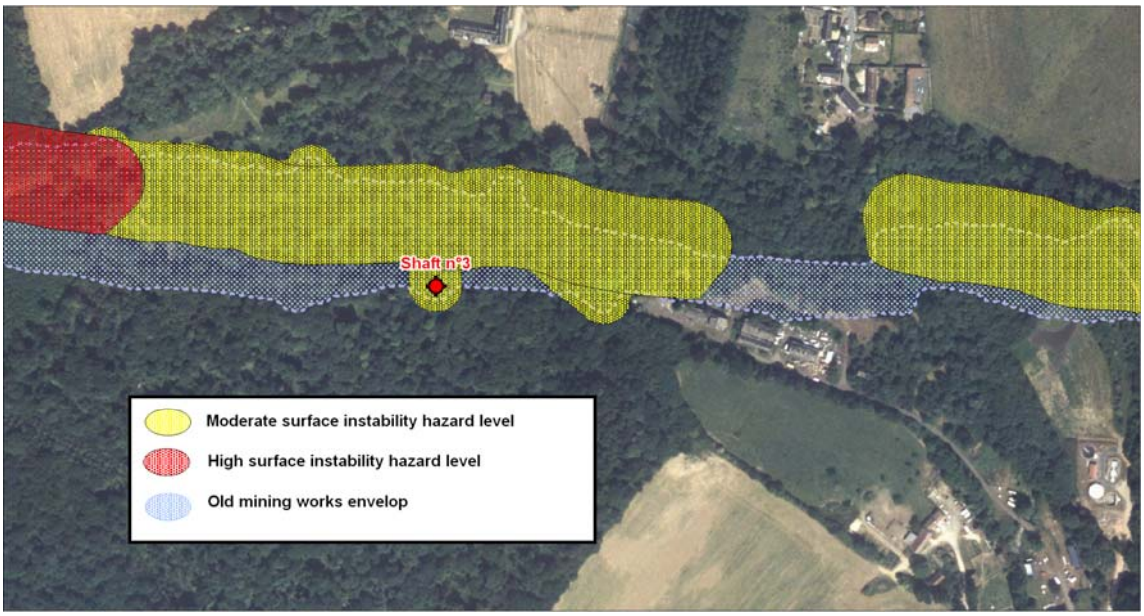


Figure 6. Example of a hazard map above abandoned iron mines (North-West of France) .

4.2. Principles of assessing and mapping the factors involved

4.2.1 Factor assessment phase

The procedure for assessing factors involved in mining risks consists of identifying the main types of land occupation or activities, both existing or future, which are likely to interfere with the risk prevention procedure. The major factors concerned will naturally include urbanised and particularly urban sectors in which the regulatory measures applied are likely to differ considerably from those defined for open land. The analysis will also identify industrial or urban wasteland which could be strategic for the development of towns with mining risk restrictions on other parts of their territory.

Assessing all the factors concerned also includes evaluating populations in danger and listing the main factors affecting safety, crisis management and vital functions in the area concerned. Therefore, public establishments, particularly the most strategic in terms of emergency aid organisation (schools, hospitals…) are identified, whether they are subject to risk or not, as well as sensitive equipment including networks (roads, electricity, gas, telephone…) so as to identify their sensitivity relative to the expected consequences of the occurrence of disorder. For example, routes used by traffic circulation which must be secured in priority to facilitate public assistance.

4.2.2 Factor mapping

The map including factors concerned is produced at the scale selected for drawing up the MRPP (often 1/10 000). It locates the main factors identified, giving them references if necessary so that descriptive sheets can be drawn up as required.

Depending on the different objectives to be reached (personal safety, future development of urbanisation…), several maps can be drawn up, giving priority to the factors most concerned by the objective in question.

5. Drawing up the zoning plan and regulations

5.1. Principles for regulatory zoning

Posting hazard and drawing up a regulatory zoning plan are two specific procedures with fundamentally different objectives. Whereas the first identifies the different types of disorder likely to develop on the surface and locates them, the second marks out the limits of the zones within which homogeneous instructions can be defined to ensure the safety of existing and future people and property.

The zones are marked out by cross-referencing hazard and factor maps, i.e. combining the type and intensity of predictable disorder with the occupation of surface land. Apart from exceptions, definition of the different zones is based on constructibility criteria (zones which are non-constructible or constructible under certain conditions…). As for hazards, the aim is to avoid multiplying the number of zones, to facilitate the legibility of the maps. For this purpose, the number of zones selected will be limited to three or four (a white zone within which requirements are minimal or non-existent, a red one for sectors considered to be non-constructible and one or two blue ones in which urbanisation remains possible but with more or less severe constraints and restrictions).

Generally speaking, priority will be given to the development of a new urban area in zones outside areas with mining-related risks. However, although this rule can be applied relatively strictly for areas not yet urbanised, constraints may be relaxed locally in urbanised areas with strong constraints due to mining-related risk over a major part of the area occupied by the communities in question. In this case, building permits may be envisaged in low or moderate risk zones.

The regulatory zoning plan must be drawn up, as far as possible, on a scale which is compatible with studies held during risk evaluation and factor assessment phases.

5.2. Drawing up the regulations

At the same time as the zoning regulations are drawn up, the State Department in charge of drafting the MRPP draws up the regulation which defines the regulatory provisions applied to each zone within the regulatory zoning area. These measures are mainly intended to improve the safety of people and property in zones subject to mining-related risks and prevent increasing vulnerability of property and activities in the most exposed zones, reducing it if possible.

The regulations must be as simple and operational as possible to make it easier for the public to understand and assimilate them. It is generally presented by type of regulatory zone (red, blue, white…) after defining the general measures applied to all the plots within the limit of the MRPP.

For each zone, it is usual to organise the measures in two groups: those designed for existing property and those intended for future projects. The different measures may take the form of prohibitions, obligations or simple recommendations.

It will be noted that one of the regulatory specificities of MRPPs, which make them a powerful tool, is their retroactive nature which means that measures can be applied to property existing before it was drawn up. However, if there is no existing restriction to future projects, the work imposed on property built before MRPP approval can only affect limited changes, costing less than 10% of the market value of the property before the risk was posted.

For successful drafting and application of the MRPP, all available expertise (administrative, technical and political) must be federated. A concertation procedure must therefore be systematically used between State Departments and local authorities, to facilitate understanding, appropriation and participation of local authorities in the risk prevention policy.

It is therefore essential to obtain the participation of local representatives when drawing up the regulatory zoning plan and regulations because they are the main authorities who will be in charge of applying it on a daily basis and explaining it to the population.

6. References

French **law n°95-101** of February 2nd 1995, relative to environment protection reinforcement (nowadays integrated through articles L.562-1 to L.562-7 to the Code of environment).The elaboration principles are described in the **edict n°95-101** of October 5th 1995.

French **law n°99-245** of March 30th 1999, also called « post-mining law ».The elaboration principles are described in the **edict °2000-547** of June 16th 2000.

L'élaboration des Plans de Prévention des Risques Miniers – Guide méthodologique. Ouvrage collectif sous la direction de l'INERIS. INERIS-DRS-04-51198/R01. 30/06/2004. 128 pages.

MANAGING THE MINING SUBSIDENCE HAZARD IN LORRAINE

DISSART Yannick[1], VERDEL Thierry[2]

[1] Groupe de Recherche en Economie Financière et Gestion des Entreprises, Pôle lorrain de gestion - 13 rue Michel Ney – CO 75 – 54037 Nancy Cedex, - France.; yannick.dissart@mines.inpl-nancy.fr

[2] Laboratoire Environnement, Géomécanique et Ouvrages, INPL – Ecoles des Mines de Nancy - Parc de Saurupt – CS 14234 - 54042 Nancy Cedex - France. thierry.verdel@mines.inpl-nancy.fr

ABSTRACT: The concept of governance makes it possible to involve three stakeholders in the management of post-mining subsidence hazards in Lorraine (East of France): the State, mining companies and the civil society. On the basis of this partition, it is possible to describe each one of them in order to study the various players through a community of logic. The study of the relationships between players shows the complexity of post mining treatment. Using an approach that takes into account not only the present but also the past makes it possible to give starts of answers regarding the non anticipation of this problem and the difficult issue it has become.

KEYWORDS: decision, governance, risk of mining subsidence, stakeholders.

RESUME : La notion de gouvernance permet de situer trois parties prenantes dans la problématique des affaissements miniers en Lorraine : l'Etat, les exploitants miniers et la société civile. Partant de cette partition, il est possible de décrire chacune d'entre elles afin d'aborder les différents acteurs à travers une communauté de logique. L'étude des relations entre acteurs montre la complexité dans le traitement de l'après mines. C'est au travers d'une approche qui prend en compte non seulement le présent mais également le passé qu'il est possible de donner des pistes de réponses quant à la non anticipation de ce problème et au dossier délicat qu'il est devenu.

MOTS-CLEFS : décision, gouvernance, risques d'affaissements miniers, acteurs.

1. Introduction

The year 1996 remains engraved in the memory of the Lorraine population. Two subsidence events occurred within a limited time, starting a large social movement.

Subsidence events are not rare. Some have been reported in Paris starting in 1776. In 1783, a mining control office is created under Louis XVI. In 1810, the mining code creates an administrative monitoring of mining exploitations in order to avoid the wasting of ore-fields and to ensure public safety and workers protection. The subsidence events induced by mining activities are thus known and regulated for over two centuries in France.

Piguet (1999), DRIRE (2003) and Forbes (2004) gave information about the first after-effects of mining subsidence in Lorraine. The first sudden collapse would have occurred in 1902 in Audun Le-Tiche, the first subsidence following the removal of mining pillars happened in Moutiers in 1954, the first subsidence due to the rupture of abandoned rooms and pillars excavations happened in Jarny between 1932 and the first reported sinkhole occurred in Thil in 1957.

Lorraine Iron Desposit has been exploited for more than two centuries. In the 1970s, the mining extraction intensity started to decrease but post-mining problems only started to emerge in the 1990s.

Today, most contributions about these problems focus on the technical side of the post-mining activity and mainly concern the identification, characterization and classification of subsidence hazard areas and the study of long-term hydro-mechanical behaviour of underground pillars.

In this paper, we would like to describe the different actors and to analyse the post-mining management in Lorraine through the concept of gouvernance. This concept enables us to describe the various stakeholders and to determine their role with respect to each other. Thus, we aim to give some elements of an answer to the question: why couldn't the consequences of mining activity be anticipated?

2. The governance principle

2.1. History of the term

The word gouvernance would have been used in the sense of “preparings” in the XIIth century It is found one century later with the meaning of steering in naval activity (Latin origin *gubernare*): to control something, to steer a ship using a rudder. The term then came to English as "*Governance*".

According to Lamy (2005), governance disappeared to the benefit of government of the State monopolizing power over a population, the governance term is then used to indicate "the way of adequately dealing with the public thing independently to the question of the capacity". A distinction then appears between power, policy and social organization modes.

Lastly, the term reappeared in the 1980s during international meetings to express a renewed need for change in decision-making processes. Peters and Savoy (2001) indicate that "governance" would have replaced "power" in order to indicate a renewed capacity of adaptation of administrations, the decision being no more concentrated in a single place.

Thus, governance requests a questioning of powers in place and a change in decision-making processes and their organization. It then requires each governmental organization to reconsider its operating modes and to have a renewed vision of itself in order to adapt to ever-increasing worldwide exchanges.

2.2. Definition of the term

The United Nations Program Development defines governance around three players, their respective roles, and reinstates people in the decision-making system: « *Under the parameters of Sustainable Human Development, sound governance has come to mean a framework of public management based on the rule of law, a fair and efficient system of justice, and broad popular involvement in the process of governing and being governed. This requires establishing mechanism to sustain the system, to empower people and give them real ownership of the process… Governance includes the state, but transcends it by taking in the private sector and civil society. All three are critical for sustaining human development. The state creates a conductive political and legal environment. The private sector generates jobs and income. And civil society facilitates political and social interaction - mobilising groups to participate in economic, social and political activities. Because each has weaknesses and strengths, a major objective of our support for good governance is to promote constructive interaction among all three* ».

The Commission des Communautés Européennes (2001) gives the following definition: « *the term "European governance" refers to the rules, processes and behaviour that affect the way in which powers are exercised at European level, particularly as regards openness, participation, accountability, effectiveness and coherence* ». This quotation underlines a system of coordination

through an organization controlled by a set of rules and behaviors in order to obtain efficiency in the decision-making model.

Wachter *et al.* (2000) give the following definition « *Governance designates a way of dealing with the question of governement which does not focus on the Art of Governing and the tools to manage actions, but on the relationships between governors and governed people, between citizens and the States.* » (translation). Regarding France, they emphasize three topics :

- The relationship between local authorities and the civil society ;
- Conditions of partnership between the public sector and the private sector;
- Citizen participation in public action, via consultation or dialogue.

We find here the articulation between the three players: the State, the Civil sector and the Private sector. They re-use the idea of citizen participation but they set it in a relationship with the local authority only.

For Biarez (1996), « *the local authority is not a single collectivity or a single political entity, it is a complex component of relationships between central structures and local leaders and heterogeous social groups* » (translation). She thus connects the State to the citizens through a complex relationship that the term 'governance' tries to translate.

2.3. Application to the Lorraine case

Refering to the principle of governance related to the post-mining subsidence problems in Lorraine, we can mention three stakeholders:

- The State, whose function was to develop economic activity and to manage post-mining hazard by taking into account technical as well as human aspects in order to fulfill his function of citizen protection;
- The mining companies, whose function was to participate to the national economic development and to secure the mining area after they have exploited them;
- The civil society which has first been employed in the local mining and metallurgical industry and which is now expecting a physical and social protection against pots-mining hazards.

All things considered, we can state that these stakeholders had in the same time both different and complementary logics as it is underlined in the definition of governance.

Now, using this scheme we can describe the various players and their role in the management of mining subsidence problem.

3. The players of the mining subsidence problem in Lorraine

After Corzani (2004), Forbes (2004) and Dissart (2005-1), it is possible to give the following description of the various players and the functioning of the organization in charge of addressing the post-mining problems in Lorraine.

3.1. The State stakeholder

In this part, we present all of the players who contribute to the protection of the individuals or their goods be they attached or not to the State by statute or contract. We only focus on players acting in a way or another in the frame of post-mining management.

3.1.1 The Prefecture

The prefecture is the legal authority representing the National Government at a local scale. Its services are in charge of implementing the policy of the State and deciding over conflicting positions.

The prefect has the power to cancel any local decision which would induce or increase a proven risk (articles L 111-1 and L 111-2 of the code of urban planning).

The state being the principal source of funding for post-mining operations, it must ensure the non-persistence of risks over the populated territories.

3.1.2 The Regional Direction of Industry, Research and the Environment (DRIRE)

The DRIRE have a direct relationship with the Prefecture.

As far as its role in post-mining management is concerned, the DRIRE is in charge of delivering a hazard map with the help of external experts (mainly GEODERIS, see below) and of carrying various studies for this purpose.

They are in charge of preparing inter-departmental conferences (CIAM) about the consequences of past mining activities.

3.1.3 GEODERIS

It is a public interest group formed by INERIS (National Institute of Industrial Environment and Risks) and BRGM (Office of Geological and Mining Research).

It aims solving the problem of post mining by gathering and comparing various information before writing the Plans of Prevention of the Mining Risks (PPMR).

3.1.4 The National Institute of the industrial Environment and the Risks (INERIS)

The INERIS is a publicly-owned industrial-commercial organization that carries out or has carried out studies and research making it possible to prevent the risks upon which economic activities weigh. It is within the framework of support for the DRIRE in order to develop PPRMs over the Lorraine territory.

3.1.5 BRGM (Office of Geological and Mining Research)

The BRGM is a publicly-owned industrial-commercial organization that brings a technical support to the DRIRE.

3.1.6 GISOS

The GISOS is a research group carrying research on the Impact and the Safety of the Underground Excavations.

It aims to develop scientific knowledge regarding post mining issues, specially as far as the subsidence hazard evaluation and their consequences are concerned. It tries, in particular, to answer to questions arised by GEODERIS.

3.1.7 Land publicly-owned establishment of Lorraine

It is a land operator acting under the responsibility of the Prefecture. When the Prefect expropriates populations, he calls upon this organization to find parcels of land for them.

3.1.8 French Agency for Environment and Energy Management (ADEME)

The ADEME is a publicly-owned commercial-industrial organization that can help other governmental organisations (DRIRE and Prefecture) as far as environmental issues are concerned.

3.1.9 The Rhine-Meuse Water Agency

Publicly-owned administrative organization of the State that carries various studies related to water ressources management.

3.1.10 Regional Direction of Environnement (DIREN)

Decentralized service of the National Government, it helps the Prefecture in proposing and instructing lawful protections. It carries out studies for decision-makers. It works in relationship with the Water Agency on environmental issues.

3.1.11 Scientific and Technical Building Center (CSTB)

The CSTB is a publicly-owned commercial-industrial organization that works on the implementation of recommendations regarding rules of constructibility in area subjected to mining subsidence.

3.1.12 Regional and Departmental Directions of the Equipment

As decentralized services of the National Government, they apply the various constraints regarding urban planning in areas subjected to mining subsidence. They directs the CSTB for the development of constructibility rules.

3.1.13 Mining Risks Prevention and Monitoring Agency

Created by decree n° 2002-353 dated March 15, 2002, it is a publicly-owned national administrative organization that collects various files and data about the mining activity and participate into regulation.

3.1.14 East pole of competence

It is an organization that carries out requests with GEODERIS for expertise in various fields. Its role is to carry competences in the other DRIRE.

3.2. The Mining Industry stakeholder

The imperial law of April 21, 1810, gave the power to the State for the choice of mining companies paving the way for the nationalization of extractive activities after the Second World War. The exploitation of the iron-ore deposit in Lorraine has never been nationalized on the contrary to the exploitation of the coal-ore deposit but the Government has always exerted its power in controlling the mining activity.

Various situations exist regarding the role of the mining industrialist when ending their excavation works :

- The mining company continues its extractive activity and is solvent. Then, it is completely responsible for the consequences of this activity;
- The mining company has stopped its extractive activity and is solvent. It then stands for all ending works required by the services of the State for making the extracting zone safe;
- The mining company has stopped its extractive activity and is not solvent. In that case, the State takes the responsibility for ensuring conformity and safety and then turns against the mining company for the payment of these operations;

- The mining company ceased its activity and disappeared. The State deals with the set of operations related to conformity and safety.

3.3. The stakeholder : Civil Society

3.3.1 The Regional Council of Lorraine

It is the first local authority acting on the basis of a contract with the State, allowing an action towards municipalities that are prone to mining subsidence events. Its interventions are at the budgetary level and cover:

- Treatment of the polluted or degraded zones, under the management of the Land Publicly-owned establishment of Lorraine;
- Urban renewal;
- Water supply under the management of the Water Agency.

The Regional Council acts as a mediator in the difficult situations and also implements a policy of voluntary town regrouping in order to achieve urban reorganization.

Lastly, it funds the poorest mining areas with a high risk for the revision of the local urban plan.

3.3.2 The General Councils

Two “General Councils” are concerned by the mining activity in Lorraine. They carried out very different actions.

The General Council of Meurthe et Moselle (south of Lorraine) offers an assistance to small municipalities that request it. Its agents advise municipalities regarding the drafting of urban planning documents or their modifications according to proven risks. They organize meetings with the services of the State so that the mayor can make a decision regarding his territory, even if that decision may be rejected by the Prefect.

The General Council of Moselle (north of Lorraine) directed its actions towards the three objectives of the Regional Council mentioned above. It is now starting to act towards the most affected municipalities.

3.3.3 The municipalities

Favored partners of the populations, they must disseminate the information regarding the risk induced by the potential collapse of mining underground excavations. They organize public discussions within the framework of collecting information for the realization of the mining risk prevention plans (PPRM).

3.3.4 Local associations

There are 14 local associations over the Lorraine territory which deal with post-mining problems. And gather people who could be subjected to them. They act as a lobby at the local level in order to affect the decision system. They can also help in collecting data regarding past extractive activities.

3.3.5 National and international associations

We can mention here the Association of Mining Cities of France (ACOM) and the European Action for Mining Communities (EURACOM).

The first one gathers the mining cities of France, on a voluntary basis, as well as various associations. It brings support in term of advices to the municipalities that request it. Lastly, it lobbies at the national level.

The second lobbies various institutions at the European level.

4. Causes of the complexity of post mining management

As we can observe through this descriptive approach, the management of post-mining subsidence hazard involved many partners and is complex.

Within the three major stakeholders that were just described, there were more than 10 players attached to the State, at least 5 for the civil society plus the mining companies. Some of them are at the disposal or are used by other players and various stakeholders.

But, besides this complexity, there are other reasons that make the post-mining management very complex. For the following paragraphs, we has refered to Dumas et al. (2003), Lorraine DRIRE (2003), Corzani (2004), Forbes (2004) and (Dissart, 2005-1).

4.1. The technical problems associated with extractive activities

4.1.1 Problems listed during the working life

- Use of polluting products, need for inventory and depollution;
- Excessive extraction ratios, difficulty to know exactly the situation for all mines;
- Cartography of extraction zones not always exact, difficulty to locate hazard zones;
- Mining extraction under urban areas with potential effects in termes of subsidence;

4.1.2 Problems listed after the working life

Here we may distinguish three types:

- Water-related problems:
  - Groundwater pollution and water treatment problems;
  - Sewage, changes in the environment and the biotope;
  - Water filling of the mining galleries which become inaccessible for later visits,
  - Water filling of the mining galleries that induces changes in local hydrology, pollution of underground water, and affects the long term behavior of pillars;
  - End of water pumping induce an extra cost to municipalities as far as their potable water supply is concerned
- Gaz-related problems:
  - The firedamp remains in the mines (coal mines), and there is a need to drain it to avoid explosions;
  - For other gases, weak O2 concentration or toxic gases, need for monitoring mine shafts and implement facilities for the degasification during the rise of water.
- Ground-related problems:
  - Residual subsidence for mines excavated by the long-wall method (coal mines)
  - Sudden or progressive subsidence for mines excavated with the methods of abandoned room and pillars

4.2. Knowledge-related problems

In this section, we can distinguish several elements:

- Evolution of scientific knowledge on the ageing of rocks and the degradation of underground cavities ;
- Loss of skills and people within the various services of the State ;
- Diffusion of the data in the human environment and difficulty of overlaying vernacular and topographic data (Decrop and Charlier, 1998).

4.3. Human-related problems

Over the years, the extractive activity created a true corporatist spirit by the hardness of work and the regrouping of immigrant miners coming from different countries. Not only had these people to endure hard work, but they also had to face the two world wars. The minors thus gave their life twice to their nation: for its economic development and for its protection.

In this context, the mining company took care of the minor's life. It gave him a salary for his work, it educated his children, it gave him holidays, it looked after and housed all his family.

Unfortunately, the end of 1960 marks a significant fall of the extractive activity in the Lorraine territory. In spite of a recovery in the 1980s, reality started to settle in: the mining company will cease its activity and will not further provide the mining tax to the local authorities (although it had been lower than the current professional tax). At the same time, the mining company progressively gave its real estate assets so that the minors may have become owners.

The consequences of mining are no longer about real estate but about individual inheritance with all the symbolic system that it supposes. Moreover, the discontinuance of business degraded the local economy with a strong social impact.

4.4. Organization-related problems

Here we may observe a difference regarding the treatment either in the presence of the absence of the mining company.

Indeed, when it is still present, the mining compagny keeps a direct bond with the local population. The contentious seem to be treated quickly by a human intervention within short times.

On the other hand, when the company ceased its activity, the bond with the local populations dispeared and the latter then had to follow administrative ways to get answers and compensations within deadlines that are lengthened. Moreover, the municipalities most affected by subsidences do not have land control of their territory any more and cannot respond to the increasing housing pressure.

5. Current treatment of the problems

We will approach this section under three perspectives:

- Symbolic, with a work of memory about an activity that made the glory of its country in its time;
- Legal, with the new mining code of 1999 ;
- Technical, with the progressive set up of the prevention plans against mining risks that integrate and transform local plans and the redevelopment of factory sites.

5.1. The symbolic system treatment of the problems

It is through various means that the various stakeholders treat the problems in a symbolic manner: the continuity of the memory of the activity.

- Development of museums about the mining history of the Lorraine Region;
- Development of teaching projects and exhibitions;
- Setting up of shows;
- Development of a literature in the local or national daily press;
- Development of fairs around the past activity or at the time of the Holy Beard, December 4.

5.2. Legal treatment of the problems

The reform of the mining code with the Mars 30, 1999 law relating to the responsibility concerning mining induced damage and the prevention of mining risks after the end of the extraction is the primary and central example.

The procedure related to mining extraction ending that governs the way mines must be closed and abandoned is now defined in articles 79 and 91. The contents of the administrative files and mandatory documents have been explained in the decrees of April 19, 1995 and September 8, 2004.

5.3. Technical treatment of the problems

The technical treatment of the problems is carried out via the related State services in partnership with the mining companies according to the procedure described by the mining code at the time of the discontinuance of the mining activity.

It consist in the installation of means for the mitigation - prevention of risks: suppression or reinforcement of underground cavities, supports of old wells, the installation of monitoring systems, etc. It also includes the production of various tools and means of constraint - knowledge: Plan of Prevention and Monitoring of the Mining Risks according to the procedure (MATE, 1997), alarm systems to prevent a disaster, development of knowledge regarding old mining works and monitoring systems of the areas at risk.

5.4. An estimated cost

In the CPER (Contrat de Plan Etat – Région, 2001), budgetary amounts are detailed as follows:

- State : 1,13 Billion Francs (172,26 M€) ;
- Lorraine Region: 520,5 Million Francs (79,34 M€) ;
- Meurthe et Moselle Departement : 268,8 MF (41 M€) ;
- Moselle Department : 476,5 MF (72,6 M€) ;
- Meuse Department : 43,6 MF (6,64 M€).

The total cost is then about 372 M€ with a distribution per year of 53 M€ to achieve the objectives of the 2000-2006 CPER: to make the territories and their resources safe, to reinforce the attractivity of the territories and to organize necessary solidarities.

5.5. Comming back to the concept of governance

As the report (DRIRE, 2003) indicates, a lack of dialogue with the local populations exists: « A permanent structure for information and discussion with elected representative and associations must be installed. It could be created from a subgroup of the CIAM (Interdepartemental Conference on Mining Activity), to be gathered regularly » (translation)

Indeed, the lack of direct bond with the local populations is obvious. The current system based on information meeting with the population could be improved in order to avoid that certain files become too complex.

A better transparency and communication appears a key-point in the management of the post mining affairs in order to move beyond individual interests as already mentioned by Foucault (1975), Beck (2001), Noiville (2003) and Delmas Marty (2004).

Then, the introduction of the concept of governance allows to have a large vision of the situation in complement of a technicist appoach. Because it brings actors face to face and situate these about the decision making like in figure 1.

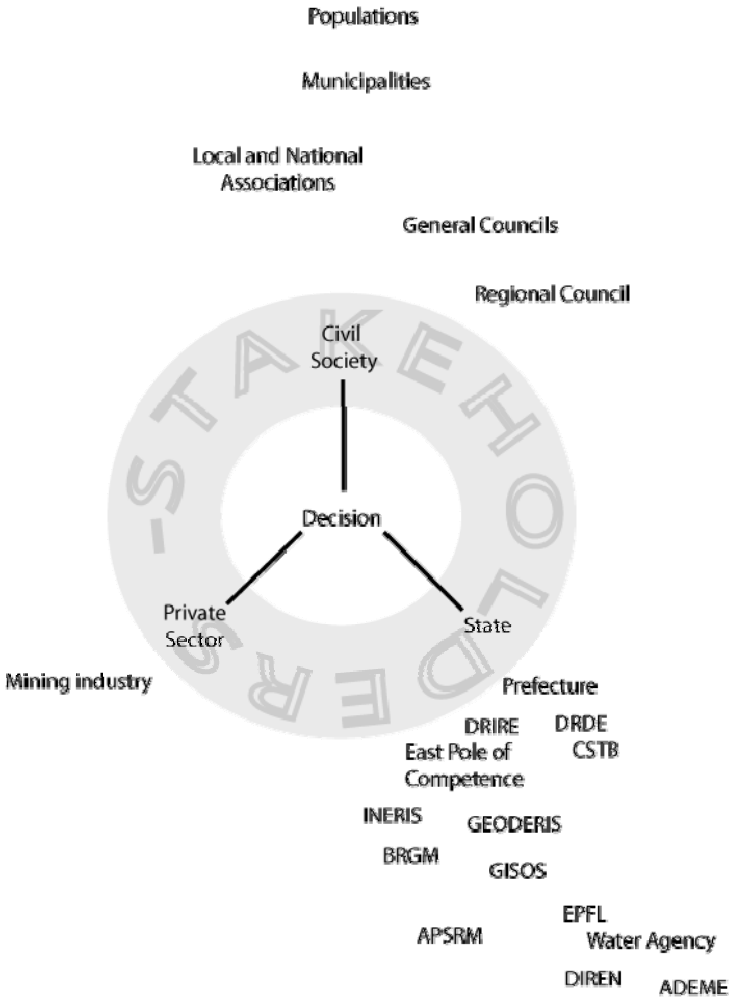


Figure 1. Actors position in relation to the decision in the management of mining subsidence hazard

We can see that the different stakeholders are situate in the relation to the decision with a large proximity of the State services and a great distance for the local populations. Here is the problem must to be solved.

6. Conclusion

The governance concept allows a human management in the problem of mining subsidence hazard by the dertemination of the role of the different actors and by their location relevant to the decision making. We can see that the current management is based on a technicist management instead of a human management. The problem of this situation was describe by (Rychen, 2002) : *« In the case where the central authority, concerned by the collective welfare, share the responsability of the public action with the competent local authorities on the reference area, in the case of a law rule, there is often an advantage to give to the central authority the informations collect and the planning of the different levels of the public actions, in charge for her to define some incitations for a sincerely communication by the local agents of the informations and a honnest sustain of recommandations. Under this hypotheses, only the arbitration is adopted between the collective efficiency and the decentralized informations. The propositions for the decentralized mecanism came on interrogations on model hypotheses ».* So, this statement makes clear that the model of the central authority capable of managing the risk by itself, by giving out information and recommendations to be followed and managed by decentralized organizations creates too many hypotheses that bring suspicion within local populations regarding the processing of the various affairs. In addition, there is complexity in the organization that deals with after mines problems and problems with the deadlines that are not understood by the victims that feel left out.

As we indicated the services of the State would gain to set up structures of dialogue in order to have a joint and understood action as suggested by the principle of gouvernance.

7. References

Beck U. (2001). *La société du risque*. Flammarion.

Biarez S. (1996). *Pouvoirs et organisations locales*. Sciences de la Société, Mai, n° 38, p. 21-47.

Bourdieu P. (2000). *Les structures sociales de l'économie*. Seuil.

Commission des Affaires économiques et du plan (1998). *Mines et carrières*. Rapport n°502, annexe au procès verbal du 17 juin 1998. Sénat.

Commission des Communautés Européennes (2001). *Gouvernance européenne, un livre blanc*. COM 428 final.

Contrat de Plan Etat – Région Lorraine (2001). *Convention d'application du contrat de plan 2000 – 2006*.

Corzani A. (2005). *Bassins miniers : Gagner l'avenir*. Conseil Général de Meurthe et Moselle.

Decrop G. et Charlier C. (1998). *De l'expertise scientifique au risque négocié*. CEMAGREF.

Delmas Marty M. (2004). *Les forces imaginantes du droit, le relatif et l'universel*. Seuil.

Direction Régionale de l'Industrie, de le Recherche et de l'Envrionnement (2000). *Historique de la législation minière*. Annexe 1.2 du dossier du Plan de Prévention des Risques Miniers.

Direction Régionale de l'Industrie, de la Recherche et de l'Environnement Lorraine (2003). *Le bassin ferrifère : « Etat des Lieux »*. 20 février 2003.

Dissart Y., Morel Guimaraes L., Chery O., Verdel T. (2005). *Aménagement des territories à risques : enjeux, acteurs et processus de decision*. 6ème congrès International Pluridisciplinaire, Qualité et Sûreté de Fonctionnement, Qualita 2005, 16 – 18 mars, Bordeaux, France, pp.179-186.

Dissart Y. (2005). *Entretiens avec les acteurs des affaissements miniers en Lorraine*. Non publié.

Dumas P., Moura P., Petit D. et Palat P. (2003). *Rapport de synthèse sur la mission après mine*. Inspection générale des Finances, n° 2003-M-032-05, Conseil Général des Mines, n°7/2003.

Forbes P-L. (2004). *La gestion des séquelles minières du basin ferrifère lorrain*. Présentation CIAM.

Foucault M. (1975). *Surveiller et punir*. Gallimard.

Lamy P. (2005). *La gouvernance, utopie ou chimère*. Revue Etudes, Paris, Février, n° 4022.

Ministère de l'Aménagement du Territoire et de l'Environnement, Ministère de l'Equipement, des Transports et du Logement (1997). *Guide général : Plan de prevention des risques naturels*, La Documentation Française.

Noiville Christine (2003). *Du bon gouvernement des risques.* PUF.

Peters G. et Savoie D.J. (2001). *La gouvernance au XXIe siècle: revitaliser la fonction publique*. Presses de l'Université Laval, Québec.

Piguet J.P. (1999). *Revue de presse*. Laboratoire Environnement, Géomécanique et Ouvrages.

Rychen F. (2002). *Gérer les risques collectifs*. Aube éditions.

United Nations Program Development (1995). *Public Sector Management, Governance and Sustainable Human Development*. United Nations, New York, january.

Verdel T. (2000). *Analyse cyndinique de la problématique des affaissements miniers lorrains*. Laboratoire Environnement, Géomécanique et Ouvrages, TV17/10/2000.

Wachter S., sous la direction de, (2000). *Repenser le territoire. Un dictionnaire critique*. Editions de l'Aube.

PSYCHOSOCIAL AND MEDICAL CONSEQUENCES OF MINING SUBSIDENCE IN LORRAINE

DODELER Virginie, TARQUINIO Cyril

Université de Metz – UFR SHA – Laboratoire de Psychologie – Ile du Saulcy 57145 METZ - virginie.dodeler@wanadoo.fr ; ctarquinio@aol.com

ABSTRACT : This study was aimed at assessing the effects on health of risky situations caused by soil subsidence and water seepage in the iron-mining basin of northern Lorraine. Psychological as well as medical aspects are considered. The results indicated that individuals subjected to mining-related problems had significantly more physical ailments and symptoms of psychological distress than persons not exposed to these problems. Among the exposed individuals, those who felt that their health had declined since the beginning of the events had more symptoms of psychological distress than the others.

KEYWORDS : Health psychology ; anxiety ; stress ; depression ; mining subsidence ; health.

RESUME : L'objectif de notre recherche était d'évaluer les conséquences pour la santé des situations de risque lié aux affaissements miniers et à l'ennoyage dans le bassin ferrifère nord-lorrain, en s'intéressant aux conséquences psychologiques et aspects médicaux. Nos résultats indiquent que les personnes confrontées aux problèmes miniers présentent significativement plus de troubles physiques et de symptômes de détresse psychologique que les personnes n'y étant pas confrontées. De plus, parmi les personnes confrontées aux problèmes miniers, celles estimant que leur état de santé s'est dégradé depuis le début des événements présentent plus de symptômes de détresse psychologique que les autres.

MOTS-CLES : Psychologie de la santé ; anxiété ; stress ; dépression ; affaissements miniers ; santé physique.

1. Introduction

For five years now, the Psychology Laboratory of the University of Metz has been conducting research on the psychosocial repercussions of mining-related problems in the Lorraine region of France. After having shown that these problems have had an impact not only on the mental health of the concerned individuals but also on their relationship to their physical and social environment, we thought it would be important to look also at physical health problems. At the beginning of 2004, we began a longitudinal study in collaboration with the French National Federation of Associations of Mining-Hazard Victims (Fédération Nationale des Associations of Victimes of Dégâts Miniers) and with physicians in the geographical area affected by these hazards.

The study was aimed at assessing the health consequences of risky situations caused by soil subsidence and water seepage in the iron-mining basin of northern Lorraine. We looked at both psychological consequences (post-traumatic stress, anxiety, depression, perceived stress, compliance with prescribed treatment), and medical aspects (heart disease, respiratory disorders, skin conditions, allergies, medication and other substance use, etc.).

From a psychosocial standpoint, the home is a place of intimacy, socialization, and physical and psychological safety (Fischer, 1997). A number of studies have shown that the properties of one's

home environment can affect human health. Evans and McCoy (1998) identified various architectural characteristics of the life space that have an impact on people's health, especially on their stress level. Evans and Cohen (1987) suggested that a state of stress can appear when there is an imbalance between environmental demands and individual resources. Warr (1987) proposed his "principal environmental influences" model, which emphasizes the importance of the environment, both physical and social, for well-being and mental health.

Traditionally studied in cases of natural or industrial disasters, degradations of the life space have been shown to trigger symptoms of post-traumatic stress, anxiety, and depression. The possibility of losing one's home -- the privileged place of psychological investment and rooting -- is thought to have an impact on the mental and physical health of individuals. The Lorraine region of France was formerly a highly industrialized area, with extensive mining operations. Today, these operations are gradually disappearing, but one of the physical repercussions of this massive exploitation is soil subsidence. The phenomenon is unpredictable and violent in the iron-mining basin, where it is causing substantial physical damage to above-ground structures, and in some cases, the inhabitants have had to relocate. It is slow and progressive in the coal-mining basin, where houses are not collapsing but are sagging, and people are forced to adapt to "tilted living" and to change their life modes. In both cases, the damages have only been environmental : no one has been wounded so far. However, the question that arises is : What might be the impact of these events on the population? How should people react to significant perturbations in their living environment, both physical and social?

Earlier studies on soil subsidence in Auboué showed that children who were disaster victims had higher anxiety and post-traumatic stress scores than children who were potential victims or control subjects (Witkowski et al., 1998; Vila et al., 2001). In a study on adults, Tarquinio (2001) noted that disaster victims had higher post-traumatic stress scores than non-victims. This was particularly true for individuals who had had to relocate ; they were experiencing very negative effects of the social uprooting brought about by their new living situation. In addition, the victims exhibited some degree of self-deprecation and a decline in health behaviors. We also showed (Dodeler & Tarquinio, 2003) that the sheer fact of residing in an area at-risk for mining-related problems increased people's anxiety level.

In the present study, we were interested in the population of individuals living in the iron-mining basin of the northern part of the Mosell Department, an area at risk for soil subsidence. Our aim was to determine the impact of this situation on the physical and mental health of the population.

2. Method

2.1. Subjects

We compared two groups of subjects :

- an experimental group made up of 143 subjects residing in the North Moselle iron-mining basin and affected by soil subsidence problems.
- a control group made up of 140 subjects not residing in a mining-risk zone and matched to the experimental group on age, gender, and homeowner or tenant status.

Table 1. Main Characteristics of the Sample

Variables		Total (n=283)
Age		M=54 ; σ =11,6 ; [24 ; 81]
Sexe	Homme	43%
	Femme	57%
Etat civil	Célibataire	8%
	Marié(e)	74%
	En concubinage	7%
	Divorcé(e)	5%
	Veuf(ve)	6%
Niveau d'études	Sans diplômes	13%
	BEPC	17%
	CAP/BEP	32%
	BAC	20%
	BAC +	18%
Situation	Locataire	18%
	Propriétaire	82%

Table 2. Main Characteristics of the Experimental Group

	Length of life in their town M = 42,5 ; σ = 20,2 ; [2;81]		Lenght of life in their house M = 28,1 ; σ = 15,7 ; [2;75]	
[0;10[	1,4%	n = 2	6,5%	n = 9
[10;20[	0%	n = 0	8,6%	n = 12
[20;50[	29%	n = 40	38,1%	n = 53
[50;80[	69,6%	n = 96	46,8%	n = 65

At the time of the study, most of the individuals had been living in the same city or town (98.6%) and in their current home (84.9%) for more than 20 years.

2.2 Materials

Psychological aspects were assessed on standard scales:

- Anxiety was measured on the STAI-Y (State-Trait Anxiety Inventory; Spielberger et al., 1983), which consists of two separate scales for evaluating state and trait anxiety. The anxiety scale contains 20 statements about what the subject is feeling at the time. It is used to assess feelings of apprehension, tension, nervousness, and worry. The trait anxiety scale includes twenty statements about what the subject feels in general. It is used to assess neurotic anxiety. Each item is rated on a 4-point Likert scale (1 to 4).
- Post-traumatic stress was assessed using the IES-R (Impacts of Event Scale Revised ; Weiss & Marmar, 1997), which contains 22 items measuring symptoms of intrusion, avoidance, and hyperarousal. Each item is rated on a 5-point Likert scale (0 to 4).

- Depression was measured using the CES-D (Center for Epidemiologic Studies - Depression Scale ; Radloff, 1977). It is comprised of 20 items for evaluating the subject's current symptoms of depression, and covers the following areas : depressed moods, feelings of guilt, helplessness and despair, psychomotor slowing, loss of appetite, and sleep disorders. Each item is rated on a 4-point Likert scale (0 to 3).
- Overall health was measured on the GHQ (General Health Questionnaire ; Goldberg), which has 28 items each rated on a 4-point Likert scale (1 to 4).
- Perceived stress was measured on Cohen's scale (1983), which has 14 items rated on a 5-point Likert scale (1 to 5).
- Compliance with medical prescriptions was measured on an adapted version of Tarquinio, Fischer, and Grégoire's scale (2000). It is composed of 16 items for assessing the individual's health-promoting behaviors, each rated on a 5-point Likert scale (1 to 5).

Medical aspects were assessed on a questionnaire developed for this purpose in collaboration with the team of physicians.

3. Results

Concerning the medical aspects measured, our results indicated that mining-related problems had an impact on people's health. The experimental-group subjects gave a lower rating to their health than the control-group subjects did ($t = -4.5$, $p < .001$). They had significantly more problems falling asleep ($t = 5.5$, $p < .001$), slept less well ($t = 6.3$, $p < .001$), woke up feeling more tired ($t = 3.5$, $p < .001$), and had more trouble concentrating ($t = 2.5$, $p < .05$). They suffered more from problems related to the respiratory system ($t = 2.4$, $p < .001$), the stomach ($t = 2.2$, $p < .05$), the intestines ($t = 3.7$, $p < .001$), the libido ($t = 3.8$, $p < .001$), and the thyroid gland ($t = -2.9$, $p < .01$). They also felt more irritable ($t = 4.2$, $p < .001$) and restless ($t = 4.5$, $p < .001$). Finally, they took significantly more anti-depressant drugs ($t = 3.5$, $p < .001$) and neuroleptics ($t = 2.1$, $p < .05$).

Concerning the psychological aspects measured, the two groups differed significantly on all scales except for compliance with prescribed treatment (see table below).

Table 3. Means (and Standard Deviations) on Mental Health Scales

	Experimental group	Control group	p
IES (Post-Traumatic Stress Disorder)	36,88 *(20,09)*	10,55 *(17,21)*	.001
Observance	70,57 *(7,15)*	69,35 *(7,91)*	ns
GHQ (General Health Questionnaire)	52,33 *(16,65)*	45,86 *(14,85)*	.001
Perceived Stress	36,62 *(9,10)*	34,36 *(9,13)*	.05
CESD (Depression)	17,35 *(11,43)*	13,45 *(10,61)*	.01
Anxiety - State	43,94 *(14,14)*	34,36 *(11,81)*	.001

Thus, it seems that the individuals confronted with mining-related problems had more symptoms of post-traumatic stress, stress in general, anxiety, and depression than the individuals in the control group. In addition, they perceived their overall state of health as being not as good. In contrast, it seems that mining-related problems did not have an impact on compliance with prescribed treatment.

Furthermore, among the victims of mining-related problems, 37% felt that their physical health had declined since the beginning of the events.

Table 4. Perceived Health Since the Onset of Mining-related Problems

Do you feel that since the water seepage and soil subsidence problems began, your health has …	… gotten worse	… remained the same	… improved
	37%	60%	3%

And it turned out that perceived health had a impact on the onset of psychological disturbances : individuals who felt that their health had declined exhibited significantly greater symptoms of stress, anxiety, depression, and post-traumatic stress than those who felt it had remained stable or had improved.

These results thus show that mining-related problems have an impact on the physical and mental health of individuals, and that these two aspects are linked. The next two phases of this study will extend these findings (the data analysis for the second phase of the study is now underway).

4. References

Cohen, S., Kamarck, T., and Mermelstein, R. (1983). A global measure of perceived stress. *Journal of Health and Social Behavior, 24*, 386-396.

Cohen, S. & Williamson, G. (1988). Perceived Stress in a Probability Sample of the United States. Spacapan, S. and Oskamp, S. (Eds.) *The Social Psychology of Health*. Newbury Park, CA: Sage.

Dodeler V. & Tarquinio C. (2003). Impacts psychosociaux des risques d'affaissements miniers : anxiété, perception de l'environnement et accès à l'information. *Après-Mines 2003 - Impacts et gestion des risques*, Colloque International GISOS, Nancy, 5-7 février 2003

Evans, G.W. & Cohen, S. (1987). Environmental stress. In : D. Stokols & I. Altman (eds). *Handbook of environmental psychology*, Vol.1, John Wiley & Sons.

Evans, G.W., & McCoy, J.M. (1998). When buildings don't work : the role of architecture in human health. *Journal of Environmental Psychology*, 18, 85-94.

Fischer, G.N. (1997). *Psychologie de l'environnement social*. Paris : Dunod. 2ème édition.

Radloff, L. (1977). The CES-D scale : a self report depression scale for research in the general population. *Applied Psychological Measurement*, 1, 385-406.

Spielberger, C.D., Gorsuch, R.L., Luschen, R., Vaag, P.R. & Jacobs G.A. (1983). *Manual for state-trait-anxiety inventory (STAI) form Y*. Consulting psychologist press inc (Palo Alto, CA).

Tarquinio, C., Fischer, G.N. & Grégoire, A. (2000). La compliance chez des patients atteints par le VIH : Validation d'une Échelle Française et mesure de variables psychosociales. *Revue Internationale de Psychologie Sociale*, 2, 61-91.

Tarquinio, C. (2001). Aspects psychosociaux dans l'étude du traumatisme. In : P. Pansu & C. Louche (eds). *Les nouvelles orientations de la psychologie sociale*. Paris : PUF.

Vila, G., Witkowski, P., Tondini, M.C., Perez-Diaz, Mouren-Simeoni M.C. & Jouvent, R. (2001). A study of psychotraumatic disorders in children who experienced an industrial disaster in the Briey region. *European Child & Adolescent Psychiatry*, 10(1), 10-18.

Warr, P. (1987). *Work, unemployment and mental health*. Oxford : Clarendon Press.

Weiss, D. & Marmar, C. (1997). The Impact of Event Scale - Revised. In J. Wilson & T. Keane (Eds), *Assessing psychological trauma and PTSD.* New York: Guildford.

Witkowski, P., Vila, G., Tondini, M.C. & Mouren-Simeoni, M.C. (1998). Etudes des troubles psychotraumatiques chez les enfants victimes d'affaissements miniers en Lorraine. *Annales Médico-Psychologiques*, 156(8), 517-528.

COPPER RECOVERY FROM THE SLUDGES OF THE LARONDE MINE, CANADA

ELAMARI Khalid[1], BENZAAZOUA Mostafa[2], BUSSIÈRE Bruno[2], ARCHAMBAULT Martin[3]

1- LABORATOIRE DE GEORESSOURCES – Faculté des Sciences et Techniques – Marrakech. B. P. 549 / 40000 Marrakech. E-mail: elamari@fstg-marrakech.ac.ma

2- UNIVERSITE DU QUEBEC ABITIBI TEMISCAMINGUE, Chaire industrielle en Environnement et Gestion des Résidus Miniers, 445 Boul. de l'Université, Rouyn-Noranda, Québec, Canada J9X 5E4. E-mail: Mostafa.Benzaazoua@uqat.ca, Bruno.Bussiere@uqat.ca

3- MINES AGNICO-EAGLE, division LaRonde, Case postale 400, Cadillac, Qc, J0Y 1C0, Canada. E-mail: martin.archambault@agnico-LaRonde.com

ABSTRACT: *The cyanide destruction process at the LaRonde mine generates a large volume of potentially polluting sludges. These sludges are rich in copper and contain traces of gold and silver. The predominant chemical elements of these sludges are: 31.4% Ca, 2.9% Si, 1.98% Na, and between 1% and 5% Cu. Calcite is the only crystallized phase, other phases are mostly amorphous and complex phases composed of Si-Ca-S, Fe-S-Ca, and Cu-S-Ca-Si, along with carbon and oxygen. Leaching tests in a sulphuric medium were conducted on these by-products in order to selectively dissolve and recover the copper from the solutions using traditional techniques (liquid-liquid extraction, electrolysis, and cementation). The results showed that it is possible to dissolve the copper completely with a good selectivity towards calcium (99% copper dissolution and less than 5% Ca). The optimal dissolution kinetic is fast (5 minutes) and the residual solid is mainly composed of gypsum containing 26.4% Ca, 18.3% S, and 0.01% Cu. The final leach solution has a content of 740 mg/l of Cu.*

KEYWORDS: *sludge, leaching, copper, cyanides treatment, gypsum.*

RÉSUMÉ : *Le procédé de destruction des cyanures à la Mine LaRonde génère des boues à potentiel polluant en quantités importantes. Ces boues sont riches en cuivre et contiennent des traces d'or et d'argent. Les éléments chimiques dominants dans ces boues sont : 31.4% Ca, 2.9% Si, 1.98% Na et entre 1 et 5 % Cu. La calcite constitue la seule phase cristallisée, les autres phases sont amorphes et complexes formées de Si-Ca-S, Fe-S-Ca et Cu-S-Ca-Si en plus du carbone et de l'oxygène. Des essais de lixiviation en milieu sulfurique, ont été réalisés sur ces produits, en vue de dissoudre sélectivement le cuivre pour ensuite le récupérer par des techniques métallurgiques classiques (extraction liquide - liquide, électrolyse, cémentation). Les résultats obtenus ont permis de mettre en évidence la possibilité de dissoudre complètement le cuivre, avec une très bonne sélectivité vis-à-vis du calcium (99% de dissolution de cuivre et moins de 5% Ca). La cinétique optimale de dissolution est très rapide (5 minutes). Le solide résiduel, formé essentiellement de gypse, contient 26,4 % Ca ; 18,3% S et 0,01% Cu. La solution de lixiviation finale titre 740 mg/l Cu.*

MOTS CLÉS : *boues de polissage, lixiviation, cuivre, cyanures, gypse.*

1. Introduction

The LaRonde property is located in Abitibi (North-West of Québec, Canada). This mine is in operation since 1989, exploiting gold, silver, copper, and, more recently, zinc. The ore, which is mined to a depth of 2300 m, is brought to the surface to feed the ore processing plant. After the fragmentation and sizing processes, the ore is submitted to a differential flotation process in order to recover the copper then the zinc, before the final flotation tailing is directed towards a cyanidation treatment to recover the remaining gold. Thirty per cent of the final tailings (after flotation and cyanidation) are used to make underground paste backfill and the rest of the tailings are pumped in a tailings impoundment. A cyanide destruction process using hydrogen peroxide was implemented at the LaRonde mine to respect environmental criteria at the final effluent imposed by the Quebec and Canadian governments.
In the mining industry, the first cyanide destruction process to be used on an industrial scale, using hydrogen peroxide, was developed by Degussa at the Ok Tedi mine in Papua New Guinea (Knorre et al., web site). The capacity of hydrogen peroxide (H_2O_2) to oxidize cyanides into non-toxic products is well-known; it oxidizes cyanide ions into cyanates at a pH ≈ 10.5 to 11:

$$CN^- + H_2O_2 = OCN^- + H_2O \qquad (1)$$

In the presence of metal-cyanide complexes, the rate of reaction with H_2O_2 depends on the dissociation rate of the complex. Metals precipitate in the form of hydroxides:

$$Me(CN)_4^{2-} + 4\ H_2O_2 + 2\ OH^- = Me(OH)_2 + 4\ OCN^- + 4\ H_2O \qquad (2)$$

The cyanate produced during the oxidation reaction forms ammonium carbonate:

$$OCN^- + 2\ H_2O = CO_3 + NH_4^+ \qquad (3)$$

Ferrocyanide complexes are too stable to be oxidized by H_2O_2, but they can be precipitated by metal ions such as copper in pH conditions similar to those of natural water:

$$2\ Cu^{2+} + Fe(CN)_6^{4-} = Cu_2Fe(CN)_6 \qquad (4)$$

The sludges produced by the Agnico-Eagle LaRonde mine cyanidation destruction process are stored in a pond of 20 hectares. These sludges are produced during the final step of residual cyanide destruction after natural destruction by UV radiation (protolysis) in the tailings pond.

The present study will concentrate on how the sludges resulting from the cyanide destruction can be processed to selectively extract the copper and recover it from the solution using traditional processes (solvent extraction, electrolysis, cementation). To do so, samples of these sludges, referenced BLT and BLT1, were first subjected to physicochemical, particle size, and mineral characterization before undergoing leaching tests in a sulphuric acid medium.

2. Material and Method

The main sludge sample (referenced BLT) used in this study contains approximately 10% of solid in suspension. This sample was kiln dried, disaggregated to separate particles, homogenized, and conditioned in hermetic plastic bags. The characterization of the initial and final products obtained was peformed using the following analysis techniques: ICP-AES for the chemical analysis of solutions and solids (after HF leaching), X-ray diffraction (XRD) for the identification of crystallized minerals, scanning electron microscopy (SEM) coupled with EDS microanalysis for the ultimate chemical analysis of solid phases, laser particle size analysis for determining the distribution and size of the particles, Fourier transform infrared spectroscopy (FTIR) for the characterization of certain amorphous

phases, and, finally, nitrogen adsorption for determining the specific surface of solids according to the BET method (Brunauer, Emmet, and Teller). More details about all these methods can be found in Villeneuve (2004).

Leaching tests on the BLT sludge were carried out using a multi-station stirrer, which allows to reproduce the same hydrodynamic agitation conditions for all the leaching tests. Erlenmeyer flasks of 250 ml were used as containers. A fixed weight (3 grams) of the BLT sludge sample were mixed with 50 ml of leaching solution made with deionized water (deionized water has a pH of 8.34 and an Eh of 889 mV). At the end of each test, the solid was separated from the liquid using a Whatmann no. 3 filter paper with a porosity of 6 µm. The residual solid was dried and weighed to determine the sample's weight loss. The residual solid and liquid were analyzed for copper, calcium, and other chemical elements to determine their dissolution rates.

3. Results and Discussions

*3.1. Characterization **of the LaRonde Sludges (BLT)***

Naked-eye observation of the BLT sample revealed two main colour components: a whitish component resembling lime, calcite, or gypsum, and a greenish component, apparently containing copper. In the polishing pond, there is a slight difference between these two components under the effect of waves. This could have an influence on the spatial and temporal distribution of copper and, therefore, on the homogeneity of these sludges in the field.

BLT sludges have a dry solid density of 2.59 and a specific surface of 30.47 m^2/g. In term of particle size distribution, these sludges have a fine particle sizing (d_{50} of 37 µm and d_{80} of 63 µm with coarse particles smaller than 300 µm). The grain-size distribution is almost unimodal with a mode of approximately 50 µm. ICP-AES analyses of the BLT sample (Table 1) show that the sludges are very rich in calcium (31.4%). This is due to the addition of lime in the cyanide destruction process used (Degussa process). The sodium, silicon, iron, and sulphur also come from the additives used during this process. The copper precipitated or trapped in these sludges amounts to 1.24%. The presence of copper in these sludges, along with that of many other chemical elements, is of paragenetic origin, depending on the deposit being processed. A part of the gold and silver that dissolved during the cyanidation process is lost in the water after the activated carbon treatment. These precious metals are therefore present in the sludges in appreciable amounts (24.6 ppm Ag and 0.24 ppm Au).

Table 1. Chemical analyses of LaRonde BLT sludges.

Element	Content	Element	Content	Element	Content
Ca (wt%)	31.4	B (wt%)	0.510	Mg (wt%)	0.367
Si (wt%)	2.9	Al (wt%)	0.278	Mn (ppm)	570
Na (wt%)	1.98	Se (wt%)	0.222	Ni (ppm)	60
Cu (wt%)	1.24	Zn (wt%)	0.138	Ba (ppm)	20
S (wt%)	0.719	Fe (wt%)	0.407	Ag (ppm)	24.6

SEM observation revealed the predominance of a well-crystallized calcium mineral that could be either calcite or lime (hydrogen not being detectable with this method). More extensive EDS analyses on large area showed the presence, in varying proportions, of the following chemical elements: calcium, carbon, copper, magnesium, silicon, iron, aluminium, sulphur, and oxygen. Other mineral phases, apparently amorphous and composed of Cu-Ca-Si-S-Mg-Fe with variable stoechiometries, depending on the mineral analyzed, were identified by punctual analyses on isolated grains (see Photo 1 and Figure 1).

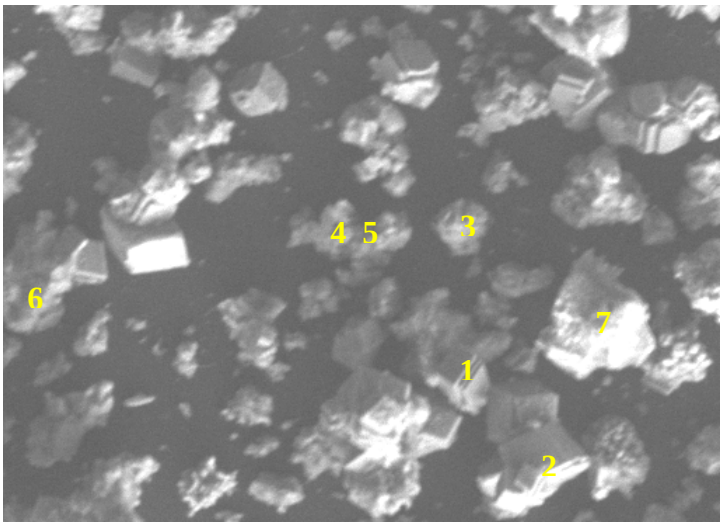


Photo 1. SEM image by retro diffused electrons, position of analysis points 1 to 7 in the BLT sample.

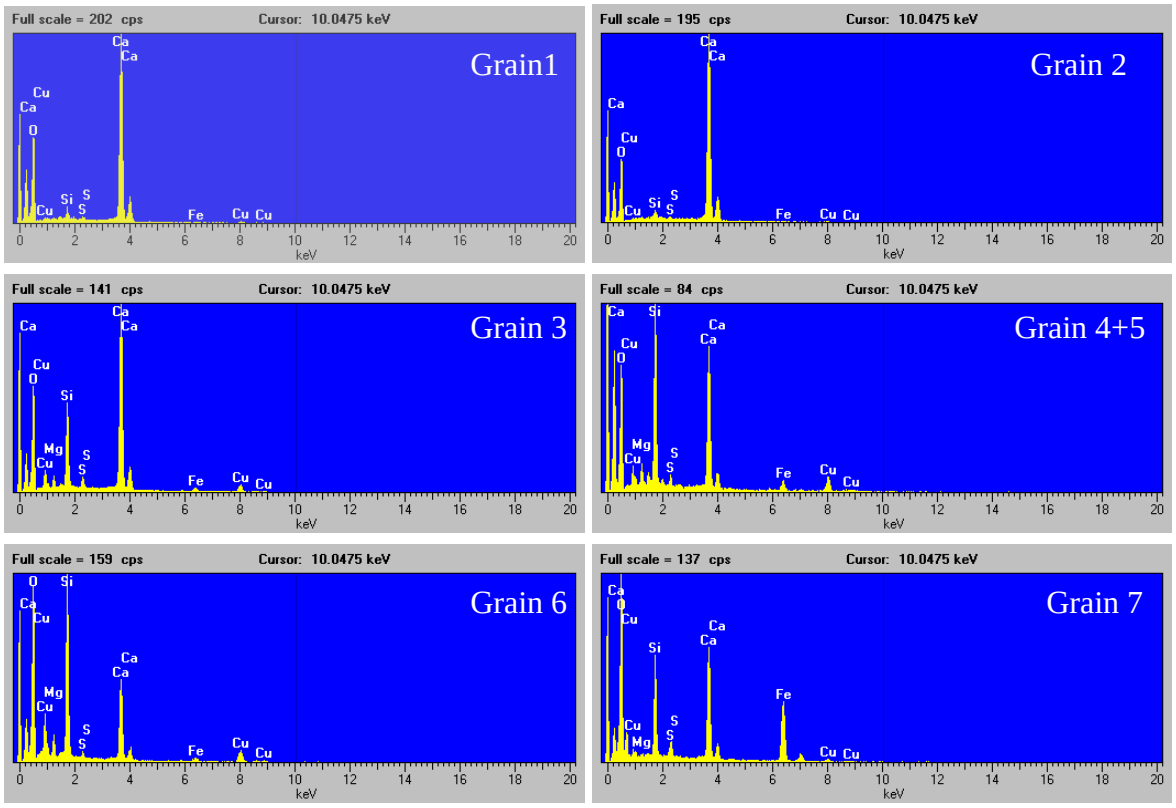


Figure 1. SEM analysis spectrums of grains 1 to 7 in photo 1.

Analyses on crystalline phases revealed the coexistence of Ca, O, and C and confirmed the presence of calcite. X-ray mapping of these elements (Figure 2) confirmed the following correlations: Si-Ca-S, Fe-S-Ca-Si, and Cu-S-Ca-Si. This can be explained by the mineral substitution, in some cases, of some chemical elements within calcite when it precipitates. In other mineral phases, calcium is found not in the form of calcite but combined with other elements in different mineral phases.

The abundance of calcium, and thus of calcite, was confirmed by X-ray diffraction (see diffractogramme in Figure 3). This Figure also shows the possible presence of a calcium silicate ($Ca_3Si(OH)_6(CO_3)(SO_4)$) that could justify the correlation between Ca, O, C, Si, and S. This confirms the scanning electron microscope observations, the calcite being the only well-crystallized mineral phase identified. No copper mineral was detected by XRD, indicating that the copper must be trapped in the calcium silicate phases or even in the calcite.

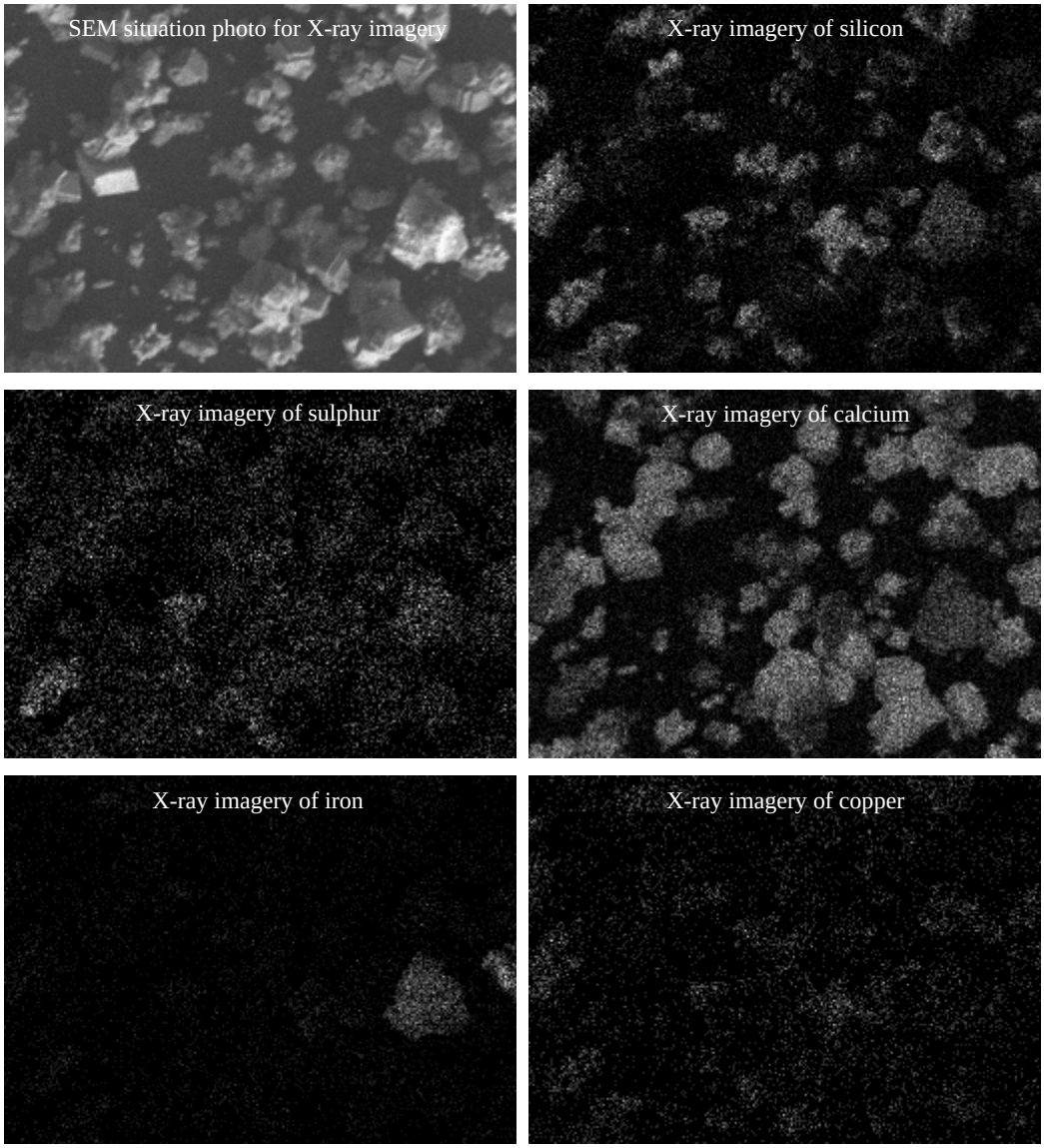


Figure 2. X-ray images of iron, sulphur, copper, calcium, and silicon in BLT sludges.

The Fourier transform infrared analysis of the BLT sludge sample (Figure 4) reveals bonds relating to water (3400 to 3540 cm^{-1} and 1620 to 1685 cm^{-1} bands), to $Ca(OH)_2$ (3640 cm^{-1} bands), to calcite (875, 710, and 1460 cm^{-1} bands), and to silica (SiO_2) (470, 780, and 1080 cm^{-1} bands). The spectrum does not show cyanides that could form dangerous hydrocyanic acid during the leaching of these sludges in an acid medium.

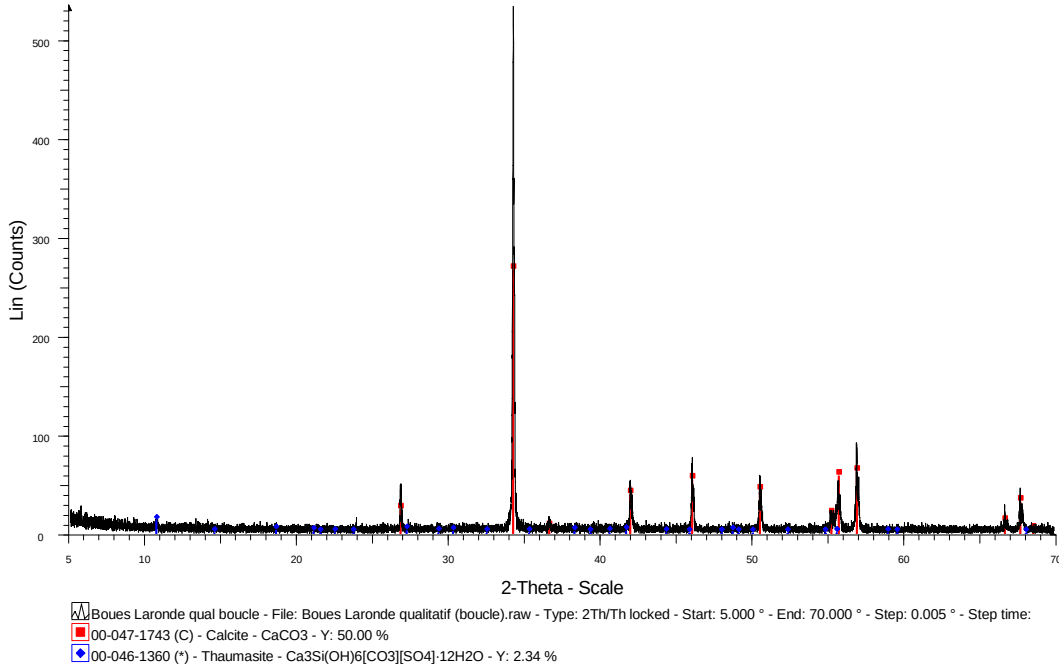


Figure 3. XRD qualitative analysis of BLT sludges.

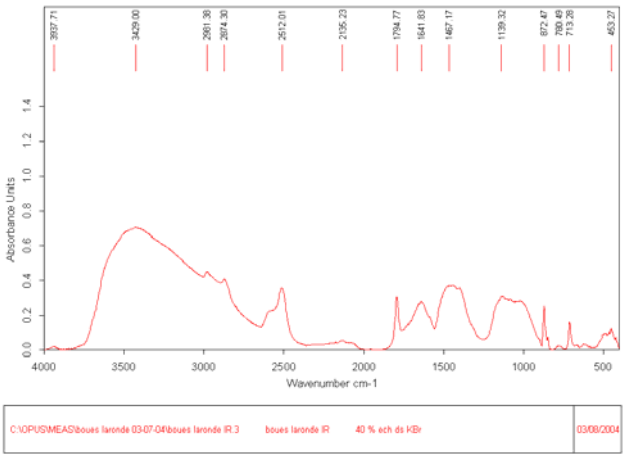


Figure 4. Fourier transform infrared analysis of BLT sludges.

3.2. Thermodynamic Considerations

The chemical and mineral characterization of LaRonde sludges revealed the association of a certain number of chemical elements in crystalline or amorphous phases. A thermodynamic study based on copper Eh-pH diagrams is imperative in order to better understand the behaviour of the copper contained in these sludges under leaching conditions and to gather more information about its stability, the degree of oxidation of the metallic element, and the ionic species it could form in the leachates. The HSC Outokumpu software (Roine, 1993) was used to produce various diagrams showed in Figure5. According to these diagrams, no matter which chemical elements are in the presence of the copper, the latter is soluble in aqueous solutions under acid and oxidant conditions. Therefore, to dissolve the copper contained in the BLT sludges, it must be put under acidic and oxidant conditions. The pH and Eh of the BLT sludges (5 g in 50 ml of deionized water) are 9.7 and 176 mV respectively.

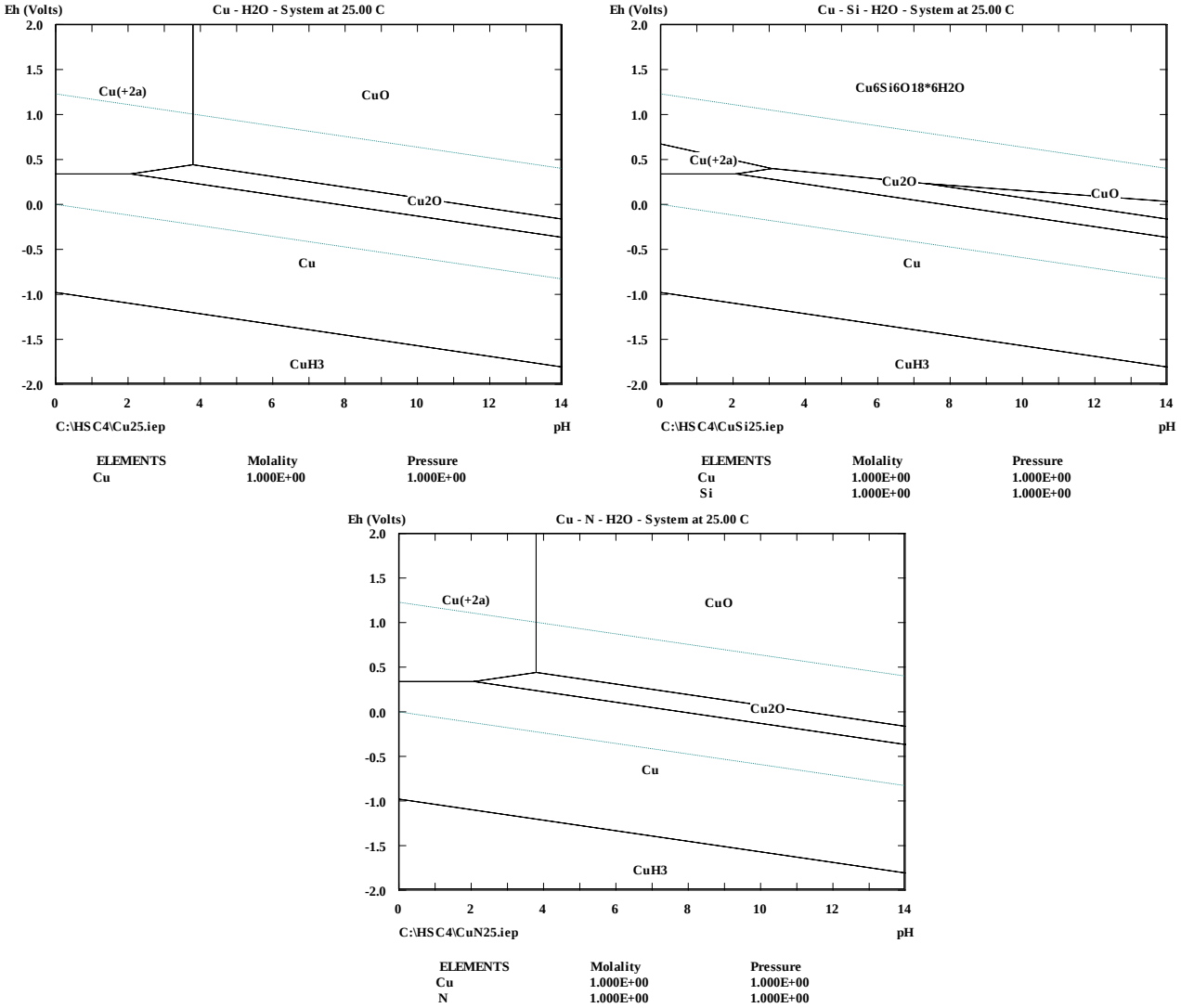


Figure 5. Eh-pH diagrams of Cu-H_2O, Cu-Si-H_2O, and Cu-N-H_2O systems at 25° C.

3.3. Leaching of the Copper Contained in the LaRonde Sludges

The leaching of the copper contained in the LaRonde sludges was carried out using acid and/or oxidant mediums. These media are ferric sulphate, known for its highly oxidant nature, and sulphuric acid, the most widely industrially used reagent due to its low-cost and the easy recovery of copper from sulphate solutions. This acid is used alone or mixed with ferric sulphate to achieve more oxidant conditions. The study focused on optimizing the main parameters of the copper extraction process, i.e. the composition of the leaching solution, the conditioning time, the solid/liquid ratio, the temperature, and the agitation.

Leaching in H_2SO_4-$Fe_2(SO4)_3$ Mixture

The tests conducted to study the effect of the composition of the leaching solution on copper dissolution were carried out under the following conditions: agitation: 250 revolutions per minute (rpm); ambient temperature: 22° C; solid/liquid ratio: 3 g/50 ml; conditioning time: 3 hours. The different extraction solutions used are described in Table 2.

Table 2. Composition of BLT sludge leaching solutions in H_2SO_4-$Fe_2(SO4)_3$ mixture.

Reagents	**Concentrations, M**															
H_2SO_4	0	0	0	0	0.5	0.5	0.5	0.5	1	1	1	1	2	2	2	2
$Fe_2(SO_4)_3$	0	0.05	0.1	0.15	0	0.05	0.1	0.15	0	0.05	0.1	0.15	0	0.05	0.1	0.15

The results presented in Figures 6 and 7 show that in the absence of sulphuric acid, the ferric sulphate has no effect upon the dissolution of copper and calcium (< 5%). The complete dissolution of copper is achieved when the concentration of sulphuric acid is increased to 0.5 M for an $Fe_2(SO_4)_3$ concentration of 0.5 M. The same results can be obtained in a sulphuric acid medium only, starting from a concentration of 1 M. This shows that the effect of adding of ferric sulphate is significant only for very low sulphuric acid concentrations.

The concentration of sulphuric acid could be reduced by adding ferric sulphate, but this addition would bring iron to the final solution, which would hamper copper recovery from this solution. The copper dissolution plateau (97%) is achieved after 20 minutes of conditioning (see Figure 7). The calcium dissolution rate does not exceed 4%. A study of the effect of the solid/liquid ratio did not make any improvement when using the sulphuric acid alone as leaching reagent.

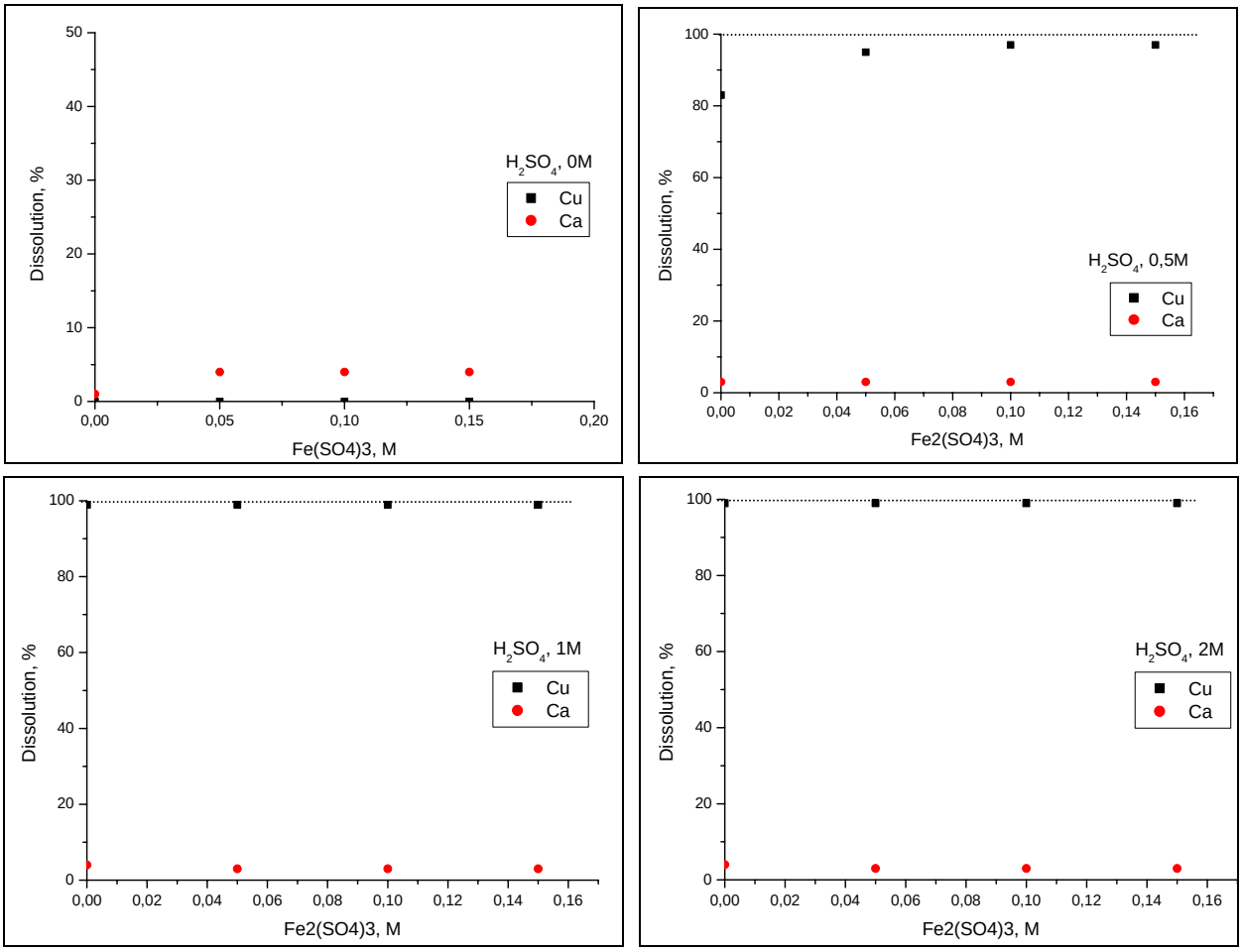


Figure 6. Effect of $Fe_2(SO_4)_3$ concentration in presence of H_2SO_4 on leaching of BLT sludges.

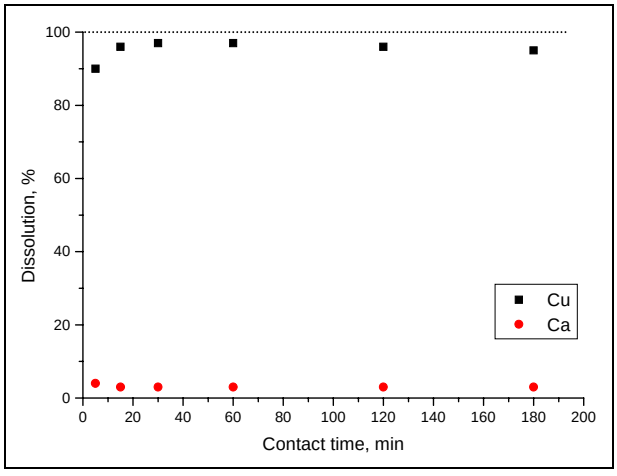


Figure 7. Leaching kinetic of BLT sludges in $Fe_2(SO_4)_3$ 0.05 M - H_2SO_4 0.5 M medium.

Leaching in H_2SO_4 Medium

A study of the effect of acid concentration on copper dissolution was conducted under the following test conditions: BLT sampling; agitation: 250 rpm; temperature: 22° C; solid/liquid ratio: 3 g/50 ml; conditioning time: 3 hours. The sulphuric acid concentration varied from 0 to 4 M. The effect of the conditioning time was also investigated. For these tests, the acid concentration was set to 2 M (concentration assumed as optimal) and the other test conditions were: agitation: 250 rpm; temperature: 22° C; solid/liquid ratio: 3 g/50 ml. The conditioning time ranged from 5 minutes to 3 hours. The last series of tests aimed at investigating the effect of the solid/liquid ratio on copper dissolution. The test conditions were: H_2SO_4 2 M; conditioning time: 2 hours; agitation: 250 rpm; temperature: 22° C. The solid/liquid ratio varied from 3 to 6 g/50 ml of solution.

During the tests it was noted that as soon as the solid and liquid came into contact, an effervescent reaction occurred. On contact with the acid, the slurry quickly turned from a greenish colour to a milky white. This is due to the dissolution of calcite which releases CO_2. The solid exchanges the carbonate (CO_3^{2-}) for the sulphate (SO_4^{2-}) to form gypsum. These observations indicate that the copper goes into solution practically instantaneously. Chemical analyses will confirm this statement.

Results presented in Figures 8, 9, and 10 show that the conditioning time needed to completely dissolve the copper is relatively short. This confirms the observations made in previous leaching tests. The solid residue in suspension quickly turns white, thus proving that the greenish component quickly disappears in contact with the sulphuric acid. A sulphuric acid concentration of 1 M is sufficient to selectively dissolve all the copper, whereas the dissolution rate of calcium does not exceed 6% in the worst case. The solid/liquid ratio can be optimized, since a solid/liquid ratio of 6 g/50 ml still allows a complete and selective dissolution of the copper. The use of a higher solid/liquid ratio is limited, because it must be taken into account the stoichiometry of the leaching reaction and the problem of CO_2 gas production.

As a follow of these results, studying the effect of temperature is no longer important, since it is possible to dissolve the copper completely at ambient temperature. Studying the effect of agitation is also no longer important if the solid and liquid mixing is progressive in order to avoid the formation of a surface crust. Also, the agitation must be sufficient to maintain all solid particles permanently in suspension.

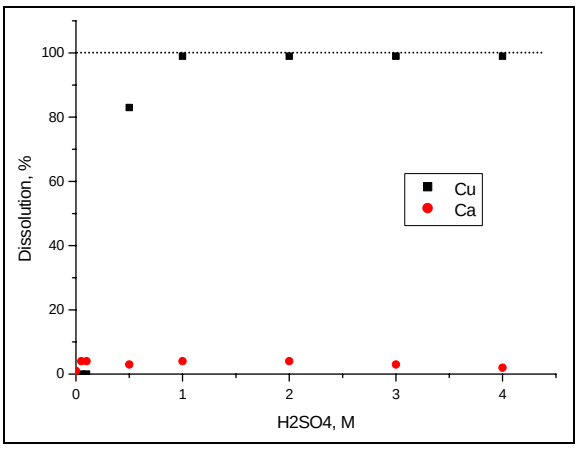


Figure 8. Effect of H_2SO_4 concentration on leaching of BLT sludges.

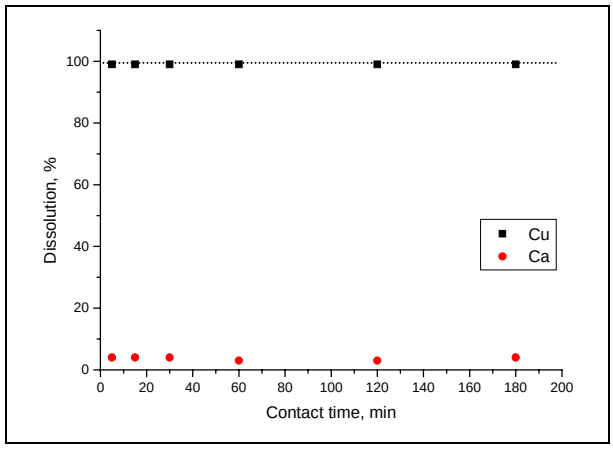


Figure 9. Effect of contact time on leaching of BLT sludges by H_2SO_4 2 M medium.

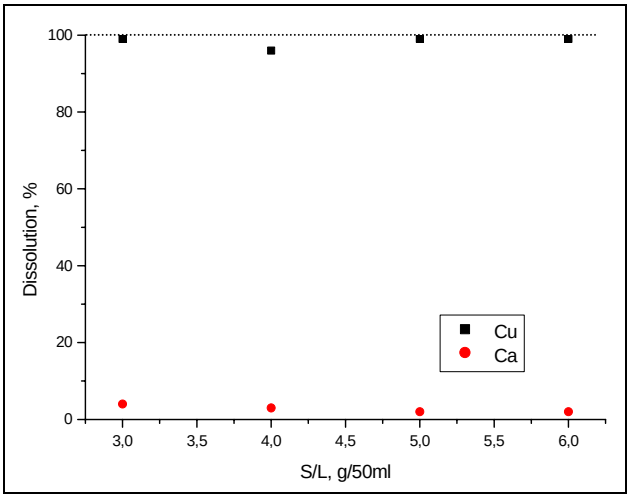


Figure 10. Effect of solid/liquid ratio on BLT sludges leaching by H_2SO_4 2 M.

Optimal Test Conditions

Good results were obtained when leaching BLT sludges in a sulphuric acid medium in optimal conditions of temperature (ambient), agitation (250 rpm), and H_2SO_4 concentration (1 M) with a conditioning time of 5 minutes and a solid/liquid ratio of 3 g/50 ml. The dissolution of copper reached 99% and that of calcium did not exceed 5%. The residual solid titrated 0.01% Cu, 0.231% Se, 26.5% Ca, 1.06% Na, and 18.3% S. The content of other elements was low to negligible (0.171% Zn, 0.042% Fe, 0.007% Mg, 0.001% Mn, and 0.001% Pb).

The enrichment in sulphur of the residual solid is due to the addition of sulphate from sulphuric acid, which precipitates with the calcium under the form of gypsum. The weight of this residual solid increased by 125% compared to the initial solid. This is due to the replacement of the CO_3 by SO_4 in the residual solid, along with the trapping of the constitutional water of the gypsum. The residual leaching solution titrates 994 mg/l Ca and 740 mg/l Cu. It is noticeable that, despite its very low

dissolution rate, calcium is still present in greater proportions than copper in the leaching solution because of its content in the initial solid. This concentration would be obtained if we were to recover the entire volume of the initial solution after filtration. In reality, however, the gypseous residual solid retains a certain amount of water, and the volume of solution recovered after the filtration of the solid is much lower than that of the initial solution. This would have an impact on the concentration of the chemical elements in the solution, meaning that the solution after filtration would be richer than the one adjusted to the initial volume and would not reflect the true dissolution rate of the elements. To obtain the true dissolution rate, the residue would need to be washed and the washing solution added to the final leaching solution. The pH of the final solution is 0.9 and its Eh potential is 738 mV.

The characterization by XRD (Figure 11) and FTIR (Figure 12) of the residual solid obtained by leaching under these conditions showed that the calcite dissolved and was replaced by gypsum. The likely persistence of a very small amount of calcite was observed in the XRD spectrum. The gypsum can be identified in the FTIR spectrums, first by the three modes of vibration of the S-O bond elongation of sulphates (SO_4^{2-}), which appear in the form of two doublets at 1145 cm^{-1} – 1120 cm^{-1} and 670 cm^{-1} – 600 cm^{-1}, and secondly by the characteristic bands of the constituent water, which appear as a large and dense doublet or triplet above 3000 cm^{-1} and which correspond to modes of vibration of the O-H bond elongation. The particle size analysis shows that the residual solid is finer than the initial sludge sample and reveals d_{50} and d_{80} of approximately 14 µm and 36 µm respectively.

From the results of chemical and mineralogical analyses, and the observations made during the leaching tests on the BLT sludges in an H_2SO_4 medium (i.e. the disappearance of the greenish colour and its replacement by a white colour, gas evolution, and selective dissolution of copper towards calcium) it can be plausibly suggest that the following chemical reaction is taking place during the leaching:

$$CaCO_3 + xCu + (1+x)\,H_2SO_4 + H_2O + x/2\,O_2 = CO_2 + CaSO_4.(2+x)H_2O + xCuSO_4 \qquad (5)$$

In this reaction, the mineral phase containing different contents and the amount of calcium that dissolves were not taken into account. The evolution of CO_2 is a factor to consider when sizing the leaching tanks.

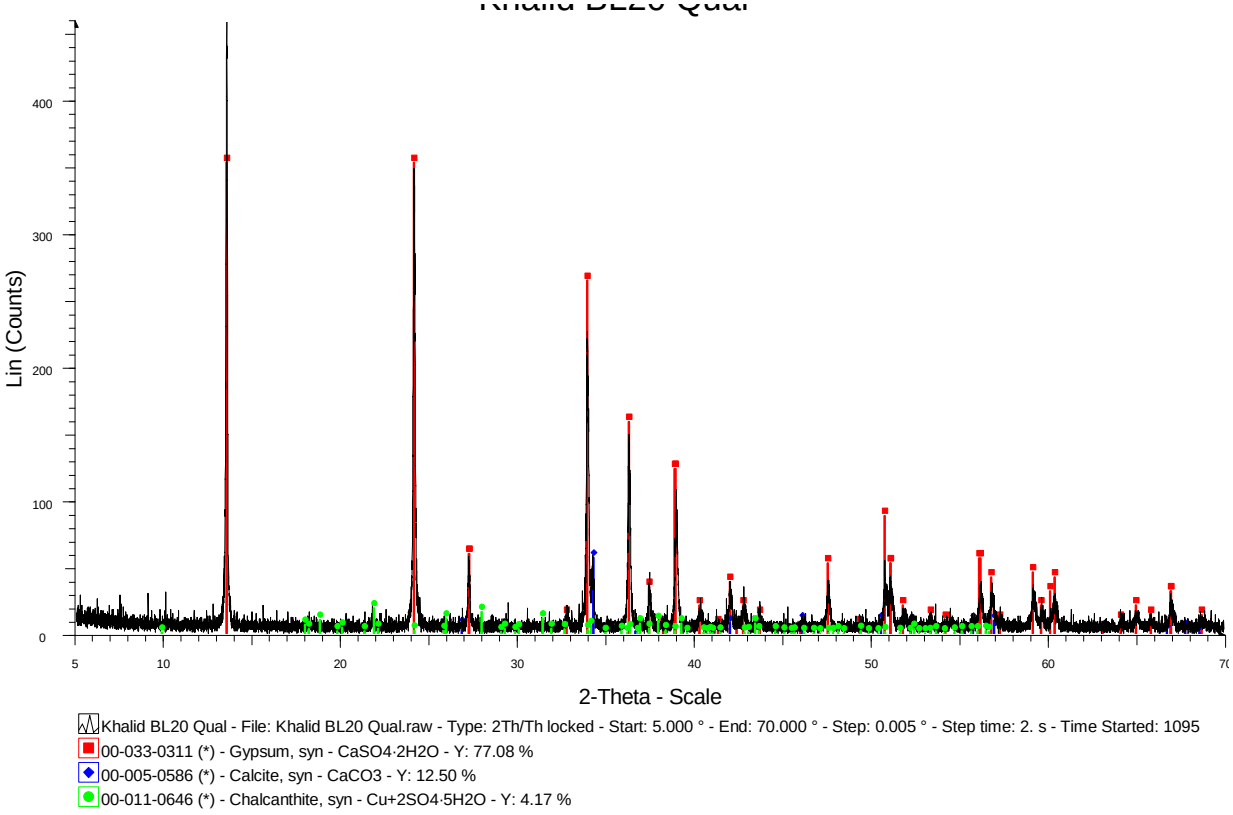


Figure 11. XRD spectrum of residue after leaching by H_2SO_4 1 M under optimal test conditions.

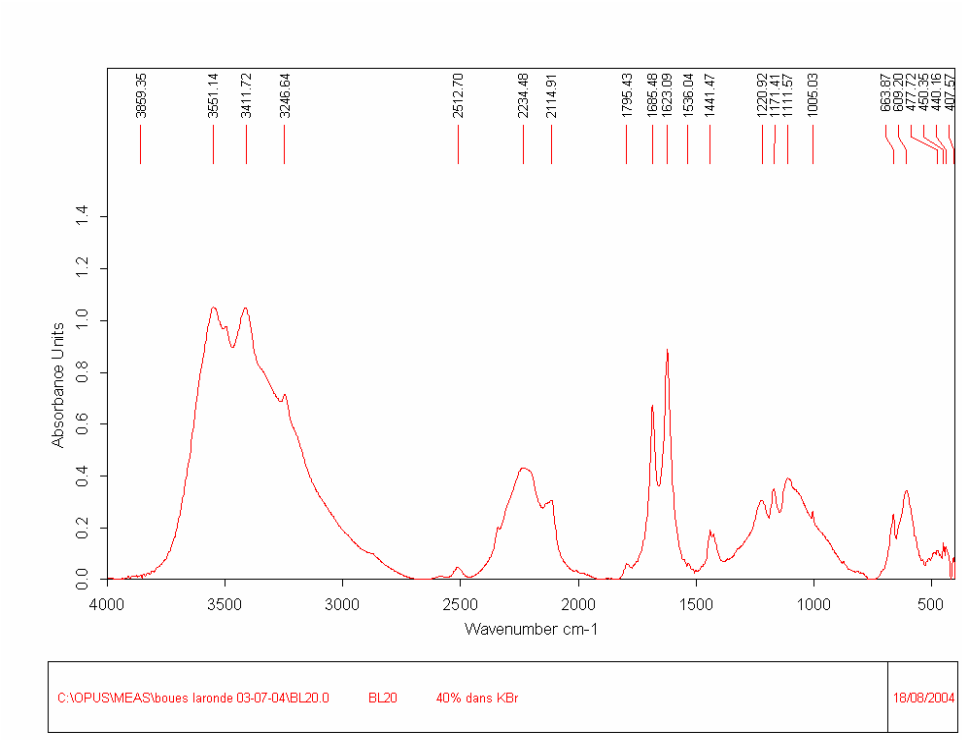


Figure 12. Fourier transform infrared spectrum of residue after leaching by H_2SO_4 1 M under optimal test conditions.

Leaching Using Sludges Richer in Copper

The extraction technique consisting in the dissolution of copper in BLT sludges using sulphuric acid having proven successful, additional tests were performed on a sludge sample (referenced BLT1) that was richer in copper and other chemical elements, and poorer in calcium than the BLT sample (see Table 3). The main objective was to confirm the good copper extraction rates obtained for poorer copper content. The BLT1 sample was taken in a greener zone in the pond than the BLT sample. The BLT1 sample was also richer in precious metals (90 ppm Ag and 0.43 ppm Au). Particle size analysis revealed that this sample had the same d_{50} (37 µm) as the BLT sample but a greater d_{80} (90 µm). Mineralogical analyses showed no difference between the two samples. The only variations might be found in the weight proportions of the sludge constituents. No phase containing copper was identified in the BLT1 sample using the SEM coupled with the EDS microanalysis.

Table 3. Chemical analyses of the LaRonde BLT1 sludge sample.

Element	Content	Element	Content	Element	Content
Ca (wt%)	20.0	Mg (wt%)	1.01	Ni (ppm)	190
Na (wt%)	1.64	Zn (wt%)	0.519	Ba (ppm)	20
Cu (wt%)	4.29	Se (wt%)	0.214	Pb (ppm)	20
S (wt%)	1.62	Mn (wt%)	0.196	Ag (ppm)	90
Fe (wt%)	1.15	Al (wt%)	0.183	Au (ppm)	0.43

Two series of tests were conducted to verify the effect of the solid concentration and the dissolution kinetic of the copper contained in the BLT1 sample. The test conditions were: 250 rpm, conditioning time of 5 minutes, H_2SO_4 1 M, 22° C for the study of the solid/liquid ratio, and 250 rpm, H_2SO_4 1 M, solid/liquid ratio of 3 g/50 ml, 22° C for the study of the kinetic. The results obtained are presented in Figures 13 and 14. One can conclude from this that the fast kinetic and the copper dissolution selectivity towards calcium are still present. A solid/liquid ratio of 6 g/50 ml also allows the dissolution of all the copper.

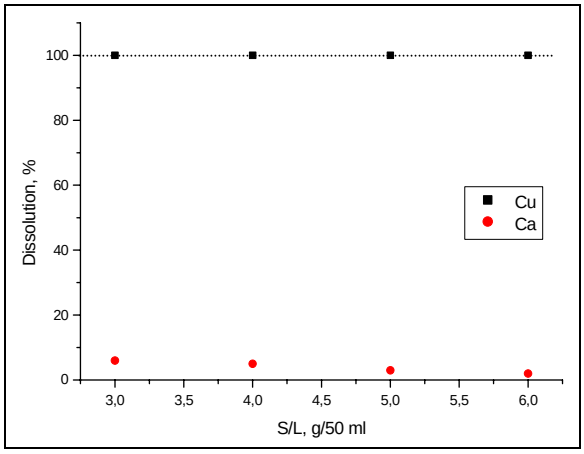


Figure 13. Effect of solid/liquid ratio on leaching of BLT1 sludges.

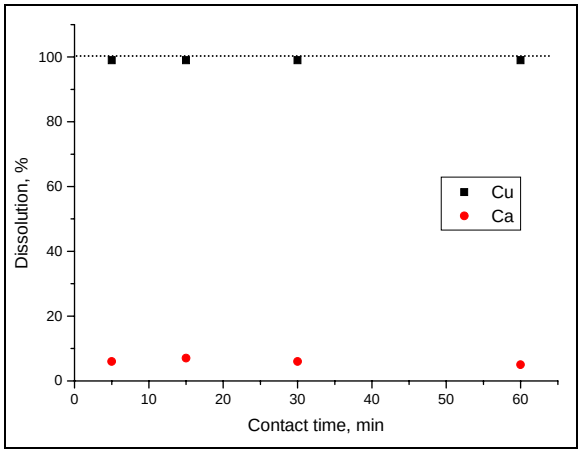


Figure 14. Leaching kinetic of BLT1 sludges in an H_2SO_4 1 M medium.

The analyses conducted on the residual solid of the BLT1 sample after leaching with sulphuric acid 1 M with a solid/liquid ratio of 3 g/50 ml revealed that its particle size is finer than that of the initial sample (d_{50} and d_{80} of around 17 µm and 30 µm respectively). This is not due to a decrease in particle size under the effect of the superficial leaching reaction, but to the formation of finer gypsum mineral particles. XRD and FTIR analyses revealed that the mineralogy of this residue is practically identical to that of the residue of the BLT sludge sample after leaching under the same conditions.

4. Conclusions and perspectives

It is possible to achieve copper dissolution with a good selectivity towards calcium by leaching sludges of the Agnico-Eagle LaRonde mine in a sulphuric acid medium. The complete dissolution kinetic is fast with high carbon dioxide production. The residual solid is essentially composed of gypsum with very low heavy metal content.

The leaching solutions containing the copper could be processed to extract this element, either by liquid-liquid extraction followed by electrolysis, or by direct electrolysis if the accompanying chemical elements are not problematic.

To follow up the present study, we plan to:

- Perform additional tests to verify the reproducibility of tests;
- Use homogenous sampling of sludges to determine the optimal fixed leaching test conditions;
- Test the possibility of using the mine's acid waters with pH adjustment to dissolve the copper;
- Test the possibility of using the leaching solution without solvent extraction if it is clean, or after extraction to activate the sphalerite in the flotation process;
- Test the possibility of using the gypsum as binding additive in the paste backfill.

5. References

Carrillo-Pedroza F.R. and Soria-Aguilar M.J (2001*). Destruction of cyanide by ozone in two gas-liquid contacting systems*. The European Journal of Mineral Processing and Environmental Protection, (2001), 1, 55-61.

Kitis M., Akcil A., Karakaya E., Yigit N.O (2005). *Destruction of cyanide by hydrogen peroxide in tailings slurries from low bearing sulphidic gold ores*. Minerals Engineering, 18 (2005) 353–362.

Knorre H., Griffiths A., Degussa AG, Werk Wolfgang. *Cyanide Detoxification with hydrogen peroxide using the Degusa Process*. Department IC-ATA, Postfach 13 45, D-6450 Hanau 1,West Germany (http://www.unr.edu/mines/mlc/conf_workshops/Cyanide/Chapter519.pdf).

Roine A. (1993). *Outokumpu HSC Chemistry for windows : Software version1.10*. Outokumpu Research, Pori, Finlande.

Villeneuve M. (2004). *Évaluation du comportement géochimique à long terme de rejets miniers à faible potentiel de génération d'acide à l'aide d'essais cinétiques.* Master Thesis of the « École Polytechnique de Montréal », Novembre 2004, 321p.

HYDRODYNAMIC STUDY OF THE LONG TERM EVOLUTION OF A SALT CAVITY AFTER COLLAPSING

FEBVAY J.B.[1], HAMM V.[2], OLTEAN C.[1], GOLFIER F.[1], FABRIOL R.[2], BUES M.[1]

[1] La EGO/ENSG, Rue du Doyen Marcel Roubault Parc – BP 40 – F 54501 Vandoeuvre-lès-Nancy, France

[2] BRGM, 1 avenue du Parc de Brabois – F 54501 Vandoeuvre-lès-Nancy, France

ABSTRACT: *The phenomenon of dissolution is commonly used to extract salt because it is easier and less expensive than traditional mining. Some exploitations continue until the collapse of cavities dug by dissolution in the salt layer. A hydraulic continuity can then be established between the salt layer and the surrounding aquifers by means of the collapsed zone. A conceptual model based on field observations is proposed to support the present work. Numerical simulations using this conceptual model are presented in order to observe the evolution of the system and to measure the influence of various parameters (permeability, velocity and inclination).*

KEYWORDS: salt, flow, transport, numerical simulation.

RESUME : Le phénomène de dissolution est très utilisée pour extraire le sel car c'est une technique plus facile est moins onéreuse que le creusement minier traditionnel. Certaines exploitations procèdent jusqu'à effondrement des cavités creusées par dissolution dans la couche de sel. Une continuité hydraulique peut alors s'établir entre la couche de sel et les aquifères environnantes par le biais de la zone effondrée. Un modèle conceptuel basé sur des observations réelles est proposé comme support de ces travaux. Des simulations numériques utilisant ce modèle conceptuel sont présentées afin d'observer l'évolution du système et de mesurer l'influence de paramètres(perméabilité, vitesse, inclinaison).

MOTS-CLEFS : sel, écoulement, transport, simulation numérique.

1. Introduction

The intense exploitation of salt in France, as in certain other European countries, raises the problem of the management and abandonment of these exploitations. The long term evolution of a site, from the ground stability point of view and also from the impact on groundwater point of view, needs to be investigated. Indeed, the annual production of extracted salt in France is about 6.3 Mt (1993-1998, source Comité des Salines de France), 90 % of which comes from salt dissolution. This is equivalent to about 3 million m^3 of cavities every year. When the exploitation of a site comes to an end, these cavities are generally abandoned. We therefore recognise the need to study their long-term evolution.

This document comes under this context and, in particular, treats the case of dissolution cavities after collapsing. The collapse of the cavity can then cause the rupture of the impermeable screen that protected the salt from the nearby aquifers. Hydraulic continuity between the saliferous formation and these aquifers are then established. Can this new system (collapsed cavity connected to the aquifer) lead in certain configurations to an unstable state with resumption of salt dissolution? Furthermore what would the consequences be on the water quality of the surrounding aquifers and on the ground stability?

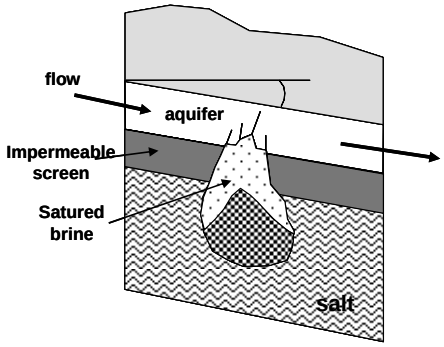


Figure 1. General representation of a salt cavity after collapsing

In order to provide answers to these questions, in a first step we will approach the salt transport in the aquifer from a hydrodynamic point of view without the dissolution phenomenon.

2. Modelling of salt cavities

2.1. Conceptual model

Collapse of a cavity will lead to structural modifications that will depend not just on the cavity dimensions but also on the stratigraphic cross-section (rock properties, thickness of various layers). Based on actual observations, two collapsing configurations are considered: one going up to the surface (Fig. 2a) and the other confined to the sub-surface (Fig. 2b). In order to neglect the porous media - fluid media coupling (Darcy-Stokes), which are related to the presence of a non-porous cavity, we focused on the configuration (a). After a numerical study based on this configuration, we will design a laboratory model.

For instance, our interest is limited to the transport phenomenon of the brine from the collapsed cavity towards the aquifer. The area of study corresponds to the configuration (a) and is delimited by the roof of the aquifer and by the roof of the salt layer. We will assume that the porous medium corresponding to the central collapsed zone has a uniform permeability higher than that of the aquifer.

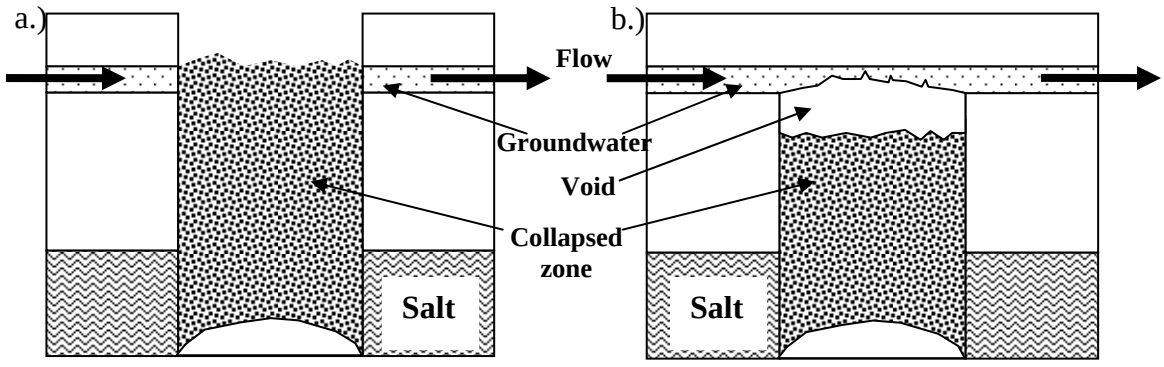


Figure 2. Scheme of a collapse (a) at the surface of the ground (b) at the groundwater level

2.2. Mathematical model

The transport of a solute by flowing groundwater can be described by the following system of equations, representing the fluid and solute mass balances, Darcy's and Fick's Laws and the equations of state for the liquid (density and dynamic viscosity):

$$\frac{\partial(\rho\varepsilon)}{\partial t} + \nabla.(\rho\varepsilon U) = \rho Q_p \tag{1}$$

$$\frac{\partial(\rho\varepsilon C_m)}{\partial t} + \nabla.(\rho\varepsilon U C_m + J) = \rho Q_p C_{m0} \tag{2}$$

$$V = -\frac{k}{\mu}(\nabla P + \rho g \nabla z)) \tag{3}$$

$$J = -\rho\varepsilon D\nabla(C_m) \tag{4}$$

$$\rho = \rho(C_m)\ \mu = \mu(C_m) \tag{5}$$

where:

∇ = gradient,

$\nabla.$ = divergence,

t = time [T],

ρ = density [ML^{-3}],

U = effective velocity [LT^{-1}],

ε = porosity [-],

Q_p = source/sink term [T^{-1}],

C_m = solute mass fraction [M/M],

k = permeability tensor [L^2],

C_{m0} = solute mass fraction in the source/sink term [M/M],

V = Darcian velocity [LT^{-1}],

J = dispersive solute flux [$ML^{-2}T^{-1}$],

P = pressure [$ML^{-1}T^{-2}$],

μ = dynamic viscosity [$ML^{-1}T^{-1}$],

z = elevation [L],

D = dispersion tensor [L^2T^{-1}],

g = gravity acceleration[LT^{-2}].

The terms of the dispersion tensor are generally defined by

$$D_{ij} = (D_m + \alpha_T|U|)\delta_{ij} + \frac{(\alpha_L - \alpha_T)U_i U_j}{|U|} \tag{6}$$

with

D_m = molecular diffusion coefficient [L^2T^{-1}],

α_L = longitudinal dispersivity of the solid matrix [L],

α_T = transversal dispersivity of the solid matrix [L],

U_i, U_j = components of effective velocity [LT^{-1}],

δ_{ij} = Kronecker's symbol [-].

According to Voss (1984) and Herbert et al. (1988), the density and dynamic viscosity are considered to vary in accordance with the solute mass fraction only:

$$\rho(C_m) = \rho_0 + \frac{\partial(\rho)}{\partial(C_m)}(C_m - C_0) = \rho_0 + \gamma(C_m - C_0) \quad (7)$$

$$\mu(C_m) = \mu_0\left(1.0 + \tau_1 C_m + \tau_2 C_m^2 + \tau_3 C_m^3\right) \quad (8)$$

where ρ_0, μ_0 and C_0 are respectively the reference density, dynamic viscosity and mass fraction concentration. γ and τ_i (i = 1,…,3) are experimental constants computed by using the data given by Weast (1977).

3. Numerical experiments

Numerical simulations based on the conceptual model were carried out with a computer code - FRIPE (LaEGO) - in order to evaluate the output of brine from the system.

3.1. Modelling support

For the remainder of the study, we will use the reduced concentration, which is defined by:

$$c = \frac{C_m}{C_{m0}}$$

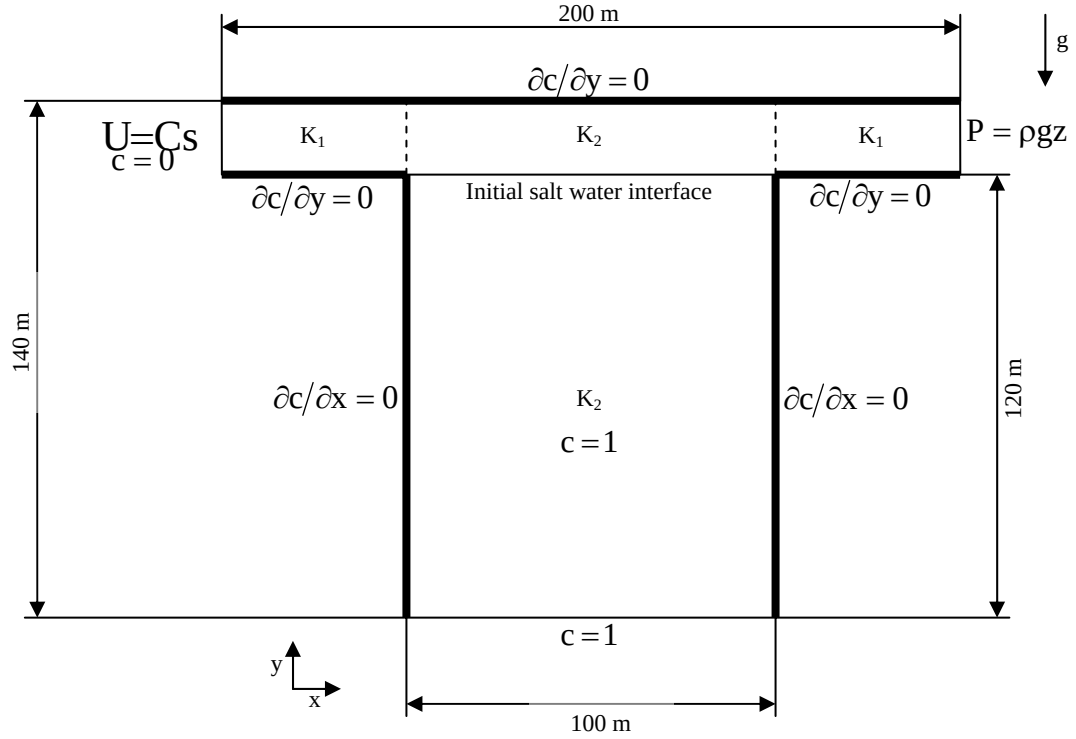


Figure 3. Modelling support

The bottom boundary is held at a constant concentration scaled to a value of 1 unit, representing an infinite source of solute. The dispersion was taken into account by setting the diffusion coefficient to a constant value and the intrinsic dispersivity to zero ($\alpha_T = \alpha_L = 0$). This simplification overlooks the variation in the dispersion coefficient as a function of the velocity.

In the initial state, the central zone is filled with brine. Indeed, when the cavity breaks down, the brine still present inside goes up through the collapsed layers. We discretise the domain using a structured, uniform grid with bilinear square elements.

Table 1. Input parameters for the numerical problem

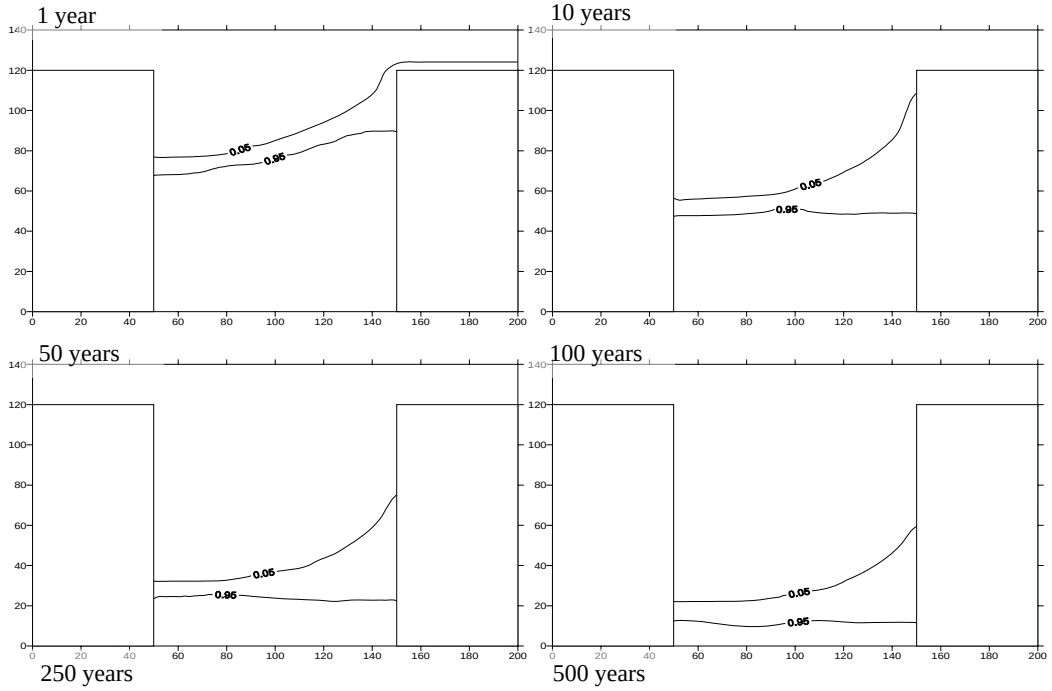
Quantity	Symbol	Value	Unit
Grid spacing	Δx	5	m
Grid spacing	Δy	5	m
Simulation length	T	500	years
Aquifer permeability	k_1	Variable	m^2
Collapsed zone permeability	k_2	Variable	m^2
Porosity	ε	0.3	
Storativity	S	0	Pa^{-1}
Diffusivity	D	1.5×10^{-8}	m^2s^{-1}
Dispersivity	α_T, α_L	0	m
Density change with concentration	γ	198.87	$kg.s^{-3}$
Acceleration due to gravity	g	9.81	$m.s^{-2}$

3.2. System evolution:

The time-space distributions of the concentration obtained for the parameters listed below are presented in figure 4.

Table 2. Input parameters

Quantity	Symbol	Value	Unit
Aquifer permeability	k_1	1×10^{-12}	m^2
Collapsed zone permeability	k_2	9.38×10^{-12}	m^2
Upstream velocity (Darcian velocity)	V	2	m per day



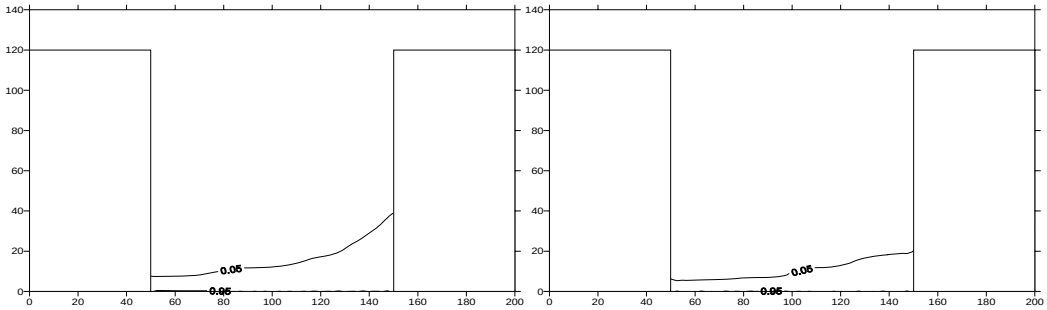


Figure 4. Isoconcentration lines (0.05; 0.95)

As may be seen, the salt water will be drawn out quickly during the first few years. The more the quantity of salt decreases in the collapsed zone, the slower its output. After a certain time, a stationary regime appears. From this moment, the quantity of salt in the system is almost constant. We may assume that, when the stationary regime is reached, a resumption of dissolution is possible because of the presence of unsaturated salt water at the bottom of the domain, i.e. at the level of the salt layer.

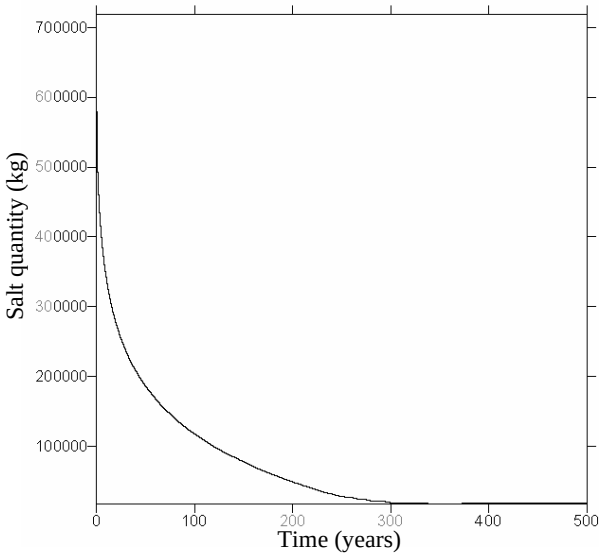


Figure 5. Salt quantity present in the domain versus time

In the case presented above, the stationary regime is reached after 300 years.

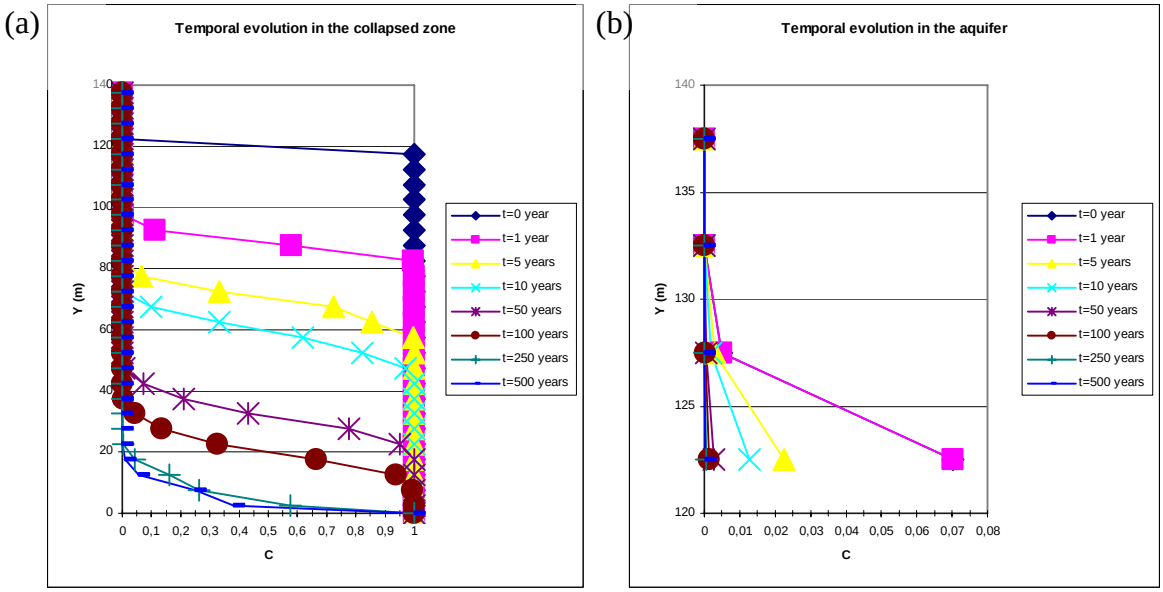


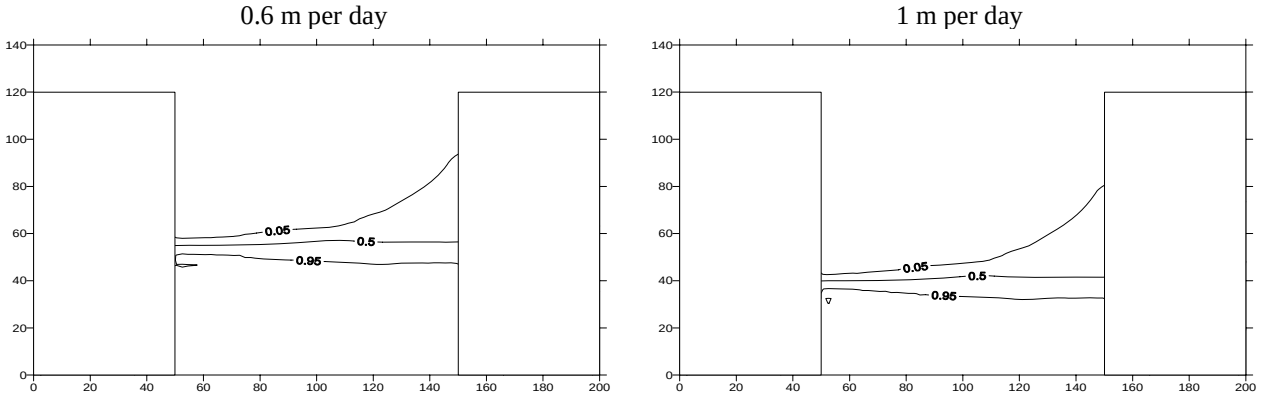
Figure 6. Concentration versus y ordinate at different times in transverse sections: (a) in the collapsed zone, x=120 m; (b) in the aquifer, x=160m

The height (y) of the mixed zone decreases with time, while the mixed zone thickness increases (figure 6a). In figure 6b, we present the profile of concentration on a section of the aquifer downstream from the collapsed zone. These concentrations are weak, but they correspond to a considerable drawing out of salt. For example, a reduced concentration of 0.01 in a 5m large mesh corresponds to a density change equal to 1.9887 Kg/m^3. If we assume the fluid moves at the imposed speed (2m per day), this corresponds to a salt output of 1.9887*5*2 = 19.887 kg per day. In conclusion, even if the fluid has a low salt concentration, it is transported continuously in significant volumes.

3.3. Velocity influence

The aquifer velocity varies considerably and can reach values close to 10 m per day. With a porosity of 0.3, the maximum corresponding Darcian velocity is 3 m per day. Input parameters are shown in table 3. The parameters used are the same as those in table 2 except for the speed, which varies.

Simulations with the Darcian velocity ranging from 0.6 to 3 m per day are presented below.



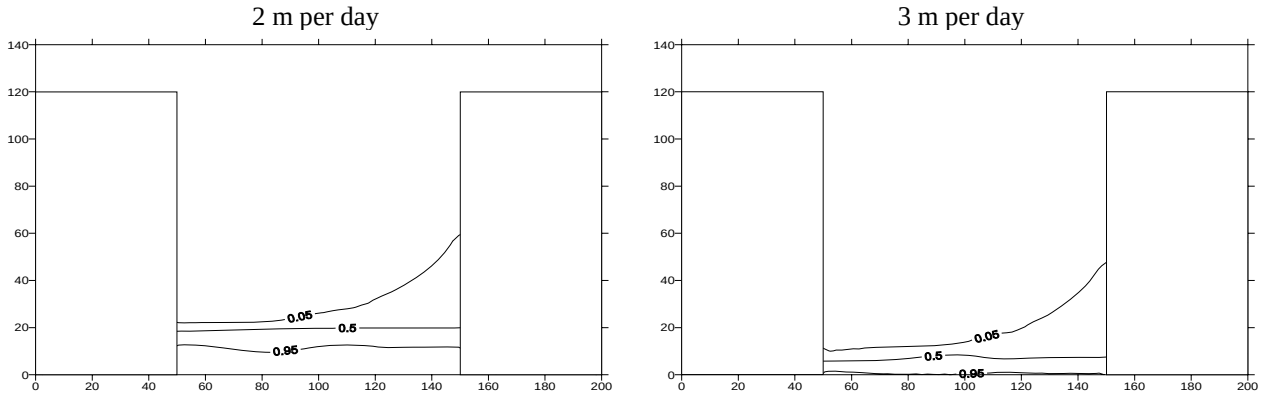


Figure 7. Isoconcentration lines (0.05; 0.5 ; 0.95) at 100 years

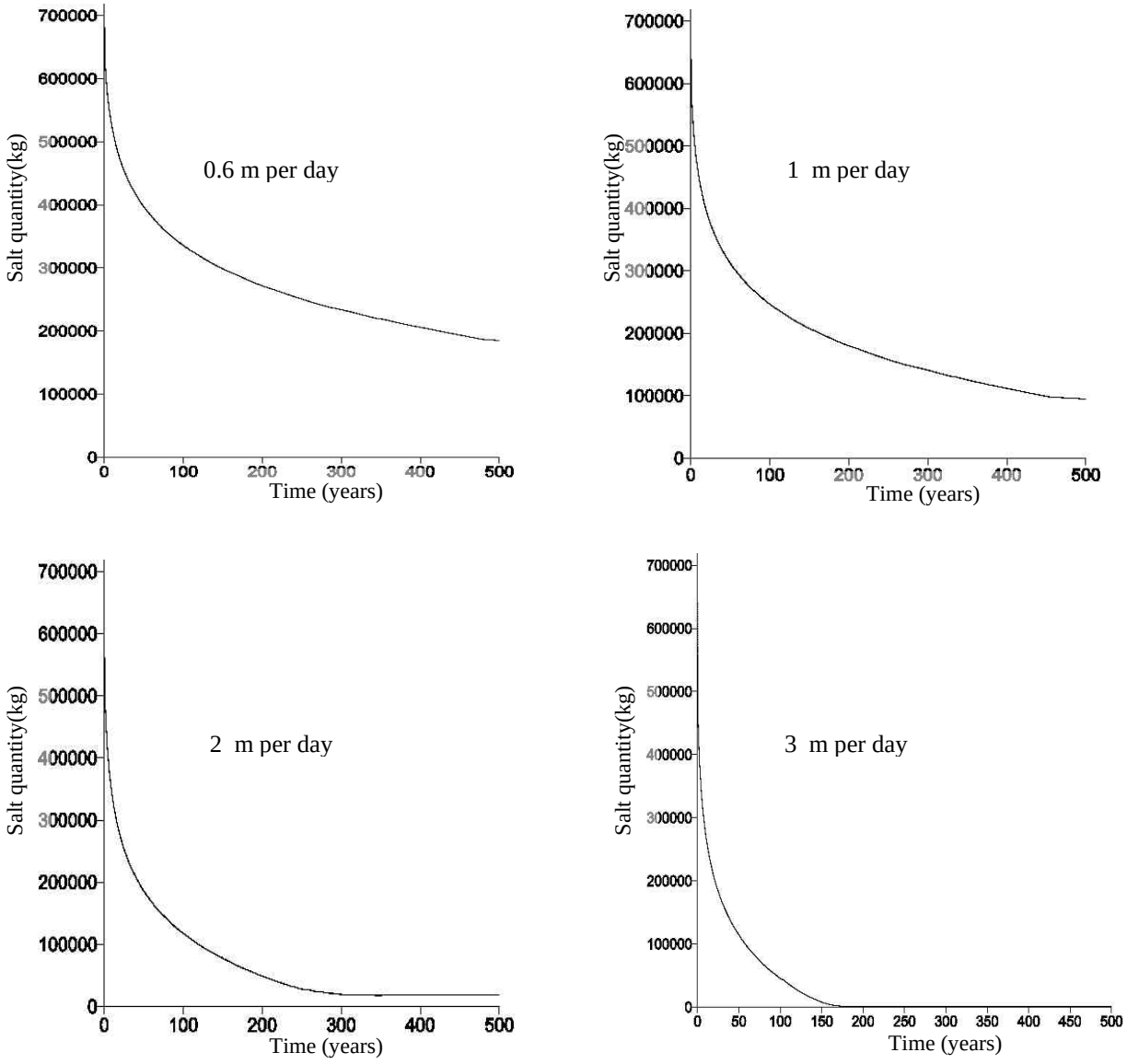


Figure 8. Salt quantity present in the domain versus time

We observe that the higher the imposed velocity, the faster the output of salt water. In certain cases, the stationary regime is not reached, even after 500 years.

3.4. Influence of permeability

Table 4. Input parameters

Quantity	Symbol	Value	Unit
Aquifer permeability	k_1	1×10^{-12}	m^2
Upstream velocity (Darcian velocity)	V	1	m per day

The results obtained with the collapsed zone permeability ranging from 1×10^{-12} to 1×10^{-10} m^2 are shown on figure 9.

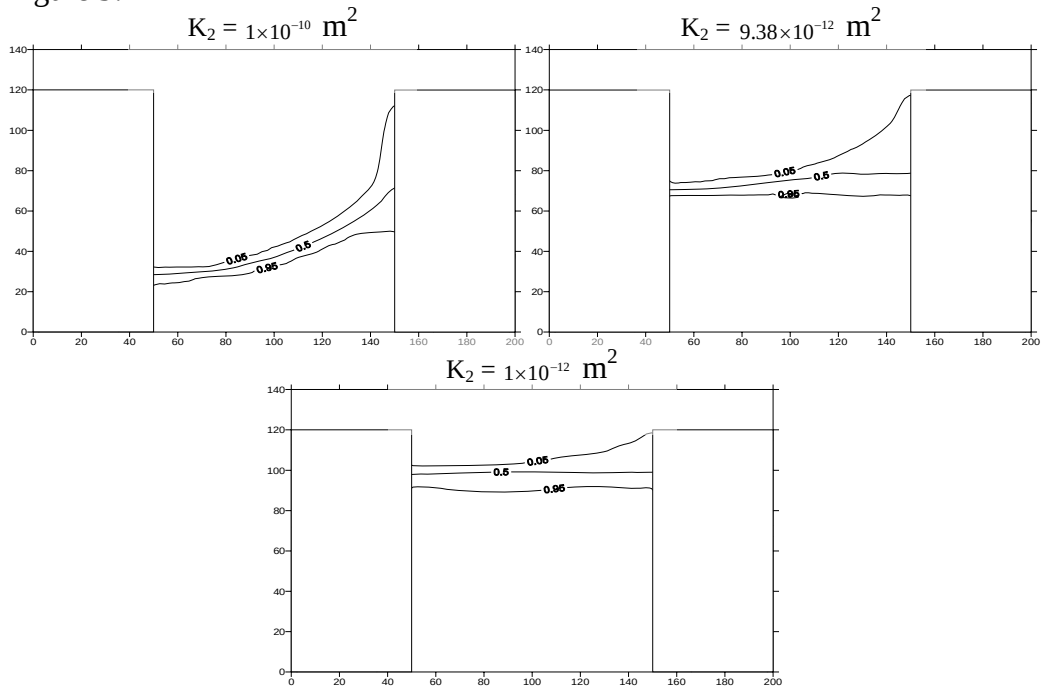


Figure 9. Isoconcentration lines (0.05 ; 0.5 ; 0.95) at 10 years

We observed that brine output is slower with a higher permeability. This can be explained by comparing the characteristic gravitational velocities:

$$V_g = \frac{\Delta\rho k g}{\mu}$$

Indeed, the gravitational velocity gets higher when the permeability increases. This will have the effect of retaining the salt water in the central zone.

3.5. Inclination effects

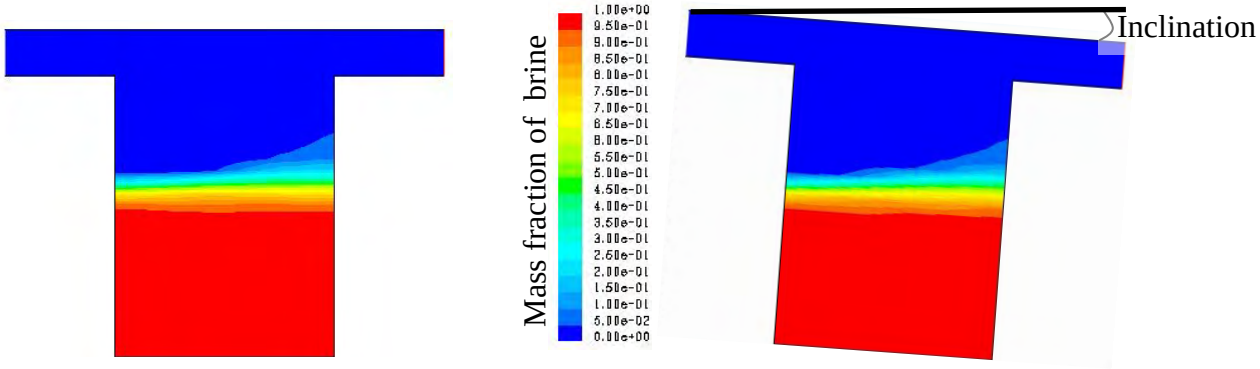


Figure 10. Mass fraction distribution

We tested the effect of an inclination going up to 10%. The results showed that the inclination has almost no effect on the quantity of exported brine. We only observed an inclination of the interface between fresh water and salt water similar to the inclination of the ground.

4. Weaknesses of the model

4.1. Influence of permeability contrast

In our conceptual model, we made the assumption that the permeability of the collapsed zone is higher than that of the aquifer. Under this consideration, it is interesting to study the effect of this permeability contrast on a 2D horizontal flow.

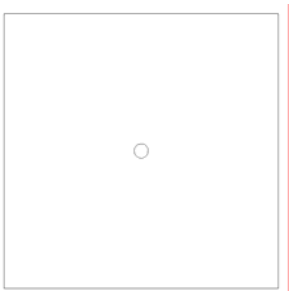


Figure 11. Modelling support

Thus, our domain is a 2 km wide square and represents the aquifer. A 100 m diameter hole is placed at the centre of the domain. The hole has a permeability higher than the aquifer. A velocity is imposed on the left side and constant pressure is imposed on the right.

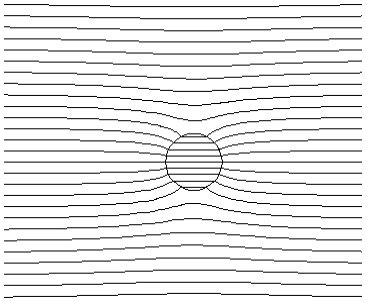


Figure 12. Example of streamlines(b)

The results in figure 12 show the velocity in the hole is higher than in the aquifer. We can observe that the relationship between the mean velocity in the hole and the imposed velocity depends only on the permeability ratio. An example of the curve obtained is presented in figure 13.

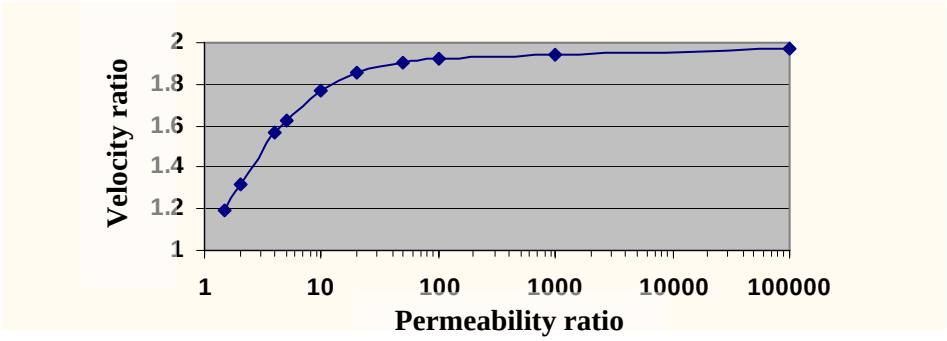


Figure13. Permeability ratio influence on the velocity ratio

It should be noted that these results depend on the domain dimensions. The velocity ratio is close to 2 for a permeability ratio greater than 50. It is necessary to take into account the higher velocity in the collapsed zone than in the aquifer.

4.2. Permeability contrast influence in our model

Contrary to the 2D horizontal model of the preceding paragraph, in our 2D vertical model there is no increased velocity in the collapsed zone related to the permeability contrast because there is no contribution of fluid in the third dimension. Indeed, we can check numerically that, in our model, the permeability imposed for the aquifer does not have any influence on the quantity of salt exported out of the system (figure 14). Consequently, we should considerer in our model that the imposed upstream velocity corresponds to the velocity in the collapsed zone and not to the aquifer velocity.

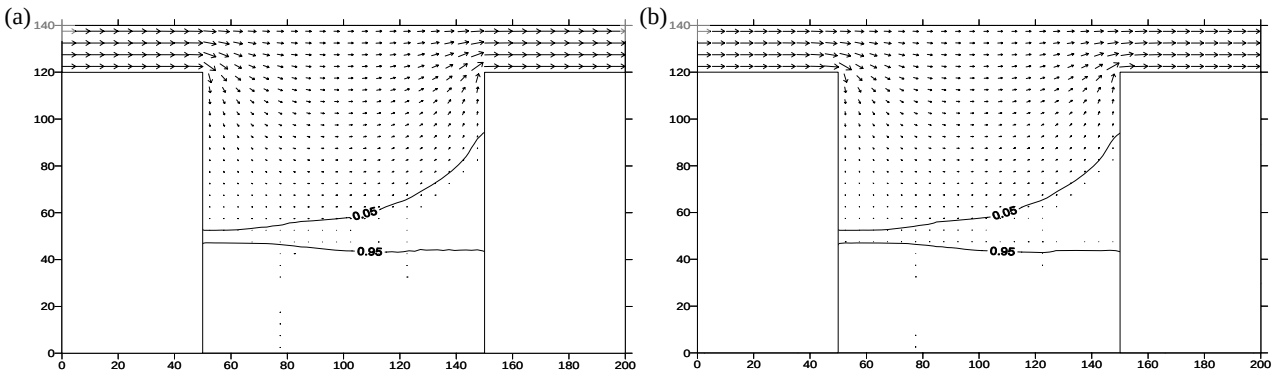


Figure 14. Fluid velocity and isoconcentration lines (0.05; 0.95): (a) aquifer permeability: 1 e-12 m^2; central part permeability 1 e-11 m^2 (b) uniform permeability 1 e-11 m^2

5. Conclusions

The results of the simulations showed that a resumption of salt dissolution should not be disregarded. Indeed, in certain configurations the output is high enough for fresh water to arrive at the salt layer after a certain time. This time depends on the hydrodynamic parameters (permeability,

velocity). The configuration is more favourable to a resumption of the dissolution when the aquifer velocity is high and the collapsed zone permeability is low. On the other hand, we were able to observe that a weak ground slope had no effect on the system evolution. Since this study was based on a configuration of fixed dimensions, we did not test their influence.
An experimental approach will enable us to supplement this study and to validate the numerical models. We will use a Hele-Shaw cell, which represents an analogue model of a two-dimensional porous medium. Constituted of two glass plates, this experimental tool allows the use of non-intrusive optical measurement techniques. The analogy is based on the possibility of expressing the average velocity through the thickness b, separating both plates, by Darcy's law. In this context, the equivalent permeability of this system is proportional to b^2. This analogy is only valid under certain conditions that we will have to respect for the dimensioning of our laboratory model. Concerning the transport in the Hele-Shaw cell, Oltean et al.(2004) defined an analogy with transport in porous media. Their study gave rise to a definition of the hydrodynamic dispersion tensor for transport in the Hele-Shaw cell. This laboratory model will be used to obtain field velocity and concentration distribution measurements over the entire domain.
At the same time, a second “experiment” on salt dissolution will be set up in order to develop a numerical model. Thereafter we will be able to numerically simulate the system by taking into account the dissolution.

6. References

M.A. BUES and C. OLTEAN, 2000, Numerical simulations for saltwater intrusion by the mixed hybrid finite element method and discontinuous finite element method, *Transport in Porous Media*, **40**, 171 – 200.

X. DAUPLEY, M. AL HEIB, A. DIOP, 2004, Typologie des mécanismes et des phénomènes de mouvement de terrain liés aux exploitations de sel, Rapport GISOS, DRS-04-56179/R01

C. FELDER ET AL., 2004, Dispersion de Taylor généralisée à un fluide à propriétés physiques variables, *C.R. Mecanique*, **332**, 223 – 229.

H.R. HERBET, C.P. JACKSON and D.A. LEVER, 1988, Coupled groundwater flow and solute transport with fluid density strongly dependent upon concentration, Water Resour. Res., **24**, 1781 – 1795.

H.-J.G. DIERSCH, O. KOLDITZ, 2002, Variable-density flow and transport in porous media : approaches and challenges, Advances in Water Resources, **25**, 899 – 944.

C. OLTEAN and M.A. BUES, 2001, Coupled groundwater flow and transport in porous media. A conservative or non-conservative form?, *Transport in Porous Media*, **44**, 219 – 246.

C. OLTEAN AT AL., 2004, Transport with very low density contrast in Hele-Shaw cell and porous medium : Evolution of the mixing zone, *Transport in Porous Media*, **55**, 339 – 360.

R.C. WEAST, 1977*, CRC Handbook of Chemistry and Physics*, 58th edn., Chemical Rubber Company Press, Boca Raton, Fle.,D-252.

COLLAPSE/SUBSIDENCE: ROLE AND INFLUENCE OF OVERBURDEN IN LORRAINE IRON MINES CASE

FOUGERON Jérôme[1], SOULEY Mountaka[2], HOMAND Françoise[1]

[1] LAEGO, Rue du Doyen Marcel Roubault – BP 40 – 54501 Vandoeuvre-lès-Nancy Cedex - France; jerome.fougeron@ensg.inpl-nancy.fr; francoise.homand@ensg.inpl-nancy.fr

[2] INERIS, Ecole des Mines - 54042 Nancy Cedex - France.; mountaka.souley@ineris.fr

ABSTRACT: This paper presents several large-scale numerical modellings of valley and tray situations with the presence or not of vertical fractures. Through these modellings, we firstly attempt to evaluate an influence zone, in terms of stress variations induced by the creation of the valley. Next we study more particularly the behaviour of a stiff overburden, according to situations, with the aim to estimate if a valley and/or the presence of subvertical fractures influence the overburden massivity.

KEYWORDS: Overburden, stiffness, stress, displacement, energy

RESUME: Ce papier présente plusieurs modélisations à grande échelle d'une situation de vallée et de plateau en présence ou non d'une fracturation verticale. A travers ces modélisations, nous tentons d'évaluer une zone d'influence, en termes de variations de contraintes induites par la création de la vallée. Puis nous étudions plus particulièrement le comportement d'une couverture raide, en fonction des situations, dans l'objectif d'estimer si une vallée et/ou une fracturation subverticale influencent la massivité du recouvrement.

MOTS-CLEFS: Couverture, raideur, contrainte, déplacement, énergie

1. Introduction

In the past, Lorraine was an important mining region leaving many empty spaces in the underground, responsible for many accidental movements. Currently 16 historical cases were recorded in the Lorraine iron ore basin, in particular 8 violent collapses and 8 progressive subsidences. It is important to distinguish violent collapses of progressive subsidences, implications in terms of person security being very different. Consequently, it is necessary to unequivocally define the meaning of these qualifiers as presented to the experts:

A collapse is qualified as violent when the four following criteria below are filled:

1. The collapse follows a seismic event of sufficient magnitude to be recorded at the Institut de Physique de Globe de Strasbourg or, for older collapses, to be felt by the population on the surface ;
2. The event results in an air blast within the mine workings ;
3. After the collapse, the surface profile is very steep and stepwise at the collapse edge ;
4. The collapse is complete in a very short amount of time (less than an hour).

A subsidence is qualified progressive if:

1. The surface profile is gradual at the subsidence edge ;
2. No seismic event precedes the subsidence ;
3. The subsidence occurs over the course of several hours instead of several minutes.

For many years, we attach an importance to the knowledge of these events and mechanisms, which are the cause of instabilities, in order to be able to prioritize them in terms of risk and in this particular case to try preventing them.

Tincelin and Sinou (1962) have proposed like collapse mechanisms:

1. A violent failure of overburden by splitting of a monolithic slab solicited in flexion
2. An overburden failure by shear of bedrock (presence of a thick and competent layer). They suppose that it is the failure of this bedrock, with a high stiffness and a high mechanical strength, which would immediately cause the failure of block rocks.

These explanations are probably too idealized and require to be re-examined on the basis of new geomechanical data and appropriate numerical modellings. Thus, in the iron ore basin, a methodological study of mining risk was led.

2. Discrimination methodology

The sixteen historical subsidence and collapse cases have ended in a methodology allowing to discriminate the both events through different criteria. There are two criteria, the one called *geometrical criterion* ant the other named *geological criterion.*

2.1. Geometrical criterion

The geometrical criterion is expressed by a discriminating function which takes into account the exploitation geometry. Ten quantitative variables were used in both PCA (Principal Component Analysis) and DFA (Discriminating Factorial Analysis) analyses.. These analyses have allowed to put in evidence a certain number of variables (extraction ratio, vertical stress in pillar, overburden thickness, mining height, pillar dimension, room dimension, surface area pillar, hydraulic radius, height-to-width ratio, abutment effect) defining the discriminating function showed on figure 1 (Thoraval, 2000).

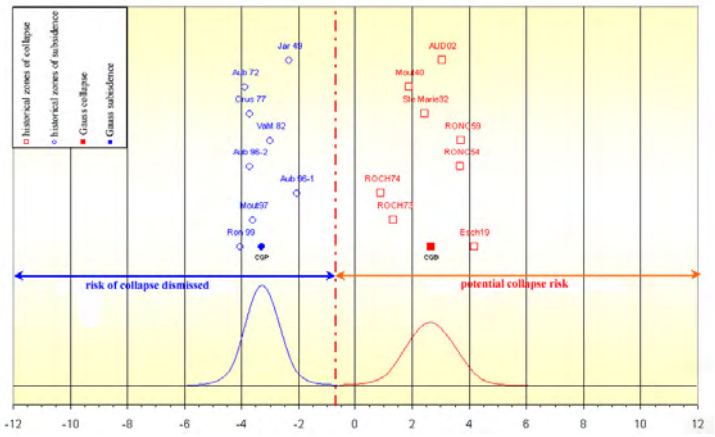


Figure 1: Discriminating function based on geometric criterion

At this stage, it was decided that for a violent collapse alea is retained, it is necessary that the discriminating function value is higher than -0.7 and it has to have the presence of stiff bedrock in the overburden. It allows the affectation of new zones to the one or the other groups without ambiguity when the projection is close to the two gravity centres.
On the other hand, this affectation becomes more delicate when the zone is projected very far from the two centres, indeed impossible when it is near to the centre. This type of analyse shows its insufficiency when we are near the critical discriminating value.

2.2. Geological criterion

For zones, where the doubt can persist, analysis based on a geological criterion is essential. A methodological study was undertaken by an expert group, based on a large geomechanical characterisation of overburden formations in the vicinity of already collapsed zones and/or zones associated a progressive subsidence (Homand, 2004). This consists of four parts:

1. to define facies-types and to emphasize the presence of a homogeneous bedrock « *in the sense of the predominant lithological facies* » with the help of geotechnical core drillings analysis ;
2. to identify the mechanical parameters from laboratory tests (average compressive strength, average Young's modulus,) for each facies-type in order to lead to an overburden characterization in the vicinity of core drillings on the base of the maximum ID value, average RQD and joint type;
3. to calculate the RMR and GSI index, for each unity, in order to evaluate of the deformability modulus at the site scale based on the well known methodologies (Barton 1980, Hoek & Brown 1982, Bieniawski 1989 and Hoek & Brown 1997) ;
4. to propose a stiff index IM.

From this large geomechanical characterisation, the total index expressing the stiffness overburden is defined by Bennani et al. 2004:

$$IM = (2A + B + \frac{C}{2}) \times \frac{f_{disc} + 5}{10} \quad (1)$$

where index A represents the total overburden behaviour by considering only stiff formations, index B is the maximal stiffness bedrock. The geometrical criterion (f_{disc}) is taken into account by the discriminating function.
Formation massivity can be defined like its total stiffness. It bases on the stiffness bedrock concept, which is not an intrinsic characteristic, but which must be evaluated in both morphological (slope, tray, etc.) and geological (fracturing, fault) contexts. The index C takes into account these criteria at a large scale. This corresponds to a morphological index describing four distinct situations encountered in the Lorraine iron basin: promontory, valley, tray and postponed valley.
Initially and hypothetically, it was decided that a tray situation would have a tendency to increase the overburden massivity by the fact that the fracture would be badly expressed imposing limited displacements (index C is equal to 1). On the contrary, it was assumed that the empty space, created by the valley, would reduce the overburden stiffness (index C is equal to 0). These basic premises must be confirmed through a large-scale numerical modelling.

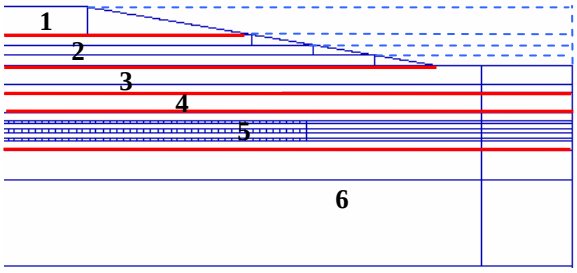
3. Geomorphological large-scale numerical modelling

The tray and valley situation with the presence or not of vertical fracture will be more particularly examined. We will examine at until which distance the valley excavation involves a disturbance of the stress field in the rock mass, the consequences on the stresses and displacements in the overburden and along the horizontal discontinuities (with or not exploitation in depth) and which role play the vertical fracture in the overburden. Finally, displacements and stresses examined in the overburden and in different configurations will be expressed into terms of massivity.
To answer of these questions, numerical modelling simulations are undertaken, which are based on the distinct element code (UDEC) within each discontinuity (interbed and vertical joints) is explicitly taken into account. The influence of numerous parameters (such as stiffness of overburden beds, mechanical properties of discontinuities, presence of vertical fractures etc.) is examined on the basis of a typical geological cross section representing both tray and valley configurations (mean dip at regional scale is 10°).

3.1. Geometrical model and loading sequences

With the aim of to more realistically represent the overburden with a stiff character (typically as certain zones in the basin), the model is basically consisted of stiff facies-types (Figure 2) : Jaumont limestone (stiff), Polypiers 1 limestone (stiff), Polypiers 2 limestone (soft), Polypiers 3 limestone (stiff), Haut-Pont limestone (stiff), Ottange limestone (soft) and Charennes marl (soft). Below marls, there is the iron layer made up of immediate roof (10 m), three iron layers (3.5 m) separated from internal waste (6.5 m) composed of limestone-marl alternation. Geologically, below the iron formation, there is the presence of marls known inferior. Between the last ore exploited layer and

the inferior marls, it has been introduced an additional layer with a power of 10 m which expresses the alternation of marls (very bad quality) and different layers of ore.



1 : Jaumont limestone 32 m (JCB)
2 : Polypiers limestone 12 m x 3 (PCGC+PCEAM+PCB)
3 : Haut-Pont (HPC) 22 m and Ottange (OTC) limestone 10 m
4 : Charennes marl 22 m (MC)
5 : iron formation
6 : inferior marl

Figure 2: Geological model

The valley formation causes the excavation of large blocks (23270 m^3 corresponding to 1100 m large and 70 m high. Few precautions about the model geometry choice must be taken into consideration. Based on several works reported in the literature, focussed on the model dimensioning in large scale slope modellings (Merrien-Soukatchoff et al. 2001) and in order to have coherent results in terms of stresses and displacements (without boundary effects), the model is 5650 m large on 2750 m high.
The vertical stress is given by the weight of overburden: $\sigma_v = \gamma\ h$. The modelling sequences are performed as follows: firstly, the model without excavation is consolidated under in situ stresses. Secondly, no horizontal displacements on the left side limit are imposed (expressing the no influence of the valley and future works to this limit) and the valley is excavated. Thirdly no displacements on the left side limit are conserved and rooms are excavated.

3.2. Mechanical properties

All materials have an average density, ρ, of 2500 $kg.m^{-3}$. For Poisson's ratio, we consider 0.3 for marls and 0.25 for limestone formations. For overburden limestone, the determination of various characteristics is based on laboratory tests. Modulus (E_m) and strength properties (C_m, ϕ_m) correspond to the rock mass scale and then fractures are already integrated. We use E_m calculated according to Hoek & Brown 97 formulation because it gives highest values, in accordance with our purpose to highlight the "stiff bedrock" role. For Charennes marls properties, it is impossible to apply Hoek & Brown 97 methodology, the spacing between each fracture not having significance. Therefore, the calculation of RMR index is impossible. We agreed to take, on the whole of geomechanical tests, the lowest measured values from laboratory tests.
Upper wall characteristics (ore layers) are equal to 75% of the formation representing the marls and not exploited ore alternation. Mechanical properties of marls at the immediate floor have weak characteristics representing the ore succession and marl internal waste of very poor qualities. They have the third of Charennes marls properties.
Inferior marls have the same characteristics of the iron formation. Finally the inferior part (or model base) is defined as being a resistant unity with mechanical characteristics four times stronger than the iron formation. Table 1 summarizes the input mechanical properties used.

Table 1: Mechanical properties

	E_m (MPa)	K (MPa)	G (MPa)	C_m (MPa)	Φ_m (°)	R_t (MPa)
JCB	21938	14625	8775	1.3	60	0.5
PCGC+PCB	26073	17382	10429	1.7	55	0.5
PCEAM	3897	2598	1559	0.5	33	0.1
HPC	25155	16770	10062	2.3	54	0.5
OTC	4690	3127	1876	0.8	29	0.2
MC	6000	5000	2308	1.0	30	0.5
Roof (immediate)	5860	3905	2343	0.9	26	0.06
Ore	7811	5207	3124	1.2	35	0.08
Marl at immediate floor	4000	3330	1538	0.7	20	0.4
Inferior marls	7811	5207	3124	-	-	-
Base	31244	20828	12496	-	-	-

3.3. Joint characteristics

Unlike the rock mass properties, it was not possible to deduct in advance the mechanical properties of joints. Therefore, the choice of these parameters presented here is based on some approaches encountered in the literature. The normal and shear stiffness K_n and K_s during the consolidation were calculated based on study reported by Kulatilake et al. (1992). In this approach, K_n and K_s depend essentially on the elastic properties of rock materials. Concerning K_n and K_s needed during excavation, it is clearly established that the mechanical behaviour of joints is generally non-linear and depend on large parameters such as: stress level, dilatancy, strength and deformability of asperities. Based on the relationships suggested by Bandis et al. (1983) and assuming that all joints have no dilatancy and their compressive strength (JCS) is equal to the uniaxial compressive strength of rock materials, the initial normal stiffness, the maximum normal closure and the shear stiffness for each discontinuity were calculated. Therefore it is possible to derive the normal stiffness (K_n) according to the normal stress level and the hyperbolic model of Bandis et al.(1983). As a first approach, we assumed that normal and shear behaviours of joints are linear and the shear stress is limited by Mohr-Coulomb criterion.

4. Influence of joint stiffness during the valley formation

Geologically, various joints, which separate formations in the overburden, can be filled with more or less clayey or marly materials. According to this filling, joints will have a more or less stiff behaviour, and both in the normal and tangential direction. For expressing this lithology in discontinuities, several sets of stiffnesses were assigned to joints: « $K_{ns\ ++}$» (« $K_{ns\ base}$ » x 100), « $K_{ns\ +}$» (« $K_{ns\ base}$ » x 10), « K_{ns} » (« $K_{ns\ base}$ »), « $K_{ns\ -}$ » (« $K_{ns\ base}$ » x 0.1) and « $K_{ns\ --}$ » (« $K_{ns\ base}$ » x 0.01).

4.1. Extent of the valley influence

For quantifying the role of a valley on the overburden behaviour, it is necessary to be able to estimate the distance where the valley disturbs stresses in the medium. Figure 3 shows the maximum perturbation rate of three stresses (expressed in % in relation to initial stresses). Initially, the valley/tray limit is set for a perturbation rate of 2% in relation to initial stresses. Beyond this zone, the geomorphology corresponds to a tray situation.

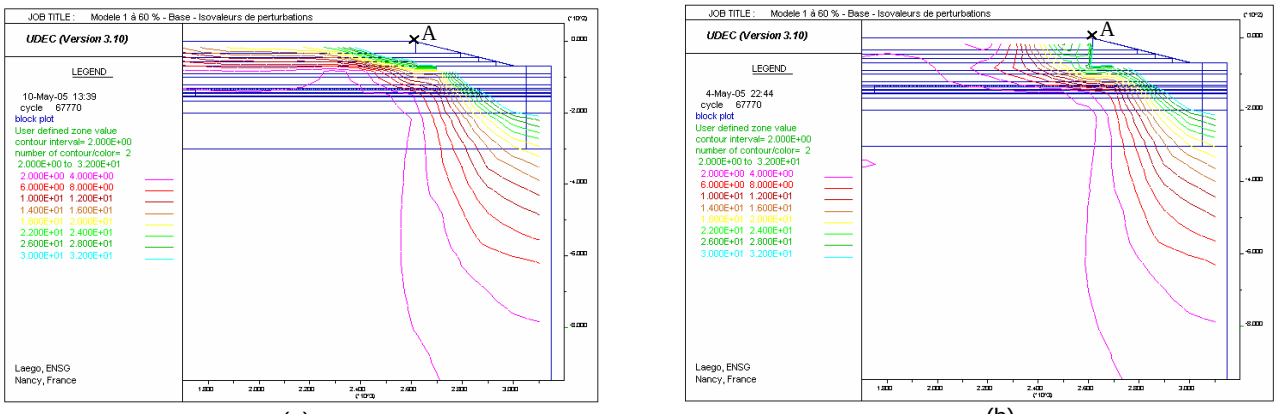


Figure 3: Maximum perturbation rate of stresses in relation to initial stresses for the « $K_{ns\ ++}$» (a) and « $K_{ns\ --}$ » (b)

The perturbation zone becomes more restricted when stiffnesses become low. Various distances found on the surface, for a rate of 2%, are specified in table 2. They are calculated from the slope rupture line (point A).

Table 2: Influence distances fixed to 2% according to different values of joint stiffness

Joint stiffness	Influence distance in relation to the valley
$K_{ns\ --}$	425 m
$K_{ns\ -}$	835 m
$K_{ns\ base}$	975 m
$K_{ns\ +}$	1020 m
$K_{ns\ ++}$	1360 m

Low stiffnesses facilitate movements and can generate released stresses within the matrix. With high characteristics, stresses will be more compressive and blocks less constrained to move toward the empty space created by the valley. Therefore influence distances will be larger for « $K_{ns\ +}$» and« $K_{ns\ ++}$» cases.

4.2. Plastic zones induced by the valley according to joint stiffness

The study of plastic zones repartition (figure 4) developed along layer limits (joints) and in the rock material allows us, at a first time, to approach of the mechanism associated to the valley excavation according to each joint stiffness set.

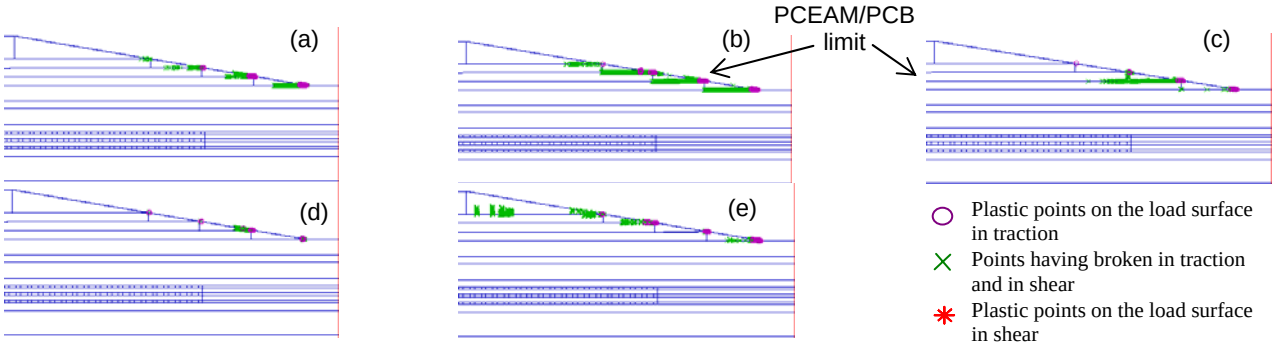


Figure 4: Plastic zones repartition for $K_{ns\ ++}$ (a), $K_{ns\ +}$ (b), $K_{ns\ base}$ (c), $K_{ns\ -}$ (d) and $K_{ns\ --}$ (e) cases

In the reference case (« K_{ns} » stiffness set), there is an important plastification near the PCEAM/PCB limit.

If joint stiffness are increased by a factor of 10 and 100 (« $K_{ns\ +}$ » and « $K_{ns\ ++}$ »), in the « $K_{ns\ +}$ » case, plastic zones appear at the layer limit level. All stiffnesses were multiplied by a factor 10 involving, therefore, more limited displacements and more high stresses along the layer limits. This plastic zone repartition is explained by the presence of shear failure occurring along joints. These failures initiate when the shear criterion $\tau_p = \sigma_n \mathrm{tg}\phi_j + C_j$ is reached, where Φ_j and C_j correspond to the joint friction angle and joint cohesion. The shear stress, on the joint, is limited by the peak value and a shear important displacement appears along the discontinuity. Proximity to the joint and in the matrix, the horizontal stress is constrained (limited also by the shear failure criterion for rock material) leading to important displacements and deformations and the appearance of plastic zones in the matrix. If joints behave elastically (by increasing the friction angle and cohesion), these broken zones would not occur on both sides of the discontinuity.

For the « $K_{ns\ ++}$ » case, plastic zones are reduced especially at the PCEAM/PCB limit. At this stage, the joint stiffness is so much higher (100 times larger) than movements are impossible further to the valley formation. From a physical point of view and compared to basic values, joints are more compressed. This does not correspond to reality, because near the valley, joints release and deteriorate, therefore increase their deformability.

Plastic zones do not develop any more in layer limits in the « $K_{ns\ -}$» case. Movements are facilitated (stiffnesses 10 times smaller than basic stiffnesses) and stresses are weaker. Layer limits do not break in shear and do not lead failures in zones on both sides of these limits.

Finally in the « $K_{ns\ --}$» case, vertical fractures appear in Jaumont limestone within rock matrix and on the valley side in PCGC. The presence of plastic zones (assimilated to vertical fractures in rock matrix) seems to be the result of an important dextral and sinistral movement on both side of the joint segments (facilitated by low stiffnesses) creating a tensile failed zone and leading to the propagation of vertical fractures in the matrix.

4.3. Relative tangential and normal displacements according to stiffnesses

The main mechanism of movement for all case of sensitive analysis on joint properties, corresponds to a dextral tangential displacement. High values of relative shear displacement are associated to the set of low joint stiffness and low values of shear stress (figure 5). For the « $K_{ns\ --}$» case, a sinistral displacement appears along the joint at 32 m in the medium (surrounded by the red dotted line, figure 5b). This is also related to the apparition of plastic zones perpendicular to joint in JCB layer. The normal displacement or joint opening increases when joint stiffness became more and more low. The opening passes in order to 4.7 µm for the « $K_{ns\ ++}$» case from 2.5 cm for the « $K_{ns\ --}$» case at the JCB/PCGC limit.

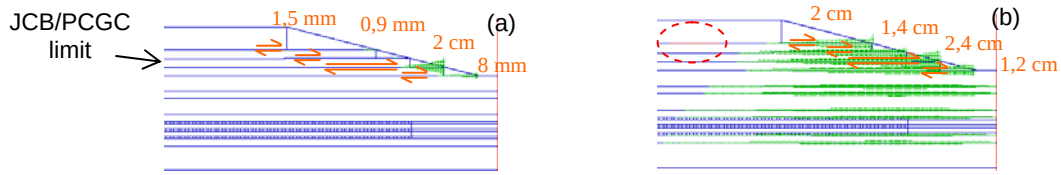


Figure 5: Relative tangential displacement for $K_{ns\ ++}$ (a) and $K_{ns\ --}$ (b) cases

4.4. Horizontal and vertical stresses within layers according to joint stiffness

The study of horizontal stress profiles (for depth of 16 m, figure 6a) according to joint stiffness shows that when the valley is excavated, the horizontal stress releases when approaching the valley. The more stiffnesses are low, the less the stress is compressive. For the « $K_{ns\ --}$» case, the horizontal stress is subject to a sudden compression in relation to with the apparition of plastic zones (§ 4.2) within the JCB block rock material (stress variation in order to 0.45 MPa). The vertical stress (figure 6b) is subject to, for all depths, a decrease near the valley. Only the stress in the « $K_{ns\ --}$» case indicates an oscillation between compression and release because of the presence of plastic zone in the layer.

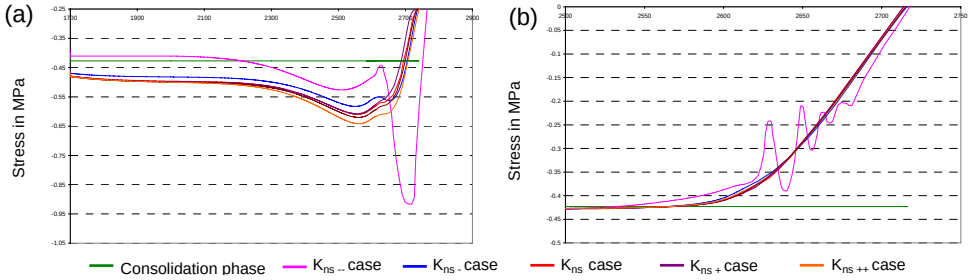


Figure 6: Horizontal (a) and vertical (b) stress profiles at a depth of 16 m (in JCB limestone)

For the other profiles in depth, the horizontal and vertical stresses also release in the vicinity of the valley with an amplitude which increases with the depth.

5. Case of an exploitation in depth: basic case

Several cases are considered: an exploitation situated under the tray (fig 9a), an exploitation situated alongside the valley (figure 9b) and an exploitation situated under the valley (figure 9c).

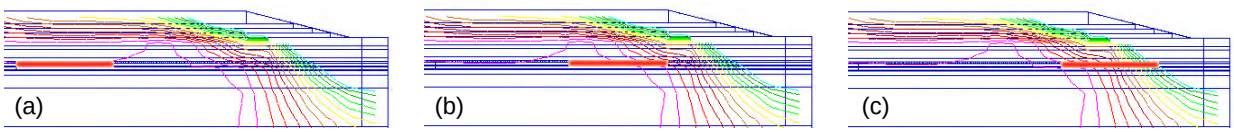


Figure 9: Different exploitation cases

The mine under the tray takes place in an undisturbed zone (rate of stress variation less than 2%). The situation is different for the mine alongside the valley where the exploitation is situated in a 7% disturbed zone at the most. The last mine under the valley takes place in a completely disturbed

zone, due to the valley presence, with a rate varying between 2% and 32%. Thus, only the mine under the valley positions completely in the perturbation zone unlike the both others.

5.1. Relative tangential and normal displacements

On both sides of the mine, the tangential displacement induced in the overburden is both dextral and sinistral as shown in figure 10a. The tangential displacement induced ($U_{s\ exploitation} - U_{s\ excavation}$) by the exploitation under valley (case a), is more important than the both others cases, in PCEAM/PCB limit (figure 10b). For exploitations under tray and alongside the valley, the induced displacement is the same ($7.18\ 10^{-5}$ m). The exploitation alongside the valley (case b) takes place finally in a not very disturbed zone by the valley even if the end of mine is excavated in a 7% disturbed zone in relation to the initial stress state. It causes in the overburden the same displacement as in the case of the mine under tray. On the contrary, for the mine under valley, the maximum tangential induced displacement recorded is of $7.78\ 10^{-4}$ m at the end of exploitation (ten times more).

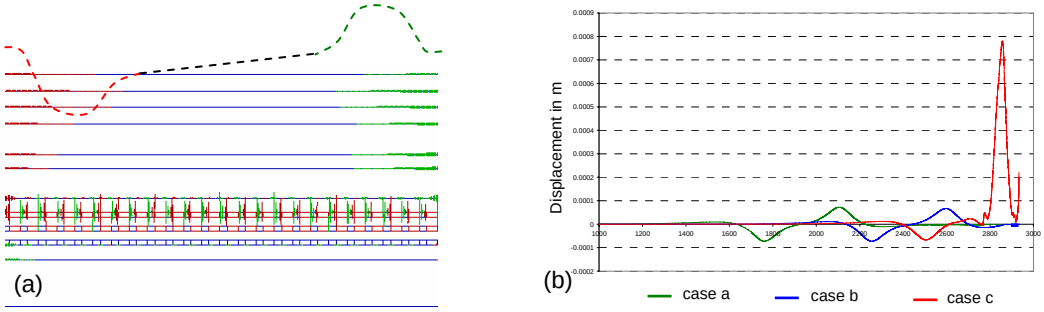


Figure 10: Relative tangential displacement

The normal displacement (fig 11a), induced by exploitations, shows a double flexion trend. It is equivalent for mines situated under tray and alongside the valley as well as the tangential displacement (fig 11b). The maximum closure, in mine edge, is of $1.5\ 10^{-5}$ m and the opening of $1.8\ 10^{-5}$ m. The exploitation under valley involves a joint opening of $2.15\ 10^{-5}$ m and showing always this double flexion trend where the magnitude is affected by the proximity of the valley.

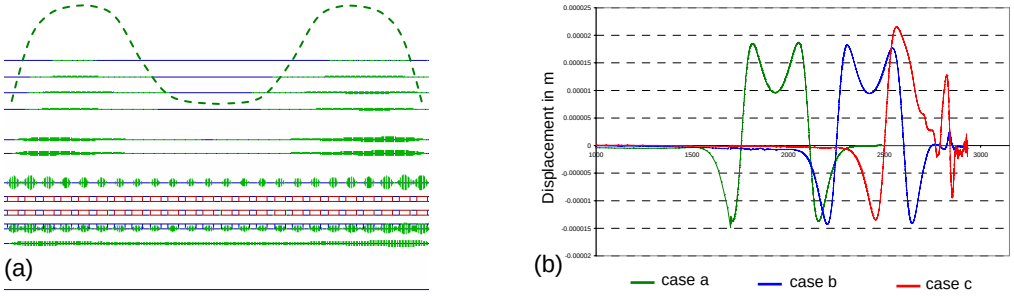


Figure 11: Relative normal displacement

At the start (without exploitation), the influence zone was defined for a stress perturbation rate of 2% (i.e. a disturbed zone until 975 m). In the presence of exploitation, the tangential and normal displacement shows that this zone must be considerably reduced, until 250 m about in the massif corresponding to a perturbation rate of 8%. This confirms that the starting criterion fixed to 2% was too large for estimating with significant and reasonable manners of the valley influence.

6. Influence of vertical fracture during the excavation valley phase

The introduction of vertical fracture aspires more to the reality even if the objective here, is not to represent it completely. The valley induces the development of fractures which are going to be more important at the approach of valley side, due to the release created by the empty space.

6.1. Influence valley zone: case of basic joint stiffness values

The vertical fracture introduction leads to a reduction of the influence valley zone (figure 12).

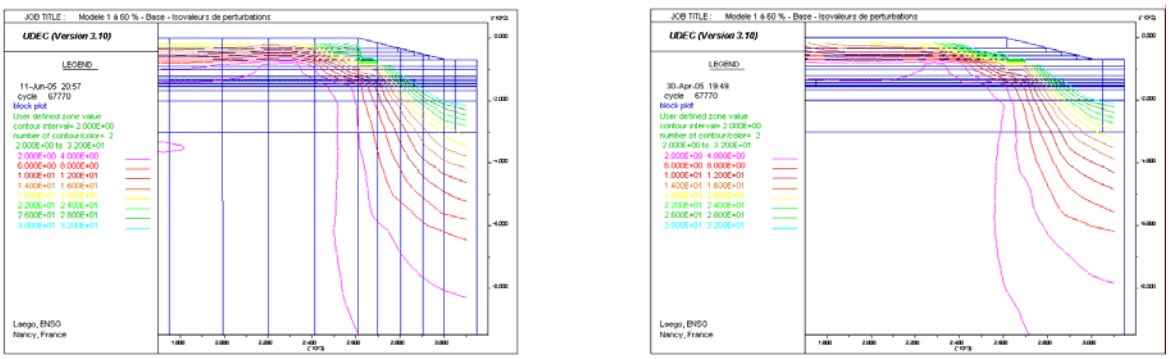


Figure 12: Influence valley zone in the case of basic stiffnesses

Vertical fractures seem to induce important displacements along vertical and horizontal joints synonymous with less compressive stresses allowing blocks to move more easily toward the empty space created by the valley. With this first analysis, the introduction of vertical fractures in the medium seems to release the sedimentary overburden.

6.2. Horizontal and vertical stresses in fractured and unfractured overburden

The horizontal stress induced by the valley excavation is less compressive (0.06 MPa), in the overburden, in fractured medium. This difference between the fractured and no fractured medium is more marked near the surface (0.11 MPa) what indicates that, superficially, the vertical fracture has a more significant effect on the horizontal stresses. Vertical stresses behave with the same manner as horizontal stresses in the sense of less compressive release than in the un fractured case in the vicinity of the valley.

6.3. Relative tangential and normal displacements in fractured and unfractured overburden

Tangential and normal displacements in layer limits are more significant in fractured medium. In the JCB/PCGC limit, the maximal displacement is five times more important (7.3 mm/ 1.4 mm) while in the PCGC/PCEAM, it is 2.5 times higher (3.8 cm/2.3 cm). An opening and a sinistral displacement appear along vertical fractures and which becomes weaker in depth. These displacements are all the more important as fractures are near the valley. Nevertheless it is low (tenth of millimetre at best) probably due to stiffnesses of vertical joints which are too high to involve large displacements along vertical fractures. All the same, this total increase of displacements is the result of a more released overburden in the fractured medium (§6.2).

6.4. Plastic zones developed in fractured and unfractured overburden

The plasticization developed along layer limits (fig 13) is more important in the fractured medium than in the no fractured medium. The failure criterion is reached more quickly in the fractured medium near the joint (because of not very compressive stresses and important tangential displacements) with a more important number of plastic zones.

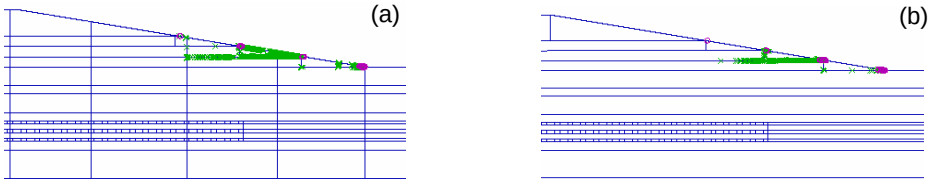


Figure 13: Plastic point repartition in fractured medium (a) and unfractured medium (b)

7. Valley influence and fractured medium in terms of stiffness on the overburden

The analysis of displacement and stress fields shows how all of the overburden limestone (consisting of a stiff bedrock) in the vicinity of the valley are subjected to the action of a vertical fracture set. The involved phenomena must be expressed into stiffness terms of overburden. Initially, it was estimated, in an intuitive way, that a free slope and the vertical fracture could have a tendency to reduce the overburden massivity. For the tray situation, the fracture is not well expressed; the corresponding overburden stiffness must be increased.

7.1. Displacements in the overburden

The tray situation can exist only at a certain distance of the slope. Initially, this situation is reached at approximately the distance of 975 m in comparison to the slope failure line (basic values of joint stiffness and a perturbation rate of 2%). This distance is variable according to the mechanical discontinuities properties and finally can be greatly reduced as seen in the paragraph 5.1 (250 m compared to 975 m in the basic case). In this zone, stresses and displacements are more released and more important. Figure 14 shows isovalues of displacements observed in the model.

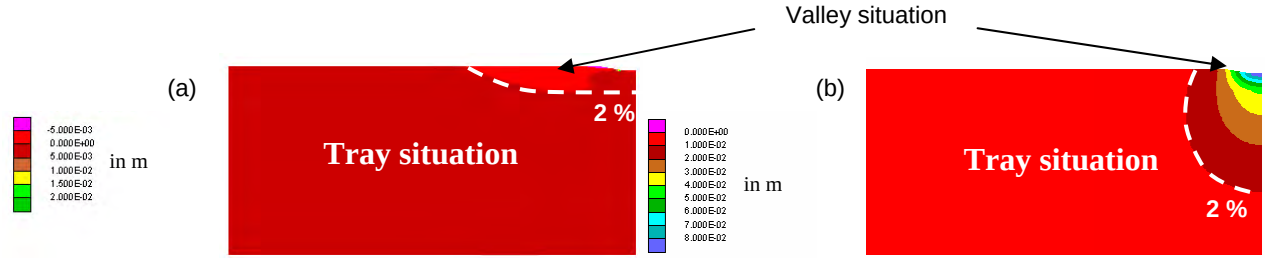


Figure 14: Horizontal (a) and vertical (b) displacement behind the valley excavation

The examination of horizontal displacement (figure 14a) shows that the observed displacement (5 mm) corresponds to the perturbation zone fixed initially to 2%. The vertical displacement (figure 14b) also underlines this zone and corresponds to movements of about 1 to 2 cm. These displacements allow in a first time to confirm the distinction between the tray and valley situation. Moreover in terms of massivity, these displacements are synonymous of an overburden less constrained near the valley and thus less stiff. This last remark comes to confirm that a free slope reduces the overburden massivity.

7.2. Vertical fracture

Harrison & Hudson (1997) have shown that the fracture had a tendency to reduce the massivity of a medium expressed through the homogeneous deformation modulus E_m:

$$E_m = \frac{\sum_i t_i}{\sum_i \frac{t_i}{E_i}} \quad \text{unfractured strata} \qquad (2)$$

$$E_m = \frac{\sum_i t_i}{\sum_i t_i \left(\frac{1}{E_i} + \frac{\lambda_i}{E_{di}} \right)} \quad \text{fractured strata} \qquad (3)$$

where λ_i corresponds to the frequency of fractures and E_{di} to the fracture stiffness in the layer i. The additional term of equation 3, $\lambda_i/E_{di,}$ shows that the fractures have a tendency to reduce the homogeneous rock mass modulus, thus to weaken the stiffness in the rock unit.
The induced horizontal displacement (figure 15) by the valley excavation is more significant for overburden in the fractured medium than in the unfractured strata. In both cases, the overburden is subject to a displacement of 5.10^{-3} m with the only difference that in the fractured medium, this displacement stretches more laterally in the massif.

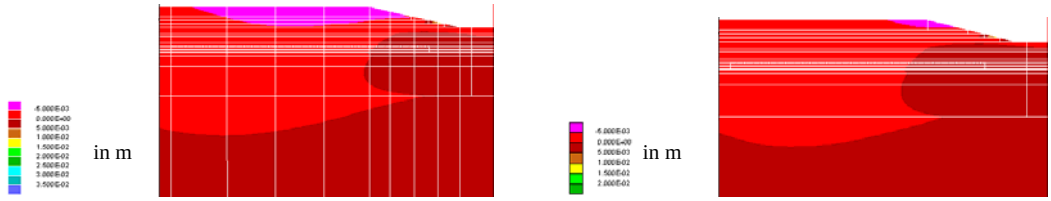


Figure 15: Horizontal displacement in fractured and unfractured medium

The vertical displacement (figure 16) is too more important in the fractured medium than in the unfractured ones. In the overburden, the valley induces a vertical displacement of about 10^{-2} to 2.10^{-2} m for the case without fractures. In the fractured medium, this same displacement reaches in the overburden a value of 10^{-2} to 4.10^{-2} m.

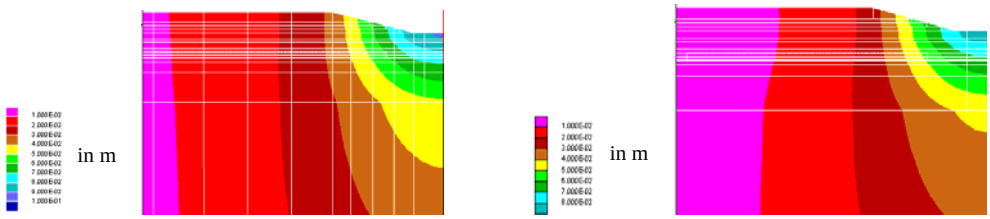


Figure 16: Vertical displacement in fractured and unfractured medium

The analysis of these displacement fields really seems to indicate that the presence of vertical fracturing causes important movements in layers, in connection with the less compressive stresses recorded (§6.2), and seems still more to reduce the massivity overburden. This is approached below in terms of strain energy balance.

8. Energy balance

Usually strain energy is stored within a block when the block is deformed under load. In the absence of energy dissipations, such as from friction or yielding, the strain energy is equal to the work done on the block by external loads. It is equal to the area under the stress-strain curve, and is a measure of the toughness of a block. The mechanisms noticed through these modellings (released stresses, displacements, plastic zones), are accompanied by a more or less important dissipation of energy. The total energy released correspond to the total dissipated strain energy in material (U_c), the total change in potential energy of the system (U_b), the total dissipated energy in joint shear (W_j) and the total dissipated work in plastic deformation of intact rock (W_p). Therefore if energy dissipations are weak in the overburden; this will be an indicator of a stiff behaviour.

8.1. Unfractured strata medium

Table 3 shows different energy dissipations between the initial state (consolidation phase in of terms of Itasca codes) and excavation phase:

Table 3: Dissipated energy according to stiffnesses between the initial state and excavation phase

	Kns --	Kns -	Kns	Kns +	Kns ++
Material strain energy U_c (J)	1563	1395	1453	1443	1455
Potential energy U_b (J)	82.63	74.17	75.76	75.24	75.58
Friction work W_j (J)	0.1739	0.0857	0.1281	0.1069	0.1064
Plastic strain work W_p (J)	$8.20.10^{-3}$	$7.25.10^{-4}$	$1.75.10^{-3}$	$1.45.10^{-3}$	$3.05.10^{-4}$
Total energy released (J)	1646	1435	1529	1518	1530

The total dissipated strain energy in material is important for the « $K_{ns\ --}$» case (1563 J) and quasi-equivalent for the other stiffnesses (≈ 1450 J) except for the « $K_{ns\ -}$» case (1395 J). The total change in potential energy is more important for the « $K_{ns\ --}$» case due to the important displacements (§4.3). Plastic strain energy (W_p) describes the deformability of the blocks. Energy is dissipated

through plastic work equivalent to irreversible deformation in the rock blocks. With the exception of « $K_{ns\,++}$» case (joints too compressed, §4.2), this energy is weaker for the « $K_{ns\,-}$» case than the other cases (figure 17a). In other words, the deformability of blocks is weaker for the « $K_{ns\,-}$» case (emphasized by the presence of few plastic points developed in layer limits §4.2).
With a less deformability or a more constrained medium, the total released energy (figure 17b), between the initial state and the excavation phase, is less important for the « $K_{ns\,-}$» case (1435 J). Therefore in this last modelling, energy dissipations are weak involving a stiffer overburden than for the other cases.

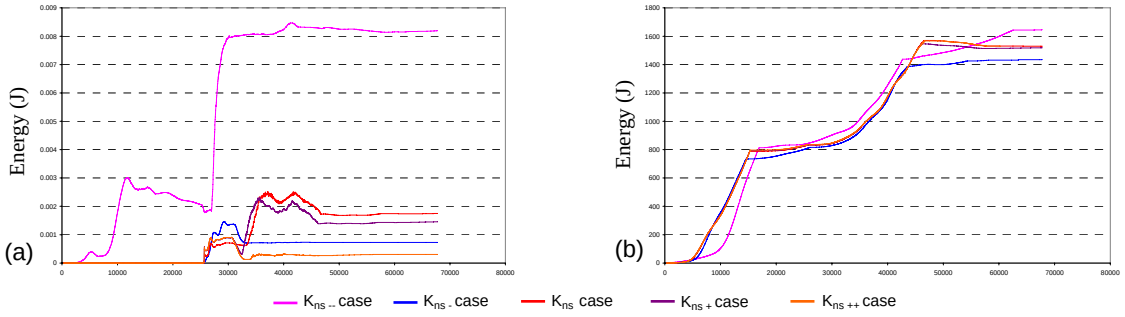


Figure 17: Evolution of total dissipated work in plastic deformation (a) and total energy released (b)

8.2. Comparison between the unfractured and fractured strata medium

Table 4 shows energy dissipations between the fractured medium and the unfractured medium:

Table 4: Dissipated energy in fractured and unfractured medium

	Fractured	No fractured
Material strain energy U_c (J)	1457	1453
Potential energy U_b (J)	300.5	75.76
Friction work W_j (J)	0.2167	0.1281
Plastic strain work W_p (J)	$8.25\ 10^{-3}$	$1.75\ 10^{-3}$
Total energy released (J)	1754	1529

The total dissipated strain energy in material is the same for both cases due to stiffnesses of vertical fractures which are too high as seen in §6.3. Even if displacements are weak along vertical joints, general displacements within rock blocks involve a released potential energy four times more important in the fractured medium in accordance with displacements observed in paragraph 7.2. Plastic strain energy does not contribute with a significant manner on the total released energy (few thousandth of joule) but it gives an idea of the deformability of the blocks. It is five times higher in the fractured medium which indicates that the fractured medium is more deformable than the unfractured medium. Consequently, the fractured medium releases an important total energy (1754 J) in comparison with the no fractured medium (1529 J). These last observations confirm the assumption that the overburden is more released with the presence of vertical fractures.

9. Conclusion

This methodology allows fixing a distance from which the valley disturbs stresses in the overburden. This distance is variable according to joint stiffnesses. For the basic case, it was fixed at 250 m (from the slope failure line) corresponding to a perturbation rate of 8% in relation to initial stresses. Beyond this zone, the geomorphologic situation is a tray situation. During the valley excavation and according to stiffnesses, stresses release, the plastic points and displacements (shear and normal) appear along discontinuities. The introduction of vertical fractures accentuates displacements, stresses are more released and plastic zones are more numerous. These induced phenomena act on the overburden behaviour in terms of stiffness. The general study of displacements and energy balances show that near the valley, the overburden is less massive than in tray situation. This release is more important in the presence of vertical fractures.

10. References

Bandis S.C., Lumsden A.C. and Barton N.R. (1983). *Fundamentals of rock joint deformation*, Int. J. Rock Mech. Min. Sci & Geomech. Abstr., 20, 249-268.

Bennani M., Homand F. (2004). *Les formations de couverture au droit des zones d'aléa d'effondrement brutal*, rapport LAEGO-GEODERIS, R2004-002_LG.FH.GEO.PSI.RPRE.04.0059.C, juillet 2004.

Harrison J.P., Hudson J.A. (1997). *Engineering Rock Mechanics, Part 2: Illustrative Worked Examples*, Pergamon, 506 pages, 1997.

Homand F. (2004). *Etude des formations de couverture au droit de zones à risque*, rapport GEODERIS, LG.FH.GEO.PSI.RPRE.03.0248.A, juillet 2004.

Kulatilake P.H.S.W., Ucpirti H., Wag S., Radberg G. and Stephansson (1992). *Use of the distinct element method to perform stress analysis in rock with non-persistent and to study the effect of joint geometry parameters on strength a deformability of rock masses*, Rock Mech. and Rock Engng., 25, 253-284.

Merrien-Soukatchoff V., Omraci K. (2000). *Détermination des conditions aux limites pour un calcul de stabilité de talus*, Revue Française de Géotechnique, 92, 3ème trimestre 2000, 31-39.

Thoraval A. (2000). *Etudes réalisées dans le cadre du GISOS et cofinancées par les fonds du CIADT pour 1999-2000*, rapport INERIS ref. DRS-00-23744/RN01, rapport GISOS n°28, décembre 2000.

Tincelin E., Sinou P. (1962). *Effondrements brutaux et généralisés – Coups de toit*, Revue Industrielle et Minérale, avril 1962.

UNDERGROUND CAVITIES DETECTION AND CHARACTERIZATION USING 2D ELASTIC FULL WAVEFORM INVERSION IN THE SPACE-FREQUENCY DOMAIN

GELIS Céline[1], VIRIEUX Jean[1], GRANDJEAN Gilles[2], OPERTO Stéphane[3], LEPAROUX Donatienne[4]

[1] GEOSCIENCES AZUR. 250 Rue A. Einstein. Sophia Antipolis. 06 560 Valbonne. France. gelis@geoazur.unice.fr, viri@geoazur.unice.fr

[2] BRGM. Dép. ARN. BP 6009. 45 060 Orléans. France. g.grandjean@brgm.fr

[3] GEOSCIENCES AZUR. Observatoire Océanologique de Villefranche-sur-mer. BP 48. 06235 Villefranche sur mer cedex. France. operto@geoazur.obs-vlfr.fr

[4] IPGP. 4 place Jussieu. 75 252 Paris cedex 05. France. leparoux@ipgp.jussieu.fr

ABSTRACT: The elastic full waveform inversion is a method dedicated to the reconstruction of soil physical parameters. Therefore buried objects like cavities may be detected and characterized. This method is based on a linearized inversion of seismic waveforms. All propagating waves are taken into account regardless their nature (body or surface waves, refracted, reflected, diffracted waves) with the help of a complete solver of the forward problem as finite difference methods. The inversion takes place in the frequency domain from low to high frequencies, because it allows a multi-scale approach and takes the non-linearity into account. Two physical parameters are simultaneously imaged, such as the P and S wave velocities, or Lamé parameters. The acquisition geometry influence is critical and preparation of the data important as well as the knowledge of the initial model. After validating the method on synthetic examples for media without free surface providing similar results as those in the acoustic formulation for body waves, we investigate influences when considering surface waves in our synthetic data. Strategies are proposed for better conditioning of the linearized scheme and potentialities for the detection and characterization of a cavity are analyzed.

KEYWORDS: Seismic imaging, linearized inversion, surface waves.

RESUME : L'inversion des formes d'onde élastique est une méthode visant à retrouver les paramètres physiques du sol. Ainsi, des objets souterrains comme des cavités peuvent être détectés et caractérisés. La méthode est basée sur une inversion linéarisée des formes d'onde sismiques enregistrées dans les sismogrammes. Cela signifie que toutes les ondes sont prises en compte quelle que soit leur nature (ondes de volume ou de surface, ondes réfractées, réfléchies, diffractées) en résolvant le problème direct complet par une méthode de différences finies. L'inversion est effectuée dans le domaine fréquentiel, permettant une approche multi-échelle et la prise en compte de la non-linéarité. Deux paramètres physiques sont imagés simultanément, comme les vitesses des ondes P et S ou les paramètres de Lamé. L'influence du dispositif d'acquisition est critique et la préparation des données ainsi que la connaissance du modèle initial sont importantes. Après avoir validé la méthode sur les exemples synthétiques sans surface libre, donnant des résultats similaires à l'approximation acoustique, nous examinons les différentes influences quand des ondes de surface se trouvent dans les synthétiques. Des stratégies sont proposées pour un meilleur conditionnement du schéma linéarisé et les potentialités pour la détection et la caractérisation d'une cavité sont analysées.

MOTS-CLEFS : Imagerie sismique, inversion linéarisée, ondes de surface.

1. Introduction

Detecting underground cavities represents nowadays a great challenge in some regions of the world, such as Lorraine, due to the natural hazard they may provoke. It is as well very important to characterize their main features, such as their size, their depth, their geometry and to determine their physical parameters.

In order to detect potentially dangerous cavities, we resort to a method based on seismic data and called the elastic full waveform inversion. Wave arrival times and amplitudes are fitted.

The corresponding forward problem is the wave propagation in a linear isotropic medium in two dimensions. The inverse problem is solved thanks to a linearized inversion (Tarantola, 1987).

2. Forward problem

The forward problem is calculated in the frequency domain. It is numerically solved with finite differences, which allows the modelling of all waves existing in the medium. The stencil of Saenger et al. (2000) is chosen because it simply and precisely simulates the free surface. The surface waves propagation is therefore particularly well modelled.

The forward problem is expressed with the matrix formalism of Stekl and Pratt (1998) and solved with a LU decomposition. This very efficiently takes multisources and multireceivers acquisitions into account.

At last, the frequency formulation allows to easily introduce some physical phenomena such as the attenuation in the medium (Stekl et Pratt, 1998).

3. Inverse problem

The inverse problem is solved with a least square linearized inversion (Tarantola, 1987 ; Pratt et al., 1998). Two parameters are simultaneously inverted. In this study, we do not invert the density since it has a weaker influence on data. We mainly focus on the P wave velocity (Vp) and the S wave velocity (Vs) or any equivalent parameters couple. Fitted data are horizontal and vertical seismograms.

Several iterations are performed at each frequency. For each iteration the optimization direction is calculated with a gradient method. The gradient contains the product (in the frequency domain, therefore a convolution in the time domain) of forward fields propagating from the source with residues (differences between calculated and observed data) backpropagated from receivers. The gradient is preconditioned with the diagonal part of the Hessien. The gradient expression depends on the chosen approximation to compute Fréchet derivatives. This approximation choice influences final images, as we will see later on.

The algorithm reconstructs the two imaged parameters differently, as illustrate figures 1 and 2. The figure 1 shows the Vp reconstruction, the figure 2 shows the Vs reconstruction. The medium parameters and the acquisition geometry are presented on figure 3. The initial model is homogeneous, as it will be the case in all other examples in this study.

The inversion is performed from low to high frequencies. Therefore, smaller and smaller wavelengths are progressively introduced in the medium, improving our knowledge of the medium

(figures 1 and 2). Furthermore, the non linearity of the problem is taken into account because low frequencies are more linear than high frequencies.

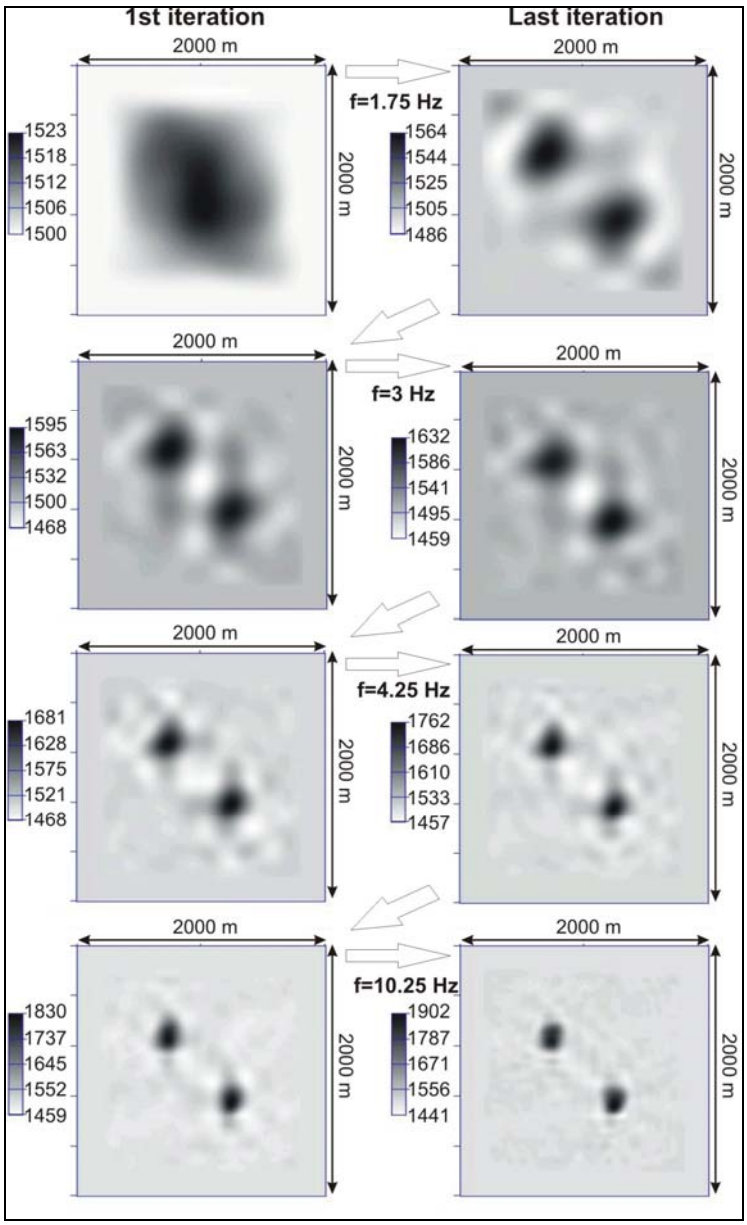


Figure 1. Vp velocity models evolution with the inverted frequency and the iteration number. Fréchet derivatives are computed with the Born approximation.

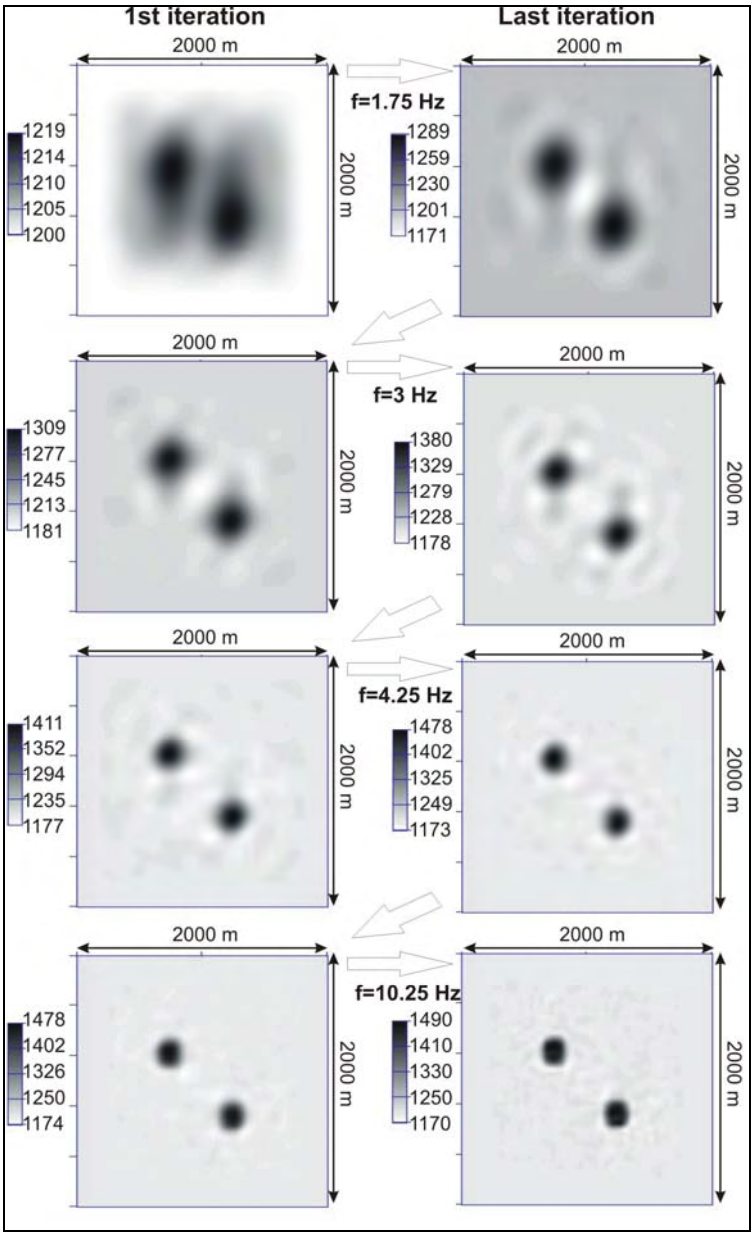


Figure 2. Vs velocity models evolution with the inverted frequency and the iteration number. Fréchet derivatives are computed with the Born approximation.

.

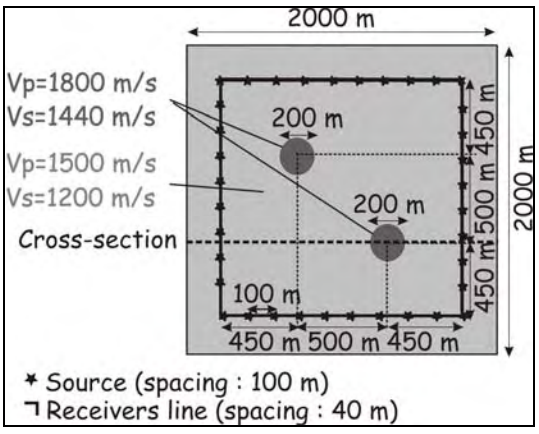


Figure 3. Modèle de vitesse à reconstruire et dispositif d'acquisition

The Fréchet derivatives included in the gradient are calculated with the Born or the Rytov approximation. In the Born approximation, perturbations of the velocity field and perturbations of physical parameters are linearly linked. In the Rytov approximation, perturbations of the complex phases of the velocity fields and perturbations of the physical parameters are linearly linked. These two approximations give different results. The figures 1 and 2 show parameters images when the Born approximation is used. The figures 4 and 5 show parameters images when the Rytov approximation is used.

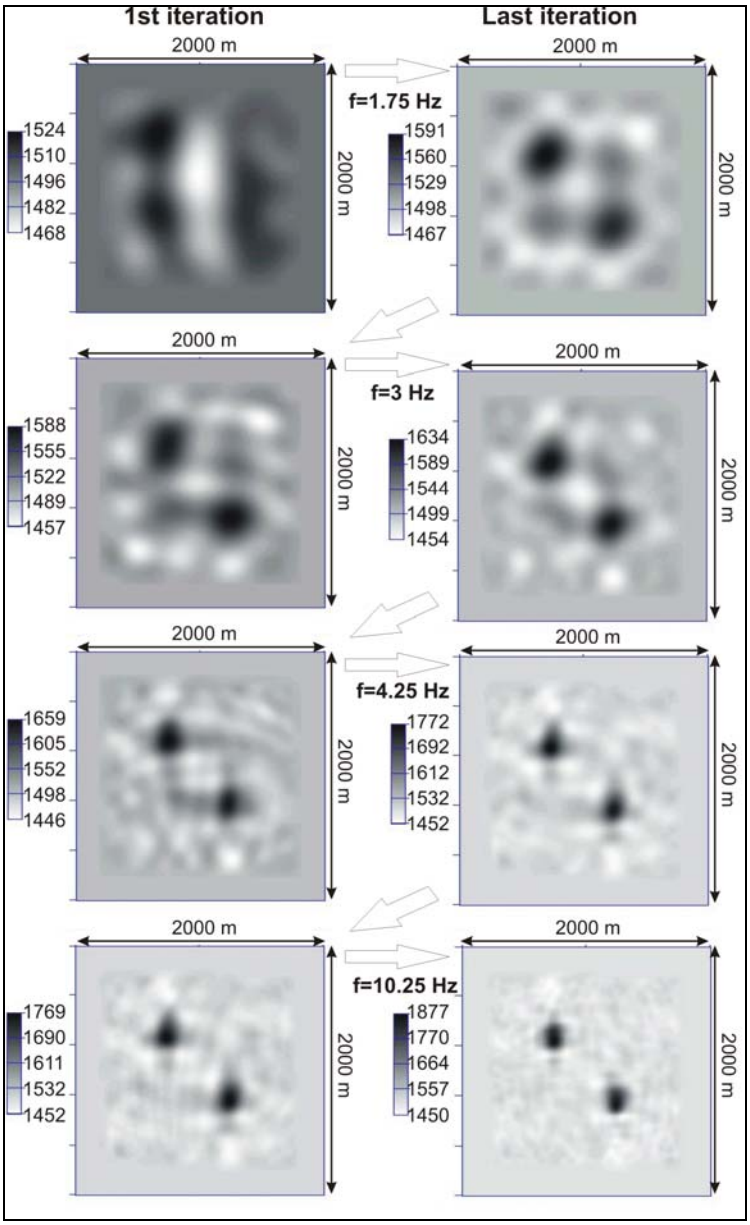


Figure 4. Vp velocity models evolution with the inverted frequency and the iteration number. Fréchet derivatives are computed with the Rytov approximation.

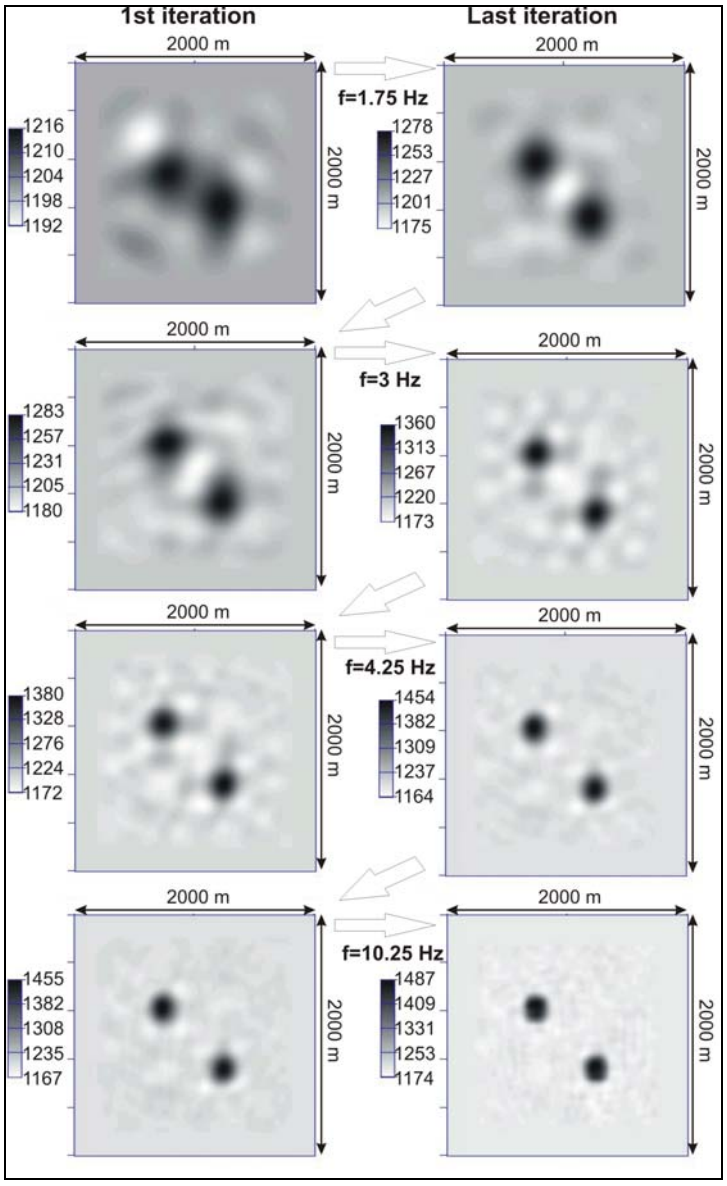


Figure 5. Vs velocity models evolution with the inverted frequency and the iteration number. Fréchet derivatives are computed with the Rytov approximation.

The inverted parameters choice plays a role as well. The figures 6 and 7 show extracted profiles from Vp and Vs final parameters images for the inversion of different parameters couples with data recorded in transmission.

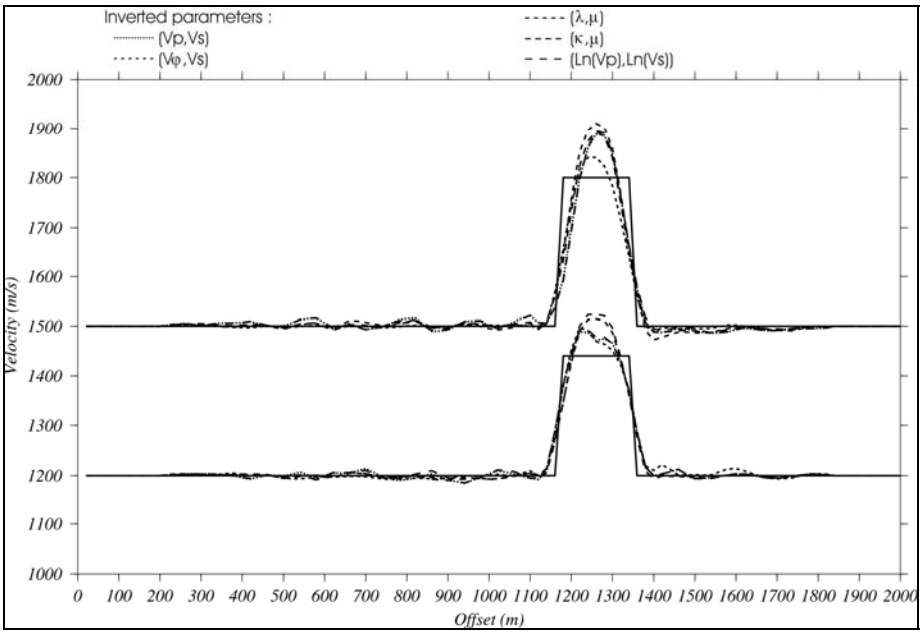


Figure 6. Horizontal cross-section (along the line in figure 3) of Vp (top) and Vs (bottom) for different inverted parameters couples with the Born approximation and a transmission acquisition geometry

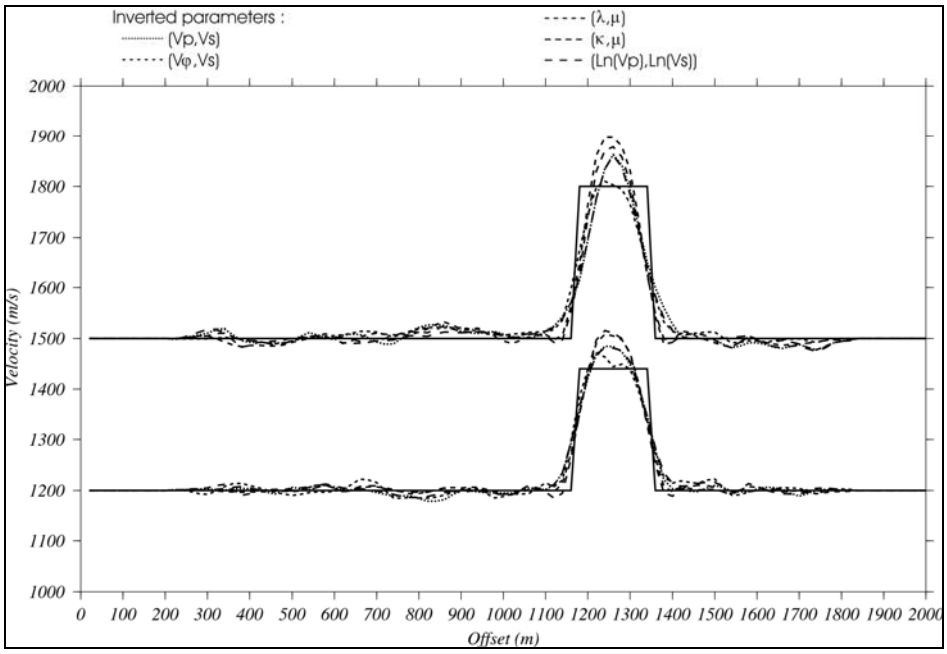


Figure 7. Horizontal cross-section (along the line in figure 3) of Vp (top) and Vs (bottom) for different inverted parameters couples with the Rytov approximation and a transmission acquisition geometry

At last, the acquisition geometry is a key parameter. The figures 8 and 9 show extracted profiles from final parameters images for the inversion of different parameters couples with data recorded in reflection. The amplitude and shape of the anomaly are not so well recovered as with a transmission acquisition geometry. The Lamé parameters inversion allows to better retrieve the maximal amplitude. The seismic velocities inversion allows to better detect the global anomaly shape.

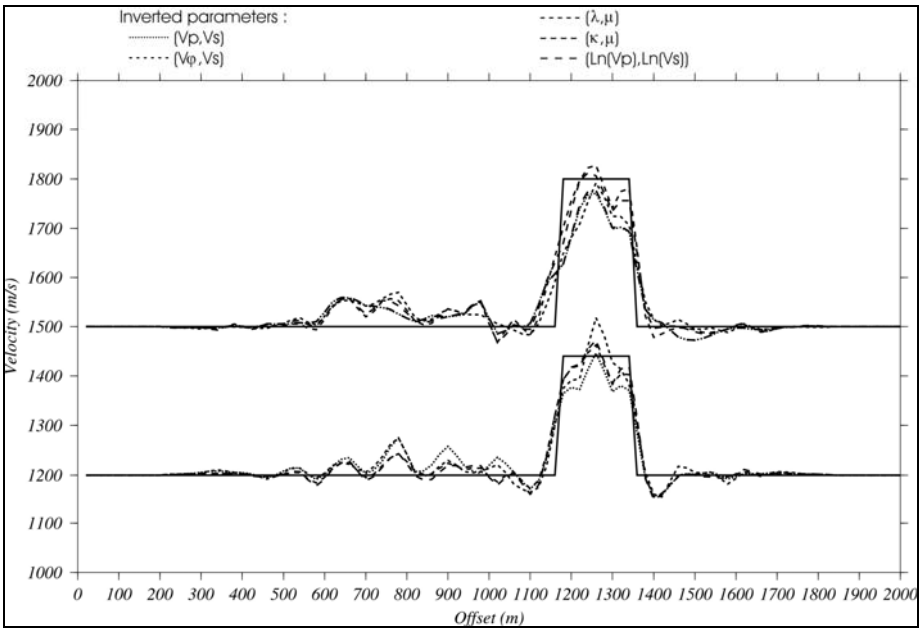


Figure 8. Horizontal cross-section (along the line in figure 3) of Vp (top) and Vs (bottom) for different inverted parameters couples with the Born approximation and a reflexion acquisition geometry

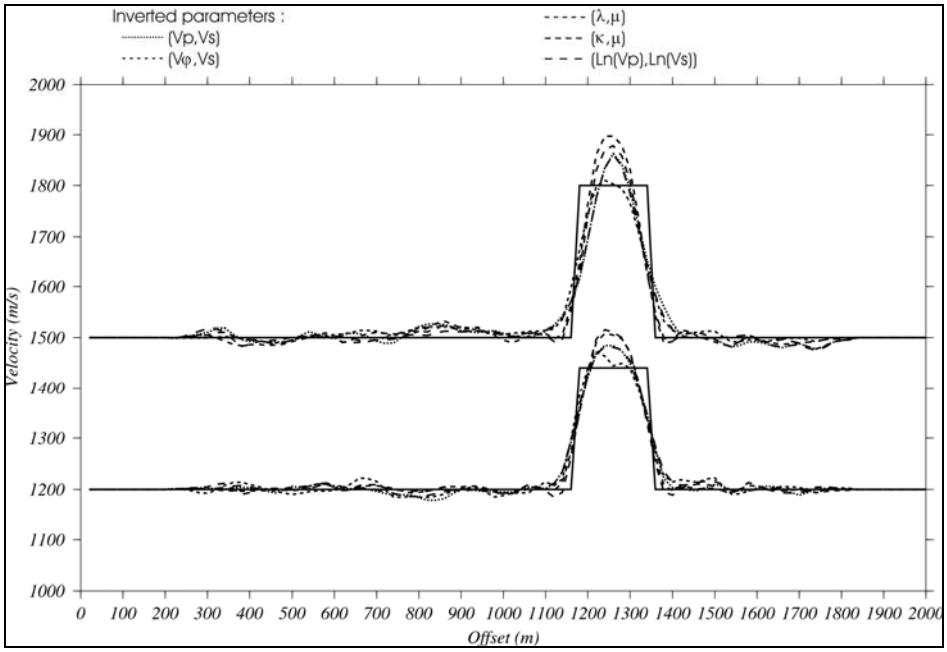


Figure 9. Horizontal cross-section (along the line in figure 3) of Vp (top) and Vs (bottom) for different inverted parameters couples with the Rytov approximation and a reflexion acquisition geometry

4. Application to anomalies detection in the presence of free surface

In real acquisitions, sources and receivers are located on the free surface. We therefore choose to perform the inversion with the Born approximation to compute Fréchet derivatives. We chose to invert the (Vp,Vs) parameters couple.

The main difficulty is to deal with surface waves containing the main part of energy and masking the diffracted body waves.

4.1. Two positive velocity anomalies

When two anomalies are present (figure 10), the algorithm reconstructs them but their amplitude and shape suffer from certain artifact.

In order to limit the surface waves influence, data are selected in such a way that we first use seismograms without surface waves. Therefore only near-offset data are selected to perform the inversion at the beginning. Then, the final parameters images serve as initial model to perform another inversion in which the maximal offset to select data is increased. Therefore, some recorded surface waves are included. We follow this flowchart and progressively introduce far-offset data. At the end, the whole dataset is inverted.

The figure 10 shows that this data preconditionning allows to get more precise parameters images.

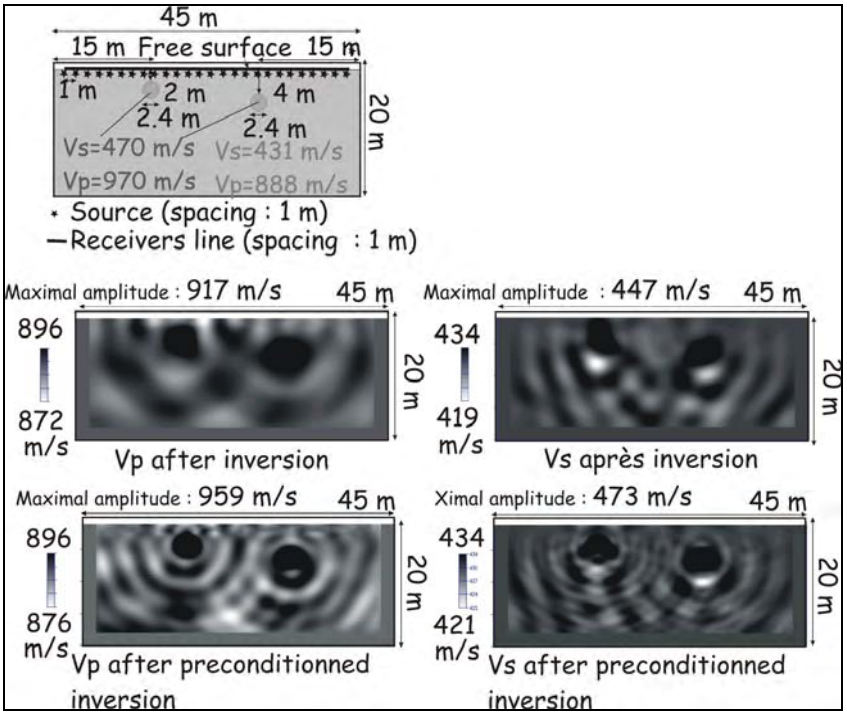


Figure 10. Medium to be reconstructed and acquisition geometry (top). Inversion performed without (middle) and with (bottom) data preconditioning. Colors are saturated to enhance contrasts.

4.2. A cavity

The application of this method to the cavity detection can be performed in two different ways. First, the full waveform inversion can be directly applied to recover the cavity main features. The previously defined strategy is performed. The figure 11 shows that the cavity is better reconstructed when data are preconditioned. Final images show that the shape, the size and the location of the cavity are well recovered. Nevertheless, as the velocity contrast is very important and as the anomaly is strongly non linear, the true amplitude is not recovered.

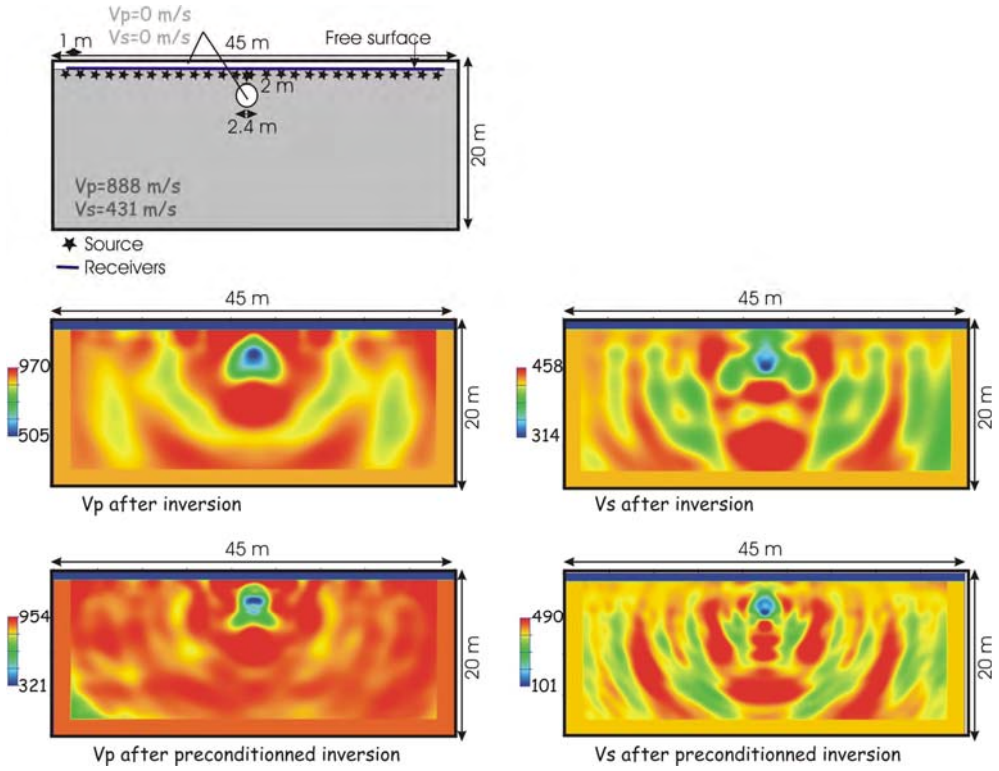


Figure 11. Medium to be reconstructed and acquisition geometry (top). Inversion performed without (middle) and with (bottom) data preconditioning. Colors are saturated to enhance contrasts

As a matter of fact, the elastic full waveform inversion can not be used strictly in this case since the anomaly to image (the cavity) is very different from the background model. The second possibility is to first compute a smooth initial model by using the traveltime tomography (Ravaut, 2003) or the surface waves spectral analysis (SASW : Spectral Analysis of Surface Waves, Nazarian et Stockoe, 1984). The elastic full waveform inversion can then be applied to precisely characterize already detected anomalies and reconstruct their shape, location and size.

5. Conclusion

The full waveform inversion allows to quantitatively determine physical parameters in the soil. This kind of study allows to detect voids and to characterize the cavity and the background by its degree of alteration and the soil decompaction. Thus, collapsing risks can be assessed.

6. References

Nazarian S. and Stokoe II K. H., 1984. *In situ shear wave velocities from spectral analysis of surface waves,* Proc. 8th Conf. on Earthquake Eng. – S. Francisco, vol. 3, 31-38.

Pratt G., Shin C. & Hicks G.J.1(998). *Gauss-Newton and full Newton methods in frequency-space seismic waveform inversion.* Geophys. J. Int., Vol. 133**,** 341-362.

Ravaut C. (2003). *Tomographie sismique haute résolution de la croûte terrestre : inversion combinée des temps de trajet et des formes d'ondes de données sismique réflexion/réfraction grand angle multitraces.* Thèse de doctorat en géophysique. Université de Nice- Sophia Antipolis

Saenger E. H., Gold N. & Shapiro S. A. (2000). *Modeling the propagation of elastic waves using a modified finite-difference grid*. Wave Motion, Vol. 31, 77-92.

Stekl I. & Pratt R.G., 1998. *Accurate viscoelastic modeling by frequency-domain finite difference using rotated operators.* Geophysics, Vol. 63, 5, 1779-1794

Tarantola, 1987. Inverse *Problem Theory : Methods for data fitting and Model Parameter Estimation.* Elsevier Sci., New York.

LONG TERM STABILITY ANALYSIS OF CAST IRON SHAFT LININGS AFTER COAL MINE CLOSURE AND FLOODING

HADJ-HASSEN Faouzi[1], BIENVENU Yves[2], NOIREL Jean-François[3], METZ Michel[4]

[1] ECOLE DES MINES DE PARIS – CGES : 35 rue St Honoré 77305 Fontainebleau – France
faouzi.hadj_hassen@ensmp.fr

[2] ECOLE DES MINES DE PARIS – CM : BP 87 91003 Evry Cedex – France
yves.bienvenu@ensmp.fr

[3] CHARBONNAGES DE FRANCE – DTN : 2 avenue Emile Huchet 57802 Freyming Merlebach – France
jean-françois.noirel@charbonnagedefrance.fr

[4]CHARBONNAGES DE FRANCE – ESA : 2 avenue Emile Huchet 57802 Freyming Merlebach - France
michel.metz@charbonnagesdefrance.fr

ABSTRACT: This paper presents the results of a study conducted to analyse the long term stability of the cast iron shaft lining after coal mine closure and flooding. The attention is mainly focused on the behaviour during the critical phase of flooding as well as the phase corresponding to the disappearance of the water pressure and the stabilization of the environment. This pluri-disciplinar study was conducted by a team combining specialists in rock mechanics who identified the main risks and the conditions of stability of the lining and specialists in metallurgy who studied the composition of the cast iron and its corrosion behaviour after exposure to mine water.

KEYWORDS: Cast iront, lining, flooding, stability, corrosion

RESUME: Cet article présente les résultats d'une étude de la stabilité à long terme des cuvelages en fonte de puits après la fermeture et l'ennoyage des mines de charbon. L'attention a été particulièrement portée au cours de cette étude sur le comportement de l'ouvrage pendant la période critique de montée de l'eau et la période qui la suit et qui correspond à la disparition de la pression hydraulique et la stabilisation de l'environnement. L'originalité de cette étude réside dans son côté pluridisciplinaire qui a mobilisé une équipe constituée par des spécialistes en mécanique de roches qui ont travaillé sur l'identification des risques encourus et des conditions de stabilité du cuvelage, et des spécialistes en métallurgie qui ont étudié la composition minéralogique de la fonte utilisée et son comportement au corrosion lorsqu'elle est exposée à l'eau de mine.

MOTS-ClEFS : fonte, cuvelage, ennoyage, stabilité, corrosion

1. Introduction

The closure and flooding of coal mines require the treatment of several aspects mainly linked to the long term stability of the surface, the new hydrogeological water regime and the management of methane. Regarding the first aspect, the behaviour of shafts and the means needed to ensure their stability constitute a major point.

In France, many shafts, particularly in the Lorraine area, have been reinforced when crossing aquiferous strata by a cast iron lining. This technique was used before the development of concrete lining (end of 19th and beginning of the 20th century). The problem arising with mine flooding concerns the behaviour if this reinforcement and its capacity to resist in the long term especially to the corrosion phenomenon induced by a water highly charged with aggressive minerals such as sulphates and chlorides. In case the stability is not guaranteed for at least a period of one century, the shaft should have a complementary treatment, for instance filling with a water resistant grout.

This paper presents the results of a study conducted to answer the question of long term stability of the cast iron lining especially in the critical phase of flooding and the phase corresponding to the disappearance of the water pressure and the stabilization of the chemical environment.

2. Shafts features and main risks

The first phase of the study was dedicated to a review of the archives in order to find the conditions of installation and the design characteristics of the cast iron lining in the two shafts concerned by the stability aspect : Hôpital shafts 1 and 2, period of sinking 1882-1886.

These two shafts were operating until 1918 and were closed in 1971 by installing reinforced concrete plugs placed on the lining heads and anchored in the surrounding rocks. The site has three important constraints which must be taken into account if a special treatment operation has to be decided to guarantee long-term stability :

- the presence of operating constructions very close to the shafts;
- shaft 2 is used as an outlet of methane with a flow rate of around 140 m^3/h, this source may induce difficulties for possible interventions in the shaft;
- the shafts contain many levels and sub-levels which may complicate the operation of treatment.

Starting from the surface, the rocks traversed by the shafts are successively the Trias sandstones with a thickness of around 130 m, the Permian sandstones with a thickness of around 100 m and the carboniferous layers. The aquifer is located in the Trias sandstones and the water table is located 20 m below the surface. The Trias sandstones are primarily constituted by the Vosges sandstones and the tests performed to characterise these rocks highlighted very low mechanical properties (cohesion around 0.1 MPa, friction angle around 40° and Young's modulus around 160 MPa).

The presence of these weak and permeable sandstones required the use of the cast iron lining whose head was installed at the level of the water table and base anchored in the resistant and impermeable Permian sandstones. The rest of the shafts was supported with a masonry lining (Fig. 1).

The stability analysis conducted to point out the main risks and to precise the safety margin showed that there are two major failure mechanisms which can occur and affect the stability of the shafts and the surface. These mechanisms can be induced either by the concrete plug or by the cast iron lining.

2.1 Failure of the concrete plug

From the mechanical point of view, the concrete plug can be modelled as a slab submitted to its weight and to the weight of the upper filling material. Analytical and numerical models taking into account the real shape of the plug and the effect of the surrounding rocks showed that the stresses developed are very low and that the conditions of stability are ensured as long as the concrete preserves its minimal properties (Fig. 2).

The risk of instability will appear in case the reinforced concrete slab would loose its mechanical characteristics under the effect of ageing and mine water corrosion during and after the flooding. The failure of the concrete plug will induce the flow of the backfilling material causing the disappearance of the shaft wall support.

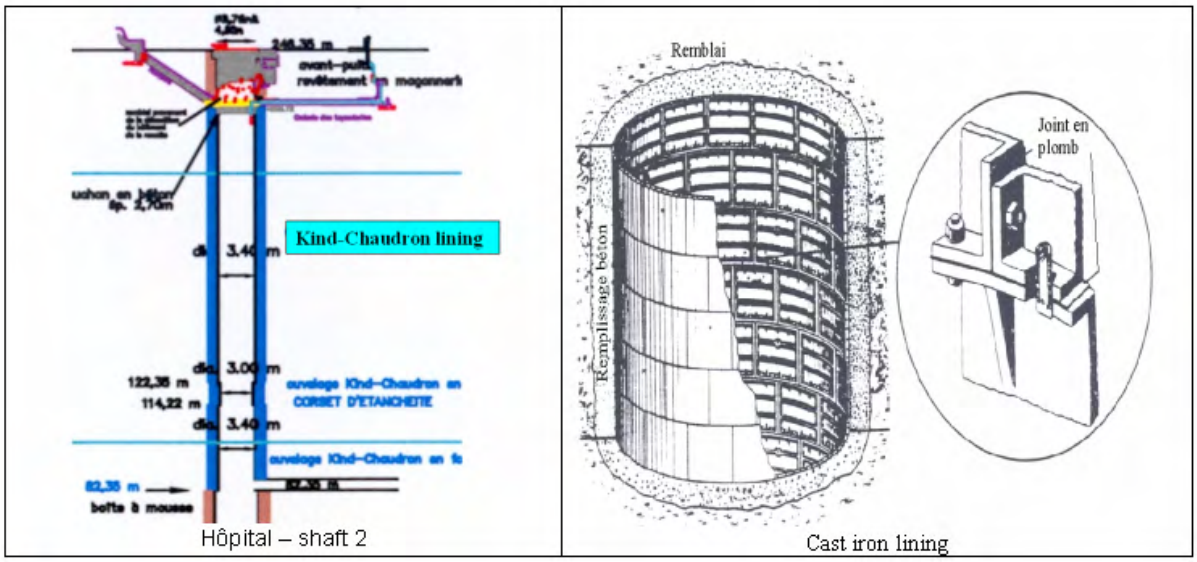


Figure 1. Cast iron lining in the Lorraine shafts

The phenomenon of concrete corrosion could be studied more in detail for a precise evaluation of the risks, but it was suggested for the treatment of this mechanism to reinforce the backfilling material in order to constitute with the concrete slab a homogeneous and coherent plug ensuring the long-term stability of the shafts and the surface.

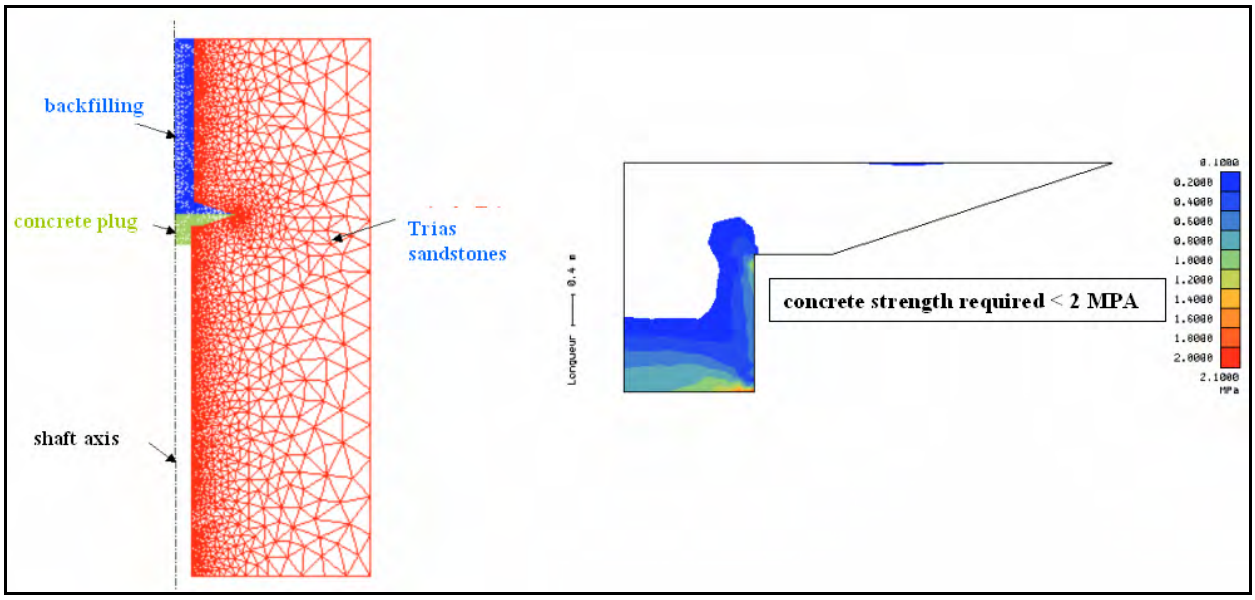


Figure 2. Analysis of the concrete slab stability with a numerical model

2.2 Failure of the cast iron lining

This instability would occur either under the effect of the ground and the water pressures or under the effect of the cast iron corrosion when exposed to the mine water. The potential risks in this case would appear in two different forms (Fig. 3):

- loss of the concrete plug support when the failure appears in the top of the lining : a deterioration of the shaft walls will take place due to the low mechanical characteristics of the Vosges sandstones and their strong sensitivity to water. The instability of the concrete slab would certainly be limited, but it would give passage to the overlying backfilling and therefore the failure could go up on the surface and give place to the

formation of a sinkhole or a subsidence whose extension and localization would depend on the quality of the backfilling and the zones of less resistance in the ground.

- failure of the lining in depth in zones where the state of the cast iron and the geotechnical conditions of the ground are unfavourable. The disappearance of support would let water flowing and leaching the sandstones. The evolution of failure is very difficult to predict. It could go up while following zones of lower resistance and creating one or more chimneys of very irregular form.

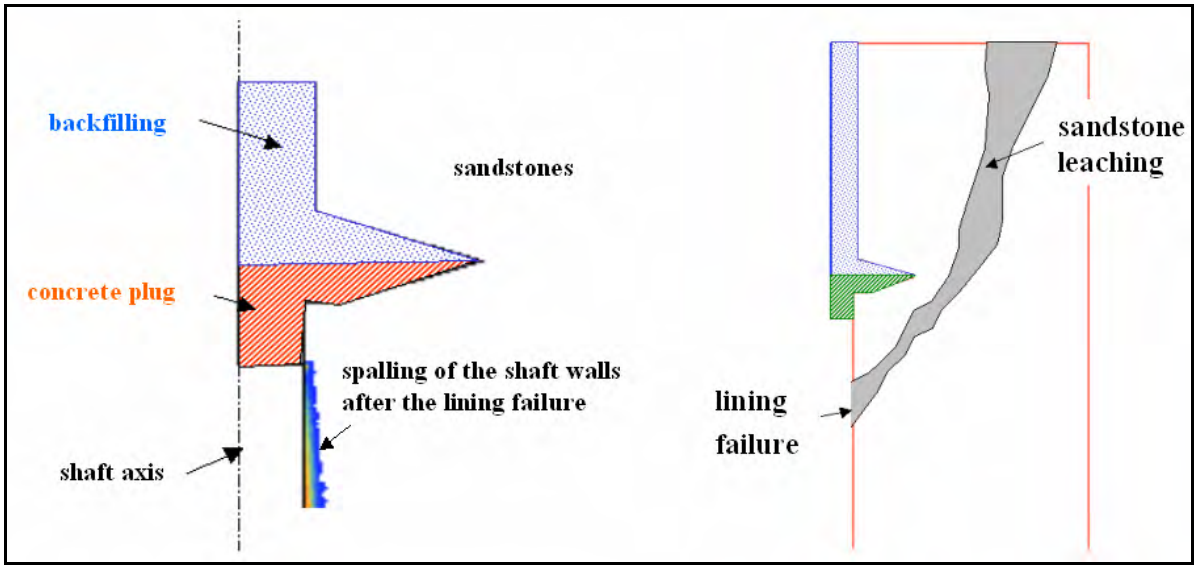


Figure 3. The two risks linked to the lining failure

This quick analysis shows that the overall stability of the shaft and the surface is mainly governed by the stability of the cast iron lining and that a metallurgical study is necessary to forecast the long term behaviour and the risks of corrosion and failure.

It is important at this stage to point out that the critical period presenting the greatest risk of occurrence of the two phenomena of failure described above is the period corresponding to the phase preceding the flooding and the phase of flooding. Once the flooding is finished, the stability conditions would become better and consequently the risks less.

3. Lining design and stability conditions

The document written by J. Chaudron in 1867 who supervised the Hôpital shafts sinking describes precisely the method used for the installation of the lining and the principle of its design. The thickness of the lining was defined according to the formula suggested by Kind and Chaudron:

$$E = 0.02 + \frac{R\,P}{500}$$

where E is the thickness of the cast iron lining in meter, R, the radius of the shaft in meter and P, the pressure applied to the lining in bar. The constant 0.02 m is introduced into this formula by safety in order to guarantee a minimal thickness of the lining.

The general method of a lining design is based on the equation which gives the compressive stress σ developed in the lining according to the external radius R and the internal radius r of the shaft and the pressure applied P ; the thickness E of the lining is thus equal to R-r:

$$\sigma = P \frac{2R^2}{R^2 - r^2}$$

To ensure the lining stability, the stress must be lower than the uniaxial compressive elastic limit σ_E of the material. The thickness E is therefore equal to:

$$E = \frac{E^2}{2R} + \frac{RP}{\sigma_E}$$

The correspondence between the 2 equations shows that the formula suggested by Kind and Chaudron introduces a safety margin on 2 levels. On the first hand, the term $E^2/2R$ was largely overestimated by considering it constant and equal to 20 mm, and on the second hand, the elastic limit of the cast iron was considered very weak (only 50 MPa) compared to its actual value (at least 120 MPa).

This rapid comparison indicates that, from the mechanical point of view, the stability of the lining is ensured as long as the cast iron conserves its mechanical properties. To conclude on the long-term stability, it was then necessary to study the effect of the mine water on the cast iron during and after the flooding phases (risk of corrosion and process of deterioration of the mechanical characteristics). The metallurgical study conducted for this purpose was carried out in three main steps: a bibliographic review in order to characterize the cast iron used in the Lorraine region during the sinking period of the two shafts, a sampling in the cast iron lining for laboratory experiments and a synthesis of the main results obtained enabling to reach a conclusion about the durability of the lining.

4. Metallurgical analysis of the cast iron

4.1 Bibliographic review

In his notice, Chaudron (1867) described the lining to be made by a grey cast iron of a second fusion with fine and homogeneous grains. In the German document of Ledebur (1895), it is found that carbon in the graphite state makes the metal porous and enables the chemical agents to penetrate deeply. It is mentioned also that very graphitic cast iron are characterised by a great resistance to rust when graphite is not in large plates and it even seems that this feature awards the cast iron a great part of its own resistance. This same document gives an average composition of the Lorraine cast iron: carbon 3.8 %, silicium approximately 2 %, manganese approximately 0.6 %, phosphorus 1.8 % and allots a tensile mechanical strength of 120 MPa. (the compressive strength would be higher).

Compared with blast furnace hot metal of the Lorraine area in the 1970's used for steel refining, the second fusion cast iron of the end of the 19th century has a higher silicon content, but is similar to the foundry iron produced by the blast furnaces of Uckange until the beginning of the 1980'. The 1930 monograph of iron alloys, indicates that, due to a better adherence of rust, the corrosion resistance of the cast iron exceeds that of all steels other than stainless.

The modern literature is richer and more quantitative regarding the behaviour to corrosion. The "Practical of Industrial Materials" document indicates that the grey ferrito-perlitic cast iron has a high resistance to corrosion and that is little attacked by water, alkaline and carbonate-ground solutions, but it is less resistant to diluted acids.

The ASM Metals Handbook confirms the features mentioned above and emphasises the low level of corrosion in grounds. It indicates that calcium carbonates can form a protective coating and that among the components of the cast iron, silicon and phosphorus decrease the speed of corrosion.

"Les techniques de l'Ingénieur" indicates that, in the absence of oxygen, water corrosion of the cast iron is very slow and that the atmospheric corrosion does not exceed 0.1 mm per annum. In the absence of oxygen the corrosion of the cast iron in water is quasi-null (justifying the use which is made of this material in hydraulic piping).

4.2 Sampling operation in La Houve Shaft

As the access to the Hôpital shafts was not possible, it was agreed with Charbonnage de France to make an operation of sampling in a cast iron lining in another shaft presenting the same characteristics (same type of lining, same installation procedures, same grounds). The choice was quickly directed towards Shaft 3 of La Houve mine where a visit was organized to observe the state of the cast iron lining and the zones of sampling.

A total of six samples were taken at three different depths in the cast iron lining for the laboratory metallurgical analysis. These samples consist of corroded material obtained by scraping, sawing or coring (Fig. 4). During the visit, no visible deformation was detected in the lining. However, a layer of calamine was observed with a thickness not exceeding 5 mm.

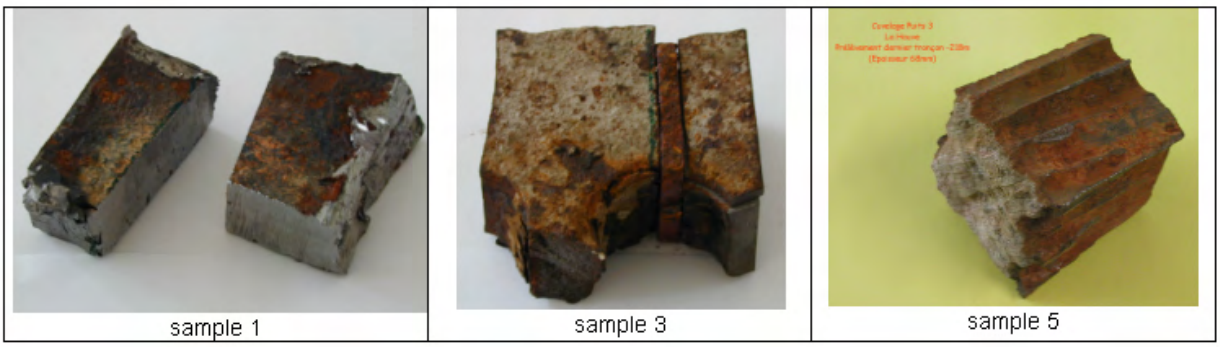


Figure 4. Photos of some samples obtained by cutting with a pneumatic band saw

Different stages of analysis were conducted on the samples. The observations were performed first with naked eyes then with a binocular and finally with an optical microscope. The quantitative microanalysis was carried out using an electron probe microanalyser in order to determine the average and the local (1-2 micrometer resolution) composition as well as the constitutive phases. The corroded material which is separated from the cast iron was also analysed separately by X-ray diffraction for phase identification.

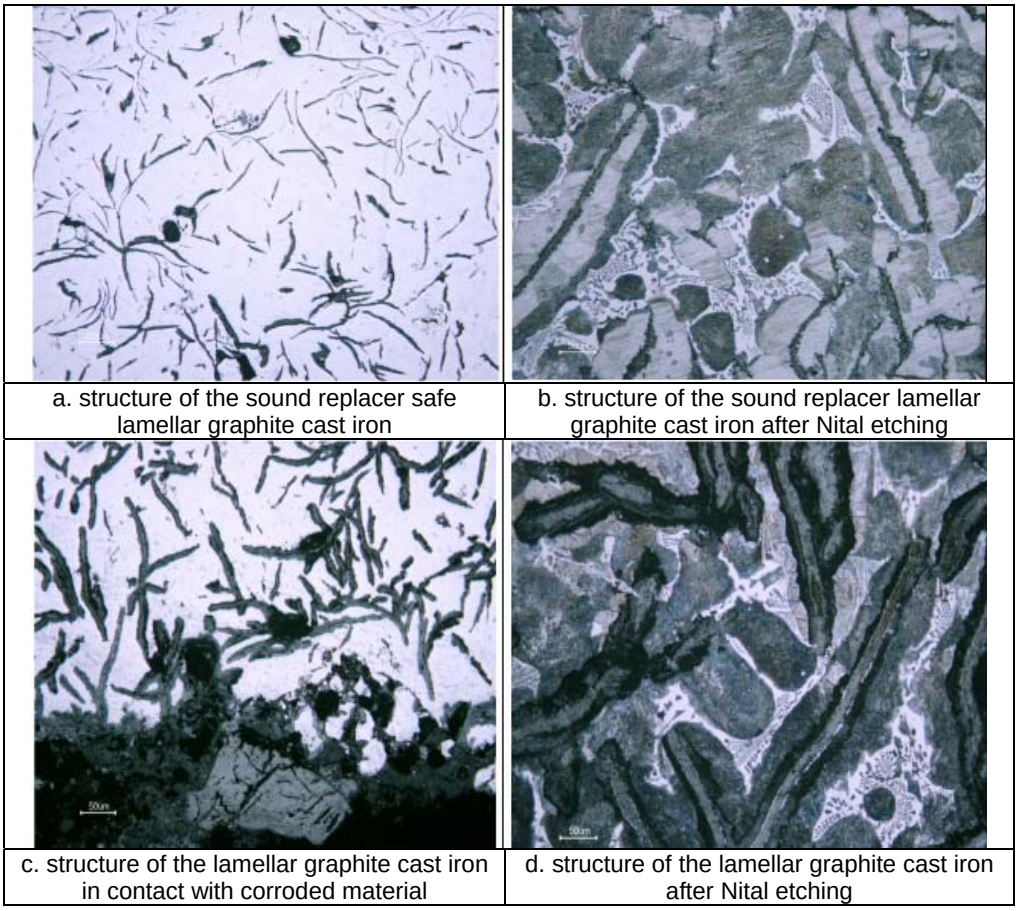
4.3 Results of the metallurgical analysis

The cast iron has a good quality, at least in the part non reached by the corrosion. It does not present porosity, cracks or exogenous inclusions of more than 5 micrometers in the cm^2 observed.

The graphite lamellae, approximately 2 microns thick and 100 microns long, are grouped in balls of 200 microns diameter. In the vicinity of the layer of corrosion, the cast iron is reached by the corrosion which progresses along the graphite lamellae that constitute a percolating network. The thickness of oxides between graphite and cast iron is of a few microns (Fig. 5).

The average global compositions of the two first cast iron samples are rather similar with more phosphorus in one than in the other. The carbon content would rather be less than 4 % for a

phosphorous cast iron which seems to be of eutectic composition. The content of the other elements is rather reliable: silicon approximately 1.6 %, manganese 0.4 %, phosphorus of about 0.5 and 1 % for two samples, sulphur approximately 0.08 % and titanium of about 0.5 % (Fig. 6).



a. structure of the sound replacer safe lamellar graphite cast iron

b. structure of the sound replacer lamellar graphite cast iron after Nital etching

c. structure of the lamellar graphite cast iron in contact with corroded material

d. structure of the lamellar graphite cast iron after Nital etching

Figure 5. Optical microscopy of the safe and corroded cast iron

Beyond the global composition, the cast iron phases were identified. The principal ones are lamellar graphite, ferrite and pearlite. Ferrite contains approximately 1.5 % Si, little carbon (<0.2 %), 0.3 % P and 0.4 % Mn. Pearlite can be distinguished from ferrite only after a metallographic etching with nital reagent. It constitutes the major component and the spacing of the cementite lamellae within the pearlite is around 1 micrometer.

Another relatively abundant phase, but not significantly detected with X-ray diffraction, is the eutectic with phosphorus, called steadite which is slightly distinguished with optical metallography without etching, but clearly in the scanning electron microscope with backscattered electrons signal. The formation of this eutectic terminates the solidification of the phosphorous cast iron towards 950° C and delimits within the structure the size of the eutectic cells (Fig. 7). The local content reaches 12 to 13 % P, 2 % C (whereas the theoretical ternary eutectic is with 7 % P, 2 % C).

One of the bolts which assemble the elements of the lining was also observed and analysed. It consists of soft steel rolled with a dense population of non metallic inclusions. Visible corrosion on the thread remained within acceptable limits.

Adherent layers of corrosion were analysed and observed in contact with the cast iron (Fig. 8). The dominating oxide is Fe_20_3 and carbon is also detected with a content close to that of the cast iron. Other oxides of Mn and Si, were found with low contents together with chlorides of Na, K and Ca as reactions products of cast iron and water.

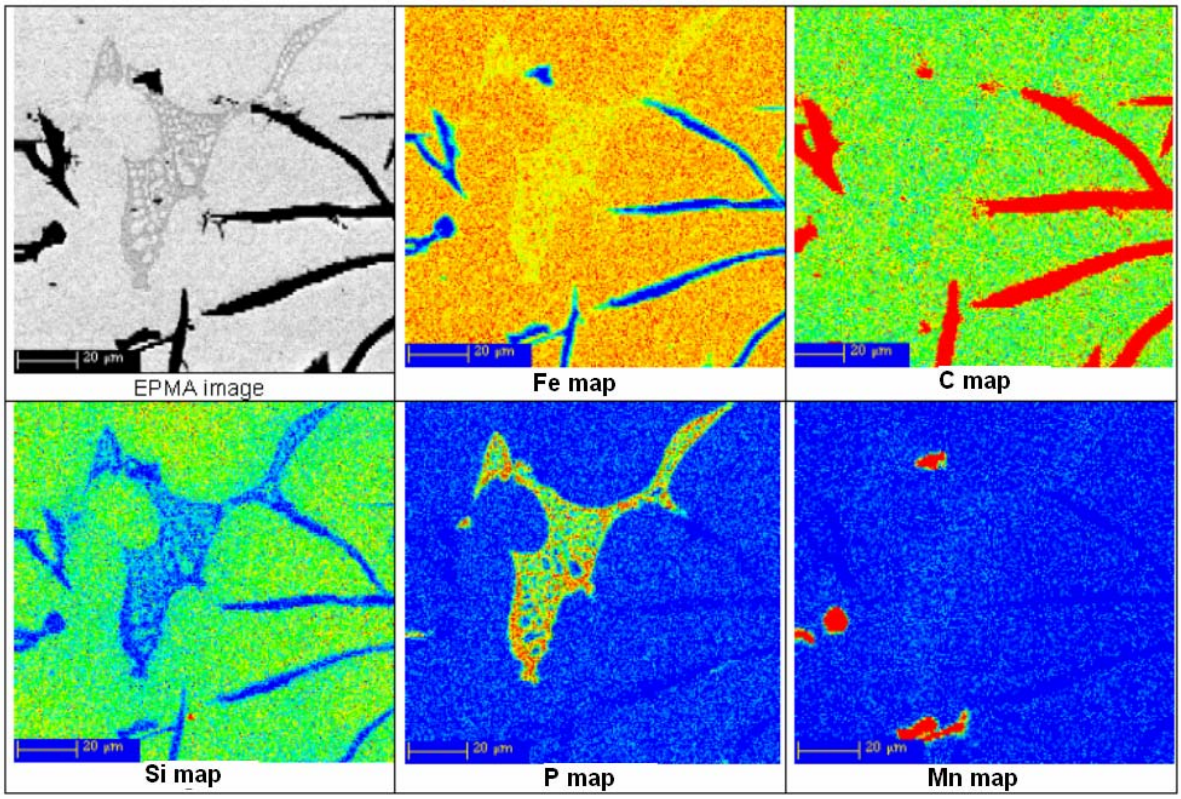


Figure 6. Example of elemental mapping obtained by the electron probe microanalyser showing the ferrous matrix, graphite lamellae and steadite

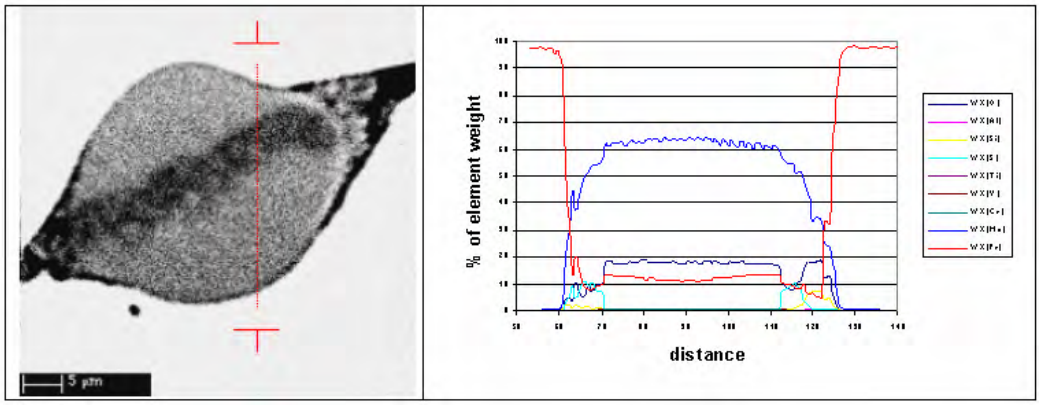


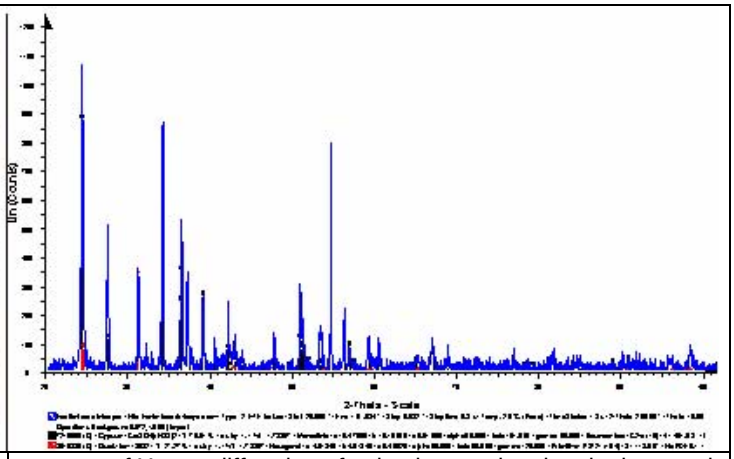
Figure 7. Image obtained with the backscattered electron band and composition profiles derived from the X-ray diffraction (oxide-sulfide inclusion)

Small zones of corroded layers in graphite and graphite lamellae are still present in the oxides. The progression of corrosion circumvents the graphite lamellae and could be of galvanic nature. The phosphorous eutectic (mainly Fe_3P) resists to corrosion, but these vestiges of cast iron do not block the progression of oxidation. The oxide is dense and it adheres to the cast iron and seems to have a reasonable mechanical behaviour.

The X-ray mapping confirmed the presence of potassium and sodium chlorides. X-ray diffraction identifies, in the separated calamines, calcite $CaCO_3$, hydrated goethite Fe_2O_3, and on the free face of calamine, gypsum $CaSO_4H_20$. The literature had presented calcite like a natural protection of the cast iron against hard water corrosion (adherent and waterproof deposit).



stratified structure of the adherent calamine to the cast iron (optical microscopy)



spectra of X-rays diffraction of calamine: scale taken in the metal side (goethite and calcite)

Figure 8. Optical microscopy and X-ray diffraction performed on the calamines

4.3 Synthesis on the metallurgical analysis

The results of the metallographic and analytical expertise performed on the cast iron lining samples are relatively coherent with the bibliographic data. They allow to make an assessment on the durability of the metal structure with respect to corrosion.

The cast iron is obtained after a second fusion and has a lamellar graphite structure. The progression of corrosion is well highlighted in the cast iron, along the graphite lamellae.

Two layers of corrosion are to be distinguished: adherent dense calamine and, beyond a thickness of less than 5 mm, a ventilated and very fragile calamine which contains iron oxides but also species deposited by water (quartz and gypsum). The description of the corrosion process proposed along the graphite lamellae (galvanic corrosion to some extent) is quite identical to that proposed by Ledebur.

The favourable role of phosphorus on the corrosion resistance is highlighted. The maximum speed of corrosion pointed out by literature is 0.1 mm per annum. Over the lifespan of the studied shaft, aqueous corrosion should consume less than 10 mm, which is a pessimistic estimate. Actually the metal consumption on the internal face of the lining would be rather about 0.03mm/year.

5. Conclusions on the long-term stability

Based on the bibliographic review and on the metallurgical analysis of the cast iron over a century in service, the maximum value of the corrosion rate was estimated to be around 0.1 mm/year. According to the security margin adopted during the design in the thickness of the lining and in the mechanical strength of the cast iron, the durability of the cast iron structure with respect to corrosion was assessed to be over at least 100 years. After flooding, the environment will be stabilised, the water will no longer be oxygenated and the mechanical stresses will be reduced. Under those conditions, the behaviour of the cast iron should be more than adequate and the long term stability would be assured.

In spite of a level of risk considered to be low or even very low, recommendations were made for the implementation of a system to monitor the two shaft stability during the critical phase of flooding. As the shafts are not accessible, a surveying operation with a dedicated borehole camera was performed to check the quality of the cast iron lining. This operation confirmed the observations made in the open shaft.

The monitoring solution suggested would consist in manufacturing a system of an umbrella which would be introduced into the shaft until the base of the cast iron lining then unfolded in order to retain the blocks which could fall.

6. References

ASM Metals Handbook, 9th edition, Vol 13

Chaudron J. (1867). *Notice sur l'établissement des puits de la Houillère de l'Hôpital*. Dunod Editeur, Paris

Dunod. *Pratique des matériaux industriels*, vol II, M. Colombié Ed., Dunod, Paris.

Ledebur (1895). *Manuel de la Métallurgie du fer*. Translated in French , Librairie Polytechnique Baudry et Cie, Paris

Sisco. F.T. (1937). *The alloys of Iron and carbon.* Graw Hill Book Company, New York and London

Techniques de l'ingénieur, Vol MB4, Fascicule M380

ENVIRONMENTAL CHARACTERIZATION OF THE ABANDONED KETTARA MINE WASTES (MOROCCO)

HAKKOU Rachid[1,3], BENZAAZOUA Mostafa[2] and BUSSIÈRE Bruno[2,3]

1- EQUIPE DE CHIMIE DES MATERIAUX ET DE L'ENVIRONNEMENT – Faculté des Sciences et Techniques – Marrakech. Univeristé Cadi Ayyad, B. P. 549 / 40000 Marrakech. E-mail : rhakkou@fstg-marrakech.ac.ma

2- UNIVERSITE EN ABITIBI TEMISCAMINGUE, 445 Boul. de l'Université, Rouyn-Noranda, Québec, Canada J9X 5E4. E-mail : Mostafa.Benzaazoua@uqat.ca

3- Canada Research Chair on Rehabilitation of Abandoned Mine Sites. E-Mail: Bruno.Bussiere@uqat.ca

ABSTRACT: *The abandoned high-sulfide mine wastes impoundment at Kettara, Morocco, wherein the tailings and waste rock have undergone oxidation for more than 20 years, was investigated using geochemical and mineralogical techniques. The Kettara waste mine contents significant concentrations of sulphur (1.2 to 14.5 wt%). The main sulfide minerals contain in the mine wastes are pyrrhotite (0 to 1.45 wt%) and pyrite (0.56 to 2.66 wt%). Acid-base accounting (ABA) static test results showed that tailings samples are considered to be highly acid-generating, with an NNP varying from -22 to -453 kg $CaCO_3$/t. The geochemical behaviour of waste rock and tailings from the abandoned Kettara mine were examined by humidity cell tests. The leachates from these tests have low pH (2.9 to 4.2) and high acidity, and sulfate and heavy metal (Cu and Zn) are in high concentrations resulting because of the acidic conditions. The environmental impacts of waste rock are more significant than that of the tailings, which showed natural coating. Indeed, waste rock continued to release acid after 378 days of leaching.*

KEYWORDS: *Mine tailings, Waste rock, Acid MineDrainage, Kettara mine site, Morocco*

RÉSUMÉ : *Les résidus et les stériles miniers issus de la mine abandonnée de Kettara, Maroc, exposés à l'altération pendant plus de 20 ans, ont été étudiés par les techniques minéralogiques et géochimiques. Leur teneur en soufre est élevée et varie entre 1,62 et 14,5 % dont une partie est déjà oxydée. Les principaux sulfures présents sont la pyrrhotite (0 à 1,45 %) et la pyrite (0,56 à 2,66 %). Les tests statiques ont montré que les rejets miniers de Kettara sont fortement générateurs d'acidité et présentent des PNN variant de -22 à -453 kg $CaCO_3$/t. Les essais cinétiques, en cellules humides ont montré que, suite au phénomène du drainage minier acide (DMA), les principaux contaminants dans les eaux de rinçage sont le pH faible (2,9 à 4,2) et les concentrations élevées en sulfates, en fer et métaux lourds (Cu et Zn). Ce sont les stériles qui posent le plus de problème environnemental. En effet, après 378 jours de lixiviation, le ralentissement de leur réactivité à la fin du test est moins important que dans le cas du résidu fin où une passivation naturelle a été observée.*

MOTS CLÉS : *Résidus miniers, Stériles, Drainage Minier Acide, Kettara, Maroc.*

1- Introduction

While mining is an important part of the industrial development in Morocco, it has frequently had, and continues to have, serious environmental consequences such as impacts on soils and water resources. Currently in Morocco there exist relatively few environmental studies on mining sites, and no national program for the rehabilitation of existing sites is presently implemented.

Acid mine drainage (AMD) is one of the most serious environmental concern facing the Morocco's mining and mineral processing industries. This problem is particularly acute for sulfide ore mines that generate wastes (tailings and waste rock) containing sulphide minerals. Oxidation of these

minerals by the ambient air and water, and catalysed by certain microorganisms, produces sulfuric acid that reduces pH and consequently solubilizes the heavy metals. This phenomena is known in the literature as the Acid Mine Drainage (AMD, or ARD for Acid Rock Drainage). Explanations of the chemical reactions by which acid mine drainage is produced from pyrite and other iron sulfide minerals can be found in Aubertin *et al.* (2002). The oxidation of sulfide minerals within mine wastes and workings may continue to release metals into the surrounding environment for decades to millennia (Blowes *et al.*, 1992; Nordstrom and Alpers, 1999; Pyatt and Grattan, 2001; Aubertin *et al.*, 2002). Thus, it is critical to identify in advance mine wastes that could potentially produce AMD in order to implement the appropriate mine waste management strategies for AMD control (SRK, 1989; Ritcey, 1989; Morin and Hutt, 1997; Bussière *et al.*, 2002; Benzaazoua *et al.*, 1998, 2001).

At the abandoned Kettara mine, tailings and waste rock have been weathering for more than 20 years. The field work performed in this study at the Kettara site was carried out in August and September 2003. At this stage, samples were taken to characterize the site and were used for a geochemical study. The primary objective of the research was to determine the acid generating potential of the wastes and the release rate of dissolved metals from the Kettara mine site. Chemical and mineralogical characterization of the wastes is a fundamental step in evaluating the environmental impact of the mine. After the characterization, the prediction of the AMD generation potential was studied on representative samples by acid/base accounting techniques using sulfur analysis and acid-base titration. Humidity cells tests were also performed to determine the rate of acid generation and metal release of two representative samples (one tailings and one waste rock sample) taken at the Kettara mine site.

2- Description of Kettara Mine Site

The abandoned Kettara pyrrhotite mine, exploited by SYPEK corporation, is located approximately 35 km north-west of Marrakech in the core of the central Jebilet mountains (see Figure 1). The mining village of Kettara and the social installations are located downstream of the tailings dump and dams (see Figure 2). According to the latest statistics (2004), the population of Kettara is approximately 2,000. The climate is classified as semi-arid with a mean annual rainfall of approximately 250 mm. It is common for rainfall to occur over short periods and with high intensity. Annual potential evaporation typically exceeds 2500 mm. Average monthly temperatures in the area range from 12° C in January to 29° C in July (ONEM, 1997).

From 1964 to 1981, the mine produced 5.2 Mt of pyrrhotite concentrate containing an average of 29% sulfur sulfide. The Kettara pyrrhotite concentrate was used in the manufacture of sulfuric acid by the company Maroc Chimie 1 (OCP group) located in Safi. Even though the ore reserves were still high, the mine was closed in June 1982, as a result of difficulties encountered in the production of the pyrrhotite and in the roasting unit of Maroc Chimie 1. Corrosion of the mining infrastructure and equipment had also been greatly accelerated by AMD.

Pyrrhotite was extracted from the ore by gravimetric separation (jigs). This activity generated a wide range of particle size fractions in the tailings. It is estimated that more than 3 million tons of mine wastes (tailings and waste rock) were stockpiled in dumps, tailings impoundments, and piles during the mine operation covering an area of about 16 hectares. Mine wastes were deposited without concern for environmental issues. During the mining operations and after the plant ceased production, mine wastes that were deposited were subjected constantly to the process of weathering. Serious AMD has occurred at the Kettara site as seen by the rust-orange colour of the oxidized tailings at the surface. Another environmental implication of the mine wastes is the physical and aesthetic changes of the surrounding environment at the Kettara mine site.

In dry periods, secondary minerals were observed in streams and at the surface of the mine wastes. The presence of these minerals in great quantities shows that the AMD is very active at Kettara (e.g. Alpers et al., 1994; Jambor, 1994). In addition to the phenomenon of AMD, which could be a source of water and soil pollution, the presence of unsafe infrastructures and the risk of catastrophic cavity deformation are also a concern.

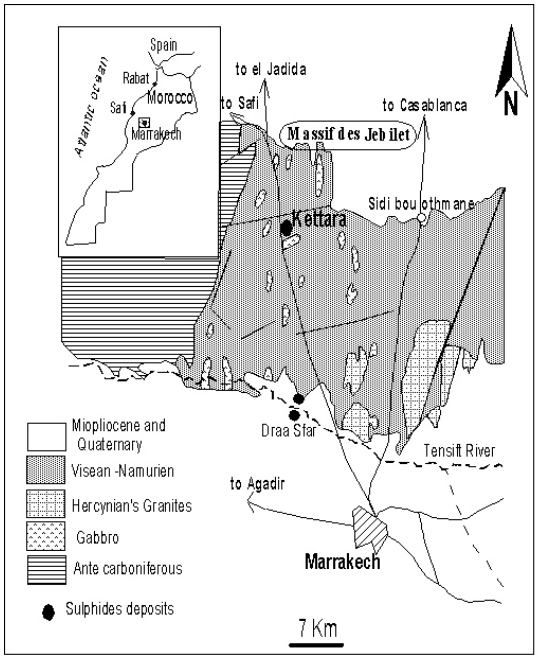


Figure 1. Location and simplified geological map of study area (adapted from Hibti, 2001)

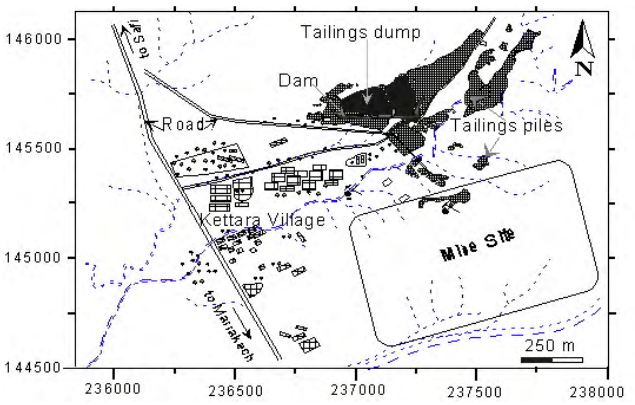


Figure 2. Schematic plan-view of Kettara mine

3. Materials and Methods

3.1. Sampling

At the Kettara mine, mine wastes can be identified into two categories: waste rock (fine gravel) deposited on the dam and piles, and tailings (silt) deposited in the tailings ponds. Two trenches were excavated in the tailings impoundment to a depth of 80 and 85 cm. In each trench, drastic variation in coloration is observed. The tailings profiles show an oxidized zone (ocherous colour) at a depths of 5 to 15 cm below the surface and a relatively unoxidized zone below the oxidation layer. Samples from each horizon were taken at both trenches. Samples were collected from the surface

and at various depths in each trench. Samples R1 to R4 correspond to the profile of the first trench. The sample of fresh tailings (R1) was taken at -80 cm (the reference 0 is the surface). Samples R2 and R3 were taken at -27 cm and -15 cm respectively. Sample R4 was collected at the surface of the tailings in the oxidized zone. Samples R5 to R8 correspond to the profile of the second trench. R5 and R6 are unoxidized tailings. They were collected at -85 cm and -15 cm respectively. R7 was collected in the oxidized zone (-5 cm), and R8 is a sample taken at the surface.

An exploratory trench of 1.10 m deep was also excavated in the principal waste rock dump. As in the tailings, extensive oxidation had occurred at the surface. Seven waste rock samples (Samples S1 to S7) were collected at equal intervals of 20 cm. The first three samples (at elevation 0, -10, and -30 cm) were affected by oxidation while the other samples (taken at -110 cm, -90 cm, -70 cm, and -50 cm) are considered fresh samples.

3.2. Acid-base accounting (static test) and kinetic test procedures

Acid-base accounting (ABA) measures the balance between the acid-producing potential (AP) and acid-neutralizing potential (NP). NP was determined using the modified procedure proposed by Lawrence (1990). This test is based on Sobek Standard ABA (Sobeck, 1978).

In this study, humidity cells tests were performed to assess the geochemical behaviour of the studied samples. Testing in the humidity cells was done following the procedure described by Morin and Hutt (1997). A mixture (1 kg) of dry tailings R1 with 60 wt% of sandy silica was placed in a humidity cell measuring 6 cm in diameter and 30 cm in height. The inert silica was added to increase the hydraulic conductivity of the tailings and hence facilitate water percolation. It is assumed here that silica will not dissolve or react during the one year test. Another humidity cell, 25 cm in diameter and 30 cm in height, was run to investigate the geochemical behaviour of the waste rock; approximately 1.83 kg (dry weight) of waste rock S1 was placed in this humidity cell. The experiment was run for 52 cycles (378 days). A full cycle consisted of 3 days of dry air at 1 L/min, 3 days of humid air at 1 L/min, and the leaching of the cells on the seventh day. The leaching was done by inundation and soaking of the waste for 4 hours with 500 mL of deionized water.

3. 3. Analytical methods

The chemical composition (Al, As, B, Ba, Be, Bi, Ca, Cd, Co, Cr, Cu, Fe, Mg, Mn, Na, Ni, Pb, S, Se, Zn, and SO_4) of the different tailings was analyzed with a Perkin Elmer Optima 3100 RL ICP-AES following a total HNO3/Br_2/HF/HCl digestion. Dilute HCl was used to extract sulfates and the solution obtained was analyzed by ICP-AES. Si and K were analyzed at the SGS Canada Inc. laboratory in Rouyn-Noranda. Content was determined by ICP-AES.

The sample's particle size distribution was determined using a Malvern Mastersizer laser particle size analyzer. The solid grain relative density (D_r) was measured with a Micromeritics Accupyc 1330 helium gas pycnometer. For the determination of specific surface area, SBET measurements of the powders were performed with Micrometrics Gemini III 2375 apparatus.

The initial tailings mineralogy was determined by a combination of X-ray diffraction spectroscopy (XRD) and Scanning electronic microscopy (SEM). XRD analyses were carried out by using a Bruker AXS D8 Advance diffractometer equipped with a scintillation detector and Co Kα radiation. The data were collected for angle between 5-70° by steps of 0.005° at a count time of 0.5 s per step. The use of the JCPDS database allows qualitative analysis (e.g., phase determination), while Rietveld method was used for the quantitative analyses of the identified phases. These phases were quantified within 0.5% error. A scanning electron microscope (SEM) equipped with a microanalysis system (Energy Dispersive Spectroscopy—EDS) was also used to study polished sections of the

mine wastes. The SEM is a pressure vacuum Hitachi S-3500N equipped with backscattered and secondary electron detectors and a Link Isis microanalysis system from Oxford Instruments.

For each kinetic test, leachate samples were filtered with a 0.45 µm nylon mesh filter immediately after collection. Metals and sulfate were analyzed by ICP-AES. Alkalinity and acidity (expressed in mg/L of $CaCO_3$) were measured by acid-base titration, to a pH of 4.5 and 8.3 respectively. The leachate's pH was measured by pH electrode with temperature compensation (Orion model 91-57). Redox potential was determined with an Orion Pt/Ag/AgCl electrode (model 920A). The results were then corrected for the standard hydrogen electrode (SHE) to obtain Eh (expressed in mV). Conductivity was determined with a conductimeter HANNA HI 8733.

4. Results and Discussion

Chemical, physcal and mineralogical properties of the mine wastes

Results of the chemical analysis are given in Table 1. As shown in this table, chemical composition varies with depth. The important constituent determining the reactivity of the tailings is the sulfur. The tailings present the highest contents of S (2.91 to 14.5 weight percent (wt%)). However, a part of the analyzed sulfur is in sulfate form, especially for the oxidized samples R4 and R8. The waste rock contains less sulfur than the tailings (1.62 to 3.66 wt%). Moreover, contrary to what was observed for the tailings, the oxidized waste rock (S7) shows higher concentration of sulfate than the fresh waste rock (S1). The iron, which is associated with the pyrrhotite and pyrite, is present in high quantities (19.3 to 40.7 wt%). The mine wastes are characterized by high quantities of magnesium (1.59 to 5.06 wt%). However, calcium is present in quantities not exceeding 0.7 wt% (between 0.35 to 0.7 wt%). In addition, silicon and aluminum are dominant elements. The silicon (6 to 15 wt%), aluminum (1.07 to 7.8 wt%), sodium (0.35 to 0.52 wt%) and potassium (0.15 to 1.18 wt%) contents indicate the presence of a relatively significant amount of phyllosilicated minerals. Table 1 shows the content of some trace elements in the different tailings materials: Mn (290 to 1200 ppm (mg/kg)), Cu (1100 to 4200 ppm), Zn (130 to 460 ppm), Cr (220 to 370 ppm), Pb (40 to 130 ppm), Co (20 to 230 ppm), As (0 to 180 ppm), Cd (50 to 90 ppm), and Ni (0 to 30 ppm).

The results of the static tests show that all the samples have no NP in accordance with the absence of neutralizing minerals such as carbonates. Based on the sulfur sulphide content, the AP values are between 51 to 453 kg $CaCO_3$/t. The NNP values range from -453 to -22.5 kg $CaCO_3$/t. Using the criteria of Miller *et al.*, (1991) or the criteria of Adam *et al*., (1997) based on the NP to AP ratio, all of the Kettara samples are potentially acid-generating.

For all materials, the main minerals found by the DRX analysis were chlorite-serpentine (Mg, $Al)_6(Si, Al)_4O_{10}(OH)_8$ (0.91 to 34.5 wt%), goethite (FeO(OH)) (3.49 to 68 wt%), quartz (SiO_2) (6 to 43.5 wt%), talc $Mg_3Si_4O_{10}(OH)_2$ (7 to 16 wt%), and muscovite $KAl_{2.20}(Si_3Al)_{0.975}O_{10}((OH)_{1.72}O_{0.28}$ (0.8 to 8 wt%). Another mineral, albite ($NaAlSi_3O_8$), presents low quantities (0 to 3.48 wt%). The carbonate content of minerals in the various samples varied from practically 0 to a maximum of 1 wt%; the main carbonate is calcite. X-ray diffraction data also indicate that the main sulfide minerals were pyrrhotite and pyrite. In the tailings, the pyrrhotite and pyrite contents are almost identical and they can reach up to 2% in the case of the R5 sample. These sulfides are accompanied by small amounts of chalcopyrite (0 to 0.45 wt%), and small amounts of galena and sphalerite.

Secondary minerals were also identified by XRD analysis. Concentrations of jarosite (K, $H_3O)Fe_3(SO_4)_2(OH)$ in the oxidized tailings sampled near the surface (R4 and R8) are significant (between 1.22 wt% and 11.4). High contents of gypsum ($CaSO_4.2H_2O$) were also detected in these samples. These secondary phases would come from the preliminary oxidation of the mine wastes of Kettara, as confirmed by the sulfate content in the samples (see Table 1). This oxidation in the

tailings dump is confirmed by the high concentration of iron oxyhydroxides represented by the goethite (0 to 68 wt%). The goethite is the dominant oxide in most samples; goethite abundance decreases with depth. Trace amounts of magnetite (0 to 0.73 wt%) were also detected.

Table 1. Chemical composition of the tailings studied

		Wt%														Wt ppm								
Sample	**Depth (cm)**	**S_{total}**	**$S_{sulfure}$**	**S_{SO4}**	**Ca**	**Si**	**Mg**	**Na**	**K**	**Ba**	**Fe**	**Al**	**B**	**Ti**	**P**	**Cu**	**Zn**	**Pb**	**As**	**Cd**	**Co**	**Cr**	**Mn**	**Ni**
R1	**80**	3.51	2.41	1.10	0.35	15	5.06	0.44	1.18	0.04	19.3	7.83	0.39	0.19	0.08	1930	430	90	0	50	60	270	1210	30
R2	**27**	2.91	0.79	2.12	0.69	15	4.1	0.45	0.36	0.01	26.8	3.2	0.26	n.d.*	n.d.	1890	130	80	0	60	40	270	480	10
R3	**15**	4.92	2.78	2.14	0.47	10	1.59	0.44	0.21	0.01	39.6	1.07	0.32	n.d.	n.d.	1380	330	100	0	90	30	350	290	0
R4	**0 (surface)**	9.47	2.96	6.51	0.46	6	2.17	0.39	0.20	0.01	28	2.34	0.33	n.d.	n.d.	2600	200	40	0	60	70	270	750	10
R5	**85**	14.5	13.63	0.87	0.41	10	2.18	0.35	0.16	0.01	40.7	3.07	0.26	n.d.	n.d.	4200	430	60	180	90	230	370	770	20
R6	**15**	5.6	4.00	1.64	0.50	13	5.24	0.45	0.50	0.02	22.1	6.3	0.39	0.16	0.068	3000	460	90	20	60	80	280	1130	30
R7	**5**	4.1	1.50	2.62	0.70	12	2.52	0.52	0.30	0.01	34.1	1.6	0.44	n.d.	n.d.	1000	190	130	30	80	20	310	360	0
R8	**0 (surface)**	9.95	3.50	6.45	0.50	7	2.13	0.41	0.16	0.01	31.4	1.57	0.25	n.d.	n.d.	1720	340	100	40	70	60	290	750	10
S1	**110**	3.22	2.49	0.73	0.86	20	3.57	0.32	0.66	0.02	17.4	6.55	0.06	0.28	0.08	1240	470	70	120	30	70	270	1090	70
S2	**90**	2.79	2.10	0.70	0.51	19	4.21	0.30	0.38	0.01	17.9	6.99	0.09	*n.d.	n.d.	1220	330	10	0	30	50	330	1130	90
S3	**70**	2.54	0.84	1.70	1.77	18	3.09	0.41	0.53	0.02	17.8	6.03	0.09	n.d.	n.d.	2660	500	30	0	30	40	250	960	60
S4	**50**	1.62	0.72	0.90	0.70	19	2.7	0.29	0.39	0.02	20.1	5.22	0.06	n.d.	n.d.	1550	430	30	70	30	30	320	790	70
S5	**30**	2.32	1.21	1.11	0.83	19	3.01	0.35	0.58	0.02	18.8	5.82	0.08	n.d.	n.d.	2240	240	50	20	30	30	240	890	50
S6	**10**	2.14	1.48	0.67	0.59	20	3.43	0.27	0.32	0.01	18.9	6.14	0.07	n.d.	n.d.	1110	300	80	20	30	50	260	930	60
S7	**0 (surface)**	3.66	3.35	0.31	0.28	17	3.02	0.27	0.36	0.01	22	5.99	0.09	n.d.	n.d.	1780	460	40	440	30	50	250	990	40

* n.d. not determined

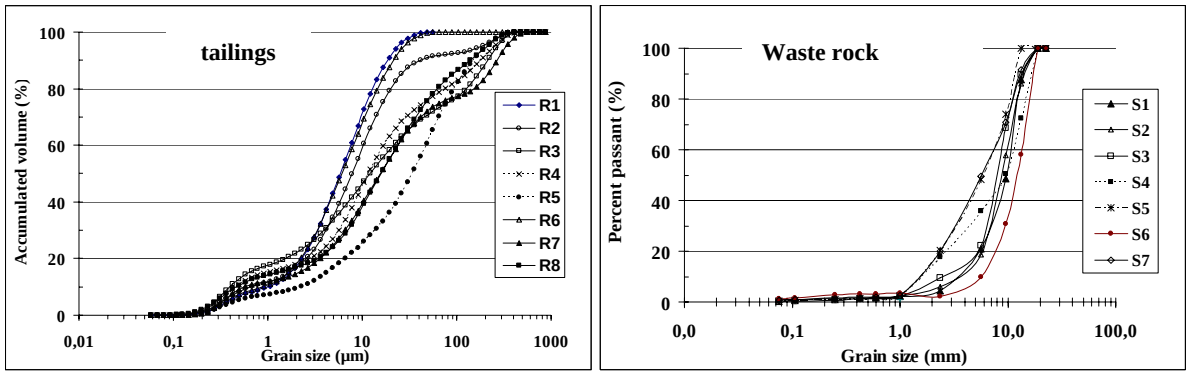


Figure 3. Size distribution for Kettara mine wastes

The non-observation of certain secondary minerals (like jarosite) in waste rock samples could be related to the fact that water flow is much greater in waste rock piles than in the tailings impoundment because of the coarser grain size distribution (more details below). The sulfates produced by the oxidation of sulfides are evacuated progressively without being able to concentrate (and precipitates) in water porosities.

The fluoroapatite ($Ca_5(PO_4)_3F$) and ilmenite (TiO_2) were identified by SEM. This correlates closely with the concentration of P and with ICP-AES analysis (see Table 1). In addition, neutralizing minerals such as calcite or dolomite have not been identified by our SEM observations.The results of DRX and SEM combined with the chemical analysis show that in the tailings of Kettara, magnesium is not associated to carbonates but rather to silicate minerals (chlorite and talc). Al is bonded with the chlorite, muscovite, and with feldspar; Si is associated to quartz, chlorite, muscovite, albite, and talc; Na is related to albite; K is associated to muscovite; Ca is present in the form of calcite or gypsum.

Figure 3 presents grain size distributions of the different studied mine waste samples. The tailings have grain size distribution typical of fine tailings from a hard rock mine (Vick, 1983; Aubertin *et al.*, 2002), with a D_{10} ranging from 0.37 to 2.09 µm and D_{80} between 12 and 150 µm. The mean particle sizes range from 7.69 to 65.39 µm. The solid grain relative densities (D_r between 2.43 and 3.32 g/cm^3) vary depending on the sample mineralogy (presence of sulfide minerals) while the specific surface area (3.2 to 20.8 m^2/g) reflects the particle size distribution and the presence of some phyllosilicates well known for their high specific surface. The fine grain size of the mill tailings leads to a large ratio of surface area to mass, hence significantly increasing the availability of sulphide minerals to oxidation. Figure 3 also shows that the Kettara waste rock (S1 to S7) have a coarse texture and has a similar grain size distribution than a fine gravel. The D_{80} is between 10.5 mm and 13 mm. The solid grain relative densities are relatively high for all samples of waste rock, ranging from 2.82 to 3.15 g/cm^3. Generally, larger sulfide content leads to higher values of D_r.

Geochemistry of leachates from humidity cell

The results of the water quality analysis for both kinetic tests are presented in this section. They include the water quality of the percolated leachate for the 52 cycles. The evolution over time of the dominant dissolved constituents and parameters involved in the neutralization and oxidation processes are presented in the figures. Figures 4a to 4o show the evolution of pH, Eh, conductivity, acidity, SO_4^{2-}, Ca, Mg, Mn, Si, Al, Na, K, Fe, Cu, Zn, and Co in the leachates from the humidity cell tests done on samples R1 and S1. The other elements (Cr, As, Cd, Ni, Pb, Mo, and Ba) are in very low concentrations or below detection limits for the ICP analysis (not presented here). The plotted values do not take into account the volume of the recovered waters or the weight of the solid sample.

As can be seen in Figure 4, the geochemical behavior of the two mine wastes is similar. After the first cycle, the leachate presents high concentrations. These high initial concentrations can presumably be related to dissolution of ultra-fine particles (Furrer and Stumm, 1986; Schott *et al.*, 1991) and dissolution at highly reactive surface sites on the fresh mineral surfaces (Wehrli, 1989). Depletion of ultrafines can be detected by the particle size distribution analysis at the post-testing characterization stage. The initial rapid dissolution can be observed for all elements and is much more pronounced for the waste rock. An additional explanation for the rapid initial dissolution is that some of the sulfides may have oxidized before the onset of the experiments. Adsorbed weathering products may then be rapidly released when the particles are immersed in water.

Figure 4a shows that for the first cycles of the experiment, the pH of the waste rock (S1) is as low as 3.1, and as low as 3.6 for the tailings (R1). The pH decreases to very acidic values (pH below 3) until the end of the experiments for S1. After 78 days in the humidity cell R1, the pH increases and

becomes stable at values between 3.25 and 3.65. These pH values are indicative of strong microbiological activity (Fe-oxidizing bacteria). The Eh ranges from 478 to 825 mV, attesting the presence of an oxidant media favorable to sulfide oxidation. The conductivity values measured on the flushed waters are often high (490 to 4390 μmhos), attesting the significant mineral dissolution. This activity is governed by oxidation and neutralization reactions.

The main acidity is generated in the leachates by the oxidation of metallic sulfide. For the tailings R1, after approximately 70 days, the acidity varies between 614 and 2245 mg $CaCO_3$/l and then decreases to very low values at the end of the experiments (figure 4c). Sample S1 produces higher acidity than R1 (3199 mg $CaCO_3$/l). It is also worth mentioning that all samples show zero alkalinity.

The sulfates are produced mainly by the oxidation of sulfides. Atmospheric oxygen and dissolved oxygen in water reacts with the sulfide minerals between the two flush cycles. Sample R1, which was tested for a longer time in the humidity cell, shows a clear decrease in sulfate production (figure 4d). After 3 cycles, the sulfate concentration reaches 9400 mg/l and decreases over time. For the tailings, only 40% of the original amount of S had been released into solution. During a kinetic test, the main variables that can influence the geochemical composition of the leachate are the depletion of the reactants, depletion of ultra-fine particles, precipitation of secondary minerals (Aubertin *et al.* 2002), and coating of the reacting minerals' surfaces by secondary phase (Cruz *et al.* 2001). However, this phenomenon was not observed in the case of waste rock (Sample S1). Due to their larger particle size, migration of water and oxygen in waste rock is rapid which increases the oxidation rate and reduces the possibility of secondary mineral precipitation (and thus coating of the sulphide minerals). It should also be noted that the evolution of sulfates in the leachates over time follows closely that of acidity.

The evolution of Mg and Mn in the flushed waters show a close correlation with sulfates (figures 4f and 4g). These metals are associated to some mineral such as chlorite and/or talc that could contribute in some extent to the neutralization of the acid produced. The geochemical behavior of Ca is different to that of Mg and Mn, as clearly demonstrated in Figure 4e. This can be explained by the fact that in Kettara mine wastes, magnesium and calcium are not associated to the same mineral. The calcium could come either from calcite or gypsum, or from the dissolution of apatite, as determined by the SEM analysis, while the magnesium is associated to chlorite and talc.

The aluminosilicate dissolution is negligible in the studied samples as demonstrate by the very low Si, Al, Na, and K concentrations within the flushed water (Figures 4h to 4k). For this study, it can be assumed, as it will be demonstrated, that the neutralization processes are not controlled mainly by carbonate dissolution but rather by aluminosilicate minerals. The very low concentrations measured in solution attest to the negligible silicate contribution to the neutralization processes.

The results of DRX and SEM combined with the chemical analysis show that in the mine wastes of Kettara, phases like chlorite, muscovite and albite control Al concentration. Si is essentially controlled by quartz, chlorite, muscovite, albite, and talc dissolution while Na and K are respectively controlled by the albite and muscovite presence. In general, it is considered that silicates have a minimal contribution to the acid neutralization process because of the slow dissolution kinetics of most of these phases compared to the oxidation of sulfides (Jambor *et al.*, 2002). Kwong (1993) classified minerals into groups of different reactivity and assigned relative reactivity values to each group. At pH 5, the dissolution or alteration of the remaining silicates in the Kettara tailings could be classified in order of importance as follows: talc and chlorite (intermediate weathering) > albite (slow weathering) > muscovite (very slow weathering). This explains the lower concentrations of Na and K which are mainly controlled respectively by albite and muscovite dissolutions. Also, K and Si (Figures 3h and 3k) do not show similar temporal variations in the leachates than the other parameters. This indicates that the dissolution of K could

also be controlled by secondary phases like jarosite. The complex assemblage of minerals controlling the Si concentration could explain the different behavior of this element.

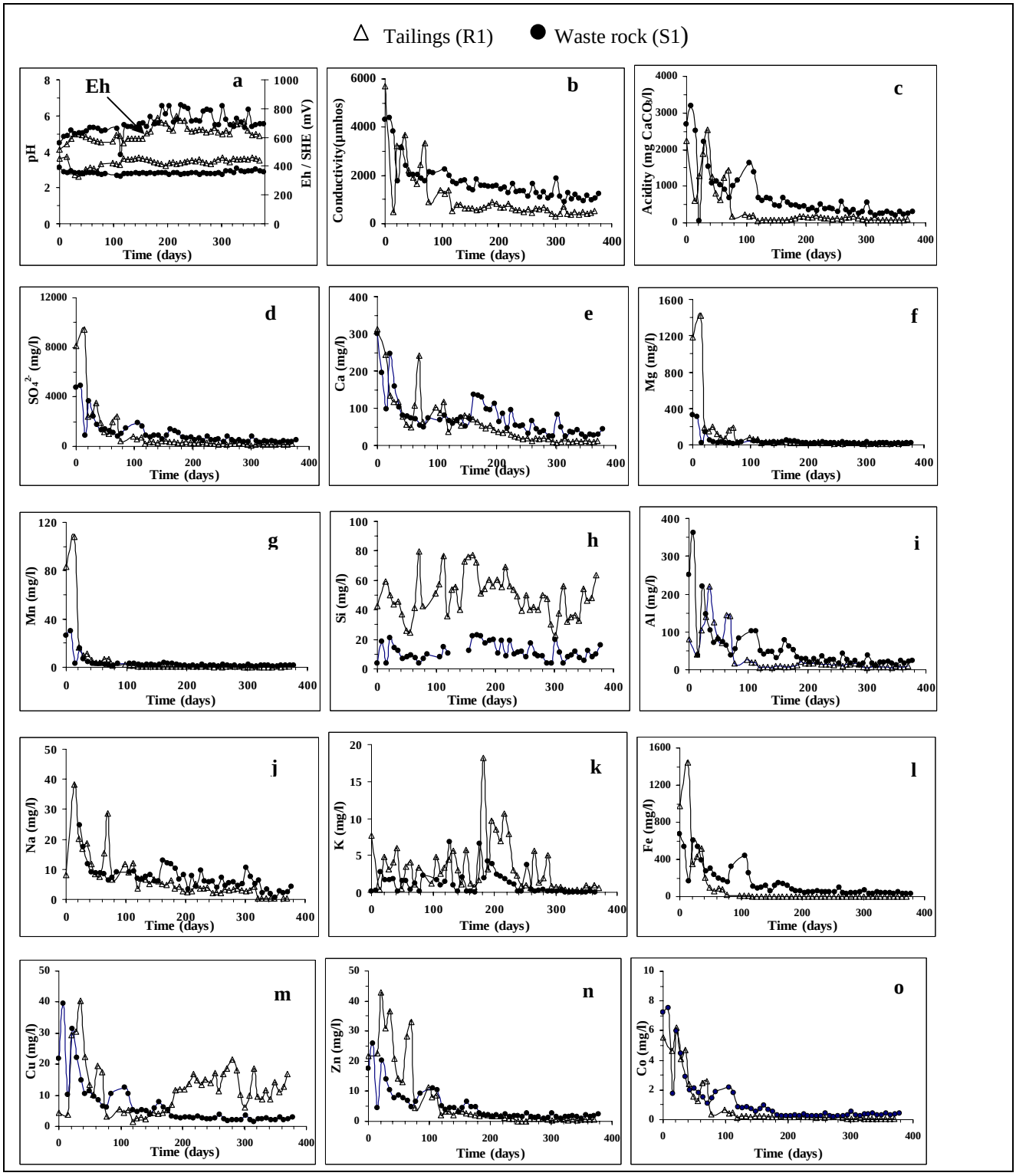


Figure 4. Water quality corresponding to humidity cell tests done on samples R1 and S1

The dissolution reactions of aluminoilicates can reduce acidity. Nevertheless, reactions with silicate minerals are relatively slow, so they typically consume only a small part of the acidity present in the solution (Crouse and Rose, 1976). The normalized NP values in kg $CaCO_3$/t of muscovite (mica group), talc, and chlorite are 0.14, 0.6, and 1.5 respectively. These values are measured using the

Sobek test and normalized to the surface area (Jambor *et al.*, 2002). The chlorite dissolution can consume acidity. Even so, Al and Fe released by dissolution will generate acidity upon hydrolysis.

Figures 3l to 3o show the concentration of Fe, Cu, Zn, and Co in solution with time. Low concentrations in Pb, Cd, Cr, and Ni (< 1mg/l or below detection limit) were observed. Iron concentrations are controlled by a complex assemblage of minerals including pyrrhotite, pyrite, chalcopyrite, goethite, and magnetite. Figure 3l shows that the iron concentrations in flushed waters from the studied samples vary between 15.1 and 1440 mg/l. These values are more than three times lower than the theoretical values obtained from the stoichiometric oxidation of pyrite or pyrrhotite. Indeed, the mean molar ratio Fe/SO_4^{2-} is 0.19 for R1 and 0.32 for S1. This suggests that iron precipitates in the humidity cells as iron oxyhydroxides. In fact, the dissolved ferric iron may contribute little to the sulfide oxidation because of its *in situ* precipitation. The characteristic orange color of iron (III) phases observed in the humidity cells, suggesting that precipitation was occurring, may explain the decrease in the cumulative release of iron in the leachates. This will be confirmed with the post-testing characterization of the humid cells (results not presented here).

Concentrations of Cu and Zn in the flushed water reached values as high as 40 and 43 mg/l (see Figures 5m and 5n). The oxidation of chalcopyrite is the primary source of dissolved Cu in the leachates, and sphalerite is the source of Zn. After 32 cycles of testing, more than 77% of Zn and 32% of Cu originally present in the tailings had been released to solution. This confirms the high weathering rate of sphalerite. The concentration of Co varies between 0.1 and 6.2 mg/l (figure 5o).

To evaluate the ability of a kinetic test to simulate acid production and consequent neutralization, the cumulative loads of Ca, Mg, and Mn (neutralization by-products) are plotted against the cumulative SO_4^{2-} (acid production product). Therefore, if neutralization is in response to acid production, Ca+Mg+Mn versus SO_4^{2-} plots should be linear as long as the reactants are not depleted and precipitation is not significant (Benzaazoua *et al.*, 2001).

Figure 5 shows the time evolution of cumulative release of SO_4^{2-} and the sulfide oxidation rate defined as the mass (mg) of SO_4 produced by sulfide oxidation per unit mass (kg) of solid material per unit time (week) (Morin and Hutt, 1997). Figure 5a shows that the cumulative release of sulfate (for the R1 sample) increased significantly until day 100. This period also corresponds to the period during which the sulfide oxidation rate was very high (between 2000 and 8000 mg SO_4/kg/week). The empirical classification scale for sulfide oxidation rates in mine wastes (Li, 2000) shows these rates to be very high and the tailings from Kettara to be highly acid-generating. After Day 100, the amount of sulfate in solution remained relatively constant, which suggested that sulfide weathering had greatly decreased or even ceased: the oxidation rate was low and varied between 600 and 78 mg SO_4/kg/week. This slightly lower oxidation rate could be explained by the depletion of ultra-fine particles and passivation of the reacting minerals' surfaces by secondary phase coating. The cumulative curve of SO_4 (figure 4d) confirms this phenomenon.

Sample R1 produced much higher concentrations of both acidity and sulfate than sample S1. Sample S1 shows a mean oxidation rate of 5379 mg/kg/week. This value is lower than the value obtained for sample R1. However, as can be seen from Figure 5c, the accumulation of released sulfates increased continuously throughout the experiment, and the waste rock continues to release acid after 378 days of leaching. Figure 5c also shows that during the first 64 days, the oxidation sulfide rate was very high (between 2400 and 560 mg SO_4/kg/week) then decreased to relatively low values (500 to 120 mg SO_4/kg/week). These results indicate that the coating phenomenon is less important for the waste rock than for the tailings.

The cumulative mass of sulfates measured in the flushed waters are plotted versus the cumulative amount of calcium, magnesium, and manganese. Sulfates represent the main oxidation product while the term Ca+Mg+Mn represents the main carbonate or silicate dissolution product. The obtained curves, called oxidation-neutralization curves, are shown in figures 5b and 5d. The Kettara

mine wastes show a linear-shaped oxidation-neutralization curves in both R1 and S1 humidity cell tests. The neutralization rate, which can also be defined as the slope of the obtained curves, varies between 0.19 and 0.10. These values are lower than those obtained generally for neutralization by carbonate dissolution (Benzaazoua *et al.*, 2004), which vary between 0.36 and 0.42.

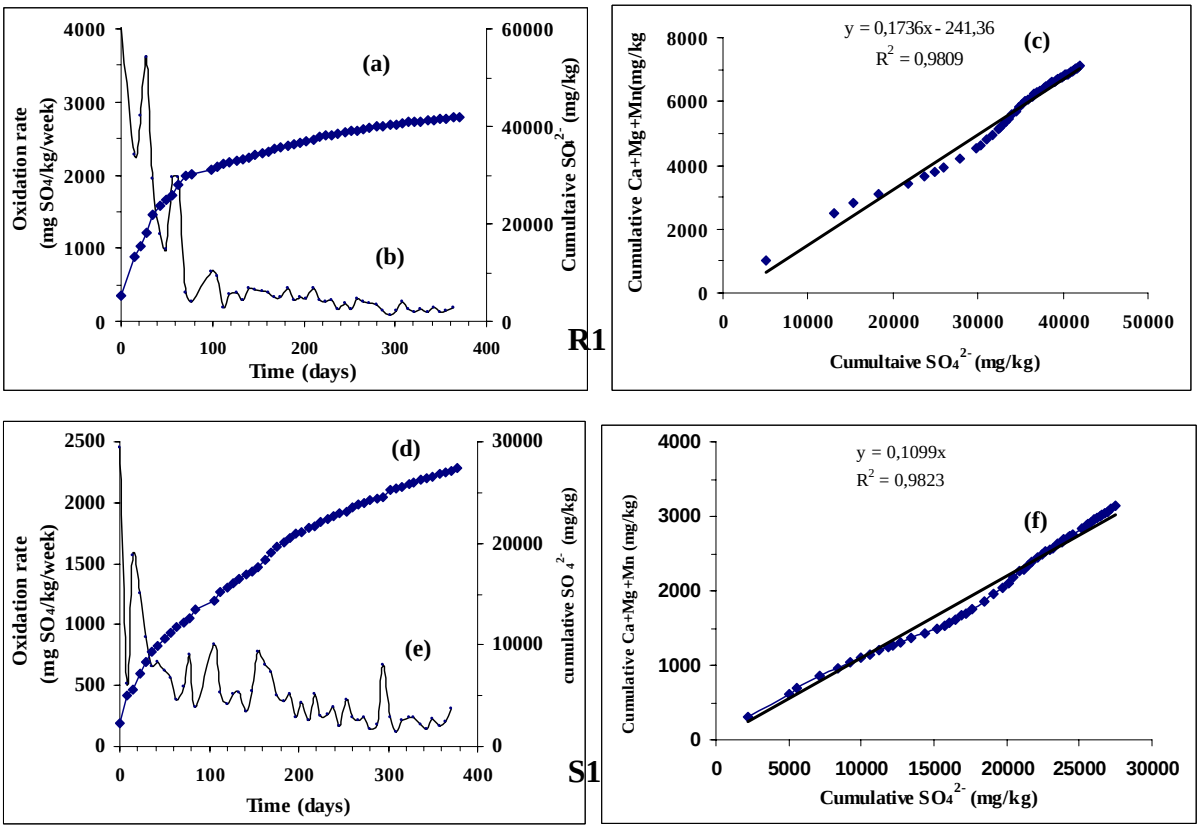


Figure 5. Evolution of cumulative sulfate loads, sulfide oxidation rate and neutralization curves obtained from water quality corresponding to humidity cell tests done on samples R1 and S1

5. Conclusion

At the Kettara mine site(Morocco), an abandoned pyrrhotite ore mine located in a semi-arid climate, more than 3 million tons of mine waste (tailings and waste rock) were deposited at the surface without concern for environmental issues. These sulfidic mine wastes produce AMD. The tailings present the highest contents of S (1.2 to 14.5 weight percent (wt%)). The main sulfide minerals in the wastes are pyrrhotite (0 to 1.45 wt%) and pyrite (0.56 to 2.66 wt%). The NNP for both samples is negative, indicating that all tailings are considered to be acid-generating, with an NNP varying from -22 to -453 kg $CaCO_3$/t.

Leaching tests performed on two representative samples in humidity cells showed that the leachates water quality is typical of AMD with low pH values, high acidity, and high concentrations in sulfate and heavy metals. Due to their larger particle size, the environmental impacts of waste rock is more important than that of the tailings; This is in agreement with field observations. Indeed, in the waste rock, the upper part of the profile is highly oxidized (75 cm). However, the alteration in the tailings dump does not extend more than 5 to 15 cm in depth from the surface. This suggests that the Kettara mine wastes will continue to release acid for a long time, at a slower rate for tailings and higher rate for waste rock.

The conclusions of this study could be applied in other mines situated in Marrakech region (Hajjar and Draa Lasfar polymetallic mines operated by Compagnie Minière des Guemassa) where similar bedrock occurs.

Acknowledgments

The authors would like to thank the Agence Universitaire de la Francophonie (AUF) which financed this project. Our acknowledgements also go to the Canada Research Chair on Rehabilitation of Abandoned Mine Site and the Unité de Recherche et de Service en Technologie Minérale (UQAT) for their financial and technical support.

Bibliographic References

Adam K, Kourtis A, Gazea B, Kontopoulos A (1997) *Evaluation of static tests used to predict the potential for acid drainage generation at sulfide mine sites.* Trans. Inst. Min. Metall. Sect. A : min. industry. 106, January-April:A1-A8.

Alpers, C.N., Blowes, D.W., Nordstrom, D.K., and Jambor, J.L. (1994) *Secondary minerals and acid mine-water chemistry, in The Environmental Geochemistry of Sulfide Mine-wastes*, Blowes, D.W. and Jambor, J.L., eds., Mineral. Assoc. Canada Short Course Notes, v. 22, p. 249-269.

Aubertin M. Bussière B and Berbier L.R. (2002) *Environnement et gestion des rejets miniers.* CD-ROM, Presses internationales de Polytechnique.

Benzaazoua M, Bussière B, Dagenais A-M (2001) *Comparison of kinetic tests for sulfide mine tailings*. In Tailings and Mine Waste 01, Balkema (Ed). Fort Collins, Colorado, USA, January, pp 263-272.

Benzaazoua M., Bussière B., Dagenais A.-M. and Archambault M. (2004) *Kinetic test comparison and interpretation for prediction of the Joutel tailings acid generation potential Environmental Geology y* 46-8 :1086–1101.

Benzaazoua M., Bussière B., Nicholson R. and Nernier L (1998) Geochemical behavior of multilayered cover made of desulphurized mine tailings. Tailings and Mine Waste 98, Fort Collins, Balkema Ed. : Rotterdam : 389-398.

Blowes, D.W., Jambor, J.L., Appleyard, E.C., Reardon, E.J., Cherry, J.A. (1992) *Temporal observations of the geochemistry and mineralogy of a sulfide-rich mine-tailings impoundment*, Heath Steele Mines, New Brunswick. Explor. Mining Geol. 1, 251–264.

Bussière, B., Aubertin, M. and Chapuis, R.P. (2002) *A laboratory set up to evaluate the hydraulic behavior of inclined capillary barriers.* International Conference on Physical Modelling in Geotechnics, St.Jonh's, Newfoundland, 391-396.

Caruccio F.T. (1967) *An evaluation of factors influencing acid mine drainage production from various strata of the Allegheny Group and the groundwater interactions in selected areas of Western Pennsylvania* , Ph.D. Thesis, The Pennsylvania State University, State College, Pennsylvania, USA.

Crouse, H.L. and Rose A.W. (1976) *Natural beneficiation of acid mine drainage by interaction with stream water and stream sediment* In: 6th Symposium on Coal Mine Drainage Research, National Coal Association/Bituminous Coal Research, Inc., pp. 237-269

Cruz, R., Méndez, B.A., Monroy, M. and Gonzalez, I. (2001) *Cyclic voltametry applied to evaluate reactivity in sulfide mining residues.* Applied Geochemistry. 16: 1631-1640.

Furrer G and Stumm W. (1986) *The coordination chemistry of weathering. I. Dissolution kinetics of Al_2O_3 and BeO*. Geochim. Cosmochim. Acta, 50, pp 1847-1860.

Hibti M. (2001). *Les amas sulfurés des Guemassa et des Jebilet (Meseta Sud-ocidentale, Maroc) : Témoin de l hydrothermalisme précoce dans la bassin Mesetien*. Ph. D. thesis, Université Cadi-Ayyad. Marrakech.

Jambor, J.L., (1994) *Mineralogy of sulfide-rich tailings and their oxidation products*. In: Jambor, J.L, Blowes, D.W. (Eds.), The Environmental Geochemistry of Sulfide Mine-wastes, Short Course Handbook 22, Mineralogical Association of Canada, May 1994, Waterloo, Ontario, Canada, 59-102.

Jambor, J.L., Dutrizac, J.E., Groat, L.A. and Raudsepp. M. (2002) *Static tests of neutralization potentials of silicate and aluminosilicate minerals*. Environmental Geology 43, 1-17.

Kwong, Y.T.J. (1993) *Prediction and prevention of acid rock drainage from a geological and mineralogical perspective* , MEND Report 1.32.1 CANMET, Ottawa, 47 p.

Lawrence, R.W. (1990) *Prediction of the behavior of mining and processing wastes in the environment. Proc. Western Regional Symposium on Mining and Mineral Processing Wastes,* Society for Mining, Metallurgy and Exploration, Inc., Littleton, C.O. 115-121.

Li, M.G. (2000) *Acid rock drainage prediction for low-sulfide, low-neutralization potential mine wastes.* Fifth International Conference on Acid Rock Drainage, 20-26 May 2000, Denver, CO. Society for Mining, Metallurgy, and Exploration, Inc. (SME), Littleton, CO. ISBN: 0-87335-182-7. Vol 1, 567-580, 2000.

Miller, S.D., Jeffery, J.J. and Wong, J.W.C. (1991) *Use and misuse of the acid-base account for "AMD" prediction*. Proc. of the Second International Conference on the Abatement of Acidic Drainage, Montreal, Canada, 3:489-506

Morin, K.A. and Hutt, N.M. (1997) *Environmental Geochemistry of Minesite Drainage : Practical Theory and Case Studies*. MDAG Publishing, Vancouver (Canada).

Nordstrom, K.D., Alpers, C.N. (1999) *Geochemistry of acid mine waters*. In: Plumlee, G.S., Logsdon, M.J. (Eds.), The Environmental Geochemistry of Mineral Deposits. Part A: Processes, Techniques, and Health Issues, Rev. Econ. Geol., 6A, pp. 133–160.

ONEM (1997) Observatoire Nationale de l'Environnement du Maroc, Monographie locale de l'environnement de la ville de Marrakech. Study carried out on behalf of the Marrakech Wilaya.Pyatt, F.B. and Grattan, P.J. (2001) *Some consequences of ancient mining activities on the health of ancient and modern human populations*. J. Pub. Health Med. 23, 235–236. Ritcey GM (1989) Tailings Management, Problems and Solutions in the Mining Industries. Elsevier.

Ritcey GM (1989) *Tailings Management, Problems and Solutions in the Mining Industries*. Elsevier.

Sobek, A.A., Schuller W.A., Freeman J.R. and Smith, R.M. (1978) *Field and Laboratory Methods Applicable to Overburdens and Minesoils.* EPA-600/2-78-054, pp. 47-50.

SRK (Steffen, Robertson and Kristen) (1989) *Guide technique préliminaire sur le drainage rocheux acide*, BC AMD Task Force, Vol.1. Centre de Recherches Minérales, Québec.

Vick, S.G. (1983) *Planning, Design, and Analysis of Tailings Dams*. John Wiley and Sons

Wehrli B. (1989) *Monte Carlo simulations of surface morphologies during mineral dissolution*. J. Colloid. Interface Sci. 132, pp 230-242.

MODELLING THE IMPACT OF BACK-FILLING MATERIAL ON THE WATER QUALITY OF FLOODED IRON MINES (LORRAINE, FRANCE)

HAMM Virginie[1], FABRIOL Robert[1], VAUTE Laurent[2], FOURNIGUET Guy[2], BAUBRON Jean-Claude[2]

[1] BRGM GISOS, Rue du Doyen Marcel Roubault – BP 40 – 54501 Vandoeuvre-lès-Nancy Cedex - France.
v.hamm@brgm.fr; r.fabriol@brgm.fr

[2] BRGM SGR/LOR, 1 av. du parc de Brabois - 54500 Vandoeuvre-lès-Nancy Cedex - France.
g.fourniguet@brgm.fr; l.vaute@brgm.fr; jc.baubron@cegetel.net

ABSTRACT: Residual voids located in the collapsed zones of mine workings present a risk of subsidence for overlying buildings. In the Lorraine iron basin (France), filling of the voids above the "Cité du Stock" with a slurry made of cement and fly ash has been envisaged. The impact of the back-filling material on the underground water quality of the flooded mine used for drinking water has been decided. Laboratory leaching tests were carried out and a model of the mining reservoir was built with a PNS ("Pipe Network System"). The results of leaching tests in columns allowed us to identify the mixture of cement and fly ash with the lowest contaminant capacity. Flow and transport modelling in galleries has shown that the concentrations of chemical elements at the supply well are within the limit concentrations for drinking water.

KEYWORDS: Flooded mine, back-filling material, leaching test, pipe network system, transport of chemical elements

RESUME : Les vides résiduels dans les zones foudroyées des travaux miniers présentent un risque d'affaissement pour les habitations sus-jacentes. Dans le bassin ferrifère lorrain (France), un comblement des vides par un coulis de ciment avec des cendres volantes a été envisagé sous la "Cité du Stock". L'impact du remblayage sur la qualité de l'eau du réservoir minier exploitée en aval pour l'A.E.P a été évalué. Des tests de lixiviation en laboratoire sur différents types de coulis ont été réalisés et un modèle du réservoir minier ennoyé a été construit sous forme d'un RDT (« Réseau De Tubes »). Les résultats des tests de lixiviation en colonne ont permis d'identifier le mélange ciment et cendres volantes le moins polluant et la modélisation des écoulements et du transport dans le réseau de galeries a montré que les concentrations en éléments chimiques à l'A.E.P sont très inférieures aux concentrations limites pour l'eau potable.

MOTS-CLEFS : Mine ennoyée, matériau de remblayage, test de lixiviation, réseau de tubes, transport d'éléments chimiques

1. Introduction

Closure of iron mines in the Lorraine basin (France) has left a dense network of underground galleries. Residual voids located in the collapsed zones present a risk of subsidence for overlying buildings. In June 2002, open mining voids were identified under the "Cité du Stock" (Thil, France). This zone was assumed to have collapsed but wide open spaces were detected (10,000 m^3) 60 m below the surface. A preliminary study was carried out to determine the possible impact of back-filling material on the underground water quality of the Godbrange flooded mine located downstream of the zone (Baubron et al. 2003). Water from the reservoir is used for drinking water supply from the Hussigny-Godbrange pumping well.

This paper presents the main results of the study: the chemical model resulting from the leaching tests on 6 mixtures of cement and fly ash, and the construction of a pipe network system for representing hydraulic and transport behaviour in flooded galleries and its application to the Godbrange mining reservoir.

2. Chemical evolution of water in contact with the back-filling material: experimental approach

2.1. The back-filling material tested

Several cement - fly ash slurries were tested in order to obtain an optimal back-filling material. The material must present a mechanical resistivity greater than 2.5 MPa, a low chemical dissolution rate in contact with water and a low cement content to reduce the cost. Two types of cement were used; CEM I and CEM III. The fly ashes were sampled from the storage of an electrical power plant (EDF, La Maxe). The slurry compositions tested are presented in table 1. Once the cement, fly ash and water had been mixed in a stirred tank, the resulting slurry was used to prepare cylindrical samples. After 90 days setting, the samples were crushed into particles to fill the leaching columns.

Table1. Composition of six cement – fly ash slurries tested

Reference	Cement (weight %)	Fly ash (weight %)	Slurry (weight in g)	Dogger water (weight in g)
CEMI 3-7	30% CEM I 52.5	70% FA	10608	7497
CEMI 2-8	20% CEM I 52.5	80% FA	9888	7772
CEMI 1-9	10% CEM I 52.5	90% FA	10164	7572
CEMIII 3-7	30% CEM III C 32.5	70% FA	9616	7617
CEMIII 2-8	20% CEM III C 32.5	80% FA	10116	7518
CEMIII 1-9	10% CEM III C 32.5	90% FA	9895	7797

2.2. Column leaching tests

Each of the six columns of the leaching system was filled with 10 kg of ground material and 7.5 kg of Dogger water (table 1). The particle size distribution was identical in each column (35 mm< S <40 mm). In a first step, the system remained closed for 14 days to approach water-material chemical equilibrium. In a second step, the system was opened to observe any chemical changes in the leaching conditions. Each column was supplied at its base with a flow of 300 ml/day of Dogger water. The water overflowed through an opening at the top of the column, where it was sampled for chemical analyses. The water conductivity and temperature in the column were measured continuously (figure 1).

Continuous monitoring of conductivity is a reliable indicator of the bulk composition of the water. The mineralisation observed after 14 days decreased gradually until 125 days of leaching, when similar chemical concentrations were obtained at the inlet (Dogger water) and outlet of the CEM III columns.

The slurries made of CEM I contaminated water more than the slurries made of CEM III. The concentration of chemical elements in the water results from the dissolution of fly ash as well as from cement. At this stage of the work, we are not able to identify the source of each contaminant in the slurry. The results of the 6 leaching tests indicate the CEM III 1-9 (10% CEM III and 90% of fly ash) is the most appropriate among the slurries tested. The chemical concentrations in water are lower than the limits defined by the French administration for drinking water supply ("*Livre III du Code de la Santé Publique*"), except for sulphate and boron at the beginning of the leaching test, and for aluminium and selenium during the leaching test period. The CEM III 1-9 is considered the more favourable among the six back-filling materials tested, and used hereafter for the chemical model.



Figure 1. Experimental device with the six leaching columns

2.3. Chemical interaction model

The column with an ascending flow may be represented as a perfectly stirred reactor described by the following mass-balance equation (Villermaux, 1993):

$$QsCs = QeCe + V(t)\, r(t) - \frac{d(V(t)C(t))}{dt} \qquad (a)$$

where:
Qs = outflow rate (l/s)
Qe = inflow rate (l/s)
Cs = outflow concentration (mol/l)
Ce = inflow concentration (mol/l)
C(t) = concentration in the reactor (mol/l)
V(t) = volume of water in the reactor (l) at time t
r(t) = production or consumption rate of a given chemical element or compound (mol/l/s)

Consider the dissolution-precipitation reaction of a mineral A_nB represented by the following equation:

$$A_nB \leftrightarrow nA^+ + B^{n-} \qquad (b)$$

The rate of this reaction is the difference between the dissolution rate and the precipitation rate:

$$r(t) = [k_{diss}\,(A_nB)] - [k_{pcp}\,(A^+)^n\,(B^{n-})] \qquad (c)$$

where:
k_{diss} = dissolution constant
k_{pcp} = precipitation constant
(A_nB) = mineral activity (1 for a pure solid)
$(A^+)^n\,(B^{n-})$ = dissolved species activity

Taking into account the relationship between the equilibrium constant of the reaction K and the kinetic constants, $K = k_{diss}/k_{pcp}$, the total reaction rate may be expressed as:

$$r(t) = k_{pcp}\,[K - (A^+)^n\,(B^{n-})] \qquad (d)$$

The conductivity of water C_w (µS/cm) is an overall function of the activity of ions. On the basis of equation (d), we assume a global reaction rate $r_g(t)$ function of C_w and empirically expressed as:

$$r_g(t) = [k_g\, M(t)^n]\, [K_g - C_w\,(t)] \qquad \text{(e)}$$

where:
k_g = overall kinetic precipitation constant
K_g = overall equilibrium constant
M(t) = total mass of chemical elements in the solid, expressed in µS/cm
n = overall order of reaction

The constants for the CEM III 1-9 kinetic model are obtained by fitting with the data from leaching column experiments.

Table 2. Constants for the CEM III 1-9 slurry

	CEM III 1-9
log K_g	+ 0.4
log k_g	- 11.75
M (µS/cm)	56.25
n	8.25

2.4. Chemical simulator

The numerical simulator was built using Matlab® software and its graphic interface, Simulink®. This interface enables the modelling and simulation of dynamic systems using a graphic representation of the block-diagram type based on bond-graphs formalism (Maschke 1992; Auroy 2000, Bequette 1998; Kervévan et al. 1998; Collon 2003, Collon et al. 2004).

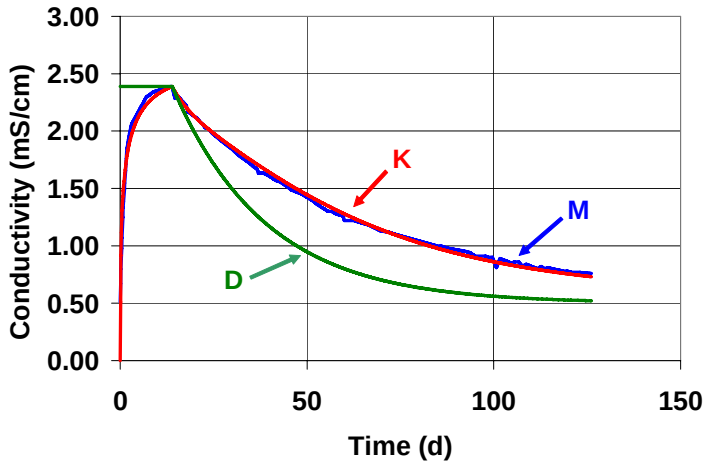


Figure 2. Calculated and measured water conductivity obtained with the CEM III 1-9 slurry. (M: measurements; D: perfectly stirred tank; K: perfectly stirred tank with kinetic)

The simulated conductivities (figure 2) are in good agreement with those measured. The kinetic effect is highlighted by comparing it with the results obtained with a perfectly mixed tank without any kinetic effect. The difference is due to the progressive dissolution of contaminant from the slurry. When comparing the change over time of contaminant concentration and water conductivity, both slopes appear similar. Consequently, the concentration is empirically calculated from the conductivity of water. This relation is used to simulate the evolution of the contaminant concentration in water. For each chemical element a proportionality coefficient is defined. Figure 3

represents the calculated and analysed selenium concentration in water. The chemical simulator built is used as a point source of contaminant in the transport model described hereafter.

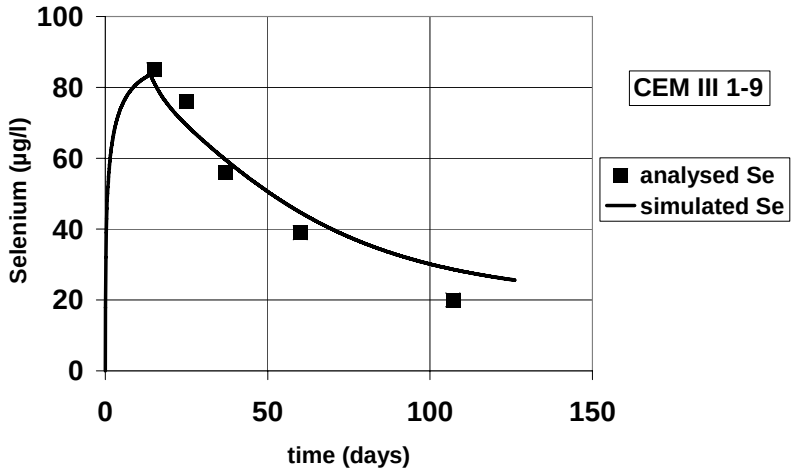


Figure 3. Calculated and analysed selenium concentration in water at the leaching column outlet

3. A Pipe Network System approach for modelling the flow and transport of chemical elements in the flooded iron mines

3.1. Pipe Network System principles: hydraulic behaviour and transport of chemical substances

The mine galleries can be modelled as connected pipes forming a pipe network system where pipes are channels used to convey water and chemical substances from one location to another. The physical characteristics of such a network include the length of the pipes, their inside diameter and their roughness coefficient.

When water is conveyed through a pipe, hydraulic energy is lost due to the friction between the moving water and the stationary pipe surface. This friction loss is a major energy loss in pipe flow and is a function of the flow rate, pipe length, hydraulic diameter, roughness coefficient and fluid properties (Sellens 1996).

The head loss associated with flow through a pipe can be expressed in a general fashion as:

$$h_L = a.q^b \qquad (f)$$

where:
h_L = head loss, m
q = flow rate, m^3/s
a = resistance coefficient
b = flow exponent

The values of the resistance coefficient and flow exponent depend on which head loss law is applied. A widely used law is the Darcy-Weisbach formula where the resistance coefficient “a” depends on a friction factor, the pipe length, the hydraulic section and diameter and the flow exponent “b” equals 2, as shown below:

$$h_L = \lambda(\varepsilon, \mathrm{Re}).\frac{L}{D_h}.\frac{1}{2gS_h^2}.q^2 \quad \text{(h)}$$

where:
λ = a friction factor that depends on the roughness coefficient ε and Reynolds number Re
L = pipe length, m
D_h = hydraulic diameter, m
S_h = hydraulic section, m
g = gravity, m/s^2
q = flow, m^3/s

The expression of the friction factor depends on the flow; indeed, for turbulent flow observed during flooding, the friction factor depends only on the relative roughness coefficient but for the laminar flow observed generally after flooding, the friction factor becomes inversely proportional to the Reynolds number (λ=64/Re) and the head loss in a pipe can be expressed as a linear function of the flow:

$$h_L = \frac{32\nu L}{gS_h D_h^2}.q \quad \text{(i)}$$

where:
ν = kinematic viscosity, m^2/s

Equation (i) can also be expressed as:

$$q_{ij} = k_{ij}.(h_i - h_j) \quad \text{(j)}$$

where:
k_{ij} = conductance of a pipe [m^2/s]. This represents the flow per unit of pipe length and depends only on the geometric characteristics of the pipe and on the flow, kinematic viscosity and gravity,
q_{ij} = flow between nodes i and j, positive for flow entering the node j ($h_i > h_j$) and negative for flow leaving the node j ($h_i < h_j$).

A second set of equations that must be satisfied is the flow continuity at each pipe junction:

$$\sum_i q_{ij} + q_{imposé,j} = 0 \quad \text{(k)}$$

where $q_{imposé,j}$ is a possible incoming or outcoming flow from external conditions.

The combination of equations (j) and (k) leads finally to:

$$h_j = \frac{\sum_i h_i k_{ij} + q_{imposé,j}}{\sum_i k_{ij}} \quad \text{(l)}$$

The hydraulic head is calculated at each node of the pipe network system and its value determines the value and direction of flow in the network. In order to solve these two sets of equations, the user must define initial and boundary conditions on hydraulic head and flow.

The transport through the pipe network is considered non reactive. This means that a substance which travels through a pipe will not react with the surrounding rock material. A dissolved substance will travel down a pipe by advection and will mix completely and instantaneously at junctions and be scattered in the entire network.
Two sets of equations describe these mechanisms: the first is the advection through a pipe, which implies a delay in the concentration of the downstream node:

$$C_{downstream}(t+\Delta t) = C_{upstream}(t-(\tau-\Delta t)) \qquad \text{(m)}$$

where:
t = actual transport time, s
Δt = time step, s
τ = transport delay through the pipe, τ = v/q where v represents the volume of the pipe (m^3) and q the flow in the pipe (m^3/s)

This equation requires that the time step is shorter than the time delay to pass through a pipe.
The second set of equations describes mixing at pipe junctions; the concentration of a substance leaving the junction is simply the flow-weighted sum of the concentrations from the inflowing pipes:

$$C_{j/x=0} = \frac{\sum_i q_{ij} C_{i/x=L} + q_{j,ext} C_{j,ext}}{\sum_i q_{ij} + q_{j,ext}} \qquad \text{(n)}$$

where:
$C_{j/x=0}$ = concentration at node j, mg/L
$C_{i/x=L}$ = concentration at the end of the link of node i, mg/L
$C_{j,ext}$ = concentration of the external flow entering the network at node j, mg/L
q_{ij} = flow through the link ij, m^3/s
$q_{j,ext}$ = external source flow entering the network at node j, m^3/s

3.2. Building the Pipe Network System: description and advantages of this approach

The software used for building the pipe network was Matlab® and its graphical interface Simulink®. The principle was to build the flow and chemical sets of equations described above by using block features provided by Simulink®. A pipe network can be represented as the repetition of a basic pattern conceived of a junction and its two connected pipes. Figure 4 below shows how pipes and nodes are modelled with Simulink® block diagrams. The node or junction in a network is represented by two blocks, one for the hydraulic head equations and the other for the water quality equations. The conductance of a pipe and the flow rate are calculated at the link between two nodes. The entry parameters for each pipe or gallery are the length, the hydraulic section, the inside diameter and a roughness coefficient for non laminar flow. This approach does not require other parameters, in contrast with porous-medium models where the user must define the intersticial permeability and a storage factor to solve hydraulic equations and the porosity and a dispersivity coefficient for the transport of chemical substances (Lanini et al. 2000). These parameters can be estimated for a porous aquifer but not for wide mining spaces. The pipe network system approach is interesting for observing what occurs inside the galleries and at the pipe wall, without modelling the rock surrounding the galleries, which is not open to water except at the collapsed zones, which are considered as refill zones.

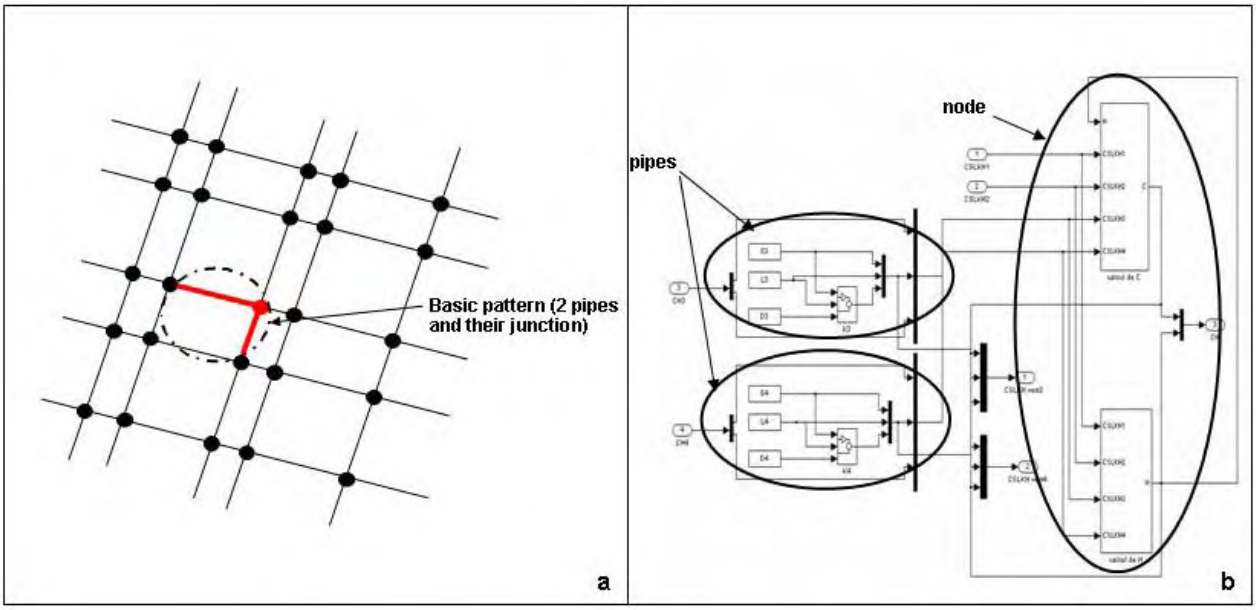


Figure 4 : Example of a basic pattern in a network (a) and its representation with Simulink® block features (b)

4. Modelling the impact of the "Cité du stock" cavity filling on the Godbrange reservoir

4.1. Godbrange mining basin: location and description

The Godbrange iron mine is located between the north part of the Lorraine iron basin and the Luxembourg border. It covers the mining concessions of Hussigny-Godbrange, Tiercelet, Brehain, Villerupt and Crusnes (figure 5). The iron-bearing formation is composed of alternating marly levels and ferruginous limestone. It is overlain by a micaceous marl layer and followed by a Dogger Bajocian limestone succession that constitutes a major karstic aquifer (Collon et al, 2002). Its floor area is estimated to be 13 km^2 and the mine water reserves are estimated at around 11,600,000 m^3. The reservoir has been flooded since 1987, due to the end of dewatering. The water level reaches the overflow point at 337 m in the north western end of the reservoir and flows into the Moulaine River. The water of the reservoir is used for drinking water at the Hussigny-Godbrange supplying well located north west of the basin.

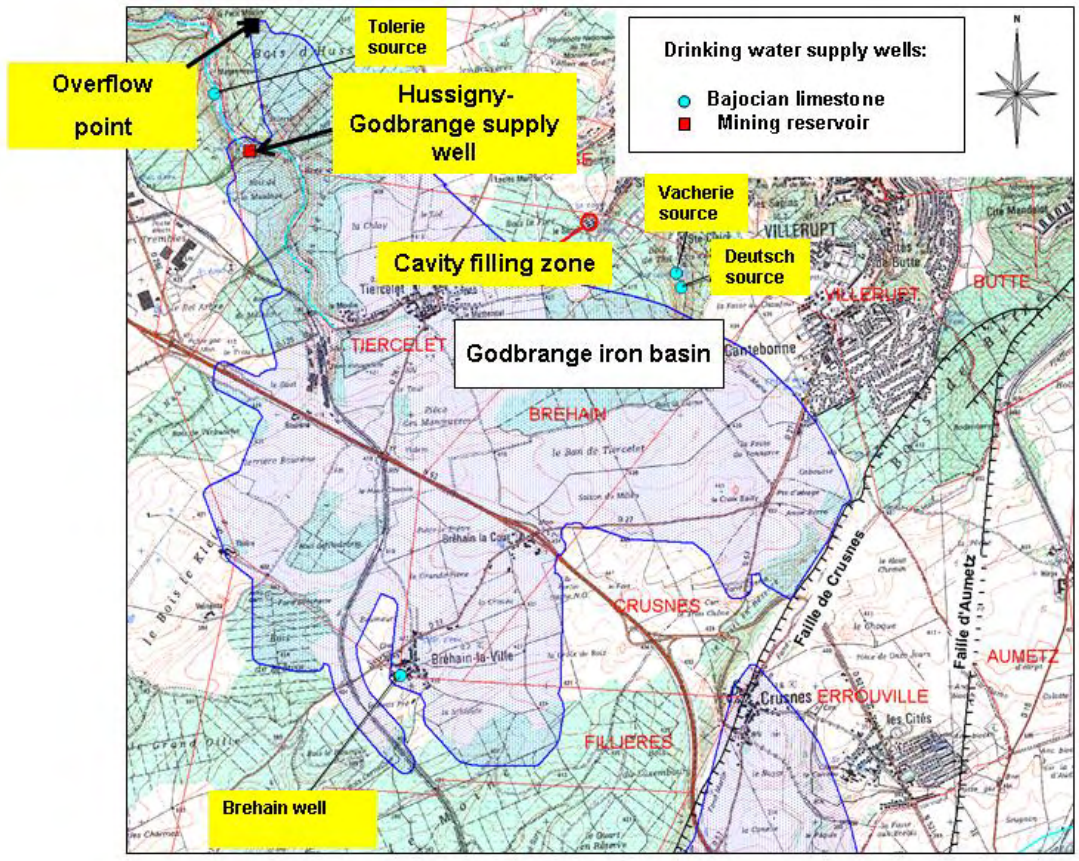


Figure 5 : Geographical location of the Godbrange iron basin

4.2. Building the Pipe Network System of the Godbrange mining reservoir

The pipe network system was built using digital planes of the Godbrange mine. The main galleries conveying water from the cavity zone to the drinking water supply well and to the overflow point were digitalized and reproduced in the conceptual network. The collapsed zones were modelled as external source flows coming from the above Dogger aquifer (refill zones). The boundary conditions of the Godbrange reservoir are represented by incoming flows due to refill zones, the values of which are proportional to the refill areas, an outcoming flow of 175 m^3/d at the pumping well and a fixed head of 337 m at the overflow point. Figure 6 below shows the conceptual model and an extract of the pipe network as it appears in the Simulink® model.
The chemical simulator described in paragraph 2.4 has been introduced in the pipe network system as a point but time varying chemical source entering in the network by the cavity filling zone.

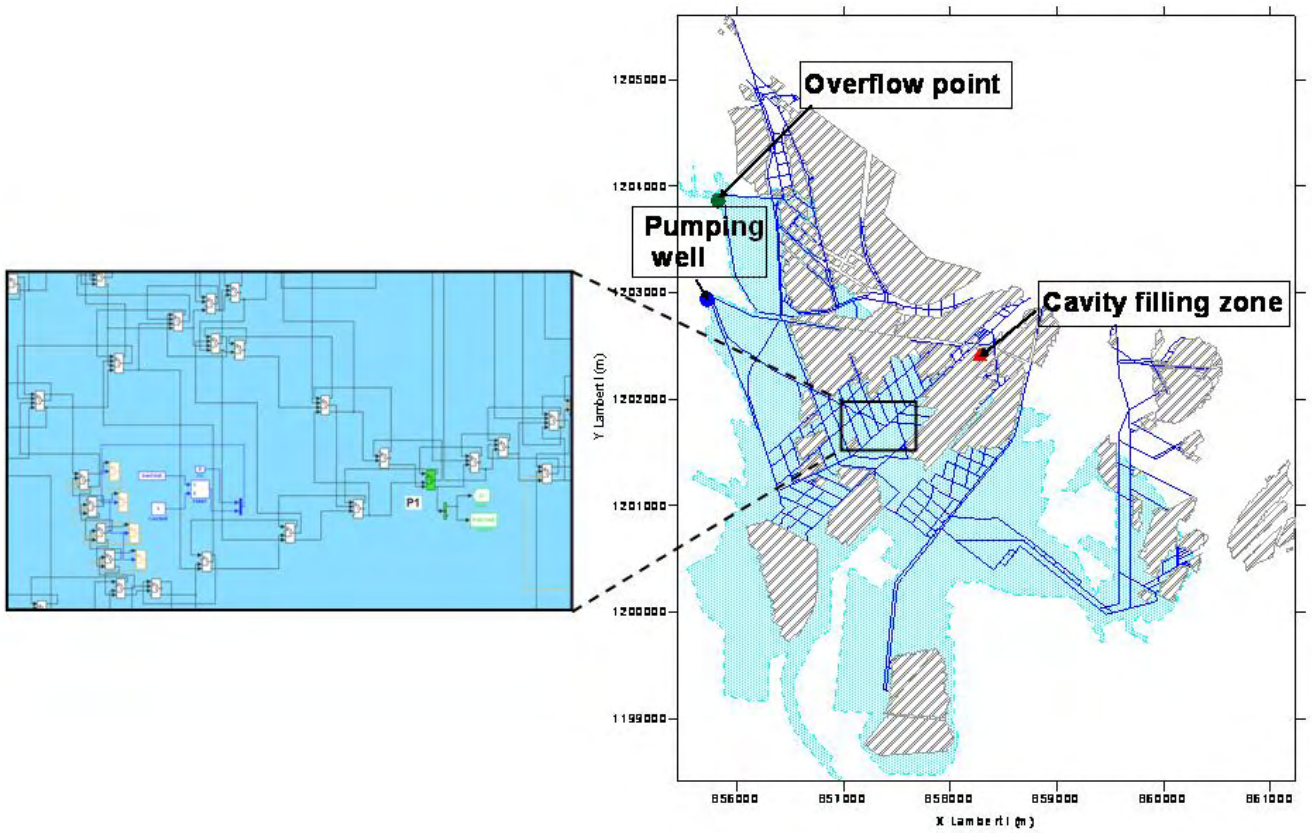


Figure 6 : The conceptual model of the Godbrange reservoir and an extract of the network in Simulink® (*dark blue: pipe network, light blue: flooded zone, striped grey: collapsed zones*)

4.3. Transport of contaminants from the cavity filling material

The simulation was performed for a total duration of 16 years after the filling of the cavity. As explained in paragraph 2.4, the proportionality between the water conductivity measurement and the contaminant concentration was used to determine the concentrations of all elements released from the filling material. Figure 7 below gives an example of the simulation for the element selenium. The concentration in the entire network was at a maximum after 1 year of simulation, and then decreased very slowly without reaching the initial state after 16 years of simulation. The limit value of selenium for drinking water was set at 10 µg/L. The simulated Se concentration exceeds this value the first year near the cavity filling, and then decreases below this limit concentration. The model shows that the pumping well for drinking water supply and the overflow point are not contaminated by any substance coming from the filling material because the contaminant travelling through the network is diluted by water refill zones with a high dilution factor.

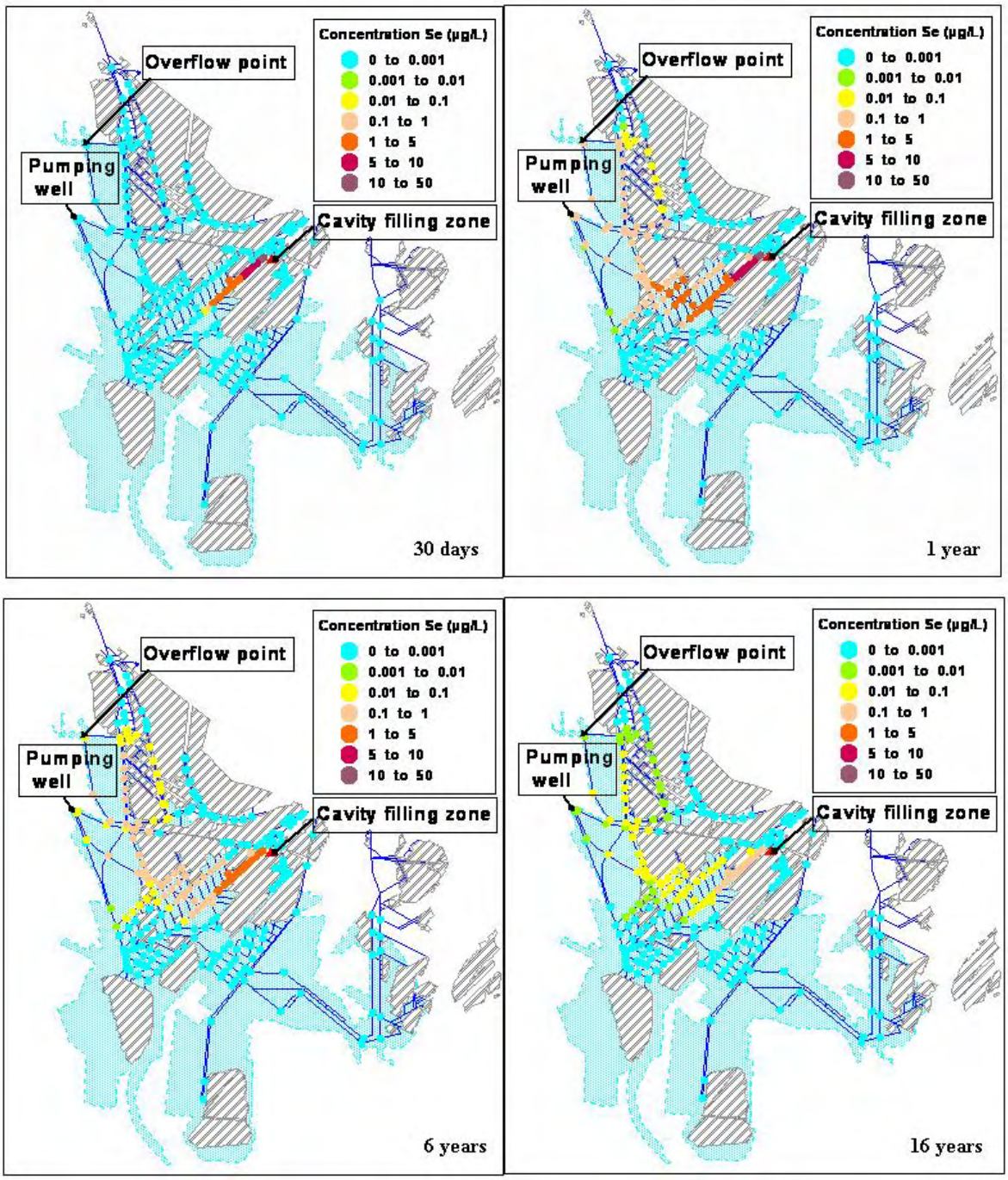


Figure 7 : Computed concentration of selenium (µg/L) in the pipe network for 30 days, 1 year, 6 years and 16 years of simulation after cavity filling.

5. Conclusions

Leaching tests performed on six different mixtures of cement and fly ash indicated that the concentration of substances dissolved from the mixture CEM III 1-9 (10% of cement and 90% of ash) were below the limit concentrations for drinking water, except for the elements boron, sulphate, aluminium and selenium. This mixture was used with its kinetic model as the cavity filling source in the pipe network system of the Godbrange mining reservoir. The results of the hydraulic and transport modelling in the flooded galleries show that the concentrations of chemical elements

at the supply well located in the north west are one thousand to one million times lower than the limit concentrations for drinking water. Furthermore, substances coming from the cavity filling material are immediately diluted after entering the reservoir and the concentrations become rapidly in line with drinking water standards.

6. Acknowledgements

This work forms part of the research programme carried out by GISOS (Research Group for the Impact and Safety of Underground Works).

7. References

Auroy M., (2000) - *Élaboration des schémas de procédés industriels*. Techniques de l'Ingénieur, traité Génie des procédés, J 6 018, 17 p.

Bequette B. W. (1998) – *Process dynamics Modeling, Analysis and Simulation.* Prentice Hall PTR, 622 p.

Baubron J-C., Fabriol R., Fourniguet G., Hamm V., Vaute L. (2003) – *Modélisation hydrogéologique du réservoir minier de Godbrange et influence d'un comblement partiel à cendres volantes.* Rapport brgm/RP-52802-FR, 73 p., 22 fig., 13 tab., 6 ann.

Collon P., Fabriol R., Buès M., (2004) - *Ennoyage des mines de fer lorraines : impact sur la qualité de l'eau - Flooding of the iron mines of Lorraine: impact on the water quality*, Comptes Rendus des Géosciences 336, p. 889-899

Collon P., (2003) - *Evolution de la qualité de l'eau des mines abandonnées du bassin ferrifère lorrain. De l'expérimentation en laboratoire à la modélisation in situ*. Thèse INPL, Octobre 2003. 247 p.

Collon P., Fabriol R., Vaute L., Pinault J-L., Buès M., (2002) - *Modelling changes in sulphate concentrations in discharge water from the abandoned iron mine of Saizerais*. Proceedings SWEMP 2002.pp 917-924.

Kervévan C., Thiéry D., Baranger P., (1998) - *SCS: Specific Chemical Simulators dedicated to chemistry-transport coupled modelling Part lll - Coupling of SCS with the hydro-transport modelling software MARTHE.* Goldschmidt Conference 1998, Toulouse, Mineralogical magazine, Vol 62 A, p. 773-774

Lanini S., Fabriol R. (2000) - *Différentes approches de modélisation des écoulements et du transport dans un réseau de tubes – comparaison avec des résultats expérimentaux*. Rapport BRGM/RP-50154-FR, 48 p., 10 fig., 1 tab., 3 ann.

Maschke B. (1992) - *Approche systémique des systèmes continus. Graphes de liaison.* Journées EEA-Electrotechnique, 26 et 27 mars 1992, Laboratoire d'Automatisme Industriel, Conservatoire National des Arts et Métiers, 35 p.

Sellens R. (1996) - *Losses in Piping*. Course of Queen's University at Kingston, Mechanical Engineering (http://me.queensu.ca/courses/MECH451/losses.htm)

Villermaux J. (1993) – *Génie de la réaction chimique, conception et fonctionnement des réacteurs*. TEC & DOC – Lavoisier, 448 p.

A STUDY OF THE EFFECT OF STRAIN RATE ON STIFFNESS AND STRENGTH IN SILTY MUDSTONE USING MULTISTAGE TRIAXIAL TESTING

HAMZA Omar[1], STACE Rod[1], REDDISH David[1]

[1] NOTTINGHAM CENTRE FOR GEOMECHANICS, School of Civil Engineering, the University of Nottingham, University Park, Nottingham – NG7 2RD, UK; omar.hamza@nottingham.ac.uk, rod.stace@nottingham.ac.uk, david.reddish@nottingham.ac.uk

ABSTRACT: The effect of strain rate on mechanical properties has been reported in literature for some types of rock using uniaxial compression tests. In this paper, the authors investigated the phenomena of strain rate dependency of strength and stiffness in a silty mudstone, from the coal measure rocks of the UK. Using multistage triaxial testing, a series of experiments were conducted on both intact and fractured rock samples to cover the two ultimate structural conditions of the rock mass. The results showed that the rate-dependency of strength and stiffness is particularly significant in the fractured samples and this dependency varies according to the level of confinement.

KEYWORDS: Time-dependent rock properties, Strain-rate, Abandoned mine, Multistage-triaxial test.

RESUME : L'effet du taux de déformation sur les propriétés mécaniques a été rapporté en littérature pour quelques types de roche en utilisant les essais de compressibilité uniaxiaux. Dans cet article, les auteurs ont étudié le phénomène de dépendance de la résistance et la raideur d'une argile schisteuse au taux de déformation. Des séries d'essais triaxiaux ont été conduites à la fois sur des échantillons de roche intacte et sur des échantillons de roche fracturée afin de couvrir les deux états limites caractérisant la structure du milieu rocheux. Les résultats ont prouvé que la taux de dépendance de la résistance et la raideur de la roche à la déformation est particulièrement significative dans les échantillons rompus et cette dépendance change selon la valeur du confinement.

MOTS-CLEFS : Effet du temps, Taux de déformation, Essais triaxiaux.

1. Introduction

In common with any rock mass, the response of coal measure rocks may be *time-independent* or *time-dependent*. Within these two main categorized responses, the material may behave elastically or yield according to the confining pressure and the applied stress level (Kaiser and Morgenstein, 1981-a). Figure 1 illustrates all these possible behaviors in rocks.

An understanding of the time-dependent properties is considered essential for further development in the field of underground mine design and long-term strata control (e.g. Singh, 1975). The effect of time has been manifested in rock specimens in laboratory tests as well as at larger scale during insitu observations. To investigate the time-dependent behaviour of rocks experimentally, researchers have used three main testing methods: (i) creep, (ii) relaxation and (iii) loading tests at different stress or strain rates. Using the third method, many experimental studies in literature have shown that stiffness and/or strength of some rocks (under uniaxial stress) can be highly dependent on *strain rate* and this dependency varies according to rock type and its condition (e.g. level of damage or fracture). Figure 2 and 3 show a copy of mechanical data from uniaxial compression

tests (Bieniawski, 1970; Peng & Podnieks, 1972) conducted on Sandstone and Tuff with various constant strain rates. The data shown in Figure 3 are similar to results from tests on other rock types reported by many authors (e.g. Wawerisk, 1973 and Peng, 1973, Yongsheng et al., 2000) where the peak strength increased as the strain rate increased.

In the field, strain may change quickly during earthquakes or due to fast mining activities; or may go slowly over many years at abandoned mine sites. Thus, possible strain rates in the rock mass can cover a wide range of magnitudes implying that a change in strain rate may have a key role in altering the rock mass response. Therefore, characterising the effect of strain rate in coal measure rocks would be significant to the mining industries helping improve their prediction and design tools.

However, it is standard procedure in most cases, for these tools to still depend on a rock characterization based on strain-controlled experiments conducted only at a single medium speed of deformation (i.e. typically between 0.002-0.005mm/s for 70mm height of cylindrical specimens). Moreover, most of the studies (e.g. Bieniawski, 1970; Peng & Podnieks, 1972) conducted to investigate the effect of strain rate have mainly utilised the uniaxial compression testing. However, the true stress condition in the ground at depth is triaxial rather than uniaxial. Therefore, the phenomenon of rate-dependency of strength and stiffness needs to be investigated under triaxial loading conditions and extended to the investigation on further rock types.

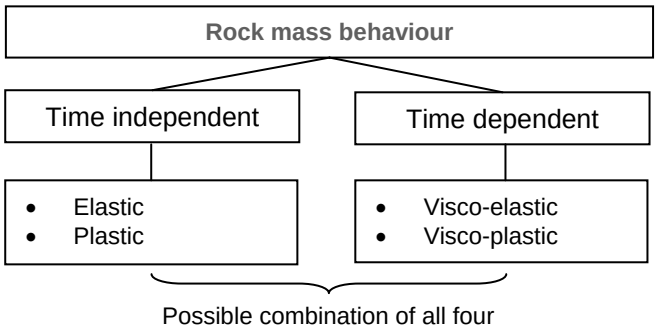


Figure 1. The common classified behaviours of rock mass

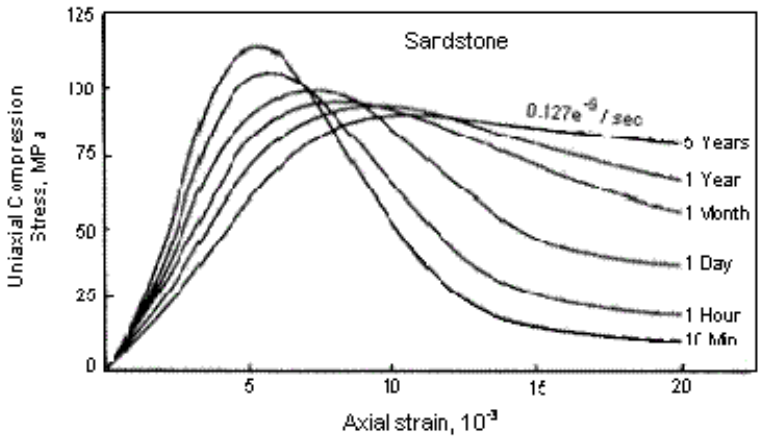


Figure 2. Stress-strain relationship from uniaxial compression tests reported by Bieniawski, 1970. Different strain rates resulted in different strength and stiffness.

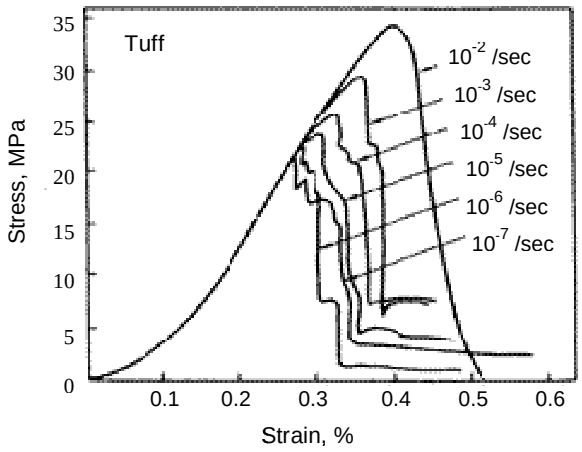


Figure 3. The relationship between stress and strain from uniaxial compression tests reported by Peng & Podnieks, 1972. Different strain rates resulted in different strength.

In this study the effect of strain rate on mechanical properties was examined in Silty Mudstone, one of the coal measure rocks in UK by conducting a series of multistage triaxial tests with different constant strain loading speeds. This testing programme was carried out on intact and fractured specimens.

Models with representative material properties are required to predict geotechnical performance and for designing purposes. Many constitutive laws considering the effect of time have been developed using (i) Experimental/empirical fitting, (ii) Mechanical models and (iii) Phenomenological models based on physical process theories. Using the experimental data, the study has indicated that it is best to use empirical models to describe the relevance of strain rate with strength and stiffness, which in turn may be used in an improved predictive tool for assessing mining stability.

2. Experimental methods

2.1. Materials and Apparatus

The tested rock material was originally obtained from an open pit mine located at Arkwright in the midlands of the UK. The rock consisted of laminated silty mudstone which is grey in color with darker bands. To reduce any possible variability in the mechanical properties, the samples were cored from carefully selected similar blocks, which were mostly dominated by a similar angle of lamination (i.e. 0^o-7^o to the horizon of specimen flat surface). After coring, the rock samples were left to dry out for 24 hours at 50^oC, and then coated with a very thin layer of flexible varnish to eliminate the effect of humidity so that the un-weathered condition of the material would be maintained over the storing and testing periods.

The tests utilised an RDP Howden servo-controlled stiff machine connected to a computer data logger. The confining stress was applied using a Hoek cell and servo controlled hydraulic pump. The axial displacement was measured by two linear voltage differential transducers (LVDTs) with a precision of 0.005mm. During the test, the computer continuously monitored and recorded the axial load, axial displacement and confining pressure.

The tests were conducted at room temperature ($\approx 23^oC$) on cylindrical samples of 74mm in height and 36mm in diameter, which were prepared in accordance with the procedure outlined by the ISRM (1981).

2.2. Experimental programme

To investigate the effect of strain rate on stiffness and strength of the silty mudstone, laboratory experiments were carried out at a strain rate varying from approximately 10^{-4} to 10^{-6} s^{-1} using the multi-stage triaxial testing technique (MSTT). In such experiments, the same rock specimen undergoes multiple triaxial tests at intervals of increasing confining pressure. Moving between the stages of confinement in the test was made manually when the operator observed significant reduction in the inclination of force-displacement curve (start of significant yield).

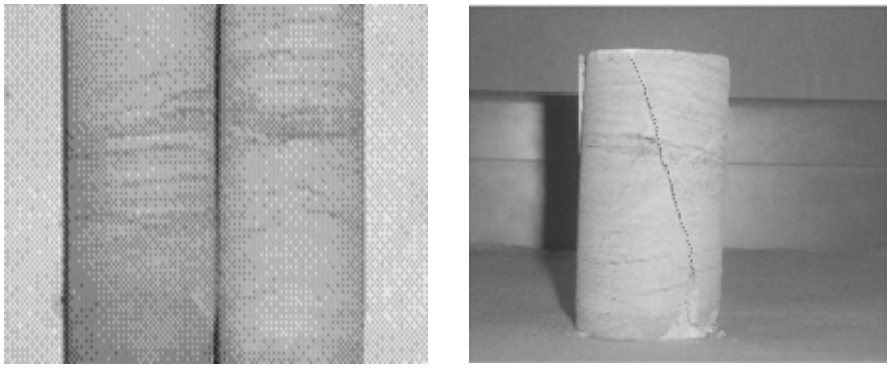
The MSTT technique enables experimenters to conserve samples and to obtain more consistent strength and stiffness data by eliminating sample variability. However the testing does not allow the post-peak behaviour to be observed, which is not our scope of investigation in this study.

The tests were conducted on dry specimens with two different structural conditions: intact and fractured. The fractured rock specimens were produced from intact rock samples after breaking them in standard triaxial compression tests with 10 MPa of confinement to simulate *confined failure* (e.g. underground excavations). The broken specimens were then left in-place to carry on the multistage triaxial testing.

Table 1 present a summary of the main experimental features and Figure 2 illustrates the two types of specimens used in the tests.

Table 1. Summary of the experimental details of: the rock samples and the testing conditions.

Rock samples		*Test details*	
Rock	Silty mudstone- Grey	Confining pressure, MPa	0-20
Structure	Intact & Fractured	Axial displacement speed, mm/s	0.074-0.00074
Unit weight, kN/m^3	24.9	Strain rate, S^{-1}	10^{-4} to 10^{-6}



(a) Intact specimens (b) Fractured specimen

Figure 4. The silty mudstone samples with two structural types used in the tests: (a) intact and (b) fractured. All specimens were cylindrical with 74mm height and 36mm diameter.

3. Results and discussion

3.1. General experimental behaviour and method of estimation: stiffness and strength

Figure 5a shows experimental results from a selected test conducted on an *intact* sample at a strain rate =1e^{-4}s^{-1} and confining pressure ranging from 2 to 15MPa. The axial stress-strain data in each stage was precisely fitted to the 6th order of a polynomial function and then the derivative, which represents the tangent modulus of elasticity, was obtained.

Basically, the tangent modulus of elasticity (E_t) represents the slope of stress-strain curve at any point. The fluctuation of this modulus throughout the multistage is shown in Figure 5b: in the first stage, E_t initially increased in magnitude until reaching a peak value (e.g. elastic-limit), where the material would be expected afterwards to deform plastically. Proceeding to the next stage by increasing the confining pressure, the tangent modulus E_t showed a jump and then typically decreased as if the material was continuing the yielding phase (inelastic deformation).

For the analysis, the strength, *S*, was taken as the maximum axial stress applied in each stage (Figure 5a), and the elastic modulus *E* in each stage was considered as the maximum value of E_t (Figure 5b). This procedure for estimating *E* may be appropriate in the first stage, however *E* can be under estimated in the following stages as the sample is likely to have experienced some plastic deformation before the proceeding to the next stage. Nevertheless that, the procedure permitted consistent estimation of stiffness between all samples, which was appropriate for the generic nature of this experimental study.

Another typical experimental behaviour, taken from a test conducted on the *fractured* rock samples, is shown in Figure 6, where the broken material did not present any significant resistance at the initial stage (i.e. σ_3 was almost zero) but persisted in its strength and stiffness during the following stages as the confining pressures progressively increased up to 20MPa.

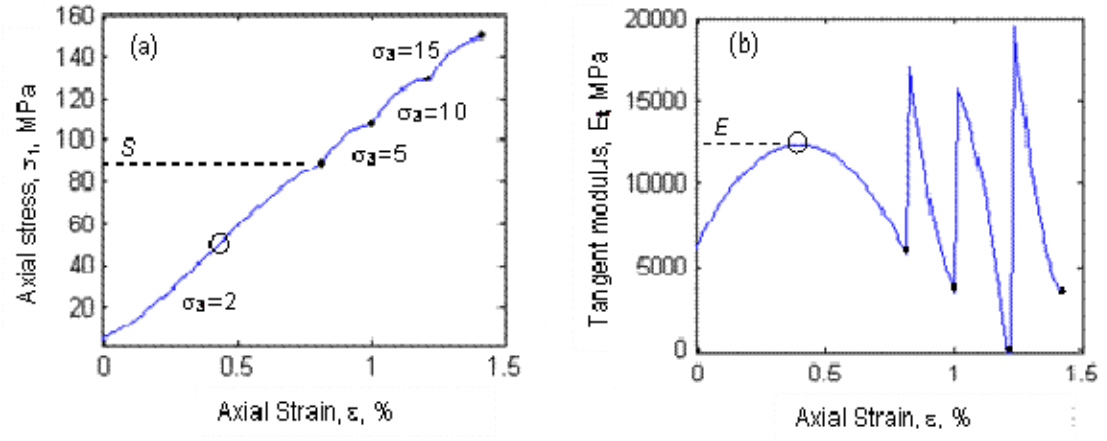


Figure 5. Four-stage triaxial compression test conducted on intact sample of silty mudstone at a strain rate equal to approximately 1e^{-4} s^{-1}. The confining pressure, σ_3, is given in MPa.

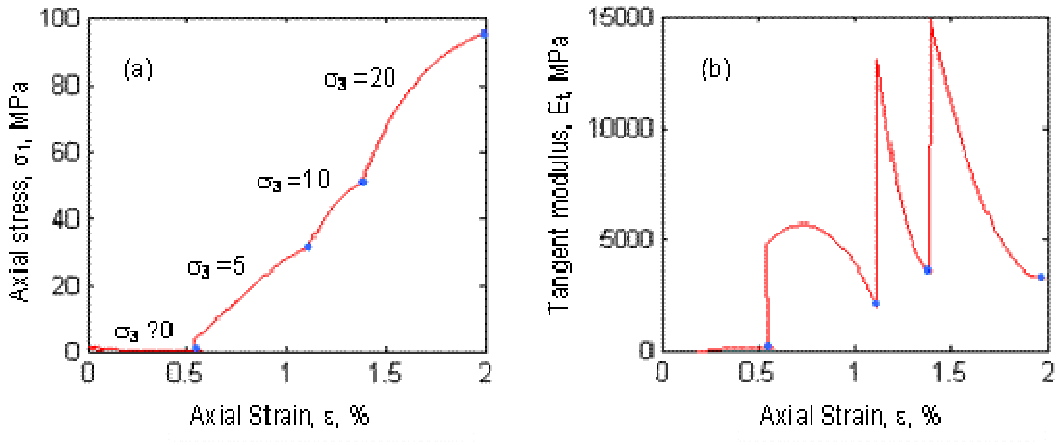


Figure 6. Four-stage triaxial compression test conducted on *fractured* sample of silty mudstone at a strain rate ≈ 5.9e^{-6} s^{-1}. The confining stress increased gradually as follow: 0, 5, 10, and 20 MPa

3.2. The effect of strain rate on strength and stiffness of intact specimens

The relationships between strain rate and rock properties are shown in Figure 7 for three four-stage triaxial tests conducted at different strain rates: 1e^{-4}, 1e^{-5} and 1e^{-6} s^{-1}. The results provided evidence that the strain rate has some effect on stiffness and strength particularly at higher confinements; the lower the strain rate the lower elastic modulus and pre-failure stress.

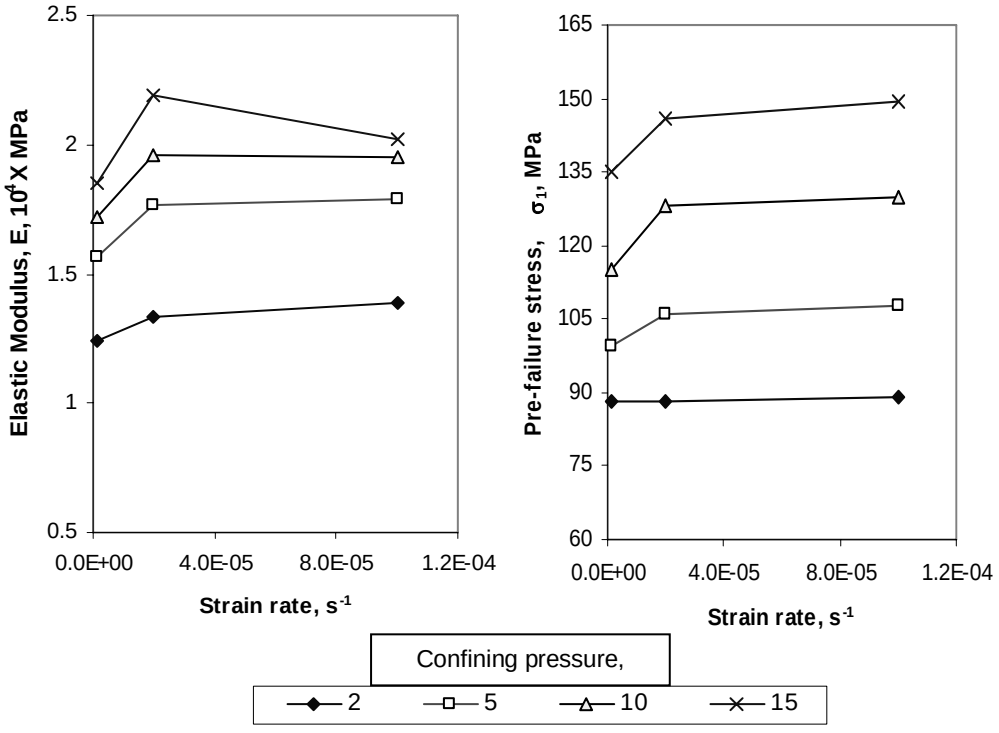


Figure 7. The relationship between the elastic modulus and confining pressure for the intact specimens.

The effect of the confinement on the elastic modules was clearly dominant, where *E* values increased with the confining pressure and then levelled out after σ_3=10MPa. It is interesting to note that at the lower strain rate the effect of confinement on stiffness is generally less.

In an attempt to obtain more findings from the results of the intact rock samples, the relationship between deviatoric stress, $q = \sigma_1 - \sigma_3$, and mean stress, $p = (\sigma_1 + 2\sigma_2)/3$ at failure is shown in Figure 8. In terms of strength changes, the figure clearly shows that the effect of time (i.e. strain rate) is not significant in the intact rock behaviour particularly al low deviatoric stress. This is consistent with previous experimental findings conducted on the same rock, where a number of *creep tests* proved that the material had insignificant viscous properties.

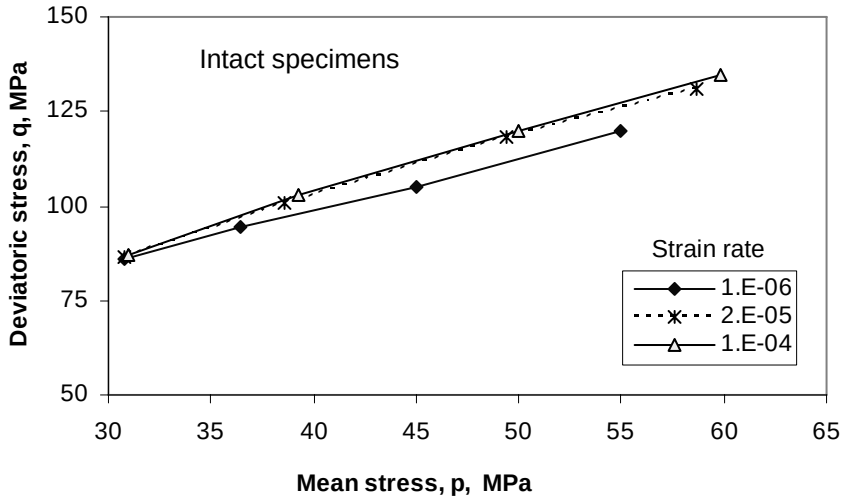


Figure 8. Deviatoric stress vs mean stress at failure for three levels of strain rate.

3.3. The effect of strain rate on strength and stiffness of fractured specimens

The fractured sample tests were performed at confining pressures varying from 0 to 20 MPa and strain rate from $3e^{-5}$ to $5e^{-6}s^{-1}$. Figure 9a shows the elastic modulus vs confining stress relations at different strain rates. The contribution of strain rate to the variation of rock deformation (stiffness) clearly increases with confining pressure σ_3 ranging from 0 to 10MPa. For example, at σ_3=10MPa stiffness decreased by more than 2.3 times when strain rate went from $1.71e^{-5}$ to $5.19e^{-6}s^{-1}$. At higher confining pressure, the influence of strain rate tends to less (e.g. level-out).

The experimental data (Figure 9a) shows also that the effect of confinement on elastic modules, *E*, is very significant. It can be seen that the values indicated by this figure imply that the confining stress had the greatest effect on *E* at 10MPa confinement, although there is a general monotonic increase in this parameter up to the maximum confining stress of 20MPa. A similar trend was observed for the rock strength properties as shown in Figure 9b.

It can be noted that the stiffness and strength properties did not coincide with the same order of the strain rates, as each rock sample may have had different joint patterns. However, there is general tendency for these properties (stiffness and strength) to decrease with the decrease of strain rate and vice versa.

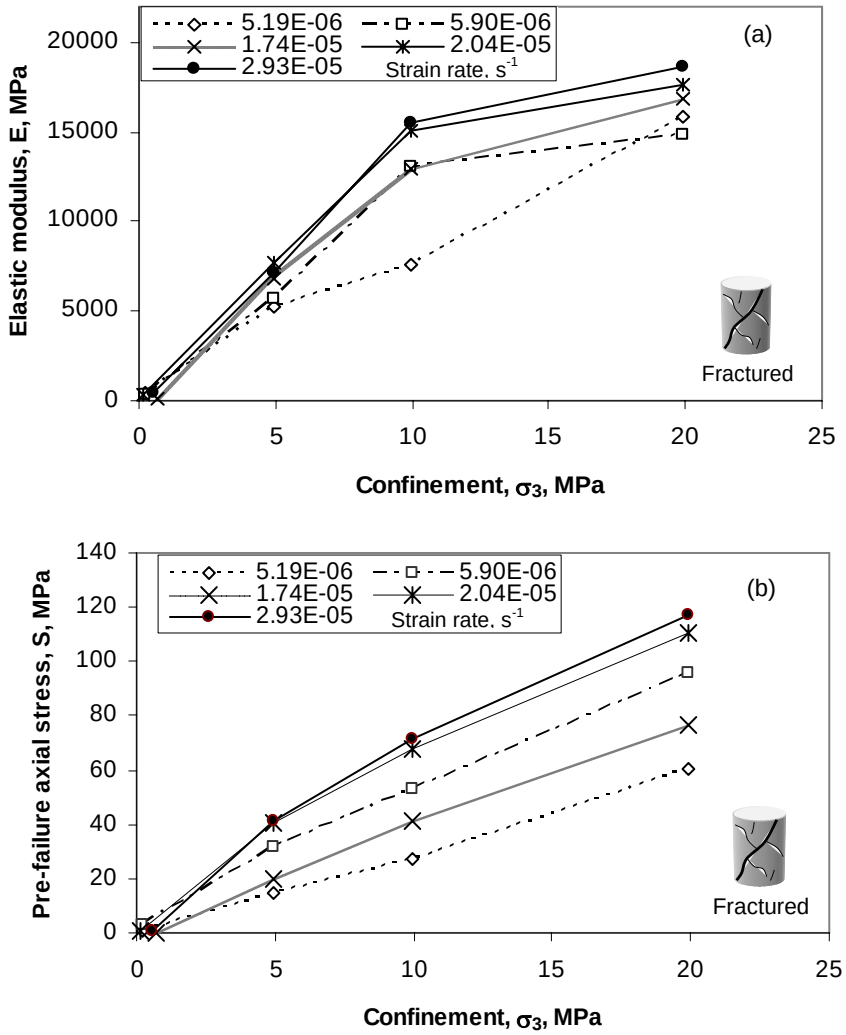


Figure 9. The effect of strain rate on: (a) elastic modulus, *E*, and (b) pre-failure axial stress, *S*, of the fractured samples.

3.4. Discussion – partial relaxation and partial creeping

Under the servo-controlled machine, the slower rate of strain loading might allow more time for *stress redistribution* and hence the rock material to *partially* creep or relax. The mechanism underlying strength reduction induced by slower strain rate can be explained on the grounds of partial relaxation: in the fractured rock sample by a movement along the pre-existed cracks or fractures (shear band) while the partial relaxation in the intact material can be attributed to crack propagation. Both mechanisms lead to a lowering of stress, hence, a lowering of the strength of the samples.

The stiffness reduction induced by slower strain rates may be explained on the grounds of partial creeping where visco-elastic deformation can contribute to the decrease in the measured stiffness. This coincides with previous conclusion that the creep can lead to a reduction in elastic modulus (Maranini and Brignoli, 1999).

It is commonly accepted that the ability of rock to relax or creep considerably increases in weaker rocks (e.g. Hobbs, 1970; Parsons and Hedley, 1966). This reinforces our hypothesis of the partial creep and relaxation which allowed the effect of strain rate to be more pronounced in the fractured rock (weak rock).

3.5. Empirical law for rock with strain rate-dependent stiffness and strength

The experimental data of the fractured samples, reporting elastic modulus and strength vs strain rate, may be fitted individually by various functional relationships. Logarithmic curve, as shown in Figure 10, was found to be the best fit among the other basic possibilities (e.g. linear, exponential and power law).

Although this initial fitting can describe the non-linear functionality of strength and stiffness in the tested range of strain rate, this simulation can lead to a deficiency in which the stiffness and strength go to infinity or a negative value if the strain rates ultimately increase or decrease in wider ranges.

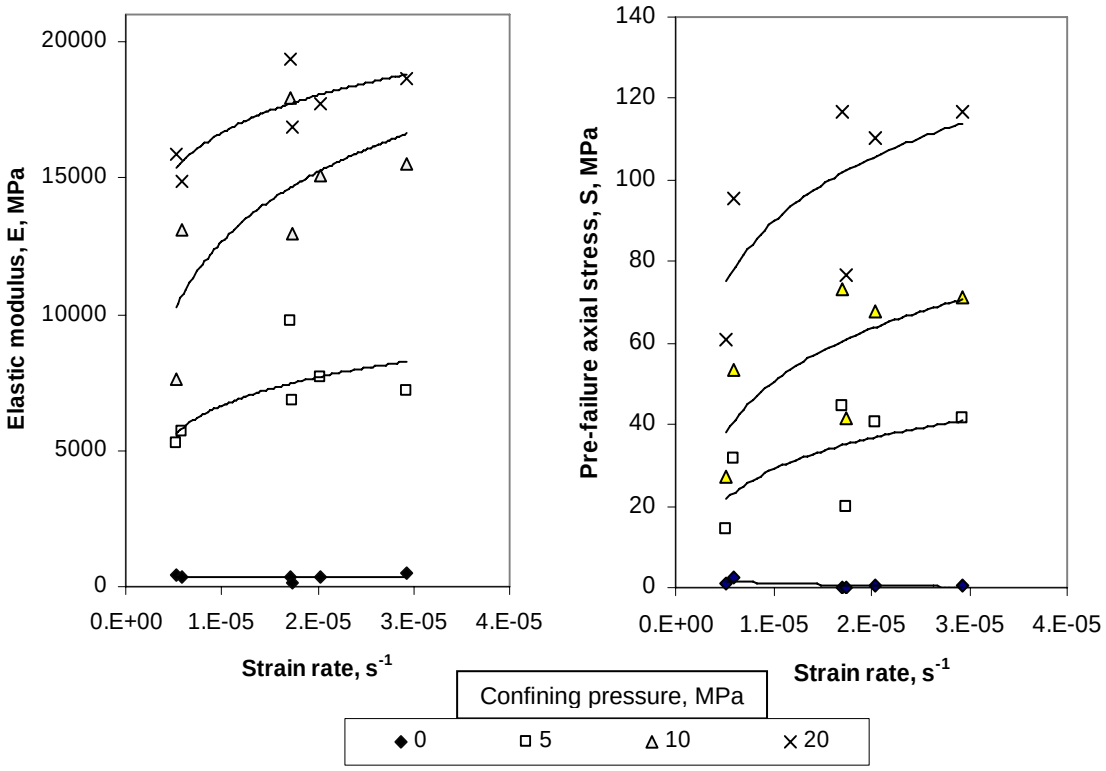


Figure 10. The effect of strain rate on elastic modulus and pre-failure axial stress at different confining pressures in the fractured rock samples. The graphs contain the actual data and their initially fitted logarithmic curves.

More sophisticated function, used by Yongsheng and Caichu (2000) to model the effect of strain rate on the uniaxial compressive strength of red sandstone, can overcome this deficiency. Therefore, a similar approach was adopted herein and particularly developed to suit our experimental data including the three dimensional stress conditions (i.e. the effect of confining pressure).

For a given strain rate ε', the stiffness (the elastic modulus, E) and strength (pre-failure axial stress, S) may be calculated for the *fractured* silty mudstone from the following equations:

$$E = A_E + B_E \text{ atan } (\log \varepsilon' + C_E) \quad (1)$$

$$S = A_S + B_S \text{ atan } (\log \varepsilon' + C_S) \quad (2)$$

where A, B and C (notated either with $_E$ or $_S$) are a function of confining pressure, σ_3.

At σ_3=10 MPa, a least square regression gives the following values: A_E =10210, B_E =4500, C_E =12.6, A_S =10210, B_S =4500, C_S =12.6; the corresponding fitted curves of the stiffness modulus, E, and strength, S, are shown in Figure 11. The figure shows clearly that stiffness and strength of the broken rock are more sensitive to strain rate in a range that starts from $8x10^{-6}s^{-1}$ downwards.

Table 2 presents the values of all these parameters at four levels of confinement. Due to the limitation of the range of observations, the evaluation here is suitable only in a narrow range of strain rates.

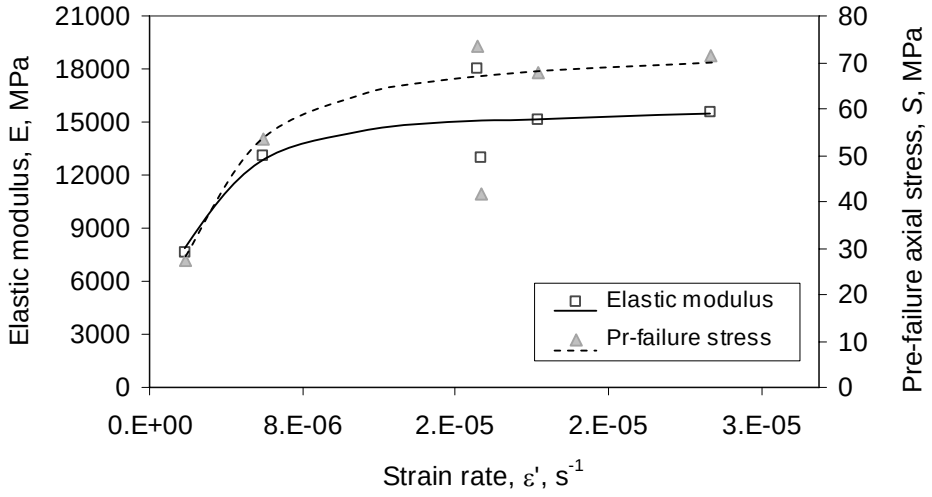


Figure 11. Fitted relationship between strain rate and both elastic modulus and pre-failure stress

Table 2. Fitting parameters for different confining pressure.

σ_3, *MPa*	Elastic modulus parameters				Strength parameters			
	A_E	B_E	C_E	*R-square*	A_S	B_S	C_S	*R-square*
0	360	1	1	0.38	2.14	1	1	0.30
5	9741	2955	10.3	0.42	21.77	17.05	12.54	0.71
10	10210	4500	12.6	0.73	41.56	25.2	12.75	0.78
20	12000	4800	13.9	0.59	71.98	35.09	12.84	0.77

4. Conclusion

This study has investigated the phenomena associated with strain rate effects on the mechanical properties of Silty Mudstone using multi-stage triaxial testing. Within a selected range of strain rate, the experiments were conducted on both intact and fractured rock specimens to cover the two ultimate structural conditions of the rock mass. The following conclusion and recommendation may be drawn from the research:

- The fundamental effect of strain rate changes in the rock constitutive behaviour is the alteration of stiffness and strength. This influence is more pronounced in the fractured rock samples implying that weak broken rocks are more vulnerable to strain rate changes than stronger ones. Although this influence was not completely proportional, a significant decrease in strain rate has resulted in a decrease in the rock properties (elastic modulus and pre-failure axial stress).
- At low confinement, the strain rate did not induce any clear changes in the properties of intact samples, a finding which contradicts with previous observation made by Peng and Podnieks (1972) on tuff. This discrepancy can be contributed to the small range of strain rate applied in our tests, suggesting that brittle rocks may require a wider range of strain rate application in order to obtain a noticeable difference in their properties. At higher confining pressure, the results have shown a slight effect of strain rate on the intact samples properties (both stiffness and strength).
- In fractured samples, the changes in rock properties with different strain rate can be noted at all confining pressures most notably at 10MPa.
- The reduction of stiffness and strength induced by a slower strain rate may be explained on the grounds of partial creeping and partial relaxation respectively. The suggested mechanisms allow the effect of strain rate to be fundamentally more pronounced in the fractured rock (weak rock).
- The experimental data describing the effect of strain rate on strength and stiffness of the fractured silty mudstone was fitted to a non-linear logarithmic function. The application of this model to other rock types and wider range of strain rates remains to be investigated. Further investigation adopting an elasto-viscoplastic constitutive model (e.g. Kaiser and Morgenstein, 1981-b) and applying the results into a case study would add on to the current study and ultimately improve the prediction tools.
- Finally, the study suggests that coal measure rocks, which comprises medium to weak rocks, might be very sensitive to strain rate changes and, thus, the stability of workings in abandoned mines as well as active mines needs to be evaluated in this regards. Ignoring these effects could lead to large discrepancies between predicted data and real field measurements.

5. Acknowledgements

The experiments were conducted in the rock mechanics laboratory of Nottingham Centre for Geomechanics (NCG) as part of a research project funded through the Research Programme of the Research Fund for Coal and Steel (RFCS).

6. References

Bieniawski Z.T. (1970). *Time-dependent behaviour of fractured rock.* Rock Mechanics, 2, 132-137.

Hobbs D W. 1970. *Stress-strain-time behaviour of a number of coal measure rocks.* International. .rock science. 7, 149-170.

ISRM (1981). *Rock Characterization Testing and Monitoring*. Brown, E.T. (ed.). Pergammon Press.113-122.

Kaiser P.K. and Morgenstein N.R. (1981-a). *Time-dependent deformation of small tunnels—I. Experimental facilities.* J Rock Mech Min Sci & Geomech. Abstr., 18, 129-140.

Kaiser P.K. and Morgenstein N.R. (1981-b). *Phenomenological model for rock with time-dependent strength.* J Rock Mech Min Sci & Geomech. Abstr., 18, 153-165

Maranini, E., and M. Brignoli. (1999). *Creep behavior of a weak rock: experimental characterization,* Int. J. Rock Mech. Min. Sci., 36, 127-138.

Parsons R.C. and Hedley D.G.F. 1966. *The analysis of the viscous property of rocks for classification*. Int J Rock Mech Min Sci. 30, 3, 325–335.

Peng S.S. (1973). *Time-dependent aspects of rock behaviour as measured by a servo-controlled hydraulic testing maching.* Int. J. Rock Mech. Min. Sci. 10, 235-246.

Peng S.S., Podnieks E.R. (1972). *Relaxation and the behaviour of failed rock*. Int. J. Rock Mech. Min. Sci. 9, 699-712.

Singh D.P. (1975). *A study of creep of rocks.* Int. J. Rock Mech. Min. Sci. & Geomech. Abstr. 12, 271–276.

Wawersik W.R. (1973). *Time-dependent rock behaviour in uniaxial compression*. Proc. 14th Symp. Rock Mechanics, Pennsylvania, 84-106.

Yongsheng Li, Caichu Xia. (2000). *Time-dependent tests on intact rocks in uniaxial compression.* Int. J. Rock Mech. Min. Sci. 37, 467-475.

POST MINING HAZARD ASSESSMENT IN NORTH RHINE-WESTPHALIA (GERMANY) AT THE EXAMPLE OF THE AACHEN HARD COAL MINING DISTRICT

Dr.-Ing. HEITFELD Michael[1], Dipl.-Ing. M.Sc. MAINZ Mark[1], Prof. Dr. SCHETELIG Kurt[1]

[1] IHS (INGENIEURBÜRO HEITFELD-SCHETELIG), Preusweg 74, D - 52074 Aachen; info@ihs-online.de

ABSTRACT: In North Rhine-Westphalia, large areas are affected by mining legacies endangering the ground surface and public safety. The problems arising and the current risk management are demonstrated at the example of the Aachen hard coal mining district. Hazards especially result from outcrops of coal seams mined at shallow depths and shafts whilst galleries usually seem to be rather unperilous due to their depth and small dimension. In this paper, the design of hazard zones and the assignment of hazard classes are described. Recent scientific developments related to the size of hazard areas are described and an outlook on future procedures is given.

KEYWORDS: Hazard, collapse feature, shallow mining, shaft, gallery.

RESUME: Des régions étendues de Rhénanie-du-Nord-Westphalie sont influées par des mines abandonnées présentant des risques pour la stabilité de la surface et la sécurité publique. La région houillière d'Aix-la-Chapelle est décrite, servant d'exemple pour ces problèmes et leur traitement. En particulier les mines proche de la surface et les puits sont plus dangereux que les galeries de taille plus faible et localisées à des profondeurs plus importante. Cet article précise le définition et l'affectation des classes de danger. Des développements scientifiques récents relatifs à l'étendue de la zone de danger sont décrits, ainsi que les améliorations futures prévues.

MOTS-CLEFS: Mines abandonnées, puits, galeries, zones de péril, classification des périls.

1. Introduction

Large parts of North Rhine-Westphalia are affected by various mining activities. Most of these mining activities ceased meanwhile and left behind large post mining areas with hazards for public safety (see fig. 1). The problems arising in North Rhine-Westphalia from former mining activity and the current risk management of the mining authorities are demonstrated at the example of the hard coal mining district of Aachen (Aix-la-Chapelle).

Within this mining district lies one of the oldest coal mining areas in Europe, the so called "Wurmrevier" (mining district of the river Wurm) with an area of about 19 km² of which approximately 14 km² are populated densely. Here, below the cities of Herzogenrath and Würselen, the Carboniferous rock lies at shallow depths up to about 25 m and dewatering galleries were driven into the rock starting from the valley of the river "Wurm" (see fig. 2). Mining activity in this valley dates back to the 12th century or maybe even back to Roman times and mapped mining information is scarce.

The resulting hazard potentials are an important obstruction to land use planning. Before building permission is given, the general possibility of the existence of mining legacies is examined in a first desk study by the mining authorities. If mining legacies possibly could affect a site, then a more detailed second desk study and, if necessary, on-site investigations are performed by expert offices. Hazard zones around shafts and above coal seams mined at shallow depths have to be remediated according to the state of the art before building projects are permitted by the authorities. Existing buildings are not affected by any examination or remediation necessity.

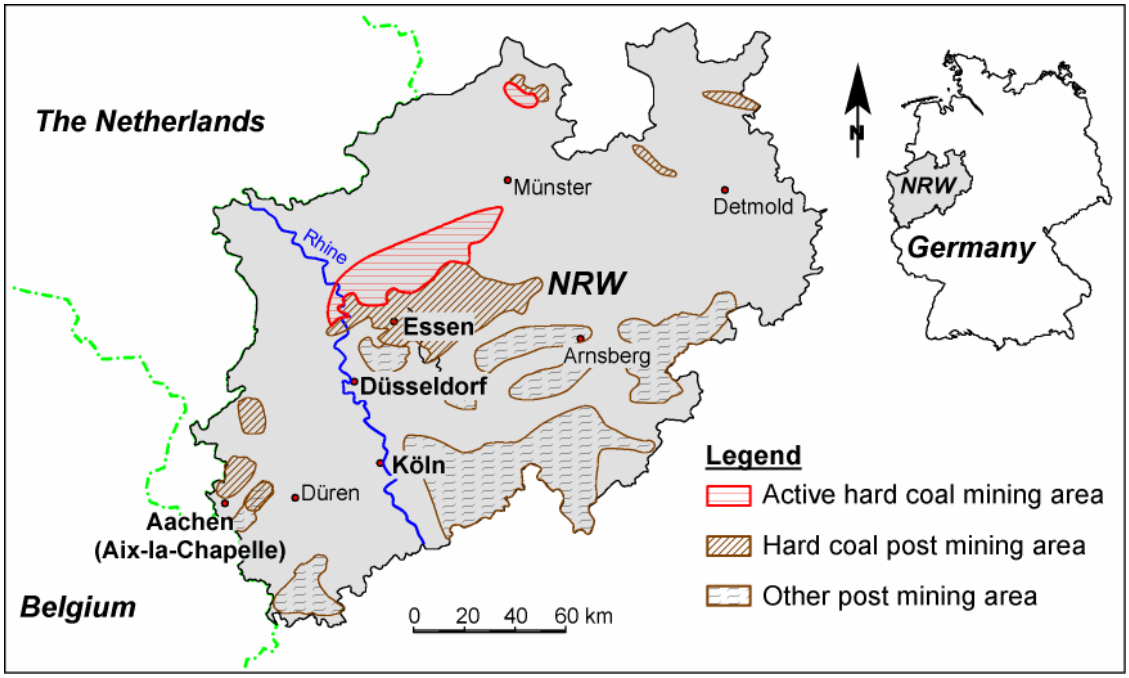


Figure 1: Mining areas in North Rhine-Westphalia (based on Welz, 2001).

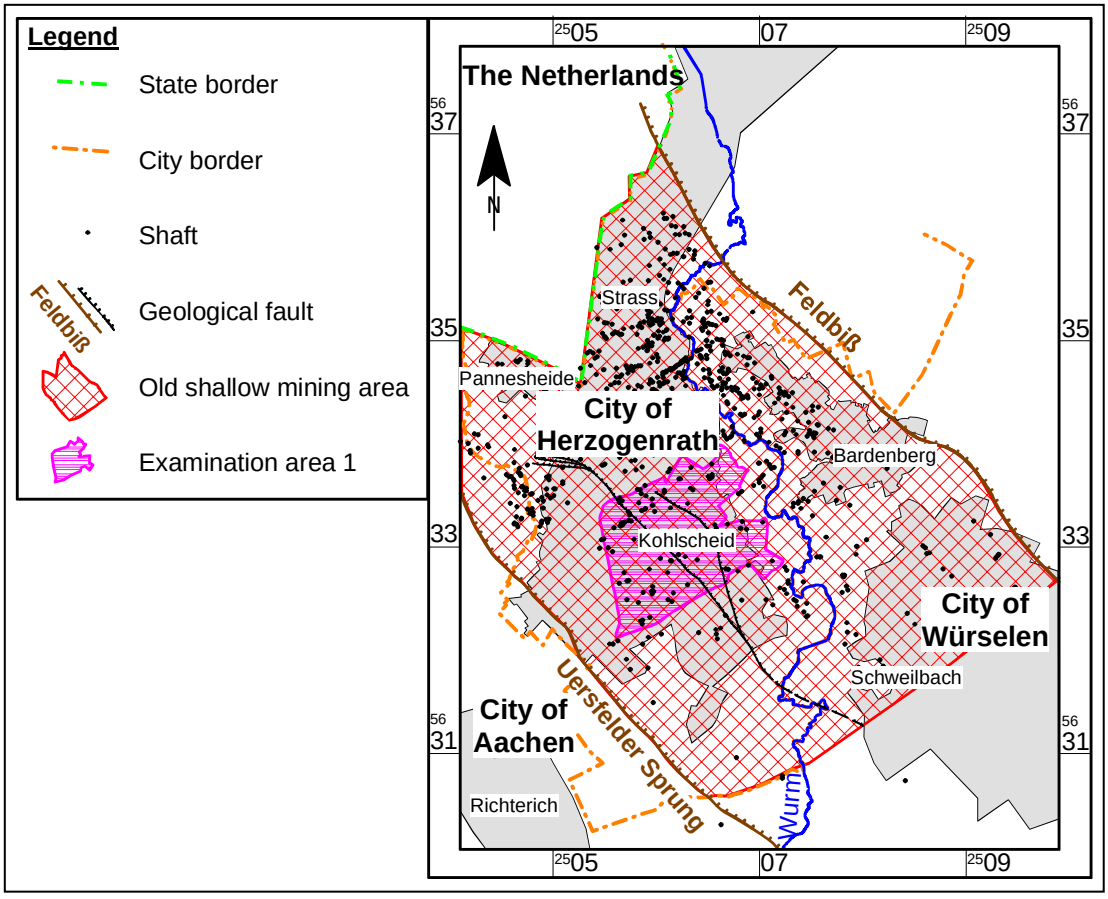


Figure 2: Area of shallow mining in the Aachen hard coal mining district.

2. Geology

2.1. Overburden

The overburden in the "Wurmrevier" consists of a thin layer of unconsolidated sediments of Quaternary and Tertiary age up to about 25 m thickness. A typical layer formation is a silty and clayey sand ("Lower Lintfort Formation") covered by Maas sand with gravel (sediments of the River "Maas") and loess loam on top. Towards the valley of the river Wurm, the overburden thickness decreases until the Carboniferous rock emerges at banking level.

2.2. Carboniferous rock

The Carboniferous rock of the Aachen mining district generally consists of sand-, silt- and claystones of Namur C to Westfal B age. The deposits are striking SW-NE and are folded quite intensively resulting in a broad variety of angles of dip of the coal seams. The enclosed coal seams have a spatial percentage of about 3 % of these sediments. Distinct geological faults strike NW-SE. East of the fault "Feldbiß" the surface of the Carboniferous rock lies significantly deeper than west of the fault. In the eastern part, mining activity did not start before the 20th century when shafts were sunk to a depth of up to 800 m.

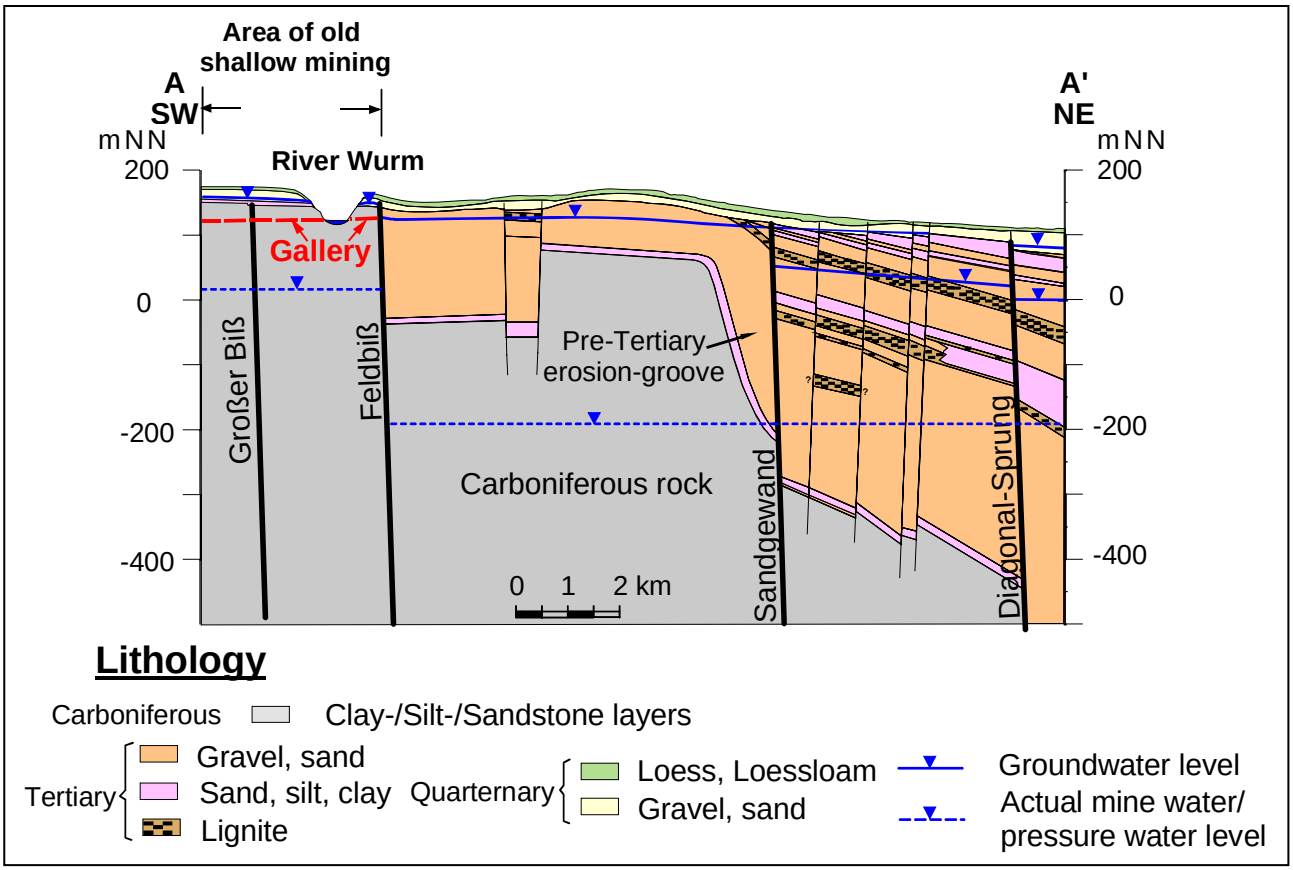


Figure 3: Geological-tectonical section of the Aachen hard coal mining district.

3. Hazard sources

Hazards within the Aachen hard coal mining district mainly result from collapse features above outcrops of dipping coal seams that have been mined at shallow depths (< 40 m) and abandoned shafts which often only have a partial and unstable filling or no filling at all. Even if the shafts have been filled, the filling material was not compacted densely. Moreover, abandoned shafts pose a risk of gas emissions.

The number of such abandoned shafts within the area of old mining activity west of the geological fault “Feldbiß” (s. fig. 3) is estimated to be more than 800. There is almost no information available on mining activity before around the year 1800 when during the French occupation mine mapping was intensified. From the year 1815 onwards Prussia kept up mapping the mining activities. Due to the very incomplete data on mining activity before 1800, a hazard of collapse features simply has to be assumed to be present along all workable coal seam outcrops.

Recent collapse feature events indicate that although the probability of collapse features may decrease with time, the principal possibility of such events is independent from time. There are a lot of long-term processes that can make a formerly stable void collapse, as e.g. decay of wooden supports, progressive failure, creep, weathering, hydraulic changes and stress redistribution.

Galleries commonly seem to pose no risk due to their depth and small dimension. Moreover, these galleries usually are partly filled up with sludge reducing the cavity volume. Rising mine water can lead to pollution of groundwater, river, lakes and soils due to its high contents of metals and salts, can make partial shaft fillings unstable by changing their cohesion and result in differential ground heave along faults. In the adjacent Erkelenz hard coal mining district, approximately 30 km north of Aachen, the mine water recovery caused a ‘damage line’ running approximately parallel to the Rurrand fault system. This ‘damage line’ has a length of about 10-12 km and differential heaves of up to 6 cm within a range of only 5 m. Until the end of 2004 damages occurred at 110 objects. Nine objects could not be repaired any more and had to be torn down (Heitfeld et al., 2004). Ground heave induced by the ongoing groundwater recovery is currently being researched within an international project group.

4. Hazard zonation

The current approach to mining legacies is linked to permission procedures for new buildings. Old existing infrastructure tended to avoid areas of former mining activity. Since such public knowledge of possibly dangerous areas is decreasing with time, it mainly is newly planned infrastructure that can be effected by mining legacies. Moreover, a large scale risk assessment and sanitation scheme for all existing buildings in NRW is an almost unfeasible task. Hence, only the most dangerous sources of hazards to existing buildings (i.e. deep shafts) are being secured by the mining authorities or the responsible mining company (if any) as a medium-term solution.

Since existing buildings are not affected by any legal constraint due to mining hazards, it is custom to only perform hazard assessments instead of risk assessments, which additionally to the possible event size and probability would respect the kind of land use and the danger to public safety related to that. The necessity of in-situ examinations and remediation measures is assessed based on a desk study and independently of the kind of building that is planned. It is assumed that either a new building is endangered by mining legacies, so that closer examination and in some cases remediation measures are needed or mining hazards to new buildings can be ruled out completely.

The desk study usually starts with an analysis of the literature on the mining history of the district and search for hints on former mining activity within old mine maps. The old mining ground maps

are being scanned and georeferentiated and then overlapped computationally with modern housing maps. Street crossings and old houses serve as weighted benchmarks. The findings thereafter are assessed as described below.

4.1. Coal seam outcrops

For assessing the hazard of collapses at banking level above outcrops of coal seams mined at a shallow depth, three hazard classes are being distinguished depending on the evidence of former mining activity, the thickness and the angle of dip of the different coal seams. It thereby is assumed that cavities show a better long term stability in seams with high angels of dip, ("steep flanks", $\alpha > 36°$) than in such dipping with lower angles ("plane flanks", $\alpha \leq 36°$). This is due to the higher vertical compaction forces acting on cavities in seams with low angles of dip making them less stable and collapse sooner. Since the main mining activity at shallow depths ceased more than 200 years ago, most surface near cavities in coal seams with a low angle of dip have collapsed meanwhile and pose no risk to the surface any more. Hence, coal seams with high angles of dip are deemed to be more hazardous today. This assumption was verified by extensive site investigations (borings) within the Aachen hard coal mining district.

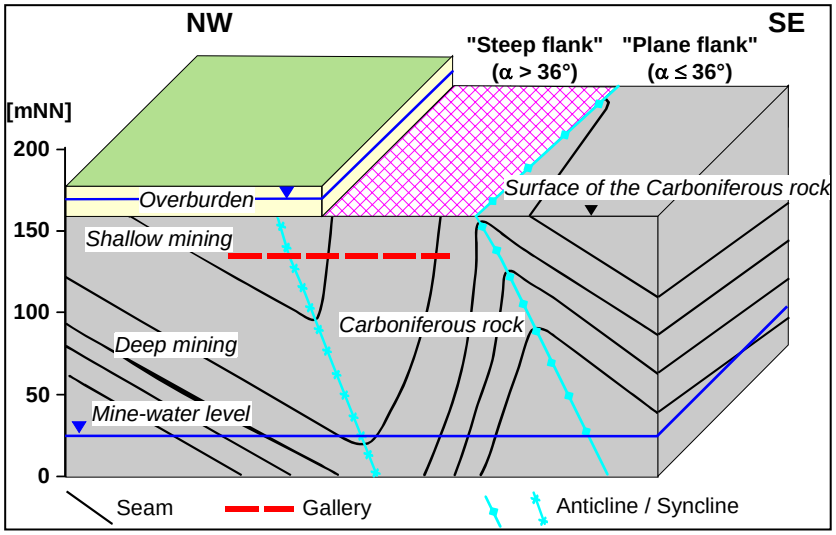


Figure 4: Model of the hard coal deposit of the "Wurmrevier".

This conception led to the following assignment criteria for the hazard class assessment above coal seam outcrops:

Table 1: Hazard class assessment above coal seam outcrops

Hazard class 1	High probability of collapse features / subsidence (evident mining activity, coal seam dipping > 36°)
Hazard class 2	Probability of collapse features / subsidence (supposed mining activity, coal seam dipping ≤ 36°)
Hazard class 3	Low probability of collapse features (mining activity can not be ruled out)
	Remediated areas / areas with proven stability

On-site investigations are necessary before building is permitted, if the hazard classes 1 or 2 are assigned. In case hazard class 3 is assigned, no on-site investigations are needed for nonsensitive buildings as e.g. housing. In case of power plants, chemical facilities etc. on site-investigations are necessary for geotechnical category 3 according to the Eurocode 7.

The width of the possibly affected area perpendicular to the strike of the coal seam outcrop is assessed based on alignment charts (Hollmann & Nürenberg, 1972), giving the endangered area on the surface of the Carboniferous rock (fig. 5). The width of the coal seam outcrop and in most cases an uncertainty related to the location of the coal seam in an order of magnitude of about 10 - 20 m has to be taken into account additionally.

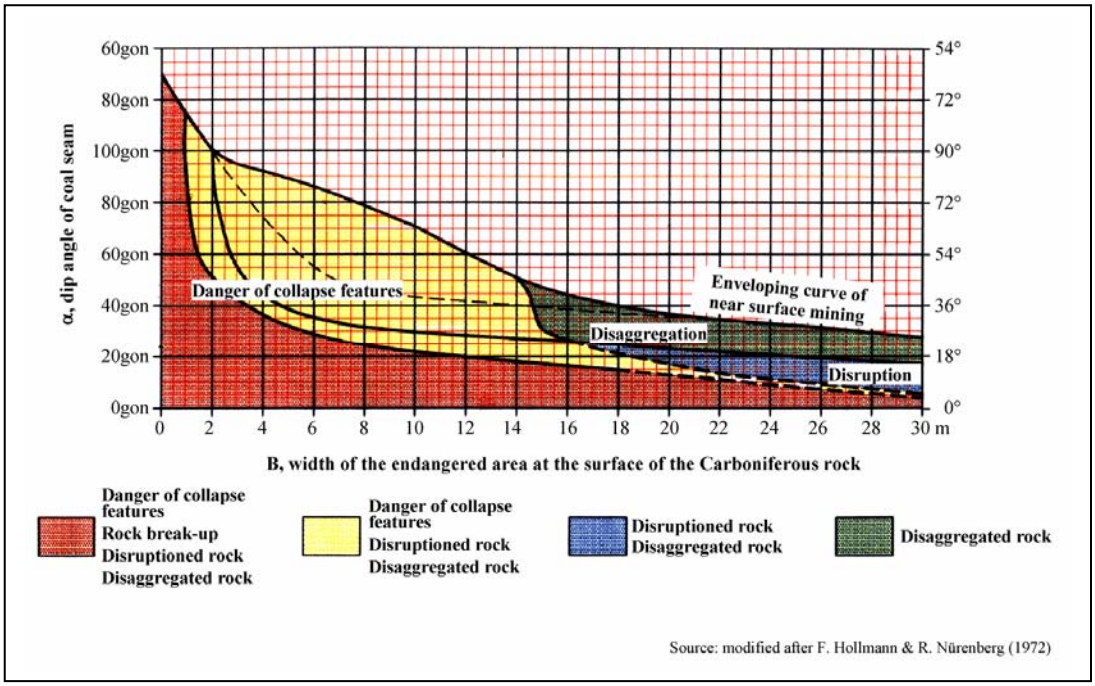


Figure 5: Width of the endangered area at the surface of the Carboniferous rock.

These hazard areas at the surface of the Carboniferous rocks then are projected towards the ground surface using a generalized angle of break of 45° within the overburden giving the width of the hazard area at banking level (fig. 6). In fact, the observed collapse features within the "Wurmrevier" show steeper slopes (also see chap. 5). A relatively low slope angle complying with the angle of friction of the soil does not develop because the collapse features usually are filled and remediated swiftly after they occurred.

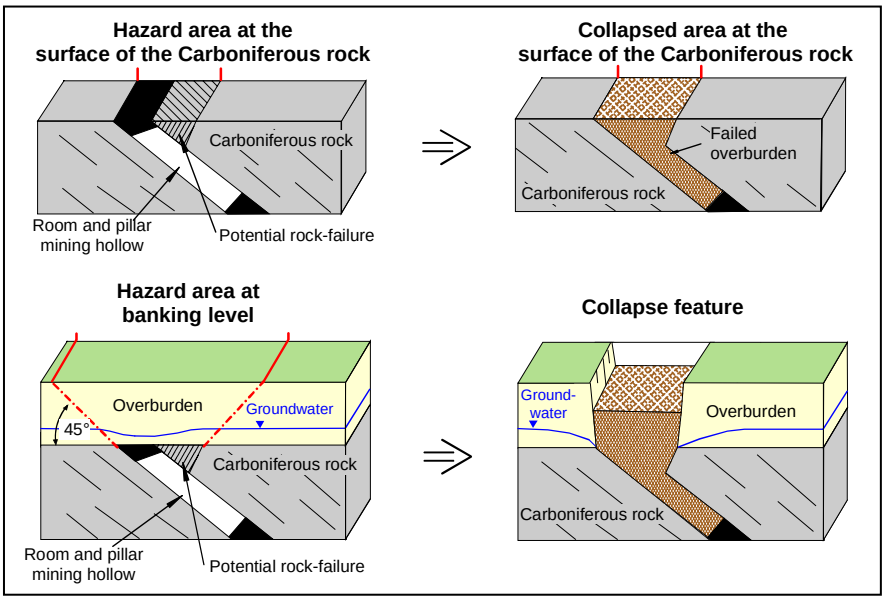


Figure 6: Hazard of collapse features above coal seam outcrops.

4.2. Shafts

The diameter of areas around unsafe shafts currently is assessed as the sum of the shaft diameter, twice the thickness of the shaft wall, twice a safety distance of 1,5 m (for disaggregation of the surrounding rock) and twice the level difference between the surface of the Carboniferous rock and banking level, also assuming an angle of break of 45° within the overburden (see fig. 7). Usually the exact location of a shaft is unknown and an uncertainty of about 10 - 20 m is to be considered, too.

No hazard classes are being distinguished within the collapse hazard zone of a shaft where building generally is not permitted as long as the shaft was not secured.

Gas hazard zones with a diameter of 40 m also are assigned to each shaft. Within this area buildings must be protected against gas using granular fill venting media and membranes. Pipes in which gas might accumulate are to be sealed.

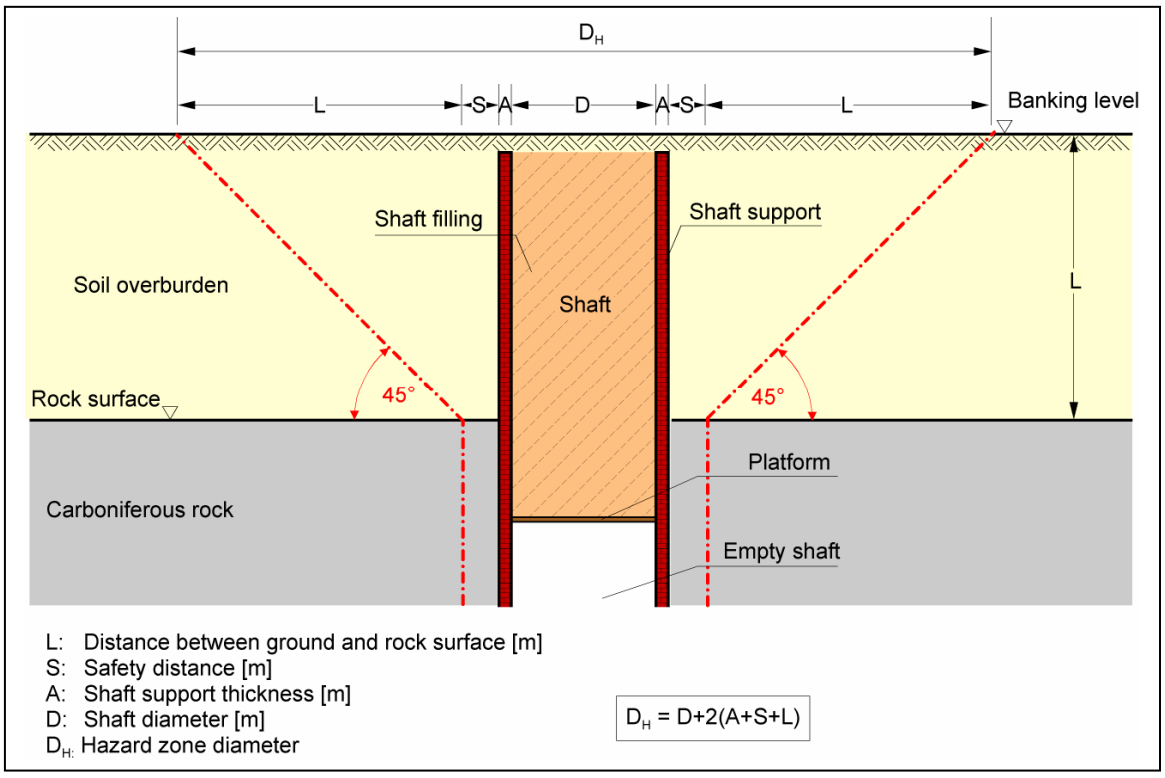


Figure 7: Shaft hazard zone.

4.3. Example of a medium scale hazard assessment ("examination area 1")

Lead by the North Rhine-Westphalian higher mining authority (Bezirksregierung Arnsberg), a first medium-scale hazard assessment for a densely populated area of approximately 1,8 km² was performed by the post mining working group of the Aachen mining district in 2002 (see fig. 2). Next to other members, this working group consisted of the responsible lower mining authority (Bergamt Düren), the local mining company (EBV AG), the geological survey (GD) and the IHS. Based on an intensive analysis of old mining ground plans and sections as well as geological-hydrogeological maps, surface projections of the deposits were elaborated and shallow mine workings and shafts were documented. Then a hazard map (see fig. 8) was worked out for coal seam outcrops using the hazard classes shown in table 1 and the chart of Hollmann & Nürenberg (1972), shown in fig. 5. This map shows hazard zones at the surface of the Carboniferous rock. In

order to gain hazard zones at banking level an angle of break of 45° within the overburden as well as coal seam location uncertainties (usually about ± 10 - 20 m) have to be taken into account additionally. In order to minimize the hazard zones at banking level for specific projects, these coal seam location uncertainties can be minimized by borings.

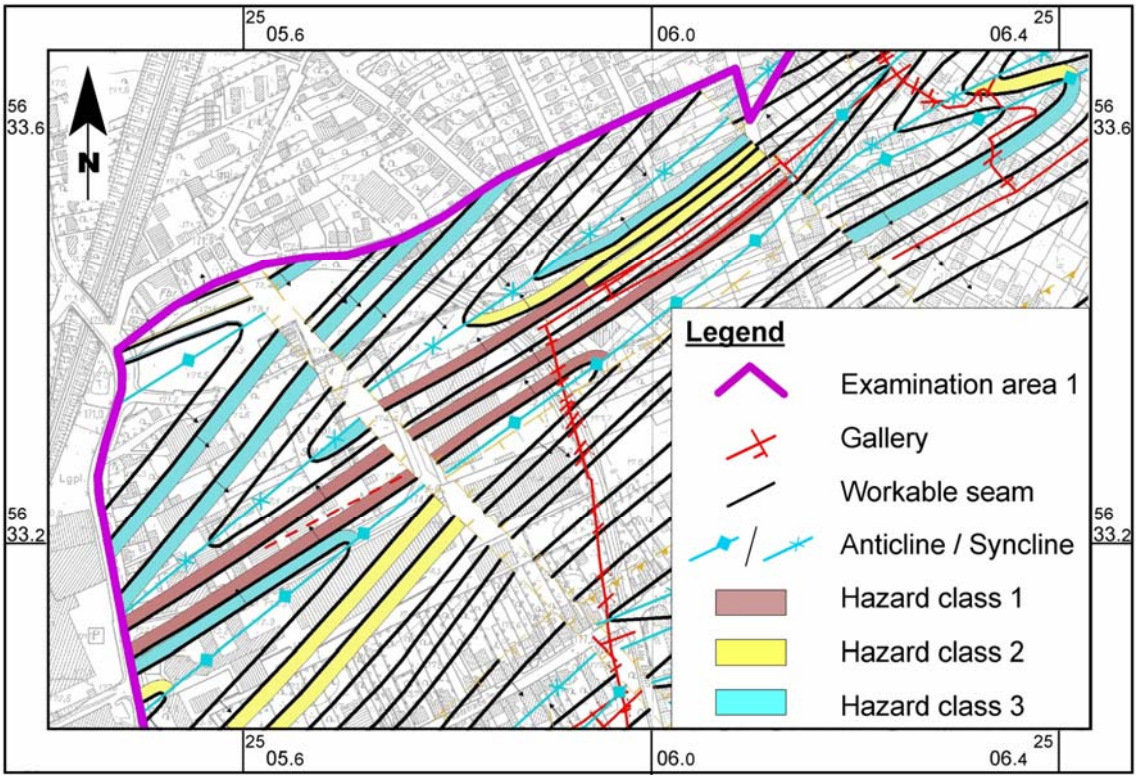


Figure 8: Detail of the coal seam outcrop hazard map at the surface of the Carboniferous rock for examination area 1

Another hazard map shows shaft hazard zones at banking level based on the design method for a shaft hazard zone described above (see fig. 7). These hazard maps now are basis for any building permission process within the examination area 1.

The local authorities of the city of Herzogenrath and the mining authorities are planning a large scale hazard assessment for the complete “Wurmrevier” within the next years. The results are meant to ease local town planning and to reduce the fear to invest in this area.

5. Outlook

The method currently used in North Rhine-Westphalia for designing hazard zones above coal seam outcrops assumes an angle of break of 45° within the soil overburden. This assumption does not take into account any soil mechanical properties of the different types of soil of the overburden.

First results of a PhD study (Mainz, see Heitfeld et al., 2005) indicate that a significant reduction of hazard zones in the Aachen “Wurmrevier” is possible considering the geotechnical properties of the overburden. Within the study collapse features where investigated using borings, penetration tests and extensive laboratory works. The study revealed, that the generalized angle of break of 45° within the overburden leads to significantly oversized hazard zones.

The on-site investigations show that the collapse process can be partitioned into single process phases with different collapse geometries depending on the soil parameters (see fig. 9). This led to a special local collapse feature model for the “Wurmrevier”.

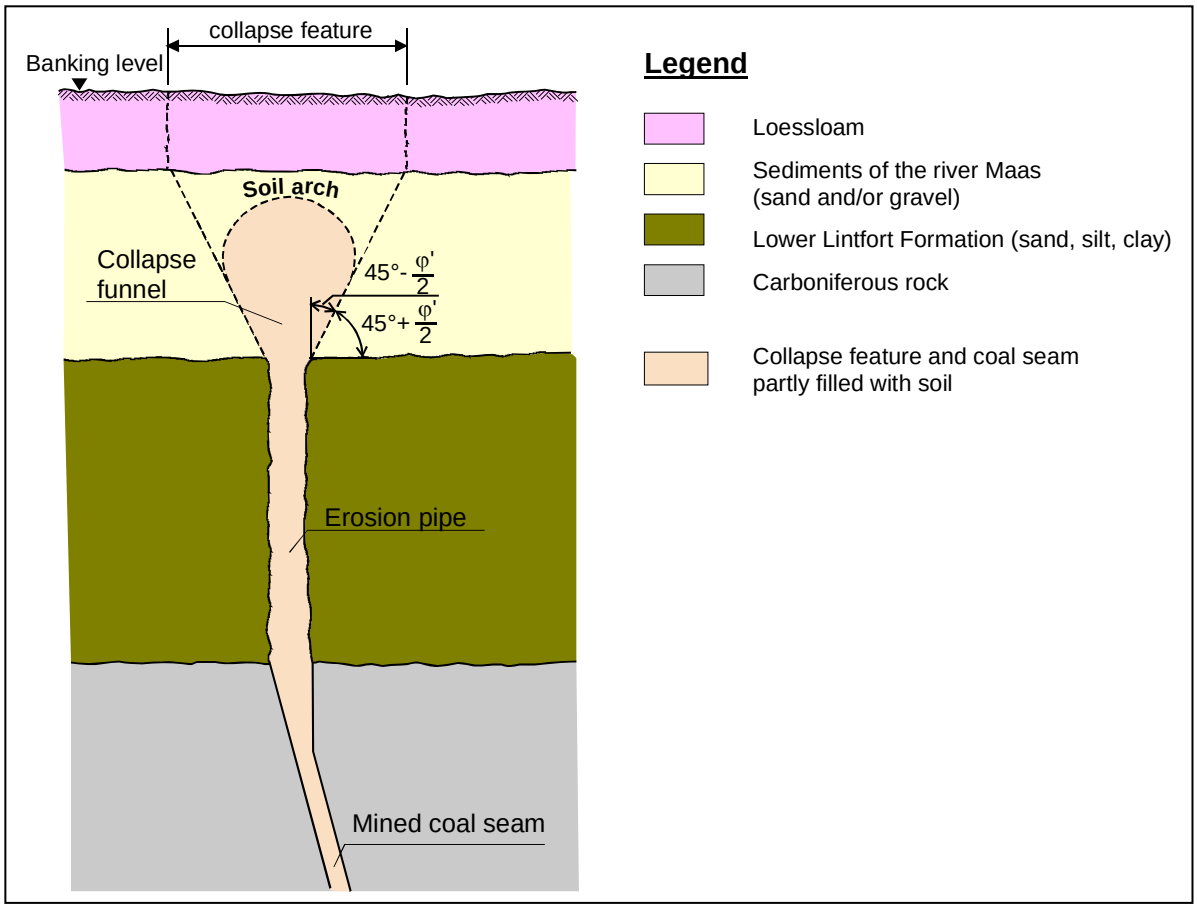


Figure 9: Collapse feature model.

Within the silty and clayey sand of the Lower Lintfort Formation no growth of the collapse towards the sides was observed. The collapse feature develops as a vertical pipe. Fig. 10 shows two stress circles for typically limiting depths of the “Lower Lintfort Formation”. None of the stress circles touches the critical state line of this cohesive soil. The Mohr-Coulomb failure criterion is not fulfilled. The upward movement of the cavity within this cohesive soil layer hence is a pure vertical erosion process.

As soon as the collapse process reaches the sand and/or gravel of the sediments of the river Maas, the soil properties change and cohesion drops. Now the stress circles for typically limiting depths, outlined in fig. 11, both touch the critical state line. Hence the Mohr-Coulomb failure criterion is fulfilled. The soil shears with an angle of break of $\beta = 45° + \varphi'/2$ resulting in a funnel shaped part of the collapse feature.

When the cavity gets too close to banking level, the soil arch above the cavity becomes unstable due to insufficient thickness and in the first instance collapses with vertical shear planes within the cohesive loess loam following the direction of gravity forces (also see Penzel, 1980).

Hence, the width of the hazard zone W_{Hazard} at banking level above coal seam outcrops in the old mining district “Wurmrevier” comprises the width of the hazard zone at the top of the Carboniferous rock and the horizontal growth within the noncohesive sediments of the river Maas along an angle of break of $\beta = 45° + \varphi'/2$.

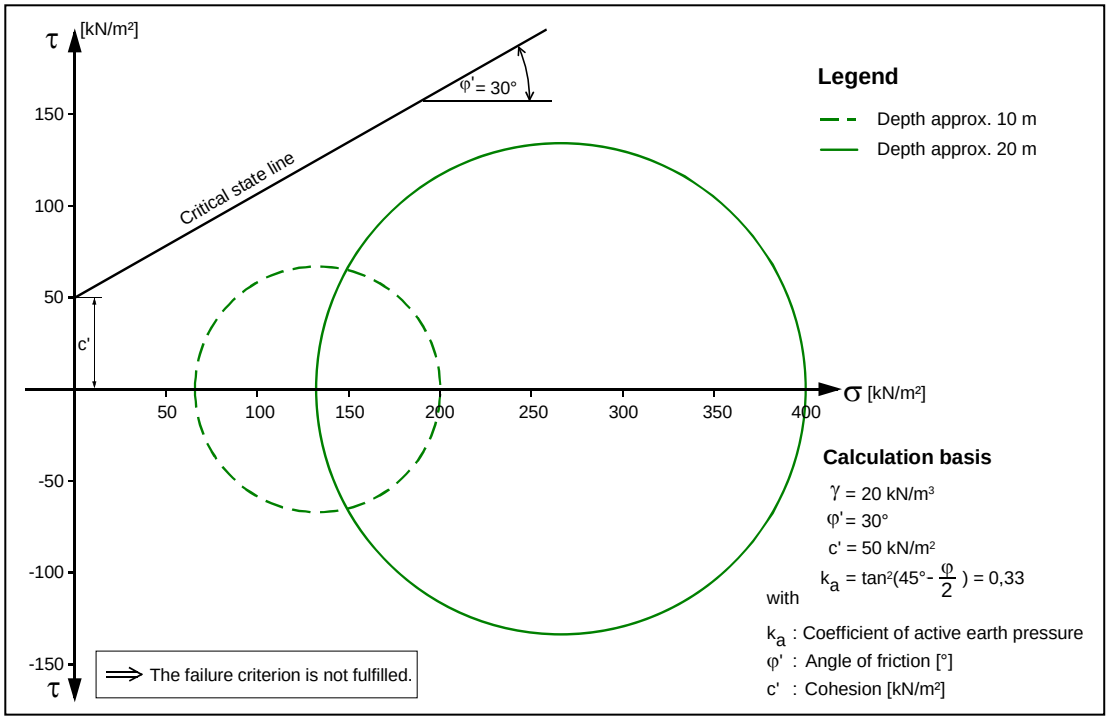


Figure 10: Mohr-Coulomb failure criterion for the Lower Lintfort Formation.

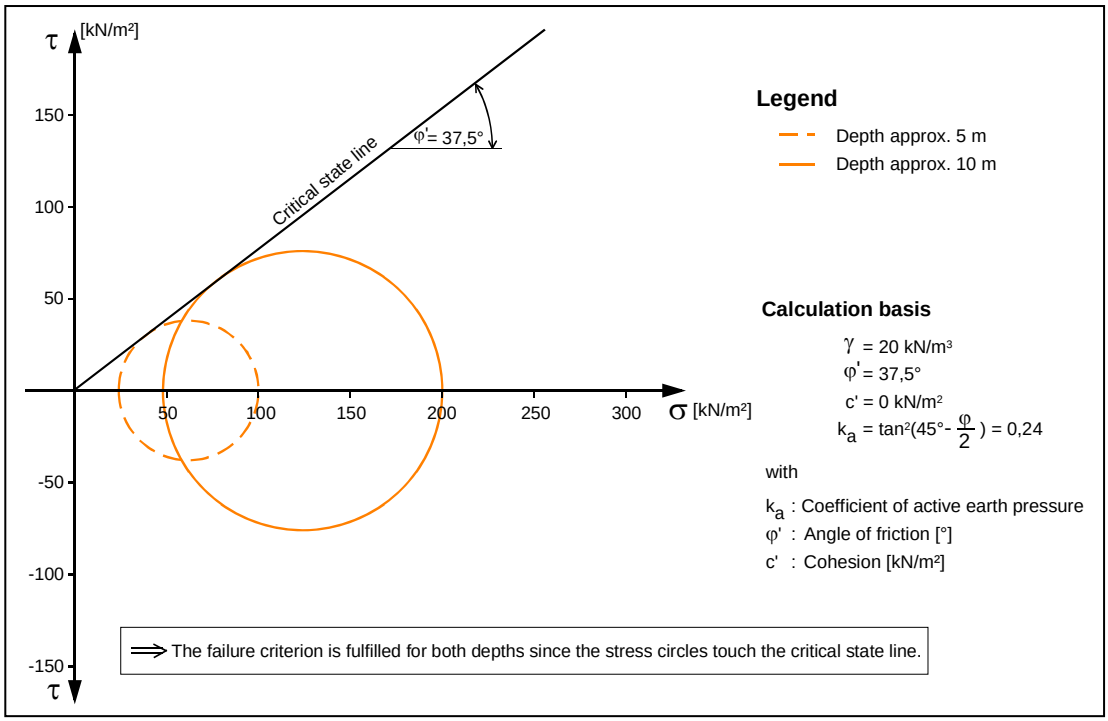


Figure 11: Mohr-Coulomb failure criterion for the Sediments of the river Maas.

In the proposed model a safety allowance for variation of the model parameters was chosen with η equal to 1,1 times the thickness of the sediments of the river Maas T_{MS} since these sediments are crucial to the prognosis of hazard zones when using the proposed model. The formula for the width of the hazard zone at banking level then is:

$$W_{Hazard} = 2*\eta * T_{MS} * \tan(45°-\varphi'/2) + W_{LLF}$$

The hazard zone width at the surface of the Carboniferous usually is assessed according to the chart of Hollmann & Nürenberg (1972, see fig. 5) plus the horizontal width of the coal seam outcrop. The width of the collapse feature within the Lower Lintfort Formation, respectively the zone within the Lower Lintfort Formation where the erosi on pipe might occur, W_{LLF} is assumed to be equal to this maximum hazard zone width at the surface of the Carboniferous. Based on the performed laboratory works, the average angle of friction φ' of the sediments of the river Maas can be assumed to be at least φ' = 35°.

The formula for the hazard zone at banking level then simplifies:

$$W_{Hazard} = 1{,}15 * T_{MS} + W_{LLF}$$

Backward analysis of real collapse features within the "Wurmrevier" showed good conformance of the model results with the real collapse feature dimensions. The model described above *can only be applied* to the "Wurmrevier" of Aachen and to the very special soil layer constellation and soil characteristics described above. These have to be verified by investigations for every single project.

When using this model, an allowance for the uncertainty of the coal seam location and the minimum distance of the planned building to the collapse feature should be taken into account additionally. This allowance is to be specified in accordance with the responsible governmental authorities.

Furthermore it has to be checked that a cohesive layer of a sufficient shear strength (φ' = 30°, c' ≥ 50 kN/m²) without major cohesion less sand layers exists, enabling a stable erosion pipe within this formation. Adequate horizontal in-situ stresses, corresponding to shallow depths, are provided. Also a sufficiently homogeneous and cohesive loessloam top layer is a prerequisite.

The transferability of the proposed model to the collapse process of shafts and other soil layer conditions within the Aachen hard coal mining district is currently being researched. The transferability of this model to other areas poses a future scientific task.

6. References

Arbeitsgruppe 4.6 der Fachsektion Ingenieurgeologie der DGGT e.V. (2004). *Geotechnisch-markscheiderische Untersuchung und Bewertung von Altbergbau*, 4. Altbergbau-Kolloquium, Appendix.

Arbeitsgruppe Altbergbau „Aachener Revier" (2002). *Untersuchungsbereich Herzogenrath-Kohlscheid – Bearbeitungsblock 1 – Stellungnahme der eingesetzten Arbeitsgruppe zu den bergbaulich-geotechnischen Verhältnissen und zur Standsicherheit der Geländeoberfläche*, Unpublished report, Ingenieurbüro Heitfeld-Schetelig GmbH.

Eurocode 7 (1996): *Entwurf, Berechnung und Bemessung in der Geotechnik*, Teil 1, DIN V ENV 1997-1.

Heitfeld M., Rosner P., Mühlenkamp M., & Sahl H. (2004). *Bergschäden im Erkelenzer Steinkohlenrevier*, 4. Altbergbau-Kolloquium, 281-295.

Heitfeld M., Krings K., Mainz M., Schetelig K. (2005). *Ein Modell zur Prognose von Einwirkungsbereichen des tagesnahen Altbergbaus auf Steinkohle für das Aachener Wurmrevier*, 5. Altbergbau-Kolloquium (in press).

Hollmann F. & Nürenberg R. (1972). *Der „Tagesnahe Bergbau" als technisches Problem bei der Durchführung von Baumaßnahmen im Niederrheinisch-Westfälischen Steinkohlengebiet*, Mitteilungen der Westfälischen Berggewerkschaftskasse, Vol. 30.

Ingenieurbüro Heitfeld-Schetelig GmbH (2003). *Bergbaulich-geotechnische Stellungnahme zu den Ursachen des Tagesbruches „Mühlenbach“ in Herzogenrath-Pannesheide,* Unpublished report in the order of the Bergamt Düren.

Ingenieurbüro Heitfeld-Schetelig GmbH (2004). *2. Bericht über ingenieurgeologisch-geotechnische Untersuchungen zur Erarbeitung von Bemessungsgrundlagen für die Ausweisung von Gefährdungsbereichen des Altbergbaus im Aachener Revier als Beitrag zum Risikomanagement,* Unpublished report in the order of the Bergamt Düren.

Penzel M. (1980). *Bemerkungen zur Erdfallgenese in Auslaugungsgebieten aus geomechanischer Sicht*, Neue Bergbautechnik 10, No. 1, 15-19.

Welz A. (2001). *Vorgehensweise bei der Grundlagenerarbeitung für die Untersuchung und Sicherung der Tagesoberfläche in Altbergbaugebieten am Beispiel „Bochum-Höntrop“*, 1. Altbergbau-Kolloquium, 58-62.

THE SPATIAL INFORMATION SYSTEM EramSIS IN THE SERVICE OF GEOTECHNICAL MONITORING

HELLER Martin[1], MAUKE Ralf[2], MOHLFELD[3] Matthias, SKRZYPPEK Jürgen[1], CROISÉ Jean[1]

[1] COLENCO POWER ENGINEERING LTD, Täfernstrasse 26 – 5405 Baden – Switzerland.
Martin.Heller@colenco.ch; Juergen.Skrzyppek@colenco.ch; Jean.Croise@colenco.ch

[2] BUNDESAMT FÜR STRAHLENSCHUTZ (BfS), Postfach 10 01 49 – 38201 Salzgitter – Germany. RMauke@bfs.de

[3] ZERNA, KÖPPER UND PARTNER (ZKP). Industriestrasse 27 – 44892 Bochum – Germany. Mo@zkp.de

ABSTRACT: Backfilling activities in the Morsleben radioactive waste repository (ERAM) began in 2003. They are necessary to stabilize the intensely mined central part of the repository. Thanks to geotechnical monitoring it is possible to ensure the local structural stability and the mandatory operational safety. The use of the integrated spatial information system EramSIS right from an early stage makes it possible to locate the great number of continuously acquired measurement results in a three-dimensional model on the computer screen. The interactive visualization proved to greatly facilitate the interpretation of the various types of information.

KEYWORDS: Geotechnical monitoring, Spatial information system, EramSIS, Interactive visualization.

RESUME : Les travaux de remblaiement de l'ancienne mine de sel et potasse de Morsleben, exploitée pour le stockage de déchets radioactifs, ont démarré en 2003. Ils sont nécessaires pour assurer la stabilité de la partie centrale de la mine dont le taux de défruitement est très important. La mise en place d'un réseau de surveillance géotechnique permet de garantir la stabilité mécanique de la mine pendant le remblayage, ainsi que la sécurité pendant l'exploitation. L'utilisation du système d'information spatial intégré EramSIS dès le démarrage des opérations permet de localiser la grande quantité de données acquises continûment par visualisation interactive tridimensionnelle, au grand profit de l'interprétation des différents types d'information.

MOTS-CLEFS : Réseau de surveillance géotechnique, Système d'information spatiale, EramSIS, visualisation interactive.

1. Introduction

The closure of the Morsleben radioactive waste repository (ERAM) is planned to involve extensive backfilling in the entire repository. Geomechanical model calculations have shown that the overall structural stability will be maintained on the long term as a result of these backfilling measures (Kreinmeyer et al., 2004 and Müller-Hoeppe et al., 2004). However, in some places individual structural elements may be partially at risk and local fracturing has to be expected (Mauke et al., 2004). As a result, additional instrumentation has been installed as part of the monitoring system in places where the model calculations have identified particularly strained horizontal and vertical pillars in order to evaluate the deformation and stress in the rock (Table 1).

By automating large parts of the data acquisition and analysis, it becomes possible to monitor processes without time delay and take immediate action, if necessary. If, for example, a certain threshold value is exceeded at a certain measurement device, a pre-defined set of counter-measures may be started off.

The temperature curves serve at least three purposes. Temperature progressions and values themselves indicate thermal strain and, thereby, may shed light on structural stability. But temperature curves are also used for calibration purposes in the analysis of data recorded by devices monitoring deformation and stress more directly. And, finally, temperature curves may enhance the re-calibration of geomechanical model calculations.

Table 1. Geotechnical monitoring devices installed in repository passages and halls.

Property	Device/Method	Purpose
Deformation	Extensometers	To determine compression and expansion in selected horizontal and vertical pillars
	Convergence cross-sections	To record convergence deformation at representative cross sections through cavities
	Fissurometers	To observe displacements along joint planes or fissures on the cavity walls
	Measurements of positional changes	To record compression, expansion, loosening and tilting along specified survey lines, section by section
Stress	Hydro-frac measurements	To determine size and direction of the least principle stress
	Stress monitoring stations	To observe thermally induced stress alterations caused by backfilling and long-term stress redistribution
	Load pressure cells	To monitor the bearing pressure as an indicator of the backfilling and hydration processes
Temperature	Temperature sensors in the rock formation, cavities and backfill	To assess the thermal strain due to backfilling and for the temperature calibration of other measuring systems and model calculations

2. Design of the spatial information system

The interpretation of geotechnical data requires a good understanding of the spatial context. A detailed 3D representation is absolutely essential – together with an interactive visualization tool. This project has relied on the comprehensive 3D model of the ERAM repository, which had been created during the planning phase. The highly complex shapes of the cavity system were modeled in AutoCAD by digitizing hundreds of paper maps and sections (Eilers, 2000). Further refinement was introduced later on by laser-scanning the most relevant halls (Busse and Kern, 2002). Also, a cadastre describing the attributes (ID, name, volume, zone, altitude, level etc.) of all the cavities was set up as a relational database.

It became evident that – to tap their full potential – the AutoCAD model and the database had to be integrated into a single application. The Toporobot approach (Heller 1983, 1994), originally developed for modeling and visualizing natural caves, offered a solution (Heller and Neumann, 2001). It had been used before to model and document prehistoric mines (Bergbaumuseum – German Mining Museum –Bochum) (Heller et al., 2002), to create an inventory of underground features in the cave of Milandre, and to build a rudimentary spatial information system of the Mont Terri Rock Laboratory (Heller and Jeannin, 2003).

The spatial information system EramSIS combines 3D visualization with a database (Heller et al., 2004). It displays the complex model of all mine passages and halls in real time and offers a fluid navigation in the 3D scene (Fig. 1 and Fig. 2). In addition, all attributes are shown tabulated in a spreadsheet. As the views are bi-directionally linked, the user can either select items from the spreadsheet and have the corresponding objects highlighted in 3D or pick a map or objects in 3D to see the associated attributes in the spreadsheet. The database table allows to sort and search, hide/show and color the objects as well as structure the scene.

The spatial information system offers specific functionality to assist with the analysis of geotechnical data. It calculates the volumes of passages or halls, displays the distance between two selected points, and finds the smallest distance between two halls. It also displays time series of measured data (Fig. 2).

Maps and profiles schematically summarizing the geological situation can be shown or hidden interactively. Figure 3 provides two similar images of the mine, one with an overlay of a selection of stratigraphic units, formation boundaries and structural elements.

The EramSIS even provides the option to generate animations by stringing together series of images portraying the evolution of a specific property or condition with time. In order to track the backfilling activities, for example, the spatial information system can be used to produce an animation of the partially filled cavities with time based on the amount of pumped backfill as recorded in the database (Fig. 4).

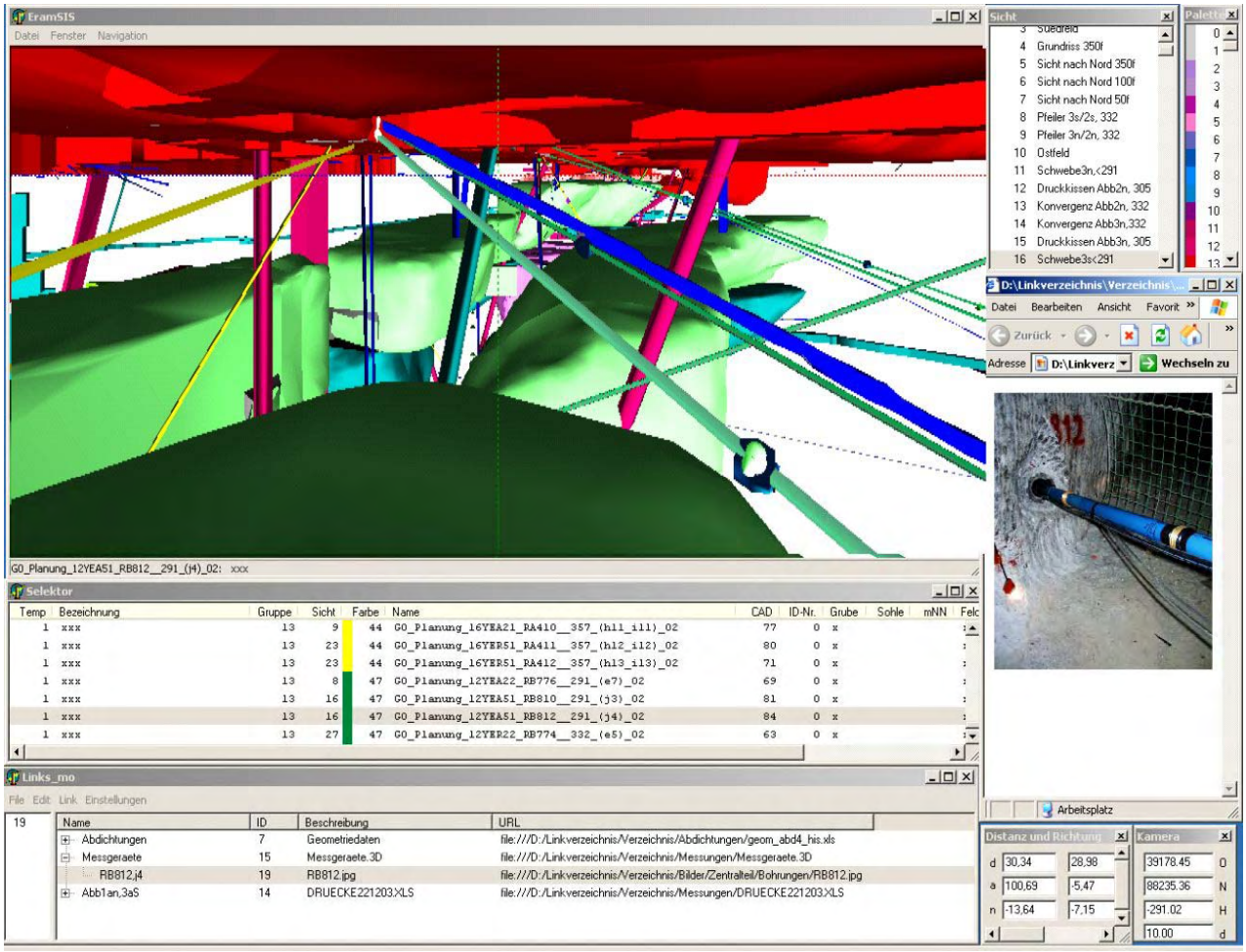


Figure 1. ERAM-SIS 3D display of filtered and linked information.

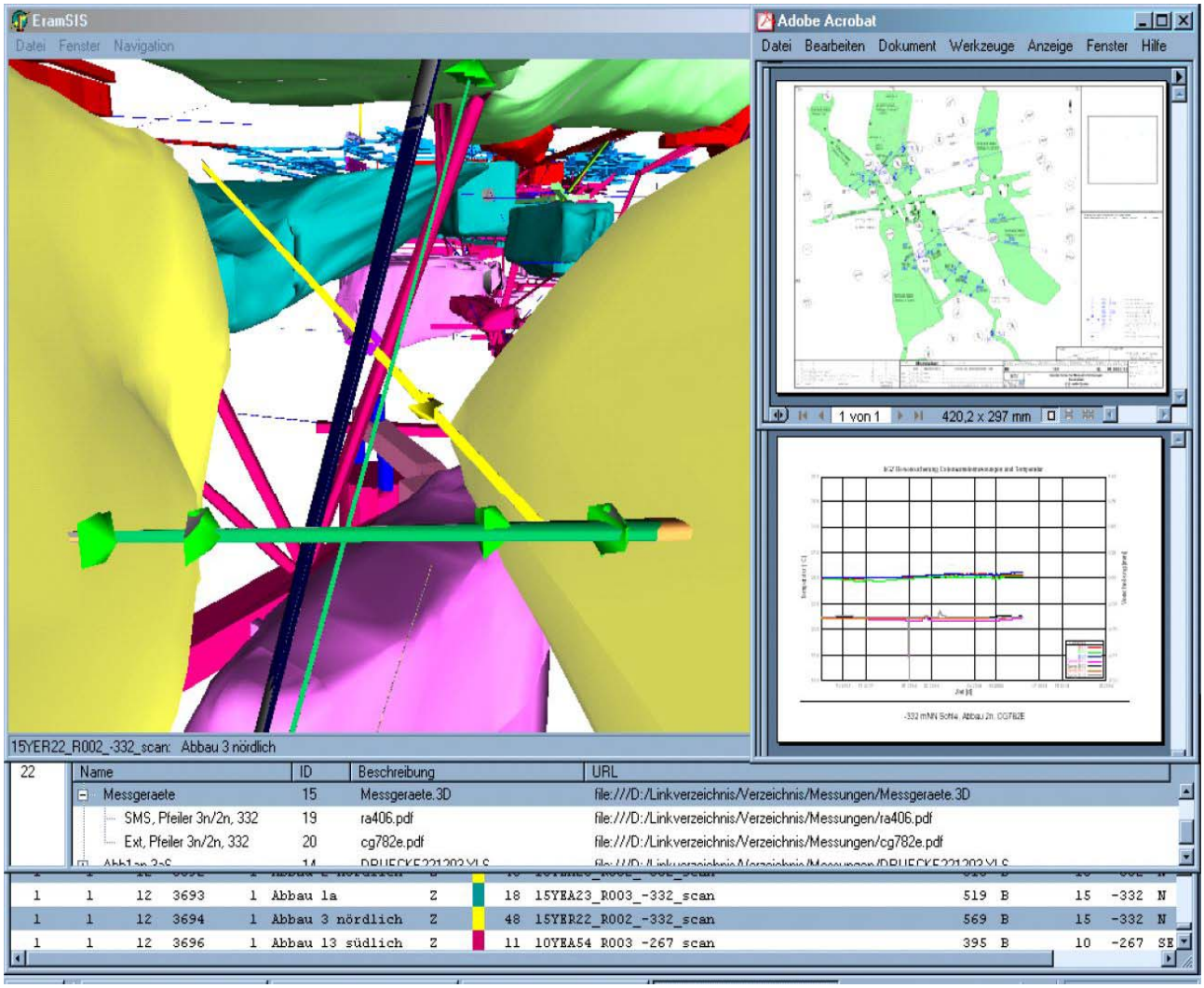


Figure 2. Illustrations of the halls and passages and results from geotechnical monitoring devices.

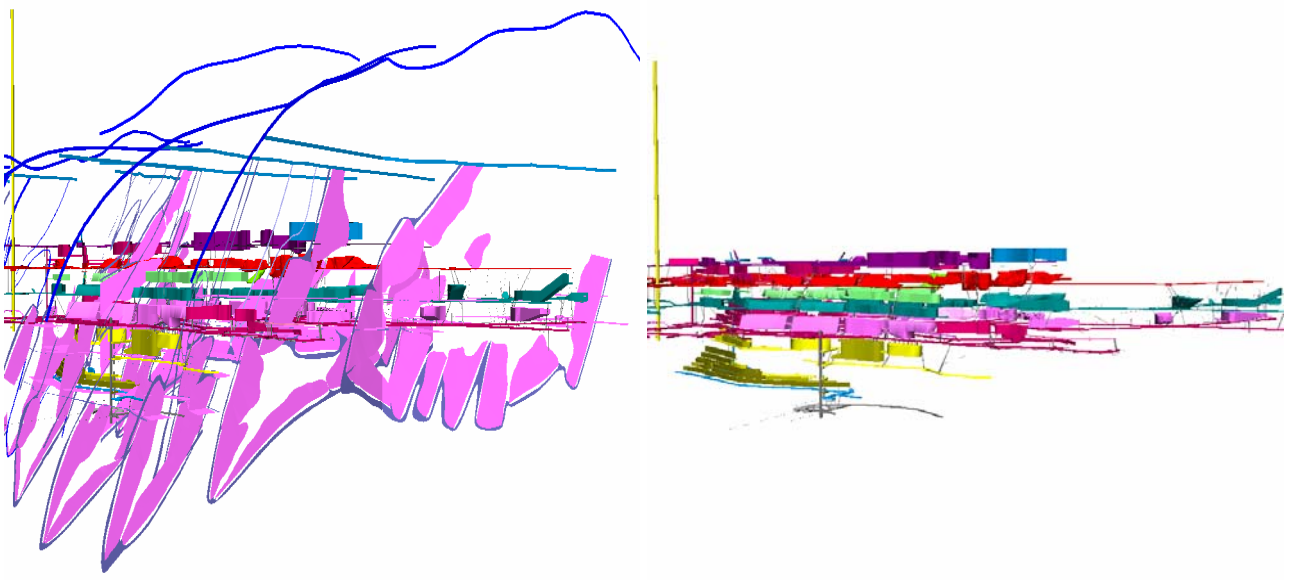


Figure 3. Example for displayed versus hidden geological information.

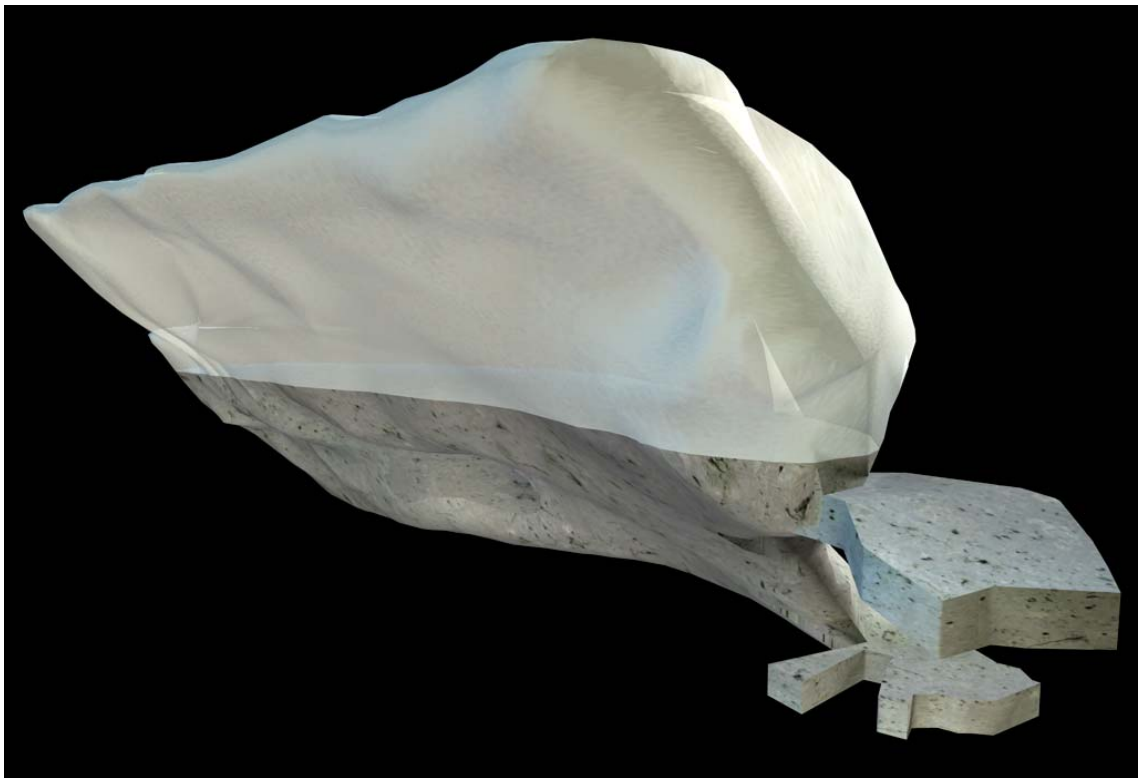


Figure 4. Image taken from an animation of the backfilling progress in a selected hall.

3. Conclusions

The spatial information system EramSIS is an interactive program designed to visualize and explore a 3D-model of the Morsleben radioactive waste repository. Such visual inspection and examination greatly assists the analysis and interpretation of geotechnical data by the following means:

- The tool may be used by a wide spectrum of users and facilitates the communication among interdisciplinary co-workers.
- Numerous sophisticated features can be integrated in an intuitive user interface.
- Different types of information sources such as measurements, borehole data, geological information, photographs, reports etc. can easily be accommodated.
- The program offers a 3D perspective of the site model along with spreadsheets displaying various attributes.
- Efficient navigation methods allow the user to examine the model interactively in three dimensions.
- Spreadsheets are used to structure objects into groups or to specify surface properties (color, transparency, etc.). Information and data may be sorted by columns, searched or filtered.
- Specific viewpoints may be stored in a list and used as bookmarks.
- Even attributes not stored in the EramSIS database may be used in the system through connections such as links to external information sources (e.g., documents, photographs, scripts).

- Users may create individual style files that save groupings, color palettes and viewpoints fine-tuned to the study of a specific aspect of the model.
- The filtered subsets of the model can be exported as groups of stylistically attributed objects in 3D formats (e.g. VRML or X3D) so that they can be used in special purpose graphics-programs or in interactive 3D web-browser plug-ins.

Using this integrated visual approach, considerable insight has been gained already, while saving time and effort.

4. References

Busse, V., Kern, P. (2002): *Nutzung von Laserscanneraufnahmen für die verbesserte Bestandsdokumentation und Verfüllplanung von Altbergbaubereichen,* 2. Altbergbau-Kolloquium 2002, TU Clausthal-Zellerfeld.

Eilers, G. (2000): *PC-based information system for the Morsleben ILW/LLW repository,* Proc. Distec 2000.

Heller, M. (1983): *Toporobot, L'ordinateur au service du spéléologue-cartographe,* Stalactite (La Chaux-de-Fonds), 33 (1), pp. 9-27.

Heller, M. (1994): *Toporobot, Logiciel d'aide à la topographie,* Spelunca Mémoires 21, Journées Norbert Casteret, Fédération Française de Spéléologie, ISSN 0242-1771.

Heller, M., Neumann, A. (2001): *Inner-Mountain Cartography – From Surveying towards Information Systems,* Proc. 20th Cartographic Conference ICA 5, Beijing 2001, pp. 3408-3417.

Heller, M., et al. (2002): *Hohlraummodellierung – von der Vermessung zum Informationssystem,* 2. Altbergbau-Kolloquium 2002, TU Clausthal.

Heller, M., Jeannin, P.-Y. (2003): *Développements en matière de SIG et de visualisation 3D à l'ISSKA,* Stalactite 2/2003.

Heller, M., Mauke, R., Mohlfeld, M., Skrzyppek, J. (2004): *ERAM-SIS: A spatial information system for visualization and management of geotechnical data,* Proc. Distec 2004.

Kreinmeyer, M. et al. (2004): *Central part of the Morsleben repository – geomechanical situation before stabilisation,* Proc. Distec 2004.

Mauke, R., Stielow, B., Mohlfeld, M. (2004): *Geotechnical control of critical construction phases in the complex mining system of the repository for radioactive waste in Morsleben (ERAM),* Rock Engineering, Theory and Practice, Proceedings of the ISRM Regional Symposium EUROCK 2004 & 53rd Geomechanics Colloquium, VGE, 2004.

Müller-Hoeppe, N. et al. (2004): *Stabilisation of the Central Part of the Morsleben Repository (bGZ),* Proc. Distec 2004.

NATURAL PROCESSES AND SYSTEM EVOLUTION DURING MINE CLOSURE: NUMERICAL SIMULATION AND VISUALIZATION

HELLER Martin[1], POPPEI Joachim[1], SCHLICKENRIEDER Liane[1], FÖRSTER Bernd[2]

[1] COLENCO POWER ENGINEERING LTD, Täfernstrasse 26 – 5405 Baden – Switzerland.
Martin.Heller@colenco.ch; Joachim.Poppei@colenco.ch; Liane.Schlickenrieder@colenco.ch

[2] GSF-FORSCHUNGSZENTRUM FÜR UMWELT UND GESUNDHEIT – SCHACHTANLAGE ASSE, Am Walde – 38319 Remlingen – Germany. Foerster@gsf.de

ABSTRACT: We have developed a numerical tool which is particularly suitable for the simulation of water and gas flow, mechanical and chemical phenomena as well as processes related to the transport of contaminants and radionuclides in underground structures over long periods of time. KAFKA was applied for investigations concerning the flooding and closure of the Asse research mine, a former salt mine. Given the complexity of the mine structure and the multitude of interconnected processes considered, the specifically designed visualization tool Assemblage is indispensable for the interpretation of intermittent and final simulation results.

KEYWORDS: Numerical simulation, Hydro-mechanical-chemical coupling, Intermittent results, Interactive visualization.

RESUME : Un outil numérique de simulation hydrodynamique de l'écoulement et du transfert de masse a été développé: écoulement diphasique eau et gaz couplé à des processus chimiques et mécaniques et transfert de radionucléides dans des cavités souterraines sur des périodes de temps longues. Le logiciel KAFKA a été appliqué pour étudier les processus lors de l'ennoyage et la fermeture de l'ancienne mine de sel allemande « Asse », utilisée comme laboratoire de recherche. Etant donné la complexité des vides miniers et des processus, il s'est avéré indispensable de réaliser un outil de visualisation nommé « Assemblage », spécifiquement conçu pour l'inspection et l'interprétation des résultats au fur et à mesure des simulations.

MOTS-CLEFS : Simulation numérique, Processus couples hydro-mécaniques-chimiques, Résultats intermédiaires, Visualisation interactive.

1. Introduction

Closing a mine bears potential consequences for fluid flow in the mine, regional groundwater flow and surficial water bodies. Equally relevant are the contaminants transported by these mine and formation waters. Understanding and being able to forecast the temporal and spatial evolution of the entire system is the key to people's and environmental protection.

Generally, the flooding is a reintegration of the mine body in the natural groundwater system. In special cases like that of a salt mine, the mining activities may alter the regional hydrogeological conditions such that formerly dry formation bodies become an active part of the groundwater system. The mobilization, retention and transport of contaminants are critical issues as the water level in the mine rises. Chemical and physical effects such as sorption, solubility, gas generation and density-driven flow may also require attention.

KAFKA, the compartment model for migration and fluid dynamics in converging underground facilities is an innovative and unique code for the simulation of multiphase flow and transport processes in open or backfilled underground structures like tunnels, mines or waste repositories. Its capacity to simulate numerically various flow processes, mechanical and chemical processes and radionuclide-specific processes is demonstrated in this paper with the example of the Asse research mine, a former salt mine which has been used for research activities concerning the disposal of radioactive wastes.

The complexity of the mine structures and the multitude of partially exponentiating or counter-active processes complicate the interpretation of computational results. One proven solution is the integration of the numerical results in an interactive visualization tool. Assemblage is the specifically designed tool linking an abstract presentation of the mine with results from KAFKA. This unique combination of numerical process simulation and 3D visualization enhances the system understanding of all project participants and supports communication among them.

2. Numerical simulation of hydro-mechanical-chemical processes

KAFKA is a hydro-mechanical-chemical coupled code that has been developed to calculate flow and transport processes in large and complex underground structures over long periods of time, a task that is very difficult for commonly used finite-element and finite-difference codes (Colenco 2004 a,b; Poppei et al. 2004). KAFKA uses an original approach that largely avoids space discretization and the construction of meshes. This and the physics considered make KAFKA an ideal tool to assess all problems involving flooding (intentional or accidental) of open or backfilled, interconnected or isolated underground cavities and the related questions of hydraulic and mechanical changes over time, transport of different species and finally the consequences of these processes on the surroundings of the cavities and the biosphere.

Table 1 lists the main features considered in KAFKA. Many different flow types can be modelled, ranging from simple one-phase Darcy flow to complex density-driven two-phase flow. Source terms for gas and dissolution of chemical species can also be considered. Mechanical coupling in terms of convergence of the modelled materials is accounted for either by supplying an external function providing the convergence behaviour, or based on creep laws allowing for a full hydro-mechanical coupling in this respect. Finally, as KAFKA was first developed to analyse the long-term behaviour of a radioactive waste repository, radionuclide transport by advection, diffusion and dispersion with consideration of decay and ingrowth as well as sorption and dissolution processes are simulated.

Table 1. Processes accounted for by the hydro-mechanical-chemical code KAFKA.

Flow processes
▪ Darcy flow ▪ Density-driven flow ▪ Two-phase flow ▪ Natural flooding incl. location, rate, duration and fluid composition ▪ Induced flooding incl. location, rate, duration and fluid composition
Mechanical and chemical processes
▪ Convergence depending on depth, material and fluid pressure ▪ Gas generation varying with time and location ▪ Dissolution processes and their effects on cavern volume and fluid density
Contaminant and radionuclide-specific processes
▪ Instantaneous and delayed mobilization of contaminants ▪ Transport with advection, diffusion and dispersion ▪ Radioactive decay and ingrowth ▪ Sorption and solubility limitations

KAFKA is based on a simplified geometric layout of the mine working and a volume-based numerical approach. It considers fluid flow and contaminant transport in a network of structural elements representing caverns, connecting passage ways such as shafts and drifts, and roof pillars that separate caverns and are located vertically one upon the other. All elements are composed of one or more materials with different geomechanical properties. This allows, for example, for elements to be specified as converging or with a constant bulk volume. The connections between caverns may be oriented in any direction. Figure 1 illustrates a simple example of a geometric network that can be modelled with KAFKA.

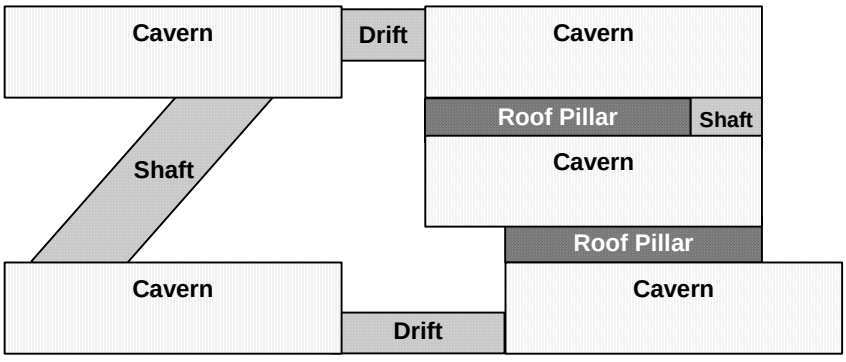


Figure 1: Example of a network of structural elements as it may be used in KAFKA.

Caverns are treated as mixing tanks and have no hydraulic resistance. As any mixing occurs instantaneously, the fluid within a cavern has homogeneous properties. Inflow into and outflow out of a cavern occurs via connecting elements, i.e. drifts, shafts or roof pillars. Liquid inflow into a gas-filled cavern is introduced from the bottom up and with the gas being displaced. Outflow takes into account the level at which the connecting element is attached to the cavern by allowing outflow to occur only once the filling level reaches the connecting element.

Drifts, shafts and roof pillars have a hydraulic resistance which depends, among other factors, on the backfill material, the mean degree of saturation and the convergence history.

The modelling approach is based on mass balances over each volume for the solution, the gas, and the liquid-phase component comprised of a solvent and a solute (density-relevant component). In addition, the time evolution of the available volumes is computed with equations describing the open volumes, pore spaces of the different compressible volumes (2 different types are possible) and the skeleton volumes.

Accordingly, one has to solve a system of 8 coupled differential equations for each volume, with 4 of these describing the time evolution of pore space. Those equations have to be solved simultaneously for all considered elements, together with the model's boundary conditions. Once the flow fields have been obtained, the transport of the radionuclides (or any other transported pollutant with no effect on fluid density) can be computed.

This is done by solving a one-dimensional transport equation for each connection between caverns based on a classical finite-volume scheme, accounting for advective, diffusive and dispersive transport and sorption, solution and precipitation as well as radioactive decay and ingrowth. In order to avoid introducing unacceptable numerical errors, it is necessary to discretize the connections for the transport calculations. This is done dynamically based on a cell Péclet criterion.

3. Modelling the Asse research mine numerically

Figure 2 shows a schematic representation of the Asse research mine. The very complex system of the mine's cavities was simplified in the KAFKA model to yield a limited number of hydraulically equivalent elements. The criteria applied for this simplification were derived from the geological situation, comparable chemical conditions, gas sources, the hydraulic behaviour of connecting structural elements and waste distribution. It was important to respect the vertical distribution of effective pore space and to include all connections that are likely to influence the flow field in order to end up with a suitable structural model of the Asse research mine.

The focus was a flooding scenario with the long-term prediction of fluid flow within the mine and of the fluid exchange with the surroundings. The simplified structural model (also in Figure 2) was designed to allow for the correct simulation of these processes while simplifying greatly the layout of the calculation domain without introducing flow artefacts. The final model comprises about 150 structural elements whose attributes were defined according to the homogenized properties of the real cavities: the chosen approach assured that every cavern, roof pillar, drift etc. in the real mine can be attributed to a clearly identified element in the simplified geometry. This guarantees that the properties of the model elements are reliably and traceably determined and that, at any time during the modelling or review process, model integrity can be shown and simplifications be clearly identified and justified.

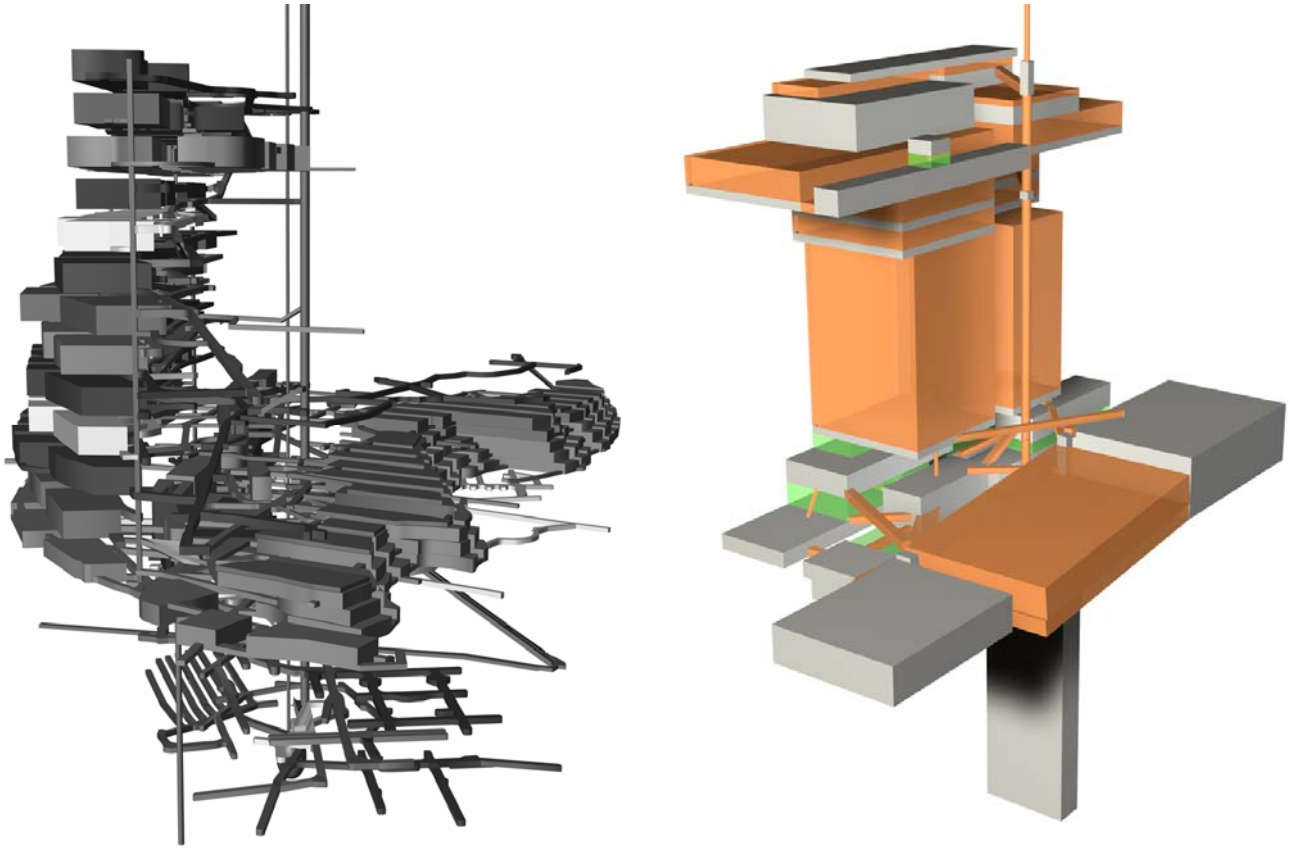


Figure 2. Schematic illustration of the Asse research mine (left)
and the geometrically simplified structural model used for numerical simulations with KAFKA (right).

4. Visualization of simulation results with Assemblage

Keeping in mind that the KAFKA computations are run with a structural model of the Asse research mine which comprises about 150 elements, the expected output of simulation results is tremendously large and their visualization indispensable. Depending on the selection of physico-chemical processes accounted for or disregarded, every single element may feature up to 10 transient parameters – such as pressure, various compressible volumes, porosities, saturation etc. – bearing influence on the flow processes. When transport processes enter the picture, the number of transient parameters grows to include, for example, tracer concentrations, contaminants in solution, possibly radionuclides and so on. For the case presented here this translates into time-dependent concentrations for more than 30 different radionuclides and 10 specific tracers.

The parameters influencing flow in the cavity system are complexly interconnected. For instance, two of the factors governing the flow of mine water and gas are the current saturation states in the respective element and the pressure difference to adjacent elements. In turn, the pressure difference depends on volume changes due to geomechanical and chemical processes. These processes may be evaluated with justifiable effort only if it is possible to illustrate the parameters and their evolution with time in any element of interest and in comparison to an adjacent element.

The specifically designed visualization tool Assemblage is fed with computation results even as the numerical simulations are still in progress. This quasi-simultaneity makes it possible to project even intermediate results into the structural model. Assemblage, therefore, provides the basis for an ongoing analysis and, if necessary, for optimizations of the computing-time intensive simulations.

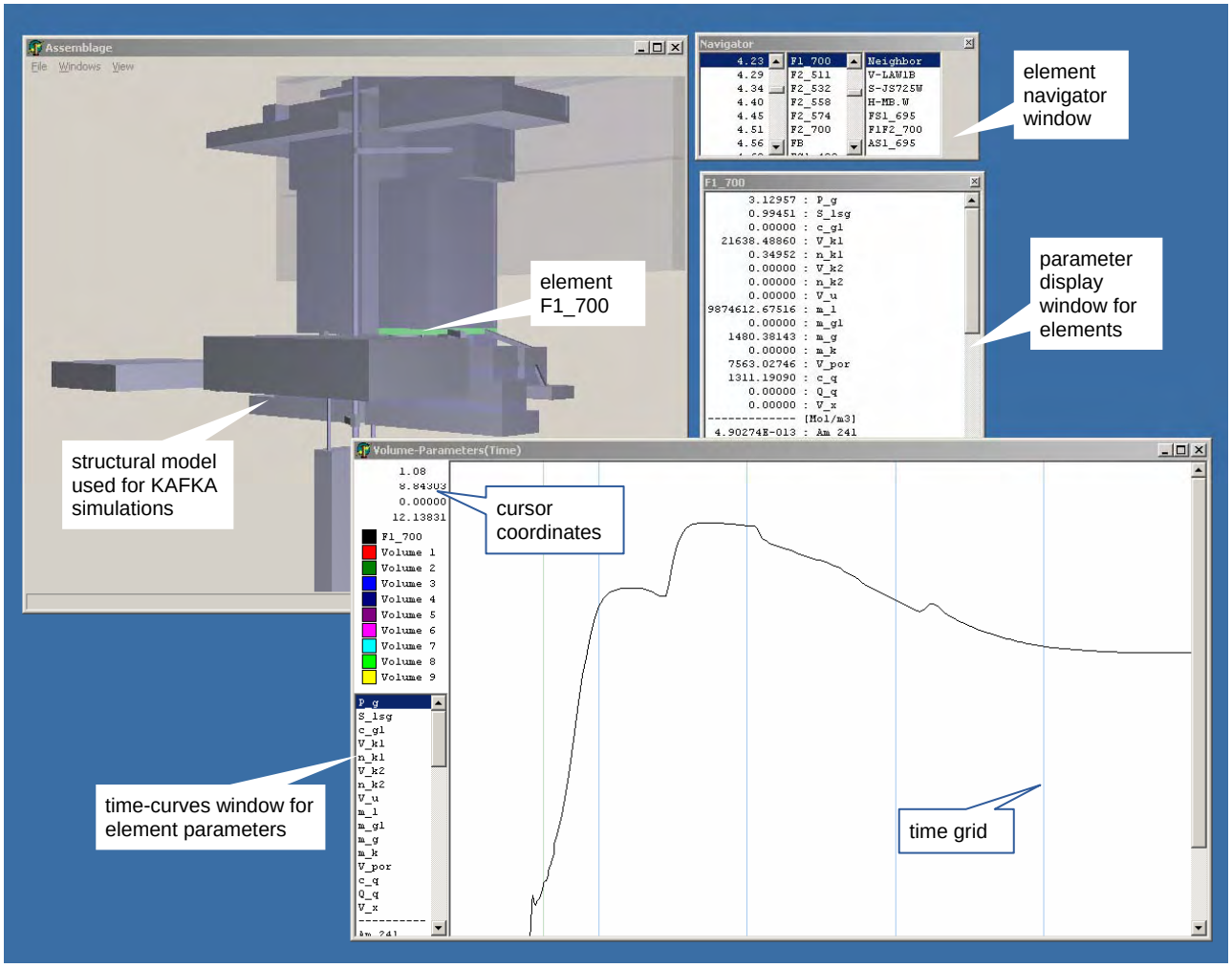


Figure 3. Assemblage screen shot with a simplified structural model presentation of the Asse research mine and various parameter displays. All displayed parameters are associated with the highlighted element F1_700.

Figure 3 shows a screen shot with several illustration options. Results pertaining to a certain structural element – in this example the element referred to as F1_700 – may be selected in the element navigator or by clicking on the element in the structural model presentation. The parameter display window lists the magnitudes of all computed parameters for the element and point in simulation time selected in the element navigator, i.e., F1_700 and 4.23 years respectively in the shown screen shot. The time-curves window displays the temporal evolution of parameters defining the selected element. In the screen shot, the time-curve corresponds to the gas pressure P_g for element F1_700. Time-curves for the same parameter but for up to 9 other structural elements may be added to the graph for easy comparison. Because comparisons are generally most telling between neighbouring elements, the right-most component of the element navigator automatically lists those adjacent to the selected element.

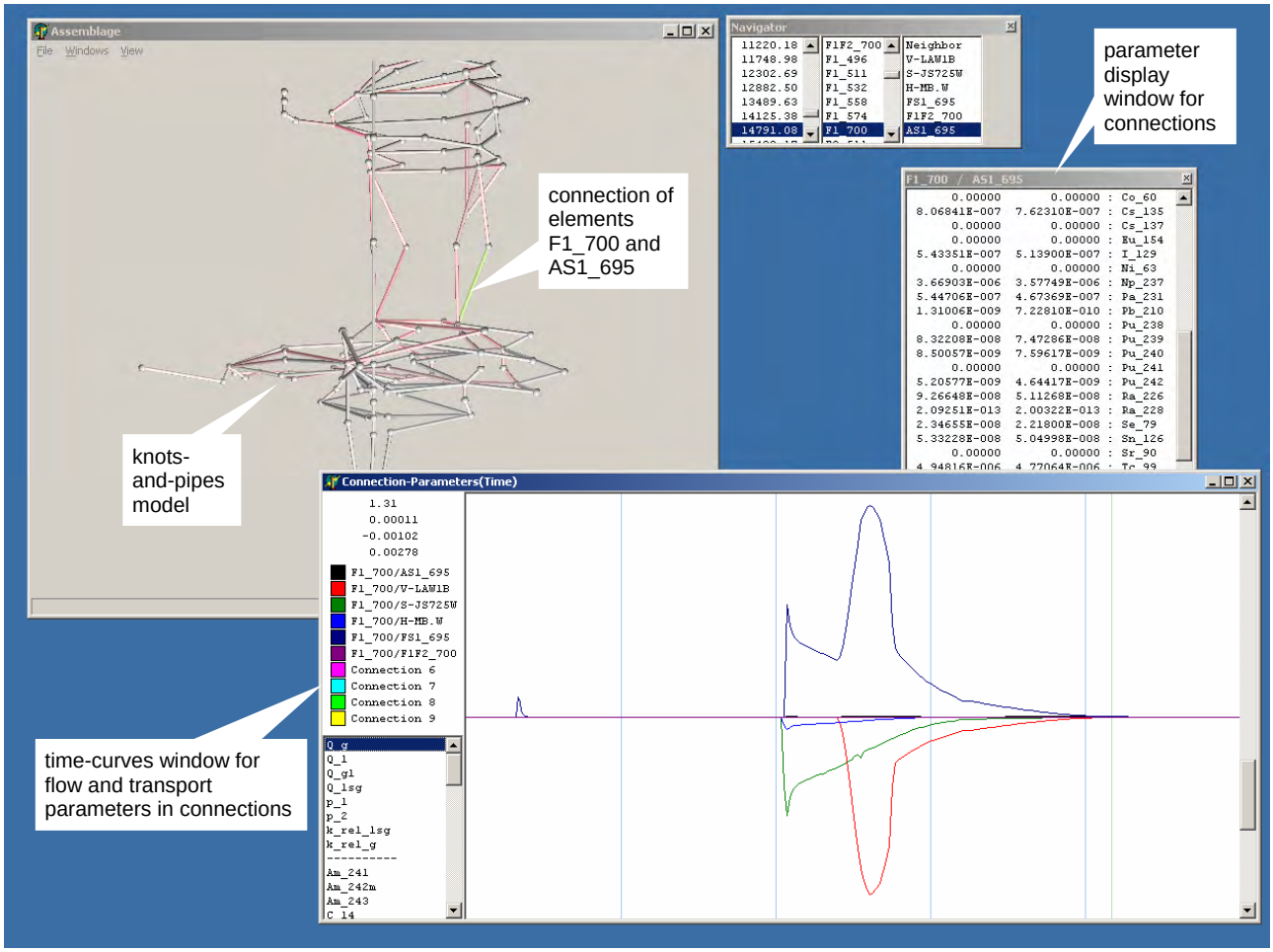


Figure 4. Assemblage screen shot with a simplified knots-and-pipes model presentation of the Asse research mine and various parameter displays. The displayed parameters are associated with the highlighted connection between the elements F1_700 and AS1_695 plus additional time curves.

Figure 4 demonstrates the distinctive feature of Assemblage to illustrate parameters concerning the fluid flow and the transport of tracers, contaminants and radionuclides between elements. These parameters are results of the numerical simulations and characterise the flow and transport processes between adjacent elements. The spatial orientation for their visualization is provided by a knots-and-pipes model whereby each knot represents one element of the structural model and every pipe represents a connection between two adjacent elements, i.e., connections are no geometric entities. The parameter display window for connections lists the parameters for the two associated elements at the point in time picked in the element navigator. In analogy to the time-curves window for element parameters, there is also a time-curves window for flow and transport parameters in connections. In the screen shot of Figure 4, the time curves concern the gas flux Q_g of the highlighted connection between elements F1_700 and AS1_695 as well as Q_g of five other connections of element F1_700.

In a broader scope it is worth noting that Assemblage is a spatial information system, that is, a tool combining the functions of visualization and data management. The advantages of a spatial information system in terms of the analysis and interpretation of geotechnical monitoring data are presented in Heller et al. (2005) using the example of EramSIS, an interactive program designed to visualize and explore a 3D-model of the Morsleben radioactive waste repository.

5. Conclusions

Using the case of the Asse research mine, the hydro-mechanical-chemical coupled code KAFKA has been found to be a suitable tool for the numerical simulation of multiphase flow and transport processes in engineered underground structures over long periods of time. The code uses a volume-based approach and accounts for numerous chemical phenomena and convergence; the latter being an important issue for an abandoned salt mine. One feasible future development is the integration of probabilistic functions for the consideration of parameter uncertainties.

Our experience with the visualization tool Assemblage has shown that a visually supported analysis enhances the understanding of complex interrelationships and greatly facilitates the interpretation of the numerical simulation results from KAFKA. Particularly the option of checking intermittent simulation results while being able to rely on model representations of the mine for spatial orientation has proven to save time and effort when investigating potential pathways for contaminants from the flooded facility to the surface along dominant pathways.

Adaptations of KAFKA in combination with an appropriately constructed spatial information system may be an equally effective combination of tools for the closure of uranium mines and underground coal workings. Be it the controlled flooding with remediation fluids or the rebound of mine waters, the achieved level of people's and environmental protection depends in large on the level of understanding of the spatially differentiated flow and transport processes and associated long-term effects ahead of time.

6. References

Colenco (2004a): *Modellbeschreibung KAFKA – Strömung und Radionuklidtransport*, Bericht 3061/44, Version 2.3, Colenco Power Engineering AG, Baden.

Colenco (2004b): *Verifikation des numerischen Programms KAFKA 2.3*, Bericht 3165/48, Colenco Power Engineering AG, Baden.

Heller, M., Mauke, R., Mohlfeld, M., Skrzyppek, J. & Croisé, J. (2005): *The spatial information system EramSIS in the service of geotechnical monitoring*, Proc. Post-Mining 2005, 16-17 Nov. 2005, Nancy.

Poppei, J., Schwarz, R., Holocher, J. & Mayer, G. (2004): *KAFKA – a numerical tool for two-phase flow and contaminant transport in converging underground facilities*, Proc. FEM-MODFLOW, 13-16 Sept. 2004, Karlovy Vary.

LONG-TERM GEOMECHANICAL STABILITY AND INTEGRITY OF THE SALT BARRIER IN THE CENTRAL PART OF THE BARTENSLEBEN SALT MINE

HEUSERMANN, Stefan[1], FAHLAND, Sandra[1]

[1]FEDERAL INSTITUTE FOR GEOSCIENCE AND NATURAL RESOURCE (BGR) - Stilleweg 2 - 30655 Hannover - Germany. heusermann@bgr.de; sandra.fahland@bgr.de

ABSTRACT : To assess the stability and integrity of the salt barrier in the old Bartensleben salt mine finite-element calculations have been made. The recent state of stress and deformation around large old rooms, humidity induced creep as well as backfilling of selected rooms have been investigated. To evaluate the results, several criteria are used concerning dilatancy, a frac criterion, allowable strain, and tensile stress. Roofs and pillars of the rooms are subjected to high creep deformation and partly to tensile stress. Extended zones of dilatancy occur in the vicinity of the rooms and in the salt rock between rooms and anhydrite layers. Long-term stability of the mine and integrity of the salt barrier can be re-established if a certain number of rooms are backfilled.

KEYWORDS : Rock salt, Integrity, Stability, Dilatancy, Modelling.

RESUME : Pour estimer la stabilité et l'intégrité de la barrière de sel à la mine de Bartensleben, on a effectués des calculs aux éléments finis. On a analysé l'état actuel des contraintes et des déformations autour de grandes et vieilles cavités, et la façon dont cet état a pu être affecté par le fluage (induit par l'humidité) et le rebouchage des cavités choisies. Les résultats acquis ont été évalués selon différent critères: la dilatance du sel gemme, son critère de rupture, sa déformation limite, sa résistance à la traction. Les toits et piliers des cavités subissent de grandes déformations de fluage et en partie des contraintes de traction. De larges zones dilatantes apparaissent à proximité des cavités, et dans la couche de sel localisée entre les cavités voisines et les bancs d'anhydrite. La stabilité à long terme de la mine et l'intégrité de la barrière de sel pourront être reconstituées si l'on rebouche un certain nombre de cavités.

MOTS-CLEFS : Sel gemme, Intégrité, Stabilité, Dilatance, Modélisation numérique.

1. Introduction

For many years the Morsleben repository was used for the disposal of low level radioactive wastes. The repository was established in the old Bartensleben mine, a former salt and potash mine consisting of several mining parts. The southern, the western, and the eastern part are located at the periphery of the mine and were used for waste disposal. However, from a geomechanical point of view, the central part which was not used as a repository is the most critical and important part of the Bartensleben mine with the most considerable degree of excavation and numerous large old mining rooms.

To assess the geomechanical stability of the underground structure as well as the integrity of the salt barrier in the central part of the mine a geotechnical safety analysis is required. Such an analysis is based on geological and engineering-geological studies of the site, on laboratory tests and in-situ measurements, and on geomechanical model calculations. Model calculations are the most important part of the geotechnical safety assessment and comprise the geomechanical modelling of the host rock to simulate as closely as possible the conditions of the site and the behaviour of the

rock, e.g. geology, repository or mine geometry, initial rock stress, as well as constitutive models and parameters (Langer, 1999).

The paper comprises the results of numerical modelling to analyse the stability of the old mining rooms and integrity of the salt barrier in the southern central part of the Bartensleben mine and to investigate the influence of humidity induced creep acceleration and the effect of backfilling of selected rooms on the integrity. To this aim, two-dimensional finite-element calculations on a characteristic cross section of the southern central part with the most unfavourable mining situation have been carried out.

2. Geological situation

The Bartensleben mine is located in the fault structure “Allertalzone” (Fig. 1). The top of the salt structure is at approximately 140 m below mean sea level, respectively about 270 m below ground surface. The thickness of the salt structure varies between 380 m and 500 m. The exploration and modelling of the geological structure of the salt rock and the overburden in several characteristic cross sections of the central part of the Bartensleben mine is based on the geological mapping of drifts, rooms, and numerous drillcores of the site as well as on ground-penetrating radar measurements (Behlau and Mingerzahn, 2001).

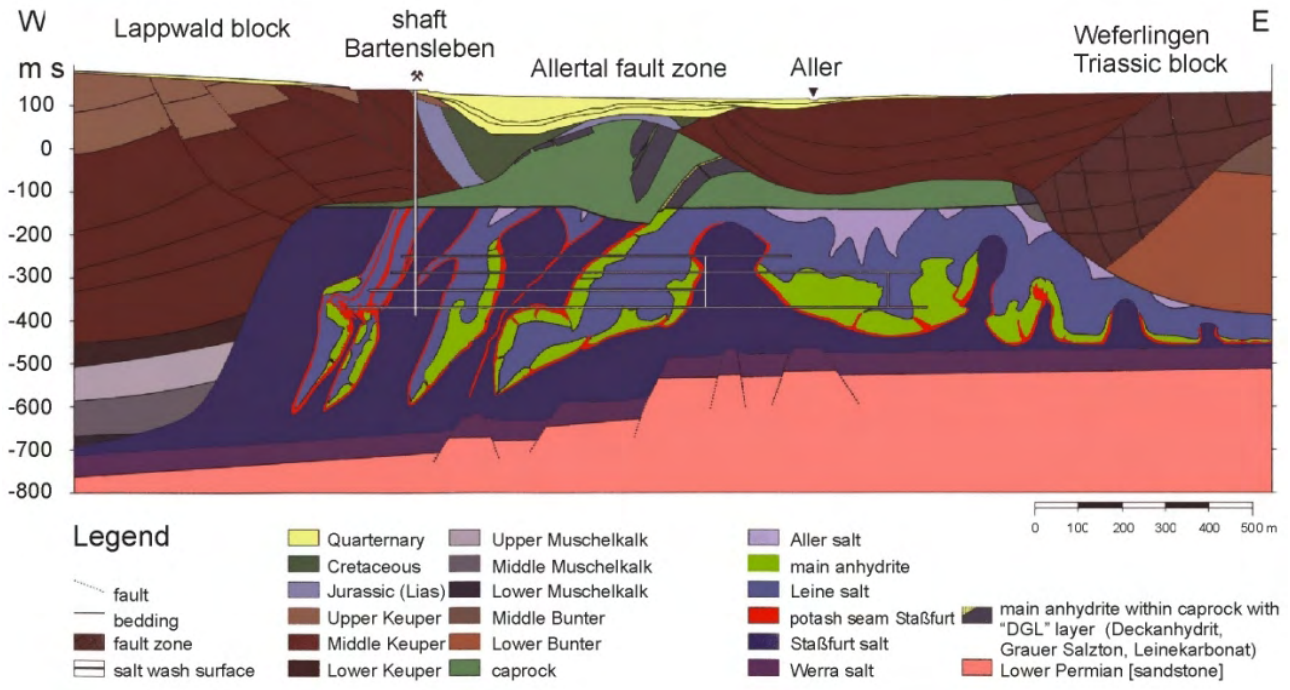


Figure 1. Geological structure in the Bartensleben mine (adopted from BfS).

The salt rock is characterised by a distinct folding of the salt layers and a high amount of main anhydrite layers (z3HA) of the Leine-sequence. The structure of the salt rock in the central part includes the main stratigraphic units of the Zechstein strata (salt layers z2HS, z2SF, z3LS, z3OS, z3BK/BD, z3AM/SS, and anhydrite layers z3HA). The structure of the overburden and country rock includes the caprock, Bunter, Muschelkalk, Keuper, Jurassic, Cretaceous, and Quaternary layers.

3. Geomechanical modelling

3.1. Idealized geological model and mining situation

The idealization of the geological structure of the salt rock and the overburden of the southern central part in the Bartensleben mine is based on a characteristic geological cross section perpendicular to the axis of the structure and the mining rooms. The main units of the Zechstein strata (salt layers z2HS, z2SF, z3LS, z3OS, z3BK/BD, z3AM/SS, and anhydrite layers z3HA) and, if necessary, composites of the main units (z3OS/BK/BD) are considered. The Hauptsalz z2HS was separated into a western part (z2HSW) and an eastern part (z2HSO), due to different creep behaviour. The structure of the overburden was idealized taken the main layers caprock cr, main anhydrite DGL (including layers of Deckanhydrit, Grauer Salzton, and Leinekarbonat) within the caprock, Keuper k, Jurassic-Cretaceous j-kr, and Quaternary q into account (Fig. 2).

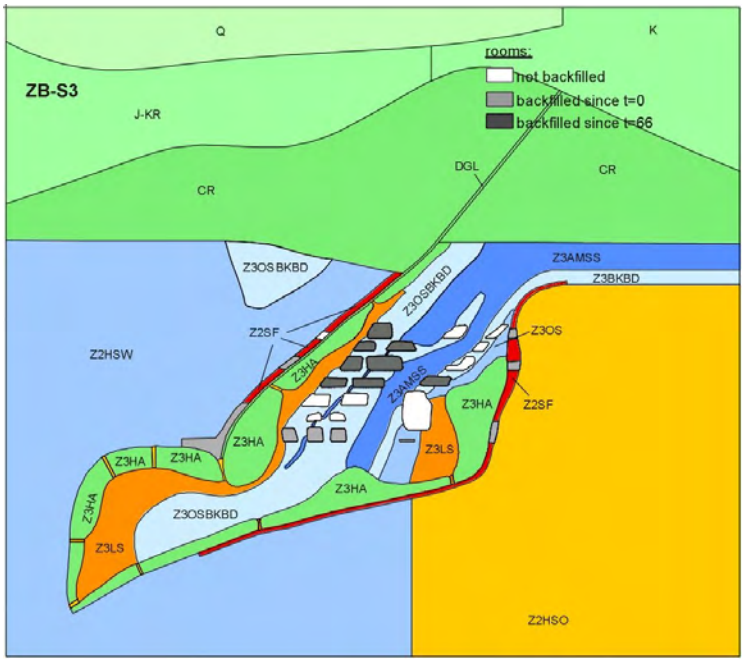


Figure 2. Idealized geological structure.

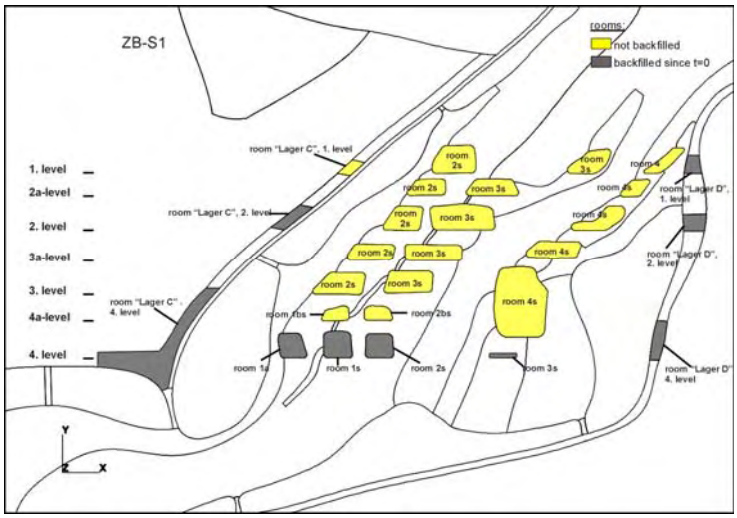


Figure 3. Configuration of old mining rooms.

The characteristic cross section used for geomechanical modelling comprises several old mining rooms excavated a couple of decades ago and located at different levels of the mine. According to the strong inclination of the salt layers the excavation rows are arranged in a steep configuration forming several pillars and roofs. The rooms as well as the pillars and roofs show different sizes and shapes determined on the basis of the mapping of the mine and by scanning the room contour. Figure 3 depicts a schematic view of the rooms which were considered in the geomechanical model. A minor part of the rooms was backfilled after excavating the potash or rock salt (Fig. 3, dark-grey coloured rooms), while the major part has been left open since excavation (Fig. 3, yellow coloured rooms).

3.2. Material behaviour and parameters

The idealized geological layers were classified with regard to their material behaviour. Anhydrite layers and the overburden were assumed to be elastic, the ductile rock salt layers were classified with respect to the steady-state creep rate. For the anhydrite layers, the modulus of elasticity was determined in laboratory tests from the post-failure stage to take the reduced stiffness of the jointed anhydrite blocks into account. Thus, a modulus of 30 GPa was used. The deformation behaviour of the ductile rock salt layers was described by a constitutive equation including both elastic and steady-state creep deformation. Additionally, the dilatant behaviour of rock salt was considered by a viscoplastic constitutive model. According to Hunsche and Schulze (1994), the effective steady-state creep rate can be calculated using:

$$\dot{\varepsilon}_{eff}^{cr} = A_{cr} \cdot e^{-\frac{Q}{RT}} \cdot \left(\frac{\sigma_{eff}}{\sigma^*} \right)^n \tag{1}$$

with R = universal gas constant (8,3143·10^{-3} kJ/mol·K), T = temperature (K), σ_{eff} = effective stress (MPa), σ^* = reference stress (1,0 MPa) and the material parameters A_{cr} = structural factor (1/d), n = stress exponent (-), Q = activation energy (54,0 kJ/mol). The several types of rock salt layers mainly differ with respect to the structural factor A_{cr}. Thus, the creep capability of the layers can be taken into account using a factor A* related to the reference value A_0 = 0,18 1/d:

$$A_{cr} = A^* \cdot A_0 \tag{2}$$

Table 1 shows the values of A* determined in laboratory creep tests on rock salt taken from the different salt layers of the Bartensleben mine.

Table 1. Relative creep capability A* .

Salt layer	symbol	*A**
Anhydritmittel-/Schwadensalz	z3AM/SS	1/32
Bank-/Bändersalz	z3BK/BD	1/16
Orange-, Bank-/Bändersalz	z3OS-BK/BD	1/8
Orangesalz	z3OS	1/16
Liniensalz	z3LS	1/8
Kaliflöz Staßfurt	z2SF	10
Hauptsalz (West)	z2HS-W	1/16
Hauptsalz (East)	z2HS-O	1/2

A viscoplastic constitutive model was used to calculate dilatant deformations of the rock salt layers. Viscoplastic flow must be considered if the stress state exceeds the dilatancy boundary. Here, the

dilatancy boundary is assumed to coincide with the yield function F which is described by a modified Drucker-Prager yield criterion:

$$F = \alpha \cdot J_1 + \sqrt{J_2^D} - k \tag{3}$$

with J_1 = 1. invariant of stress tensor (MPa), J_2^D = 2. invariant of stress deviator (MPa^2), α = fictive angle of friction (-), k = fictive cohesion (MPa). The parameters α and k were determined to α = 0,2887 and k = 0.

4. Numerical calculations

4.1. Finite-element modelling

The finite-element model of the southern central part of the Bartensleben mine was established on the basis of the idealized structure of the geological layers (Fig. 2) and the geometry of the old mining rooms (Fig. 3). For reasons of simplification, a two-dimensional plane-strain model was used in spite of the distinct three-dimensional development of stresses and strains around the rooms. This is valid since the rooms have a considerable length in the normal direction and the stress and deformation state calculated in a 2-D model is more unfavourable and "conservative" with respect to the assessment of the stability and integrity of the structure.

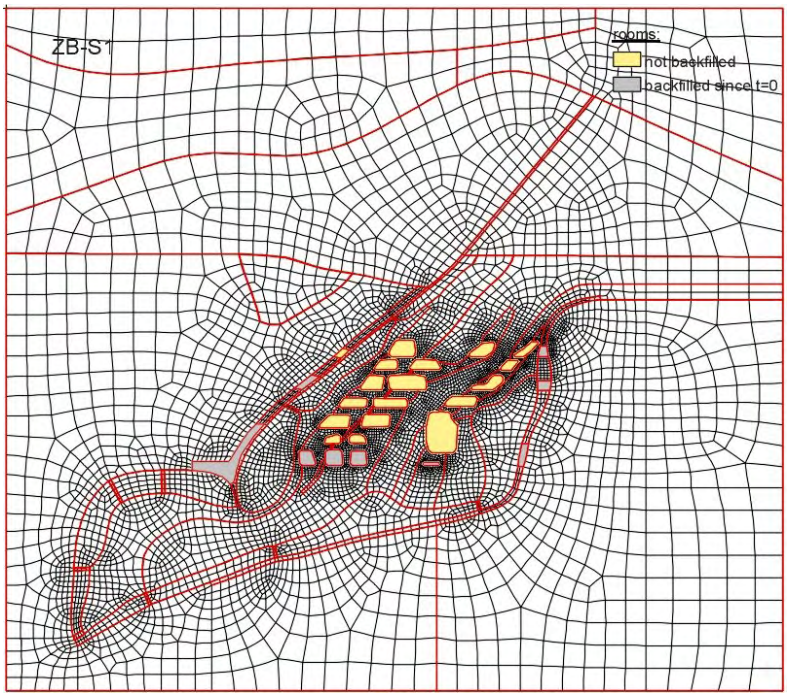


Figure 4. Two-dimensional plane-strain finite-element model.

Figure 4 shows a plot of the entire FE model, 750 m in height and 850 m in length, comprising 30675 nodal points, 10178 isoparametric 8-node elements and approximately 50000 degrees of freedom. The rooms were assumed to be excavated instantaneously in the year 1940. Thus, up to now a time elapse of about 65 years must be regarded to analyse the recent stress and deformation state. The total time elapse considered in the model amounted 100 years up to the year 2040. A minor part of the rooms (Fig. 3, dark-grey coloured) was backfilled after extracting the potash; they were assumed to be backfilled with crushed salt with a low stiffness directly after excavation.

Model calculations were made using the finite-element code ANSALT I (Nipp, 1991) and included the following steps: First, the recent stress and deformation state of the structure was analysed including the determination of dilatant rock zones in the salt rock and the effective stress and strain in the roofs and pillars of the rooms. Second, the influence of humidity induced creep acceleration on the stability and integrity was investigated. Third, the backfilling of a number of selected rooms was simulated due to the concept of advanced backfilling of the central part of the Bartensleben mine; this model variation served to study the long-term reduction of dilatant rock zones and the improvement of the stress conditions for healing of the salt barrier. The results of model calculation were evaluated using the pre- and postprocessor INCA/PATRAN.

4.2. Assessment of stability and integrity

The stability of the mine and its components has to be analysed at the following scales:

- Stability of local and medium size areas of the salt rock, considering the risk of roof fall and the collapse of mine components like pillars and roofs,
- overall stability and integrity of the entire structure, including the impact of potential damage zones in and around the mine.

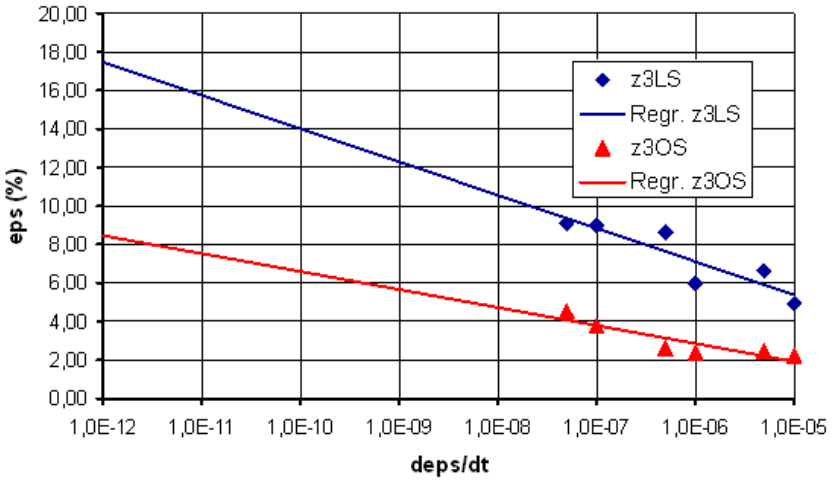


Figure 5. Maximum allowable deviatoric strain at different strain rates for rock salt types z3LS and z3OS.

To analyse the stability of the mine at small and medium scales, two criteria are taken into account. First, critical areas of tensile stress in the salt rock are determined with respect to the very low tensile strength of rock salt. Second, the deformation state in roofs and pillars in terms of the deviatoric strain is calculated and compared to the maximum allowable deviatoric strain measured in the laboratory and extrapolated to the strain rate conditions occurring in situ. As an example, Figure 5 shows the results of short-term deformation tests on rock salt samples from the Bartensleben mine. The laboratory tests were performed on z3LS and z3OS samples at different strain rates $d\varepsilon/dt = 5.0 \cdot 10^{-8} - 1.0 \cdot 10^{-5}$. The regression lines calculated from the measured ultimate deviatoric strain values and plotted in the semi-logarithmic diagram yield maximum allowable deviatoric strains ε of approximately 8.5 % (z3OS) and 17.5 % (z3LS) at the estimated in-situ strain rate of $d\varepsilon/dt = 1.0 \cdot 10^{-12}$.

To analyse the integrity of the salt rock barrier from a geomechanical point of view, the following criteria were used (Langer and Heusermann, 2001):

- Dilatancy criterion: The geomechanical integrity of the barrier is guaranteed if rock stresses do not exceed the dilatancy boundary (Schulze et al., 2001); if this boundary is exceeded, micro-cracks will form and will cause progressive damage and increasing permeability of the salt rock.
- Hydraulic criterion: The geomechanical integrity of the barrier is guaranteed if the hydrostatic pressure of an assumed column of brine extending to the ground surface does not exceed the minimum principal rock stress at the considered location of the salt body contour (e.g. top of the salt structure, contact area between salt and anhydrite blocks connected hydraulically to the overburden).

Additionally, the surface subsidence and inclination was calculated to analyse the long-term deformation behaviour of the entire mine and to assess the risk of damage above ground caused by creep closure of the mining cavities.

4.3. Results

To calculate the recent stress and deformation state of the southern central part of the Bartensleben mine a reference model was used taking into account the “best-estimate” model and material parameters. The main results are as follows: The salt rock around the old mining rooms, especially in the roofs, is subjected to increased stresses and deformations.

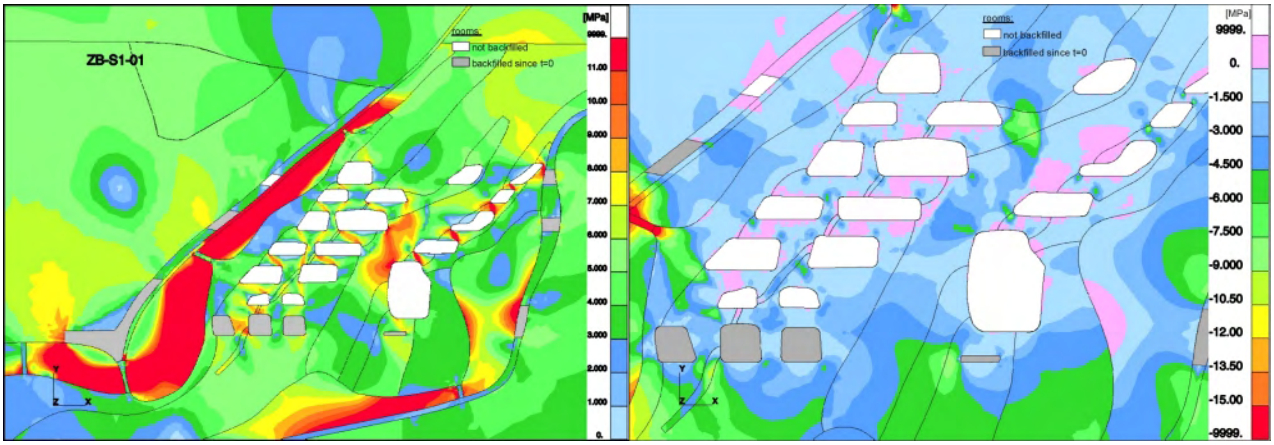


Figure 6. Calculated stresses 65 years after excavation, a) deviatoric stress (left), b) minimum principal stress (right).

Figure 6a shows the distribution of deviatoric stress and minimum principal stress at time t = 65 years after excavation. High deviatoric stress values especially occur in the roofs of the rooms of the eastern excavation row (fourth row with rooms no. 4s at levels 1, 2a, 2, 3a, and 4a, see Fig. 3) as well as in wide parts of the anhydrite blocks caused by creep of the salt structure and subsequent accumulation of stress in the anhydrite. Due to the unfavourable shape and spatial arrangement of the rooms, numerous roofs of the mine are partly subjected to tensile stress (Fig. 6b, pink coloured areas) indicating an unfavourable stress state with respect to the very low tensile strength of rock salt.

In Figure 7, the calculated deviatoric strain at time t = 65 years is plotted for the fourth excavation row with rooms no. 4s. The more or less diagonal configuration of the rooms and the resulting characteristic asymmetric deformation of the roofs between the rooms cause a significant shear and bending zone reaching diagonally from the left corner in the floor of the upper room to the right corner in the roof of the lower room. These strain values increase with time due to the creep of the salt rock. Comparing the deviatoric strain to the maximum allowable strain determined in the laboratory (Fig. 4) it must be stated that the calculated values have reached more or less the ultimate

values. For the long term, creep and dilatant deformation of the roofs will cause microcracks or, in case of accumulated microcracks, a single or a few macrocracks. Recent observations of fractures in numerous roofs of the central part of the Bartensleben mine confirm the results of modelling.

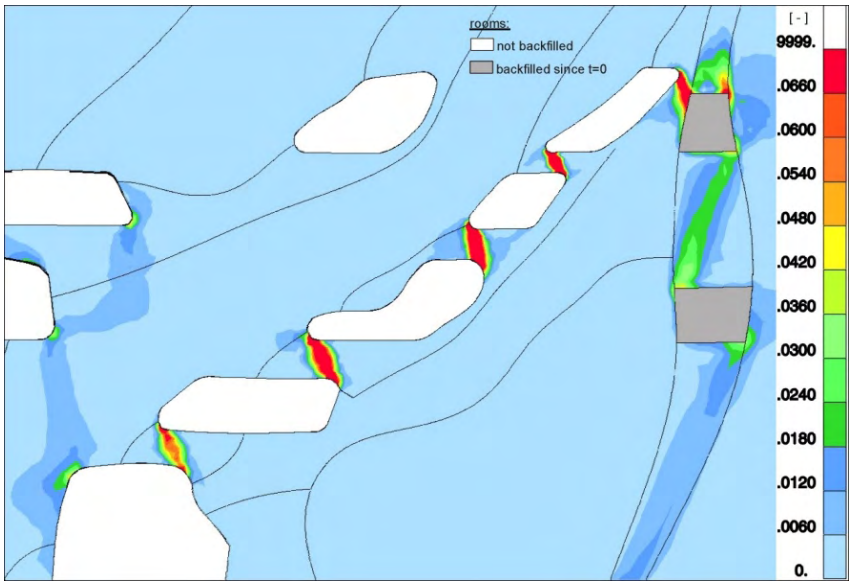


Figure 7. Calculated deviatoric strains (t = 65 years).

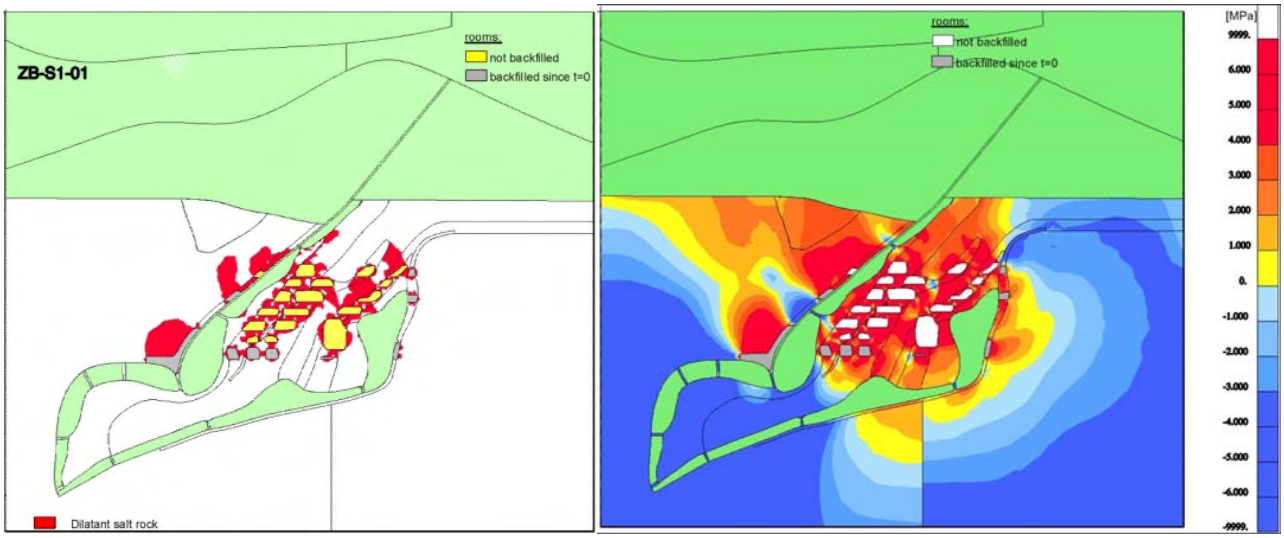


Figure 8. Proof of the integrity of the salt barrier, a) calculated dilatant zones (left), b) hydraulic criterion (right).

The dilatant rock zones calculated with the reference model for a time elapse of 65 years after excavation are plotted in Figure 8a. Excavation effects and creep of the salt rock cause the development of dilatancy around all rooms, as to be expected. The major part of the roofs and pillars between the rooms as well as larger rock zones between some rooms and the anhydrite layers are dilatant. Nevertheless, the salt barrier at the top of the salt dome shows no dilatancy. The development of dilatant rock zones with time is very slow. Regarding the hydraulic criterion, the calculations show wide zones around the cavities of the central part with a distinct reduction of the minimum principal stress. Thus, the stress conditions appear to be unfavourable with respect to a hypothetical brine pressure which exceeds the minimum principal stress in the contact zone between salt and anhydrite blocks (Fig. 8b, yellow to red coloured zones). Since dilatancy occurs in this zone, integrity of the barrier is not guaranteed and migration of brine from the caprock via the anhydrite layers and dilatant salt rock into the mining rooms cannot be excluded.

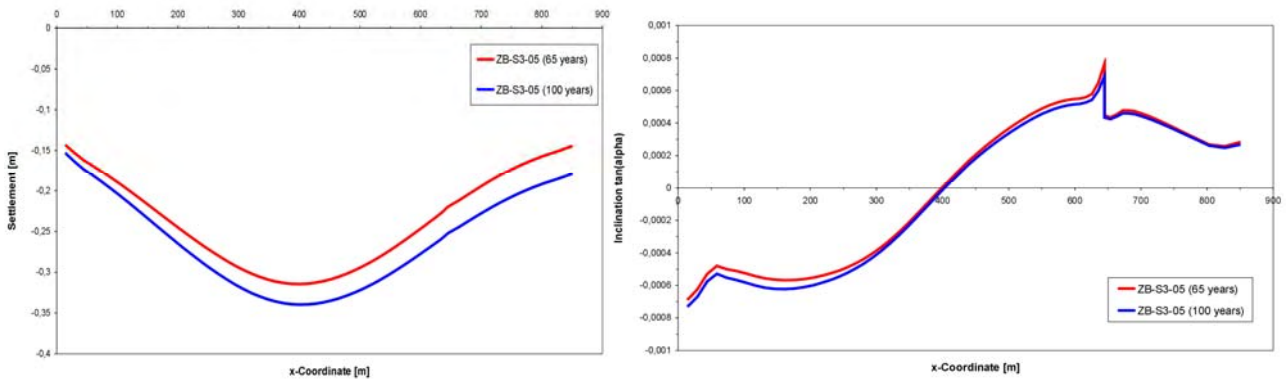


Figure 9. Calculated deformation at ground surface, a) subsidence (left), b) inclination (right).

The surface subsidence is plotted for t = 65 and 100 years in Figure 9a. At present (t = 65 years), a maximum settlement of about 0.32 m is calculated occurring directly above the central part. Figure 9b depicts a diagram of the surface inclination. Maximum values of inclination occur at the left and right side of the subsidence trough, as to be expected, and amount up to 0.007. This value is considerably lower than the maximum allowable value of 1/300 for the inclination of usual buildings (Skempton and McDonald, 1956). Subsidence and inclination will increase with time due to the creep of the salt rock and the time-dependent closure of the mining rooms.



Figure 10. Calculated dilatant salt rock zones assuming humidity induced creep.

Humidity induced creep was taken into account to study the effect of air humidity and migration of humidity into dilatant salt rock on the integrity of the salt barrier. As a first approach, it was assumed that the complete dilatant zones of the salt rock calculated with the reference model (Fig 8a) are affected by humidity. In the near vicinity of the rooms up to a distance of about 1-2 m from the room contour it was assumed that the humidity induced creep rate is ten times higher than the creep rate of the dry rock salt of each salt layer. For dilatant rock zones at larger distances from the rooms the humidity induced creep was assumed to be five times higher. Both values are in satisfactory agreement with observations in the laboratory.

As an example, Figure 10 shows the calculated dilatant salt rock zones for t = 65 years. According to the humidity induced creep acceleration, dilatancy occurs in wider parts of the salt rock than in the reference model (Fig. 8a). In contrast to the reference case, a dilatant path occurs which extends from the mining rooms up to the top of the salt structure.

The long-term stability of the mining rooms and integrity of the salt barrier can be significantly improved by backfilling the rooms with a suitable material. With respect to the actual backfilling concept, a selected number of rooms were assumed to be backfilled in the model (Fig. 2, dark-grey coloured rooms). The stiffness of the backfill material was taken to E = 3500 MPa corresponding to a medium stiffness. In the model calculations the backfilling was assumed to take place at present (65 years after excavation). Results were obtained for a time elapse of up to 35 years starting from now.

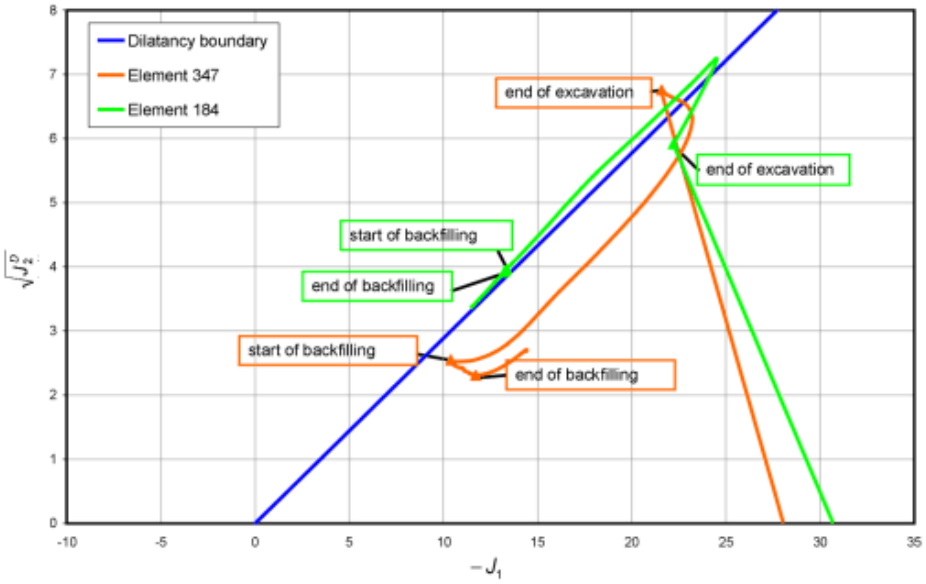


Figure 11. Exemplary stress paths depending on excavation and backfilling of mining rooms.

To demonstrate the effect of backfilling on the stress state of the salt rock, Figure 11 depicts the stress path of two selected points located in the salt rock in the vicinity of the mining rooms. It can be seen that high deviatoric stresses are caused by excavation with subsequent decrease or increase due to creep and stress redistribution of the structure. Starting of backfilling leads to an additional decrease of deviatoric stress with time (Fig. 11, element 347).

As an example, Figure 12 shows the zones of dilatancy calculated for a time t = 75 and 100 years after excavation (corresponding to 10 and 35 years after starting of backfilling) and assuming humidity induced creep of the salt rock. Comparing these results to the results at 65 years before backfilling (see Fig. 10), it can be seen that a distinct reduction of dilatant zones in the salt rock occurs. Most of the previous dilatant zones are disappeared, especially around the backfilled rooms. Dilatancy is calculated only locally in the vicinity of the non-backfilled rooms, between some backfilled rooms and the anhydrite blocks, and in some upper parts of the salt barrier. Variation of the stiffness of backfill material shows that a higher stiffness leads to an acceleration of the decrease of dilatant zones. A lower stiffness will delay the reduction.

Considering the effect of backfilling of selected rooms on the surface subsidence and inclination, Figure 9 compares the values calculated for t = 65 years (just before starting of backfilling) to the values calculated for t = 100 years (35 years after start of backfilling). The maximum subsidence of 0.32 m before backfilling increases slightly to 0.34 m after a time elapse of 35 years. The surface inclination shows only a slight increase with time.



Figure 12. Calculated dilatant salt rock zones after backfilling of selected rooms, a) t = 75 a (left), b) t = 100 a (right)..

5. Summary and conclusions

To assess the stability of old mining rooms and the integrity of the salt barrier in the southern central part of the Bartensleben mine of the Morsleben repository, geomechanical model calculations have been carried out. A two-dimensional model of a characteristic cross section of the mine was used based on an idealized model of the geological structure. The calculations comprised the analysis of the recent status of the rooms and the salt barrier and the evaluation of stability and integrity based on several criteria taking tensile stress, maximum allowable strain, surface subsidence and inclination, dilatancy, and a hydraulic criterion into account. Additionally, the effect of humidity induced acceleration of creep of dilatant rock salt was considered. Finally, the backfilling of selected rooms was analysed to demonstrate the effectiveness of backfilling and the decreasing of dilatant rock zones.

The following results could be obtained by means of finite-element modelling:

- The analysis of the recent status of the southern central part of the mine shows that the local and medium-scale stability of the mine is strongly influenced by an unfavourable shape of the rooms and steep configuration of excavation rows. Thus, tensile stress, high deviatoric strain and dilatancy occur especially in the roofs between the mining rooms. Fractures in the roofs with subsequent roof fall cannot be excluded in such cases since tensile stresses and high deviatoric strains. Recent observations of several fractures in numerous roofs of the mine are in good agreement with the results of numerical modelling. However, this local phenomenon does not affect considerably the present large-scale stability and integrity.
- The integrity of the salt barrier is given for most parts of the salt rock, especially at the top of the salt structure. However, significant zones of dilatancy occur around the rooms and between the rooms and the anhydrite layers. Thus, potential migration of brine from the caprock into the mining rooms via the anhydrite layers and the dilatant salt rock cannot be excluded. Humidity induced acceleration of creep of the salt rock causes an increase of the development of dilatant zones.

- If a number of selected rooms in the mine are backfilled with a suitable material, a distinct reduction of dilatant rock zones will occur within a couple of years or a few decades depending mainly on the stiffness of the backfill material.

6. References

Behlau, J., Mingerzahn, G. (2001). *Geological and tectonic investigations in the former Morsleben salt mine (Germany) as a basis for the safety assessment of a radioactive waste repository*. Eng. Geol., 61, 83-97.

Hunsche, U., Schulze, O. (1994). *Das Kriechverhalten von Steinsalz*. Kali und Steinsalz, 11(8/9), 238-255.

Langer, M. (1999). *Principles of geomechanical safety assessment for radioactive waste disposal in salt structures.* Eng. Geol., 52, 257-269.

Langer, M., Heusermann, S. (2001). *Geomechanical stability and integrity of waste disposal mines in salt structures.* Eng. Geol., 61, 155-161.

Nipp, H.-K. (1991). *Testbericht und Freigabemitteilung für das Programmsystem ANSALT I (Release 1991-1)*. Bericht, Archiv-Nr. 108586, BGR, Hannover.

Schulze, O., Popp, T., Kern, H. (2001). *Development of damage and permeability in rock salt undergoing deformation.* Eng. Geol., 61.

Skempton, A.W., McDonald, D.H. (1956). *The allowable settlement of buildings.* Proc. of the Institution of Civ. Engs., Part 3, Vol. 5, 727-768.

A STUDY OF SINKHOLE HAZARD AT AREA OF LOCKED COLLIERY

KOTYRBA Andrzej

CENTRAL MINING INSTITUTE, 40-159 Katowice, Pl. Gwarków 1, Poland;
a.kotyrba@gig.katowice.pl

ABSTRACT: Transformations of polish industry began the process of mine closures. Among various mines being in process of abandoning, there are a large number of collieries, which exploited coal since 17th century. The depth of mining openings ranged from some to hundreds meters. The height of primary mining openings ranged from 1 to 9 m. Mining operations have left in geological basement large number of cavities, which still create a hazard to the surface stability. Post mining deformations of the surface can take continuous and discontinuous forms. The last ones are the topic of paper. Although those deformations can take various forms, they are commonly called as sinkholes. In paper, the sinkholes hazard has been analyzed in a scale of selected one mine area, in regard to various parameters. The selected "Siemianowice" mine is located in northern part of the Upper Silesian Coal Basin. A database containing full set of sinkholes, recorded within area of mine in a period of 50 years, has been tested in geomechanical and statistical approaches.

KEYWORDS: Mine closure, Voids, Sinkholes, Hazard, Risk,

RESUME: La fermeture de mine a commencé avec la transformation de l'industrie polonaise. Parmi les mines en train d'être fermées, on trouve de nombreuse mines de charbon exploitées depuis le 17e siecle. La profondeur de travaux miniers varie de quelques mètres à plusieurs centaines de mètres. La hauteur des galeries principales est comprise entre 1 et 9 m. Les opérations minières ont laissé dans le terrain beaucoup des vides qui sont toujours une menace pour la stabilité de surface. Les déformations de surface induites par l'instabilité des anciens travaux miniers peuvent avoir une forme continue ou discontinue. Les déformations discontinues sont le sujet de cet article, elles sont généralement appelées fontis. Dans cet article, on a analysé le risque de fontis en terrain minier dans le cas de la mine de charbon de « Siemianowice » localisée au nord du Bassin Houiller de Haute-Silésie. On a examiné, du point de vue géomechanique et statistique, une base des données concernant les fontis qui se sont produit dans le secteur depuis 50 ans.

MOTS -CLEFS: Fermeture des mines, Vides, Fontis, Alea, Risque

1. Introduction

The study concerns the post-underground mining-induced surface subsidence hazard. This hazard arises from the mined-out voids left, following the mine closure. The void-related ground surface subsidence can occur at an indefinite time after the mine closure, and especially is essential for the sinkhole process formation. The post mining subsidence events can be tested in regional and local scale. Usually, only local scale is a matter of interest due to economic reasons. It leads to simplified solutions and limitation of subsidence hazard only to sinkhole events. The regional scale studies should be undertaken especially in areas, where still operating mines coexist with locked ones in which (as it is in Poland) are observed also distant, continuous effects [Kotyrba et al. 2004].

The sinkhole processes are the cause of characteristic surface disturbances, that usually bring about breaking out of the strata continuity and lead to formation of the local ground surface subsidence phenomena such as funnels, troughs, steps and cracks. In the majority of cases, they can suddenly occur at the surface without advance warning (typical sinkhole process). In some cases however, the subsidence formation process develop during a longer period of time and can be indicated by progressive ground surface subsidence.

None of the past mining techniques, in particular exploitation conducted on shallow depths (range from 0 to 100 m) have offered a total self-backfilling of the old mine workings in coal seams. Many old mine workings neither have undergone caving at all nor they have been backfilled in the mine closure phase. Because of the afore-mentioned factors, leaving the voids in massive rock body should be considered to be a persistent element of the altered and degraded geological environment that creates hazard for the post-mine ground surface stability both at present and in the future. In methodology of the surface hazard assessment over voids various approaches are applied. Generally they are based on theoretical assumptions, geophysical/geological testing, surveying and observational data. In one mine case described in presented paper, theoretical and observational data are compared and analysed.

2. Geology and mining

In geology of the studied area anthropogenic, quaternary, Triassic and carboniferous sediments take part. The anthropogenic soils in many parts are thick up to 10 m. They consist of different origin wastes. Most frequently the wastes come from mines (stone) and metallurgical plants (slag). They are also frequently mixed. The thickness of quaternary sediments ranges between 2 to 60 metres. Those glacial origin soils occur in form of sands, sandy clays, clays and clayey sands. The occurrences of particular soils are irregular. Therefore quaternary sediments are generally permeable for water. The Triassic sediments in form of limestone and dolomites occur in the northern part of mine area. Their thickness increases to the North and ranges from some to 200 m. The outcropping on the terrain surface younger geological strata is shown on fig.1 [Buła and Kotas, 1994]. All three stratigraphic units mentioned form the overburden to the carboniferous strata, which consist of sandstones, mudstones, shale stones and coal beds. Coal seams thickness ranges from 1 to 11 m.

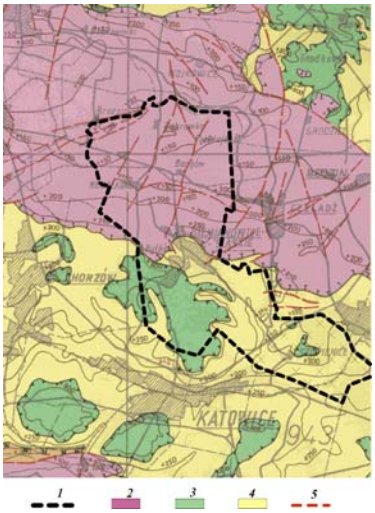


Fig. 1. Stratigraphic units in the overburden of coal deposit at the area of “Siemianowice” mine.
(1 - mine lease area border, 2 – Triassic, 3 - quaternary sediments of thickness not exceeding 2 m, 4 – quaternary sediments of thickness exceeding 2 m, 5 - faults).

The surface of the carboniferous formation is not even and has been created by tectonic movements and erosion. Tectonic movements uplifted the central part of area creating saddle. Therefore the dipping of carboniferous beds has different directions. In the northern part of area dominant is dipping to the north. In southern parts, the beds are dipping generally to the south. The dip angle ranges from 8 to 15 degrees. Tectonic movements left in rock formation numerous ruptures (faults). Some of them are visible on the Triassic surface (fig.1). The faults cut the rock formation mainly on directions SW-NE and NW-SE. Less numerous are faults spreading parallel to latitude.

The water conditions in area are shaped by geological structures. Water horizons have been recorded in quaternary, Triassic and carboniferous sediments. Those waters are drained by central pumping system designed to keep the water on the level, which is regarded as safe for operating mines located in the vicinity.

The earliest information on organized hard coal mining in the Upper Silesia Coal Basin (USCB) area dates back to the second half of the 18th century. At that time there were simple, small-sized mines supplying local blacksmith's shops, brickyards, breweries and Limestone quarries with coal. Rapid development of the coal mining industry began on the turn of the 18th century. It was caused by the rising demand for hard coal needed in the iron and lead smelters, for generating steam in machine boilers and mostly, in the zinc smelters. The border of Siemianowice mine lease area shown on fig 1, illustrates the state on the date of mine closure. This line changed many times in the past according to divisions mining region among smaller mines. Filed records of that mining activity are known from the end of XIXth century. In the early phases of mining, the coal seams were being opened out by the two following methods:

1. Sinking of vertical shafts from the surface.
2. At first, opencast mining, next driving a dip heading (inclined shaft) after the overburden became thick enough, and then extraction galleries along strike were driven from the dip heading.



Fig. 2. The layout of mining works in coal seam 501 at the southern part of the Siemianowice mine.

The similar method of coal exploitation was used in many parts of the Siemianowice mine area even in XX century. On fig.2 is shown the mining map from year 1943, showing the shallowest exploitation performed in southern part of studied mine area (site cross hatched on fig.1) in so called "wide galleries" system. Anyway, the dominant systems of exploitation performed in depth range from 0 to 100 m b.g.l., were based on room and pillar scheme (early stages of XIX and beginning of XX century).

3. Description of sinkholes recorded

One of the methods, which characterize quantitatively the hazard of the discontinuous deformations, is a detailed study of events, which have occurred in the past. The polish mines were obliged to keep a so-called "register of discontinuous surface deformations". Those data can serve as a valuable tool, both for the risk assessment and creation of future scenarios of surface stability (prediction). The use of registers for quantitative analysis is limited only to a few polish mines, which filled them in proper form (full data about time, deformation type and dimensions, geological and mining conditions).

One, such a register has been analysed in the study. The selected " Siemianowice" mine has been locked finally in the year 2000. The register contains data gathered in period of fifty years (1952-2002). Not all, separate records in register are complete. Anyway, they allow building a data set for further analysis. Distribution of the events on the area of shallow exploitation (depth from 0 to 80 meters), performed within mining lease area, is shown on fig. 3.

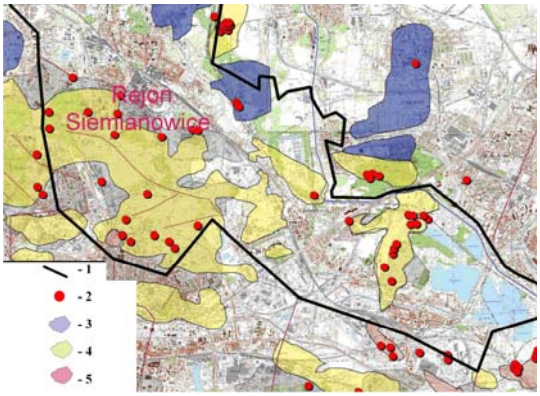


Fig. 3. Distribution of sinkholes (red dots) recorded within or near by the mine border
(1- mine lease border, 2 – location of sinkhole, 3,4,5 - areas of mining works in depth range 0 – 80 m marked in 3 point hazard rating scale – low, medium, high).

It can be observed, that near all deformations, have been recorded within extraction panels or nearby their borders in the southern part of mine area, where the carboniferous strata are over lied by quaternary sediments (southern part of the mine area shown on fig. 1) The largest sinkhole occurred at the site of an old shaft "Piaskowy II", used in the past for sand transport to deeper parts of mine (fig.4).

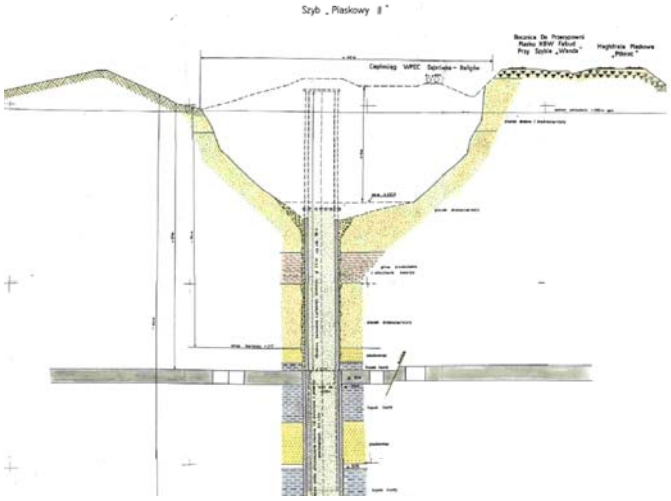


Fig. 4. A sinkhole at location of shaft "Piaskowy II" (approximate diameter 40 m, depth 15 m).

Although within analysed area, there were recorded also three cases, in which deformations of the surface had a form of fissures, those records were rejected from the data set. The origin of two events is not clear and difficult to determine. In third case (which has occurred in 1971 in Katowice), the fissure was due to the spontaneous fire in extracted coal seam residues. In the air out flowing from the fissure, the increased content of gases CO, CO_2 has been observed. The temperature of the out flowing air was also relatively high. This event caused serious damages in the building structure located at the area, due to subsidence of the foundations.

The sinkholes can occur within all types of mining openings (extraction panels, shafts, adits, caving zones) and can induce spontaneous fires in coal residues what creates gas hazards to humans. In all cases the primary reason of sinkhole process the presence of void within geological basement.
There are generally four methods, which can be used to assess the surface hazard due to cavities, left in rock strata by mining operations (theoretical approach, experimental approach, statistical approach, geological approach).

4. Theoretical approach

Among various geo-mechanical concepts regarding the assessment of surface deformation hazard due to shallow mining void migration phenomena, the most interesting is the method based on theory of pressure vault [Jarosz and Janusz 1976; Chudek et al. 1988; Kwiatek 2002]. In this method all phenomena in mined rock overburden are due to the static pressure distribution. The theoretical intersection of the strata with mining void is depicted on fig. 5. The primary, rectangular void in vertical plane of width 2*a* is done on whole thickness of the coal seam (*g*). Over the void is a layer of hard rock of thickness *h*, over lied by soils of thickness h_n. The rock in the void roof relieves the stress creating the elliptical distressed zone. Over that zone the static pressure in rock strata distributes in form of “pressure vault”. Circular, horizontal shape of the void allows foe assumption, that the pressure vault has a form of rotational ellipsoid.

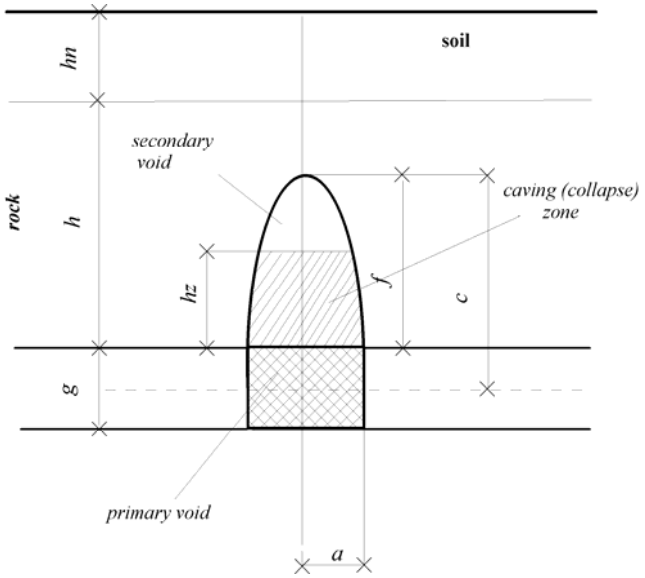


Fig. 5. Model of coal mining void in pressure vault theory.

The vertical, longer half axis of ellipsoid has dimension *c*. The horizontal half axis has dimension *b* and equals to the half width the primary void. The ratio of half-axes can be expressed in equation 1.

$$n = \frac{c}{a} = \frac{1}{2}\left[\left(m-2\right) + (m-1)\frac{R_r}{p_z}\right] \tag{1}$$

Where:
m=1/ν - Poisson number (ν-Poisson's ratio)
R_r – tensile strength,
P_z – vertical pressure at the half height of void,

Making additional assumption, that the tensile stresses are absent in the rock over void (R_r =0), we get formula 2.

$$n = \frac{m}{2} - 1 \tag{2}$$

It is assumed further, that the rock inside pressure vault tends to fissuring and crushing and falls down on the void bottom at the end, creating the caving zone of height h_z. Over the caving zone a secondary void is created. The caving process can be multiplied to the moment, when the void is fully filled with crushed rock (void migration process). If the pressure vault reach the roof of hard rock, it's possible that the soil from overburden fill the void. In result, the deformation of the ground surface can occur. The deformation will not occur if the following inequality is filled:

$$\mathrm{f} = \mathrm{c} - \frac{\mathrm{g}}{2} < \mathrm{h} \tag{3}$$

The width of primary void (l_c) which fills this inequality, can be expressed by condition 4:

$$\mathrm{l_c} = 2\mathrm{a} < \frac{2}{\mathrm{n}}(\mathrm{h} + \frac{\mathrm{g}}{2}) \tag{4}$$

Due to safety reasons, the recommended permissible width of void (l_p), should not exceed 0.5 l_c. It leads to condition 5:

$$\mathrm{l_p} = \frac{1}{\mathrm{n}}\left(\mathrm{h} + \frac{\mathrm{g}}{2}\right) \tag{5}$$

The use of theory in practice is difficult, because usually we don't know the width of void left in mined strata. Nevertheless, described model shows that in geomechanical approach very important are two following parameters:

h_z - caving height (void migration height),
k - bulk ratio (defined as a ratio of volume of caved rock to volume of primary void).

The height of caving zone (vertical half axis of pressure vault) increases with primary void width. It can be proved that there is such a horizontal width of void at which the void can be self filled. Using parameters from theory it can be derived a condition for total backfilling of the void with caved rock (maximum void migration height) written as formula 6.

$$\mathrm{h_z} = \mathrm{h_{z\,max}} = \mathrm{g}\left[\frac{6}{\pi(\mathrm{k}-1)} + \frac{1}{4}\right] \tag{6}$$

In such a case, the height of caving equals *f* on fig. 5. If the width of void increase further, the height of pressure vault increase too. In the absence of secondary void, the rock above the caving zone gets only fissured, creating a *zone of fissures* of height h_{as}. According to theory, the fissures can propagate to the height of 1.5 h_{zmax}. If the pressure vault reaches the rock over this height, the strata can deflect up to the ground surface only.

On the base of pressure vault theory, there are following cases in which the surface deformations can be met:

- $h_s \le h_{z\max}$, Discontinuous deformations of the surface can occur,
- $h_{z\max} < h \le 1.5h_{z\max}$ and $h_n \le 30m$, discontinuous deformations of the surface can occur,
- $h_{z\max} < h \le 1.5h_{z\max}$ and $h_n > 30m$, discontinuous deformations will not occur but it can be met local, continuous subsidence of the surface,
- $h > 1.5h_{z\max}$, Discontinuous deformations of the surface will not occur but the continuous subsidence is probable.

For geological conditions of the studied area, where the exploited layers of coal ranged between 1 and 9 m, the possible void migration height is shown on fig.6. The voids migration height depends highly on bulk ratio. If this parameter is low, the largest voids can migrate up to the heights over 100 m. It can be assumed that weak, soft, brittle rocks (eg.shales, thin sandstone beds, coal beds) have high bulking ratios (k=1.4). The hard (stiff) rocks (e.g. mudstones, sandstones) have low bulking ratios (k=1.1-1.2 and exceptionally less). Plot from fig. 6 can be applied for theoretical assessment of void migration height, if the mining and geological data are known. It should be noted, that in described theory, the soil stratum covering the bedrock acts as a safety pillow. If it is enough thick (>30 m), it can split the deformation process.

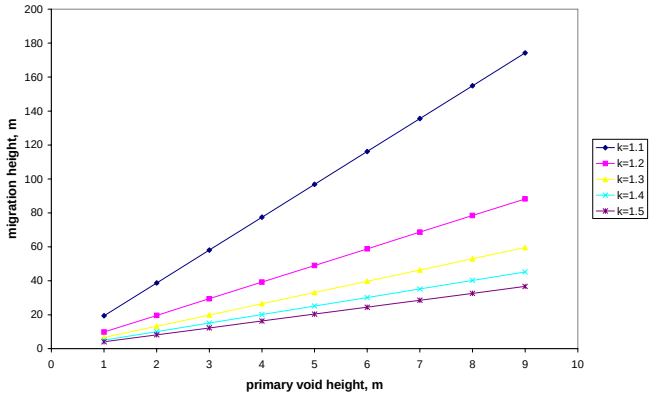


Fig. 6. Plot of mining voids migration height versus primary void thickness in the pressure vault theory (k – bulk ratio).

On fig.7 is depicted plot between fissuring zone height and the primary void height for the same as on fig. 6, range of void heights. It can be noted that fissures in exceptional cases (g = 9m), can propagate up to the height of 260 m, above the void.

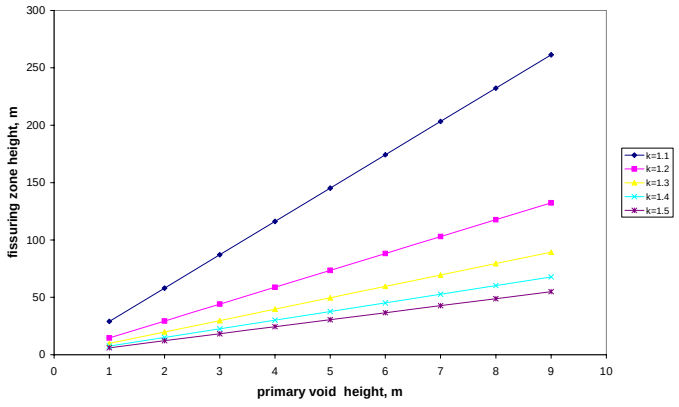


Fig.7. Plot of fissuring zone height versus primary void thickness with bulk ratio as a parameter.

5. Analysis of sinkhole data set

For the study needs, the two-layer model of geological basement with post mining void, migrating from the extraction level to the surface, has been analysed [Kotyrba et al. 2004, Kotyrba 2005]. The top model layer consists of quaternary sediments and due to difficulties with thickness determination is treated similarly to bedrock (fig.8). On base of that model various mining and geological parameters have been set or calculated as shown in tab.1. Some of them come directly from the mine register such as year of exploitation completion, year of sinkhole event, coal seam number identification, diameter or shape of event, deformation depth and the depth to extracted coal seam.

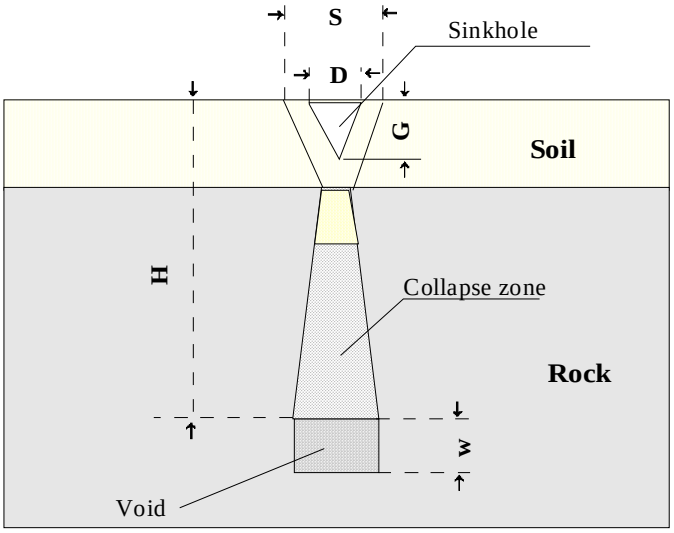


Fig. 8. Descriptive model of sinkhole process for data set from the "Siemianowice" mine.

The rest of parameters have been calculated according to preliminary data (the area of deformation) or model (time elapsed, migration parameter – H/w, collapse parameter G/w).

The shaft collapse event shown on fig. 4 has been rejected from the data set. The variability ranges of analysed geometrical parameters are summarized in table 2. It should be noticed relatively low values of collapse ratio and relatively high values of migration parameter. In specific geological conditions (where the rock outcrops on the terrain surface) the collapse ratio, could determine how many collapses of mining void roof can occur.

Table 1. Data set of sinkholes recorded at area of the “Siemianowice” mine.

Nr of Event	Year of event	Year of exploitation end	Time Elapsed	Nr of coal seam	Extracted Coal Thickness	Deformation Diameter	Deformation Depth	Deformation Area	Depth of shallowest seam extracted	Deformation Shape	Parameter H/ w_0	Parametr G/w_0
					W_0, m	D, m	G, m	S, m^2	H, m			
1	1952	1952	0	501	3	17 x 3	8	51	33	Trench	11	2,666667
2	1954	1952	2	501	2,4	10	3	78	20	Sinkhole	8,3	1,25
3	1959	1957	2	510	5	11	3	95	48	Sinkhole	9,6	0,6
4	1959	1957	2	510	8	8	2	50	59	Sinkhole	6,5	0,25
5	1966	1958	8	510	7	4	3	12,5	42	Sinkhole	6	0,428571
6	1967	1883	84	501	5	1,5	5	1,8	30	Sinkhole	6	1
7	1967	1889	90	501	5	5	3,5	19,7	30	Sinkhole	6	0,7
8	1968	1873	95	501	4,2	3	8	7	55	Sinkhole	13	1,904762
9	1968	1957	11	510	8,5	3	1	7	40	Sinkhole	4,7	0,117647
10	1969	1953	16	501	4	8,5	5	57	55	Sinkhole	13,8	1,25
11	1969	1954	15	501	5	9,5	7,5	71	60	Sinkhole	12	1,5
12	1970	1933	37	501	2	4	2	12,6	18	Sinkhole	9	1
13	1970	1880	90	501	7,5	4	8,94	12,6	125	Sinkhole	16,7	1,192
14	1971	1899	82	510	6	1	1	0,8	15	Sinkhole	2,5	0,166667
15	1971	1899	82	510	6	15	7	177	15	Sinkhole	2,5	1,166667
16	1971	1928	43	501	3	0,4	2	0,1	140	Sinkhole	46,7	0,666667
17	1971	1928	43	501	3	1	4	0,8	140	Sinkhole	46,7	1,333333
18	1971	1888	20	501	7	0,8	5	0,5	20	Sinkhole	2,9	0,714286
19	1972	1953	19	501	4	6	3	28	22	Sinkhole	5,5	0,75
20	1972	1883	89	501	5,5	4	4	12,6	10,5	Sinkhole	1,9	0,727273
21	1974	1916	48	501	6	1,5	1	1,7	30	Sinkhole	5	0,166667
22	1974	1885	89	501	7	3	1,8	7,1	35	Sinkhole	5	0,257143
23	1974	1933	41	501	2	2,5	5	4,9	16	Sinkhole	8	2,5
24	1976	1859	117	501	6	3	11	7,1	46	Sinkhole	9,1	1,833333
25	1977	1875	102	501	5	5	9	19,6	45	Sinkhole	9	1,8
26	1977	1845	122	501	5,5	3	8	7,1	30	Sinkhole	5,5	1,454545
27	1979	1884	95	501	7	4	8	12,6	60	Sinkhole	8,6	1,142857
28	1983	1880	103	501	7	2	6	3,1	30	Sinkhole	4,3	0,857143
29	1987	1874	113	501	4,5	3	2	7,1	35	Sinkhole	7,8	0,444444
30	1989	1900	89	501	6	8	3	50	58	Sinkhole	9,7	0,5
31	1989	1886	103	501	7	3,5	3,7	9,6	32	Sinkhole	4,6	0,528571
32	1989	1859	140	501	5,5	11	10	95	18	Sinkhole	3,3	1,818182
33	1991	1890	111	501	6,5	10	2	78,5	41	Sinkhole	6,3	0,307692
34	1992	1894	98	510	5,5	3,5	7	9,6	16	Sinkhole	2,9	1,272727
35	1994	1882	112	501	5	2,6	7	5,3	69	Sinkhole	13,8	1,4
36	1996	1924	72	504	1,7	1	0,6	0,8	42	Sinkhole	24,7	0,352941
37	1997	1859	138	501	5	15	7	177	18	Sinkhole	3,6	1,4
38	1998	1878	120	501	3	6	14	28	34	Sinkhole	11,3	4,666667
39	2002	1872	130	504 510	8	6	6	28	12	Sinkhole	1,5	0,75

Tab.2. Variability ranges of geometrical parameters shown in table 1.

Statistic parameter	*Geometrical parameters*					
	Deformation diameter, m	*Deformation depth, m*	*Deformation area, m^2*	*Depth to extracted coal seam*	*Parameter H/w (Depth/thickness of coal extracted*	*Parameter G/w (Deformation depth/thickness of coal extracted*
Maximum value	15	14	177	140	46,7	4,7
Minimum value	0,4	0,6	0,1	10,5	1,5	0,12
Average value	7,7	7,3	88,55	75,25	24,1	2,4

As opposite to above conclusion, high values of migration parameter indicate that also other than analysed factors influence the sinkhole processes. Note should be given also to the similarity of average values for the deformation diameter and depth.

To assess the correlation between specific parameters of the data set, a basic trend analysis has been performed. The results of analysis of the relations between area of deformation and basic mining factors, such as depth of exploitation and thickness of coal extracted (fig.9, 10), show that there are no correlations between them.

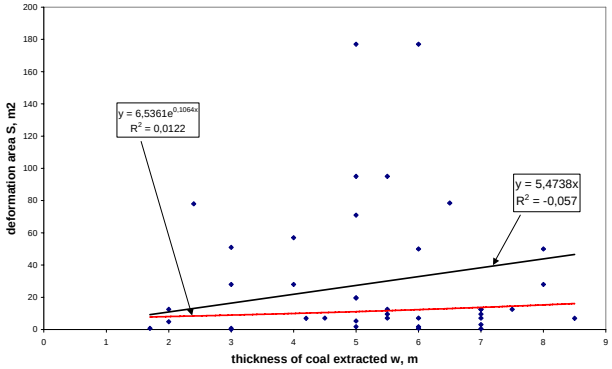


Fig. 9. Plot between deformation (sinkhole) area and thickness of extracted coal for the data set from the “Siemianowice” mine. Trend approximated by straight and exponential lines.

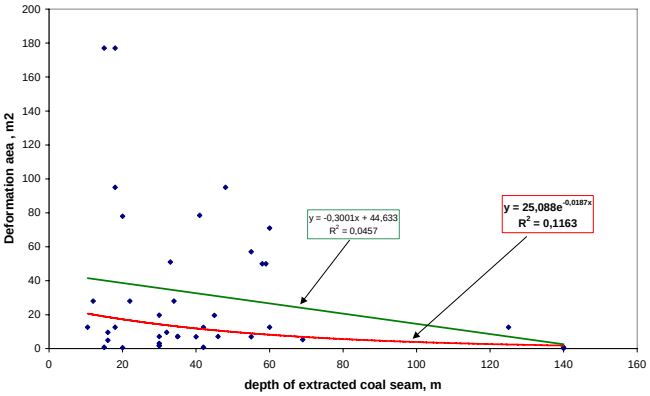


Fig. 10. Plot between deformation (sinkhole) area and depth to extracted coal seam for the data set from the “Siemianowice” mine. Trend approximated by straight and exponential lines.

The correlation plot of sinkhole diameter versus depth of extracted coal area is shown on fig. 11. It can be observed, that correlation between them is only a little better, than between parameters described earlier.

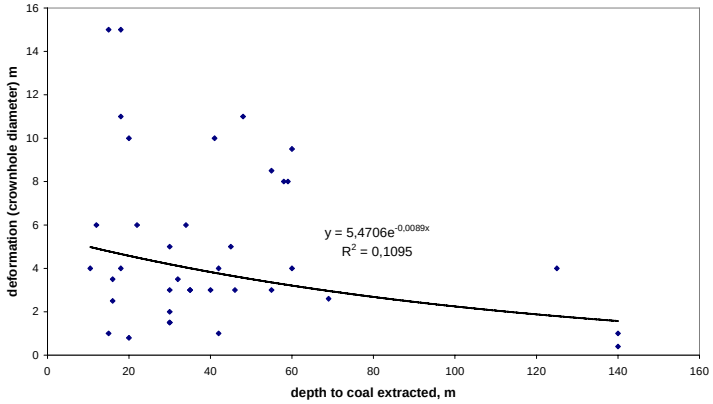


Fig. 11. Plot between deformation diameter and depth to extracted coal seam for the data set from the “Siemianowice” mine. Trend approximated by exponential line.

The similar is observed when we compare the vertical size of sinkholes (G) versus the depth to extracted coal seam (fig.12).

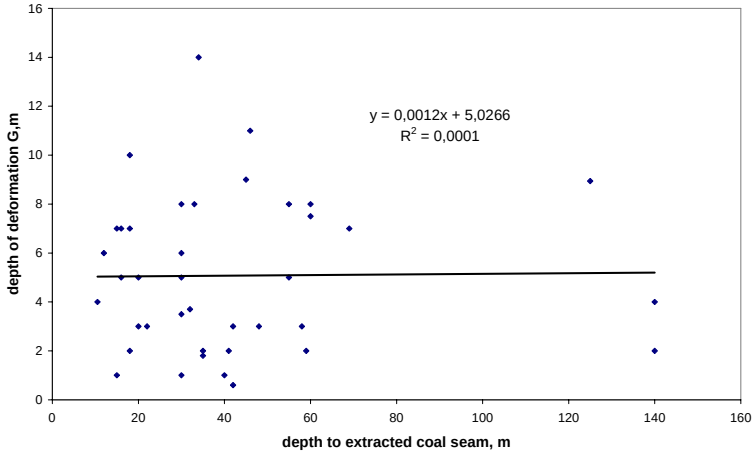


Fig. 12. Vertical size of sinkhole (depth of hole) versus the depth of extracted coal seam plots for the data set from the “Siemianowice” mine. Trend approximated by straight line.

Two indirect geometrical parameters, which are usually used in theoretical analyses of surface stability over void, have been tested (migration ratio, collapse ratio). The first one parameter (fig.13) characterizes the ability of void migration to the surface (depth to extracted coal seam thickness). The second one (fig.14) intermediately, shows the ability for natural backfilling of void (deformation depth/thickness of coal extracted).

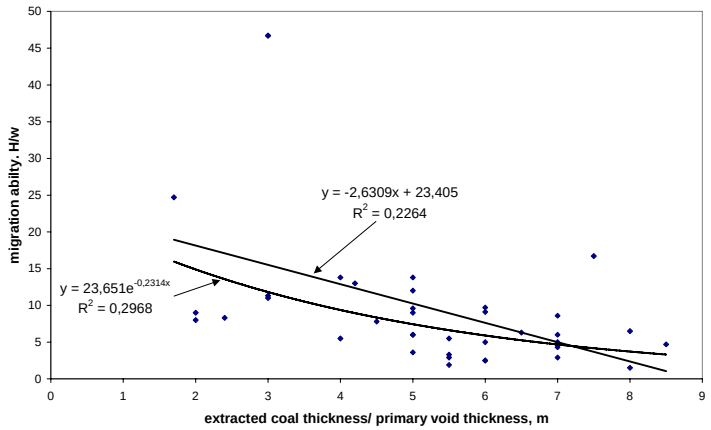


Fig.13. Plot between migration ability (parameter H/w) and thickness of coal extracted for the data set from the "Siemianowice" mine. Trend approximated by straight and exponential lines.

On plot shown on fig. 13, it can be observed that in prevailing number of events, migration ratio does not exceed a number of 15. Similarly, analysing plot shown on fig. 14 it can be concluded, that in prevailing number of recorded events, collapse ability (height of collapse in units of extracted coal seam thickness) does not exceed a number of 5. This parameter is connected with natural ability of rock strata to backfill the void by defragmented rock particles and soils on its migration way.

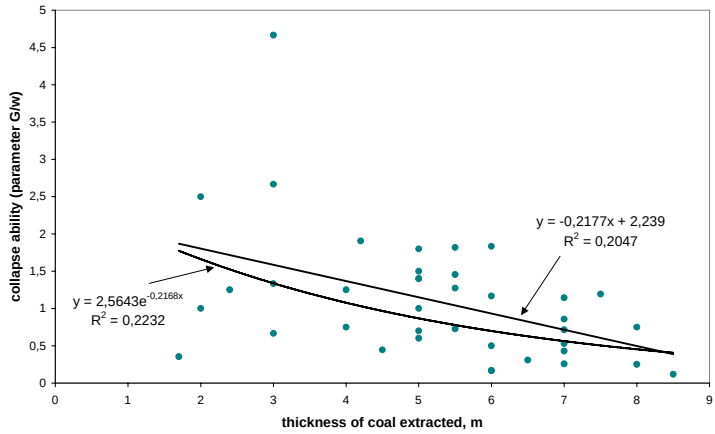


Fig. 14. Collapse ability (parameter G/w) versus extracted coal thickness (primary void height). Trend approximated by straight and exponential lines.

The correlation ratios squared (power ratios) for both plots are of order 0.2. Although the results of approximation show, that the correlation ratios are low, it should be noted that they are relatively higher than for parameters analysed earlier. Nevertheless, on both plots is observed that migration and collapse ratios tend to decrease with the thickness of extracted coal (primary void thickness). It can indicate, that smaller voids have higher ability for collapses and migration phenomena.
The last one analysed was the dependence of the area of deformation and time, which elapsed from exploitation completion (fig.15).

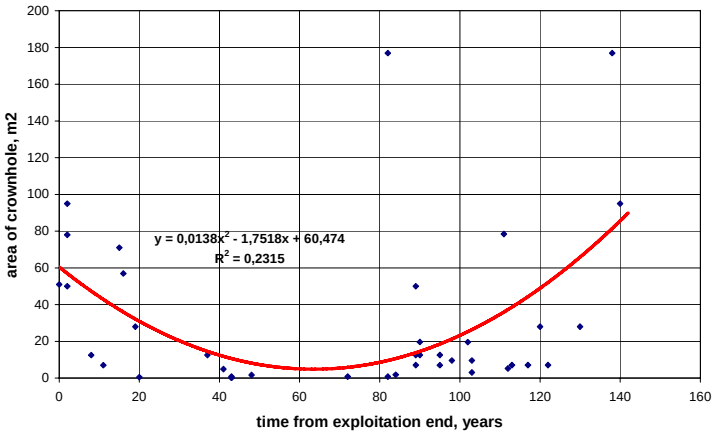


Fig. 15. Plot between area of surface deformation and time, which elapsed from exploitation end for the data set from the "Siemianowice" mine. Trend approximated by polynomial of second order.

Although the correlation between analysed parameters is also weak, the power ratio obtained is the highest comparing to others. On plot depicted on fig.15, three intervals can be distinguished, which are characterized by following trends:

1. Period 0 – 40 years – the size of crown holes decreases,
2. Period 40 – 80 years – the size o crown holes is stable and low,
3. Period > 80 years – the size of crown holes increases.

The 3rd period is most interesting for long-term assessments of post mining voids behaviour. According to plot, the number of sinkhole events shows increasing trend with time, which elapses from exploitation end.

6. Sinkhole hazard in statistical and probabilistic terms

The void migration parameter can be used out for estimation of the surface deformation hazard analysis in statistical terms. On fig. 16 a block chart, between the numbers of sinkholes (as a percentage of total number of events), which have been recorded at the Siemianowice mine area, in a function of parameter H/w classes, is presented. On chart, the location of two points, in which the number of separate events, divided by total number of events in data set, overcome 90 and 95 percents are marked. The corresponding values of migration parameter are respectively 14 and 26.

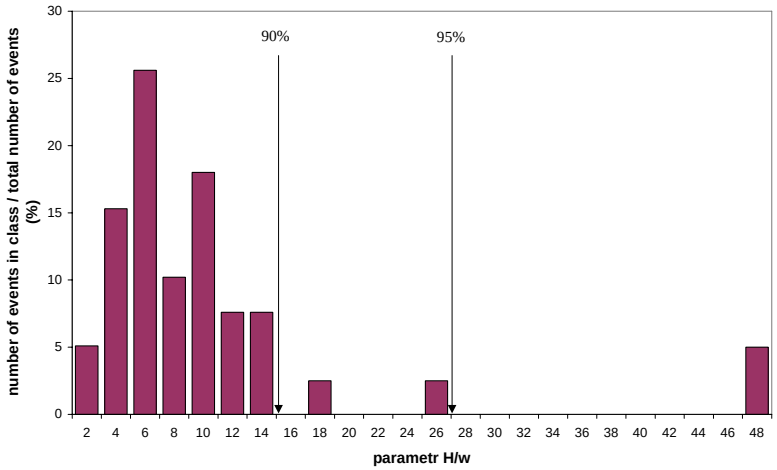


Fig. 16. Plot between the number of events in classes (percent) and values of parameter H/w (depth of exploitation/thickness of coal extracted) for the data set from the Siemianowice mine (arrows indicate the values of parameter for which percentage of events is 90 and 95 percent - confidence levels).

The chart can be used for estimation the limits of mining depths (which respectively to confidence levels) are likely to create the sinkhole hazard for the surface in a function of typical thickness of coal seams, exploited in the "Siemianowice" mine (table 3).

Table 3. Estimated values of mining parameters, which can generate deformation (sink holing) effects on the surface.

Thickness of extracted coal W, m	Depth limit, m H_g (90 % confidence level)	Depth limit, m H_g (95 % confidence level)	Depth limit H_g(100 % confidence level)
1	14	26	48
2	28	52	96
3	42	78	144
4	56	104	192
5	70	130	240
6	84	156	288
7	98	182	336
8	112	208	384
9	126	234	432

It should be noted, that the estimated values of depth limits are higher, than those which have been usually taken for division of exploitation for shallow and deep (up today 80 metres in polish collieries). Performed analysis shows that new depth criteria should be determined, in accordance with values set in table 3. It should be pointed also, that exploitation depth limits which can be hazardous for the surface, depend on the thickness of coal extracted (primary void height) and should not be generalised. It's questionable, which confidence level should be taken in hazard assessment tasks.

From engineering point of view, the horizontal size of deformation is the most important in hazard assessment for structures. It characterizes the area of ground at which the foundation can loose support. The depth of ground displacement has a minor effect. The frequency plot showing the percentage of deformations and corresponding areas is shown on fig.17. It can be observed that near 50% of deformations, have the area lower than 10 m^2 (app. diameter equal to 3 m). Nevertheless, 95% level of confidence is met for the set of events, which area is less than 100 m^2 (approximate diameter 33 m).

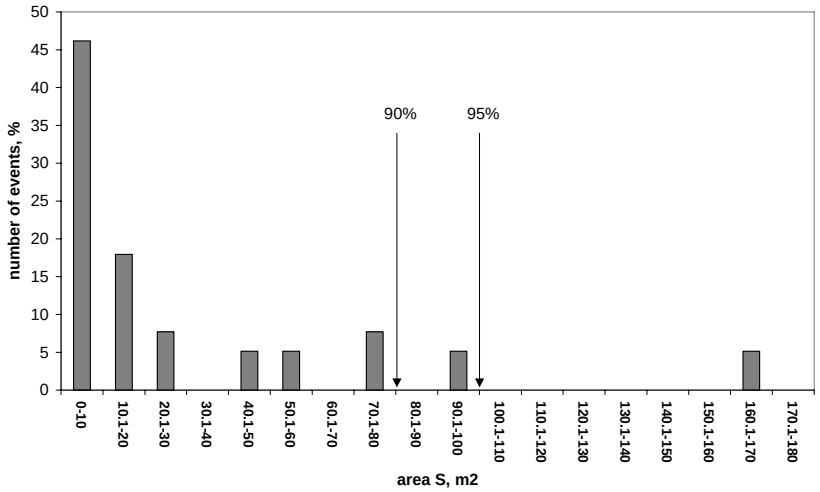


Fig.17. Plot between the percentage of events and area of deformations for the Siemianowice mine data set (arrows indicate the values of parameter for which percentage of events is 90 and 95 percent - confidence levels).

Tested data allow estimating the probability of sinkhole event occurrence within mine's area. The probability (p), that such incident will occur at any site of shallow exploitation, can be calculated from formula 7.

$$p = n_i \times \frac{a_i}{t \times a_c} \qquad (7)$$

Where:
p – probability,
n_i – number of incidents recorded (39),
t – time period (50 years),
a_i – area affected by one incident (32.5 m^2)
a_c – area of shallow exploitation (10 km^2).

In result of calculations we get, that probability of incident occurrence equals $p=2.5x10^{-3}$ *per annum*. The reference value for the whole area of shallow exploitation in the Upper Silesian Coal Basin (Poland) equals $p= 1.53\ x10^{-6}$ *per annum* [Kotyrba et al 2004]. The corresponding value for the South Wales Coalfield in United Kingdom is $1\ x\ 10^{-7}$ *per annum* [Statham and Scott, 1994]. This shows, how regional approach can give fictious results, when we deal with specific area (in studied case one mine area). High probability value for the "Siemianowice" mine area is due to geology of coalfield overburden. It is composed mostly of thick, competent sandstone layers (saddle beds), not suitable for defragmentation. That type conditions are characteristic for the northern part of the Upper Silesian Coal Basin.

7. General conclusions

Comparing theoretical solutions and experimental data presented in the study one can see that they fit only in rough range. This remark applies mainly to the possible void migration height. It is difficult to set a terminal value of depth below which the void would not create the sinkhole hazard to the surface. This is due to differences of modelled and real geological environments. Dynamic processes shape the equilibrium of geological strata in post mining period. Therefore, all geological and mining parameters, which derived from geomechanical, static model of mining void show weak correlation. Relatively low horizontal sizes of sinkholes can idicate that in post mining period, they have rather fissure than the void roof collapse origin. Neverthless, the analysis of data set allow to e the sinkhole hazard at the mine area in three degrees scale, on the base of void migration ability parameter (tab.4).

Table 4. Sinkhole hazard ranking at area of the "Siemianowice" mine.

Category	Hazard rank	Void migration ability parameter (H/w)
I	Low	> 20
II	Moderate	10 – 20
III	High	< 10

The sinkhole data set recorded in the "Siemianowice" mine area enables to assess the risk for structures in probabilistic terms. Performed study reveals that the hazard and related risk for structures located at mine area is higher than in the rest of Silesia Region. The value of probability equals $p=2.5x10^{-3}$ *event per annum* (whereas for whole Upper Silesian Coal Basin is equal to $1.53\ x10^{-6}$ *per annum*).

The study results order clear-sighted examination of post mining lands with voids ine bedrock. Procedures of examination should include a wide variety of data and "in situ" testing methods. Special attention should be given to neogenic rock movements and dynamic loads such as rainfall water circulation, seismic tremors and parasesimic vibrations.

7. References:

Buła Z., Kotas Z. (1994). *Geological Atlas of the Upper Silesian Coal Basin. Part III. The Structural, Geological Maps.* Polish Geological Institute. Warsaw.

Chudek M., Janusz W., Zych J. (1988). *The study of formation and prediction of discontinuous deformations due to subterranean mining*. Zeszyty Naukowe Politechniki Śląskiej, z. 141. Gliwice.

Janusz W., Jarosz A. (1979): *Discontinuous deformations of the surface due to shallow mining*. PAN. Oddział w Katowicach. Komisja Ochrony Terenów Górniczych.

Kotyrba A. Cumming E., Hole B., Martinez P., Onions K., Rollin C. (2004) *Assessment and Sustainable Reclamation of Mining Sites for Post Mining Use.* ECSC Project 7220-PR-095 Final Report. Brussels.

Kotyrba A. (2005) *Collapse sinks hazard and risk of the terrains of the Upper Silesian Coalfield.* Wiadomości Górnicze nr 7-8. Katowice, 348-358

Kwiatek J. (2002). *Building structures on mining lands.* Główny Instytut Górnictwa. Katowice.

Statham I., Scott M (1994)*: An analysis of drill and grout records from the South Wales Coalfield* Arup Geotechnics.

CONTRIBUTION TO IMPROVE PILLAR ANALYSIS IN ABANDONED ROOM AND PILLAR SATL MINES

LAOUAFA Farid, GHOREYCHI Mehdi

Institut National de l'Environnement Industriel et des RISques (INERIS), Parc technologique alata BP2, 60550 Verneuil-en Halatte, France ; farid.laouafa@ineris.fr ; mehdi.ghoreychi@ineris.fr.

ABSTRACT: The long-term behavior of old abandoned salt mine openings is an important question from a safety assessment viewpoint. For room and pillar mines, a simple is proposed method to improve the accuracy of the classical pillar stability analysis methods. The first part of this method deals with pillar behavior by taking into account the mechanical interactions "pillar-roof" and "pillar-floor". This is achieved by means of finite element computations. These computations allow to perform a substantial correction of the classical pillar's failure criterion. The comparison of results of various finite element analyses with those of real cases validated this method.

KEYWORDS : Salt mines, room and pillars, stability, finite elements, creep

RESUME : Le comportement à long terme d'anciennes exploitations de sel est une question primordiale du point de vue de la sécurité. Nous proposons une méthode simple pour l'analyse des mines de sel exploitées par la méthode des chambres et piliers abandonnés. La méthode prend en compte la contribution mécanique du sommet et de la base des. Au vu du caractère non homogène et non-linéaire du problème aux limites, l'objectif est atteint en ayant recours à la modélisation numérique. Les abaques issus de cette méthode permettent une correction significative de la sollicitation évaluée par la méthode de l'aire tributaire. La méthode proposée est validée par la comparaison de résultats issus de cette nouvelle méthode avec des mesures effectuées in-situ.

MOTS-CLEFS : Mines de sel, chambres et piliers, stabilité, éléments finis, fluage

1. Introduction

Several salt deposits in France were exploited using different methods (solution-mining, room and pillar mines, etc.). The depth of a salt deposit can be different from one site to another (several hundred meters). Many salt mines are more than one century old. After several decades of exploitation, many of salt's mines in France have been abandoned, leaving significant residual voids underground. The existence of such voids, with various sizes, raises the question of the long-term stability of those mines as well as their potential impact on safety of population and structures located on surface. This paper deals only with abandoned room and pillar salt mines.

Within the framework of geomechanical stability analysis of salt mines, "time" is a significant parameter since rock salt is characterised by a well-known strongly time-dependent behavior. The classical method used in order to assess pillars stability, in room and pillar mines, is usually based upon the *tributary area method*. From a safety viewpoint, this method is well appropriated when it is applied within a design framework. Nevertheless, its formulation is not accurate enough for checking or establishing the current stability of old abandoned room and pillar mines.
In fact, the formulation of this method is based on two major assumptions. The first one considers the overburden, whatever its mechanical features, as a simple dead load. The weight of overburden layers is so fully supported by the pillars. The second assumption, the one analysed in this paper,

deals with pillar-roof and pillar-floor interactions. In fact, the *tributary area method* considers perfectly smooth contacts, with no shear stress at the pillar's ends (contact surfaces).

In this paper the authors focus on the second assumption. The shear stresses acting at the ends of the pillar are in general not negligible. They can in fact increase significantly the strength or the stability of the pillar by reducing deviatoric stresses, regarding plasticity framework, and decrease the creep strain, in a viscoplastic framework. The value of deviatoric stress strongly depends on the geometry of the pillar, more exactly, on the slenderness ratio (λ). This one is defined as the ratio of the height H of the pillar over its width L : $\lambda = H / L$.

One could easily bypass these two major assumptions by performing a numerical computation of such mechanical problems (finite element computation for instance). Unfortunately, the geometrical sizes of a mine and its mechanical history are such, as it becomes almost impossible to perform an accurate numerical modelling of the overall problem. In order to improve, the *tributary area method*, we propose a simple method to correct the classical method through factors identified numerically on a single pillar. These correcting factors take into account the interaction between pillar and roof and pillar and floor. This method is developed in the case of plasticity and also in the case of viscoplasticity by taking creep into account.

When taking into account the shear strength acting at pillar boundaries, it is observed that the reduction factors are non-linear functions of slenderness ratio. Several numerical computations have been performed for different slenderness ratio, material parameters and loading cases. The validity of this method was checked successfully by comparing results of various finite element analyses with data related to real cases.

2. Current method for assessing salt mine pillar stability

This section is devoted to a brief description of the classical *tributary area method* and its main assumptions.

We suppose, for sake of simplicity, that the strata layers and the mine are horizontal. Under this assumption, the *tributary area method* states that the stress acting in the pillar is:

- Homogeneous $\underline{\underline{\sigma}}(x, y, z) = \underline{\underline{\sigma}}, \forall (x, y, z) \in \Omega_{pillar} \subset \mathbf{R}^3$,

- The second order Cauchy stress tensor is completely defined by only a single component:

$$\boldsymbol{\sigma} = \begin{pmatrix} \sigma_{xx} & \sigma_{xy} & \sigma_{xz} \\ \sigma_{xy} & \sigma_{yy} & \sigma_{yz} \\ \sigma_{xz} & \sigma_{yz} & \sigma_{zz} \end{pmatrix} = \begin{pmatrix} 0 & 0 & 0 \\ 0 & 0 & 0 \\ 0 & 0 & \sigma_z \end{pmatrix}$$

The value of the stress component σ_z depends on the thickness of the overburden layers and the extraction ratio (τ) which is classically defined as follows:

$$\tau = 1 - \frac{(Lp)^2}{(Lp + w)^2} \tag{1}$$

where Lp and w are respectively the widths of the pillar and of the room. The overburden thickness

H_r is a purely weighing stratum (dead load). Under these considerations, the averaged vertical stress σ_z is then equal to:

$$\sigma_z = \sigma_{TAM} = \frac{\gamma H_r}{1-\tau}, \tag{2}$$

Where γ is the specific weight of the overburden. Let us call σ_{TAM} this vertical stress defined by the Tributary Area Method. In stability analysis framework, currently, the averaged stress σ_{TAM} is compared with the uniaxial compression strength Rc, which is expressed in the framework of a Mohr-Coulomb failure criterion as follows:

$$Rc = \frac{2C\cos(\phi)}{1-\sin(\phi)} \tag{3}$$

C is the cohesion and ϕ the angle of internal friction of the pillar material.

3. Factors of correction of the classical method for assessing stability of salt mines pillars

In the short description of the Tributary Area Method below, one can note that neither the contribution of the roof nor the pillar form are taken into account in the expression. The mechanical contribution of the overburden is very difficult to measure. It depends on several geometrical and mechanical parameters such as, geometry of the exploitation, the geomechanical characteristics of the overburden, the history of the exploitation (phases of extraction) etc. The ends of pillars are assumed with no shear stress and no kimenatical constrains (acting or prescribed).

In order to improve, the tributary area method, we propose to apply a multiplying correction factor to the averaged stress σ_{TAM}, as follows:

$$\bar{\sigma} = C_{RE} \times C_P \times \sigma_{TAM} \tag{4}$$

In this expression C_{RE} is a factor, which takes into account the mechanical contribution of the overburden. The value of the coefficient $C_P \leq 1$ expresses the mechanical contribution of the pillar shear acting on its ends, leading to a confining pressure (in average). The first factor C_{RE} deals with the intensity of the loading applied to the pillar. It can be considered as a *loading factor*. The second factor C_P is linked to the *structural* pillar strength. It can be considered as a *strength factor*.

The expression (4) is more explicit when written as follows:

$$\bar{\sigma} = C_P \times \left(C_{RE} \times \sigma_{TAM}\right) \tag{5}$$

Since C_P and C_{RE} are known, in order to assess stability of the pillar or to perform a creep analysis of the pillar, σ_{TAM} will be substituted by $\bar{\sigma}$.

We suppose in the following development that $C_{RE} = 1$.
The factor C_P is determined numerically using finite element computations. This is principally due to the difficulty to express analytically the solution of such non homogeneous IBV (initial non-linear boundary value) problems.

4. Definition and values of C_P : assumptions and methods

The figure below shows a schematic representation of a typical room and pillars mining: pillar, rooms, floor, roof and overburden.

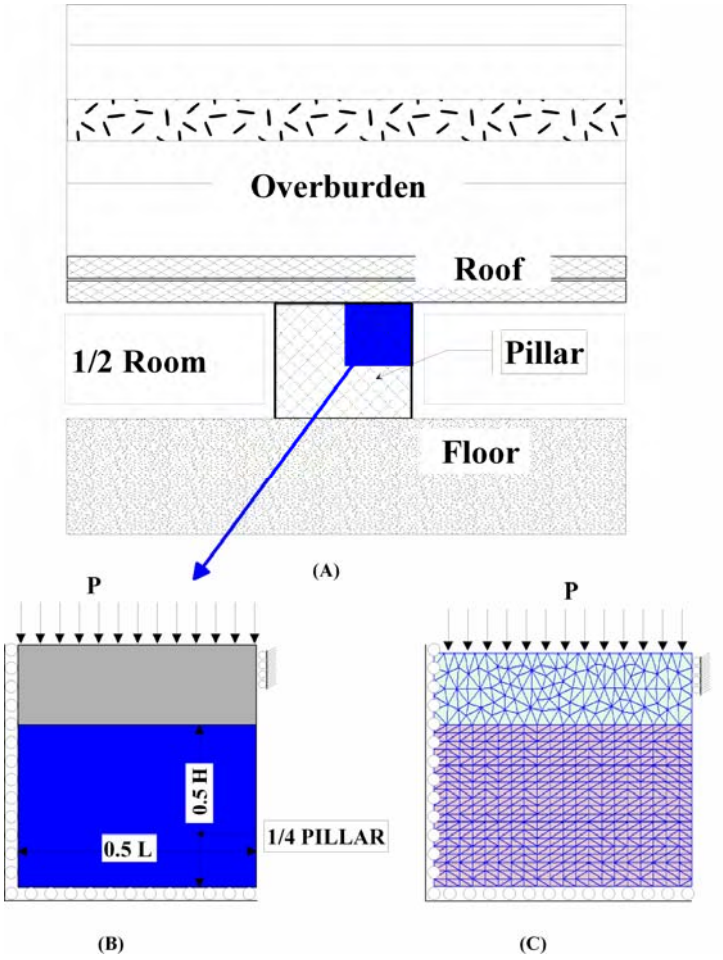


Figure 1. Schematic plan of the pillar and the overburden (A), geometric model (B), finite elements model (C).

Finite element analysis is performed in axisymmetric condition. The width of the pillar corresponds then to the diameter of the model. We assume also the existence of a symmetric plane perpendicular to the pillar. Thus only ¼ of the pillar is modelled. An elastic domain with variable Young modulus (Figure 1C) replaces the overburden. A *dead load P* is applied on the top. The boundary conditions are also shown in Figure 1C. Since basically the pillar behaviour view is considered, roof and floor have been supposed to be stable.

4.1. Elastoplatic analysis

In an elastoplastic analysis framework, the load *P* is increased smoothly until the failure of the pillar is reached. The pillar failure criterion is then defined by the lost of convergence of the iterative process used in order to solve the non-linear problem. $\bar{P}$ is called the load leading to failure of the pillar. It is to be noticed that, in this present approach, no bifurcation analysis as defined by Rice (1974) or Hill (1958) was performed. In plasticity, a Mohr-Coulomb model is used to describe the local failure criterion.

When the pillar failure is reached, C_P is defined as follows:

$$C_P\left(\phi,C,E,\nu,\lambda\right)=\frac{Rc}{\bar{P}} \text{ with } \lambda=\frac{H}{L} \tag{6}$$

In elastoplastic analysis, the factor $C_P(\phi,C,E,\nu,\lambda)$ should depend on friction angle ϕ, cohesion *C*, Young modulus *E*, Poisson's ratio ν and slenderness ration λ of the pillar. Many finite element computations have been performed, and the parametric analysis performed through these computations concluded that C_P is mainly function of λ and ϕ. In other words, for a pillar with fixed ends (no slide at the interfaces), $C_P \equiv C_P(\phi,\lambda)$.

4.2. Elasto-vicoplastic or creep analysis

This study deals with salt mine pillars. Among different constitutive models of salt (Cristescu & Hunsche, 1991,1998), we choose the Lemaitre power-law model (Lemaitre,1988) expressed in rate form as follows:

$$\frac{\partial \boldsymbol{\varepsilon}^{vp}}{\partial t}=Ae^{\left(\frac{-B}{T}\right)}\left(\frac{\sigma_{eq}}{\sigma_0}\right)^{\boldsymbol{n}}\left(\varepsilon_{eq}^{vp}\right)^{\boldsymbol{m}}\frac{\partial\sigma_{eq}}{\partial\boldsymbol{\sigma}} \tag{7}$$

Where $\boldsymbol{\varepsilon}^{vp}$ is the second order vicosplastic strain tensor, $\boldsymbol{\sigma}$ the Cauchy stress tensor , σ_{eq} the Von Mises equivalent stress ($\sigma_{eq}=\sqrt{\frac{3}{2}\boldsymbol{s}:\boldsymbol{s}}$) where $\boldsymbol{s}$ is the deviatoric stress tensor $\left(\boldsymbol{s}=\boldsymbol{\sigma}-\frac{tr(\boldsymbol{\sigma})}{3}\mathbf{I}\right)$. The hardening parameter is the equivalent viscoplastic strain defined as $\varepsilon_{eq}^{vp}\left(\varepsilon_{eq}^{vp}=\sqrt{\frac{2}{3}\boldsymbol{\varepsilon}^{vp}:\boldsymbol{\varepsilon}^{vp}}\right)$. σ_0 is the reference stress value (1 MPa), and, finally, T is the temperature in Kelvin. In the finite code VIPLEF, used in our study and in the following development, the model will be rewritten as follows (1-D case) :

$$\varepsilon^{vp}=10^{-6}\left(\frac{\sigma_{eq}}{K}\right)^{\beta}t^{\alpha},\quad\left[\frac{m}{m}\right] \tag{8}$$

The authors emphasize on the fact that choosing the over-mentioned constutive model, one can easily get the well-known Norton law for wich $\alpha=1$ or *m*=0. This is why, in this study we preferred to use the general expression rather than the specific case of Norton law which is very common for salt.

In presence of viscosity, the mechanical problem becomes obviously a time-dependent or rate depend problem. The corrected value of the average vertical stress σ_{TAM} leads to the following scalar equation:

$$\varepsilon=\frac{CV}{H}=\varepsilon=\varepsilon^{e}+\varepsilon^{vp}=\frac{C_{RE}C_P\sigma_{AT}}{E}+\left(\frac{C_{RE}C_P\sigma_{AT}}{K}\right)^{\beta}t^{\alpha} \tag{9}$$

Where CV is the floor-roof closure, and ε the averaged axial or vertical strain.

The expression of C_P does also depend on several parameters such $C_P=f\left(E,\nu,\lambda,\alpha,\beta,K,t\right)$. Many finite element computations have also been performed in this case. The parametric analysis performed

through these computations concluded that C_P is only function of λ and t, in other words $C_P = C_P(\lambda,t)$, at short term and C_P is only function of λ at long term. In fact, C_P quickly reaches an asymptotic value. The value of $C_P(\lambda,t)$, for a given pillar geometry defined by λ and at a given time t_n, is the solution of the following non-linear scalar equation:

$$\frac{C_P(t_n,\lambda)\sigma_{AT}}{E} + \left(C_P(t_n,\lambda)\right)^{\beta}\left(\frac{\sigma_{AT}}{K}\right)^{\beta} t_n^{\alpha} - \bar{\varepsilon}(t_n) = 0 \qquad (10)$$

5. Factors of correction

The figures below shows the finite element computation of C_P both, in the cases of a creep and plasticity analyses.

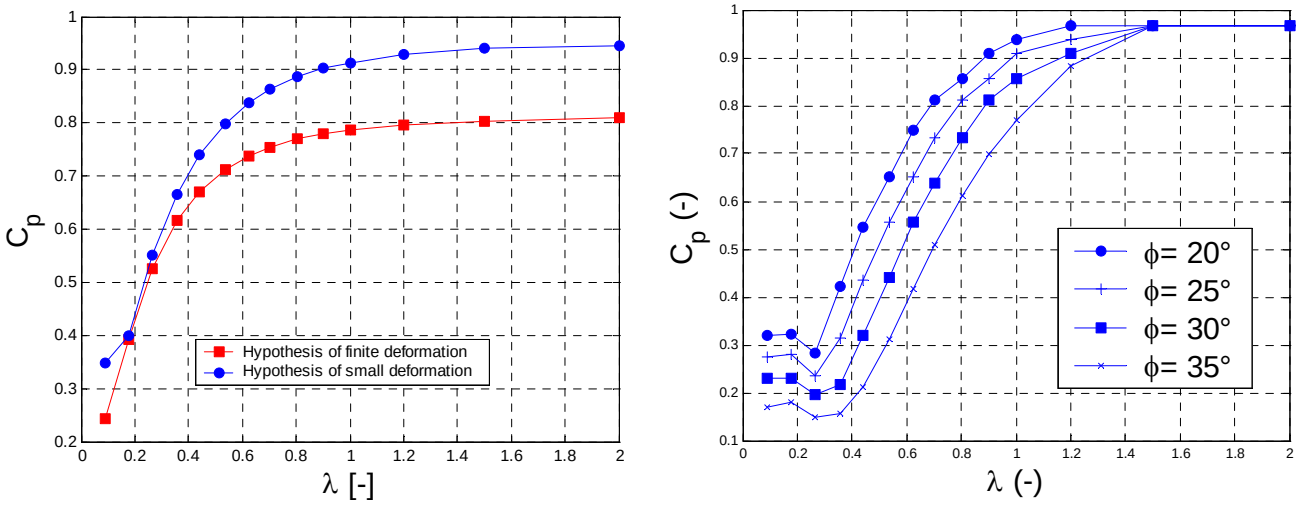


Figure 2. Factor of correction C_P for creep analysis (left) and plastic analysis (right).

One can notice the strong influence of the slenderness ratio λ on C_P and also its dependence on the friction angle ϕ. This last contribution is naturally linked to the fact that the shear stress acting on the boundaries of the pillar generates a non homogeneous confining pressure inside the pillar, and thus it will move out the average stress state far from the Mohr-Coulomb failure plane.

6. Example of application in case of salt pillars creep

This example deals with a real case of a salt mine exploited by room and pillars method. This mine is located in the East of France. The pillar height is 4.5 meters and the extraction ratio τ is equal to 75%. A part of the mine of about 110 years old: this is located at about 135 m deep. In this area the pillars are of square section of 10 by 10 meters. A thick salt layer has been left in the roof. The second part of the mine of about 70 years old is located at about 143 m of depth. In this area the pillars are of square section of 15 by 15 meters. A thick salt layer has been also left in the roof. Two analyses were performed in order to describe evolution of the axial (vertical) *averaged* pillar strain

(deformation).

The first one used finite element analysis (Fig. 3)

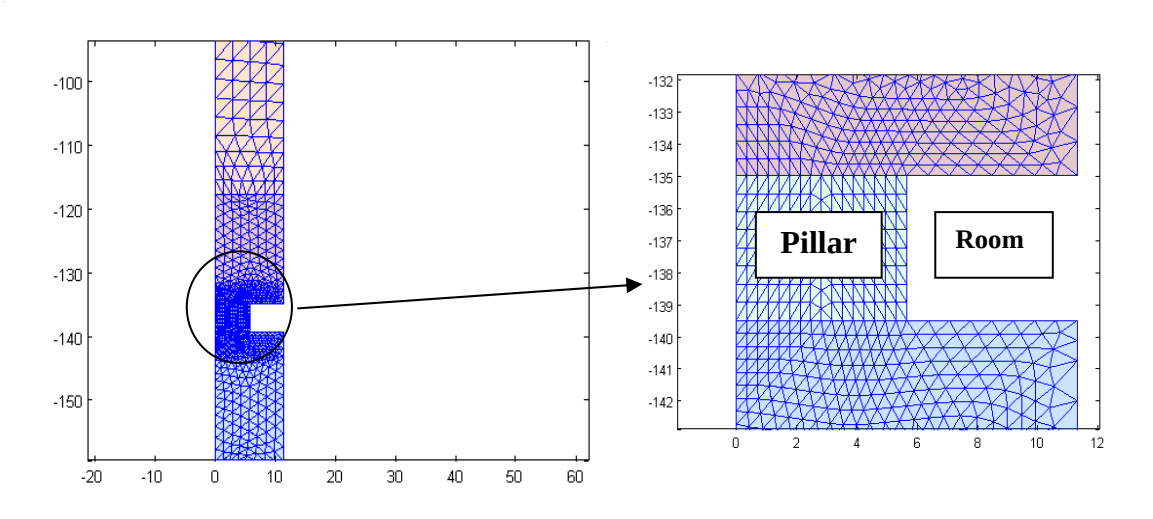


Figure 3. Finite element mesh of the mine (pillar-roof-room, left-hand) and detail of the pillar mesh (right-hand).

The second computation used the corrected method described below. The comparsion of the résults are shown in Figures 4 and 5.

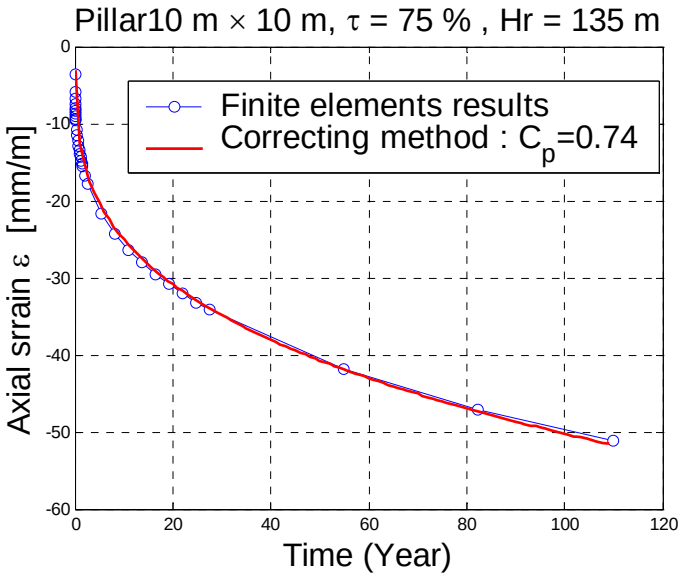


Figure 4. Comparison of the result obtained with finite element computation and the proposed correcting method.

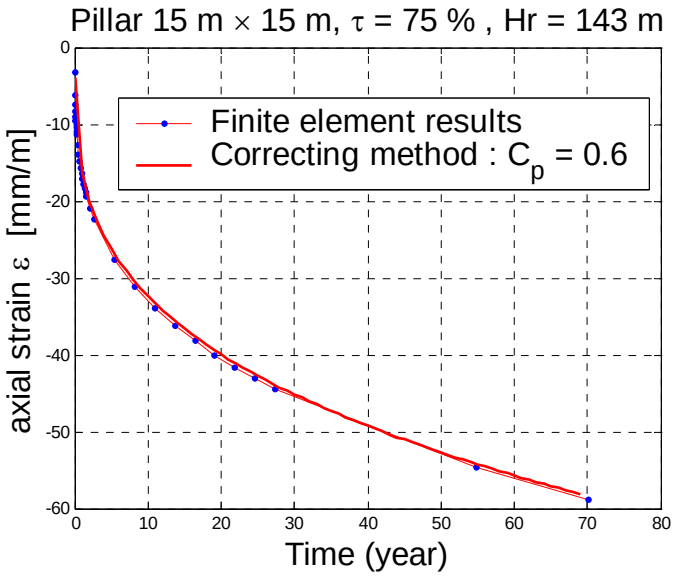


Figure 5. Comparison of the result obtained with finite element computation and the proposed correcting method.

One can realise that, through the simple analytical method proposed above, the results are almost the same as those obtained using a complex finite element modelling. The current strain rates, measured in situ, are the following: 0.148 mm/m/year for the first case and 0.214 mm/m/year for the second case. With the factor of correction and using tributary area method we obtain: 0.142 mm/m/year for the first case and 0.252 mm/m/year in the second one. Indeed the suggested method fits quite well with field data.

7. Conclusion

The results presented above show up clearly that for the purpose of long term analysis of room an pillar salt mines, both mechanical stability and time-dependent displacement of the pillars can easily be evaluated using the suggested method. This method has been elaborated by a series of finite element computations in elastoplasticity (pillar stability) and in viscoplasticity (pillar creep). The results allowed to express correcting factors than can be used together with the classical tributary area method.

The suggested method has been validated by data from real salt mines. It can be applied successfully to room and pillar salt mines without any complicated numerical computations (F.E. method). Nevertheless, the results are very accurate and the method is very easy to use.

In this study, the overburden is assumed as a dead load applied to the pillars. The mechanical contribution of an overburden containing stiff layers requires further studies leading to a complementary correcting factor.

8. References

Cristescu N., Hunsche U. (1991), A constitutive equation for salt, 7th Int. Cong. Rock Mech., Aachen, Sept. 16-20, Balkema.

Cristescu N., Hunsche U. (1998), Time effects in Rock Mechanics, Wiley.

Ghoreychi M.(1990) Conséquences du comportement thermomécanique du sel pour la conception et la sûreté d'un enfouissement de déchets radioactifs. Stockage en Souterrain, Presses des Ponts et Chaussées, 229-243.

Ghoreychi M., Daupley X. (2003). Devenir à long terme d'exploitations abandonnés de sel. Revue Française de Géotechnique, Vol. 106-107, 73-83.

Hill R. (1958). A general theory of uniqueness and stability in elastic-plastic solids. J. of Mech. and Phys. of solids, 6:239-249.

Lemaitre J., Chaboche (1988) J.L. Mécanique des matériaux solides. Dunod, Paris.

Rice J.R. (1974). The localisation of plastic deformation. Theoretical and applied mechanics, W.T. Koiter ed, North Holland, 207-220.

BROOKS UNDER COLLIERY HEAPS IN THE WALLOON REGION

LARDINOIS Jean-Pierre [1], FLAMION Bruno[2], Yves ZECH[3].

[1.] Ingénieur, IGRETEC, Boulevard Mayence, 1, 6000 Charleroi – Belgique. jean-pierre.lardinois@igretec.com.
[2] Ingénieur des mines et géologie, Direction générale des Ressources naturelles et de l'Environnement. Direction des Eaux souterraines, Avenue Prince de Liège, 15 – 5100 Jambes – Belgique. b.flamion@mrw.wallonie.be
[3] Professeur, Université catholique de Louvain, Unité de Génie civil, Place du Levant, 1 – 1348 Louvain-La-Neuve, zech@gce.ucl.ac.be

ABSTRACT: Several studies are presently under progress in the Walloon Region so as to assess the long term environmental impact caused by the closing of coal mines. Among the effects on water resources management, mining wastes deposits in the major bed of small rivers becomes a concern since the lack of maintenance of the works leads to difficulties of drainage in period of storm and to situations at risk for the vicinity. A first characterization carried out by the IGRETEC at the request of the Walloon Region leads to the selection of nine spoil heaps for more detailed investigations. The purpose is to update the administrative data by establishing the profile and cross sections of the works, to collect hydrological data and to evaluate measures to be proposed according to the risks and to the dimensioning of the works. The in situ investigations called upon specialized speleologists and the use of video cameras.

KEY-WORDS: mines- environmental impact – guttered brooks - floods- spoil heaps.

RESUME: Plusieurs études sont actuellement en cours en Région wallonne afin d'étudier l'incidence environnementale de l'arrêt de l'exploitation des mines de charbon. Parmi les conséquences sur la gestion des eaux figure le dépôt des déchets miniers dans le lit majeur de cours d'eau préalablement mis sous pertuis. Cette pratique était particulièrement courante dans le bassin minier de Charleroi, où une vingtaine de terrils recouvrant près de six kilomètres de voûtements ont été répertoriés. L'absence d'entretien des ouvrages conduit à des difficultés d'évacuation des eaux en période d'orage et à des situations à risque pour le voisinage. A l'issue d'une première caractérisation menée par l'IGRETEC à la demande de la Région wallonne, neuf sites ont été sélectionnés en vue d'investigations plus détaillées. Il s'agit notamment d'effectuer un relevé précis des voûtements afin d'établir les profils en long et en travers des ouvrages en vue de déterminer leurs paramètres (ou capacités) hydrauliques. En fonction des données hydrologiques du site, le dimensionnement des ouvrages est vérifié et les risques d'obstruction évalués afin de définir les mesures à prendre pour éviter des inondations en amont. Les investigations in situ ont fait appel à des spéléologues spécialisés et à l'utilisation de caméras vidéo et de matériel antidéflagrant.

MOTS-CLEFS : mines – incidence environnementale – ruisseaux canalisés - inondations – terrils.

1. Review and links between mines heaps and river management

1.1. Consequences of Mine closure on water management in the Walloon Region

Since a few years, the Walloon Region has undertaken various studies about the consequences of After mine on water management. These studies could be born thanks to the "Comité wallon de démergement", scientific committee created in 1927 in order to advise the studies and supervise works undertaken in order to prevent the floods in land subsidence area due to mining activities, works having taken the name of "démergement" in the Walloon Region.

The first concerns were devoted to the troubles related to water table rebound following the stop of the drainage of coal mines (ARNOULD and FLAMION, 2003). Although various spoil heaps slides had occurred and retained attention because of the determining part played by water, it is only some years ago that the need for a general study relating to the links between heaps and small rivers management has emerged, more particularly in the dewatering zone of CHARLEROI.

1.2. Inventory of the situations at risk related to the spoil heaps in CHARLEROI area

In the area of CHARLEROI, the spoil heaps made up of the residues of the mining activity modified appreciably not only the landscape but also the natural hydrographic network.

Indeed, by easiness, local coal industry has, as of the surroundings of 1850, filled by its waste numbers talwegs and valleys of small tributaries of Sambre river.

In order not to deviate or alter the brooks pathway, those were channelled and arched before being covered by the heaps.

At the time of coal mines closure, which spread out essentially between 1960 and 1982, the management of the works and their maintenance hitherto ensured by the coal companies, stopped. The responsibility fell very often with the communes lacking the necessary means or owners little concerned about assuming their responsibility.

By wear, loss of stability, lack of maintenance or repair, the arched brooks ("voûtements") subside, or even break down, making obstacle to the flow continuity and being likely to cause obstructions and then floods upstream, they were even source of heap instability, as described by the guide of the holders of colliery heap (PAQUETTE et LAVERSSANE, 2003).

The communal and inter-commune authorities are facing many complaints which need to be adressed. Because of its competences as regards floods mitigation in zone of mining subsidence, the IGRETEC (Association of communes of CHARLEROI and surroundings working in particular in the fields of sanitation and regional planning) was charged by the Walloon Region and the concerned communes to carry out an inventory of the brooks channelled under spoil heaps.

At the end of this mission carried out in 2002, twenty one heaps covering channelled brooks were identified, the conduits having a total length of approximately six kilometers (LARDINOIS, 2003).

This preliminary study also made it possible to determine the catchment area (S) of the various brooks as well as, in a rudimentary way, the average runoff coefficient (φ). The stormflow to be evacuated by the arched brooks could thus be calculated on the basis of the simplified formula: $Q = \psi \varphi A S$ (where A = 172 l/s ha and $\psi = 0,75$).

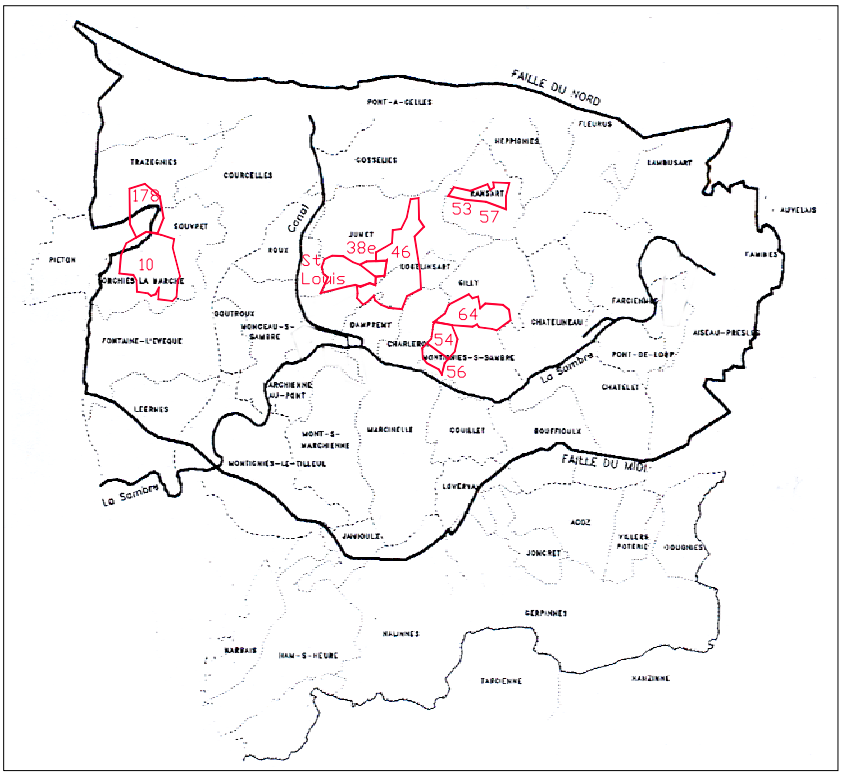
Knowing the apparent section and the slope of the brooks, the easily flooded zones observed on the ground could then be explained by collapses or contracted sections, not visible without further inspection.

Nine sites requiring prior complementary investigations were thus identified by the scientific Committee in charge of the evaluation of the results.

2. Liability and study of the prior hazardous zones

After an examination of the regulatory aspects of the situation, the Walloon Region agreed to finance a study for the prior areas. It was a question to allow the IGRETEC:

- to map the risks;
- to carry out in situ surveys ;
- to set up devices for hydrological monitoring;
- to define guidelines for an integrated management.



Map 1. Dewatering area of CHARLEROI and catchments of priority arched brooks (no scale).

2.1. Regulatory aspects to take into account

With regard to the preliminary legal aspects, two questions arose first of all: on one hand what was the responsibility for the Walloon Region, on the other hand what were the authorizations required to undertake the in situ work investigations.

With the first question, it was clearly answered that, within the framework of the legislation on the nonnavigable rivers, the responsibility falls to the owner or to the guardian of the work set up on the river, the duty of the Public Authority being to take care to ensure the water run-off of the river concerned, and, if the need arises, to enforce the urgent works at its own expenses, with later recovery for the costs.

In the current state of the Walloon legislation, the only public authorities entitled to intervene on the brooks listed by the IGRETEC are the Province and the communes.

It has to be mentioned that, with regard to the mining law, spoil heaps are not anymore considered to be part of the colliery. Except when they were the subject to a valorization grant, these heaps are ordinary private properties not subjected to administrative monitoring, except what is said in article

74 of the mining laws with regard to the power to be exerted by the mining engineers for the conservation of the buildings and the safety of the ground.

With the second question, it results from what precedes that the access to the heap must be obtained in theory from their owner and occupants, as for any private ground. However, for the small rivers involved, the commune or the Province according to the importance of the water course, benefits from a right of access to exert the monitoring, right of access of which they can make profit to the IGRETEC.

The study was thus considered to be essential to allow the Walloon Region and the communes to advise and if necessary to enforce the measures to be taken by the private owners in charge to limit the risks and harmful effects related to the possible breakdown of the arched brooks (floods, heaps slide).

2.2. Aims of the study

The study covers the dewatering zone of CHARLEROI and extends to the catchment areas from the brooks listed in chart 1 below.

Chart 1. Priority list of channelled brooks under spoil heaps.

IGRETEC reference	*Lenght of the arched brook*	*Commune*	*Spoil Heap Name*	*Responsible of the brook management*
21	510 m	FONTAINE-L'EVÊQUE (Forchies-La-Marche)	N° 10 Les Bans	Province du Hainaut
11	200 m	CHARLEROI (Montignies sur Sambre)	N° 54 Résolu	Private owner
12	460 m	CHARLEROI (Montignies sur Sambre)	N° 56 Résolu n°2	Private owner
4	360 m	CHARLEROI (Gilly) /CHÂTELET (Châtelet)	N° 64 Les Viviers	Province du Hainaut
14 15	370 m	CHARLEROI (Ransart)	N°53 La Flanière N°57 St-Charles	Private owner / Ville de CHARLEROI
7	320 m	CHARLEROI (Gosselies et Jumet)	Fosse St-Louis	Province du Hainaut / Ville de CHARLEROI
8	420 m	CHARLEROI (Lodelinsart)	N° 46 Sacré Français	Province du Hainaut
6	330 m	CHARLEROI (Jumet)	N° 38e Bois de la Coupe	Ville de CHARLEROI
19	650 m	COURCELLES (Trazegnies)	N° 178 Terril n° 5	Private owner

The studied area includes the communes of CHARLEROI, CHÂTELET, COURCELLES, FARCIENNES and FONTAINE-l'EVEQUE. Its delimitation is shown in red on map 1 above.

The purpose of the study comprises in particular the cartography of the affected zones, the determination of the causes of the floods and if possible the installation of hydrologic networks, the description of the works conditions based on in situ investigations, the evaluation of the inherent risks due to the floods, proposals of guidelines for technical solutions taking into account the hydrological, social, environmental and economic aspects including, if necessary, a comparison between various possible solutions (rehabilitation of the arches; putting back of the brooks to the open sky; construction of storm basins...).

The purpose of the mission entrusted to the IGRETEC is primarily to help the managers of the rivers and the communes to bring solutions to problems of safety badly encountered by the residents, being of course that the Walloon Region does not take any responsibility in the realization of work possibly necessary.

The study began on December 1, 2003 and should enclose at the beginning of 2006. Some results can already be presented.

3. Preliminary results of the study

3.1. Risk mapping

The potentially flooded zones upstream of the heaps were mapped by first of all simulating an obstruction inside the arched brooks, then by determining the flooded zone and the new pathway of water according to the most recent and most reliable digitized topographic data (data of the Walloon Ministry of Equipment and Transport), finally while carrying out the field checks with the topographers.

No analysis was still carried out to represent the sliding risks of the heaps in the event of obstruction of the drains under it (creep rupture of the supporting soils saturated with water or rupture by plasticization of materials of the deposit subjected to wetting cycles).

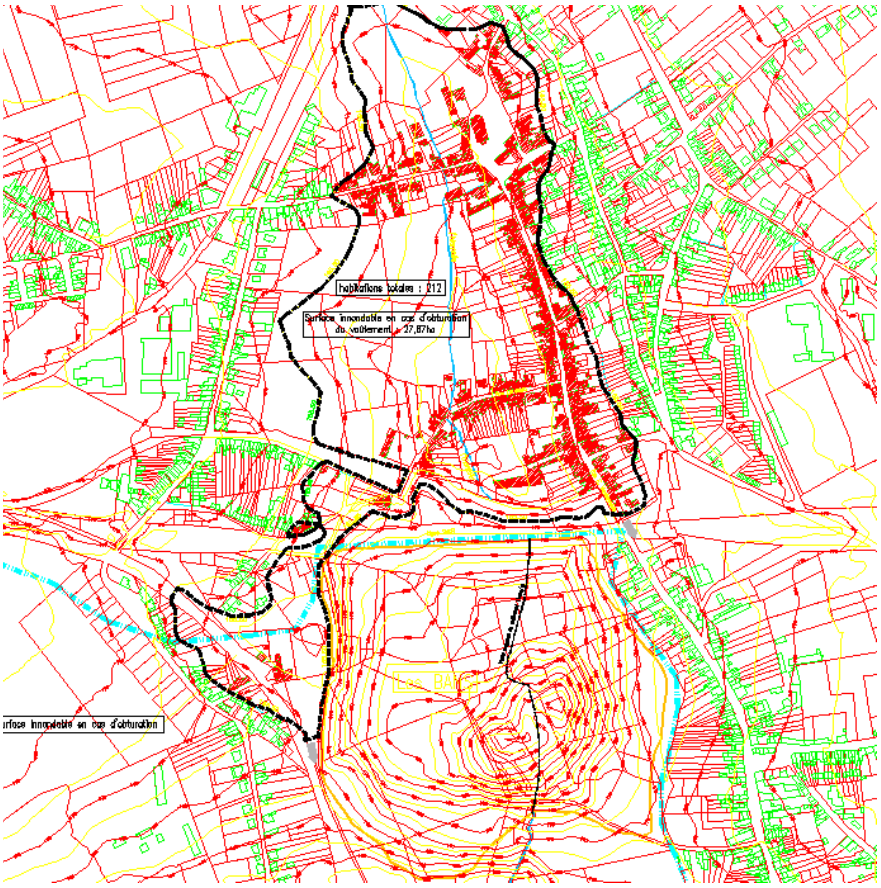
The zone most affected in terms of number of inhabitants is that of Forchies-La-Marche, with 212 houses included in the potentially flooded zone (map 2). The majority of the houses being relatively close to the spoil heap, the risks remain significant (photograph 1).

The field investigations show that in certain cases (Bois-de-la-Coupe; Viviers) the floods are due to the water rising through the sewers.

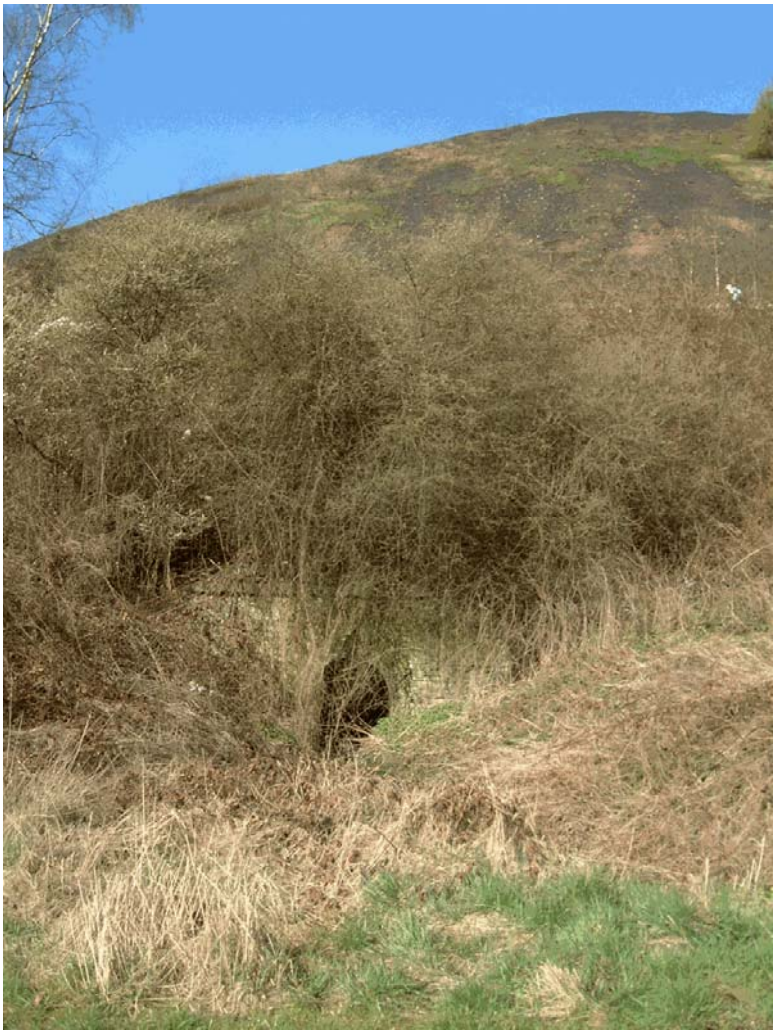


Photograph 1. Flooded area near spoil heap "Les Bans" (FONTAINE-L'EVÊQUE Forchies-La-Marche).

Elsewhere, the number of dwellings is rather low, but the situation is alarming because of the vicinity of the dwellings and the heap (seven houses in Saint-Charles at Ransart, spoil heap in addition in combustion: photograph 2).



Map 2. Flooded area in case of obstruction at "Les Bans" (FONTAINE-L'EVÊQUE Forchies-La-Marche)..



Photograph 2. Downstream "St-Charles" spoil heap in combustion near dwellings at CHARLEROI (Ransart).

3.2. Pluviographic data at short time step

Only the data of two permanent recording rain-gauges (IRM recording rain-gauge at Gosselies airport and SETHY recording rain-gauge at Monceau lock) are available to determine the project rains and to analyze the behaviour of the brooks catchments.

Two additional recording rain-gauges were thus established. The comparison of the Intensity Duration curves shows significant differences between the various recording rain-gauges, probably because of the orographical effect (proximity of the heap; effect of valley).

Taking into account the recording mode, the time step available to gather the data (10 minutes) is not entirely satisfactory in order to draw up for the future the curves Intensity-Duration-Frequency valid for small catchments (less than 200 ha).

In the framework of the study, the possibility of gathering data with a short time step was thus investigated, trough tipping bucket recording rain-gauges with readings every two minutes.

For various reasons (difficulty in complying with the rules of placement of the recording rain-gauges; availability of the material) this wish could not be concretised and the installation of a network of recording rain-gauges adapted to urban hydrology remains a challenge for the Administration and the organizations in charge of sanitation in the Walloon Region.

3.3. Flow meters

Within the framework of the study, each brooks has been equipped with a flowmeter, its location being strongly dependant of accessibility constraints. At "Terril N° 5" for example, there is a marsh upstream (photograph 3). In order to check the good choice of location of the probes of measurement, the longitudinal and cross-section measurement profiles were drawn up and the measurement sections were checked before to fulfill the calibration curves.



Photograph 3. Marsh upstream "terril N°5" at COURCELLES (Trazegnies).

Collected data are now being processed.

3.4. In situ investigations methodology

One of the most important result of the study was the realisation of in situ investigations based on a methodology and terms and conditions outlined in the general and special specifications prepared for the call for tenders to carry out the work under extremely particular conditions.

Seven "voûtements" arched galleries of an overall length of almost 3500 m were selected to be the subject of the inspections.

Taking into account the problems of safety in confined space (lack of oxygen, explosion and/or fire hazard, risks of intoxication and brutal rise in the temperature), all measures were enforced to carry out work in full safety:

- experienced personnel (of which a first-aid worker and a foreman) and equipped (gas-detector in particular);
- personnel in a sufficient number and well distributed: a person remaining outside to take part in the security of the operations, a team of two men for the beaconing and of cleaning or clearing

out work necessary to the passage of the camera or the personnel in charge of the description of the"voûtement" and a team of two men for the land surveys and the photographs.

Work consisted in:

- taking all measurements to make safe the access to the works being primarily in roadway system;
- taking photograph in order to illustrate degradations and anomalies (section and changes of slope, cracks, breaks, perforations, erosions, obstructions...) and locating the pictures in cumulated and orientation, at a rate of at least a photograph every 20 meters (3 million pixels, minimum, for A4 prints)
- carrying out underwater picture if required when the water level is too important;
- measuring the length of the work and to locate in cumulated all degradations and anomalies;
- recording the levels and the orientations every 20 meters minimum and to establish of them the sights in plans, longitudinal and cross section profiles;
- sending a camera on carriage or "raft" in the inaccessible parts by the team, according to possibilities.

For each arched gallery, a video tape (numerical color) of approximately an hour was carried out, a synthesis being also prepared to illustrate the present paper.

4. Results of the in situ investigations and first conclusions

4.1. In situ investigations

A first inspection took place on September 16, 2004 at Forchies-La-Marche.

The results made it possible to validate the methodology, while bringing some little adaptations in order to better hold account of the field realities (painted marks on the arches for filming identifications; adaptation of the number of photoshots according to the constraints of batteries lighting; improvement of the waterproofing of the apparatuses).

The arches under the heap "the Bans" obviously were carried out progressively with the erection of the heap, the central part being the oldest and the most deteriorated.

There are many changes of section, without relationship to the requirements of water flow. The materials and the modes of realization vary and the junctions are very often badly carried out.

Settlements due to undermining operations and concretion formations (hardness of the underground water: 44°F) could be located (photograph 4). There is no more no maintenance, in particular for the metal parts.



Photograph 4 concretion formations and partial obstruction of Ernelles brooks under spoil heap "Les Bans" (FONTAINE-L'EVÊQUE Forchies-La-Marche).

The closing of the topographic data is good after 600 meters with the electronic compass (9 m into horizontal and 0,6 m into vertical). The roughness of the various sections could be estimated.

Counterslopes due to soil subsidence and hydraulic problems (obstructions; shrinkages) sounded out at the time of the inventory thus could be specified. The results were synthesized in a file established for each site and comprising photographic statements.

The logistic support brought by firm DEBACKRE and URGYAN proved to be excellent. These visits were however particularly tough. Important problems (temperature higher than 60°C and dangerous atmosphere) were encountered at the St-Charles, requiring the venting of the principal galery. The visit shows that the upstream of the arch inside of the St-Charles was voluntarily blocked, not preventing however water from cutting through a path through masonry.

In Ransart, the inspection has to be done by the downstream because of an obstruction.

With the Vivier, the visit was stopped upstream by the total coal dust plugging and downstream because of the insufficiency of oxygen and the coal dust plugging, of unspecified origin in absence of physicochemical analysis.

4.2. First conclusions

In a general way, the state of the works does not assure for the future. This situation challenges. The in situ investigations show that the absence of maintenance is seldomly the only cause of the bad flow, which is also due to the design of works carried out at various periods and to the location of these works. Indeed, the investigations showed:

- changes of hydraulic parameters caused by the variations of the sections and the diversity of the principles of construction;
- destruction of the works by general outdatedness (corrosion of the steel structure) or by ground pushing on the walls.

With regard to the preventive and corrective measures which are essential, the recommendations of PAQUETTE and LAVERSSANE (op. cit.) should inspire the Public Authorities concerned so:

- to impose prohibitions to build in the zones at the risk;
- to avoid the proofings in slope stake;

- to regularly control the existing conduits under heaps in order to carry out necessary repairs.

The proposals for an improvement of the voûtements should however not be carried out if there is a possible alternative, so as to deviate the brook.

5. Perspectives

These problems of arched brooks (voûtements) are not limited with collieries heaps, because number of brooks were channelled in other circumstances, then covered by the urbanization.

In addition, it is not because there is no noted problem that the "voûtements" is satisfactory. A collapse occurred recently on one voûtement not mentioned in the priority study.

In the particular case of the mines heaps, the results currently obtained could be used to establish a classification of the heaps according to the risks which they present for the environment and their vicinity, taking into account the European directive on mining waste in process of adoption.

One of the challenges for the future is thus to complete the investigations for the whole of the voûtements listed on the brooks, which represents a work to be planned in the long run.

References

ARNOULD R., FLAMION B. (2003) *L'après-mines en Région wallonne: le point de vue du démergement et de la gestion des eaux.* Actes du Colloque Après-mines 2003, 5-7 Février 2003, Nancy

LARDINOIS, J-P (2004) *Etude des ruisseaux canalisés sous terrils dans la zone de démergement de Charleroi*, Les techniques de l'Industrie minérale, N° 23, octobre 2004, pp 27-28.

Ministère wallon de l'Equipement et des Transports (2005) *Projet informatique de Cartographie Continue (PICC).* http://cartographie.wallonie.be/PortailCarto/Maquette/admin_prof/menu_diff_donnees.php

PAQUETTE, Y et LAVERSSANE, J. (2003) *Guide du détenteur de terrils et autres dépôts miniers issus de l'activité charbonnière (verses, bassins de décantation, dépôts de cendres).* Les fascicules de l'Industrie minérale, 39p.

MANAGEMENT OF MINING-RELATED DAMAGES IN ABANDONED UNDERGROUND COAL MINE AREAS USING GIS

U. J. Lee[1], J. A. Kim[1], S. S. Kim[1], W. K. Kim[2], S. H. Yoon[2], J. K. Choi[2]

[1] COAL INDUSTRY PROMOTION BOARD, 80-6 Susong-dong Chongro-gu -110-727 Seoul, -Korea

[2] SSANGYONG INFORMATION & COMMUNICATION CORP., 24-1 2-ga Jeo-dong Jung-gu -100-748 Seoul, -Korea

ABSTRACT : The mining-related damages such as ground subsidence, acid mine drainage(AMD), and deforestation in the abandoned underground coal mine areas become an object of public concern. Therefore, the system to manage the mining-related damages is needed for the effective drive of rehabilitation activities. The management system for Abandoned Underground Coal Mine using GIS includes the database about mining record and information associated with the mining-related damages and application programs to support mine damage prevention business. Also, this system would support decision-making policy for rehabilitation and provide basic geological data for regional construction works in abandoned underground coal mine areas.

KEYWORDS: Abandoned underground coal mine, Ground subsidence, Acid Mine Drainage (AMD), Shafts and drifts, Abandoned Mine GIS (AMGIS)

RESUME :Les dommages relatifs aux mines, comme l'affaissement de terrain, le drainage dans des mines acides et le déboisement dans une région à l'aplomb de mine de charbon abandonnée, sont devenues une préoccupation publique. En conséquence, un système de gestion des dommages est nécessaire pour l'organisation de la remise en état. Le système d'information géographique (SIG) utilisé pour les Mines de Charbon Souterraine Abandonnées inclut une base de donnés à propos des enregistrements relatifs à l'activité minière et des informations associées avec des dommages miniers, ainsi que des programmes de support aux travaux de prévention contre ces dommages. Ce système supportrait aussi une politique de décision pour la réhabilitation des secteurs miniers et fournirait des donnés géologiques pour des travaux de construction éventuels.

MOTS-CLEFS : Mine de charbon abandonée en souterrain, Affaissement, Drainage dans des mines acides(AMD), Abandoned Mine GIS(AMGIS)

1. Introduction

Due to decrease of coal demands and closure of the 336 coal mines, safety accidents and environmental contaminations caused by mining-related damages such as ground subsidence, acid mine drainage(AMD), and deforestation in abandoned underground coal mine areas have been socially issued.

That is the reason why the Coal Industry Promotion Board(CIPB) has continuously carried out mining-related damages restorations and environmental improvements.

Also, CIPB has plan to establish AMGIS(Abandoned Mine GIS) for mining-related damages for 336 abandoned underground coal mines (1,121 ㎢) in South Korea from 2003 to 2009. This system will work out analytical management and synthetic prevention for countermeasures against mining-related damages.

2. Mining-related Damage Restoration by CIPB

2.1. Ground Subsidence Prevention

The project of ground subsidence prevention is composed of primary and detailed investigation, survey measurement, reinforcement work, and verification of effectiveness in order to prevent the safety accident caused by ground subsidence in abandoned underground coal mine areas.

Primary and detailed investigations are the processes that survey and evaluate the ground subsidence probability for surface and subsurface geological condition through mining record, geological mapping, geophysical prospecting and drilling for the site beneath which abandoned underground coal mines may exist.

After the investigations, survey measuring the deformation of surface and bedrock overlying shafts and drifts by measuring instruments is conducted. Based on the results of the surveys, ground reinforce-ment using grouting material such as cement mortar and cement milk is conducted and its effectiveness is verified by drilling or survey measurement.

2.2. Remediation of Acid Mine Drainage(AMD)

Most coal mines are located in mountainous areas, particularly the Gangwon Province from where the uppermost of the Nakdong and Han rivers are originated. CIPB has applied the natural purification engineering method to treat AMD caused by heavy metal leaking from mine opening. The AMD is purified by SAPS (Successive Alkalinity Producing System) I and II to neutralize acidic mine water, and reduce and settle iron; at the swamp, remaining iron is removed by sulfate reducing bacteria.

Also, it applies physico-chemical purification method to the site where the natural purification engineering method is hard to apply because the volume of waste water and the degree of contamination are too high.

2.3. Restoration of Forests

Forest restoration before 1995 was simply for preventing waste stone from being washed away, so it could not achieve afforestation over time but rather the restored area was washed away or the view was ruined.

The CIPB adopted an engineering method considering the characteristics of waste stone and vigorous trees. Using the method, the restored areas were protected from torrential downpours and afforestation was achieved in a short period.

3. Geographic Information System for Mining-related Damages

AMGIS includes building database and developing an expert system which can support decision-making policy for rehabilitation in abandoned underground coal mine areas and provide basic geological data for regional construction works.

To the 2nd period of the project(~ 8. 2005), CIPB built up spatial and attribute data for 52 abandoned underground coal mines in Samcheok and Taebaek City, and developed application programs to analyze and estimate the mining-related damages. Fig. 1 shows the system configuration of AMGIS. The server side consists of ArcSDE for management of spatial database

and Oracle RDBMS. The client side consists of workstations where the client applications based on ArcGIS are loaded.

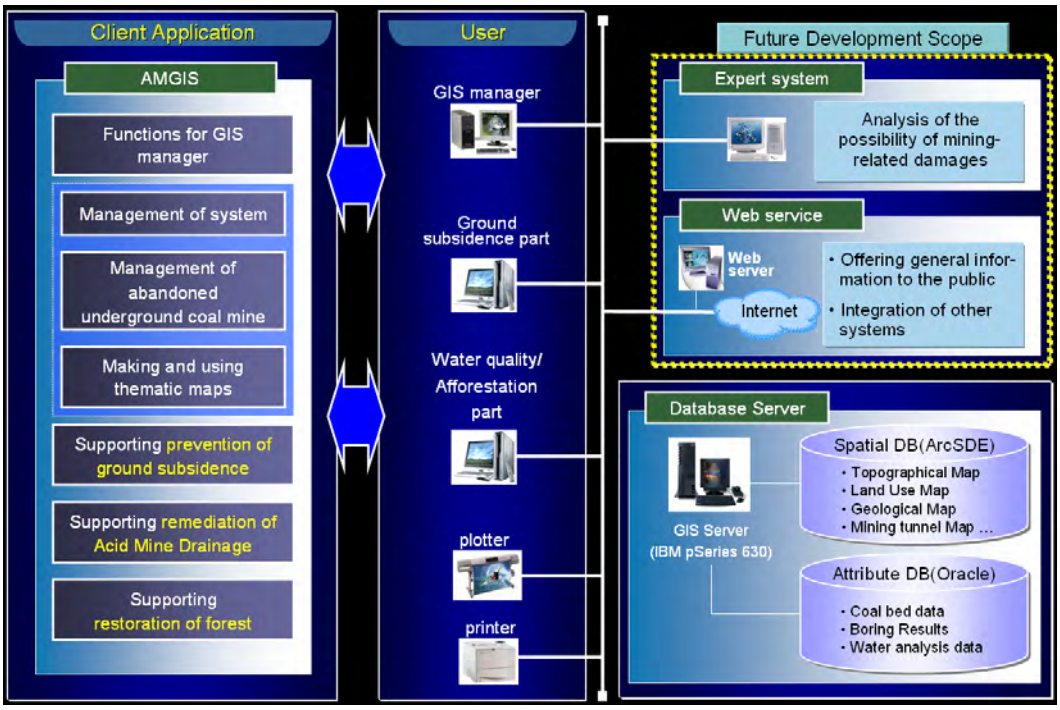


Fig. 1. System configuration of AMGIS

3.1. GIS Spatial Database

(1) Topographical map : road, railroad, river, building, administrative districts, height contour etc., 1;5,000 scale, published by NGII (National Geographical Information Institute)

(2) Land Use Map : represents the land use based on land registration map, 1;5,000 scale, published by NGII

(3) Geological Map : geological unit, boundary, structural line, strike and dip etc., 1;50,000 scale, published by KIGAM(Korea Institute of Geoscience and Mineral Resources)

(4) Mine Lot Map : represents mining land registration, overlay of unit and free style mine lot map

(5) Mining Tunnel Map : represents the location, depth, and width of shafts, drifts, and mine opening. mine openings were surveyed by GPS for the use of Ground Control Points

(6) Satellite Image : Ikonos and landsat-7 ETM+ image

(7) Spatial data from mining-related damages prevention project : areas of investigation, reinforcement work, and remediation facility, cross-lines for geological and geophysical interpretation, and drilling point, etc.

3.2. GIS attribute Database

(1) Abandoned underground coal mine Information : Mining record, information of shafts and drifts, etc.

(2) Geological Interpretation Data : coal bed, field survey data, cross section interpretation, etc.

(3) Geophysical Prospecting Interpretation Data : seismic, electrical resistivity, GPR, etc.

(4) Borehole Data : Standard Penetration Test(SPT), water pressure test, borehole lateral load test, Rock Mass Rating(RMR), BIPS, Numerical Analysis, etc.

(5) Results of Survey measurement : Multi Point Borehole eXtensometer(MPBX), Slope Inclinometer, etc.

(6) Reinforcement Work Data : Grouting material, method, etc.

(7) Purification of mine wastewater : information of facilities, water quality, and pollution status, etc.

(8) Restoring the ruined forest : ruined status, afforestation information, etc.

3.3. Application development

(1) System administration :
- registering and editing users and codes
- managing the system privileges of users
- setting up the work areas and group layers
- managing functions of spatial and attribute data

(2) Management of abandoned underground coal mines :
- searching and editing abandoned underground coal mine data and maps(mine lot map, geological map, etc.)
- making the charts and reports of abandoned underground coal mine data

(3) Management of abandoned underground coal mining-related damages :
- managing the mining-related damages data and prevention work results
- searching and viewing the individual survey and prospecting data

Fig. 2 shows the windows for the management of the database related with ground subsidence area and work of forest restoration.



Fig. 2. management of mining-related damages

(4) Making the thematic maps :
- Making the various complex map of mining layers

(5) 3–D visualization of mining tunnel map :
- Visual analysis between underground tunnel and surface facilities

Fig. 3 shows the window where satellite image, mining tunnel map and some topographical elements built 3 dimensionally were overlayed.

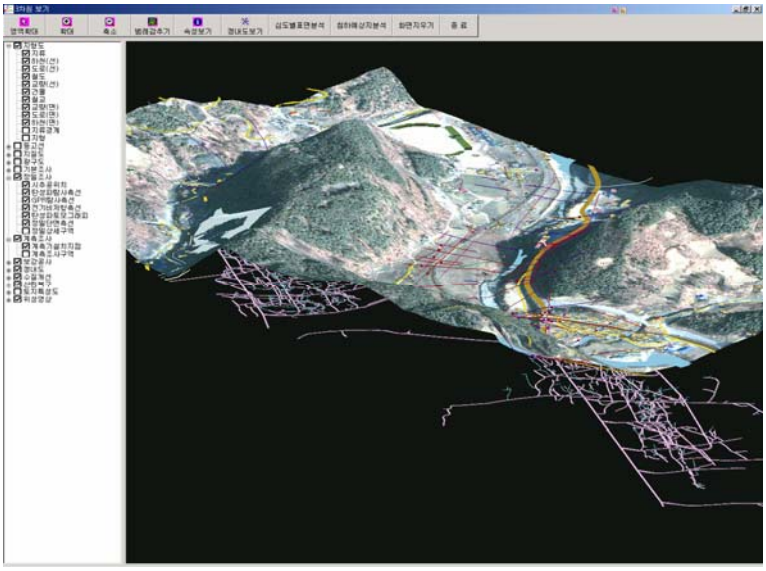


Fig. 3. 3-D satellite image and mining tunnel map

(6) Analysis of the possibility of ground subsidence :
- 2-D and 3-D cell-based analysis by calculating distance between tunnels and each cell
- analysis by the theory of subsidence such as the theory of angle of draw and the theory of volume expansion

Figure 4 represents 2-D analysis according to the depth from surface to drifts. The red areas have high possibilities of ground subsidence. Figure 5 shows the result of analysis of the ground subsidence possibility by the subsidence theories.

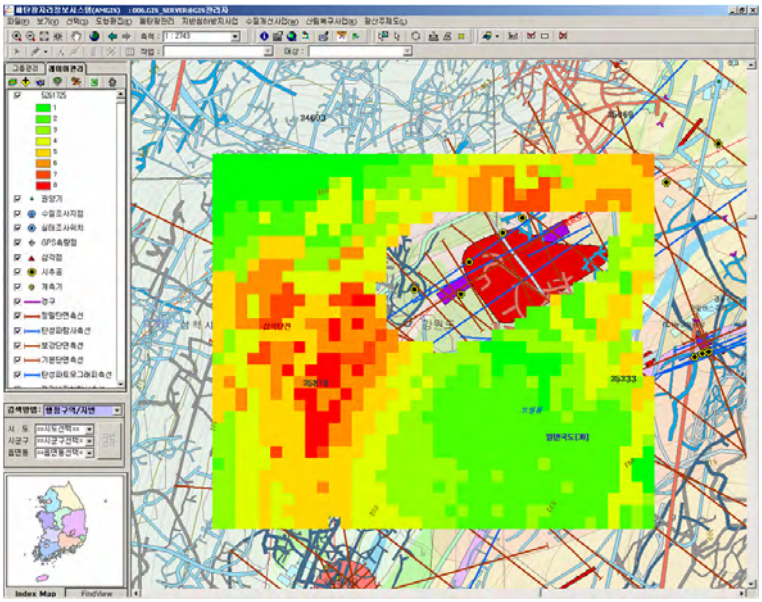


Fig. 4. 2-D cell-based analysis of ground subsidence

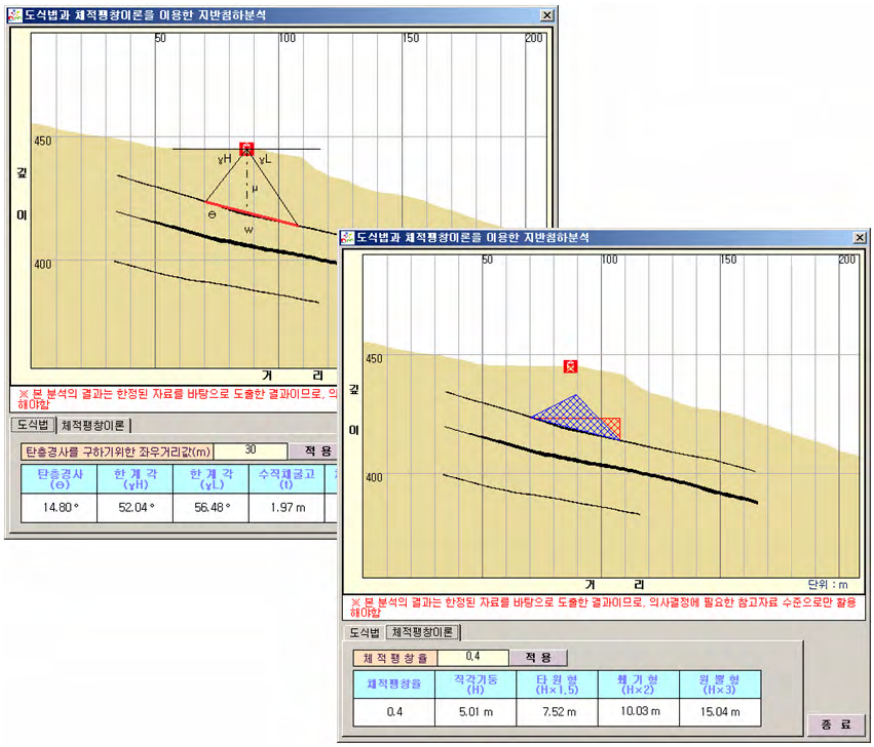


Fig. 5. Analysis by the theory of subsidence.

4. Discussion and Conclusion

AMGIS is the first implementation to analytically manage the problems associated with abandoned underground coal mines and mining-related damages in Korea. Through building database for 52 abandoned underground coal mines and developing application programs to support internal business of CIPB, it is shown that GIS is very effective tool for managing mining-related damages. Also, we can have foundation to develop an expert system such as estimation and trend analysis of ground subsidence and verification of remediation of AMD, etc.

The 3rd year(2005. 12 ~ 2006. 11) of the AMGIS project is about to start for 65 abandoned underground coal mines in the Jeongseon, Gohan and Sabuk City, and the application programs will be improved as more valuable, analytical and visualized system for experts in the field of mining related business.

In the future, database for all 336 abandoned underground coal mines in South Korea will be built and AMGIS will be expanded and stabilized. The client application will be extended for all sections related with mining-related damages in CIPB. And the expert system that can analyze the possibility of ground subsidence and AMD will be developed. Also, the web GIS system for offering general information to the public will be built by the year 2009.

The contents of database and application programs in AMGIS can be applicable not only to coal mines but also to metalliferous and non-metallic mines. AMGIS will be a supporting system to propose the most effective solution of mining-related damages.

TECHNICAL AND LEGAL ASSESSMENT OF A DISUSED UNDERGROUND QUARRY IN THE NEIGHBOURHOOD OF SAUMUR (FRANCE)

MATHON David[1]

[1] CETE de l'OUEST – LRPC ANGERS – 23 avenue de l'amiral Chauvin – BP20069 – 49136 LES PONTS DE CE Cédex

ABSTRACT: During the survey of undulation assessment in the Saumur countryside (France), difficulties were met to translate hazards due to presence of disused underground quarries. Indeed, ruin of these quarries can imply depression or even collapse of the surface level. It is not easy to diagnose hazard intensity without having precise maps of the quarry. A lawful solution was concluded in agreement with the Departmental Direction for Infrastructure by rating these areas as "presumed high level hazard" zones. The article will show the stages of the dialogue with the local communities especially the management of a "presumed high level hazard " area, which intersects spaces that were planed to be built.

KEYWORDS: undulation assessment, disused underground quarries, hazard, dialogue.

RESUME : Dans le cadre de l'étude du Plan de Prévention des Risques Mouvement de terrain du Coteau du Saumurois, des difficultés ont été rencontrées pour traduire l'aléa lié à la présence d'anciennes carrières souterraines abandonnées. En effet, la ruine de ces carrières peut se traduire en surface par un affaissement voire un effondrement. Il est très délicat de diagnostiquer une intensité d'aléa sans disposer de plans précis de l'exploitation du fait de l'impossibilité de se situer précisément dans cet environnement. Une parade réglementaire a été choisie en accord avec la Direction Départementale de l'Equipement en affectant à ces zones un aléa « présumé fort » par application du principe de précaution. L'article reprendra les étapes de la concertation avec les collectivités locales notamment dans la gestion d'une zone d'aléa présumé fort qui recoupait des espaces à bâtir au Plan d'Occupation des Sols.

MOTS-CLEFS : PPR, carrières souterraines abandonnées, aléa, concertation.

1. Introduction

Following the collapse of the North East rampart of Saumur's castle in 2001, the French government (urged by local authorities) ordered a general survey to assess undulation hazard between Saumur and Montsoreau (a town by the River Loire located on the border between Indre-et-Loire and Maine-et-Loire in France).

Consequently, in January 2002, the Prefect ordered a study on how to tackle undulation hazard. The area concerned by this survey is located on the hillside between Saumur and Montsoreau. It concerns 5 towns (or cities) and about 12 linear kilometres of hillside. The Departmental Direction for Infrastructure (Natural hazards survey department) is in charge of the survey which will be carried out by the LRPC from the neighbouring city of Angers.



April 22nd 2001 : collapse of the rampart

Saumur's hillside is a fairly low cliff – under 40 metres high - made up of soft Turonian limestone called tufa ("tuffeau" in French). In this area, this particular geological stratum is severely undermined because the "tuffeau" was used as building stone for cities like London, for example. Two types of caves are to be found:

- Small caves (cave-dwellings for example…)

- Large caves like underground quarries that are generally disused.

2. Initial process

The survey consisted in a thorough study to determine how stable the caves were by observing the rock massif and estimating the depth between the surface and the cave-roof. In fact, locating underground quarries, some of which were disused, proved difficult.

So, we tried to estimate how large these underground quarries were:

- firstly, through indirect information such as ventilation shafts, verbal accounts, toponymy or local surface details that might testify that an underground collapse occurred (subsidence or other signs..)



Ventilation shaft in the vineyard

- secondly, through direct information such as quarry-maps (sometimes there was one…) or if need be, by drawing up our own map by simple means of a compass and a laser beam.

As a result, these areas were rated "presumed high level hazard" as a precautionary measure.

3. Dialogue with the local authorities:

These hazard maps were shown to the mayors of the towns at risk. The relevance of the diagnoses was not questioned, nor were the precautionary measures which applied to the undermined areas. Nevertheless, a particular problem was met with one “presumed high level hazard” area as it was to be part of the local land use plan.

4. Carrying out a more thorough survey:

The Departmental Direction for Infrastructure (Direction Départementale de l’Equipement) decided to carry out a more thorough study in order to get further information on the disused quarry which was under the building land. It consisted in:

1. First of all, the drawing up of a map of the excavation by a team of topographers (it took about 2 weeks).

2. Afterwards, two geologists made a geological survey of the quarry and noted every sign of instability to establish a geotechnical zoning.

3. Finally, another diagnosis was made by an expert from the CETE in Lyons to ratify the previous one.

Drawing up a topographic map allowed us estimating how large this underground quarry was. Then, this map was used to localize every instability signs that were found in the quarry. As a result, hazard zoning was easier with this map.

We began the first diagnosis from the southern entrance of the quarry, which was running as mushroom beds 10 years ago. Firsts hectometers are safe; the main gallery was concreted to support the traffic of vehicles transporting mushrooms. The draught is getting trough 2 ventilation shafts.

Vaults of rooms seem to be safe; the tufa is homogeneous and rarely affected by fractures. The quarry was run according to the "rooms and pillars" way. We watched spans reaching 25 meters. Pillars are generally about 3 meters thick. This zone therefore presents an excavating rating (that is the ratio between the surface of extracted materials with regard to total surface) included between 80 and 85 %.

In order to support some vault’s cracks, operators built some pillars. Some others pillars were built to relieve overloaded pillars that might break by unconfined compression. Over the whole quarry, the caprock (that is rock included between cavity’s roof and the surface) represents about 25 meters thick.



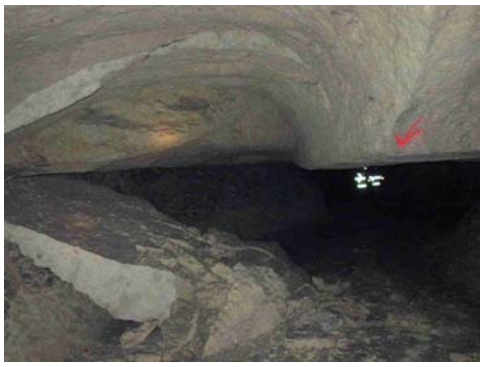
An overloaded pillar which was propped up

Considering these observations and the thickness of the residual caprock, this part of the quarry was rated as a middle level hazard zone

Deeper and as we get closer to the hillside, the rock appearance evolves. For safety reasons, the topographic drawing up was therefore arrested. The location of the observations was made on the basis of a progress raised in the compass and in the laser beam.

We realized this traverse from North entrance (from the hillside), by heading towards the most constant possible direction in order to “connect" the known part of the quarry. The precision of this method is therefore less important but the presence of a ventilation shaft allowed to re-prop up our measures (the error was about 10 meters after covering 300 meters in underground galleries).

The rock presents two networks of orthogonal tectonic fractures (North / South and Est/Ouest orientation). This fracturing associated to the sub-horizontal stratification of the tufa is responsible for numerous falls of roof sometimes implying important blocks and evolving at least in 2 places as bell holes measuring 10 meters high.



Fall of roof due to tectonic fractures and stratification

In this broken zone, rooms are sharply less wide (4 or 5 meters at the most), but the excavating rating remains high (always about 80 %).

Pillars show evident signs of weakness. They are affected by important shear stress and therefore spalling phenomenon is observed (diabolo’s forms). Consequently, the workers propped up (during quarry running) by solid packing near broken pillars.



Propping up by solid packing

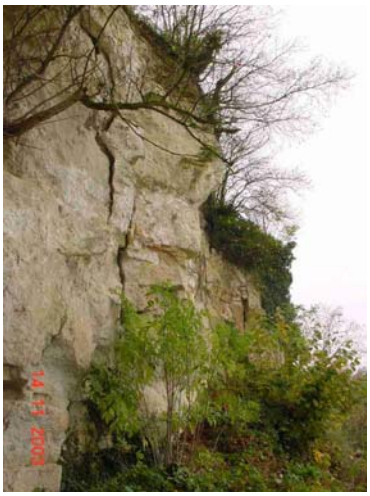
Vertical walls are therefore widely broken up. We watched few cracks on the vault (except where there were fall of roof…).



Vertical walls showing weakness signs

Considering these observations, this part of the quarry was rated as a high-level hazard zone

Finally, northern extremity of the quarry was rated as a very high-level hazard zone because of the proximity of the hillside. In this area, there is a phenomenon of grounds decompression that occurred a network of larges fractures parallel to hillside.



decompression fracture of the hillside

5. Results

This new survey led us to produce a new hazard map which was different from the first one. In fact, instead of just the “presumed high level hazard” area, there were now 3 types of hazard areas: a middle level hazard zone, a high-level hazard zone and a very high-level hazard zone.

In terms of regulations, the differences between each hazard level were important. That is to say: a high or very high or “presumed high level hazard” area became a red zone so that no new construction would be allowed on this area. On the other hand, a middle level hazard area became a blue zone that allowed new constructions subjected to technical conditions like doing a geotechnical study including drillings for example.

6. Conclusions

First, it emerged from this survey that the application of the precautionary principle is generally well accepted by local managers in the areas where there are no equipment or projects.

Secondly, it emphasizes that good communication and dialogue with local authorities involves a (positive) critical vision of hazard-zoning surveys and reinforces technical credibility of the survey.

Thirdly, quality of the rock massif hardly depends of his localisation in comparison of the hillside.

Finally, this example illustrates the following theory about the quality of a natural hazard-zoning survey :

· it depends on the technical capacities of the geologist team.

· it also depends on the communication between various people or organisations such as the State authorities, the geologist, the local managers and the people that live in dangerous areas.

7. References

Mathon D., Leducq M, Huet M, Delporte F (2005) *Plan de Prévention des risques mouvement de terrain du coteau entre Saumur et Montsoreau*

Potherat P, *Compte-rendu de visite du 20/9/2005 à Dampierre sur Loire*, 4 octobre 2005.

EVALUATION OF POST MINING AREAS IN AUSTRIA WITH METHODS OF MINE SURVEYING AND MINING SUBSIDENCE ENGINEERING.

Gerhard MAYER, Reinfried PILGRAM, Bahman RANDJBAR,

Department Mineral Resources and Petroleum Engineering, University of Leoben, Franz-Josef-Str. 18, A-8700, Leoben, Austria

ABSTRACT: In this contribution, different functions of mining subsidence engineering investigations of old mines are shown and discussed afterwards. From this resulting the present situations of old mines is described. On this basis a systematic evaluation regarding the potential of influence on surface of old mines in Austria is developed.

KEYWORDS: Old mines, Austria, Mining subsidence engineering, Mine surveying, Land use

RESUME: Dans cette contribution, nous montrons et discutons des investigations faites concernant les affaissements d'anciennes mines qui nous permettent de décrire la situation actuelle. Sur cette base, une evaluation systématique du potentiel d'influence à la surface d'anciennes mines autrichiennes est développée..

KEYWORDS: Anciennes mines, Autriche, Affaissements miniers, Occupation des sols

1. Introduction

Cause for this paper is the frequency of the mine damages like slips, changes of water levels, caves to the surface, sink holes and deepenings on the surface due to possible long-term effects of old mines. In many surface dedication plans of the municipalities former mining districts, without preceding investigations, are proven as endangerment ranges and are very often also much too largely, whereby considerable economical damage can develop. In contrast to this numerous cases often buildings are in the direct effect and endangerment range of old mines.

During the closing period of mines in Austria, like as in other countries, usualy precautions were taken for the security of the surface generally within the range of the mining gallery openings, because one assumed that the rest of the mine would be either stable or would collapse soon without effects for the surface. In the old mining districts today the surface is used to a large extent very intensively. The timbering and walling collapses – as far as the cavities are not permanent stable - by long-term stress after decades and at the surface locally concentrated soil deformations and in extreme cases, caves on the surface appeare due to cavity collapses or sink holes in combination with the seeping part of the precipitation. Therefore the local hydrogeological conditions are very important.

However in the period of 1949 to 2004 more than 100 mining industry enterprises in Austria were shut down (Österreichisches Montan-Handbuch, 2000). Likewise a large number of unsecured bomb shelters exist from wartime in our federal territory. This paper refers exclusively to old mines in such depth that can cause surface fractures, because in Austria more than 90 % of the old mines are very near to surface type of mines.

2. Definition of the terms “old mine” and “very near to surface mine”

Old mines are defined as the whole of all mining cavities (mine working) including drill holes as well as open pit mines and dumps, which are no more used for mining activities and also any other subterranen cavities as cellars, caves, bomb shelters and tunnels (Meier, 2004).

From the view of mining subsidence engineering these mining cavities can be devided in groups:

· Mining causing surface fracture (very near to surface mines)
· Mining causing prevailing subsidences (near to surface mines and deep mines)

In more recent time this is defined using the thickness of excavated rock in relation to the overburden. This graduation depends among other things on the characteristics of rock and the overburden. The hazard potential of sand and gravel layers is larger than of solid rock (Hollmann, 1968, Randjbar, 2001).

3. Effects and aftereffects of old mines on the surface

The aftereffects of the old mining industry on the surface cannot be regarded overall. In the sense of mining subsidence engineering it must be distinguished between the effects of the mining causing prevailing subsidences with a deposit-dependent induction period and the mining causing surface fracture with temporally practically unlimited aftereffects.

Environmental damages caused or released by old mining industry are usually due to

· directly on the production of the underground cavities and the redistribution of stress resulting from cavities or
· indirectly to the rerise of the lowered groundwater.

Table 1: Some aftereffects of old mines

Mining activity	Effects
Deep mines	· Sink holes · Changes in the distance from ground water to surface
Near to surface mines	· Compression of soil · Subsidences
Very near to surface mines	· Caves on the surface · Surface fractures, Caves on the surface and sink holes caused by the rerise of the lowered groundwater

4. Evaluation of old underground mines with methodes of mine surveying and mining subsidence engineering

Before old mining areas can be evaluated, a stocktaking has to be made of all facts concerning topography, geology, the mineral deposit and mining activities. This stocktaking can be accomplished by means of a check list, which to former Institute for Mine surveying and mining

subsidence engineering of the Leoben university has developed generally (Randjbar, 2001) and particularly for old mining industry in the eastern alps (Hollmann, 1997).

For this check list the following data has to be acquisited:

· official and operational documents
· geological, geotechnical and mine surveying documents
· geological and hydrogeological conditions
· general documents (without mining maps)
· responsibility
· kind of material resources
· type of mineral deposit
· excavation activities
· development of the mine

The result of all pre-working must be a clear overview of the mining development of the area, so that for the evaluation a clear borderline of possible endangerment zones can be drawn.

4.1. Investigation and detection of unknown mining cavities

In the following chapter the possibilities of the investigation of cavities near to the surface will be shown up briefly. Missing or incomplete documents about the mining activities require, in particular in inhabited areas, careful detection and investigation of such cavities.

In the case of a "recent" old mining industry, historical aerial photographs as well as questionings of time witnesses and adjacents resident can be helpful. Every now and then the area morphology gives information about old mining. For a first wide laid out search for "suspicion surfaces" the use of airplane and satellite-based remote sensing systems can be helpful.

If from the document search as well as from the evaluations mentioned above the suspicion on cavities being present has consolidated and is locally clearly limited, pursuing methodes of investigation and detection can be used. These methodes can be divided into direct, indirect and special methods, and are predominantly typically geotechnical and geophysical procedures:

· direct methodes (drilling, exploring, ...)
· indirect methodes (geophysical procedures including piling samples, ...)
· special methods (tracer methodes scanning water and air, camera probes, ...)

Drillings can be made as single drillings, drilling rasters or drilling fan. In principle core drillings offer a substantially increase of information. Since a long time these investigations are no longer limited to drillings, but are supplemented by geophysical investigations.

Using geophysical methods physical parameters of the rock are measured from the surface as well as from boreholes. Geophysics as science of the study of the physical characteristics of the earth, supply elastic, electrical, magnetic, electromagnetic, radioactive, gravimetric and thermal parameters. The quality of the results of these procedures is dependent, among other things, on the geological conditions, a professional measurement and the applied evaluation methods.

4.2. Evaluation of old mines using mine maps

Old maps and plans of the investigation area have frequently fatal lacks. Usualy they are copies and are not in a perfect condition. Especially the completeness of the entries is hardly to verify. Talking

about “old maps" in this meaning all documents are concerned, which are of importance for the maps. This can also be field records, draft versions, computation minutes, photos (including aerial photographs), statements of persons (e.g. staff) an so on. It occurs that damage areas must judge with only insufficient maps or sometimes even without any maps.

4.3. Surface mining damages

As long-term impairments we can find, among others, subsidences of the surface, changes of the groundwater corridor distances, cracks and fissures. Mining very close to the surface can effect break deformations and in particular caves to the surface. In steep deposits and with shafts the most frequent reason for caves to the surface is the moving of the filling material into the deeper areas. In sink hole areas this effect can be natural, particularly by grain migration in natural cavities or also by solution activity in salt -, gypsum and lime layers. A comparison with the mine maps is essential in such cases.

For the evaluation of the effects of mining influences a complete chronological documentation is required, including effects (damages) observed and safeguards already accomplished so far. Occurred mining damages have to be mapped and a evaluation is to be accomplished.

5. Evaluation of possible endangerments

One of the principal purposes of the evaluation is to indicate possible damage ranges in the examined mining area with the greatest possible security. The hazard potential has to be evaluated using 3 criteria:

· evaluation of mining iduced impacts and effects
· evaluation of geologically iduced impacts and effects
· evaluation of other impacts and effects

To the technical bibliography after Prof. Spickernagel (Randjbar, 2004) regarding the protection of the surface for Austrian old mining areas two danger zones were introduced: Danger zone 1 as "caves to the surface surely endangered " and danger zone 2 as "caves to the surface probably endangered".

During the investigation of different case studies the impairment ranges were specified in 3 zones by the authors. Independently of the kind of mines shafts, gallery crossings, adit openings as well as mining sections with an overlay of less than 20 m were assigned to the zone 1. Zone 1 is to be always regarded "caves to the surface surely endangered ". This demand applies also to not stable filled old shafts.

Zone 2 is in the first step specified by outlining the borders of mining areas, galleries an so on, without zone 1. This range is extended using the angle of break. Zone 2 is to be regarded as probable endangerment range, in particular for sink holes.

Zone 3 can be found by extending zone 2 using the limit angle or the effective angle. Zone 3 is to be regarded as possible endangerment range, whereby the use of the surface for building activities under curtain conditions is possible.

Table 2. Hazard potential zones of old mines

zone	mine	area	surface use
1	· shafts · gallery crossings · adit openings · overlay of less than 20 m	· circle with 10 m diameter · circle with 10 m diameter · circle with 10 m diameter · outline	building activities combined with permanent safeguards; qualified agriculture
2	whole mine area without zone 1	extended outline using the angle of break (without zone 1)	building activities combined with subsoil rehabilitation; agriculture
3	whole mine area without zones 1 and 2	extended outline using the limit angle (without zones 1 and 2)	building activities combined with structural measures; agriculture

6. Prospects

Lately several reports show mining damages on the surface, especially caves to the surface. These damages many times result from the fact, that when mines in Austria were closed, the safety of the surface was not considered sufficiently.

A systematic evaluation of all available information is the basis of an estimation of the surface endangerment as a result of mining activities. The discussed check list can be used for this purpose.

It is important to determine surface endangerment ranges of old mines with greatest possible security with the goal of implementation into surface dedication plans for local purposes.

For an effective protection of the surface, for the security of people, buildings and the public traffic the hazardous zones of old mines should be brought in a stable condition.

We have to create the bases for an efficient information system to support research und analysis possibilities.

7. References

1. Kratzsch : „*Bergschadenkunde*“, Nachruck der korrigierten 3. Auflage von 1997, Deutscher Markscheider Verein e.V., Bochum 1997
2. Hollmann F., *Tagesnaher Bergbau und Bebauungsplanung im Niederrheinisch-Westfälischen Steinkohlengebiet*, Bergfreiheit 33 (1968), S. 109 – 117
3. Hollmann F.: *Stand der Sicherungsmaßnahmen im Niederrheinisch-Westfälischen Steinkohlengebiet bei getätigtem tagesnahen Bergbau.* Neue Bergbautechnik 22 (1992), S. 96 bis 100

4. Hollmann F.: *Nutzungsrelevante bleibende Überprüfungen der Gefügestrukturen im Senkungstrog. Ein Beitrag zum Verhalten des geschichteten Gebirges unter bergbaulicher Zwängung*. – Festschrift o. Prof.Dr.-Ing. Spickernagel, Institut für Markscheide- und Bergschadenkunde der MU Leoben, 1994, S. 58 - 81
5. Hollmann F.: *Zur bleibenden Beeinträchtigung der Nutzung von Boden und Baugrund im Senkungstrog nach Einstellung bergbaulicher Tätigkeit bzw. nach Auslaufen bergbaulicher Bodenbewegungen*. – Bergbau 46 (1995), S. 76 bis 82
6. Hollmann F., Kremser F., Landmann H., *Altbergbau in den Braunkohlenrevieren der Ostalpen unter den bergrechtlichen Randbedingungen der Republik Österreich*, 5. der Schriftenreihe der GDMB, Gesellschaft für Bergbau Mettallogie, Rohstoff – und Umwelttechnik Heft 97, S. 87 – 107
7. Meier G.; *Die bisherige Tätigkeit des Arbeitskreises 4. 8 „Altbergbau-geotechnische Erkundung und Bewertung" und dessen zukünftige Aufg*aben. 4. Altbergbaukolloquium 2004 Montanuniversität Leoben 7-12
8. Österreichisches Montan-Handbuch 2000, Verlag Ferdinand Berger & Söhne, Horn/Wien
9. Randjbar, B.: *Bergschadenkundliche Bewertung untertägiger Altbergbaue in Österreich*, Berg- und Hüttenmännische Monatshefte (BHM), 146. Jg. (2001), Heft 12, S. 478 – 483
10. Randjbar, B.: *Bergschadenkundliche Bewertung im Hinblick auf das Gefährdungspotential auf der Tagesoberfläche bei aufgelassenen Altbergbauen in Österreich*. 2. Altbergbaukoqium 2002 TV Clausthal 336 – 346
11. Randjbar. B. : *Das Bergbaukartenwerk als Grundlage der Beurteilung von Altbergbaue in Österreich*, BHM,149 Jg. (2004) heft 12 S.428-432
12. Randjbar, F Hollmann, , F. Kremser, Helmuth Landsmann *Standwasser im Grubengebäude minimiert Bergschäden*, BHM,149 Jg. (2004) heft 12 S.424-428,
13. Spickernagel H.: *Folgewirkungen eines tagesnahen Abbaus auf die Erdoberfläche. Bodenbewegungen und Bergschaden*, Kolloquium, Berlin, Oktober 1972, S. 144 bis 162
14. Berggesetz 1975 (BergG1945).-*Bundesgesetz vom 13.05. 1975 über den Bergbau und die Änderung der Gewerbeordnung 1973*. – i.d.F. 1997, 125 Seiten
15. Mineralrohstoffgesetz – MinroG 1999.- *Bundesgesetz über mineralische Rohstoff, über die Änderung der Arbeitnehmerinnenschützgesetzes und des Arbeitsinspektionsgesetzes 1993 in der Fassung der Mineralstoffgesetznovelle 200*1, Manzsche Verlags- und Universitätsbuchhandlung, 359 Seiten, Wien 2002
16. Weber & Weiss: „*Bergbaugeschichte und Geologie der Österreichischen Braunkohlenvorkommen"* –Archiv für Lagerstättenforschung, Hersgb. Geologische Bundesanstalt Wien, Bd. 4, Oktober 1983

INDUCED SEISMICITY IN A SALT MINE ENVIRONMENT EVALUATED BY A COUPLED CONTINUUM-DISCRETE MODELLING.

MERCERAT Diego[1], SOULEY Mountaka[2] , DRIAD Lynda[2], BERNARD Pascal[3]

[1] LAEGO – Parc de Saurupt, Ecole des Mines de Nancy, 54000 Nancy cedex, France; diego.mercerat@mines.inpl-nancy.fr

[2] INERIS – Parc de Saurupt, Ecole des Mines de Nancy, 54000 Nancy cedex, France; Mountaka.Souley@ineris.fr, Lynda.Driad@ineris.fr

[3] Laboratoire de Sismologie - IPGP, 4 Place Jussieu, 75005 Paris cedex, France; bernard@ipgp.jussieu.fr,

ABSTRACT: With the objective to better understand the induced microseismicity in a salt mine environment due to an underground solution mining, an in situ experiment is undertaken by GISOS[1] in the Lorraine salt basin. The overburden overlying the salt cavity is characterized by the presence of two competent layers where most microseismic events are expected. This paper presents a coupled continuum-discrete modelling to simulate the mechanics of fracture initiation and propagation in the rock mass overlying the cavity: discrete approach for the competent layers and continuum approach for marls, salt and other rocks and soils. For the competent layers, numerous calibrations of the model microparameters based on the laboratory results are firstly performed. The first coupled modelling results suggest that the mechanism of fracturing in the competent layers is predominantly tensile as it could be expected. The results also show that the microseismic events associated to the progressive damage in the competent layers through microcraks development can be modelled. This opens interesting perspectives to assess the feasibility of seismic monitoring of underground cavities by comparing, in the future, the numerical modelling results with the recorded seismicity of the study area.

KEYWORDS: Induced seismicity, salt cavity, competent layer, in situ, continuum-discrete modelling, , microcraks,

RESUME : Dans l'objectif de mieux comprendre la microsismicité induite dans des mines de sel, une expérimentation in situ a été entreprise par le GISOS sur une cavité saline de la région Lorraine. Le recouvrement est caractérisé par la présence de deux bancs raides dans lesquels l'essentiel de l'activité microsismique est attendue lors de la reprise de l'exploitation. Ce papier présente une modélisation basée sur une approche couplée : continue (pour les marnes et le sel) et discrète (pour les bancs raides) pour évaluer les mécanismes de développement des fractures dans le recouvrement. De nombreuses calibrations des microparamètres du modèle discret à partir des paramètres macroscopiques ont été nécessaires. Les résultats de la modélisation montrent que le mécanisme de fracturation dans les bancs compétents résulte essentiellement d'efforts en traction. Les premiers résultats montrent aussi que les évènements microsismiques peuvent très bien être mesurés à travers la formation des microfissures. Ceci ouvre des perspectives intéressantes pour des confrontations avec les mesures qui seront enregistrées lors de l'effondrement provoqué.

MOTS-CLEFS :: Sismicité induite, cavité saline, banc raide, in situ, modélisation continue-discrete, microfissures

---

1 GISOS (Groupement de recherche sur l'Impact et la Sécurité des Ouvrages Souterrains) réunissant l'INPL, le BRGM, l'INERIS et l'Ecole des Mines de Paris

1. Introduction

A research project within the GISOS program has been launched in order to assess the feasibility of seismic monitoring of underground growing cavities due to salt dissolution (solution mining). Within such framework, this specific project focus on two main complementary axes : (a) the validation of induced seismicity monitoring techniques in salt mine environments, and (b) the numerical modelling of deformation and failure mechanisms with their associated acoustic emissions as well as the induced microseismicity.

Previous studies on induced seismicity of underground growing cavities (Johnston and Einstein 1990, Mendecki et *al.* 1999) confirm the presence of microseismic events associated with the progressive damage of the overburden until its final collapse. Continuous monitoring of such microseismicity may provide crucial information for stability analysis of the area surrounding the cavity. In order to validate such seismic monitoring techniques, a microseismic network has been installed over a site test at Cerville-Buissoncourt (Lorraine, France), where a stable brine cavity is nowadays found. When the salt exploitation restarts, the spatial and temporal evolution of the seismic event locations can firstly be recorded and secondly be correlated with the results of mechanical modelling.

Numerical modelling of such complex process requires a large scale model which takes into account both the cavity evolution within the salt layer and the mechanical behaviour of the overburden layers where high deformation and fracturing are expected. To achieve this scientific challenge (experimental and numerical through geophysics and geomechanics fields), a coupled continuum and discrete modelling strategy is then adopted.

This paper focus on the feasibility to achieve the previous scientific objective and presents the preliminary numerical results of induced microseismicity evolution in the competent layers through the microcracks distribution.

From numerical point of view and in order to take into account the elasto-brittle behaviour of the competent layers where most seismic damage is really expected, we use the code PFC2D (Particle Flow Code in two dimensions) based on the discrete element method. To describe the behaviour of the other layers (mainly composed of marls and salt) which present more ductile and/or viscoplastic behaviour, a continuum approach based on the bidimensional Fast Lagrangian Analysis of Continua code (FLAC) is used allowing for different and more complex constitutive laws.

Numerous calibration process are firstly performed to estimate the microparameters used in PFC2D to reproduce the macroscopic stress-strain curves obtained from laboratory tests (macroscopic behaviour from uniaxial and triaxial tests).

A large scale continuum model assuming an elastic perfectly plastic behaviour of the competent layers is firstly built in order to establish the suitable boundary conditions with regard to the brine cavity sizes. Finally, a fully coupled continuum-discrete model is developed (coupling between FLAC and PFC2D domains is achieved through a special function written in the internal language of both codes), as well as a comparison with the previous continuum approach.

2. Site test of Cerville-Buissoncourt

2.1. Brine cavity and overburden characteristics

The brine cavity of Cerville-Buissoncourt (Lorraine, France) is actually located within a salt layer at about 180 m depth and it presents an irregular shape but in a first approximation, it can be

considered as a cylindrical cavity of 100 m of diameter and 50 m high. An schematic geological section of the study area is shown in Figure 1. Typically, the overburden is characterized by the presence of a series of intercalated anhydritic marls lying over the salt layer, and on top of them, the presence of two competent layers of 8.5 m thickness with an elasto-brittle behaviour located approximately 50 m above the salt layer. These layers correspond to what is known as the Beaumont dolomite (a dolomite of 5 m thick and an anhydrite of 3.5 m thick).

2.2. Microseismic network

A microseismic network has been installed over the underground brine filled cavity of Cerville-Buissoncourt. The network includes four 3D components and three 1D component seismometers located at different depths in cemented boreholes distributed around the study area. A velocity model of the area, from the processing of a 2D seismic line (work in progress), will allow us to obtain an accurate location of microseismic events when the salt exploitation restarts . The spatial and temporal evolution of the seismic event locations can then be correlated with mechanical modelling results, and therefore a quantitative analysis of seismic and non-seismic deformation will be available.

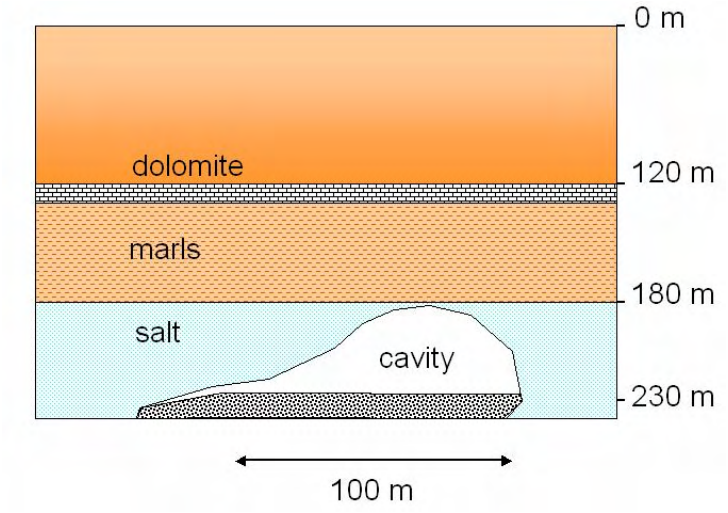


Figure 1. Schematic section of the salt cavity and main geological facies.

3. Geomechanical laboratory characterization

A large number of laboratory tests have been carried out on SOLVAY S.A samples to characterize the geological formations of interest. Some of them are available (by courtesy) for this study. In particular, the Beaumont dolomite and the anhydrite facies present a rather high Young modulus (~80 GPa) and uniaxial compressive strength (UCS ~200 MPa) for typical sedimentary rocks. The tensile strength measured by Brazilian tests is also high. The acoustic properties of these competent layers are quite elevated.

On the other hand, the mean values found for samples extracted from the marls located between the salt layer and the Beaumont dolomite are much lower, with extremely low tensile strengths measured in some samples.

The results of this geomechanical laboratory characterization are used to choose the physical and mechanical parameters of the numerical model, and to obtain the appropriate microproperties, by means of a calibration process that will characterize the PFC2D inclusion within the continuum. For

numerical modelling purposes, we do not differentiate between the two competent layers (Beaumont dolomite and anhydrite facies).

4. Modelling strategy

4.1. Philosophy and coupling continuum-discrete modelling

When the salt exploitation restarts, the cavity will progressively grow leading to develop irreversible damage within the upper layers until the final collapse. Numerical modelling of such a complex process requires a large scale model which takes into account both the cavity evolution within the salt layer and the mechanical behaviour of the overburden layers where high deformation and fracturing are expected.

From previous mechanical laboratory investigations, both competent layers exhibit a clear elastic and brittle behaviour. To keep the elasto-brittle behaviour of the competent layers where most of seismic damage is expected and in order to directly compare the acoustic emission (AE) events, we use the PFC2D code. That allows us to represent the damage within the competent layers directly by the formation and tracking of microcracks. A detailed description of the PFC2D model and the theory is provided elsewhere (see for example Hazzard et al. 2000 ; Potyondy and Cundall 2004). Below we briefly present the main characteristics of this code.

To describe the behaviour of the other layers (mainly consisted of marls and salt) which present more ductile and/or viscoplastic behaviour, a continuum approach based on the code FLAC (a 2 dimensional finite difference code widely used by the scientific and industrial communities) is employed. This leads to approach more complex rheological behaviours based on continuum mechanics (elastoplastic with or without hardening and softening, viscoelastic or viscoplastic). Hence, the brittle layers are modelled in PFC2D as an inclusion of bonded circular particles embedded in a classical FLAC grid, the applied forces received from PFC2D act on the grid points along the inclusion boundary. The translational velocities of these boundary particles are received from FLAC. The full coupling between FLAC and PFC2D boundaries is achieved through a special function written in the internal *FISH* language.

4.2. Short description of PFC2D code

The PFC2D code models the rock mass as an assembly of particles bonded together to reproduce cohesion. The bond that connects two neighboring particles can break apart if the normal or shear stress at the bond exceeds its normal or shear strength, respectively. This corresponds to the explicit formation of a microcrack, with the spontaneous generation of a stress wave that can propagate outward from the crack. Therefore, PFC2D was extensively used to model acoustic emission in rock specimens (Hazzard and Young, 2002, 2002b) and to simulate fault zones (Hazzard et al., 2002). Interesting studies were conducted to associate many cracks that occur very close in space and time, into one microseismic event of spatial dimension of several broken bonds (Hazzard and Young, 2002b). This allows to explicitly assign seismic source parameters, such as moment tensor or magnitude values, emergent from the modelled material that can be compare with those obtained from observations.

However, in our numerical simulations, not all zones in the numerical model are necessarily submitted to large stress variations and exhibit contact breaks. Apart from that, despite the extensive use of PFC to model elasto-brittle failure in rock and some other interesting progress (Dedecker et al., 2004), it is not clear at the present time how to model more complex rheological

behaviours in PFC2D. Only the competent layers overhanging the salt cavity will be modelled with this code.

4.3. PFC2D microproperties calibration

In PFC2D, the particle contact stiffness, the contact coefficient of friction and the contact bond model between different particles govern the mechanical behaviour of the material. These are known as the microparameters (or microproperties) of the bonded particle model. They must be chosen in order to reproduce the relevant material properties measured in the laboratory tests (at a macroscale) of the rock specimen to be modelled. This calibration process is not specified a priori and a trial-and-error procedure is generally used. Nevertheless there is some knowledge and guidance based on previous research on PFC2D calibration (Kulatilake et al. 2001; Potyondy and Cundall, 2004) about the relation between each microparameter and its effect on mechanical properties (Table 1).

Following this guidance and using the previous laboratory results, we have calibrated our discrete model of the Beaumont dolomite by simulating a Brazilian test and three biaxial compression tests (at 0.1, 2 and 5 MPa of confining pressure). We used a parallel bonded model material because it seems to well approximate the mechanical behaviour of a brittle elastic cement joining two bonded particles.

This calibration process is firstly performed on the more realistic particle arrangement; say a random packing arrangements around a mean grain size. However, when the specimens are created using a random packing of particles, an extra effort is needed to obtain a uniform stress state within the sample with low 'locked-in' stresses, and to eliminate 'floaters' (particles with less than three contacts with neighbouring particles). For this reason, the calibration process is also performed on a regular hexagonal packing of particles. Some differences in the microparameters and tensile-shear microcrack initiation thresholds are therefore to be expected, particularly for microcrack densities which are dependent on the porosity of the particle packing arrangement.

Table 1. Relations between microparameters and mechanical properties.

Microproperties	**Macro mechanical property**
Normal (k_n) and shear (k_s) contact stiffness	Young's modulus (E) and Poisson's ratio (ν)
Normal ($\underline{\sigma}c$) and shear ($\underline{\tau}c$) bond strengths	Uniaxial Compression Strength (UCS)
Friction coefficient (μ) – Particle clustering Ratio shear/normal bond strength	Slope of failure envelope
Mean bond strength ($\underline{\sigma}c$) – Particle radius	Brazilian strength (σ_t)

4.3.1 Random packing

We have firstly verified the independence of the mechanical properties to the mean particle radius by performing ten different biaxial test simulations with similar microproperties. For each mean particle radius, we only change the random number generator. As expected, when increasing the resolution (increasing the number of particles along the shortest dimension of the model), the coefficient of variation (ratio of standard deviation to mean) of each material property decreases as

it was confirmed by Potyondy and Cundall (2004). From these tests, the retained microparameters are given in Table 2 and the emergent macroproperties are shown in Table 3.

Table 2. Model microproperties for the competent layers samples (parallel bonded model). Random packing.

Particles	**Cement**
ρ = 2820 kg/m^3	$\underline{E}_c$ = 65 GPa
D_{max}/D_{min} = 1.5 D_{avg} = 0.5 cm (D: particle diameter)	$\underline{k}_n/\underline{k}_s$ = 2.5
$E_c = k_n/2$ = 65 GPa	$\underline{\sigma}c$ = 120 ± 60 MPa
k_n/k_s = 2.5 μ = 0.5	$\underline{\tau}c$ = 240 ± 60 MPa

Table 3. Macroproperties of the PFC2D model of the competent layers samples (80 x 160 mm^2 specimens).

Property	**PFC2D model D_{avg} = 0.5 cm (number of samples = 10)**
E (GPa)	78.3 ± 2.4
ν	0.261 ± 0.031
UCS (MPa)	173.2 ± 8.6
ϕ (deg)	42 ± 4
c (MPa)	37.9 ± 5.1
σ_t (MPa)	44.1 ± 4.5

4.3.2 Regular hexagonal packing

The calibration of a regular hexagonal packing model was carried out starting from the retained values of the previous model shown in Table 2 for Davg (average particle diameter) of 0.5 cm. This regular arrangement of particles allows a straightforward installation of a required uniform stress within the sample by slightly modifying the particle radius. This may be useful for later applications regarding the coupling with FLAC code.

As expected, the stiffness and unconfined compressive strength of a regular packing specimen are much higher than those corresponding to a random packing specimen. For this reason, in order to keep an identical response, we drastically decrease both the bond strengths and stiffnesses of the regular hexagonal model (compare Tables 2 and 4). Similar behaviour in terms of independence of microparameters with particle radius and upscaling to regional dimensions are obtained. In Table 4 we show the retained microparameters for the hexagonal packing bonded particle model that reproduce the mean elasto-brittle behaviour of the Beaumont dolomite.

Finally, Figure 2(a) compares the simulations of uniaxial test with random and regular particle packing and the observed ones. Figure 2(b) illustrates the development of microcracks at different stage of axial stress (pre-peak corresponds to 50% of peak; peak and post-peak related to the end of test).

Table 4. Model microproperties for the competent layer samples. Hexagonal packing.

Particles	**Cement**
ρ = 2820 kg/m^3	$\underline{E_C}$ = 30 GPa
D = 0.5 cm	$\underline{k_n}/\underline{k_s}$ = 2.5
$E_C = k_n/2$ = 30 GPa	$\underline{\sigma}c$ = 25 ± 10 MPa
k_n/k_s = 2.5 μ = 0.5	$\underline{\tau}c$ = 50 ± 10 MPa

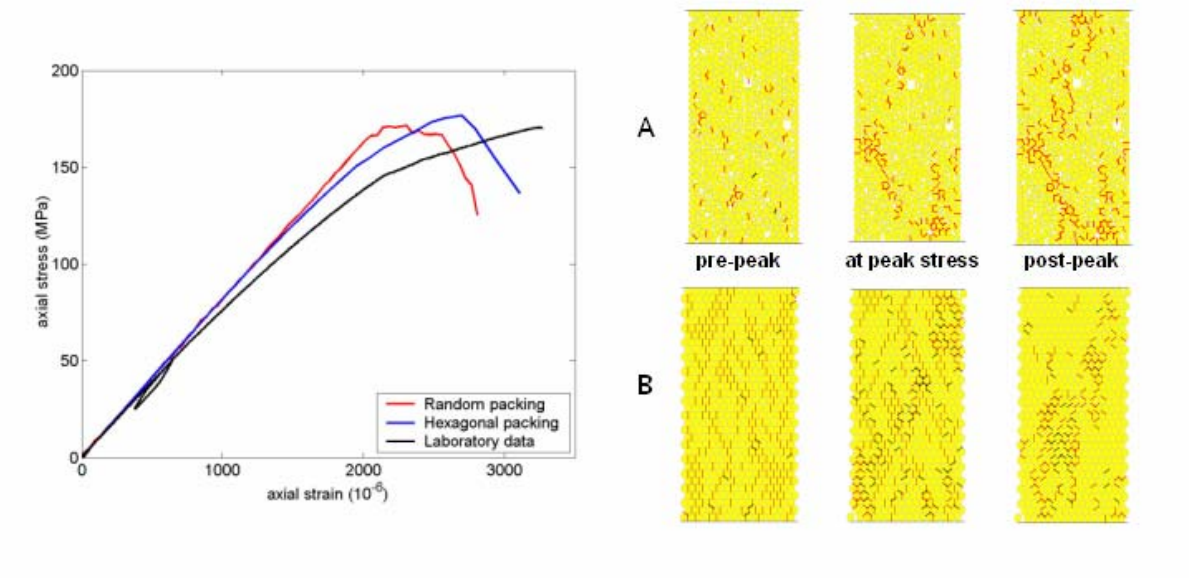


Figure 2. Uniaxial compressive test : (a) Example of axial stress-strain curve for regular and random packing and the experimental curve, (b) Microcracks distribution (A random packing, B regular hexagonal packing) at three different stages of axial stress (tensile cracks in red, shear cracks in black)

4.4. Geomechanical model

The geometrical model shown in Figure 3 is essentially composed of :

- the salt formation extending from the bottom boundary of the model up to the actual brine cavity roof,
- on top of the salt layer, a formation of intercalated marls composed of thin anhydritic to clayley marls with relatively weak mechanical characteristics,
- and the overburden characterized by two competent layers (dolomite and anhydrite level), followed by a series of carbonates, sandstones and marls layers up to the surface.

The geomechanical characteristics of the salt, the competent layers and the intercalated marls are known from the laboratory tests whereas the characteristics of the other materials are inspired on the literature of these basins. For the PFC2D inclusion (in the coupled scheme) we use the microproperties previously calibrated. The inclusion is also represented in the model.

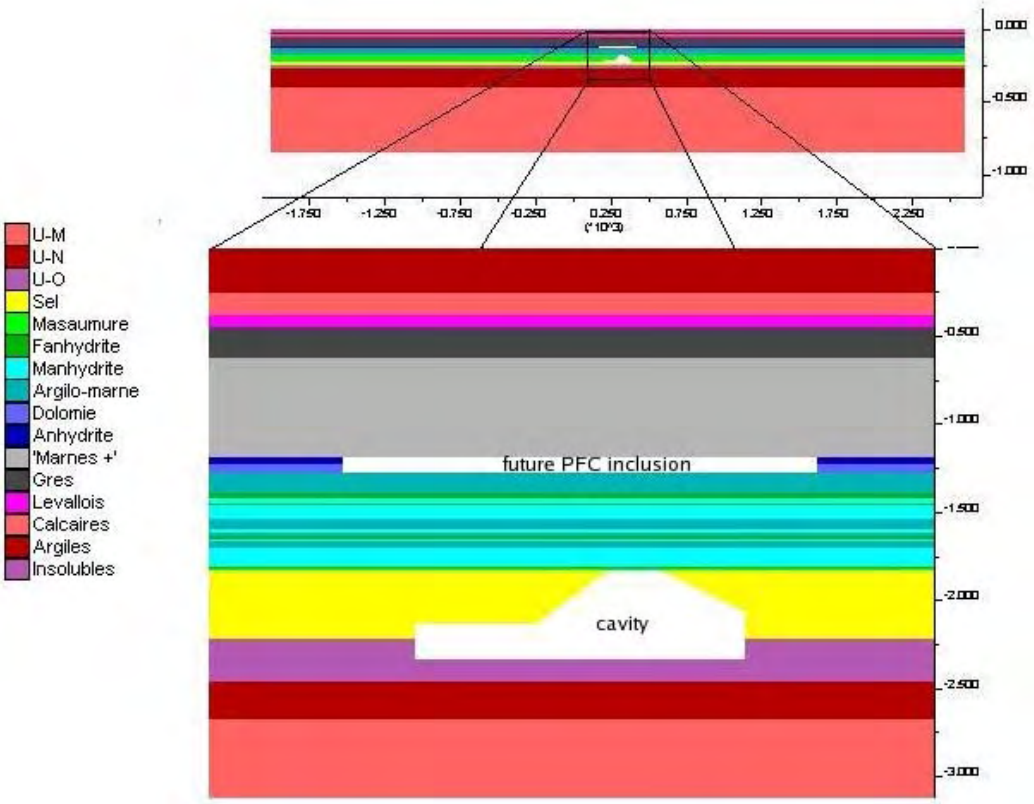


Figure 3 – Detail of the geomechanical model used in this study: the cavity in the salt layer and the PFC inclusion (used later in the coupled scheme) within the competent layers are shown.

In a first time and in order to calibrate the boundary conditions, many simulations have been carried out using an elasto-plastic behaviour for the competent layers, the corresponding optimal geomechanical model is then used in this study. The final geometrical model is 4600 m large and 850 m high.

Because of the absence of symmetry of the cavity, the problem is thus three-dimensional. In spite of its three-dimensional nature and for reasons of simplicity, we chose to perform our analysis in 2D for these first calculations. While considering a section in the greatest dimension of the cavity, we place ourselves in conditions of plane deformations. Consequently, the boundary conditions are:

- no vertical displacement at the bottom boundary of the model (assumption of fixed substratum).
- no horizontal displacement at the lateral boundaries (they are placed far enough to neglect any influence from the cavity filling out process).

The initial stress state is assumed to be isotropic: this assumption is well justified within the salt layer where null initial deviatoric stress is expected. In absence of data concerning the initial stresses in the other materials, we also admit that they are isotropic (a sensitive analysis on the stress anisotropy ratio in such formations can be undertaken on the basis of the literature data). Finally, the vertical stress is equal to the overburden weight.

The initial conditions within the PFC inclusion and in the cavity before the exploitation restarts:

- we established an unifrom isotropic stress of 3 MPa within the PFC domain corresponding to the approximate initial stress found at the inclusion depth due to the overburden weight .
- When the cavity is full of brine, a normal stress acting on the cavity walls equal to $\lambda\ \sigma_0$ is imposed (σ_0 is the overburden weight at the corresponding depth, and λ=0.5). The progressive filling out of the cavity is modelled by progressively reducing λ from 0.5 to 0 (empty state of the cavity).

5. Results of large scale modelling

5.1. Fully continuum approach

As previously mentioned in the continuum approach, we assume that all off the competent layers are viewed as an elastoplastic material. The aim of this assumption is: (a) to guarantee the type of boundary conditions (applied forces or fixed normal displacements) that will be specified, as well as the external model dimensions with regard to the cavity size, and (b) to keep the model reaction (global response under the initial conditions and when filling out the cavity).

The vertical displacement evolution on top of the Beaumont dolomite and the subsidence at the topography surface are illustrated in Figure 4 as a function of the brine pressure within the cavity: (a) $\lambda = 1$ virgin rock mass, (b) $\lambda = 0.5$ initial state of the cavity full of brine, (c) $\lambda < 0.5$ simulating a progressive filling out of the cavity ($\lambda = 0$ representing the empty state of cavity).

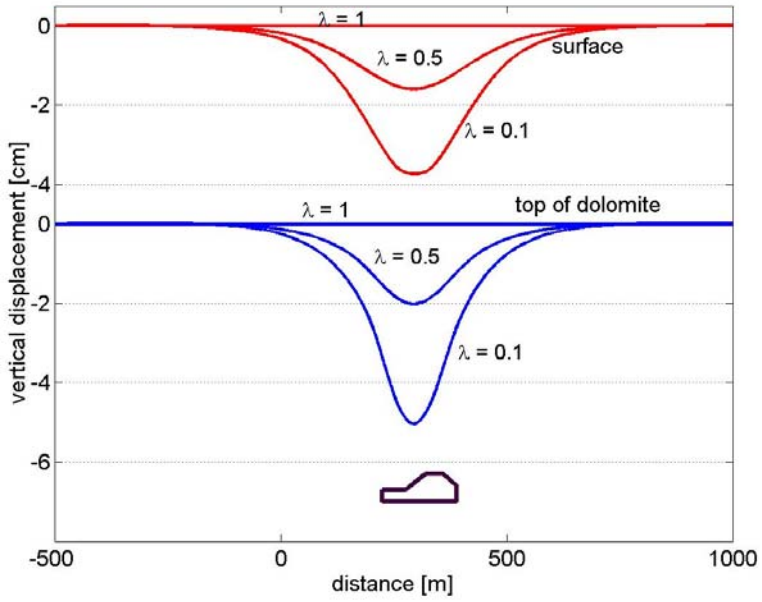


Figure 4. Vertical displacement evolution at the surface and at the top of dolomite (the salt cavity is schematically shown).

In Figure 5, we can appreciate the state of the plastic zones through the layers lying on top of the cavity for λ around of 0.1. The competent layers remain stable and the plasticity migrates from the weakest layers within the intercalated marls and located at the immediate roof, up to the base of the

competent layers. For $\lambda = 0$, most rock materials intercalated between the salt formation and the dolomite fail, leading to a significant stress report in the competent beds.

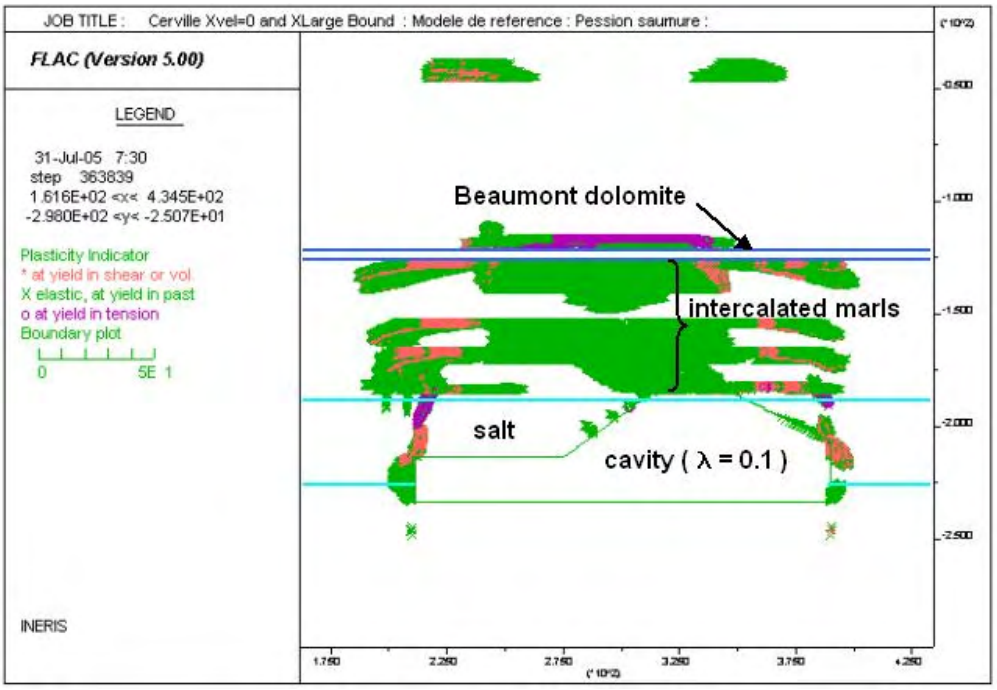


Figure 5. State of plasticity in the overburden layers for $\lambda = 0.1$. The competent layers remain stable (without plastic points).

5.2. Coupled continuum-discrete approach

The coupling scheme embeds a PFC2D inclusion region within the FLAC grid (the complementary domain of the inclusion in the competent beds where microseismic events are not expected is modelled as a continuum domain). A PFC2D material must be created to confirm the inclusion region such that a single layer of particles overlaps the boundary as illustrated in Figure 6. The applied forces received from PFC2D act on the grid points along the inclusion boundary. The translational velocities of these boundary particles are received from FLAC after one step of calculation (*i.e.* after the motion calculation where velocities and displacements are computed based on the internal and external forces acting on the gridpoints).

Using the calibrated hexagonal parallel bonded model[2], a rectangular PFC2D inclusion within the FLAC model has been created. As a first step, we decided to limit the inclusion to the region where the greatest variation in ambient stress are produced due to the cavity growing. The inclusion centred on top of the actual cavity, is 260 m long by 8.5 m thick, and it covers the dolomite and the anhydrite levels (see Figure 3). Filling this area with circular particles of 0.5 m diameter gives a total number of 10800 particles forming the inclusion. A detail of the coupled model can be seen in Figure 6.

Before establishing the coupling process, a uniform isotropic compressive stress of 3 MPa is obtained within the PFC2D inclusion prior to its connection to the FLAC grid. This allows faster convergence of the initial coupled model to be stabilized. For the rest, the coupled FLAC-PFC2D

2 Due to difficulties encountered in installing an initial stress state near 3 MPa with a random particle packing, we have use for this feasibility study the regular particle packing, some differences are therefore to be expected.

scheme is run with similar boundary and initial conditions as the fully FLAC simulations specified in the previous section.

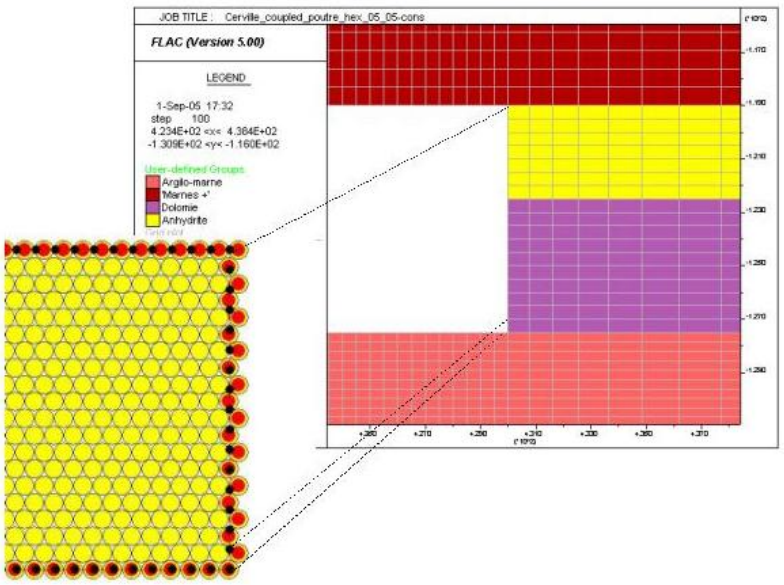


Figure 6. Detail of the right limit of PFC2D inclusion within the FLAC grid. Boundary particles (red) and grid node positions (black) are shown in the PFC2D domain.

The resulting force distribution in the cement between particles of the PFC inclusion can be seen in Figure 7. From $\lambda = 0.5$ down , we can appreciate the increasing zone in tension at the middle of the inclusion, where almost all microcraking occurs. A number of tensile cracks develop first with a random spatial distribution and concentrating later in the central part of the inclusion (just on top of the cavity). The number of microcraks (also shown in Figure 7) increases from about 20 at $\lambda = 0.5$, up to more than 100 at $\lambda = 0.1$. There is a sudden rise up between $\lambda = 0.3$ and $\lambda = 0.1$ manifesting the failure instability within the stiff layer. However, a clear tensile fracture can not be identified at this stage, as it was the case for the fully continuum modelling approach (see Figure 5).

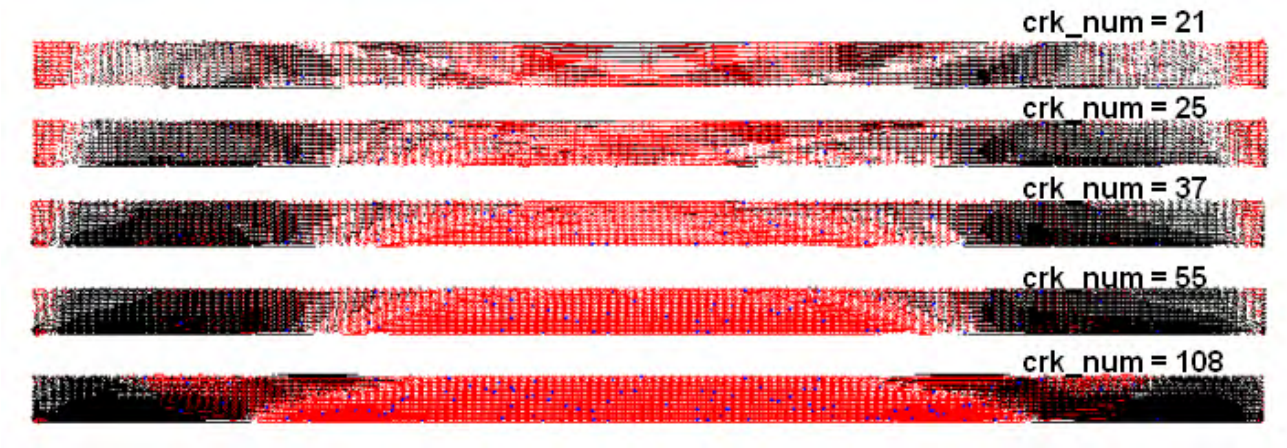


Figure 7. Bond forces in the cement between particles (black = compression, red = in tension) of the PFC inclusion at (from top to bottom) $\lambda = 0.5$, 0.4, 0.3, 0.2 and 0.1. Tensile cracks are shown in blue.

6. Concluding remarks

We have presented a preliminary investigation of a coupled continuum-discrete modelling strategy to analyse a complex geomechanical and geophysical process in a salt mine-environment. This involves the fracturing and deformation of the overburden due to brine pumping out and the consequent pressure decrease in the underground cavity.

Based on the results of a laboratory geomechanical characterization, we have calibrated the microproperties of the PFC2D model to be used as the discrete inclusion within the competent layers in the overburden. We used both a random and hexagonal particle packings to create the parallel bonded specimens. The influence of the particle size and the scale effect was analysed. We do not notice any drastic change in the emergent mechanical properties of the modelled materials at both the laboratory and regional scale. This suggests that the use of PFC for modelling the elaso-brittle behaviour of competent layers at the regional scale should be satisfactory.

On the other hand, the effect of particle packing seems to be extremely important in the macro response of the modelled material. The samples created with an hexagonal regular packing are stiffer than those created with a random packing. Also the former present much higher compressive and tensile strengths while keeping the same microproperties for both specimen types. That forced us to perform another calibration process of microparameters for this form of particle packing.

We obtained the first results with the coupled FLAC-PFC2D scheme using an hexagonal PFC2D inclusion 260 m length by 8.5 m height embedded in the Beaumont dolomite layer. The development of microcracking is in accordance with the predicted tensile zone obtained with a fully continuum approach. On the other hand, the sudden rise up of the microcracks number can be interpreted as the damage initiation within the competent beds. A conclusive statement about the failure mechanisms could be achieved when information about real microseismic event locations will be available.

Let us notice that this work is a preliminary one in such complex geomechanical modelling field. In addition, the presented results remain specific to several simplified assumptions taken compared to reality; in particular for the cavity geometry and its evolution, but also for the geomechanical properties of certain materials at the immediate roof and in the overburden, which influence the behaviour of the competent layers.

This research opens many new perspectives in modelling the induced seismicity of the study area. The following steps should be: (a) after installation of the initial stress state in the PFC2D inclusion by assuming a more realistic particle packing (random packing), to perform a sensitive analysis on the microcrack threshold, and evaluate its effect on the mechanism of microcrack growth, while computing the associated AE; (b) to compare these numerical modelling results with those of the measurements recorded in situ after restarting of salt exploitation in a few months.

ACKNOWLEDGEMENTS : This works has been performed within the GISOS framework. We acknowledge with gratitude the financial support of the MEDD and MinEFI French ministries. to subventions. The authors also thank the company SOLVAY S.A. for the site, the technical support at the time of the experiments and the data of the site characterization

7. References

Cundall P. A., Strack O (1979). *A discrete element model for granular assembies.* Geotechnique, 29, 47-65.

Dedecker F., Billaux D. *Evaluation of damage-induced permeability in the bure site using a three dimensional adaptive continuun/discontinuum code*, in Clays in Natural end Engineered Barriers for Radioactive Waste Confinement. Tours 2nd International Meeting, March 14-18, 2005.

Hazzard J. F., Young R. P., Maxwell (2000). *Micromechanical modelling of cracking and failure in brittle rocks*. Journal of Geophysical Research, Vol 105, 37555-37569.

Hazzard J. F., Collins D. S., Pettit W. S., Young R. P. (2002). *Simulation of unstable fault slip in granite using a bonded particle model*. Pure and Applied Geophysics 159, 221-245.

Hazzard J. F., Young R. P. (2002b). *Moment tensors and micromechanical models*. Tectonophysics, 356(1-3), 181-197.

Itasca Consulting Group. (1999) *PFC2D (Particle Flow Code in 2 dimensions)*. Minneapolis, Minessota: Itasca Consulting Group, Inc.

Itasca Consulting Group. (1999) *FLAC (Fast Lagrangian Analysis of Continua)*. Minneapolis, Minessota: Itasca Consulting Group, Inc.

Johnston, J. C., Einstein, M. H., 1990, *A survey of mining associated seismicity*; Proc 2nd Int Symp Rockbursts and Seismicity in Mines, Minneapolis, Fairhurst (ed), Rotterdam:, A.A. Balkema, 121-127.

Kulatilake P., Malama B., Wang J. (2001) *Physical and particle flow modelling of jointed rock block behavior under uniaxial loading*, International Journal of Rock Mechanics and Mining Sciences 38, 641-657.

Mendecki, A. J., van Aswegen, G., Mountfort, P., 1999 *A guide to routine seismic monitoring in mines*, in A Handbook on Rock Engineering Practice for Tabular Hard Rock Mines, Jager and Ryder (eds) SiMRAC, Cape Town, South Africa.

Potyondy D, Cundall P. (2004) *A bonded particle model for rock*. International Journal of Rock Mechanics and Mining Sciences, 41(8), 1329-1364.

FROM DISCOVERY TO BACK FILLING OF POTENTIALLY UNSTABLE MINING VOIDS: THE CASE OF THIL (54).

MIDOT Dominique[1], MARNET Alain[2], GIONTA Jean-Philippe[2], TREBUCQ Sébastien [1]

[1]GEODERIS, 1 rue Claude Chappe, BP25198–57071 Metz Cedex 3– France.

[2]DRIRE, 15 rue Claude Chappe, BP 95038 – 57071 Metz Cedex 3 – France. ,

Abstract: The mining cavities located under the Stock housing estate in Thil (54) were discovered in June 2002 by GEODERIS, as part of the programme of surveying areas with a risk of subsidence related to mining works in the Lorraine iron-ore field. These cavities, with a volume of about 10,000m3, are located at an average depth of 62m, in an area that was indicated, in the 1/5000th scale abandon drawings, as fully stoped and caved in.
The first stage involved setting up video camera surveillance to ensure the safety of persons. In parallel and in accordance with the law of 30 March 1999, a comparative analysis between the cost of treatment of the mining works and the value of the property concluded in the feasibility of treatment compared with the cost of expropriation, leading to the Prefect taking the decision to back fill.
The back filling work began in August 2004 and were completed in March 2005. About 15,000m3 of grout were injected in the cavities i.e. 50% of grout losses in the stopes. The estimated final cost of the operation is about €2.7million, which corresponds to a cost per m^3 of injected grout, of about €180.

KEY WORDS: mining cavities,back filling, fly ash.

RESUME : Les cavités minières situées sous la Cité du Stock à Thil (54) ont été découvertes en juin 2002 par GEODERIS, dans le cadre du programme d'étude des zones à risque de fontis liées aux exploitations minières du bassin ferrifère lorrain. Ces cavités, d'un volume d'environ 10 000m3, sont situées à une profondeur moyenne de 62m, dans une zone qui était indiquée, sur les plans d'abandon au 5000ème, comme intégralement dépilée et foudroyée.
La première étape a consisté à mettre en place une surveillance par caméra vidéo afin d'assurer la sécurité des personnes. Parallèlement et conformément à la loi du 30 mars 1999, une analyse comparative entre le coût de la mise en sécurité des travaux miniers et la valeur des biens a conclu à la faisabilité d'une mise en sécurité par rapport au coût d'une expropriation, conduisant le préfet à prendre la décision de combler.
Les travaux de comblement ont débuté en août 2004 pour s'achever début mars 2005. Environ 15 000m3 de coulis ont été injectés dans les cavités soit 50% de pertes de coulis dans les dépilages. Le coût final de l'opération est estimé à environ 2,7 M€,ce qui correspond à un coût par m^3 de coulis injecté, d'environ 180€.

MOTS-CLES : cavités minières, comblement, cendres volantes.

1. Introduction

The mining cavities located under the Stock housing estate in Thil were discovered in June 2002 by GEODERIS, as part of the programme of risk analysis related to mining works located at low depth (<50m): areas with a risk of sinkholes. This programme, which provides for the detailed surveying of about 177 hectares of undermined areas, began in 2000 and is due to be completed in 2009. The areas with a risk of subsidence located in the town of Thil, which are considered as a priority, were among the first to be surveyed.

The aim of this article is to describe the sequence of work to be carried out which, from the risk analysis and reconnaissance phases, led the treatment while guaranteeing, throughout the process, the safety of persons.

2. Geographical, geological and mining frameworks

The town of Thil is located in Meurthe et Moselle at 70 km to the north west of Metz and 15 km to the south of Longwy, near the Luxembourg border. It is located in the northern part of the Lorraine iron-ore field or Briey-Longwy field. The Lorraine iron deposit is of sedimentary origin dating back to the late Toarcian and Aalenian periods and extends of more than 130 km. The iron-ore formation, with an average thickness of 30m, contains up to 9 workable layers, sloping slightly towards the west (3%). In general, minerals have only been worked in a few layers or even a single layer as in Thil. Under the Stock housing estate, the mining works date back to the end of the 19th century and beginning of the 20th century, and the methods used are of the tracing and "widening" type following by stopes. During the Second World War, the main gallery was used for military purposes (assembly of V1 rockets), which led to its gauge being increased considerably. This widening caused two sinkholes which took place in 1946 and 1957.



Figure 1. Sinkhole of 1946. To the left: surface view, to the right: bottom view.

3. Risk analysis and reconnaissance, setting up of monitoring

It was when continuing the underground reconnaissance of mining works, beyond the 50m coverage limit, that the three cavities were discovered, at about 1km from the mine entrance, in an area indicated as fully stoped and caved in the 1/5000th scale drawings of the abandon folders.

The main cavity, of dimensions 90mx50m, is characterised by a high proportion worked (90%), small slim pillars (12m x 6m maximum), large roof (up to 30m) and a ceiling height of 2.5m. There was a very advanced general state of degradation with intensely fractured or even partially ruined pillars and spectacular roof collapses (figure 2). The two other significantly smaller cavities (950m3 and 50m3), were discovered by drilling (ST04 and ST01), during additional exploration phases. All the cavities are located above the water table.



Figure 2. State of degradation of the pillars and roof of the main cavity

The mining cavities are located at an average depth of 62 m under the Stock housing estate. The stability calculations concluded that there was a potential instability in the massif with a risk of sudden collapse of all the terrains located above the cavities. The potential hazards area covered 1.4 hectares and included 9 buildings, 2 collective garages, in other words a large part of the Stock housing estate, and a water tower (figure 3). 27 homes including 65 people are concerned by this risk.

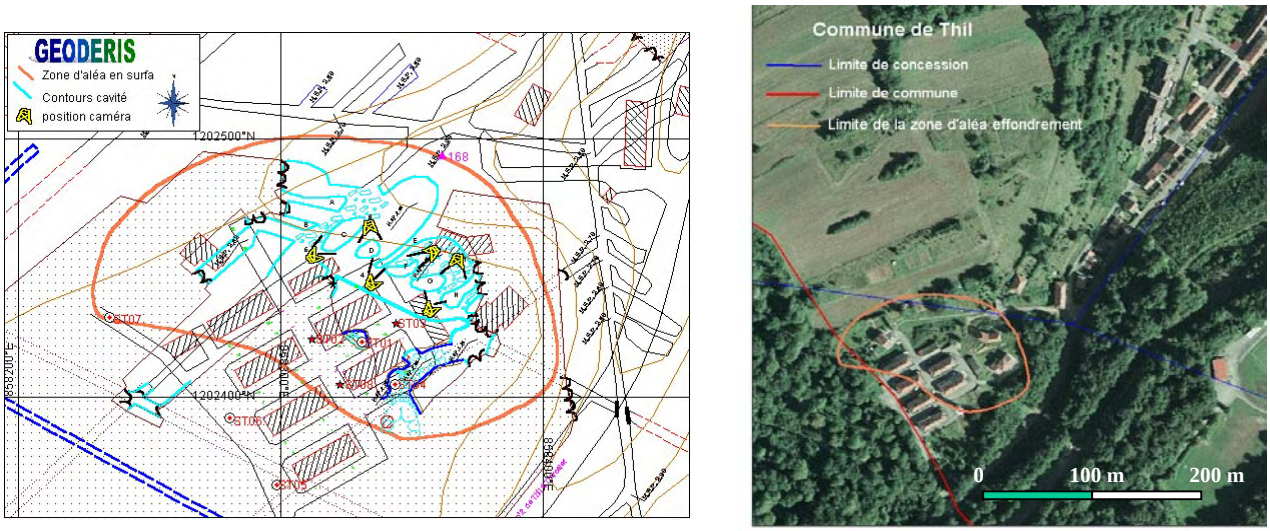


Figure 3. Mapping of cavities and plotting of the potential hazards area.

The sudden collapse phenomenon, due to the damage it causes to buildings, is a physical risk to occupants. Thus, from mid August 2002 onwards, in other words less than 2 months after the discovery of the cavities, a monitoring device was operational.
This device consisted of six video camera which allowed changes in the degradation of pillars to be monitored. The images were sent to the GEODERIS office in Metz over a telephone link where the image of the day was compared with the image of the previous day 7 days a week. In parallel, the images were recorded on the spot, on video tape, in sequences of 35 seconds per camera, thus forming a bank of images providing a trace of any event at any time of the day or night.
The monitoring procedure allowed 65 people to be evacuated from the Stock housing estate within 4 days at the most of an aggravation of the situation being observed and the alert to be initiated. Monitoring was maintained during the filling phase with a double frequency (2 viewings per day) and ended with the total filling of the cavity, at the beginning of 2005.

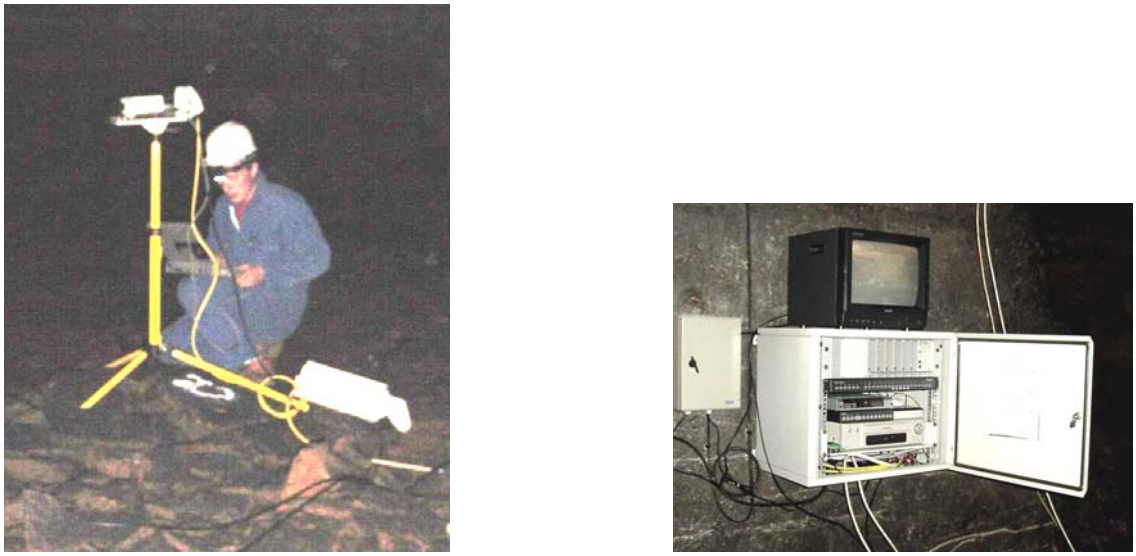


Figure 4. Setting up of the video surveillance system: camera and multiplexer.

4. Comparison between the cost of treatment (remediation) and value of the property

The cost of treatment and the value of the property were compared jointly with the setting up of the monitoring and in accordance with the law of 30 March 1999. Indeed, article 95 of this law indicates that, in the event of a mining risk posing a serious threat to the safety of persons, the property exposed to this risk may be expropriated by the State, when the means of safekeeping and protecting populations proves to be more costly than expropriation.

The financial assessment of the property was carried out by the Service des Domaines (domain department).

The technical/economic feasibility survey for the treatment of the site was given to the INGEROP Grand Est design office.
The choice of the filling method and materials had to meet the following criteria:

- a mechanical criterion: the filling product had to have an eventual compression strength of at least 2.5 MPa, and this behaviour must not deteriorate over time,

- an environmental criterion: the contamination of infiltration water percolating through the filled in area had to be as low as possible so as not to contaminate the AEP collection of the Hussigny-Godbrange well, located 1km downstream,
- the processing method had to be able to be implemented in an urban environment, without relocating populations and without interrupting the surveillance.

It was also stipulated in the specifications that the elimination of the risk of sudden collapse did not call for the neighbouring stopes to be keyed or impregnated.

In the feasibility survey, two back filling methods and several types of materials were examined.

The back filling of cavities from underground was quickly eliminated on account of the prohibitive cost of stabilizing about a kilometer of gallery. The filling by injection from the surface was thus opted for.

Various types of filling materials were envisaged:
- non cohesive materials: sand, pure fly ash,
- cohesive materials: fly ash/cement or bentonite/cement based grout and sand/cement (and bentonite) based mortars.

The use of non cohesive materials proved to be technically difficult and not cost effective due to the water consumption during filling (10 to 15 times the volume filled in) and the difficulty of confining materials properly from the surface, as required to obtain the desired strength.
Cohesive materials were selected in accordance with the mechanical and environmental criteria indicated above as well as for their ease of use, their cost and their availability.
Sand and cement based (and bentonite) mortars and bentonite/cement based grout were not selected as:
- they are difficult to use as mortars: they only run over 5 to 10m compared with 50m to 70m for grout, which calls for the number of injection boreholes to be increase,
- the cost of the material for bentonite/cement grout is high: about €34/m^3 ex. tax compared with €18 to 24 /m^3 for fly ash/cement grout and €26 -€27/m^3 ex. tax for mortars (excluding implementation).

On completion of the technical/economic feasibility survey, the solution selected was to back fill from the surface by injection of fly ash and cement based grout. The use of fly ash from the La Maxe EDF power plant field was opted for because of its proximity (52 km from Thil) and the availability of the material throughout the year.

As the cost of this solution proved to be slightly lower than the expropriation cost, the Prefect took the decision to back fill.

5. Surveys prior to back filling work

Having confirmed the feasibility of a solution of back filling in by injection of fly ash based grout, it remained to assess the potential effect of filling in on the environment and more particularly on underground resources, the area to be filled in being located in the future protection perimeter, away from the Hussigny-Godbrange drinking water collection areas. This impact survey was carried out by BRGM in cooperation with GISOS and LAEGO. It involved:

- the physical/chemical characterisation of the fly ash and in particular of the content of potentially contaminating elements,
- the survey of the long term behaviour of a flying ash/cement grout, from both the mechanical and chemical standpoint,
- the survey of the mining reservoir hydrogeological context.

The physical/chemical characterisation of fly ash was determined using 95 samples taken from eight substratum boreholes, representing the whole field No. 4 of the La Maxe EDF power plant.
The samples were analyzed by portable X fluorescence spectrometry (Niton 723S), monitored by laboratory analysis by ICP/MS. The distribution of concentrations according to depth showed, for the whole field, a stratification significantly marked with a higher content of sensitive contaminating elements at depth (mainly lead and arsenic): the concentrations were higher than the usual sensitive VCI (impact observation value) at a depth greater than 2.5m for arsenic and 4.5m for lead. On the basis of these results, it was thus decided only to use fly ash located at a depth of less than 1.5m to manufacture the grout. A finer mapping of the concentrations in terms of sensitive contaminating elements contained in the field was carried out during the filling work preparation phase. The results are presented in paragraph 6.1.

The mechanical behaviour was studied for three fly ash/cement (CV/C) proportions: 90/10, 80/20 and 70/30 and two types of slag cement: CEMI and CEMIII.
The simple compression tests showed that the required strength (2.5MPa) was just achieved after 90 days for a CV/C proportion of 90/10 (RC: 2.52MPa) but it was largely exceeded for grout richer in cement with strengths of 4.82 MPa for grout with a 80/20 proportion and 7.10 MPa for grout with a 70/30 proportion.

The chemical behaviour was investigated by means of lixiviation tests in columns, carried out on crushed grout with a grain size of between 3.5cm and 4 cm. The water used was similar in composition to that of the site. The lixiviation tests were first carried out in a closed system for 14 days for the water to be balanced chemically with the grout, and then in an open system with a supply rate of 300ml/day, also for 14 days.
The results showed that, for equal formulation, the grout made with CEMI cement was significantly more contaminating than the grout made with CEMIII, notably in terms of chromium, cobalt and arsenic. On the other hand, and for a given type of cement, there is no systematic link between the release quantity of an element and the grout V/C proportion, which would seem to indicate that the elements can be released by either ash or cement.

On the basis of these results, it was concluded that a grout containing 85% CV and 15% CEMIII type cement should meet both the strength criterion (2.5 MPa) and the environmental criterion (minimum release of contaminating elements).

And finally, to assess the potential effects of the filling in on the Hussigy-Godbrange AEP collection, located at 1km downstream, the transfer of chemical elements from the filling washing was modelled. For this purpose, the mining reservoir was assimilated to a network of tubes in which most of the run off takes place via the galleries, the surrounding terrains being considered as impermeable. In this model, the water supply points are formed by the stoped off and caved in areas and the output points coincide with the current overflow and AEP collection point.
The results of the modelling indicate dilution rates of the washing water at the AEP collection point of between 30 and 260. This means that the Hussigny-Godbrange AEP collection point cannot be contaminated by the filling in of cavities; the concentrations calculated at the AEP will be about a thousand to a million times lower than those of the drinkability standard.

6. Back filling work

The work began in mid August 2004 by a preparatory phase followed from November 2004 onwards, by the filling phase proper which was completed at the beginning of March 2005. The contracting authority was DRIRE Lorraine, project leadership was provided by the INGEROP Grand Est office and the injection work was carried out by the Soletanche-Bachy company. Arcadis was in charge of the external check and GEODERIS acted as advisor to the contracting authority.

6.*1) Characterisation of the stock of fly ash of La Maxe field No. 4*

The preliminary survey of the field ash had concluded, with a small number of boreholes, that the field ash could be used provided the depth is limited to 1.5m. However, before using this ash on a wider scale, the distribution of the most penalising elements should be accurately defined.

85 boreholes, with a unitary length of 1.5m, were made using a portable lanterned core barrel, using a 10m by 10m mesh. The ash was analyzed routinely for six elements (arsenic, barium, copper, manganese, lead, zinc). 10 monitoring samples were subjected to multi-elementary analysis for 23 elements.



Figure 5. Field fly ash. To the left, lanterned core barrel sampling for samples. To the right, clod breaker.

Most of the samples showed levels of sensitive contaminating elements (As, Pb and Cu) lower than usual sensitive VCIs except for 4 samples in which the arsenic concentrations were greater. The

corresponding plots were not used to make grout. About 10,000t of ash was excavated, the clods broken on the spot down to a grain size of 20mm and then transported by truck to the site.

6.2) Boreholes and laser examinations

26 boreholes each 70m long were drilled including 14 for the dams, 6 for injection and 6 to check the rise of the grout. The maximum authorized deviation was 1.5% (i.e. 1m for 70m bored) and this was checked by inclinometry. The boreholes were fitted with PVC tubes of dimensions 112mmx125mm for injections and passing the various sensors.

The geometry of the cavities was then checked by laser shots, coupled with video images. The position and range of the stop edges were thus able to be located and the cavities were positioned accurately relative to the surface elements (frame and infrastructures).

Following the examinations, the selected volume of the cavities is distributed as follows:

- main cavity: 9000m^3
- ST04 cavity: 950m^3
- ST01 cavity: 50m^3

i.e. 10,000m^3 in all.

6.3) definition of the formulations of grout and variations in strengths

The best performance, and in particular as regards strengths, is obtained by seeking the best proportioning between fly ash and cement. The proportions of the filling grout proposed under the contract, for each m3 of grout, were 144 kg of cement and 818 kg of fly ash but the tests, carried out within the framework of the project, showed that the required compression strength of 2.5MPa could not be obtained within 90 days. The quantity of cement was thus increased to 171 kg, with, for each m^3 of grout, 727 kg of fly ash (i.e. an ash/cement ratio of 81/19) and 619 l of water.

The proportions of the rigidified dam grout were 300kg of cement, 700 kg of ash and 10% of silicate plus water. To provide better control over the mixture and avoid untimely setting in the conduits, the silicate was injected at the foot of the borehole.

The simple compression strength tests (Rc) carried out on 31 May 2005 within the framework of the external check (Arcadis) are shown in the graph below.

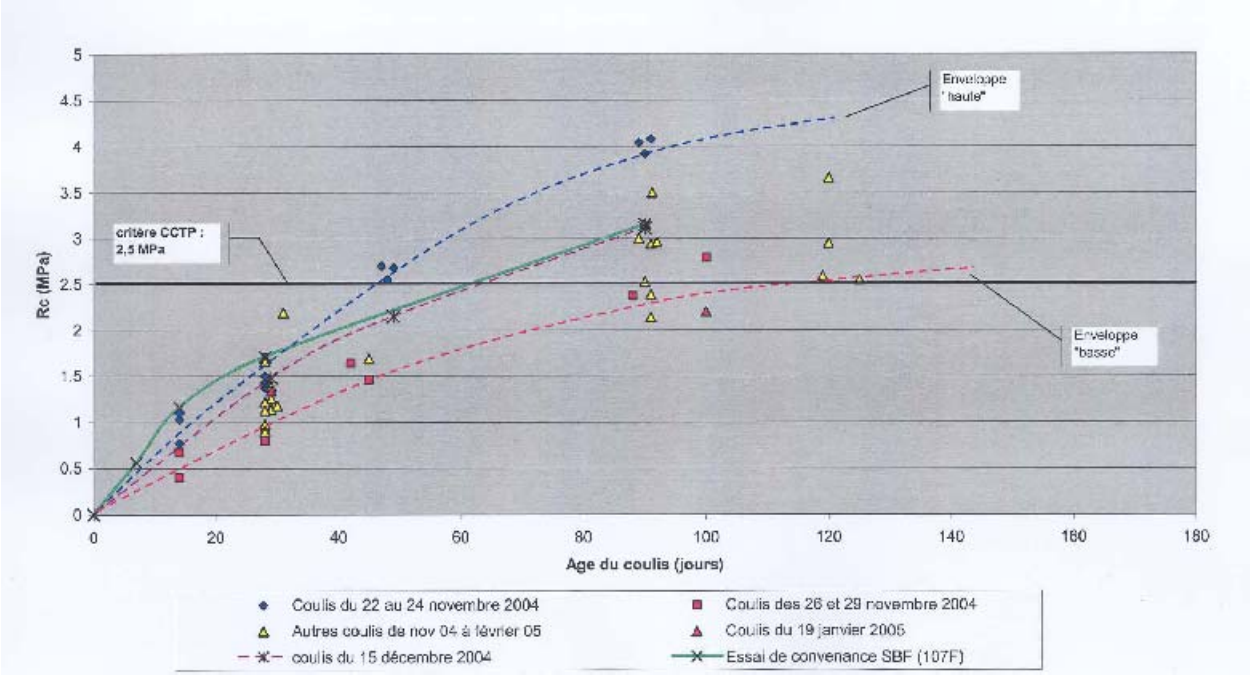


Figure 6. Results of the simple compression tests on the filling grout (source Arcadis)

This graph shows that virtually all the samples tested will in the end exceed the acceptance criterion (2.5 MPa). It can, however, be seen that there is a fairly wide dispersion of the values between an upper range with Rc of 1.4MPa and 4.0MPa at 28 days and 90 days and a lower range showing lower strengths with Rc of around 0.8 MPa and 2.5MPa at 28 days and 90 days. Most of the low values correspond to low density grout (<1.5) due to an excess of water. It would appear that the dispersion of values is not due to variations in the mineralogical composition of the ash but reflects more the difficulty of controlling the water content in the event of significant variations in the hydrometry of the ash. With a doubling or even a tripling of the strengths, the fly ash pozzolanic effect seems to have played its full role between the 28th day and the 90th day.

6.4) Manufacturing and injection of grout and monitoring of back filling

Back filling was carried out by gravity injection of grout from the surface through the boreholes. Grout based on fly ash was made on the spot as and when needed, in a mixer with a maximum capacity of 3m^3, mounted on spring balances and controlled by a programmable logic controller, into which water, cement and damp fly ash were successively added. The quantity of water added was calculated according to the hydrometry of the ash, which was measured twice each shift (at the beginning and in the middle of the shift). In addition to the hydrometry, the density and viscosity of the fresh grout and the liquating after 3h were regularly checked on the site, with a tolerance of:

- from 1.50 to 1.54 for the density,
- from 8s to 10s for the viscosity (at T0 and at the 10mm nozzle),
- from 1.5% to 2.0% for the liquating.



Figure 7. To the left, injection plant. To the right, regulation programmable logic controller.

To prevent grout losses, the borders of the main cavity were enclosed by dams of rigidified grout except for one side, which was left open, on an experimental basis, at the start of filling, to determine the grout distribution distance in the stopes.
The main entry was sealed off by a bricked wall the building of which called for the access gallery to be stabilized at several points by angled timbering.

The widest dams along the stopes called for several injection boreholes, spaced by 2m. The dams were erected at the same time as the filling grout, slightly above the grout level. The erection of the dams was monitored by a video camera during boring.

The filling grout was injected alternatively via several boreholes distributed over the whole extent of the cavities so as to obtain a regular rise of grout. The grout rise was monitored on a daily basis by means of six ultrasonic sensors located in the boreholes. The video surveillance cameras also proved very helpful in viewing the rise of the grout.



Figure 8. Monitoring of grout rise: to the left by ultrasonic sensor, to the right by video camera

On the basis of the quantity of grout injected and the height of the rise given by the ultrasonic sensors, an extended surface was then calculated and compared against the real area of the cavities, thereby allowing the losses to be assessed. In the event of observed losses, corrective action involving decreasing the injection rate, lengthening the waiting time between two injections, thereby ensuring better setting of the grout and, if need be, the injection of more viscous grout.

The volumes of grout injected for each cavity are summarised in the table below.

	Cavity volume (m^3)	*Volume of grout injected (m^3)*	*Losses (%)*
Main cavity	*9 000*	*12 123*	35%
ST04 cavity	*950*	*2 283*	140%
ST01 cavity	*50*	*620*	1140%
Total	***10 000***	**15 026**	**50%**

Table 1. Volumes of grout injected versus volumes of cavities

The total volume of grout injected comes to 15,000m^3 for a cavity volume of 10,000m^3 i.e a loss of grout in the stopes of about 5,000^3 equivalent to 50% of the initial volume. Due to the grout losses, the average injection rate throughout the filling duration was only 286m^3/day for a nominal capacity of 450m^3/day.

In the main cavity, accessible from the bottom and by far the best known, the losses were only 35% (equivalent of about 3,000m^3 of grout). They were proportionally significantly greater in the other two cavities, which were not accessible, which accounts for voids or particularly permeable stopes which were not able to be identified during laser examinations and video camera during boring.

The estimated final cost of the operation is €2.7million i.e. a cost of €180 per cubic meter of injected grout.

7. Trials

The back filling of the mining cavities located under the Stock housing estate in Thil provides a unique opportunity to monitor the *in-situ* variation of filling based on flying ash grout and its effect on the natural drainage in the environment. Several actions were thus taken on a trials basis, in particular concerning the mechanical and chemical behaviour of grout and its dispersion in stopes.

The examination of the mechanical behaviour of grout will involve carrying out simple compression strength tests on samples of boring cores that will be sampled a year after the laying of the grout, over the whole thickness of the filling and over the whole extent of the cavities. A good image of the distribution of strengths within the grout monolith will thus be obtained. Its dispersion in the stopes will be examined by means of horizontal core boring carried out underground, from the entry of the main cavity and in the direction of the stopes.

The examination of the chemical behaviour will be based on the fluids from the fresh grout (so called liquating) and the infiltration water percolating through the filling. A device consisting of 5 resistivity sensors, 2 temperature sensors and an acquisition unit was installed before the filling phase. This arrangement will allow variations in the water composition to be monitored continuously over fifteen months after the end of filling. Chemical analysis will also be carried out regularly.

8. Conclusion

The Thil case provides a perfect illustration of the problem of managing the aftermaths of the closing of mining works. More than two and a half years of surveys and work costing several millions euros were needed to identify the mining risk, and monitor and eliminate this risk by work to establish safety.
Thil also provides a unique experience dealing with the risk of land movement by back filling in deep mining cavities by injection from the surface, of fly ash based grout. The lessons learned in terms of rheological and chemical behaviour of grout, confinement techniques, injection and follow up of filling, will be extremely valuable for future safety establishing work.
Thil is also an example in terms of cooperation between the Public Authorities and the various participants in the post mining era where the safety of populations has always been at the centre of concerns.

9. Acknowledgements

We would like to thank the INGEROP Grand Est, EDF, Solétanche-Bachy and Arcadis companies for making this information available. The authors also benefited from the surveys carried out by and BRGM, GISOS and LAEGO.

10. Bibliography

Arcadis (2005). *Mechanical compression strength of hardened grout. Memo No. 72 0559 002 CL 03 B.*

Baubron J-C, Fabriol R, Fourniguet G., Hamm V., Vaute L. (2003). *Hydrogeological modelling of the Godbrange mining reservoir and the effect of partial filling with fly ash. Report brgm/RP-52802-FR, 67p., 22 fig., 12 tab., 6 ann.*

Géodéris (2002). *Assessment of the risks of localised collapsing under the Stock housing estate, in the town of Thil (54).* Géodéris memo No. N2002/077.

Géodéris (2002). *Proposal of a video-surveillance system permanently installed at the bottom.* Stock housing estate, town of Thil (54). Géodéris memo No. N2002/038.

Géodéris (2002). *Determining of areas with a potential risk of subsidence in the town of Thil (54).* Géodéris memo No. N2002/025.

Ingérop région Grand Est (2003). *Filling in of mines in Thil. Preliminary survey.* Report No. SW03010.

ELECTRICAL METHODS FOR DETECTING AND CHARACTERIZING DISTURBANCES CAUSED BY SALT MINING: EXAMPLE OF THE LA MADELEINE SALT CONCESSION (MEURTHE-ET-MOSELLE).

MIEHE Jean-Marc[1], MATHIEU Francis[1], FEUGA Bernard[2] and FABRIOL Hubert[1]

[1]BRGM, 3 av. Claude Guillemin, BP 6009 – 45060 ORLEANS Cedex 02 – France. jm.miehe@brgm.fr; f.mathieu@brgm.fr; h.fabriol@brgm.fr

[2]GEODERIS, 1 rue Claude Chappe, BP 25198 – 57075 Metz Cedex 3 – France. bernard.feuga@industrie.gouv.fr,

ABSTRACT: Methodological geophysical investigations carried out in 2002 and 2003 at the La Madeleine experimental site near Nancy (Lorraine, France) have shown that certain electrical techniques such as the resistivity rectangle method and 2D resistivity profile method are wholly suitable for locating and characterizing salt-formation disturbances caused by solution mining. The resistivity rectangle enables one to determine the geological structure, visualize the extent of the salt-water body overlying the salt formation, and detect conductive anomalies with larger amplitudes than those caused by the presence of the salt-water body. The resistivity profiles supplement the resistivity rectangle mapping by enabling one to confirm and clarify the boundaries of the salt-water body, determine the geometry of the geological structures, and resolve the uncertainty concerning the origin of conductive anomalies revealed by the rectangle.

KEY WORDS: geophysics, salt cavities, electrical sounding, rectangle method, electrical imagery.

RESUME : Les investigations géophysiques à caractère méthodologique effectuées en 2002 et 2003 sur le site expérimental de La Madeleine près de Nancy (Lorraine, France) ont démontré que certaines méthodes électriques comme le rectangle de résistivité et le panneau de résistivité étaient tout à fait adaptées à la localisation et à la caractérisation des modifications apportées à la formation salifère par l'exploitation du sel par dissolution. Le rectangle de résistivité a permis d'appréhender la structure géologique, d'imager les extensions de la nappe salée située au toit de la formation salifère et de détecter des anomalies conductrices d'amplitude plus importante que celles provoquées par la présence de la nappe salée. Les panneaux de résistivité complètent la cartographie élaborée à partir du rectangle de résistivité en permettant de confirmer et de préciser les limites d'extension de la nappe salée, d'appréhender la géométrie des structures géologiques et de lever l'indétermination quant à l'origine des anomalies conductrices mises en évidence par le rectangle.

MOTS-CLEFS : géophysique, cavités salines, sondages électriques, méthode rectangle, imagerie électrique.

1. Introduction

BRGM has carried out a methodological geophysical study on the La Madeleine salt concession (Lorraine, France). The experimental site, provided by Novacarb and C.I.M., lies at the western edge of the town of St-Nicolas-de-Port, 10 km southeast of Nancy. The salt formation of the Lower Keuper from Lorraine was there intensively exploited in the past (Table 1). This study has been carried out for the account of the public agency GEODERIS, in the framework of its validation program of methods for the detection of cavities arising from former salt mining activities. 2D electrical profiles had already been recorded in 2001 for the LR 45 cavity in the neighbouring Art-

sur-Meurthe concession (Miehé et al., 2004). Solution mining of the La Madeleine deposit has involved 130 exploitation boreholes since 1881 and is characterised by the existence of:

- brine-filled residual cavities,
- partly collapsed residual cavities (migration to the base of the Beaumont dolomite) filled with insolubles (sandstone, clay) and dipping in brine,
- collapse cones filled with variably compacted heterogeneous material,
- a "salt-water body" located at the top of the salt formation —a thin solution zone (about a metre thick) that probably comprises anastomosing channels filled with saturated brine. This salt water body is not of natural origin, but developed due to chimney collapse with permeabilization of the decompressed zone in the overlying marl.
- a regional-scale fault or flexure (the Meurthe fault) that could be the seat of the salt-water circulation.

Table 1. Lithostratigraphic section of the Lorraine Keuper

AGE	FORMATION	THICKNESS		LITHOLOGY
LIAS	Promicroceras Clay	~ 25 m		Mudstone
	Gryphaea Limestone	~ 15 m		Marl and Limestone
RHETIAN	Levallois Clay	~ 10 m	~ 30 m	Mudstone
	Rhetian Sandstone	~ 20 m		Fine-grained Sandstone, Siltstone
UPPER KEUPER "Marnes irisées sup."	Upper variegated Clay	25 to 35 m	40 to 45 m	Mudstone (+ Limestone, Dolomite, Gypsum)
	Chanville Clay	10 to 15 m		Mudstone (+ Dolomite, Gypsum)
MIDDLE KEUPER "Marnes irisées moy."	Beaumont Dolomite	5 (to 10 m)	20 to 30 m	Dolomite (Top : Anhydrite)
	Medium variegated Clay	~ 5 m		Mudstone
	Reed Sandstone	~ 10 m		Fine-grained clayey Sandstone or Mudstone
LOWER KEUPER "Marnes irisées inférieures"	Anhydrite Marl	5 to 20 m	30 to 50 m	Mudstone (+ Anhydrite, Dolomite, Gypsum)
	1st unit	20 to 40 m	100 to 150 m Salt-bearing formation	80% Salt + Mudstone, (Anhydrite)
	2nd unit	~ 25 m		40% Salt, + Mudstone, (Anhydrite)
	3rd unit	~ 25 m		80% Salt + Mudstone, (Anhydrite)
	4th unit	~ 25 m		Mudstone, little Salt, (Anhydrite)
	5th unit	~ 30 m		50% Salt + Mudstone, (Anhydrite)
	Pseudomorphoses Sandstone	~ 25 m		Mudstone (+ Dolomite, Anhydrite)
LETTENKOHLE	Upper Dolomite	2 to 5 m		Dolomite

The geophysical study had several fixed objectives, which were to:

- detect and characterize the residual cavities remaining from the salt solution mining and the hydraulic connections linking the cavities,
- investigate the extent of the "salt-water body" located at the top of the salt formation at a depth of some 150 to 200 m,
- locate and characterize the Meurthe Fault and determine possible salt-water circulation within the fault.

This article describes the acquisition and interpretation of the electrical measurements made in 2002 and 2003.

2. Field measurements and interpretation

The following geophysical methods were used to meet the objectives (Mathieu, 2002, 2003):

- electrical sounding for characterizing the different geological formations in terms of resistivity,
- resistivity sounding (rectangle method) for locating the various disturbances induced underground by salt mining,
- resistivity profiling (2D electrical resistivity imagery) for determining the geometry of the cavities and the Meurthe Fault.

The map on Figure 1 shows the locations of the different measurement points.

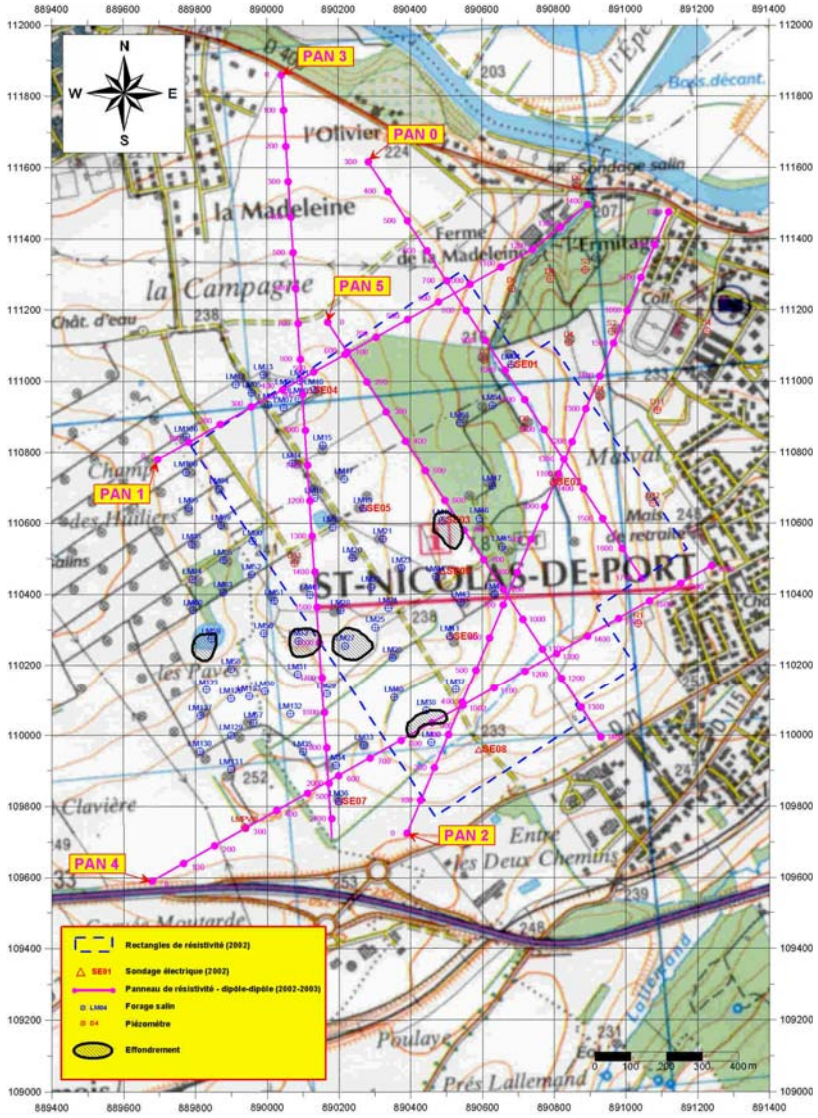


Fig. 1: Measurement points

2.1. Electrical soundings

A number of environment-related constraints meant that the electrical soundings could not be made under the best conditions. The AB injection lines could not exceed 1200 m because of major roads, the town of St-Nicolas-de-Port, the Meurthe river and the Novacarb factory at La Madeleine; this AB length was, however, sufficient to give an investigation depth to slightly below the top of the salt formation. Similarly, it was not possible to respect the planned N-S orientation of the lines because of the same environment-related constraints and of the presence of a fairly dense network of metal pipes (piping for the mined salt brine and a gas pipeline). Eight of the nine completed electrical soundings were located over boreholes where the geological succession is perfectly known. These soundings were therefore interpreted with the constraint of a fixed depth for certain geological interfaces:

- The base of the salt formation (extrapolated value based on an average thickness of 150 m for this formation),
- The top of the salt formation,
- The base and top of the Rhaetian sandstone, located itself at the top of the upper Keuper.

The results of these calibrations show that the true resistivities of the different formations vary greatly from one electrical sounding to the next; a variability that is due to lateral effects caused by conductive 3D heterogeneities. Given these conditions, and taking into account the equivalence principle of the electrical sounding method, it was impossible to show whether or not a thin conductive horizon (salt-water body) exists at a depth of around 200 m. However, a certain amount of information, which could be useful in the future (for electrical and electromagnetic modelling), came out of the 1D interpretation of these electrical soundings:

- The resistivity of all the clay-marl formations at the top of the salt and at the top of the Rhaetian sandstone is of the order of 10 to 15 ohm.m,
- The bed of massive Rhaetian sandstone is a resistive layer with a resistivity between 50 and 200 ohm.m,
- The bed of massive Beaumont dolomite (middle Keuper), due to its relative thinness (8 to 10 m) and its depth (130 to 150 m), cannot be individualized by electrical sounding,
- The true resistivity of the salt formation has probably not been determined, the AB spacing being much too short. Various models taking into account a 150-m-thick salt formation comprising interbedded resistive layers (salt at 10^5 ohm.m) and conductive layers (marl at 20 ohm.m) show that, in order to determine the true resistivity of the formation, the AB/2 of the electrical soundings needs to be of the order of 5 to 10 km.

2.2. Resistivity rectangle

Two resistivity rectangles with an area of 1000 x 700 m were required. The characteristics of these rectangles were: injection dipole: AB = 2000 m; reception dipole: MN = 100 m; measurement grid: 50 x 50 m for rectangle no. 1 and 100 x 50 m for rectangle no. 2. The resistivity map (Fig. 2) shows a conductive zone occupying the centre and the NW and SW borders of the study area, whilst the NE and SE borders are represented by a resistive zone. This picture correlates perfectly with the local geology, which is represented by a synclinal closure whose core contains a marly formation (conductive response) that is absent on the limbs, in which there is an uplift of the salt formation (resistive response).

Within the conductive and resistive zones of geological origin, however, we find a number of short wavelength (~100 m) conductive anomalies. To better individualize these anomalies, which would be of anthropic origin (cavity, collapse, or salt-water body), a specific processing (theoretically applicable to potential field techniques) was carried out on the resistivity map. A "regional field" comparable to the geological response was subtracted from the resistivity map in order to obtain a "residual anomaly" map (Fig. 3). This map shows:

- Conductive areas on the SE border and in the NE corner of the study area which are due to a poor assessment of the "regional field" (boundary effects). These conductive anomalies are thus not to be taken into account.
- Large-amplitude conductive anomalies C1 and C2 that correlate perfectly with the LM27 and LM48 collapses (Fig. 5)
- Conductive anomalies with fairly similar amplitudes to C1 and C2:
    - C3 located between boreholes LM16 and LM18
    - C4 centred on the group of boreholes LM05 to LM13
    - C5 associated with LM44
    - C6 centred on LM45
    - C7 centred on LM04

  By analogy with C1 and C2, these conductive anomalies could be related to cavities filled with brine and/or brine-saturated insolubles, the top of which would have risen into the marl overlying the salt formation.

- A conductive envelope that contains all the conductive anomalies as well as most of the exploitation boreholes. This conductive envelope could reflect the extent of the salt-water body. A certain number of elements supports this assumption:
  - the existence of a certain correlation between the conductive envelope and the cumulated zones of subsidence (Fig. 5)
  - the presence of salt water identified at LM04 (old borehole used for dissolution mining at the top of the salt formation)
  - the presence of salt water in the BRGM observation well,
  - the existence of a hydraulic connection between this observation well and boreholes LM44 and LM45 (as pointed out by piezometric recordings made by BRGM in 1985).
- The absence of a significant conductive anomaly for the LM38 – LM39 collapse. The geophysical study can provide no tangible explanation for this absence, and further investigation would be necessary to find the answer.
- A certain NE-SW pattern (elongation axis of the conductive envelope, plus two resistive axes framing this conductive envelope) whose explanation is probably geological (fault or flexure direction).

2.3. Resistivity profiles (2D electrical resistivity imagery)

To determine the location and the geometry of the Meurthe Fault, and also to detect the possible circulation of salt water within this fault, two resistivity profiles (PAN 1 and PAN 2) were carried out (Fig. 1). The proximity of the urban area of St-Nicolas-de-Port considerably limited the possibilities for running these two profiles. The Meurthe Fault being located just at the western edge of St Nicolas de Port meant that neither PAN 1 nor PAN 2 extended far enough to the east to correctly intersect the structure.
The purpose of resistivity profile PAN 3 was to confirm the presence of cavities below conductive anomalies C3 and C4 revealed by the rectangle method (2002 survey). This profile also intersected conductive anomaly C1, which correlates with the LM32 – LM27 collapse. Resistivity profile PAN 4, which is shown as an example in Figure 4, was aimed at resolving the uncertainty concerning the LM38 – LM39 collapse in view of the fact that no conductive anomaly (2002 rectangle) was recorded over this disturbance. Resistivity profile PAN 5 was run across the LM48 collapse which, unlike the LM38 – LM39 collapse, does correlate with a conductive anomaly (C2).
The resistivity profiles were also aimed at confirming and determining the extent of the salt-water body revealed by the rectangle method.

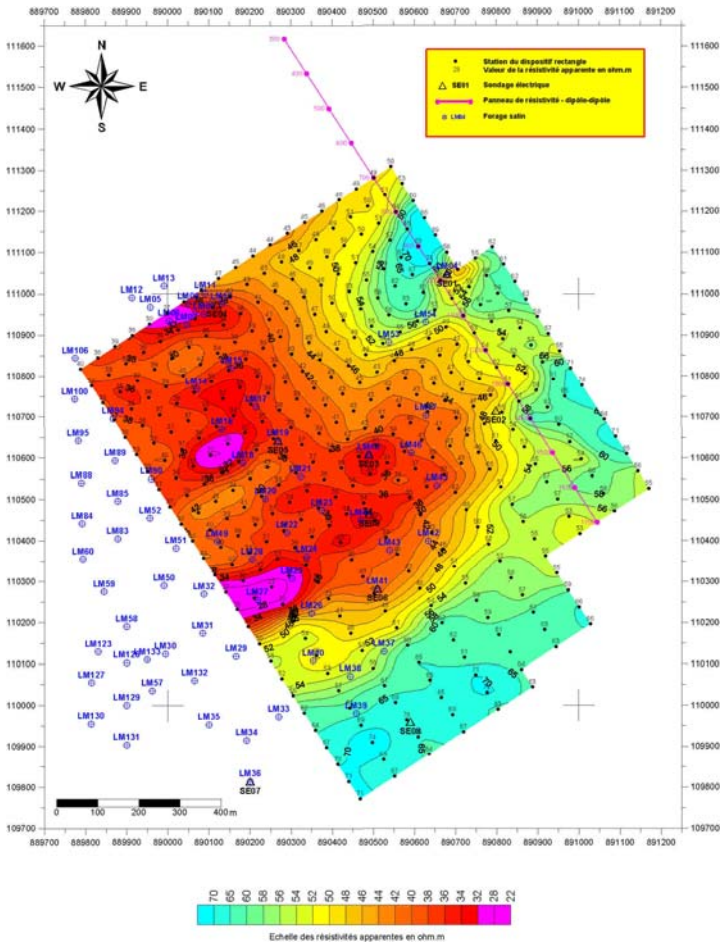


Fig. 2: Rectangle method: apparent resistivity map

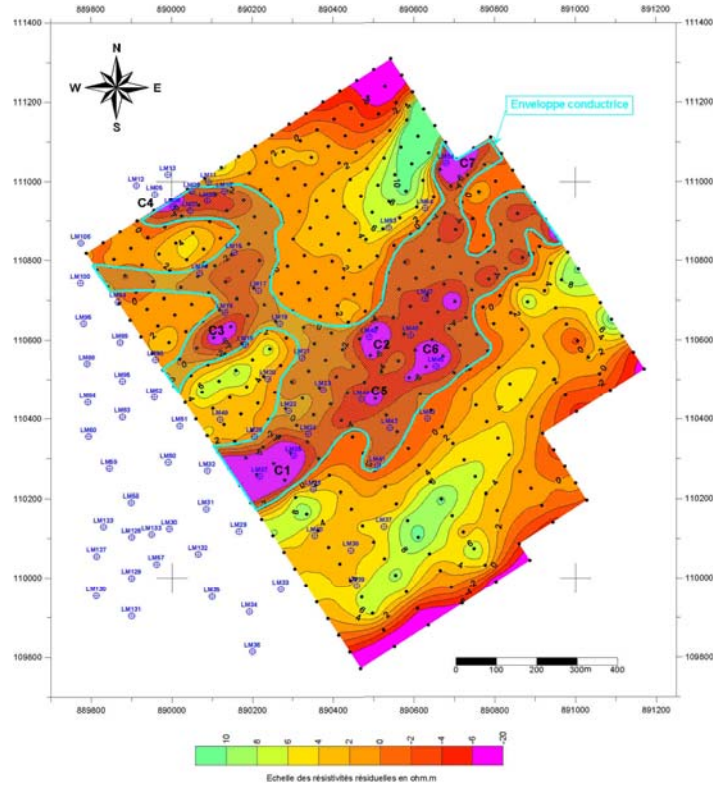


Fig. 3: Rectangle method: apparent-resistivity residuals map

The pseudo-sections were interpreted by inversion using the RES2DINV software (Loke et al., 1996). Inversion makes it possible to establish a "true" resistivity section according to the directly interpretable depth in terms of geological formations. The six inverted resistivity sections globally show the same geoelectric pattern, i.e. from the top down (Table 1):

- a resistive unit (>30 ohm.m) comprising the Pliesbachian Amaltheus marl and ochre limestone;
- a conductive unit (<15 ohm.m) corresponding to a geological succession of three beds: the Promicroceras clay (Pliesbachian), the Gryphaea limestone (Hettangian, Sinemurian) and the Levallois clay (Rhaetian),
- a resistive unit (>50 ohm.m) comprising the geological formations between the bottom of the Beaumont dolomite and the top of the Rhaetian sandstone, i.e. the Beaumont dolomite, the Chanville clay, the upper Keuper marl and the Rhaetian,
- a conductive unit corresponding to the upper, middle and lower Keuper marl. The resistivity of this unit varies according to whether or not salt water is present: it is greater than 25 ohm.m where salt water is absent and less than 20 ohm.m where salt water is present at the top of the salt formation. The Keuper marl overlying the salt-water body is saturated with brine over a certain thickness,
- the last geoelectric unit of the profile corresponds to the upper part of the salt formation. Where this formation has not been dissolved, the inverted resistivity is greater than 100 ohm.m. It is obviously not the true resistivity of this formation which could not be determined by the measuring device; it is too low, given that the resistivity of salt is of the order of 100,000 ohm.m. However, where cavities and hydraulic channels linking cavities are present and filled either with brine or with a mixture of brine and insolubles, the resistivity of this unit is between 10 and 20 ohm.m.

The interpretation of the 2D resistivity profiles has enabled us to:

- locate and characterize the Meurthe flexure, which is represented by at least three faults. The width of this structure is about 250 m with a throw between 50 and 100 m;
- show a probable circulation of salt water within this structure (Cf. PAN 1 and PAN 2). The salt-water circulation would only be present in the northern part of the flexure; the presence of salt water was not detected in the southern part, around PAN 4;
- confirm the existence of a hydraulic channel, located at the top of the salt formation, between the Meurthe Fault (northern area) and the mined area (Cf. PAN 1, PAN 2 and PAN 0);
- show the presence of salt water over the entire mined area. This salt-water body is located in the lower Keuper marl overlying the salt formation and also in the salt formation itself (cavities and inter-cavity channels);
- individualize several cavities whose tops would be close to the Beaumont dolomite:
  - C12 near borehole LM04
  - C9 near borehole LM34 (Fig. 4)
  - C4 – C11 near borehole LM42
  - C8 between boreholes LM16 and LM 18.
- show that saline pollution affects the aquifers of the Beaumont dolomite, the upper Keuper marl and the Rhaetian sandstone. This saline invasion is related to the LM 05 to LM 16 group of boreholes;
- show that no brine-filled cavity occurs where collapse has occurred. The conductive anomalies revealed near these disturbances are due to decompression of the collapsed rock and fill material (preferential circulation of meteoric water).

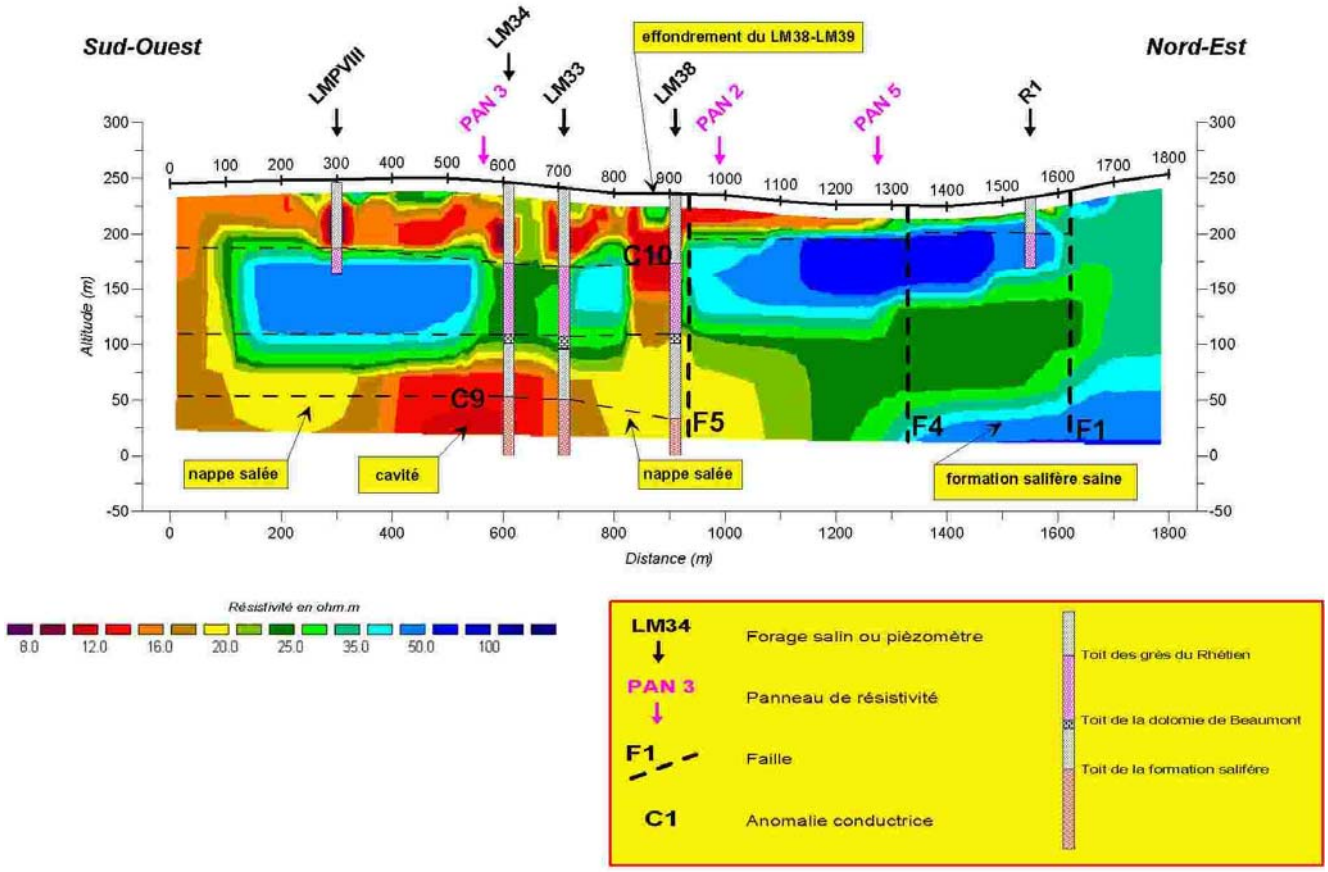


Fig. 4: PAN 4 inverse resistivity section

3. Conclusion

The methodological geophysical investigations carried out in 2002 and 2003 on the La Madeleine experimental site have shown that certain electrical methods, such as the resistivity rectangle and 2D resistivity profile, are perfectly suited to locating and characterizing disturbances induced underground by salt mining. Figure 5 synthesizes the results obtained during the 2002 and 2003 campaigns. The resistivity rectangle and profiles revealed the presence of a hydraulic connection (salt water body) between the Meurthe Fault and the mined area. A good correlation exists between the boundary of the salt-water body determined from interpretation of the 2D resistivity profiles and the area containing the cumulated collapses. This map also shows that the conductive anomalies shown by the interpretation of the resistivity rectangle are due either to collapse (RC 1 and RC 2), or to zones contaminated by salt water (RC 4), or to cavities (RC 3 and RC 7). It thus confirms the value of combining the rectangle and profile methods for determining the origin of conductive anomalies.

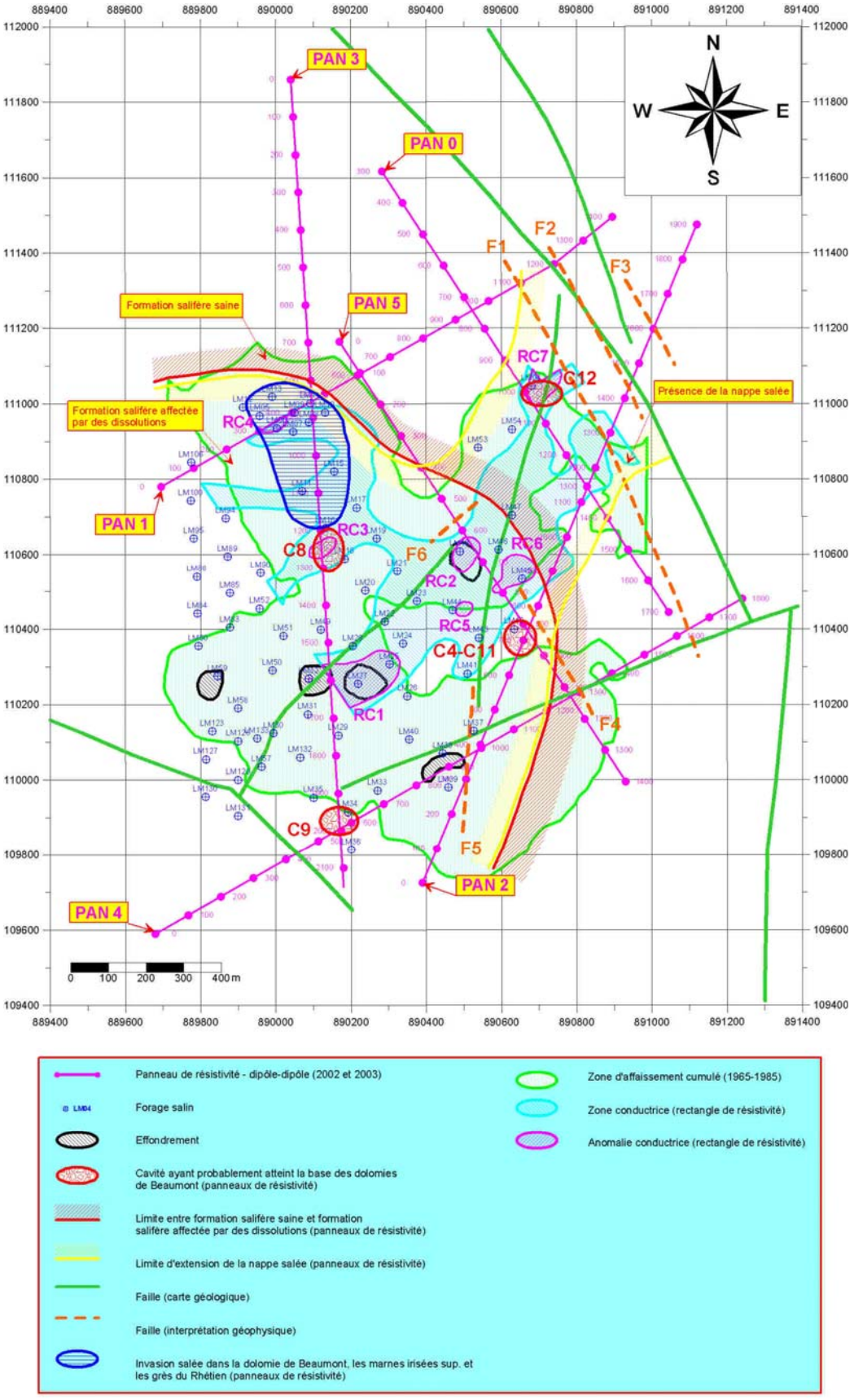


Fig. 5: Integrated interpretation of the electrical methods

The resistivity rectangle enabled us to understand the geological structure, image the extent of the salt-water body located at the top of the salt formation, and detect conductive anomalies with larger amplitudes than those caused by the presence of the salt-water body and whose origins could be one of three:

- decompression of the rock in the collapse zones (preferential circulation of meteoric water),
- saline invasion of the aquiferous formations overlying the salt formation (pollution due to the solution mining or from the reinjection of saline muds),
- presence of cavities filled with brine or brine-saturated impurities located at the top of the salt formation or having migrated to the base of the Beaumont dolomite.

The 2D resistivity profiles complete the mapping of the disturbances located by the resistivity rectangle in providing confirmation and precision concerning the limits of the salt-water body, in determining the geometry of the geological structures (faults, flexures, contacts, formation thicknesses), and in resolving the uncertainty as to the origin of the conductive anomalies revealed by the rectangle:

- the conductive anomaly due to collapse extends from the ground surface down to the salt formation;
- the conductive anomaly caused by a saline invasion correlates perfectly with the aquiferous formations located above the base of the Beaumont dolomite;
- the cavities filled with brine and/or brine-saturated insolubles are characterized by large-amplitude conductive anomalies located in the upper part of the salt formation and may extend to the base of the Beaumont dolomite.

The present study concerns a former salt mining area where the top of the salt formation was exploited. The case where cavities within the salt formation have a layer of salt at their top was not examined during this study, and thus the uncertainty concerning the validity of these electrical methods for detecting cavities located in such a context remains unresolved. Although the electrical sounding method adopted in 2002 did not give convincing results concerning the detection of the salt-water body, the results of the 2003 campaign show that all the electrical soundings were situated within the area of the salt-water body. To truly conclude on the applicability of electrical sounding for detecting a salt-water body, it will be necessary to calibrate the method in a virgin area (i.e. no salt-water body and no salt mining).

4. Acknowledgements

We are grateful to NOVACARB and CIM to give us access to the La Madeleine site. GEODERIS funded the study in the framework of its validation program of reconnaissance methods of cavities.

5. References

Loke, M.H., Barker, R.D., (1996). *Rapid least-square inversion of apparent resisitivity pseudosections by a quasi-Newton method*, Geophys. Propect., 44, 131-152.

Mathieu, F. (2002). *Reconnaissance géophysique à caractère méthodologique sur la concession saline de la Madeleine, Meurthe-et-Moselle,* BRGM/RC-51883, 61 p., 7 fig., 1 tabl., 3 ann.

Mathieu, F. (2003). *Reconnaissance géophysique à caractère méthodologique sur la concession saline de la Madeleine, (54) Phase 2,* BRGM/RC-52583, 41 p., 10 fig., 1 tabl., 1 ann.

Miehé, J.M., Feuga, B. et Vachette C. (2004), *Détection d'une cavité remplie de saumure par imagerie électrique,* Rev. Française de géotechnique, N° 106-107, 23-29.

MONITORING THE FLOODING OF A MINE GALLERY IN LORRAINE THROUGH ELECTRICAL-RESISTIVITY AND SASW SURVEYS – TRESSANGE PILOT SITE

MIEHE Jean-Marc [1], BITRI Adnand [1], FABRIOL Hubert [1], GRANDJEAN Gilles [1], LEBERT François [1], MATHIEU Francis [1], RICHALET Gérard [1]

[1]BRGM, 3 av. Claude Guillemin, BP 6009 – 45060 ORLEANS Cedex 02 – France.
jm.miehe@brgm.fr, a.bitri@brgm.fr, h.fabriol@brgm.fr, g.grandjean@brgm.fr, f.lebert@brgm.fr, f.mathieur@brgm.fr, g.richalet@brgm.fr

RESUME : Dans le cadre du GISOS et des travaux concernant la surveillance des anciennes structures minières ennoyées, le BRGM a réalisé une série de mesures de résistivité électrique et de sismique en ondes de surface (SASW) à l'aplomb d'une galerie de mine ennoyée à Tressange, avant pendant et après l'ennoyage. L'objectif était de qualifier l'état de l'intercalaire marneux et d'étudier la capacité des méthodes géophysiques à détecter l'influence de l'eau sur l'évolution des paramètres physiques mesurés pour appréhender la dégradation des propriétés mécaniques de l'intercalaire liée au lessivage. Les deux méthodes d'auscultation montrent que le cycle ennoyage-dénoyage provoque des effets irréversibles notamment à la base de l'intercalaire. Par ailleurs le centre de l'intercalaire semble être en état de compression après dénoyage, comme l'indique les augmentations de résistivité et de vitesse S.

MOTS CLES : Imagerie électrique 2D, Résistivité, vitesse des ondes S, ennoyage, dénoyage.

Abstract: In the context of GISOS and studies concerning flooded former mines, BRGM carried out a series of electrical resistivity and seismic surface wave (SASW) surveys over a flooded mine gallery at Tressange, before, during and after the flooding. The objectives were to determine the initial state of gallery's marly base and to test the potential of the geophysical methods for detecting the water's influence on the measured parameter changes in order to understand the mechanical degradation of the marly base due to leaching. Both methods shed light on the irreversible effects of the flooding-dewatering cycle on the marly base. The central part of this base seems to be in state of compression after dewatering, as indicated by increased electrical resistivity and S velocities.

KEY-WORDS: 2D electrical imaging, resistivity, S velocity, flooding, dewatering.

1. Introduction

In the context of GISOS (Scientific Interest Group for the Surveillance of Underground Structures) and studies concerning flooded former mines, BRGM carried out a series of electrical resistivity and seismic surface wave (SASW) surveys over a flooded mine gallery at Tressange, before, during and after the flooding. The objective was to determine the initial state of gallery's marly base and then to test the potential of the geophysical methods for detecting the water's influence on the measured parameter changes in order to understand the mechanical degradation of the marly base due to leaching. The test site forms part of the *Terres Rouges* iron-ore mine (Tressange crown pillar) and lies at a depth of 250 m. Mining ceased in 1997. Once all activity within the mine has completely finished, the mine drainage pumps will be stopped. The phreatic groundwater will then re-establish its natural level, consequently flooding the mine galleries. The purpose of the pilot site was to recreate and study the effects of such an event at a reduced scale. The mine, at the pilot site, was worked on three levels —the yellow layer, the grey layer and the brown layer. The current

operation consisted in isolating a reservoir with 70 m sides using a set of watertight barriers to ensure that two pillars (F and G in Figure 1) were completely flooded.

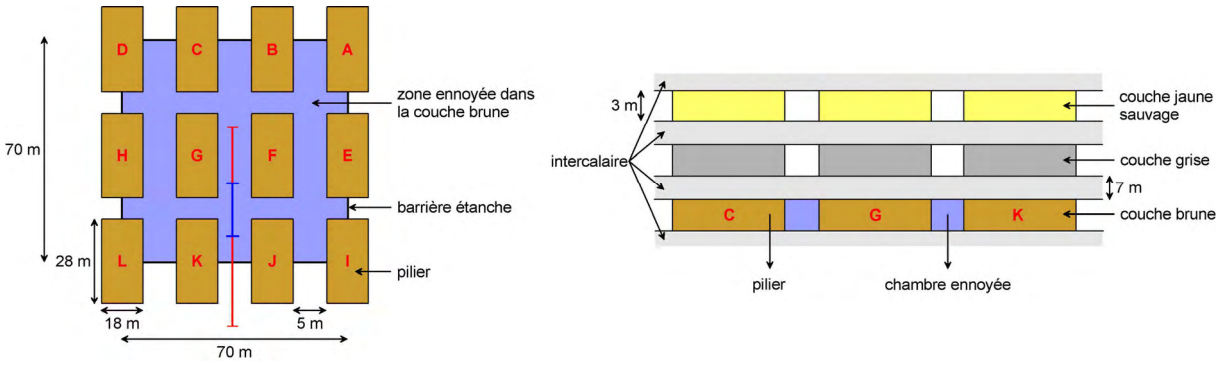


Figure 1. Geometry of the pilot site. Plan view (left) and section view (right). The red line indicates the position of the electrical array, the blue line the position of the SASW system.

2. Measuring devices

The electrical resistivity survey with continuous current injection used a Wenner-type array of 64 electrodes spaced at 1 m intervals. Eight surveys were run between January 2002 and December 2003. The SASW survey allowed us to calculate the distribution of the shear-wave velocities Vs versus depth, and thus the shear module G. The device used was equivalent to a seismic refraction array with a pulse source at each end of a line of geophones. Six tests were made between January 2002 and December 2003. The instruments were centred on the gallery intersection between pillars GFKJ. The choice was motivated by the fact the intersections correspond to the zones most sensitive to instability.

3. Results

The resistivity readings are presented as apparent-resistivity (Figure 2) and interpreted-resistivity (Figure 3) cross sections.

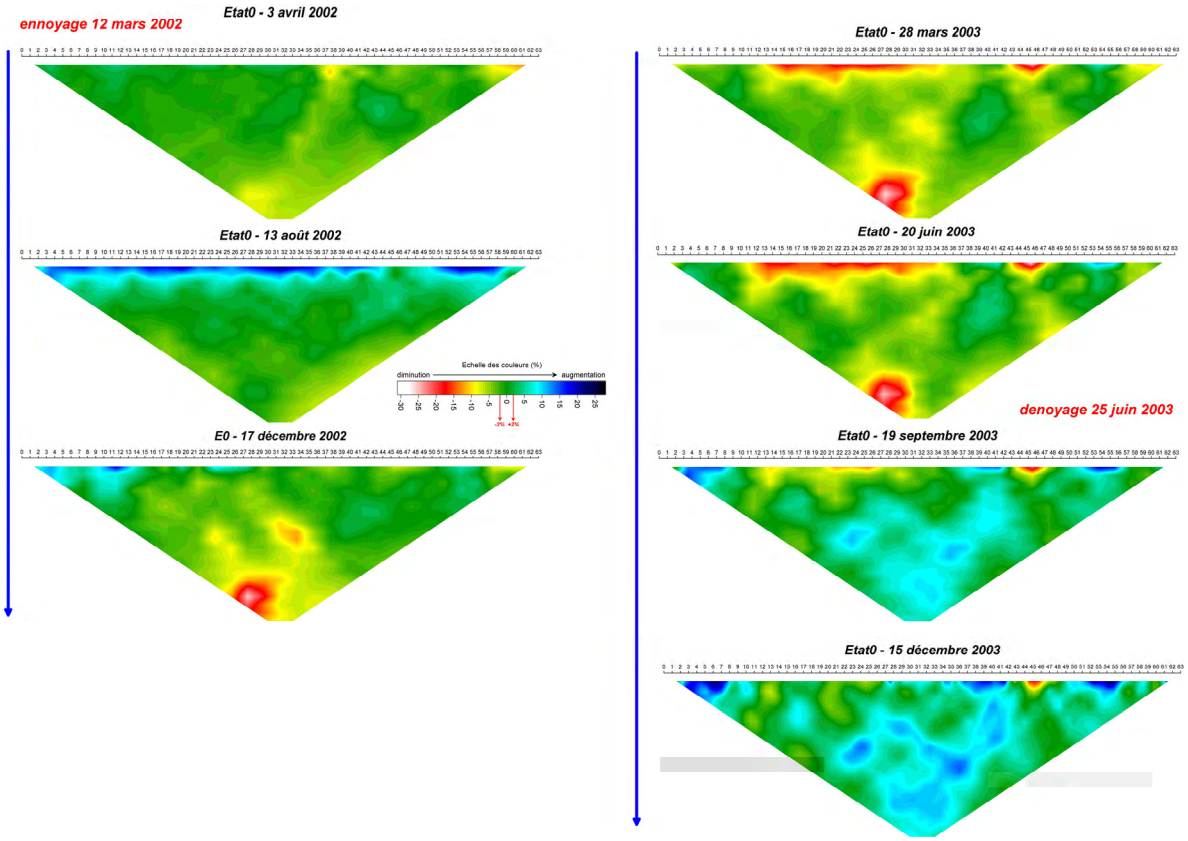


Figure 2 - Evolution of the apparent resistivity in relation to the initial state.

The measurement precision is of the order of 1%. Repeated measurements over two days before the flooding showed variations of the order of 2%. Therefore only variations greater than 2% in absolute value were considered as significant. The interpreted sections are reliable within the first 5 to 10 metres, below which artefacts appear due to the 3D room-and-pillar configuration whose effects could not be taken into account with a single linear array.

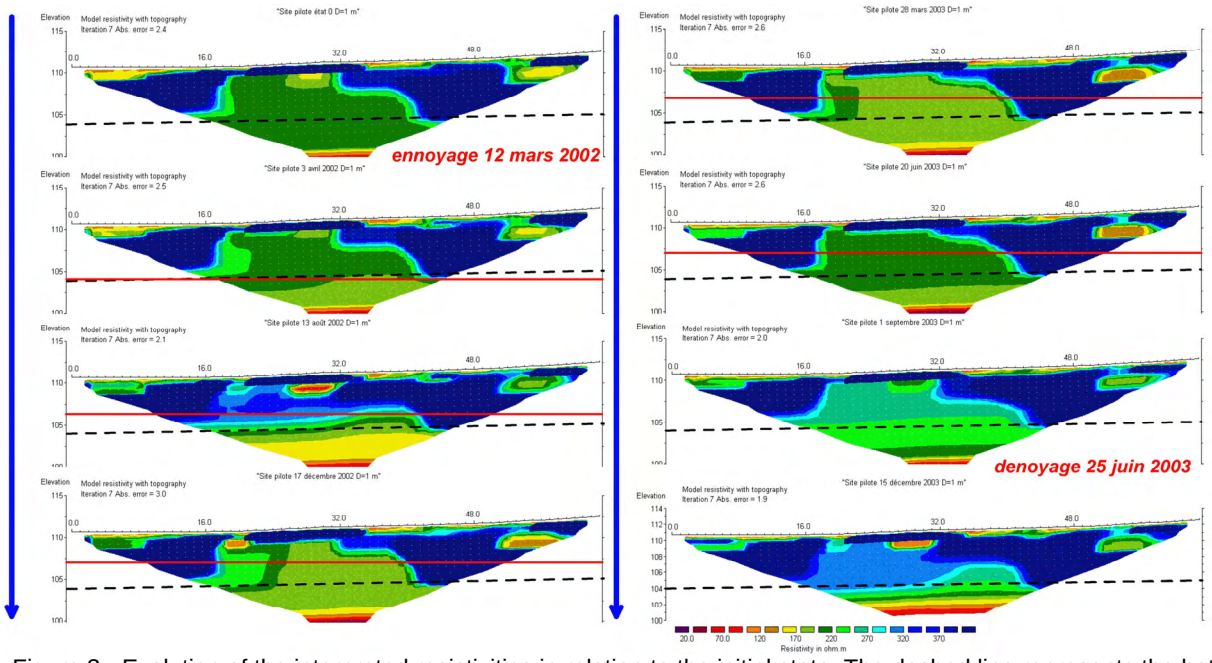


Figure 3 - Evolution of the interpreted resistivities in relation to the initial state. The dashed line represents the bottom of the marly base layer, the red line corresponds to the water level within the base layer.

For each of the six SASW seismic tests we calculated the dispersion curve (variation of the phase velocity with frequency) of the S waves (Figure 4). Uncertainties due to different measurement noises on the pick of the dispersion curve can be quantified by the thickness of the set of curves at the ends of the frequency band being considered (50 Hz and 200 Hz). The dispersion curve was interpreted in 1D by iterative inversion with a tabular velocity-distribution model (Figure 5). Only the shots whose source position was between pillars C and B and beyond were used. Below 6 m depth, the models are difficult to interpret, because the recording takes into account all of the 3D room-and-pillar structure below and around the array.

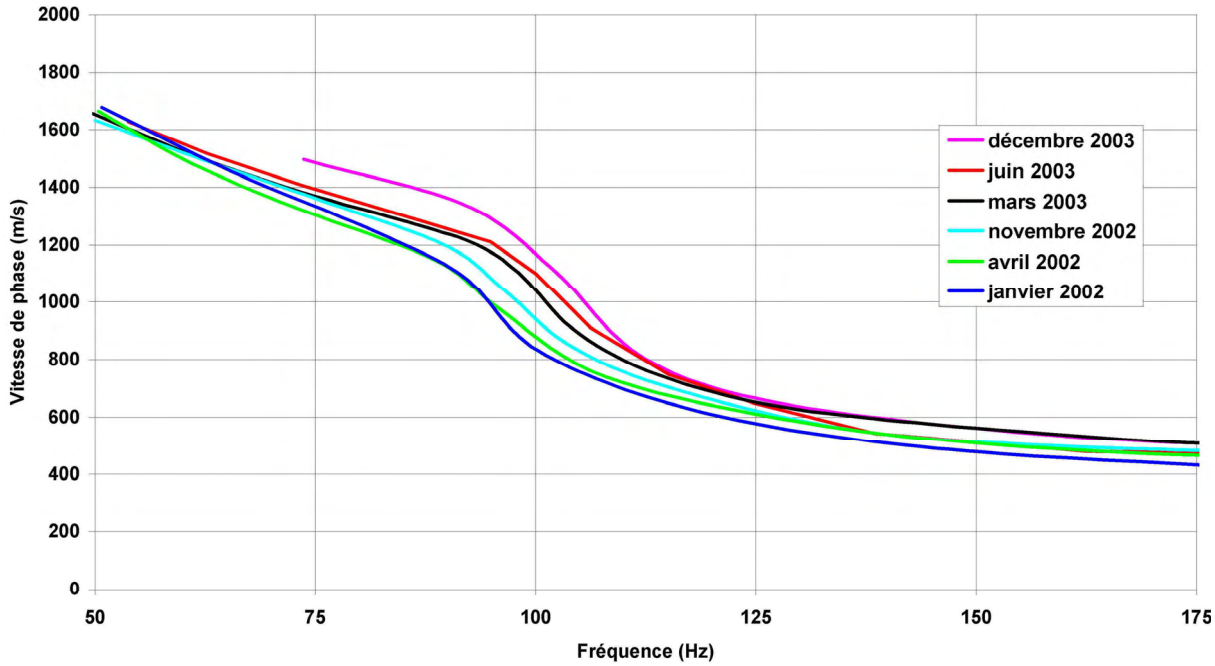


Figure 4 - Variation of the SASW dispersion curves with time

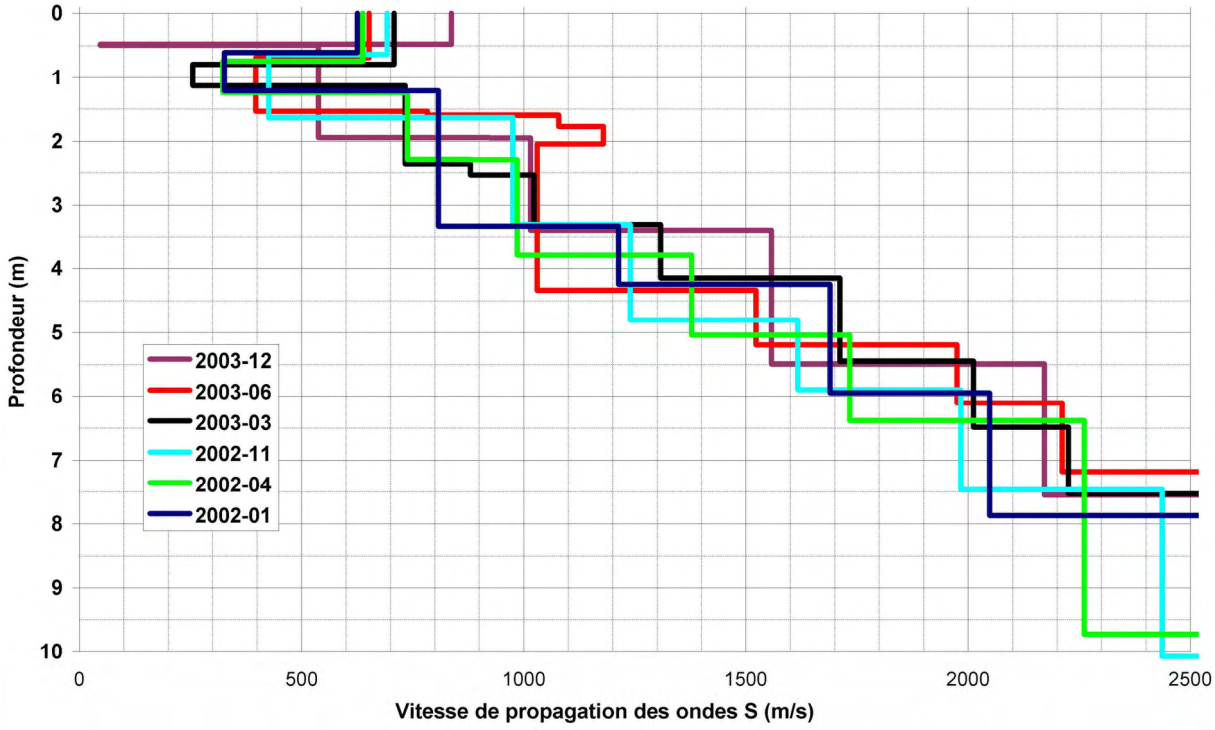


Figure 5 - Variation of the S-wave velocity models.

The evolution of the marly base layer was characterised by comparing the initial state with the states during and after flooding.

3.1. Before flooding

The interpreted resistivity section reveals the presence of an inhomogeneity in the marly base layer. This strong inhomogeneity has also been observed elsewhere by P-wave velocity interferometry. Between stations 0 and 16, the resistivity section shows a three-layer structure that corresponds approximately to the three known facies, i.e. calcarenite, arenite and argillite from the top down.

The SASW indicates that the velocity Vs of the rocks making up the floor of the gallery increase regularly from 500 m/s at around 1.5 m depth to 2000 m/s at around 6 m depth, with a velocity inversion in the topmost metre.

3.2. During flooding

The variations in apparent resistivity show a 5 to 20% lowering of the values with time in the deepest part tested by the instrument. This lowering is unquestionably linked to the presence of water in the cavity and its rise within the marly base layer. The interpreted sections show lateral resistivity variations in the marly base layer that vary with time, in agreement on the one hand with presence of inhomogeneities at the zero state, and on the other hand with a differentiated flowpath of the groundwater during flooding.
Two observations are to be noted in the dispersion curves obtained by the SASW:

- a small variation between 50-75 Hz and 115-175 Hz,
- a time offset of the curves between 80 and 115 Hz, corresponding to an increase in the velocity Vs between January 2002 and the completion of flooding at around 4.0-4.5 m depth.

The inversion of the dispersion curves shows that the models are close, if not indiscernible from one another, and are therefore not able to show the velocity increases revealed quantitatively on Figure 4.

3.3. After dewatering

The resistivity remains weakest at the top of the brown layer. This result can be attributed to open and incompletely drained fractures. In the centre of the marly base layer, however, the increased vertical stress closed the fractures, leading to an increase in the resistivities (up to 10% of the initial apparent-resistivity values). This effect began in June 2003 and is clearly seen on the interpreted section of December 2003. The resistivity increase is accompanied by an increase in the S-wave velocity at around 4.0-4.5 m depth.

4. Conclusion

The two sounding methods show that the flooding-dewatering cycle has caused irreversible effects, notably at the bottom of the base layer, probably due to damage in the brown layer. Moreover, the centre of the base layer seems to be in a state of compression after dewatering, as indicated by the increases in both resistivity and S-wave velocity.

5. List of references

Cahyna F., Mazac O., Venhodova D. (1990). *Determination of the extend of cyanic contamination by surface geoelectrical methods*. In Geotechnical and Environmental Geophysics, Ward, S.H. (ed), v. 2, Environmental and Groundwater, Society of Exploration Geophysicists, Tulsa , 97-99

Dam van J.C., Meulenkamp, J.J. (1967). *Some results of the geo-electrical resistivity method in ground water investigations in the Netherlands. Geophysical prospecting*, 15(1), 92-115

Edwards L.S. (1977). *A modified pseudosection for resistivity and induced-polarization*. Geophysics, 42, 1020-1036

Keller G.V., Frischknecht F.C. (1966). *Electrical methods in geophysical exploration*. Pergamon, New York, 519 p.

Loke M. H., Barker R.D. (1996). *Rapid least-squares inversion of apparent resistivity pseudosections by a quasi-Newton method*. Geophysical Prospecting, 44, 131-152

Loke M.H., Barker R.D. (1996). *Practical techniques for 3D resistivity surveys and data inversion*. Geophysical Prospecting, 44, 499-523

Ogilvy A.A., Kuzmina E.N. (1972). *Hydrogeologic and engineering geologic possibilities for employing the method of induced potentials*. Geophysics, 37(5), 839-861

Reynolds J.M. (1997). *An introduction to applied and environmental geophysics*. John Wiley & Sons Ltd., England, 796 p.

Summer J.S. (1976). *Principles of induced polarization for geophysical exploration*. Elsevier Scientific Publishing Company

Tweeton D.R., Cumerlato C .L., Jay C., Kuhlman H.HL.(1991). *Field test of geophysical techniques for predicting and monitoring leach solution flow during in situ mining*. Geoexploration, 28, 251-268.

Vacquier V., Holmes C.R., Kintzinger P.P., Lavergne M. (1957). *Prospecting for ground-water by induced electrical polarization*. Geophysics, 22(3), 660-687

Ward S.H. (1990). *Resistivity and induced polarization methods*. In Geotehnical and Environmental Geophysics, Ward, S.H. (ed), Society of Exploration Geophysicists, Tulsa, OK, 147-149

Yaramanci U.(2000). *Geoelectric exploration and monitoring in rock salt for the safety assessment of underground waste disposal sites*. Journal of Applied geophysics, 44, 181-196

RE-STABILISATION OF THE CARNALLITIC WORKING AREAS IN THE MERKERS POTASH MINE

MINKLEY Wolfgang, MÜHLBAUER Jan

IFG INSTITUT FÜR GEBIRGSMECHANIK GMBH, Friederikenstraße 60, D-04279 Leipzig, - Germany.; wolfgang.minkley@ifg-leipzig.de; jan.muehlbauer@ifg-leipzig.de;

ABSTRACT: In the Merkers potash mine those working areas which in the past had not been dimensioned in a stable way are now stabilized by inserting rock salt as stowing material. This procedure concerns predominantly such working areas which have been opened in the carnallitite of the Thuringia seam following the room-and-pillar technique. The purpose of this type of stowing is to provide a permanent stabilization of the mine layout and thus to prevent rock burst danger. This purpose is fulfilled by limiting the de-strengthening processes running in the pillars since several dozens of years.

KEYWORDS: Potash mining, carnallitite, rock burst, stowage, system stability.

RÉSUMÉ: Dans la mine de potasse de Merkers ceux champs d'abbattage qui n' ont pas été dimensionnés de manière stable maintenant subissent d'un procédé de stabilisation par mettre en place de sel gemme comme matériaux de remblayage. A ce sujet, il s'agit surtout des champs d'abattage creusés dans le carnallitite de la couche appelée Thuringe et abattus en exploitation par chambres et piliers. Le but de cettes mesures de remblayage consiste en garantir une permanente stabilisation de l'ossature de la mine par la limitation des procédés de déstabilisation qui sont avancées depuis plusieres dizaines d'années et, par conséquence, de prevenir le danger des coups de terrain.

MOTS-CLEFS: Exploitation des sels de potasse, carnallitite, coup de terrain, remblayage, stabilité du système.

1. Introduction

Since more than 100 years in the Werra-Fulda region in the German federal countries of Thuringia and Hessen potash salts are mined (Eisenbach and Paulinyi, 1998). The salt formations of the Werra-Fulda region have been formed about 255 millions of years ago, i. e. in the Upper Permian formation (Zechstein). The two potash seams which are called Thuringia and Hessen are located within the evaporite sequence which has a total thickness of several hundred metres. The potash seam Thuringia exists mainly in a carnallitic form whereas the seam Hessen consists of kieseritic hard salt. During the basaltic volcanism in the Tertiary formation 15 to 20 millions of years ago, liquid phases as well as watery solutions and gas mixtures consisting mainly of carbon dioxide penetrated into the evaporite layers where they gave rise to different conversion processes. Due to such processes, a part of the original carnallitite rock has changed its mineralogic and chemical material composition and has been transformed into kieseritic hard salt and into sylvinite.

Owing to the specific conditions of this deposit in the Werra-Fulda region, already very early the potash mining in this region has been confronted with the risks of sudden outbursts of carbon dioxide and salt, with hydrologic dangers and rock burst risks. Major rock bursts occurred in 1953 at Heringen (magnitude $M_L = 5$), in 1958 at Merkers ($M_L = 4.8$), in 1961 at Merkers ($M_L = 3.7$), in 1975 at Suenna ($M_L = 5.2$), and in 1989 at Voelkershausen ($M_L = 5.6$). These rock bursts have been

called so according to the names of the overlaying places (Fig. 1). By these rock bursts mainly the carnallitic working areas of the second floor in the Thuringia seam were affected. Then, salt was mined following the long-room technique, later-on, following the room-and-pillar method without stowing.

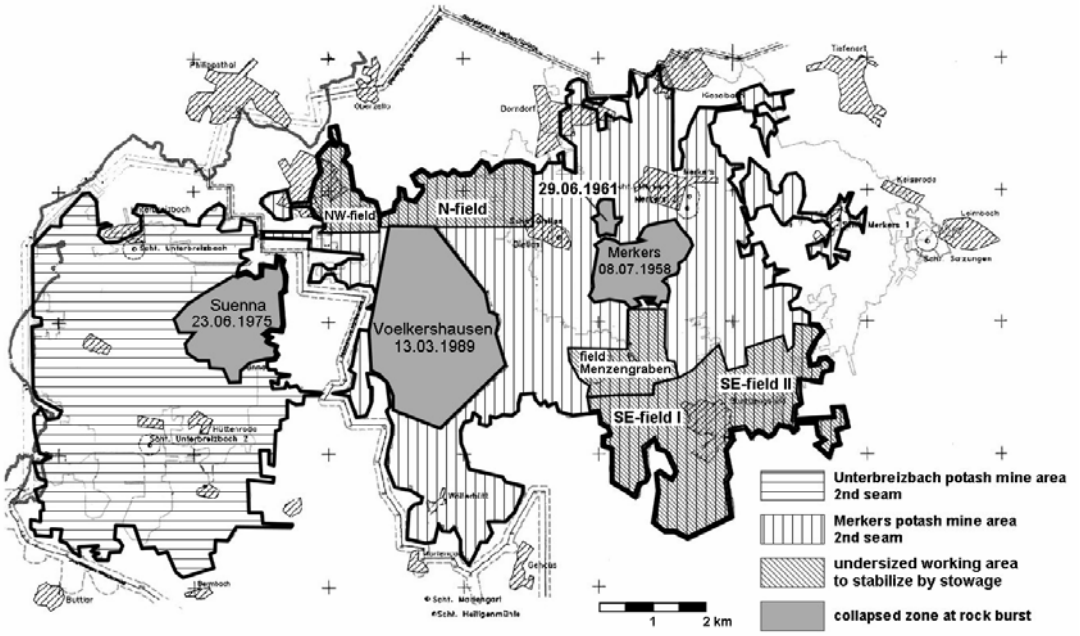


Figure 1. Working areas of the Unterbreizbach and Merkers mine in the Werra-Fulda potash deposit.

The last rock burst in the Werra potash region occurred on 13.03.1989 below the place of Voelkershausen (Fig. 2). This rock burst belongs to the most energetic seismic events which have ever occurred worldwide in mining regions. It was mainly this rock burst which compelled to tackle the causes of such events in order to permit an estimation of the stability of those working areas which have been left in an apparently intact state and to take measures, if necessary, to stabilize them. As a consequence, a specific visco-elasto-plastic constitutive model has been elaborated (Minkley et al., 2001) for being in the state to describe the behaviour of carnallitite with respect to its de-strengthening and brittle rupture. This constitutive model allowed to perform successfully a trace-back calculation referring to the rock burst at Voelkershausen. This trace-back calculation has shown that this rock burst had been initiated by a blast process (30 kg of Dekamon) which had been carried out in an already pre-damaged carnallitite pillar. Starting from this predominantly local instability the rupture process propagated within only several seconds in the manner of a chain reaction throughout the whole working area measuring 6.5 km².

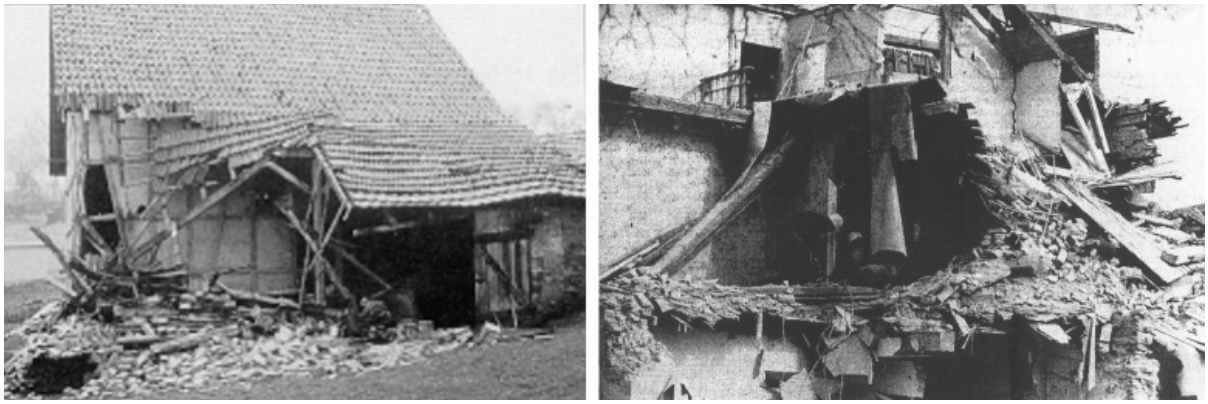


Figure 2. Destroyed buildings in the village of Voelkershausen directly above the fracture zone of the rock burst 1989.

This event resulted in the destruction of 3200 carnallitite pillars at depths between 750 to 900 metres. The above-mentioned calculation model provides a consistent explanation of the rupture process which had occurred as well of the failure of the Lower-Werra rock salt by CO_2 gas frac during the dynamic relaxation of the floor when the working area collapsed (Minkley, 2004).

2. Visco-elasto-plastic material model

In order to be able to adequately simulate the brittle fracture process in rock mechanic model, an elasto-plastic material model with degradation needed to be developed. The shortcoming of the linear Mohr-Coulomb model is the effective strength increasing infinitely at a rising confining pressure (σ_3):

$$\sigma_{1B} - \sigma_3 = \sigma_D + \left(N_\phi^L - 1\right) \cdot \sigma_3 \tag{1}$$

with

$$\sigma_D = 2 \cdot c \cdot \sqrt{N_\phi^L} \qquad N_\phi^L = \frac{1 + \sin\phi}{1 - \sin\phi} \tag{2}$$

in which σ_D is uniaxial compressive strength, c cohesion, ϕ the friction angle, σ_3 minimum principal stress and σ_{1B} maximum principal stress at failure.

Since an infinite effective strength is not realistic physically, a strength limit was introduced for $\sigma_3 \rightarrow \infty$, the maximum effective strength σ_{MAX}. Hence, the modified Mohr-Coulomb model can be written in the form:

$$\sigma_{1B} - \sigma_3 = \sigma_D + \frac{\sigma_3}{\dfrac{1}{N_\phi^L - 1} + \dfrac{\sigma_3}{\sigma_{MAX} - \sigma_D}} \tag{3}$$

The new non-linear fracture hypothesis contains the linear Mohr-Coulomb model as the limiting case for $\sigma_{MAX} \rightarrow \infty$. By introducing the parameter

$$\sigma_\phi = \frac{\sigma_{MAX} - \sigma_D}{N_\phi^L - 1} \tag{4}$$

the relation (3) can be written in the form:

$$\sigma_{1B} - \sigma_3 = \sigma_D + \frac{\sigma_{MAX} - \sigma_D}{\sigma_\phi + \sigma_3} \cdot \sigma_3 \tag{5}$$

For the description of strain hardening and strain softening the parameters σ_D and σ_ϕ depending on the plastic shear deformation are applied.

The elasto-plastic model is linked to a modified non-linear Burgers model. The developed visco-elasto-plastic model (Fig. 3) with hardening/softening and dilatancy can be utilized in UDEC, 3DEC, FLAC2D and FLAC3D as user defined model (Minkley et al., 2001). The constitutive model was used in the recalculation of the rock burst in Voelkershausen for the description of the mechanic characteristics of the saliniferous rocks.

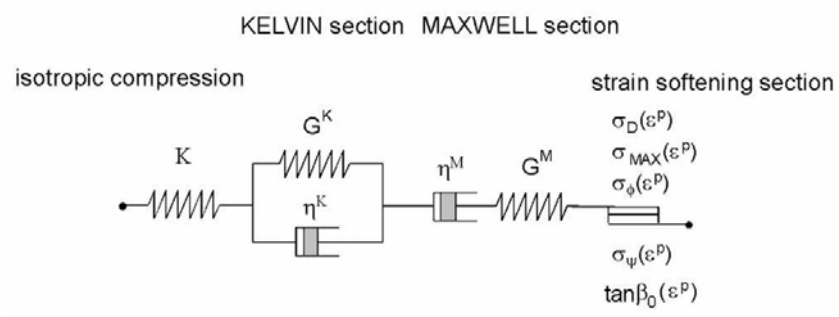


Figure 3. Visco-elasto-plastic model.

3. Back-calculation rock burst Voelkershausen 1989

The rock mechanical structure model is 3450 m wide and depicts the geological profile from the surface to the Lower Permian in a depth of -700 m sea level (Fig. 4).

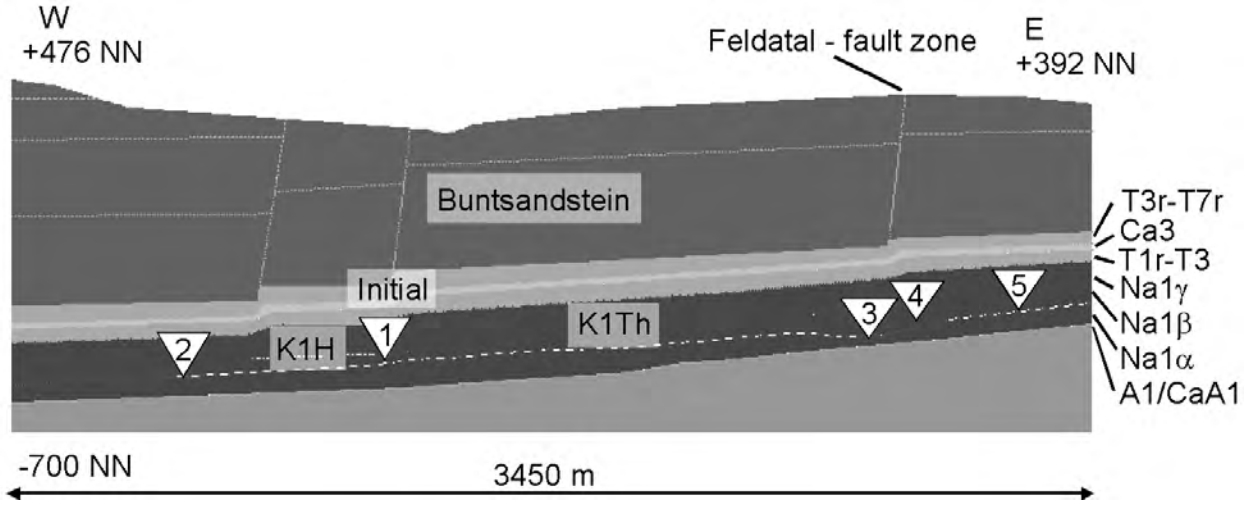


Figure 4. Development of pillar failure in carnallitite at 2nd seam - rock burst simulation in model (K1H = seam *Hessen*, hard salt; K1Th = seam *Thuringia*, carnallitite).

The saliniferous strata series of the Obere Leine-clay (T3r) at the base of the Buntsandstein overlying rock to the Lower Werra-anhydrite (A1) located in the subjacend bed is described uniformly in the rock mechanic model with the visco-elasto-plastic model including the typical characteristics of the individual saliniferous rocks for hardening/softening and dilatancy as well as the viscous characteristics determining the rocks' creeping behavior.

In the numerical model the blasting was simulated at the carnallitic pillar below the mining face of the 1st seam (Fig. 4) with unsymmetrical load distribution by applying a pressure impulse and a progressive pillar fracture process occurred. The pillars in the mining district neighboring in the east hold the heavily reduced additional load without failure (Fig. 5, curve 5). According to the calculation the fracture process for the 1600 m from the dynamically stimulated pillar to the eastern rib lasted approximately 2.2 seconds (Fig. 5, curve 3).

The seismological investigations also concluded that the propagation of the fracture process across the entire mining district occurred within a time span of 2…3 seconds (Ahorner, 1998). Thus, the chain-reaction-like pillar fracture process in the dynamic calculation is in good accordance with the real sequence of the rock burst process.

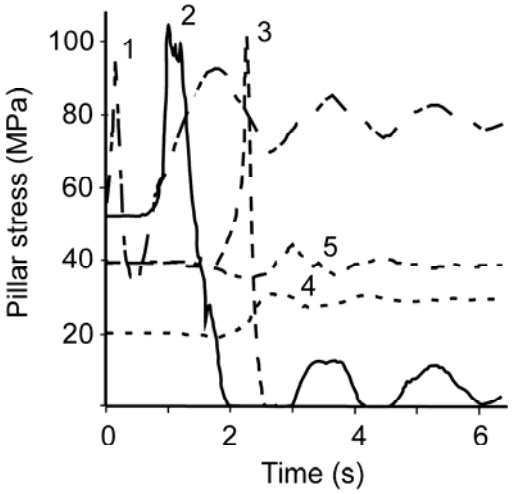


Figure 5. Pillar stress vs. time - rock burst simulation (location see Fig. 4).

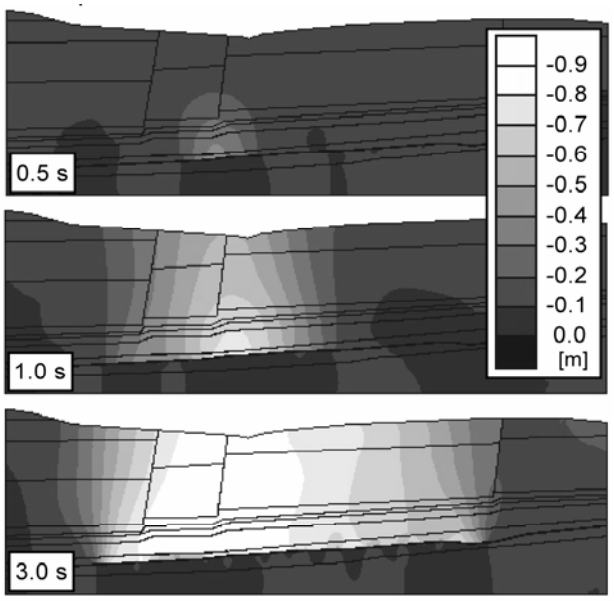


Figure 6. Vertical-displacements at 0.5, 1.0 and 3.0 s after rock burst initial - model simulation.

Figure 6 shows the calculated vertical displacements in the rock mass at different points in time. According to the calculation, the subsidence of the surface, which occurred dynamically, reaches about 1 m in the subsidence center after the oscillation has stopped. This is the same amount as yielded in the subsidence measurement conducted after the rock burst.

In connection with the convergence jump in the mining horizon the minimum principal stress at the base of the Lower Werra-rock salt Na1α in the area of the thinned zone below the Feldatal-fault zone decreases suddenly by 20 MPa to a few Megapascal (Fig. 7) after the pressure surge has gone through in front of the fracture front.

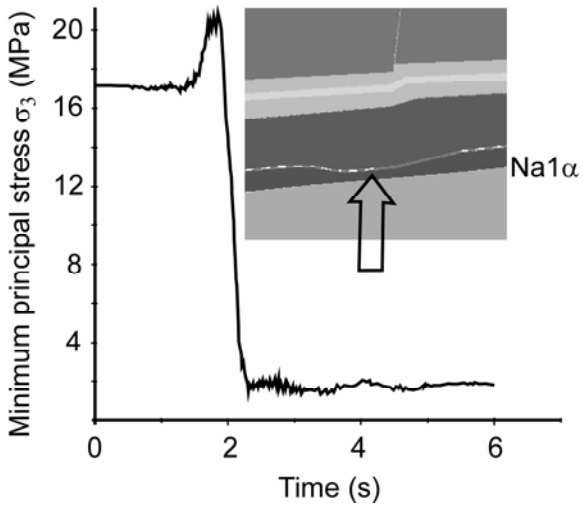


Figure 7. Decrease of minimum principal stress σ_3 at base of Lower Werra rock salt Na1α - rock burst simulation.

The permeability in the superjacent protective layer was calculated using a permeability-porosity-correlation (Minkley, 2004).

The primary permeability in the rock salt of $K = 10^{-22}$ m^2 is significantly increased in the areas below the rooms' seams due to destrengthening and dilation. However, a highly permeable zone

with $K \approx 10^{-4}$ m^2 has formed exclusively in the balk area of the rock salt rising up to the upper edge of the Lower Werra-anhydrite. Immediately after the rock burst CO_2 was detected escaping from clefts and gaps in the gallery level at the south-eastern rib of the fracture zone.

4. Requirements on stabilization measures

What was needed was a suitable scale for assessing the stability of working areas in the Thuringian mines of Merkers and Unterbreizbach which have comparable dimensions. Then, as such only the dimensioning method as applicable to the Hessian mines was available. This method had been elaborated by Uhlenbecker (1971) and had proven as a safe method by experience. This dimensioning method is based on short-period tests carried out on models of carnallitite pillars to be carried out for determining the failure strength as a function of the width-to-height ratio of the pillars. In dimensioning the pillars, scale effects existing between the pillar model and the situation in situ as well as the time-depending de-stabilisation behaviour have been taken into consideration by introducing an empiric safety factor of

$$S = \frac{\sigma_{\text{failure}}^{\text{model}}}{\sigma_{\text{in situ}}^{\text{pillar}}} = 3 .$$

Experts' inspections with respect to the state of dimensioning of the carnallitic working areas of the Thuringian Werra region as carried out by Wittke (1993) and Wilke (1994) have shown that there exist in part essentual gradual deviations from the required value of the safety factor S = 3. These deviations concern both the calculated values of single pillars and the application of an array rule aiming at compensating local undersizing. As a result of the inspection regarding the pillar dimensioning, in 1993 for six working areas the competent Mining Office has directed the duty of stowage which had to be accomplished by inserting stowing material in an amount of about 30 millions of tons. As stowing material only rock salt was the possibility, since the must urgent working areas in the Merkers mine which were concerned by the stowage duty required really about 13 millions of tons, i. e. an amount which, due to limitation in time, could not by acquired in the form of suitable residual materials. At first, only complete stowing was considered to be the most effective measure beyond all doubt. Thus, the working rooms were completely stowed so that the carnallitic pillars were completely embedded in the stowing material. This was moistened before and then compacted by bulldozing tractor shovels and afterwards pressed up to the roof to reach engagement. The rock salt stowing material was mined in an especially prepared working field having a room-and-pillar supporting system with pillars sized for long-period stability.

For optimizing the work necessary to guarantee safety, in 1998 the IfG – Institute for Rock Mechanics Leipzig – was instructed by the Federal Agency for Special Tasks in the Connection with the Re-Unification to investigate the properties of rock salt stowage and to provide the evidence of the efficiency of stowing as a function of the height of the filled-in stowing material by carrying out adecuate calculations. With regard to the carnallitic working areas of the Merkers potash mine the aim of filling these working rooms with stowed rock salt consists in eliminating the potential rock burst danger. If the method of embedding should prove successful in altering the supporting behaviour of the carnallitite pillars in such a way that the necessary condition for a dynamically occurring failure process (brittle rupture) will be eliminated then any release of seismic energy would not any longer be possible. In the sense of mechanics this means that the characteristic diagram of load-bearing capacity will rise steadily and no decrease in the load-bearing capacity will occur. By completely stowing the working room using the cohesive rock salt stowing material the above-mentioned condition will be fulfilled by the fact that the embedded carnallitite pillars show a

deformation behaviour which is characterized by increasing strengthening. The complete elimination of the liability of carnallitic support elements to brittle rupture (i. e. elimination of the necessary condition for a release of energy) by filling-in stowing materials, however, presents rather a conservative and expensive way. It is to be appreciated that a release of seismically relevant amounts of energy cannot be expected any longer even if the liability to brittle rupture is not completely prevented by stowing, provided that the sufficient condition will not be fulfilled any longer. Partially stowing the working rooms will generally impede the fulfillment of the sufficient condition for initiating a rupture – i. e. exceeding the load-bearing limit – by the fact that the maximum load-bearing capacity of the pillars will increase with a simultaneous reduction of the de-strengthening modulus (Fig. 8).

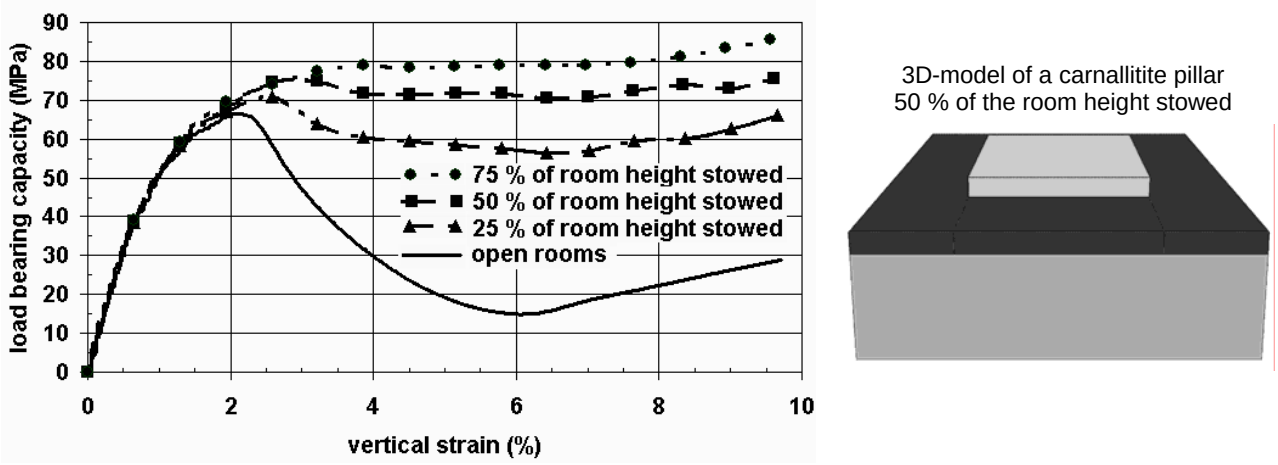


Figure 8. Calculated load bearing capacity of a carnallitite pillar by different stowage levels.

In the case of a single pillar it is not possible to settle to what extent the liability of the support element to brittle rupture and thus to an energy release must be reduced and the excitation threshold must be raised to secure that an energy release does not take place when the rupture development is in progress. Therefore, the conclusions made on the basis of calculations as carried out for single pillars have been supplemented by calculations concerning actual working systems and considering dynamically occurring stress conversions. Experience won in the practice shows that also under the conditions of a limited release of seismic energy (local instability, stress drop > 0) a breakdown of the working area will not occur if the dynamic excitation threshold for a failure of the system is sufficiently high, i. e. if there still exists a sufficient reserve in load-bearing capacity. Therefore, the task consisted in investigating which are the actual conditions on which a local instability transforms into system instability and how this mechanisms can be effectively blocked by embedding the carnallitite pillars by means of rock salt stowage. Therefore, an optimisation of stowing work was possible only on the basis of considerations concerning the dynamic system stability of actual working areas.

5. Experimental studies

A quantitative assessment of the stabilising effect of stowage required experimental tests to be carried out on this stowing material which consisted of rock salt which was mined in the Eastern area of the Merkers mine and filled in the respective carnallitic mine areas. Rock salt stowing is characterized by building up cohesive bonds that due both to the chosen filling technology using previous moistening followed by compaction carried out by tractor shovels and to the wide grain

size range of the materials won by blasting. This fact allowed to win drill core samples from the stowed mass in the south eastern field of the Merkers mine (Fig. 9) and to determine the values of cohesion and friction angle which are of importance from the viewpoint of strength mechanics.

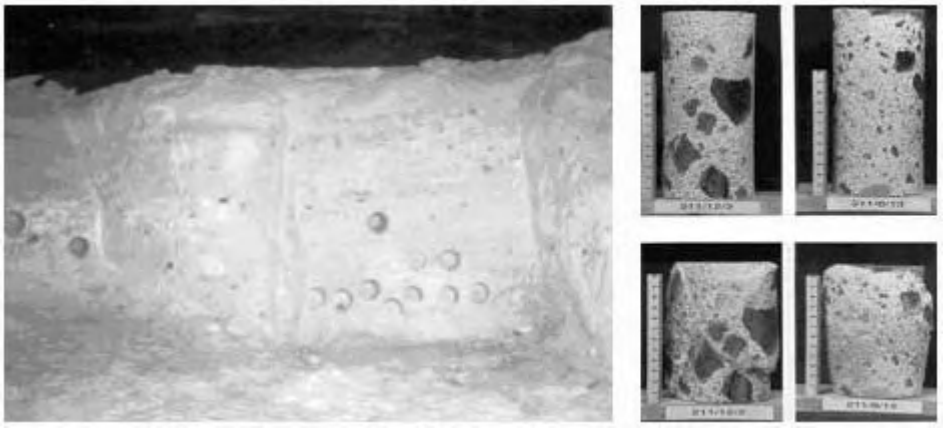


Figure 9. Compacted stowed mass in the SE-field of the Merkers mine and sampled drill cores to determine the strenght values of cohesion and friction by rockmechanical laboratory tests.

As a result of these rock mechanical tests, the stowing material sample has been subdivided into two densitiy classes, namely $\rho > 1.6$ g/cm³ and $\rho < 1.6$ g/cm³ (Table 1), the stowing material with the lower density having been found mainly in the upper layers of the stowed material.

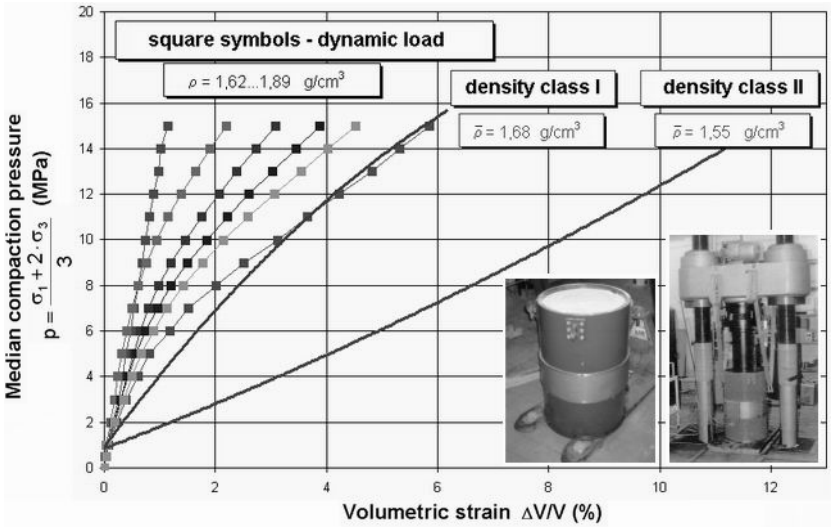


Figure 10. Test results of study the compaction behavior of the inserted rock salt stowing material.

The compaction behaviour has been studied in a pressure cell designed for stowing materials and having a volume of 160 litres (Fig. 10). The rock salt stowing material was pre-compacted to such density values as found under in-situ conditions and filled into the mentioned cell. The compaction rate of the stowing material during the quasi-static laboratory tests was several orders of magnitude above the rate at which the stowing material is compacted in situ by underground cavity convergence. The pressure of storage that builds up during loading depends on the compaction rate. The higher the compaction rate the quicker will rise the resistance of the stowing material. For verifying this pressure behaviour of the stowing material, also some tests have been carried out using rock salt stowing material from the Merkers mine and applying dynamic pre-compaction of the stowing material.

Table 1. Rock salt stowage in the Merkers mine.

Type of stowing material	Density ρ [g/cm³)	Friction angle ϕ [°]	Cohesion c [MPa]
Class I	> 1,6 (1,68)	41	0,73
Class II	< 1,6 (1,55)	39	0,21

The graphs of the stowing material pressure which have been determined under dynamic loading are generally above those graphs as determined under quasi-static load conditions (Fig. 10). It is to be emphasized that the aim of the long-term storage by embedding undersized carnallitite pillars in rock salt stowing material in the Merkers potash mine consists in the prevention of rock burst dangers, i. e. dynamically running processes. When in the calculations carried out for assessing the dynamic system stability of the stowed working areas that pressure diagram of the stowing material which has been determined under quasi-static load conditions has been presumed so represents this quite a conservative approach.

For determining rock mechanical material parametres in laboratory tests rock specimens have been sampled from pillars in the respective working area. The sampling sites are located in such supporting pillars where also stress measurements and drill hole sampling have been carried out. The rock mechanical studies on the carnallitite specimens have been carried out with the aim to determine such mechanical parametres which allow to describe both the time-dependant viscous behaviour and the de-strengthening behaviour of the solid carnallitite varieties which leads to brittle rupture (Fig. 11). The basis for the mechanical description was the visco-elasto-plastic constitutive model which has been developped especially for carnallitite. By applying the elasto-plastic part of this model (de-strengthening model by Minkley (1997)) the rupture strength, the deformation-depending de-strengthening, and the dilatancy of the rock material are covered by a not-associated yield law. This way, the prerequisites have been created which allow to image the de-strengthening brittle-rupture processes which are typical for carnallitite in the rock mechanical model as a function of the actual deformation state and the effective constraining conditions.

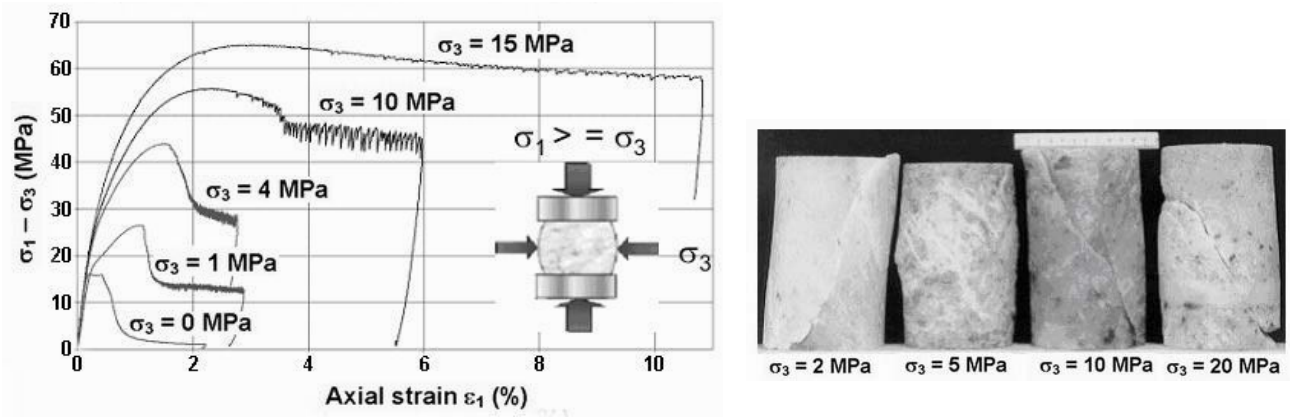


Figure 11. Results of several triaxial strength tests at different confining pressures to determine the failure boundery and the strain softening behavior of carnallitite

Triaxial constraining of the carnallitite pillars is determined mainly by the shear strength on the contact surfaces between the pillar rock and the rock salt of the roof and the floor. Therefore, specimen blocks with layer transitions from carnallitite to rock salt have been mined in situ to carry out direct shear tests in the laboratory. For modeling the cohesion loss on the layer surfaces a shear model has been applied which has been developped especially for salinar bedding planes (Minkley et al., 2005).

6. Calculations on the load-bearing performance of pillars embedded in stowing material

The liability of carnallitite pillars to brittle rupture can be restricted or eliminated by embedding them in stowing material. The decision whether partial or complete stowing will be sufficent for their stabilisation depends on the mechanical properties of the stowing material and on the dimensions of the respective pillars. Examples for insufficient stowage are the rock bursts in 1916 at Angersdorf and in 1940 at Teutschenthal which have been initiated in partially stowed working areas still during the operative phase by blasting work for salt working. The trace-back calculation of a long pillar in the 1940 rock burst field which had been stabilised in stowing material, provided the result that the slender pillars (width-to-height ratio = 0.6) are still able to fail in a brittle manner at a height of the stowing material of 75 per cent when dynamically loaded. As a result of its dynamic loading the unstowed upper portion of the pillar having a ratio of width to free height equal to 2.5 showed an intense de-strengthening of the contour and destruction phenomenae reaching to the pillar core. In the pillar region embedded in stowing material the de-strengthening of the contour is significantly reduced. Partial stowing was not suited to prevent the 1940 rock burst having the magnitude $M_L = 4.3$ and causing a sudden subsidence at the surface of about 0.2 metres.

On pillars having a higher width-to-height (W/H) ratio the embedding in rock salt stowing material shows a significantly higher stabilizing effect even at lower heights of the stowing material. When exposed to dynamic loading and after exceeding the load-bearing limit at about 45 MPa a carnallitite pillar having a W/H ratio equal to 3 and embedded up to half of its height in rock salt stowing material shows a response consisting in a moderate stress reduction before the load-bearing capacity begins to rise after reaching a pillar deformation of about 4 per cent which is due to the resistance of the stowing material (Fig. 12a). This means that because of the de-stabilising deformation behaviour (reduction in load-bearing capacity) during the failure process, there exists still the possibility that energy can be released to a limited extent. At a height of the stowing material of 75 per cent a compact pillar having a W/H ratio = 6 will be sufficiently stabilised (Fig. 12b). The graph of the load-bearing capacity shows a stabilising deformation behaviour which means that an energy release will not occur.

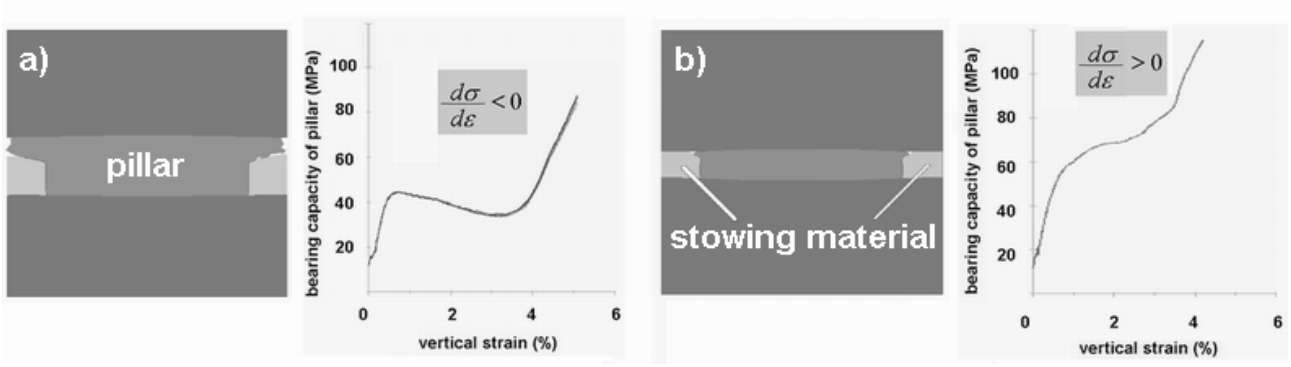


Figure 12. Model calculations to study the bearing capacity of carnallitite pillars embedded in rock salt stowing material a) W/H ratio = 3 and 50 % of the room height filled b) W/H ratio = 6 and 75 % of the room height filled.

Apart from calculations on single pillars also the dynamic system stability of pillar arrays has been studied using 3D-models. The calculation example shows a severely undersized array of 9 carnallitite pillars at a depth of 710 m which have safety factors S = 0.75…1.75 and W/H ratios = 2.7…4.6 (Fig. 13). The pillar having the lowest safety coefficient S = 0.75 (PF 96) was dynamically excited ($M_L \approx 2.5$) and the response of the unstowed system to this excitation was studied. As a result, all pillars fail and the de-strengthened carnallitite is shifted for several metres towards the working rooms (Fig. 13 below), this shifting being farthest in the case of such severely undersized

pillars having safety coefficients S < 1. For the purpose of a numerical analysis of the stabilizing effect of rock salt stowing the pillars have been embedded up to half of their heights in stowage material. After dynamic excitation having the same magnitude the failure is limited to the excited pillar and to the neighboured severely undersized pillars. The remaining pillars show only contour damages. The horizontal shifts observed on the pillar contours reach only a maximum of 0.4 m in comparison with 3.4 m in the unstowed room-and-pillar system.

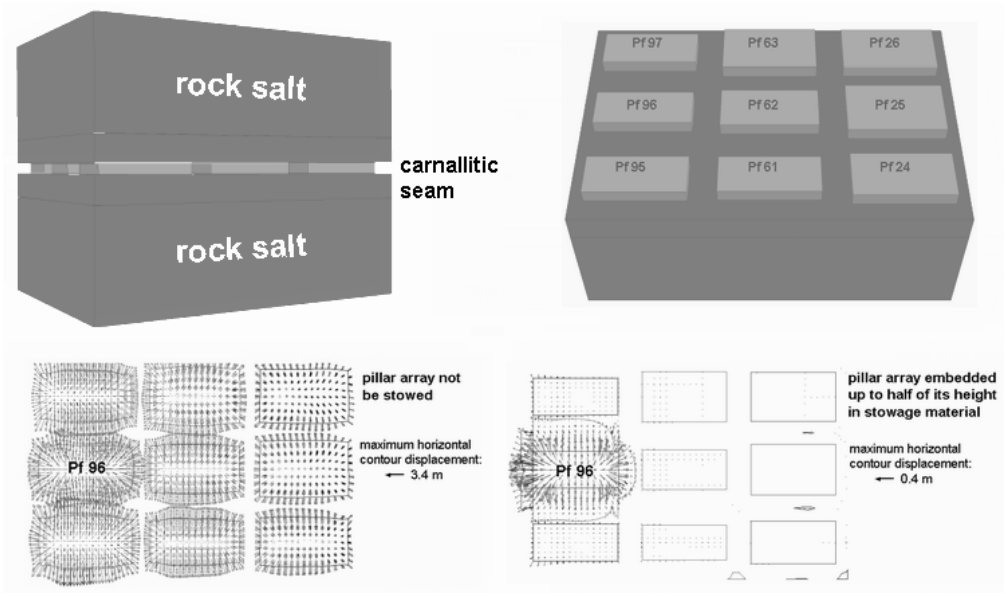


Figure 13. 3D-model calculations to analyse the system stability of a pillar array by dynamic stimulation.

7. Calculations for increasing the system stability by stowage

In the following, rock mechanical calculations will be presented which have been used to study the dynamic system stability of open and stowed room-and-pillar working systems in carnallitite by using typical partial working fields characterized by long-room workings and situated south of the rock burst field of the 1958 rock burst in the Merkers potash mine. These calculations refer to a working block having relatively high working heights reaching up to 12 m with correspondingly slender pillars (W/H ratios = 0.8…1.7). This block is the partial field which shows most severe undersizing in the eastern working field of Menzengraben. It is just the block above which the highest subsidence values have been measured. When dynamically excited, the system will collapse and the working rooms will be stowed by the caved carnallitic material (Fig. 14).

Subsidence values up to a maximum of 0.8 metres would occur at the surface if the rupture process extends over a major area. When applying a height of the stowed material equal to 50 per cent of the pillar heights, however, above the stowed material the pillar contours will show a comparatively severe de-strengthening when dynamically excited. Through shear zones will develop in the pillars. Potential subsidence values will reach several centimetres at the surface which values would correspond to a release of a still quite high amount of energy ($M_L \approx 3.5$). A significantly favourable dynamic system behaviour will be expected when the height of the stowed material exceeds 75 per cent (Fig. 14). Then, the subsidence values at the surface will reach less than a half centimetre. Considering eventual imponderables, therefore, complete stowing has been recommended to stabilize those severely undersized partial areas characterized by slender pillars.

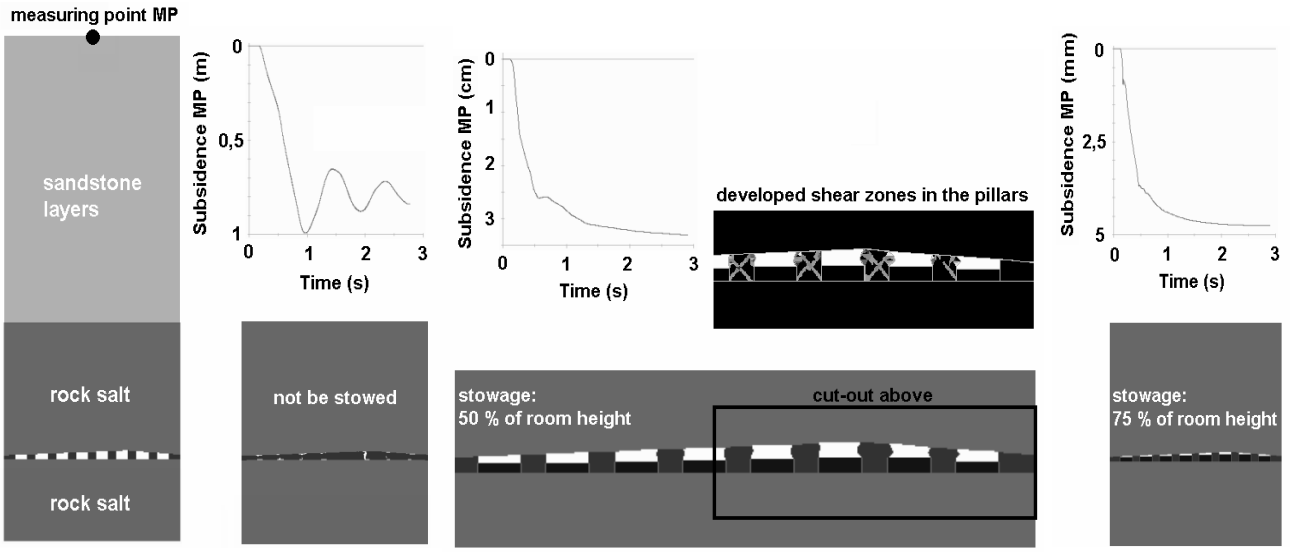


Figure 14. Results of numeric model calculations to determine the dynamic system stability of a undersized pillar assembly in carnallitite by different levels of stowage.

The working areas situated north of the field of the 1989 rockburst at Voelkershausen have been subjected to a stability assessment, too. The regarded region is preceded towards north the eluviation depression of Oberzella which represents a zone of eluviation extending over an area of about 25 km². At a large-area scale here more than 100 metres in salt thickness are missing. A hydrologic danger may proceed from the fact that the established and supposed thickness values of the Lower Werra rock salt formation at several places fall short and when fluids would rise from the sub-salinar layers due to a collapse of the working area, a situation similar to the failure of the floor barrier at the margin of the afflicted field of the rock burst dated 13.02.1989. In the northern field of the Merkers potash mine 69 per cent of the total number of 1779 pillars have shown to be undersized as assessed following the dimensioning method developped by Uhlenbecker. In the carnallitic field parts 57 per cent of the pillars have calculated safety coefficients $S < 2$ and 13 per cent have savety values $S < 1$. As a whole, the situation can be judged that the northern field is characterized by quite different working parametres showing partially a severe undersizing but also including parts having certain reserve in load-bearing capacity. In the sylvinite layers and in regions having alternating layers of carnallitite/sylvinite the undersizing results in higher deformation values (higher compliance values). In several inspections carried out in situ, massive rupture phenomenae have been observed in the sylvinite layers and in regions having such alternating layers of carnallitite/sylvinite. Among the factors which reduce the load-bearing capacity there are also frequently appearing gas or liquor impregnations as well as layer surfaces having separating properties. These cause a quick reduction of the triaxial constraint of the pillars due to increased lateral strain and thus the reduction of the reserves in load-bearing capacity in the course of time. The observed contour ruptures which have occurred in major parts of the northern field indicate that still existing stability reserves will be continuously consumed. This process can be counteracted in a suitable manner only by controlled stowage. The reason is that, due both to the partially high pillar loads ranging from 40 to 50 MPa and to the comparatively low width-to-height ratio, the time-depending de-strengthening process will not come to a stop by itself and therefore may give rise to a certain danger.

Rock mechanical calculation models with regard to the system behaviour of the northern field of the Merkers mine have allowed to show that there is in fact a certain possibility that within a significantly undersized pillar supported system a progressively running rupture process will develop out of a local instability. In transition zones to sylvinitic facies this rupture process comes

to a stop thanks to the significantly lower liability of the sylvinite to brittle rupture in comparison to that of carnallitite. As can be seen from the rock mechnical calculations, in the case of dynamic loading the possibility that the floor barrier will suffer from a loss of impermeability cannot be excepted. As a result of the studies carried out with regard to a specific working area and the rock mechanical calculations the following basical recommendations for performing the required stowage work have been presented:

- Sylvinite and mixed salt regions which already show severely damage by rupture events ought not be included in the stowage measures.
- The accessible underground carnallitite regions have to be filled predominantly up to 75 per cent of the opened room heights.
- Strongly oversized pillar arrays must not be stowed.

For other undersized working areas in the Merkers mine a geomechanical assessment of their state regarding mine safety has been performed, too. As a result, for several working areas subjected to the duty of stowage could be established that partial stowage up to a range between 50 per cent and 75 per cent of the working height will secure to reach permanent stability. The studies and calculations have shown, too, that in the south eastern field II which is situated at a small depth of 500 m (there 73 per cent of the pillars have safety values of $S < 3$) a parcellation of the working area by stowage barriers of 200 m in width in which the pillars are embedded up to 75 per cent of the room heights in stowing material will be sufficient to stabilise them (Fig. 15). This is due both to the fact that there the pillars have a stratified structure of carnallitite, hard salt and rock salt and to the existence of un-mined dead grounds.

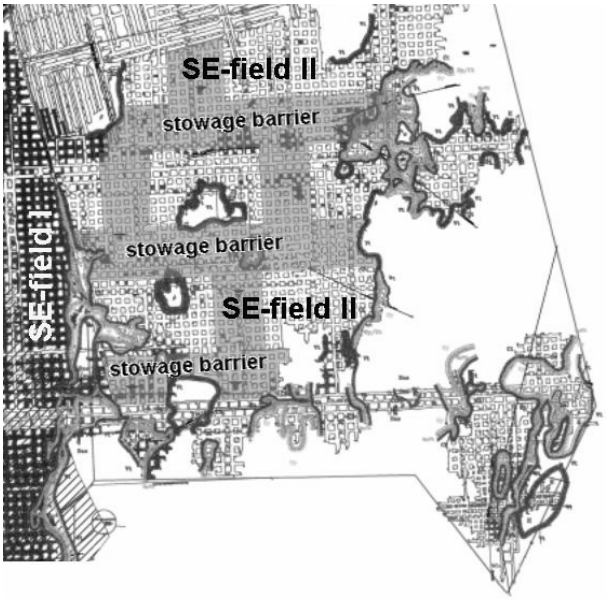


Figure 15. Parcelling the working area of the SE-field II Merkers mine by build up several barriers in which the undersized pillars are empedded up to 75 % of the room heights in rock salt stowing material.

8. Conclusion

Apart from the re-opening of the working areas according to the state of the art, from the assessment of their state with respect to specific working areas and from the mining of the rock salt stowing material, geomechanical studies on the load-bearing behaviour of carnallitite pillars embedded in rock salt as well as on the system stability of stowed room-and-pillar working systems

form to the prerequisites which are required for carrying out the demanded stowage measures in an optimal manner. Rock mechanical calculations have been carried out using a visco-elasto-plastic constitutive model to describe the de-strengthening and brittle rupture behaviour of carnallitite. As a result, for 4 working areas out of 7 working areas of the Merkers mine these calculations have allowed to recommend partial stowage – instead of complete stowage – to stabilise them. Thus, all carnallitic working areas of the Merkers mine which have a certain long-term liability to de-strengthening and to instability can be included in the global stowage measure without the need of essentially expanding the available total amount of stowage material of 30 millions of tons. By rock salt stowing the following geomechnical aims are pursued:

- Raising the dynamic excitation threshold for local pillar failure.
- Increasing the stability level in the respective working area to block off any transition of local system stabilities to system instability and thus to eliminate any rock burst danger.
- Reducing the convergible cavity volume and decreasing the strain in the geologic protective layers of the roof and the floor as well as reducing subsidence and thus limiting the effects at the surface to an acceptible extent.

The mining activities required for stabilizing the carnallitic working areas in the Merkers mine will terminate probably in 2015.

9. References

Ahorner L. (1998). *Entstehung und Ablauf des Gebirgsschlages von Völkershausen am 13. März 1989 im Kalibergbaugebiet des Werratales, Thüringen, aus seismologischer Sicht.* Geologisches Jahrbuch, E 55, 25-46

Eisenbach U., Paulinyi A. (1998). *The potash industry in the Werra and Fulda region.Hessisches Wirtschaftsarchiv.* Scripts on Hessian economic and company history, Nr. 3, Darmstadt

Minkley W. (1997). *Brittle rupture behaviour of carnallitite and its impact on long-term safety of underground disposal spaces.* Reports FZKA-PTE Forschungszentrum Karlsruhe GmbH, Nr. 5, 249-275

Minkley W., Menzel W., Konietzky H., te Kamp L. (2001). *A visco-elasto-plastic model and its application to solving static and dynamic stability problems in potash mining.* Proc. 2nd Int. FLAC Symposium Lyon, 29-31 October 2001, 21-27

Minkley W. (2004). *Back analysis rock burst Völkershausen 1989.* 1th Int. UDEC/3DEC Symposium, Bochum, 29.09.-01.10.2004

Minkley W., Mühlbauer J., Naumann D., Wiedemann M. (2005). *Prognosis of the dynamical long-term stability of mine layouts in the salinar considering discontinuities and bedding planes.* Final report from IfG to FZKA-PTE Forschungszentrum Karlsruhe GmbH, FKZ 02C0892

Uhlenbecker F. W. (1971). *Rock mechanic studies carried out in the potash plant of Hattorf (Werra region).* Kali und Steinsalz 5, Heft 10, 345-359

Wilke F. L. (1994). *Gutachterliche Stellungnahme zum Gefährdungspotential Grube Merkers.* Technische Universität Berlin, Institut für Bergbauwissenschaften, unpublished

Wittke W. (1993). *Gutachten über den Einfluß der vorhandenen Abbaufelder auf die Tagesoberfläche - Teil IV Grube Merkers.* WBI - Wittke Beratende Ingenieure für Grundbau und Felsbau GmbH Aachen, unpublished

PLACE OF A SOCIO-ECONOMIC APPROACH IN THE WATERSHED-SCALE POST-MINING MANAGEMENT: EXAMPLE OF THE GOLD MINING DISTRICT OF ST-YRIEIX, FRANCE

ORRU Jean-François[1], RECOCHE Gilles[1], ITARD Yann[1]

[1] BRGM 3, Avenue Claude Guillemin – BP 6009 – 45060 Orléans Cedex 2, - France.

jf.orru@brgm.fr; g.recoche@brgm.fr; y.itard@brgm.fr

ABSTRACT: In post-mining period management, socio-economics contribute to the understanding of the constraints and assets of a space defined by multiple criteria (economic, cultural, social, environmental, landscape, etc.) that are often interrelated. The BRGM, within the scope of its AREDIE research project, is working on a novel, overall approach on a pilot site, the Saint-Yrieix area in France, by combining the biochemical aspects of the flow of pollutants, societal dynamics and territorial mutations in order to further understanding. The aim of this interdisciplinary approach is to contribute, through a multi-faceted (spatial and temporal) and participative approach, to a better understanding of the social and economic aspects linked to the closure of mines in the Saint-Yrieix area. The synthetic analysis could be used by decision makers in their land development strategies.

KEYWORDS: Socio-economics; post-mining period; governance; reconversion; territory; Saint-Yrieix.

RESUME : Dans la gestion de l'Après-mine, la socio-économie contribue à la compréhension des contraintes et des atouts d'un espace défini par des critères multiples (économiques, culturels, sociaux, environnementaux, paysagers…) qui sont souvent en interrelation. Le BRGM, dans le cadre de son projet de recherche AREDIE s'inscrit dans une approche globale novatrice sur un site pilote : le secteur de Saint-Yrieix, en associant à la compréhension des aspects bio-chimiques des flux de polluants, les dynamiques sociétales et les mutations territoriales. La finalité de cette démarche interdisciplinaire est de contribuer par une approche multi-échelles (spatiales et temporelles) et participative à une meilleure compréhension des aspects sociaux et économiques liés à la fermeture des mines du secteur de Saint-Yrieix. L'analyse synthétique pourra servir aux décideurs dans leurs stratégies de développement territorial.

MOTS-CLEFS : socio-économie, après-mine; gouvernance; reconversion; territoire; Saint-Yrieix.

1. Introduction

Although the phase of mine exploitation marks the most important part of the development of a region, it is effectively in the post-mining phase that the integration of a mining project will finally be judged as part of a sustainable development process. It is only at this stage that the cost-benefit analysis can be drawn. For a long time, most research work focused on the problems related to the post-mining period and its impacts through separate approaches; by distinguishing the physical effects (mining collapses and mechanical instabilities), environmental aspects (water and soil pollution) and health and social aspects (Lacoste & Spinosi, 1998).

In France, the importance of economic and social consequences of the closure or the end of mine workings in the Nord-Pas de Calais or Lorraine mining regions (Convert & Pinet, 1992; Laversanne & Faille 1999) has led to carry out numerous studies mainly focused on the socio-economic dimension. Over the last decades, important funding has been liberated allowing a large implication of all stakeholders and regional associations. In spite of this investment, the reconversion programmes have had difficulty compensating for the imbalances caused (Meilliez, 1998; Mazade, 2000; Leconte, 2000).

On the other hand, in the metal mining sectors, environmental considerations have largely occult the socio-economic dimension of the post-mining management. Unemployment problems and the loss of financial returns concern relatively small communities (small towns, villages) meeting with difficulties for grouping their efforts in solution finding. In such case, the place of socio-economy, instead of being preponderant, can usefully contribute to an integrated watershed approach. It is the goal of the multi-disciplinary research project "AREDIE" developed by BRGM and presented in this paper.

2. The AREDIE project: watershed approach of a post gold mining situation

The general objective of this project is to build up knowledge and mastery of risk assessment tools in order to be able to propose to local decision makers, a management aid tool for former mining sites on the scale of a catchment area. The specificity of AREDIE project is to study the residual mining risks through an integrated approach at small watershed scale combining chemical, biological, mineralogical and human sciences.
AREDIE comes within the framework of research work on the socio-economic theme (elaboration of sustainable development indicators, management of conflicts, modelling and scenarios, land developments) carried out over the last few years by the BRGM.

The choice of the study zone has fallen on the southern Limousin region in the Haute-Vienne Department of France, in the upper part of the Isle watershed. This pilot site, with a surface area of 200 km^2, covers part of the gold-bearing district of Saint-Yrieix la Perche (south of Limoges) extending over 2300 km^2. Nearly 90 gold lode deposits are known in this region and around sixty veins have been mined to a greater or lesser extent in the area, some since the Celtic period (Cauet, 1991a, 1991b & 1994). The sector upstream of the Isle basin comprises ten or so gold mines, now shut down.

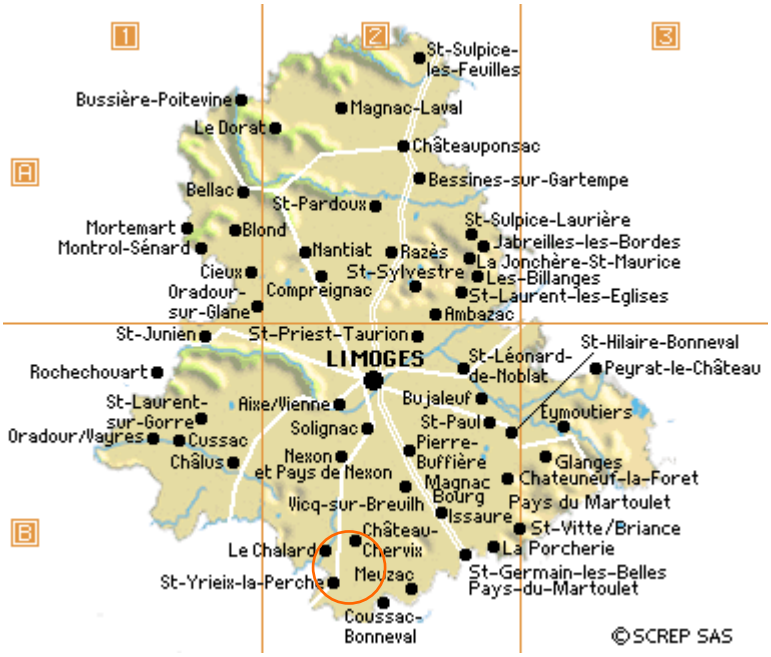


Fig. 1 : location of St Yrieix district in the Haute Vienne Department.

.

Most of these mines were worked in two stages, at the start of the 20th century then more intensively from 1980 onwards, for around twenty years. During this last period, around 25 tons of gold have been produced, representing 20% of the national production during this period.

The employment basin corresponding to the mining district is mainly based on agricultural/arboricultural activities. Tourism is one of the pillars of the local economy and the low level of industrial activities gave an important relative weight to the extractive industry sector. At the scale of the project the main administrative structure is the community of municipalities of St Yrieix, grouping 10 rural and 1 urban municipalities.

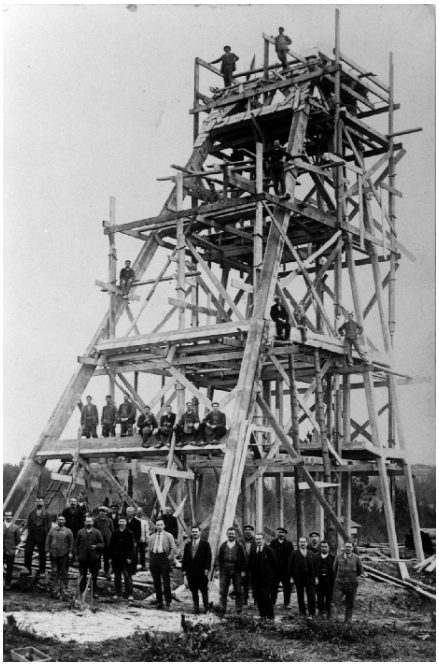


Fig. 2 : Mine Pit of Douillac(1920), St Yrieix district.

In the AREDIE research project, economic and social sciences are the subject of a module, the objective of which is to contribute to a better apprehension of complex dynamic phenomena (mutation of the space used, lived in and perceived) in an integrated logic in order to escape from the shackles of conventional specific approaches and to establish the link between biochemical environmental studies and social and economic studies. This overall approach, favourable to the production of synthetic analyses, could serve as a support for deliberations (relative viewpoint, predisposed to mediation and negotiation) regarding land use management.

Thus, beyond the study of the pilot site chosen for AREDIE, it is indeed a question of the problem of managing the social and economic situations of the post-mining period. Through the analysis of territorial mutations, it involves evaluating the impact of the closure of mines on the local socio-economic context.

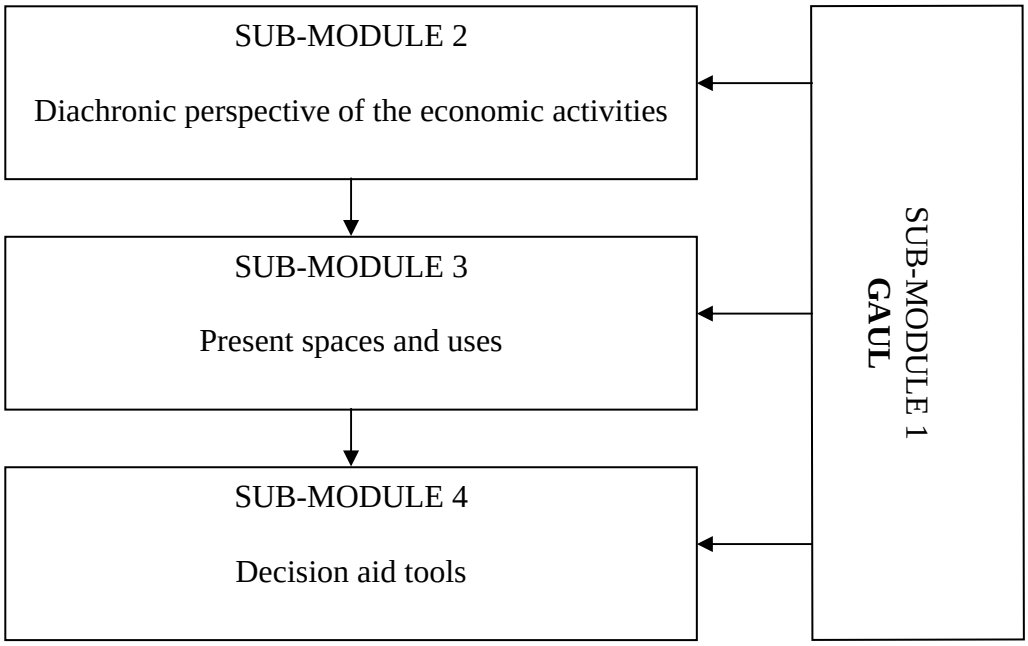
Three principal study themes are envisaged:

- The diachronic perspective (before, during and after) of economic activities, the principal objective of which is to take account of the change in the relative importance of the mines within the local economic infrastructure.
- The characterisation of the present situation, not just in terms of the demographic panorama and economic activities but also in terms of land-use restrictions.
- These two approaches will highlight the key parameters of the mutation and will make it possible to develop an analytical approach for constructing tools for evaluating socio-economic mutations (reviews) and conceivable perspectives (scenarios).

From an organisational point of view, the socio-economic module of the AREDIE project is broken down into four sub-modules, namely:

- A sub-module corresponding to the implementation of an interactive communications cell and think tank known as GAUL (Local Stakeholders and Users Group).
- Two research sub-modules, one focused on an analysis of the historic perspective of economic activities and the social context and the other on a diagnosis of the state of the present situation.

- Finally, the fourth sub-module concerns the manner in which this approach may be extended to other post-mining situations, through the development of monitoring and decision making aid tools.



3. Participative approach: issues and constraints

Given the historic importance of mines in the life of local communities and the current issues and challenges in terms of reconversion, this type of project is not restricted to a limited exchange between scientists and administrators. Indeed, the inhabitants of the sector, whether users or not of the natural environment, are also concerned and interested, not only in the present situation but also in the future of their community and their region. First and foremost, they are the living memory of history and the best persons to recount the lived-in space and the perceived space. We therefore considered it essential to establish the project in a participative approach.

The objective of the socio-economic approach, linked to the environmental and biochemical studies, is to create this research – community link by setting up a **group of local users and stakeholders** (GAUL). This cell is not intended to act uniquely as a focus for exchange, but instead as a think tank in which the voluntary participants can, throughout the lifetime of the project, provide their contributions through their knowledge and their view of land development (present situation, testimonies from the past, vision of the future).

As part of a research project concerning a problem that is both sensitive and topical, calling on the services of an interactive cell (comprising administrators, local elected representatives, economic stakeholders representing associations and the general public) poses the risk of getting bogged down in a militant debate given the amount of pitfalls and hazards (unemployment, pollution, land easements, etc.). Therefore, the decision to make this cell a working group as much as an objective, scientifically rigorous structure for dialogue is primordial and should make it possible to avoid purely descriptive shortcomings or partisan arguments.

It is in striving to appreciate the value of local history by gathering testimonies from a period that formerly enjoyed a certain influence, by accepting this past that has now gone by rather than pushing it away like a phantom from the past that we will be able to establish, in a dispassionate manner, the solid bases to assure a transition and move towards the construction of a new territory and a new socio-economic context.

This reconnaissance work is essential in order to reflect on the constraints of the present situation and the future outlook, because the characteristics of the post-mining period did not just appear as such, but instead form part of a historic continuum spanning several generations and for which the countryside is, after all, the only witness from "start to end". Therefore, the point will not be to take part in a critical view of mining but instead to begin to become aware of the history and lessons that former periods can provide in order to build a better future.

Given the necessary structuring of the working themes to be covered within the GAUL, this structure will be activated when the initial results of the historical and socio-economic research sub-modules are available concerning the evolution of the activities and communities and on the characterisation of the present situation of the spaces and uses of the land. Moreover, avoiding partisan debates has required, on our part, sufficient knowledge of the various players involved, work that was carried out in the first few months of the project.

4. Diachronic perspective of economic activities

The starting point for the historic analysis has been set at the start of the 20th century, which corresponds to the first concession applications in the Saint-Yrieix area. The study of documentary archives over a century has several objectives:

- To establish a diachronic economic record of the different activity sectors and thereby to assess the relative and comparative evolution during the mine working period.
- To take account of the socio-economic effects of the mining activity on the population (demographic fluctuations, repercussions on the habitat, on the infrastructures, etc.)
- To establish the zero condition necessary for evaluating the impact of the closure of the mines.

From a methodological point of view, this involves collecting, summarising and representing data. The data will be processed and structured so as to highlight the key periods and representative parameters (importance of activity areas, breakdown of assets per sector, inhabitants of the communities concerned, migration, etc.). This classified information will make it possible to carry out a comparative temporal analysis and to evaluate the impact of the mining activity on local socio-economic development, on the scale of the "basin".

The collection of bibliographic data concerning the economic and social aspects of the zone under study (administrative reports, university dissertations, archives, etc.) has already begun with various bodies (departmental archives, university archives, etc.). Several criteria guide these investigations, such as professional activities (mining activity, breeding, arboriculture, vegetable crops, cereal crops, forestry, tourism, etc.), leisure activities (fishing, hunting, walking, panning for gold, etc.) and other uses of the environment (existing habitat, land-use and town planning , etc.). The economic aspects (direct and indirect participation of mines in land use management and in socio-cultural and leisure activities) are also evaluated. Finally, the collection of data also takes into

consideration the demographic aspects [INSEE studies (French National Institute for Statistics and Economic Studies)].

With regard to the initial syntheses of the qualitative (accounts, narratives, interviews, descriptions, etc.) and quantitative data (number of people, production results, etc.), the information collected reveals a certain heterogeneity. Indeed, some data is quantified and other data not, some data covers the period in question relatively well while other data leaves wide information "gaps". This observation reinforces the interest in involving the GAUL in this task.

In so far as the existence of data (plans of mining sites, aerial photographs, spatial imaging, etc.), historical information such as the evolution of the amount of land acquired by mining works during the different mine working phases, then the monitoring of obsolete industrial zones and any land developments or rehabilitations undertaken since the cessation of activities will be dealt with by period, in order to take account of the evolution of the landscape.
Cartographic documents could therefore reconstruct the social imprint of the mines throughout their history, up to the present easements.

5. Land-use/land-cover: present and future.

The purpose of this sub-module is to establish a typology of the spaces (used, exploited and under easement) and to establish the panorama of present uses associated with them and likely to be impacted by contamination from a mining source (farming, breeding, fishing, etc.). This sub-module will be based on the results of other modules (characterisation of sources and characterisation of transfers and receptors) for the determination of the contaminants and the media likely to be contaminated, in order to determine the "sensitive" uses. Such uses will be localised, spatialised and documented.
Medium resolution spatial imaging (SPOT 2-3-4) and aerial imaging will also be used in this sub-module to analyse the land use. Thus, from maps drawn up on the basis of the historical evolution, it will involve re-transcribing the modifications in the use of the environment (constraints zones, extension of the habitat, farming areas to the profit of leisure zones, industrial zones, etc.) and the strategic planning objectives for land development and economic re-dynamisation (thematic projection maps).

To achieve the objective, two lines of investigation have been retained:

- The first concerns uses of land linked to the potential risks of contamination of the environment or easements with regard to the spaces. This involves firstly defining a socio-economic investigation methodology. The criteria enabling an inventory to be made and information gained on the different uses will be defined for drawing up an investigation protocol. This protocol will be tested by the GAUL. The community land registers and data of the Chamber of Commerce and Industry will provide complementary information on the economic activities. The associative sphere will also be considered as a source of information on the leisure aspects of uses of the environment. The services of the GAUL will be called on in this task of carrying out an inventory of the use of land and access to information.

- The second line of research of this sub-module will be devoted to taking stock of the economic situation induced by the closure of the mines. By referring to the economic data described and quantified in the previous sub-module on the contributions (financial and other) of mining companies to local development (maintenance of infrastructures, planning of public spaces, etc.)

and the operation of public and private services (support to associations, etc.), the closure of the mines will be evaluated in accordance with a cost-benefit logic. This work will make it possible to review the situation, firstly with regard to the real cost of the induced constraints (immobilization of certain spaces, drop in communal and associative revenues, no longer maintaining certain infrastructures, etc.) and secondly with regard to the envisaged economic substitution measures (rehabilitation plan, palliative subsidies, etc.).

6. Towards the development of decision aid tools

The aim of the AREDIE project is to evaluate, over time and space, modifications to the equilibrium and flows brought about by the end of the mining activity. The aim of the socio-economic module is to lead to the elaboration of socio-economic indicators for monitoring the territories and communities concerned by the closure of the mines (indicators that may be transposed elsewhere in France and in Europe). This approach will provide additional socio-economic elements for assessing and managing risks.

The definition of indicators is based on the choice of parameters stemming from the data and information processed in the research sub-modules, tested and validated by the participative approach. The model proposed for the elaboration of indicators is that of an approach based on consultations with local stakeholders through the activities of the GAUL. Meetings and thematic workshops will make it possible to define the issues at stake and the fields of measurement, choose the objectives, identify the variables, define the measurable parameters and, finally, select the relevant, consensual indicators. These indicators will serve as the basis for the prospective approach.

By relying on the historic analysis and the present findings, it will involve elaborating scenarios on the different situations with which society may be confronted in the future on the theme of the management of post mine working situations. The modelling tools will be used in this prospective work from the results acquired and will provide to the decision makers decision aid tools (multi-criteria scenarios and associated recommendations).
The prospective modelling will devote itself, from the chosen variables, to envisage different scenarios for which the users will be able to simulate future situations by exploiting the data on different variables (demography, economic activities, etc.).

7. References

Alvarez Areces M. A. (1998). *Les conséquences socio-économiques de la fermeture des mines aux Asturies*, annales des Mines, Collection "Responsabilité et environnement" n°12, octobre 1998, pp.75-89

Bassin Miniers Nord Lorrains (2000). *Directive Territoriale d'Aménagement Rapport des études préalables : les propositions du Préfet de la Régions lorraine*, Préfecture de la région Lorraine, 88 p.

Cauet, B. (1991a). L'Exploitation de l'or en Limousin, des Gaulois aux Gallo-Romains, *Annales du Midi*, Toulouse, T.103, n°194, 1991, p.149-181

Cauet, B. (1991b).Aurières du Limousin: état des recherches dans le district de Saint-Yrieix-la-Perche (Hte-Vienne), *Mines et métallurgie antiques et médiévales de la France méridionale*, Journées de Perpignan, Fev.1987, Perpignan, 1991, p.53-7

Cauet B. (1994) Les mines d'or gauloises du Limousin. Ed. Culture & Patrimoine en Limousin, Limoges 36 p.

Convert, B. & Pinet, M (1992). L'art d'accommoder les restes : reconversion économique et changements social dans le bassin minier Nord Pas de Calais. Thèse de 3e cycle, EHESS.

Haney M.and Shkaratan M. (2003). *Mine Closure and its Impact on the Community : five years after mine closure in Romania, Russia and Ukraine*, World Bank Policy Research Working Paper 3083, june 2003, 61 p.

Joly N., (2000). *Le renouveau territorial des régions minières : un projet de territoire. Les exemples du parc paysager de Duisbourg-Nord et du site du 11/19 de Loos-en-Gohelle*, Actes du Colloque international de Béthune, IFRESI - CNRS, 24-26 mai 2000, pp 185-194.

Lacoste O. et Spinosi L. (1998). *Santé et mutations sociales dans « l'après-mine » du bassin houiller du Nord-Pas-de-Calais*, annales des Mines, Collection "Responsabilité et environnement" n°12, octobre 1998, pp.70-73

Laversanne J. et Faille J. (1999). *Les enjeux de la fermeture d'un grand bassin houiller : l'exemple du Nord-Pas-de-Calais*, annales des Mines, Collection "Responsabilité et environnement" n°13, janvier 1999, pp.55-60.

Leconte G. (2000) Le passage de la mine au chantier conversion et socialisation d'anciens mineurs. In : Actes du Colloque international de Béthune, IFRESI – CNRS 24-26 mai 2000, pp 357 - 380.

Mazade O. (2000) La reconversion des agents des Houillères du bassin du Nord – Pas-de-Calais (HBNPC). In : Actes du Colloque international de Béthune, IFRESI – CNRS 24-26 mai 2000, pp 335 – 356.

Meilliez F. (1998). *Un exemple fructueux de développement non durable : le bassin minier Nord-Pas-de-Calais*, annales des Mines, Collection "Responsabilité et environnement" n°12, octobre 1998, pp.53-60.

HIGH RESOLUTION IMAGING OF GROUND SUBSURFACE: APPLICATION TO MINING SITES

PIWAKOWSKI Bogdan[1], BARREZ Fréderic [2], MEILLIEZ Francis[3] et MANIA Jacky [2]

(1) Groupe Acoustique - Electronique, Ecole Centrale de Lille (IEMN DOAE UMR 8520 CNRS) 59651 Villeneuve d'Ascq ; Bogdan.Piwakowski@ec-lille.fr

(2) Laboratoire de Mécanique de Lille (UMR CNRS 8107), Polytech'Lille, 59655 Villeneuve d'Ascq Cedex ; jacky.mania@polytech-lille.fr

(3) Laboratoire PBDS (UMR CNRS 8110), Sciences de la Terre 59655 Villeneuve d'Ascq Cedex ; francis.meilliez@univ-lille1.fr

ABSTRACT: The paper presents the examples of the successful use of the high resolution seismic imaging used in order to investigate the geological structure of three post-mining sites. The studies aimed in determination of the spatial limits of exploration, in evaluation of the state of the terrain (sound or collapsed) and in detection the geological faults which presence may affect the hydro-geological system.

KEYWORDS: High resolution seismic, acoustic imaging, voids, detection, mines, faults, cavities,.

RESUME : La communication présente les exemples de l'application réussie de la sismique haute résolution à la détermination de la structure géologique de trois sites miniers distincts. L'objectif des travaux est triple: il s'agit de confirmer les limites d'exploitation, d'évaluer l'état du site (terrain sus-jacent sain ou effondré), et de localiser des failles éventuelles dont la présence peut affecter considérablement l'hydrosystème crayeux.

MOTS-CLEFS : Sismique haute résolution, imagerie acoustique, détection, mines failles, cavités

1. 1. Introduction

The seismic reflection method, a powerful geophysical exploration technique (Dobrin,1983), which has been in widespread use in the petroleum industry for more than 60 years, has been also used since about 30 years for shallower targets (Knapp et Steeples, 1986, Mari et al.,1998). Recent advances in microelectronics have resulted in construction of seismographs and microcomputers allowing cost effective acquisition and processing of seismic data, relative to drilling tests, have permitted the appearance of the high resolution seismic reflection (HRS) technique, adapted for imaging at shallower depths.

It should be pointed out that the decrease of the depth of interest does not facilitate, as it could be expected, the work to be done. The signals reflected from shallow targets (layers, tunnels, faults) are generally mixed with a background of coherent noise, i.e. surface waves, groundroll, refractions, air coupled waves. This requires some experience in the data acquisition and processing in comparison with the "classic" deep seismic methodology, and non observance of the specific HRS principles can even lead to serious errors. That is why the progress in HRS is measured by the decrease of the shallowest prospected depth.

The rigorous discussion parameters of the HRS requires considering a seismic image in terms of a general pulse-echo imaging system, and to analyze principal parameters of the image, which are the depth and lateral resolution. (Piwakowski et al., 2003). In terms of pulse-echo imaging device, the

seismic image is equivalent to the sounding with the synthetic aperture array of dimension *D*, focussed (by using normal move-out correction) at the subsurface point at depth *d* and moving along the prospected profile (Fig.1).

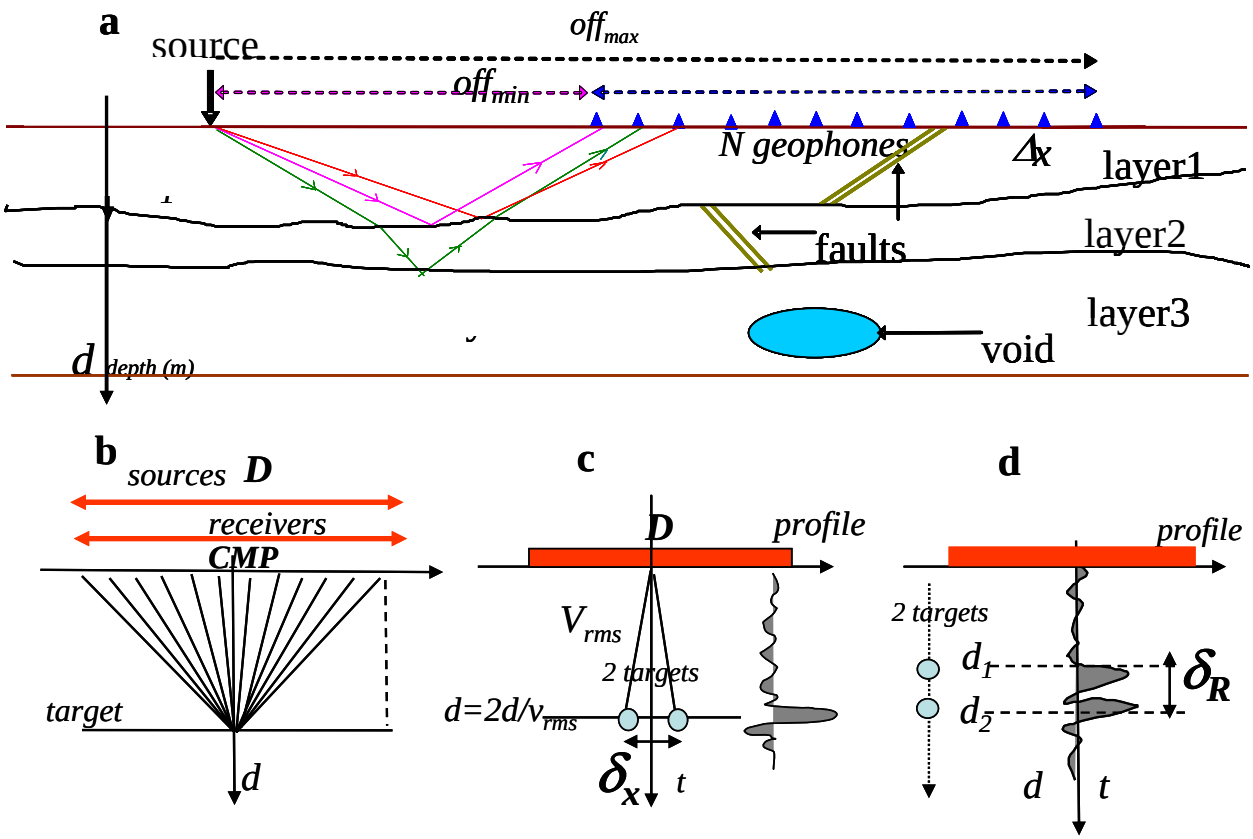


Figure.1. Operation of the High Resolution Seismic Imaging in terms of the pulse-echo imaging device; **(a)** acquisition geometry ; **(b)** CMP gather– Synthetic aperture of dimension D focused at depth d. **(c)** equivalent probe, characterised by angular resolution δ_θ; and lateral resolution δ_x **(d)** illustration of the depth resolution δ_r

According to general imaging principles, the focussed linear array yields angular resolution $\delta_\theta=\lambda_a/D$, where λ_a is the apparent acoustic wavelength $\lambda_a=V_{rms}/f$, V_{rms} is the stacking velocity and f is the dominant signal frequency. The lateral resolution which expresses the ability to resolve two point targets spaced by δ_x is then found as

$$\delta_x = \delta_\theta d = \frac{\lambda}{D} d = \frac{v_{rms}}{fD} d \qquad (1)$$

(in deep seismic it is assumed that δ_x is equal to the Fresnel radius $(\lambda d/2)^{0.5}$). The depth resolution, δ_r may be estimated as to be equal to

$$\delta_r = (1/4 \approx 1/2)\lambda \qquad (2)$$

The high absorption of the ground, which strongly increases with frequency, requires the use of the low frequencies, generally lower than it is required in Eq.1. The spectrum exploited in practice varies from several dozen Hertz (deeper imaging, depths of several hundreds of meters) to several hundred Hertz (high resolution shallow imaging, depth of dozen of meters). This implies the use of specific seismic sources to generate the acoustic waves (explosives, weight-drops, vibrators, (Miller et al., 1986) and of the geophones (acoustic velocity sensors) as the receivers.

The use of the synthetic aperture methods for the resolution enhancement requires the use of the specific geometry for the acquisition of the data. An example of such geometry is illustrated in Fig.1.a. The acoustic field is recorded along the sounded profile by the N-channel Δx spaced acquisition array, for a given start position of the seismic source. The source and the receiving array are moved by ΔS and the acquisition is repeated. The obtained records are then processed in laboratory. The results of processing are equivalent to sounding with the point acoustic probe, moving along the profile, focused at a given depth at a given position known as CMP point (Common Middle Point). The probe is thus characterised by the angular resolution δ_0 given in Eq.1. The set of traces presented as a function of CMP position gives the final output image. The distance between the traces (ΔCMP) is a function of the acquisition geometry. In the light of this discussion, the HRS may also be considered as the particular realisation of the sonar or of the ultrasonic non destructive testing probe, adapted for the detection in ground.

The chose of the minimal and maximal offsets off_{min} et off_{max} should provide the so called "optimum offset window" (Cook, 1965). In this window the researched reflections from targets display the optimum signal/noise ratio. Generally the definition of these parameters requires preliminary test records.

2. 2. Acquisition and processing

For the all examples presented in this paper the acquisition of the seismic data was carried out using a 48 channel seismograph and end-off geometry (as illustrated in Fig.1.a). The closest offset off_{min} and the geophone spacing Δx, were set individually to each profile in order to approach the optimum offset window and to fulfil the spatial sampling condition. (Piwakowski,2004). The parameters and geometry used to carry out profiles presented in this paper are illustrated in Table 1. The processing included the high resolution "optimum offset window" operations flow (Mari et al., 1997, Yilmaz, 1987).

Table.1 Acquisition parameters applied at profiles presented in section 3.

	Distance Δx (m)	Profile Length (m)	Source type	Offset min (m)	Resolution ΔCMP (m)
Site I Fig.2	3	300	Downhole/buffalo gun	30	1,5
Site II, Fig.3	5	600	Downhole/dynamite 200 g	50	2,5
Site III, Fig.4	5	500	Downhole dynamite 200 g	50	2,5

3. 3. Practical example

In this section we present the successful application of the HRS for the characterization of coal exploration sites located in north of France, being now unexplored. The objective of these surveys is to check the HRS capacity for imaging of mines, voids and of neighbouring faults, and to provide several information concerning the site structure, its state (collapsed or not) and to evaluate its hydro geological system.

3.1. Site I, Condé sur Escaut

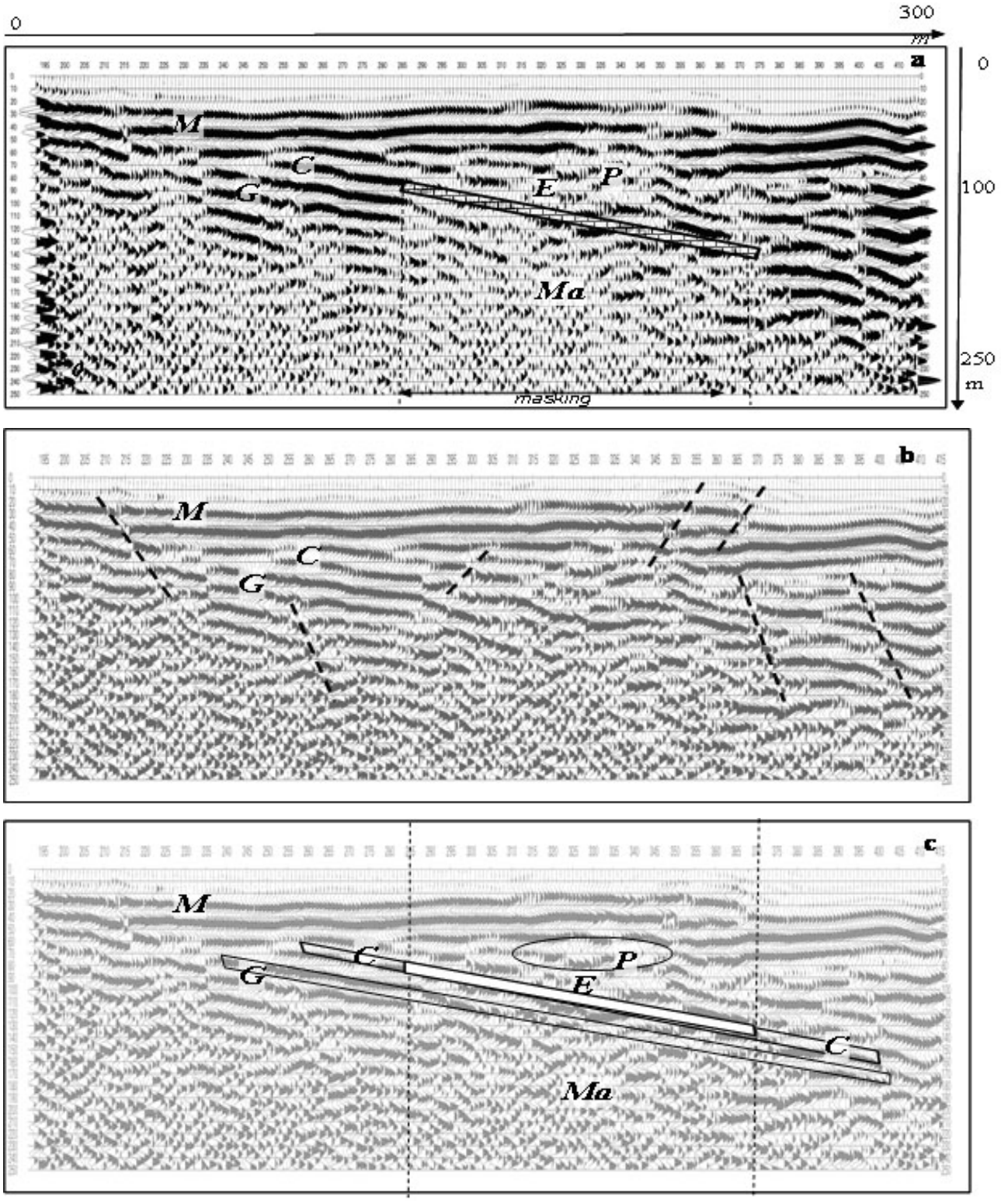


Figure 2 Seismic section obtained at site I (Condé sur Escaut ;Nord de France). (**a**) Main section, C-coal, M-Marl, G-Gres, E – known position of the mine, P zone of anomalies, Ma- zone of masking (**b**) section showing the faults, (**c)** geological interpretation of (a) and (b) and notation of the area of interest

The objective of this survey, was to obtain the seismic image of the geological structure of old coal exploration site and in the particularity, to detect and locate the geological faults which presence could affect the hydro geological system. The aimed depth of the survey was in order of 300m; the

mine occurring at a depth varying from 30 to 70 m below the regular structure, composed of 20 m thick layer of marl.

The obtained results, shown in Fig.2.a., rest in excellent agreement with the a priori known geological structure (Meilliez et Lamand ,1995). This structure includes the horizontal layer of marl (*M*) and dipping layers of coal (*C*) and gres (*G*), (Fig.2.c). The mine (*E*) is located precisely at its true (known a priori) position. The location is performed *indirectly* by means of the mine-induced masking of the deeper layers (shadow region, masking zone *Ma*). The numerous faults detected are shown in section (b). The anomalies over the mine consisting in discontinuity of geological structure and in the weakening of signal (*P*) could be interpreted as the mine induced upward propagating collapses. Notice that the presence of the fault *B* could give an explanation why the exploration was suddenly stopped.

3.2. Site II: Mares à Goriaux

The second example concerns the seismic profile is carried out over mines occurring at a depth varying from 120 to 400 m. The plan of site and the location of the profile are shown in Fig.3.a. This site is collapsing and the results of the collapse are clearly observed at the surface. For example, as the effect of the ground collapses, the surface of lake shown in figure increased about 3 times, during last 100 years. The embankment (*Em*) was realized especially in order to protect the neighbouring railway and highway against an inundation. The mine positions are here quite irregular; the tunnels occur at different floors, display the relatively high dip and are followed by numerous faults (Fig.3b).

The obtained result and their interpretation are shown in figures 3.c;d As it could be expected from known general structure, the seismic image for depths smaller than 120m (i.e. over mines) yields the regular horizontal structure including the layers of sand, tuff, chalk (*Ch*) and marl (*M*). Notice that the not explored zone (*NE*) yields regular and clear lines for all layers and also for coal zone *C.* In the contrary, within the explored area (*E)* the mines (*C*) and faults appear as the perturbations of the deeper sections, inducing the same *masking effect* (*Ma*) as this observed already in site I. The marl layer is there also not regular and perturbed.

Interesting information obtained is the appearance of the discontinuity of the chalk/marl and the base of marl interfaces. The most realistic interpretation of this phenomenon is that these perturbations are caused by the successive collapsing of the mines which propagates upward (Driad and Piwakowski, 2002). The line which joins the observed discontinuities can be thus interpreted as the collapse limit *(CLL*). The position of this line (Fig.3.d) shows that in three locations the upward propagating collapse reaches already the interface chalk/marl. This interpretation well correlates with the mentioned before collapses occurring at the surface and points out that, in future, when that phenomenon will reach the shallower structure, supplementary collapses could be expected.

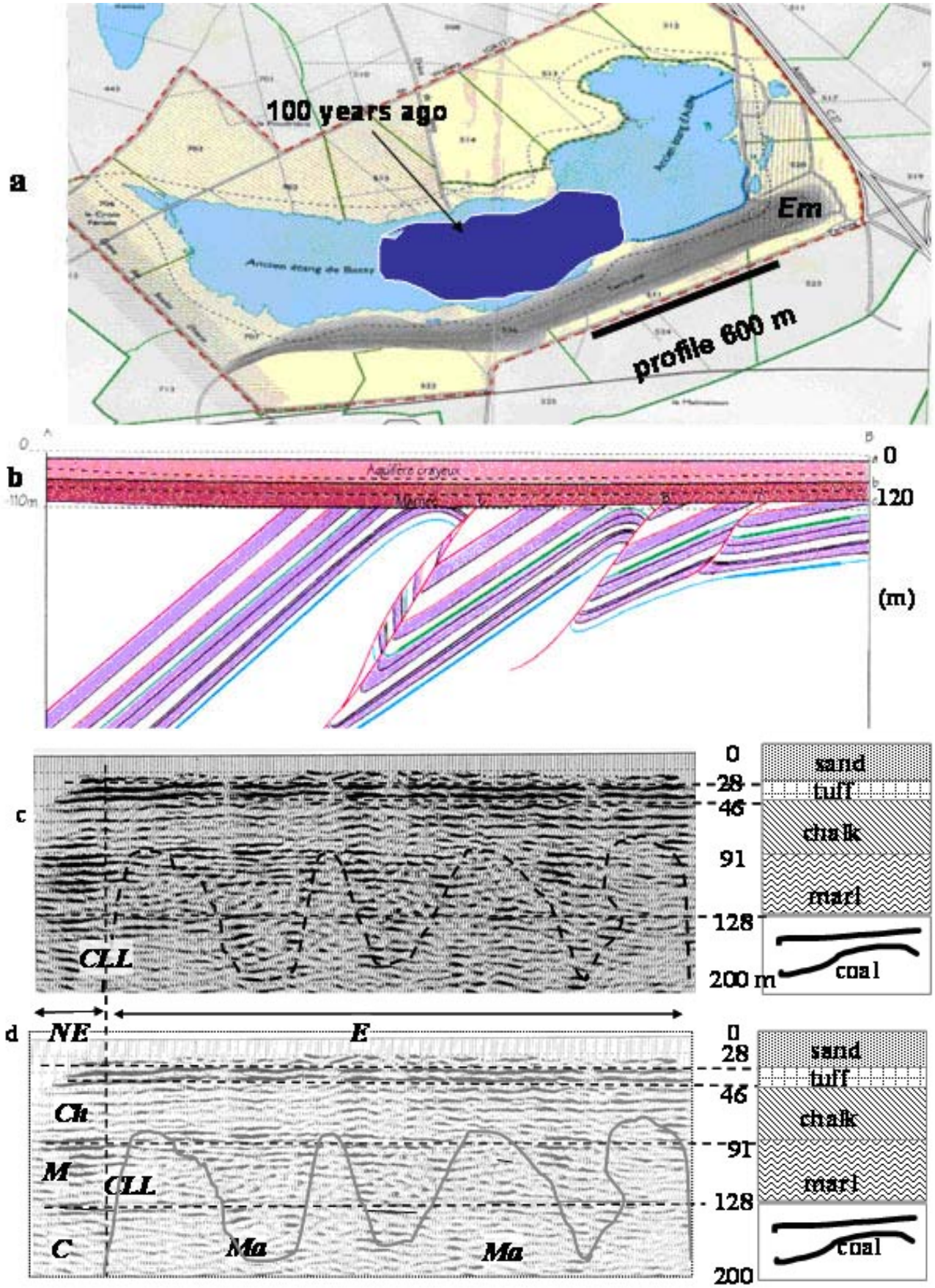


Figure 3 Site II : Mares à Goriaux . (**a**) ;Plan of site and position of the profile, *Em* indicates the embankment , **(b)** General geological structure including upper horizontal layers and dipping coal seams. **(c**) Seismic section obtained, **(d)** interpretation of (c) ;Ch-chalk; C-coal, M-Marl, Ma- mine induced zone of masking ,CLL – collapse limit line, NE-non explored zone, E-explored zone

3.3. Site III : Evin Malmaison.

This study has been carried out at Evin-Malmaison (Pas-de-Calais, France). Its main objective was to define fracture zone in the chalk aquifer situated in the region of the old mining exploration. The mines occurs here at the depths greater than 300m

This work was performed in three stages

(1) The high resolution seismic profile was defined and carried out using the parameters given in Tab.1.. The global seismic image obtained is presented in Fig.4.a. For depths smaller than 300 m (i.e. over mines) the seismic section shows the regular horizontal structure including the layers of sand, chalk (*Ch*), chalk/marl (*Ch/M*), and gres/schistes (*G/S*). As expected this part yields regular and quasi horizontal lines. In the contrary the zone of mines (depth>300 m figure displays the "chopped" reflectors. Such result may be characteristic to the network of not collapsed (so strongly reflecting acoustic waves) tunnels (Kourkafas and Goulty, 1996). Notice that observed effect has a different character than the *masking effect* observed for both previous sites I and II: which was there associated wit the strong weakening of signal (due to the absorption of acoustic wave in fractured medium), Additionally, the continuity of the *G/S* layer proves that there is no upward propagating collapse phenomena, as it was observed in site II.

(2) The upper part of seismic image (d<300 m) was zoomed and post-processed in order to enhance the resolution (Fig.4.b). The obtained result was than interpreted for the anomalies (Fig.4.c) and analyzed in order to choose the location of the most fractured zone. This position was found as the superposition of events *A1, A2, M, C1,* and *C2*. The detailed interpretation of this stage may be found in Barrez et al., 2005a. Finally the location *F* (Fig.4.c) was chosen as the best position for the boreholing tests.

(3) The fracture zone in the chalk aquifer was determined from the bore holing, using the TeleViewer, temperature and conductivity profiles. The result of these tests is shown in Fig.5. Notice excellent agreement of the depths found from seismic (Fig.5.a) et the depths found from bereholing (Fig.5.b).The boreholing show that the main markers in section Fig.4.b are the *Hardground* (Chalk- Chalk/Marl interface) and the top of Westphalian. The *hardground* layer (depth 71 m) is the base of the water reservoir, and this is confirmed by temperature and conductivity tests and TeleViever (Figs.5.c,d,e).

In conclusion, the interpretation of the anomalies from seismic image enabled to locate successfully the adequate borehole location. In the light of interpretations of sections I and II, the anomaly *M*, (not investigated by boreholing) can indicate the fractured zone. As well, the top of Westphalian (150 m) can be considered as the future potential reservoir of water. More detailed analysis of illustrated above problem can be found in Barrez et al.,2005b (see this proceedings).

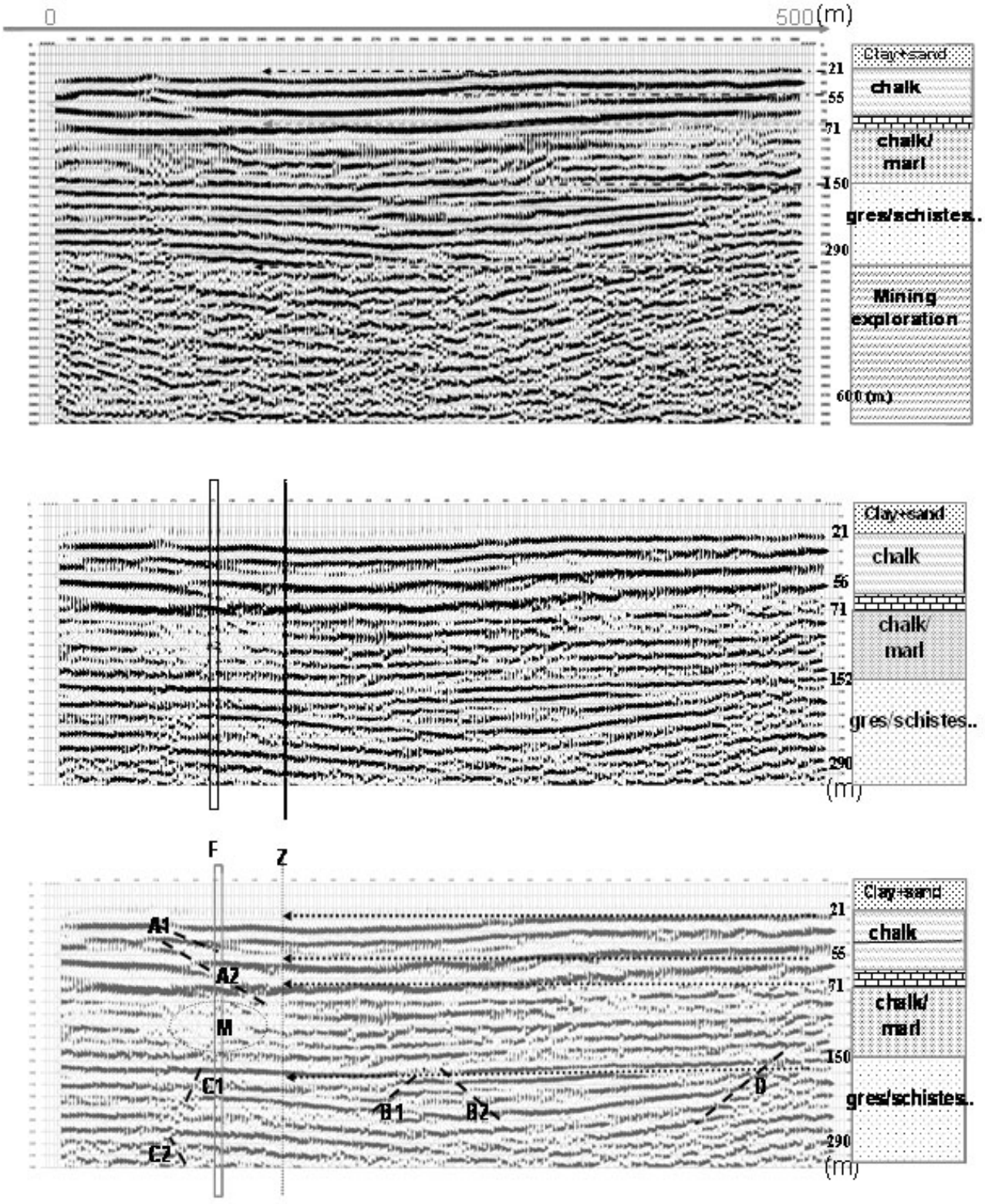


Figure 4 Site III :Evin- Malmaison . **(a)** ; Seismic section obtained, **(b)** Zoom of (a) for depths 0-300 m processed in order to enhance the resolution **(c)** Interpretation of (a) and (b) ;A1 ,A2,B1,B2,D – faults, C1,C2 non identified anomalies (fractured zone?) M- fractured zone, Z position for interpretation of depths, F location of borehole

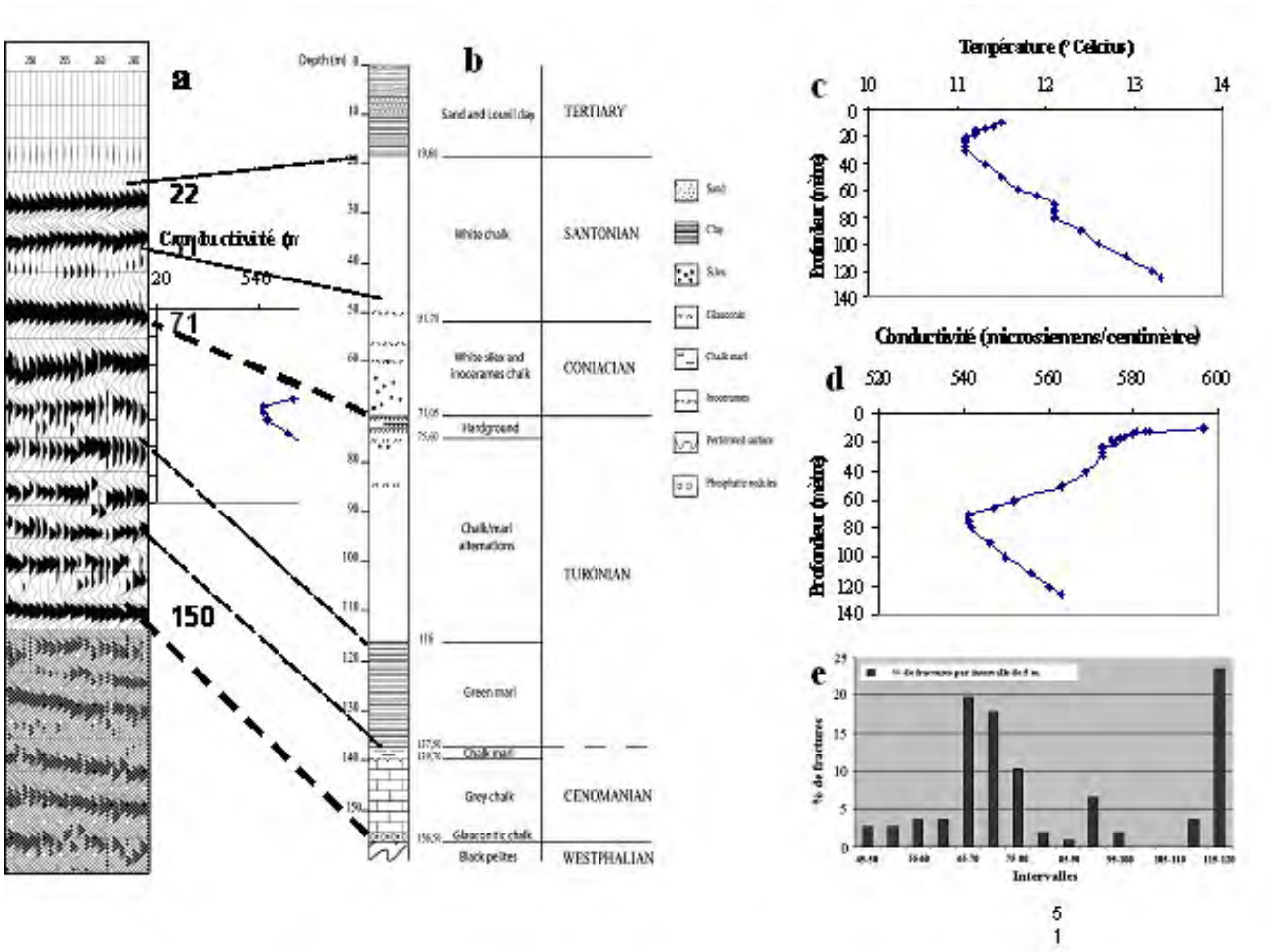


Figure 5 :Site III **(a)** Zoom of the seismic section at position Z (ref. Fig.4)); **(b)** Borehole results obtained at position F (ref.Fig 4), **(c)** temperature versus depth; **(d)** Conductivity versus depth; **(e)** fractures versus depth

4. Conclusion

The high resolution seismic imaging can be considered as the useful tool for the solution and understanding the problems related with mining exploration associated with the post mining problems. In the light of the presented examples our conclusions can be summarizes as follows:

(1) The HRS enables to visualize the mine-induced effects, and their interpretation and comparison with the a priori known geological structure. Fall all presented profiles a very good correlation with the known regular geological structure was obtained. The obtained precision of the depth is better than 5%.

(2) The mine can be located precisely. The location is performed indirectly by detection of the mine-induced masking of the deeper targets, in the regular seismic pattern.

(3) HRS is an efficient mean, capable not only to evidence the presence of voids but also to recognise their state (stable or collapsed). Our experience shows that in the case where a void is collapsed:

- The seismic image of masked marker evidences total loss of signal coherence and an important drop in the signal level.
- If the collapse propagates upward, the same effect is observed on the upper markers.
- However, the recognition of such effects requires the image of the intact geological structure which can be considered as a reference.

(4) The HRS can considerably help in the water investigation i.e. in the detection of potential sources of water and in positioning of boreholes. The imaging of chalk aquifer has been proved a very useful tool to the understanding of its hydrodynamics.

5. Acknowledgements

The authors are grateful to Charbonnages de France for their assistance and to Nord-Pas-de-Calais Region and the European Union for their financial support

6. References

Barrez,F., Mania,J., Mansy J-L.,Piwakowski B. (2005a) *"Quelques outils géophysiques pour la détection de zones fracturées dans la craie "* colloque *GEOFSCAN Orléans, 20-21 .09*

Barrez F., Mania J., Mansy J-L., Piwakowski B. (2005b) *"Influence of Coal Mine Tips On The Chalk Aquifer. Sampling Methods For Three Dimensional Sulphate Infiltration Study"., Post-Mining* 2005, November 16-17, Nancy, France

Cook, J.,C. (1985) *Geophysics*, **30** (527-538).

Driad,L., Piwakowski,B.(2002) *" Detection And Characterisation Of Underground Cavities Using High Resolution Seismic (HRSR)"* 8thCongress of European Section Environmental & Engineering Geophysical Society, Vo1, Lisbona

Dobrin, M.B., (1983*) Introduction to Geophysical Prospecting*. Mc Graw Hill N.Y.

Knapp, R.W.and Steeples, D.W., (1986) *"High resolution common-depth-point seismic reflection profiling: field acquisition parameter design"*. Geophysics **51**, (283-294).

Kourkafas P. & Goulty N.R. (1996) *"Seismic reflection imaging of gypsum mine working at Sherburn-In-Elmet,Yorkshire, England" European Journal of Environmental and Engineering"* Geophysics **1**, (53-63).

Mari, J-L, Arens, G., Gaudiani, P.et Chapellier D. (1998) *« Méthodes de géophysique de gisement appliquées au génie civil ».* Publications de l'Institut Français du Pétrole, éditions TECHNIP, Paris

Mari, J-L., Glangeaud, F., Coppens, F., (1997*) "Traitement du signal pour géologues et géophysiciens"*. Publications de l'Institut Français du Pétrole, éditions TECHNIP, Paris

Meilliez F. & Lamand D. (1995) *" Paramétrage géométrique pour la modélisation géomécanique des cavités minières abandonnées"* 2ème rencontre du *Réseau de Laboratoires GEO*, Aussois, France.

Miller R.D., Pullan S.E., Waldner J.S. & Haeni F.P. (1986) *"Field comparison of seismic sources"* Geophysics **51** (2067-2092).

B.Piwakowski, Ch.Leonard, I.Shahrour *"La sismique réflexion haute résolution, un outil pour la reconnaissance des couches superficielles"* Revue Française de Géotechnique 2003 N°101 pp 23 –33

Piwakowski, B; (2004) *"From high resolution land seismic imaging to very high resolution: state of the art, limits and field examples"* Présentation invitée session spéciale. Proceedings of *International Symposium of European Association of Exploration Geophysicists*, Paris, June 6-10

Yilmaz O, (1987) *"Seismic Signal Processing"*, Society of Exploration Geophysicists,

CAVITIES AS THE SOURCES OF ACID MINE PROCESS IN THE NIWKA-MODRZEJÓW COAL MINE (POLAND)

PLUTA Irena[1], MAZURKIEWICZ Maciej[2]

[1]CENTRAL MINING INSTITUTE, Plac Gwarków 1, 40-116 Katowice, irena-pluta@wp.pl

[2]ACADEMY MINING AND METALLURGY, Al. Mickiewicza 30, 30-059 Kraków, mamaz@agh.edu.pl

ABSTRACT: Acid mine process is one of the most significant sources the pollution of surface water. The intensive process was discovered in the Niwka-Modrzejów Coal Mine at the level 100-130 m. In this paper the method of prevention by the filling cavities of wastes from energy plants was proposed.

KEYWORDS: Acid mine process, Coal mine, Wastes from energy plants

RESUME: Les eaux de mine acides sont une des sources de pollution des eaux la plus importante. Cette pollution s'est révélée très importante dans la mine de charbon « Niwka-Modrzejów » (étage 100-130 m) aujourd'hui fermee. Dans cette publication, on présente la méthode de prévention de la pollution qui a été adoptée et qui consiste en un comblement des vides d'exploitation à l'aide de résidus industriels de production de l'énergie.

MOTS-CLEFS: Eaux de mine acides, Mine de charbon, Résidus industriels de production de l'énergie

1. Introduction

Acid mine drainage is one of the most significant environmental challenges and a major source of water pollution worldwide (Frost 1979; Younger 1995; Wood et al., 1999). Particularly acid mine processes constitute a notable problems at abandoned coal mines. The intensive acid mine process were discovered in the Niwka-Modrzejów C.M. in the Upper Silesian Coal Basin in Poland. (Pluta et al., 2002; Pluta, Jackowicz-Korczyński, 2003). In this paper the diagnosis of sites of acid mine process and method its prevention is presented.

2. Sampling area and its geology

The Upper Silesian Coal Basin (USCB) is located in the southern part of Poland. Sixty six hard coal mines were situated in this region (Fig. 1). The coal has been mined since the second half of the 18th century. One of the oldest coal mine is the Niwka-Modrzejów Coal Mine, which was active since 1810 to 2002. This mine was situated in the eastern part of the USCB (Fig. 1). Carboniferous formations consist of a complete profile of sediments from Namur A to Westfal B which is composed of claystones and sandstone and mudstones with layers of hard coal. This sediments are covered with formations of Quaternary formations of different seam thickness like fine and coarse sands, sand-gravel mixed interbedded with clay and loam. Carboniferous formation lie on the majority of coal area

almost on the surface but Quaternary sediments lie mainly on lower parts of river valleys where their seam thickness reaches up to about 50 m.

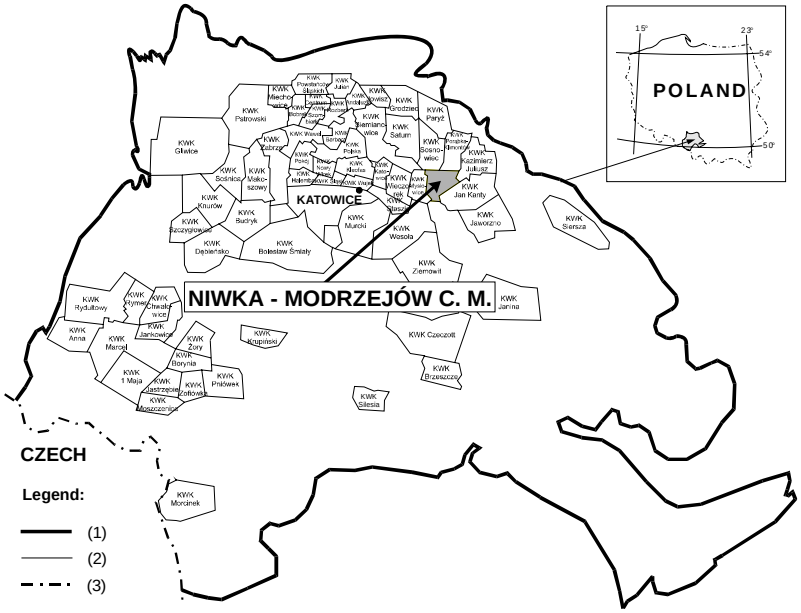


Figure 1. The coal mines of the Upper Silesian Coal Basin (Poland) (1-base of Carboniferous- bearing deposits, 2- coal mine boundaries, 3- boundary of Poland

3. Cavities in the Niwka-Modrzejów Coal Mine

The intensively mining in the Niwka-Modrzejów C.M. came into being old mine workings in the Carboniferous formation. The capacity of these cavities in three regions close to the surface (I 450.000 m^3, II 1.260.000 m^3, III 1.870.000 m^3) is about 3,5 mln m^3 (Fig. 2).

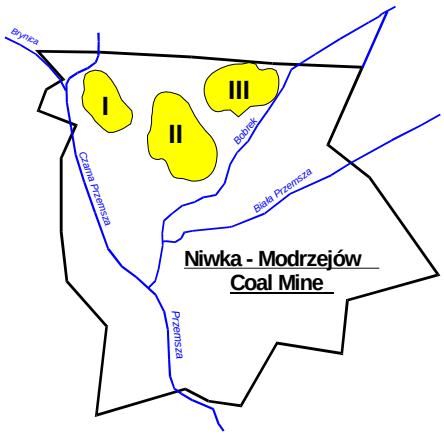


Figure 2. Location of cavities in three regions on the coal mine area of the Niwka-Modrzejów C.M.

4. Acid mine process in the Niwka-Modrzejów Coal Mine

Acid mine processes have been recognized in the Niwka-Modrzejów C.M. for about fifty years. One of the most intensive is located in cavities at the level of 100-130 m. Water from this level has pH between 2,5 and 3,8 and the temperature about 20°C. Concentrations of iron ions reach up to 1350 mg/dm^3 and of sulphate ions up to 4440 mg/dm^3.

5. Prevention of the acid mine processes

Prevention of the acid mine process in the Niwka-Modrzejów is necessary. Methods aiming at elimination of sulphide oxidation at the level of 100-130 m, which are significant sources of acid mine drainage and the pollution of surface water, should be used. The rocks containing the sulphide minerals must be separated from oxygen and waters. The potential risk of acid mine processes can be determined by filling of cavities in old mine workings up to level of 100-130 m. Implementation of appropriate prevention reduce the potential risk of sulphide oxidation has been determined by introduction of large quantities industrial wastes. Mostly kinds are fine-grained wastes from energy plants: fly-ashes of coal burning or flu gas desulphurization products.

6. Conclusions

In this paper the diagnosis of acid mine process and method its prevention in the Niwka-Modrzejów Coal Mine is presented. Acid mine process at the level of 100-130 m can be determined by filling the cavities in old mine workings by fine-grained wastes from energy plants.

7. Acknowledgements

Studies were financed by MNiI (Ministerstwo Nauki i Informatyzacji) under Project No. 4T12B04428.

8. References

Frost R.C., (1979). *Evaluation of the rate of decrease in the iron content of water pumped from flooded shaft mine in County Durham. England*. Journal of Hydrology, 40, 101-111.

Pluta I., Jackowicz-Korczyński J., (2003). *Acid mine process in polish coal mines, Niwka-Modrzejów Coal Mine example. In: Mine water and the environment.* 9th International Mine Water Association Congress 2003, 37-41.

Pluta I., Mazurkiewicz M., Widuch T., Sitko F., (2002). *Koncepcja ograniczenia wpływu zagrożenia hydrogeochemicznego wód likwidowanej kopalni "Niwka-Modrzejów" (in Polish).* In: Doświadczenia z likwidacji zakładów górniczych, Mysłowice 2002, 107-112.

Wood S. C.; Younger P. L., Robins N. S., (1999). *Long-term changes in the quality of polluted minewater discharges from abandoned underground coal workings in Scotland.* Quarterly Journal of Engineering Geology, 32, 69-79.

Younger P. L., (1995). *Hydrogeochemistry of mine waters flowing from abandoned coal workings in County Durham.* Quarterly Journal of Engineering Geology, Vol. 28, S101-S113.

GAS MIGRATION FROM CLOSED COAL MINES TO THE SURFACE. RISK ASSESSMENT METHODOLOGY AND PREVENTION MEANS

Zbigniew POKRYSZKA[1], Christian TAUZIÈDE[1] and Candice LAGNY[1],

Yves GUISE[2], Rémy GOBILLOT[2], Jean-Maurice PLANCHENAULT[2], René LAGARDE[2]

[1] INERIS, Parc Technologique ALATA - BP N°2 - 60550 Verneuil-en-Halatte – France;
zbigniew.pokryszka@ineris.fr, christian.tauziede@ineris.fr.

[2] Charbonnages de France, 100 avenue Albert 1er - BP 220 - 92503 Rueil-Malmaison - France,
yves.guise@charbonnagesdefrance.fr, remy.gobillot@charbonnagesdefrance.fr

ABSTRACT: French law as regards renunciation to mining concessions calls for the mining operator to first undertake analyses of the risks represented by their underground mining works. The problem of gas migration to the surface is especially significant in the context of coal mines. This is because mine gas can migrate to the earth's surface, then present significant risks: explosion, suffocation or gas poisoning risks. As part of the scheduled closure of all coal mining operations in France, INERIS has drawn up, at the request of national mining operator Charbonnages de France, a general methodology for assessing the risk linked to gas in the context of closed coal mines. This article presents the principles of this methodology. An application example based on a true case study is then described. This is completed by a presentation of the preventive and monitoring resources recommended and usually applied in order to manage the risk linked to gaseous emissions.

KEYWORDS: gas, coal, mine, closure, risk.

RESUME : La réglementation française en matière de renonciation aux concessions minières prévoit que l'exploitant minier réalise au préalable des analyses des risques présentés par ses travaux miniers souterrains. La problématique de remontée de gaz en surface est particulièrement importante dans le contexte des mines de charbon. En effet, le gaz de mine peut migrer vers la surface du sol et présenter alors des risques importants : risques d'explosion, d'asphyxie ou d'intoxication. Dans le cadre de l'arrêt programmé de l'ensemble des exploitations de charbon en France, l'INERIS a établi, à la demande de Charbonnages de France, une méthodologie générale d'évaluation du risque lié aux gaz dans le contexte des mines de charbon arrêtées. L'article présente les principes de cette méthodologie. Un exemple d'application sur un cas concret est ensuite exposé. Il est complété par la présentation des moyens de prévention et de surveillance préconisés et appliqués habituellement pour gérer le risque lié aux émissions gazeuses.

MOTS-CLEFS : gaz, mine, charbon, fermeture, risque.

1. Introduction

French law as regards renunciation to mining concessions calls for the mining operator to first undertake assessment of the risks represented by their underground mining works in terms of people, property and the infrastructure present on the surface. In cases where significant levels of risk are identified, the operator must furthermore define and implement the appropriate preventive measures.

The problem of gas migration to the surface represents one of the major aspects of this risk assessment, especially in the context of coal mines, for these works very often combine the

three components needed to trigger the appearance of the feared phenomena:

- the presence of residual mining voids which, together with the natural porosity of the strata, forms underground reservoirs. Taken together, given the conditions of French coal seams, these reservoirs could represent 25 to 35% of the total volume of coal extracted (Degas and Wojtkowiak, 2003),
- the presence of dangerous gases,
- the possibility that these gases could accumulate and migrate, in significant concentrations, to the surface.

2. Mine Gas and the Dangers Linked to its Presence

Coal seams very often contain significant amounts of endogenous gas (firedamp), whose main component is typically methane and sometimes carbon dioxide. Firedamp can be released from unmined parts of the seam for a relatively long time after the end of mining operations.

It accumulates in residual mine spaces at the same time as other gases from the transformation of materials present in the old workings and/or in the air that may still be able to circulate through the old workings (nitrogen, carbon dioxide, carbon monoxide, hydrogen sulphide…). The combinations of these gases form a mixture called "mine gas". Very often, this mixture is severely lacking in oxygen or even virtually oxygen free.

Mine gas can migrate to the surface where its presence can then induce significant risks: risks of explosion, suffocation or poisoning. In France and in other coal mining countries affected by mine closures, a number of accidents and incidents linked to releases or build ups of mine gas have been reported in the literature (Sizer *et al*, 1996; Burrel and Friel, 1996; Kral *et al*, 1998; Jackson, 2000; Łukowicz and Walter, 2000; Pokryszka and Tauzièdе, 2000; Robinson, 2000; Novotny *et al*, 2001).

The most common situations that have caused these incidents or accidents are:

- Local, concentrated, releases of mine gas through a direct path between the old workings and the surface (mining opening, faults, crack...);
- A build up of gas in confined or semi-confined spaces (basements or underground locations, or in buildings themselves as well as in underground networks, etc.);
- The unintentionally connection of a post-mining voids to the atmosphere (e.g. due to drilling or excavating work conducted close to old workings...).

3. Mine Gas Migration to the Surface

The transfer of gas from post-mining voids to the surface may be driven by a number of mechanisms:

- the rising water level within the old workings;
- feeding the reservoir with gas by its release from the coal left in place;
- variations in barometric pressure;
- natural draft.

These different possible causes of gas releases on the surface may occur simultaneously. Nevertheless, the period during which the water level rises once pumping stops represents the most critical phase.

The possible appearance and intensity of gas emissions on the surface from old workings will essentially depend on three main factors:

- the gaseous (firedamp) nature of the post mining reservoir present, especially represented by the type of gas that is present, the importance of its "production" in the reservoir and the volume of the voids;
- the degree of differential pressure between the reservoir and the surface generated in combination by the various mechanisms mentioned above;
- the resistance of the environment to gas migration, simultaneously represented by former mine-surface links and by the covering strata, including water bearing horizon within it.

This shows the importance of knowing the underground mining reservoir (the structure and distribution of any residual voids, their position in relation to the surface…), their geological environment and their hydro-geological behaviour, so as to best appreciate the problem posed by the migration of mine gas to the surface.

Gas may rise to the surface:

- preferably through former works linking the mine and the surface (shafts, adits, access galleries) which constitute individual gas emissions points, if they have remained open or are not sufficiently tightly sealed off;
- through the covering ground itself, especially in areas of only slight thickness and/or where permeability is greatest. This is because a slight thickness in the covering ground, when naturally permeable (with high built-in permeability, the presence of cracks…) or made permeable as a direct consequence of mining operations (induced fracturing), is the situation that is most likely to favour gas releases;
- to a lesser extent, through water release or with the water from mine drainage (dissolved gas).

Figure 1 illustrates the various possible paths used by mine gas when migrating towards the surface.

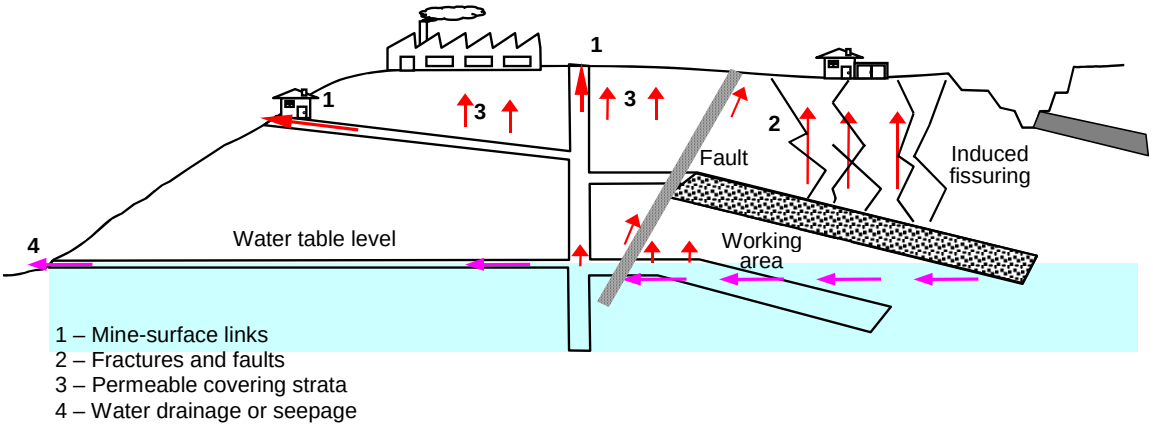


Figure 1 Mine gas migration paths towards the surface

4. Risk Assessment Methodology

Considering the shutdown of all coal mining operations in France, INERIS at the request of Charbonnages de France, drew up a general methodology for assessing gas related risks. This methodology, drawn up in its initial version around 1995 for the specific context of coal mines closure has since been improved and expanded to take into account the experience gained from handling a larger number of real life cases.

The methodology is based on taking into account and analysing various types of information and data:

- Data relating to the underground reservoir: the firedamp characteristics of the seams, the volume and extent of the residual mining voids, their position in relation to the surface...;
- Data relating to covering strata: type, structure and overall thickness of the covering strata, thickness of the various specific bedrocks and their permeability. The latter parameter may be strongly dependent on the fissuring induced by the workings;
- Information relating to hydrogeology: type, thickness, shape of the water bearing horizons, their position in relation to the mine workings and their evolution over time;
- Elements relating to seam structure: here the aim is especially to identify any possible presence of formations likely to encourage the accumulation and migration of mine gas;
- Data relating to ground occupation: geographic position and density of built up areas for rising gases result in a risk that is all the more significant if there is a human presence in the area and a possibility that gas will accumulate on the surface.

The superimposition and mapping of the various data and information is carried out on a map background using a scale chosen to obtain a result that provides enough overall coverage while being sufficiently precise.

This work is performed in line with the following major steps:

- collecting the knowledge available on the firedamp nature of the mining concession studied, from archive documents completed by any reconnaissance and measurements taken on field;
- information on the mine workings and the geological and hydro-geological context;
- identification of areas that may potentially release gas, based on geological and hydro-geological data and on working characteristics that are specific to the mining area;
- identification of risky areas, based on surface occupation;
- definition of the means of prevention and/or monitoring applied to manage the risk.

In cases where the hydrodynamic situation of the studied area has not yet stabilised (the water table is rising and the former workings are progressively flooded), the analysis of the problem of gas migration to the surface is performed separately for the two consecutive hydro-geological configurations:

- for the rising water level phase, and
- for the phase that follows the stabilisation of the hydrodynamic situation.

This general approach is presented in graphic format in Figure 2.

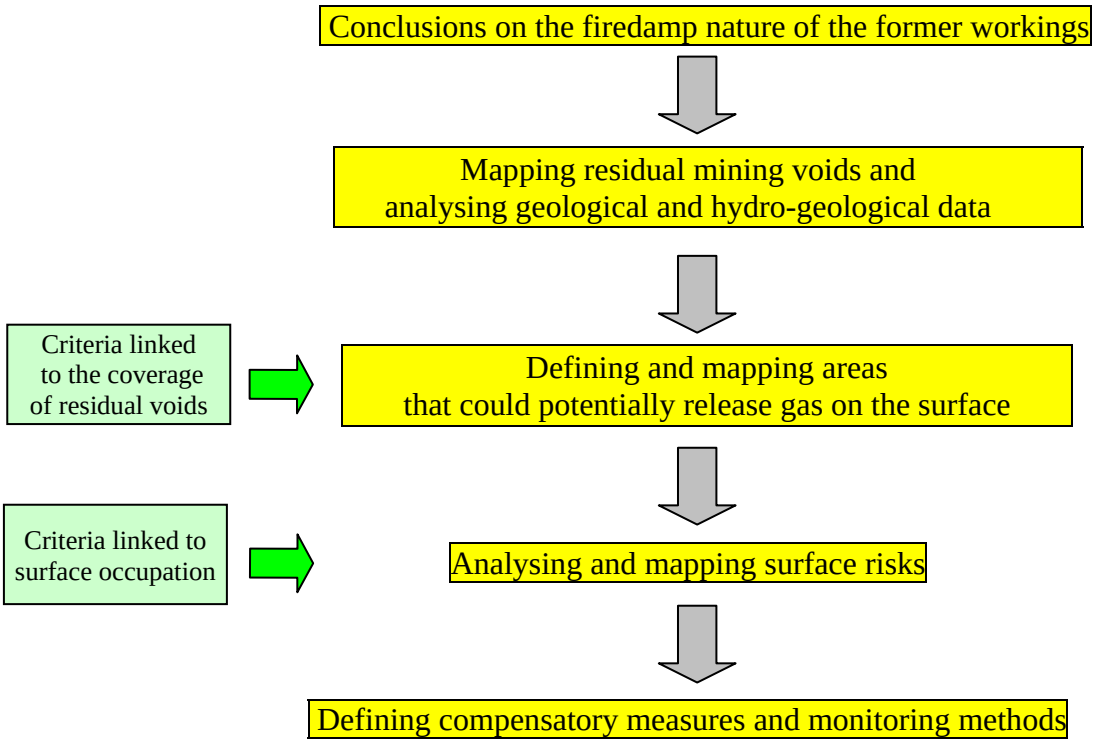


Figure 2. General approach applied to the analysis of the problem of mine gas rising to the surface

4.1. Conclusions on the Firedamp Nature of the Former Workings

This step aims to define the potential for former mine workings to release and to accumulate mine gas as well as to identify the type of gas likely in time to transit to the surface.

The analysis is performed through the search for numerous quantitative or simply qualitative data. The following especially should be retained:

- reports of the appearance of firedamp in the underground workings as stated in the reports filed by the operators or the authorities in charge of supervising the mines, or even various works describing the history of the mining operations.
- administrative ranking of workings in relation to firedamp that appeared in France towards the end of the 19th. Century.
- implementation during mining operations of firedamp prevention measures: safe explosive, safe lamps, mechanical ventilation, firedamp meters…
- reports on firedamp related accidents.
- results of the various measurements taken of firedamp releases during mining operations.

This data can be collected, more or less exhaustively, from the various archives available, those kept by mining operators, the mining administration or national or local public archives. This approach can be completed by reconnaissance on field and especially taking gas release measurements from mining openings where this is still possible.

The data collected is then compared and summarised so as to determine to what extent the workings being studied and their various sectors are affected by the presence of mine gas.

4.2. Mapping Residual Mining Voids and Analysing Geological and Hydro-geological Data

This work comprises analysing and summarising the various elements relating to the workings considered and are necessary to evaluate the sensitivity of the old mine being studied to gas accumulation and its transfer towards the surface, namely:

- a cartographic presentation of the main working areas and any underground links that may exist between these areas,
- identifying the upper mined out areas in the former mine workings that form "potential mine gas traps" and their position in space,
- the thickness of the overlying covering strata in the upper mined out areas,
- information relating to the structure, type and aeraulic characteristics of this covering strata as well as the degree of fissuring affecting it (both natural and that induced by the workings),
- information relating to overlying water tables above the upper mined out areas,
- current hydrological situation and the way it changes over time and in space, for the rising water phase as well as the future stabilised phase,
- the presence of any geological structures that favour the accumulation and/or migration of gas.

4.3. Defining and Mapping Areas that could potentially release Gas on the Surface

This step serves to locate and to set out a hierarchy, where possible, those areas that may contain mine gas and release it to the surface. This work is performed using the data acquired during the previous step.

The analysis requires setting out a number of criteria, the two main ones being:

- thickness and type of soil covering the upper mined out areas in the post-mining reservoir.

  From a general point of view, a covering thickness of more than 200 meters is sufficient to obstruct the rise of gas in any way other than in a diffuse way. This limit thickness has been adopted on the basis of models developed in Europe for predicting the release of firedamp from a coal exploitation by caving longwalls, one that is the most penalising in terms of weakening the overlying strata.

  These models consider that there is no significant influence by mine workings on the aeraulic properties of the covering strata in excess of a height of some 150 to 170 meters above the seam (Gunther, 1965; Coal Directorate, 1980; Pokryszka, 1992).

  Depending on the refinement of the analysis, it is also possible to introduce intermediate limits in the covering thickness thereby ensuring partial protection in relation to gas migration.

  At the same time, depending on the hydro-geological context of studied mining area, one takes into account when setting out the criteria, the existence in the covering strata of impervious beds (clay for example) or even water bearing beds, on condition that these are thick enough and continuous in order to form an efficient obstacle to rising gases.

- degree of flooding in the former workings still in contact with the unmined seam.

  This aspect is especially relevant for the stabilised hydrodynamic phase, in cases where the workings or some of its parts remain insufficiently flooded. This is because, in this case, the gas contained in unmined seams may potentially continue to be released and transit to the surface.

  For lack of studies or relevant past data, dedicated research work has been undertaken in order to be able to propose criteria relating to this aspect. This study covered the behaviour of the gas (methane) adsorbed in the coal in the presence of a hydraulic load created by the flooding water.

  Experiments performed in the laboratory showed that finely split flooded coal, with no significant hydrostatic pressure may still, despite this, release gas. However desorption kinetics are very weak, some ten times less than with dry (not flooded) coal.

  When the hydrostatic pressure caused by the flooding rises, the gas release kinetics falls. If the water pressure approaches that of the adsorbed gas, then the quantities of gas released become highly insignificant: they are in this case in the order of a few percent of the volume that can be desorbed. Figure 3 shows and example of the results obtained.

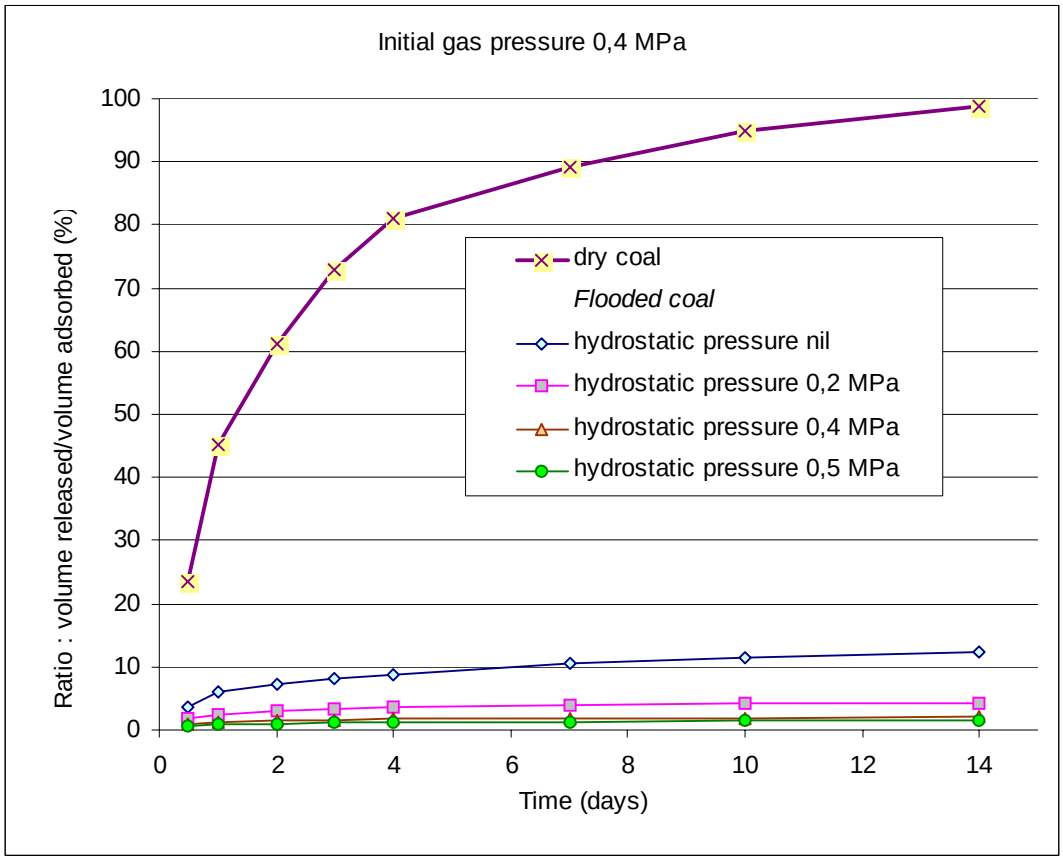


Figure 3. Example of the influence of water on coal gas desorption kinetics. Laboratory experiment using finely split coal.

All of these results have made it possible to detail the notions of "coal seam gas pressure" and the "minimum flooding level" as the basis for setting out criteria that correspond to the degree of flooding affecting former workings.

Applying these criteria makes it possible, for example, to eliminate from the rest of the risk assessment, those areas that are sufficiently flooded at a given time, by considering that in this configuration, the water present effectively inhibits any significant release of firedamp from the residual coal still in place.

In the analysis of areas that may potentially release gas, it is also considered, in parallel with the upper areas in former underground workings, those geological or tectonic structures that favour the accumulation or the migration of gas towards the surface (porous and permeable layers, anticlines, faults…).

This entire step leads to drawing a map of "areas likely to release mine gas". As an example, Figure 4 shows an excerpt of the mapping of such areas for a part of the French Nord-Pas-de-Calais coal mining area, representing some 13 square kilometres.

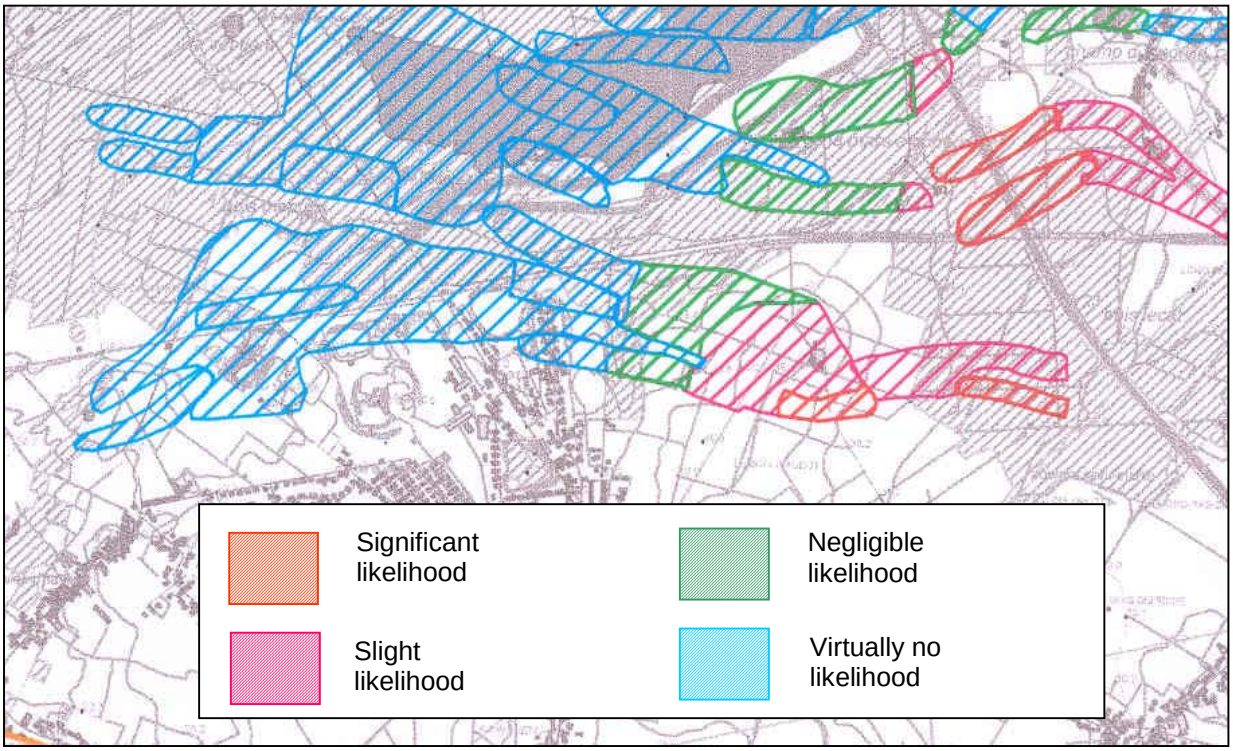


Figure 4. Excerpt from the mapping of areas potentially likely to release gas produced for the Eastern part of the Nord-Pas-de-Calais coal mining area

4.4. Analysing and Mapping Surface Risks

This step comprises identifying, from among those areas that could potentially release mine gas, those which are occupied on the surface by gas sensitive elements. This analysis is done by superimposing the aforementioned map of areas that could potentially release mine gas over a surface occupation map.

In this analysis, special consideration is of course given to built up areas occupied by buildings and industrial installations, for any release of gas can all the more frequently result in accidental events when there is a human presence and possibilities for mine gas to accumulate in buildings or in surface infrastructures. Built up areas therefore increase surface vulnerability and consequently, with the same likelihood of gas releases, the degree of risk.

Consequently, when enough information is available, the analysis is conducted so as to result in a hierarchy of risk, based on geographic location, the type and density of vulnerable areas. It should be noted that the risk mapping that is generated in this way is valid for the occupation of the surface in question, as it was when the study was conducted.

This step results in a so-called map of "mine gas emissions risk area". Figure 5 illustrates the result of this mapping effort drawn up for the same part of the French Nord-Pas-de-Calais coal mining area as presented in the preceding subsection.

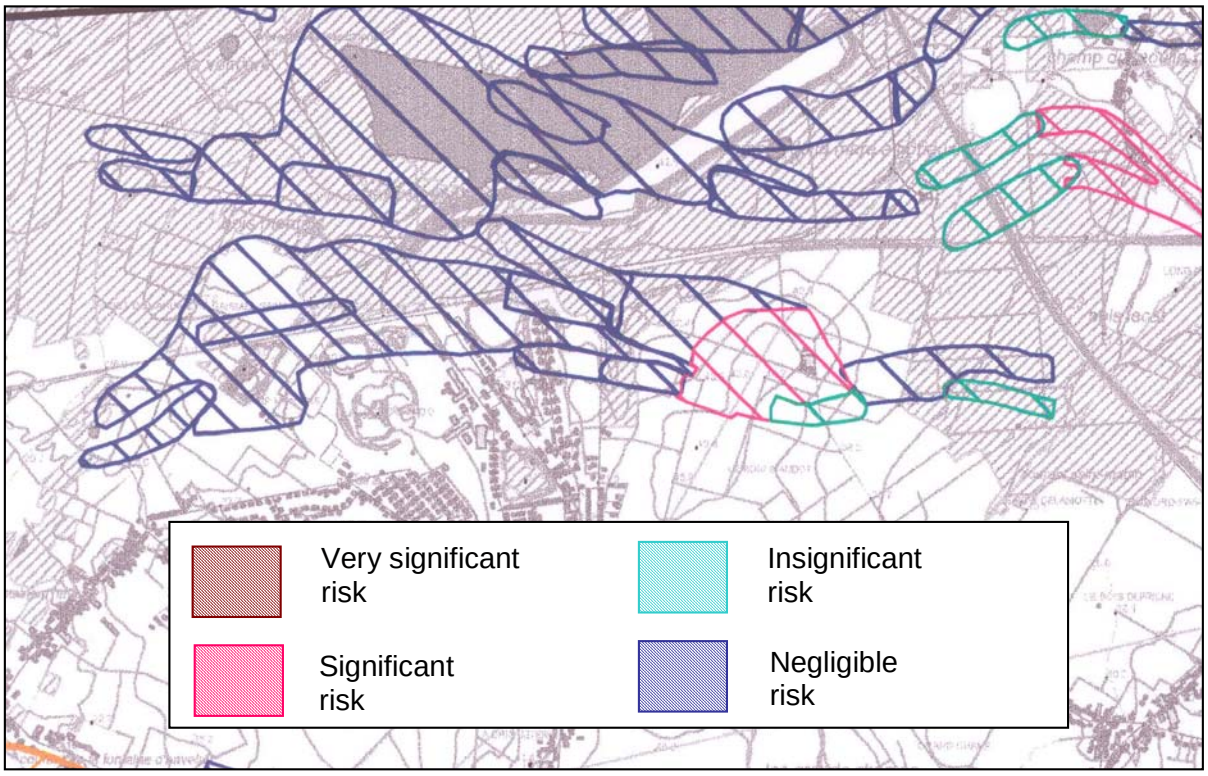


Figure 5. Excerpt from the mapping of areas with a mine gas emissions risk produced for the Eastern part of the Nord-Pas-de-Calais coal mining area

4.5. Defining Compensatory Measures and Monitoring Methods

4.5.1 Compensatory Measures

Once the risk linked to the rise of gas to the ground's surface is quantified and mapped, it is necessary to define the preventive or compensatory measures well suited to the context. These measures should make it possible to reduce the risk to a technically and financially acceptable minimum.

Two types of measures are possible to minimise the rise of gas to the surface: active treatment and passive treatment of the mine gas.

Capturing firedamp (drainage) from the surface represents an especially efficient active treatment of the problem. It usually creates a more or less significant vacuum in the mine reservoir compared with the surface level, but one that is sufficient to stop any uncontrolled release of gas on the surface. For example, large scale gas capture installations have been set up in the Nord-Pas-de-Calais mining area where a majority of the former mine workings are now under a vacuum of up to –500hPa.

This costly and complex method is most often practised in very gassy mining areas in order to industrially capture the gas and it is technically difficult to apply to low firedamp content seams. It is however possible, in some cases, to set up a local capture station intended to avoid any uncontrolled gas releases at local level (Robinson, 2000) or even a mobile installation that can be temporarily connected to capture points set up ahead of time in those areas where mine gas periodically appears on the surface (Novotny *et al*, 2001).

In mines where firedamp collection systems have been set up in the past during mining operations, whether for safety reasons or gas exploitation, it may be interesting to keep such mechanisms in service even after coal mining stops, so as to control the water flooding phase for as long as possible. This is the case with the capture installations operating in the eastern and central parts of the Lorraine coal mining area.

Passive treatment comprises implementing, in areas of risk, priority escape routes for the gas, by building decompression installations (existing shafts suitably fitted out or drilling performed specially). This is because it is necessary for the gas contained in the reservoir to find a priority escape route to the outside atmosphere, i.e. one that considerably less resistant than the former mine-surface connections that are closed off or the covering strata.

The drilling required, which does not necessarily necessitate a very large diameter to be efficient, must aim for the high parts in the mining reservoir, in order to favour the decompression of the voids that are the closest to the surface and to allow the release of gas for as long as possible during the rising water phase.

Figure 6 illustrates the operating principle of a decompression borehole connected to a flooding post-mining reservoir. Given the normally very limited level of the unitary gas flows involved, one can easily assume that the releases from all of the system components (post-mining reservoir, covering, shafts and decompression works) are mainly laminar (Couillet *et al*, 1998).

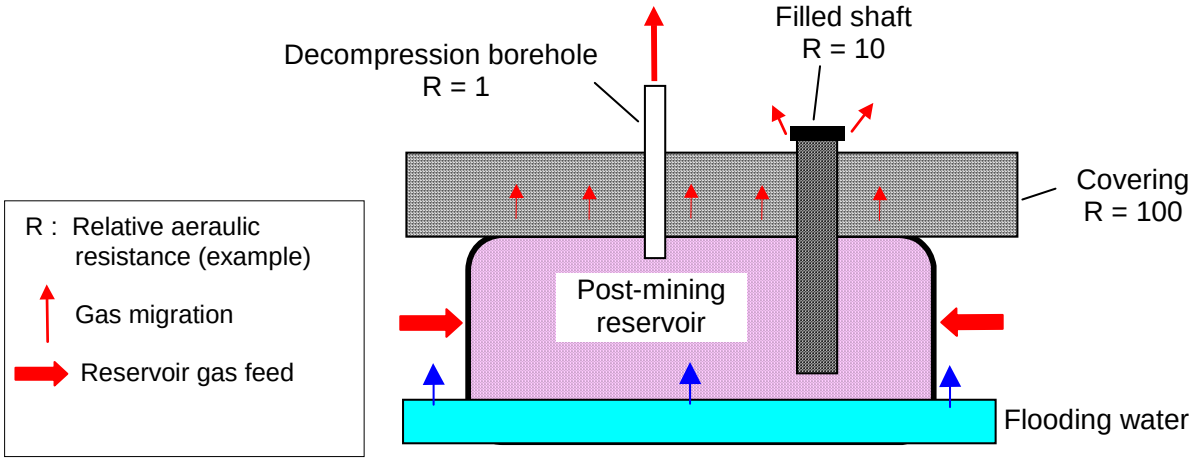


Figure 6. Operating principle of a decompression borehole linking a post-mining reservoir that is flooding

In this case, the distribution of the gas flow migrating to the surface spread among the three possible paths, i.e. the covering strata, the former adits or shafts and the decompression works will take place proportionally to the relative aeraulic resistance of each of these paths. The gas will therefore generally be released mainly by the one or more decompression devices as these offer the circuit with the least resistance.

It should be noted that prevention systems of this type have been proposed and/or implemented in a number of mining countries: in France, but also in Germany, Great Britain

(Jackson, 2000), in Poland (Łukowicz and Walter, 2000), in the Czech Republic (Novotny *et al*, 2001; Prokop, 2001), etc.

Installing decompression works requires implementing specific safety measures in relation to the risks linked to the gas that can emerge from the post-mining voids (inflammation, suffocation, poisoning). In the same way, once completed, these works must be made safe in view of their often long term operation by fitting them with safety equipment such as cut off valves, flame arrestors…, and made inaccessible to the public.

For those drillings where it is assumed that they will become highly active, it is also necessary to establish a protection area that takes into account the above mentioned risks. An example of how to define this area in relation to the thermal effects caused by accidental gas (methane) inflammation conducted by INERIS on a drilling in the Lorraine coalfield, is presented in Figure 7.

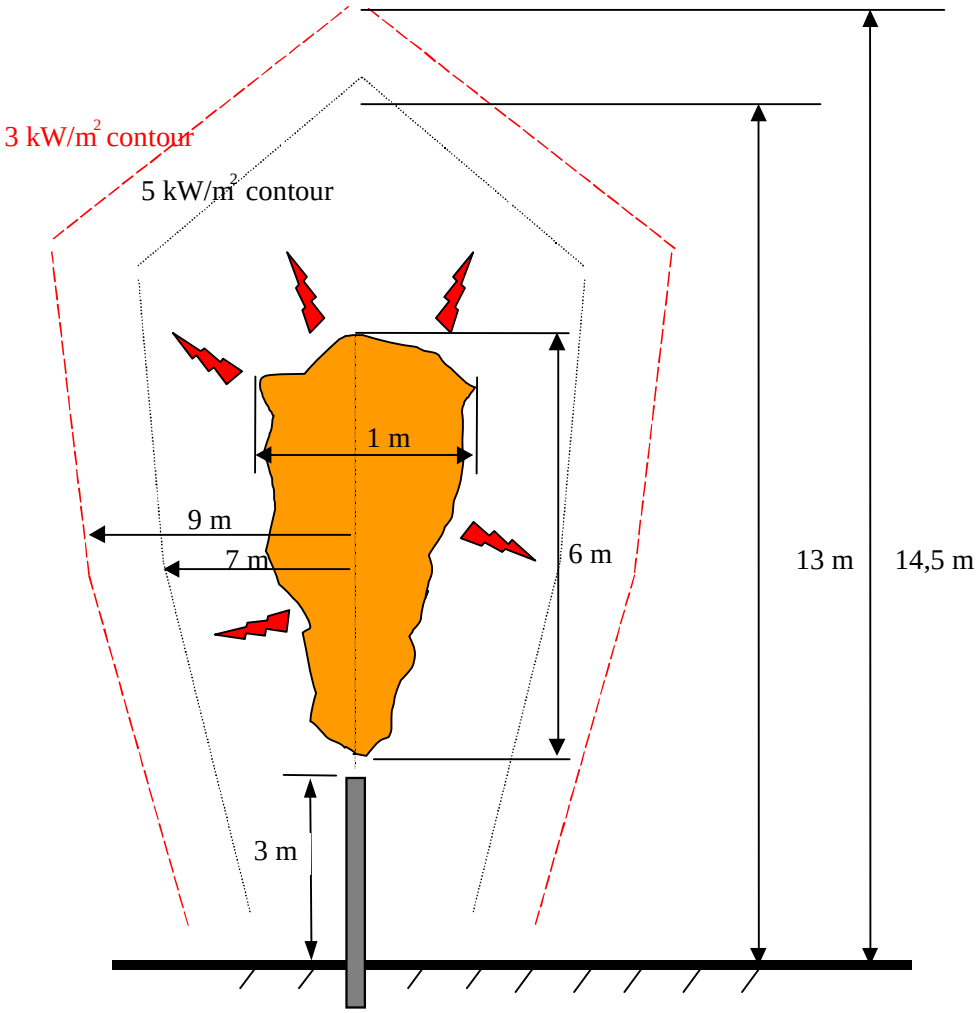


Figure 7. Example of the definition of the protection area around a highly active decompression drilling in relation to the thermal effects linked to accidental gas inflammation (methane outflow 0,3 m^3/s)

It should be noted that these decompression installations should play a part during the entire time taken to flood the underground works, the most critical phase, but that they may also need to be retained in situations where flooding of post-mining voids will never be complete.

As an example, Figure 8 presents the change, over a three-year period, to the activity of a decompression borehole placed into service in Cransac in France's Decazeville coalfield that is flooding.

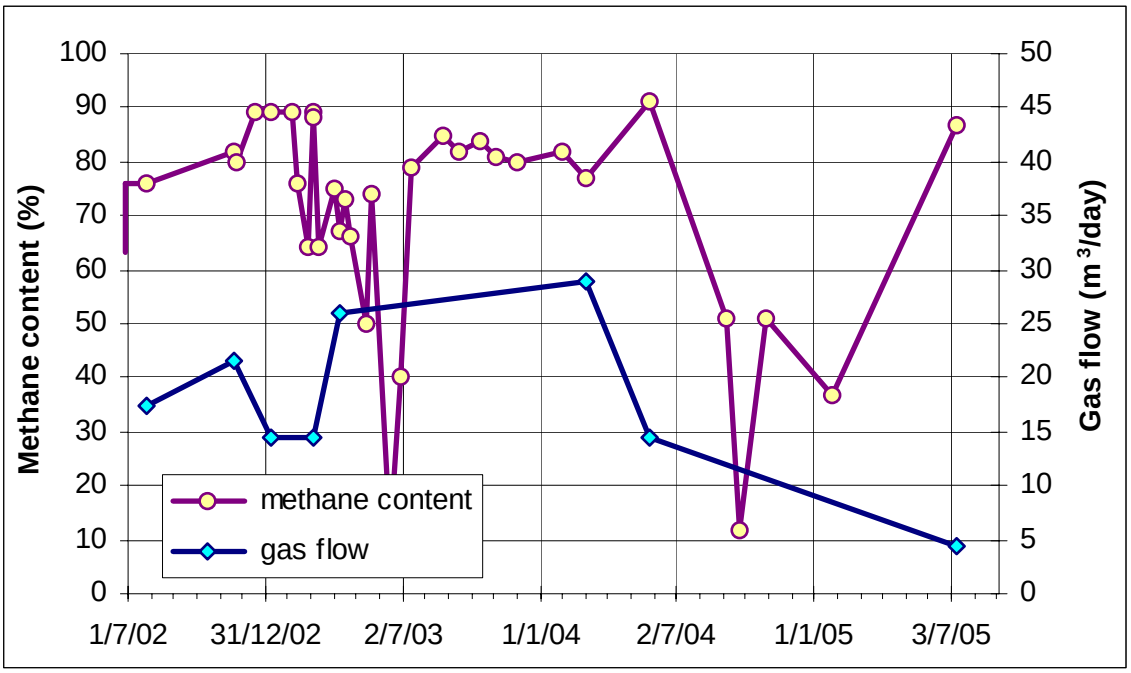


Figure 8. Example of the activity of a decompression borehole in the Decazeville coalfield

The intensity of the gaseous release from this borehole, as established from one-off measurements of the methane content and gas flow clearly show the beneficial effect that this kind of installation can have in terms of reducing the pressure level in the post-mining reservoir and in reducing the amount of gas likely to migrate uncontrollably to the surface.

4.5.2 Special Measures and Land Management

In those special cases where implementing efficient prevention methods is technically impossible or where the action of all of the means implemented turns out to be insufficient, the appropriate administrative approach must be undertaken as regards the urban development of those areas classified as being the most likely to release gas to the surface.

Depending on the local context, this may require:

- temporarily ruling out any urban development in the affected areas or the banning of new building projects without any additional preventive measures, at least during the rising flood water phase;
- the mandatory inclusion as part of any building permit, of technical and/or constructive measures that inhibit the penetration and accumulation of gas within the buildings envisaged.

These measures which have to be set out on a case by case basis, must come with the appropriate inspection and monitoring procedure.

4.5.3 Inspection and Monitoring Means

Whatever the treatment mode chosen and implemented, monitoring the operating parameters of the underground mining reservoir and the presence of any mine gas on the surface is necessary to ensure that the preventive measures taken are effective.

It is especially necessary to regularly check the correct operation of the decompression shafts or boreholes (or the gas drainage system) so as to be sure that the reservoir is not placed under pressure. This check must be carried out throughout the service life of the system.

Post-mining site monitoring can be performed by:

- manual checks and measurements (covering gas content, pressure, direction of release, flow...) performed periodically at strategic locations or those that are most exposed (decompression boreholes, former mine-surface links, locations where build-ups may occur such as in underground networks and basements…), using portable devices;
- implementing automated measurement or remote monitoring systems. A system of this kind has, for example, been installed by Charbonnages de France in the Nord-Pas-de-Calais coalfield, to monitor the overall behaviour of the post mining reservoir from some twenty observation points;
- direct measurements of gas flows on the surface. These measurements are especially effective in assessing the importance of the actual transfer of gas towards the surface (Pokryszka and Tauziède, 1999). This is recommended for sensitive built up areas, if the presence of gas is observed using the aforementioned monitoring measures.

The means available for use in checking and monitoring post-mining sites are described in greater detail in a communication dedicated to this problem (Besnard and Pokryszka, 2005).

5. Conclusions

The risks linked to the rise of mine gases to the surface represents a problem that is especially important in the context of closed coal mines. This aspect should be taken into consideration during regulatory investigations prior to a mining operator relinquishing their mining concessions.

A methodology for analysing and assessing this risk has been developed by INERIS in cooperation with Charbonnages de France. It is based on compiling and analysing multiple data relating to the studied mining area: historical data, the characteristics and the behaviour of the post-mining reservoir, the geological and hydro-geological characteristics of the seam… It results in a quantified mapping of risks and in defining those preventive measures that should possibly be implemented.

This method has been applied to all closed down mines belonging to Charbonnages de France in the various French coalfields where an analysis of the risk relating to migration to the surface of mine gas turned out to be relevant.

Furthermore, even if there remains a number of phenomena that are insufficiently understood[1], the development and research work undertaken in the context of establishing this methodology have made it possible to improve knowledge of gaseous phenomena in the

[1] For example: the evolution of gaseous properties of post-mining voids and their hydro-chemical behaviour over the long term, the durability of decompression works…

context of shutdown coal mines and to move along the understanding of the behaviour of post-mining reservoirs in a complex geological and hydrological environment.

The knowledge acquired and those elements of the methodological approach established can be used or derived to evaluate the risks linked to gases in other post-mining contexts other than closed coal mines. It can be also used in the context of setting out Mine Risk Prevention Plans (Plans de Prévention des Risks Miniers or PPRM) described in a communication dedicated to this regulatory tool (Didier and Leloup, 2005).

6. Bibliography

Burrel R., Friel S. (1996) – *The effect of mine closure on surface gas emission* – Proc. of the conference on the environmental management of mine operations – IBC (eds), London (UK)

Besnard K. and Pokryszka Z. (2005) - *Gases emission monitoring in a post-mining context* - Actes du Colloque International Après-mine 2005, 16-17 November, Nancy (France)

Coal Directorate of the Commission of the European Communities (1980) - *Firedamp Drainage – Handbook for the coalmining industry in the European Community* – Verlag Glückauf, Essen (Germany) – ISBN 3 7739 0254 9

Couillet J.-C., Pokryszka Z., Tauzième C., Prince M. (1998) - *Mathematical model for firedamp reservoirs* - Proc. of the International Conference on Coal-bed Methane Technologies of Recovery and Utilisation – GIG (eds) – Katowice (Poland)

Degas M. and Wojtkowiak F. (2003) - *Stabilité de la surface après l'exploitation totale du charbon et l'arrêt des pompages d'exhaure minière,* Actes du Colloque International Après-mine 2003, 5-7 February 2003, Nancy (France)

Didier C. and Leloup J. (2005) – *The MRPP: A powerful operational regulatory tool to prevent and manage post-mining risk* - Actes du Colloque International Après-mine 2005, 16-17 November, Nancy (France)

Gunther J. (1965) - *Mécanisme et prévision du dégagement grisouteux* – Publication CERCHAR n°1588, Verneuil-en-Halatte (France)

Jackson N.W. (2000) – *Our mining heritage* – Presidential address delivered to the North-East branch of the Institution of Mining and Metallurgy on 21 Oct. 1999 at Newcastle upon Tyne (UK) – IM&M – July 2000 - pp 185-190

Kral V., Paletnik M, Novotny R. (1998) - *Methane from closed-down mines in the soil* – Proc. of the International Conference on Coal-bed Methane Technologies of Recovery and Utilisation – GIG (eds) – Katowice (Poland)

Łukowicz K. and Walter P. (2000) – *Prévision et prévention du risque lié au grisou à la surface de mines fermées* – Bulletin de l'Institut Central des Mines, Gornictwo n°1, ISSN 1507-5206, Katowice (in Polish).

Novotny R., Platenik M., Takla G., Kral V. (2001) – *Reduction of uncontrollable mine gas emission in the Czech part of Upper Silesian hard coal basin devastated by past mining activity* - Proc. of the 7th international mine ventilation congress – Research & Development Center EMAG (eds) – Cracow (Poland) – ISBN 83 913109 1 4

Pokryszka Z. (1992) - *Estimation of the extension of the zone of increased permeability in the goaf. Application to mine gas drainage techniques* - Workshop on the recovery and end-use of coal-bed methane – Katowice (Poland)

Pokryszka Z., Tauzième C. (1999) - *Method of measuring surface emission of methane* - Proc. of the International Conference on Latest Achievements in the Field of Mine Ventilation - Fire and Methane Hazard Fighting - GIG (eds) - Katowice-Szczyrk (Poland)

Pokryszka Z., Tauzième C. (2000) - *Evaluation of gas emission from closed mines surface to atmosphere* – Proc. of the 6th international conference on environmental issues and management of waste in energy and mineral production, Calgary (Canada) – Balkema (eds) – ISBN 90 5809 085 X

Prokop P. (2001) – *Gas leak effects on environment of Ostrava basin* - Proc. of the 7th international mine ventilation congress – Research & Development Center EMAG (eds) – Cracow (Poland) – ISBN 83 913109 1 4

Robinson R. (2000) - *Mine gas hazards in the surface environment*. Transactions of the institution of mining and metallurgy, section A, Mining technology, vol 109, September - December 2000, pp228-238.

Sizer K., Creedy D., Sceal J. (1996) - *Methane and other gases from disused coal mines : the planning response* – Technical report for the department of the environment – Wardell Armstrong – The Stationery Office (eds) – London (UK)

MODELING AND ASSESSMENT FOR SUBSIDENCE HAZARD IN INCLINED IRON MINING.

RENAUD Vincent[1], TRITSCH Jean-Jacques[2], FRANCK Christian[3]

[1] INERIS LAEGO - Ecole Nationale Supérieure des Mines de Nancy, Parc de Saurupt – F 54042 Nancy Cedex, France. vincent.renaud@ineris.fr

[2] INERIS, Parc Technologique Alata, B.P. 2, 60550 Verneuil-en-Halatte, Jean-Jacques.Tritsch@ineris.fr

[3] GEODERIS, Avenue de Tsukuba, 14209 Hérouville Saint-Clair, christian.franck@industrie.gouv.fr

ABSTRACT: *The old iron mines of the North-West of France have geometrical and exploitation configurations appreciably similar, with dips varying between 30° and 90°. Within the framework of the establishment of risk maps related to these exploitations, the observation of subsidence in certain basins leds us to try to better know the conditions of occurrence and the consequences on the surface of these phenomena, and in particular the influence of the dip on their relevance. A modeling was thus undertaken, consisting initially of back-analysis of a subsidence trough observed and studied, in order to seek the initiating mechanism within mining work and to appreciate the influence and the degree of reliability of the parameters, and in the second time the parameterised analysis of the zones of potential failure according to the dip, the opening of the mine seam, the extraction ratio and the thickness of the overburden. The contribution of this modeling and the experience feedback of other mining basins allowed to fix the principles of evaluation of the subsidence alea, in terms of intensity and occurrence, of these deposits.*

KEYWORDS: hazard, subsidence, inclined seams, iron mine, modeling.

RESUME : *Les anciennes mines de fer du Nord-Ouest de la France présentent des configurations géométriques et d'exploitation sensiblement similaires et des pendages variant de 30° à 90°. Dans le cadre de l'établissement de cartes d'aléas liées à ces exploitations, l'observation de cuvettes d'affaissement dans certains bassins a incité à mieux apprécier les conditions d'apparition et les conséquences en surface de ces phénomènes et notamment l'influence du pendage sur leur pertinence. Une modélisation a ainsi été entreprise, consistant d'abord en la rétro-analyse d'une cuvette d'affaissement observée et étudiée, afin de rechercher le mécanisme initiateur au sein des travaux miniers et apprécier l'influence et le degré de fiabilité des paramètres et, dans un second temps, l'analyse paramétrée des zones de rupture potentielle en fonction du pendage, de l'ouverture de la couche exploitée, du taux de défruitement et du recouvrement. L'apport de cette modélisation et le retour d'expérience d'autres bassins miniers ont permis de fixer les principes d'évaluation de l'aléa affaissement, en termes d'intensité et d'occurrence, de ces gisements.*

MOTS-CLEFS : aléa, affaissement, gisement penté, mine de fer, modélisation.

1. Introduction

In the framework of the assessment and the prevention of mining hazards, the establishment of risk maps related to the movements above the iron deposits exploited in the North-West of France (figure 1) highlighted their relative homogeneity and singularity.

These basins indeed have geological and exploitation characteristics of formation relatively homogeneous. In addition, and mainly because these exploitations have an important dip (between 30° and 90°), it quickly appeared during the information collection and the first observations of disorders on the surface that the risk evaluation of ground movement, and especially of subsidence occurrence, had to take into account the singularity of these deposits and could not be completed with the analyses made for horizontal mining works.

This article initially describes the characteristics specific to these exploitations. Then, the objectives are presented, steps and results of the modeling made on the basis of back-analysis of an observed subsidence phenomenon. Finally the transcription of these results and the evaluation of the subsidence risk are discussed.

2. Characteristics of North Western iron mining exploitations

The risk analysis is developed for studies at the scale of a whole basin of risk, even several risk basins, if they present strong analogies. It is the case of the iron deposits of the synclinals of Soumont, May/Orne, La Ferrière-aux-Etangs (Normandy) and Segré (Pays-de-Loire).

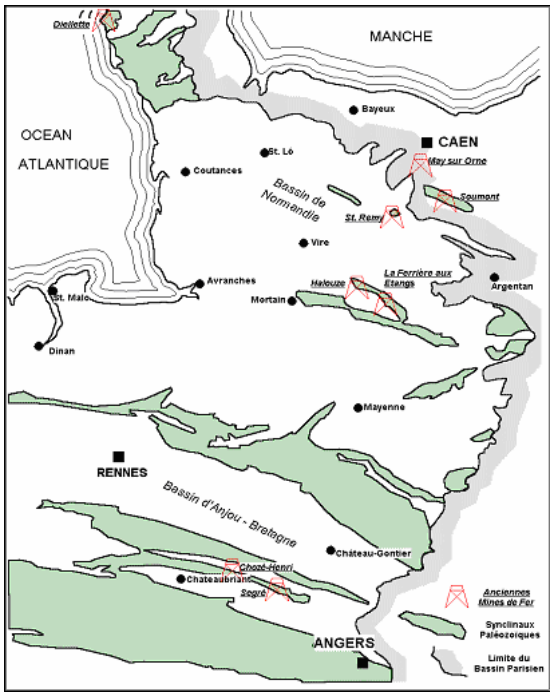


Figure 1. Localisation of the iron-bearing basins of the North-West of France (Varoquaux and Gerard, 1980).

The various basins present much analogies on the geological and exploitation aspects. These deposits fit in the dissymmetrical synclinal whose periods of deposit (Ordovician or Silurian) and of crumpling are near on a geological scale. They are fairly to strongly slopes (figure 2), located at very close depths (between 10 and 600 m) and hold one or two veins of low or average thickness (overall 2 to 4 m, locally more).

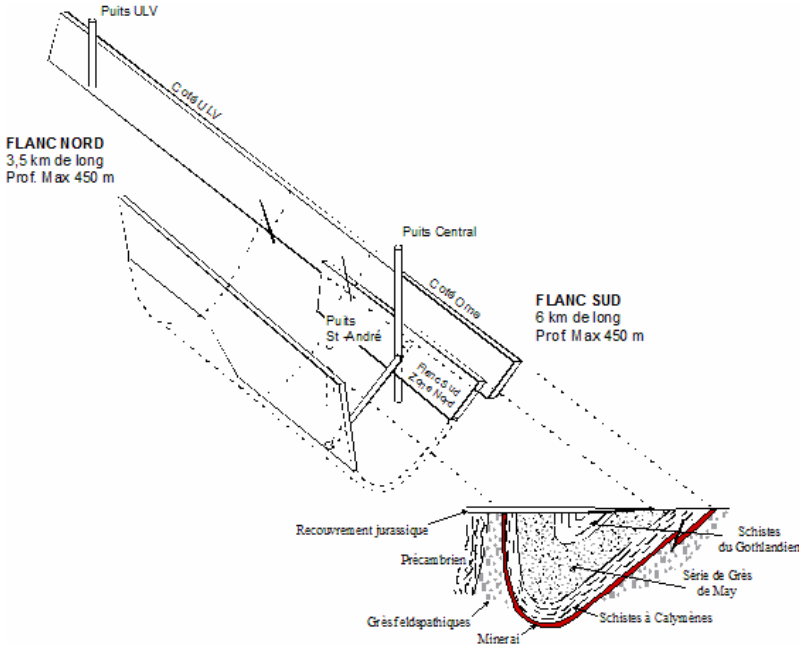


Figure 2. Example of the mine configuration of May-sur-Orne (according to Maury, 1972).

The nature and the strength of the iron ore are relatively variable. The ore is mainly constituted of haematite at May-sur-Orne and at a shallow depth under the calcareous overthrust of Soumont. The ore is carbonated in-depth in others basins, like at Segré and La Ferrière-aux-Etangs. The compressive strength of the ore is about 100 MPa at May-sur-Orne and 200 MPa (perpendicular to the bedding plane) at La Ferrière-aux-Etangs.

The mining methods used in those several basins are appreciably similar (figure 3). The oldest mining sites were exploited by short dip faces also called stops, then by dip strike faces. Thereafter, one systematically applied the method of the rise faces or the mechanised strike faces for the mining sites with low slopes (dip lower than 50°) and the shrinkage method for the mining sites slopes to high slopes (dip higher than 50°). These works are connected by level galleries connected to the works of ore extraction, and spaced of 30 m to 75-80 m in altitude, according to the basins and the methods used.

The observed disorders (table 1) in these various basins are similar (primarily some localized sinkholes by crown section rupture, shaft or raise clearings, or collapses of galleries). One notes however the existence of collapses of important districts at the bottom, in production run, in general without repercussions on the surface, except for Soumont and La Ferrière-aux-Etangs. The observed disorders on surface are traditional depressions with spread out board, with opened cracks but without frank breaks of shearing, which can be connected with subsidence troughs.

On the other hand, the documentary analyses do not identify any accident of huge collapse type: the only events known in the western French basins are exclusively the fact of slate exploitations whose common factors are their complex geometry, very different from iron mining works, and the presence of important residual voids (Tritsch, 2000).

Table 1: Comparative analysis of various Western iron-bearing basins

Basin	**MAY-SUR-ORNE**	**SOUMONT**	**LA FERRIERE-AUX-ETANGS**	**SEGRE**
Dates of exploitation	1896 - 1968	1907 - 1989	1905 - 1970	1907 - 1984
Maximum depth	450 m	650 m	400 m	490 m
Mining methods	stoping, dip faces, shrinkage	Rise faces, shrinkage, strike faces or “stoping”	Stopings, rise faces, retreating workings, shrinkage	shrinkage
Dip	45° to 90°	30° to 60°	25° to 45°	60° to 90°
Number of worked seams	1 (very locally 2)	1	1	2 (intercalated bed of 40 to 50 m thickness)
Dominant nature of the iron ore	Facies haematite	Haematite under calcareous overthrust, Carbonated and siliceous in-depth	Chlorito-carbonated. Little haematite	Carbonated
Content of iron	35-50%	36-50%	35-50%	Average 52%
Compressive strength of the ore	100 MPa	115 MPa	80 MPa parallel to the bedding plane, 200 MPa perpendicular to the bedding plane	???
Thickness	3.5 to 4.0 m (locally: 6 to 7 m)	3 m (locally: 6 m)	3 to 4 m (locally: 5 m)	1 to 2 m
Discordant overburden	0 to 60 m (Jurassic limestone)	0 to 50 m (Jurassic limestone)	missing	missing
Zone of deterioration of the ore	20 to 50 m	20 to 50 m	20 to 80 m	20 to 80 m
Types of observed disorders	Sinkholes (rupture of crown section), shaft collapses or raise clearing	Subsidence (roof failure), sinkholes	Subsidence (roof failure), collapses (rupture of crown section), sinkholes (directly above not very deep galleries)	Sinkholes, collapses (rupture of crown section)

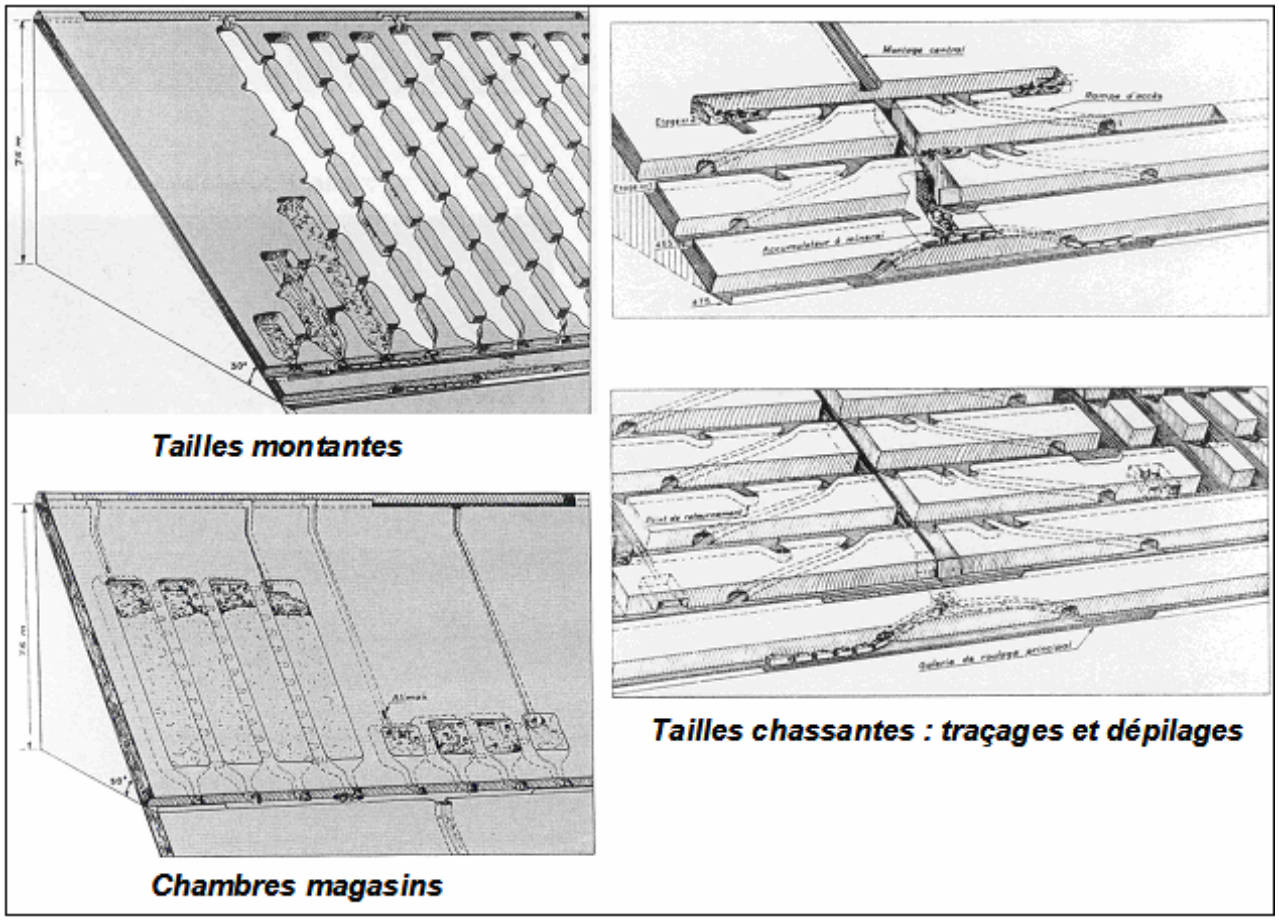


Figure 3. Mining methods of the basin of Soumont (according to Perrotte and Lidou, 1983).

3. Modeling of the inclined deposits of the West of France

3.1. Modeling approach

The study of modeling, using code UDEC (2D calculations in discontinuous medium), was organised in two stages:

- the back-analysis of a subsidence trough in Soumont developed in 1966 above a well delimited underground collapse;
- parametric analysis of the zones of potential failure (extension, amplitude) according to the dip (30 to 65°), the extraction ratio (70 to 90 %), the layer thickness (1.5 to 5 m), and thickness of the formations of overburden in discordance (0 to 50 m).

3.2. Back-analysis of the subsidence phenomenon of Soumont appeared in 1966

Several collapses occurred in the mine of Soumont between 1929 and 1966. They mainly induced subsidence troughs on the surface (figure 4). The latest one is the most documented for underground visits and analyses of the causes were carried out in close connexion with this collapse. Thus this event has been selected for the back-analysis. Collapse occurred between the levels -120 and -250 m, 40 years after the exploitation of this sector of mining works. The dip of the layer is 30° and the extraction ratio is high (80-85 %).The maximum subsidence measured at that time was 65 cm.

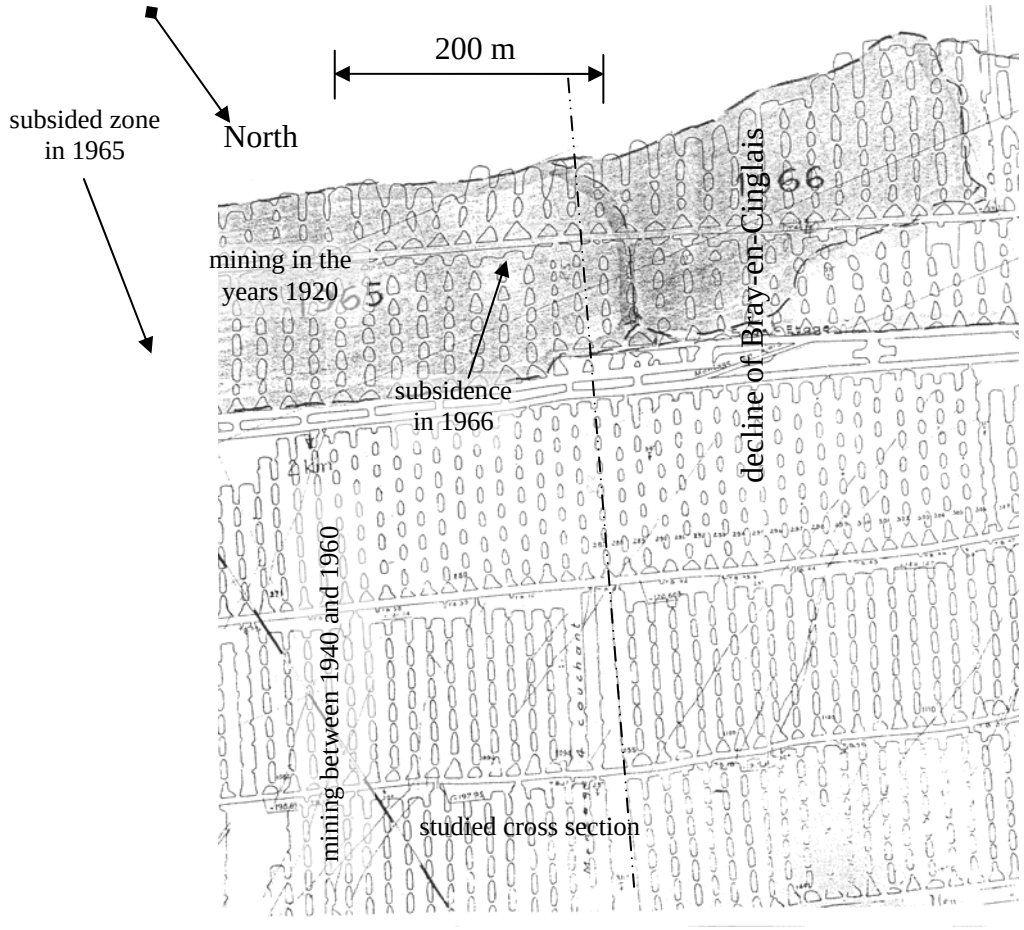


Figure 4. *Plane view of the seam worked by rooms and pillars at Soumont in the collapse zone of 1966*.

The back-analysis was based on a modeling on the collapsed district scale. The objective was to specify the conditions which were at the origin of collapse and the most relevant mechanisms. This work was carried out by respecting the three following checking points:

- A subsidence amplitude of 0.65 m was measured on surface;
- The absence of collapse in work of depth higher than 220 m;
- The stability of the mining works exploited with the same depth by shrinkage, to the west of the collapsed districts.

3.2.1 Description of the mining conditions

The extraction ratio of the lower stages decreases with depth. The section of the way is trapezoidal and the opening of these levels is 4.5 m. The pillar width of the lower stages varies between 4.5 m and 6 m. Above the ore layer, one meets massive and resistant schist beds for a total thickness of 120 m, then sandstone beds over 95 m, then a schist alternation and sandstone of weak thickness (10 m) and finally again sandstone. In lower part of the ore layer, there is a 10 m thick schist bed then a series of sandstones. The whole of these formations is covered by a calcareous slab whose thickness can be evaluated to 30 m at the location of the concerned sector (Tincelin & Vouille, 1992).

3.2.2 Geomechanical characteristics

The geomechanical characterisation of various materials of the southern side of the mine of Soumont is not complete. Only the iron ore and its immediate roof and floor have been tested in laboratory. Hence we estimated the data according to various sources:

- values obtained in laboratory: bibliographical study carried out at the time of the preliminary phase (Delaunay & Renaud, 2003);
- data resulting from a study on the slate mine of Misengrain (Tritsch, 2000);
- data from the database by Fine (1993);
- data (for the sandstone) resulting from the synthesis of the mechanical characterisations for the HBL (Mery & Thoraval, 1998);
- data from the geological map of Mézidon (BRGM);

The values of strengths (tensile and compressive) were then degraded while taking into account:

- the scale effect being estimated at 0.47: according to Bieniawski & Van Heerden (1979), referring to a curve obtained on unconfined iron ore samples;
- the 2D aspect of modeling by preserving the strength/stress ratio for the pillar in 2D and 3D by decreasing the compressive strength of the seam (equation 1):

$\sigma_{pillar} = \frac{\rho g z}{1-\tau_{3D}} = \frac{1}{\alpha}\frac{\rho g z}{1-\tau_{2D}}$ that is to say $\frac{1}{\alpha} = \frac{1-\tau_{2D}}{1-\tau_{3D}}$, α: coefficient of correction.

$$\tau_{2D} = \frac{L_{room}}{L_{room}+L_{pillar}} \text{ and } \tau_{3D} = 1 - \frac{{L_{pillar}}^2}{\left(L_{room}+L_{pillar}\right)^2} \text{ thus } \alpha = \sqrt{1-\tau_{3D}} \quad (1)$$

Let us recall that for square rooms and pillars:

- the time influence on the material (by estimating that the coefficient of reduction of strengths is founded on a ratio elastic strength/ peak strength).

Table 2 shows a synthesis of all strengths values obtained according to the various effects taken into account. The behaviour law retained takes into account a hardening then softening post-failure behaviour.

Table 2. Synthesis of the compressive strengths for various materials of the study.

		Iron ore			
	Extraction ratio	85% (upper stage)	82% (stage between z = -202 and z = -302 m)	76% (stages lower than z = -302 m)	Other materials
instantaneous strength	initial strength of the sample in laboratory (MPa)	Rc^0 (= 115 MPa)			
	taking into account of the scale effect (MPa)	0.47 Rc^0			
1966	effect 2D/3D (MPa)	0.182 Rc^0	0.199 Rc^0	0.230 Rc^0	0.47 Rc^0
	long-term strength (MPa)	0.084 Rc^0	0.092 Rc^0	0.106 Rc^0	0.216 Rc^0

3.2.3 Initial state of stresses

The assessment of the series of stress measurements carried out in situ in 1979 (TINCELIN & Vouille, 1981) showed that $\sigma_h/\sigma_v = 0.5$. However, many stress measurements carried out in the West of France, within synclinal structures, show that the horizontal stress is always higher or equal to the vertical stress. For the sites of Grais (May/Orne) and St-Sigismond (Maine-et-Loire), the ratio σ_h/σ_v varies between 1 and 1.5 (Burlet, 1991). The stress tensor being of doubtful validity, we considered three values for the ratio σ_h/σ_v: 0.5, 1 and 2.

3.2.4 Results

The solutions being able to explain the collapse of 1966 being plural, some certain data input were regarded sure (extraction ratio, dimensions of the various stages, width of the stage pillars, exploitation thickness, geology, geomechanical characterisation of materials other than the iron ore) and others were regarded as variables of the study.

Each method of calculation of this study was analysed in terms of subsidence on surface, distribution of plasticity, displacements, principal stresses and plastic deformation in five tested pillars (figure 5). To sum up, the different methods of calculation carried out made it possible to study the influence of the:

- stress field with the ratio σ_h/σ_v (3 values: 0.5, 1 and 2);
- density of the roof stratification;
- friction angle of the bedding planes;
- effects of faults on the collapse mechanism;
- joint behaviour law;
- strength of the pillars;
- panel width;
- opening effect.

The various calculations allow to reproduce a mechanism and explain the subsidence observed on surface in 1966. It is due initially to the relative compressions of pillars and then to the deflection of the roof. These two zones are the place of strong shear mechanisms which imply a potential failure by shearing up to surface.

The three checking points (collapse of 1966 in the upper stage, stability of the lower stages and shrinkage stability) were checked.

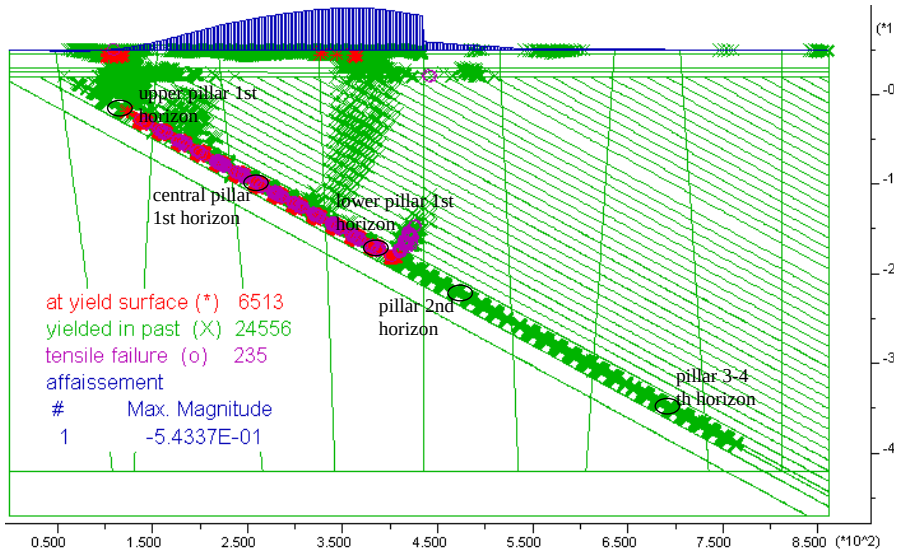


Figure 5: Distribution of plasticity: joint spacing of 10 m + variation of subsidence on the surface

3.2.5 Conclusion

Works completed showed that the height/width ratio and the strength of the pillars and the roof stratification are the essential parameters which allow to carry out this back-analysis. This work let us draw some conclusions and clear tendencies:

- the length of the plastic zone cannot exceed 200 m**.** The mechanism highlighted cannot thus be repeated in the lower stages;
- the verification of the 2nd checking point showed the importance of the strength value of the barrier pillars. The pillar strength must be higher (51 MPa) than that of the pillars of the higher stage (34 MPa) for the mechanism to occur. That is compatible with the fact that the iron ore of the lower stages is more carbonated (so more resistant);
- for σ_h/σ_v = 0.5 and 1, we notice that the value of maximum subsidence on the surface is close to that measured in 1966: 65 cm;
- the state of the initial stresses has a relatively weak influence on the thresholds of pillar strength of the lower stages;
- the characteristics (spacing and friction angle) of the stratification network parallel to the dip are essential parameters in the mechanism which we highlighted: the increase in spacing between the joints inhibits the mechanism of collapse. It is the same for the friction angle;
- the values of strengths which we introduced into our models are compatible with the intervals of variation of the in-situ characteristics [instantaneous value ; value in the long term integrating the effect of time].

3.3. Parametric analysis

The second part of this study consisted in carrying out a numerical modeling on the scale of the mine in order to develop the back-analysis collapse (of Soumont in 1966) and to evaluate the criteria to specify the risk by carrying out a parametric study (allowing a valorization on the whole inclined deposits of the same type). We thus studied the sensitivity of four parameters by carrying out twenty calculations:

- the dip (between 30 and 65°);
- the extraction ratio (between 70 and 90 %);
- the exploitation thickness (between 1.5 and 5 m);
- the height of overburden (between 0 and 50 m).

The analysis of these twenty calculations was focused on the extension of the zones of potential failures (plasticity), on the value of maximum displacement in the pillars and on the value of the maximum subsidence on the surface. This reveals that the mechanism identified at the time of the back-analysis can be reproduced under the geometrical conditions synthesised in table 4. In addition, we noticed that the subvertical faults can inhibit or amplify the mechanism of failure by shearing. Moreover, the reduction of the height/width ratio of the pillars (or thickness reduction) has a very significant positive role on the exploitation stability.

4. Evaluation of the “subsidence” hazard

The hazard assessment is classically made by combining the awaited intensity of the phenomenon with its probability of occurrence, this being the predisposition of the site with respect to the dreaded phenomenon.

4.1. Qualification of the intensity

It is recognised that the characteristics of depression which materialise the most severe damage for the goods located on surface are the horizontal differential strains and movements of ground inclined setting rather than maximum vertical subsidence in itself. Table 3 gives indicative values of the strains and slopes which make it possible to evaluate the phenomenon intensity.

Table 3: Classes of intensity of the risk “subsidence” (purely indicative values)

Classify intensity	**Horizontal differential strains ε (in mm/m)**	**Surface inclination μ (in %)**
Negligible	$\varepsilon < 1$	$\mu < 0.2$
Very low	$1 < \varepsilon < 5$	$0.2 < \mu < 1$
Low	$5 < \varepsilon < 10$	$1 < \mu < 2$
Medium	$10 < \varepsilon < 30$	$2 < \mu < 6$
High	$\varepsilon > 30$	$\mu > 6$

The value of these two parameters can be appreciably influenced by different factors studied before.

It appears so that value of maximum subsidence is in the form: $A_{max} = 0.3.\ w.\tau$, with:

- A_{max} = maximum subsidence;
- w = exploited thickness (in the districts exploited by shrinkage);
- τ = extraction ratio (or recovery factor).

It can be easily deduced from them the values from the strains (ε_{max}) and slopes (μ_{max}) starting from the following traditional relations: $\varepsilon_{max} = \alpha\ .\ A_{max} / P$

$$\mu_{max} = \beta\ .\ A_{max} / P$$

Where:

- P is the average depth of the panel;
- α and β of the coefficients estimated respectively at 1.5 and 5 in the western iron basin.

The values of the coefficients α and β are deduced from the studies in experience feedback carried out on the Iron Mines of Lorraine and adopted for their drastic security character.

4.2. Qualification of the occurrence probability

In the inclined exploitations of the iron deposits of the West of France, it is mainly the stability of the barrier pillars, the slabs or the pillars left in place to ensure the behaviour of the immediate strata which controls the subsidence predisposition. To evaluate the long-term stability of the under-mined surface, main factors that have to be take into account are:

- dimensions of the panels;
- dip of the layers;
- extraction ratio;
- opening (height exploited between immediate strata);
- strength of pillars.

In a more precise way, the parametric analysis described previously provides fundamental indications on the configurations of layer and exploitation for which the occurrence of a subsidence can be excluded (table 4, below).

Table 4: conditions of exclusion of the process of subsidence (according to Renaud, 2004)

Dip	Extraction ratio (τ %)	Thickness (W)
> 55°	≤ 90%	≤ 4 m
	≤ 85%	≤ 5 m
45° to 55°	≤ 90%	≤ 3 m
	≤ 80%	≤ 5 m
30° to 45°	≤ 80%	≤ 3 m
	≤ 70%	≤ 5 m

The influence of an increase in the dip appears by a displacement of the zones of failure toward the surface (or of the outcrop): the greater the dip value, the more one affects the grounds close to surface (plastic points).

In addition to these configurations of exploitation, other conditions must be taken into account for a reduction of the hazard level, like:

- condition n° 1: for a subsidence to occur entirely, it is necessary that dimensions of the mining sites (width L) reach or exceed the depth (H) (that is: L ≥ H), which represents, in the context of these exploitations, a width along the dip from 250 to 290 m (depth lower than 220–250 m). In lower part (L < H), subsidence is all the more, the hazard level is lower;
- condition n° 2: it is considered that there are no repercussions on surface (non perceptible subsidence) if the mining site has a width L < 0.4 H;
- condition n° 3: if the minimum depth of mine working is higher than 250-300 m (according to the geometry of the mining sites), it is considered that the failure zones are not likely to reach surface.

Table 5: Classes of predisposition of the site for the risk “subsidence”

Site predisposition	Ratio L/H	Depth (H)
Very sensitive	L/H > 1	< 250 m
sensitive	L/H # 1	< 250 m
Not very sensitive	0.4 < L/H <1	< 250 m
negligible	L/H < 0.4	< 250 m
	L/H ≥ 1	> 250-300 m

4.3. Hazard zoning

The limits materialising on surface the zone influenced by subsidence are established, taking in account an angle called “influence angle”, measured from the vertical, which connects the end of the panel, at the bottom, to the points of surface where subsidence, strains or slopes are regarded as unperceivable or null. Although an single influence angle (γ) value of 30° to 35° is retained for flat veins, three angle limit values are defined for inclined layers (exploitations) These are:

- the limiting angle value (γ), in the direction of drivage which is equal to the limiting angle in flat vein;
- the “upstream” angle value, lower than the angle γ ;
- the “downstream” angle value, always greater than the angle γ ;

Looking at the data obtained in Soumont, it can be noticed (table 6) that the values of failure angles measured upstream and downstream (on average respectively about 7° and 30°), for a dip ranging between 30° and 40°, are very close to the corresponding values of the abacuses of the Lorraine coalfields or the Nord Pas-de-Calais region (Proust, 1964). Hence, it can be deduced that the influence angles must be also very close and take for the layer of Segré some values of influence angle equal to 30° (upstream side) and 45° (downstream side).

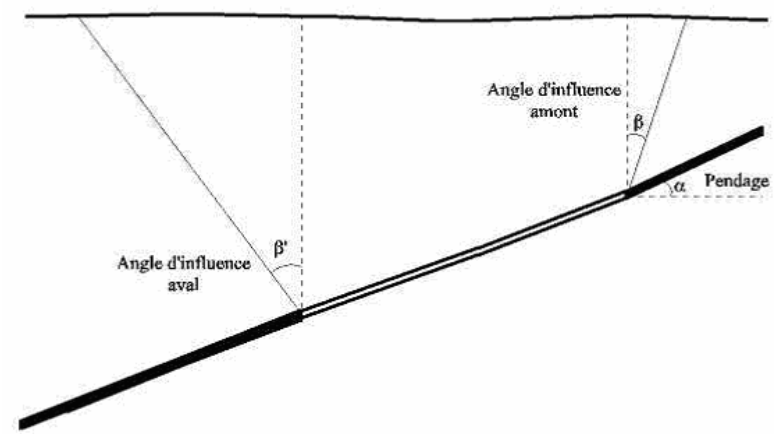


Figure 6: Diagram showing the dissymmetry of the upstream and downstream influence angles in inclined deposit

Table 6: Values given in the subsidence abacuses of Nord/Pas-de-Calais, Saar and Lorraine basins

Dip values		0°	15°	25°	30°	**40°**	50°	60°
Angles of rupture giving the limits of fracturing on the surface	Upstream angle	18	14	12	11	9	7	6
	Downstream angle	18	22	25	27	30	33	36
Angles of influence giving the limits of null subsidence	Upstream angle	35	32	30	30	**30**	28	27
	Downstream angle	35	38	40	43	**45**	47	48

Let us specify that the downstream influence angle is taken at the base of the exploited panels, and the upstream influence angle at the higher part of the panels.

5. References

Bieniawski, Z.T., Van Heerden, W. L. (1979). *The significance of in-situ tests on large rock specimens*. Int. J. Rock Mech. Min. Sci., 12, 101-113.

Burlet D. (1991). *Détermination du champ de contrainte régional à partir de tests hydrauliques en forages, résultats de neuf expérimentations in-situ réalisées en France*. Thèse de doctorat de Géophysique Interne à l'université de Paris VII.

Delaunay T., Renaud V. (2003). *Phase préliminaire à la réalisation d'une modélisation numérique sur les gisements pentés des bassins ferrifères de Soumont, May-sur-Orne et Segré (Calvados et Maine-et-Loire)*. Rapport INERIS DRS-03-49161/R01.

Fine J. (1993). *Le soutènement des galeries minières*. Ed. Armines, Centre de Géotechnique et d'Exploitation du Sous-sol.

Itasca (2000). *UDEC 3.01 User's Guide and Command Reference*. Itasca Consulting Group Inc. Minneapolis, USA.

Maury V. (1972). *Aménagement de la mine de May-sur-Orne en stockage souterrain d'hydrocarbures*. Revue de l'Industrie Minérale. Cahier 4 du Comité Français de Mécanique des Roches, 73-84.

Mery C., Thoraval A. (1998). *Synthèse des caractérisations géomécaniques*. Rapport INERIS SSE-CMe/ATh-98-25EP51.

Perrotte A. et Lidou B. (1983). *Diverses variantes de chambres avec piliers abandonnés dans la mine de fer de Soumont*. Industrie Minérale – Les Techniques, p.74-78, février 1983.

Proust A. (1964). *Etude sur les affaissements miniers dans le Bassin du Nord et du Pas-de-Calais*. Revue de l'Industrie Minérale, juin-juillet 1964, n° 6 et 7, 68.

Renaud V. (2004). *Contribution à l'analyse des conditions d'effondrement des gisements pentés des bassins ferrifères de Soumont, May-sur-Orne et Segré (Calvados, 14 et Maine-et-Loire, 49)*. Rapport INERIS DRS-04-50864/RN01.

Tincelin E., Vouille G. (1981). *Société des mines de Soumont - Projet d'exploitation des Etages 560-475 et 650-560 - Etude de stabilité.* Rapport de l'Ecole Nationale Supérieure des Mines de Paris – Centre de géotechnique et d'exploitation du sous-sol. R81/21.

Tincelin E., Vouille G. (1992). *Mine de Soumont - Mesures à entreprendre pour prévoir l'imminence d'un risque d'effondrement survenant à l'aplomb des routes nationales n°158 ou départementales n°43.* Rapport de l'Ecole Nationale Supérieure des Mines de Paris – Centre de géotechnique et d'exploitation du sous-sol. R92/12.

Tritsch J.-J. (2000). *Assistance technique à l'élaboration d'un dossier de demande d'abandon, carrières de Misengrain – site de Noyant, ardoisières d'Angers*. Rapport INERIS DRS-00-25078/R01.

Varoquaux J.-A., Gérard E. (1980). *Les gisements de minerai de fer français.* Annales des Mines, juillet-août 1980, 135-154.

LONG-TERM BEHAVIOUR PREANALYSIS OF THE BODOVALLE MINE (GALLARTA-VIZCAYA, SPAIN)

RODRIGUEZ Ramón[1], MARTIN DE LA ESCALERA Federico[1], ELORZA F. Javier[1], DEL OLMO Carlos[2], SAMPER Adolfo[3]

[1] ETSI MINAS - UNIVERSIDAD POLITÉCNICA DE MADRID_C/ Ríos Rosas 21 – 28003 Madrid, Spain; rodripons@dmami.upm.es ; FMARTIN@aero.gamesa.es ; jelorza@dmami.upm.es

[2] INGEMISA C/ Santo Angel 81. P4.1ºA – 28043 Madrid, Spain ; cdelolmo@ingemisa.com

[3] AGRUMINSA Bº Loredo s/n. Abanto y Ziervana – 48500 Vizcaya, Spain ; abraindustrial@infonegocio.com

ABSTRACT: The main purpose of this work is to evaluate, using the available information, the viability of design, development and verification of a prediction system in terms of long-term prediction of both loads or stresses distribution and displacements in zones in the vicinity of mined chambers of the Bodovalle mine, by means of computational techniques. In this respect, these works have begun selecting a representative zone of the underground mine system of chambers and pillars. For this sector, a preliminary 3D mathematical model has been developed.

KEYWORDS: Long term prediction, Simulation, Risk management, Mine closure.

RESUME : L´objectif de ce travail, est d´évaluer à l´aide de la bibliographie disponible, la viabilité de la conception, du développement et la vérification, d´un système permettant la prédiction á long terme du champ de contrainte et de déplacement autour des exploitations par chambres et piliers de la mine de Bodovalle à l´aide la modélisation numérique (méthode aux éléments finis). Dans ce sens, le travail a commencé par la selection d´un secteur représentatif des chambres et de piliers de la mine, en réalisant, tout d´abord un modèle mathematique préliminaire en trois dimensions.

MOTS-CLEFS : *Prédiction du comportement à long terme, Simulation, Gestion des risques, Fermeture des mines.*

1. Introduction

The mine of Bodovalle was active from 1961 to 1993 producing iron carbonate. It is placed at Vizcaya (Spain). The mineral was extracted from underground and opencast mining. Two companies were authorized to work there, Franco-Belga and Agruminsa. The latter now manages the maintenance and the design of the Bodovalle Mine Closure Project; this closure plan will be developed until the beginning of the next decade.

The underground mine presents big cavities and chambers, and a continued pumping for nearly 40 years from the lowest mine level, -185m. A consequence of the stop of water pumping, will be flooding of the mine, beginning from the deepest chambers and arriving to the shallow cavities, affecting also the opencast mine. In this situation, a new hydraulic equilibrium would be reached and the piezometric level would be place at +48m, where drainage gallery is situated.

Therefore, the Bodovalle Mine Closure Project considers the filling of some chambers and the development of complementary support studies with the objective of increasing the available knowledge with respect to the coupled hydro-mechanical-chemical behaviour of the chambers and

pillars system once the mentioned flooding would take place. In order to predict this long-term behaviour, different numerical simulations are foreseen. In this frame is placed the work here presented.

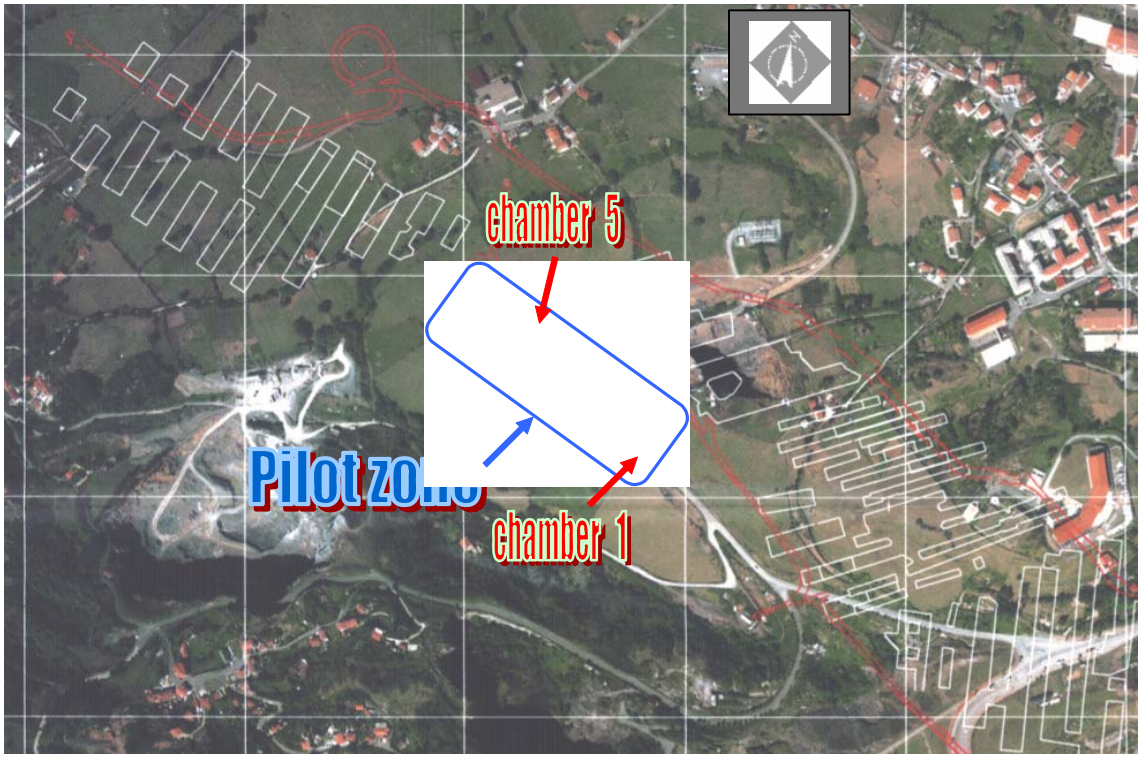


Figure 1. Bodovalle Mine aerial landscape. Chambers and pillars system is superposed. UTM grid (250m x250m)

2. Antecedents and context

The Closure Project objective of Mine Bodavalle is to guarantee the absence, in the long term, of unacceptable effects at surface that were mine closure consequences –particularly when infiltrated water pumpings were finished– using best practices and all available knowledge, minimising, at the same time, the economic resources needed for Project realization.

Due to limited available information about the hydromechanical mine behaviour, the Closure Project establishes a suite of preliminary studies, previous to the closure, having as objective:

- To evaluate the influence of water in the rock behaviour (mineral pillars, marl roofs,…), from the point of view of the local stability of each one of the mined structures and from the point of view of the global stability.
- To determinate the temporal evolution of the hydromechanical effect over the rock materials behaviour in order to evaluate the underground chambers long term evolution once the mine will be flooded.
- To study the impact of the old mine works over the underground and superficial water quality and to guarantee the absence of environmental affections.

So that could be possible to determine with precision the mine structures long term behaviour once the mine will be flooded.

Conservative approximations has been chosen (INGEMISA, 2004) to formulate the needed actions due to the quite limited available information, starting from the hypothesis that, in the long term, as consequence of the mine flood, breaches of pillars, with safety coefficients minor or equal than 4, will be produced. In this case, inadmissible lengths in the roofs, from the point of view of their stability, will appear increasing traction strain up to cause the breaking. Depending on the geological structural context (fault network complexity), where roof breaking is produced, the transmission of holes to the surface can be produced, in form of chimney (Ramirez Oyanguren, 2003) or, gradually, in form of sag sinking, with self-backfilling of the created cavity, that –in case of chambers placed at larger depths– could be possible that it will not reach out due to the produced expansion when terrain break up. The best way to limit the hole transmission is by chamber backfilling, with higher backfilling coefficients as the structural complexity of the potential break area increases.

In consequence, the Closure Project of Bodovalle Mine, consist of the following working phases:

2.1. Preclosure works

The previous works will be developed, fundamentally, between 2005 and 2008, although some tasks will take place till 2011. This phase has as main objective to reduce conceptual uncertainties about underground structures long term behaviour, when the pumping stoppage will take place, by means the improving hydrogeological, geochemical and, fundamentally, geomechanic knowledge of the mineral deposit. These tasks will be achieved through the correspondent studies. During their development, underground and surface instrumentations are foreseen, together with “in situ” and laboratory tests. Numerical models will help to develop prediction and integration information tools.

2.2. Closure works: Phase 1

They have as objective to study, at true scale, the mine flooding influence on roofs and pillars. They will be developed between 2009 and 2010. These works are previous studies continuation, in which phenomenological information will have been obtained by laboratory and “in-situ” tests. This information will contribute to the numeric models progress.

The works that are to be developed are based in the monitoring, by means an adequate instrumentation, of a mine zone called “pilot area” (Figure 2). In this area, it would be studied the behaviour of the backfilling, the roofs and the pillars in the more similar possible conditions to flood. After several visits to the mine, it has been observed that chambers 2, 3 and 4 placed in the NO1Sur block are the chambers with better conditions to be used as a pilot experience:

- They are chambers that must be refilled.
- They are chambers with relative easy access from mine interior to place instrumentation in their pillars.
- They are chambers with water presence.
- It should be possible, by adapted roofs maintenance works, drill from collector gallery to the chambers roof and to the pillars axes.

Moreover, the collector gallery instrumentation shows an additional advantage: it is a gallery designed at the most tectostructural complex area of the mine and has been traced, in some zones, in the roof marls, fact which will facilitate studies of this kind of material. At last, this is the nearest

accessible area to the subsidence area, that would allow its eventual use as control element in case of potential extension of subsidence areas of block “NO1Norte”.

However, if mentioned “NO1Sur” chambers were considered inadequate for the pilot experience, would be possible the use of other minor structures: for instance, the chambers and pillars area –that could be flooded under control– or any of the “NO Sur” chambers already operated, placed under the old mine, and that probably, they will have some water or they will be easy to flood.

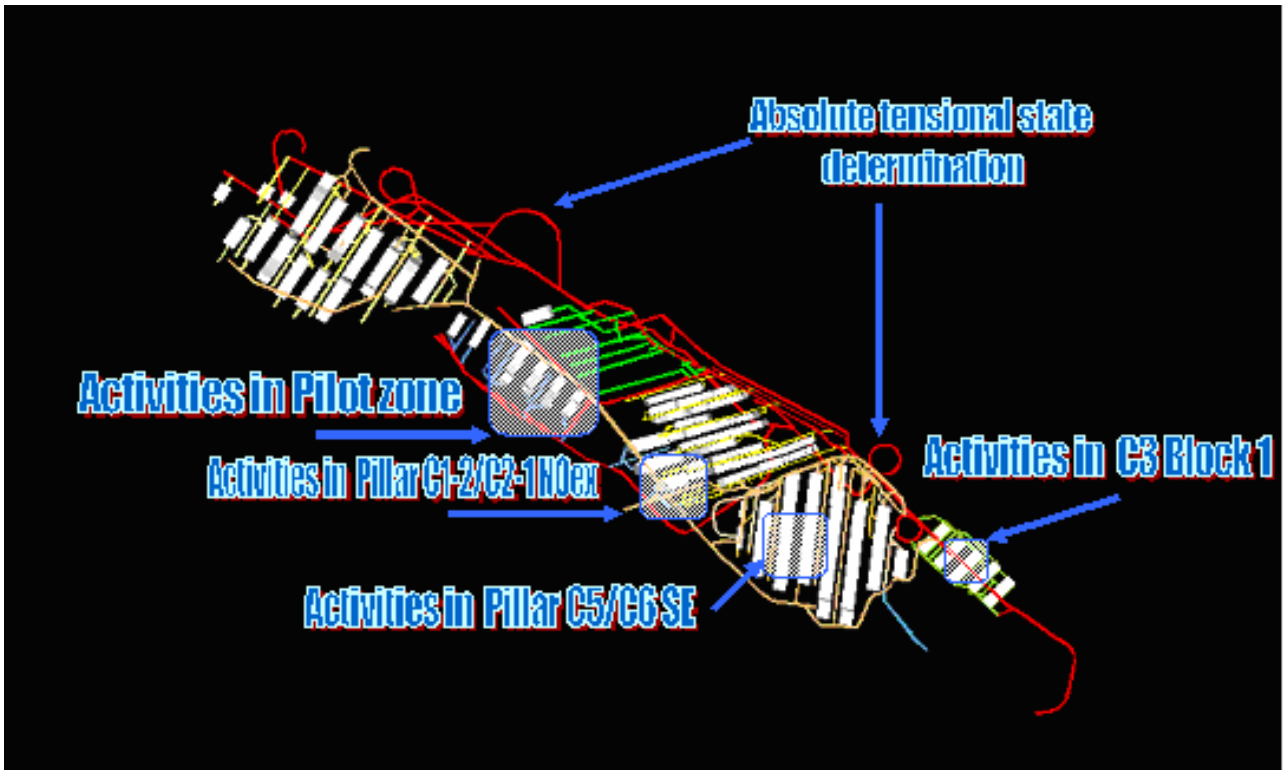


Figure 2. Planned actions in the underground mine system showing the “Pilot zone”

2.3. Closure works: Phases 2 and 3

The closure works will be developed between 2011 and 2013. Closure works will be developed under the accumulated experience during the six years of previous works. The works will consist in the backfill, by optimized methods, of those areas that were considered unstable, machinery and installations dismantling, and shafts and galleries closure.

3. Objective of job here presented

Inside of the Bodovalle Mine Closure Project, concretely at the denominated “preclosure works” phase, is foreseen to integrate all the available information, fundamentally geomechanical and hydrogeological, by numerical modelling. In this context, a preliminary modelling of a representative sector of the chambers and pillars system of the mine, at the selected pilot area, is presented here (Figure 3 and 4). The numerical technique used is based on the finite elements method.

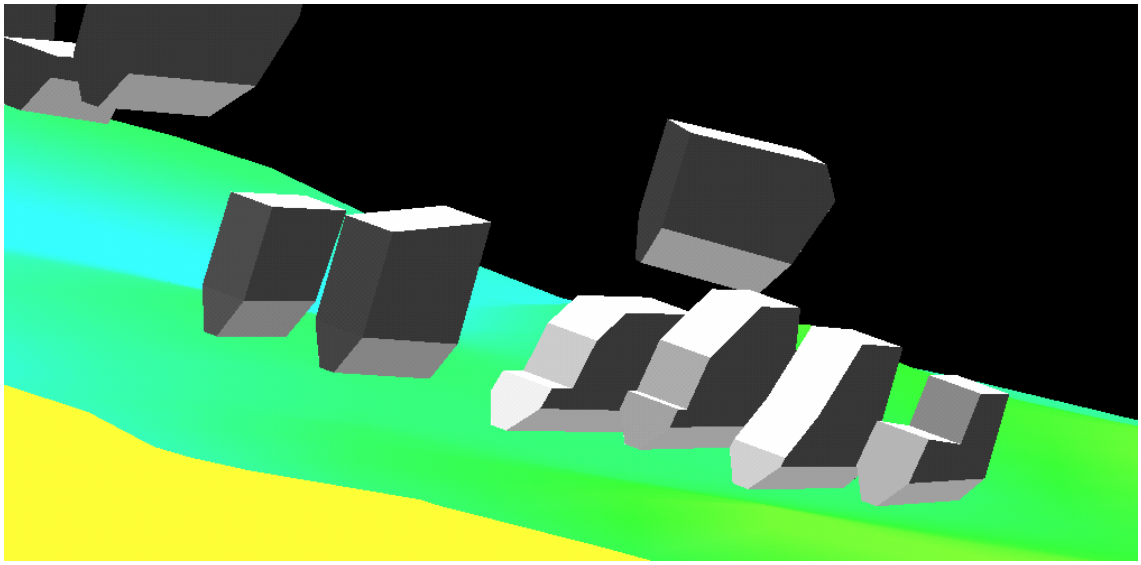


Figure 3. 3D mine model. Detail at 300 meters deep, with chambers nº 1 to nº 7. The chamber nº5 is already backfilled

In this way, it is hoped to develop a model, local at first request and amplified later, that contributes to improve the knowledge of the geomechanical and hydrogeological deposit behaviour. Moreover, the model will allow reduce the existing conceptual uncertainties about the underground structures long term behaviour and set and evaluate the possible and necessary corrector dispositions.

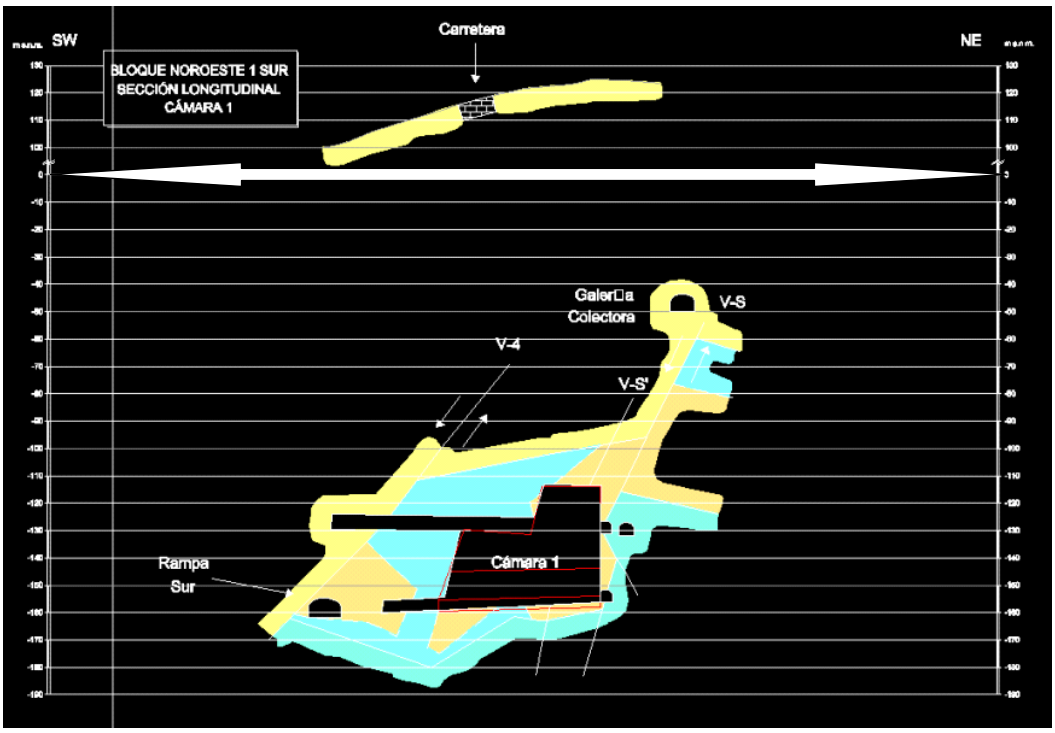


Figure 4. Geometric and geologic detail. Longitudinal section (SW – NE) of chamber nº 1 placed in block “N01SUR”. The arrow indicates 0 meters level

4. Modelling of the selected zone

4.1. 3D modelling set up

The selected sector, in which the numerical model has been developed, is composed of seven chambers (Figures 3), one of them –chamber nº 5– had been previously refilled as consequence of subsidence problems in the area. When establishing numerical modelling domain, it has been started from chamber nº 1 transversal geological section. This section (Figure 5), simplified, has been taken as generatrix section, allowing generating all the simulation domain by an extrusion whose directrix is normal to the chamber nº 1 section. Then, a realistic space distribution of the different materials has been realized: argillites, and upper limestones, the iron mineral –siderite–, the lower limestones and sandstones**,** together with the filling material used in chamber nº 5.

The geological and geomechanical available information of the deposit has allowed to define the different materials by lineal constitutive laws from their elasticity module and their Poisson coefficient.

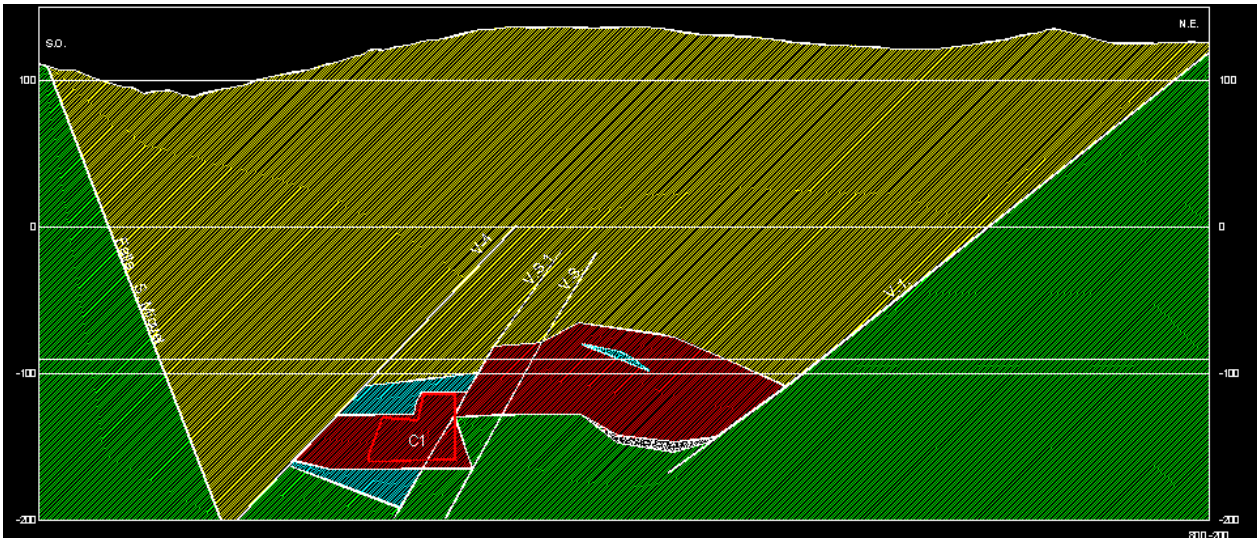


Figure 5. Geological cross section (SW – NE) simplification through chamber nº 1

In this way, a modelling domain of dimensions 800 x 309,30 x 866,6 meters has been defined (Figure 6), in which seven chambers have been placed and the most important faults have been also considered: San Miguel fault and VI fault. From the reference level 0 (sea level), a 110 metres material cover has been considered.

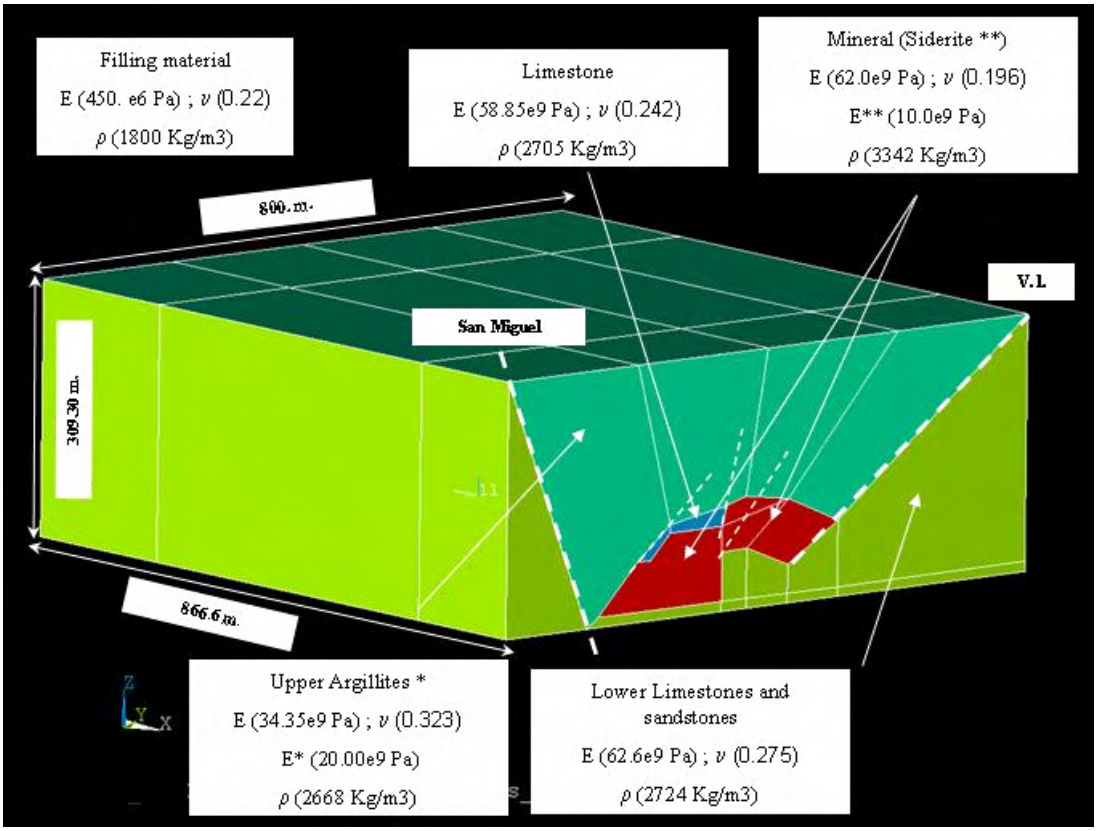


Figure 6. Materials and lithologic model distribution. Dimensions of the domain modelled

From the definition of the sub-volumes that form the simulation domain and once excavated the cavities correspondent to the chambers, the discretization of the domain has been done (Figures 8, 9 and 10). The modelization volume has been spatially discretized by means an automatic meshing of 54500 3D finite elements and 47000 nodes, with three degrees of freedom per node. The elements used are tetrahedrons and a reference system (Figure 7) has been defined in order to express on it both the displacements field and the stresses field placed in the elements (element centroid). The boundary conditions are the following: all the nodes placed in the lower base of the simulation domain are limited in their z displacement –simple support in z direction–, meanwhile the nodes placed in the lateral faces of the calculus domain can not displace in the normal directions to their respective faces. The unique load applied to the model has been the own weight of the solid materials, from the known densities of the different materials of the geological domain.

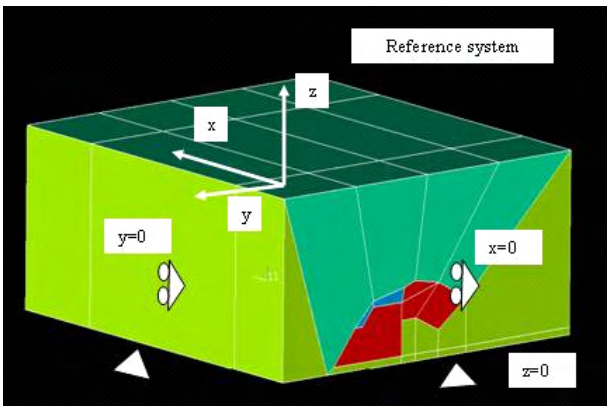


Figure 7. Reference system and boundary conditions

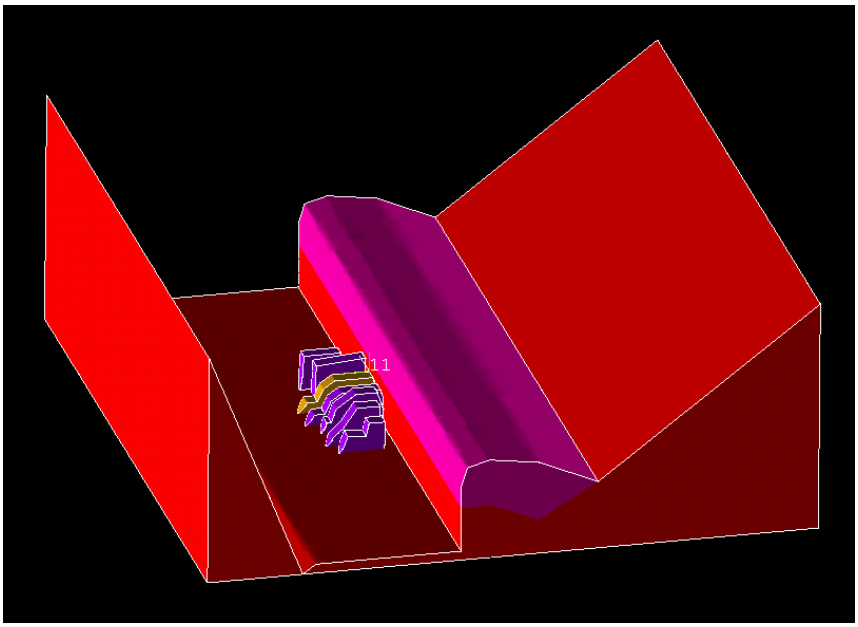


Figure 8. 3D geometrical model of the pilot area showing the chambers situation

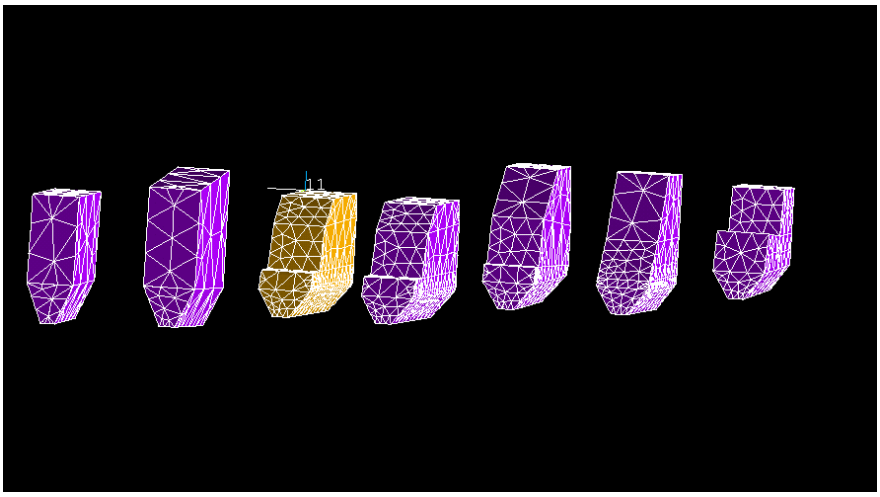


Figure 9. Spatial mesh of the 7 chambers. Chamber nº 5 is backfilled

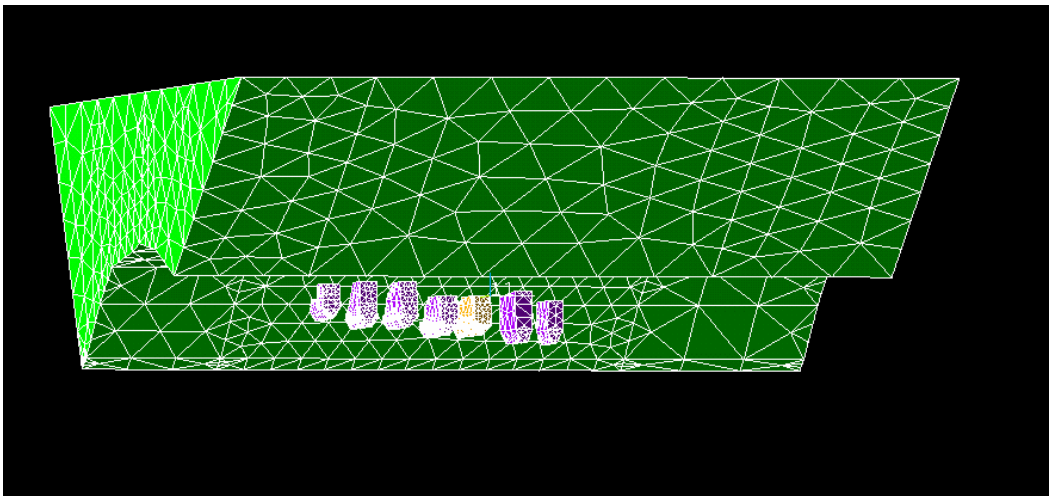


Figure 10. 3D geometrical model. Spatial mesh above the chambers

4.2. 3D modelling results

The results here presented are referred to the field of stresses and to the field of displacements, comparing the distributions obtained before and after the excavation of the chambers. These results of the 3D modelization point towards the viability to predict, in the first steps with the data available, the mine long-term geomechanical behaviour by means of numerical techniques.

Let see the results. In the next figures (Figures 11 and 12) it can be observed that there is a concentration of stresses (Pa unit) in the vicinity of the chambers, especially in the zone placed at the bottom of the chambers. It can be also observed that in the chamber nº 5, that has been filled, there is a stress relaxation. This relaxation is a simulation artifice and it is a consequence of the way in which the backfilling has been simulated.

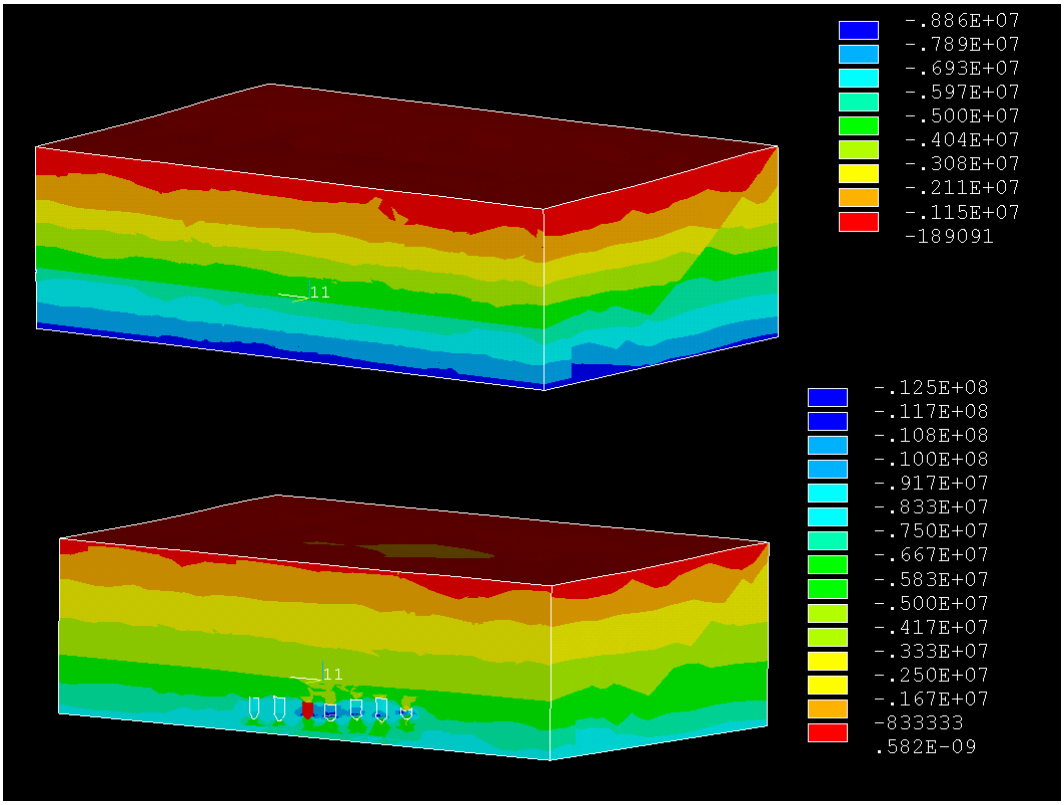


Figure 11. Stresses field before and after excavating chambers

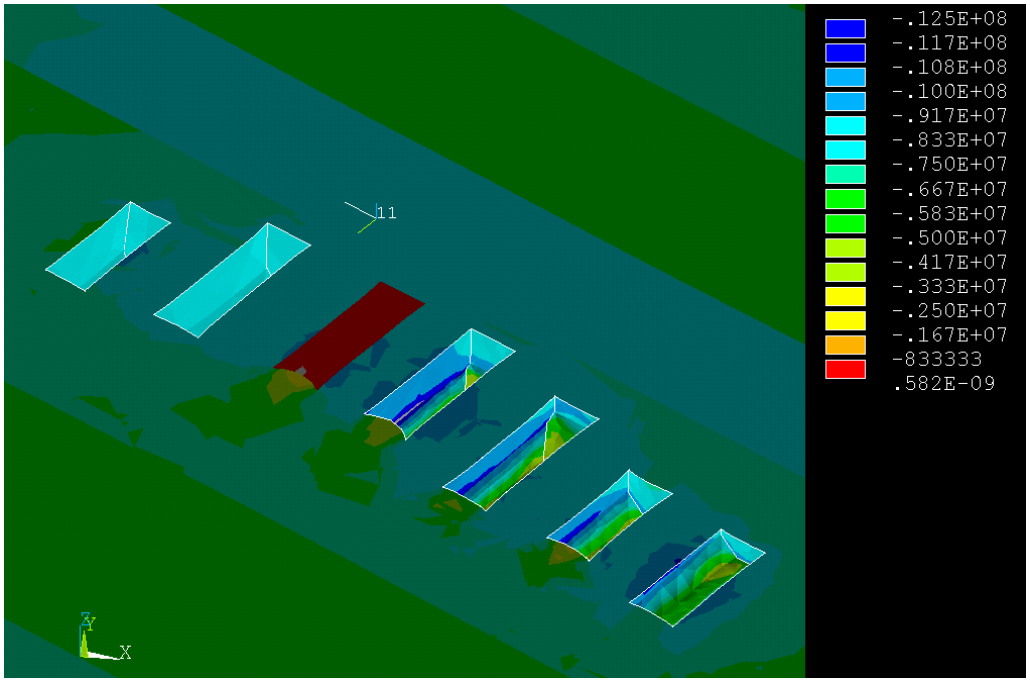


Figure 12. Detail of the stresses field at the chambers level

In respect of the displacement field (m unit), in the next figures (Figures 13, 14 and 15) it can be notice the effect of the chambers excavation in the surface of the domain modelized. The maximum vertical displacement observed, the maximum subsidence, is in the range of centimetres, around 5 cm. In the vicinity of the chambers the larger subsidence takes place in the upper zone, as it was expected.

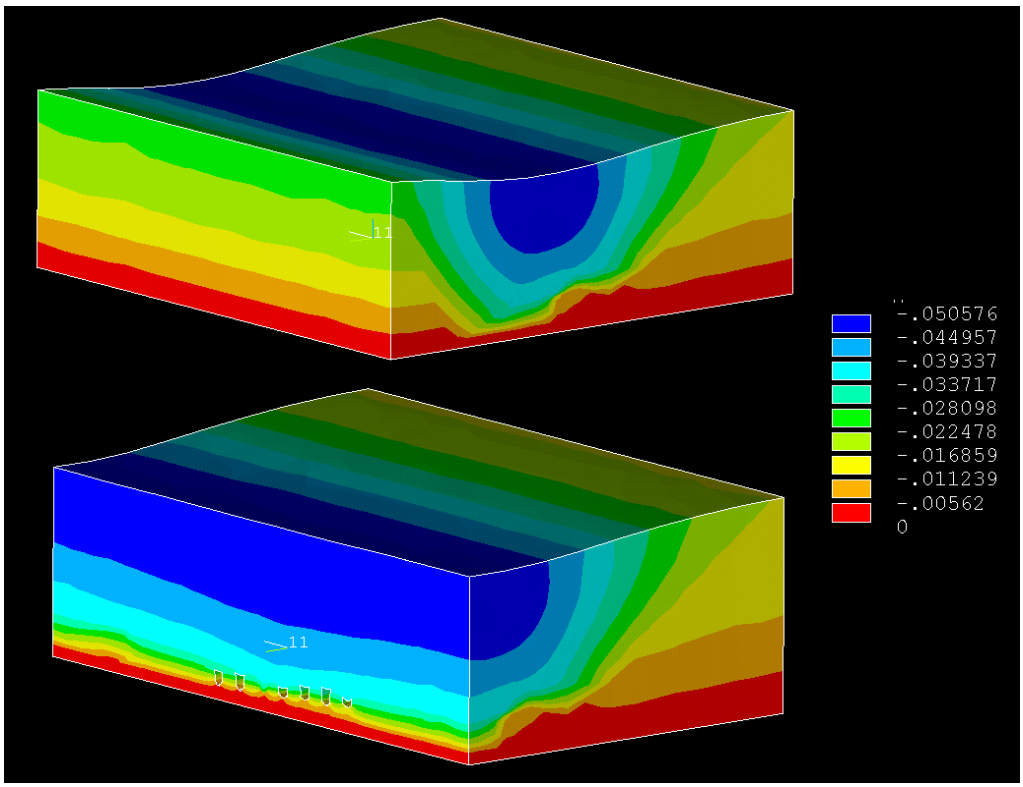


Figure 13. Displacement field before and after excavating chambers

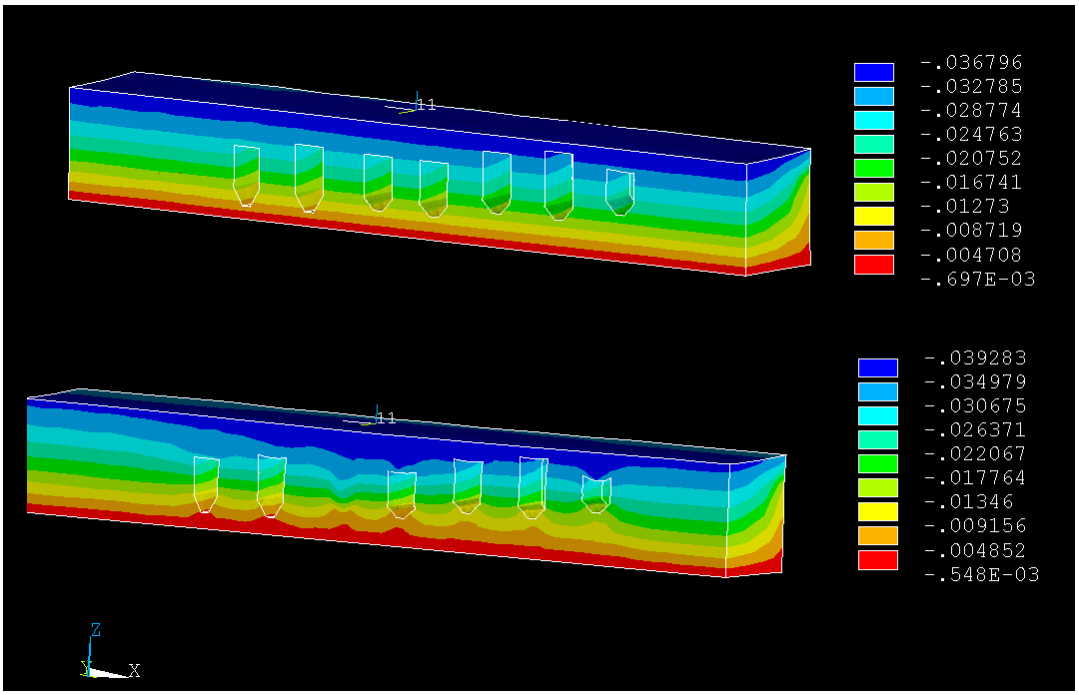


Figure 14. Detail of the displacement field before and after excavating chambers

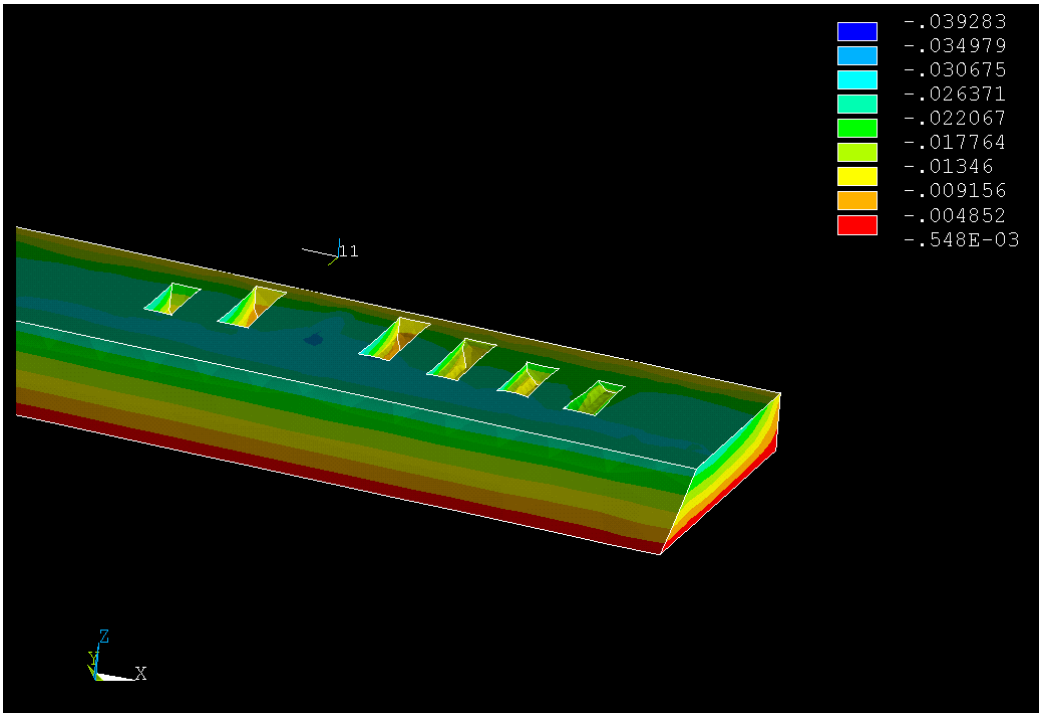


Figure 15. Detail of the displacement field at the chambers level. Chamber nº 5 is backfilled.

5. Conclusions

Numerical modelling is a good way to increase the knowledge of the behaviour of the Bodovalle Mine system here posed, and, therefore a good way to verify the viability of the different actions that can be established in each phase of the Bodovalle Mine Closure Project. This methodology permits develop long-term predictions of the system in terms of both loads or stresses distribution and displacements in zones in the vicinity of mined chambers.

Selecting a pilot zone, a representative underground mine sector, makes possible monitoring suitably the principal variables, stresses and the displacements, and also permits to model the area in an effective and efficient way. In both cases, the available information and its quality is the beginning point to get a realistic mine system knowledge and the possibility that the numerical results and predictions will be reliable.

Once the materials monitoring information were available, it would be necessary to define a constitutive model more realistic, a non lineal model that approximates in better way the geological materials behaviour. This monitoring information will also permit to calibrate the model. Moreover, the numerical model of the system will be able to represent sequential excavation and backfilling in order to reproduce adequately in each moment both the stresses and displacements fields.

A 3D model, as the one here presented, permits to integrate all the information available referred to the geometry of the chambers, distances between them, heterogeneity of lithologies distribution, etc. When the information of the pilot area flooding is available, also the coupled hydro-mechanical-chemical effect of water presence will be considered in the model. The backfilling modelization will be improved by means the use of “contact” finite elements.

6. References

Adams R., Younger P-L. (1999). *The application of Groundwater and Surface Water Modelling Systems to the Simulation of Groundwater Rebound in Abandoned Coalfields*. Proc. ModelCare99, 649-654

Dell’Angello L. N., Olgaard D. L. (1995). *Experimental deformation of fine-grained anhydrite : evidence for dislocation and diffusion creep*, J. of Geophysical Research, Vol. 100, 15425-15440.

INGEMISA (2004). *Proyecto de Clausura de la Mina Bodovalle.* Cliente: AGRUMINSA.

Peltzer, G., Rosen, P., Rogez, F., Hudnut K., (1996), *Postseismic rebound in fault step-overs caused by pore fluid flow*, Science, 273, 1202-1204.

Ramirez Oyanguren P. (1993). *Estudio geotécnico de la mina subterránea Bodovalle.* DERMOS/UPM. Informe para AGRUMINSA.

Ramirez Oyanguren P. (2000). *Análisis de estabilidad de la mina subterránea Bodovalle.* DERMOS/UPM. Informe para AGRUMINSA.

Ramirez Oyanguren P. (2001). *Estudios sobre fracturación en diversos sectores de la Mina Bodovalle.* DERMOS/UPM. Informe para AGRUMINSA.

Ramirez Oyanguren P., Laín R. (2003). *La stabilité des mines de fer de la région de Bilbao (España)*. Après-mine 2003. INPL. Nancy.

Szeki A., Potts E.L.J. (1971). *A Report on the Testing of Rock Samples from the Bodovalle Iron Ore Mine. (*Confidential Report for AGRUMINSA)

AN INTEGRATED CAVITY FILLING TECHNIQUE FOR ABANDONED UNDERGROUND ROOM AND PILLAR LIGNITE MINES AND UNDERGROUND QUARRIES

SAKAMOTO, Akio[1], YAMADA, Noritoshi[1], SUGIURA, Kenrou[1], HAMADA, Masanori[2]

[1] TOBISHIMA CONSTRUCTION COMPANY, Nagoya Branch, Japan.; Akio_Sakamoto@tobishima.co.jp; Noritoshi_Yamada@tobishima.co.jp; ,kenrou_sugiura@tobishima.co.jp

[2] WASEDA UNIVERSITY, Tokyo, Japan. ; hamada@waseda.jp

ABSTRACT: The authors involved with the cavity filling for some time in Tokai region, where the extensive extraction of lignite was carried by room-pillar technique until 1960s and they have developed their own integrated cavity filling technique. The cavity filling technique involves several fundamental steps such as exploration of dimensions of cavities, establishing the filling plant facilities, filling and monitoring. The non-harmfull industrial by-products are also utilized as filling materials. In this article, the authors describe their integrated cavity filling technique with some emphasis on the development of new cavity filling materials utilizing industrial by-products.

KEYWORDS: Abandoned mine, Lignite, Filling technique, Industrial by-products.

RESUME : Les auteurs sont impliqués dans le travaux du comblement des cavités dans la région de Tokai, où l'extraction de la lignite a été réalisée par la méthodes des chambres et piliers jusque dans les années 60. Les auteurs ont développé leur propre technique de comblement des cavités. Cette technique implique plusieurs étapes fondamentales telles que l'exploration des dimensions des cavités, la mise en place de l'usine à remblai, les opérations de remblaiement et de contrôle. Des sous-produits industriels sans danger ont été également utilisés comme produit de remblayage. Dans cet article, les auteurs décrivent leur technique de comblement des cavités en insistant sur le développement de nouveau matériaux de remblayage à partir de sous-produits industriels.

MOTS-CLEFS : Mine abandonnée, Lignite, Technique de remblayage, Sous-produits industriels

1. Introduction

The extraction of lignite using the room and pillar mining technique was extensive in various parts of Japan until 1960s. These mines are abandoned and some of these areas have become urbanized since then. Tokai region in Central Japan is a well-known example for such a case. It is now considered to fill these abandoned mines in urbanized areas because of great concerns on the risk of collapse and/or subsidence of ground above these abandoned mines. The authors involved with the cavity filling for some time in Tokai region (Sakamoto et al. 2005a, 2005b; Sugiura et al. 2003, 2005) and they have developed their own integrated cavity filling technique.

The selection and supply of filling materials are important items of the filling operations. Since a great cost involved with the filling material in Japan, the utilization of non-harmful industrial by-products (re-cycling materials) may reduce the cost as well as to ease the disposal problem of such by-products.

In this article, the authors describe their integrated cavity filling technique developed for abandoned lignite mines in Tokai region as well as abandoned underground quarries. Some emphasis is also

given to the development of new cavity filling materials utilizing non-harmful industrial by-products.

2. Integrated Cavity Filling Technique

The cavity filling technique involves several fundamental steps such as the exploration of dimensions of cavities to be filled, establishing the filling plant facilities, filling and constructional and environmental monitoring and surveying. All these steps must be performed with due considerations of environmental restrictions and regulations. Figure 1 shows the schematic flow-chart of the integrated cavity filling technique. The details of the filling technique are given in the following sub-sections.

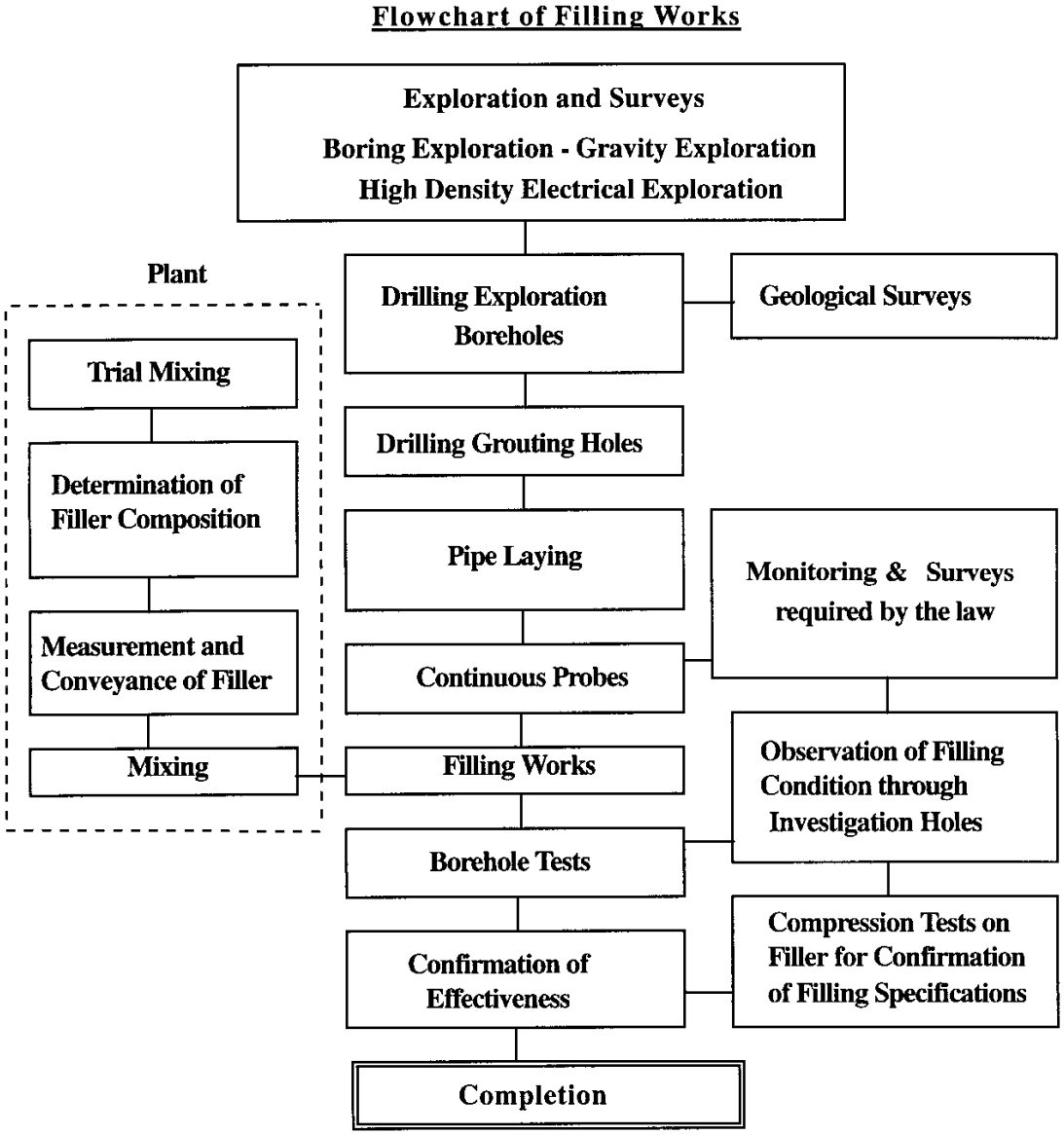


Figure 1. A schematic illustration of the integrated cavity filling technique.

2.1 Exploration and Surveys

Explorations and surveys involve the determination of layouts and spatial distributions of cavities to be filled and underground water conditions. Although some mining plans submitted to the authorities at the time of mining operations are available, these documents do not generally coincide with actual mining layouts. Furthermore, the geometry may change with partial degradation and collapses of pillars and roof layers in abandoned mines as time goes by.
In order to perform underground filling works effectively, the following exploration and surveys are conducted.

1) Site investigations for cavities to be filled, plant-yards, offices, etc.,
2) Investigations for pre-existing cracks in exterior walls, ground floors and elevations of nearby buildings and of the presence of wells,
3) Examination of groundwater and waters of rivers and wells,
4) Investigation of buried structures,
5) Collection and analysis of existent

- data on topography, strata, and geology,
- Treatises and documents issued by public offices, and
- Legwork.

The authors utilize several exploration techniques such as borings, gravity exploration, high-density electrical resistivity technique, sonar exploration technique depending upon the geological and environmental conditions. The most efficient method is the boring technique together with sonar exploration technique through drillholes. Figure 2 illustrates the sonar exploration technique utilizing a drillhole and its typical output. This system can be used under submerged underground environments for determining the geometry of cavities along the project routes.

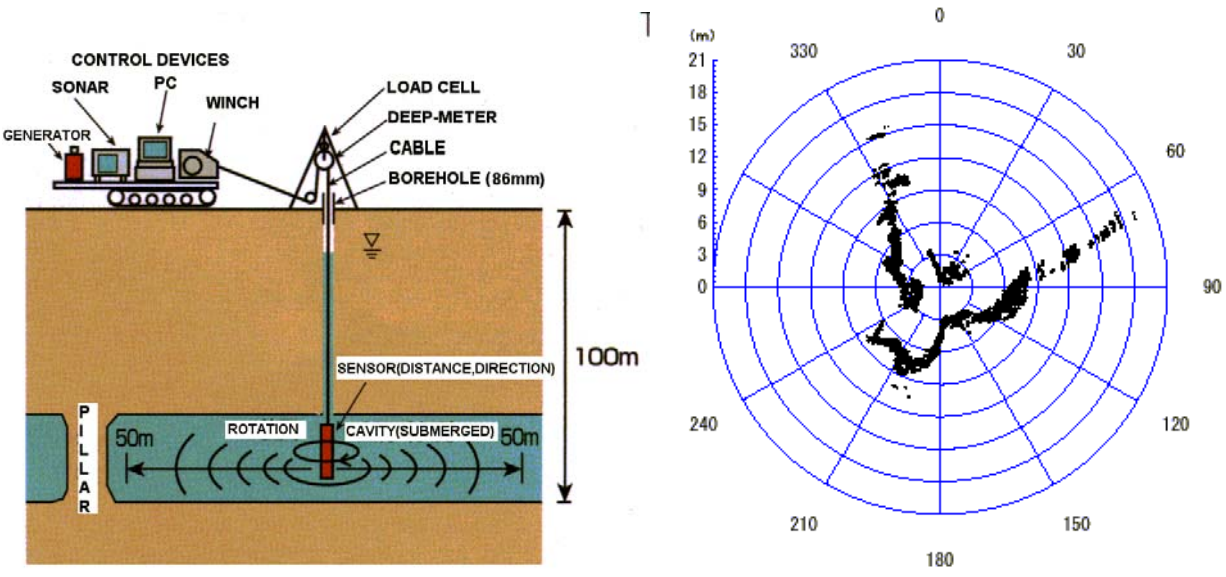


Figure 2. Sonar exploration technique and its application to abandoned lignite mine.

2.2 Design of Grouting and Monitoring Drillholes

The next step is to design the layout of drillholes for grouting and piping. Grouting drillholes (Figure 3) should be drilled at points about 0.5m away from exploration drillholes, where the

existence of caverns is confirmed. Although the spacing between drillholes depends upon the characteristics of filling material, an area with a radius of about 20m can be filled through a single grouting drillhole with use of filling materials used by the authors. Therefore the spacing distances between the grouting boreholes can be chosen as approximately 40m. However, if there are much deposits in caverns or the area is densely urbanized, the spacing of grouting boreholes should be less than 40m in order to control grouting pressure.

The water level in other grouting drillholes should be continuously monitored through probes after infusing water into some grouting boreholes. Through the monitoring of water level, it is possible to confirm if the drillholes are linked with each other. These probes also serve to know whether cavities are connected to each other or independent, and it is possible to determine the filling order. The ground settlement or uplift is also measured continuously through probes as shown in Figure 4.

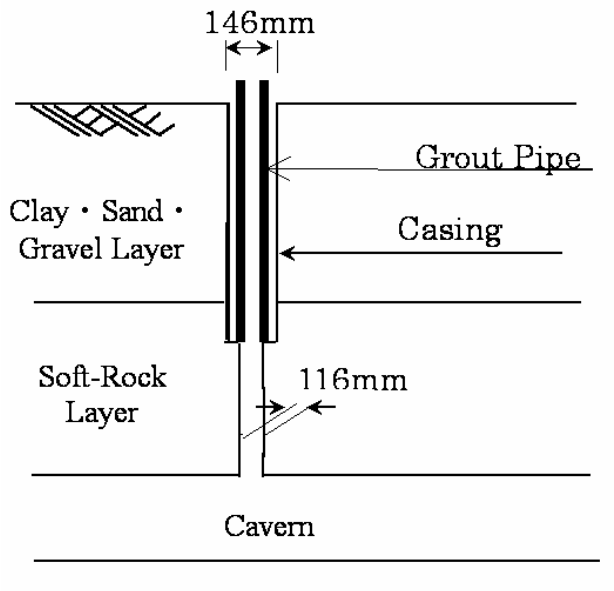


Figure 3. An illustration of dimensions of drillholes.



Figure 4. A monitoring probe for grouting.

2.3 Filling Plant

A typical filling plant basically consists of suppliers of scums, agitators, mixers and slurry pumps as illustrated in Figure 5 and Figure 6. The capacity of the plant depends upon the size of the site, the period of filling and the usable space. For example, a plant with a maximum mixing capacity of 300m^3 per day should have an area of about 2000m^2, through the consideration of the filling materials, which are transported into the plant by 10 to 20 dump trucks with 11 tonnages per day, and the materials, which should be stocked for a few days.

Mixers are used to mix the various scums before pumping filling material in cavities. Mixers can dissolve even viscous materials like clay scum in a short time and mix them easily. The maximum mixing capacity ranges between 20 and 550m^3 per day depending upon the plant size. However, the usual mixing capacity ranges between 10 and 300m^3 per day. The amount of filling per day also depends on cavern conditions.

Slurry pumps are used to pump the mixed slurry of filling material and they have the capability of conveying slurry with a density ranging between 1.3 and 1.5kg/cm^3 even though grouting drillholes may be about 1000m far away from the location of the pumps.

2.4 Underground Cavity Filling Procedure

Filling materials are pumped into cavities. The priority is given to cavities at lower elevation. During the filling operation, the utmost attention is paid to pressure rise in the grouting holes in order to prevent accidents such as spurts of filler or protuberances caused by overfilling. Any of the following monitoring items are used to infer the complete filling (Figure 7).

a. To confirm the slurry flow by filler sensors or tape measurement in connected cavities
b. The overflow from grouting holes changes from water to slurry
c. The water pressure rise in cavities

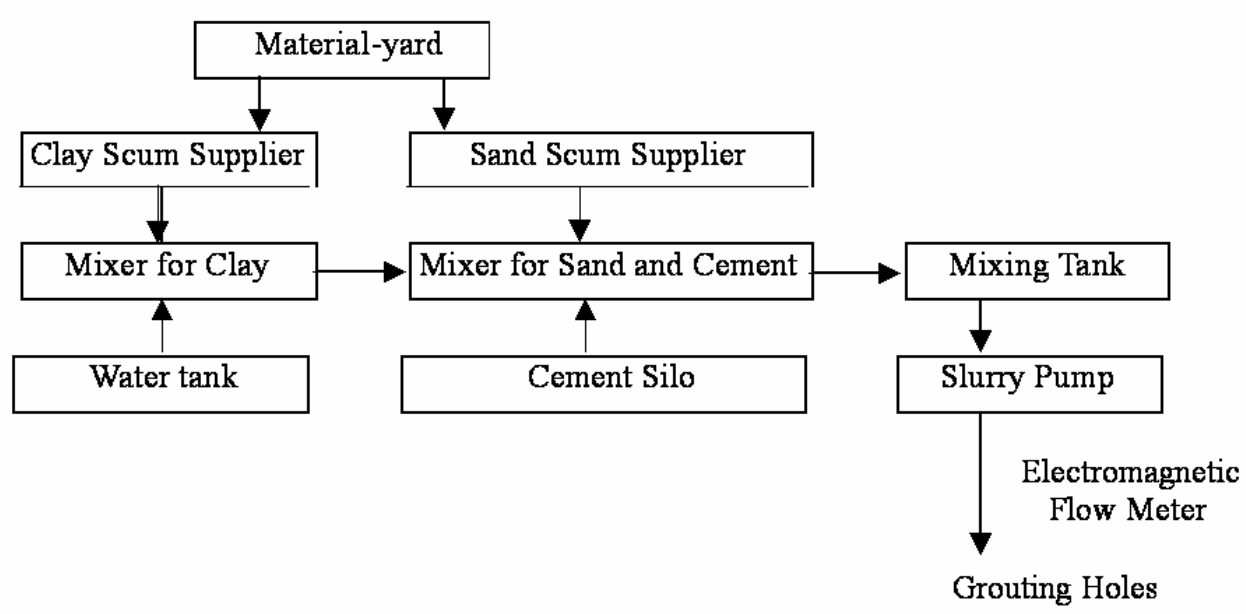


Figure 5. Flowchart of the filling plant.

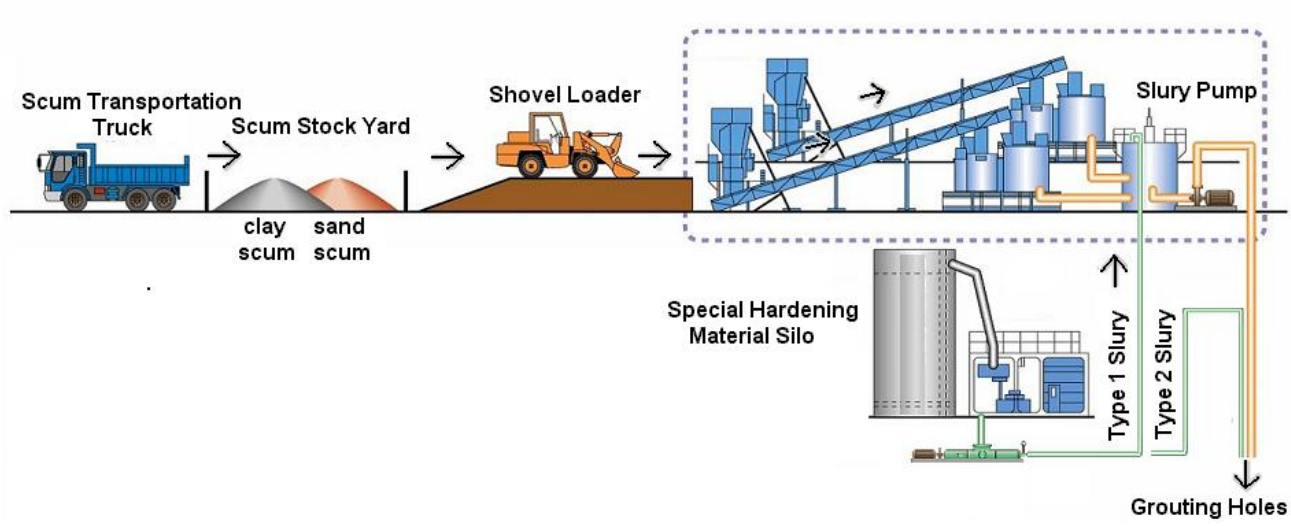


Figure 6. An illustration of the filling plant and filling operation.

2.5 Safety measures and Monitoring

The environmental monitoring involves the ground deformations due to filling operations, the solvents in underground water migration as well as groundwater levels. Protuberances caused by overfilling are prevented by monitoring the pore water pressure, the tape measurement of the slurry level in grouting boreholes, and monitored changes through tilt-meters and crack-meters on the ground.

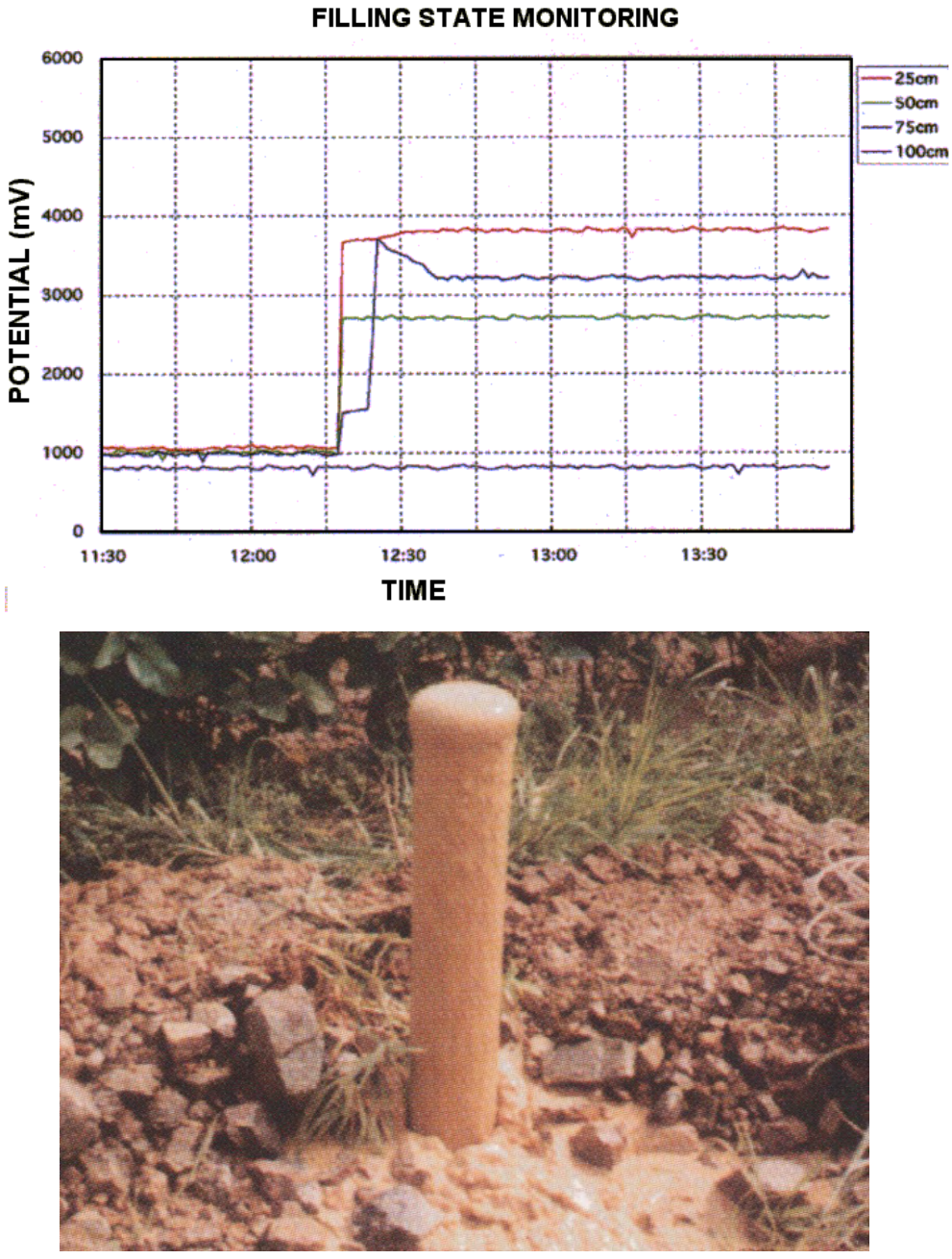


Figure 7. Monitoring result for cavity filling state and the inference from the overflow of wells.

The spurts of water from grouting boreholes after neutralizing are drained. The spurts of slurry with sand pumps and vacuum are pumped up, and the wastes are discarded after required processing.

pH value of ground water, solvents are monitored to assess the effects of grouting on the environmental conditions of ground water. To ensure the quality of grouting and filling state, several tests and measurements are carried as listed in Table 1.

Table 1. Criteria of Quality Control.

A List of Tests	Criteria of Quality Control
Flow Value	9 - 14 seconds
Bleeding Rate	3% or less than
Uniaxial Compressive Strength after 28 Days	Uniaxial strength cured samples in water should be 50 kPa or more Uniaxial strength from the boring cores should be 20 kPa or more
Analysis of Toxic Materials	Less than the statutory criteria

3. Characteristics of Filling Materials

The filling material used in the integrated system developed by the authors is initially in a slurry state and it solidifies with time after filling the cavities. The main materials of slurry are by-products produced at neighboring factories. Furthermore, the authors have also involved with developing new non-harmful cavity filling materials from various industrial by-products such as coal fly ash, filter press cake, paper sludge ash, sewage incineration ash and molten slag. The filling material basically consists of silicious clay-size and sandy-size scums, water and hardening agents such as cement, slaked lime, plaster. Figure 8 shows grainsize distributions of scums used as filling materials. Table 2 compares the mixture compositions (by weight per unit volume) of filling materials before 1975 and at present, used in Tokai Region.

Table 2. Example of mix proportion of filling materials.

(a) 1975 age

Clay scum (kg)	350
Sand scum (kg)	150
Plaster (kg)	50
Lime (kg)	30
Water (l)	776

(b) Present

Clay scum (kg)	400
Sand scum (kg)	200
Cement (kg)	50
Water (l)	759

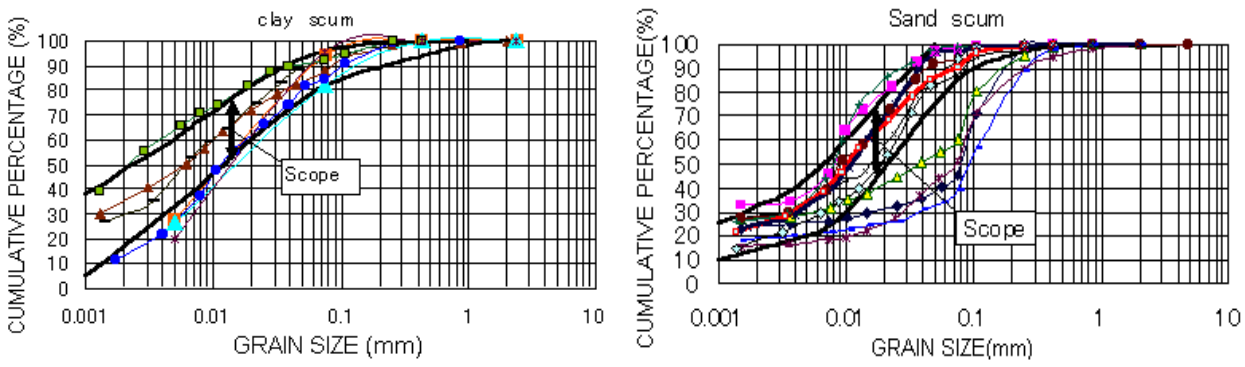


Figure 8. Grainsize distribution of scums.

The physical and mechanical characteristics of filling materials containing various industrial by-products (recycling materials) such as coal fly ash, filter press cake, paper sludge ash, sewage incineration ash and molten slag differ from each other. Various tests were carried out to measure the characteristics of such filling materials and results are given in Table 3.

Table 3. Physical and mechanical characteristics of various filling materials.

Kind of main materials		Quantity (kg/m^3)				Results of experiments		
Recycling materials	Control materials	Main material: Recycling material	Main material: Control material	Cement	Water	Funnel flow time (sec)	Bleeding ratio (%)	Compressi strength (kN/m^2)
Clay scum (1)	Sand scum	320	160	60	799	11.5	0.7	61
Clay scum (2)		420	0	60	822	11.2	0.65	63
Filter press cake (1)		450	0	60	815	10.9	0	84
Filter press cake (2)		600	0	90	749	10.2	0.34	75
Filter press cake with lime (3)		600	0	120	738	11.7	1.33	110
Filter press cake (4)		570	0	90	761	10.3	1.47	70
Filter press cake (5)		570	0	90	762	10.8	1.36	75
Coal fly ash (1)	Clay scum	300	300	60	725	10.6	2	143
Coal fly ash (2)	Clay scum	650	150	60	629	12.5	2.5	202
Paper sludge ash (1)		570	0	60	753	12.6	1.24	141
Paper sludge ash (2)		570	0	60	753	10.8	0.13	397
Surplus soil (1)		460	0	60	813	9.3	0.43	258
Surplus soil (2)		480	0	60	793	9.5	0	475
Sewage incineration ash (1)	Clay scum	175	325	120	789	10	0	104
Sewage incineration ash (2)	Clay scum	57	513	60	766	13.6	0.77	74
Sewage incineration ash (3)	Clay scum	114	456	120	744	13.5	0	440
Molten slag	Filter press cake	400	400	60	690	10.5	0.56	144
Shirasu	Filter press cake	420	420	60	632	10.1	1.78	340
Criteria of quality control						9 ~ 14	≦ 3	≧ 50

Table 4. Chemical analyses of filling materials utilizing some industrial by-products.

		Unit	Environmental standard for soil	Filling material using coal fly ash	Filling material using sewege incineration ash	Filling marerial using molten slag
Mixture composition	Recycling material	kg/m^3		112.5	114	400
	Control material	kg/m^3		337.5	456	400
	Cement	kg/m^3		60	60	60
Results of dissolving experiments	Cd	mg/L	0.01	< 0.001	< 0.001	< 0.001
	CN	mg/L	ND	ND	ND	ND
	Pb	mg/L	0.01	< 0.005	< 0.001	< 0.005
	Cr_{VI}	mg/L	0.05	< 0.01	< 0.005	< 0.04
	As	mg/L	0.01	< 0.005	< 0.001	< 0.005
	Hg	mg/L	0.0005	< 0.0005	< 0.00005	< 0.0005
	Cu	mg/kg	125	< 0.5	< 1	< 0.5
	B	mg/L	1	0.4	0.06	0.08
	Se	mg/L	0.01	< 0.002	< 0.003	< 0.002
	F	mg/L	0.8	0.6	< 0.01	0.4
Suitable				○	○	○

One of important aspects in utilizing industrial by-products as filling materials requires their chemical stability as well as not causing harmful effects on the environment. They should satisfy the criteria of regulations. The authors conducted some chemical analyses of filling materials utilizing various industrial by-products. Results are given in Table 4. As seen from the table, the utilization of such industrial by-products, the disposal of which is urgently needed, satisfy the environmental criteria set by the Environmental Ministry of Japan.

4. Limited Area Filling Method

When a limited area, which may arise during the construction of roadways, railways or new complex development over abandoned mines or existing underground cavities, has to be filled, it is necessary to fill only the area of concern. For this purpose, the authors extended their integrated filling technique to such circumstances and they called it as the limited area filling technique. In this technique, the outer walls are first constructed and the space between the outer walls is then filled (Figure 9). As a result, the physical and mechanical characteristics of filling materials and hardening processes would be different for outerwalls and inner space filling materials. Furthermore, the strength characteristics of the filling materials may be required to be different depending upon the constructional and environmental conditions. Table 5 gives mixture proportions for outer and inner filling materials for lower and higher strength requirements. The rest of procedures except the way of outer-wall construction would be the same as those described in the previous section.

Table 5. Examples of mix proportions of filling materials (Limited area type).

	Low strength type		High strength type	
	Outside	Inside	Outside	Inside
Clay scum (kg)	360	340	360	360
Sand scum (kg)	180	170	180	180
Cement (kg)	90	100	120	150
Silicate grout (kg)	48.8	12.2	48.8	24.4
Water (l)	724	763	715	725

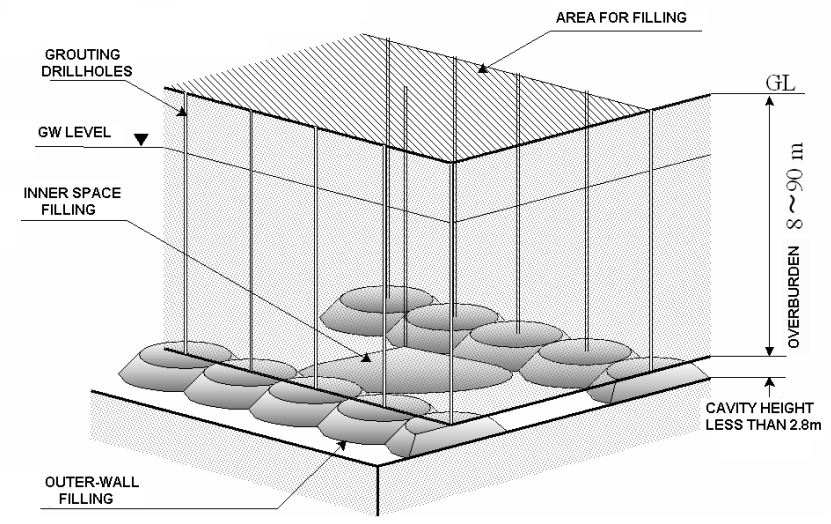


Figure 9: Illustration of limited area filling technique

5. Conclusions

The authors described an integrated cavity filling technique with its extension to the limited area filling with due considerations of construction conditions and environments. The technique integrates every stages involved in a cavity filling operation. The operation utilizes a filling material in a slurry state during transportation from the plant to the filling site and it solidifies with time after filling the cavities. The filling material is a mixture of the scum of by-products from a macadam plant, cement and water. Since the slurry has a high fluidity characteristic, it is possible to transport it to distant places in a cave from one filling hole. Furthermore, it is possible to homogenously to fill cavities even though they may have complicated geometries. In some particular circumstances, it may be necessary to fill only limited areas.

Acknowledgements

The authors sincerely thank Prof. Dr. Ömer AYDAN of Department of Marine Civil Engineering of Tokai University for his editorial help and advices during the preparation of this article. We also thank Emeritus Prof. Dr. Toshikazu KAWAMOTO of Nagoya University for his invaluable suggestions and encouragement for the development and application of this integrated cavity filling technique utilizing also recycling materials.

6. References

Sakamoto, A., Yamada, N., Sugiura, K., Kawamoto, T. (2005a). *Some examples of the cavity filling along transportation routes above abandoned room and pillar lignite mines in Tokai Region.* Post-Mining 2005, Nancy.

Sakamoto, A., Yamada, N., Iwaki, K., Kawamoto, T. (2005b). *Applicability of re-cycling materials to cavity filling materials.* Zairyo, Japan Society of Material Science (in print).

Sugiura, K. and Yamada, N. (2003). *On the completion of the cavity filling works of Tokai By-Pass Expressway (in Japanese).* Juten, Journal of Japan Grouting (Juten) Association. No.44, 8-17.

Sugiura, K., Ishiai, N., Wada, S. (2005). *Cavity filling in urbanized area: Changes and state of construction environment in cavity filling works (in Japanese).* Juten, Journal of Japan Grouting (Juten) Association. No.47, 8-13.

SOME EXAMPLES OF THE CAVITY FILLING ALONG TRANSPORTATION ROUTES ABOVE ABANDONED ROOM AND PILLAR LIGNITE MINES IN TOKAI REGION

SAKAMOTO, Akio[1], YAMADA, Noritoshi[1], SUGIURA, Kenrou[1], KAWAMOTO, Toshikazu[2]

[1] TOBISHIMA CONSTRUCTION COMPANY, Nagoya Branch, Japan.; Akio_Sakamoto@tobishima.co.jp; Noritoshi_Yamada@tobishima.co.jp; ,kenrou_sugiura@tobishima.co.jp

[2] NAGOYA UNIVERSITY, Emeritus Professor, Nagoya, Japan. ; choman@poem.ocn.ne.jp

ABSTRACT: The authors describe the applications of the integrated cavity filling technique to abandoned lignite mines in Tokai region. These abandoned lignite mines were in operation until 1960s and the routes of Tokai By-Pass Expressway and the linear motor car railway line for Aichi Exposition pass over these abandoned mines. Since the size of abandoned mines were much larger than the route of the expressway and the elevated monorail, limited areas relevant to their stability had to be only filled. This article describe the details of cavity filling operations in these two projects, which may be some valuable examples for assessing the methods how to deal problems associated with mine closures in long term.

KEYWORDS: Abandoned mine, Lignite, Filling technique, Mitake, Nagakute

RESUME : Les auteurs décrivent les applications d'une technique de remblayage des cavités aux mines de lignite abandonnées dans la région de Tokai. Ces mines abandonnées ont été exploitées jusqu'à dans les années 60. L'autoroute et la ligne ferroviaire construites pour accéder à l'Exposition d'Aichi sont ensuite passées à l'aplomb de ces mines abandonnées. La taille des mines abandonnées étaient beaucoup plus grande que l'itinéraire de l'autoroute et du monorail, seuls des secteurs d'extension relativement limitée ont dû être remblayé. Cet article décrit les détails des opérations de remblayage des cavités dans ces deux projets. Ceci peut être considéré comme des exemples instructifs de traitement de problèmes liés aux fermetures de mine dans le long terme.

MOTS-CLEFS : Mine abandonnée, Lignite, Technique de remblayage, Mitake, Nagakute

1. Introduction

The extraction of lignite using room and pillar mining technique was widespread in Tokai region of Central Japan until 1960s (Figure 1). These mines are abandoned since then and some of these areas have become urbanized. Furthermore, some transportation routes such as Tokai by-pass expressway and Aichi Exposition linear motor car line pass over the abandoned lignite mines. Since the areas of old-mining operations are much larger than those of the routes, it was necessary to fill limited areas required by these respective projects.

The authors involved with cavity filling for some time in Tokai region and they have developed their own integrated cavity filling technique (i.e. Sugiura & Yamada, 2003; Sugiura et al., 2005; Sakamoto et al. 2005a, 2005b). This technique was also further advanced to carry out cavity filling operations on limited areas required by a given project. The integrated cavity filling technique for a limited area involves several fundamental steps such as the exploration of dimensions of cavities, establishing the filling plant facilities, building outer-walls and filling of required space and monitoring. All these steps must be performed with due considerations of environmental restrictions and regulations.

In this article, the authors describe two specific examples of cavity filling operations in Tokai region of the Central Japan. The details of these two cavity-filling operations may be some valuable examples for assessing the methods to deal problems associated with mine closures in long term.

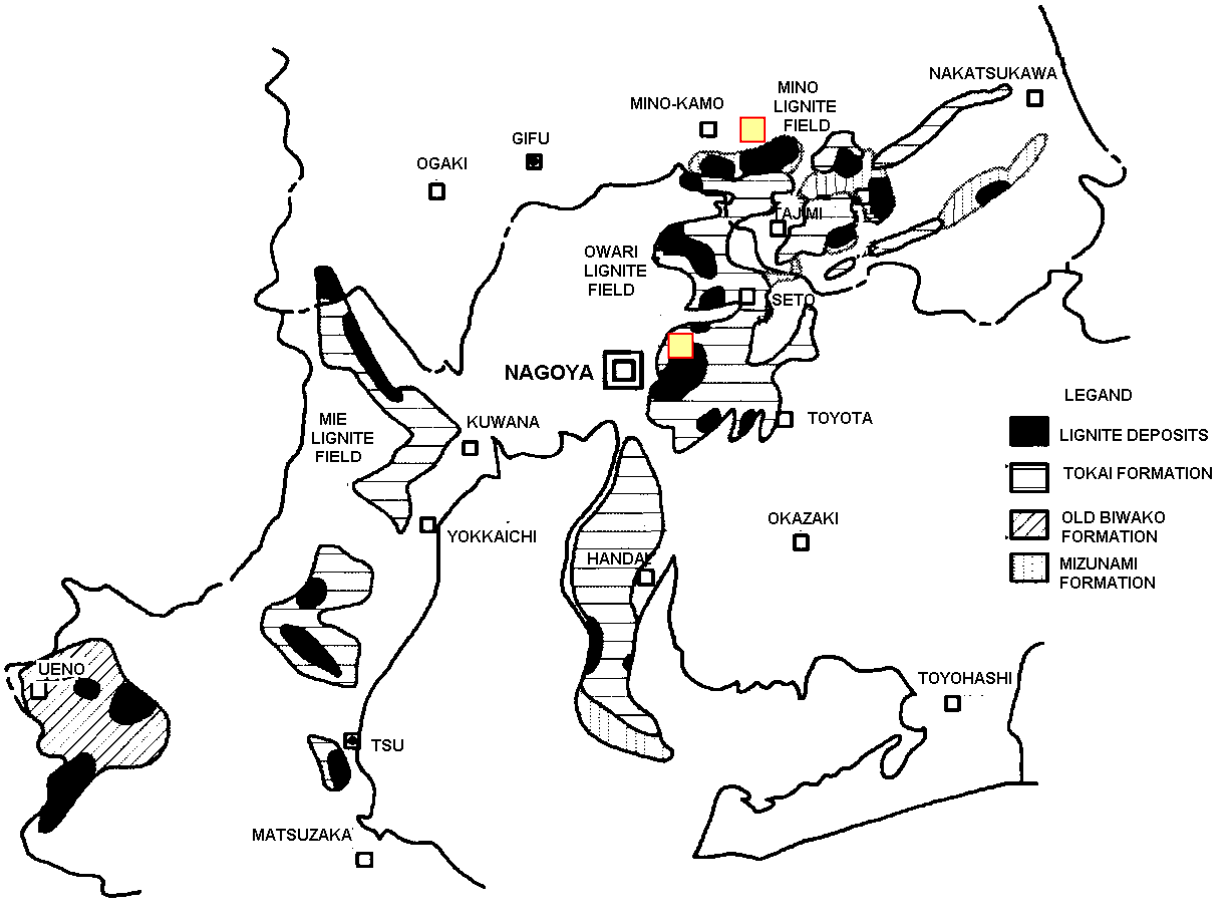


Figure 1. Lignite deposits in Tokai region and locations of sites.

2. Outline of Limited Area Filling Technique

When the filling of abandoned mines is necessary for a limited area, the outerwalls are first constructed and the space between the outerwalls is then filled (Figure 2). The outerwall has higher strength and solidifies much more rapidly. These outerwalls act as barriers for lower strength inner space filling material while it solidifies. All these operations utilize some constructional and environmental monitoring. The constructional monitoring is associated with controlling the filling state of cavities and maintaining the quality of filling while environmental monitoring involves the ground deformations due to filling operations, the variation of characteristics of underground water as well as its levels.

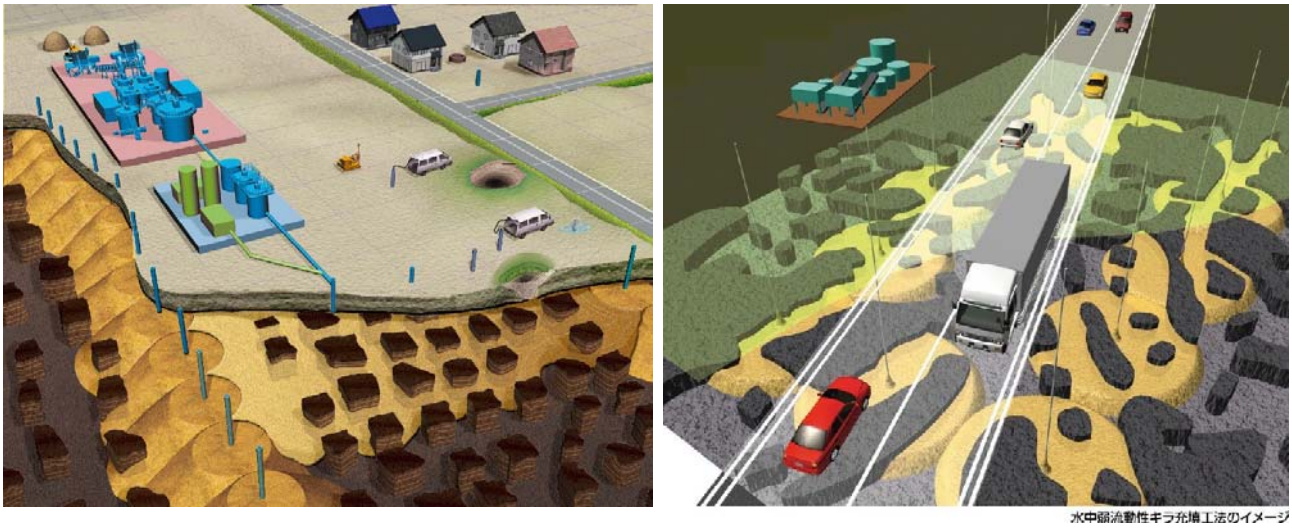
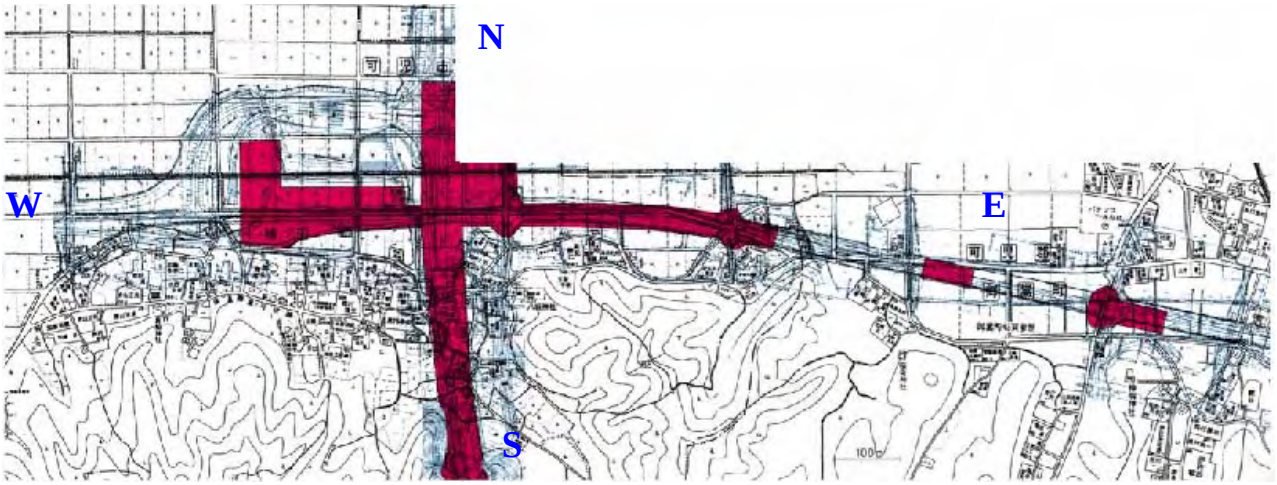


Figure 2. Illustration of actual cavity filling operations of limited areas.

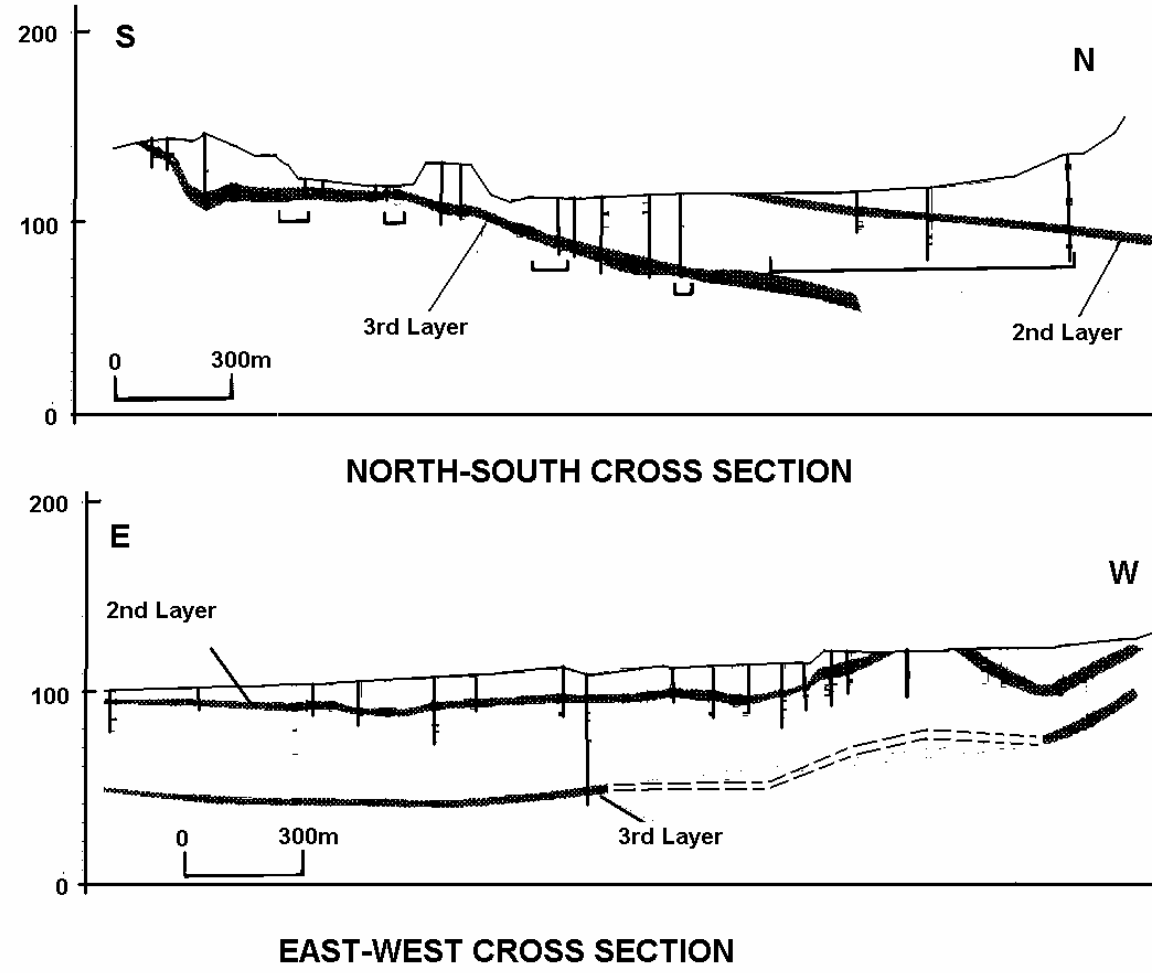
3. Application to Tokai By-Pass Expressway

The first example is associated with the cavity filling of abandoned lignite mines in Mitake town and Kani city at an interchange on the route of Tokai By-Pass Expressway. A plan view and geological cross sections are shown in Figure 3. The N-S section coincides with the alignment of the Nagoya-bound Expressway while E-W section is aligned with the local roadway. Figure 4(a) shows an artist illustration of the interchange and filling works. In the same figure, a part of the abandoned lignite mine, which was uncovered, is also shown (Figure 4(b)). One of the challenging problems associated with cavity filling operations is how to determine the exact geometry of cavities to be filled. Although some mining plans submitted to the authorities at the time of mining operations are generally available, these documents do not coincide with actual mining layouts. Furthermore, the geometry may change with partial degradation and collapses of pillars and roof layers. Figure 5 shows the distribution of cavities and pillars beneath the interchange area of the Tokai By-Pass Expressway obtained from sonar exploration method through drillholes, which was carried out as an experimental filling operation.

Since a limited area has to be filled, the limited area filling technique is employed. The composition of the filling materials for outerwalls and inner space differ from each other. Thus, their strengths are also different from each other (Table 1). Furthermore, the composition of the filling materials differed depending upon the characteristics of the superstructure. Higher strength filling materials are used beneath the foundations of viaducts of the expressway. Besides clay and sand scums, the amount and type of hardening materials differed according to the required strength characteristics of the filled space in relation to the type of superstructures of the expressway. The diameter of drillholes for grouting was 100mm and the average spacing of the drillholes for grouting was 15m. The volume of experimental filling operation was 2,155m^3. However, the total volume of experimental filling operation was 81,000m^3Figure 6 shows the areal distribution of outerwall filling and inner space filling at this particular location.

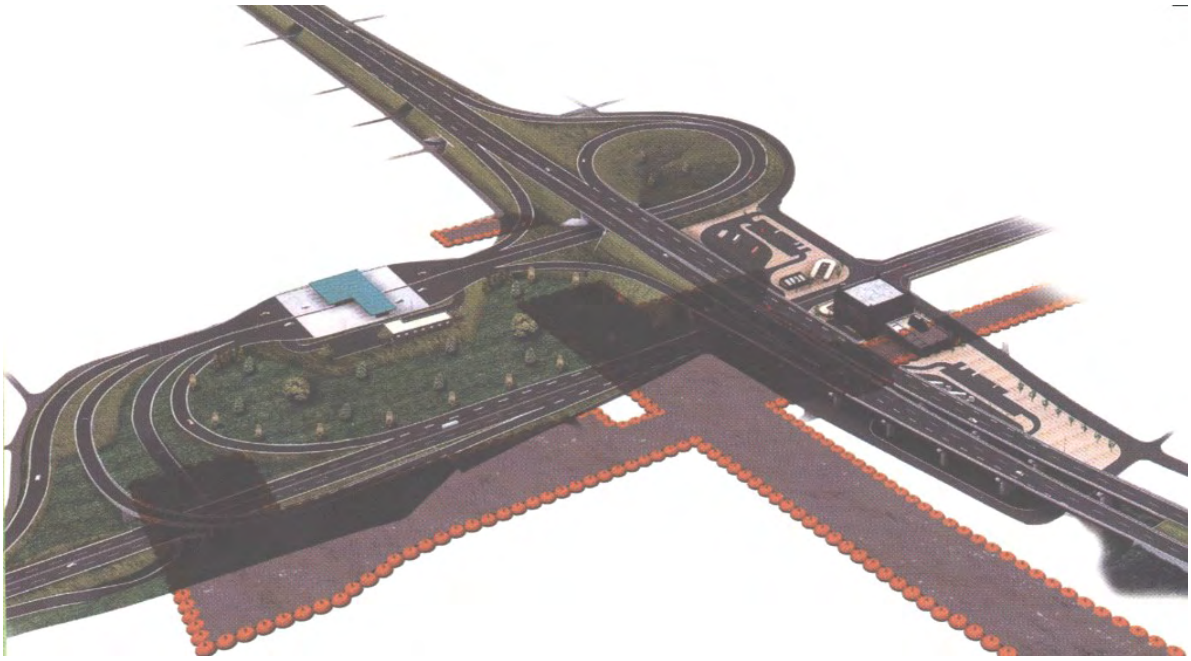


(a) Plan view



(b) Cross sections

Figure 3. Geological cross sections at the vicinity of the interchange of Tokai By-Pass Expressway.



(a) Artist illustration of cavity filling and constructed Interchange at Kani City



(b) Exposed abandoned lignite mine

Figure 4. Tokai Expressway passing through abandoned mines in Mitake-Kani area.



Figure 5. The distribution of pillars and cavities obtained from sonar exploration technique.

Table 1. Composition of mixtures of filling materials depending upon superstructures.

Materials	Beneath Embankment Low strength (>100kPa)		Beneath Viaduct Foundations High strength (>400kPa)	
	Outerwall	Inner Space	Outerwall	Inner Space
Clay scum (kgf)	360	340	360	360
Sand scum (kgf)	180	170	180	180
Special hardening agent (kgf)	90	100	120	150
Special Sodium Silica (kgf)	48.8	12.2	48.8	24.4
Water (kgf)	724	763	715	725

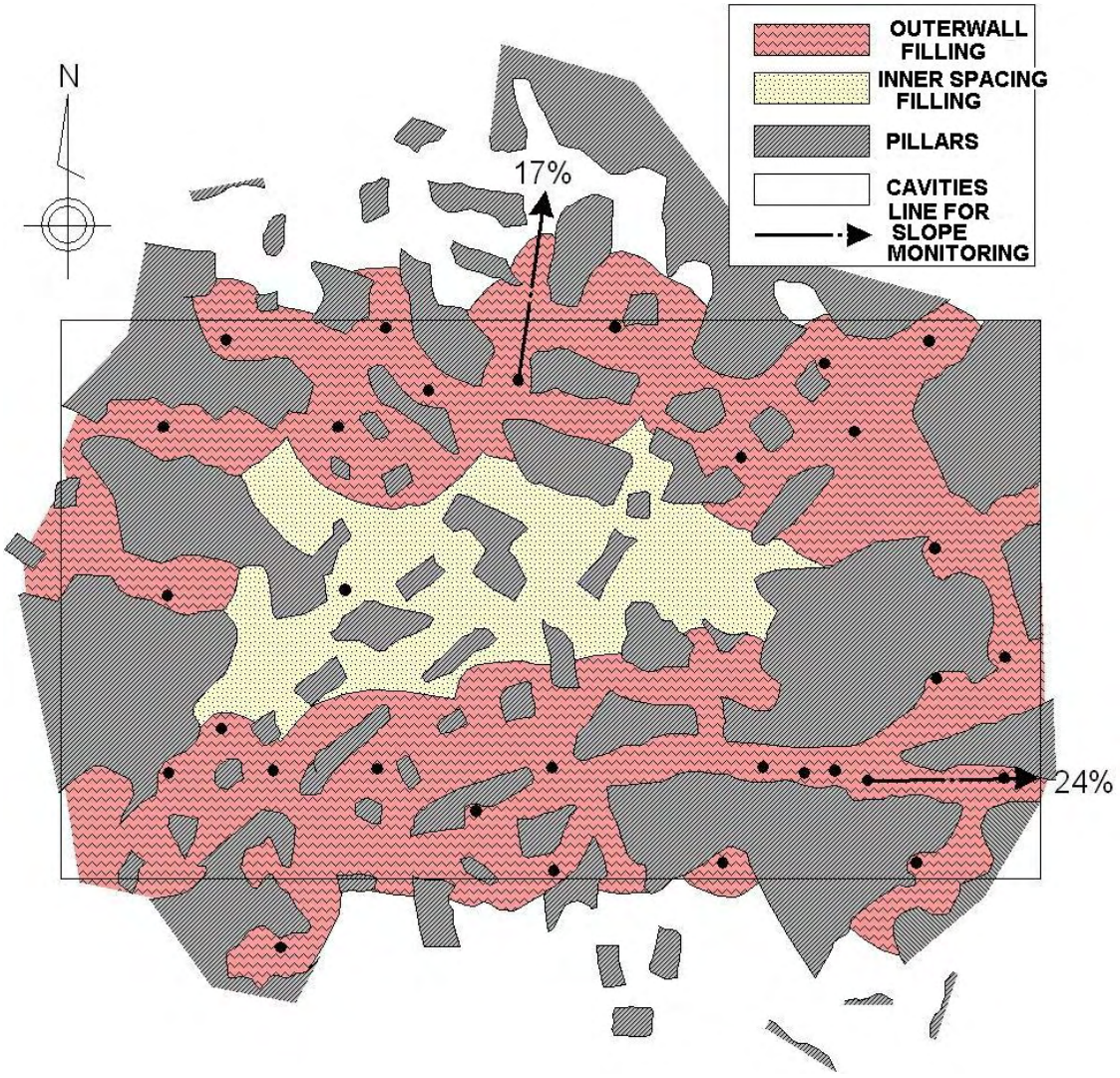


Figure 6. Distribution of outerwall and inner space filling.

Various Monitoring was carried out for measuring ground tilting, outerwall gradient, filling state and quality control of filling materials and ground water characteristics during the filling work.

4. Application to Aichi Exposition Linear Motor Car Railway Project

The second example is associated with the route of Aichi Exposition linear motor car transportation system in Nagakute town of Aichi Prefecture, Japan. The railway passes over Nagakute lignite deposits, which were extracted until 1950s (Figure 7). The railway is elevated through viaducts and the lignite seams dips west. The length of the line having cavities beneath is about 1km and the depth of cavities ranges between 6 and 57m. The average height of the extracted lignite seam was about 1m and tributary area ratio was 65%.

Since Aichi Exposition linear motor car route passes through a highly urbanized area, the construction space is very limited. The total volume of grouting was 19000m^3 and 990 drillholes (total length of drillholes 35.7km) were bored. The drillholes for outerwall and inner space had to be bored from the central pavement of the existing roadway (Figures 8 and 9). The filling materials

denoted as type A and type B are prepared separately at two plants and they were mixed just before grouting into the drillholes. Their compositions are given in Table 2. The distance between the plants and grouting locations was up to 630m.

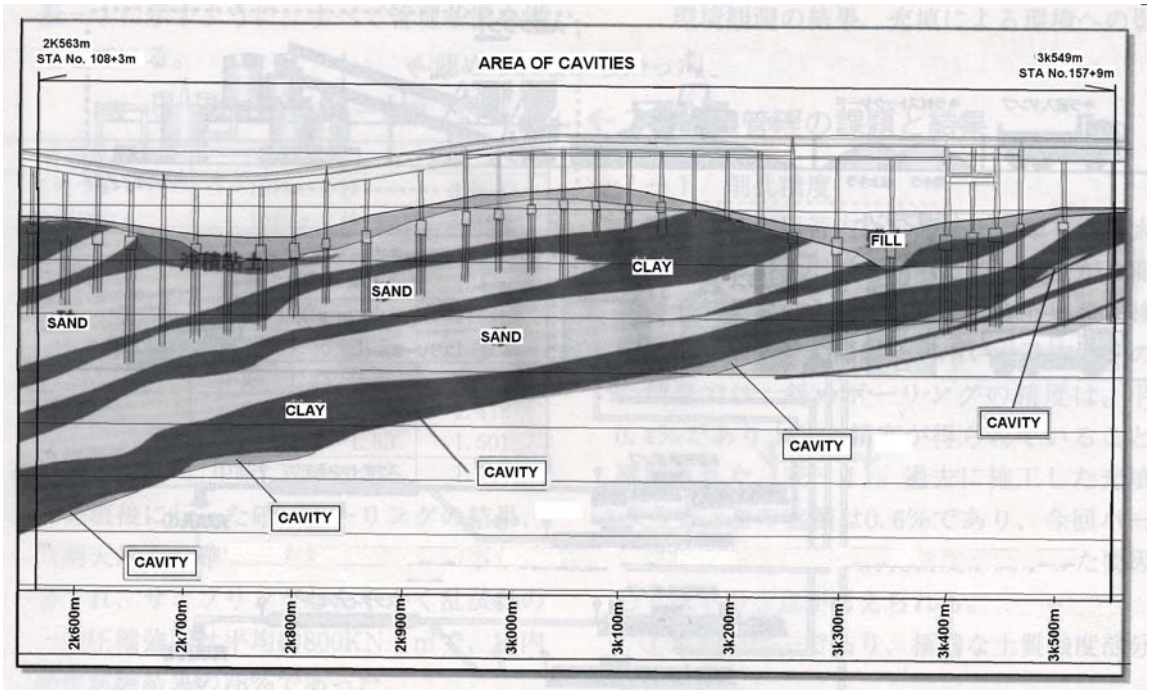


Figure 7. Geological cross section and locations of viaducts of the monorail and cavities.

Table 2. Composition of filling materials (unit kgf/m^3).

Filling Materials	Required Strength (kPa)	Type A Filling Material (Plant A)				Type B Filling Material (Plant B)		
		Clay Scum	Sand Scum	Special Sodium Silica	Water	Special Hardening Agent	Water	Retarder
Outerwalls	400	360	180	48.8	595	120	120	C x 0.5%
Inner space	400	360	180	24.4	575	150	150	C x 0.5%

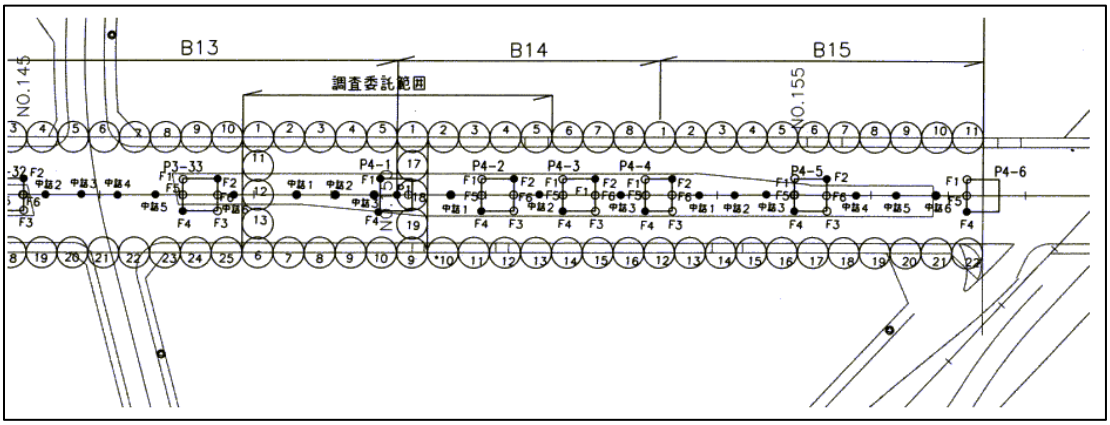


Figure 8. Planned layout of drillholes for outerwalls and inner space filling works.

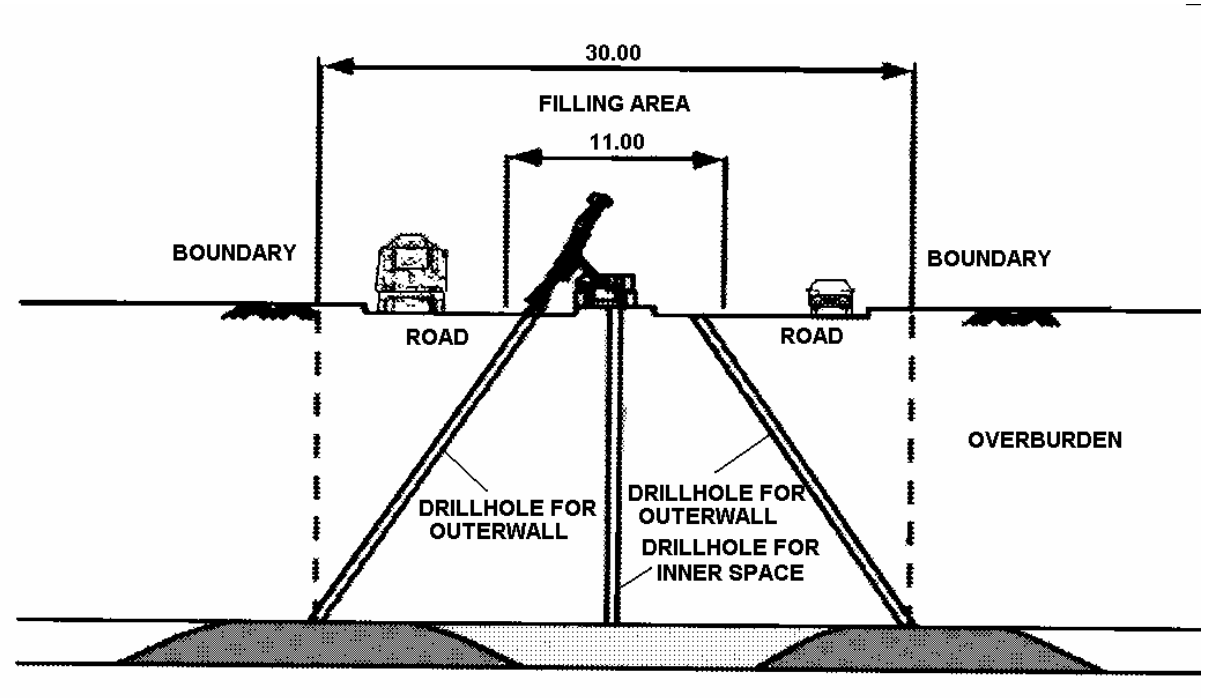


Figure 9. An illustration of how drillholes for outerwalls and inner space filling works are bored.

Deviation of drillholes, grouting performance, ground tilting, outerwall gradient, filling state and quality control of filling materials and ground water characteristics were monitored. Figure 10 shows some of the results.

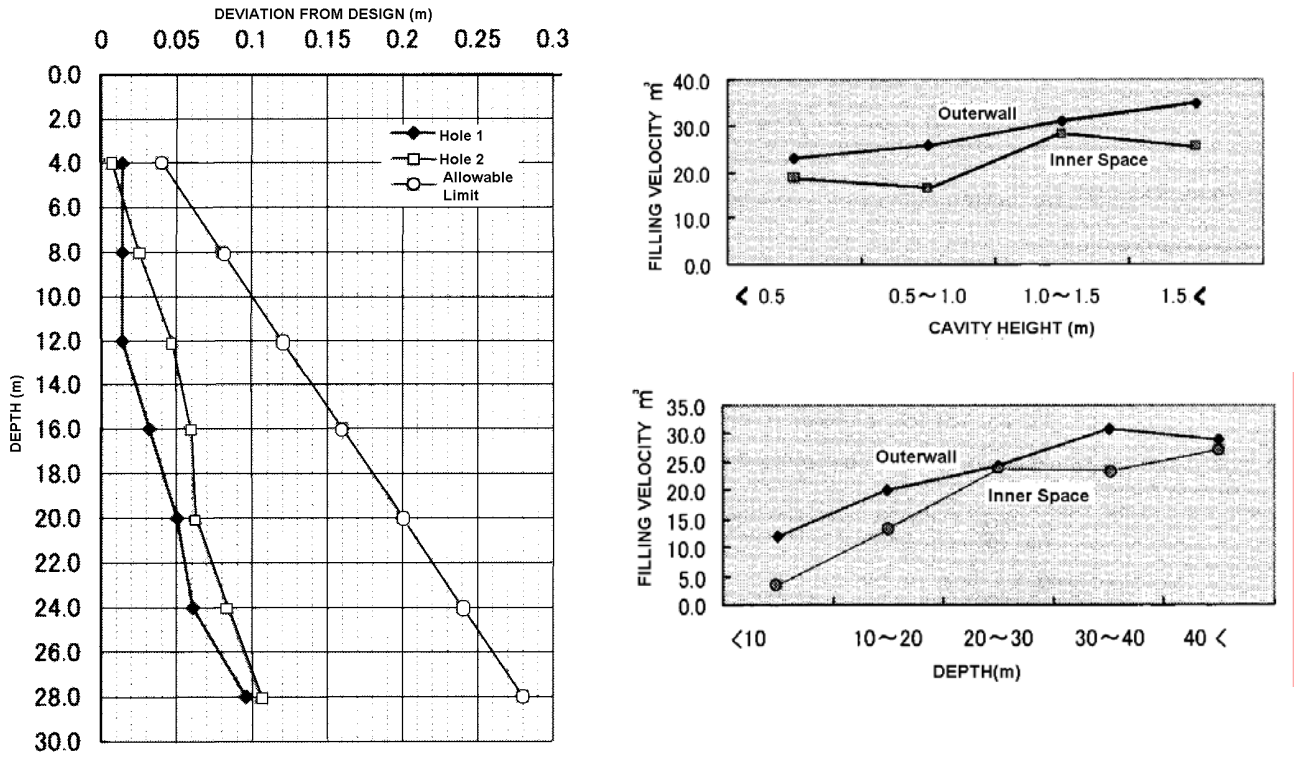


Figure 10. Monitoring results of some parameters.

6. Conclusions

The authors presented some applications of an integrated cavity filling technique with its extension to the limited area filling to the filling of abandoned lignite mines beneath an expressway and a railway in Tokai Region of Japan. The details of these two cavity-filling operations may be some valuable examples for assessing the methods how to deal problems associated with mine closures in long term.

Acknowledgements

The authors sincerely thank Prof. Dr. Ömer AYDAN of Department of Marine Civil Engineering of Tokai University for his editorial help and advices during the preparation of this article. We also thank Prof. Dr. Masanori HAMADA of Waseda University for his invaluable advices.

7. References

Sakamoto, A., Yamada, N., Sugiura, L., Hamada, M. (2005a). *An integrated cavity filling technique for abandoned underground room and pillar lignite mines and underground quarries.* Post-Mining 2005, Nancy.

Sakamoto, A., Yamada, N., Iwaki, K., Kawamoto, T. (2005b). *Applicability of re-cycling materials to cavity filling materials.* Zairyo, Japan Society of Material Science (in print).

Sugiura, K. and Yamada, N. (2003). *On the completion of the cavity filling works of Tokai By-Pass Expressway (in Japanese).* Juten, Journal of Japan Grouting (Juten) Association. No.44, 8-17.

Sugiura, K., Ishiai, N., Wada, S. (2005). *Cavity filling in urbanized area: Changes and state of construction environment in cavity filling works (in Japanese).* Juten, Journal of Japan Grouting (Juten) Association. No.47, 8-13.

SAFETY ASSESSMENT FOR THE LAND SURFACE IN THE VICINITY OF THE POTASH SHAFT NEUSTAßFURT VI

SALZER Klaus, MINKLEY Wolfgang

IFG INSTITUT FÜR GEBIRGSMECHANIK GMBH, Friederikenstraße 60, D-04279 Leipzig, Germany.; klaus.salzer@ifg-leipzig.de; wolfgang.minkley@ifg-leipzig.de

ABSTRACT: In the 70's the former potash mine Neustaßfurt VI/VII located in the northeast flank of the Staßfurt Salt Anticline was flooded initiating sinkholes around the shaft Neustaßfurt VI until today. At the end of the 90's a safety assessment was desired to estimate the risk for the land surface. Underground exploration found a leaching cavern in the vicinity of the shaft. To assess the stability of this cavern and of the shaft itself a comprehensive rock mechanical study based on laboratory tests and numerical investigations with 3DEC *was performed. The calculations show that the overburden of the leaching cavern remains stable but the shaft stability and its surrounding is threatened when the shaft lining will be destroyed.*

KEYWORDS: Safety Assessment, Flooding, Potash Mine, Sinkhole.

RESUME : Dans les années 1970, la mine de potasse de Neustassfurt V//VI, située au flanc nord-est de l'anticlinal salin de Stassfurt, a été ennoyée. Cette ennoyage a eu comme conséquence, jusqu'aujourd'hui, l'initiation de dolines d'effondrement autour du puits de Neustassfurt VI. Vers la fin des années 1990, une expertise de sécurité a été demandée pour apprécier les risques d'instabilité de surface. Des sondages, réalisés à cet effet, ont révélé une caverne de lixiviation au voisinage du puits. Pour apprécier la stabilité de cette caverne et du puits lui-même, une étude de mécanique des roches a été conduite à partir d'essais de laboratoire et d'investigations numériques avec le logiciel 3DEC. Les simulations montrent que les morts-terrains restent consistants, tandis que la consistance du puits et de son entourage seront mis en danger en cas de destruction du revêtement du puits.

MOTS-CLEFS : Expertise de sécurité, Ennoyage, Mine de potasse, Doline d'effondrement.

1. Introduction

The origin of the worldwide potash mining is located at the Staßfurt region. This region suffers from the post mining consequences most of all other potash mining regions in Germany. The potash mining mostly at carnallitite began in 1858 underneath the downtown of Staßfurt in the southwestern flank of the Staßfurt Salt Anticline.

Due to some rockbursts fresh water invaded in the mines and even at the beginning of the 20th century the potash mines in the southwest flank of the Staßfurt Salt Anticline at the area of the town of Staßfurt had been flooded and three sinkholes had been arisen. Figure 1 gives an overview about the mining induced surface damage at the area of the Staßfurt Salt Anticline. The filled dark circles indicate the locations of the flooding-induced sink-holes. Figure 3 shows a characteristic geological profile across the Staßfurt Anticline and the potash mining in its flank.

Between September 5th 1973 and April 27th 1979 the potash mine Neustaßfurt VI/VII located in the northeast flank of the Staßfurt Salt Anticline was flooded with partial saturated salt brine as a preventive measure to avoid surface damage in the Staßfurt town. Figure 1 shows the situation of

the potash mine Neustaßfurt VI/VII and mining induced surface damage at the area of the Staßfurt Salt Anticline. Due to its high solubility the carnallitic material in the mine was extensively leached off respectively destroyed. These processes resulted in the occurrence of a large sinkhole (surface caving) in the area between the shafts Neustaßfurt VI and VII. Figure 2 shows the large sinkhole in the year 1975 immediately after its occurrence. The sinkhole had a diameter of about 100 m.

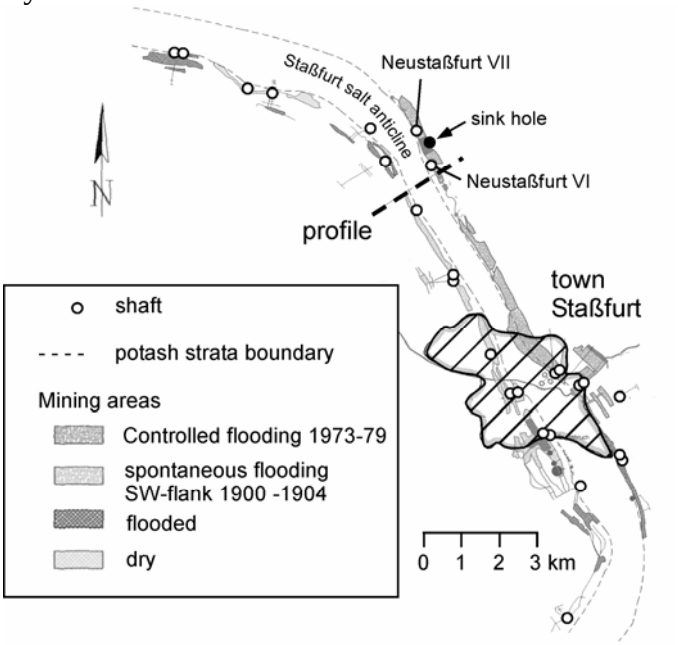


Figure 1. Mining and mining-induced surface damage at the area of the Staßfurt Salt Anticline.

In the following years the large sinkhole had been increasing and in 1998 in the vicinity of the large sinkhole three smaller sinkholes arose. This temporal evolution implies that in the carnallitic parts of the safety pillar around the shaft Neustaßfurt VI leaching and destruction processes took place until today. Therefore, the mining authority desired to perform a new safety assessment for the land surface around the shaft Neustaßfurt VI, where an industrial park is located.

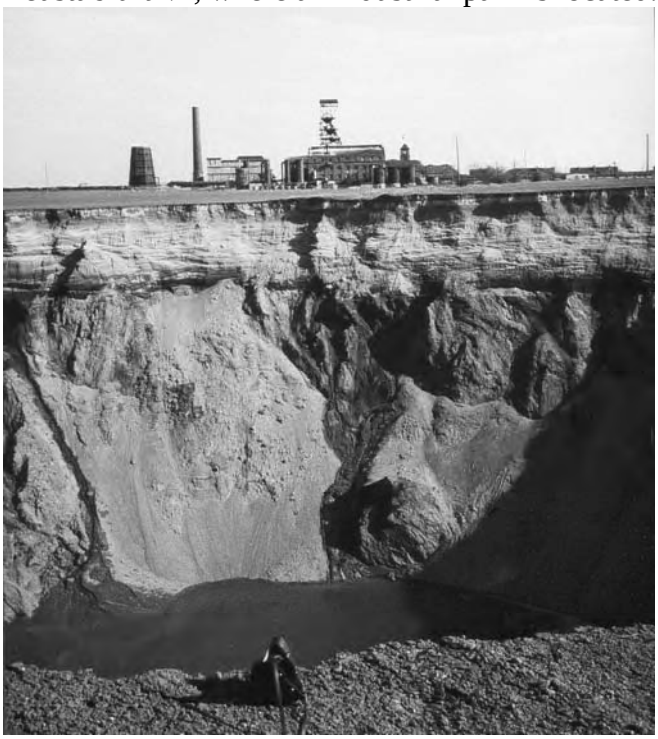


Figure 2. Sinkhole in the area between the shafts Neustaßfurt VI and VII in the year 1975 immediately after its occurrence.

A geological SW-NE profile across the Staßfurt Salt Anticline and the shaft Neustaßfurt VI is given in Figure 3. As first estimate of existing underground openings an ultrasonic survey of the flooded shaft tube was performed. In the depth where the carnallitic layer intersects the shaft tube a leaching cavern was found. In order to improve existing stratigraphical information a borehole that meets the top of the cavern was drilled nearby the shaft and a second ultrasonic survey was performed. The top of the cavern in the carnallitic layer was located in a depth of 251.4 m. The cavern height was 67 m with a width of 65 m. The explored shape of the leaching cavern in the carnallitic layer together with the shaft tube is also included in figure 3.

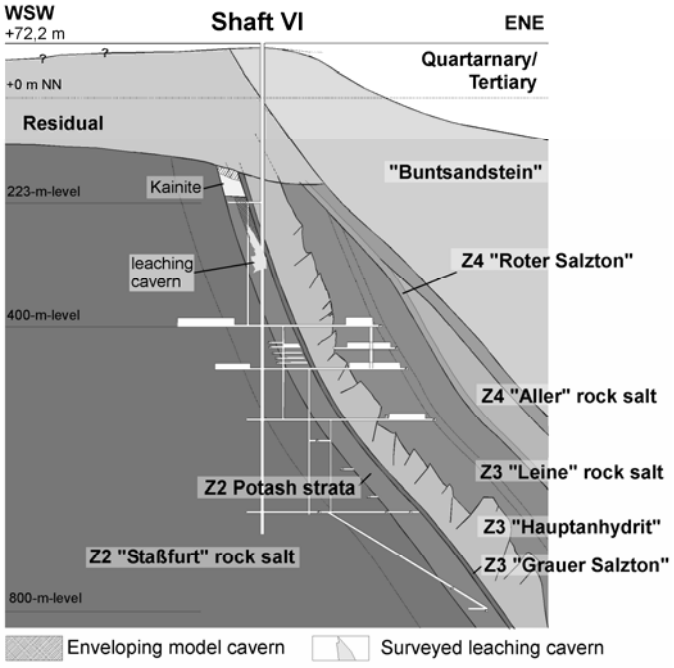


Figure 3. SW-NE-profile across the Staßfurt Salt Anticline in the vicinity of the shaft tube Neustaßfurt VI (ARGE 2004).

For a prognosis of forthcoming surface variations induced by underground processes, this paper reports results from rock mechanical laboratory investigations and numerical calculations considering the spatial dimension of the cavern, the structure and properties of the surrounding rocks and, in addition, the effect of varying humidity.

2. Laboratory Investigations

The site-specific rock parameters are a prerequisite for a relevant numerical modeling. As shown in figure 3 the investigated rock units mainly cover the saliniferous strata Zechstein 2 and 3, each composed of anhydrite (“Hauptanhydrit”), rock salt and potash salt (mainly carnallitite) followed by younger salt strata and the overburden cap rocks. They consist of insoluble residual salt components (gypsum aggregates and Hauptanhydrit) and mesozoic sediments (e.g. “Buntsandstein”) and are overlapped by younger tertiary and quaternary material.

Cap rock material was collected from the exploration drill cores and tested in triaxial and shear tests. Results are summarized in Table 1.

To determine the failure criterion of Kainite and Grauer Salzton (T3), which were unknown before, we used the shear testing equipment of the IfG (MTS Systems Corporation model 816). As main advantage, it allows new types of testing procedures for direct shear tests with different boundary conditions (for experimental details see Blümel 2000). Especially the multiple failure state testing

was found to be a powerful technique for the determination of a failure criterion of joints and intact rocks in only one experiment (for example see Fig. 4).

Table 1. Geomechanical parameter for the overburden determined by own investigations.

rock strata	strength		residual strength	
	c [MPa]	φ [°]	c [MPa]	φ [°]
Bundsandstein				
dry	1.4	30	0.37	28
moistened			0.001	26
Residual	4.0	35	0.52	33
Hauptanhydrit A3	22.0	38	0.56	41
Grauer Salzton T3	0.41	49	0.01	39

Special attention has been paid to the influence of moistening the overburden Buntsandstein. Our investigations document a drastically loss of cohesion c and a reduction of the friction angle φ due to the embedment of water in the clay particle (not shown here).

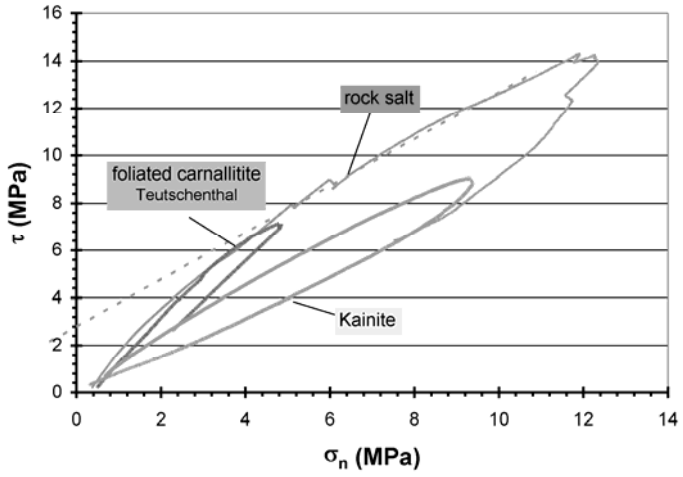


Figure 4. Shear tests with no dilation allowed on various salt rocks.

Since no core material suitable for rock mechanical investigations of carnallitite and rock salt could be obtained from the exploration drill we took rock mechanical parameters determined for the same strata in the Teutschenthaler Salt Anticline which geological situation is equivalent to that of the shaft Neustaßfurt VI.

3. Visco-elasto-plastic Model

To investigate the stability of the leaching cavern located in the vicinity of the shaft tube numerical calculations were performed with *3DEC*. Modeling of the creep- and failure behavior of the saliniferous strata carnallitite and rocksalt was accomplished with a specially developed visco-elasto-plastic constitutive model (Minkley et al. 2001). The remaining part of rock strata does not show any creep. So their material behavior was described with the Mohr-Coloumb flow- and failure criteria.
A non-linear failure criterion on the basis of a modification of the Mohr-Coulomb model was developed by Minkley (1997):

$$\sigma_{1,B} = \sigma_D + \left(1 + \frac{\sigma_{MAX} - \sigma_D}{\sigma_\phi + \sigma_3}\right)\sigma_3 \quad (1)$$

respectively

$$\sigma_{eff,B} = \sigma_D + \frac{\sigma_{MAX} - \sigma_D}{\sigma_\phi + \sigma_3}\sigma_3 \quad (2)$$

Where σ_3 = minimum principal stress, $\sigma_{1,B}$ = maximum principal stress at failure, $\sigma_{eff,B} = \sigma_{1,B} - \sigma_3$ = maximum effective stress at failure, $\sigma_D(\varepsilon^P)$ = uniaxial compressive strength, $\sigma_{MAX}(\varepsilon^P)$ = maximum effective strength, $\sigma_\Phi(\varepsilon^P)$ = curvature parameter for strength surface, $\sigma_D(\varepsilon^P)$ = uniaxial compressive strength and ε^P = plastic shear deformation.
Exemplary for all the saliniferous strata described with this model the measured and calculated failure envelope for carnallitite is shown in figure 5.

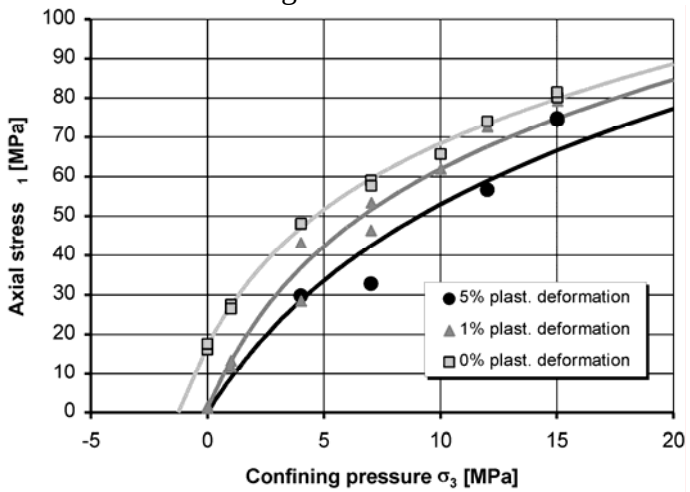


Figure 5. Measured and calculated failure envelope for carnallitite C60.

For volume increase (dilation) induced by softening is valid:

$$\frac{\Delta V}{V} = \varepsilon^p_{vol} = \left(N_\psi - 1\right)\cdot\varepsilon^p \quad (3)$$

N_Ψ is the dilation function:

$$N_\psi = 1 + \sigma_\psi \frac{\left(\sigma_{MAX,\psi} - \sigma_D\right)}{\left(\sigma_\psi + \sigma_3\right)^2} \quad (4)$$

For $\sigma_3 = 0$, it follows from equations 3 and 4:

$$\frac{\varepsilon^p_{vol,0}}{\varepsilon^p} = \tan\beta^0 = \frac{\sigma_{MAX,\psi} - \sigma_D}{\sigma_\psi} \quad (5)$$

where $\tan\beta^0$ is the slope of the volume deformation curve in the dilation area under uniaxial load. Therefore, the dilation function can be written as:

$$N_\psi = 1 + \frac{\sigma_\psi^2}{\left(\sigma_\psi - \sigma_3\right)^2}\cdot\tan\beta^0 \quad (6)$$

where $\tan\beta^0$ and σ_Ψ depend on the plastic deformation ε^P.

Analogous to the failure envelope the measured and calculated volume change for carnallitite is shown in figure 6 to be exemplary for all the saliniferous strata described with this model.

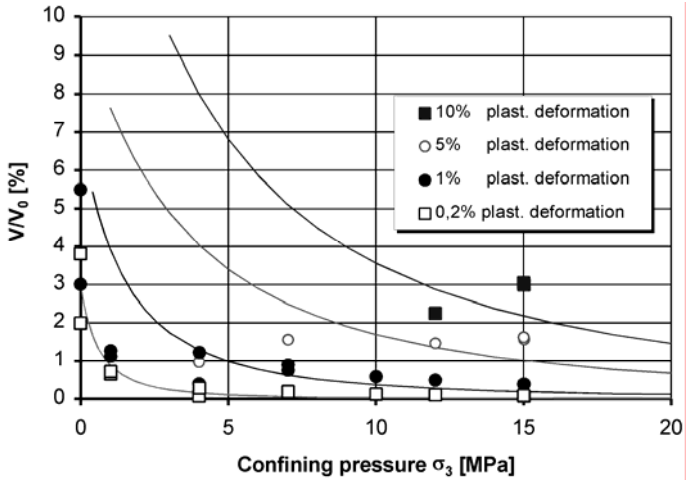


Figure 6. Measured and calculated volume change for carnallitite C60.

The elasto-plastic model, which describes softening and dilatancy depending on stress and deformation, is combined with a non-linear Burgers model to get a visco-elasto-plastic model. The primary creep phase is modeled by the Kelvin-Model with Kelvin shear modulus G^K and Kelvin viscosity η^K. The secondary creep phase is controlled by the Maxwell viscosity η^M. If $\eta^K \rightarrow \infty$ and $\eta^M \rightarrow \infty$ the material model coincides with the time-independent elasto-plastic model. Within the visco-elasto-plastic model the stress dependency of the creep rate is governed by the exponential dependency of the Maxwell viscosity on the deviatoric stress σ_V:

$$\eta^M = \eta_0^M \cdot e^{m \cdot \sigma_V} \tag{7}$$

The creep parameters for the Teutschenthal potash mine could be applied directly for this model because the numerical investigations show the calculated development of the surface subsidence corresponds to the measured in the vicinity of the shaft Neustaßfurt VI. The used creep parameters are summarized in Table 2.

Table 2. Creep parameters for the saliniferous strata.

Rock strata	Kelvin-body		Maxwell-body	
	G^K [GPa]	η^K [MPa x d]	η^M [MPa x d]	m [MPa^{-1}]
Roter Salzton (T4)	7.3	3.8×10^4	3.7×10^4	0.0
Rocksalt	63.0	1.7×10^5	4.0×10^7	0.33
Carnallitite	2.0	1.0×10^4	2.5×10^5	0.17

The material model is available as a DLL-application for the codes *FLAC*, *FLAC*^{3D}, *UDEC* and *3DEC*.

4. *3DEC* Modeling

The spatial geomechanical model includes a cross section of 231×231 m^2 (Fig. 7), i.e. this area corresponds with the whole surface area to be assessed. The shaft tube itself coincides with the center of this area. The lower model boundary corresponds with the 400 m-level of the mine. The x-axis of the model corresponds with the line of strike, the z-axis lies normal to the x-axis and the y-axis is directed perpendicular upward.

All essential geological strata are included in the assembly of the model. The layers between the Roter Salzton and Z6 are combined in one material region with the material properties of the Roter

Salzton. Also the series of strata between Deck-Steinsalz and Grauer Salzton are united in one material region with the Grauer Salzton rock mechanical properties. The rock mechanical parameter sets of all included material regions are summarized in table 3.

Table 3. Rock mechanical parameters for the material regions.

material region	elastic properties		Mohr-Coulomb properties	
	E [GPa]	ν [-]	c [MPa]	φ [°]
Quaternary/Tertiary	0.15	0.33	0.015	20
Bundsandstein	3.5	0.17		
dry			0.37	28
moistened			0.001	26
Residual	25.0	0.24	0.52	33
Roter Salzton T4	10.0	0.26	*	
Hauptanhydrit A3	30.0	0.23	0.56	41
Grauer Salzton T3	30.0	0.23	0.01	39
Rocksalt	25.0	0.25	*	
Carnallitite	10.0	0.25	*	

* visco-elasto-plastic model

The shaft tube is modeled as a 7 m-diameter tube, i.e. in a conservative approach the effect of the cement phase corrosion of brickwork shaft lining is taken into consideration. Due to the possibility of continuing leaching and disintegration in the carnallitite layer by long term processes the today located leaching cavern was assumed that will increase up to the lower border of the Kainit layer (217 m-level). The Kainit is not soluble in the salt brine analyzed in the leaching cavern and assumed there in the long term. Furthermore all possibly disintegrated rock areas in the vicinity of the located leaching cavern were included in an enveloping model cavern that is included in the numerical model. This model cavern has a horizontal cross section area with a semi-elliptic shape (axis length 20 m: 30 m cross section area 940 m^2). The large axis coincides with the lower border of the insoluble Grauer Salzton. A volume of 97,000 m^2 can be calculated with the geometry of the model cavern, which is around four times as high as the surveyed volume.

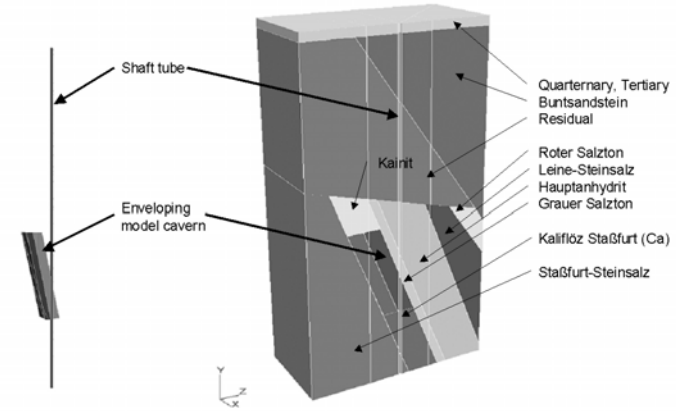


Figure 7. Structure of the *3DEC* model (material regions).

Due the symmetry of the rock volume to be assessed it is possible to reduce the model to the northwestern half of the original volume. So the number of zones and the numerical effort could be reduced. Despite this reduction the number of zones totals 277,494.
The maximal edge lengths in the model are summarized in table 4. In the vicinity of the shaft tube a smaller zone size was chosen.

Table 4. Maximum zone size (edge length) in the 3DEC model.

distance to the shaft [m]	maximum zone size [m]
8.0	1.0
18.0	2.0
55.0	4.0
>55.0	10.0

An homogenous primary stress state was assumed in the entire model with an average stress gradient 24 kPa/m and a lateral pressure coefficient $\lambda = 1$. Underground measurements and methodical calculations show these assumptions are a good approximation for the saliniferous layers in the salt anticline and its vicinity and for the overburden in the sense of a conservative approach. Furthermore, an average fluid and pore pressure gradient of 12 kPa/m was assumed in the entire model.
The numerical simulation of the model behavior was performed in the following steps:

- In the first step the primary stress state was simulated and the unbalanced forces were balanced.
- In the second step a standing time of 100 years was simulated whereby the creep and failure processes around the model cavern and the shaft tube took place.
- In the third step the failure properties of the Buntsandstein were changed from dry to moistened to estimate consequences.

5. Numerical investigation Results

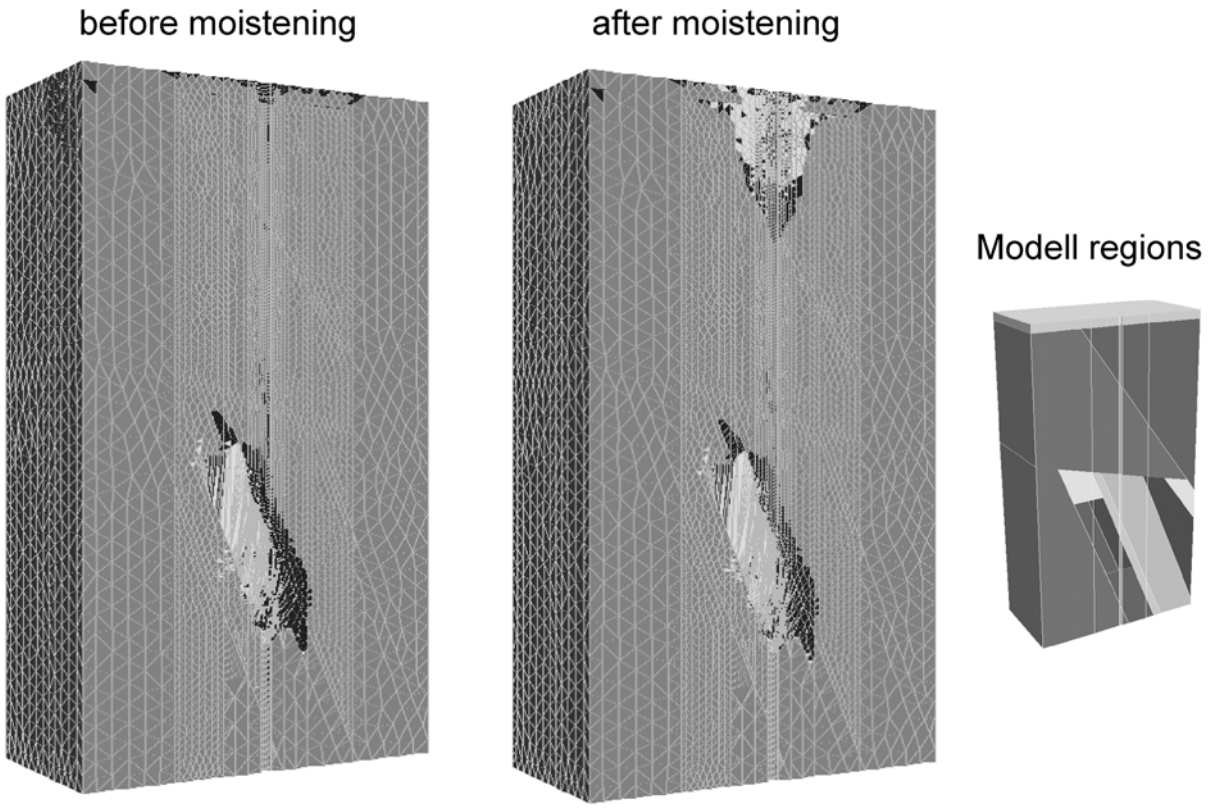


Figure 8. Distribution of the failure indicator immediately before and 1 year after moistening the Buntsandstein.

The distribution of the failure indicator for a standing time of 100 years is shown on the left side of figure 8. The entire layer of the Grauer Salzton in the vicinity of the model cavern is in the state of tensional failure (light regions) whereas the adjoining parts of the Hauptanhydrit and the triaxial stressed parts of the Grauer Salzton are in a permissible state after their failure and stress redistribution (dark regions).

In the vicinity of the unlined shaft tube only single zones in the regions of the residual and the Buntsandstein reached the failure state (dark regions).. Only in the region of Quaternary and Tertiary sediments the unlined shaft tube is not stable(dark regions).
In order to investigate the effect of moistening the Buntsandstein in the case of failure of the brickwork shaft lining the failure properties of the entire region of Buntsandstein were reduced in accordance with the results of the laboratory tests and the calculation was continued up to a standing time of 101 years.
The distribution of the failure indicator for a standing time of 101 years is shown on the right side of figure 8. Inside a breaking-in funnel with an aperture angle of around 60° the Buntsandstein shows complete failure and moves into the shaft tube (light regions). It means an area around the shaft with a diameter of about 100 m takes some risk. This process begins in the calculation procedure immediately after changing the properties of the Buntsandstein. This result is illustrated by vertical displacements of some points near the shaft tube in different model depths (Fig. 9). In reality the process of moistening the argillaceous components of the Buntsandstein due to the destruction of the brickwork shaft lining takes a longer period.

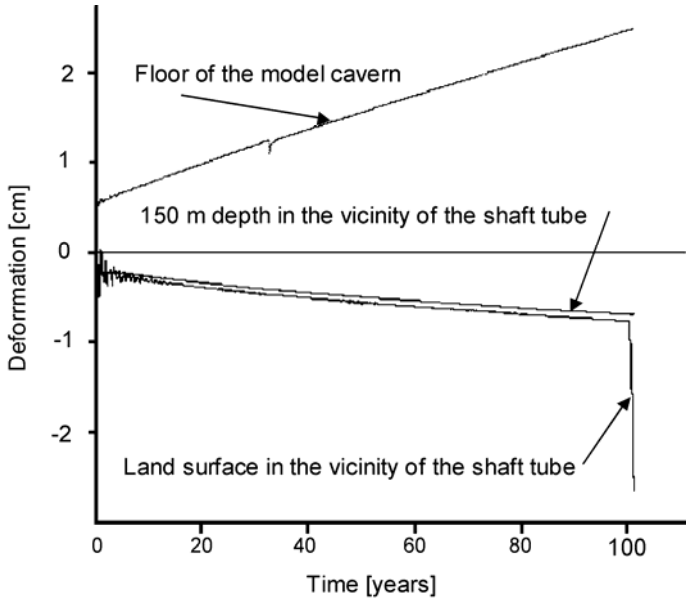


Figure 9. Evolution of vertical displacements in the vicinity of the shaft tube.

6. Conclusions

The stability of the leaching cavern in the vicinity of the flooded potash shaft tube Neustaßfurt VI and the shaft tube itself could be simulated in various numerical calculations with *3DEC* based on a rock mechanical laboratory program performed for the adjacent rocks.
The specially developed visco-elasto-plastic constitutive model of Minkley was found to be an adequate tool for modeling of the creep- and failure behavior of the saliniferous strata, e.g.

carnallitite and rocksalt. Because the remaining parts of rock strata do not show any creep, their material behavior was sufficiently considered with the Mohr-Coloumb failure criteria.
The numerical investigations demonstrate that the overburden of the leaching cavern remains stable over a lifespan of 100 years. Only in the case of break down of the brickwork shaft lining, which can occur in a longer life span, moistening of the Buntsandstein will result in a drastic loss of its strength as indicated in laboratory tests. Under such conditions the calculations clearly indicate that in these regions and, particularly, in the unconsolidated Tertiary and Quaternary sediments the shaft tube is not stable resulting in accelerated land surface subsidence around the shaft.

Acknowledgement

This study is part of the safety assessment for the land surface around the shaft tube Neustaßfurt VI commissioned by the GVVmbH. We thank the GVVmbH for their financial and technical support. The project benefited from many helpful discussions with the colleagues of ERCOSPLAN Erfurt and KUTEC Sondershausen.

References

ARGE (2004). (ERCOSPLAN Erfurt, IfG Leipzig). *Gefährdungsabschätzung auf der Grundlage einer Szenarienanalyse mit Gebirgsmechanischer Modellierung für den Schacht Neustaßfurt VI*. 15. January 2004, unveröffentlicht.

Blümel, M., (2000). *Improved procedures for laboratory rock testing*. Proc. ISRM Symposium EUROCK 2000, Aachen, 573-578.

Minkley, W. (1997). *Spödbruchverhalten von Carnallitit und seine Auswirkungen auf die Langzeitsicherheit von Untertagedeponien.* Forschungszentrum Karlsruhe GmbH, Wissenschaftliche Berichte FZKA-PTE-Nr. 5, 249-275.

Minkley, W., Menzel, W., Konietzky, H & te Kamp, L. (2001). *A visco-elasto-plastic softening model and its application for solving static and dynamic stability problem in potash mining*. In Billaux et al. (eds.), Proc. of the 2nd International FLAC Symposium, FLAC and Numerical Modeling in Geomechanics Lyon, France, 29-31 Oct. 2001. Rotterdam: Balkema, 21-27.

Salzer, K., Jost, G. & Landsmann, O. (2003). *Geomechanische Untersuchungen und Gefährdungsabschätzung für das geflutete Grubengebäude am Schacht Neustaßfurt VI*. In Hartmann & Schönberg (eds.), Kali-, Steinsalz und Kupferschiefer in Mitteldeutschland IV; Vorträge zum 15. Treffen des Arbeitskreises Bergbaufolgelandschaften, Magdeburg, 26.-27. September 2003, 9-24.

ASSESSMENT OF THE WATER INFLOW TO THE MINE WORKINGS BY NUMERICAL MODELLING

SHENG Yong [1], REDDISH David [2]

1. School of Civil Engineering, University of Leeds, Leeds, LS2 9JT, U.K.

Email: y.sheng@leeds.ac.uk

2. School of Civil Engineering, University of Nottingham, Nottingham, NG7 2RD, U.K.

Email: david.reddish@nottingham.ac.uk

ABSTRACT: A numerical model is developed in FLAC to assess the potential path of the water inflow to the mine workings with particular references to the influence of geological fault and old mine workings. A typical case study has been carried out by using the developed model. Numerical results are presented and discussed in this paper. The general trend of the numerical results has been found to agree with the site observations, thus the numerical model is validated and can be modified to simulate more complicated problems associated with the ground water recharge.

KEYWORDS: Water inflow, geological fault, shear band, numerical modelling, FLAC

1. Introduction

In the past few decades a significant number of deep coal mines have been abandoned in the UK and groundwater has begun to rise. It has been normal practice in some cases to allow this recharge to take place and to deal with the consequences as they become apparent. However this strategy is beset with logistical difficulties and expense related to ongoing water treatment. Allied to these problems is the potential for further subsidence events relating to rising ground waters and flooding near-surface mine workings. Water inflow is a common problem that can be observed in the closed mines and current active mine workings, which sometimes can cause great safety concerns and even halt the production of the mine workings. Therefore, it is of significant practical and economical importance to predict and prevent water inflows. Although some researches has been carried out with particular considerations of the strata failure characteristics and hydraulic conductivity changes due to mining activities (Ardejani F.D. and Singh R.N., 2004, Zhang J. and Shen B., 2004, Shi L.Q. and Singh R.N. 2003); however, the mechanism of water inflows is still not well understood.

The changing of geological and hydrological conditions attributes to the most water inflow problems. The main factors often concerned in the analysis of the causes of the water inflow are strata pressure, water pressure, geologic structures and mining parameters (such as mining width and advancing distance, etc.) (Zhang J. and Shen B., 2004). Strata pressure can be significantly altered by mining-induced in situ stress redistributions. The geologic structures, particularly faults, are one of the main causes of water inrushes. Due to the fact that the rock strength in the fault zone is much lower than that of normal rocks, rocks in faulted zones fail easier, and may create a larger failure zone in which the hydraulic conductivity increases (Xiao HT and Xu HY, 2000). Furthermore existence of a fault may reduce the distance between the seam and aquifer, if the faulted zone is permeable and reaches the aquifer, it will cause water inflow through the fault into the mine workings. Despite of the great influence of the geological fault on the water inrush problems, few studies had counted for it.

As part of the European Commission RFCS research program for managing the impacts of changing hydrological regimes surrounding closed underground coal mines (7220-PR-136), a numerical model is developed in FLAC to assess the effect of the geological fault and the mining

activities on the ground water inflow to the mine workings. The numerical model can also be used to study the interaction between an abandoned deep longwall workings and shallow, partial extraction workings. A typical case where the inflows of water into the coal mine workings happened due to a new working face above an old working in a mine area in North Yorkshire, U.K. has been selected and studied to validate the numerical model. Model construction and the discussion of the numerical results are presented in the context of this paper. The information on the extent of failure zones, strain distributions and the fracture plane development during the extraction of panels for the entire block concerned in the model has been obtained in the modelling, which can be used to determine the potential path of the water inflow.

The trend of the numerical results has been qualitatively validated by the site observations, the possible water path indicated in the numerical results generally match the reported positions of water inflow.

2. Model description

A typical case associated with the water inrush problem in a U.K. mine area has been selected and the numerical model was constructed using the geometrical and geological data collected from mine site. The general model arrangement is shown in Fig 1. The numerical modelling consisted of constructing a large scale model across the panels to allow a general understanding of the interaction between the system of panels, the geological fault and the surrounding rock strata. The overall model was based on a vertical plane with the dimensions of 900 metres vertically by 800 metres horizontally. There are two mine workings in the model, the old one in Barnsley seam has been closed, and the new one is in the above Stanley main seam where the large amount of water inflow was reported during the early stage of the excavation. There is an aquifer in the Woolley edge sandstone stratum directly above mine workings and connected with the nearby geological fault. Therefore, the geological fault is considered as the primary cause of the water inflow in this case. However, the modelling of the fault plane itself represented a new challenge. A sensitivity analysis of the effect of a range of different fault criteria (cohesion and angle of friction) was conducted. In the model, it was assumed that the fault was a single plane with a throw of 10 metres.

Due to the large extent of the area modelled, a relatively coarse grid was utilized to produce general details with respect to strains, and stresses and possible shear band formations. The modelling began with the building of the complete grid in FLAC, followed by the simultaneous extraction of panels in the Barnsley seam. This represented the general situation that was met at the commencement of mining in the Stanley Main seam. Then each panel within the Stanley Main seam was sequentially removed with the redistribution of stress and shear planes allowed to occur around that panel prior to the mining of the next panel in the series. This was undertaken to simulate the actual process of mining.

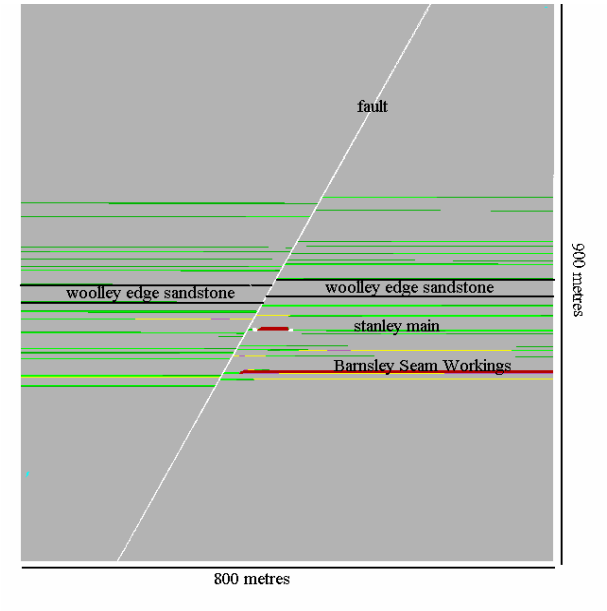


Fig.1 General Model Arrangement

Figure 2 provides an enlargement of the grid around the Stanley Main seam workings, noticing that the grid has been refined around the goaf area in order to obtain more accurate predictions of the redistribution of the strata stress.

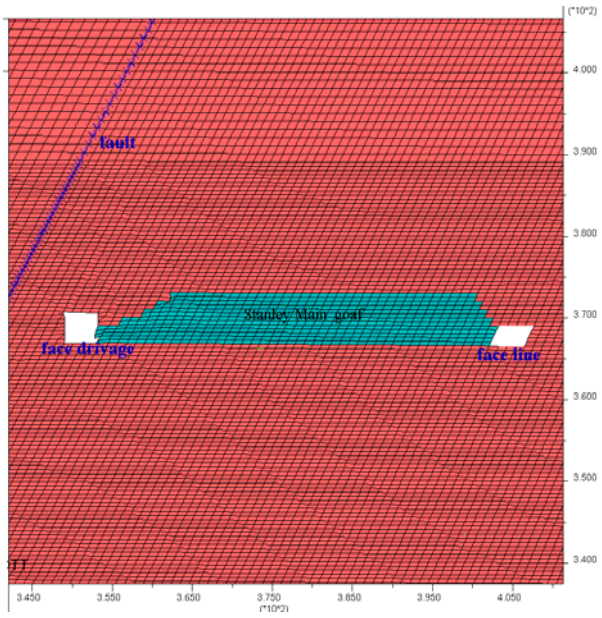


Fig.2 Details of Model Grid Around Stanley Main Seam

Modelling the influence of the fault using FLAC included input parameters based on data supplied by the mine, plus strength data on typical coal measure rocks collected at the mine site, using correction factors following the application of Rock Mass Classification.

Knowledge of joint performance in coal measure rocks based on test information gathered at the University of Nottingham led to the selection of a friction angle of 28^o and cohesion of 0.398 MPa for the fault. In order to test the significance of this choice, models were also run in which at one extreme the fault was 'glued' by the model allowing no shear, and at the other extreme, a friction angle of 10^o and a cohesion of 0.1 MPa was chosen.

3. Modelling results and discussions

The model outputs have been expressed in terms of shear strain distribution. As a qualitative assessment, the greatest concentrations (and highest levels) of shear strain are highlighted in zones with bright colours in the cross-section of the model.

Laboratory testing of coal measure strata indicates that a shear strain of approximately 3mm/m should be taken as the level where shear movement would have created rock failure and sufficient post-failure shear movement necessary to provide a preferential pathway through strata for methane gas (Lowndes I.S. et al, 2002). Whether this level also applies to water flow is conjectural, but the 3mm/m level is a useful guideline to apply. Each of the diagrams of model output highlights those areas of shear strain greater than the 3mm/m level. All areas of shear strain less than 3mm/m are shown in the base colour.

An initial model was developed for the Barnsley seam workings of panels in order to simulate the initial situation prior to the commencement of mining in the Stanley Main seam. Figure 3,5,7 show the result of this initial model in terms of shear band development around the Barnsley seam prior to the mining of the Stanley Main seam.Figure 4,6,8 show the shear strain development around the pillar and sides of the panel in the sequential modelling in which workings in the Stanley Main seam has also been started. Fig 3 and 4 show model outputs when the original fault parameters (friction angle of 28^o and cohesion of 0.398 MPa) were applied. In Fig 3 a pattern of shear strain associated with the working of the Barnsley seam only has been shown. In Fig 4, these strains were superimposed with those developed by the Stanley Main Workings. Figs5-8 show similar information for the two extreme fault property cases.

To illustrate the relative position between the shear bands and the overlying Woolley Edge sandstone and Stanley Main seam, the level of the Stanley Main seam and the Woolley Edge sandstone has been added to the figures. It can be seen from the Figure that the models predict that shear horizons parallel to the bedding will be present at several elevations above the Barnsley seam with some shear horizons occurring above the Woolley Edge sandstone. As would be expected the pattern of the strains were similar for different fault properties but the magnitude of strain changes. Shear areas above the Barnsley were contained within the proximity of the four thin coal seams that lie between it and the Stanley Main and at the Stanley Main level itself. The magnitude of these strains increased as the fault was made less strong and the development of a shear fracture above the Barnsley seam face start line is shown clearly by the model for the friction angle of 10^o and cohesion of 0.1 MPa case, as shown in Figure??. Strain development above the Stanley Main level before it was worked were less significant being restricted to thin coal seam levels again. In all cases, linkage to the fault (as a possible water flow channel) following the working of the Barnsley seam was restricted to the strata below the Stanley Main level, as can be observed in Figure 3,5,7.

The shear bands that formed during the computer modelling can be subdivided into sub-horizontal horizons parallel to bedding and subvertical shear zones associated with the pillar edges. The sub-horizontal horizons are usually associated with weaker strata units such as coal seams and seatearths. In general the modelling indicates that greatest shear along these horizons occurs in the regions overlying the goaf and the rib sides of the panels.

Sub-vertical shear horizons originating from the edges of the panel workings have also been predicted by the modelling. These dipping shear bands, by intercepting the horizontal shear horizons, potentially generate continuous pathways for water movement from above water bearing horizons into the roadways of the panel. In the modelling the sub-vertical shear bands terminated at a horizontal shear horizon approximately 20 metres above of the Stanley Main seam. Therefore it would be anticipated, from the modelling, that water flow into the mine workings from the roof strata would only occur if water-bearing horizons were present within 20 metres height of the Stanley Main seam. However, in this case, the aquifer is known to be in the Woolley Sandstone stratum, which is some 400 meters above the Stanley Main seam. Numerical results indicate that water was not directly broken through the roof rook strata above the goaf.

However, below the Stanley Main panels the modelling predicts the development of continuous shear bands extending down to the Barnsley seam workings which could provide a continuous potential water pathway between the Stanley Main and Barnsley seams.

Once the Stanley Main panel was worked in the model, the sheared areas above the Stanley Main were accentuated and, in each case, an inclined shear fracture, parallel to the plane of the fault formed above the face entry area. Linkage between the Stanley Main level, the fault, the beds between the Stanley Main and the Woolley Edge Rock and the Rock itself, especially on the downthrow side of the fault became possible, with almost any properties chosen for the fault. To assess if continued retreat of the panel would generate further shear planes that may provide additional potential pathways for water ingress, the model was extended to represent a retreat distance of approximately 390 m. The model indicated that the pattern and extent of the shear bands that developed around the face drivage area and in the vicinity of the fault were not significantly altered with further extraction of the panel.

Fig 9 illustrates data taken from the model in the preferred fault properties case (friction angle of 28^{o} and cohesion of 0.398 MPa). It shows that shear displacement along the fault plane itself when only the Barnsley seam was worked was restricted largely to small areas between the two seams. Once the Stanley Main was worked in the model, substantially greater displacements were found above the Stanley Main seam, which can cause fracture of the rock mass to form a linkage between geological fault and mine workings. These linked weak zones can act as potential paths for the groundwater to beak through.

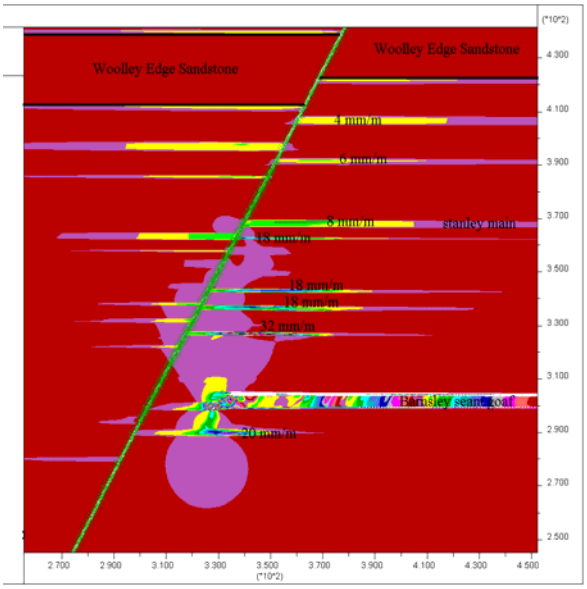


Figure 3 Shear Strain Development after working Barnsley seam

(Fault 28^{o} friction angle and 0.398 MPa Cohesion)

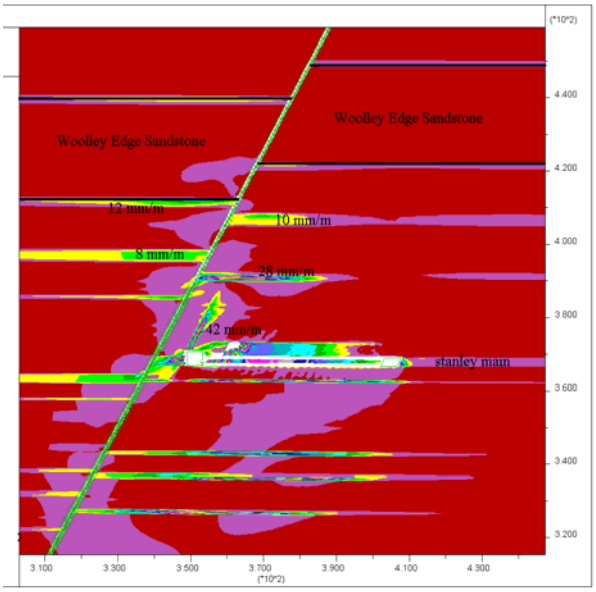


Figure 4 Shear Strain Development after working Barnsley seam and Stanley Main

(Fault 28^{o} friction angle and 0.398 MPa Cohesion)

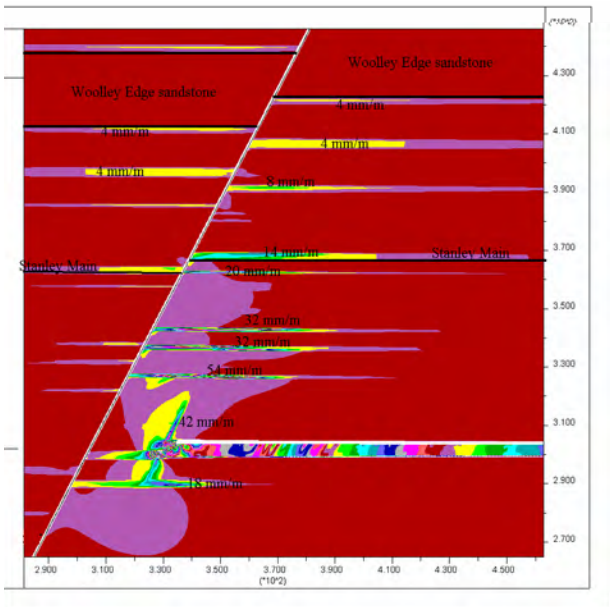


Figure 5 Shear Strain Development after working Barnsley seam
(Fault 10^{o} friction angle and 0.1 MPa Cohesion)

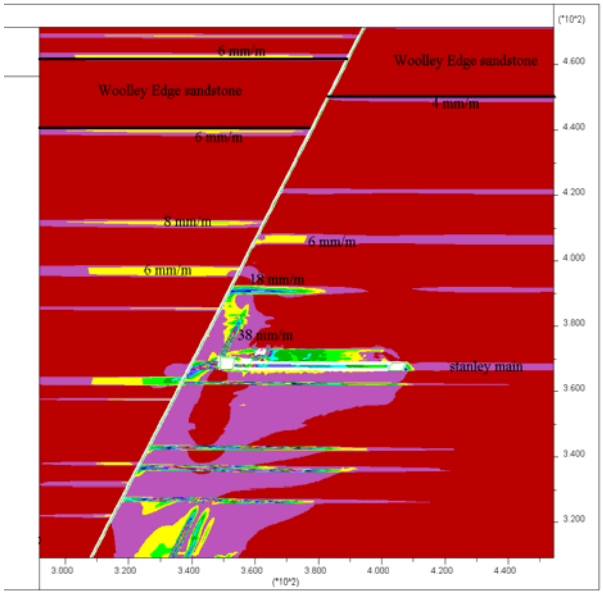


Figure 6 Shear Strain Development after working Barnsley seam and Stanley Main
(Fault 10^{o} friction angle and 0.1 MPa Cohesion)

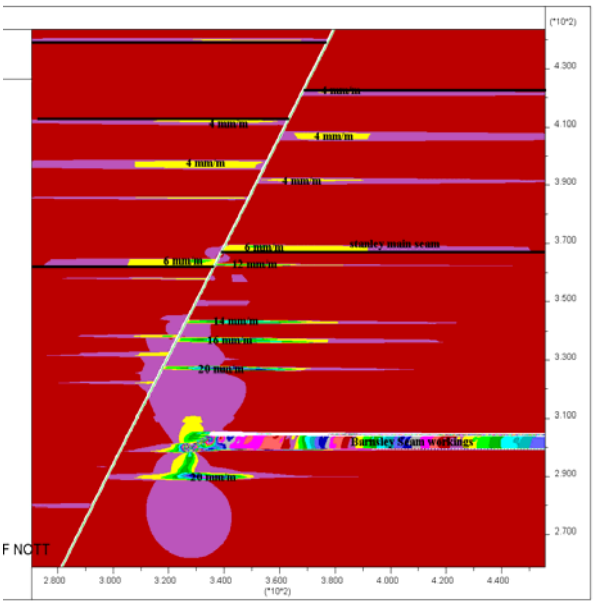


Fig. 7 Shear Strain Development after working Barnsley seam

(Fault Glued)

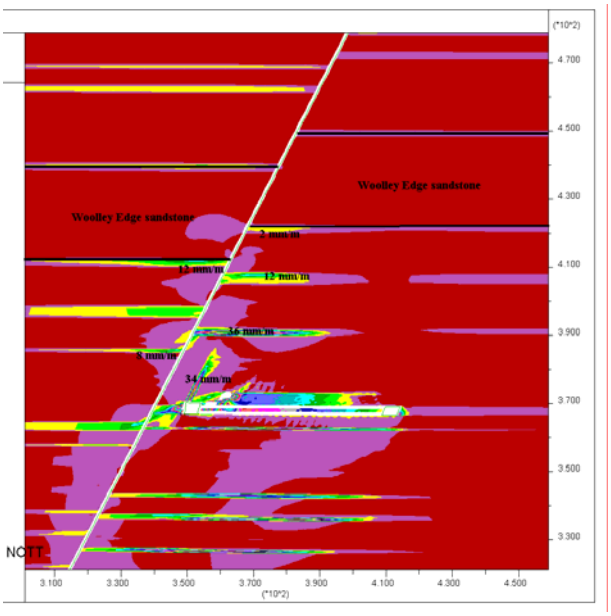


Fig.8 Shear Strain Development after working Barnsley seam and Stanley Main Seam

(Fault Glued)

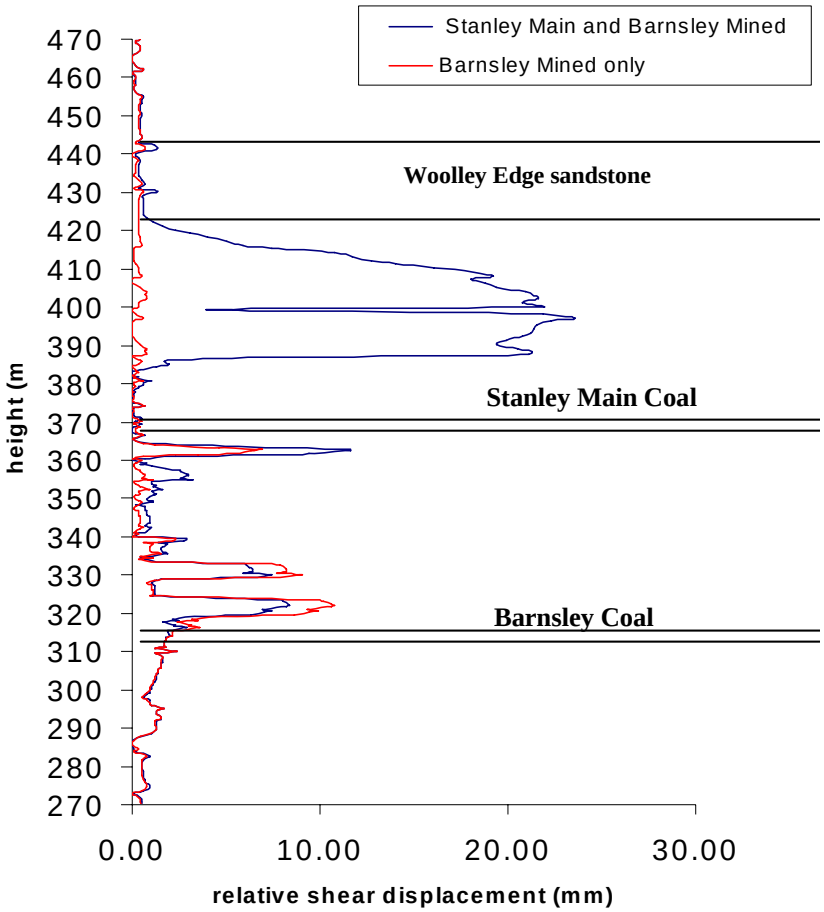


Fig.9 Relative slip along the fault

5. Conclusion

As a conclusion, FLAC result shows that the working of the Barnsley seam alone was unlikely to have created flow paths between the Stanley Main level and the Woolley Edge rock (the aquifer). However, shear strain values at certain weaker strata levels above the Stanley Main could have risen to the point that charging with water from the aquifer could have taken place at these levels over a period of time prior to the working of the Stanley Main. It is also indicated in the FLAC result that the subsequent working of the Stanley Main seam could introduce significant water flow paths via the fault plane and vertical breaks from the Stanley Main face start line to those horizons mentioned above which could have already become charged with water.

Through this typical case study, the numerical model in FLAC is validated to be able to simulate the interaction of new and old mine workings, and to predict the potential flow path within the strata between geological fault and mine workings. However, the model developed here is restricted as a 2D plain strain model. In order to recreate the situations and conditions of the mine site in the numerical model, and achieve more realistic simulations, 3D model is essentially anticipated to be developed. The deteriorative effect of water on the material properties of rock mass will also be introduced into the model to modify the stress and strain state in the rock, and eventually to give better prediction of the rock failure and the pattern of the flow path.

This numerical model can be modified and further applied to the assessment of geomechanical response of the abandoned mining area while groundwater recharging occurs, and can be used as a numerical tool to predict the potential geological hazards such as land subsidence.

6. Reference

Ardejani F.D., Singh R.N. (2004). *Assessment of groundwater rebound in backfilled open cut mines using finite element method*, J of Rock Mech. & Tunnelling Tech., , **10**(1), 1-16

Zhang J., Shen B. (2004). *Coal mining under aquifers in China: a case study*. Int. J Rock Mech. Min Sci., **41**(4):629–39.

Wu Q, Wang M, Wu X. (2004). *Investigations of groundwater bursting into coal mine seam floors from fault zones*. Int. J Rock Mech. Min Sci, **41**:557–71.

Shi L Q, Singh R.N. (2003). *Mine water inrush prediction using the probability index method*, J of Rock Mech. & Tunnelling Tech., **9**(1), 1-10

Wang J-A, Park H.D. (2003). *Coal mining above a confined aquifer*. Int J Rock Mech Min Sci **40**:537–51.

Lowndes I.S., Reddish D. J., Ren T.X., Whittles D. N. and Hargreaves D. M. (2002) *Improved modelling to support the prediction of gas migration and emission from active longwall workings*, Proceedings of the North American/ Ninth US Mine Ventilation Symposium, pp 267-272

Xiao HT, Xu HY. (2000) *In situ permeability measurements to establish the influence of slice mining on floor rocks*. Int. J Rock Mech. Min Sci. **37**:855–60.

Acknowledgement

This project is supported by the European Commission RFCS research program 7220-PR-136.

INTERFEROMETRY OF SPATIAL RADAR IMAGES FOR POST-MINING SURVEILLANCE: EXPERIMENT FEEDBACK

SIMONETTO Elisabeth[1,2], RAUCOULES Daniel[1], CARNEC Claudie[1]

[1] BRGM, Service Aménagement et Risques Naturels, 3 avenue Claude Guillemin - BP 6009 - 45060 ORLEANS Cedex 2 - France.; e.simonetto@brgm.fr; c.carnec@brgm.fr; d.raucoules@brgm.fr

[2] ESGT, Laboratoire de Géodésie et Géomatique, 1 Bd Pythagore, Campus Universitaire, 72000 Le MANS – France.; elisabeth.simonetto@esgt.cnam.fr

ABSTRACT: For several years, satellite radar differential interferometry (DInSAR) has proven its efficiency for the detection of ground deformation with vertical precision measured by centimetres to millimetres. Currently, the technique can provide measurements on large areas of 100x100 km² with a 20m mesh or less. In this presentation, the validity of the DInSAR technique for post-mining risk assessment is evidenced from several interferometric studies. For that purpose, we propose a synthesis of already known interferometric products corresponding to various mining contexts (iron, coal, salt). It turns out that interferometric results are compatible with existing in situ measurements. In a complementary way of these last methods, DInSAR, in favourable cases, provides dense and historical ground movement information over large areas.

KEYWORDS: Interferometry, ground deformation, post-mining surveillance, remote sensing.

RESUME : Depuis plusieurs années, l'interférométrie différentielle d'images radar satellite (DInSAR) a prouvé son efficacité pour la détection de la déformation du sol avec une précision verticale sub-centimétrique. Actuellement, la technique fournit des mesures sur de larges zones de 100 par 100 km avec un pas d'au moins 20m. Dans cette présentation, la validité de la technique DInSAR est mise en évidence à partir de plusieurs cas d'études. Dans ce but, nous proposons ici une synthèse de produits interférométriques déjà obtenus dans des contextes miniers différents (fer, charbon, sel). Il s'avère que les mesures interférométriques sont compatibles avec les mesures pouvant être effectuées sur le terrain. Complémentairement à ces dernières méthodes, le DInSAR, dans les cas favorables, fournit une information dense et historique sur de larges zones.

MOTS-CLEFS : Interférométrie, déformation du sol, surveillance après-mine, télédétection.

1. Introduction

For several years (Massonnet et al., 1993), satellite radar differential interferometry (DInSAR) has proven its efficiency for the detection of vertical ground deformation. The technique provides measurements on large areas of 100x100 km² with a 20m mesh. More recently, the advanced Permanent Scatterer (PS) technique leads to a dense network of points on a mesh of around 10m. This advanced method is based on DInSAR where the deformation parameter inversion only relies on the most pertinent pixels (Ferretti et al., 2000). These ones generally turn to be artificial or natural corners such as building/ground or rock/ground. Several limitations are known: data availability over the site, atmospheric artefacts, measurement along the sensor-antenna direction only and failure over rapid changing surface such as vegetated areas or most landslides. However, the radar database (ERS, RADARSAT, ENVISAT-ASAR, JERS) beginning in 1991, allows assessing historical measurements of the deformation under study. Such technique is also of great

interest in many cases where *in situ* measurements are missing, costly, or difficult to perform. Moreover, the current repetitive image acquisition on a same site should allow the monitoring from space of a given deformation.
BRGM has realised interferometric studies for more than 10 years, in particular for the assessment of urban and mining subsidence phenomena resulting from various anthropic or natural causes. In this presentation, the validity of the DInSAR technique for post-mining risk assessment is evidenced from several interferometric studies at BRGM and with collaborators. For that purpose, we propose a synthesis of interferometric products relative to the mining contexts (iron, coal, salt) in France. We focus on past or recent works at BRGM with collaborations, although, of course, many other examples can be found in the literature. This synthesis allows us to assess main advantages and pertinence of DInSAR for mining surveillance.

2. Experiments in Provence-Alpes-Côtes d'Azur

In this region, coal mining activity occurred near Gardanne at North of Marseilles since 17th century and stopped in 2004. Thirteen ERS images were processed, covering the period 1992-1995 and in a second project nineteen on the 1996-2000 period (Carnec and Delacourt, 2000). These studies supported by ESA, consisted in analysing each interferogram (produced from 2 images) with temporal baseline less than 6 months. Indeed, the context rather difficult (lots of vegetation) prevented from analysing interferogram with large temporal baseline. Several subsidence halos were detected. It was shown that the derived deformation maps correlate well with the underground activities (mined blocks) and lithologic formations (figure 1). In this example, DInSAR helped to the understanding of mining activity impact on geological environment.

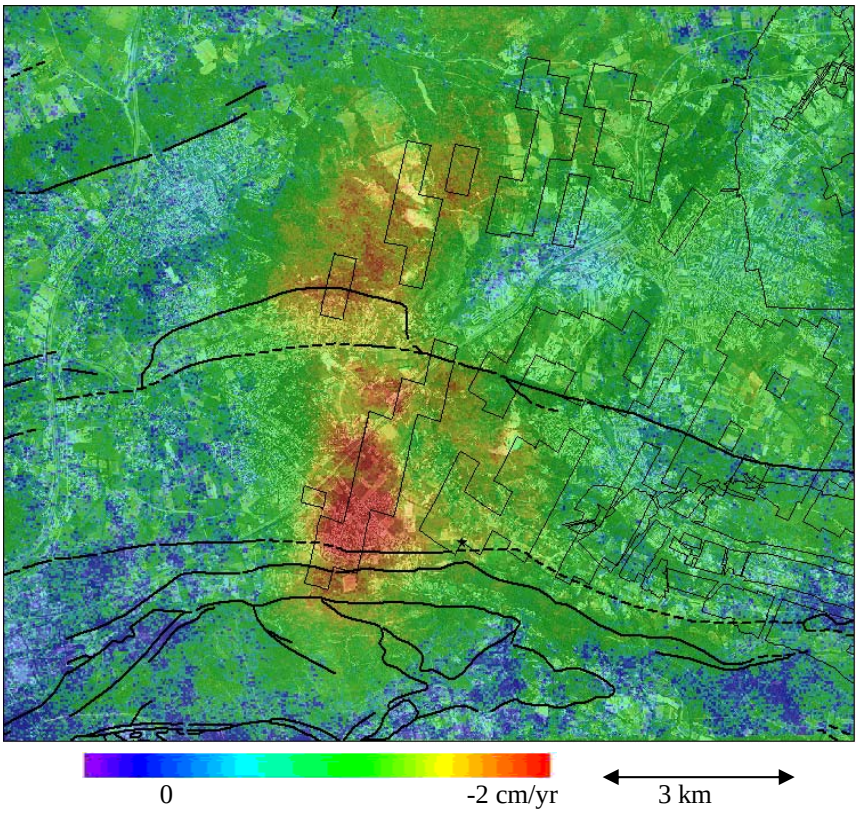


Figure 1 : Subsidence (velocities) map on the area of Gardanne derived from INSAR on the period 1996-2000 overlaid with mining map, superficial formations and an aerial orthophoto (source IGN). The eastern pannels were the last exploited (after 1995).

3. Experiments in Nord/Pas de Calais

In the region of Nord/Pas de Calais in North of France, coal exploitation occurred between 1750 and 1990. Since then, underground water pumping ended and surface deformation was expected due to the increase of the underground water level. Supported by CNES and the French Research Ministry (RTE, RGCU), an interferometric study on this area has been performed in the framework of the RESUM project (http://resum.brgm.fr), that deals with the surveillance of urban and mining subsidence by radar interferometry. Using ten ERS images ranging from 1992 to 2000, individual interferograms reveal subsidence phenomena over 4 cities: Lens, Billy-Montigny, Courrières, and Ostricourt (Raucoules et al., 2004; Raucoules et al., 2005). Measured subsidence rates are ranging from -3 to -4.5cm/year between 1992 and 2000 (Figure 2). A further observation of interferograms showed that deformation occurred until 1995-1996 and after 1996, the terrain stabilised. Levelling measurements in Courrières were also available. They showed a stable period until 1996 followed by uplift until 2001. DInSAR maps proved that the levelling point used as reference of the network was in a moving area, explaining the disappearance between both techniques. Changing the levelling reference point then led to compatible measurements. Thus, DInSAR can efficiently help field missions by providing the deformation spatial area.

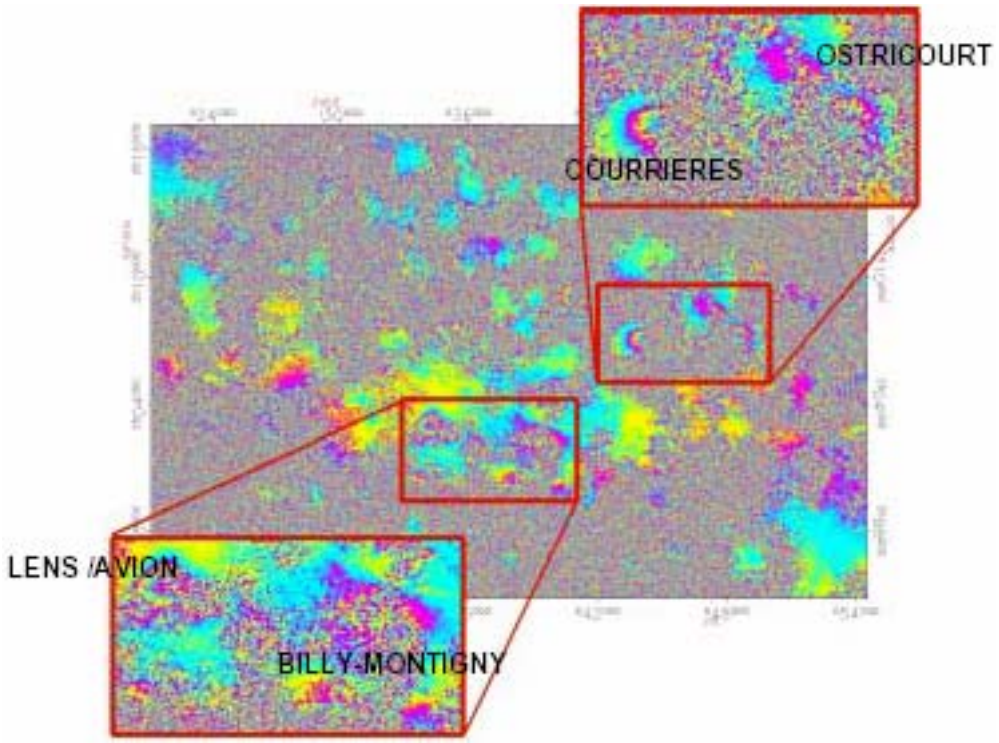


Figure 2. A deformation map obtained by DInSAR in Nord/Pas de Calais between 1992 and 2000. One fringe corresponds to a deformation of about 3cm. Noisy areas contain no information and correspond to non-urbanized areas such as vegetation. Adapted from (Raucoules et al., 2004; Raucoules et al., 2005).

4. Experiments in Bourgogne

In Montceau-Les-Mines, terrain uplift was detected by radar interferometry between 1995 and 1998 (Carnec et al., 2001). This phenomenon was most likely linked to the increase of water level after the end of exploitation. *In situ* piezometric measurements also confirm the observation (figure 3).

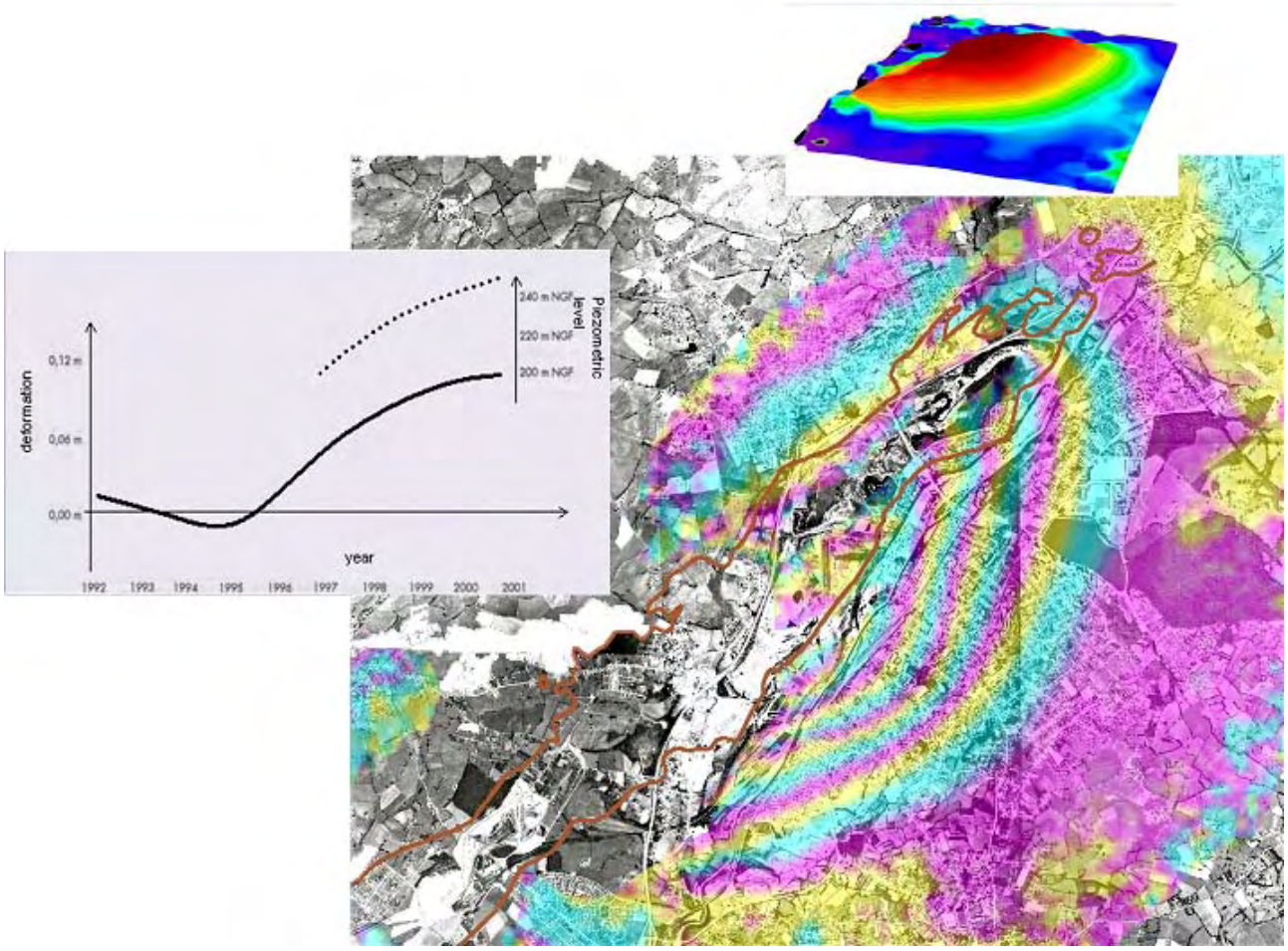


Figure 3. Example of deformation maps obtained by DInSAR in Montceau-Les-Mines. The curves show that DInSAR measurements are compatible with the piezometric level variations. Adapted from (Carnec et al., 2001).

5. Experiments in Languedoc-Roussilon

In the framework of the RESUM project, a study was carried out in order to survey an underground salt mine in South of France near the city of Vauvert (Raucoules et al., 2003). The processing is based on solution mining aiming at dissolving the salt and pumping the brine. 16 ERS data were used covering the period 1993-1999. The stack of three interferograms showed a 8 km large deformation bowl with around 15cm of maximal total subsidence at its center (more than 2cm/yr of displacement rate). Levelling was performed between 1995 and 1998 along black lines on figure 4. Levelling along white lines was used as reference points. One can observe that the reference points are in the moving area. DInSAR showed here how the technique could help *in situ* mission preparation. A new levelling profile (in blue) was then proposed. Deformation rates have been compared between levelling and DInSAR results. A good agreement was achieved between measurements with a RMS error of 2mm/yr, which is compatible with both technique precision.

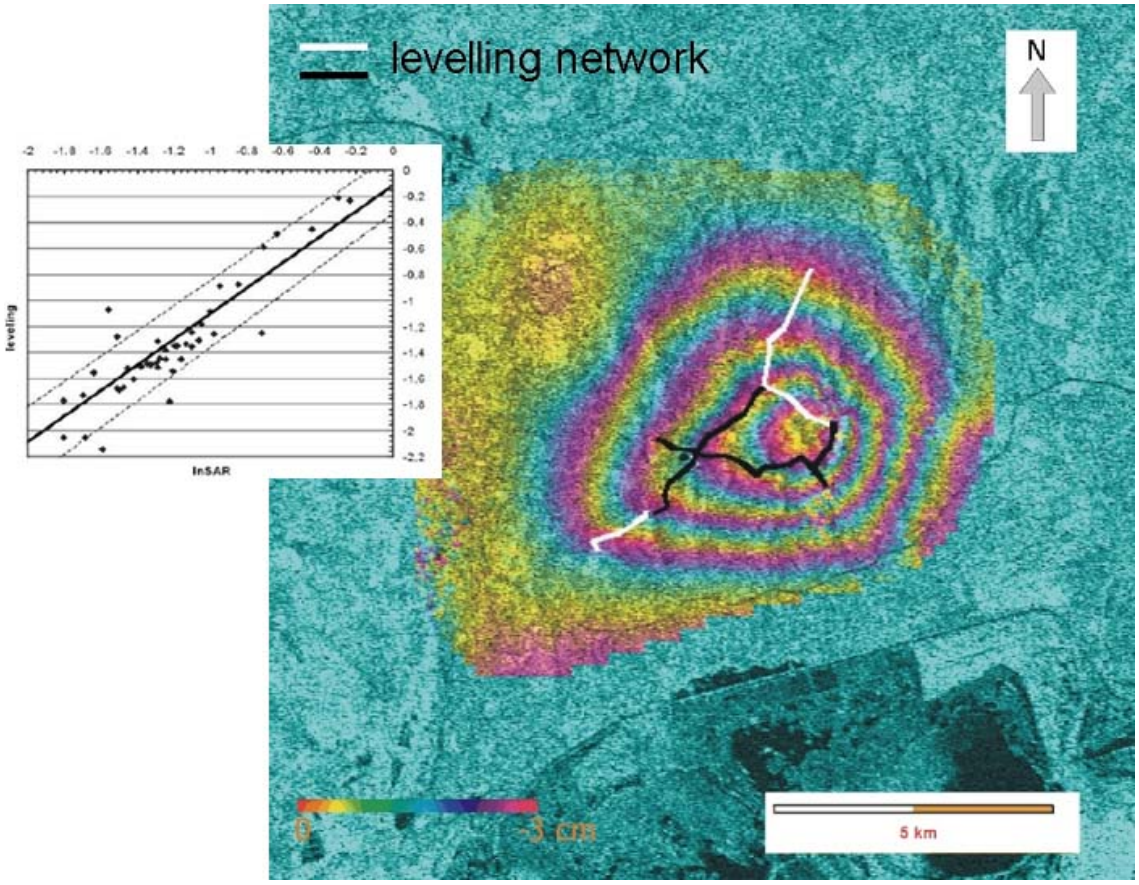


Figure 4. Example of deformation maps obtained by DInSAR near Vauvert in France. The curves accompanying map show that DInSAR measurements are compatible and complementary with the existing levelling network. Adapted from (Raucoules et al., 2003).

6. Experiments in Lorraine

In the East of France, in Lorraine, we were interested in several mining sites: an iron basin near Roncourt and a large coal basin including the cities of Merlebach, Morbach and Forbach. These studies were also conducted for the RESUM project.

In Roncourt, subsidence bowls and sudden collapses are likely to occur due to intensive iron ore exploitation since about 1870 using the chamber and pillar method. The PS technique was applied by the Italian company TRE (Tele-Rilevamento Europa), using 57 ERS images, acquired between 1995 and 2000 (Colesanti et al., 2004). Apart from the mean deformation rate map, the most remarkable result of this study was the detection of precursor signs 10 months before a major collapse that occurred in 1999, whereas no ground measurements were available yet to our knowledge (Figure 5). This result showed how DInSAR could be used for monitoring. After this date, field measurements using optical levelling were then registered. As the phase is measured modulo 2π, the displacement field is measured modulo 3cm with ERS. As consequence, if the amplitude of the deformation is more than 1.5cm during the time period separated two image acquisition dates, ambiguity errors can occur when one wants to 'unwrap' the information. This phenomenon has typically occurred in Roncourt (Carnec et al., 2004). On figure 5, it appears that the DInSAR technique was not able to resolve the inherent 2π ambiguity without *a priori*

information. However, with the optical levelling measurements, this ambiguity was easily corrected. It shows how both techniques cooperate.

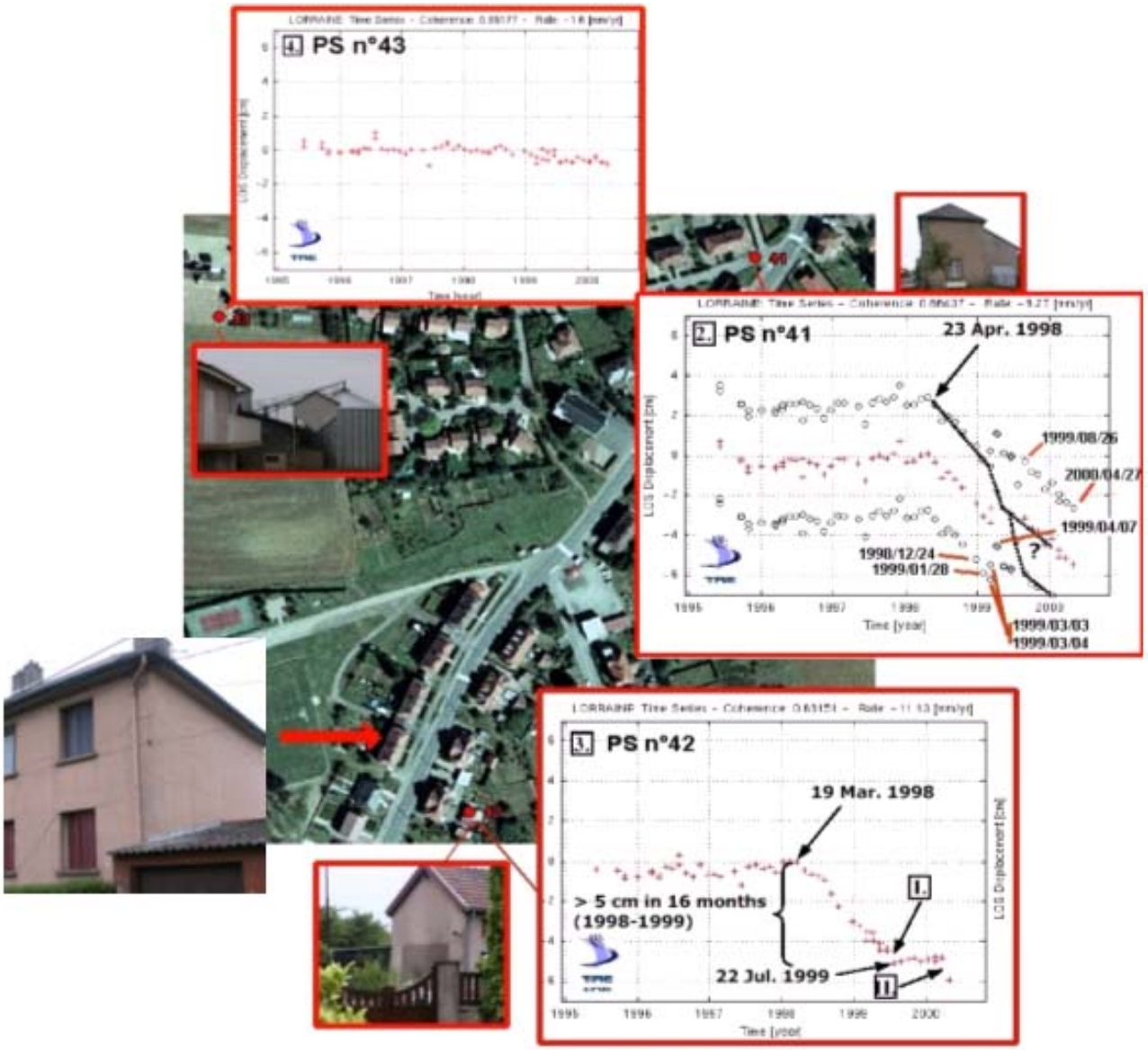


Figure 5. Cumulative displacement for three PS in Roncourt, localised on IGN orthophoto, between 1996 and 2000. The curves showed precursor signs of a major collapse in February 1999, since March/April 1998. For the PS 41, three temporal series are represented: the measured one and two others with an error of respectively one and two phase cycles (ambiguity errors). Black lines indicate potential real movement after manual correction of the ambiguity. Adapted from (Colesanti et al., 2004 ; Carnec et al., 2004).

In the coal basin of Lorraine including Merlebach, Morsbach and Forbach, conventional DInSAR has been applied using 18 ERS images acquired between 1993 and 1999 (Carnec and Raucoules, 2000). Individual interferograms revealed subsidence bowls with maximal amplitudes ranging up to 15cm/an at Merlebach, that are likely to be linked to the past coal exploitation (figure 6). However, interferometric application was unsuccessful in non-urban areas because, in all likelihood, of vegetation growing and surface humidity variation. This example shows the opportunity of using DInSAR for surveillance in urban area. In the meantime, it also shows the limitation of the technique in non-urbanized areas.

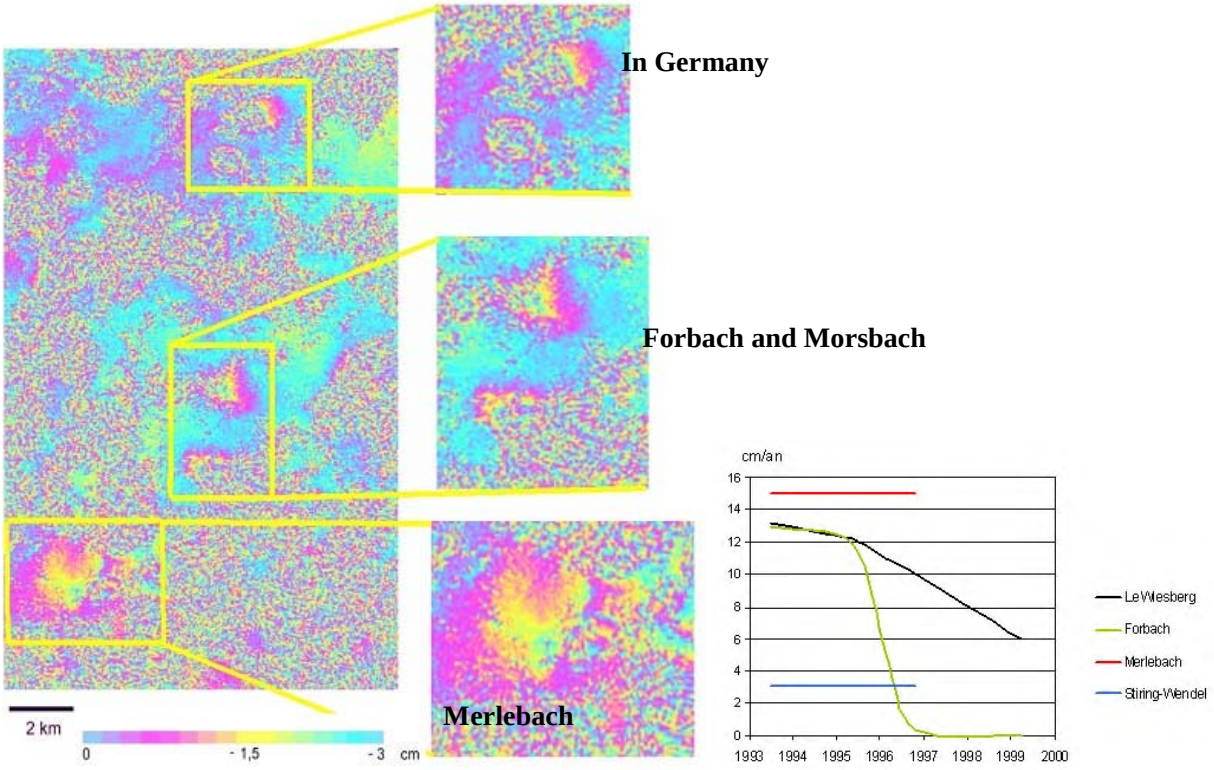


Figure 6. Interferometric map obtained using two images acquired in 1993 between June and August, and maximal displacement rate observed above four cities between 1993 and 2000. Two curves after 1997 stop because measurements were too noisy. Adapted from (Carnec and Raucoules, 2000).

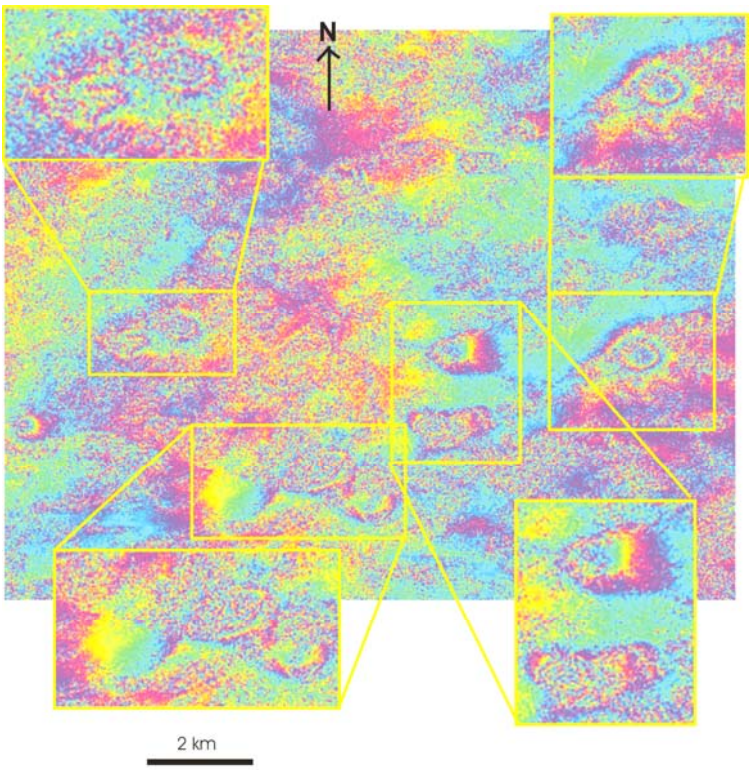


Figure 7. JERS-1 interferogram on the mining area of la Lorraine (same sector that Figure 6). Acquisition dates 24/03/1993 - 11/03/1994. 1 fringe ~ 11.5 cm of vertical deformation. Additional subsidence bowls undetected on figure 6 are observed. Adapted from (Raucoules at al., 2005b).

However, an experiment has been carried out using JERS (figure 7, Raucoules at al., 2005b) data from the Japanese Space Agency. This satellite was equipped with a sensor working with L-band (22cm wavelength), instead of C (5.6cm wavelength) as for ERS or ENVISAT. As a result, interferometric measurement is less sensitive to temporal variation linked to vegetation or surface humidity and provide a complement to the C-band interferometry on vegetated areas.

7. Experiments in Paris

A precedent experiment over Paris revealed a deformation around Montmartre hill. This study was performed in the framework of the RESUM project. 30 ERS images acquired between 1992 and 2000 have been processed using an advanced stack technique, based on classical DInSAR (Le Mouelic et al., 2005). DInSAR showed an averaged subsidence of -2mm/yr for this period on the West and South parts of the mound. Compaction over filled up gypsum quarries was the first explanation retained. However, more recently, a 3D geological model showed that unconsolidated backfills above old gypsum quarries are only one of the potential causes explaining the terrain displacement (figure 8). Up to 25m of backfill thickness can be found at this place. Two other factors may also participate: the slope of the terrain and a perched water table on the sannoisian clay on charge toward west, leading to the destabilization of the unconsolidated backfills (Thierry et al., 2004).

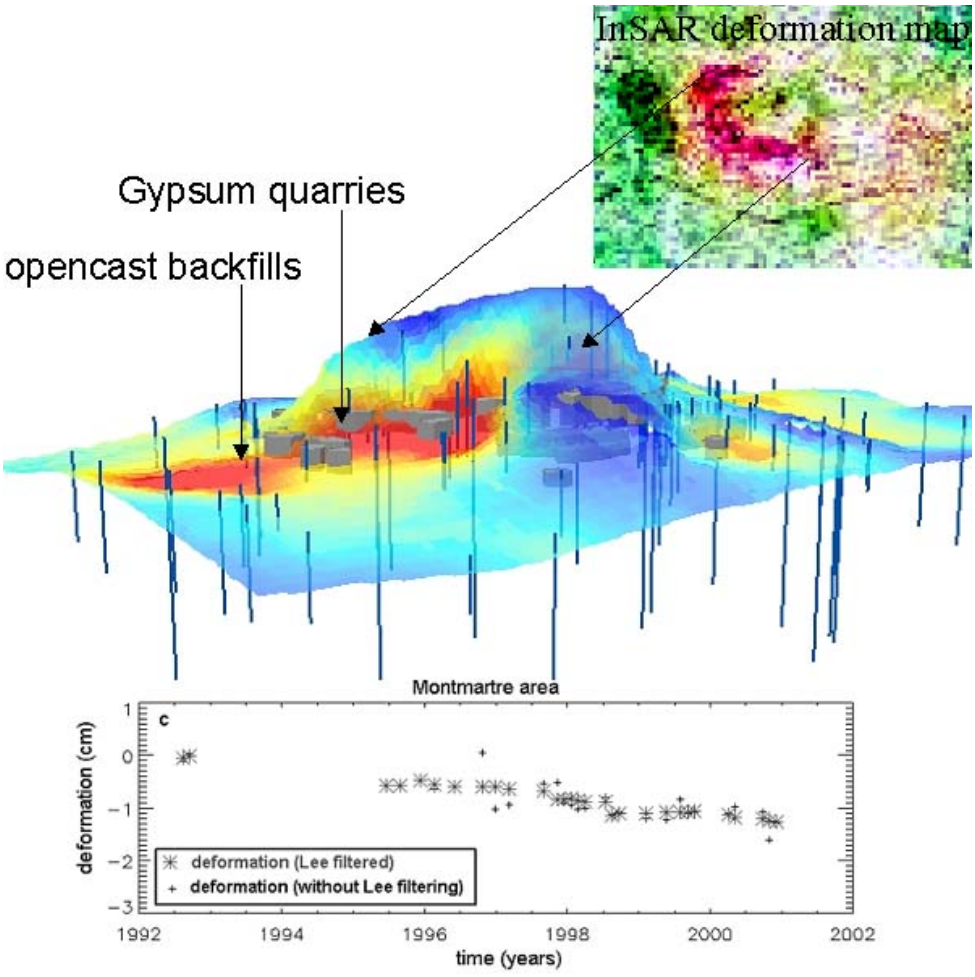


Figure 8. DInSAR map of the mean displacement rate between 1992 and 2000 in Paris, Montmartre mound. A 3D geological model shows that backfills around old gypsum quarries is one of the causes of the deformation in Montmartre. Backfill layer is represented according to its thickness (blue to red) and mapped on a DEM with a vertical exaggeration. The area is 1.5kmx2.2km. Temporal profiles of the deformations occurring in Montmartre area. Plus symbols correspond to the direct output of the least squares inversion method. Asterisks correspond to the values filtered using a Lee filter

with a window of 5 pixels (in time) to reduce the atmospheric component, which is completely random from one image to the next. Adapted from (Le Mouélic et al., 2005).

8. Conclusions

The DInSAR technique presents great advantages for mining and post-mining surveillance. It provides dense and historical deformation maps, precise measurements (mm/yr) and is complementary to field auscultation. Previous studies showed the compatibility of the InSAR measurements with existing *in situ* topometric data. Besides, in certain cases precursor signs of the deformation could also be detected. This remote sensing technique allows the survey of a site with no *a priori* information and no devices on the terrain. Of course, some *in situ* measurements (like GPS) are necessary to validate the InSAR measurements and calculate the absolute deformation field.

Here, one can also notice that the methodology has evolved and is still improved in the framework of research projects. Firstly, individual interferograms were analysed, then interferograms have been stacked allowing to increase the signal to noise ratio. Currently, the PS technique is expected to be the most promising.

It must be noted that the technique can be used only in a favourable context leading to pertinent measurements (data availability, terrain geometry, vegetation, deformation characteristics). Due to the dependence on the launch of a satellite and its characteristics, the method actually suffers from a lack of visibility to insure long-term measurements. Currently, an archive of 15 years of radar interferometric images exits (ERS and ENVISAT from ESA) since 1991. ENVISAT should yet go on some years.

Radar interferometry could also be opportune for other applications such as civil engineering, gas or petrol field surveillance, aquifer system analysis, and in earth science (seismic activity, volcano).

9. Aknowlegdements

The works presented in this paper have been carried out with the support of the research division of BRGM, the RESUM network (funded by the French Ministry of Research and CNES) and ESA.

10. References

Carnec C., Raucoules D. (2000). *Etude de faisabilité: détection et suivi de déformations de surface liées à l'existence de cavités minières souterraines par interférométrie radar différentielle: région de Faulquemont, bassin houiller lorrain*, rapport BRGM RP-50228-FR, 54p.

Carnec C., Delacourt C. (2000). *Three years of mining subsidence monitored by SAR interferometry, Gardanne, France*, Applied Geophysics, Vol.43, 43-54.

Carnec C., King C., Raucoules D., Guise Y., Paquette Y. (2001). *Suivi de mouvements résiduels sur sites miniers par interférométrie radar : perspectives et applications*, SIM Environnement, N.14, 21-23.

Carnec C., Le Mouelic S., Raucoules D., Colesanti C., King C. (2004). *Avancées des technologies spatiales radar appliquées à la détection des déformations de surface d'origine minière*, Revue Française de Géotechnique, N°106-107, 15-22.

Colesanti C., Le Mouelic S., Bennani M., Raucoules D., Carnec C.,Ferretti A. (2004). *Detection of mining related ground instabilities using the Permanent Scatterers technique - A case study in the East of France*, International Journal of Remote Sensing, accepted.

Ferretti A., Prati C., Rocca F. (2000). *Nonlinear subsidence rate estimation using Permanent Scatterers in differential SAR interferometry*, IEEE Transactions on Geoscience and Remote Sensing, N.38, 2202-2212.

Le Mouelic S., Raucoules D., Carnec C., King C. (2005). *A least-squares adjustement of multi-temporal InSAR data – Aplication to the ground deformation of Paris*, Photogrammétric Engineering and Remote Sensing, vol. 71(2), 197-204.

Massonnet D., Rossi M., Carmona C., Adragna F., Peltzer G., Feigl K., Rabbaute T. (1993). *The displacement field of the Landers earthquake mapped by radar interferometry*, Nature, N.364, 138-142.

Raucoules D., Maisons C., Le Mouélic S., Carnec C., King C., Hosford S. (2003). *Monitoring of slow Ground Deformation by ERS Radar Interferometry on the Vauvert Salt Mine (France). Comparison with Ground Based Measurement*, Remote Sensing of Environment, Vol.88, 468-478.

Raucoules D., Guise Y., Le Mouelic S., Carnec C. (2004). *Mesure des mouvements post-mine sur le bassin houiller du Nord/Pas de Calais par interférométrie radar*, Journées Nationales de Géotechnique et de Géologie, Lille, 2004.

Raucoules D., Le Mouelic S., Carnec C., Guise Y. (2005). *Monitoring post-mining subsidence in the Nord/pas de Calais coal basin (France). Comparison between SAR interferometric results and levelling*, International Journal of Remote Sensing, submitted.

Raucoules D., Colessanti C. and Carnec C (2005b), *Use of SAR interferometry for detecting and assessing ground subsidence*, submitted to Comptes rendus Geosciences.

Thierry P., Raucoules D., Felenc J., King C. (2004). *Vertical movements in Paris : coupling 3D geological model and SAR interferometry results*, in IGC 32nd - International Geological Congress, Florence, Italy.

HIGH RESOLUTION MICROGRAVITY INVESTIGATIONS FOR THE DETECTION AND CHARACTERISATION OF SUBSIDENCE ASSOCIATED WITH ABANDONED, COAL, CHALK AND SALT MINES

STYLES Peter[1], TOON Sam[1], BRANSTON Michael[1], ENGLAND Richard[1], THOMAS Ewan[2], McGRATH Richard[2]

[1] APPLIED AND ENVIRONMENTAL GEOPHYSICS GROUP, School of Physical and Geographical Sciences, Keele University, Keele, Staffs, ST5 5BG UK, (p.styles@keele.ac.uk);
[2] GEOTECHNOLOGY, 5 Cefn-yr-Allt, Aberdulais, Neath, UK, SA10 8HE1, (geo.technology@cableol.co.uk)

ABSTRACT: The closure and decay of industrial activity involving mining has scarred the landscape of urban areas and geohazards posed by subsurface cavities are ubiquitous throughout Europe. Features of concern consist of natural solution cavities (e.g. swallow holes and sinkholes in limestone gypsum and chalk) and man-made cavities (mine workings, shafts) in a great variety of post mining environments, including coal, salt, gypsum, anhydrite, tin and chalk. These problems restrict land utilisation, hinder regeneration, pose a threat to life, seriously damage property and services and blight property values. This paper outlines the application of microgravity techniques to characterise abandoned mining hazard in case studies from Coal, Chalk and Salt Mining environments in the UK.

KEYWORDS: Microgravity, Subsidence, Chalk, Salt, Coal.

RESUME : La fermeture et l'affaiblissement de l'activité industrielle liée à l'exploitation minière a marqué le paysage de secteurs urbains et les dangers posés par les cavités proches de la surface sont omniprésents en Europe. Cela concerne des cavités de dissolution (par exemple des dolines et des fontis apparaissant dans le gypse et la craie) et des cavités creusées par l'homme (exploitation minière, puits) dans une grande variété d'environnements, comme le charbon, le sel, le gypse, l'anhydrite, l'étain et la craie. Ces problèmes limitent l'aménagement des terrains de surface, freinent la régénération, expose la population à un risque qui peut être mortel, endommagent sérieusement les propriétés individuelles et les services. Cet article décrit l'application des techniques de microgravité pour caractériser la présence d'exploitation minière abandonnée dans des secteurs d'exploitation de charbon, de craie et de sel au Royaume -Uni.

MOTS-CLEFS : Microgravité, Affaissement, Craie, Sel, Charbon..

1. Introduction

The microgravity technique consists of measuring minute changes in the gravitational pull of the Earth and interpreting the presence of subsurface density variations, such as those produced by voids and cavities, from an analysis of these readings. These gravity anomalies are superimposed onto much larger variations produced by elevation, topography, latitude and regional geological variations and are, usually, almost undetectable by conventional gravity investigations. microgravity surveying has developed considerably over the last ten years with the development of modern, high resolution instruments, prudent field acquisition procedures, sophisticated data reduction methods and advanced analysis techniques. Qianshen et al. (1996) presents a thorough review of the microgravity technique. It is now possible to detect and interpret anomalies as small as 10 microgal with a repeatability of a few microgals under favourable site conditions (the

microgal is the commonly used unit for microgravity surveying; 1 microgal = 10^{-6} cm s^{-2}). Not only can the isolated anomalies reveal the location of mines, caverns and voids, either natural or man-made, but they also provide information on their depths, shapes and morphology. Through the use of Gauss's theorem, the 'missing mass' associated with the void can be calculated in order to provide vital information for the development of remediation strategies and, ultimately, the costs associated with cavity filling. Through the targeted use of post-remediation surveys, assessments can be made on the success, or not, of the remediation process and help verify the location and distribution of materials used to 'grout up' the void space. These attributes have led to the method becoming widely used in hydrogeological, engineering and geotechnical investigations with the significant advantage of leaving the ground completely undisturbed.

2. Microgravity as a tool for the detection and characterisation of subsurface cavites

The presence of karstic features or mining-related cavities in the rock mass often leads to severe restrictions in land utilization and a variety of subsidence-related problems for both current and future users of that land. Cavities constitute a hazard to both development and redevelopment as their migration to the surface, as sinkholes or fractured and disturbed ground, may seriously damage property, services and, in some cases, cause significant groundwater contamination problems. Features of interest usually consist of natural and/or man-made cavities and are generally termed 'targets'. The most common natural targets in karst environments are solution related features such as voids, extended cavern systems and the collapse/drainage features associated with swallow holes (or sinkholes). Man-made cavities, which include mine workings, shafts and tunnels, are just as important and, in fact, can be even more prevalent than natural features, particularly in industrialized environments. Prior to the development (or redevelopment) of a site, the most common method of site investigation has been to drill an extensive pattern of boreholes over the target area in an attempt to locate and then define the spatial extent of any cavities. Indirect techniques such as geophysics can give a cost effective, non-invasive method of cavity delineation with targeted drilling used as a verification tool rather than a primary search technique. A cavity usually has a lower density than the surrounding material and may also be filled with air (i.e. a void), water, sediment, collapse material, or a mixture of all of these. The existence of the cavity alters the physical state of the strata and results in a contrast between the cavity and the host stratum that can be detected using suitable geophysical methods if the contrasts are large enough and the features are of a sufficient size (McDowell et al. 2002).

The microgravity survey technique is a powerful cavity location method. Because a void represents a mass deficiency in the subsurface, a small reduction in the pull of the Earths gravity is observed over the cavity, which is called a negative gravity anomaly. Although the method is simple in principle, measurement of the minute variations in the gravity field of the Earth requires the use of highly sensitive instruments, strict data acquisition procedures, stringent quality controls, careful data reduction and sophisticated digital data analysis techniques in order to evaluate and interpret the data. Conventional site investigation techniques are then employed, as directed by the microgravity results, to verify the areas deficient in mass. In order to detect a target using microgravity there must be a difference in density between the target and its surroundings, resulting in a significant deficiency in mass, otherwise the target will be undetectable using microgravity and other geophysical methods may be more suitable. However, cavities usually do provide significant density contrasts with their surroundings with air filled cavities offering the largest anomaly condition because of the complete absence of material. The simplified picture of a solitary cavity described above is not usually the case for natural or man-made cavities. This is primarily because the rock surrounding the cavity is often disturbed and extensively fractured, particularly in the case

of natural cavities and unsupported mines. The fractured zone may extend for two or more diameters away from the cavity (Daniels 1988) and a similar effect is often observed with karst cavern systems due to the development of sinkholes, collapse features, passages, dissolution and the enlargement of faults/joint systems, etc. consequently , the 'effective' size of the target is dependent not only on the strict volume of the cavity, but also its connectivity with the surrounding rocks. This secondary effect (or cavity enhancement) is often termed a 'halo' and serves to increase the effective target size, meaning the cavity may be indirectly sensed (Chamon & Dobereiner 1988; Bishop et al. 1997; Patterson et al. 1995).

The detectability of cavities in salt beds using gravity is well documented by (Speed, 1970). The detectability was assessed by comparing maximum anomaly amplitudes as a function of cavity depth, diameter thickness and ellipticity with values of precision of measurement and uncertainty of gravity background. The literature records some early examples of the application of microgravity techniques to detect cavities (Colley 1963; Arzi 1975). Neumann (1967) performed a microgravity survey to locate a buried concrete water tank reservoir, and also succeeded in tracing the existence of a subsurface gallery during the survey of an old quarry. Fajklewicz (1976) describes the application of vertical gravity gradient measurements for the detection of tunnels and rock caverns beneath Polish towns, whilst Butler (1984) applied microgravity and gradient techniques to the detection and delineation of shallow subsurface cavities and tunnels. Chamon and Dobereiner (1988) evaluated gravity, resistivity, magnetic and very low frequency (VLF) electromagnetic techniques over a mapped sandstone cavern system in the Amazon sedimentary basin. They concluded that: 'From all the methods used, the gravity survey was the only one which detected the presence of the cavern. It was observed that small caverns in sandstones, in the range of two to five meters in diameter, 40 to 50 metres below the surface can be detected by the microgravity method. It is important to mention that the gravity attraction of such small cavities would escape the sensitivity of the gravity meter. However, due to features associated with the cavern (dolines, collapsed structures, caves, porosity, etc.) it could be indirectly sensed…'. The cavity was subsequently investigated by topographic surveying and theoretical gravity profiles calculated from the known volume of the caverns. The observed microgravity anomalies were twice as large as those predicted from theory, again demonstrating the enhanced anomaly which is caused by secondary effects surrounding the cavity.

Al Rifaiy (1990) describes the use of microgravity to detect the presence of cavities associated with sink-holes in the Eocene Dammam Limestone in the Al-Dahr area 27 km south of Kuwait City. Negative gravity anomalies between -20 to -80 microgals were associated with the presence of sink-holes and their upward propagation through the overlying Kuwait group which consists of poorly cemented sands and gravels. Ghatge (1993) reports on the use of a small microgravity trial to detect shallow (only 2 to 3m below the surface) abandoned mine workings in New Jersey. Lyness (1985) discusses how gravity measurements can be used to detect mining subsidence. Most of these surveys relied upon data gathered along discrete profiles which can often fail to adequately sample the anomaly caused by a mass deficiency at depth. Emsley et al. (1992) and Bishop et al. (1997) describe the utilisation of the microgravity technique using gridded maps of data in the detection of both Karstic and man-made cavities. The papers also describe how the resulting data can be enhanced by image processing to better define the anomalies associated with the targets. In particular they describe how the microgravity data which we collected in Kuwait and which was described by Al-Rifaiy (1990) can be enhanced by subsequent data processing.

Yule et al (1998) describe the use of microgravity for the detection of cavities in a switchyard with the results confirmed by investigatory drilling. Patterson et al (1995) describe the use of the microgravity technique for the detection of dissolution subsidence in gypsiferous Permo-Triassic strata in Yorkshire. They assess the realistically achievable accuracy of their measurements to be c 4 microgals and on this basis postulate that voids as small as 4 metres diameter might be detected in

the right circumstances down to 12 metres. Recently the technique has been used with great success in the detection of old partially filled abandoned stope workings in Kalgoorlie Consolidated Gold Mines Open Pit even in the presence of very large terrain corrections caused by the topographic effect of the 250m deep excavations associated with the open-cut workings (Closed-File Report to KCGM 1997). A very valuable piece of information about an area which is underlain by cavities, is the amount of material which has been removed or lost from this area, in other words the mass deficiency. It is particularly useful in estimating the total mass deficiencies due to the presence of subsurface voids and is used to calculate the amount of grout required to fill the voids. This mass deficiency, which is the cause of the negative gravity anomaly, can be estimated by a mathematical theorem known as Gauss' theorem directly from the anomaly map without any prior knowledge of the exact location or nature of the targets.

The identification of the cause of the subsidence (i.e. a cavity or solution feature) is only the first objective of a site characterisation program. The stability and potential hazard posed by the migration to the surface and possible collapse of such a feature is an integral part of the remediation process. Time-lapse microgravity is a technique in which repeated microgravity surveys can be used to identify sub-surface density contrasts and monitor their development over time. The use of time-lapse microgravity to track the development of sub-surface density contrasts can provide a fast, real-time, cost-effective, monitoring technique, which has little or no impact on the residents or environment. Although microgravity surveys have become accepted practice in site investigations over the last ten years, time-lapse microgravity remains a relatively new discipline although examples of its use exist in the literature. Repeated microgravity surveys were used by Poeter (1990) to locate textural heterogeneities within the cone of depression caused by pumping in an unconfined aquifer. Pool and Eychaner (1995) also used time-lapse microgravity to monitor the movement of groundwater. In this case temporal-gravity surveys were used to directly measure aquifer-storage change and estimate values of specific yield. A forward inversion was performed by Hare et al. (1999) to investigate the potential of time-lapse microgravity to monitor the success of a proposed water injection in the Prudhoe Bay reservoir, Alaska. However, until recently (Rybakov et al, 2001), time lapse microgravity has not been used to detect and then monitor areas of low density in unstable environments. Rybakov et al. used repeated microgravity surveys to monitor the evolution of sinkholes at the western edge of the Dead Sea. Recent refinements have been made to this technique, including its application in a 4-D (temporal) mode, by the Applied and Environmental Geophysics Group at Keele University and these are reported in a number of papers, for example: (Styles 2003, 2004, Styles et al 2005) and in this paper.

3. Case Studies

3.1 The use of microgravity for the detection of abandoned Coal workings.

Extensive areas of the UK Coalfields were worked with shallow mining in the 19th C with few or no records kept of their abandonment. We have carried out many successful surveys to detect the presence, and state of stability of coal workings all over the UK.

3.2 Case Study: Shallow Coal Mining, Bristol

A major redevelopment scheme was proposed for the Longwell Green area of Bristol. The site was known to be underlain by abandoned shallow pillar and stall coal mine workings in the form of seams, tunnels and drifts and voids had been proved at depths of between 12 and 18m below ground level by rotary drilling. Typical void sizes ranged from 0.5 to 3.5m and clearly posed a significant hazard to the proposed development a retail Park with steel portal frame structures.

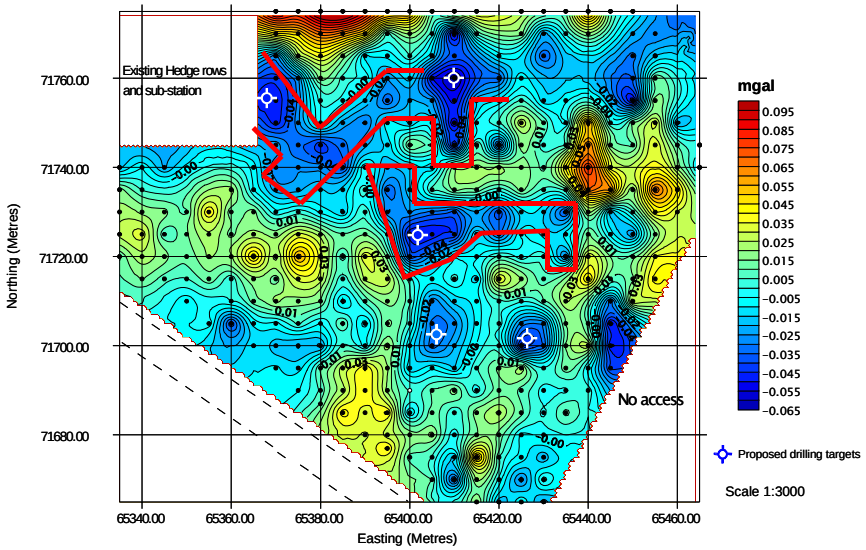


Figure 1 Microgravity map and drilling results showing an area of abandoned coal workings in Bristol, UK

A microgravity map at a 5-metre grid produced the above map after data reduction and clearly shows the presence of significant negative gravity anomalies. Drilling targets were selected on the basis of this map and the mine workings outlined in red were confirmed with voids identified at 12m to 14m below surface and the analysis of the gravity map predicts that the total mass missing from beneath the site was 995 tonnes which is a useful guide to the amount of remedial grouting required to stabilise the site.

4 Case Study The legacy of Chalk mining in the UK

Chalk has been extracted extensively in the United Kingdom for more than 4,000 years with excavations for flints at Grimes Graves, near Thetford in Norfolk probably being the earliest. From as early as Roman and Saxon times the flint was initially mined for building purposes while in later years the chalk bedrock itself was extracted and burnt to make lime for producing mortar and agricultural dressings and to aid the disposal of bodies from the epidemics which ravaged Britain in the period 1348 to 1666. Many parts of Kent and Sussex are pock-marked by ancient workings called dene-holes which are underground structures consisting of many small chalk mines entered by a vertical shaft. Several major towns have extensive areas which are underlain by historic Chalk

workings, most notably Reading, Norwich and the Blackheath and Lewisham districts of south east London.

4.1 Case Study : A2 Collapse Greenwich London

In April 2002 a major collapse occurred within the A2 (London to Dover road) where it climbs Blackheath Hill in southeast London. The collapse occurred after subsoil washed away triggering subsidence of chalk pits dating from the mid-Fifteenth Century (and possibly Roman times) through to the mid-Nineteenth Century. The collapse caused traffic chaos with extensive diversions for many months, a number of people were evacuated from their homes, and investigation and remedial works spanning ten months was carried out at a cost of several million pounds. An extensive microgravity survey was carried out along the spine of the road and in adjacent areas of land. After correction for the terrain effects of a number of low-rise residential blocks, the data revealed the presence of areas where chalk had been historically excavated primarily from beneath the edges of the road. It also indicated areas of the road underlain by undisturbed ground. Approximately 150 boreholes were sunk to prove the results of the gravity survey which showed excellent correlation with the identified areas of mass deficiency.

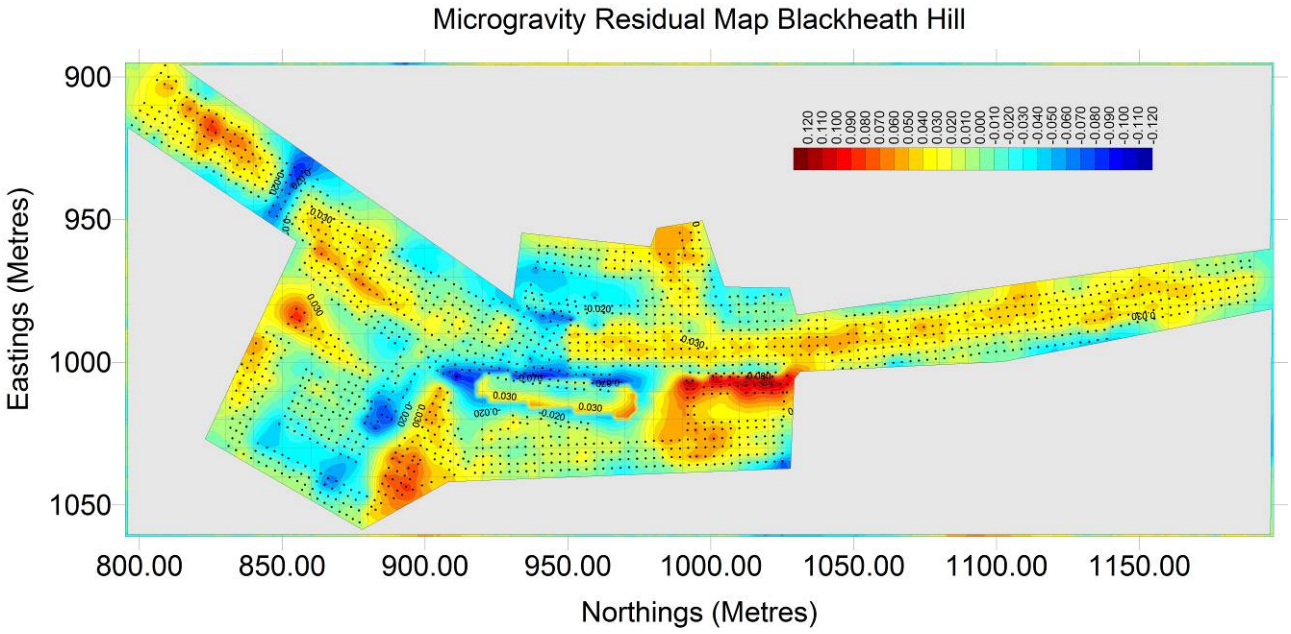


Figure 2 Residual microgravity map of a region of the Roman Road (A2) into London showing areas where chalk was excavated after the Black Death in the C15th and which recently collapsed

Similar microgravity surveys have been carried out in Norwich, Norfolk and Hatfield, Hertfordshire (Figure 3) where extensive areas of old chalk mines and quarries are present and chalk related subsidence has occurred since the last Century.

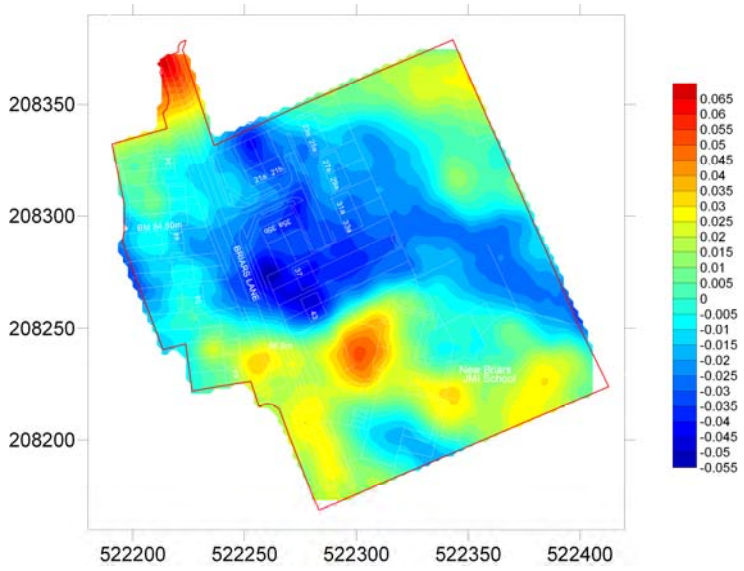


Figure 3. Microgravity Map showing an extensive area of chalk workings beneath Hatfield, Hertfordshire

5 Case Study Salt Mine Characterisation

5.1 Salt Mine stability evaluation using microgravity in Northwich Cheshire

Rock salt was first discovered in Great Britain in 1670 near Northwich UK. However, it is difficult to determine the exact number of mines that were sunk in the area as no official records were kept until 1873. Mining in Northwich was continuous and important from 1791 to 1928. Although the salt industry brought work and wealth to Northwich, the exploitation of the rock salt deposits has been accompanied by the serious problem of subsidence. Initially mining was concentrated in the upper salt bed, about 30m below the surface in a seam 30m thick. Later a second seam, also 30m thick, was found at a depth of 60m. Most of the upper level mines flooded and subsequently collapsed leaving large crater like holes. The likelihood of collapse was increased, as once the water running into the mineshafts became saturated, the “Bastard Brine” was pumped out in order to satisfy the continuing demand. The consequence of this action was the repeated drawing of fresh water into the mine dissolving the supporting pillars resulting in catastrophic collapse. The pumping of Bastard Brine became popular and many brine pumping shafts were established in the Northwich area. Again this accelerated the dissolution of salt at “Wet Rock Head” i.e. the area where the termination of the salt bed is in contact with groundwater. (If the salt bed terminates below the level of the local groundwater this surface is termed “Dry Rock Head”). More importantly however, the dissolution was uncontrolled and often occurred some distance away from the Pumping station. Subsidence was common throughout the town in the late 19th and early 20th Centuries and many of the houses built in that era were mounted on jacks so that they could be raised to the level of the road after a subsidence event. The town centre of modern Northwich is underlain by abandoned salt workings, which has led to significant planning blight and the threat of continued subsidence. We have used microgravity successfully in Northwich Cheshire to monitor upwards-propagating subsidence in Permian marls associated with salt dissolution occurring at the interface between marls and salt (wet rock-head). In this case the cause is continuing brine pumping which has led to the dissolution of salt at wet rock head and the associated collapse of the overlying Keuper Marls. In order to discriminate anomalies of this small magnitude careful field procedures, data reduction (including correction for the terrain effects of buildings) and interpretation procedures must be followed. However, with these procedures it is then possible to distinguish both the presence and the state of stability of most shallow and hazardous abandoned mine workings .



Figure 4 Location of Northwich, Cheshire, UK and specifically Peter Street where three repeat microgravity surveys have been acquired from 1998 through to 2002

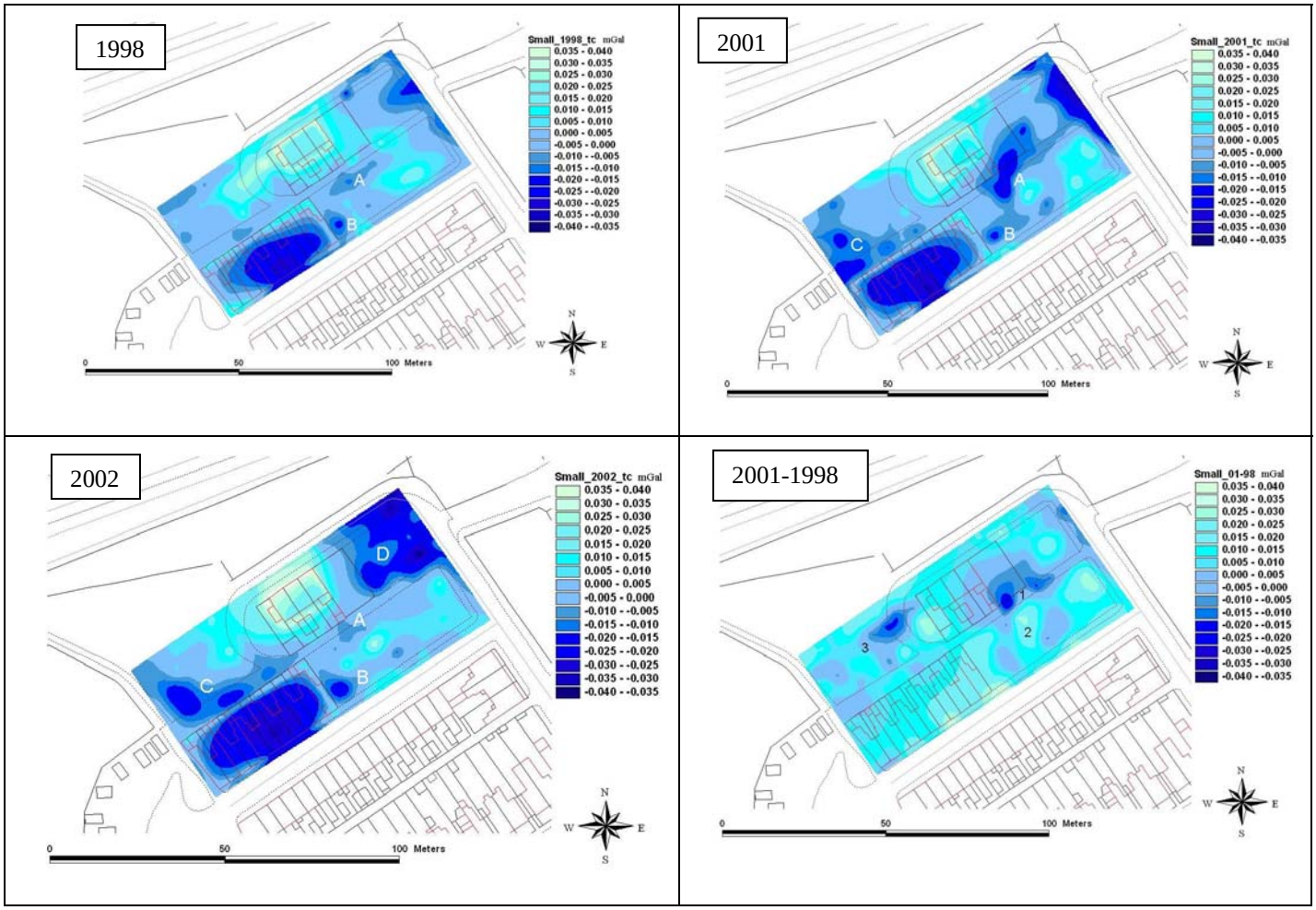


Figure 5 Contour map of the gravity data acquired in 1998, 2001 and 2002. The later surveys covered a larger area but extractsa which coincide with the original more limited survey have been selected. A first order polynomial has been removed from each set of data after the gravitational effect of the buildings has been corrected for. Negative gravity values are denoted by dark shades of blue. The final figure shows a contour map of the gravity change between 1998 and 2001.

A new variation called time-varying differential microgravity has considerable potential for detecting changes in mass distribution beneath an area and has the advantage that only a limited sub-set of the original survey need to be re-sampled to detect the time-varying part of the signal. This is particularly appropriate when known cavities or voids are being monitored to detect the onset or development of instability. Branston and Styles (2003) describe the use of time lapse microgravity in Northwich, Cheshire, UK (Figure 4). Peter Street is an area of terraced housing suffering from subsidence that was thought to be mine related. Microgravity and resistivity profiling were used on Peter Street to as non-invasive techniques to investigate the cause of subsidence. The first microgravity survey was carried out in the Peter Street area in 1998 (Simon Emsley and Sarah Corrie of Golder Associates) and in 2001 and again in 2002 by Keele University. The 1998 survey was carried out using a Scintrex CG-3M Microgravity Meter with three readings taken at each point in quick succession to ensure repeatability. The 2001 and 2002 surveys were carried out a Lacoste and Romberg D Meter (D-141), on a 5m by 5m grid with repeat readings at each point for repeatability and topographic heights of survey points measured to within 2mm for Free Air Corrections. In both surveys base readings were taken at the start and end of each day, and at hourly intervals between. Both surveys were processed to produce a residual Bouguer gravity map where the effect of drift, elevation and topography are removed. These are shown in Figure 5.

The 1998 survey detected an negative gravity anomaly (A) coincident with the reported area of subsidence,. Its amplitude is approximately -15µGal and the anomaly extends in a NE-SW direction. The results of the 2001 survey shows the main feature is a negative anomaly (B to C) of amplitude -60µGal trending from the NW to the SE which has grown in amplitude and steepened in gradient. A second anomaly (A) branches off this and trends towards the NE, the principal area of recorded subsidence. Through the use of various modelling techniques it has been shown how this change in the anomalies characteristics corresponds to a shallowing of the causative body. The results of the 2002 survey again show the main feature identified in the 2001 survey, a large negative anomaly trending NW-SE. Again a second linear anomaly can be seen to branch off this main anomaly towards the NE. However, the amplitude of this anomaly (A) has become less negative over the monitoring period, i.e the anomaly has reduced in amplitude and volume. This has been attributed to further shallowing and a reduction in volume of the body due to progressive collapse and infilling. A second, more localised anomaly (B), was recorded south of anomaly A. Anomaly B has an amplitude of -20µGal and is circular in extent. When we consider the 2002 survey some interesting aspects emerge. Although the monitoring period is shorter, it is evident that the area has also been active during this period. Interestingly, anomaly A has decreased in amplitude to -12µGal.. Anomaly B remains consistent with the 1998 and 2001 surveys. Its amplitude and extent has remained relatively constant. Alarmingly, anomaly C has continued its growth and now has an amplitude of -30µGal. The NE of the grid is the second area where the value of gravity has continued to decrease. Anomaly D appears to be the development of the NE extension of anomaly (A) seen in the 2001 survey. It has a large extent, some 20m^2, with maximum amplitude of -35µGal. Concentrating on the area of the 2001 microgravity survey that is coincident with the 1998 survey (it becomes evident that the area has been mobile between 1998 and 2001. Anomaly A has grown in amplitude and extent. Its amplitude is now -25µGal, and it has broadened towards the NE, extending onto the waste ground left by the demolition of the houses in 1985. Anomaly B is still evident although it appears to remain relatively constant in amplitude and extent. However, the area to the west has become increasingly negative resulting in anomaly C. The maximum amplitude in this area is -20µGal. Figure 5.d shows that there is a high degree of negative change in the area around the principal subsidence (1). The area of negative change also extends southwards towards Peter Street. At its maximum a change of -35µGal has been recorded This is well above the expected error of a time-lapse microgravity survey (~15µGal), and so we must conclude that the causative body, or zone has been active during this time period. Interestingly, there has also been a positive change in the area (2). This is also present in the difference plot

between 2002 and 1998. The cause of this will be investigated during the interpretative modelling. The other area of interest is in the west of the survey area (3). This area also shows a negative change with a maximum of -25µGal.

Branston and Styles 2003 found that Peter Street had subsided by up to 23cm between July 1998 and July 2001. The microgravity surveys showed that this subsidence is coincident with a low density gravity anomaly, and time-lapse microgravity shows that this low density anomaly has grown in size over the 3 year period. Modelling shows that the propagating edge of the low density body has risen by approximately 4m in the 3 years between surveys. Resistivity profiling supported the conclusions drawn from gravity data, suggesting an anomalous area coincident with the gravity and topographic lows.

6 Future planned work

The Institut National de l'Environnement Industriel et des Risques (INERIS), France, have identified an experimental site for the geophysical survey of salt cavities as part of the BCRD research program “Underground reconnaissance using geophysical methods applied to sounding and the detection of underground cavities” (Program BCRD-DRS-04/01). The site ‘Pistes de la Rape’ near Art-sure-Meurthe, Loraine, France is made up of 29 wells split into three main tracks that were mined by dissolution between 1971 and 1993. The resulting salt cavities are at depths of 110 to 180m in various shapes and sizes. Argillites overlie the salt roof and, as a result of a successive argillite disintegration mechanism, the cavities have migrated until a more resistant layer was reached. The cavities have been classified into 3 groups according to their location in relation to the geological formations:

1. The roof of the cavity is located along the base of the dolomite bed.
2. The cavity is entirely within the argillites.
3. The cavity has reached the salt roof.

An extensive programme of geophysical techniques in planned for Summer 2005 to determine their efficacy in characterising the stability parameters of salt mines. As part of the BCRD research program (BCRD-DRS-04/01) described above, the Applied and Environmental Geophysics Research Group of Keele University will carry out a microgravity surveys (normal and time lapse) at ‘Pistes de la Rape’, near Lenoncourt, Art-sure-Meurthe , Lorraine In July/August 2005. There are several different type of cavities exhibiting differing behaviours and they will be surveyed in order to differentiate the characteristic of these stability environments

1 **Zone 51. Piste 3** This is a zone of active collapse where a large cavity has breached the surface. The lateral extent of this cavity is uncertain and a set of profiles at 3 metres spacing will be collected to attempt to identify the spatial configuration of the subsurface void.

2 **Zone 31 Piste 1** This is not thought to be particularly active but a considerable number of other geophysical techniques will be trialled here and it is useful to have a complementary microgravity survey for integration into the synthesis of the interpretation. This area will be chosen for a 3-d grid of gravity data at 5 meters spacing over a zone of c 100 metres by 100 metres.

3 **Zone 41 Piste 2** This is a zone where activity is though to be high and which is likely to have significant on-going dissolution with associated instability. This area will be chosen for a 3-d grid of microgravity gravity data at 5 meters spacing over a zone of c 100 metres by 100 metres.

A second survey will be carried out over the same area Zone 41 in July/August 2006 using the same equipment and techniques in order to determine the changes in microgravity which have taken place and the associated changes in sub-surface void configuration.

7 Conclusions

A wide range of microgravity investigations have now been carried out in the UK over many types of abandoned shallow mines including coal, chalk, tin and salt. In all of these environments the microgravity method has proved to be a useful tool for the detection, delineation and characterisation of subsurface cavities and this has been validated by extensive progammes of drilling (150 boreholes for the A2 collapse in London). The agreement between predicted and proven cavities has been extremely good, leading to the technique becoming widely used in site investigations where abandoned mine-workings are suspected to exist.

In selected areas, it has been possible to carry out repeated surveys in order to investigate the temporally varying componet of the microgravity field. Over intervals as short as a year significant changes in gravity have been deteced and have been shown to be assoiated with areas of enhanced subsidence. This technique has the advantage of removing the need for terrain and geological corrections as they are identical between surveys. Areas of maximum subsidence and potential collapse can be identified and treated by grouting to stabilise the area.

The technique has equivalent application for karst cavities as shown by Styles et al (2005) and also for the detection of piezometreic changes in aquifers and mine-water rebound.

References

Arzi, A. (1975). *Microgravity for engineering applications*. Geophysical Prospecting, 23, 408-25.

Bishop, I., P. Styles, S. J. Emsley and N. S. Ferguson., (1997), *The Detection of Cavities Using the Microgravity Technique: Case Histories From Mining and Karstic Environments* in “Modern Geophysics in Engineering Geology”,

Branston M. W. and Styles, P., (2003), *The application of Time-Lapse Microgravity for the Investigation and Monitoring of Mining Subsidence*. QJEG, 36, 231-244).

Butler, D. K. (1984). *Microgravimetric and gravity gradient techniques for the detection of sub-surface cavities*. Geophysics, 49, 1084-96.

Chamon N. and Dobereiner L. (1988). *An example of the uses of geophysical methods for the investigation of a cavern in sandstones*. Bulletin of the International Association of Engineering Geology, No. 38, Paris, 37-43.

Colley, G. C. (1963). *The detection of caves by gravity measurements*. Geophysical Prospecting, 11, 1-10.

Cripps, J. C., McCann, D. M., Culshaw, M. G. and Bell, F. G. (1988). *The use of geophysical methods as an aid to the detection of abandoned shallow mine workings*. Institute of Mining Engineers, MINESCAPE 88, Harrogate.

Daniels, J. (1988). *Locating caves, tunnels and mines*. Geophysics: The Leading Edge of Exploration, 7, No. 3, 32-7.

Emsley, S. J., Summers, J. W. and Styles, P., (1992). *The detection of subsurface mining related cavities using the micro-gravity technique*. Proc. Conf. Construction over Mined Areas, Pretoria, South Africa., May 11-12 1992., 10p.

Fajklewicz, Z. (1976). *Gravity vertical gradient measurements for the detection of small geologic and anthropogenic forms*. Geophysics, 41, 1016-30.

Ghatge S. L. (1993). *Microgravity method for detection of abandoned mines in New Jersey*. Bulletin of the Association of Engineering Geologists, 30, 79-85.

Hare, J. L, Ferguson, J. F., Carlos, L., Aiken, and Brady, J. L. (1999). *The 4-D microgravity method for waterflood surveillance: A model study for the Prudhoe Bay reservoir, Alaska*. Geophysics 64 No 1, 78-87.

Lyness, D. (1985). *The gravimetric detection of mining subsidence*. Geophysical Prospecting, 33, 567-76.

McGrath, R.J., Styles, P., Thomas E. and Neale, S., (2002), *Integrated high resolution geophysical investigations as potential tools for water resource investigations in karst terrain*, Environmental Geology, 42: 552-557.

Neumann, R. (1967). *La gravimetrie de haute precision - application aux recherches de cavities.* Geophysical Prospecting, 15, 116-34.

Patterson, D. A, J.C. Davey, A.H. Cooper, & J.K. Ferris, (1995). *The investigation of dissolution subsidence incorporating microgravity geophysics at Ripon, Yorkshire*. Quart. Jour. Eng. Geol. 28, 83-94.

Poeter, E. P. (1990). *A new tool: delineation of textural heterogeneities in unconfined aquifers, using Microgravity surveys during pumping*. Bulletin of the Association of Engineering Geologists, 27, No 3, 315-325.

Pool, D.R., and Eychaner, J.H., (1995), *Measurements of aquifer-storage change and specific yield using gravity surveys*. Ground Water, v. 33, no. 3, p. 425-432.

Rybakov, M., Goldshmidt, V., Fleischer, L., and Rotstein,Y., (2002). *Cave detection and 4-D monitoring: A microgravity case history near the Dead Sea*. The Leading Edge 20, no. 8, 896-900.

Speed, R. C., (1970).*Gravity Anomalies from Cavities in Salt Beds. I. The surface Field*. Northern Ohio Geol. Soc. Third Symposium on Salt, 2, 367 – 385.

Styles P. (2003). *Environmental geophysics: a site characterization tool for urban regeneration in the post-mining era*. Geology Today, 19 (5), 173-178.

Styles P. (2004). *Detection of Caves by Microgravity Geophysics, Bahamas*, in Sinkholes and Subsidence, (Waltham, Bell and Culshaw Eds.), Springer, 317-321.

Styles, P., McGrath, R., Thomas E and Cassidy N.J. (2005), *The use of microgravity for cavity characterisation in Karstic terrains*. Quart J Eng Geology., 38, 155-169.

Yule, D., E., Sharp, M., K., and Butler, D., K., (1998), *Microgravity investigations of foundation conditions.* Geophysics, 63, No. 1, 95-103.

SOLUTION OF UNDERGROUND MINE GAS EMISSIONS ON SURFACE OF ABANDONED MINING SITES WHERE STEEP DEPOSITED COAL SEAMS HAVE BEEN EXPLOITED

TAKLA Georges[1], FROML Karel[1]

[1] OKD, DPB, a.s. Rude armady 637, 739 21 Paskov, Czech Republic. gtakla@dpb.cz; kfroml@dpb.cz

ABSTRACT: The solution of uncontrolled gas emissions from abandoned underground coal mine sites in Ostrava-Karvina coalfield to surface ground in connection with old mine shafts and drifts and with old mining workings in horizontal and inclined coal seams has many forms. It varies according to geological and mining conditions and the disposition of the site surface. Since four years the gas emission risk has appeared in the area of former exploited vertical coal seams within the historical centre of Orlova town, which is protected by State Monument Protection office. A project based on such special nature of mining-geological and urban conditions was elaborated and already implemented.

KEYWORDS: mine gas, emissions, degassing boreholes

RESUME: Les émissions de gaz non-controllés provenant de mines de charbon souterraines abandonees dans la gisement d'Ostrava-Karvina et se propageant dans les terrains de surface par l'intermédiaire des anciens puits et d'anciens travaux miniers dans des couches horizontals ou inclines, prennent des formes différentes. Elles varient selon les conditions géologiques ou minières et la disposition de la surface. Depuis 4 ans, un risqué lié aux emissions de gaz est survenu dans des zones autrefois exploitées verticalement dans le centre historique de la ville de Orlava, protégée par l'office national de protection des monuments. A project base sur la nature spécifique des conditions urbaines, minières et géologique a donc été élaboré et déjà implémenté.

MOT-CLEFS: gaz de mine, emissions, sondage de dégasage

1. Introduction

The Ostrava-Karvina coalfield (OKR) is the most significant Czech coal deposit. It covers an area of about 1,600 square kilometres. This area constitutes to about 20 % of the Upper Silesian Coal Basin, which straddles the Polish / Czech frontier. Within that area, about 335 km^2 belong to mining claims of individual collieries.

Some of the collieries are already closed. Coalmines closure does not mean that methane liberation into the underground abandoned areas would be stopped.

After closure water level in the abandoned Mines is being kept at a level of about 600 m under the surface in order to prevent the flooding of the water into the active mines via many natural and manmade communications. The water is being pumped in two sites by means of submersible pumps installed in unused mine shafts.

During this stage some mine gas may leak to the surface via natural migration channels and old mine shafts. This migration is greatly influenced by rapid drops in atmospheric pressure. A risk of explosion or fire would occur in the basements of buildings or industrial plants in the densely populated regions of Ostrava and Karvina. A complete system of gas extraction, gas monitoring and

safety measures is being built to prevent the uncontrolled gas emissions to the atmosphere and to ensure the inhabitants safety.

Due to divers mining geological conditions in particular endangered zones any universally applicable procedures for effective reducing of such danger cannot be defined

As a consequence of rock forming processes in distant geological past changes of situation of parts of originally horizontal deposited Carboniferous sedimentary coal bearing measures occurred in such a way that these measures were loaded by rock stress effects, lifted, deformed and their horizontal deposition was transformed to an inclined, steep or even opposite dip deposition. At the same time a number of divers tectonic zones with various parameters arose.

There are coal-bearing measures with steep deposition of coal seams in Ostrava-Karvina coalfield such as its western periphery (western saddles) and eastern periphery of Orlova structure (opposite dip fold). With no Miocene overburden (outcrops) – see Figure 1.

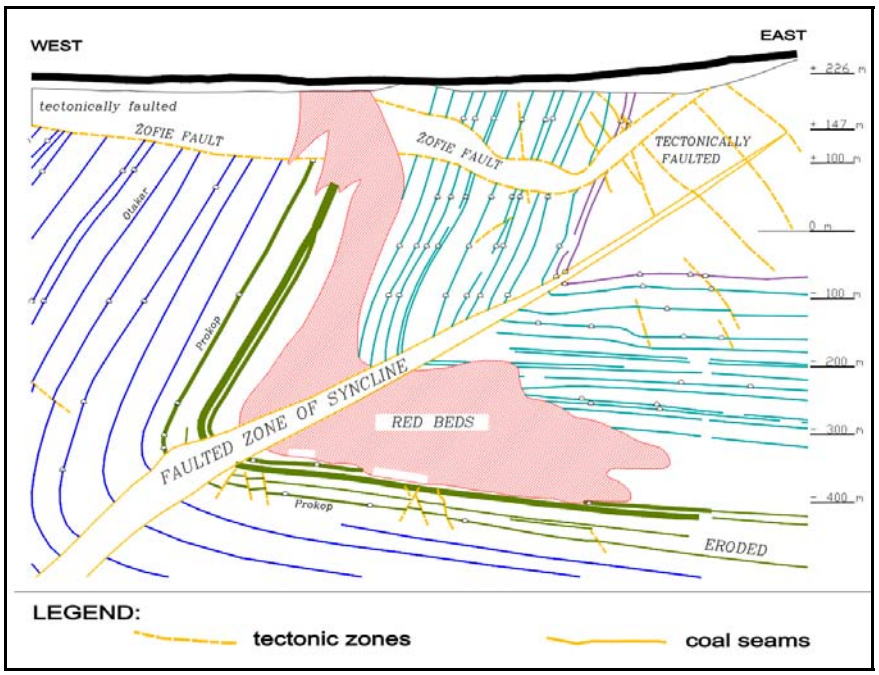


Figure 1. Vertical geological east-west section below historical centre of Orlova City

Above the eastern periphery of Orlova fold structure with discontinuously mined out coal seams the historical centre of the town of Orlova extends, this centre is protected by State Monument Protection Office.

Beginning of exploitation of hard coal below the historical centre of Orlova town is dated in 1817. Mining of coal seams outcrops was concerned. In 1841 next to a „Carboniferous window“ (outcrops) among other the prospecting shafts Jirí N^{o} II and Shaft N^{o}3 – Racok were sunk. They should be basis of future underground coalmine. Due to enormous methane emission mainly from the Shaft Jirí II they were interconnected by a tracing drift underground. However, any coal mining did not start and the shafts were filled about 1860.

Due to methane emissions in this area and to gradually verified complicated geological structure of Carboniferous formation the coal mining below historical centre of Orlova town started only at fifties of last Century.

At the end of the seventies of last century coal working in steep coal seams was terminated and the centre of town was influenced by mining of the same group of coal seams of flat development eastwards of syncline of opposite dipped Orlova fold – see Figure 1. In professional literature a number of locations are mentioned where methane from Carboniferous formation was emitted freely to surface ground and this circumstance was the reason of several ignitions and explosions that caused burns of some persons and destruction of premises.

The first written reports about such events are dated at the end of XIXth Century. After termination of controlled removal of methane from underground areas by means of main ventilation and of gas drainage (degasification) and after subsequent closure of underground coal mines intense mine gas emissions were detected during 2001 in several areas of the town of Orlova – see Figure 2.

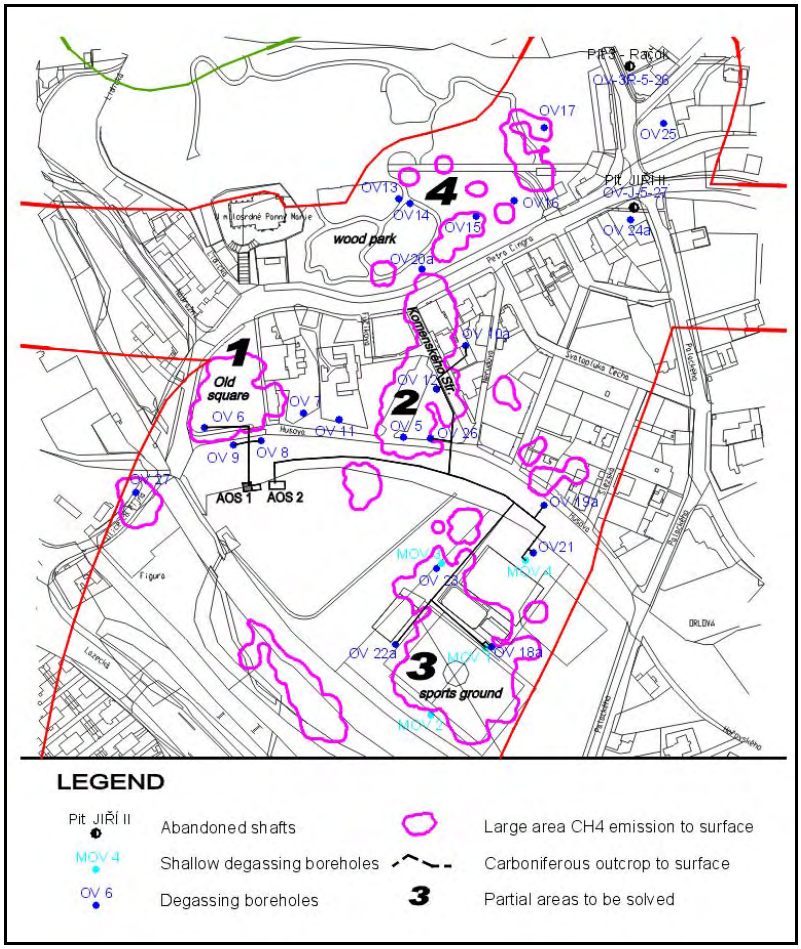


Figure 2. Purpose.-aimed map of historical centre of the town of Orlova

2. Geological structure and scope of mining – out of coal seams

Below the area of interest in Orlova town a coal-bearing Carboniferous formation approaches to earth surface by its Ostrava-Karvina ridge, which runs across total coal deposit in east-west direction. The Carboniferous emerges to earth surface through Carboniferous outcrops, out of which a single one enters from northwest the overburden below the built-up area of Orlova town centre. Here a mean thickness of only 4 meters of overburden overlying the Carboniferous formation has been detected. The overburden consists here exclusively of Quaternary mostly sandy sediments and by made-up grounds. Tertiary, Miocene sediments participate in structure of overburden formation

only northeastwards from Orlova town centre. Carboniferous formation of the area was enormously loaded and transformed in its geological past. By rock forming processes the deposit was folded and structured by tectonic faults. Between today Orlova and Petrvald municipalities the Orlova fold was shaped. Therefore, the originally horizontal coal seams have been deposited steeply, vertically or even toppled over to opposite dip, see Figures 1 and 3. The centre of the town of Orlova is located above the eastern wing of toppled-over Orlova fold. The layers of strata including coal seams are oriented from southeast to northwest. However, they are faulted in east-west direction by the Sophia fault with dipping of strata southwards. This tectonics and a near almost parallel demarcation between mine fields of former Sophia and Doubrava collieries did not allow to mine out the coal seams continuously. Therefore, residual pillars remained within coal seams between the demarcation and the Sophia fault.

Beginning at about 80 m depth below earth surface 16 coal seams were mined out in a variable extent – see Figure 3. In north-south direction the coal seams were structured due tectonic causes or also due to solving of spatial relations between the two mines (work on demarcation boundary) into two or three mining blocks. Mining of other coal seams of such measures was advanced only at greater mining depth.

The Sophia fault enters the Carboniferous relief between Old Square and church in the historical centre of the town and it is continued further eastwards.

The mined-out underground areas were as a rule backfilled. In the oldest ones marl balls were applied, further then sand, filled marl or eventually filled stone.

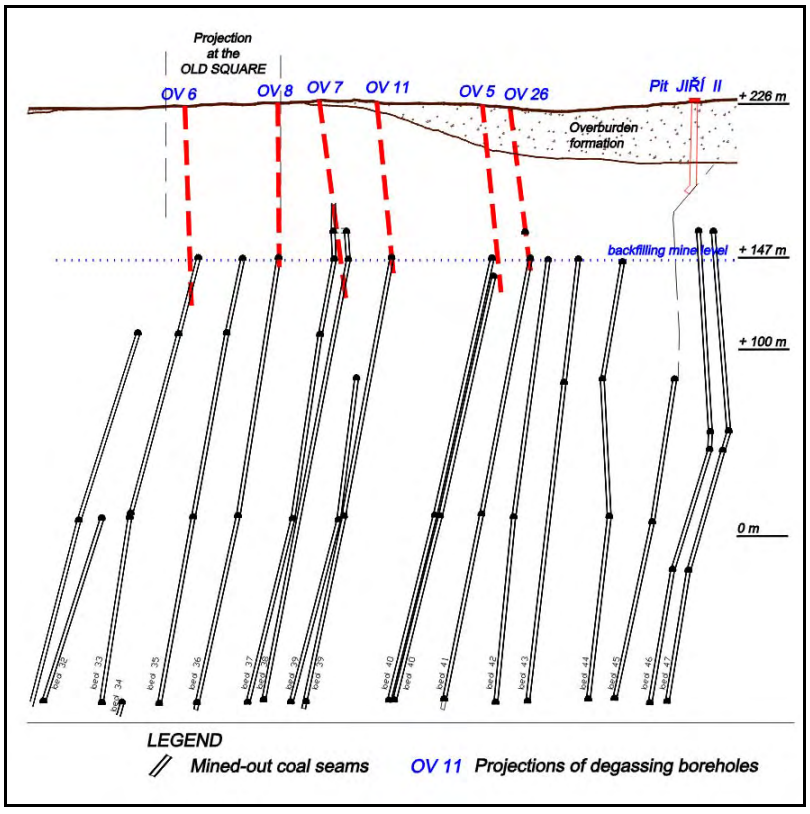


Figure 3. Schematic geological east-west section below the town of Orlova with projections of degassing boreholes

3. Principal solution of uncontrolled mine gas emissions to the surface

The main factor influencing the uncontrolled mine gas emissions to the surface are the natural (tectonic faults) and artificial manmade (shafts, drifts etc.) communications between the surface of abandoned mines area and the gobs in their underground. The intensity of such emissions depends on the differences of air pressure and temperature between the surface and the underground. The changes of barometric pressure and their gradient have the principle influence.

The risk of mine gas migration to the surface is higher in abandoned mines areas where gobs are near the surface. In the methodology of the classification of the ground surface from the point of view of the potential risk of mine gas migration, worked out by the Authors´ Company, two critical limits are being accepted

- the thickness of the overburden of the Carboniferous layers is less or equal to 50 m. These areas are classified as imperilled
- the depth of the gobs under the surface is less or equal to 100 m and simultaneously the first condition (limit) is fulfilled. These areas are classified as dangerous. Also the area within 25 m around the old mine shafts is considered as dangerous.

This classification has to be verified by so called methane screening which is a atmogeochemical measuring of CH_4 and CO_2 contents in the soil in 1,2 m deep test pits. This measuring is usually done when a drop of barometric pressure is registered.

In the dangerous area a system based on the assessment of geological and mining situation is implemented. This system consists of following items.

- Drilling of degassing boreholes into the upper gobs.
- Long-term gas exhausting tests on drilled down degassing boreholes and their complex evaluating in relation to reaching scope of applied under pressure and to identification of existing communication ways of mine gas migration among the boreholes themselves and among them the and complex of adjacent gobs.
- A controlling methane screening is applied to verify the effectiveness of degassing boreholes.
- If the results of the methane screening don’t confirm that the already drilled boreholes are effective, other complementary boreholes are drilled and/or the boreholes are connected to exhausting station.
- A special attention is drawn to looking over the state of the buildings on the dangerous areas to assess the risk of mine gas penetration into their interiors. If such risk exists the identified premises of buildings are maintained and/or equipped with CH_4 sensing units with signalling of exceeding of limit values.

4. Hitherto the measures that have been realised in Orlova

In order to have the mine gas emissions to the surface under control and to protect the inhabitants and the buildings in the historical centre of Orlova town the following measures and activities have been implemented.

- Searching for and definitive securing of 10 old mine shafts in cadastre territory of Orlova in accordance with special rules issued by the Czech Mining Authority in Prague.
- Basic surface survey by measurement of CH_4 and CO_2 concentrations in soil air (methane screening) by application of atmogeochemistry method within an area of about 70 ha.

- According to configuration of evidenced CH_4 surface emissions the centre of Orlova was structured into the following 4 zones – see Figure 2:
  1. Old Square,
  2. Environs of Komensky Street,
  3. Sports ground,
  4. Wood park.
- Drilling of particular degassing boreholes has been proposed in view to structuring of gobs and to surface situation in the above-mentioned 4 zones of town centre, i.e. it is a compromise between mining geological situation, layout of built-up area and ground configuration. A selected compromise, however, should guarantee the assumed effectiveness of degassing boreholes – see Figure 3.
- Drilling down of 4 shallow and 23 deep degassing boreholes into gobs of exploited seams – see Fig. 2.
- Performing of 25 exhausting tests including their evaluation.
- Building and installation of two gas exhausting systems AOS 1 and AOS 2 connecting 3 and 8 degassing boreholes to exhausting stations. The results of the exhausting tests and of the continuous monitoring of degassing boreholes, buildings and sewerage have demonstrated that the passive function of the degassing boreholes in connection with the changes of barometric pressure does nut ensure the safety of the surface buildings and inhabitants – see Figure 4.



Figure 4. Gas exhausting station of AOS 1

- Evaluating of basements of buildings and of sewerage system in view of risk of methane penetration and implementation of their ensuring against methane penetration and/or their partial reconstruction.
- Installing of 22 methanometric central units and of 56 methane-sensing units in endangered buildings and their regular monitoring (among them 18 electronic units with remote transmission).

- Realization of architectonic solution of fences of newly installed constructions in order to be in accordance with the requirements of State Monument Protection office – see Figure 5.
- Continuous safeguarding of emergency service for solving of extraordinary events.



Figure 5. Architectonic solution of fence of the chimney of degassing borehole

5. Results and recommendations

Based on evaluation of work on controlling of large area mine gas emissions to surface in historical town centre of Orlova which extends above gobs of steep deposited coal seams the following results can be formulated and recommendations.

- Communications between gobs of particular coal seams, the distances between which oscillate within range of 1 to 50 m, have a very low permeability for mine gas mixtures. This reality has been proved by measurement.
- The gobs of longwalls in steep deposited coal seams indicate a very high consolidation, i.e. they have a very low gas permeability – this knowledge results from low gas permeability of degassing boreholes if they did not contact return roadways or connecting drifts.
- Due to the above-mentioned experiences it is necessary to drill down boreholes to gob roadways in every particular coal seam or to connecting drifts.
- The number of degassing boreholes is to be specified by means of checking measurements of mine gas components in soil air and their reaching range during exhaust tests.
- Based on results of checking measurements of CH_4 and CO_2 concentrations in soil air and on evaluation of exhaust tests the necessity of installing of local autonomous exhausting systems on suitable degassing boreholes is not excluded.

- The measures gradually implemented in Orlova town since the second half of year 2001 have proved their eligibility. In 2005 the maximal content of CH_4 in sewerage system has never exceeded the value of 2 %. This is an excellent result in comparison with the content of CH_4 measured in 2001: 16 % in the buildings, 60 % in the sewerage network and 80 % in the soil.
- The recently installed system consisting of CH_4 and CO_2 monitoring and exhausting has to be kept in operation probably for many years. This depends on the future of actually active collieries, which need not to raise the level of water in the underground as stated in chapter 1 of this presentation.

6. Conclusion

The complex system implemented in Orlova town to control the mine gas emissions to the surface in the area of abandoned coalmines has proved its eligibility.

In the nineties of last century the question of methane migration to the surface was solved only after some accidents and emergencies linked with this problem.

In the year 2002 the government of the Czech Republic decided to give an important sum of 800 million Czech Crowns (about 27 million Euros) to elaborate and realize a project of protection of about 30 km^2 in Ostrava-Karvina region from the risk of uncontrolled mine gas emissions to the surface.

The measures taken in Orlova are considered as a pilot project within the mentioned project in the region. In the time being this project has been already elaborated with an important contribution of Authors´ Company. It is expected that its realization would start in the beginning of the year 2006.

MICROSEISMIC MONITORING OF ABANDONED SALT MINES BENEATH NORTHWICH, CHESHIRE, UK.

TOON Samuel[1], STYLES Peter[1]

[1] APPLIED & ENVIRONMENTAL GEOPHYSICS RESEARCH GROUP, Keele University, School of Physical & Geographical Sciences, Keele, Staffordshire, ST5 5BG, United Kingdom; s.m.toon@esci.keele.ac.uk; p.styles@esci.keele.ac.uk

ABSTRACT: Northwich town centre is underlain by abandoned salt mines that are in imminent danger of collapse. The mines are being filled with grout in the next 3 years. We started microseismically monitoring the mines in 2001 to evaluate the stability of the mines before, during and after the remediation process, which should be completed in 2007.

KEYWORDS: Salt-Mine, Microseismic, Regeneration.

RESUME : Le centre de la ville de Northwich se situe à l'aplomb de mines de sel abandonnées en danger imminent d'effondrement. Les mines vont être remblayées avec un coulis, dans les 3 années à venir. Nous avons commencé une surveillance microsismique en 2001 pour évaluer la stabilité des mines avant, pendant et après le processus de remédiation, qui devrait être achevé en 2007.

MOTS-CLEFS : Mine de sel, Microsismique, Régénération.

1. Introduction

The Cheshire Salt Field has been the site of salt mining and wild brine pumping from Roman times for industry on Merseyside and Cheshire. Whilst mining under Northwich ended in 1928 there has been a history of continuing subsidence. Salt and brine extraction formed the basis of mid-Cheshire's chemical industry, the primary economic force for the area, up to the 1960's. Since then progressive and continuing re-structuring of that industrial sector has presented local authorities with severe social and economic regeneration issues. The ability to respond to these challenges has been jeopardised by the presence of large areas of unstable land extending beneath parts of Northwich's shopping, commercial and residential centre. Vale Royal Borough Council and English Partnerships commissioned work to attempt to identify the remedial action necessary to secure permanent ground stability and money (£30,000,000) has now been allotted to deal with remediation of this area.

Many mines are experiencing the onset of potential pillar failure. Saturated brine has been pumped into the cavities at certain times to arrest dissolution by freshwater from the River Weaver, of the salt pillars supporting the town centre. A magnitude 1.5 earthquake (11/9/1997 at 52.23 N, 2.42 W) just to the south-east of Northwich is likely to be associated with incipient instability underlining the threat to the town centre either by direct impact on the substructure or by disturbance of groundwater regimes. Until 1988 there were no indications of the mines becoming unstable. However, geotechnical engineering consultants, on behalf of a commercial developer undertook some initial investigations into Baron's Quay Mine, concluding the mine would eventually become

unstable. This alerted the Borough Council and application was made to the DOE and English Partnerships for derelict land grants to carry out further investigations into the four mines to establish their life expectancy and to examine stabilisation materials and techniques. An analysis of the data from sonar measurements in a further series of boreholes has confirmed the conclusion that the condition of the salt pillars which support the roof of the mines is deteriorating and may result in the eventual collapse of the mines and that in the case of the Witton Bank mine the salt pillars supporting the roof may well have entered the tertiary creep phase and subsidence at the surface may start to occur within the next 5-15 years. The subsidence may lead to structural damage to buildings affected by the mines.

The mines will be remediated by a programme of grouting using PFA grout which will be pumped into the ground at specified sites to support the roof while the brine will be withdrawn and removed from the site for reprocessing. The remediation started in early 2005. In order to monitor the state of stability of the area before, during and after the remediation phase, a network of up to ten microseismic stations has been deployed over the area of the mines to detect any changes in ambient microseismicity.

2. Seismic network

We have deployed a network of up to 10 seismic stations around Northwich town centre. The network is shown is Figure 1. Each station has either 1 or 2 4.5Hz or 30Hz triaxial geophones deployed in a borehole at depths varying from 50 to 120 metres. The data is acquired using ISS SAQS intelligent seismometers at the surface, with telemetry communication via radio modems to a central Run Time System (RTS) computer in Northwich. The individual SAQS log all detected events to hard disk, and also transfer the data to the RTS. The RTS associates the data from each station into events, which are automatically processed to give a preliminary location and magnitude. The events are then emailed to a processing system at Keele University for further analysis. The RTS can raise alarms based on various criteria which are then emailed and/or sent as SMS text messages to a mobile phone. The SAQS work in standalone mode and continue to log data even if they lose communications with the RTS. The network has been operational from July 2001 and it is planned that it will continue to operate until a year after the infilling of the mines has finished in mid 2007.

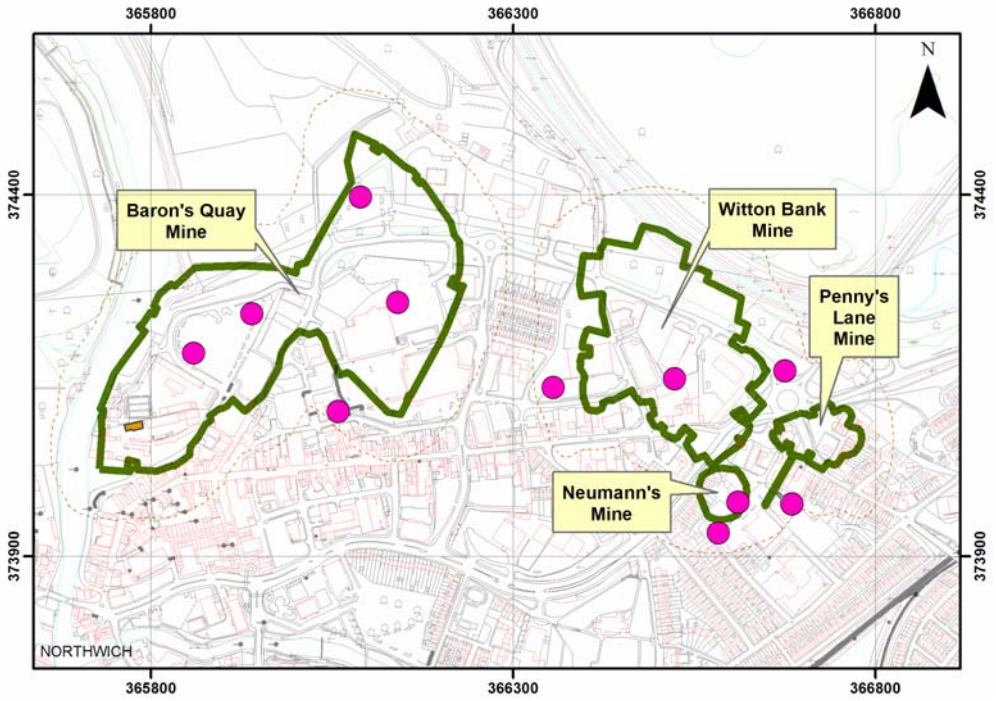


Figure 1 – Map showing the location of the seismic stations in Northwich town centre. The mines are shown by the thick green lines. Basemap © Crown Copyright Ordnance Survey. An EDINA Digimap/JISC supplied service.

3. Seismicity

We have detected low levels of seismic activity around the mines. Most of the events are so small that we only detect them at 1 or 2 stations. Most of the events occur in the Penny's Lane area and there also appears to be cyclicity to the event rate during the week (Figure 2). The seismicity rate shows clear peaks on Wednesday and Friday. It is unclear what is causing this cyclicity, but it may be related to wild brine pumping in the area.

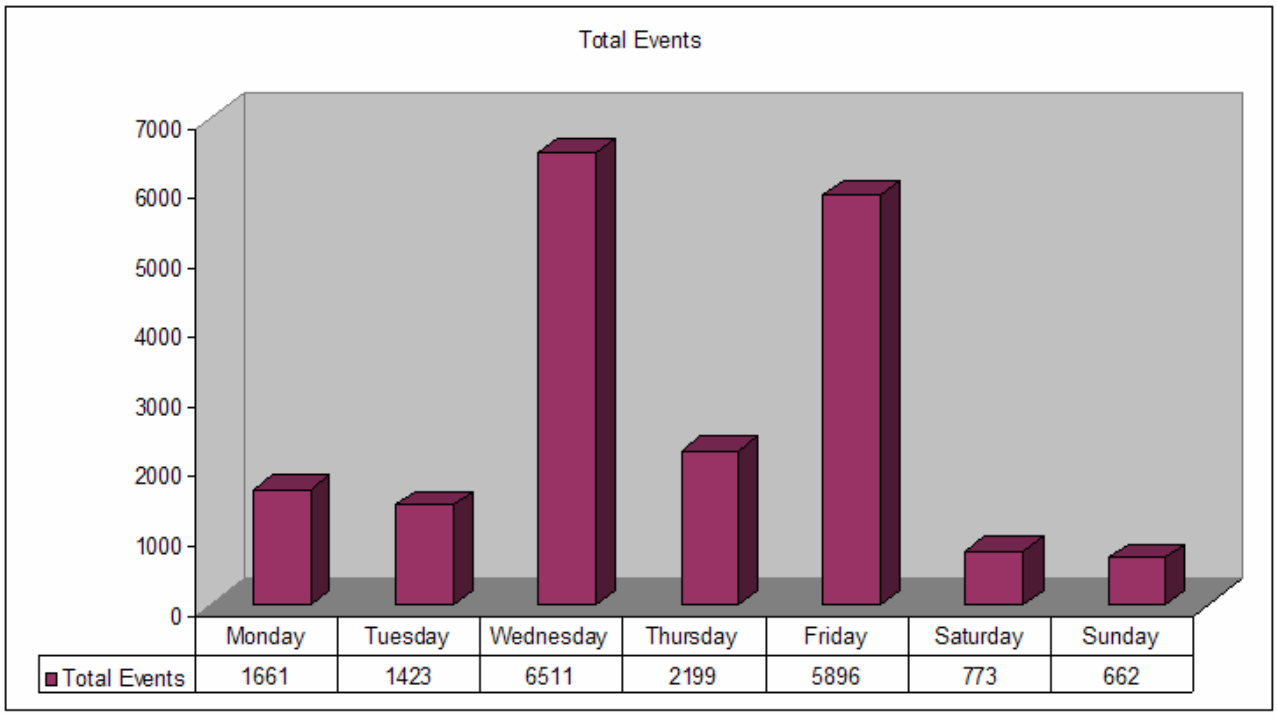


Figure 2 – Number of events per day (to 21/08/2005). There are clear peaks in the number of events on Wednesday and Friday.

4. Source Mechanisms

Two distinct types of seismicity have been detected during this monitoring. The first, but rarer event family, has normal shear type mechanisms and corresponds to MODE II failure, i.e. no-volume change mechanisms. We expect these in any mining situation where reasonably large tri-axial stress systems become established and have seen them often associated with microseismicity around long-wall coal mines (Bishop et al 1994, Jackson et al 1997, Ren et al 2001. An example of this type of event is shown in Figure 3. The fault plane solution for this event is a vertical fault with vertical slip downwards which would suggest roof failure as the mode of failure.

The second family, which comprise small but frequent events such as we see in the Penny's Lane area of the mines are most likely to be MODE I, dilatational failures, associated with bed separation in the marl roof overlying the salt. An example of this type of event is shown in Figure 4. They are associated with volume change and are common where dilatant micro-fracturing is occurring. We have observed this type of "harmonic tremor" activity associated with outbursts of methane in anthracite mines (Styles 1995). In this context we think that their geomechanical implication is the progressive spalling of the marl roof over a propagating void which is migrating, albeit slowly in this case, toward the surface. Time-varying Microgravity observations (Branston and Styles 2003) have shown this type of behaviour over a region of significant subsidence outside the main area of mining.

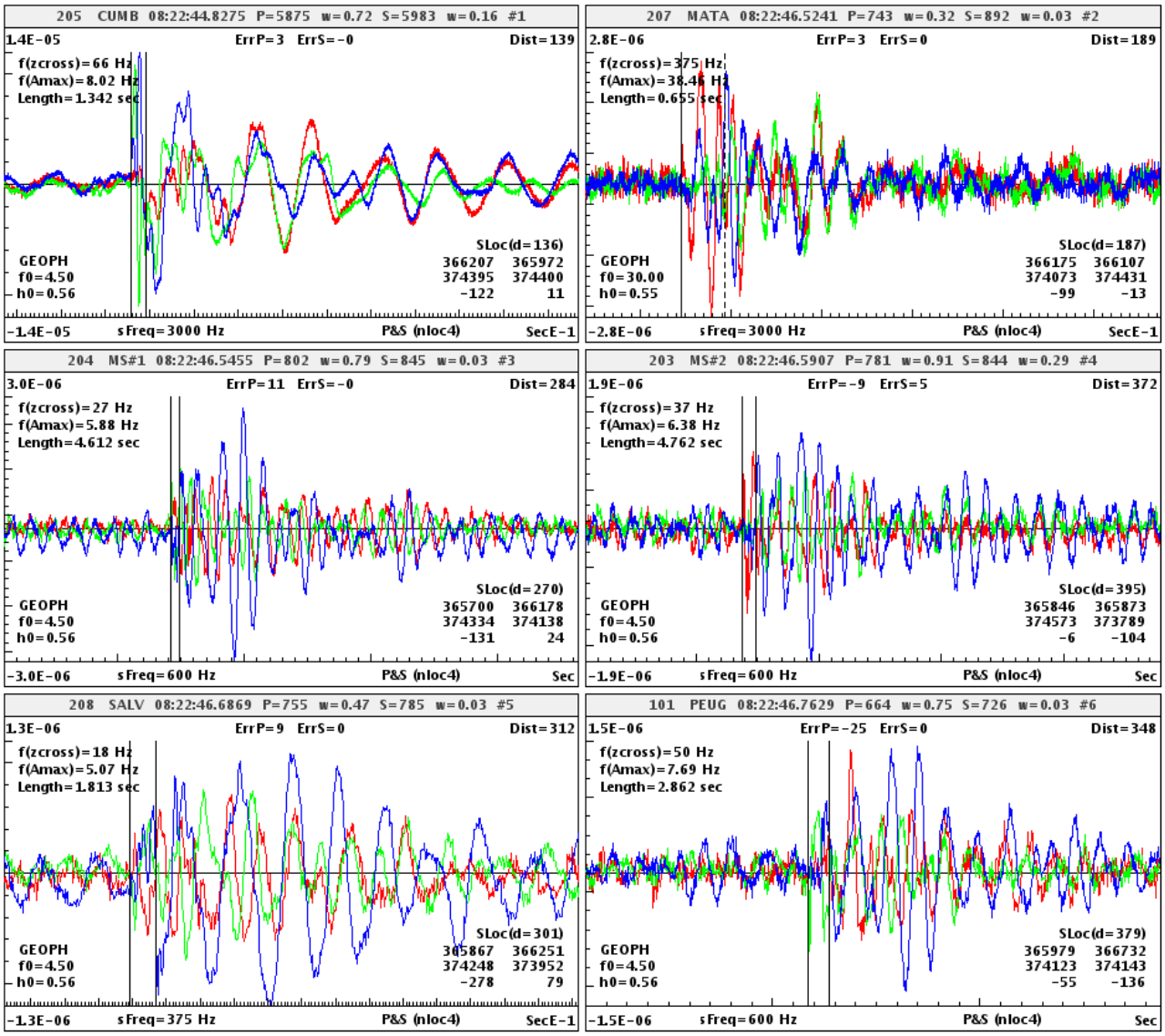


Figure 3 - A shear type event detected on 11th March 2003 on most stations in the network. This event was located below an area of high subsidence at ground level.

5. Conclusions

There are low levels of seismic activity around the mines and therefore from a seismic point of view the mines appear to be stable. There are a few hot-spots of seismic activity but apart from the activity in the Penny's Lane area, none of them are long term. The seismicity generally falls into two categories of event – Shear type (Mode II) events that we would normally expect around a mine and dilational (Mode I) failures that may be associated with bed separation in the roof above the mines.

Microseismic monitoring can be a powerful tool to use to monitor abandoned mines and cavities as it is a passive technique and samples the whole rock mass rather than specific points as in conventional geotechnical techniques.

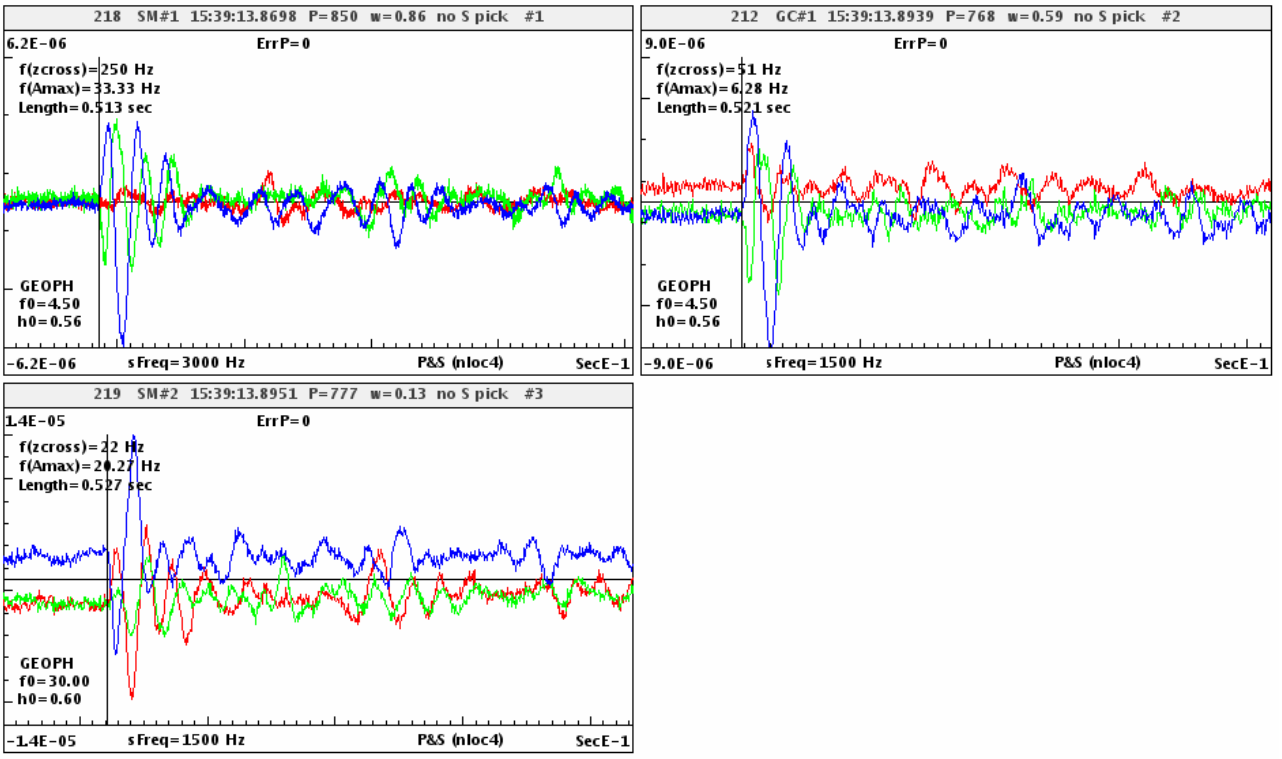


Figure 4 – Event from Penny's Lane area showing emergent onset and no clear S-wave arrival. These events may be due to bed separation.

6. References

Bishop, I, Styles, P. and Allen, M. (1994). *Mining Induced Seismicity in the Nottinghamshire Coalfield.* Q. J.Eng. Geol. 26 (4), 253-279.

Branston M. W. and Styles, P., (2003) *The application of Time-Lapse Microgravity For The Investigation And Monitoring Of Mining Subsidence.* QJEG, 36,231-244).

Jackson. P.J., Styles. P., Toon. S. J., and Bryan-Jones., A., (1997). *Seismic Monitoring of Longwall Mines to provide a better understanding of Overburden Behaviour.*, Proc. 27th International Conference of Safety in Mines Research Institutes., New Delhi., India., 867-893.

Ren, T.X., Reddish D. J and Styles P., *Numerical modelling and microseismic monitoring to improve strata behaviour*. 29th APCOM April 25-27, 2001, Bejing, P.R. China

Styles, P, (1995), *Harmonic Tremor Precursors and their implications for the mechanisms of Coal/Gas Outbursts.* in 'Management and Control of High Gas Emission and Outbursts in Underground Coal Mines', Lama, R., (Ed), Balkema: Rotterdam. 123-131

DEVELOPMENT AND VALIDATION OF A METHOD TO PREDICT COAL PILLAR LIFE IN SOUTH AFRICA.

VAN DER MERWE J.N.[1]

[1] Department of Mining Engineering - University of Pretoria – South Africa; nielen@postino.up.ac.za

ABSTRACT: One of the most difficult aspects of mine closure procedures, is to predict the long term stability of pillars in the case of coal mining. In South African coal mining, pillars have been designed since the late 1960's with the aid of a pillar strength formula based on statistical analysis of failed pillar cases by the well known team of Salamon and Munro. They developed the widely used power formula for pillar strength. Since that time, however, the data base of failed pillars has effectively doubled in size and re-analysis of the new data indicated that the original pillar strength of small pillars may have been over estimated. The data was then extensively re-analysed and a more effective linear formula for pillar strength was found. The most important differences between the two formulae are that the predicted strength of small pillars are lower and the strength of larger pillars, higher with the new formula. However, neither of the two methods explicitly cater for the prediction of the expected time of stability of coal pillars. No direct correlation between the safety factors and the period of stability of pillars could be found. It was then determined that the most frequent mode of pillar failure was by progressive scaling. Using the new formula to determine a minimum value of pillar safety factor (i.e. the safety factor at which failure can be taken as guaranteed to occur), the final sizes – after scaling - at which the failed pillars had to be in order to fail, were determined. The differences between the original dimensions and the postulated final dimensions were then used to calculate a rate of pillar scaling. The rate was then re-applied to the original data bases of both failed and intact pillar cases and distinct differences were found. The projected lives of the failed pillars were substantially shorter than the projected lives of the intact pillars. While this inspired confidence in the procedure, it was still based on an assumed and unproven rate of pillar scaling. The next step was then to measure the actual amounts of scaling on unfailed pillars underground. This was done on a large number of pillars in a variety of conditions. The measurements showed sufficiently close correspondence with the assumed values, to confirm the assumptions and by consequence, the life prediction procedure. With the aid of the real measurements, it was also possible to statistically determine confidence and accuracy levels of the procedure.

KEYWORDS: Coal pillar, Statistical analysis, Factor of safety, Rate of pillar scaling, Life prediction.

RESUME : La prédiction à long terme de la stabilité des piliers abandonnés est, parmi les travaux à réaliser lors de la fermeture d'une mine de charbon, l'un des plus difficiles. Dans les mines de charbon d'Afrique du Sud, le dimensionnement des piliers repose depuis la fin des années 60 sur des formulations analytiques établies sur la base d'une analyse statistique faite par Salamon et Munro. Elle a conduit à une formule, aujourd'hui largement utilisée, pour l'estimation de la résistance des piliers. Une actualisation de cette analyse (depuis 40 ans, le nombre de cas d'instabilité introduits dans la base des données a doublé) a montré que la résistance des petits piliers avait été surestimée et celle des grands piliers sous-estimée. Cependant ceci ne permet pas encore de prédire la durée pendant laquelle le pilier restera stable. En effet aucune corrélation n'a pu être établie entre le facteur de sécurité et la durée de vie du pilier. Après avoir constaté que le mode de rupture le plus fréquent du pilier était la diminution progressive de sa largeur, la taille critique des piliers avant effondrement a alors été déterminée. La différence entre les tailles réelles et critiques des piliers a permis de déterminer la potentialité de diminution en taille de chaque pilier. L'application de ces résultats à un ensemble de cas de piliers stables et instables a montré

que l'on pouvait prévoir que la durée de vie des piliers effondrés était significativement plus faible que celle des piliers encore en place. Des mesures complémentaires fait sur un grand nombre de piliers sollicités de manières variées ont permis de déterminer statistiquement la confiance et la précision du modèle prédictif.

MOTS-CLEFS : Pilier de charbon, Analyse statistique, Facteur de sécurité, Taux de diminution progressive de sa largeur, Durée de vie.

1. Introduction

Failure of pillars in bord and pillar panels in South Africa more often than not results in surface subsidence. This is due to the combination of mining depth, being in the range 40 m to 160 m, panel width, of the order of 80 m to over 200 m and mining height, ranging from 1.5 m to over 4 m.

It is known that over time, coal pillars lose strength and that at some or other time in the future, the failure of pillars that were stable at the time of mining, is possible. From the points of view of planning for mine closure and undermining of surface structures with bord and pillar mining, it is important to have some knowledge of how long coal pillars will be stable for, if they are to fail.

The approach that is normally adopted in situations where surface structures are to be undermined, is to leave larger pillars with higher safety factors underneath those structures. It comes down to making a "stable" situation "even more stable", thereby decreasing the probability that failure may occur due to unknown weakness of the pillar material or any other cause. However, the safety factor on its own offers no method of estimating the likely period of stability.

It is shown that the safety factors of coal pillars do not quantifiably correlate with their lives. Broadly speaking, under identical conditions, pillars with higher safety factors are likely to last longer than ones with lower safety factors. However, beyond this broad statement, nothing more can be said about the relationship between safety factors and coal pillar lives.

This paper describes the development of a prediction method, based on observation of coal pillar failure by progressive weakening from the outer edges of the pillars towards the inner core. It is postulated that at some or other time, the remaining core of the pillar will be too small to bear the weight of the overburden and failure will then occur. The rate of weakening is determined for different areas and seams in South Africa and the time of failure is then predicted. The predicted time of failure is compared with the actual life-spans of pillars in the data base of failed pillar cases.

Following the initial development, underground measurement of the amount of scaling on pillars was used to verify the method. A close correlation was found between the predicted scaling rates and the actual ones found by direct measurement.

Note that in the context of this paper, the term "pillar failure" refers to the failure of a large number of pillars in a panel and not to the failure of individual pillars. The area of failure is at least equal to a circle with diameter equal to the panel width. It should also be understood that pillar failure in South Africa is a rare occurrence. It is estimated that less than 0.3% of the pillars that have been created, have failed.

2. Previous attempts to predict pillar life

Van Besien and Rockaway (1988) published a formula based on pillar stress, yielding the time delay between mining and the possible onset of pillar failure. They postulated that if failure had not occurred by the predicted time, it would not happen. The method is purely empirical, based on case studies in the USA, without reference to a mode of failure.

Hao and Chug (1992) published the results of an analysis of 24 bord and pillar subsidences in Ilinois. They concluded that failure of the floor was the most likely subsidence mechanism and then developed a formula to predict the pillar life. As this method only relates to floor failure, as occurs commonly in the Illinois basin in the USA with soft floor, its application to South Africa is not relevant.

Van der Merwe (1993) observed and analysed pillar failures in the Vaal basin and concluded that progressive pillar scaling was the predominant mode of pillar failure. He found a correlation between mining height and the rate of scaling. Combined with the scaling distance required to reduce the safety factor to a value of 0,3 (the minimum value at which all the failed pillars in the data base had failed), this yielded a method to predict the Pillar Life *Index*, specifically not called a pillar *life* because of the restrictions of the method. This method was only valid for the Vaal Basin.

Salamon et al (1998) investigated van der Merwe's method further, developing a statistical procedure to predict the probability of failure at a given point in time. Their method, however, used the probability of failure of pillars using the original mining dimensions at different times of failure. This is not valid for pillars after scaling had taken place and at a specific point in time, as the pillar dimensions at the time of failure were not the same as at the time of mining.

3. Postulated mode of pillar failure

Coal pillars may fail as a result of several mechanisms, including progressive scaling, fire and foundation failure. Fire is regarded as a special case and will be excluded from the study. Foundation failure has been observed in South Africa only on isolated occasions and is likewise discarded.

It has been stated that in weak roof areas like the Vaal Basin no 3 Seam, pillars may fail as a result of roof collapse and the consequent increase in pillar height. While this mechanism cannot be excluded as a possibility, it has to be seen in the correct context. The author has several years' experience of underground work in the Vaal Basin, and while roof falls did occur more frequently there than elsewhere, they were still rare occurrences when seen in the overall context. They tended to be directional and confined to certain roadways, very seldom occurring in a general and widespread fashion that was likely to affect pillar stability over any appreciable area. By contrast, pillar scaling was seen to occur generally and almost everywhere, like in the examples in Figures 1 and 2 from different mining areas in South Africa.



Figure 1. Typical view of an old pillar in the Vaal Basin, known to have weak coal.



Figure 2. Pillar scaling on the Ermelo B-Seam in a 90-year old area, where pillar scaling is generally considered to be a less serious problem.

Model of pillar failure

It is postulated that the majority of the pillars in South Africa fail by progressive weakening of the pillars, by a process that starts at the pillar edges and works its way into the pillar core, thereby reducing the effective sizes of the pillars. Eventually it reaches the stage where the loss of strength is sufficient to result in failure of the pillars.

If the original pillar width is *w* and it scales by an amount *d*, then the effective pillar width is $w - d$. At the same time, the bord width *B* will increase to $B + d$, while the pillar centre distance, *C*, equal to $B + w$, will remain unaffected. Figure 3 illustrates the principle.

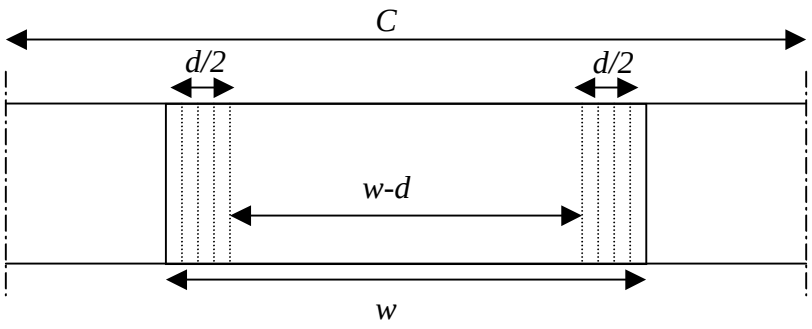


Figure 3. Cross section through a pillar, illustrating some of the nomenclature.

Due to the change in dimensions, the Safety Factor, *S*, will be affected. According to van der Merwe (2003), the pillar strength prior to scaling is:

$$Strength(MPa) = 3{,}5\frac{w}{h} \quad (1)$$

where *h* is the pillar height and *w* the pillar width.

The pillar load, using the tributary area theory, is:

$$Load(MPa)=.025H\left[\frac{C_2}{w_2}\right] \quad (2)$$

where H is the mining depth and C the pillar centre distance.

The Safety Factor, S, is

$$S=\frac{Strength}{Load}, \text{ or}$$

$$S=3.5\frac{w}{h}\left[\frac{w^2}{.025HC^2}\right] \quad (3)$$

After scaling by a distance d had taken place, the new Safety Factor, S_n, will be:

$$S_n=3{,}5\frac{(w-d)}{h}\left[\frac{(w-d)^2}{0{,}025HC^2}\right] \quad (4)$$

If the minimum Safety Factor, S_m, at which failure has to occur, is reached when the critical scaling distance equals d_c, then it is possible to transpose Equation [4] to calculate d_c as follows:

$$d_c=w-\left[0{,}00714S_mHhC^2\right]^{0{,}333} \quad (5)$$

The average rate of scaling over the life of the pillar at the time of failure, R, can be determined for each case of pillar failure where the actual life, L, is known, as follows:

$$R=\frac{d_c}{L} \quad (6)$$

4. The Data Base

In all empirical investigations, the composition of the data base is of prime importance. For this analysis, the extended data base that was used by van der Merwe (2003) to derive the optimum pillar strength formula for South African conditions was used as a base, while the collapse cases from the so-called “Weak coal areas” were included. That data base already excluded the failures that were suspected to have been caused by floor or roof failure. All the failures that occurred within less than a year after mining were then excluded from the data base, as were the ones where the actual pillar lives could not be determined due to a lack of data.

Figure 4 shows the failures as a function of the safety factors, confirming that there is no quantifiable correlation between the safety factors and the times of failure. The differences between the different mining areas are also apparent, with the Klip River and Vaal Basin exhibiting failures relatively soon after mining, at high safety factors. The analysis that followed, therefore differentiated between the different mining areas.

Figure 5 shows the frequency distribution of actual pillar lives for all the pillars in the data base of failed pillars. It is clear from the figure that the majority of failures occurred relatively quickly, within the first ten years of their formation. Thereafter the rate of failures diminished.

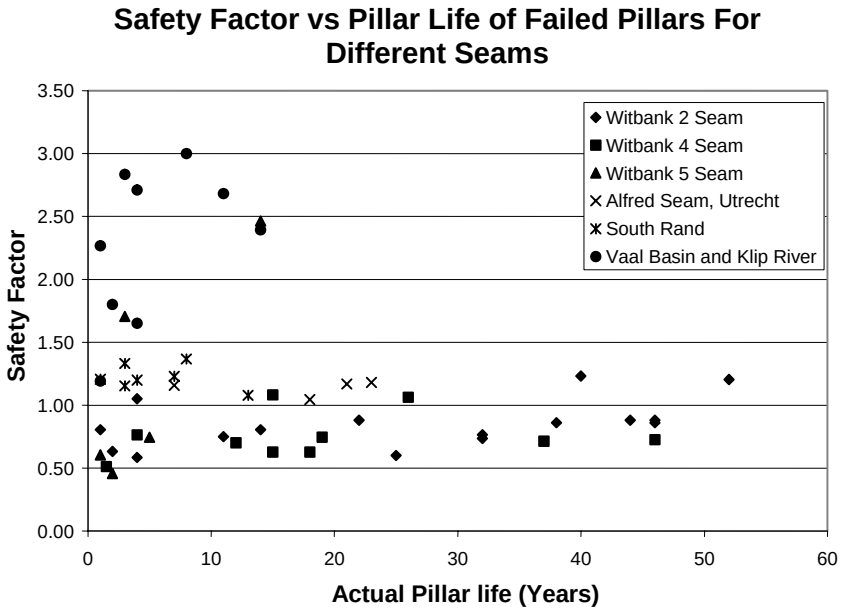


Figure 4. Pillar Life as a function of safety factor, illustrating that the safety factor on its own does not correlate with pillar life. The differences between the different seams are also apparent.

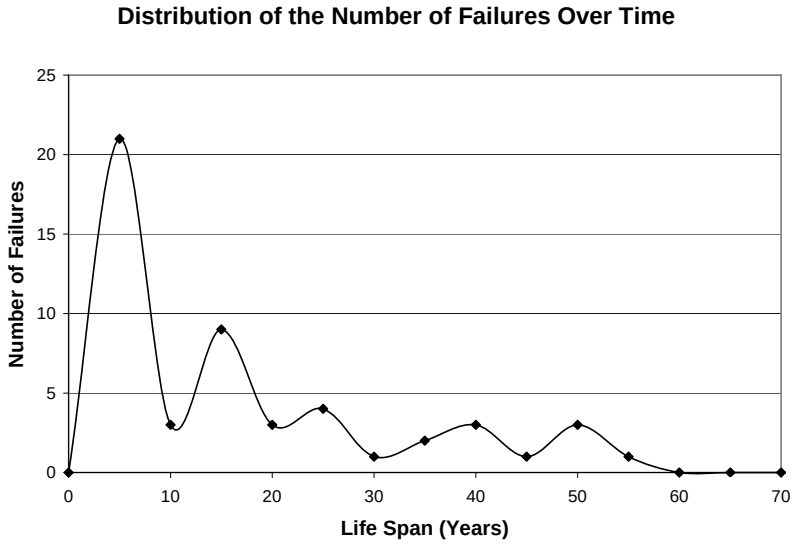


Figure 5. Frequency distribution of pillar failure cases over time, indicating that most of the failures that did occur, occurred within the first ten to twenty years.

At this point, it has to be explained that the strength of the pillars and consequently their safety factor, was derived statistically. A safety factor of 1.0 merely implies that at that value, 50% of the pillars in the data base had failed. It does not mean that pillars with safety factors less than 1.0, will fail and ones with greater safety factors will be stable. The spread is due to a combination of several unknowns such as the exact strength of pillars in specific regions and variations in the exact dimensions of pillars.

The minimum safety factor that was found in the data base of failed pillars was 0,46. None of the pillars in the data base failed immediately. It can then be assumed that some scaling had to take place before failure occurred, even for the pillars with low safety factors. It was thus decided to use

a value of 0,4 for S_m, as at that value failure has to occur. No pillar with a lower safety factor in the data base of failed pillars had survived.

5. Method of Analysis

5.1. Determination of scaling rate

Equations (5) and (6) were used to calculate the average scaling rates for all the failed cases in the data base. Correlations between the scaling rates and other measurable parameters were then sought. It was found that the scaling rates did not correlate with the safety factor, pillar widths, pillar stress or the width-to-height ratio. Note that this remark does not refer to whether or not pillars are likely to fail or to the extent of scaling, but merely to the *rate* of scaling.

However, there was a strong inverse relationship with time, see Figure 6, and less well developed relationships with the mining height, see Figure 7.

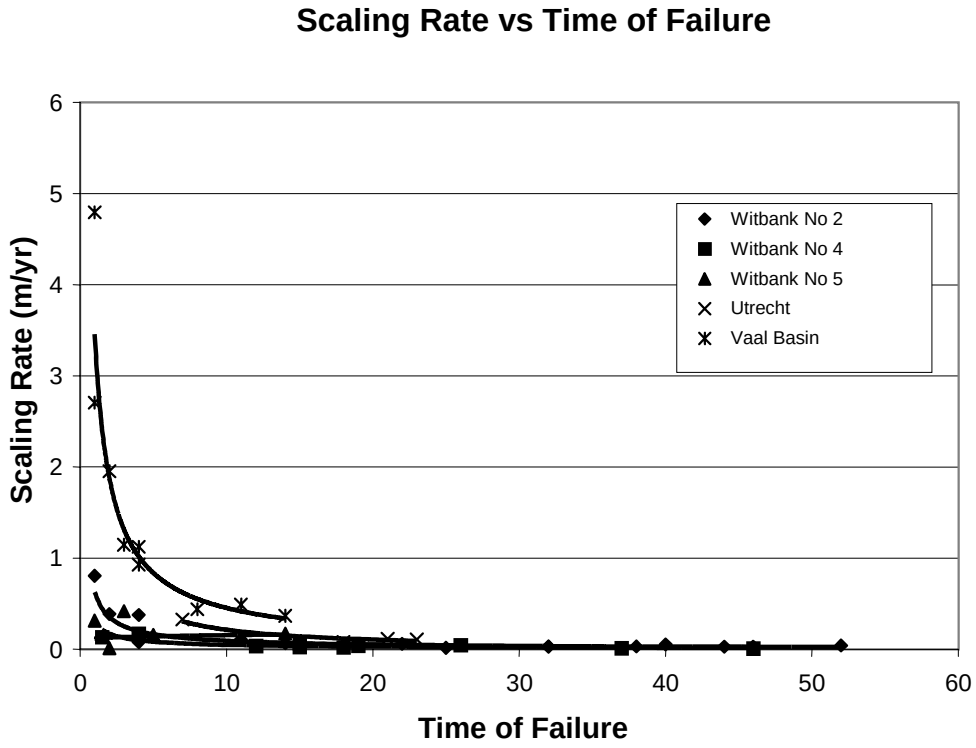


Figure 6. Relationship between the scaling rates of pillars that had failed and time for the different mining areas.

Figure 6 shows that the scaling rate decreased rapidly with time. The different mining areas exhibited the same trends. The grouping of mining areas was based on the similarity of scaling rates.

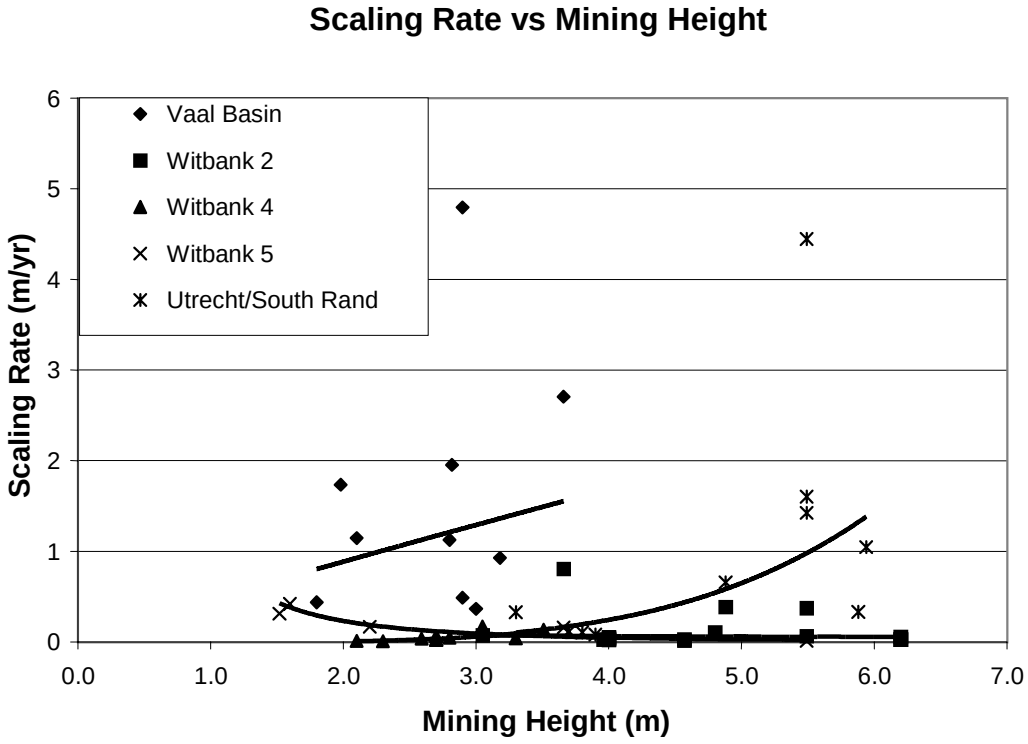


Figure 7. Relationships between mining height and scaling rates for the different mining areas.

It is seen from Figure 7 that in the broad sense, there was a direct, if in some cases weakly developed, relationship between mining height and scaling rate. Table 1 summarises the correlation coefficients between scaling rate, mining height and time for the different areas. These correlations were only apparent when the data was grouped according to the different mining areas.

Table 1. Correlation coefficients between scaling rate, time and mining height

Area	Time	Mining Height
Utrecht/South Rand	0,83	0,53
Witbank No 4 Seam	0,74	0,64
Witbank No 5 Seam	0,01	0,8
Vaal Basin	0,95	0,06
Witbank No 2 Seam	0,83	0,05

5.2. Determination of relationships between time, mining height and scaling rate.

As the data indicated that there was a direct relationship between scaling rate and mining height and an inverse relationship between scaling rate and time, the correlations between scaling rate and the *h/T* (mining height over time) parameter were investigated. The results are shown in Figure 8.

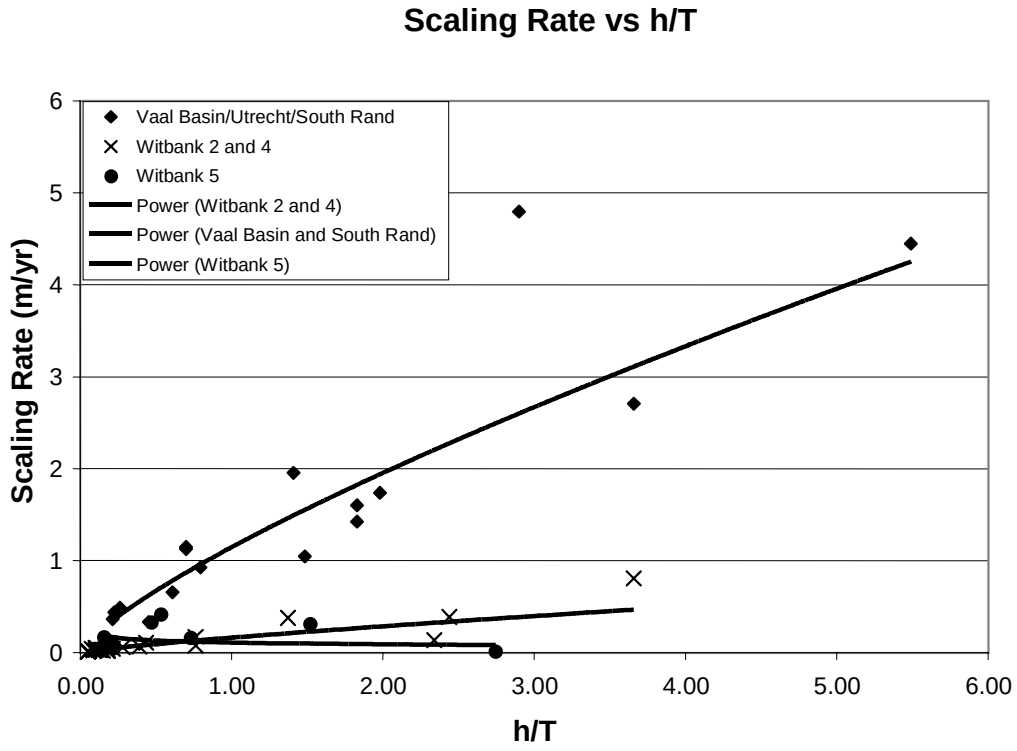


Figure 8. Relationships between scaling rate and the h/T parameter.

Several different groupings of the data were investigated. It appeared that the Vaal Basin, Klip River, Utrecht and South Rand failures displayed similar trends and they were consequently grouped together, henceforth referred to as the Vaal Basin group. The Witbank No 2 and No 4 seams were likewise included in a single grouping. The Witbank No 5 Seam was kept separate. Figure 8 clearly shows that the different groupings displayed different behaviour.

The relationships all had the form:

$$R = m\left[\frac{h}{T}\right]^{x} \tag{7}$$

where *m* and *x* are dimensionless constants.

Table 2 contains the *m* and *x* values as well as the correlation coefficients of scaling rate with *h/T* for the different groups.

Table 2. Correlation coefficients, *m* and *x* values for the different areas.

	m-Value	**x-Value**	**R^2**
Vaal Basin	1,3888	0,804	0,94
Witbank No 2 and 4 Seams	0,1624	0,8135	0,81
Witbank No 5 Seam	0,105	-0,3061	0,09

5.3. Prediction of time of failure

Substituting T for L in Equation [6] and combining with Equation [7], the life-spans of the pillars, T, can be determined as follows:

$$T = \left[\frac{d}{mh^{x}} \right]^{\frac{1}{1-x}} \tag{8}$$

By using the area specific values for m and x from Table 2 in Equation [8], the life spans of pillars can now be predicted. This was done for the cases of known failure in the different areas and the results are shown in Figures 9, 10 and 11.

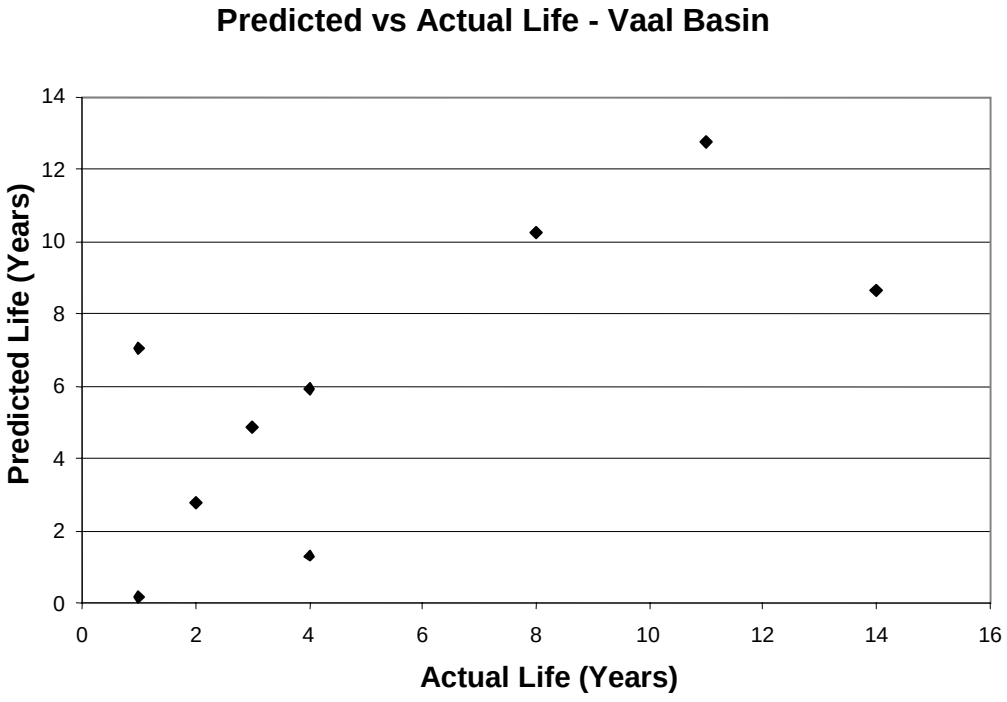


Figure 9. Comparison of predicted to actual life for failed pillars in the group comprising the Vaal Basin and Klip River. The correlation coefficient in this case is 0,53.

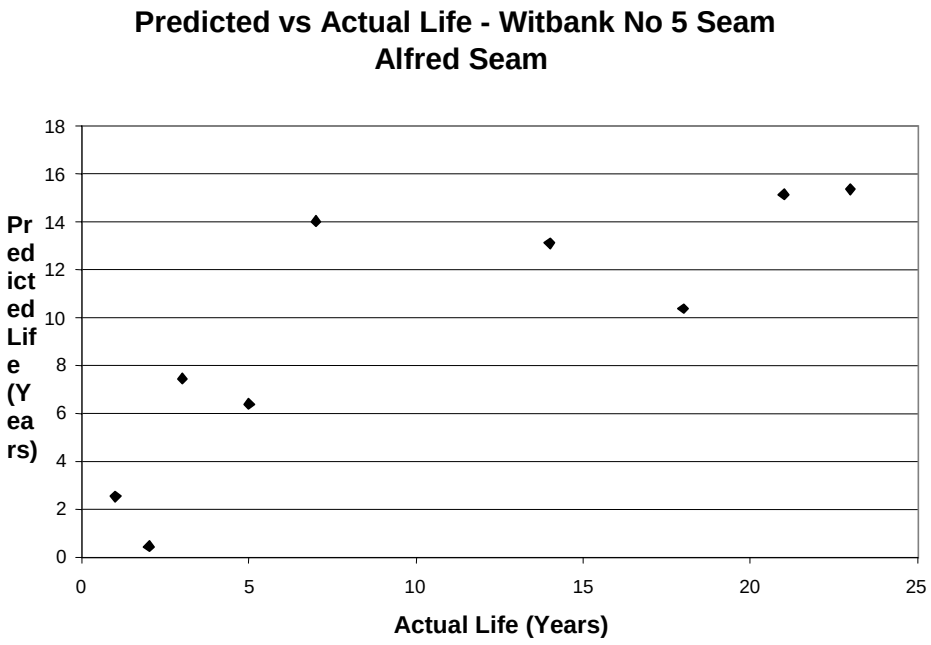


Figure 10. Comparison of predicted to actual life for failed pillars in group comprising the Witbank No 5 Seam and the Alfred Seam in the Utrecht Coal Field. The correlation coefficient in this case is 0,66.

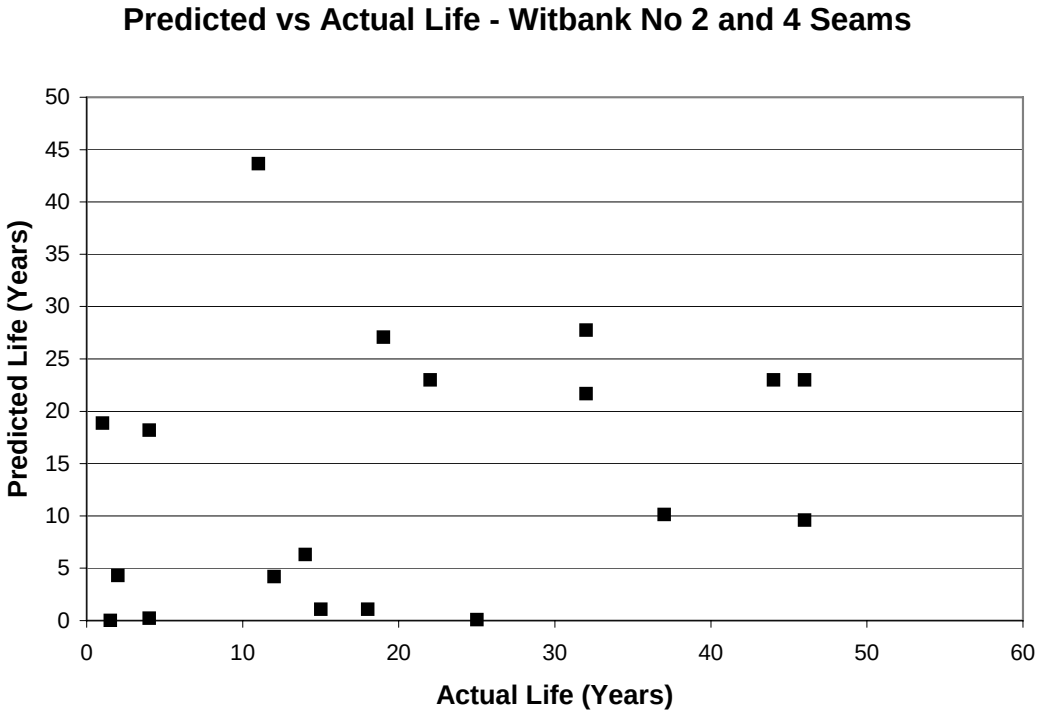


Figure 11. Comparison of predicted to actual life for failed pillars in group comprising the Witbank No 2 and 4 Seams. The correlation coefficient in this case is 0,16.

In the cases of the Vaal Basin and Witbank No 5 Seam groups, the correlation coefficients are satisfactory. Even in the Witbank No 2 and 4 Seam group, with a much lower correlation coefficient, it is apparent that the predicted lives of 22 out of 26 cases were in an acceptable time frame. For the sake of clarity of the diagram, 4 out of the 26 predictions were not plotted, as they were in the range of thousands of years and therefore obviously anomalous. All the other data was plotted.

No satisfactory prediction could be made for the South Rand coal field, possibly because the 5 available cases displayed very little variation with regard to the mining heights and scaling rates. It could also indicate that for that coal field, the hypothesis of failure by progressive scaling does not hold true and that another failure mechanism was responsible for the pillar failures.

6. Comparison with failed and stable data bases.

It was shown in Figure 5 that the pillar failures tended to occur quickly, with almost 70% of the failed pillars failing within the first 15 years. Figure 12 is a comparison between the frequencies of predicted and actual failures of all the data in the data base of failed pillars.

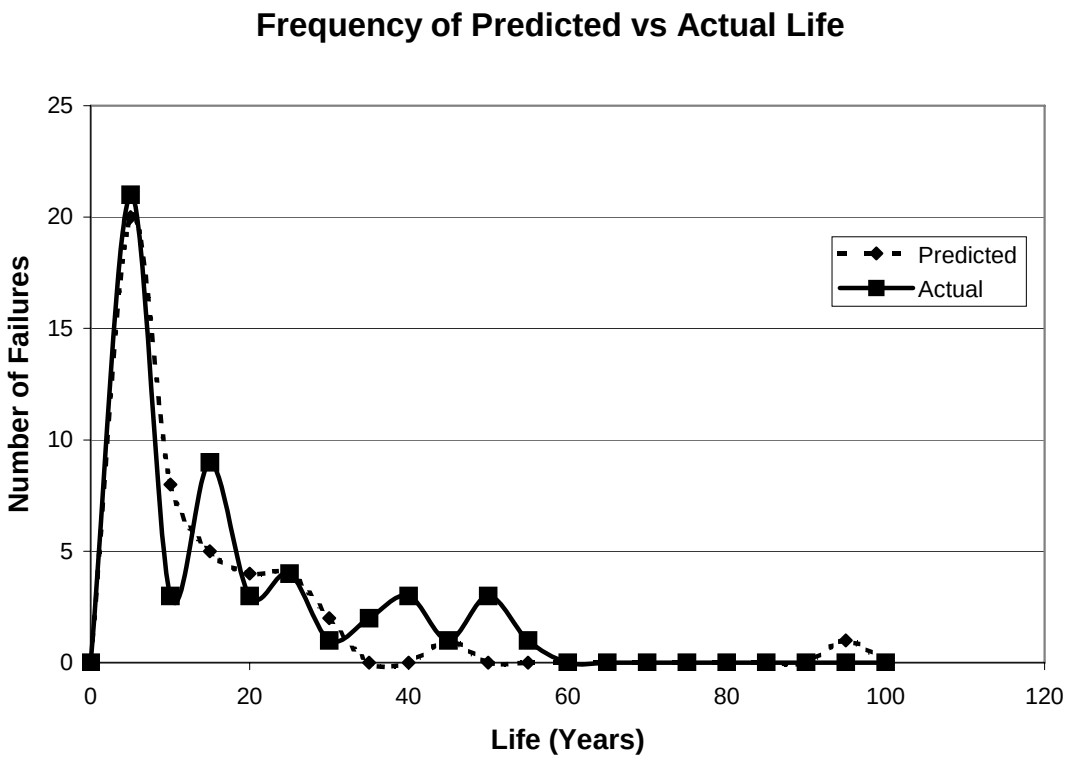


Figure 12. Comparison between the predicted and actual frequencies of pillar failures of failed pillars in all the areas. Note that four anomalous predictions were omitted from the data.

The figure makes it clear that the procedure developed during this investigation results in a profile of frequencies of failure over time period that is very close to the observed data.

As a final test, the procedure was applied to pillars that had not failed. For this purpose, the data base of intact pillar cases that was collected by Salamon and Munro (1967) was used, as that was accepted as representative of pillars that had not failed. The results are shown in Figure 13 together

with the frequency of the failed pillars. Note that because the average predicted lives of the intact pillars was 44 000 years, the time scale in the figure is logarithmic to provide a clear visual comparison.

For the prediction of pillar lives of the intact pillars, a higher scaling rate than the one derived for the Witbank No 2 and 4 Seams was used – the *m* and *x* values were respectively 0,1203 and 0,7049, which were the constants for the No 2 Seam only. The reason for doing this was that the localities of all the pillars in the stable data base was not known and therefore the maximum rate that was found was used.

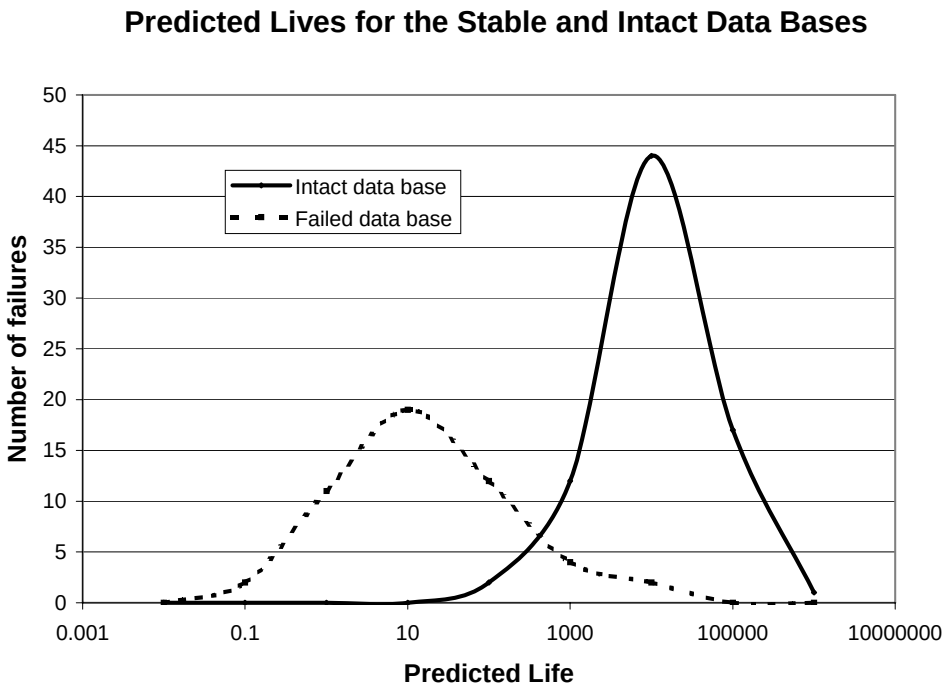


Figure 13. Predicted lives for the data bases of failed and intact pillar cases. The data base of intact pillars is only a sample of the total population of pillars that had not failed, while the data base of failed pillars include all the known cases of failed pillars. The overlap area in the figure is thus not significant.

Figure 13 shows a distinct difference between the predicted lives of the failed and the intact pillar data bases. The predicted lives of the majority of failed pillars is for all practical purposes confined to a 100 year period while the predicted lives of the intact pillars extends to several thousands of years.

7. Volume restriction

Salamon et al (1998) argued that provided the debris resulting from pillar failure was not removed, further pillar scaling could be prevented by choking of the excavation in certain cases. They developed expressions to calculate the pillar width at which choking would occur, hypothesizing that it would happen at the stage when the debris had built up to the roof of the excavation along the edges of the pillars. They stated that this would only stop further scaling in the absence of a stress driven mechanism of deterioration.

However, pillar failure where the debris had indeed built up to the roof had been observed, as shown in Figure 14. It is thus confirmed that the postulation by Salamon et al (1998) should not be applied in the practical situation, where failure is invariably stress driven.



Figure 14. Illustration of a case where pillars had failed even though the scaling debris had reached roof height. The original road width in this case was more than 6 m, while the width at the top of the cavity after failure was less than 4 m.

Nonetheless, it is known that lateral confinement does increase the strength of pillars and therefore the basic argument must be sound, even if the proposed limits can be questioned. Quantification of the strengthening effect would be extremely complex and will require extensive further research. For this investigation, the argument was simplified by assuming, for the purposes of demonstration, that the failure process will stop when the coal debris had been compressed to result in an effective bulking factor of 1.05 from the estimated 1.3 in the uncompressed state and the angle of repose had been flattened to 30^o from the estimated 35^o in the undisturbed state. This is shown in Figure 15.

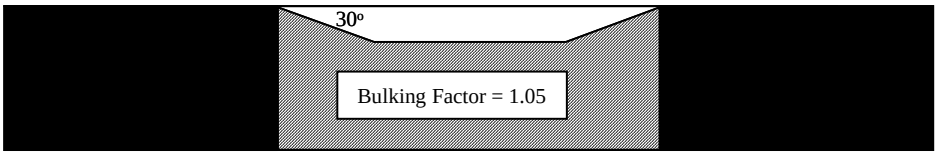


Figure 15. Schematic cross section through scaling pillars showing the build-up of confining debris against the pillar sides.

For each case, the volume of coal material that was available to fill the excavation, resulting from scaling, was calculated at the stage when failure was predicted to occur. If the available space, based on the geometry shown in Figure 14, was then less than the volume resulting from scaling, it was postulated that failure would not occur.

This test was applied to all the cases in both the failed and intact data bases. It was found that none of the cases in the failed data base would be restricted by this consideration while 30% of the cases in the intact data base would be restricted and can then be considered to be “infinitely stable”.

Due to the nature of the assumptions in this argument, this result should not be used for practical design purposes, but it does indicate that there may be merit in further investigation.

8. Verification by Direct Measurement

Up to this stage, there are two fixed points in the sequence of the argument used to predict pillar life, namely the pillar dimensions at the time of mining and the elapsed time between the creation of the pillars and their eventual failure. In between those two points, the scaling rate is linked to the assumption of the minimum safety factor, as the minimum safety factor determines the scaling distance that is required to result in failure. For instance, if the real minimum safety factor is greater than the assumed value of 0.4, then the scaling distance would be smaller and the rate also lower, because the age of the pillar at the time of failure is fixed. Conversely, if the minimum safety factor is less than 0.4, then the real scaling distance would be greater and the rate consequently higher.

This would not have a dramatic effect on the pillar life prediction, as any change in the real minimum safety factor would be compensated for by an accompanying change in the scaling rate. Nonetheless, it remained an unproven assumption in the procedure.

The assumption could be proven by direct measurement of either one of the two unknowns, i.e. the real minimum safety factor or the rate of scaling, as they are linked. The real pillar dimensions at the time of failure could not be measured, but the rate of scaling of existing intact pillars, prior to failure, could be determined.

The rest of the paper describes an investigation into the rate of scaling by measuring the amount of scaling of pillars of which the original dimensions could be determined and of which the time of mining was known.

9. Method of measurement

The measurements were taken by Mr Christophe Baron, final year engineering student at the Nancy School of Mines in France, assisted by Mr Gary Prohaska of CSIR Miningtek. The data was supplemented by measurements which were taken by the mine surveyors and staff of the Department of Minerals and Energy at the Leeuwfontein Colliery.

Due to the differences in pillar shapes after some scaling had occurred, it was necessary to decide where the measurements should be taken – mid height, position of maximum scaling, etc. This decision was based on observation and is covered in the paper. It was also necessary to determine whether there were preferential scaling directions, and therefore it was first necessary to measure all around the pillars to determine if there was a preferential direction. The other issue was to decide how to handle the pillar corner scaling, as it has often been observed visually that pillar corners are more prone to scaling than the mid span areas. This is also addressed in the paper.

There were two methods of measurement. One was to determine the original position of the pillar edge by direct observation of for instance continuous miner pick marks in the roof. The other was to measure the road width and to compare the new dimensions with the original pillar offsets obtained from the mine survey departments or measured directly from survey plans.

It is known that pillars in the centres of panels are subjected to higher loads than ones at the edges where they are protected by the larger inter panel pillars and therefore care was taken to obtain measurements over a representative spread of the areas.

Measurements were conducted at 13 sites on 6 mines in the Secunda and Highveld coalfields. The No 2 and No 4 Coal seams were investigated, 3 on the No 2 Seam and 10 on the No 4 Seam. More than 1 800 measurements were taken. The areas where observations were taken are shown in Table 3 and the measurements in Table 4. It was shown by van der Merwe (2003) that the No 2 and No 4 Seams were sufficiently similar to be treated as one group.

Table 3. Characteristics of data collection areas

Mine	Area	Seam	Mining Method	Year of Mining (m)	Air Way	Original Height (m)	Original Road Width (m)	Pillar Centers (m)	Mining Depth (m)
Blinkpan		2	D&B	1963	Intake	2.92	6.03	20*20	
Delmas	Open	2	D&B	1983	Intake	2.80	6.80	17*17	94
	Sealed	2	D&B	1983	Sealed	3.00	6.78	17*17	94
Matla	A1	4	CM	1980	Intake	3.85	6.37	17*17	73
	E	4	CM	1997	Return	3.93	6.79	17*19	72.6
	G	4	CM	1981	Intake	3.96	7.14	17*20	72
	Last	4	CM	1988	Intake	3.25	6.32	17*17	70
	Q	4	CM	1997	Return	4.00	7.05	17*19	71
	T	4	CM	1996-1997	Intake	4.03	6.24	20*30	72
	U1	4	CM	1979-1980	Return	4.86	7.19	17*16	77
Secunda		4	D&B	1989-1990	Intake	2.58	6.19	28*28	169
Tweefontein		4	D&B	1980-1981	Intake	2.88	6.02	17*17	51.8
Leeuwfontein		4	D&B	2002	Intake	3.48	6.83	14*14	43

Table 4. Summary of measurements taken

Mine	**Area**	**No of measurements**	**No of pillars measured**	**No of road width measurements**	**No of mining height measurements**
Blinkpan		207	33	69	69
Delmas	Open	185	25	75	12
	Sealed	78	10	38	49
Matla	A1	192	24	57	57
	E	240	30	51	49
	G	18	5	5	4
	Last	111	14	18	18
	T	63	30	15	9
	U1	41	19	13	7
Secunda		165	33	51	51
Tweefontein		483	73	142	26
Leeuwfontein		281	56	212	69
Total		**2547**	**352**	**746**	**420**

The measurement instruments were a hand held electronic device with an accuracy of 1 mm over a distance of 10 m and survey tapes.

9.1. Observed Pillar Shapes

Some examples of pillar shapes after scaling are shown in Figures 16 and 17.

It was soon seen that *(e)*, in other words maximum scaling at mid height, represented the most common shape. Shapes *(b)* and *(c)* occurred where obvious planes of weakness were present in the coal, while *(d)* occurred where prominent slips dominated the pillar failure mode. Shape *(a)* was not common, although it was observed. The decision was then taken to take all measurements at mid height unless if the pillars were severely distorted into another shape.

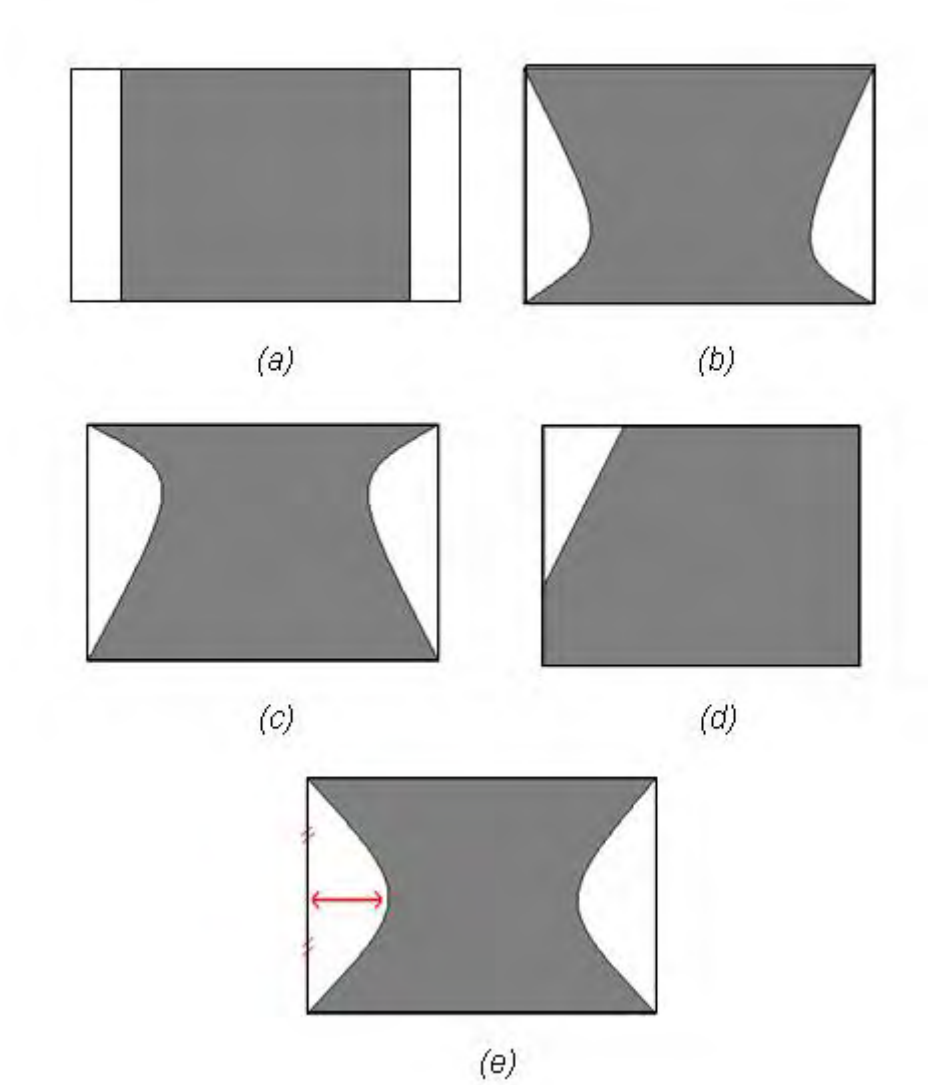


Figure 16. Examples of post scaling pillar shapes.

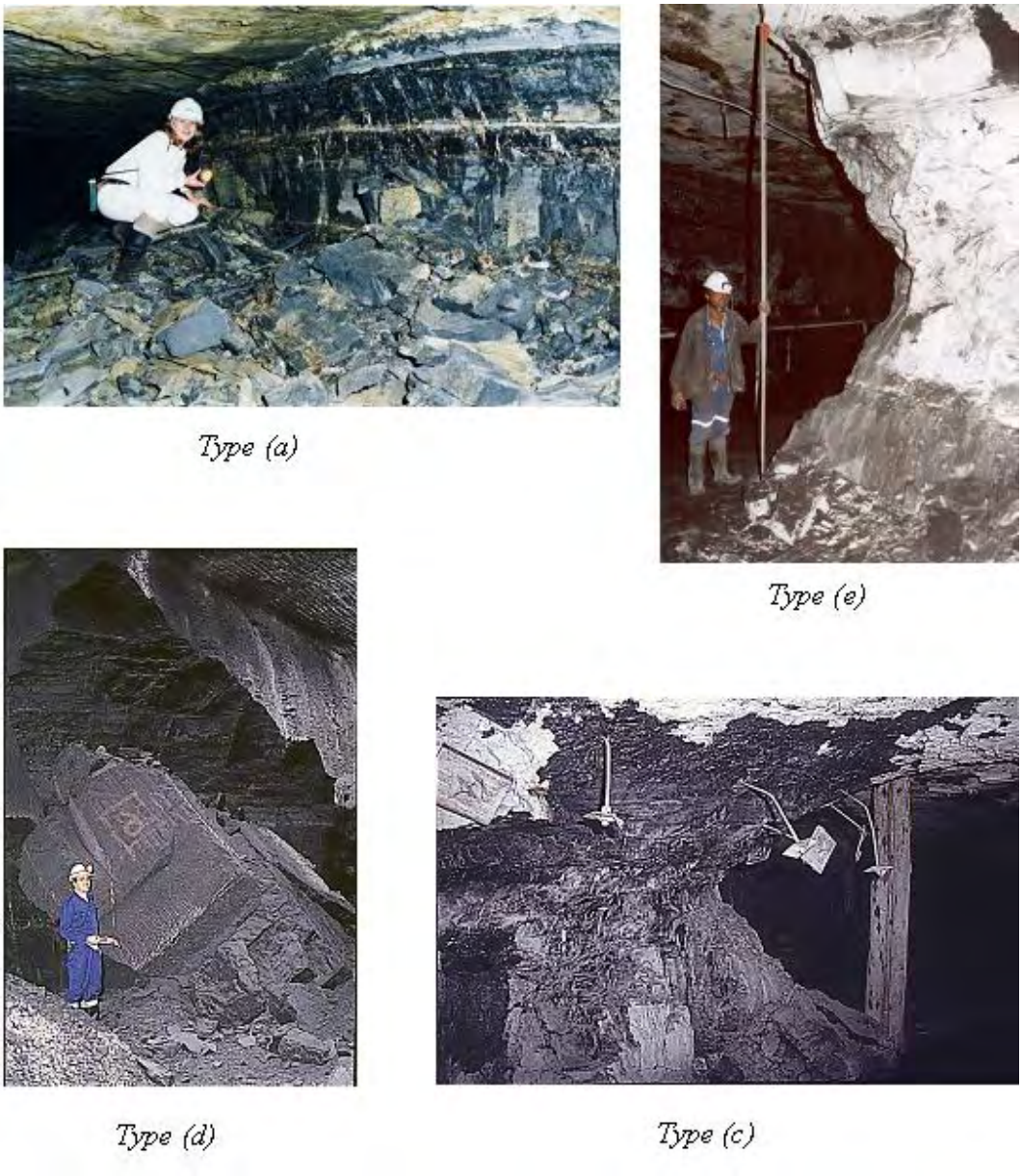


Figure 17. Underground examples of the basic pillar shapes shown in Figure 16. Type (e) is the most common shape.

9.2. Preferential Scaling Directions

Scaling distances were measured all around the pillars at 12 of the sites to determine whether there was a preferential scaling direction. The results from 182 pillars are summarised in Table 5.

Note that in Table 5, there is no reference to the age of the pillars studied or anything other than just the total amount of scaling on different sides of the pillars. It indicates that there are no significant differences.

As a consequence, the data gathering exercise could be simplified, as it was clear that scaling measurements taken on one side of a pillar could be transferred to the other sides without appreciable error.

Table 5. Scaling distances on different sides of pillars

		Average Sidewall Scaling (m)			
		North	*East*	*South*	*West*
No 2 seam	Blinkpan	0.460	0.380	0.380	0.460
	Delmas - open	0.330	0.330	0.330	0.320
	Delmas - sealed	0.720	0.650	0.750	0.710
Average No 2 seam		*0.503*	*0.453*	*0.487*	*0.497*
No 4 seam	Matla - A1	0.510	0.505	0.480	0.490
	Matla - E	0.220	0.265	0.265	0.220
	Matla - G	0.705	0.815	0.580	0.470
	Matla - Last	0.290	0.330	0.300	0.260
	Matla - T	0.450	0.435	0.480	0.495
	Matla - U1	0.570	0.585	0.625	0.610
	Secunda	0.310	0.390	0.360	0.380
	Tweefontein - 1	0.390	0.410	0.430	0.410
	Tweefontein - 2	0.270	0.290	0.300	0.280
Average No 4 seam		*0.413*	*0.447*	*0.424*	*0.402*
Average all pillars		**0.435417**	**0.44875**	**0.44**	**0.425417**

9.3. Pillar corner scaling

It is widely believed that pillar corners are more prone to scaling than the mid pillar areas. The question that had to be answered was whether this was an illusion caused by visual observation, or whether it was real, and if real, how much additional scaling occurs at the corners?

The method of investigation employed in this instance was to take direct measurements of the pillar corners and to compare that with the scaling of the sidewalls, as shown in Figure 18.

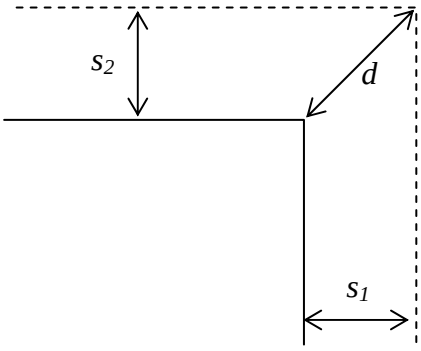


Figure 18. Measurement of pillar corner scaling.

Logically, the pillar corners are more highly stressed than the mid pillar areas and have two free surfaces, therefore the expectation is that they should scale more than the mid pillar areas.

If there was no additional scaling at the pillar corners, then using the symbols shown in Figure 18,

$$d = \sqrt{s_1^2 + s_2^2}\ , \tag{9}$$

Table 6 was constructed using the information obtained from 182 pillars that were measured. In the table, the parameter δd indicates the additional scaling at the corners, defined by:

$$\delta d = d - \sqrt{s_1^2 + s_2^2} \ . \tag{10}$$

The scaling distances s_1 and s_2 were taken at the mid pillar positions. It is seen., rather surprisingly, that on average, there is no significant difference between the mid pillar sidewall scaling and the corner scaling.

The conclusion drawn here is that the stress concentration on the pillar corners is, in general, not significantly greater than in the mid pillar areas. This is possibly due to the fact that the road widths are invariably narrower than the pillar widths and that the layouts are regular. The reason for the perception that corners scale more is not clear – it is possible that it exists because the scaling tends to begin at the corners and one is used to seeing cracks in the corners of fresh pillars.

Another possible explanation is that at the corners, one visually observes the diagonal of the scaled area which is by definition longer than the perpendicular distance one observes in the mid pillar areas.

Table 6. Observation of pillar corner scaling.

	Mine - Area	**Average of additional corner scaling δd (m)**	**Average of additional corner scaling (%)**
No 2 seam	Blinkpan	- 0.13	- 22 %
	Delmas - open	+ 0.02	+ 3 %
	Delmas - sealed	- 0.17	- 17 %
Average No 2 seam		*- 0.09*	*- 12 %*
No 4 seam	Matla - A1	+ 0.02	+ 3 %
	Matla - E	+ 0.27	+ 79 %
	Matla - G	+ 0.06	+ 7 %
	Matla - Last	+ 0.09	+ 21 %
	Matla - T	+ 0.18	+ 28 %
	Matla - U1	- 0.01	- 1 %
	Secunda	- 0.04	- 8 %
	Tweefontein - 1	- 0.19	- 33 %
	Tweefontein - 2	- 0.13	- 32 %
Average No 4 seam		*+ 0.03*	*+ 7 %*
Average All Pillars		**-.003**	**-2%**

9.4. Direct Measurement Vs Comparison With Original Off-Sets

It was found in 4 of the cases where the newly measured road widths were compared to the original average off-sets obtained from the mines, that the pillars had actually increased in size. This is clearly not possible. While the reason for this could not be established, it was decided not to use that data but to rely only on the direct measurements of scaling underground.

While this meant that some data was lost, there was still sufficient left to complete the analysis. The data that was retained for use in the scaling rate analysis, is summarised in Table 7. The data that was used was collected from 352 pillars in 12 panels. The data used for the indirect analysis comprised 19 panels on the combined No's 2 and 4 Seams.

Table 7. Data used for the scaling rate analysis

Mine	Area	Coal Seam	No of pillars measured
Blinkpan		No 2	33
Delmas	Open	No 2	25
	Sealed	No 2	10
Matla	A1	No 4	24
	E	No 4	30
	G	No 4	5
	Last	No 4	14
	T	No 4	30
	U1	No 4	19
Secunda		No 4	33
Tweefontein		No 4	73
Leeuwfontein		No 4	56
Total			**352**

10. Determination of Scaling Rates

The average scaling rates were then determined for each of the cases and compared to the predicted rate as a function of the mining height to pillar age ratio (*h/T*), as previously described. The scaling distances were the measured distances as shown in Table 5. Note that the distances shown in Table 5 reflect the individual measurements taken on each side of the pillar. The scaling distance of the pillar is the sum of the scaling on opposing sides, being the total distance by which the pillar width is decreased. Table 8 summarises the results.

Table 8. Comparison of Measured and Predicted Scaling Rates

Mine	Area	Age (Years)	Height (m)	H/T	Measured Scaling Distance (m)	Measured Rate (m/yr)	Predicted Rate (m/yr)
Blinkpan		39	2.92	0.0749	0.84	0.0215	0.0197
Delmas	Open	19	2.80	0.1474	0.66	0.0347	0.0342
	Sealed	19	3.00	0.1579	1.42	0.0747	0.0362
Matla	A1	22	3.85	0.1750	1.00	0.0455	0.0393
	E	5	3.93	0.7860	0.48	0.0960	0.1335
	G	21	3.96	0.1886	1.28	0.0610	0.0418
	Last	14	3.25	0.2321	0.6	0.0429	0.0495
	T	5.5	4.03	0.7327	0.94	0.1709	0.1261
	U1	22.5	4.86	0.2160	1.20	0.0533	0.0467
Secunda		12.5	2.58	0.2064	0.72	0.0576	0.0450
Tweefontein		21.5	2.88	0.1340	0.58	0.0270	0.0316
Leeuwfontein		.67	3.48	5.1940	0.30	0.4500	0.6204

The average scaling rates based on the measurements, as a function of time, confirms the trends found previously, using data inferred from the ages of pillars at the time of collapse. In both cases, the maximum rate occurs in the very beginning and it then decreases sharply over a short period of

time. One can almost regard this as a bi-linear trend with the highest rate in the period 0 to 5 years, which then decreases rapidly for the rest of the time.

This is shown in Figure 19, a comparison using the measured average scaling rates shown in Table 7 and the inferred data for the No's 2 and 4 Seams in Figure 6. It is shown that the two data sets are practically overlapping at all stages. The correlation coefficients between the measured and inferred data sets was 0.98.

The original scaling rate, R_I, as a function of time, T, using the inferred data, was

$$R_I = 0.45T^{-0.79} \tag{11}$$

Using the measured data, the expression is

$$R_M = 0.44T^{-0.77} \tag{12}$$

The close correspondence between the two expressions points to the similarity of the measured and the inferred data sets.

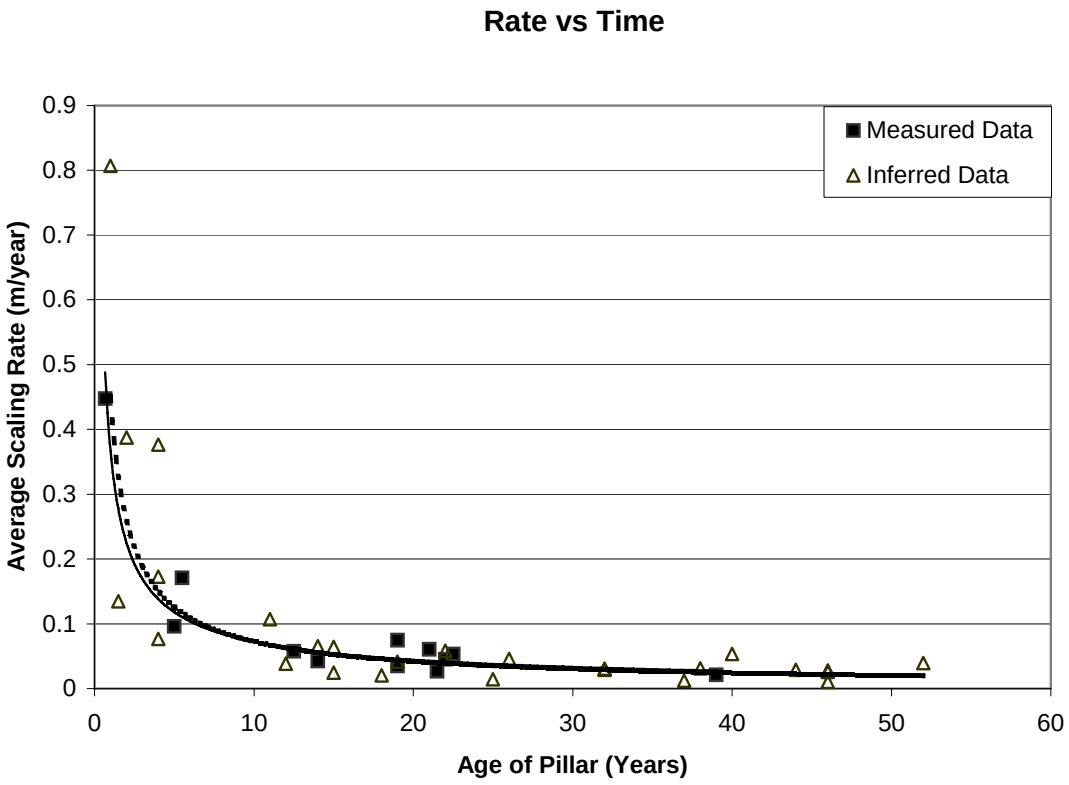


Figure 19. Comparison of the average scaling rates using the measured data and the inferred data.

It is seen from Table 8 that there is close agreement between the measured and the predicted scaling rates (using Equation 7) as a function of the *h/T* parameter. The correlation coefficient between the predicted and measured rates is 0.98. This could be seen as an "inflated" correlation coefficient, due to the good agreement between the values for the Leeuwfontein case, which is a remote point on the graph, see Figure 20. Discarding that single data combination, the correlation coefficient reduces to 0.85, which is still an indication that the data is very well correlated. The high correlation coefficients can be regarded as further indication that the original assumptions and the derived scaling rates have been validated by measurement.

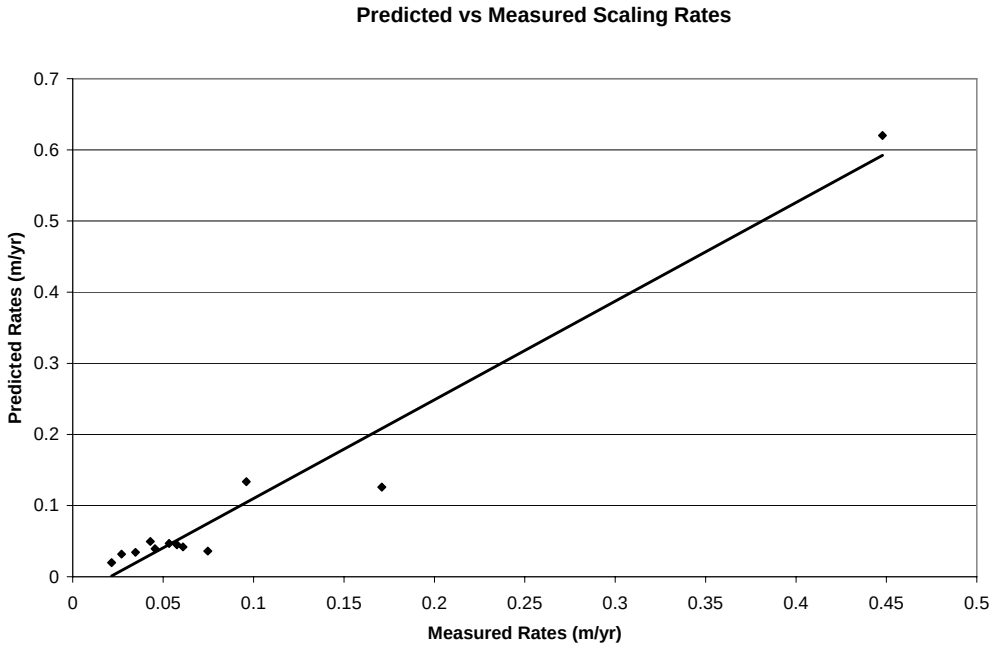


Figure 20. Comparison of predicted and measured scaling rates.

When the last two columns of Table 8 are compared on a point by point basis, it is apparent that there is one point where the measured scaling rate is significantly greater than the predicted rate. That is the third point, from "Delmas sealed". It is noteworthy that the only point with a much greater than expected scaling rate – it is more than double – is also the only one where measurements could be taken in a sealed panel. All the others were ventilated. It has often been remarked that the amount of scaling appeared to increase when panels were sealed, but whether this was a perception caused by lack of cleaning up operations or real, could never be ascertained.

A single data point is not sufficient to base any conclusion on, but it indicates a direction for further investigation.

11. Confidence and significance

In an empirical study, one of the most important issues is the size of the sample, as together with the amount of scatter, it affects the level of confidence that can be attached to the results.

In this particular case, the central issue is the rate of scaling, which has been seen to correspond to the predicted scaling rates with a high correlation coefficient. To test the validity of the results, standard statistical procedures were used, specifically as described by Bowker and Lieberman (1959).

For convenience, the scaling results that were found by measurement as compared to the predicted rates, are reproduced here in Table 9 with the addition of the ratio of predicted to measured scaling rates. The single data point from the sealed panel, "Delmas Sealed" has been omitted as it is obviously anomalous. Eleven cases are thus considered.

Table 9. Statistical parameters relevant to the scaling rates.

Mine	Area	Measured Rate (m/yr)	Predicted Rate (m/yr)	Ratio of Measured to Predicted Rate
Blinkpan		.0215	.0197	1.0924
Delmas	Open	.0347	.0342	1.0156
Matla	A1	.0455	.0393	1.155
	E	.0960	.1335	.7190
	G	.0610	.0418	1.4582
	Last	.0429	.0495	.8658
	T	.1709	.1261	1.3553
	U1	.0533	.0467	1.1424
Secunda		.0576	.0450	1.2803
Tweefontein		.0270	.0316	.8524
Leeuwfontein		.4478	.6204	.7218
Mean (μ)		.0962	.1080	1.0599
Standard Deviation (σ)		.1238	.1740	0.2499

It was hypothesised that the ratio of predicted to measured scaling rates equals a value of 1.0.

The rules for acceptance are that the Type I Error (i.e. the probability of rejecting the hypothesis if it is indeed true) should not exceed 5% (i.e. α = 0.05) and the type II Error (i.e. of accepting the hypothesis if it is indeed incorrect) should not exceed 20% (i.e. β = 0.2). The maximum margin of error is 20% either side of 1.0, or the prediction should be 80% correct.

The parameter *d*, defined as

$$d = \frac{|\mu_1 - \mu_0|}{\sigma}, \tag{13}$$

is then found to be 0.8 and the required sample size, *n*, is 12.

The hypothesis will be accepted if the statistic *U*, defined as

$$U = \frac{(\bar{x} - \mu_0)\sqrt{n}}{\sigma}, \tag{14}$$

falls within the range $-K_{\alpha/2}$ *to* $K_{\alpha/2}$, or 1.96 to -1.96. As *U* is found to be 0.795 with values of 1.0599 and 11 for *x* and *n* respectively, the hypothesis can be accepted for the stated limits and conditions. In other words, one can be 80% certain that the ratio of predicted to actual scaling rates differs by less than 20%.

12. Discussion and Conclusions

12.1. The safety factor is a poor predictor of pillar life

It was shown in Section 4 of the paper, and particularly by Figure 4, that the safety factor on its own cannot be used in a quantifiable manner to predict pillar life.

12.2. The differences in behaviour between the coals in different seams and areas have to be taken into account

It was found that without differentiation of the data base, no useful trends could be found that could enable a prediction method of pillar life to be developed. This finding corresponds with the recent work done on laboratory strength tests of coal samples from different areas - van der Merwe, (2003b) - and the derivation of an optimum formula for pillar strength - van der Merwe, (2003) - where it was shown that the differences in behaviour between the different areas are quantifiable. This finding corresponds with the experience of underground coal miners in South Africa. There is now ample evidence to allow differentiation between the different areas. More work on the reasons for the differences and boundaries of the groupings will be of benefit.

12.3. The majority of pillars in South Africa fail by a process of progressive pillar scaling

The results obtained by the method based on the assumption that pillars fail by progressive scaling, indicates that the assumption is probably correct. This is backed up by observation over several years in different coal mining areas of South Africa.

12.4. The rate of scaling decreases over time

It was shown that the initial scaling rate is the highest and that it decreases rapidly with time. This conforms with the observation that the majority of known failures occurred relatively soon after the formation of the pillars. It is also in accordance with the observations by van Biesien and Rockaway (1988) in the USA.

12.5. The scaling rate is directly proportional to the mining height.

It was shown that there is a general trend that the higher the mining height, the greater the rate of scaling. The rate of scaling does not correlate with other measurable parameters like pillar stress or width-to-height ratio.

12.6. The time of pillar failure depends on the maximum amount of tolerable scaling

It was shown that failure occurs when the amount of scaling reaches the maximum tolerable amount by which the pillar width can be decreased. This indirectly brings the safety factor into play. With the safety factor comes all the related matters like pillar load, width-to-height ratio, etc that in isolation, do not play a discernible role in the time of failure. The higher the safety factor, the greater the amount of scaling that can be tolerated. In this context, the term “scaling” implies the distance into the pillar by which there is a loss of strength. Whether this is always due to physical detachment of portions of the pillar sides or merely the loss of strength caused by oxidation or other processes is not yet known and should be researched.

12.7. The proposed method to predict pillar life corresponds with the characteristics of both the failed and intact pillar case data bases in South Africa.

It was shown that the proposed method results in frequencies of failure over time that match the frequencies of observed pillar collapses in South Africa to a high degree. It was also shown that the method is successful in distinguishing between the cases of failed and intact pillar cases. The predicted lives of failed pillars matched their observed lives, while the predicted lives of the intact pillars were orders of magnitude greater.

12.8. Pillars that have not failed soon after mining can be expected to be stable for a very long time.

In this context, "soon after mining" means within 20 or 30 years. The reason for this is that the rate of scaling decreases rapidly over time and if the critical scaling distance is not reached within the period of high scaling rates, it will take ever longer to reach it. This has major implications for the undermining of structures by high safety factors and for the provision of funds to cater for post mine closure mitigation of damage due to subsidence. It means that if failure does not occur during the first few decades after mining, the pillars may be expected to be stable for much longer periods than is usually catered for in human planning. The periods of expected stability will probably span millennia in several instances. It was also shown that there is considerable merit in conducting further research into the possibility that choking of the excavations can permanently halt the failure process.

12.9. There is now potential to predict the probability of failure of pillars over time.

The overlap between the populations of failed and thus far stable pillar cases can be used to calculate the probability of failure of pillars as a function of time. For this to be done, the data base of intact pillars has to be revised in the light of the most frequent mining conditions over the last few decades. The intact pillar data base of Salamon and Munro (1967) is useful to demonstrate the ability of the prediction method to distinguish between failed and stable pillar cases as it is an accepted collection of representative intact pillar cases, but for actual probability of failure predictions, it will have to be extended.

12.10. New philosophy for pillar design

Instead of designing pillars to a specific safety factor, it would be more practical to design around a desired pillar life. It has been shown that the method to predict pillar life presented in this paper, albeit crude, can distinguish between cases of failed and intact pillars at a given point in time, which is what a safety factor formula should logically do. It is known that the concept of pillar stability is dependant on time – what is stable today may not be stable in a decade or a century. With further refinement, it may become possible to develop a procedure to design pillars to be stable for a specified time period. For instance, pillars underneath structures that require protection may be designed as "10 000 year pillars" while production panels without any surface or safety related constraints may be designed as "10 year pillars".

12.11. There is no clear preferential direction for pillar scaling

The data indicated that although there were minor differences in the scaling distances measured on the different sides of a pillar, there was no clear directional preference. Also, the differences were relatively small and not in the range likely to affect pillar stability or induce appreciable error if measurements are not taken all around a pillar. This has important bearing on future data collection.

12.12. Pillar corners do not scale appreciably more than the sides

This rather unexpected conclusion indicates the danger of relying on visual observations which are not confirmed by measurement. The reasons for the incorrect perception that the corners are more prone to scaling are difficult to ascertain. It can be speculated that it could be because one observes the diagonal of two perpendicular scaling sets at intersections, that cracks are more visible at the corners or that the process starts at the corners. This conclusion may confirm that the pillar edge stresses are not significantly greater than the stresses deeper inside the pillar.

12.13. The pillar scaling rates previously inferred, have been confirmed by measurement within certain limits of confidence.

This is the most important conclusion of the study. The central goal of the investigation was to determine whether the scaling rates inferred by the original report were correct or whether adjustments were required. Confirmation of the inferred scaling rates by direct measurement on pillars that have not failed, by implication means that the assumptions regarding the minimum safety factor of a pillar prior to failure (0.4 using the linear formula of van der Merwe 2003a), is also in the correct range. The previously developed procedure for the prediction of pillar life spans, can thus be used with more confidence as the key assumptions have now been validated by measurement.

The limitations are that the predicted rate can only be assumed to be correct to within 80% and that there is a 20% probability of accepting an incorrect scaling rate as the correct one. These are obviously broad limits, but one has to bear in mind that there are several reasons for the amount of scatter observed in pillar behaviour.

12.14. The influence of sealing panels should receive urgent attention

It has been remarked, Madden (2003) that once a panel is sealed off, the scaling tends to increase. It was only possible to take measurements in one panel that had been sealed and that single data point exhibited a much greater scaling rate than was anticipated. This cannot be regarded as conclusive evidence, but in the light of the serious ramifications if sealed panels do in fact have much greater scaling rates, this matter should receive urgent attention.

12.15. The mechanism of pillar deterioration should be researched

The work described in this paper focussed on the observations of pillar scaling without attempting any explanations for the phenomenon. Whether it is due to chemical changes taking place or mere material fatigue under the conditions of elevated stress and sufficient space into which to expand, remains unknown. The matter will only be fully understood once the causes are known. It is also important from the point of view of preventing pillar collapse – for instance, are pillars with higher sulphur content in the coal prone to higher scaling rates? What role does the moisture content play? How important is the oxygen level in the underground atmosphere? Are there changes in coal composition at the edges of pillars that have been exposed to the atmosphere?

These questions indicate a new direction of research into long-term pillar stability.

13. Acknowledgements

The permission and assistance of managements of the following mines where data was collected, is greatly appreciated:

- Matla Mines
- Tweefontein Colliery
- Delmas Colliery
- Blinkpan Colliery
- Secunda Collieries
- Leeuwfontein Mines.

Mr Christophe Baron performed the measurements as an exchange student between the University of Pretoria and the Nancy School of Mines, facilitated by CSIR Miningtek. The cooperation of the three institutions to make this work possible is gratefully acknowledged.

The input and assistance of Mr Ismet Canbulat of CSIR Miningtek – both professionally and in the administrative sphere - and the professional assistance rendered by the greatly experienced Mr Gary Prohaska of CSIR Miningtek are deeply appreciated.

This work was sponsored by the Coaltech 2020 research initiative, whose support is gratefully acknowledged. The contribution of Mr Bill Abel of Anglo Coal, through in depth discussion, is likewise acknowledged.

This paper is essentially a combination of two papers that were previously published in the *Journal of the South African Institute of Mining and Metallurgy*.

14. References

Van der Merwe J. N. (2003). *A Linear Coal Pillar Strength Formula for South Africa.* J. South Afr. Inst. Min & Metall. June 2003.

Van der Merwe J. N. (2003a). *Predicting Coal Pillar Life in South Africa.* J. South Afr. Inst. Min & Metall. June 2003.

Van der Merwe J. N. (2003b). *A Laboratory Investigation Into the Effect of Specimen Size on the Strength of Coal Samples From Different Areas.* J. South Afr. Inst. Min & Metall. June 2003.

Bowker, A. H., Lieberman J. L. (1959). *Engineering Statistics pp 96 – 119.* Prentice-Hall Inc, Englewood Cliffs, N.J.

Madden B. J. (2003) *Personal communication.*

Salamon M. D. G., Munro A. H. (1967). *A Study of the Strength of Coal Pillars.* J. S Afr Inst Min Metal. September 1967.

Salamon M. D. G., Ozbay M.U., Madden B.J. (1998). *Life and design of bord and pillar workings affected by pillar scaling.* J. S Afr Inst Min Metal. May 1998.

Van Besien A.C., Rockaway J.D. (1988). *Influence of Overburden on Subsidence Development Over Room and Pillar Coal Mines.* In Engineering Geology of Underground Movements. Ed. Bell, FG et al. The Geological Society, London.

Hao Q-W., Chug Y. P. (1992). *An Engineering Approach to Predict Subsidence Likelihood Over Abandoned Coal Mines in Illinois.* In Proc. 3rd Subsidence Workshop Due to Underground Mining. Ed SS Peng West Virginia University, Morgantown, West Virginia, USA.

Van der Merwe J. N. (1993). *Revised Strength Factor for Coal in the Vaal Basin.* J S Afr Inst Min Metal March 1993.

Van der Merwe J. N. (1998). *Prediction of pillar life in the Vaal Basin, South Africa.* Proc 17th Intnl Conf Ground Control in Mines, Morgantown, West Virginia, USA 1998.

Appendix A: Data base of failed pillars used for the time of failure study

In this appendix, the prefix "s" in the case numbers refers to cases collected by Salamon and Munro (1967), "m" refers to cases collected by Madden and "n" refers to cases collected after 1995.

Case no	Colliery	Seam	Coal Field	Depth	Pillar width	Bord width	Mining height
s12	Coronation	W1	Witbank	25.9	3.7	8.5	3.1
s16	M Steam	W2	Witbank	21.3	4.0	8.2	4.6
s17	Wolvekrans	W2	Witbank	29.6	5.2	7.0	5.5
s40	Wolvekrans	W2	Witbank	33.5	6.1	6.7	5.5
s41	Crown Douglas	W2	Witbank	30.5	4.6	7.6	3.7
s57	Koornfontein	W2	Witbank	88.4	7.2	6.6	4.9
s116	Waterpan	W2	Witbank	61.0	6.1	6.1	4.6
s118	Waterpan	W2	Witbank	57.9	6.1	7.6	4.0
m149	Koornfontein	W2	Witbank	90.0	7.5	6.0	4.8
m151	Tweefontein	W2	Witbank	62.0	7.5	6.4	4.0
m162	Tweefontein	W2	Witbank	62.0	7.3	6.2	4.0
m166	Tweefontein	W2	Witbank	62.0	6.1	6.1	4.0
m167	Tweefontein	W2	Witbank	62.0	6.1	6.1	4.0
n171	Wolvekrans	W2	Witbank	41.0	6.4	6.4	6.2
n172	Wolvekrans	W2	Witbank	41.0	6.4	6.4	6.2
n173	Wolvekrans	W2	Witbank	41.0	6.4	6.4	6.2
n200	New Largo	W4	Witbank	43.0	4.8	6.2	2.8
s9	New Largo	W4	Witbank	30.5	3.4	6.4	2.6
s64	South Witbank	W4	Witbank	61.0	4.7	6.9	3.5
s119	W. Consolidated	W4	Witbank	41.1	4.3	6.4	3.1
m148	New Largo	W4	Witbank	28.5	3.8	5.8	2.7
m148a	New Largo	W4	Witbank	34.0	3.5	6.7	2.7
m148b	New Largo	W4	Witbank	34.0	3.5	6.7	2.7
m163	South Witbank	W4	Witbank	56.0	5.1	6.5	3.3
n198	New Largo	W4	Witbank	32.0	3.3	6.4	2.3
n199	New Largo	W4	Witbank	32.5	3.2	6.5	2.1
s42	South Witbank	W5	Witbank	53.3	5.2	6.4	3.7
s55	Blesbok	W5	Witbank	68.6	3.4	5.8	1.5
s58	South Witbank	W5	Witbank	57.9	5.2	6.4	5.5
m165	Springbok	W5	Witbank	22.0	3.5	6.5	1.6
n174	Matla	W5	Witbank	35.5	5.5	5.5	2.2
n185	Umgala	Alfred	Utrecht	101.0	9.0	6.0	3.8
n186	Umgala	Alfred	Utrecht	100.0	8.5	6.5	3.3
n187	Umgala	Alfred	Utrecht	97.0	9.0	6.6	3.7
n188	Umgala	Alfred	Utrecht	51.5	6.0	6.0	3.9
s66	Springfield	Main	South Rand	193.2	15.9	5.5	5.5
s67	Springfield	Main	South Rand	184.7	15.9	5.5	5.5
s122	Springfield	Main	South Rand	167.6	15.9	5.5	5.5
m168	Springfield	Main	South Rand	165.7	15.0	5.0	5.9
m169	Springfield	Main	South Rand	195.0	17.0	6.0	4.9
m170	Springfield	Main	South Rand	205.0	17.0	6.0	5.9
s126	Vierfontein	Main	Free State	87.8	6.1	6.1	2.0
n175	Springlake	Bottom	Klip River	70.0	7.5	5.0	1.8
n176	Springlake	Bottom	Klip River	63.5	7.5	5.0	2.1
s120	Cornelia	OFS1	Vaal Basin	128.0	9.8	5.5	3.7
m157	Sigma	OFS2	Vaal Basin	112.0	10.6	6.5	2.8
m159	Sigma	OFS2	Vaal Basin	108.0	10.6	6.5	3.2
n180	Sigma	OFS3	Vaal Basin	82.0	10.0	5.0	2.8
n181	Sigma	OFS3	Vaal Basin	96.0	12.0	6.0	2.9
n184	Sigma	OFS2a	Vaal Basin	112.0	11.5	5.5	2.9
n196	Sigma	OFS2a	Vaal Basin	104.0	12.0	6.0	3.0

DEVELOPMENT OF TOOLS FOR MANAGING THE IMPACTS ON SURFACE DUE TO CHANGING HYDROLOGICAL REGIMES SURROUNDING CLOSED UNDERGROUND COAL MINES (ECSC COAL RTD PROGRAMME, CONTRACT 7220-PR-136)

VESCHKENS Mathieu[1], UNLAND Werner[2], KORIES Holger[2]

[1] ISSeP, Rue du Chéra, 200 – B 4000 Liège, - Belgium. ma.veschkens@issep.be

[2] DMT, Am Technologiepark,1 – D 45307 Essen, - Germany. Wener.Unland@dmt.de, Holger.Kories@dmt.be

ABSTRACT: This paper demonstrates how box model approach and FE and box mixed model approach allow to better understand and model water flows in complex mined coal measures and interactions between shallow aquifers and flooded coal measures. Benefits of these approaches are illustrated on the basis of case studies in Liège and Ruhr coal basins.

KEYWORDS: Water rebound, Box model, Mixed model, Coal mines, RFCS

RESUME : Cet article montre l'apport de l'approche de type « box model » et de la combinaison de modèles de type éléments finis et de type « box » dans la compréhension et la modélisation des écoulements dans les massifs charbonniers exploités complexes et des interactions entre les eaux minières et les aquifères adjacents. Les avantages sont illustrés à l'aide de cas d'étude choisis dans les bassins houillers de Liège et de la Ruhr

MOTS-CLEFS : Ennoyage, Modèle de type Box, Modèle mixte, Mines de charbon, RFCS

1. Introduction

Closed underground mines may induce risks for the environment and for the safety and health of the population living at the surface around the mine or nearby. Some of these risks are linked to the modification or the shut down of the mine water pumping operations leading to a groundwater rebound, they include: the pollution of underground or surface water, the flooding of zones subsided below the water table level, additional surface movements in relation with collapse of shallow mine workings or even surface heave, accelerated mine gas emissions.

These risks exist after the mine closure in the short term but especially on the long and very long term depending on the quantity and flow of water involved and the volume of the mine workings concerned.

In order to better understand the three inter-related phenomena: water rising in mining areas, stability issues relating to the flooding of shallow mine workings and surface responses to groundwater rebound, a project called "Development of tools for managing impacts due to changing hydrological regimes surrounding underground coal mines" (contract 7220-PR-136) has been performed in the framework of a research programme of the Research Fund for Coal and Steel (RFCS).

The most important tasks of this project conducted by a consortium composed of AIDE[1], Armines[2], DMT[3], University of Nottingham[4] and ISSeP[5] consisted in: back analysis of case studies, detailed

[1] Association Intercommunale de Démergement et D'Epuration. Rue de la Digue, 25 B 4420 Saint Nicolas. Mr R. De Schrijver

[2] Association pour la Recherche et le Développement des Méthodes et Processus industriels, 60, boulevard Saint Michel, F-75272 Paris. Dr F. Hadj-Hassen

site analysis of selected pilot sites, lab experimental works and development of modelling tools.

This paper will only focus on highlighting the work parts related to the development of numerical tools aiming at better understanding and modelling water flows in complex mined coal measures and interactions between shallow aquifers and flooded coal measures. Results related to other aspects of the project will also be presented by other authors on the occasion of Post-Mining 2005. (Shenk and Reddish, 2005), (Wadim, Hadj-Hassen, and al., 2005)

The hydraulic situation in underground coal mines is fundamentally different from the situation within an ordinary continuous aquifer system. In underground mines, drifts, adits and shafts provide practically no resistance to mine water flow and facilitate equal hydraulic heads over long distances, standard groundwater flow models are thus not suited to represent such conditions.

Recently numerical models for mine water flow and rebound have been developed on the basis of the "box model" approach. This type of approach consists in dividing the study zone in a series of boxes, each one representing a working zone drained by a network of galleries. These compartments are separated by unworked layers of rocks acting as a barrier. It is nonetheless possible that the compartments are interconnected by means of galleries or faults.

The mass conservation principle is applied to each of these compartments: the differences between inputs (pluviometric recharge, input from other compartments,…) and outputs (pumping, outflow in the waterways, export towards other compartments,…) express themselves by a variation of the water stock in the compartment and by variations of the water level, function of the porosity characterizing the compartment. The exchanges between compartments are represented by simple transfer equations (function of the load difference).

This approach has the advantage of taking into account, globally, the distinctive features of the mining system without requiring a comprehensive description and a too considerable quantity of data. At the beginning of the project, it was already used in Germany and in other countries to model flooding processes of underground coal mines (Sherwood and Younger, 1997), (Banks, 2001) but ready made models were not available on the market..

It thus appeared useful to build such a model in order to better understand the water table variations in the mined coal measures of river valleys even where the rebound process due to the shut down of the pumping operations is supposed to be ended.

On the other hand, as it was clear that when mine waters interact with other aquifers, the assumptions made in the box model approach did not allow to identify all the impacts linked with total water rebound with the requested accuracy, DMT and ISSeP, with the help of the University of Liège, decided to try to combine models based on box approach and models developed on more traditional approaches (FE and FD). This part of the project has been performed in view of forecasting the interactions between flooded mines and shallow aquifers in Ruhr area, for DMT and of identifying the potential changes in water level and flows within mined coal massif affected by drainage pattern modifications, for ISSeP and the University of Liège.

---

[3] Deutsch Montan Technologie

[4] University of Nottingham, School of Civil engineering. Centre for Geomechanics, University Park NG7 2 RD Nottingham. Dr Y Sheng

[5] Institut Scientifique de service Public

2. Study of water table variations in the mined coal measures of the Liège coal basin by means of a box model approach

Recent experiences in the Liège coal basin showed that different mechanisms could lead to important secondary water rising. This situation can be encountered in coal basin located in valley areas. The shut down of the pumping operations induced a first water rising, the water table reaching the level of the drainage galleries emerging at the level of the river flowing in the valley. The water table remains constant as long as the gravity drainage allows the evacuation of the water volume percolating through the fissured coal measures and the mining works. If for some reasons, one part of the mining works is disconnected from the drainage galleries or if the flow in the drainage gallery itself is impeded, the water starts rising again up to a level depending on the level of new outlets. Due to this additional rising, new impacts appear such as: water emergence at the foot of the valley slopes; the loading of the alluvial aquifers, an increase of the pore-fluid pressure within the rock massif.

2.1 Analysis of the available data. Selection of a modelling approach

At the beginning of the project, scientific information on the flows within the mined coal measures of the Liège coal basin did not exist. Neither recent piezometry maps nor water budgets were available. Monitoring of the drainage galleries had been abandoned for more than 15 years. It is the reason why the first stage of the study consisted in selecting a relevant pilot site, analysing all the geological, hydrological and mine information related to this site and assessing water budgets

Detailed studies of mining plans led to locate a great number of underground works used for the drainage of carboniferous massif. The analysis of the position of all these galleries demonstrated the existence of 5 networks not directly inter-connected. Connections between these networks trough the fracturing of the rocks induced by the exploitations and trough deeper works can however not be excluded.(Fig. 1)

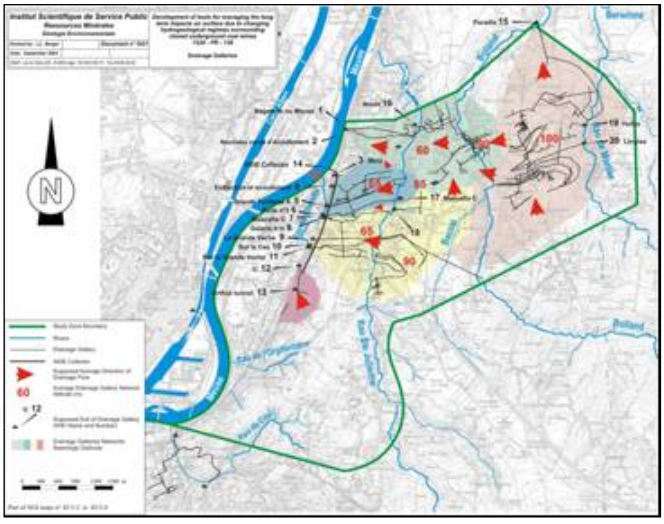


Figure 1. Liège coal basin. Identification of the 5 blocks within the pilot site.

A cross analysis of all the available information led ISSeP to consider that from the hydraulic point of view the mined coal measures are composed of different blocks with their own behaviour. Hence, conceptually, the mined coal measures above the drainage level was considered as a network of boxes connected more or less between themselves and by galleries to the surface water,

recharged by rain infiltration trough overlying quaternary or strata and potential river seepage and fitted with junctions trough which water withdrawal can occur.

2.2 Selection of a modelling tool (Gardin and Brouyère, 2005)

Despite the efforts spent on the analysis of the available data, information collected on several features (connection between different mining areas, flow exchange with the areas bordering the pilot site, spatial distribution of the remaining voids, …) remained too incomplete to formulate a single conceptual model. To get round these difficulties, it was decided to try to model the phenomena with the help of a simplified box model, to compare the results obtained with the measurements supplied by monitoring campaigns and then according to the matching degree to go on with the assumptions or to assess new ones.

When a box approach is used for modelling flow, the major assumption consists in considering that from the hydraulic point of view the rock massif is composed of boxes to which a unique water level can be attributed and which are connected between themselves by a network of galleries. A situation which is very similar to the one of a network of tanks connected with pipes provided the fact that the volumes attributed to tanks correspond to the global porosity (the intrinsic porosity plus the remaining voids created by mining operations) of the boxes.

For this reason it was decided to test the EPANET program[6]which is a tool developed by EPA[7]in order to model flow in water supply networks. EPANET models water supply networks as a collection of links collected to nodes. The links represent pipes, pumps and control valves. The nodes represent junctions, tanks and reservoirs. EPANET components and the governing equations used for modelling flow according to the other variables appeared suitable for developing models based on a box model approach.

With EPANET, flow within a network is governed by two laws:

- the first one links the flow rate between two nodes (between two boxes, between a box and a drainage point,…) by the following relationship:

$$H_i - H_j = h_{ij} = A\ Q_{ij}^{\ B} \quad (1)$$

  Where
  h_{ij} = headloss between node i dand j
  Q_{ij} = flow rate between node i and j;
  A = resistance coefficient, for the resistance coefficient;
  B = flow exponent, different values can be used for the flow exponent

- the second one expresses the water balance equation (or conservation of mass) at each node of the network.

$$\sum j = Q_{ij} - D_i \quad (2)$$

  Where
  Q_{ij} = flow rate between node i and j;
  D_i = recharge or withdrawal rate by a pumping or injection well.

[6] http://wwww.epa.gov.ORD/NRMRL/wswrd/epanet.html
[7] Environment Protection agency. http//www.epa.gov

However, in order to yield a water table as close as possible to the reality from a box model, it is also necessary to take into account that the porosity ratio varies according to the vertical location. In EPANET it can be done by allowing storage tanks diameter which are cylindrical volumes to vary according the z coordinate. As far as its height is concerned, it is fixed by the distance between the water drainage level and the mined massif top.

In EPANET, receiving surface water is represented by reservoir elements which are supposed to be infinite external sinks of water and are characterized by hydraulic heads not affected by what happens in the network. However heads can be made to vary with time (by assigning a time pattern) in order to take into account the variations in the drainage level related to modifications in the receiving surface water regime. Recharge is modelled by junctions which are points of the network where water enters or leaves the network. They are characterized by a rate of recharge which can vary with time or which can be made dependent on a pressure gradient. Finally tanks (boxes) are connected between themselves or to receiving water by means of pipes which are characterized by their status (open, closed) and the headloss they cause.

2.3 Development, calibration and identification of the capacity of models based on EPANET program

Each of the parts of the pilot site mined coal measures drained by one of the five networks identified in the survey stage has been considered as a tank the volume of which corresponds to the global porosity of the zone. In a first stage, as the spatial distribution of the remaining void is not known accurately, the tank is represented by a simple cylinder. Its height corresponds to the distance between the drainage level (+/- 55 m) and the top of the coal measures (+/- 130 m). (Fig.2)
The model has been calibrated on the basis of both the piezometric levels and drainage flows measured by the monitoring network in service since three years and the water budgets established on the pilot site and by adjusting the resistance coefficient $A_{i,j}$ of the connections of the different boxes between themselves and with the water surface.

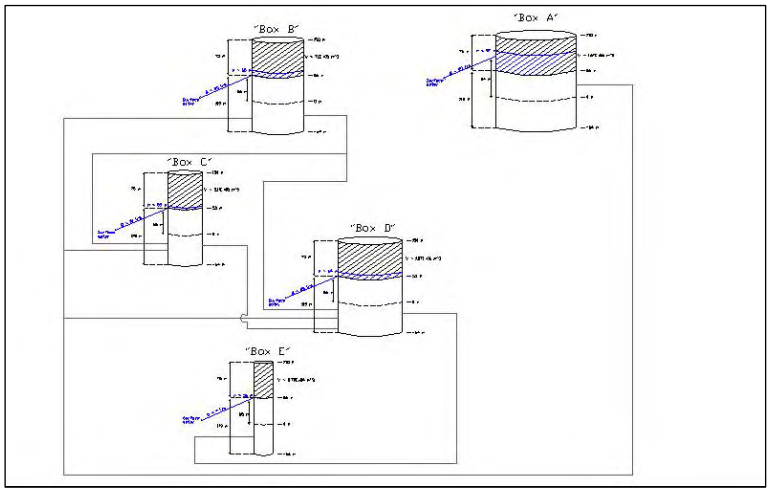


Figure 2. Liège coal basin. Conceptual model of the pilot site.

Once a good matching was reached between the measured water levels and drainage flows and those calculated reached, the model was used to simulate water rising which is supposed to have taken place after the closure of the pumping operations. Although this process was not followed up it was necessary to check that the results supplied by the model correspond to the punctual observations performed at that time. According to the model, the rebound phase lasted about three years in Box A and between one and three years in the other boxes. These results are consistent

with the observations. Moreover at the end of the rebound phase, the water levels and drainage flows supplied by the model still correspond to the measures for the recharge ratio attributed to the study area.

At this stage, data are missing for validating further the model, it was thus decided to compare the results supplied by EPANET with those derived from other validated tools like MIFIM (Banks,D. 2001) Comparisons showed that the two tools give similar results.

Additional model runs demonstrated the capacity of EPANET for performing sensitivity analysis, for clarifying the role of the different parameters in the rebound processes induced by variations taking place within gravity drained coal mines and hence for identifying the risk of flow inrush according to the measures supplied by the monitoring network.

Table 1. Comparison of calculated and measured water levels and drainage flow within the five boxes of the pilot site.

Parameters	BOX A	BOX B	BOX C	BOX D	BOX E
Water level measured (m)	97,00	65,00	59,00	64,00	56,00
Water level calculated (m)	96,73	64,66	58,89	63,54	55,67
Difference	0,27	0,34	0,11	0,46	0,33
Drainage flow measured (l/s)	23,00	25,00	21,00	29,00	?
Drainage flow calculated (l/s)	20,30	24,50	19,80	25,90	2,20
Difference	2,70	0,50	0,20	4,10	

Besides these positive aspects, it has to be admitted that models developed on the basis of EPANET do not allow to represent accurately enough the water level variations in less well drained zones which does not allow to interpret correctly the piezometric map derived from the monitoring work. To reach this aim it is necessary to combine box model and more traditional approaches (see point 3.2)

3. Combining box model and traditional approach

3.1 Study of the interactions between flooded mines and shallow aquifers in Ruhr area

At the beginning of the 7220-PR-136 project, the applicability of numerical box models was already proven in predicting groundwater rebound and in simulating water management in a large section of the Ruhr coal mine district, called Emschermulde.

If the accuracy of such models allowed mining operators to define adequate pumping strategy, it was suspected that it was not sufficient for simulating the impacts of complete groundwater rebound on shallow aquifer in terms as well as of water level rising as of discharge quality of mine water.

It is the reason why DMT has proposed to assess different ways for combining box model and traditional models on a pilot site the Schwarzbach catchment area (part of the Emschermulde area). Figure 3 shows an overlay of the box-model “Emschermulde” with the Schwarzbach catchment area.

As combining both models required balancing water flow in the two models, the seepage rate from the shallow aquifers to the mine workings Q_m (in the shallow aquifer model) had to be set equal to the recharge rate of the mine workings from the shallow aquifer Q_g. (in the box model)

In the existing models of shallow aquifers in the Ruhr area the seepage of groundwater into the deeper underground was usually described by a fixed rate of seepage at the bottom of the aquifer. In the same way, recharge of groundwater into the box model at the top of the Carboniferous layer was up to now defined as a fixed recharge rate. However, in order to use combined models for assessing total water rebound, seepage and recharge rates have to be adjusted according to varying shallow aquifers and flooded mines situations. DMT proposed to make match these situations by Cauchy boundary conditions (leakage boundary condition) such as

$$Q_m = Q_g = A * k_{fv} * (h_g - \max(h_m, C_t)) / m_o \quad (3)$$

Where

Q_g = seepage rate into the deeper underground (m^3/s),
A = area of seepage into the deeper underground (m^2),
k_{fv} = vertical hydraulic conductivity (m/s),
h_g = groundwater level (m),
h_m = mine water level (m),
C_t = top of the Carboniferous layer (m),
m_o = thickness of the water saturated overburden (m).

From this relationship, it can be stated that mine water levels, calculated by the box model, become the leakage potentials of the FE model and the groundwater levels, calculated by the FE model, become the leakage potentials for the box model.

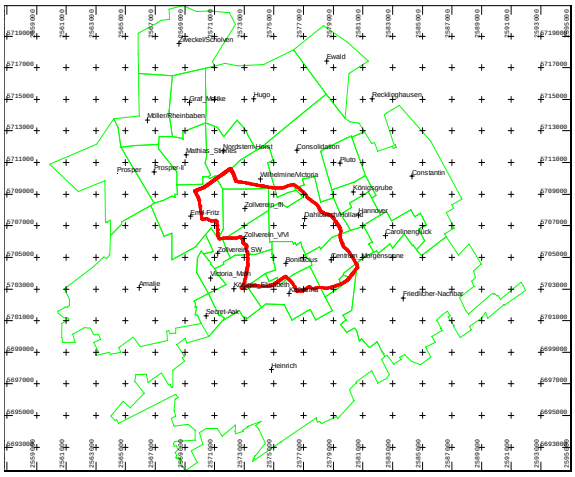


Figure 3. Projection of the Schwarzbach catchment area on the Emschermulde box model.

In the framework of the project, DMT decided to assess the two following solutions to develop an adequate coupling between box models and standard FE models:

- sequential run of the two models and adjustment via boundary conditions (batch approach);
- transformation of FE models into box models by keeping the structure of FE models (unified approach)

The objective followed in the first approach was to couple the two separate models by preserving their original status to the extent possible, using appropriate boundary conditions and exchange data files for the transfer between the models.

The principle of the model coupling by sequential run and adjustment of the boundary conditions consists in making run the two models in a sequential way using a batch process. The linear equation systems involved are normally solved in an iterative way. After each iteration sequence the necessary groundwater levels h_g, calculated by the FE groundwater model, are handed over to the box model and the mine water levels h_m, calculated by the box model, are handed over to the groundwater model.

This is done by writing each simulation result (hydraulic heads) into a specified result file, so that these data can be read by the other program. The batch process used is illustrated in the schematic flow diagram of Figure 4.

This sequential execution of both models is repeated until a certain termination condition is fulfilled (e.g. only minimal changes in mine water and groundwater levels or a maximum number of calculation steps).

Usage of this concept based on batch processes for coupling the separate models via boundary conditions depends on the possibility to execute both models in some sort of batch mode, which requires no manual user input. The two most widely spread groundwater modelling packages in Germany using the FE-method, i.e. SPRING and FEFLOW as well as the box model program offered this option.

The major work of DMT consisted in writing of programs used in the batch process (building of a element-box allocation table, procedures for adjusting the boundary conditions according to the new water levels calculated, conversion programs, graphical subroutine, program checking the termination conditions the routines for exchanging)

The validity of the approach with the Spring and Feflow programs has been controlled by checking the fact that after coupled simulations had been run leakage rates of shallow aquifer remained equal to recharge rates of the flooded mines and by comparing the water levels obtained with those supplied by the calibrated models run separately. For both cases, only slight differences were noticed.

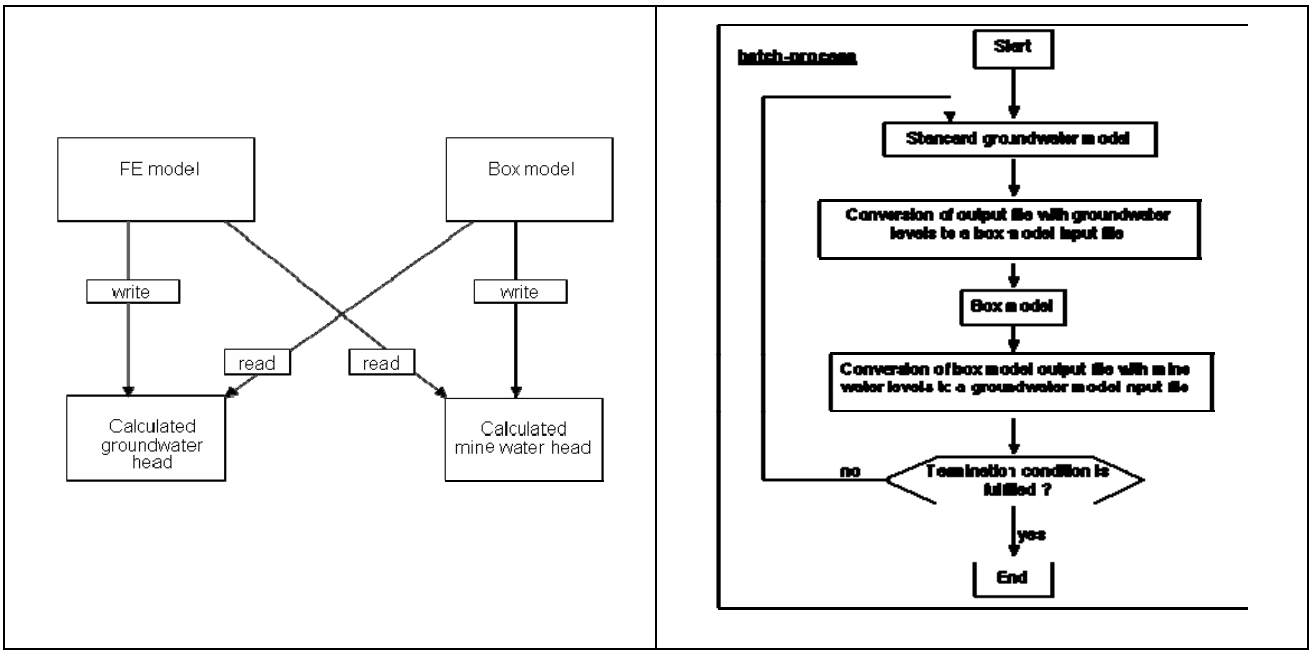


Figure 4. Schematic flow diagram of the FE-Box model coupling by batch process

For the second approach, the method chosen was to convert FE models into special box models supposed to form the uppermost layer of the existing flooded mine box models (unified model). As

the boxes used in a box model approach can adopt theoretically any closed polygonal shape, they can be defined so that they correspond to cells created by FE mesh generators.

However, the main difficulties encountered when converting a FE model into a box model are caused by the different numerical approaches the programs use to solve the flow equations. The FE models discretize the simulation domain in triangular and quadrangular elements over which the differential flow equations are integrated. They are based on parameters and variables, defined for the FE's area (element parameters) and for the nodal points of the FE-grid (nodal parameters). In contrast, the volume balance method used by the box model defines all parameters and variables at the centres of the boxes and balances flow between these boxes. Therefore, transformations of nodal and element parameters of the FE-model to box-centred parameters of the box model has to be made.

Basically, two concepts for transforming a FE-grid to a box model structure could have been considered: adopting the FE-grid using each finite element as a corresponding box structure or building boxes around the nodal points

Since the first approach required the distribution of the nodal parameters over all adjacent boxes, which led to the fact that discrete and exact point information at well-defined locations (e.g. wells, rivers) would not have been represented in an adequate way any more, only the second approach was assessed further.

Building boxes around FEM nodes can be done by connecting all centres of the elements surrounding grid nodes. A special treatment has to be given to nodal points situated at the borders of the FE-grid, because they are not completely surrounded by finite elements.

Once boxes built around the nodal points of the FE-grid, nodal parameters can be easily converted into box-centred parameters. Element parameters can also readily be distributed over all corresponding boxes by using weighted values.

Box models obtained from the conversion of FE models have a much higher spatial resolution than the traditional general box model used for water mine management purposes but their overlapping with traditional box models using coarser box structure does not however cause any special difficulties, as it has been demonstrated by DMT with the Emschermulde unified model.

For the Emschermulde model, the integration of the shallow aquifer and the flooded mines models also requested to find a way for representing the seepage described by Cauchy boundary conditions between boxes of the uppermost and the lower layers. This has been solved by using special connection elements (part of the box model concept) used for the simulation of hydraulic connections between mine fields.

For each of the elements with underground seepage one special connection element with a leakage rate L was created. The lower endpoints of these connection elements were set to coincide with the top of the Carboniferous formation (C_t) so that the underground seepage rate can be correctly calculated as

$$Q_g = L^*(h_g - \max(h_m, C_t) \quad (4)$$

The validity of the unified model has been validated on its capability to represent the present situation. Therefore the reproduction of the calibrated situations obtained separately served as an indicator.

Figure 5 shows the contour lines of the shallow aquifer (Schwarzbach) heads obtained from a unified model after conversion of the FE model compared with those supplied by the calibrated model developed on the basis of the Spring program. It can be stated that differences are very well acceptable.

Different scenarios with partially flooded mine workings including (or not) dewatering measures have been investigated. All these scenarios were considering increased pumping levels. For all scenarios the new pumping levels were chosen in a way that some mine water levels below the Schwarzbach catchment rise to elevations above the top of the Carboniferous formation and hence are affecting the seepage of groundwater into the deeper underground.

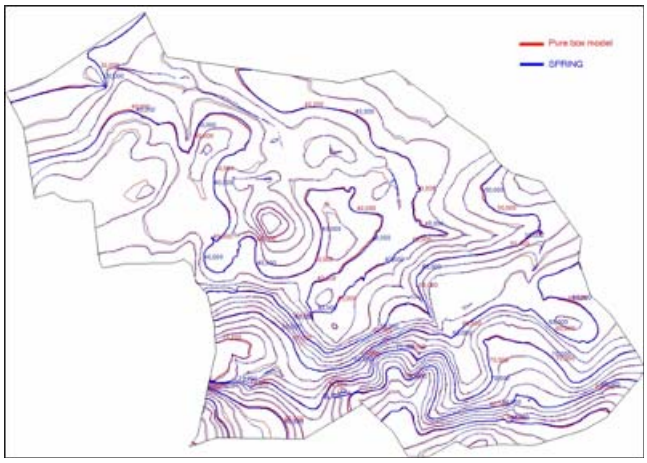


Figure 5. Schwartzbach pilot site. Comparison of groundwater contour lines of the pure box model simulating the present situation with those of the SPRING model

Simulated scenarios with high pumping levels result in elevated mine water levels in the different boxes as illustrated in Figure 6. Noticeable are the small differences in the mine water levels of the different boxes for each scenario, which are a direct consequence of all the hydraulic mine field connections assumed active at these higher water levels.

As far a the shallow aquifer is concerned, the different coupling techniques produce identical results. For this reason, only the results supplied by the batch combined approach (box model – Spring model) for scenarios where it is assumed that mine waters rise up to - 30 masl and dewatering facilities are or are not operational are presented.

Figure 7 shows that due to water rebound in mine workings the water levels of the shallow aquifer rise from values ranging from 0,25 to 2 m so that in numerous areas, the depth of the water table is not greater than 1,5 m which exposes building to ponding effects. They demonstrate also the capacity of the coupled model to simulate the impacts of dewatering measures and hence its usefulness for planning and designing the dewatering strategy to be developed in order to manage surface impacts.

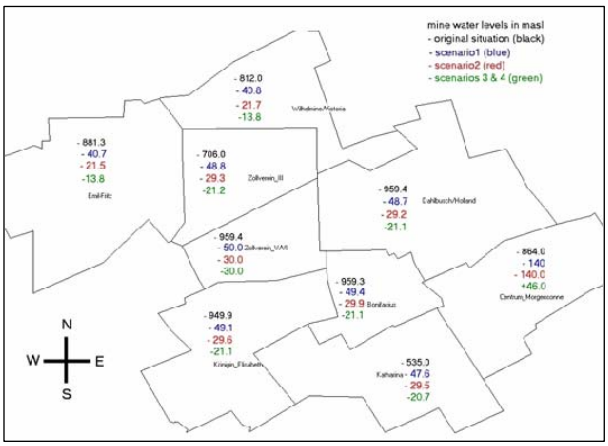


Figure 6. Schwartzbach pilot site. Mine water levels in the different boxes of the Emschermulde model according to the final pumping level

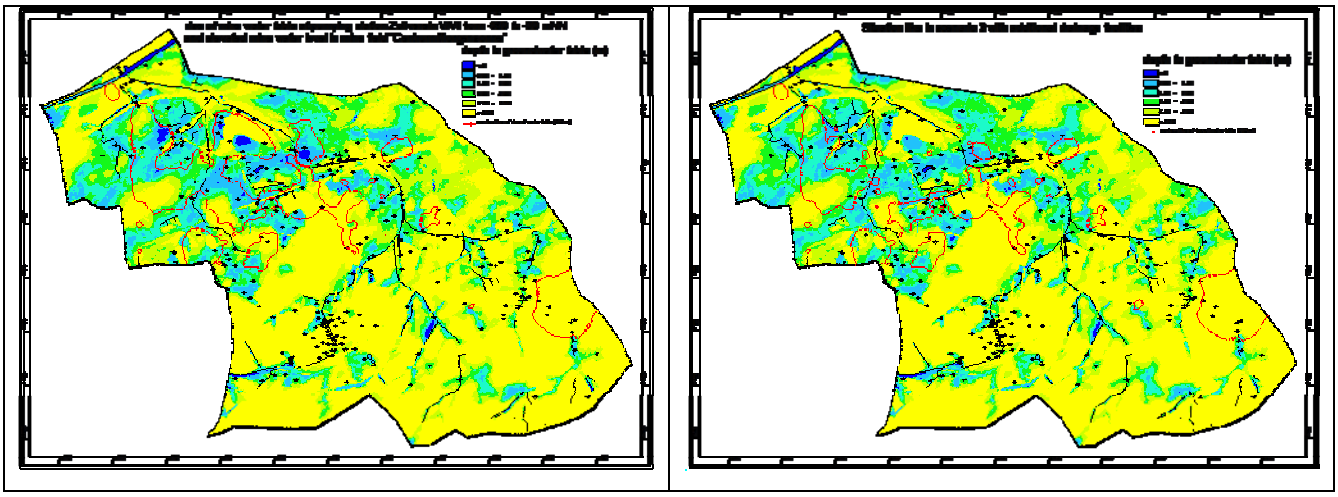


Figure 7. Schwarzbach pilot site. Depth of the water level (in red area were depth < 0,5 m) for scenario where the pumping level is fixed at -30 masl and without (left) or with (right) dewatering facilities

3.2 Study of the changes in water level and flows within mined coal massif affected by modifications in the flow pattern. Liège coal basin case study

Box model approach does not allow to represent flows in mined massive composed of a set of adjacent well and not well drained areas with the accuracy required. To achieve this aim, it is necessary to go trough a mixed approach. In the framework of the study devoted to the Liège coal basin pilot site, the mixed approach proposed consisted into using FE tools and defining, within the model, sub-domains where flow governing equations can be expressed by different mathematical relationships ranging from transfer function to more traditional differential equations.

When the sub-domains have to be considered as linear tanks, the flow governing law only comes to the relationship that expresses that the outflow varies in a linear way according to the water level in the sub-domains.

$$Qs = V_s * (\delta\theta/\delta t) = S * A_s * \delta(H-H_s)/\delta t + q \quad (5)$$

Where

V_s = sub-domain volume
θ = water volumetric ratio in the sub-domain
S = storage coefficient of the sub-domain
H = average height in the sub-domain (dependent variable)
H_s = average drainage level in the sub-domain
A_s = the average surface of the sub-domain
q = recharge/withdrawal coefficient

In the other sub-domains, the governing law is expressed as :

$$F* (\delta h/\delta t) = \nabla *(K * \nabla (H+Z)) + q \quad (6)$$

Where

F= generalized storage coefficient
K = hydraulic conductivity tensor
H = pressure potential
Z = gravity potential
q = recharge/withdrawal coefficient

Spatial discretization can be adapted according to the available information and thus to the mathematical (numerical) approach which can be applied. Sub-domains can even not be discretized at all and treated as a unique box. Water exchanges between each hydraulically connected sub-domain are modelled by means of internal boundary conditions defined along the interfaces.

Later on, in case more detailed information on the hydraulic behaviour of a sub-domain was collected, its model could be updated on the basis of a finer discretization and more complex flow governing laws using for spatially distributed parameters and directly integrated in the global model without requiring any modification of the other sub-domains.

In practice, these concepts are implemented in the SUFT3D program by this way:

A global mesh is generated on the overall area to be modelled (including well and non well drained areas) by means of a traditional dedicated tool (GMS). Then for sub-domains to be considered as a unique box (tank), the cells are grouped together by means of adequate criteria. In each sub-domain the nodes and elements are re numbered in order to duplicate those common to adjacent sub-domains. The equations expressing the flow governing laws are solved iteratively within each sub-domain, dedicated routines taking in charge the transfer of water volumes exchanged and boundary conditions between sub-domains interfaces.
Conceptually the pilot site will be divided into six sub-domains: one sub-domain for each of the five blocks drained by independent networks and one for the rest of the area. The first five sub-domains are presently considered as unique boxes whereas the last one is sub-divided in three layers: two for representing the overlying strata (alluvium with locally terraces, chal) and one for the coal measures. (Fig. 8)

At this stage development work of the mixed approach is still under progress and calibration and simulation processes have not started yet.

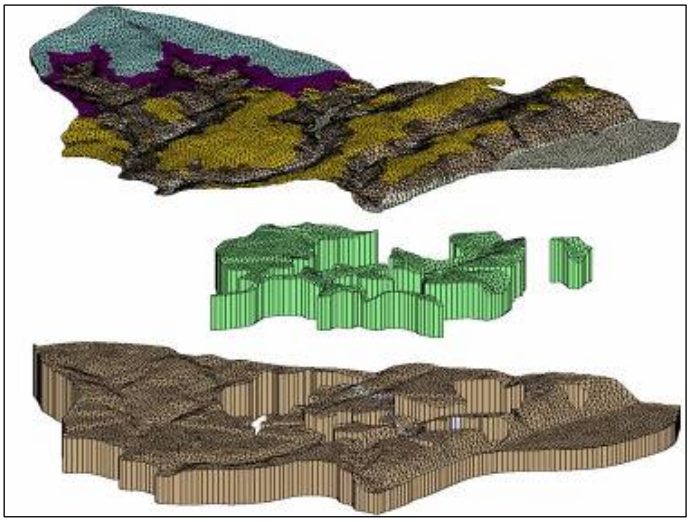


Figure 8. Liège coal basin pilot site. Mixed approach. In brown parts modelled with FE elements, in green the five parts considered as box

4. Conclusions

Once again, it has been demonstrated that the box model approach represents a satisfying method for modelling underground water rebound in mined coal measures even in special situations where water rising is caused by modifications of the gravity drainage conditions. Advantages of the EPANET software in order to implement this approach like: existence of a gravity interface,

capacity of representing drainage pumping operations or the porosity variations according to the depth by adjusting the tank area have been illustrated. Moreover as it allows to model water inrush, it can be viewed as a valuable tool for predicting such phenomena.

However, when interactions between mine waters and other aquifers have to be taken into account more accurately, box model approach has to be combined with traditional approach. Three combining ways have been assessed: batch process with boundary conditions adjustment, transformation of FE models into box models in order to build a unified model, mixed approach dealing with sub domains where flow governing equations and discretization degree can be adapted according to the available data. Each of them offer potentiality for modelling complex situations.

5. References

Banks D. (2001) *A variable volume, head dependent mine water filling model.* Journal of ground water. Vol. 39, number 4.

Gardin N., Brouyère S. (2005) *Modélisation de la remontée des niveaux piézométriques dans les massifs affectés par des travaux miniers dans l'ancien bassin charbonnier de Liège.* Rapport d'étude Géomac, non publié.

Shenk Y., Reddish, D. (2005) *Assessment of the water inflow to mine workings by numerical modelling.* Postmining 2005, Nancy

Sherwood J.M., Youger P.L. (1977) *Modelling groundwater rebound after coalfield closure.* Congress of the International Association of Hydrogeologists. Groundwater in the urban environment. Process and Management

Watkin J., Hadj-Hassen F. and ale (2005) Effects of water on the mechanical behaviour of argillaceous shales. Postmining 2005, Nancy

EFFECT OF WATER ON THE MECHANICAL BEHAVIOUR OF SHALES

WAKIM Jad[1], HADJ-HASSEN Faouzi[1], TIJANI Michel[1], NOIREL Jean-Francois[2]

[1] Ecole des Mines de Paris – CGES, 35, rue Saint-Honoré, 77305 Fontainebleau - jad.wakim@ensmp.fr

[2] Charbonnage de France – DTN, 2, avenue Emile Huchet, 57802 Freyming Merlebach

ABSTRACT: This paper aims to presenting the results of a research conducted in order to study the effect of water on the mechanical behaviour of the Lorraine Basin Colliery shale. The work performed can be divided into four main parts. The first part is dedicated to classical tests and it includes geological and mineralogical analysis as well as mechanical laboratory tests. The second part is devoted to the phenomenon of shale swelling under water effect. New procedures and equipment of testing were set up in order to characterise this swelling behaviour and to determine its model parameters. The tests performed in this second part are allowed to develop a phenomenological model which describes the elasto-visco-plastic behaviour of shales before and after saturation. The last phase of the work is dedicated to implement the new model in the finite element code VIPLEF in order to apply in tunnel excavated in swelling anisotropic rocks.

KEYWORDS: shale, swelling, anisotropy, strength weakening, creep, tunnel.

RESUME : L'objectif de l'article est de présenter l'influence de l'eau sur le comportement mécanique des schistes argileux de la houillère du basin de Lorraine. Le travail effectué est composé en quatre parties. La première partie concerne les caractéristiques géologiques et minéralogiques ainsi que les caractéristiques mécaniques des schistes argileux. La deuxième partie a pour but d'appréhender le gonflement des schistes sous l'effet de l'eau. Dans ce contexte, des nouveaux dispositifs expérimentaux ont été développés pour étudier et modéliser le gonflement. Les essais effectués nous ont permis à développer un modèle phénoménologique qui caractérise le comportement élasto-visco-plastique des schistes avant et après saturation. La dernière partie concerne à implanter le modèle développé dans un code de calcul par éléments finis VIPLEF pour l'appliquer sur un tunnel excavé dans une roche anisotrope gonflante..

MOTS-CLES : schiste argileux, gonflement, anisotropie, ramollissement, fluage, tunnel.

1. Introduction

Shale is the major constituent of sedimentary rocks covering approximately three-fifths of the terrestrial surface of earth. Shale may induce many geotechnical problems when they are put in contact with water or humidity. Unfortunately, these problems are found in many underground works such as radioactive waste disposal, mines, tunnels, oil wells and others.

Shale contains fine-grained less than $2\,\mu m$ in diameter of clays. Clays have a very high specific surface area and a residual imbalanced of electrical surface charge. The combination of these factors is the reason why clay particles adsorb polar molecules - like water - and therefore have a high affinity for polar liquids. The results of these factors are the creation of double diffuse layer that has a tendency to separate clay particles. The creation of double diffuse layer has a consequence to induce the macroscopic swelling. Other phenomena can coexist in shale such osmosis and capillarity. These phenomena are often known under the name of total suction.

The swelling of shale can lead to deterioration of the linkage between the layers in the clay particles resulting to reduction of mechanical properties such a Young's modulus and compressive strength. Basically, the increase of water content is the major factor for swelling. Swelling is strongly influenced by microscopic and macroscopic factors. On the microscopic scale, these factors are very complex and mainly depend on the mineralogical properties of the clayey materials and the chemical properties of the pore fluid. Another problem is the geometrical distribution of clayey layers that make the anisotropic swelling.

Although the swelling phenomenon takes place at the microscopic scale, it is a macroscopic approach that is used for prediction of the swelling.

2. Geotechnical properties of shale

The shale, present in the Lorraine Basin Colliery at 900 meters depth, is a sedimentary anisotropic rock. The density of this shale is 2.65. The mineralogical analysis by X-ray diffraction reveals that the rock is composed of 70 % of clayey minerals of which (40/55 %) of illite, (20/45 %) of chlorite and (5/35 %) of kaolinite, the remaining percentage being composed of quartz and feldspars. Both kaolinite and illite are known for being low to moderately expansive materials. The initial water content is 1.2 %. This value corresponds to well preserved samples after coring.

Mechanically, the uniaxial compressive strength is the order of 25 MPa and the indirect tensile strength is 3.7 MPa. The Young modulus, for a direction normal to bedding plan, is equal to 4000 MPa.

3. Effect of water on the Lorraine shale

In this paper, the effect of water on the rock is studied under the following two cases:

- Deterioration of the mechanical property,
- Swelling.

3.1. Deterioration of the mechanical property

The Lorraine shale is strongly sensitive to the variation of his water content. This reactivity has been initially verified by compressive wave velocity test, which effects in a normal direction to bedding plane, for different samples at different water contents. A linear decrease with increasing water content observed in the figure 1 for normalized p-wave velocity is due to apparition of micro cracks. Fooks and Dusseaulet (1996) found some similar linear variation in case of the Pierre shale.

Triaxial compression tests have been done on the Lorraine shale samples for two conditions of saturation. The first corresponds to the initial state before the saturation of the sample and the second corresponds to the saturation state where the water content is 5 %. The figure 2 presents the Coulomb failure envelopes for two water contents. We can conclude that there is a 70 % loss in the uniaxial compression strength, a 78 % loss in the friction angle and 45 % loss of the cohesion when the water content varies from 1.2 % to 5 %. In the elastic domain, an 80 % loss in the Young modulus has been observed. However, the Poisson ratio has the same value.

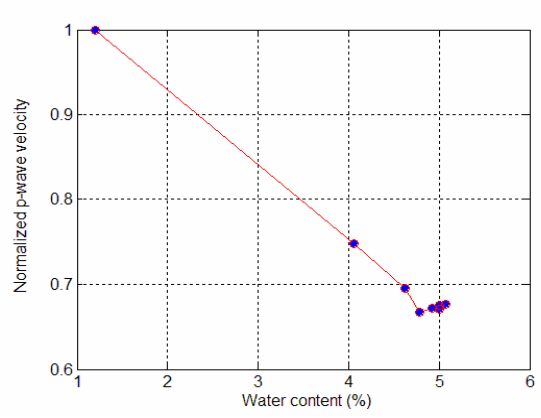


Figure 1. Normalized p-wave versus water content

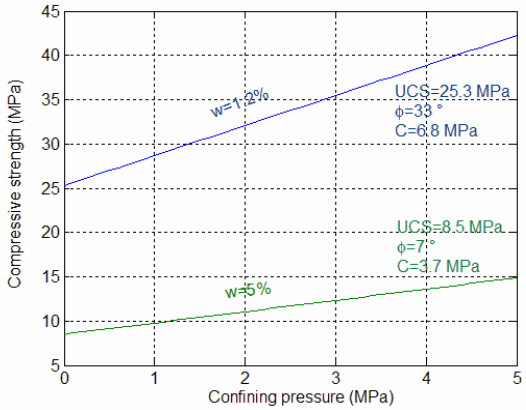


Figure 2. Mohr-Coulomb failure criteria for two water contents

The Fooks and Dusseaulet model considers that the Mohr-Coulomb failure criteria depends on the water content and it can be written as the following equation:

$$\frac{\sigma_1 - \sigma_3}{2} = \left(-\alpha_1.w + \alpha_2\right).\frac{\sigma_1 + \sigma_3}{2} - \alpha_3.w + \alpha_4 \qquad (1)$$

Using this model, we can estimate, as a function of the water content, the reduction of: uniaxial compressive strength (UCS), friction angle and cohesion (figure 3).

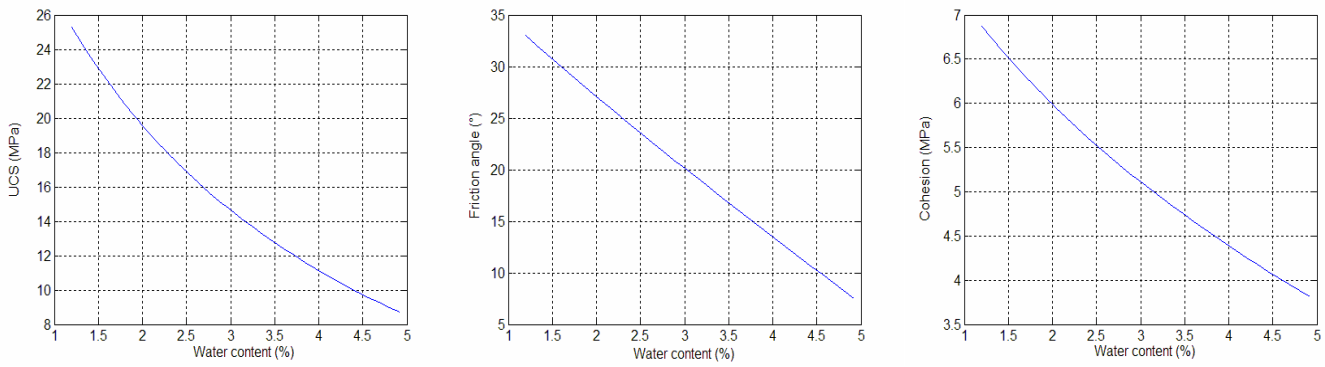


Figure 3. UCS, friction angle and cohesion versus water content

The parameters of model are: α_1=11.12; α_2=0.67; α_3=53.3 and α_4=6.40.

3.2. Swelling

Swelling depends on different macroscopic parameters such as the initial water content, the chemical properties of solution and the applied stress.

This paper will concentrate on the influence of the stress in three-dimensional anisotropic swelling of shale.

From the bibliographic researches, three contradictory cases are cited to explain and to model the three-dimensional swelling of argillaceous materials:

1- Independence of swelling following a principal direction with the stress following the other directions (Zhou et al., 1992; Kiehl, 1989; Froehlich, 1987),

2- Increase of swelling following a principal direction with the stress following the other directions (Yesil et al., 1993; Windal, 2001),

3- Decrease of swelling following a principal direction with the stress following the other directions (Hawlader, 2003; Wong, 1997; Lo. 1989).

These different observations have directed us to conduct different experimental tests in order to understand the swelling behaviour of the Lorraine shale.

4. Experimental apparatus

The experimental program is completed from different apparatus that are:

- *Triaxial apparatus:* it allows to apply different paths of axial and radial stress and to measure the axial swelling or the axial swelling pressure generated after blocking completely or partially the axial displacement. The sample has a 50 mm in diameter and 25 mm in height. The axial stress is applied by a hydraulic piston with a rate of deformation equal to 120 micron/m/min and the confining pressure is applied by an oil injector. This pressure is then transmitted to the sample by an impervious silicone jacket. The saturation of the sample is assured by the injection of water from bottom to top through the porous stone.

- *Uniaxial apparatus*: This apparatus can measure the axial swelling and the radial swelling for different paths of axial pressure. The diameter of samples is 50 mm and the height is 35 mm. The axial swelling is measured by two LVDT sensors while the radial swelling is measured diametrically by a steel ribbon surrounding the sample and linked to a LVDT sensor.

- *Zero swelling apparatus*: This cell allows to measure the axial swelling pressure of a sample prevented to swell axially and laterally. The device is constituted of a rigid metallic ring with interior diameter of 63.1mm. The height of samples can vary from 10 mm to 20 mm.

- *Free swelling apparatus*: it can measure the axial and radial swelling of a sample with a 50 mm in diameter. The height can vary between 20 to 60 mm.

5. Laboratory swelling behaviour of the shale

The purpose of this experimental study is to show the influence of a lateral condition or an axial stress on the axial swelling or a radial swelling. In this study, the sample show transverse isotropy.

5.1. Influence of the deviator stress and the mean stress

Two tests of axial swelling measurement have been done for the same deviator stress $Q = \sigma_1 - \sigma_3$:

- Free swelling test ($\sigma_1 = \sigma_3 = 0$),

- Triaxial swelling stress ($\sigma_1 = \sigma_3 = 1$).

For the free swelling test, the axial swelling normal to the bedding plane is 3 %. On the other hand, the axial swelling observed in the triaxial test is 0.3 %. These results show that the deviator stress does not affect a swelling.

Globally, for anisotropic shaly rocks, the swelling in a direction is not affected by the mean stress. This stress can have an effect on the clayey soils generally presenting an isotropic behaviour.

5.2. Influence of the radial tolerated swelling on the axial swelling pressure

To study the influence of the radial tolerated swelling on the axial swelling pressure normal to the bedding plane a sample of which diameter is 61 mm. The tolerated radial swelling is then extensively elevated with regard to the free radial swelling.

On the figure 4 we can note that, even though the radial swelling is prevented or not, the axial swelling pressure is for each situation nearly comparable to 0.65 MPa.

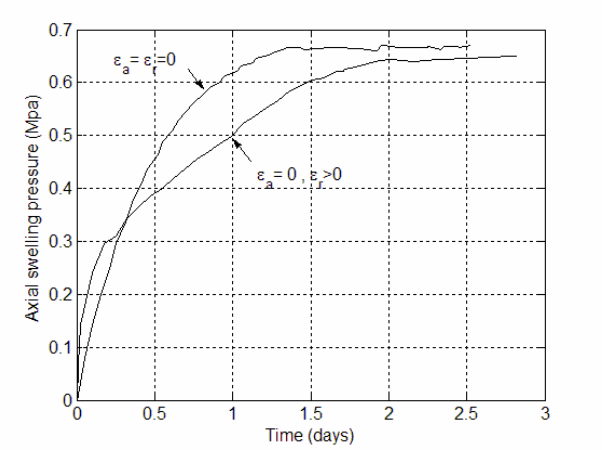


Figure 4. Swelling pressure versus time for two differents lateral confinement

5.3. Influence of the axial pressure on the radial swelling

Two tests have been carried out for different steps of unloading of the axial stress measuring simultaneously the radial swelling and the axial swelling.

Chosen stress paths are the following:

- 0.7, 0.4, 0.2 and 0.1 MPa
- 1.01, 0.7 and 0.5 MPa

These two tests are illustrated on the figure 5.

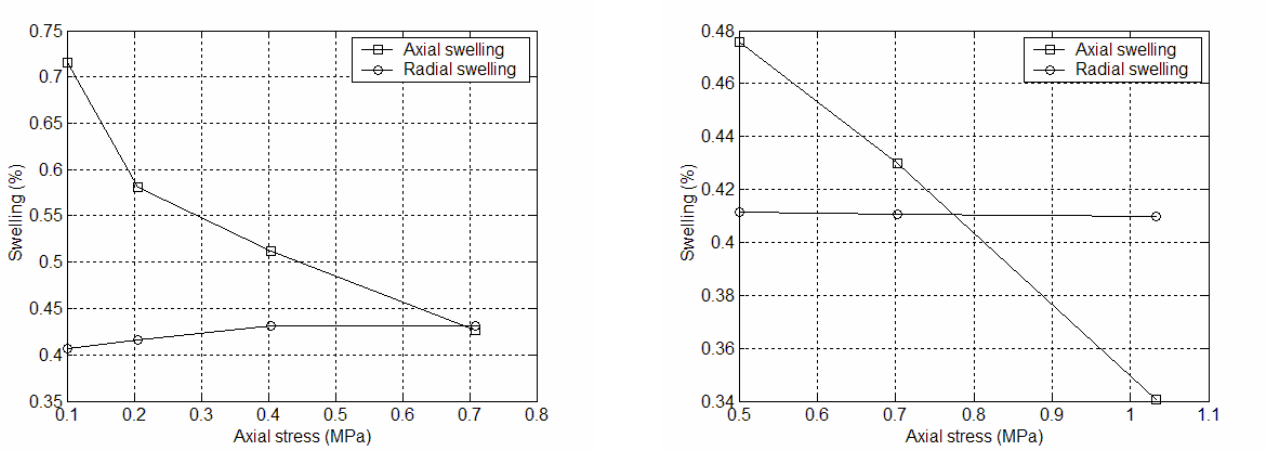


Figure 5. Axial swelling and radial swelling versus axial stress

For these tests, although the axial swelling increases with the reduction of the axial stress, no considerable difference of radial swelling has been observed. We can deduce that the lateral swelling is not influenced by the applied axial stress and by the path of axial stress.

The figure 6 presents two tests one of them done with oedometric apparatus and the other by uniaxial apparatus.

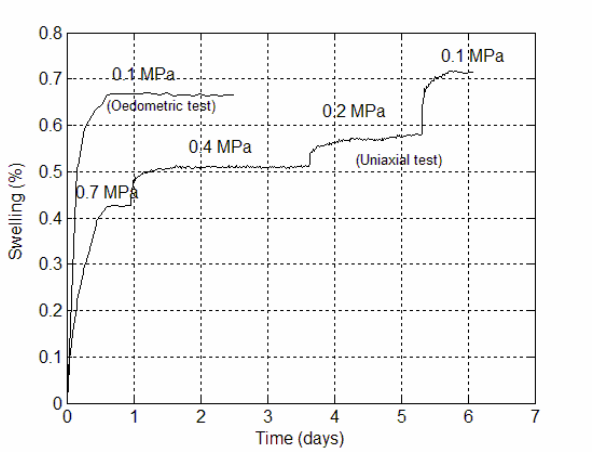


Figure 6. Comparison between unaxial test and oedometric test for 0.1 MPa of axial stress

For the same axial stress of 0.1 MPa, the axial swelling is approximately the same whatever is the lateral confinement.

To confirm the previous results, a swelling test conducted in triaxial apparatus in conditions of isotropic stress of 1 MPa generates an axial swelling of 0.3 %. A uniaxial swelling test with an axial stress equal to 1 MPa generates an axial swelling equal to 0.34 %. This value is approximately similar to the axial swelling measured by triaxial cell.

These results illustrate that the axial swelling is independent from the applied confining pressure.

5.4. Study of the reversibility of swelling

Two triaxial tests, for the same confining pressure of 1 MPa, have been done for different steps of unloading of the axial stress. The applied axial stresses are:

- 4.5-3.5-2.5 MPa

- 3.5-2.5-1.5 MPa

These tests present the two identical stress which are 3.5 and 2.5 MPa. For the same axial stress, the difference of axial swelling between the two tests is small in the order of 0.03 %.

In addition to the previous tests, the two uniaxial tests presented on the figure show that for the same stress of 0.7 MPa the difference of deformation is 0.01 % which is negligible.

6. Rheological model

The presented theoretical model concerns to study the evolution versus the time of the strain of the anisotropic shaly rock before saturation and after saturation by water.

These strains are clearly presented in the figure 7 that represented a uniaxial test with measuring of axial strain normal to the bedding plan. The applied axial pressure is equal to 1.2 MPa.

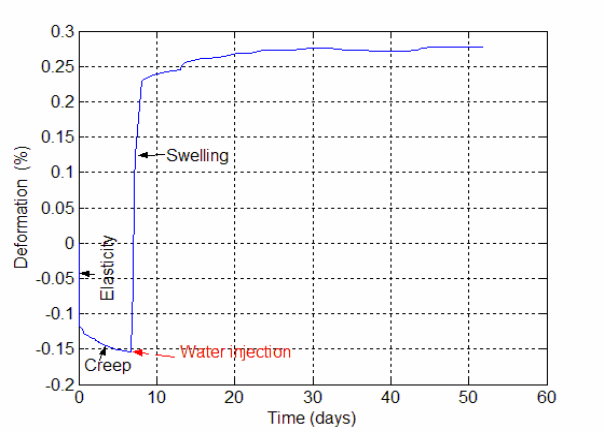


Figure 7. Three phases of deformation

These three phases can be summarised as following:

- Elastic phase

- Creep phase

- Swelling phase

A phenomenological model has been developed to predict the elasto-visco-plastic behaviour of the shale and can be summarized by the following equation:

$$\varepsilon(t) = \left[\varepsilon^{e} + \varepsilon^{vp}(t)\right].He(t_s - t) + \varepsilon^{s}(t).He(t - t_s) \qquad (2)$$

where ε^{e} , ε^{vp} and ε^{s}: are respectively the elastic, the visco-plastic, and the swelling strain at a given time t, t_s : the time of saturation and He : the Heaviside function.

6.1. Creep

The presented creep model is inspired by the Lemaître's visco-plastic law but it is generalized to anisotropic materials (Tijani, 2004). In case of triaxial stress, the creep in the vertical direction is:

$$\varepsilon_3^{vp}(t) = -\sqrt{A}.\left(\frac{\sigma_1 - \sigma_3}{k_\theta}\right)^{\beta}.t^{\alpha} \qquad (3)$$

With,

$$k_\theta = \frac{k}{A^{\left(1+\frac{1}{\beta}\right).\frac{1}{2}}} \text{ and } A = 1 + \frac{w}{4}.\sin^2(2\theta)$$

w designs the anisotropic creep and θ is the angle between the vertical axis and the normal vector to bedding plane. β , α and k are the same parameters of Lemaître's law.

6.2. Swelling

Based upon the results of swelling tests, the law of swelling is based on the following assumption:

- Reversibility of swelling,

- The direction of principal swelling $\varepsilon_{i\infty}^{s}$ (i=1, 2, 3) coincides with the direction of principal normal stress σ_i ,

- The main swelling $\varepsilon_{i\infty}{}^{s}$ only depends on the principal stress σ_i,

- The anisotropic of swelling can be deduced by a geometrical transformation.

(The notations s, i and ∞ corresponds respectively to swelling, to the direction of swelling and to the stabilization time).

For time t=∞, the following equation describes the relationship between swelling and the stress following a principal direction "i" (Wong et al., 1997).

$$\varepsilon_{i\infty}{}^{s} = A_i.\left[1-\left(\frac{\sigma_i}{\sigma^s{}_i}\right)^{c_i}\right].He\left(\sigma^s{}_i-\sigma_i\right) \qquad (i=1,2,3) \tag{4}$$

where $\varepsilon_{i\infty}{}^{s}$ and σ_i : the maximal swelling strain and stress parallel or perpendicular to the anisotropy and $\mathrm{A_i}$ $\sigma^s{}_i$: the free swelling and the swelling pressure parallel or perpendicular to the anisotropy, c_i : the power factor parallel or perpendicular to the anisotropy and.

It is necessary to note that in this case the swelling pressure doesn't correspond to the one measured by zero swelling test. The method used to estimate this pressure is identical to the parallel stress method.

6.3. Integration of the time

The rate of swelling vector $\left\{\dot{\varepsilon}^{s}(t)\right\}$ is expressed by the following expression:

$$\left\{\dot{\varepsilon}^{s}(t)\right\} = \frac{1}{n_s}.\left[\left\{\varepsilon_{i\infty}{}^{s}\right\}-\left\{\varepsilon^{s}(t)\right\}\right] \tag{5}$$

n_s is the kinetic of swelling and $\left\{\varepsilon^{s}(t)\right\}$ is the swelling vector in the local cartesian system .

For $t\to\infty$, the rate of swelling reaches zero.

For one loading step, the principal swelling in "i" direction is:

$$\varepsilon_{i,1}{}^{s}(t) = F_1.\left[1-\exp\left(\frac{-t}{n_s}\right)\right] \tag{6}$$

For several unloading steps, the swelling is:

$$\varepsilon_{ik}{}^{s}(t) = \varepsilon_{i,1}{}^{s}(t)+\sum_{k=2}^{n}\Delta F.\left[1-\exp\left(\frac{t_{k-1}-t}{n_s}\right)\right].H_e(t-t_{k-1}) \tag{7}$$

With,

$\Delta F = F_k - F_{k-1}$

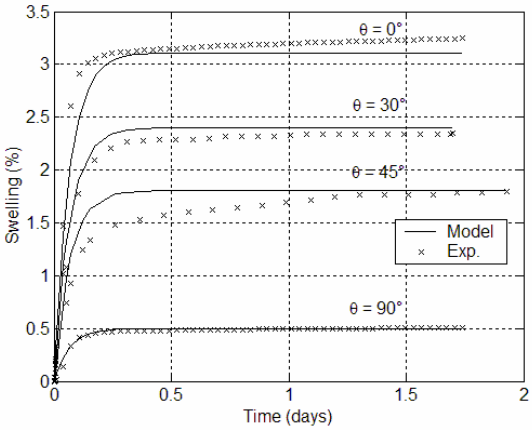
$F_k = A_i.\left[1-\left(\frac{\sigma_{i,k}}{\sigma^s{}_i}\right)^{c_i}\right]$

k corresponds to the number of loading steps and t_k is the beginning time of the loading step $k+1$.

6.4. Validation of the proposed model

The presented model has been adjusted on different tests with axial measuring:

- Free swelling for four orientations (0°, 30°, 45°, 90°)
- Uniaxial tests for two orientations (0°, 90°)
- Maximal swelling for different axial stress and for two orientations (0°, 90°)



. Figure 8. Free swelling.

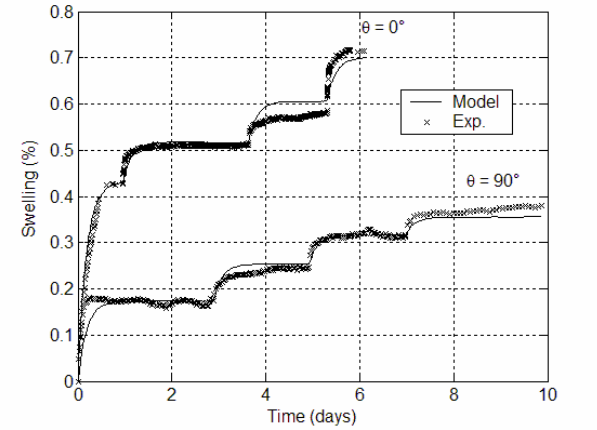


Figure 9. Uniaxial swelling.

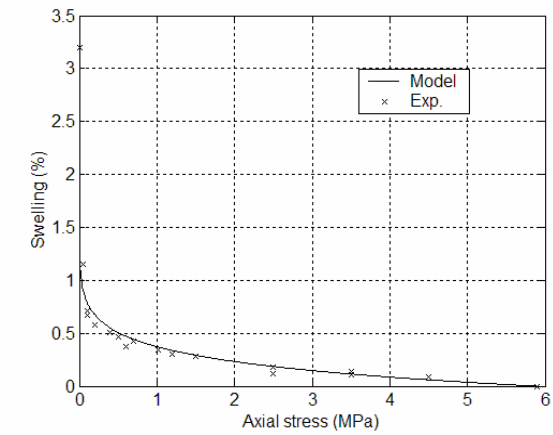


Figure 10. Maximal swelling for $\theta = 0°$.

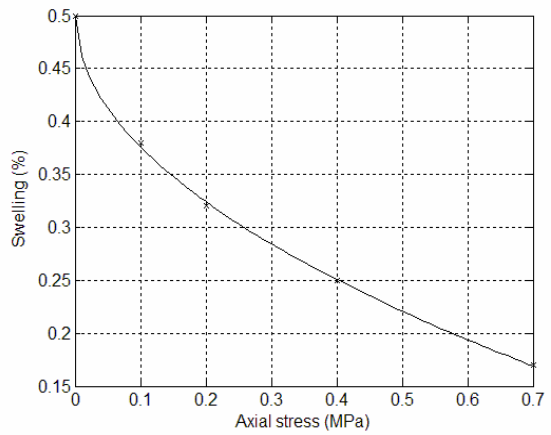


Figure 11. Maximal swelling for $\theta = 90°$.

For combined test creep-swelling, the model has been applied to one uniaxial test:

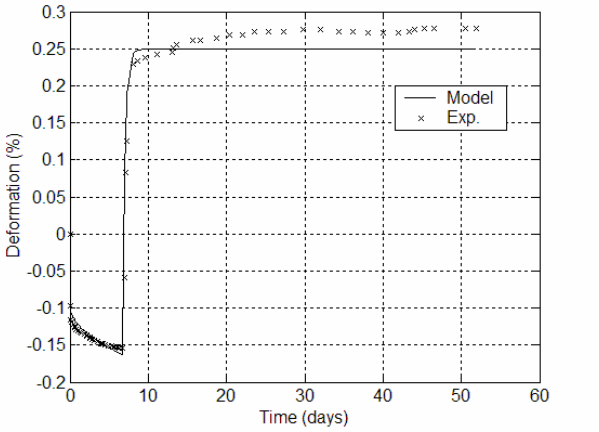


Figure 12. Combined test for $\theta = 0°$

The parameters of proposed model are illustrated in the following table:

Table 1. Parameters for model (stress in MPa and time in days)

Swelling parameters	**Value**
Free swelling $(\theta = 0°)$	0.032
Free swelling $(\theta = 90°)$	0.005
Swelling pressure $(\theta = 0°)$	6 MPa
Swelling pressure $(\theta = 90°)$	2.1 MPa
C $(\theta = 0°)$	0.068
C $(\theta = 90°)$	0.504
Mean n_g	0.1
Creep parameters	**Value**
β	1.236
α	0.496
k	$1.573.10^3$

6.5. Simulation of swelling with VIPLEF

The model developed has been integrated in finite element code VIPLEF. The objective of this part is to show results of simulation the anisotropic swelling behaviour of the ground with a shistosity inclined at 20° regarding the horizontal and especially around a tunnel. The tunnel has a-400 meter height of overburden. The initial overburden pressure is approximately equal to 10 MPa.

The tunnel has an arch shaped cross section (Figure 14). The tunnel is located with the invert in shale and with the crown in a limestone which elastic behaviour. After excavation and installation of 50 cm thick of the reinforced concrete lining, the rock mass underneath the tunnel was watered.

A cross-section view of the plane strain element finite mesh used in the analyses is shown in figure 13.

Appropriate boundary conditions were applied at the boundaries (in the extremity of works u=0 for lateral boundary and v=0 for bottom boundary).

The simulation has been executed in two phases:

- Excavation of tunnel in elastic domain,
- Swelling.

The figure 14 presents the displacement due to swelling of lining, we show that the swelling is not symmetric because the anisotropic swelling primordial in the direction normal to bedding plan.

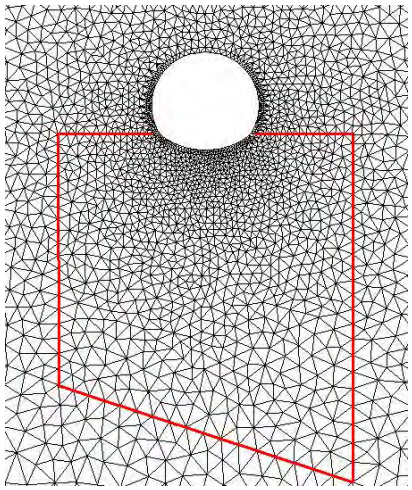


Figure 13. Detailed of the mesh used in modelling

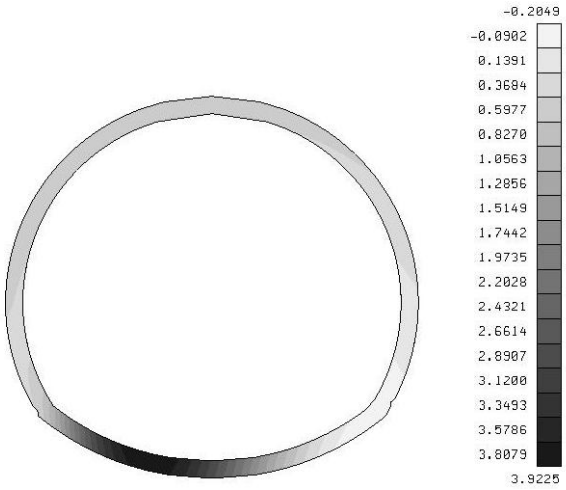


Figure 14. Vertical displacement of lining (mm)

The figure 15 presents the normal swelling along invert section, the maximum swelling is 3.5 mm at 3.2 m from left extremity of inverted arch. In fact, in the centre of inverted arch, the swelling is 2.1 mm.

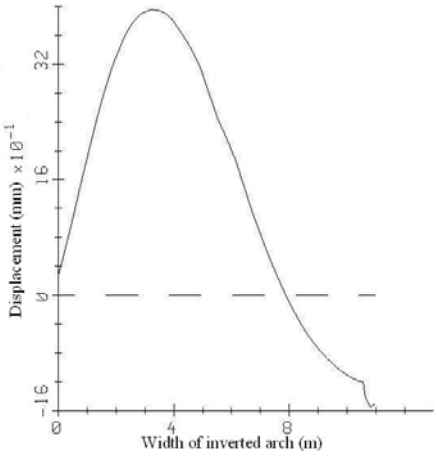


Figure 15. Normal displacement to invert (mm)

7. Conclusion

Lorraine shale is very sensitive to water as a result swelling and reduction of mechanical property are observed.

The accomplished experimentations have permitted to develop a phenomenological swelling model. This model has been applied on different experimental tests and a good agreement has been found with the theory.

The integration of the model in VIPLEF has allowed to visualize the anisotropic swelling along the invert of the tunnel.

For the future research, some new experimental tests need to be conducted to analyse the effect of the chemistry solution on the swelling.

8. References

Fooks J.C., Dusseault M.B. (1996). *Strength of Pierre I shale as function of moisture content.* Eurock 96, Eds. Barla, 77-82.

Froelich O.B (1978). *Anisotropic swelling behaviour of diagenetic consolidated claystone* . Commision of swelling rock. Int. Soc. Rock. .Mech., 1487-1488.

Hadj-Hassen F, Gordine .D, Accarie H. (2002). *Rapport sur le gonflement des schistes argileux. Rapport interne.* CGES-ENSMP.

Hawalader B.C, Lee Y.N, Lo K.Y (2002). *Three-dimensional stress effects on time-dependent swelling behaviour of shaly rocks*. Canadian Geotechnical Journal, Vol. 40, 501-511.

Kiehl J.R (1990). *Ein dreidimensionales quellgesetz und seine anwendung auf den felshohlraumbau*. Proc. 9th Natn. Felsmechanik Symp.,Aachen Germany, 185-207

Lo K.Y, LEE Y.N (1989). *Time dependent deformation behaviour of Queenston shale*. Canadian Geotechnical Journal, Vol. 27, 461-471.

Tijani M. (2004). *L'aisotropie transverse*. Note interne CGES, Ecole des Mines des Paris, 2004.

Windal T. (2001). *Etude en laboratoire du gonflement des sols: mise au point d'un oedomètre flexible et étude du gonflement tridimensionnel*, Phd Thesis, laboratoire de Mécanique de Lille, Université des .Sciences et Technologie, 128 pages.

Wong R.C.K, Wang E.Z (1997). *Three-dimensional anisotropic swelling model for clay shale – A fabric approach.* Int. J. Rock. .Mech. Min. Sci.. Vol. 34, 2, 187-189

Yesil M.M., Pasamehmetoglu A.G. et Bozdag T. (1993). *Technical Note, A Triaxial Swelling Test Apparatus*, Int. J. Rock. .Mech. Min. Sci, Vol. 30, 4, 443-450.

Z.H.Zhou, R.Z.Huang, Y.F.Chen (1992). *Constitutive equations of shale and clay swelling: Theoretical model and laboratory test under confining pressure*, Society of petroleum engineering , 22382, 529-540.

MINE WATER MANAGEMENT AND THE WATER FRAMEWORK DIRECTIVE

Wolkersdorfer Christian

Technische Universität Bergakademie Freiberg, Lehrstuhl für Hydrogeologie, Gustav-Zeuner-Str. 12, D-09596 Freiberg/Sachsen, Germany ; c.wolke@tu-freiberg.de

ABSTRACT: The European "Water Framework Directive" meant a significant change in the administration of many water catchment areas. That change also affected the administration of mine water discharges and in consequence the necessary measures of mine operators or regulatory authorities to manage those discharges. Due to the differences in the water and especially mine water legislation in the European countries the EU FW6 project ERMITE (Environmental Regulation of Mine Waters in the European Union) investigated those differences by addressing the many facets of Nations and disciplines involved.

KEYWORDS: mine water management; Water Framework Directive; European Union; mining

RESUME : La directive européenne sur l'eau a induit un changement significatif dans la gestion administrative des bassins captifs. Ce changement a aussi affecté la gestion des eaux d'exhaure et par conséquent les mesures à prendre par les opérateurs miniers et les autorités de régulation pour gérer ces rejets. En raison des différences de législation des pays européens dans ce domaine, le projet EU FW6 ERMITE (Environmental Regulation of Mine Waters in the European Union) a été lance pour les étudier à travers les différentes politiques nationales et les disciplines impliquées.

MOTS-CLEFS : gestion des eaux de mines, directive européenne sur l'eau, Union européenne, activité minière

1. Introduction

Mine water are all waters emanating from active, abandoned, or closed surface or underground mines. This definition includes water draining through dewatering adits, mine dewatering pumps, open pit mines, or raw material handling facilities on the site of a mining operation (ERMITE Consortium et al. 2004). Some countries, such as Germany or Sweden, do not categorize mine water as waste water, whereas many other countries, such as Finland or Poland, categorize mine water as waste water (Wolkersdorfer 2001; Plinke and Wildhagen 2003) Under strict interpretation of the European waste legislation, mine water has to be considered as waste as long as it is not produced or pumped for a special purpose. The EU Council Directive 75/442/EEC on waste, amended 91/156/EEC states in Art. 1(a): "'Waste' shall mean any substance or object in the categories set out in Annex I which the holder discards or intends or is required to discard" and in Annex I, Category Q16: "any materials, substances or products which are not contained in the above categories". Yet, this strict interpretation should be avoided as many mine waters are of good chemical and biological quality and can therefore directly be discharged into surface streams without further treatment.

On the other hand, polluted mine water is one of the largest single waste streams in the European Union. Though no comprehensive investigation of all mine water impacted surface streams or groundwater bodies in the European Countries exists so far, a total length of several thousands of kilometres of affected surface water can be assumed. As a result of the European Water Framework

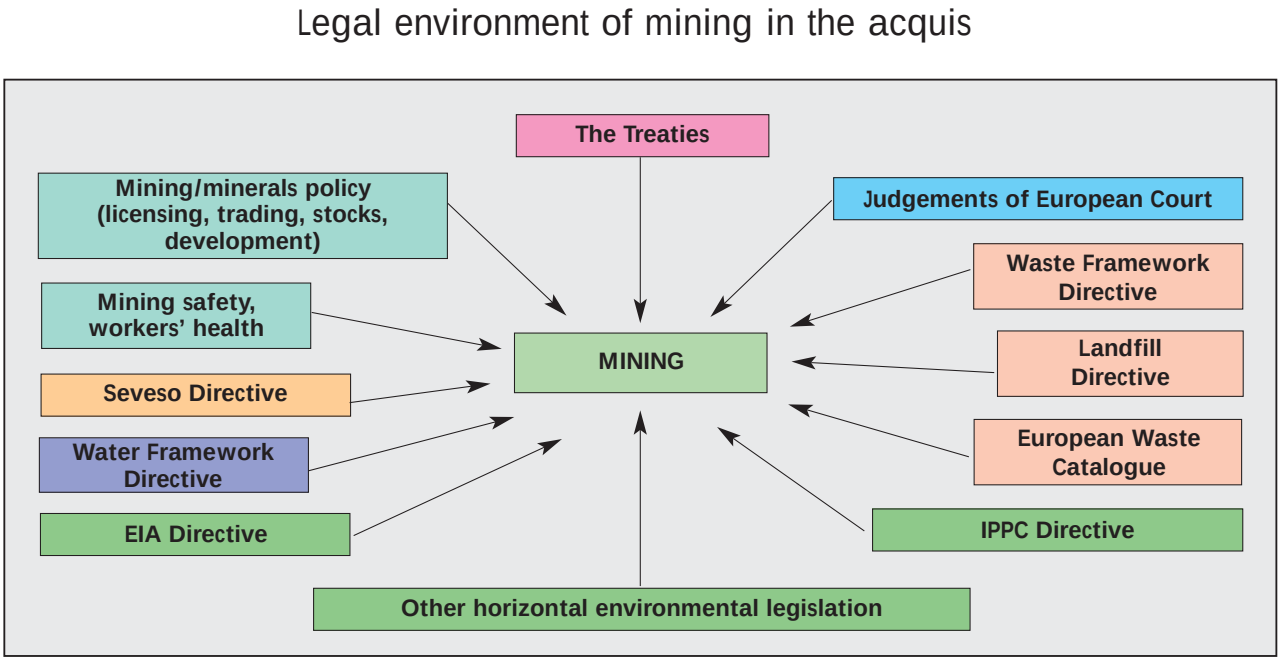


Figure 1. Legal framework of mining in the European Union (from Hámar et al. 2002).

Directive (2000/60/EC; European Commission 2000), which is meant to be a general framework for the protection of all waters including rivers, lakes, coastal waters, and groundwaters river basin management plans have to be set up until the year 2009. A key aim of the Water Framework Directive is to reach a good chemical and ecological status of all water bodies in the European Union. It is meant to be a framework and therefore does not regulate every issue into detail, but will be amended if necessary, one of those amendments being the proposed Groundwater Directive. Besides the Water Framework Directive, other regulatory elements affect European mining. They have been partly studied by Hámar et al. (2002) and shall not be further discussed here (Fig. 1). A thorough discussion of the EU regulations and legislative measures in the context of mine water and mine safety has been given by Kroll et al. (2002 a, b).

Mining, and consequently mine water, is not directly mentioned in the Water Framework Directive. The only reference to mining is article 11(3)j, which allows the injection of water for hydrocarbon exploration and exploitation and the reinjection of pumping water from mining or quarrying operations (European Commission 2000):

Member States may authorise

- *injection of water for technical reasons into geological formations from which hydrocarbons or other substances have been extracted or into geological formations which for natural reasons are permanently unsuitable for other purposes;*
- *reinjection of pumped groundwater from mines and quarries or associated with the construction or maintenance of civil engineering works;*

Nevertheless, because polluted mine water does affect surface water and ground water, mine water is covered by the Water Framework Directive and therefore need a thorough management in accordance with the targets set out by the directive.

2. Water Framework Directive – Some Insights

On December 12 2000 the European Water Framework Directive was set info force and after a timescale of 7—13 years this directive substitutes 7 other EU directives relating to water. As can be seen from table 1 the Water Framework Directive consists of different steps and monitoring procedures which shall ensure that the good chemical and ecological status of all European water bodies will be met in 2027.This stepwise approach includes to identify potential mine water related water quality problems within relevant coupled groundwater and surface water catchments and investigate all possible means of improving water quality in affected water environments. In consequence this means to choose the preferred economic decision rule for actual allocation of water quality improvement measures within each catchment. Furthermore, the coordination of policy programmes for mine water pollution abatement has to be based on economic principles aimed at making the best use of society's scarce resources for water quality protection and improvement. Finally, strategic steps for economically optimal management programmes have to be taken in mine water pollution abatement programmes (adopted from a presentation of Destouni, G.). Such management programmes, especially in remote areas or where no responsible mine operator can be allocated, can include the use of passive treatment options (PIRAMID Consortium 2003) as well as natural attenuation or enhanced natural attenuation options.

A basis for decision making is the priority list which is part of the Water Framework Directive and lists potentially dangerous substances. Furthermore, the Water Framework Directive mentions basic and supplementary measures to reach a good status of waters. Specifically, it refers to diffuse pollution and actions to address such diffuse pollution. In addition, all regulators and researchers must understand that under the Water Framework Directive it will become more important to manage chronic pollution from abandoned metal mines.

One of the first issues in most countries was to define the good ecological status of the river catchments in the single Member States. Furthermore, a list with heavily impacted or artificial waters had to be provided. The latter waters might be excluded from the Water Framework Directive if it has been proven that a good ecological or chemical status can't be reached. Such an example is the Rio Tinto area where any treatment options for cleaning the Rio Tinto are either impossible or would be economically not feasible. The French situation and the implementation of French water legislation by the "*Projet de Loi sur L'Eau*" has been described in Bongaerts (2002). But also other countries had to amend their water laws to mirror the context of the Water

Table 1. Time-line of the European Water Framework Directive.

Year	Issue	Reference
2000	Directive entered into force	Art. 25
2003	Transposition in national legislation	Art. 23
	Identification of River Basin Districts and Authorities	Art. 3
2004	Characterisation of river basin: pressures, impacts and economic analysis	Art. 5
2006	Establishment of monitoring network	Art. 8
	Start public consultation (at the latest)	Art. 14
2008	Present draft river basin management plan	Art. 13
2009	Finalise river basin management plan including programme of measures	Art. 13 & 11
2010	Introduce pricing policies	Art. 9
2012	Make operational programmes of measures	Art. 11
2015	Meet environmental objectives	Art. 4
2021	First management cycle ends	Art. 4 & 13
2027	Second management cycle ends, final deadline for meeting objectives	Art. 4 & 13

Framework Directive, such as Germany. Sweden, for example, has already changed their water law to meet most of the issues addressed in the Water Framework Directive (Salmon and Destouni 2001).

Before the Water Framework Directive came into force, most discharges or polluters were seen individually, but not within a catchment scale and transboundary impacts or consequences were usually not taken into account, some exceptions as the Rhine or the Oder/Neiße catchments being a nice example of what could be done. This was true for most European countries. According to the Water Framework Directive all countries within a specific water catchment have now to work together in a transboundary approach, whereas the use of GIS applications is an integrated part of this approach (Timmermann and Langaas 2004). Some of those water catchments, such as the Elbe or Rhine river water catchment, include one of the intensively mined European regions (Fig. 2). In the case of the Rhine River those are – to name some of them – the Swiss mountains, Black Forest, Vosges, Saar Basin, Rhenish lignite mining, Ruhr valley coal mining, and the Rhenish Schiefergebirge (Wolkersdorfer and Bowell 2005).

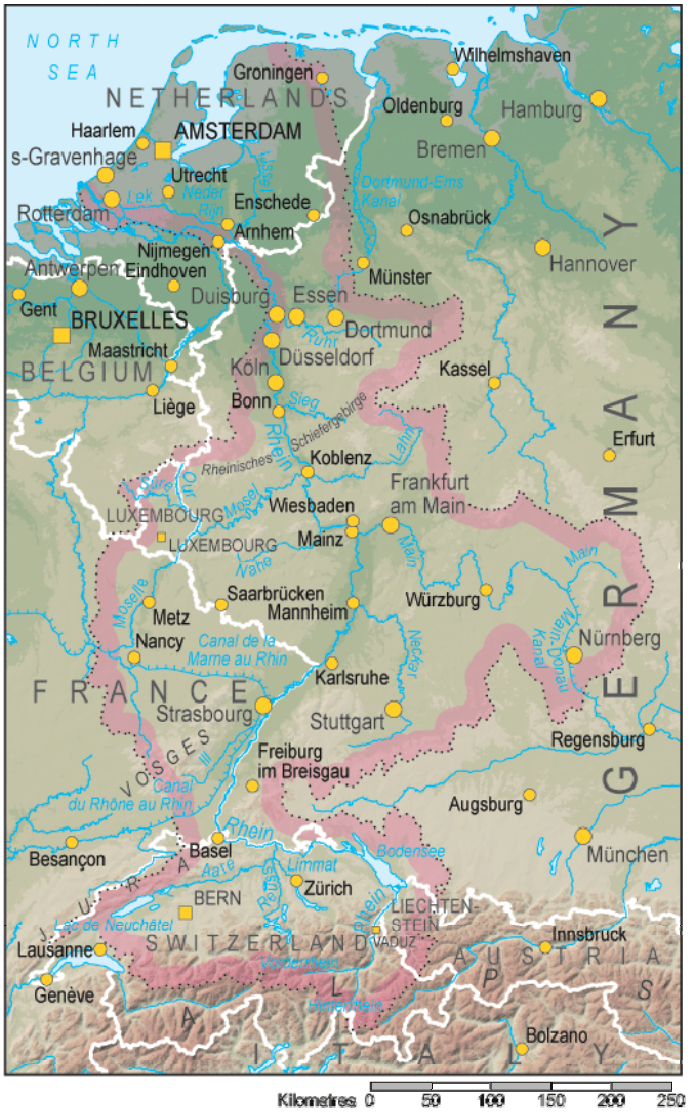


Figure 2. The borders of the river Rhine catchment which lies partly in Switzerland, Austria, Vaduz, France, Germany, Luxembourg, Belgium, and the Netherlands.



Figure 3. Untreated, polluted mine water discharging from the abandoned Gernrode/Germany (Harz Mountains) fluorspar mine.

3. Mining in Europe

Within the last decades many European mines had to close as a result of economic or environmental pressures on the metal market and due to national or European legislation. Nonetheless, there are still many hundreds of mining and thousands of quarrying operations with potentially polluted mine water discharges (Wolkersdorfer and Bowell 2005). All of those mining operations have to meet the standards outlined in the Water Framework Directive or as a result of national legislation. As long as a mining operation is active, the mine operator has to guarantee that the quality standards of the discharged water are met at all times. Even after mine closure water treatment has to be conducted as long as the mine water could cause negative impacts on the receiving water course. Yet, as has been seen from the Aznacollar and Baia Mare accidents, large scale pollution of our environment can only be reached if all parties involved in mining inform each other within short notice. Furthermore, everybody has to work according to the highest standards available, as has been outlined by the BATNEEC principle, which means “best available technology not entailing excessive costs” (Environmental Protection Agency of Ireland 1997).

From a water perspective view, those active mining operations can’t be seen as a problem. Other the polluted discharges from abandoned mines, for which in many, but not all, cases, no one can or will be made responsible. Currently, no exact number of those “uncontrolled” discharges is known, but on the basis of several local studies, it must be assumed, that those point or diffuse discharges can be counted by tens of thousands (ERMITE Consortium et al. 2004). Furthermore, most European key mining regions are within the boundaries of metallogenetic provinces where surface and ground water have already naturally enriched concentrations of metals or metalloids. For those regions it might be problematic to define the pre-mining good ecological status and Neitzel et al. (2002) have discussed, if those regions would need special consideration within the Water Framework Directive. Cave et al. (2003) described how the Water Framework Directive might affect the management of a metal-rich catchment and its coastal area.

4. Mine Water Management and the Water Framework Directive

Mine water management, according to the Berlin guidelines (United Nations Department of Technical Co-operation for Development and Development Policy Forum of the German Foundation for International Development (1992) and their amendments in 2002) and the recommendations of the ERMITE Consortium et al. (2004), has to start before any exploitation on the mine site starts. Already during the exploration, and especially during the planning phase mine operators must bear in mind the post-mining situation. That means that mine water management and the mine closure as well as the post-closure phase have do be conducted in that way that no unacceptable negative effect on the water catchment will be encountered. During the active mining phase, water treatment is usually no problem, because in accordance with the "polluter pays" principle the mine operator can be forced to treat his discharged water. This is slightly more complicated for the thousands of untreated discharges from abandoned mines (Fig. 3), because the legal owner often is not able to cover the treatment costs. Younger (2002) claimed that all mine operators closing down their mine should "[pass] prior to the closure of the mine … certain minimal information to those authorities which are responsible for implementing the Water Framework Directive". In Germany, according to the Bundesberggesetz (Federal Mining Law, its relation to water legislation is discussed in Reinhardt 1999) and in Austria according to the Mineralrohstoffgesetz (Mineral Raw Material Law, see discussion in Randl 1998/99) every mine operator has to pass those information to the regional mining authorities where it is available even decades, and sometimes centuries after the mine's closure.

For abandoned mines the UK Coal Authority and the Environment Agency gave examples of how to minimize the impacts caused by abandoned mines. They constructed several tens of passive treatment plants in order to reduce the pollutant load into the receiving streams (Brown et al. 2002, Younger 2002, Wolkersdorfer and Younger 2002). Not all of those treatment plants clean the water down to the commonly used discharge standards for most metals, but at least they reduce the negative impacts on the receiving water courses and consequently the whole catchment area. Because it is economically impossible to treat all mine water discharges from abandoned mines to values accepted by all regulators, the installation of passive treatment plants for abandoned mines is therefore a valuable means to meet the demands of the Water Framework Directive.

As can be seen from those demands, the protection of our water catchments from polluted mine discharges could be a costly matter for the authorities involved. Baresel et al. (2003) investigated the necessary measures for the calculation of different rehabilitation procedures on the basis of the Swedish Dal river catchment. Though the measures discussed therein are no applicable for all cases of mine water discharges, the investigation clearly shows that a thorough understanding of the site and potential remediation options is necessary to calculate the potential remediation costs.

5. Concluding remarks

As has been shown above – and only a small aspect of the interaction between mine water issues and the Water Framework Directive has been addressed – a key issue of today's mining is the water management from the first day of exploration and mine planning. Taking into consideration the potential impacts of polluted mine water after the mine's lifetime guarantees in most cases a thorough protection of the river catchment, in which the mine operations are situated.

Concerning the thousands, possible tens of thousands of point or diffuse pollutions from abandoned mines, for which no one wants to take over responsibility, the situation is still unclear. As long as those sources of pollution are not treated or at leased minimized in their impact, a good ecological and chemical status of some river catchments can't be reached within the timeframe given by the

Water Framework Directive. The example of the UK, where the responsible authorities invest in passive treatment schemes – at least to minimize the impacts of mine water discharges – is a good example of how such problems might be solved in other Member States.

In conclusion, the Water Framework Directive – though it does not mention mining or abandoned mine voids in particular – can be seen as an sufficient tool to manage such sources of stress on our water environment. For the still unclear situations with either naturally elevated metal concentrations or, especially, abandoned mine voids further actions seem to be necessary.

6. Acknowledgements

Parts of the work presented here have been financed by the European Union Framework 6 R&D projects PIRAMID (EVK1-CT1999-00021) and ERMITE (EVK1-CT-2000-00078).

7. References

Baresel C., Larsén K., Destouni G., Gren I.-M. (2003). *Environmental Regulation of Mine Waters in the European Union – D 5 Economic Analysis Of Mine Water Pollution Abatement On A Catchment Scale*: *ERMITE Report – EU R&D Project EVK1-CT-2000-00078*. 34 p., Stockholm (Royal Institute of Technology).

Bongaerts J. C. (2002). *European Water Law: water policy and water resources management in France: the project de loi sur l'eau*, Europ. Env. Law Rev. (8—9, 10), 239—244; 260—270.

Brown M., Barley B., Wood H. (2002). *Minewater Treatment – Technology, Application and Policy*. 500 p., London (IWA Publishing).

Cave R. R., Ledoux L., Turner K., Jickells T., Andrews J. E., Davies H. (2003). *The Humber Catchment and its Coastal Area: from UK to European Perspectives*, Sci. Total Environ., 314, 31—52.

Environmental Protection Agency of Ireland (1997). *Integrated Pollution Control Licensing – BATNEEC Guidance Note for the Extraction of Minerals*. 28 p., Wexford (Environmental Protection Agency).

ERMITE Consortium, [eds. Younger P., Wolkersdorfer Ch. (2004). *Mining Impacts on the Fresh Water Environment: Technical and Managerial Guidelines for Catchment Scale Management*, Mine Water and the Environment, 23 (Supplement 1), S2-S80.

European Commission (2000). *Directive 2000/60/EC of the European Parliament and of the Council of 23 October 2000 establishing a framework for Community action in the field of water policy*, Official Journal of the European Communities, L 327, 1—72.

Hámar T., D'Allessandro M., Bidaglio G. (2002). *Legislation on Mining Waste Management in Central and Eastern European Candidate Countries* **EUR 20545 EN**. 196 p., Ispra (Joint Research Centre of the European Commission).

Kroll A., Amezaga J. M., Younger P. L., Wolkersdorfer Ch. (2002a). *Regulation of Mine Waters in the European Union: Contribution of Scientific Research to Policy Development*, Mine Water and the Environment, 21 (4), 193—200.

Kroll A., Betlem G., Brans E., Getliffe K., Groen F., Santamaría L., Lucas M., López B. (2002b). *Environmental Regulation of Mine Waters in the European Union – D 4 European Policies and*

Mine Waters: *ERMITE Report – EU R&D Project EVK1-CT-2000-00078*. 189 p., Sevilla (Institute for Prospective Technological Studies).

Neitzel P. L., Schneider P., Schlumprecht H. (2002). *Physico-chemical surface water conditions of catchments with metallogenic origin: A contribution to the establishment of the EC Water Framework Directive 2000/60/EG in Germany*. In: Merkel B. J., Planer-Friedrich B., Wolkersdorfer Ch.: *Uranium in the Aquatic Environment*, 77—83, Heidelberg (Springer).

PIRAMID Consortium (2003). *Engineering Guidelines for the Passive Remediation of Acidic and/or Metalliferous Mine Drainage and similar Wastewaters*. 166 p., Newcastle Upon Tyne (University of Newcastle Upon Tyne).

Plinke M., Wildhagen E. (2003). *Mining and water in Germany – Legal framework and technical aspects*. In: Nel P. J. L.: *Mine Water and the Environment*, 279—286, Johannesburg (Proceedings, 8th International Mine Water Association Congress).

Randl H. (1998/99). *Die Neuordnung des Bergrechts durch das Mineralrohstoffgesetz (MinroG)*, JAP – Juristische Ausbildung und Praxisvorbereitung, 5, 248—257.

Reinhardt M. (1999). *Bergrechtliche Determinanten wasserbehördlicher Entscheidungen*. In: Danwitz T. v.: *Bochumer Beiträge zum Berg- und Energierecht* **32**, 57—81, Stuttgart u.a. (Boorberg).

Salmon S. U., Destouni G. (2001). *Environmental Regulation of Mine Waters in the European Union – D 1 National Case Studies – Sweden*: *ERMITE Final Report – EU R&D Project EVK1-CT-2000-00078*. 21 p., Stockholm (Royal Institute of Technology).

Timmermann J. G., Langaas S. (2004). *Environmental Information in European Transboundary Water Management*. 258 p., London (IWA Publishing).

United Nations Department of Technical Co-operation for Development, Development Policy Forum of the German Foundation for International Development (1992). *Mining and the Environment – The Berlin Guidelines – A study based on an international Round Table in June 1991*. 180 p., London (Mining Journal Books).

Wolkersdorfer Ch. (2001). *Environmental Regulation of Mine Waters in the European Union – D 2 Overview of the EU and Eastern Europe*: *ERMITE Final Report – EU R&D Project EVK1-CT-2000-00078*. 5 p., Freiberg (TU Bergakademie Freiberg).

Wolkersdorfer Ch., Bowell R. (2005). *Contemporary Reviews of Mine Water Studies in Europe*, Mine Water and the Environment (electronic edition), 24 (3), 1—76.

Wolkersdorfer Ch., Younger P. L. (2002). *Passive Grubenwassereinigung als Alternative zu aktiven Systemen*, Grundwasser, 7 (2), 67—77.

Younger P. L. (2002). *Coalfield closure and the water environment in Europe*, Trans. Inst. Min. Metall. Sect. A, 111, A201—A209.

Younger P. L. (2002). *Mine waste or mine voids: which is the most important long-term source of polluted mine drainage?*, United Nations Environment Programme, Mineral Resources Forum, paper Nov—Dec 2002, 12.